2015

ANNUAL PROGRESS REPORT

DOE Hydrogen and Fuel Cells Program

U.S. DEPARTMENT OF ENERGY

DOE/GO-102015-4731
December 2015

U.S. Department of Energy
1000 Independence Avenue, S.W.
Washington, D.C. 20585-0121

FY 2015
PROGRESS REPORT FOR THE DOE HYDROGEN AND FUEL CELLS PROGRAM

December 2015

DOE/GO-102015-4731

Approved by Sunita Satyapal, Director, Hydrogen and Fuel Cells Program

NOTICE

This report was prepared as an account of work sponsored by an agency of the United States government. Neither the United States government nor any agency thereof, nor any of their employees, makes any warranty, express or implied, or assumes any legal liability or responsibility for the accuracy, completeness, or usefulness of any information, apparatus, product, or process disclosed, or represents that its use would not infringe privately owned rights. Reference herein to any specific commercial product, process, or service by trade name, trademark, manufacturer, or otherwise does not necessarily constitute or imply its endorsement, recommendation, or favoring by the United States government or any agency thereof. The views and opinions of authors expressed herein do not necessarily state or reflect those of the United States government or any agency thereof.

Available electronically at http://www.osti.gov/bridge

Available for a processing fee to U.S. Department of Energy
and its contractors, in paper, from:

U.S. Department of Energy
Office of Scientific and Technical Information
P.O. Box 62
Oak Ridge, TN 37831-0062
Phone: (865) 576-8401
Fax: (865) 576-5728
Email: mailto:reports@adonis.osti.gov

Available for sale to the public, in paper, from:

U.S. Department of Commerce
National Technical Information Service
5285 Port Royal Road
Springfield, VA 22161
Phone: (800) 553-6847
Fax: (703) 605-6900
Email: orders@ntis.fedworld.gov
Online ordering: http://www.ntis.gov/ordering.htm

Printed on paper containing at least 50% wastepaper, including 20% postconsumer waste

Table of Contents

I. Introduction . . . I–1

II. Hydrogen Production . . . II–1

II.0 Hydrogen Production Sub-Program Overview . . . II–3

II.A Hydrogen Production Analysis . . . II–11

II.A.1 Strategic Analysis, Inc.: Hydrogen Pathways Analysis for Solid Oxide Fuel Cell (SOFC) and Dark Fermentation . . . II–11

II.B Electrolysis . . . II–18

II.B.1 National Renewable Energy Laboratory: Renewable Electrolysis Integrated Systems Development and Testing . . . II–18

II.B.2 Giner, Inc.: High-Performance, Long-Lifetime Catalysts for Proton Exchange Membrane Electrolysis . . . II–23

II.B.3 Proton OnSite: Low-Noble-Metal-Content Catalysts/Electrodes for Hydrogen Production by Water Electrolysis . . . II–28

II.B.4 Giner, Inc.: High Temperature, High Pressure Electrolysis . . . II–31

II.C High-Temperature Thermochemical . . . II–35

II.C.1 Sandia National Laboratories: High Efficiency Solar Thermochemical Reactor for Hydrogen Production . . . II–35

II.C.2 University of Colorado Boulder: Flowing Particle Bed Solarthermal Redox Process to Split Water . . . II–41

II.C.3 Savannah River National Laboratory: Electrolyzer Component Development for the HyS Thermochemical Cycle . . . II–46

II.C.4 National Renewable Energy Laboratory: High Efficiency Tandem Absorbers for Economical Solar Hydrogen Production . . . II–50

II.C.5 University of Hawaii: Wide Bandgap Chalcopyrite Photoelectrodes for Direct Water Splitting . . . II–56

II.C.6 University of Colorado: Accelerated Discovery of Advanced RedOx Materials for Solar Thermal Water Splitting to Produce Renewable Hydrogen . . . II–60

II.D Photoelectrochemical . . . II–67

II.D.1 The University of Toledo: New Metal Oxides for Efficient Hydrogen Production via Solar Water Splitting . . . II–67

II.D.2 Rutgers, the State University of New Jersey: Tunable Photoanode-Photocathode-Catalyst Interface Systems for Efficient Solar Water Splitting . . . II–72

II.E Biological . . . II–76

II.E.1 National Renewable Energy Laboratory: Fermentation and Electrohydrogenic Approaches to Hydrogen Production . . . II-76

II.E.2 National Renewable Energy Laboratory: Improving Cyanobacterial O_2-Tolerance Using CBS Hydrogenase for H_2 Production . . . II–81

II.F Separations and Bio-Feedstock Conversion . . . II–84

II.F.1 Pacific Northwest National Laboratory: Monolithic Piston-Type Reactor for Hydrogen Production through Rapid Swing of Reforming/Combustion Reactions . . . II–84

II.F.2 FuelCell Energy, Inc.: Reformer-Electrolyzer-Purifier (REP) for Production of Hydrogen . . . II–90

III. Hydrogen Delivery . . . III–1

III.0 Hydrogen Delivery Sub-Program Overview . . . III–3

III.1 Argonne National Laboratory: Hydrogen Delivery Infrastructure Analysis . . . III–9

III.2 Oak Ridge National Laboratory: Vessel Design and Fabrication Technology for Stationary High-Pressure Hydrogen Storage . . . III–13

III.3 Sandia National Laboratories: Hydrogen Embrittlement of Structural Steels . . . III–18

III. Hydrogen Delivery (Continued)

III.4 Savannah River National Laboratory: Fiber Reinforced Composite Pipeline . . . III–22
III.5 Hexagon Lincoln: Development of High Pressure Hydrogen Storage Tank for Storage and Gaseous Truck Delivery . . . III–25
III.6 NanoSonic, Inc.: Cryogenically Flexible, Low Permeability H_2 Delivery Hose . . . III–28
III.7 Southwest Research Institute®: Hydrogen Compression Application of the Linear Motor Reciprocating Compressor (LMRC) . . . III–33
III.8 Oak Ridge National Laboratory: Steel Concrete Composite Vessel for 875 Bar Stationary Hydrogen Storage . . . III–40
III.9 Wiretough Cylinders, LLC: Low Cost Hydrogen Storage at 875 Bar Using Steel Liner and Steel Wire Wrap . . . III–45
III.10 FuelCell Energy, Inc.: Electrochemical Hydrogen Compressor . . . III–50
III.11 Sandia National Laboratories: Reference Station Design . . . III–53
III.12 Argonne National Laboratory: Hydrogen Fueling Station Precooling Analysis . . . III–57
III.13 National Renewable Energy Laboratory: 700-Bar Hydrogen Dispenser Hose Reliability and Improvement . . . III–60
III.14 Pacific Northwest National Laboratory: Magnetocaloric Hydrogen Liquefaction . . . III–65

IV. Hydrogen Storage . . . IV–1

IV.0 Hydrogen Storage Sub-Program Overview . . . IV–3

IV.A Analysis . . . IV–11
IV.A.1 Argonne National Laboratory: System Analysis of Physical and Materials-Based Hydrogen Storage . . . IV–11
IV.A.2 Strategic Analysis, Inc.: Hydrogen Storage Cost Analysis . . . IV–17

IV.B Engineering – HSECoE . . . IV–22
IV.B.1 Savannah River National Laboratory: Hydrogen Storage Engineering Center of Excellence . . . IV–22
IV.B.2 Ford Motor Company: Ford/BASF SE/UM Activities in Support of the Hydrogen Storage Engineering Center of Excellence . . . IV–27
IV.B.3 Oregon State University: Microscale Enhancement of Heat and Mass Transfer for Hydrogen Energy Storage . . . IV–32
IV.B.4 United Technologies Research Center: Advancement of Systems Designs and Key Engineering Technologies for Materials-Based Hydrogen Storage . . . IV–36
IV.B.5 Pacific Northwest National Laboratory: Systems Engineering of Chemical Hydrogen Storage and Cryo-Sorbent Storage, Pressure Vessel, and Balance of Plant for Onboard Hydrogen Storage . . . IV–44
IV.B.6 National Renewable Energy Laboratory: System Design, Analysis, Modeling, and Media Engineering Properties for Hydrogen Energy Storage . . . IV–49
IV.B.7 Hexagon Lincoln Inc.: Development of Improved Composite Pressure Vessels for Hydrogen Storage . . . IV–53
IV.B.8 Los Alamos National Laboratory: Chemical Hydride Rate Modeling, Validation, and System Demonstration . . . IV–56
IV.B.9 General Motors R&D Center: Testing, Modeling, and Evaluation of Innovative Hydrogen Storage System Designs . . . IV–59

IV.C Hydrogen Storage Materials . . . IV–63
IV.C.1 Lawrence Berkeley National Laboratory: Hydrogen Storage in Metal-Organic Frameworks . . . IV–63
IV.C.2 National Renewable Energy Laboratory: Hydrogen Sorbent Measurement Qualification and Characterization . . . IV–70
IV.C.3 National Institute of Standards and Technology: Neutron Characterization in Support of the DOE Hydrogen Storage Sub-Program . . . IV–76
IV.C.4 Ames Laboratory: High-Capacity Hydrogen Storage Systems via Mechanochemistry . . . IV–81
IV.C.5 Savannah River National Laboratory: Electrochemical Reversible Formation of α-Alane . . . IV–84

IV. Hydrogen Storage (Continued)

IV.C Hydrogen Storage Materials (Continued)

IV.C.6 Ardica Technologies, Inc.: Low-Cost α-Alane for Hydrogen Storage IV–88

IV.C.7 Boston College: Novel Carbon(C)-Boron(B)-Nitrogen(N)-Containing H_2 Storage Materials IV–92

IV.C.8 HRL Laboratories, LLC: Boron-Based Hydrogen Storage: Ternary Borides and Beyond IV–97

IV.C.9 Lawrence Livermore National Laboratory: Improving the Kinetics and Thermodynamics of $Mg(BH_4)_2$ for Hydrogen Storage IV–101

IV.D Advanced Tanks IV–108

IV.D.1 Sandia National Laboratories: Innovative Development, Selection, and Testing to Reduce Cost and Weight of Materials for BOP Components IV–108

IV.D.2 Lawrence Livermore National Laboratory: Thermomechanical Cycling of Thin Liner High Fiber Fraction Cryogenic Pressure Vessels Rapidly Refueled by LH2 Pump to 700 bar IV–113

IV.D.3 Pacific Northwest National Laboratory: Enhanced Materials and Design Parameters for Reducing the Cost of Hydrogen Storage Tanks IV–118

IV.D.4 Materia, Inc.: Next Generation Hydrogen Storage Vessels Enabled by Carbon Fiber Infusion with a Low Viscosity, High Toughness System IV–122

IV.D.5 Oak Ridge National Laboratory: Melt Processable PAN Precursor for High Strength, Low Cost Carbon Fibers (Phase II) IV–126

IV.D.6 PPG Industries, Inc.: Achieving Hydrogen Storage Goals through High-Strength Fiber Glass . . .IV–134

IV.D.7 Composite Technology Development, Inc.: Optimizing the Cost and Performance of Composite Cylinders for H_2 Storage Using a Graded Construction IV–138

IV.E Basic Energy Sciences IV–143

IV.E.1 Ames Laboratory: Complex Hydrides – A New Frontier for Future Energy Applications IV–143

IV.E.2 Savannah River National Laboratory: Elucidation of Hydrogen Interaction Mechanisms with Metal-Doped Carbon Nanostructures IV–144

IV.E.3 University of California, Davis: Activation of Hydrogen under Ambient Conditions by Main Group Molecules. IV–145

IV.E.4 Virginia Commonwealth University: Elucidation of Hydride Interaction Mechanisms with Carbon Nanostructures and the Formation of Novel Nanocomposites IV–146

V. Fuel Cells V–1

V.0 Fuel Cells Sub-Program Overview. V–3

V.A Catalysts & Electrodes V–9

V.A.1 National Renewable Energy Laboratory: Extended, Continuous Pt Nanostructures in Thick, Dispersed Electrodes V–9

V.A.2 Argonne National Laboratory: Nanosegregated Cathode Alloy Catalysts with Ultra-Low Platinum Loading V–13

V.A.3 Brookhaven National Laboratory: Contiguous Platinum Monolayer Oxygen Reduction Electrocatalysts on High-Stability, Low-Cost Supports V–20

V.A.4 Illinois Institute of Technology: Synthesis and Characterization of Mixed-Conducting Corrosion Resistant Oxide Supports V–25

V.A.5 Northeastern University: Development of Novel Non-PGM Electrocatalysts for Proton Exchange Membrane Fuel Cell Applications. V–29

V.A.6 University of South Carolina: Development of Ultra-Low Platinum Alloy Cathode Catalysts for PEM Fuel Cells V–37

V.A.7 Los Alamos National Laboratory: Non-Precious Metal Fuel Cell Cathodes: Catalyst Development and Electrode Structure Design. V–43

V.A.8 Argonne National Laboratory: High-Throughput Synthesis, ORR Activity Modeling, and Testing of non-PGM PEMFC Cathode Catalysts. V–51

V.A.9 Proton OnSite: Non-Platinum Group Metal OER/ORR Catalysts for Alkaline Membrane Fuel Cells and Electrolyzers. V–56

V. Fuel Cells (Continued)

V.A Catalysts & Electrodes (Continued)
V.A.10 pH Matter, LLC: Non-Precious Metal Bi-Functional Catalysts . . . V–60

V.B Membranes & Electrolytes . . . V–64
V.B.1 3M Company: New Fuel Cell Membranes with Improved Durability and Performance . . . V–64
V.B.2 Colorado School of Mines: Advanced Hybrid Membranes for Next Generation PEMFC Automotive Applications . . . V–69

V.C MEAs, Cells, & Other Stack Components . . . V–73
V.C.1 3M Company: High Performance, Durable, Low Cost Membrane Electrode Assemblies for Transportation Applications . . . V–73
V.C.2 Argonne National Laboratory: Rationally Designed Catalyst Layers for PEMFC Performance Optimization . . . V–80
V.C.3 TreadStone Technologies, Inc.: Novel Structured Metal Bipolar Plates for Low Cost Manufacturing . . . V–86
V.C.4 National Renewable Energy Laboratory: Advanced Ionomers and MEAs for Alkaline Membrane Fuel Cells . . . V–92

V.D Balance of Plant Components . . . V–96
V.D.1 Eaton Corporation: Roots Air Management System with Integrated Expander . . . V–96

V.E System, Stack, and Component Operation & Performance . . . V–101
V.E.1. Los Alamos National Laboratory: Durability Improvements through Degradation Mechanism Studies . . . V–101
V.E.2 Lawrence Berkeley National Laboratory: Fuel-Cell Fundamentals at Low and Subzero Temperatures . . . V–108
V.E.3 National Renewable Energy Laboratory: Effect of System Contaminants on PEMFC Performance and Durability . . . V–113
V.E.4 Hawaii Natural Energy Institute: The Effect of Airborne Contaminants on Fuel Cell Performance and Durability . . . V–119
V.E.5 Ballard Power Systems: Open Source FCPEM-Performance and Durability Model: Consideration of Membrane Properties on Cathode Degradation . . . V–125

V.F Testing and Technical Assessment . . . V–130
V.F.1 National Renewable Energy Laboratory: Optimal Stationary Fuel Cell Integration and Control . . . V–130
V.F.2 Argonne National Laboratory: Performance and Durability of Advanced Automotive Fuel Cell Stacks and Systems . . . V–133
V.F.3 Strategic Analysis, Inc.: Fuel Cell Vehicle and Bus Cost Analysis . . . V–141
V.F.4 Oak Ridge National Laboratory: Characterization of Fuel Cell Materials . . . V–147
V.F.5 National Institute of Standards and Technology: Neutron Imaging Study of the Water Transport in Operating Fuel Cells . . . V–152
V.F.6 Battelle: Stationary and Emerging Market Fuel Cell System Cost Analysis—Primary Power and Combined Heat and Power Applications . . . V–158
V.F.7 Lawrence Berkeley National Laboratory: A Total Cost of Ownership Model for Design and Manufacturing Optimization of Fuel Cells in Stationary and Emerging Market Applications . . . V–162
V.F.8 Redox Power Systems: Affordable, High Performance, Intermediate Temperature Solid Oxide Fuel Cells . . . V–167
V.F.9 FuelCell Energy, Inc.: Smart Matrix Development for Direct Carbonate Fuel Cell . . . V–170
V.F.10 National Renewable Energy Laboratory: Fuel Cell Technology Status—Degradation . . . V–174
V.F.11 Giner, Inc.: Ionomer Dispersion Impact on Advanced Fuel Cell and Electrolyzer Performance and Durability . . . V–179
V.F.12 Argonne National Laboratory: Novel Non-PGM Catalysts from Rationally Designed 3-D Precursors . . . V–184

V. Fuel Cells (Continued)

V.F Testing and Technical Assessment (Continued)

V.F.13 Savannah River National Laboratory: PGM Free Catalysts for PEMFC V–189
V.F.14 Pacific Northwest National Laboratory: High Performance and Durable Low PGM Cathode Catalysts V–194
V.F.15 Oak Ridge National Laboratory: Magnetic Annealing of Pt-Alloy Nanostructured Thin Film Catalysts for Enhanced Activity V–198
V.F.16 Oak Ridge National Laboratory: High Conductivity Durable Anion Conducting Membranes. . . . V–203
V.F.17 Los Alamos National Laboratory: Advanced Hydroxide Conducting Membranes V–205
V.F.18 Sandia National Laboratories: DOE's High Acid Content Diels-Alder Poly(Phenylene)s for High Temperature and Low Humidity Applications V–211
V.F.19 Los Alamos National Laboratory: Engineered Low-Pt Catalyst Layers V–218
V.F.20 Brookhaven National Laboratory: Semi-Automated MEA Fabrication with Ultra-Low Total PGM Loadings V–223

VI.0 Manufacturing R&D VI–1
VI.0 Manufacturing R&D Sub-Program Overview. VI–3
VI.1 National Renewable Energy Laboratory: Fuel Cell Membrane Electrode Assembly Manufacturing R&D VI–7
VI.2 Westside Industrial Retention & Expansion Network NE: U.S. Clean Energy Hydrogen and Fuel Cell Technologies: A Competitiveness Analysis VI–12

VII. Technology Validation VII–1
VII.0 Technology Validation Sub-Program Overview VII–3
VII.1 National Renewable Energy Laboratory: Hydrogen Component Validation VII–9
VII.2 Lawrence Livermore National Laboratory: Performance and Durability Testing of Volumetrically Efficient Cryogenic Vessels and High Pressure Liquid Hydrogen Pump. VII–13
VII.3 National Renewable Energy Laboratory: FCTO INTEGRATE Stack Test Bed and Grid Interoperability VII–17
VII.4 National Renewable Energy Laboratory: Fuel Cell Electric Vehicle Evaluation VII–21
VII.5 National Renewable Energy Laboratory: Technology Validation: Fuel Cell Bus Evaluations VII–26
VII.6 National Renewable Energy Laboratory: Material Handling Equipment Data Collection and Analysis VII–31
VII.7 Sandia National Laboratories: Development of the Hydrogen Station Equipment Performance (HyStEP) Device. VII–36
VII.8 California Fuel Cell Partnership: Station Operational Status System (SOSS) 3.0 Upgrade VII–41
VII.9 Proton OnSite: Validation of an Advanced High Pressure PEM Electrolyzer and Composite Hydrogen Storage, with Data Reporting, for SunHydro Stations VII–44
VII.10 Gas Technology Institute: Performance Evaluation of Delivered Hydrogen Fueling Stations VII–50
VII.11 National Renewable Energy Laboratory: Hydrogen Station Data Collection and Analysis VII–53
VII.12 California State University Los Angeles: CSULA Hydrogen Refueling Facility Performance Evaluation and Optimization VII–58
VII.13 National Renewable Energy Laboratory: Stationary Fuel Cell Evaluation VII–61
VII.14 Idaho National Laboratory: Dynamic Modeling and Validation of Electrolyzers in Real Time Grid Simulation. VII–65

VIII. Safety, Codes & Standards VIII–1
VIII.0 Safety, Codes & Standards Sub-Program Overview VIII–3
VIII.1 Sandia National Laboratories: Hydrogen Behavior and Quantitative Risk Assessment VIII–7
VIII.2 National Renewable Energy Laboratory: Component Standard Research and Development VIII–13
VIII.3 Sandia National Laboratories: R&D for Safety, Codes and Standards: Materials and Components Compatibility. VIII–17

VIII. Safety, Codes & Standards (Continued)

VIII.4 Los Alamos National Laboratory: Hydrogen Fuel Quality VIII–21
VIII.5 National Renewable Energy Laboratory: NREL Hydrogen Sensor Testing Laboratory VIII–26
VIII.6 Pacific Northwest National Laboratory: Hydrogen Safety Panel, Safety Knowledge Tools and First Responder Training Resources VIII–31
VIII.7 National Renewable Energy Laboratory: Fuel Cell Technologies National Codes and Standards Development and Outreach VIII–38
VIII.8 Fuel Cell & Hydrogen Energy Association: Fuel Cell & Hydrogen Energy Association Codes and Standards Support. VIII–42
VIII.9 National Renewable Energy Laboratory: Hydrogen Contaminant Detector VIII–46
VIII.10 Sandia National Laboratories: Enabling Hydrogen Infrastructure Through Science-Based Codes and Standards VIII–49
VIII.11 Los Alamos National Laboratory: Hydrogen Safety, Codes and Standards: Sensors VIII–53
VIII.12 Lawrence Livermore National Laboratory: Hands-On Hydrogen Safety Training VIII–60

IX. Systems Analysis IX–1

IX.0 Systems Analysis Sub-Program Overview IX–3
IX.1 Argonne National Laboratory: Impact of Fuel Cell System Peak Efficiency on Fuel Consumption and Cost IX–13
IX.2 Oak Ridge National Laboratory: GPRA Analysis: Impact of Program Targets on Vehicle Penetration and Benefits IX–19
IX.3 National Renewable Energy Laboratory: Pathway Analysis: Projected Cost, Lifecycle Energy Use and Emissions of Emerging Hydrogen Technologies. IX–24
IX.4 Argonne National Laboratory: Performance and Cost Analysis for a 300 kW Tri-Generation Molten Carbonate Fuel Cell System. IX–29
IX.5 Argonne National Laboratory: Employment Impacts of Infrastructure Development for Hydrogen and Fuel Cell Technologies IX–34
IX.6 Argonne National Laboratory: Life Cycle Analysis of Water Use for Hydrogen Production Pathways IX–37
IX.7 Sandia National Laboratories: Hydrogen Analysis with the Sandia ParaChoice Model IX–41
IX.8 The University of Tennessee: Status and Prospects of the N.A. Non-Automotive Fuel Cell Industry: 2014 Update IX–44
IX.9 University of California, Irvine: Tri-Generation Fuel Cell Technologies for Location-Specific Applications IX–48
IX.10 Argonne National Laboratory: Analysis of Incremental Fueling Pressure Cost IX–54
IX.11 Oak Ridge National Laboratory: Analysis of Optimal On-Board Storage Pressure for Hydrogen Fuel Cell Vehicles IX–58
IX.12 National Renewable Energy Laboratory: Infrastructure Investment and Finance Scenario Analysis IX–61
IX.13 The University of Chicago: The Business Case for Hydrogen-Powered Passenger Cars: Competition and Solving the Infrastructure Puzzle IX–65
IX.14 Kalibrate: Retail Marketing Analysis: Hydrogen Refueling Stations. IX–67

X. Market Transformation. X–1

X.0 Market Transformation Sub-Program Overview X–3
X.1 Plug Power: Ground Support Equipment Demonstration. X–7
X.2 Sandia National Laboratories: Maritime Fuel Cell Generator Project X–10
X.3 Center for Transportation and the Environment: Fuel Cell Hybrid Electric Delivery Van Project X–14
X.4 Hawaii Natural Energy Institute: Hydrogen Energy Systems as a Grid Management Tool X–18
X.5 US Hybrid Corporation: Demonstration and Deployment of a Fuel Cell-Electric Refuse Truck for Waste Transportation X–21

XI. Small Business Innovation Research (SBIR) Fuel Cell Technologies Office New Projects Awarded in FY 2015 . . . . XI–1

XI.0 Small Business Innovation Research (SBIR) Fuel Cell Technologies Office New Projects Awarded in FY 2015 . . . . XI–3

Phase I Projects XI–4

XI.1 US Hybrid Corporation: Fuel Cell-Battery Electric Hybrid for Utility or Municipal MD or HD Bucket Trucks (H2BT) XI–4

XI.2 Mainstream Engineering: Cross-polarized Near-UV Detector for In-line Quality Control of PEM Material XI–4

XI.3 Proton OnSite: Non-Platinum Group Metal OER/ORR Catalysts for Alkaline Membrane Fuel Cells and Electrolyzers XI–4

XI.4 PH Matter, LLC: Non-Precious Metal Bi-Functional Catalysts XI–5

XI.5 Southwest Sciences, Inc.: Diode Laser Sensor for Contaminants in Hydrogen Fuel XI–5

XI.6 Sustainable Innovations, LLC: Hydrogen Contamination Detection XI–5

Phase II Projects XI–6

XI.7 Giner Inc.: Ionomer Dispersion Impact on Advanced Fuel Cell and Electrolyzer Performance and Durability XI–6

XI.8 Tetramer Technologies, LLC: New High Performance Water Vapor Membranes to Improve Fuel Cell Balance of Plant Efficiency and Lower Costs. XI–6

XI.9 GVD Corporation: Flexible Barrier Coatings for Harsh Environments. XI–6

XI.10 Giner Inc.: High Performance Long Lifetime Catalyst for Proton Exchange Membrane Electrolysis XI–7

XI.11 Tetramer Technologies, LLC: New Approaches to Improved PEM Electrolyzer Ion Exchange Membranes XI–7

XII. Acronyms, Abbreviations, and Definitions XII–1

XIII. Primary Contacts Index XIII–1

XIV. Hydrogen and Fuel Cells Program Contacts XIV–1

XV. Project Listings by State XV–1

XVI. Project Listings by Organization XVI–1

I. INTRODUCTION

I.0 Introduction

The U.S. Department of Energy's Hydrogen and Fuel Cells Program (the Program) engages in comprehensive efforts across a range of technical and non-technical areas to enable the widespread commercialization of hydrogen and fuel cell technologies. The Program is coordinated across the U.S. Department of Energy (DOE or the Department), incorporating activities in the offices of Energy Efficiency and Renewable Energy (EERE) (led through the Fuel Cell Technologies Office [FCTO]), Science, Nuclear Energy, and Fossil Energy. The Program's efforts are aligned with the Administration's "all-of-the-above" approach to energy and the President's Climate Action Plan and will spark the type of innovation that drives economic growth and creates American jobs, while moving our economy toward cleaner, more efficient forms of energy that will cut our reliance on foreign oil.

With emphasis on applications that will most effectively strengthen our nation's energy security and improve our efforts to cut carbon emissions, the Program conducts research, development, and demonstration (RD&D) leading to critical improvements in hydrogen and fuel cell technologies, as well as diverse activities to overcome economic and institutional obstacles to commercialization.

The year 2015 was a landmark year for hydrogen and fuel cells. After decades of research and development (R&D) and the demonstration of various generations of prototype fuel cell electric vehicles (FCEVs) by a number of global automakers, this year saw the first commercial FCEVs in history, being *sold* to regular consumers. These accomplishments are directly in line with directives in the Energy Policy Act of 2005: "to enable a commitment by automakers no later than year 2015 to offer safe, affordable, and technically viable hydrogen fuel cell vehicles in the mass consumer market" (Public Law 109-58, Title 8, Sec. 805). To garner more public visibility, Congress established the first National Hydrogen and Fuel Cell Day in 2015—on October 8th (chosen for the atomic mass of hydrogen, 1.008)—with industry, government, and laboratories across the nation commemorating accomplishments and progress on that inaugural day. Against that backdrop, DOE continued to make substantial progress toward its goals and objectives, working with industry and other stakeholders to enable the widespread, commercially viable adoption of hydrogen and fuel cell technologies.

In Fiscal Year (FY) 2015, Congress appropriated approximately $117 million for the DOE Hydrogen and Fuel Cells Program in addition to $30 million for solid oxide fuel cell related activities. More detailed discussions of Program activities and plans can be found in the Hydrogen and Fuel Cells Program Plan, as well as in the plans of the program offices—FCTO's Multi-Year RD&D Plan; Office of Fossil Energy's Hydrogen from Coal RD&D Plan; and the Office of Science's Basic Research Needs for the Hydrogen Economy.[1]

In addition to summarizing examples of key R&D accomplishments, this report highlights major programmatic accomplishments, including launching the $1 Million H2 Refuel H-Prize; demonstrating the world's first fleet of hydrogen fuel cell airport ground support equipment; establishing national-laboratory-led consortia in key R&D areas; and supporting the public-private partnership, H2USA, through national-laboratory-led efforts developing financial assessment tools for hydrogen infrastructure and critical equipment to validate the performance of hydrogen stations as they come on line.

PROGRESS AND ACCOMPLISHMENTS BY KEY ACTIVITY

This report documents more than 1,000 pages of accomplishments achieved by DOE-funded projects in the last year. The following summaries include only a few examples. More details can be found in the individual sub-program introductions, subsequent project reports, and in the corresponding 2015 Annual Merit Review and Peer Evaluation Report.[2]

Fuel Cells

The Fuel Cells sub-program supports RD&D of fuel cell technologies for transportation applications, as well as enabling stationary and early market applications, with a primary focus on reducing cost and improving durability. Efforts include R&D of fuel cell stack components, system balance-of-plant (BOP) components, and subsystems, as well as system integration. The sub-program seeks a balanced, comprehensive approach to fuel cells for near-, mid-, and longer-term applications.

[1] www.hydrogen.energy.gov/roadmaps_vision.html
[2] http://www.hydrogen.energy.gov/annual_review15_report.html

Cost

One of the most important fuel cell metrics is the projected high-volume manufacturing cost for automotive fuel cells, which the sub-program tracks on an annual basis. This year, the cost of an 80-kW_{net} automotive polymer exchange membrane (PEM) fuel cell (FC) system based on next-generation laboratory technology and operating on direct hydrogen was projected to be \$53/kW_{net} when manufactured at a volume of 500,000 units/year (Figure 1) and \$60/kW_{net} when manufactured at 100,000 units/year. (For comparison, the expected cost of automotive PEM fuel cell systems that are based on current technology is approximately \$280/kW when manufactured at a volume of 20,000 units/year.)[3]

To enable commercially competitive fuel cell vehicles, the sub-program is targeting a cost reduction to \$40/kW by 2020. Long-term competitiveness with alternative powertrains is expected to require further cost reduction to \$30/kW, which represents the sub-program's ultimate cost target.

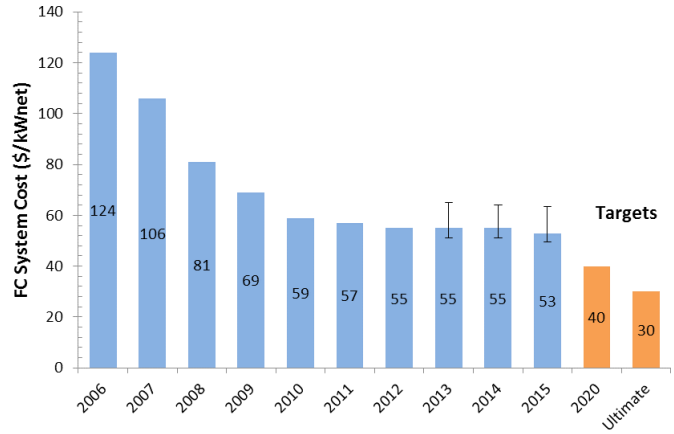

FIGURE 1. Modeled cost of an 80-kW_{net} PEM fuel cell system based on projection to high-volume manufacturing (500,000 units/year) (Source: FY 2015 Fuel Cell System Cost Record: http://www.hydrogen.energy.gov/program_records.html#fuel_cells)

Development of Best Practices and Protocols Impacting the Electrocatalyst Research Community

In addition to progress in fuel cell performance, cost, and durability, a key accomplishment in 2015 was finalization of standard protocols for rotating-disk electrode (RDE) testing to assess catalyst activity. This is an example in which the Program can impact the broader scientific community and bring together both basic research scientists and the applied research stakeholders to enable accurate and reproducible measurements that can subsequently be evaluated and taken to the next stage of development.

RDE testing is a standard tool to evaluate catalyst performance before determining whether membrane electrode assemblies (MEAs) should be fabricated, and it is widely used by thousands of researchers across academia, industry, and national labs worldwide. However, as brought to our attention by the Naval Research Laboratory (NRL), results can be highly irreproducible even when identical catalysts are used. A key to obtaining high and reproducible oxygen reduction reaction (ORR) activity measurement using the RDE technique is the formation of a uniform catalyst film on a glassy carbon electrode. However, uniformity of the film and hence results depend on how the film is deposited. As noted by NRL and coworkers, rotational drying can be used to eliminate the "coffee ring" structure typically seen when using stationary drying (Figure 2).[4] Discrepancies in activity values reported between research groups and the

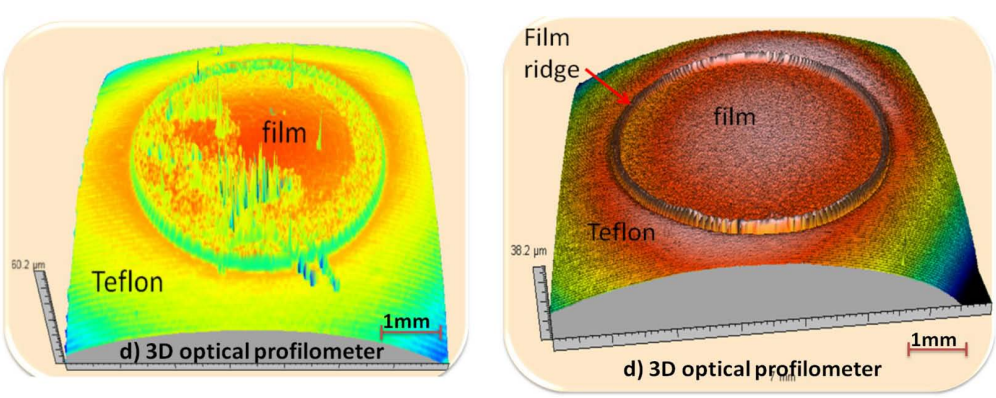

FIGURE 2. View of uniform film (right) vs. coffee ring structure and lack of uniformity (left)

[3]DOE Program Record #15015, http://www.hydrogen.energy.gov/pdfs/15015_fuel_cell_system_cost_2015.pdf
[4]Y. Garsany, I.L. Singer, K.E. Swider-Lyons, S.S. Kocha, Impact of film drying procedures on the RDE characterization of Pt/VC electrocatalyst, *J. Electroanal. Chem*. 662 (2011) 396–406.

fact that improved protocols have not been uniformly adopted result in inaccurate and unreliable catalyst screening and benchmarking being reported in the literature. For example, activity values reported over the last decade for the same catalyst tested in different laboratories have varied by as much as 200%.

The National Renewable Energy Laboratory (NREL) and Argonne National Laboratory (ANL) established standardized RDE test protocols and best practices to allow for more precise and reproducible data and reliable comparisons to be made by catalyst and fuel cell developers when evaluating novel synthesized catalysts in small quantities. Figure 3 shows reproducible results at three different laboratories using catalysts from three different suppliers. Details on the protocols can be found in the references below.[5] Given the importance of reporting accurate results in the literature, the new protocols and best practices are highlighted here for broader awareness.

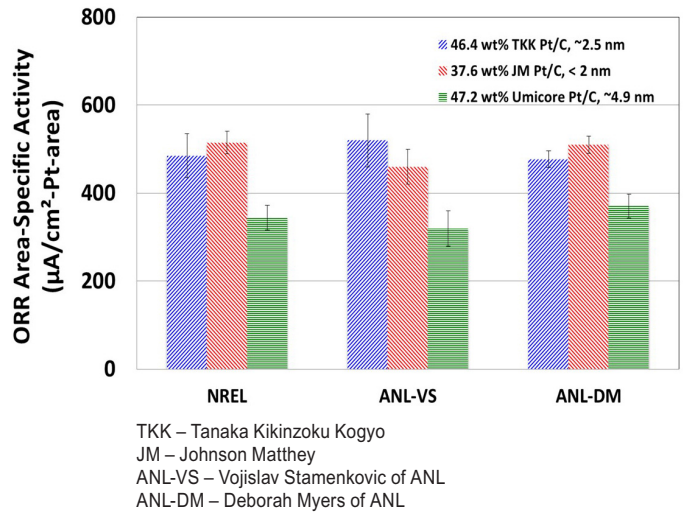

FIGURE 3. Catalyst activity results demonstrating reproducibility

Catalyst and MEA Advances

FY 2015 saw additional improvements in the integration of fuel cell components based on nano-structured thin film catalysts into high-performance MEAs. Power output per gram of platinum group metal (PGM) at rated power increased to 6.5 kW/gPGM (improved from 2.8 kW/gPGM in 2008 and 6.2 kW/gPGM in FY 2014) and is on track to achieve the 2020 target of 8 kW/gPGM.

Since catalysts comprise nearly half of the high-volume cost of automotive fuel cells, catalysis R&D continues to be a focus. Last year marked a significant step towards developing cathode catalysts with ultra-low platinum content with the development of $PtNi_3$ nanoframe catalysts at ANL. Synthesized by a novel spontaneous corrosion and annealing procedure, the resultant Pt-coated nano-framework, when integrated in an MEA, increased MEA performance by three-fold in comparison to a Pt/C catalyst under low-loading conditions (Figure 4).

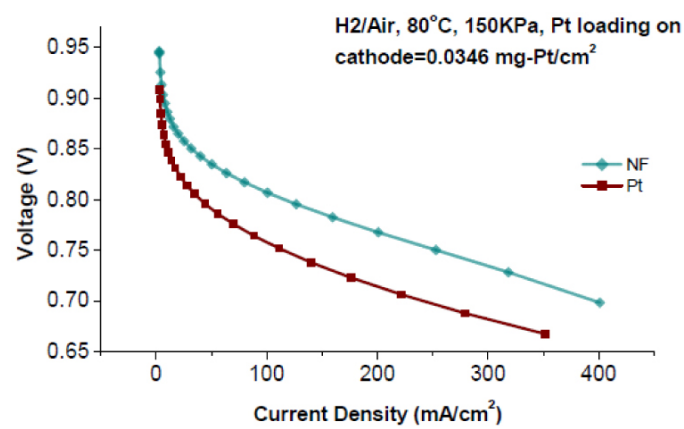

FIGURE 4. Performance of the nanoframes (NFs) relative to a traditional Pt/C catalyst (V. Stamenkovic, P. Yang et al., *Science*, 343 (2014) 1339)

This year also brought advances in catalyst design that resulted in further improvements over last year's nanoframe project, including the development of catalysts based on non-precious metals like iron that were coordinated into carbon and nitrogen-containing matrices. Current densities as high as 110 mA/cm^2 were achieved in air with these PGM-free catalysts, representing a significant improvement over the benchmark of 75 mA/cm^2 set in FY 2014, and demonstrating good progress toward achieving the targeted performance levels for platinum-based catalysts with less costly metals. Durability studies of these materials are underway, but initial ex situ testing has already demonstrated high stability.

Finally, the sub-program established a lab-led consortium project—Fuel Cell Performance and Durability (FC-PAD)—to further advance progress in improving performance and durability of fuel cell systems. Funding opportunities for adding industry, university, and other national lab projects to FC-PAD are planned for FY 2016.

[5]S. Kocha, et al., *Journal of The Electrochemical Society*, **162** (10) F1144–F1158 (2015); *Journal of The Electrochemical Society*, **162** (12) F1384–F1396 (2015). http://www.hydrogen.energy.gov/pdfs/review14/fc111_kocha_2014_o.pdf

Hydrogen Production

In FY 2015, the Hydrogen Production sub-program continued to focus on developing technologies to enable the long-term viability of hydrogen as an energy carrier for a range of applications with a focus on hydrogen from low-carbon and renewable sources. Progress continued in several key areas, including electrolysis, photoelectrochemical, biological, and solar-thermochemical hydrogen production.

In October of 2014, the Program announced the launch of the $1 million H2 Refuel H-Prize, consistent with the H-Prize authorization in the Energy Independence and Security Act of 2009 and with feedback from numerous stakeholders and the Program's federal advisory committee. This two-year competition challenges America's engineers and entrepreneurs to develop affordable systems for small-scale, non-commercial hydrogen fueling. Successful entries will install and test systems that generate hydrogen from resources available at most homes, like electricity or natural gas, and provide the hydrogen to fuel vehicles. The team that demonstrates the best system will win the $1 million cash prize. Initial system designs were due October 29, 2015, and the winner will be announced in late 2016.[6] This effort will complement the current focus by states and industry to deploy retail hydrogen fueling stations and will incentivize opportunities for small-scale hydrogen generation.

Efforts in the solar-thermochemical hydrogen (STCH) production area were directed toward performance characterization of water splitting by novel, non-volatile metal-oxide-based reaction materials and the development of new reactor concepts to optimize efficiency of the reaction cycles. Of particular note, more than 1,000 possible binary perovskites were screened, of which nearly 200 materials show potential for use in STCH production.

Also in FY 2015, the Program completed a stochastic analysis to establish the hydrogen fuel cost at which FCEVs will be competitive with internal combustion engine vehicles (ICEVs) in the near-term (2015–2020). The cost calculation was achieved by varying the price of gasoline, fuel economy values of ICEVs and FCEVs, and incremental cost of ownership of FCEVs within bounds determined by data from the Energy Information Administration, ANL's Autonomie vehicle simulation system, current state and federal incentives, and current sales prices of vehicles. The analysis determined that FCEVs are likely to be competitive with ICEVs at a hydrogen cost of about $7.00/gge.[7] The RD&D targets for the Program are being modified for consistency with this approach and result. The cost target for 2017 has been set at $12.00/gge (including production, delivery, and dispensing at low volumes).

Hydrogen Delivery

The goal of the Hydrogen Delivery sub-program is to reduce the costs associated with delivering hydrogen to a point at which its use as an energy carrier in fuel cell applications is competitive with alternative transportation and power generation technologies.

In FY 2015, the Hydrogen Fueling Infrastructure Research and Station Technology (H2FIRST) project published "The Reference Station Design Report"[8] that describes the designs and costs of hydrogen stations that are expected to be viable in the near-term (Table 1). The report includes detailed piping and instrumentation diagrams, bills of material, and layouts for five stations. The report additionally describes the impact of several key variables (station utilization rate, capacity, number of hoses, and supply method) on capital costs, levelized costs of hydrogen, and station footprint. These analyses are then used to provide recommendations for future research on station components, codes and standards, and business practices. The project completed much of its analysis using the Hydrogen Refueling Station Analysis Model (HRSAM), which was created at ANL in FY 2015.

TABLE 1. Station Designs Detailed in H2FIRST Reference Station Design Report

Delivery Method	Daily Capacity (kg)	Target Market	Site Type	Installed Capital Cost ($K)	Fuel Cost ($/kg)
Gaseous	300	High Use	Gas Station or Greenfield	$1,265	$6.03
Gaseous	200	High Use		$1,179	$5.83
Gaseous	100	Intermittent		$1,098	$13.28
Liquid	300	High Use	Greenfield	$2,007	[a]
Future Liquid	300	High Use	5	$1,551	$7.46

[a] This station type was not available in HRSAM as of this analysis and fuel cost could not be estimated. It has been included in the current version of the model.

[6] http://energy.gov/eere/fuelcells/articles/h2-refuel-h-prize-guideline-update
[7] DOE Program Record #15015, http://www.hydrogen.energy.gov/pdfs/15015_fuel_cell_system_cost_2015.pdf
[8] H2FIRST Reference Station Design Task, http://www.nrel.gov/docs/fy15osti/64107.pdf

HRSAM allows a user to determine the levelized cost of hydrogen dispensing for a given fueling station design and projected utilization rate. The model estimates the costs of station equipment based on recent vendor data and allows users to simulate gaseous stations, along with near-term and futuristic liquid stations. By the end of FY 2015, a modified version of the Hydrogen Delivery Scenario Analysis Model will also be made publicly available. The model will incorporate recent cost data from vendors and applications to the California Energy Commission and will include the ability to simulate varying annual station utilization rates, near-term and futuristic liquid hydrogen stations, and impacts of market penetration on component costs.

Finally, the H2FIRST project's major accomplishment in FY 2015 was to develop a prototype device that could be used to validate hydrogen fueling station performance (HySTEP – Hydrogen Station Test Equipment Performance device). HySTEP will allow station owners and operators to validate station performance and save millions of dollars over time by avoiding the need for automakers to individually take FCEVs to each station to verify fueling performance. The HySTEP unit is now undergoing testing at NREL and will be shipped to California for service in FY 2016. State agencies in California have already committed cost share for its implementation, demonstrating an effective partnership between federal and state programs.

Hydrogen Storage

The Hydrogen Storage sub-program's objective is to develop technologies that provide sufficient onboard hydrogen storage to allow fuel cell devices to provide the performance and run-time demanded for the applications. In the near-term, automotive companies plan to commercialize FCEVs that use 700 bar compressed hydrogen storage systems onboard, with system cost being one of the most important challenges to commercialization. In fact, two automotive original equipment manufacturers have started to offer FCEVs for lease or commercial sale this year in California with 700 bar compressed hydrogen systems onboard the vehicle.

In FY 2015, the Program updated the cost projections for 700 bar compressed hydrogen storage systems to $14.69/kWh, an overall cost reduction of approximately $2/kWh from the baseline cost of $16.76/kWh established in FY 2013. The analysis reflects recent technology advancements to reduce the cost of carbon fiber (CF) precursor and resin and to integrate BOP components. The analysis also includes changes in the tank design to better reflect commercially manufactured pressure vessels, which increase projected costs. Specific changes to the 700 bar pressure vessel system cost calculation include use of a low-cost carbon fiber precursor based on high-volume textile fiber processes; BOP component revisions to reduce the number of fittings; and use of a low-cost, low-density resin. The analysis this year also explicitly accounts for cost increases associated with manufacturing design changes suggested by industry, including the removal of pre-woven endcaps and increased composite layer thickness to account for a more robust assessment of manufacturing variations. The relative cost impact of each component change is presented in Figure 5.

The Hydrogen Storage Engineering Center of Excellence is completing its Phase III activities, with a focus on evaluating two hydrogen adsorbent system designs that differ in heat exchanger concept and completing the validation and posting of their complete system models for use by the research community. The two prototype hydrogen adsorption systems have been built and are undergoing evaluation. One prototype (hexcell) uses a flow-through concept where excess hydrogen removes the heat of adsorption as it passes through the adsorbent that is packed within an aluminum hexagonal honeycomb structure. The second prototype uses a "Modular Adsorption Tank Insert" microchannel heat exchanger that is cooled by flowing liquid nitrogen through it.

In FY 2015, the sub-program awarded five new individual projects and set the foundational framework for future materials efforts in hydrogen storage using a lab-led consortium approach: HyMARC (Hydrogen storage Materials Advanced Research Consortium).

Manufacturing R&D

The Manufacturing R&D sub-program supports activities needed to reduce the cost of manufacturing hydrogen and fuel cell systems and components. FY 2015 saw a number of advancements in the manufacture of fuel cells, including new algorithms for automated defect detection (Figure 6). The Program also expanded its previous demonstration of optical inspection for fuel cell electrodes by developing algorithms that can automatically detect defects of various types from the real-time inspection data. The algorithms were shown to have no false positives on sample materials from General Motors. This work supports improved technology transfer to industry and addresses Program milestones for MEA inspection.

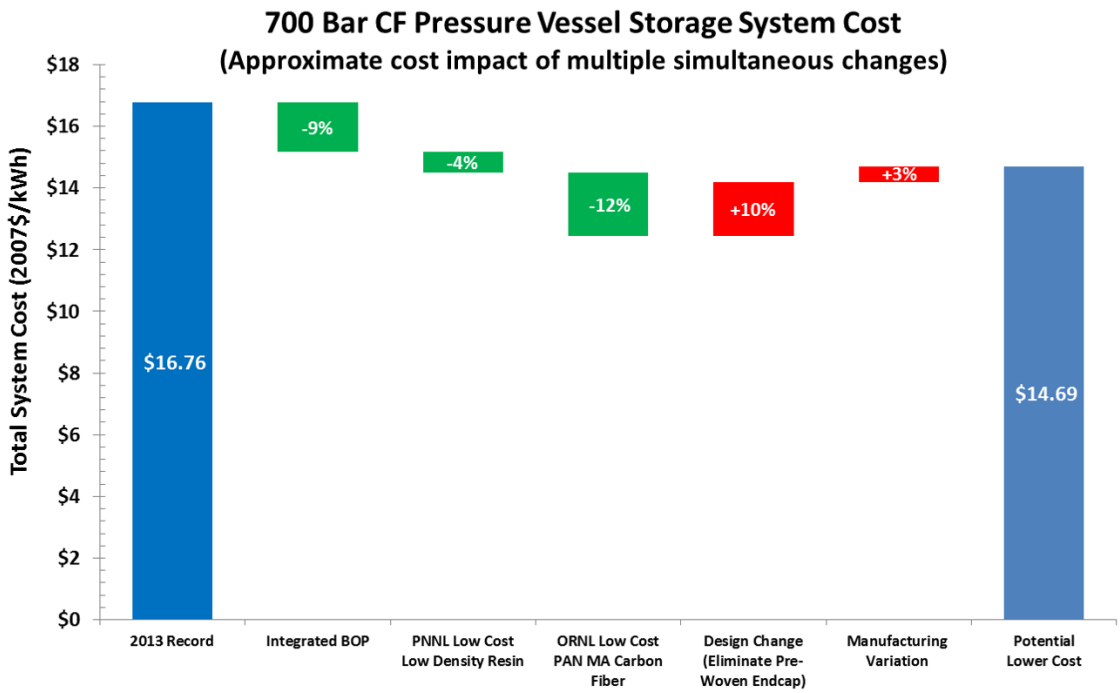

PNNL – Pacific Northwest National Laboratory; ORNL – Oak Ridge National Laboratory; PAN MA – polyacrylonitrile with methyl acrylate

FIGURE 5. Revised projected costs for 700 bar compressed hydrogen storage systems for light-duty vehicles at 500,000 systems per year, comparing analyses between 2013 and 2015

Aligned with EERE's Lab Impact Initiative, the Program offered NREL's optical defect detection technology as a Tech Transfer Opportunity (TTO) through the Small Business Innovation Research (SBIR) and Small Business Technology Transfer (STTR) programs. TTOs provide opportunities for small businesses to commercialize technologies by licensing national lab intellectual property. This TTO, which is one of the first within EERE, was awarded to Florida-based Mainstream Engineering to develop a low-cost optical detector for continuous analysis of membranes for PEM fuel cell MEAs based on a licensing agreement with NREL.

Also in FY 2015, the Program demonstrated its reactive impinging flow (RIF) technique in which the reactive gas ($H_2/O_2/N_2$) flows onto conductive fuel cell roll goods; heat from the chemical reaction is then detected. Lab researchers modeled the RIF process with gas diffusion electrode material and predicted changes in the material's temperature (due to reactive excitation and heat generation) as a function of the width of the defect for three different defect depths—results can be seen in Figure 7. Clearly, at any defect width, the more the catalyst layer thickness is reduced, the higher the temperature change from the bulk material. If the lines are extrapolated down to $\Delta T = 1$ K or 2 K, the width of the minimum detectable defect can be determined. This work is highlighted as an example that can have broad impact across the manufacturing community through improved quality control and manufacturing processes. Rather than funding the development of just one specific catalyst, for instance, the limited funding for the sub-program focuses on enabling technologies or processes that can advance widespread commercialization across areas.

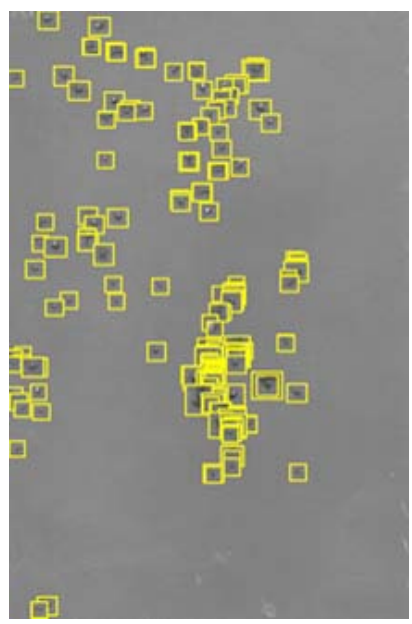

FIGURE 6. Image of intentionally created scuffs and scratches on fuel cell membrane. Defects were detected using optical reflectance. The scanning system operated on sheet materials at 10 feet per minute. Algorithms were developed and demonstrated for automated detection as illustrated by the yellow boxes. The debris images (dots) were magnified 10x for ease of viewing.

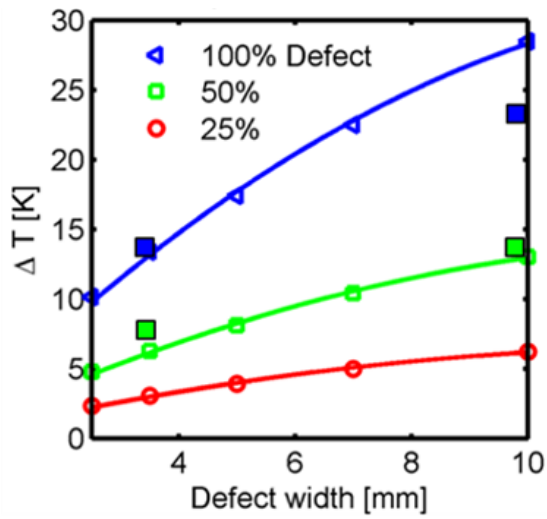

FIGURE 7. Change in temperature of gas diffusion layer material as a function of defect width following reactive excitation for three different defect thicknesses. 100% defect means that all the reactive material is gone and only a bare spot is left. 50% means that the thickness of catalyst layer is reduced by one half, and 25% means the thickness is reduced by one quarter. The solid symbols represent experimental data while the hollow symbols are model predictions. The solid lines were drawn to guide the eye through the modelled data points.

Basic Research

The Basic Energy Sciences (BES) program in the DOE Office of Science supports fundamental scientific research addressing critical challenges related to hydrogen storage, hydrogen production, and fuel cells. These basic research efforts complement the applied R&D projects supported by the other offices in the Program. Progress in any one area of basic science is likely to spill over to other areas and bring advances on more than one front.

The subjects of basic research most relevant to the Program's key technologies are as follows.

- Hydrogen Storage: Nanostructured materials; theory, modeling, and simulation to predict behavior and design new materials; and novel analytical and characterization tools.
- Fuel Cells: Nanostructured catalysts and materials; integrated nanoscale architecture; novel fuel cell membranes; innovative synthetic techniques; theory, modeling, and simulation of catalytic pathways, membranes, and fuel cells; and novel characterization techniques.
- Hydrogen Production: Approaches such as photobiological and direct photochemical production of hydrogen.

By maintaining close coordination between basic science research and applied R&D, the Program ensures that discoveries and related conceptual breakthroughs achieved in basic research programs will provide a foundation for the innovative design of materials and processes that will lead to improvements in the performance, cost, and reliability of fuel cell technologies and technologies for hydrogen production and storage. This is accomplished in various ways—for example, through bi-monthly coordination meetings between the participating offices within DOE, and at the researcher level by having joint meetings with participation from principal investigators who are funded by the participating offices.

In June 2015, the Program's Annual Merit Review and Peer Evaluation meeting included presentations and posters from BES-funded researchers on fundamental-science-related topics in conjunction with presentations by EERE and Advanced Research Projects Agency-Energy funded researchers.

In FY 2015, the Office of Science re-competed the Joint Center for Artificial Photosynthesis and announced a future forum on electrochemical carbon reduction. Future efforts will include coordinated activities between EERE and BES.

Technology Validation

The Technology Validation sub-program demonstrates, tests, and validates hydrogen and fuel cell technologies and uses the results to provide feedback to R&D activities. In addition to validating light-duty FCEV and hydrogen infrastructure technologies, continuing efforts include the real-world evaluation of fuel cell electric bus (FCEB) technologies at various transit authorities and monitoring performance of fuel cells in stationary power, backup power, and material handling equipment (MHE) applications.

Six major automakers (General Motors, Honda, Hyundai, Mercedes-Benz, Nissan, and Toyota) are demonstrating advanced light-duty FCEVs, with data being collected from up to 48 vehicles. During the data collection period of October 2012 through December 2014, the 48 FCEVs traveled over 2.4 million miles, demonstrating an average on-road fuel economy of 51 miles/kg and an average fleet voltage durability of 3,930 hours. A maximum of 5,605 fuel cell operation hours (which surpasses the 2020 DOE target of 5,000 hours) was also demonstrated. These results, along with previous ones, reveal that steady progress has been demonstrated over the past 10 years, with improvements especially in fuel cell durability, range, and fuel economy.

During FY 2015, data from 15 FCEBs at two transit agencies, AC Transit (Oakland, California) and SunLine (Thousand Palms, California), were collected and analyzed. FCEBs continue to show improved fuel economy (ranging from 1.7 to 2.1 times higher) compared to baseline (diesel and compressed natural gas) buses in similar service. The average fuel economy for the fuel cell power plants was 7.26 miles per diesel gallon equivalent (DGE), approaching the Federal Transit Administration's performance target for FCEB fuel economy of 8 miles per DGE. The top fuel cell power plant accumulated over 19,000 hours of operation, surpassing the DOE/U.S. Department of Transportation target of 18,000 hours for 2016, while 67 percent of fuel cell power plants accumulated over 8,000 hours. Values for fuel cell system miles between road calls—a measure of reliability—surpassed the 2016 target and were found to be approaching the ultimate target.

Over the period from the first quarter of 2009 to the fourth quarter of 2014, data collected on 10 hydrogen stations revealed that a cumulative amount of more than 62,700 kg of hydrogen was dispensed (43 percent improvement over the previous year's cumulative), with average dispensing rates of 0.6 kg/min. Average fill time was found to be 5.6 minutes, with 49 percent of fills taking less than five minutes, and 20 percent taking less than three minutes.

During the past year, the electrolyzer-based hydrogen fueling station at California State University, Los Angeles (CSULA), part of DOE's Technology Validation sub-program, was the first in the United States to receive the seal of approval for commercial sale of hydrogen fuel. The CSULA station may in fact have been the first in the world with the sufficiently high-accuracy metering technology required for the commercial sale of hydrogen—a requirement to ensure customers get the amount of fuel for which they pay. Although meter accuracy requires further improvement, the current status allows sale to the public using routine credit card purchases. Since then, California state funding has enabled two additional stations that can sell hydrogen fuel, with more on the way. Power meters, flow meters, and buffer tanks were installed, and performance evaluation data are being provided. Gas Technology Institute's West Sacramento, California, station—using liquid hydrogen and 900 bar ionic compression technology—was commissioned in December 2014, and instrumentation is now installed, allowing for data collection. These examples show how the Program enables first-of-a-kind real-world installations, taking technology from the laboratory to the field, followed by partner funding (such as California state agencies), resulting in further replication and deployment.

DOE has established a Grid Modernization program, a cross-cutting effort involving various offices within DOE, with the objective to help set the nation on a cost-effective path to an integrated, secure, and reliable grid that is flexible enough to provide an array of emerging services while remaining affordable to consumers. Hydrogen-based energy storage could provide value to many applications and markets, and electrolyzers may be utilized as a controllable electrical load that can provide real-time grid services. The Program is exploring these value-added services. An electrolyzer stack test bed was designed, built, commissioned, and is now in operation at NREL. The first-of-its-kind real-time digital simulator (RTDS)-to-RTDS communications network between labs was established for hardware-in-the-loop simulations with electrolyzer hardware.

Market Transformation

To ensure that the benefits of the Program's efforts are realized in the marketplace, the Market Transformation sub-program continues to facilitate the growth of early markets for fuel cells used in stationary, specialty-vehicle, and truck fleet applications. Program activities are helping to reduce the cost of fuel cells by enabling economies of scale through early market deployments; these early deployments also help to overcome a number of barriers, including the lack of operating performance data, the need for applicable codes and standards, and the need for user acceptance. The Program also partners with other federal agencies and stakeholders to deploy fuel cell systems in applications such as marine cargo transport operations.

One of the key accomplishments of the Program in FY 2015 was deploying the world's first fleet of zero-emissions, hydrogen-powered airport ground support equipment (GSE) trucks. This project is demonstrating the value proposition of using fuel-cell-powered tow tractors as a cost-competitive and more energy-efficient solution compared to incumbent internal-combustion-engine-powered vehicles. In April 2015, the project commissioned a fleet of 15 GSE units, which are now operating at the Federal Express hub at the airport in Memphis, Tennessee. Federal Express has more than 1,300 baggage tow tractors at its Memphis facility to manage ~270 flights per day. In the long term, such early markets could offer the potential for hubs of hydrogen infrastructure for applications such as shuttle buses, fleet vehicles, rental cars, taxis, and retail consumer vehicles.

Finally, in coordination with the Technology Validation sub-program, two new efforts were initiated for fuel cells as range extenders and hybrid systems for parcel delivery vans with Federal Express and United Parcel Service. Similar to the strategy from previous years with forklifts and backup power units, the Program aims to develop and demonstrate fuel cell systems for other early markets that are commercially viable and help pave the way for broader deployment and creation of infrastructure. Another example is an SBIR Phase 1 project to assess the feasibility of fuel cell refuse trucks that could potentially provide the range currently not available with pure battery electric trucks.

Education

Although the Program relies on prior year resources for the Education sub-program's activities, education and outreach continue to be important for hydrogen and fuel cell technology. With the advent of commercial systems, industry has taken the lead on education, but stakeholders still rely on DOE for providing technically accurate and objective information to key target audiences both directly and indirectly involved in the use of hydrogen and fuel cells. In FY 2015 the Program published more than 100 success stories through news articles, blogs, press releases, and media announcements and conducted more than 20 webinars, averaging more than 150 attendees per webinar. Activities reached at least 3,000 people at key conferences and meetings, and the FCTO monthly newsletter reached more than 11,800 subscribers. The Program is also continuing to train middle school and high school teachers based on prior year funding through "H2 Educate!," reaching a total of 12,000 teachers in 35 states; 90% of participants have stated that the training resources increased the effectiveness of their lesson plans.

Safety, Codes and Standards

The Safety, Codes and Standards (SCS) sub-program identifies needs and performs high-priority R&D to provide an experimentally validated, fundamental understanding of the relevant physics, critical data, and safety information needed to define the requirements for technically sound and defensible codes and standards. During the past year, the sub-program continued to identify and evaluate safety and risk management measures that can be used to define the requirements and close the gaps in codes and standards in a timely manner.

In FY 2015, the Hydrogen Risk Assessment Models (HyRAM) were released for alpha testing by various stakeholders, including industry representatives. This software enables quantitative risk assessment (QRA) and performance-based design and incorporates hydrogen behavior models also developed through the Program. A model for release of liquid hydrogen was validated and will be used, along with the QRA tool, to inform separation distances in the 2019 code cycle for National Fire Protection Association 2/55.

The Program continues to share current safety information and knowledge with the community through the launch of H2Tools.org, which, in addition to consolidating existing resources (i.e., Hydrogen Lessons Learned Database), serves as a centralized resource for hydrogen safety information, news, and user-specific content. This is a major accomplishment because it allows for a "one stop shop" online rather than requiring stakeholders to navigate numerous other websites and resources.

The Program has now educated more than 35,000 code officials and first responders across the nation, allowing for greater familiarity with emerging hydrogen and fuel cell technologies. In addition, the efforts of the Program's Safety Panel have been commended by stakeholders worldwide for its work in assessing numerous projects and safety plans to ensure that a high degree of attention is paid to safety and risk mitigation.

Systems Analysis

The Systems Analysis sub-program focuses on examining the economics, benefits, opportunities, and impacts of hydrogen and fuel cells through a consistent, comprehensive, analytical framework. The team made several significant contributions to the Program during FY 2015.

The Hydrogen Financial Analysis Scenario Tool (H2FAST) was developed to provide in-depth financial analysis of hydrogen refueling stations and is available in two formats: an interactive online tool and a downloadable Microsoft Excel spreadsheet. The spreadsheet version of H2FAST offers basic and advanced user interface modes for modeling individual stations or groups of up to ten stations. It provides users with detailed annual financial projections in the form of income statements, cash flow statements, and balance sheets; graphical presentation of financial performance parameters for 65 common metrics; life-cycle cost breakdown for each analysis scenario; and common ratio analysis results such as debt/equity position, return on equity, and debt service coverage ratio. The online H2FAST tool can be used to explore the impact of basic financial performance metrics by varying up to 20 user inputs as illustrated in Figure 8. The tool was thoroughly peer reviewed and issued to the public.[9] The sub-program also evaluated the

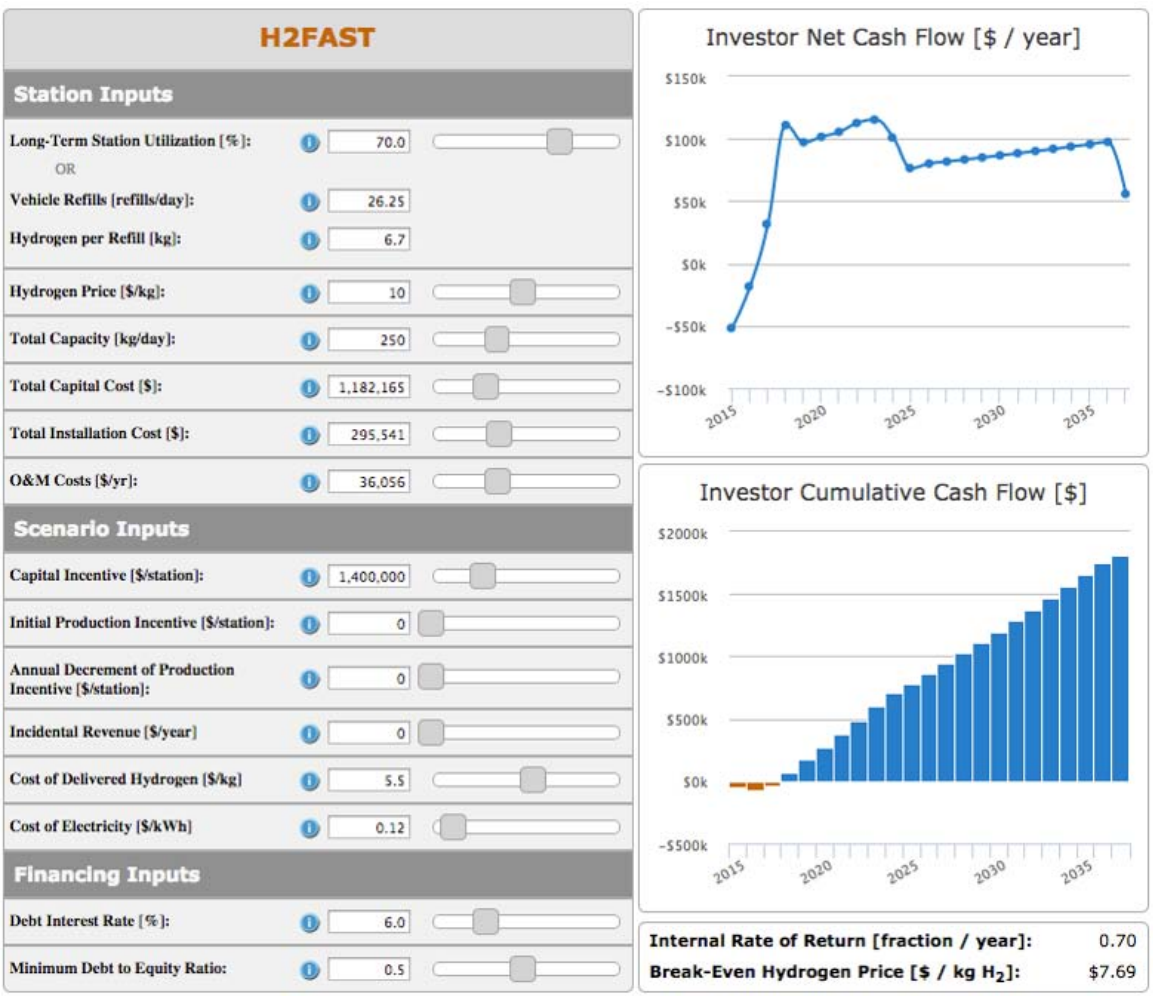

FIGURE 8. H2FAST model input screen

[9] http://www.nrel.gov/hydrogen/h2fast/

impact of improving fuel cell efficiency and FCEV performance on the cost of fuel cell and hydrogen storage systems, showing the potential to decrease the cost of onboard hydrogen systems by ~80% and fuel cell systems by ~70%.

The JOBS model was used to assess employment and economic impacts of infrastructure development for the early market penetration of fuel cell vehicles in California. The California roadmap projects approximately 100 hydrogen refueling stations will be built between 2016 and 2023. This station development is estimated to create 1,000 to 1,400 jobs and yield an economic impact of $230 million by 2023.

The Greenhouse gases, Regulated Emissions, and Energy use in Transportation (GREET) model continues to be enhanced for the analysis of greenhouse gas emissions, petroleum use, and water consumption for conventional and renewable hydrogen pathways on a life-cycle basis. The Program expanded the GREET model's life-cycle analysis capabilities in FY 2015 to examine water consumption for hydrogen production and delivery pathways from natural gas, water electrolysis, and other fuels such as gasoline and ethanol (Figure 9). A methodology for allocating water consumption to hydropower generation was also developed.

An early market cost target was developed to guide and prioritize R&D for the Program. The early market hydrogen cost target, a pathway-independent target to guide R&D for production and delivery technologies for hydrogen fuel, is set at $7/gge, untaxed and dispensed at the pump. This target is based on a "top-down" analysis of the cost at which hydrogen fuel for FCEVs is projected to be competitive on a cost per mile basis with gasoline fuel for gasoline ICEVs in the early market timeframe of 2015 to 2020. The target considers a range of vehicle technologies, performance, fuel economy values (for both FCEVs and the competing ICEVs), and the federal and regional incentives

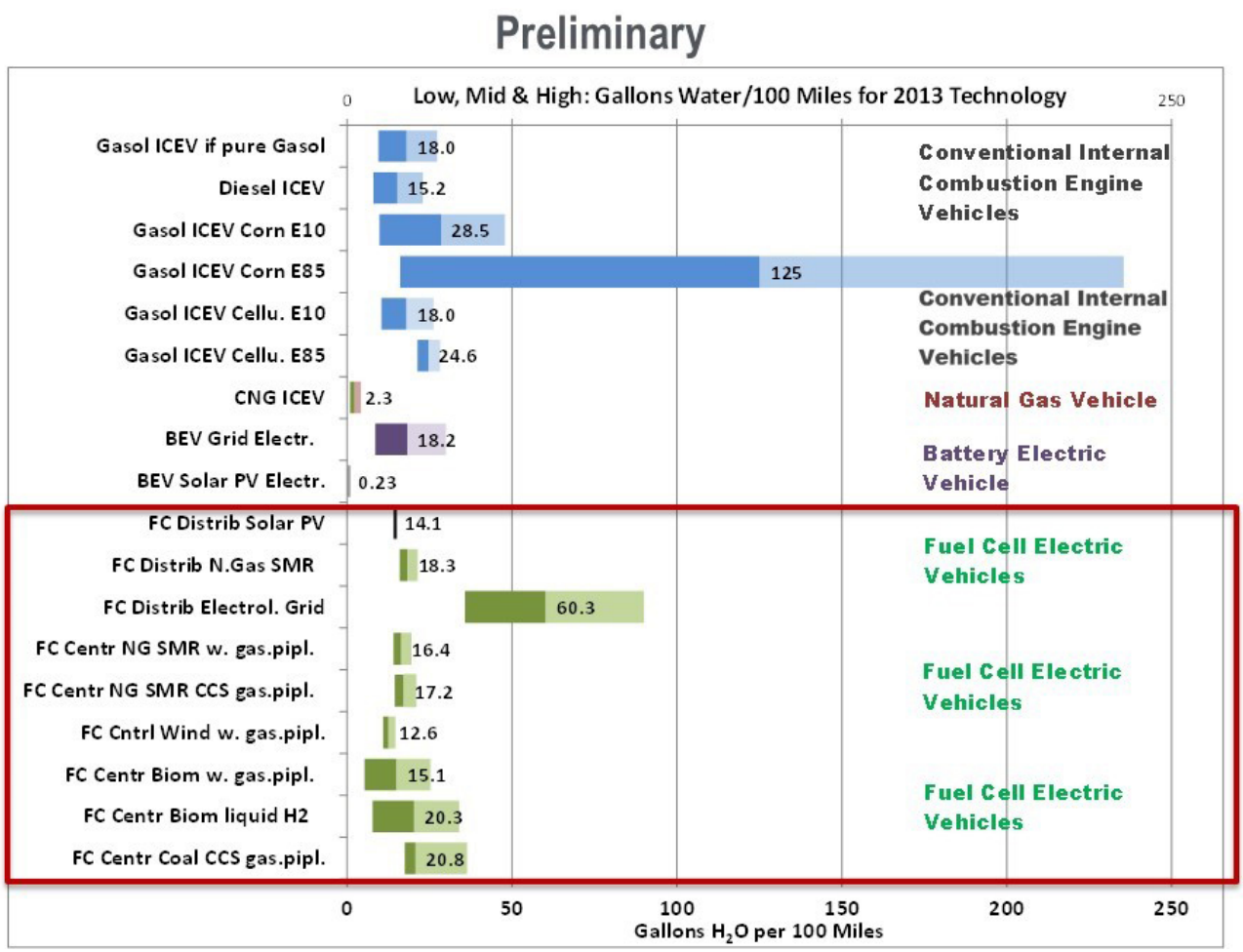

CCS – carbon capture and sequestration; CNG – compressed natural gas; NG – natural gas; PV – photovoltaic; SMR – steam methane reformer

FIGURE 9. Water consumption of hydrogen pathways comparable to conventional fuels

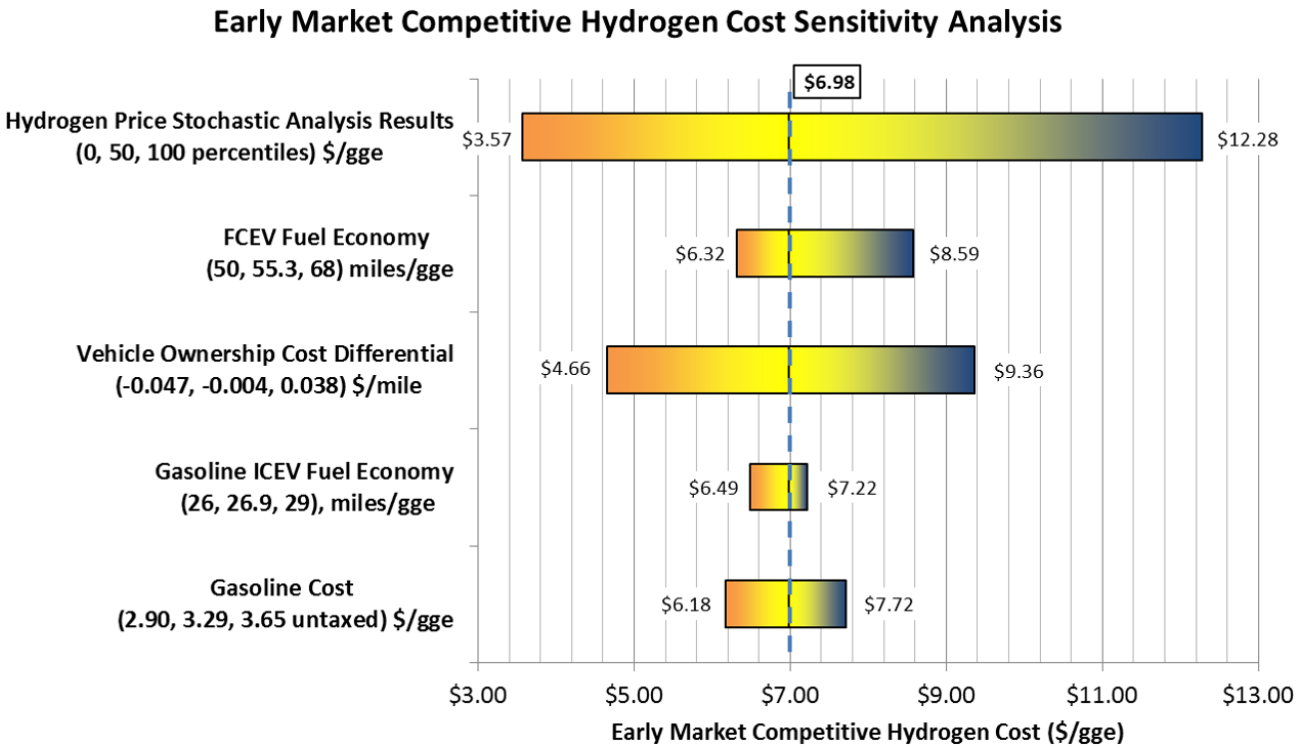

FIGURE 10. Sensitivity of the early market hydrogen cost (untaxed) to gasoline cost, vehicle ownership cost differential, and vehicle fuel economy

currently in place as well as the gasoline market prices in the regions analyzed (Figure 10). A DOE Program Record on this subject was was developed, peer reviewed, and issued.[10]

American Recovery and Reinvestment Act Projects

The American Recovery and Reinvestment Act of 2009 (Recovery Act or ARRA) has been a critical component of the Program's efforts to accelerate the commercialization and deployment of fuel cells in the marketplace. As of October 2015, all of the original twelve projects have been successfully completed, and 100% of the Recovery Act project funds have been invoiced by the projects. A total of 1,330 fuel cell units were deployed—824 fuel cell backup power systems for cellular communication towers, 504 fuel cell lift trucks, and 2 stationary power systems—surpassing the original deployment goal of up to 1,000 fuel cells. The National Fuel Cell Technology Evaluation Center (NFCTEC) at NREL has established data reporting protocols with Composite Data Products (CDPs) and Detailed Data Products showing progress to date. The CDPs are available on the NREL NFCTEC website.

Successful DOE deployments of fuel cells (including deployments from ARRA funding as well as Market Transformation projects) have led to industry orders of more than 8,300 fuel cell forklifts and more than 5,500 fuel cell backup power systems, with no additional DOE funding.[11] In addition, a study by ANL[12] found that DOE's ARRA investments led to the creation or retention of over 1,400 direct, indirect, and induced job-years for U.S. workers.

OTHER PROGRAM ACTIVITIES AND HIGHLIGHTS FROM FY 2015

Tracking Commercialization

One indicator of the robustness and innovative vitality of an RD&D program is the number of patents granted, as well as the number of technologies commercialized. The Program continued to assess the commercial benefits of

[10]DOE Program Record #14013, http://hydrogen.energy.gov/pdfs/14013_hydrogen_early_market_cost_target.pdf
[11]DOE Program Record #15004, http://www.hydrogen.energy.gov/pdfs/15004_industry_bup_deployments.pdf and DOE Program Record #15003, http://www.hydrogen.energy.gov/pdfs/15003_industry_lift_truck_deployments.pdf
[12]Economic Impact of Fuel Cell Deployment in Forklifts and for Backup Power under the American Recovery and Reinvestment Act, http://energy.gov/eere/fuelcells/downloads/economic-impact-fuel-cell-deployment-forklifts-and-backup-power-under

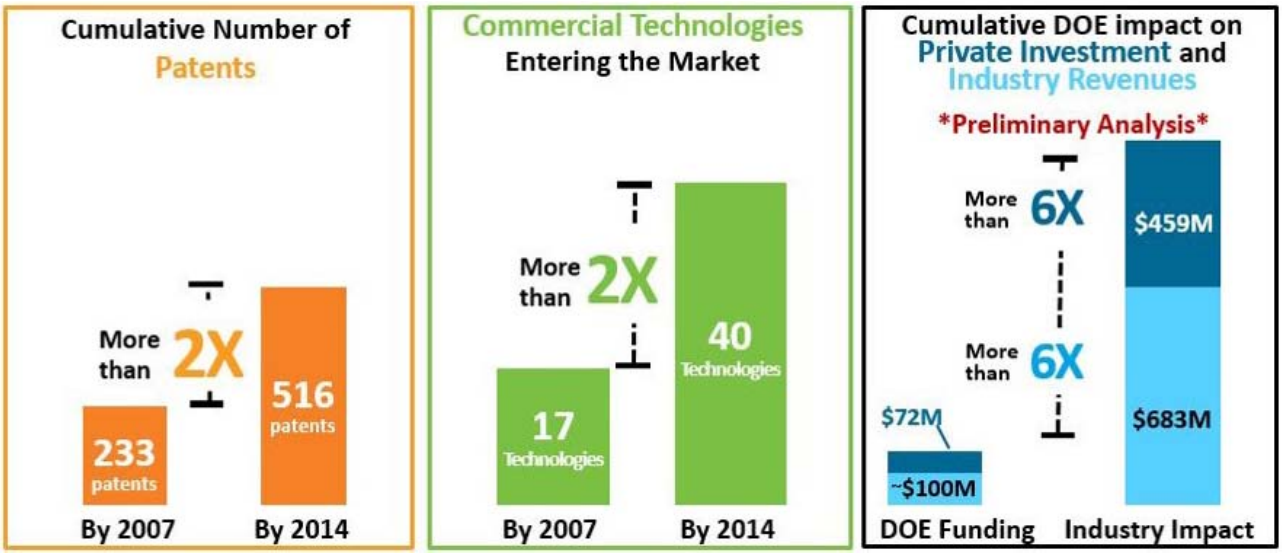

FIGURE 11. RD&D efforts funded by FCTO have resulted in 515 patents, 40 commercial technologies in the market, and 65 technologies that are projected to be commercialized within three to five years (as of October 2014).

funding by tracking the commercial products and technologies developed with the support of FCTO. RD&D efforts funded by FCTO have resulted in 515 patents, 40 commercial technologies in the market, and 65 technologies that are projected to be commercialized within three to five years (as of October 2014, Figure 11).[13]

In addition, the Program's investment of $100 million in specific hydrogen and fuel cell projects led to more than $683 million in revenue, and investments of approximately $72 million in specific projects led to nearly $459 million in additional private investment. These values are periodically updated based on industry input and their feedback on which technologies resulted from DOE support.

Awards and Distinctions

During the last year, a number of researchers within the Program were recognized through various awards. For example:

- Proton OnSite was presented with the President's "E" Award for Exports by the U.S. Secretary of Commerce, Penny Pritzker, during a ceremony in Washington, D.C.
- Rod Borup of Los Alamos National Laboratory won the 2015 Research Award presented annually by the Energy Technology Division of the Electrochemical Society.
- Drew Higgins, University of Waterloo, was awarded the Grand Prize for the 2014 Dr. Bernard S. Baker Student Researcher Award for Fuel Cell Research.
- Y. F. (John) Khalil of the United Technologies Research Center was awarded the Institution of Chemical Engineers Senior Moulton Medal for best technical and meritorious paper for his research in experimental and theoretical investigations for mitigating $NaAlH_4$ reactivity risks during postulated accident scenarios involving exposure to air or water.
- Lawrence Berkeley National Laboratory's and Argonne National Laboratory's nanoframe catalyst project was a finalist for R&D Magazine's 53rd Annual R&D 100 Awards.
- Proton OnSite was recognized in U.S. Senator Chris Murphy's (D-Conn.) weekly series (August 3, 2015) called "Murphy's Monday Manufacturer."
- Ian M. Robertson of the University of Wisconsin–Madison was awarded the 2014 ASM Edward DeMille Campbell Memorial Lectureship award in recognition of seminal contributions for the understanding of hydrogen embrittlement of metals and alloys.

[13]Pathways to Commercial Success, http://energy.gov/eere/fuelcells/market-analysis-reports#mkt_pathways

- Adam Weber, Lawrence Berkeley National Laboratory, was selected as a Kavli Fellow of the National Academy of Sciences for 2014.
- Piotr Zelenay received the Fellows Prize for Outstanding Research from Los Alamos National Laboratory. He also received the honorary title of Professor in Chemistry from Poland's President Bronisław Komorowski during a June 23 ceremony at the Presidential Palace in Warsaw.

Key Reports and Publications

Every year, the Program commissions a number of key reports, providing vital information to industry and the research community. Some of these are released on an annual basis—such as the Market Report (2014 Fuel Cell Technologies Market Report), the commercialization report (2014 Pathways to Commercial Success: Technologies and Products Supported by the Fuel Cell Technologies Office), and the State of the States: Fuel Cells in America 2014 report—while others are published when studies are complete, projects have ended, or key milestones have been reached. Key examples include the following:

- The ***2014 Fuel Cell Technologies Market Report*** finds that the hydrogen and fuel cell market continues to grow rapidly. According to the report, the industry grew by almost $1 billion in 2014, reaching $2.2 billion in sales—up from $1.3 billion in 2013. In addition, more than 50,000 fuel cells were shipped worldwide in 2014.[14]
- ***States of the States: Fuel Cells in America 2014***, the sixth annual report on state activities, details fuel cell and hydrogen activities and policies in the 50 states and the District of Columbia.[15]
- ***Pathways to Commercial Success: Technologies and Products Supported by the Fuel Cell Technologies Office***, the Program's annual commercialization report, indicates that FCTO efforts have successfully generated more than 515 patents, 40 commercial technologies, and 65 technologies that are expected to reach commercial scale within the next three to five years.[16]
- ***The Business Case for Fuel Cells*** illustrates how top American companies are using fuel cells in their business operations to advance their sustainability goals, save millions of dollars in electricity costs, and reduce carbon emissions by hundreds of thousands of metric tons per year.[17]
- The ***Hydrogen Fueling Station in Honolulu, Hawaii, Feasibility Analysis*** assesses the technical and economic feasibility of developing a vacant, undeveloped General Services Administration-owned property into an income-producing site equipped with a hydrogen fueling station and a covered 175-stall parking structure with roof-top solar panels.[18]
- The ***Mass Production Cost Estimation of Direct H_2 PEM Fuel Cell Systems for Transportation Applications: 2013 Update*** is the seventh annual update of a comprehensive automotive fuel cell cost analysis conducted by Strategic Analysis, Inc.[19]
- The ***A Total Cost of Ownership Model for Low Temperature PEM Fuel Cells in Combined Heat and Power and Backup Power Applications*** report describes a total cost of ownership model for emerging applications in stationary fuel cell systems.[20]
- The ***Backup Power Cost of Ownership Analysis and Incumbent Technology Comparison*** report identifies the factors impacting the value proposition for fuel cell backup power and presents the estimated annualized cost of ownership for fuel cell backup power systems compared with the incumbent technologies of battery and diesel generator systems.[21]

[14]2014 Fuel Cell Technologies Market Report, http://energy.gov/eere/fuelcells/market-analysis-reports#mkt_program
[15]State of the States: Fuel Cells in America 2014, http://energy.gov/eere/fuelcells/market-analysis-reports#mkt_state
[16]Pathways to Commercial Success: Technologies and Products Supported by the Fuel Cell Technologies Office, http://energy.gov/eere/fuelcells/market-analysis-reports#mkt_pathways
[17]The Business Case for Fuel Cells, http://energy.gov/eere/fuelcells/market-analysis-reports#mkt_business
[18]Hydrogen Fueling Station in Honolulu, Hawaii Feasibility Analysis, http://energy.gov/eere/fuelcells/downloads/hydrogen-fueling-station-honolulu-hawaii-feasibility-analysis
[19]Mass Production Cost Estimation of Direct H2 PEM Fuel Cell Systems for Transportation Applications: 2013 Update, http://energy.gov/eere/fuelcells/downloads/mass-production-cost-estimation-direct-h2-pem-fuel-cell-systems
[20]A Total Cost of Ownership Model for Low Temperature PEM Fuel Cells in Combined Heat and Power and Backup Power Applications, http://energy.gov/eere/fuelcells/downloads/total-cost-ownership-model-low-temperature-pem-fuel-cells-combined-heat-and
[21]Backup Power Cost of Ownership Analysis and Incumbent Technology Comparison, http://energy.gov/eere/fuelcells/downloads/backup-power-cost-ownership-analysis-and-incumbent-technology-comparison

- The ***Economic Impacts Associated with Commercializing Fuel Cell Electric Vehicles in California: An Analysis of the California Road Map Using the JOBS H2 Model*** summarizes an analysis of the economic impacts associated with commercializing FCEVs in California.[22]

Workshops and Events

In FY 2015, the Program organized a number of workshops and events valuable to both stakeholders and to the DOE, including those below:

- The ***Transitioning the Transportation Sector: Exploring the Intersection of Hydrogen Fuel Cell and Natural Gas Vehicles*** report includes the proceedings from a September 2014 workshop that considered common opportunities and challenges in expanding the use of hydrogen and natural gas as transportation fuels.
- On Tuesday, November 11, 2014, FCTO hosted several ***Tech-to-Market events at the Fuel Cell Seminar and Energy Exposition*** in Los Angeles, California, to foster increased collaboration between national labs and industry. Events included a plenary presentation by Deputy Assistant Secretary for Transportation Reuben Sarkar, a panel discussion aimed to demystify the process of working with the national labs, presentations highlighting national labs' unique capabilities, and a poster session.
- On January 27–28, 2015, FCTO held the ***DOE Materials-Based Hydrogen Storage Summit: Defining Pathways to Onboard Automotive Applications*** workshop. The objectives of this meeting were to (1) present and discuss recent results from DOE's hydrogen storage system modeling efforts and their implications for hydrogen storage materials development efforts and (2) gather input from various stakeholders to identify hydrogen storage materials development pathways and areas of research needed.
- On March 18–19, 2015, FCTO held the ***Hydrogen, Hydrocarbons, and Bioproduct Precursors from Wastewaters Workshop*** and gathered 30 experts from academia, government, and industry to share information and identify the current status and potential RD&D possibilities for production of hydrogen and higher hydrocarbons (containing four or more carbon molecules) from wastewaters using biological, biochemical, and other techniques.
- On June 22, 2015, EERE hosted ***Sustainable Transportation Day*** at the Energy Department's headquarters in Washington, D.C. Together, the Bioenergy, Fuel Cell, and Vehicle Technologies Offices showcased how EERE's strategic investments in sustainable transportation technologies are improving vehicle efficiency and advancing the use of alternative fuel vehicles. The event was kicked off by remarks from Deputy Assistant Secretary for Transportation Reuben Sarkar.
- On October 8, 2015, FCTO celebrated the first ***National Hydrogen and Fuel Cell Day***. The day included announcements and events all over the country, a DOE blog authored by Principal Deputy Assistant Secretary David Friedman, and a press release announcing FCTO's office-wide Funding Opportunity Announcement selections.
- On October 12 and 13, 2015, FCTO hosted several ***Tech-to-Market events at the Electrochemical Energy Summit 2015*** in Phoenix, Arizona, including a plenary presentation by Under Secretary for Science and Energy Lynn Orr, a panel discussion aimed to demystify the process of working with the national labs, and a poster session highlighting the national labs' unique capabilities and opportunities in fuel cells and electrochemical systems.

New Funding Opportunity Announcements (FOAs) and Awards

The Program conducted FOAs and selected new projects consistent with the overall portfolio and congressional budget justification language and appropriations.

- **$21.5 million** was awarded to ten projects to advance fuel cell and hydrogen technologies and enable early adoption of fuel cell applications such as light-duty FCEVs. Selected projects are located in Oregon, Minnesota, Michigan, Colorado, Illinois, Massachusetts, New York, and California.
- **$10 million** in incubator funding was awarded to eleven projects to support innovations in fuel cell and hydrogen fuel technologies. The intent of the incubator FOA, implemented across EERE, was to spur innovation in higher-risk and high-impact areas slightly outside each program's roadmap. Selected projects are located in Connecticut, Georgia, Illinois, Massachusetts, California, Delaware, New Mexico, Colorado, and Virginia.

[22]The Economic Impacts Associated with Commercializing Fuel Cell Electric Vehicles in California: An Analysis of the California Road Map Using the JOBS H2 Model, http://energy.gov/eere/fuelcells/downloads/economic-impacts-associated-commercializing-fuel-cell-electric-vehicles

- **$4.6 million** was awarded to four projects to develop advanced hydrogen storage materials that have potential to enable longer driving ranges and help make fuel cell systems competitive for different platforms and sizes of vehicles. The projects are located in Iowa, California, Texas, and Michigan.
- **$2 million** was awarded to two projects for clean energy supply chain and manufacturing competitiveness analysis for hydrogen and fuel cell technologies. Selected projects are located in Ohio and Virginia.

The Program participated in a number of SBIR FOAs and awards.

- **2015 SBIR/STTR Phase I** Release 1 award winners included three projects focusing on non-platinum catalysts for fuel cells and detection of contaminants in hydrogen. Selected projects are located in Connecticut, New Mexico, and Ohio.
- **2015 SBIR/STTR Phase I** Release 2 award winners included projects that will evaluate opportunities for fuel cell-battery electric hybrid trucks and develop a real-time, in-line optical detector for the measurement of fuel cell membrane thickness. Award winners are located in California and Florida.
- **2015 SBIR/STTR Phase II** Release 1 award winners included three Office of Science-funded projects focusing on hydrogen production from electrolysis and hydrogen systems supporting FCEVs. Selected projects are in Massachusetts and South Carolina.
- **2015 SBIR/STTR Phase II** Release 2 award winners included projects focused on fuel cell durability, performance, and efficiency, with the ultimate goal of lowering costs. The projects are located in Massachusetts and South Carolina.
- **2016 SBIR/STTR Phase I** Release 1 topics included hydrogen production from organic waste streams and fuel cell membranes, funded through the Office of Science. Applications were due October 19, 2015.

The Program also coordinated with other offices, and the following FOA from FY 2015 is relevant.

- **$20 million** was awarded through the Small Business Voucher Pilot, a public-private partnership that will connect clean energy innovators across the country with the top-notch scientists, engineers, and world-class facilities at our national laboratories. Five national laboratories were competitively selected to lead the $20 million pilot, including Oak Ridge National Laboratory ($5.6 million), National Renewable Energy Laboratory ($4.9 million), Lawrence Berkeley National Laboratory ($4.2 million), Sandia National Laboratories ($2.8 million), and Pacific Northwest National Laboratory ($2.7 million). Small businesses will be competing to receive "vouchers" allowing them to work with a national lab of their choice to accelerate progress in key areas.

Requests for Information (RFIs)

The Program uses RFIs to solicit feedback from the stakeholder community in an open and transparent process that serves to inform the Program and develop future plans. Key examples included collecting feedback on the following topics:

- Hydrogen production and hydrogen delivery RD&D activities aimed at developing technologies that can ultimately produce and deliver low-cost hydrogen. (October 2014)
- Gas clean-up for fuel cell applications. (June 2015)

Webinars and Blogs

The Program held a number of webinars throughout the year (Table 2). These are archived on the Program's website, providing valuable information to the entire stakeholder community.[23]

The Program also published multiple blogs focused on hydrogen and fuel cell activities (Table 3).

[23]http://energy.gov/ eere/fuelcells/2014-webinar-archives

TABLE 2. Program Webinars Offered to Stakeholders in FY 2015

Date	Title	Summary
September 11, 2014	Introduction to SAE Hydrogen Fueling Standardization	This webinar provided an overview of the SAE Standards J2601 and J2799 and how they are applied to hydrogen fueling for FCEVs. Validated in the lab and proven in the field over the last decade, the SAE J2601 hydrogen fueling protocol standard, coupled with the SAE J2799 FCEV communications standard, provide the basis for hydrogen fueling in the first generation of infrastructure worldwide.
October 21, 2014	Opportunities for Wide Bandgap Semiconductor Power Electronics for Hydrogen and Fuel Cell Applications	This webinar featured representatives of Cree Inc., who provided an overview and roadmap of silicon carbide (SiC) power electronic technology and highlighted opportunities for product development responsive to the market pull of the hydrogen and fuel cell technology applications.
November 6, 2014	2014 and 2015 Hydrogen Student Design Contests	This webinar covered the results of the 2014 Hydrogen Student Design Contest and introduced the theme for the 2015 contest. The teams from Washington State University and Humboldt State University presented their winning designs. The 2014 contest teams were challenged to design a hydrogen fueling module that fulfills the requirements of low cost, easy permitting, low maintenance, mass production, and transportability in order to create a model for a reliable, convenient, and reasonably priced refueling experience for all hydrogen fuel cell vehicle customers.
November 18, 2014	An Overview of the Hydrogen Fueling Infrastructure Research and Station Technology (H2FIRST) Project	This webinar reviewed the objectives, approach, and structure of H2FIRST and provided a progress update on active and proposed technical tasks. The H2FIRST project focuses on technical tasks in support of H2USA to ensure that fuel cell vehicle customers have a positive fueling experience similar to conventional gasoline/diesel stations as vehicles are introduced (2015–2017) and we transition to advanced fueling technology beyond 2017. Led by the National Renewable Energy Laboratory and Sandia National Laboratories, the project leverages core capabilities at the national laboratories to address the technology challenges related to hydrogen refueling stations.
December 2, 2014	Materials Genome Initiative	DOE supports the use of the Materials Genome Initiative (MGI) tools and methodologies to accelerate the discovery and development of materials in the clean energy technologies space. The approach centers on coordinating research efforts in theory, synthesis, characterization, and information management, and uses the latest combinatorial and high-throughput techniques in both computation and experimentation. This webinar described current directions in the evolution of the clean energy MGI and showcased several exciting DOE projects, mainly in the Fuel Cell Technologies Office, that have been early adopters of MGI methods.
January 13, 2015	Highly Efficient Solar Thermochemical Reaction Systems	This webinar focused on DOE's investments in micro- and meso-channel reactors and heat exchangers, which have led to the development of a highly compact reaction system that efficiently converts concentrated solar energy into chemical energy. The webinar described the evolving status of the technology with a focus on near-term, anticipated applications that include fuel cells, combustion gas turbines, and the production of various chemical products.
March 10, 2015	2nd International Hydrogen Infrastructure Challenges Webinar	This webinar summarized the second international information exchange on the hydrogen refueling infrastructure challenges and potential solutions to support the successful global commercialization of hydrogen FCEVs. The information exchange took place in May 2014 at Toyota's Torrance, California, facility as a follow-up to the previous June 2013 workshop in Berlin, Germany. Participants included topical experts from Germany, Japan, the United States, Scandinavia, and the European Commission. The webinar focused on the station requirements necessary to meet the latest SAE J2601 protocol and the development of alternative fueling protocols; maintaining and measuring purity to the SAE J2619 fuel quality standard; the availability and accuracy of meters for hydrogen dispensing for 700 bar onboard fueling; and the current status of key hardware for 700 bar refueling.
March 10, 2015	Overview of Funding Opportunity Announcement DE-FOA-000224: Hydrogen and Fuel Cell Technologies Research, Development, and Demonstrations	This webinar outlined information regarding Funding Opportunity Announcement DE-FOA-0001224: Hydrogen and Fuel Cell Technologies Research, Development, and Demonstrations. This FOA covers a broad spectrum of the FCTO portfolio with areas of interest ranging from research and development to demonstration and deployment projects.
March 24, 2015	National Hydrogen Safety Training Resource for Emergency Responders	This webinar discussed the launch of a new, free, online national hydrogen safety training resource for emergency responders. Developed by the Pacific Northwest National Laboratory and the California Fuel Cell Partnership, the resource provides a single repository of credible and reliable information related to hydrogen and fuel cells that is current and accurate and eliminates duplicative efforts among various training programs.
May 12, 2015	Overview of Station Analysis Tools Developed in Support of H2USA	This webinar provided a basic introduction to two new models—HRSAM and H2FAST—developed by ANL and NREL, respectively. The tools were designed to address key technical and financial barriers to hydrogen fueling infrastructure deployment. HRSAM will help to assess the impact of station design on the economics and incorporates a station's capital and operating costs based on key design variables such as station capacity and mode of hydrogen delivery. To complement HRSAM, H2FAST provides in-depth financial analysis, including cash flow and return on investments for hydrogen fueling stations, based on key financial inputs such as station capital cost, operating cost, and financing mechanisms.

TABLE 2. Program Webinars Offered to Stakeholders in FY 2015 (Continued)

Date	Title	Summary
May 14, 2015	H2 Refuel H-Prize Technical Data Collection Requirements	This webinar provided testing specifications and plans for FCTO's $1 million H2 Refuel H-Prize competition, a two-year competition administered by the Hydrogen Education Foundation that challenges America's engineers and entrepreneurs to develop systems for small-scale hydrogen fueling. The testing specification documents are intended to inform potential contestants about the type of data that will need to be provided and how to ensure that it is compatible with the data collection system. For more information on the H2 Refuel H-Prize competition, visit hydrogenprize.org.
June 25, 2015	H2 Refuel H-Prize Overview and Q&A	This webinar focused on the $1 million H2 Refuel 2014–2016 H-Prize competition, which challenges America's innovators to deploy an on-site hydrogen generation system, using electricity or natural gas, that can be used in homes, community centers, retail sites, or similar locations to fuel hydrogen vehicles. The entry that meets all the requirements and scores the highest on the technical and cost criteria will win $1 million. The H-Prize is administered by the Hydrogen Education Foundation and sponsored by the U.S. Department of Energy.
August 6, 2015	H2 Refuel H-Prize Safety Guidance	This webinar included a discussion on safety planning and what information should be included in the safety plan document for FCTO's $1 million H2 Refuel H-Prize competition. As part of the design submission for finalist selection, contestants must include a safety plan and a hazard analysis. There also was a general discussion on codes and standards and the need for local fire/building approval requirements. Members of the Hydrogen Safety Panel led the discussion and answered questions.
August 11, 2015	Analysis Using Fuel Cell Material Handling Equipment (MHE) for Shaving Peak Building Energy	This webinar explored the synergy between a facility's use of hydrogen fuel cell forklifts and its reduction of electric grid time-of-use energy charges. Electric fuel cell forklifts use electricity generated from hydrogen fuel and can be used for either mobility or to offset grid charges associated with peak facility demands. The analyzed scenarios focused on how different buildings can benefit from offsetting their peak energy demands by connecting fuel cells to their internal power systems. The webinar included a techno-economic analysis as well as competitive analysis for the alternative peak-shaving apparatus.

TABLE 3. EERE Blog Posts in FY 2015 Focusing on Hydrogen and Fuel Cell Activities

Date	Title	Summary
December 29, 2014	H2 Refuel H-Prize Aims to Make Fueling Hydrogen Powered Vehicles Easier than Ever[24]	The H2 Refuel H-Prize is challenging America's innovators to develop systems that make it easier and convenient to fuel hydrogen powered vehicles.
January 9, 2015	Fuel Cell Technologies Office Reaches Major Patent Milestone[25]	Fuel cells are an emerging technology that can provide heat and electricity to buildings and power for vehicles while emitting nothing but water. The Energy Department's Fuel Cell Technologies Office (FCTO) within the Office of Energy Efficiency and Renewable Energy supports research and development (R&D) that improves the performance and lowers the cost of these systems. The office recently reached a major milestone, with 500 patents resulting from FCTO-supported R&D.
January 27, 2015	Washington Auto Show Spotlight: How Fuel Cell Electric Vehicles Work[26]	Fuel cell electric vehicles (FCEVs) are quickly becoming a commercially viable sustainable transportation option for Americans. Unlike gasoline-powered cars, these cutting-edge vehicles are fueled by hydrogen and emit only water. The latest and greatest FCEVs are on display this week at the Washington Auto Show. Learn more about how FCEVs work and what the Energy Department is doing to make them even more energy efficient and cost effective.
April 10, 2015	EERE Energy Impacts: You Can Now Drive a Fuel Cell Electric Vehicle[27]	Fuel cell electric vehicles (FCEVs) are now commercially available, so car buyers have the option to drive these vehicles that run on hydrogen gas rather than gasoline and emit only water from the tailpipe. FCEVs have the potential to significantly reduce our nation's dependence on foreign oil and lower harmful emissions that contribute to climate change—just one of EERE's Energy Impacts.
April 21, 2015	H2USA Accomplishments Push Hydrogen Infrastructure Forward[28]	The U.S. Department of Energy (DOE) has announced new tools developed in support of H2USA focused on hydrogen fueling infrastructure analysis. H2USA is a public-private partnership founded in 2013 by DOE, along with automakers and other stakeholders, to address the key challenges of hydrogen infrastructure. H2USA's mission is to promote the introduction and widespread adoption of FCEVs across America.
June 5, 2015	Annual Merit Review Evaluates Impact of Sustainable Transportation Projects[29]	This week from June 8 to 12, the Vehicle Technologies Office and Hydrogen and Fuel Cells Program are simultaneously holding their Annual Merit Review and Peer Evaluation Meeting in Washington, D.C., where hundreds of Energy Department-funded projects will be put to the test.
June 10, 2015	World's First Fuel Cell Cargo Trucks Deployed at U.S. Airport[30]	A ribbon-cutting ceremony held at Memphis International Airport on April 9, 2015, marked the start of a two-year demonstration of the world's first zero-emissions, hydrogen fuel cell powered ground support equipment.
June 24, 2015	Sustainable Transportation Day Drives Innovation Forward[31]	On June 22, the Office of Energy Efficiency and Renewable Energy (EERE) hosted Sustainable Transportation Day at the Energy Department's headquarters in Washington, D.C. Together, the Bioenergy, Fuel Cell, and Vehicle Technologies Offices showcased how EERE's strategic investments in sustainable transportation technologies are improving vehicle efficiency and advancing the use of alternative fuel vehicles.
August 25, 2015	Garbage In, Power Out: South Carolina BMW Plant Demonstrates Landfill Gas to Hydrogen Fuel[32]	In a first-of-its-kind demonstration, the Energy Department, BMW, and project partners Ameresco, Gas Technology Institute, and the South Carolina Research Authority powered some of the facility's fuel cell forklifts with hydrogen produced on-site from biomethane gas at a nearby landfill.
October 8, 2015	Stacked for Success: Celebrating National Hydrogen and Fuel Cell Day[33]	Do you know the atomic weight of hydrogen? It's 1.008, which makes today, October 8, a great day to celebrate National Hydrogen and Fuel Cell Day! But at the Department of Energy, we're not just celebrating the confluence of the calendar and the periodic table. We're starting to see a hydrogen future to our roads today.
December 10, 2015	First Commercially Available Fuel Cell Electric Vehicles Hit the Street[34]	Fuel cell electric vehicles are now widely available in the United States. These passenger vehicles have the driving range, ease of refueling, and performance of today's gasoline-powered cars while emitting nothing but water.

[24] http://energy.gov/eere/articles/h2-refuel-h-prize-aims-make-fueling-hydrogen-powered-vehicles-easier-ever
[25] http://energy.gov/eere/articles/fuel-cell-technologies-office-reaches-major-patent-milestone
[26] http://energy.gov/eere/articles/washington-auto-show-spotlight-how-fuel-cell-electric-vehicles-work
[27] http://energy.gov/eere/articles/eere-energy-impacts-you-can-now-drive-fuel-cell-electric-vehicle
[28] http://energy.gov/eere/articles/h2usa-accomplishments-push-hydrogen-infrastructure-forward
[29] http://energy.gov/eere/articles/annual-merit-review-evaluates-impact-sustainable-transportation-projects
[30] http://energy.gov/eere/articles/worlds-first-fuel-cell-cargo-trucks-deployed-us-airport
[31] http://energy.gov/eere/articles/sustainable-transportation-day-drives-innovation-forward
[32] http://energy.gov/articles/garbage-power-out-south-carolina-bmw-plant-demonstrates-landfill-gas-hydrogen-fuel
[33] http://energy.gov/eere/articles/stacked-success-celebrating-national-hydrogen-and-fuel-cell-day
[34] http://energy.gov/eere/articles/first-commercially-available-fuel-cell-electric-vehicles-hit-street

INTERNATIONAL ACTIVITIES

International Partnership for Hydrogen and Fuel Cells in the Economy

The International Partnership for Hydrogen and Fuel Cells in the Economy (IPHE) includes 17 member countries (Australia, Austria, Brazil, Canada, China, France, Germany, Iceland, India, Italy, Japan, Norway, the Republic of Korea, the Russian Federation, South Africa, the United Kingdom, and the United States) and the European Commission. IPHE is a forum for governments to work together to advance worldwide progress in hydrogen and fuel cell technologies. IPHE also offers a mechanism for international R&D managers, researchers, and policymakers to share program strategies. IPHE members embarked upon a second 10-year term in November 2013. An independent Secretariat was established during the past year, and the Chair of IPHE transitioned from Japan to France. The U.S. continues its strong role as a Vice Chair. In FY 2015, the IPHE Steering Committee met in Rome, Italy (December 2014), and in Wuhan, China (May 2015), to share progress and plans related to hydrogen and fuel cells. IPHE related workshop topics in FY 2015 included education, smart cities, and fuel cell backup power.[35]

International Energy Agency

The United States is also involved in international collaboration on hydrogen and fuel cell R&D through the International Energy Agency (IEA) implementing agreements and is a member of both the Advanced Fuel Cells Implementing Agreement and the Hydrogen Implementing Agreement. These agreements provide a mechanism for member countries to share the results of R&D and analysis activities. The DOE Hydrogen and Fuel Cells Program is a strong contributor to numerous IEA tasks and activities. During FY 2015, the United States, along with other representatives of the Hydrogen and Fuel Cell Technology Roadmap steering committee, supported the IEA in preparation of the first IEA Technology Roadmap on Hydrogen and Fuel Cells, published in the summer of 2015.

EXTERNAL COORDINATION, INPUT, AND ASSESSMENTS

H2USA Partnership

To help address the challenge of hydrogen infrastructure, in 2013 DOE co-launched H2USA, a public-private partnership focused on the widespread commercial adoption of FCEVs. H2USA currently consists of 45 participants, including the state of California, as well as developers, car companies, and hydrogen providers. The number of partners has increased more than four-fold since its launch.

In April 2014, the Program announced two new tools developed in support of H2USA to help address technical and financial barriers to hydrogen fueling infrastructure deployment. The Hydrogen Refueling Station Analysis Model will help to assess the impact of station design on station economics. The model optimizes station component size to meet demand while minimizing cost. It estimates capital and operating cost based on design variables such as station capacity and mode of hydrogen delivery. The Hydrogen Financial Analysis Scenario Tool provides in-depth financial analysis, including cash flow and return on investments for hydrogen fueling stations, based on financial inputs such as station capital cost, operating cost, and financing mechanisms.

In direct support of H2USA, DOE launched the Hydrogen Fueling Infrastructure Research and Station Technology (H2FIRST) project in 2014 to leverage capabilities at the national laboratories to address the technology challenges related to hydrogen refueling stations. Jointly led by Sandia National Laboratories and NREL, H2FIRST is a strong example of DOE's efforts to bring national lab capabilities and facilities together to address immediate and mid-term challenges faced by the industry.

H2FIRST recently released two critical reports. The Reference Station Design report[36] details engineering models and economic analyses of five hydrogen refueling station templates that can meet near-term market needs. The Hydrogen Contaminant Detection report[37] describes the current commercial state-of-the-art technologies in contamination detection. These tools and reports will identify and accelerate near-term solutions that will help industry address the challenges of hydrogen infrastructure.

[35] http://www.iphe.net/
[36] H2FIRST Reference Station Design Task, http://www.nrel.gov/docs/fy15osti/64107.pdf
[37] H2FIRST Hydrogen Contaminant Detector Task, http://www.nrel.gov/docs/fy15osti/64063.pdf

Hydrogen and Fuel Cells Technical Advisory Committee (HTAC)

As required by the Energy Policy Act of 2005, HTAC was created in 2006 to advise the Secretary of Energy on issues related to the development of hydrogen and fuel cell technologies and to provide recommendations regarding DOE's programs, plans, and activities, as well as on the safety, economic, and environmental issues related to hydrogen and fuel cells. HTAC members include representatives of domestic industry, academia, professional societies, government agencies, financial organizations, and environmental groups, as well as experts in the area of hydrogen safety. HTAC met twice in FY 2015. In May 2015, HTAC released its seventh annual report, which summarizes hydrogen and fuel cell technology, domestic and international progress in RD&D projects, commercialization activities, and policy initiatives.

Currently, the Committee has two established subcommittees, both started in 2013. The Advanced Manufacturing Subcommittee conducted an assessment of the state of manufacturing techniques that are, or could be, used to benefit commercialization in the fuel cell and hydrogen generation industries. Their written report, "Advanced Manufacturing Status and Opportunities to Accelerate Growth in Fuel Cell and Hydrogen Products," was submitted to the Secretary of Energy in January 2015. The Retail Infrastructure Subcommittee will track the progress of the worldwide rollout of FCEVs and examine the evolving business case for retail hydrogen fueling stations, including the effects of technology advancement and government policy. It is anticipated that this subcommittee will prepare a written report detailing its accomplishments and findings to the full Committee in FY 2016.

Federal Inter-Agency Coordination

The Hydrogen and Fuel Cell Interagency Task Force (ITF), mandated by the Energy Policy Act of 2005, includes senior representatives from federal agencies supporting hydrogen and fuel cell activities, with the DOE/EERE serving as chair. The Hydrogen and Fuel Cell Interagency Working Group (IWG), also chaired by DOE, supports the initiatives and actions passed down by the ITF. The IWG meets monthly to share expertise and information about ongoing programs and results, to coordinate the activities of federal entities involved in hydrogen and fuel cell RD&D, and to ensure efficient use of taxpayer resources. A key example of interagency collaboration included work with the Environmental Protection Agency's (EPA's) Diesel Emission Reduction Act program to broaden program rules to allow fuel cell alternatives. DOE worked with EPA to show how fuel cell applications can replace diesel power trains. DOE and the Department of Transportation's Maritime Administration commissioned an operational testing project for an auxiliary maritime power system that can provide power for ocean vessels both pier-side and onboard. Finally, further collaboration with the Federal Aviation Administration and the Department of Defense to identify locations for future hydrogen stations is also helping support the early FCEV and hydrogen fuel infrastructure markets.

The National Academies

The National Research Council (NRC) of the National Academies provides ongoing technical and programmatic reviews and input to the Hydrogen and Fuel Cells Program. The NRC has conducted independent reviews of both the Program and the R&D activities of the United States Driving Research and Innovation for Vehicle efficiency and Energy sustainability (U.S. DRIVE) partnership. Formerly known as the FreedomCAR and Fuel Partnership, the U.S. DRIVE partnership advances an extensive portfolio of advanced automotive and energy infrastructure technologies, including batteries and electric drive components, advanced combustion engines, lightweight materials, and hydrogen and fuel cell technologies. Plans were developed for future reviews.

Clean Energy Manufacturing Initiative

The Clean Energy Manufacturing Initiative (CEMI) is a strategic integration and commitment of manufacturing efforts across EERE's clean energy technology offices and DOE's Advanced Manufacturing Office (AMO), focusing on American competitiveness in clean energy manufacturing. The objectives are to increase U.S. competitiveness in the production of clean energy products by strategically investing in technologies that leverage American advantages and overcome disadvantages, and increase U.S. manufacturing competitiveness by strategically investing in technologies and practices to enable U.S. manufacturers to increase their competitiveness through energy efficiency, combined heat and power, and taking advantage of low-cost domestic energy sources.

The DOE announced selections from a recent FOA, including a project to develop innovative, low-cost processes for manufacturing fiber reinforced composite pipe that eliminates O-ring failure and is capable of carrying hydrogen at 100 bar, is durable for 50 years, and has a reasonable leak rate. The project should lead to installed fiber reinforced

plastic costs that are equivalent to or lower than the cost of installing a natural gas pipeline of the same size and be scalable to high-volume manufacturing.

At the American Energy and Manufacturing Competitiveness Summit held in Washington, D.C., in September 2015, DOE's Assistant Secretary for Energy Efficiency and Renewable Energy, David Danielson, announced the Clean Energy Manufacturing Analysis Center (CEMAC) at NREL. CEMAC will harness NREL's analytical and modeling capabilities to provide detailed data on all aspects of manufacturing (material and labor costs, interest rates, trade flows, tariffs, etc.) so that companies can select the most favorable place to initiate their next manufacturing plans. In FY 2015, FCTO's Manufacturing R&D sub-program expanded its global competitiveness analysis project on hydrogen and fuel cells with the Great Lakes WIND Network to include activities with CEMAC.

The Program also supported CEMI's technologist in residence pilot initiative for personnel exchange to help national laboratories identify issues in industrial manufacturing processes while industry will learn about the capabilities and facilities of the national labs. The result of the initiative will be a long-term plan for the team to increase collaborative R&D.

As discussed earlier under FOAs, the FCTO is involved in EERE's Small Business Voucher pilot to increase access of small businesses to the expertise and infrastructure of DOE's national labs; small businesses will apply for and use vouchers to work with the labs to tackle industry-wide problems.

FY 2015 Annual Merit Review and Peer Evaluation (AMR)

The Program's AMR took place June 8–12, 2015, in Arlington, Virginia, and provided an opportunity for the Program to obtain expert peer reviews of the projects it supports and to report its accomplishments and progress. Under Secretary Franklin "Lynn" Orr kicked off the meeting, and former Senator Byron Dorgan (ND-D) gave the keynote plenary presentation. For the seventh time, this meeting was held in conjunction with the annual review of DOE's Vehicle Technologies Office. During the AMR, reviewers evaluate the Program's projects and make recommendations; DOE uses these evaluations, along with other review processes, to make project funding decisions for the upcoming fiscal year. The review also provides a forum for promoting collaborations, the exchange of ideas, and technology transfer. This year, approximately 1,800 participants attended, and more than 370 experts peer-reviewed 120 of the Program's projects—conducting a total of more than 600 individual project reviews, with an average of more than six reviewers per project. The report summarizing the results and comments from these reviews is available.[38] The 2016 Annual Merit Review and Peer Evaluation Meeting will be held June 6–10, in Washington, D.C.

Funds Saved through Active Project Management

The AMR is a key part of the Program's comprehensive approach toward active management of its projects. Termination of underperforming projects—identified through the AMR as well as through go/no-go decisions (with criteria defined in the project scope of work)—helped the Program redirect $0.6 million in funding in FY 2015, $3.0 million in funding in FY 2014, and over $32 million over the past five years.

DOE Cross-Cutting Activities

Hydrogen Energy Storage (HES)/Grid Integration: HES may provide a broad range of energy services and typically involves the production of hydrogen from electricity via electrolyzers. Increasing capacity for variable renewable energy technologies (e.g., wind and solar) on the grid is going to be a major challenge facing future deployment as these technologies make up a larger portion of the power generation portfolio. FCTO is contributing significant funding to the Grid Modernization program (a cross-cutting effort involving various offices within EERE and the DOE Office of Electricity Delivery and Energy Reliability) with an objective to help set the nation on a cost-effective path to an integrated, secure, and reliable grid that is flexible enough to provide an array of emerging services while remaining affordable to consumers. Activities were described under the Technology Validation sub-program.

Carbon Fiber: Carbon fiber composites are expected to play an important role across many clean energy technologies, such as in high-efficiency, longer wind turbine blades; lighter-weight, higher-fuel-economy vehicles; and high-pressure gaseous fuel storage systems. EERE's cross-cutting carbon fiber initiative aims to lower the cost of carbon fiber for clean energy applications through higher-energy-efficiency manufacture, higher piece production throughput, lower-cost raw materials, and increased recyclability. For high-pressure gaseous fuel storage systems, such as for hydrogen and compressed natural gas, high-strength carbon fiber is required and is a major contributor to cost of

[38] www.hydrogen.energy.gov/annual_review15_report.html

the storage systems. The polyacrylonitrile (PAN) precursor fibers used to produce high-strength carbon fiber account for over 50% of the final carbon fiber costs. An approach FCTO has taken to lower the cost of carbon fibers has been to focus on alternative, lower-cost PAN precursors. In FY 2015, Strategic Analysis Inc. updated the cost projections for 700 bar compressed hydrogen storage systems. The updated analysis projects a system cost of $14.69/kWh, an overall cost reduction of approximately $2/kWh from the baseline cost of $16.76/kWh established in FY 2013. The analysis reflects recent technology advancements to reduce cost of carbon fiber precursor and resin, and through balance of plant components integration. The analysis also includes changes in the tank design to better reflect commercially manufactured pressure vessels, which result in increased projected costs.

Wide Bandgap Semiconductors for Clean Energy Initiative: Wide bandgap (WBG) semiconductor materials allow power electronic components to be smaller, faster, more reliable, and more efficient than their silicon-based counterparts. These capabilities make it possible to reduce weight, volume, and life-cycle costs in a wide range of power applications, including fuel cells and hydrogen production technologies. EERE's technology offices, through AMO, are working together to harness these capabilities to lead to dramatic energy savings in industrial processing and consumer appliances. The flagship of this cross-cutting effort is the PowerAmerica partnership, a 2014 addition to DOE's National Network for Manufacturing Innovation (NNMI) focused on accelerated development of next-generation WBG semiconductor products. FCTO has identified numerous applications of hydrogen and fuel cell technologies that could benefit from the development of next-generation WBG power electronics, including fuel-cell-powered MHE and FCEVs in the transportation sector and large-scale grid integration of fuel cells and electrolyzers in the stationary power sector. FCTO is working with PowerAmerica and with leading innovators in the WBG electronics industry to explore opportunities for product development responsive to the market pull of these hydrogen and fuel cell technology applications.

Energy Materials Network: In FY 2014, FCTO initiated an effort to explore the use of high-throughput computational and experimental methods toward the accelerated discovery and development of critical materials for hydrogen and fuel cell technologies. This approach leverages the scientific methodologies of the Presidential Materials Genome Initiative (MGI) launched in 2011. In FY 2015, several DOE offices identified complementary MGI-related research interests in several key material domains, with plans to align their materials research through the establishment of broad research consortia supporting teams of industry, academic, and national lab partners and conducting focused research within these domains. Together, these consortia will form the Energy Materials Network (EMN), a resource network with capabilities in materials design, synthesis, characterization, manufacturing, and digital data management and informatics. One important thrust of the FCTO pilot effort in EMN is the accelerated development and optimization of alternative low-cost, high-performance, PGM-free catalysts integrated into membrane electrode assemblies for PEM fuel cells and electrolyzers. The EMN-related efforts at FCTO, which have already included roundtable meetings of experts, RFIs and workshops, are expected to continue through FY 2016 and beyond.

IN CLOSING …

The need for clean, sustainable energy and the need to reduce emissions have come together to form a global imperative—one that demands new technologies and new approaches for the way we produce and use energy. Widespread use of hydrogen and fuel cells can play a substantial role in a portfolio of clean energy technologies that will overcome key energy challenges. In addition, growing interest and investment among leading world economies, such as Germany, Japan, and South Korea, underscores the global market potential for these technologies.

The Program's latest Fuel Cell Technologies Market Report[39] shows that the fuel cell industry continues to grow at an unprecedented rate, totaling more than $2.2 billion in sales in 2014. Globally, fuel cell shipments increased by around 37% over 2013, and the number of megawatts (MWs) shipped grew by about 7%. More than 50,000 fuel cells, totaling over 180 MW, were shipped worldwide in 2014. This continues to uphold the consistent 30% annual market growth rate over the last few years. EERE-funded R&D has resulted in 515 patents, 40 commercial technologies, and 65 technologies that are projected to be commercialized within three to five years.[40]

With so much FCTO-supported activity in the last year, only a few highlights are summarized below.

In January, Energy Secretary Moniz gave plenary remarks at the 2015 Washington Auto Show and toured a number of FCEV original equipment manufacturer displays. A slideshow featuring highlights from Secretary Moniz's tour of the 2015 Washington Auto Show was posted on the Energy Department's blog. Featured fuel cell vehicles

[39]Fuel Cell Technologies Market Report, http://energy.gov/eere/fuelcells/downloads/2014-fuel-cell-technologies-market-report
[40]Pathways to Commercial Success, http://energy.gov/eere/fuelcells/market-analysis-reports#mkt_pathways

included Toyota's Mirai, Hyundai's Tucson fuel cell vehicle, and the Honda FCV concept car.[41] Soon after the tour, Secretary Moniz test drove the Mirai, which was filmed and posted online.[42]

In February the Program launched a new, free, online national hydrogen safety training resource for emergency responders. The resource provides a single repository of credible and reliable information related to hydrogen and fuel cells that is current and accurate and eliminates duplicative efforts among various training programs. To date, the resource has been downloaded more than 300 times by people from 35 states and six continents. It has also been translated into Japanese.[43]

In August, the industry celebrated 50 years of fuel cells in space. On August 21, 1965, the National Aeronautics and Space Administration launched the Gemini 5, the first manned spacecraft to use fuel cells. Using fuel cells to power onboard electronics allowed the United States to break the world's spaceflight endurance record by traveling for eight days. Fuel cells were then used on all subsequent American manned space missions through the Gemini, Apollo, and Space Shuttle programs.

This year the program has had a strong focus on tech-to-market activities and encouraging industry to work with national labs to bring technology to the real world faster. On November 11, 2014, at the Fuel Cell Seminar and Energy Exposition in Los Angeles, California, and again on October 12, 2015, at the Electrochemical Energy Summit in Phoenix, Arizona, the Program hosted several events to foster increased collaboration between national labs and industry. The events included keynote addresses from Deputy Assistant Secretary for Transportation Reuben Sarkar and Under Secretary for Science and Energy Franklin "Lynn" Orr, respectively. Both events also included panel discussions that worked to demystify the process of working with national labs and the mechanisms put in place to put labs to work on industry problems. These panels were followed by presentations and poster sessions that highlighted the capabilities of the national labs.

On Thursday, October 8, 2015, the industry celebrated the first National Hydrogen and Fuel Cell Day. The day was marked by events across the country, including a National Renewable Energy Laboratory hydrogen station ribbon cutting and announcements from multiple national laboratories and industry partners. Aptly chosen for the atomic weight of hydrogen (1.008), National Hydrogen and Fuel Cell Day was recognized by the U.S. Senate.[44]

The most notable development of the year was the launch of commercially available FCEVs. The Department of Energy's fuel cell program began in the 1970s after the first oil embargo, when a group of researchers met at Los Alamos National Laboratory. Eventually, national lab researchers developed breakthrough methods of fabricating fuel cell electrodes that spurred worldwide research and development on PEM fuel cells. Forty years later, we see the impact of those early pioneers as car makers around the world develop fuel cell cars. In November 2014, Hyundai started leasing its Tucson FCEV, and in October 2015, Toyota announced FCEVs for sale, right on track with DOE's original plans for R&D resulting in commercial decisions being made in the 2015 timeframe. Several other companies also plan to release FCEVs very soon, including Honda, GM, Daimler, and BMW.[45]

This is a critical time for fuel cells and hydrogen. The DOE Hydrogen and Fuel Cells Program will continue to work in close collaboration with key stakeholders and will continue its strong commitment to effective stewardship of taxpayer dollars in support of its mission to enable the energy, environmental, and economic security of the Nation. In support of these efforts, the following nearly 1,000 pages document the results and impacts of the Program in the last year.

Sunita Satyapal
Director
Fuel Cell Technologies Office
U.S. Department of Energy

[41] http://energy.gov/eere/articles/washington-auto-show-spotlight-how-fuel-cell-electric-vehicles-work

[42] http://energy.gov/eere/fuelcells/test-driving-toyota-mirai

[43] https://h2tools.org/fr/nt/

[44] http://energy.gov/eere/articles/stacked-success-celebrating-national-hydrogen-and-fuel-cell-day

[45] http://energy.gov/eere/articles/first-commercially-available-fuel-cell-electric-vehicles-hit-street

II.0 Hydrogen Production Sub-Program Overview

INTRODUCTION

The Hydrogen Production sub-program supports research and development (R&D) of technologies that will enable the long-term viability of hydrogen as an energy carrier for a diverse range of end-use applications, including transportation (e.g., specialty vehicles, cars, trucks, and buses), stationary power (e.g., backup power and combined heat and power systems), and portable power. A portfolio of hydrogen production technology pathways utilizing a variety of renewable energy sources and renewable feedstocks is being developed under this sub-program.

Multiple DOE offices are engaged in R&D relevant to hydrogen production, including the following.

- The Fuel Cell Technologies Office (FCTO), within the Office of Energy Efficiency and Renewable Energy (EERE), is developing technologies for distributed and centralized renewable production of hydrogen, including conversion of biomass-derived feedstocks, advanced water splitting (including high temperature/pressure operations and novel catalyst/membranes), direct solar water splitting (including thermochemical and photoelectrochemical [PEC] processes), and biological processes.
- The Office of Fossil Energy (FE) is advancing the technologies needed to produce hydrogen from fossil fuel resources, including co-production of hydrogen and electricity. FE is also developing technologies for carbon capture, utilization, and storage, which could ultimately enable reduced-emissions pathways for hydrogen production from fossil resources.
- The Office of Science's Basic Energy Sciences (BES) program conducts research to expand the fundamental understanding of processes and mechanisms relevant to hydrogen production, including biological and biomimetic hydrogen production, photoelectrochemical water splitting, catalysis, and membranes for gas separation.
- The Office of Nuclear Energy (NE) is currently collaborating with EERE on a study of nuclear-renewable hybrid energy systems. Many of the systems being evaluated by this study use hydrogen as a form of energy storage or as an input to industrial processes.

GOAL

The goal of the Hydrogen Production sub-program is to develop low cost, highly efficient hydrogen production technologies that utilize diverse domestic sources of energy, including renewable resources (EERE), coal with sequestration (FE), and nuclear power (NE).

OBJECTIVES

The objective of the Hydrogen Production sub-program is to reduce the cost of hydrogen dispensed at the pump to a cost that is competitive on a cents-per-mile basis with fuels used in competing vehicle technologies. Based on current analysis, this translates to a hydrogen cost target of <$4/kg hydrogen (produced, delivered, and dispensed, but untaxed) by 2020[1], with <$2/kg apportioned for production only[2]. Technologies are being developed to achieve this goal in timeframes appropriate to their current stages of development.

The objectives of FE's efforts in hydrogen production are documented in the *Hydrogen from Coal Program Research, Development and Demonstration Plan* (September 2010)[3]. They include proving the feasibility of a near-zero emissions, high efficiency plant that will produce both hydrogen and electricity from coal and reduce the cost of hydrogen from coal by 25% compared with current technology by 2016. The objectives of NE's collaborative efforts with FCTO are documented in the report: *Rethinking the Future Grid: Integrated Nuclear Renewable Energy Systems*[4].

[1] *Hydrogen Threshold Cost Calculation*, Program Record (Office of Fuel Cell Technologies) 11007, U.S. Department of Energy, 2012, http://www.hydrogen.energy.gov/pdfs/11007_h2_threshold_costs.pdf
[2] *Hydrogen Production and Delivery Cost Apportionment*, Program Record (Office of Fuel Cell Technologies) 12001, U.S. Department of Energy, 2012, http://hydrogen.energy.gov/pdfs/12001_h2_pd_cost_apportionment.pdf
[3] *Hydrogen from Coal Program Research Development and Demonstration Plan*, Office of Fossil Energy, U.S. Department of Energy, September 2010, http://fossil.energy.gov/programs/fuels/hydrogen/2010_Draft_H2fromCoal_RDD_final.pdf
[4] *Rethinking the Future Grid: Integrated Nuclear Renewable Energy Systems*, National Renewable Energy Laboratory, December 2014, http://www.nrel.gov/docs/fy15osti/63207.pdf

FISCAL YEAR (FY) 2015 TECHNOLOGY STATUS AND PROGRESS

Recent and current status for the high-volume projected costs of hydrogen production for several of the near- to mid-term production pathways is shown in Figure 1. The figure highlights the reduction in costs in recent years resulting from R&D. It is seen that natural gas reforming is the only technology meeting the FCTO cost target of <$2/kg. Ongoing R&D is exploring ways to accelerate development and reduce cost in all available hydrogen production technology pathways, including the mid- to long-term renewable pathways.

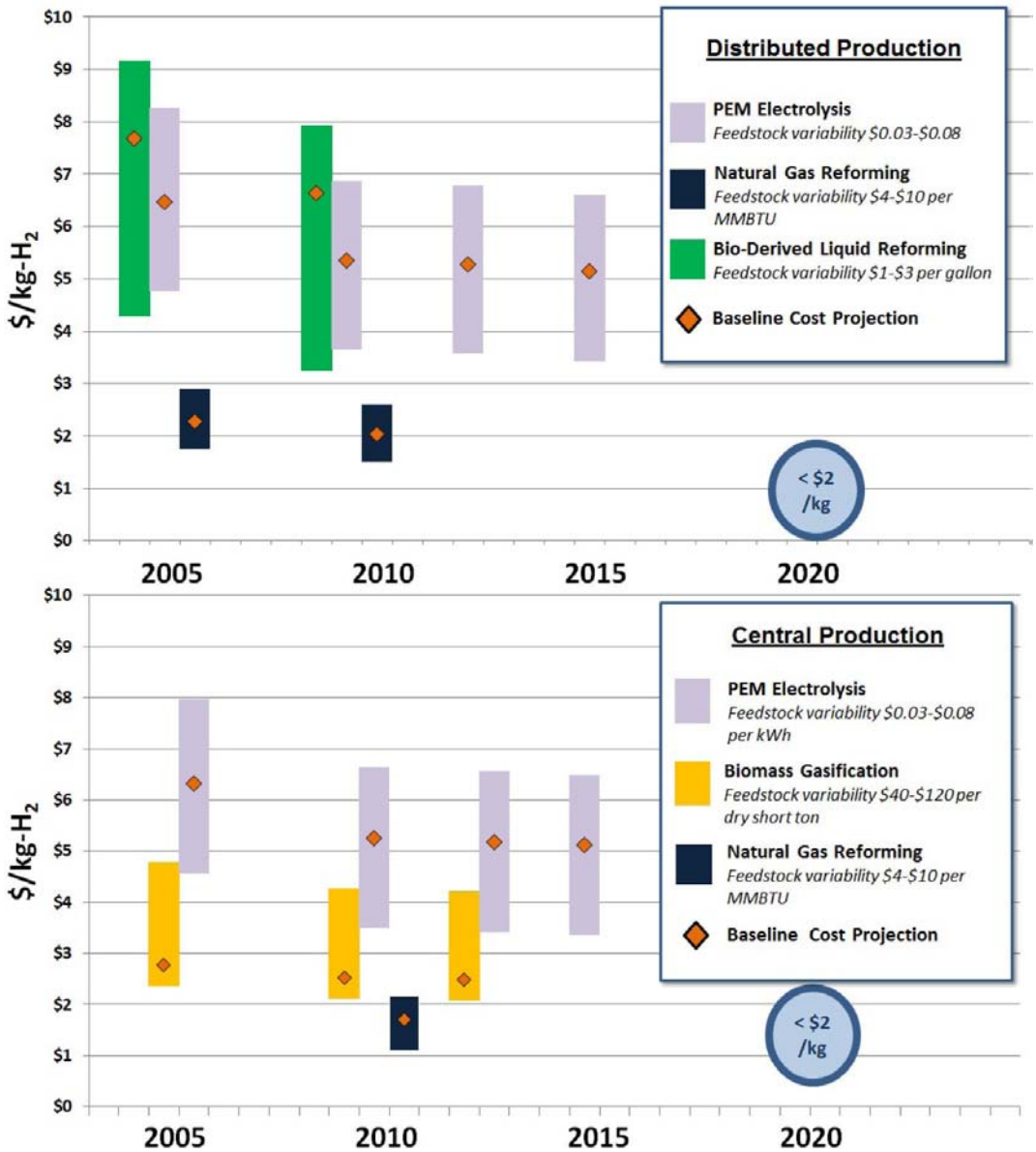

PEM – Polymer electrolyte membrane

FIGURE 1. Range of hydrogen production costs, untaxed, for near- to mid-term distributed and centralized pathways. The high end of each bar represents a pathway-specific high feedstock cost as well as an escalation of capital cost, while the low end reflects a low feedstock cost and no capital escalation. Bars for different years in the same pathway represent improvements in the costs of the specific pathway, based on specific reference data for the appropriate year and pathway. Detailed information is included in the DOE Hydrogen and Fuel Cells Program Record #14005[5].

[5] DOE Hydrogen and Fuel Cells Program Record #14005 Hydrogen Production Status 2006-2013, under development

In FY 2015, significant progress was made by the Hydrogen Production sub-program on several important fronts. Highlights include the following.

- The second H-Prize competition, H2 Refuel, was launched in October 2014. This $1 million competition challenges America's innovators to deploy an on-site hydrogen generation system to fuel hydrogen-powered vehicles. The system may use electricity or natural gas and can be sited in homes, community centers, small businesses, or similar locations.
- The H2A (Hydrogen Analysis) Tool was enhanced to include an updated economic basis and easy-to-read results containing tornado and waterfall plots.
- A joint workshop was held by FCTO and the Bioenergy Technologies Office (BETO) in March 2015, titled *Hydrogen, Hydrocarbons, and Bioproduct Precursors from Wastewaters*. The workshop presentations have been posted online[6], and a workshop report will be posted in FY 2016. A Request for Information to solicit public input will follow.

Detailed FY 2015 progress in the Hydrogen Production sub-program is described below.

New Project Selections

In FY 2015, an Incubator funding opportunity announcement (FOA) was released to support R&D efforts to address critical challenges and barriers to hydrogen production and delivery technology development, and specifically the long-term goal of hydrogen production at <$2/kg hydrogen. Innovative materials, processes, and systems are needed to establish the technical and cost feasibility for renewable and low carbon hydrogen production and delivery. Specifically, the Incubator FOA sought research on game-changing technologies that could reach FCTO targets but were under-represented in the Program's Multi-Year Research, Development, and Demonstration Plan targets and/or research portfolio. The four selected projects are as follow.

- Proton OnSite, Wallingford, Connecticut, will advance alkaline-exchange-membrane-based electrolysis technology by developing durable and efficient precious group metal (PGM)-free electrolysis cells.
- Versa Power Systems, Littleton, Colorado, will develop hydrogen production technologies using high temperature solid oxide electrolysis capable of operating at high current densities (i.e., high hydrogen production rates) and high efficiencies.
- University of California, Irvine will develop a novel photocatalyst particle-based slurry reactor with the potential for low cost renewable hydrogen production via solar water splitting.
- Virginia Polytechnic Institute and State University, Blacksburg, Virginia, will develop a cell-free biological hydrogen production technology based on an in vitro synthetic biosystem composed of numerous thermoenzymes and biomimetic coenzymes.

Four *solar water splitting* projects awarded in FY 2014 under the National Science Foundation (NSF)/FCTO joint solicitation NSF 14-511: NSF/DOE Partnership on Advanced Frontiers in Renewable Hydrogen Fuel Production, were initiated. The four projects are listed below.

- The University of Toledo, Toledo, Ohio, initiated the project titled: New Metal Oxides for Efficient Hydrogen Production Via Solar Water Splitting.
- Stanford University, Stanford, California, initiated the project titled: Engineering Surfaces, Interfaces, and Bulk Materials for Unassisted Solar Photoelectrochemical (PEC) Water Splitting.
- The University of Colorado (CU) at Boulder, Boulder, Colorado, initiated the project titled: Accelerated Discovery of Advanced RedOx Materials for Solar Thermal Water Splitting to Produce Renewable Hydrogen.
- Rutgers University, New Brunswick, New Jersey, initiated the project titled: Tunable Semiconductor/Catalyst Interfaces for Efficient Solar Water Splitting.

[6] *Hydrogen, Hydrocarbons, and Bioproduct Precursors from Wastewaters*, Joint workshop of DOE's FCTO and BETO, March 2015, http://energy.gov/eere/fuelcells/hydrogen-hydrocarbons-and-bioproduct-precursors-wastewaters-workshop

H2A Technoeconomic Case Studies

Industry-vetted case studies of hydrogen production costs via solid oxide electrolyzer cells (SOEC) and fermentation were completed using the H2A v3 tool, and these studies are being made publically available on the DOE website. In these studies, representative SOEC and fermentation systems were modeled based on input from several key industry collaborators with commercial experience. Both technologies were analyzed as centralized production facilities with a capacity of 50,000 kg/d, and both were evaluated at two technology years (current: 2015 and future: 2025). The technoeconomic case study process included soliciting relevant, detailed information from the companies followed by synthesizing and amalgamating the data into base parameters and sensitivity limits that were vetted by the industry collaborators. Results included the following.

- The results of the SOEC case studies show hydrogen production costs (at high volume, untaxed) of $4.21/kg and $3.68/kg for current and future cases, respectively. Key cost drivers were identified and quantified, including electricity cost, electrical efficiency, and capital cost.
- The results of the fermentation case studies show hydrogen production costs (at high volume, untaxed) of >$100/kg for the current case, but reduced to $4.62/kg for the future case. The cost of the current case is dominated by utility heating cost. The heat requirement of the future case is projected to be offset by using heat from burning lignin in the system.

(Strategic Analysis, Inc., National Renewable Energy Laboratory [NREL], Argonne National Laboratory)

Electrolytic Hydrogen Production

The major emphases of the electrolysis projects were on cost reduction and efficiency improvement through leveraging catalyst development. Work on alkaline membrane electrolysis is showing promise to deliver electrolyzer systems with very low PGM loading. Additional work is needed to reduce electrolyzer system costs by reducing balance of plant losses, such as dryer losses. Technical progress included the following.

- A large active area stack electrolyzer test bed (sub-megawatt scale) and dryer skid were installed to allow independent performance testing. Preliminary variable-flow drying demonstrations suggest that over 1,000 kg H_2/yr would be saved, compared to traditional drying methods, by coupling the electrolyzer stack with 1 MW wind electricity. (NREL)
- High pressure electrolysis with stable performance was demonstrated for 1,000 h at 95°C and for 500 h at 95°C and 1,000 psi in advanced PEM electrolysis membranes. (Giner, Inc.)
- Three different types of low PGM loaded (<0.5 mg/cm^2) anode catalysts were developed that have comparable performance to Giner's standard anode (4 mg PGM/cm^2). (Giner, Inc.)
- A manufacturable ultra-low PGM loaded cathode was developed with greater than 500 h durability. Core shell catalysts were demonstrated to have activity advantages by enabling lower loadings at equivalent performance. (Proton OnSite)

PEC Hydrogen Production

The main focus of projects in this area was on using state-of-the-art theory, synthesis, and characterization tools to develop viable PEC material systems and prototypes with improved efficiency and durability. Technical progress included the following.

- Greater than 460 hours of stabilized device operations were demonstrated for III-V semiconductor PEC tandem devices using an NREL-developed ion bombardment surface passivation process (patent pending). This result represents an important step forward toward demonstration of stabilized solar-to-hydrogen conversion efficiencies >20% using PEC devices. (NREL)
- Photoactive $CuInGaS_2$ with controlled composition and tunable bandgap in the 1.5–2.4 eV range was successfully fabricated. Initial demonstration of chalcopyrite surface protection with MoS_2 was also demonstrated. (University of Hawaii)

Thermochemical Bio-Feedstock Conversion Production

The technical focus of projects in this area was on using thermochemical methods to produce hydrogen from biomass-derived feedstocks. Technical progress included the following.

- Cell performances with >30% increase in hydrogen production and >20% increase in hydrogen purity were achieved through implementation of an electrolysis step (compared to the base process without the electrolysis step). (FuelCell Energy, Inc.)
- Two promising carbon dioxide (CO_2) sorbents were identified for respective low-temperature and high-temperature sorption, and two promising low-temperature reforming catalysts were identified through modeling and bio-oil reforming tests. (Pacific Northwest National Laboratory)

Biological Hydrogen Production

The broad focus of the projects in the biological hydrogen production portfolio was to address key barriers such as oxygen sensitivity and feedstock utilization using molecular biology and genetic engineering techniques along with improved systems engineering. Technical progress included the following.

- Hydrogen production at an average rate of 757 mL H_2/L/d from de-acetylated and mechanically refined feedstock was demonstrated. (NREL)
- Roles of the two different sets of hydrogenase maturation genes, *hyp1* and *hyp2*, were confirmed. Also, a *Synechocystis* strain expressing the non-native CBS hydrogenase and maturation proteins was developed. (NREL)

Solar Thermochemical Hydrogen (STCH) Production

Efforts in these projects were directed toward performance characterization of water splitting by novel, non-volatile metal-oxide-based reaction materials and development of new reactor concepts to optimize efficiency of the reaction cycles. Technical progress included the following.

- A prototype 3 kW cascading pressure reactor/receiver was designed, and the approach to material discovery and engineering of thermochemical properties was extended such that greater than 50 new compounds have been developed. (Sandia National Laboratories)
- A solar hybrid sulphur process was designed that uses a bayonet acid decomposer and thermal energy storage, including an Aspen Plus® flowsheet and performance evaluation. (Savannah River National Laboratory)
- A flowing particle reactor design was completed, including Aspen Plus® process modeling. More than 2 g of hercynite active material was synthesized by spray drying. This material was characterized for composition, particle size, and surface area. (CU Boulder)
- 1,045 possible binary perovskites were screened, of which 199 materials show potential for use in STCH. (CU Boulder)

BUDGET

The FY 2015 appropriation for the Hydrogen Production and Delivery sub-programs was $19.6 million. Funding was distributed approximately evenly between Production and Delivery, with Production allocated $9.8 million. This split reflects the priority to maintain a balanced R&D portfolio focused both on near- and longer-term technology options. The request for Production and Delivery in FY 2016 is $23.6 million, with $12 million slated for Production. The estimated budget breakdown for Production funding in FY 2015 and FY 2016 is shown in Figure 2.

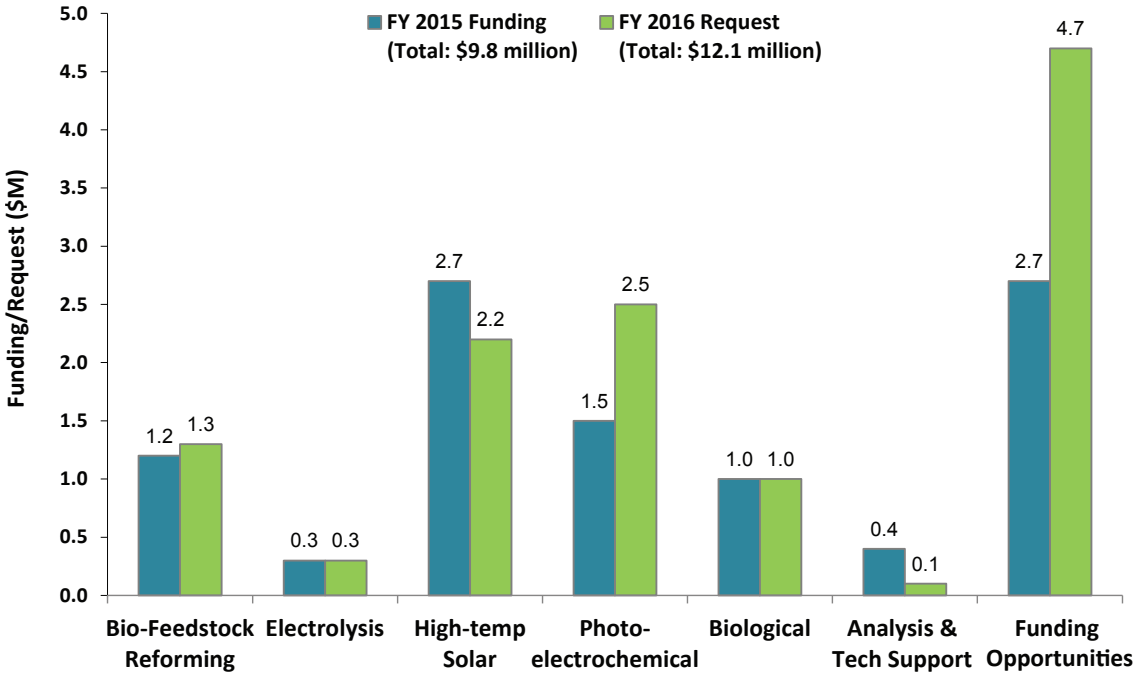

FIGURE 2. Hydrogen Production R&D Funding. Subject to appropriations, project go/no-go decisions, and competitive selections. Exact amounts will be determined based on research and development progress in each area and the relative merit and applicability of projects competitively selected through planned funding opportunity announcements.

With the near-term emphasis on forecourt stations and infrastructure in the Delivery portfolio, and with natural gas reforming a viable option for supplying near-term hydrogen demands, the Production R&D portfolio has increasingly focused on mid- to longer-term, renewable pathways such as advanced conversion of bio-derived feedstocks, advanced water-splitting, direct water-splitting through PEC, and solar-thermochemical processes. The R&D emphasis on a balanced portfolio of long-term and nearer-term renewable technologies is expected to continue into FY 2016. Projects selected in a FY 2014 FOA in areas of bio-derived feedstock conversion and photoelectrochemical and solar thermochemical water splitting will continue, supplemented by the four joint NSF/FCTO projects in solar water splitting and the five new Incubator projects. In addition, a new laboratory consortium on renewable hydrogen production will be initiated on advanced water-splitting technologies, including enhancement of core capabilities in materials-device and system-level development for advancing technology readiness level (TRL) in technologies including photoelectrochemical and solar-thermochemical water splitting.

FY 2016 PLANS

General Hydrogen Production program plans for FY 2016 include the following.

- Continue to demonstrate substantial progress in the six Production projects selected in the FY 2014 FOA; demonstrate initial progress in the five new projects selected under the 2015 Incubator FOA and in the four advanced water-splitting projects selected under the FY 2014 NSF/FCTO joint solicitation.
- Continue emphasis on materials durability, production efficiency, and process optimization for all pathways, and develop and refine materials characterization protocols and performance metrics for early development technologies.
- Assess the sustainability of incumbent hydrogen production technologies (e.g., steam methane reforming and carbon sequestration), as well as renewable alternatives. Baselines will be developed through collaboration with industry and reviews of existing literature, including H2A case studies and life-cycle analyses.
- Continue collaboration with the NSF and BES and Advanced Research Projects Agency-Energy.

- Initiate the new laboratory consortium on advanced water-splitting technologies, including enhancement of core capabilities in materials-device and system-level development for advancing TRL in technologies including PEC and solar-thermochemical water splitting.

Important pathway-specific milestones planned for FY 2016 in the Hydrogen Production sub-program projects include the following.

- Demonstrate >500 hours of hydrogen production from bio-derived liquids with in situ CO_2 capture and >90% pure H_2.
- Design a megawatt-scale STCH production plant for 100,000 kg/d, and show, through modeled performance analysis, the capability to meet the $2/kg cost target.
- Develop photovoltaic-grade wide band gap thin film absorbers with photoelectrochemical solar photocurrent densities ≥13 mA/cm^2 to enable 16% solar-to-hydrogen conversion efficiency.

Eric Miller
Hydrogen Production and Delivery Program Manager
Fuel Cell Technologies Office
Office of Energy Efficiency and Renewable Energy
U.S. Department of Energy
1000 Independence Ave., SW
Washington, D.C. 20585-0121
Phone: (202) 287-5829
Email: Eric.Miller@ee.doe.gov

II.A.1 Hydrogen Pathways Analysis for Solid Oxide Fuel Cell (SOFC) and Dark Fermentation

Brian D. James (Primary Contact),
Daniel A. DeSantis, Jennie M. Moton,
Cassidy Houchins
Strategic Analysis, Inc.
4075 Wilson Blvd., Suite 200
Arlington, VA 22203
Phone: (703) 778-7114
Email: bjames@sainc.com

DOE Manager
Eric Miller
Phone: (202) 287-5829
Email: Eric.Miller@ee.doe.gov

Contract Number: DE-EE0006231

Project Start Date: March 15, 2013
Project End Date: March 14, 2016

Overall Objectives

The objectives of this project are to:

- Analyze hydrogen production and delivery (P&D) pathways to determine the most economical, environmentally benign and societally feasible paths for the P&D of hydrogen fuel for fuel cell electric vehicles (FCEVs).
- Identify key technical and economic barriers to the success of these pathways, primary cost drivers, and remaining R&D challenges.
- Assess technical progress, benefits and limitations, levelized hydrogen costs, and potential to meet U.S. DOE P&D cost goals of <$4 per gasoline gallon equivalent (gge) (dispensed, untaxed) by 2020.
- Provide analyses that assist DOE in setting research priorities.
- Apply the Hydrogen Analysis (H2A) production model as the primary analysis tool for projection of levelized hydrogen costs (U.S. dollars per kilogram of hydrogen [$/kg H_2]) and cost sensitivities.

Fiscal Year (FY) 2015 Objectives

In 2014–2015, these overall project objectives were applied to:

- Develop hydrogen pathway case studies for hydrogen generation via:
  - Dark fermentation of bio-feedstocks.
  - High temperature electrolysis using solid oxide electrolysis cells (SOEC).
- Select additional hydrogen pathways, gather information on those hydrogen pathways, and define those hydrogen pathways for future case study development.

Technical Barriers

This project addresses the following technical barriers from the Hydrogen Production section of the Fuel Cell Technologies Office Multi-Year Research, Development, and Demonstration Plan:

Hydrogen Generation by Water Electrolysis

(F) Capital Cost

(G) System Efficiency and Electricity Cost

(K) Manufacturing

Fermentative Hydrogen Production

(AX) Hydrogen Molar Yield

(AY) Feedstock Costs

(AZ) Systems Engineering

Technical Target

This project conducts cost modeling to attain realistic cost estimates for the production and delivery of hydrogen fuel for FCEVs. These values can help inform future technical targets.

- U.S. DOE P&D cost goals <$4/gge of H_2 (dispensed, untaxed) by 2020

FY 2015 Accomplishments

- Completed hydrogen pathway cases to determine the projected cost of hydrogen generated via high temperature SOEC.
  - Solicited and analyzed data from industry and research organizations on likely current and future SOEC technology and plant configurations.
  - Developed SOEC case studies representing current and future cases of a central plant producing 50,000 kg H_2/day. Case studies prepared using H2A Production Model (Version 3.1).
  - Validated the case studies through performance modeling, vetting with industry, and written supporting documentation. Made H2A cases

and documentation publicly available at http://www.hydrogen.energy.gov/h2a_prod_studies.html.

– Projected hydrogen cost via SOEC:
  - Current case: \$4.21/kg H_2 (\$3.21 to \$5.06/kg H_2 with 90% confidence)
  - Future case: \$3.68/kg H_2 (\$2.76 to \$4.57/kg H_2 with 90% confidence)

– Quantitatively demonstrated that the three main cost drivers for the levelized hydrogen cost from SOEC are (1) electricity price, (2) electrolyzer capital cost, and (3) heat price.

- Completed hydrogen pathway cases to determine the projected cost of hydrogen generated via dark fermentation of biomass.
  – Completed literature review for dark fermentation of corn stover for hydrogen production. Data was drawn heavily from past related reports [1,2] design and capital cost data.
  – Work closely with National Renewable Energy Laboratory (NREL) researchers to analyze and project fermentation performance and reaction kinetics.
  – Developed fermentation case studies representing current and future cases of a central plant producing 50,000 kg H_2/day. Case studies prepared using H2A Production Model (Version 3.1).
  – Validated the case studies through performance modeling, heat and energy balances, analysis of potential byproduct sales, and written supporting documentation. Made H2A cases and documentation publicly available at http://www.hydrogen.energy.gov/h2a_prod_studies.html.
  – Projected hydrogen cost via fermentation:
    - Current case: ~\$578/kg H_2 (due to non-economical fermentation broth concentration)
    - Future case: \$3.78 to \$5.47/kg H_2
  – Quantitatively demonstrated that the three main cost drivers for the levelized hydrogen cost from fermentation are (1) fermentation broth concentration, (2) feedstock cost, and (3) capital cost.
- Initiated case studies for the monolithic piston reactor and molten carbonate electrolysis reformer pathways.

✧ ✧ ✧ ✧ ✧

INTRODUCTION

This report reflects work conducted in the second year of a three year project to analyze innovative hydrogen production and delivery pathways and their potential to meet the U.S. DOE hydrogen P&D cost goal of <\$4/gge by 2020. Work in the first year of the project concentrated on hydrogen production from proton exchange membrane electrolysis. Work in the second year has focused on SOEC technology and dark fermentation. The analysis methodology utilizes DOE's H2A Distributed and Central Hydrogen Production models [3]. Those models provide a transparent modeling framework and apply standard mass, energy, and economic analysis methods agreed upon by DOE's Hydrogen and Fuel Cell technology teams.

APPROACH

The following steps summarize the analysis methodology applied to each of the hydrogen production pathways examined in the project.

- Conduct literature review
- Develop, circulate, and analyze results from an industry survey covering the targeted technology
- Define generalized cases for systems of different sizes and technology readiness levels
- Run H2A models with general case input data to calculate the levelized cost of hydrogen (\$/kg H_2)
- Perform sensitivity analyses (including tornado and waterfall charts) to identify key cost drivers
- Document case study results
- Vet case study results with DOE, industry, and team partners
- Repeat these steps until agreement attained among project partners

Specific Approach to SOEC Analysis

A questionnaire spreadsheet was circulated to six research and industrial groups to gather data on SOEC performance and cost. Collected data included H2A model input parameters necessary for developing cases and covered engineering system definition, stack and balance of plant (BOP) capital costs, and other economic parameters. The data was analyzed and used to synthesize generalized cases reflecting realistic parameters and a representative production scenario while protecting proprietary technical information.

Two public generalized cases were developed:

- Current Central
- Future Central

Both cases are based on "Central" production at 50,000 kg H_2/day. Two technology development time horizons are considered: "Current" representing a Year 2015 technology and "Future" representing a Year 2025 technology. Current Central cases assume a short-term technology readiness projection from technology that has been demonstrated already in the lab. Future Central cases assume an advanced development of the technology via better materials, capabilities, efficiencies, lifetimes, and/or costs. Both Current and Future cases are based on projected system capital costs for mature, developed markets (i.e., not one-of-a-kind plant pricing).

The SOEC cases are based on high temperature (800°C) SOECs splitting steam into H_2 and O_2. The H_2 is separated from the steam and captured for transport. The O_2 is vented (and thus is not assumed to generate any byproduct sales revenue). The stacks operate near the thermo-dynamic neutral point: 1.34 volts/cell for the Current case and 1.28 volts/cell for the Future case. Heat is added to the system to maintain the 800°C reactants stack entry temperature. Heat price is based on burning of natural gas but the analysis is meant to be heat agnostic, i.e., the results are not tightly tied to the source of heat. Primary differences between the Current and Future cases are: slightly lower electrical usage, higher pressure operation allowing electrical generation from exhaust gases, and a higher current density. Further details of the two cases appear in Table 1.

Data from the two generalized cases were used to populate the H2A Model (Version 3.1) and to generate estimates of the levelized hydrogen cost. The electrolyzer

TABLE 1. SOEC Input Parameters

Parameter	Current Central	Future Central	Cost Basis
Plant Capacity (kg/day)	50,000	50,000	H2A
Total Uninstalled Capital (2012$/kW)	$820	$430	Ind. Questionnaire
Stack Capital Cost (2012$/kW)	$287	$99	Ind. Questionnaire
Balance of Plant (BOP) Capital Cost (2012$/kW)	$533	$331	Ind. Questionnaire
Total Energy Usage (kWh/kg)	50.9	46.6	Ind. Questionnaire
Stack Voltage (V)	1.34	1.28	Ind. Questionnaire
Current Density[1] (mA/cm^2)	1000	1500	Ind. Questionnaire
Net System Energy Efficiency[2]	66%	72%	Ind. Questionnaire
Stack Electrical Usage (kWh/kg)	33.49	34.05	Ind. Questionnaire
System Electrical Usage (kWh/kg) (% LHV H_2)	36.8 91%	35.1 95%	Ind. Questionnaire
System Heat Usage (kWh/kg)	14.1	11.5	Ind. Questionnaire
Electrolyzer Power Consumption (MW)	76.6	73.1	Eng. Calculation
Average Electricity Price over Life of Plant[3] (2007¢/kWh)	6.24	6.89	AEO/Eng. Calc.
Electricity Price in Startup Year (H2A Default Values)[4] (2007¢/kWh)	5.74	6.59	AEO/Eng. Calc.
Thermal Energy Cost (2007$/GJ)[5] (2007¢/kWh)	10.1 3.64	11.5 4.13	AEO/Eng. Calc.
Hydrogen Outlet Pressure (MPa)	2.1 (300 psi)	4.8 (700 psi)	Ind. Questionnaire
Installation Cost (% of uninstalled capital cost)	12%	10%	H2A
Replacement Interval (years) [Stack/BOP]	4/10	7/12	Ind. Questionnaire
Replacement Cost of Major Components (% of installed capital cost)	15%	12%	Ind. Questionnaire

[1]Current density is not used directly within the H2A analysis but is included here as a representative value to allow comparison between the Current and Future cases.
[2]Efficiency is defined as H_2 product output energy/input electrical and heat energy. H_2 product energy is based on the lower heating value (LHV) of H_2.
[3]Average electricity price over life of plant (40 years for Central cases).
[4]H2A Default Values from Energy Information Administration (EIA) Annual Energy Outlook (AEO) data.
[5]The thermal energy cost is based on the average EIA's AEO 2009 reference case costs for natural gas over the plant life, a combustion efficiency of 85.7%, and burner capital costs over the plant lifetime of ~$0.01/GJ.

companies vetted the generalized cases, H2A model results, sensitivity limit parameters and results, and resulting documentation.

Specific Approach to Fermentation Analysis

A questionnaire spreadsheet was circulated to various research and industrial groups to gather data on dark fermentation performance and cost. Unfortunately, industry response was limited and the academic group responses reflected both the low technology maturity of the systems as well as diversity of feedstock and organism approach. Consequently, it was decided to focus on dark fermentation of corn stover based primarily on the approach and experimental results from researchers at the NREL. NREL data sources were used to develop detailed mass and energy balance which provided input parameters for H2A analysis.

Two public generalized cases were developed:

- Current Central
- Future Central

Data from the two generalized cases were used to populate the H2A Model (Version 3.1) and to generate estimates of the levelized hydrogen cost. The fermentation questionnaire respondents vetted the generalized cases, H2A model results, sensitivity limit parameters and results, and resulting documentation.

The fermentation cases are based on a corn stover feedstock, hemicellulous pre-treatment, fermentation reaction using a *Clostridium thermocellum* consortium, pressure-swing adsorption for hydrogen gas purification, and waste water treatment of the liquid effluent. Data for the *C. thermocellum* bacteria was provided by NREL. The fermentation capacity for the Current case is taken from existing NREL lab results. The Future case data is extrapolated from similar NREL data and has a higher fermentation capacity (producing more hydrogen for each molecule of sugar) than the Current case. Undigested solids (primarily lignin) are combusted to generate process heat. Biogas (methane) generated in the waste water treatment facility is combusted for process heat in the Current case or is fed to a turbine generator to produce electricity for byproduct sale in the Future case.

The primary differences between the Current and Future cases are (1) higher feedstock-to-hydrogen conversion, (2) higher fermentation broth concentration, and (3) generation of byproduct electricity. Further details of the two cases appear in Figure 1.

RESULTS

All cases studied demonstrate a production price between approximately \$3/kg H_2 to \$5/kg H_2 with the exception of the fermentation Current case, which has a cost of approximately \$577/kg H_2. Figure 2 details the cost breakdown of both SOEC cases and the fermentation Future case. From Figure 2, the SOEC cost drivers are seen to be variable costs such as electrical price and thermal energy price or the fixed installed capital cost. In Figure 3, these cost drivers are further identified to be electricity price, thermal energy price, and the capital cost. The electricity price averages 6.8¢/kWh and 6.97¢/kWh for the Current and Future cases, respectively. Results of a Monte Carlo analysis for the SOEC technology indicate a probable H_2 cost range of \$3.21/kg H_2 to \$5.02/kg H_2 for the Current case and \$2.76/kg H_2 to \$4.57/kg H_2 for the Future case. These ranges represent 90% confidence, i.e., the middle 90% of possible outcomes.

Costs for the fermentation cases are \$578/kg H_2 and \$4.62/kg H_2 for the Current and Future cases, respectively. The Current case cost is extremely high due to the fermentation reaction being carried out with a low concentration (5 g/L) fermentation broth, a concentration level more appropriate for lab scale research than commercial operation. The Future case, modeled with a fermentation broth concentration of 300 g/L (60 times greater than the Current case fermentation broth concentration), yields a more competitive H_2 cost of \$4.62/kg H_2. As shown in Figure 2, this cost is dependent on a byproduct credit received from converting excess lignin and biogas to thermal energy which is then converted to electrical energy and selling it back to the grid at industrial rates. Figure 4 identifies the primary cost drivers of the fermentation case as feed stock cost, capital cost, and broth concentration. In reality, broth concentration is a vital factor and is not the top parameter in Figure 4, only because it is bound between 100 g/L and 400 g/L. As the broth concentration decreases, it affects the cost of hydrogen production significantly more than any other cost driver. Molar yield is also a critical parameter but is not identified specifically as it is incorporated in several of the other parameters due to its use in the mass balance. Due to the extremely wide range of the various input parameters, as well as overlapping influences of the parameters on the cost model, a Monte Carlo analysis was not conducted as it would yield a final hydrogen cost range so wide that it would hold little meaning.

CONCLUSIONS AND FUTURE DIRECTIONS

In its second year, this project made key observations and important achievements.

- Representative pathway analysis cases were completed for hydrogen generation from SOEC and fermentation using the H2A Production Model (Version 3.1).
- Large capital cost reductions are predicted between Current and Future systems for both pathways.

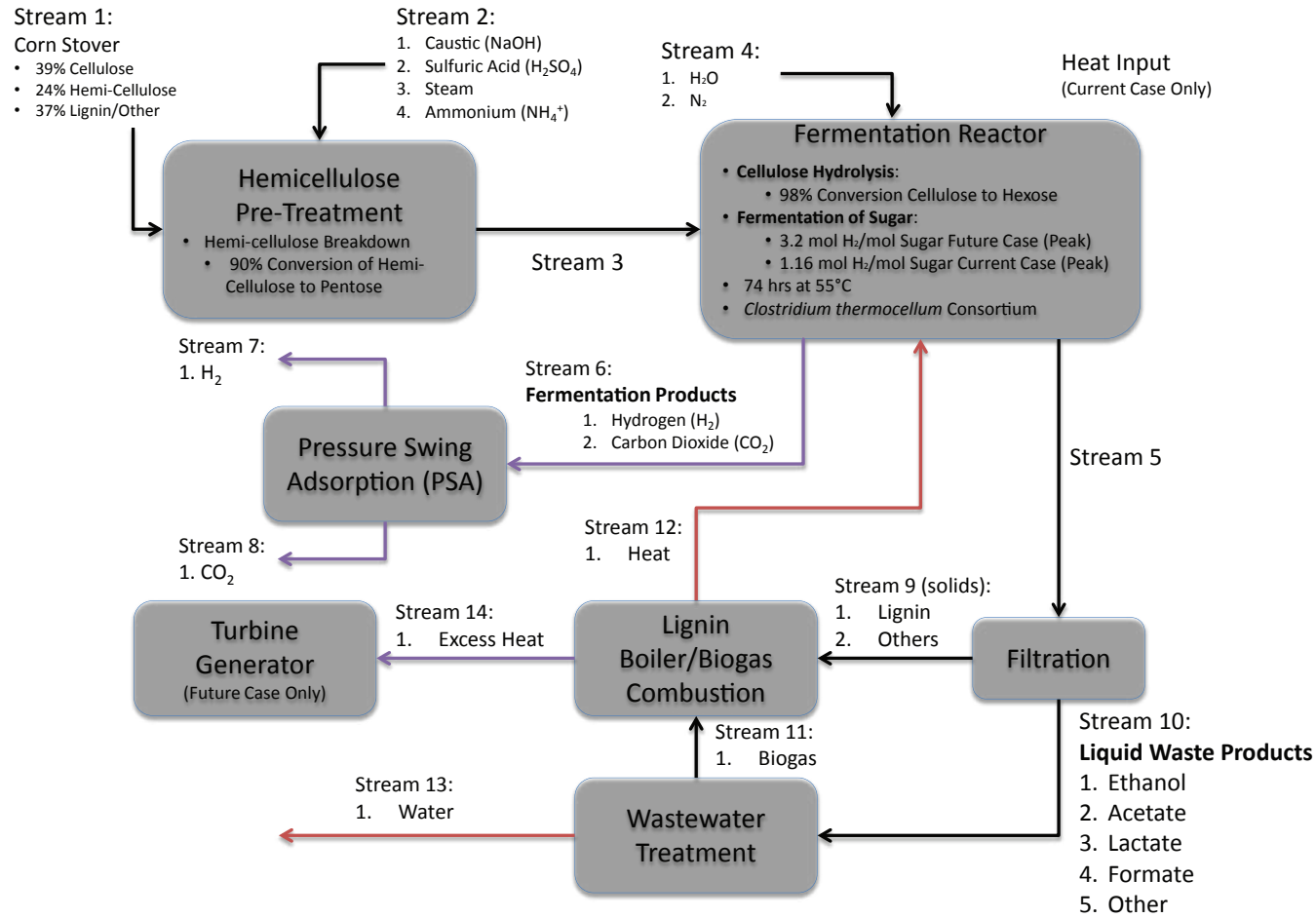

FIGURE 1. Dark fermentation process flow diagram

- Predicted SOEC hydrogen production costs are ~\$4.21/kg H_2 (Current case) and \$3.68/kg H_2 (Future case).
- Predicted fermentation hydrogen production costs are ~\$578/kg H_2 (Current case) and \$4.62 /kg H_2 (Future case). The Current cost is elevated due to use of a low concentration fermentation broth density.
- Further research is needed to demonstrate systems in which high molar yields (approaching 3.2 mol H_2/mol hexose) are possible with high broth concentrations (~300 g/L).

FY 2015 PUBLICATIONS/PRESENTATIONS

Presentations

1. James, B.D. DeSantis, D.A. Moton, J.M "*H_2 Pathways Project Update to DOE,"* Delivered remotely from Arlington, VA, 2015/02/27.

2. James, B.D., Moton, J.M, DeSantis, D.A., Houchins, C., "*Benchmarking Transformational Energy Technologies,"* Chicago, IL, 2015/5/28

3. James, B.D., DeSantis, D.A., Moton, J.M., "*Analysis of Advanced H_2 Production Pathways,"* 2015 DOE Hydrogen and Fuel Cells Program and Vehicle Technologies Office Annual Merit Review and Peer Evaluation Meeting, Arlington, VA, 2015/6/10.

4. Colella, W.G., James, B.D., Saur, G., "*Technical and Economic Performance of Next Generation Solid Oxide Electrolysis Cell (SOEC) Systems for Hydrogen Production,"* Hydrogen Production Technical Team Meeting, 1/6/2015.

REFERENCES

1. James, B.D., Baum, G.N., Perez, J., and Baum, K.N. *Technoeconomic Boundary Analysis of Biological Pathways to Hydrogen Production. Production* (2009). at http://www1.eere.energy.gov/hydrogenandfuelcells/pdfs/46674.pdf.

2. Davis, R. *et al. Process Design and Economics for the Conversion of Lignocellulosic Biomass to Hydrocarbons: Dilute-Acid and Enzymatic Deconstruction of Biomass to Sugars and Biological Conversion of Sugars to Hydrocarbons Process Design and Economics for the Conversion*. (2013). doi:10.2172/1107470.

3. "DOE H2A Analysis," at http://www.hydrogen.energy.gov/h2a_analysis.html.

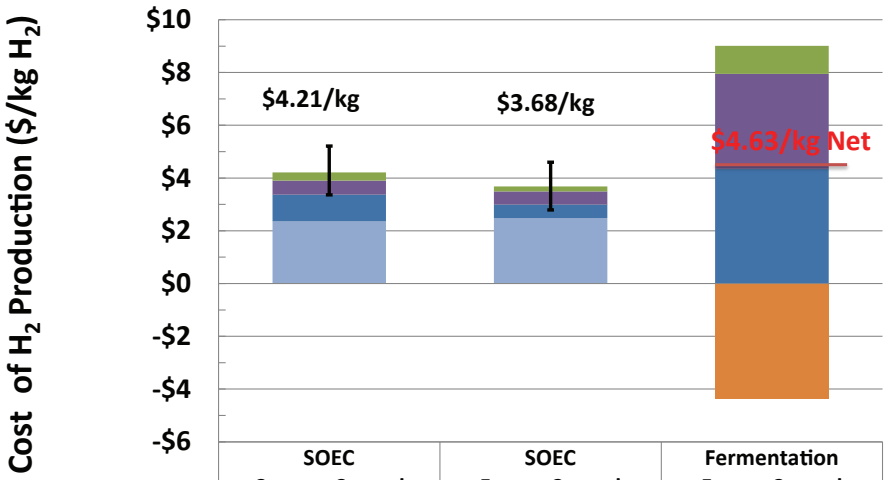

	SOEC Current Central	SOEC Future Central	Fermentation Future Central
Byproduct Cost	$0.00	$0.00	-$4.38
Other Raw Material Cost	$0.00	$0.00	$0.00
Fixed O&M	$0.31	$0.19	$1.06
Feedstock Cost	$0.53	$0.49	$3.60
Decommissioning Cost	$0.00	$0.00	$0.01
Installed Capital Cost	$1.02	$0.52	$4.34
Other Variable Cost	$2.36	$2.48	$0.00

FIGURE 2. Cost breakdown of analyzed systems

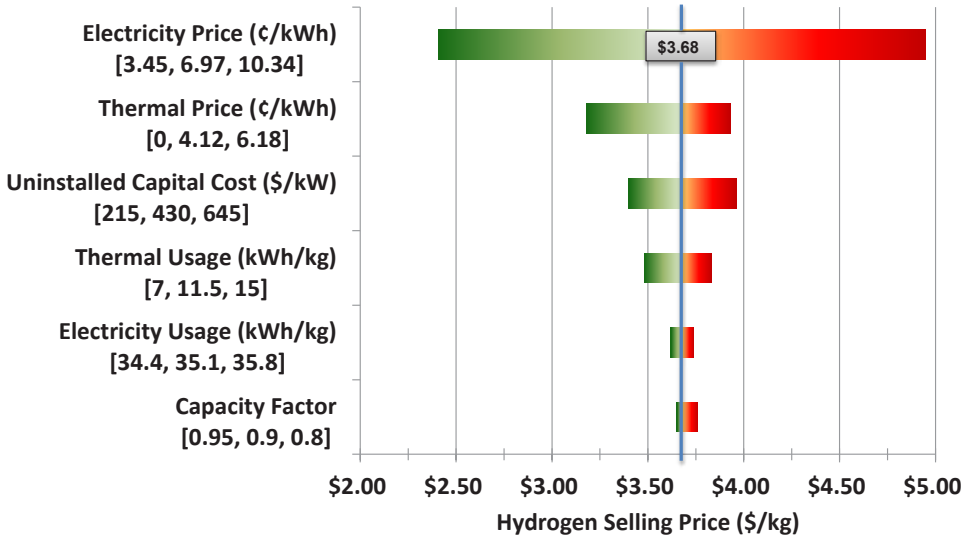

FIGURE 3. Tornado chart for SOEC future case sensitivity study

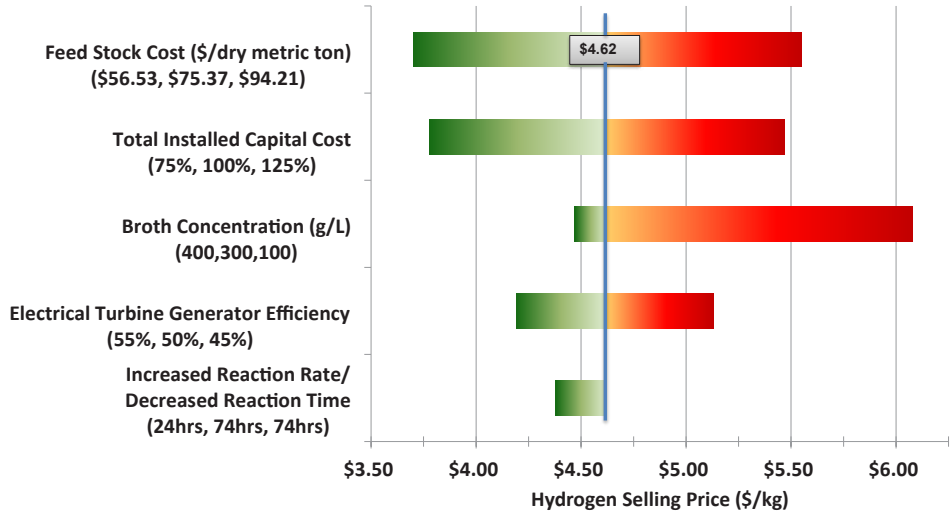

FIGURE 4. Tornado chart for fermentation future case sensitivity study

II.B.1 Renewable Electrolysis Integrated Systems Development and Testing

Mike Peters (Primary Contact), Kevin Harrison, Huyen Dinh
National Renewable Energy Laboratory (NREL)
15013 Denver West Parkway
Golden, CO 80401-3305
Phone: (303) 524-0864
Email: Michael.Peters@nrel.gov

DOE Manager
David Peterson
Phone: (720) 356-1747
Email: David.Peterson@ee.doe.gov

Subcontractor
Spectrum Automation Controls, Arvada, CO

Project Start Date: October 1, 2003
Project End Date: Project continuation and direction determined annually by DOE

Overall Objectives

- Collaborate with industry to research, develop, and demonstrate improved integration opportunities for renewable electrolysis systems for energy storage, vehicle refueling, grid support, and industrial gas end uses
- Design, develop, and test advanced experimental and analytical methods to validate electrolyzer stack and system efficiency, including contributions of sub-system losses (e.g., power conversion, drying, electrochemical compression), of advanced electrolysis systems

Fiscal Year (FY) 2015 Objectives

- Compile detailed information on multiple hydrogen drying techniques used in electrolyzers
- Test NREL's variable flow drying technique on large active area polymer electrolyte membrane (PEM) stacks provided to NREL as part of the Integrated Network Testbed for Energy Grid Research and Technology Experimentation (INTEGRATE) project
  - Drying apparatus will be procured through INTEGRATE with instrumentation and data collection/analysis happening as part of the Integrated Systems Development and Testing FY 2015 funding
- Continue long-duration testing on the three 10-kW PEM stacks from Proton OnSite, comparing decay rates of variable operation versus constant powered operation

Technical Barriers

This project addresses the following technical barriers from the Fuel Cell Technologies Office 2012 Multi-Year Research, Development, and Demonstration (MYRDD) Plan, Section 3.1.5:

(G) System Efficiency and Electricity Cost

(J) Renewable Electricity Generation Integration (for central production)

(M) Control and Safety

Technical Targets

This project is conducting applied research, development, and demonstration (RD&D) to reduce the cost of hydrogen production via renewable electrolysis for both distributed and central production pathways to help meet the following DOE hydrogen production and delivery targets found in the MYRDD plan (2011–2020).

Technical Targets: Central Water Electrolysis Using Green Electricity (Table 3.1.5)

- Stack efficiency:
  - 44 kWh/kg H_2 (76% lower heating value [LHV]) by 2015
  - 43 kWh/kg H_2 (78% LHV) by 2020
- System efficiency:
  - 46 kWh/kg H_2 (73% LHV) by 2015
  - 44.7 kWh/kg H_2 (75% LHV) by 2020
- By 2015 reduce the cost of central production of hydrogen from water electrolysis using renewable power to \$3.00/gge at plant gate; by 2020, reduce the cost of central production of hydrogen from water electrolysis using renewable power to ≤\$2.00/gge at plant gate

FY 2015 Accomplishments

- The project team designed, instrumented, and commissioned a pressure swing adsorption drying system capable of drying hydrogen to the SAE J2719 fueling standard. The dryer is capable of handling hydrogen flow rates up to 135 kg/day and pressures up to 1,000 psig.
  - NREL modified the hydrogen dryer by adding two linear actuated valves to optimize hydrogen drying losses under variable stack power operation.
- By the end of FY 2015, we will finalize a report on NREL's variable flow drying technique by finishing data

collection and analysis of variance (ANOVA) on data collected.

- The Energy Systems Integration Facility electrolyzer stack test bed was commissioned through the INTEGRATE project, expanding NREL's capabilities to perform large active area stack and balance of plant testing.
  - The electrolyzer stack test bed provides a test platform that the Renewable Electrolysis Integrated Systems Development and Testing project will be able to use for years to come to test PEM electrolyzer stacks (up to 500 kW) under variable or renewable power operation.

✧ ✧ ✧ ✧ ✧

INTRODUCTION

The capital cost of commercially available water electrolyzer systems, along with the high cost of electricity in many regions, limits widespread adoption of electrolysis technology to deliver low cost hydrogen production. PEM electrolyzer manufacturers are working to scale up into the megawatt range to increase system energy efficiency and reduce capital cost. Along with capital cost reductions and efficiency improvements, both alkaline and PEM technologies are developing utility-scale electrolyzers capable of advanced grid integration functionality and better integration with renewable electricity sources. An integrated system with advanced sensing and communications will enable grid operators to take advantage of the controllable nature of distributed and central water electrolysis systems to maintain grid stability. Electrolytic production of hydrogen, where fossil fuels are the primary electricity source, will not lead to significant carbon emission reduction without carbon sequestration technologies.

Renewable electrolysis is inherently distributed, but large-scale wind and solar installations are being planned to take advantage of economies of scale and achieve system-level energy efficiencies less than 50 kWh/kg. Renewable electricity sources, such as wind and solar, can be closely—and in some cases directly—coupled to the hydrogen-producing stacks of electrolyzers to reduce the energy conversion losses and capital cost investment of this near zero carbon pathway.

APPROACH

Results and insights gained from this RD&D project aim to benefit the hydrogen-based industry and relevant stakeholders as the market for this equipment expands. Results from the project have demonstrated opportunities to improve efficiency and capital cost of an integrated renewable-coupled electrolysis system.

The Xcel Energy/NREL Wind-to-Hydrogen and Energy Systems Integration Laboratory RD&D project is helping to advance the integration of renewable electricity sources with state-of-the-art electrolyzer technology. Real-world data from 24/7 daily operation are demonstrating opportunities for improved system design and novel hardware configurations to advance the adoption of this technology. Lessons learned and data-driven results provide feedback to industry and to the analytical components of this project. Finally, this project provides independent testing and verification of the technical readiness of advanced electrolyzer systems by operating them from the grid and renewable electricity sources.

RESULTS

Variable Flow Drying Technique

The main focus for this project in FY 2015 was looking into system efficiency improvements of hydrogen dryers under a variable or renewable profile. NREL's variable flow drying approach aims to reduce hydrogen drying losses through electrolysis to an equal percentage of stack flow. The testing compares the variable flow drying technique versus the standard orifice operation under variable and renewable profiles. In FY 2015, NREL tested two types of photovoltaic profiles, a wind profile, and two different regulation profiles. An ANOVA will be used to compare the two techniques using dew point sensors to track hydrogen quality. The variable flow approach will aim to keep drying losses at 3.5% of stack flow. Commercially available electrolyzer systems have typical hydrogen losses in the 5–10% range; this project aims to reduce those down to 3.5%. An annual milestone report summarizing key findings from the drying testing and results of the ANOVA will be published at the end of FY 2015. Figure 1 shows the hydrogen drying system, and Figure 2 shows four of the five profiles used in variable mode.

The most common form of hydrogen dryer used in today's electrolyzers is a pressure swing adsorption (PSA) dryer. The goal of the dryer is to dry the hydrogen to less than five parts per million by volume (ppmv) of H_2O in H_2. The 5 ppmv threshold is set by SAE J2719, which is the hydrogen fuel quality standard adopted for light-duty fuel cell vehicles.

A PSA drying system consists of a handful of control valves and two desiccant beds combined in parallel on the output of the H_2-H_2O separator and before the back pressure regulator. The saturated hydrogen comes out of the H_2 separator and travels through one of the desiccant tubes to dry the hydrogen. At the outlet of the active desiccant tube, some of the dry hydrogen is used to dry the inactive desiccant bed. The dry hydrogen is used as a sweeping gas to get the moisture off of the desiccant in the inactive bed. In a fixed flow system there is an orifice between the two desiccant beds that allows limited flow of hydrogen between

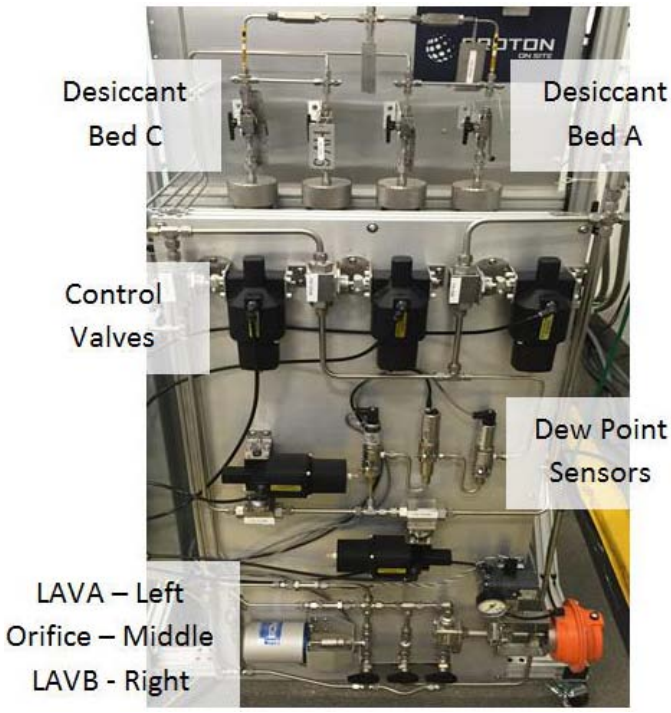

FIGURE 1. PSA dryer

the two. The flow of dry hydrogen through the inactive bed is a function of the orifice size and the back pressure regulator setting. The hydrogen used to dry the desiccant bed is not recoverable and is vented off to the atmosphere; this is what is considered the electrolyzer drying losses.

The fixed orifice drying system, employed in commercially available electrolyzer systems today, allows a constant flow of hydrogen to be lost through the orifice independent of how much hydrogen the stack is producing. This approach is not optimal in an electrolyzer system operating with variable stack power, because the percentage of hydrogen lost will increase as stack power drops below maximum operating power. During renewable operation of an electrolyzer the stack is operated below full power most of the time, which means the hydrogen flow rate is less than when it is operated at full power; however, the same amount of hydrogen will be lost through the fixed orifice during the drying process. With a fixed orifice dryer, if the flow decreases while still losing the same amount of hydrogen, there is a higher percentage of hydrogen lost to drying.

PEM Electrolyzer Long Duration Testing Update

NREL is conducting side-by-side testing and comparison of stack voltage decay rates between constant and variable power operation. Three 34-cell stacks (labeled A–C) for

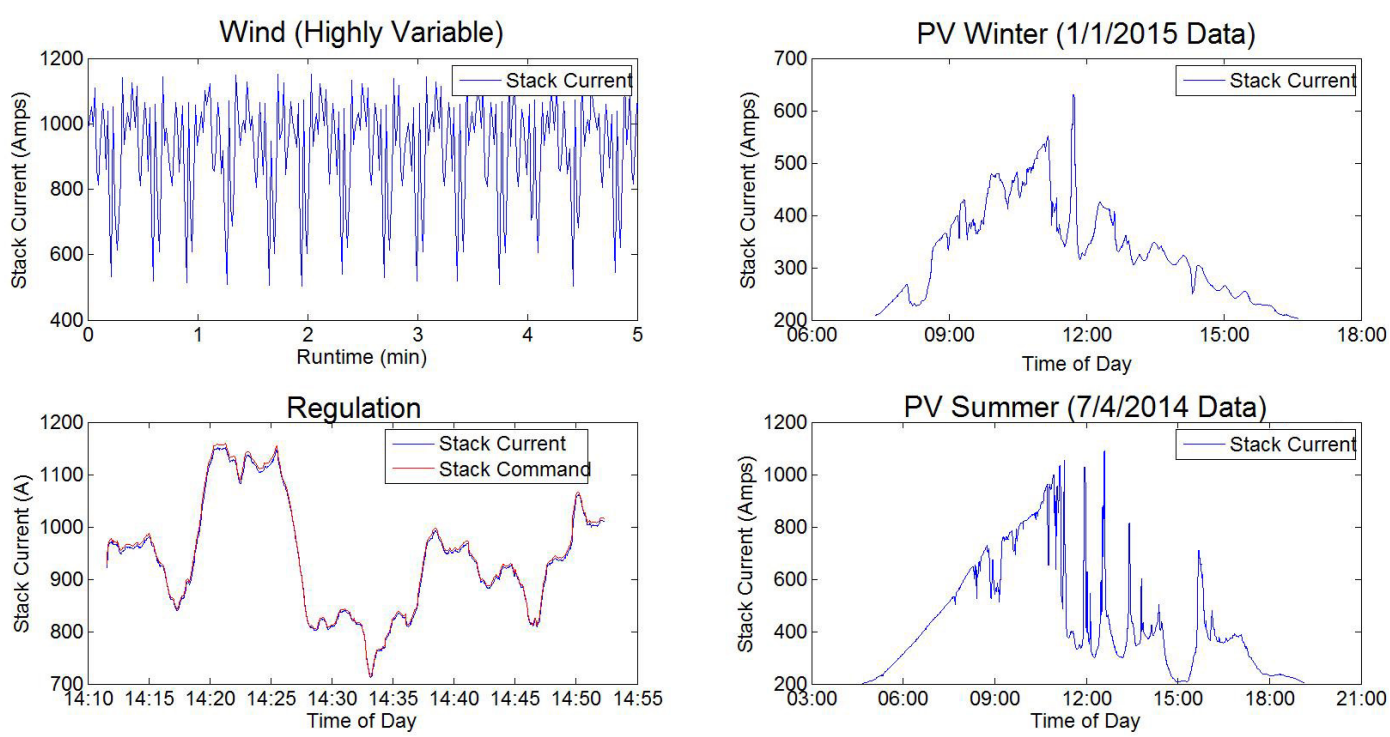

PV - photovoltaic

FIGURE 2. Variable and renewable stack profiles

the H-Series PEM electrolyzer from Proton OnSite were obtained in FY 2015. Two of the stacks (A and B) have 6,500 hours of operation to date and one of the stacks (Stack C) has 3,500 hours of operation. Stacks A and C are being operated in variable mode and Stack B is being operated in a constant power mode. Stack decay rates are being tracked and Table 1 shows a snapshot of decay rates that was reported at the 2015 DOE Annual Merit Review, at that time Stack C was only being operated in constant power mode. The table shows slightly higher decay rates than expected, with no significant difference observed between the two operating modes. In past testing Proton OnSite has stated that the decay rates should be better than 9 microvolts per cell-hour (μV/cell-h); however, the testing so far has indicated a slightly higher decay rate than expected.

TABLE 1. Snapshot of Stack Decay Rates

Operating Mode	Stack Identifier	Decay Rate (μV/cell-h)
Variable Power	Stack A	11.5
Constant Power	Stack B	12.6
Constant Power	Stack C	21.6

Long duration testing of the three stacks will continue through the end of FY 2015. When the goal of 7,500 hours is met, the stack decay rates at that time will be reported again.

Electrolyzer Stack Test Bed

The electrolyzer stack test bed located in the Energy Systems Integration Laboratory was designed, built, and commissioned in FY 2014/FY 2015. The test bed was funded under NREL's INTEGRATE task and was commissioned in September 2014 as a collaboration with Giner, Inc. The stack test bed features a modular design that allows testing of different PEM electrolyzer stacks (up to 500 kW) and electrolyzer balance of plant components. The test bed provides an essential platform for this project looking at both stack performance and system efficiency improvements under renewable operation as electrolyzer stacks scale up to the megawatt size.

In collaboration with Proton OnSite, NREL designed, instrumented, and commissioned a hydrogen drying system on the electrolyzer stack test bed. The hydrogen dryer is capable of handling flows up to 135 kg/day and pressures up to 1,000 psig. The dryer was procured from Proton OnSite using funds from INTEGRATE; this project funded activities such as adding control valves and dew point sensors, and programming the dryer operation. Figure 3 shows the electrolyzer test bed in the Energy Systems Integration Laboratory.

CONCLUSIONS AND FUTURE DIRECTIONS

- **Conclusion:** Testing of NREL's variable drying technique is on-going. Preliminary results indicate that 3.5% drying losses may be hard to maintain over long operation but the annual milestone report will finalize the data analysis.
- **Future direction:** We will submit an annual milestone report with an ANOVA comparing the two methods toward the end of FY 2015. Optimization of hydrogen drying will continue into FY 2016 using the electrically actuated linear actuated valve.
- **Conclusion:** Long duration constant versus variable power stack testing showed higher-than-expected stack

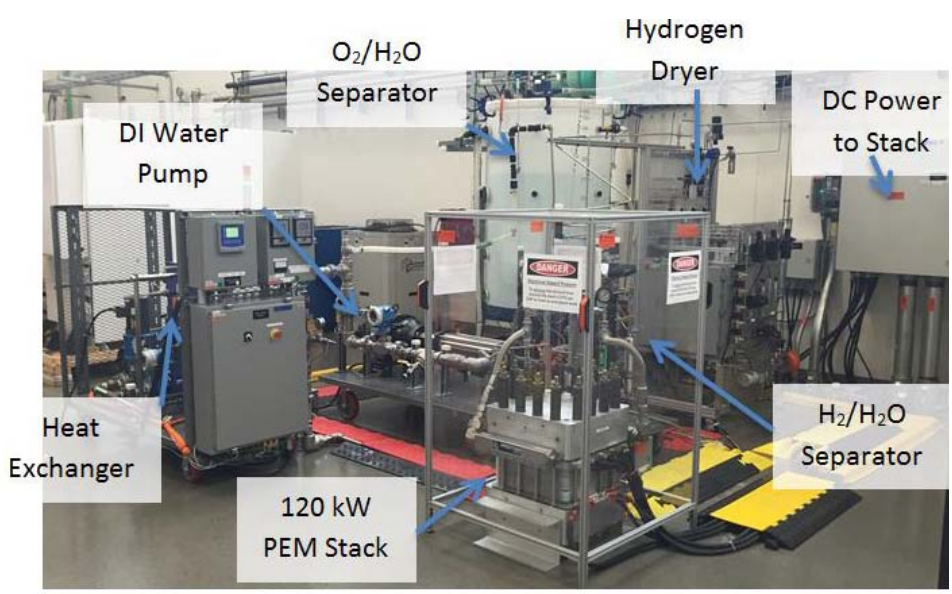

FIGURE 3. Electrolyzer stack test bed

decay rates, but no significant difference between the two methods was observed so far in the testing.

- **Future direction:** Stack testing up to 7,500 hours will continue through the end of FY 2015.
- **Conclusion:** Design, build, and commissioning of the Energy Systems Integration Laboratory electrolyzer stack test bed was completed as a collaboration with the INTEGRATE project.
- **Future direction:** The electrolyzer stack test bed will be used as a platform for renewable electrolysis testing for years to come.

FY 2015 PUBLICATIONS/PRESENTATIONS

1. Peters, Michael. "Renewable Hydrogen Production for Use in Hydrogen Fuel Cell Vehicles," Presentation at the ACT Expo, Dallas, TX, May 2015.

2. Peters, Michael, Kevin Harrison, and Danny Terlip. "Renewable Electrolysis Integrated System Development and Testing," Presentation at the DOE Hydrogen and Fuel Cells Program Annual Merit Review and Peer Evaluation Meeting, Arlington, VA, June 2015.

II.B.2 High-Performance, Long-Lifetime Catalysts for Proton Exchange Membrane Electrolysis

Hui Xu (Primary Contact), Brian Rasimick, and Michael Riera-Smith (Giner)
Bryan Pivovar, Shaun Alia, and K.C. Neyerlin (NREL)
Krzysztof Lewinski and Sean Luopa (3M Company)
Giner, Inc.
89 Rumford Ave.
Newton, MA 02466
Phone: (781) 529-0573
Email: hxu@ginerinc.com

DOE Manager
David Peterson
Phone: (720) 356-1747
Email: David.Peterson@ee.doe.gov

Subcontractors
- National Renewable National Laboratory (NREL), Golden, CO
- 3M Company, St. Paul, MN

Contract Number: DE-SC0007471

Project Start Date: April 22, 2013
Project End Date: April 21, 2015

Overall Objectives

- Develop various synthetic routes to make iridium (Ir) based oxygen evolution reaction (OER) catalysts with enhanced surface area, oxidation resistance, performance and durability
- Screen the OER catalyst powders via rotating disk electrode (RDE) to determine corrosion resistance and initial catalytic activity
- Physically characterize the catalysts with good RDE activity using microscopy and X-ray techniques to elucidate their structure and particle size distribution
- Evaluate the performance and the durability of membrane electrode assemblies (MEAs) (1,000 hours) in Giner's laboratory commercial proton exchange membrane (PEM) electrolyzers
- Determine the category of catalyst that is most efficient and economically feasible

Fiscal Year (FY) 2015 Objectives

- Further develop synthetic routes to make Ir-based OER catalysts to lower Ir loading or enhance PEM electrolysis efficiency
- Examine the performance of synthesized OER catalysts in operating PEM electrolyzers
- Test the durability of selected OER catalysts in 1,000-hour PEM electrolyzer operations
- Characterize structure changes of selected catalysts after durability tests to analyze their degradation mechanisms
- Evaluate the scalability and processablity of catalyst synthesis via short production runs of selected catalysts

Technical Barriers

This project addresses the following technical barriers of PEM water electrolysis from the Hydrogen Production section of the Fuel Cell Technologies Office Multi-Year Research, Development, and Demonstration Plan.

(F) Capital Cost

(G) System Efficiency and Electricity Cost

Technical Targets

The targets of this project are to develop high performance and long lifetime OER catalysts that may help meet the technical targets of DOE distributed forecourt water electrolysis as shown in Table 1. Included in this table is Giner's status as of 2013.

TABLE 1. Technical Targets: Distributed Forecourt Water Electrolysis [1]

Characteristics		Units	2015[1]	2020[1]	Giner Status (2013)
Hydrogen Levelized Cost[2]		$/kg-$H_2$	3.90	<2.30	3.64[3] (5.11)[4]
Electrolyzer Cap. Cost		$/kg-$H_2$	0.50	0.50	1.30 (0.74)[5]
Efficiency	System	%LHV (kWh/kg)	72 (46)	75 (44)	65 (51)
	Stack	%LHV (kWh/kg)	76 (44)	77 (43)	74 (45)

[1] 2012 MYRDD Plan. [2]Production Only. [3]Utilizing H2A Ver.2. [4]Utilizing H2A Ver.3 (Electric costs increased to $0.057/kW from 0.039$/kW) . [5] Stack Only
LHV - lower heating value

Accomplishments

- Ir supported on tungsten doped titanium dioxide ($Ir/W_xT_{1-x}O_2$) reduced anode PGM loading by an order of magnitude while retaining performance comparable to the industry standard (with high PGM loading).
- Ir deposited on nanostructured thin film (Ir/NSTF) anode catalyst significantly lowered the catalyst loading

while enabling the water electrolysis operations at extremely high current density (>10 A/cm^2).

- Both Ir/$W_xT_{1-x}O_2$ and Ir/NSTF anode catalysts demonstrated minimal performance decay after 1,000-hour PEM electrolyzer tests.
- Ir-metal (Ni or Co) nanowire OER catalysts simultaneously enhanced mass activity and specific activity compared to commercial Ir black in RDE tests.
- Structures of Ir/$W_xT_{1-x}O_2$ catalyst based anodes were characterized after durability tests, providing some insights on catalyst degradation mechanisms.
- Roll-to-roll production of Ir/NSTF catalysts was achieved, showing processability and scalability of catalyst synthesis.

✧ ✧ ✧ ✧ ✧

INTRODUCTION

Current hydrogen production from electrolysis is only a small fraction of the global hydrogen market, due to the high cost that results from expensive materials (membrane, catalyst, and bipolar plate) and electricity consumption. The two largest efficiency losses in PEM electrolysis are the anode over-potential and the ohmic losses from the membrane resistance. Anode over-potential is a source of major inefficiency in the entire region of current densities, originating from poor OER kinetics. The only way to lower the over-potential at the anode is to utilize a better catalyst, increase the catalyst loading, or operate at a higher temperature. Iridium and its oxide (IrO_2) represent the current state of the art for oxygen evolution catalysts in electrolysis applications where both performance and durability are important. State-of-the-art PEM electrolyzers relying heavily on Ir black have high Ir loading and low system efficiency (high electricity consumption/per kilogram hydrogen). Therefore, our project aims to develop advanced Ir-based catalysts that enhance OER catalysis and the efficiency of PEM electrolyzers.

APPROACH

Three distinct catalyst approaches have been explored in this project. The first approach is iridium dispersed on tungsten-doped titanium oxide (Ir/$W_xT_{1-x}O_2$) at Giner. The second approach is iridium nanostructured thin film from 3M (Ir/NSTF). The third approach uses NREL's iridium on Ni or Co nanowire technology (IrCo or IrNi); the developed catalysts have been screened by RDE for corrosion resistance and activity and selected catalysts will be made into MEAs and tested in Giner's state-of-the-art electrolyzer test stations to evaluate their performance and durability. Scaled-up production of selected catalysts was conducted.

RESULTS

Giner efforts have focused on increasing mass-specific activity by dispersing Ir nanoparticles (NPs) on appropriate supports, similar to what has been achieved with carbon supported Pt for fuel cells (see Figure 1a). One example is Ir/$W_xT_{1-x}O_2$ catalyst that have been characterized by high angle annular dark field-scanning transmission electron microscopy (HAADF-STEM) and energy dispersive X-ray spectroscopy (EDS) images (see Figure 1b) at Oak Ridge National Laboratory (ORNL). Figure 1b demonstrates typical morphology of Ir NPs (bright areas) on surfaces of agglomerated $W_xTi_{1-x}O_2$ support plates. Most of the $W_xTi_{1-x}O_2$

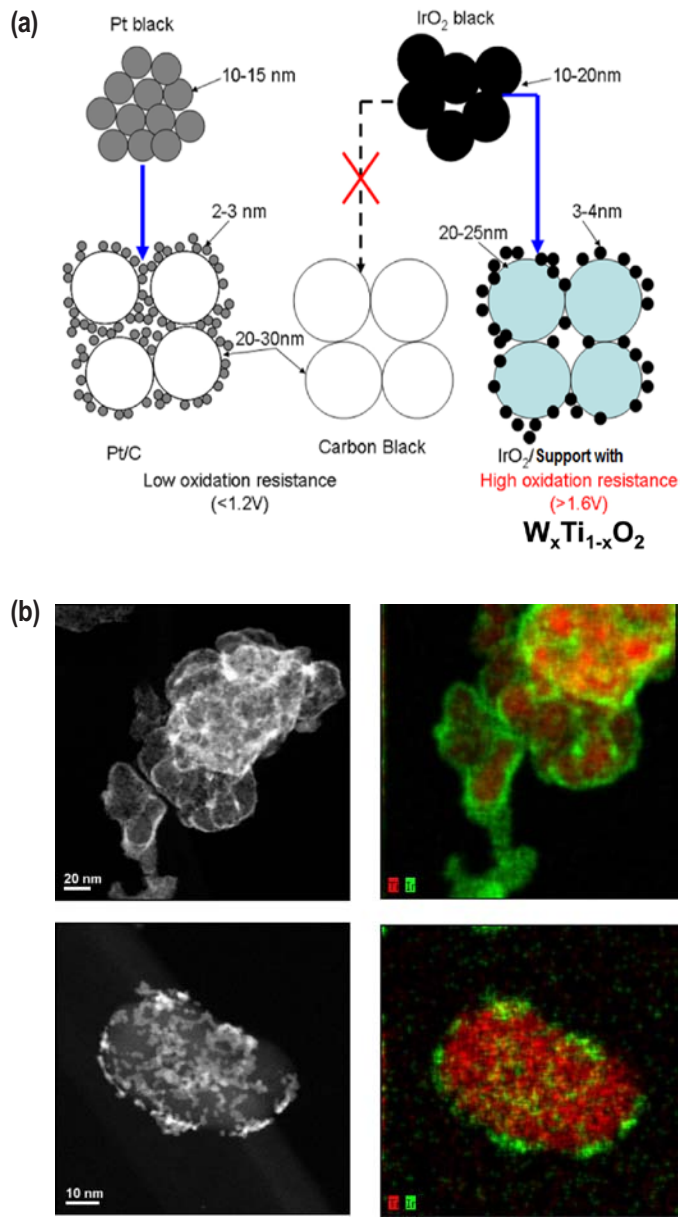

FIGURE 1. Ir/$W_xT_{1-x}O_2$ catalyst development at Giner. (a) Illustration of supported Ir nanoparticle catalyst development. (b) HAADF-STEM images of Ir supported on $W_xTi_{1-x}O_2$ taken by Dr. Karren More at ORNL.

particles are thin plates and are "bean-shaped or elongated." The corresponding EDS map (Ti = red, Ir = green) shows that Ir does not form a continuous coating on the surface of $W_xTi_{1-x}O_2$, but Ir NPs form a "lacey or chain-like" network of interconnected NPs (1.5–2.5 nm) on the surface of the $W_xTi_{1-x}O_2$.

The performance and durability of the Ir/$W_xT_{1-x}O_2$ catalyst are shown in Figure 2. The anode of Group 3 cells (4, 5, and 6) is made of Ir/$W_xT_{1-x}O_2$ catalyst with low Ir loading (0.25 mg/cm^2) where Group 1 cells (1 and 2) use the industry standard anode (Pt+Ir loading 2 mg/cm^2). Low loadings of the new catalyst performed significantly better than standard iridium black containing twice as much PGM and approached the performance of the Giner standard anode containing eight times the PGM loading (Figure 2a). A single cell containing Ir/$W_xT_{1-x}O_2$ catalyst at the anode remained relatively stable during a 1,000-hour operation at 1.5 A/cm^2 with 20 mV voltage loss (Figure 2b). HAADF-STEM images of test MEAs (data not shown) indicate that partial Ir agglomeration and Ir migration into the membrane occur, which may account for the performance loss.

3M created a new NSTF anode that uses iridium without any platinum. The catalyst loading is 0.25 mg/cm^2. 3M anodes with this low Ir-loading (Ir/NSTF) demonstrated performance comparable to industry standard anodes. Furthermore, they also enabled extremely high current densities up to 16 A/cm^2 (Figure 3a). No signs of impending transport limitations have been observed at these very high current densities. The ability to operate at high current density is significant as it may help to reduce the size, and

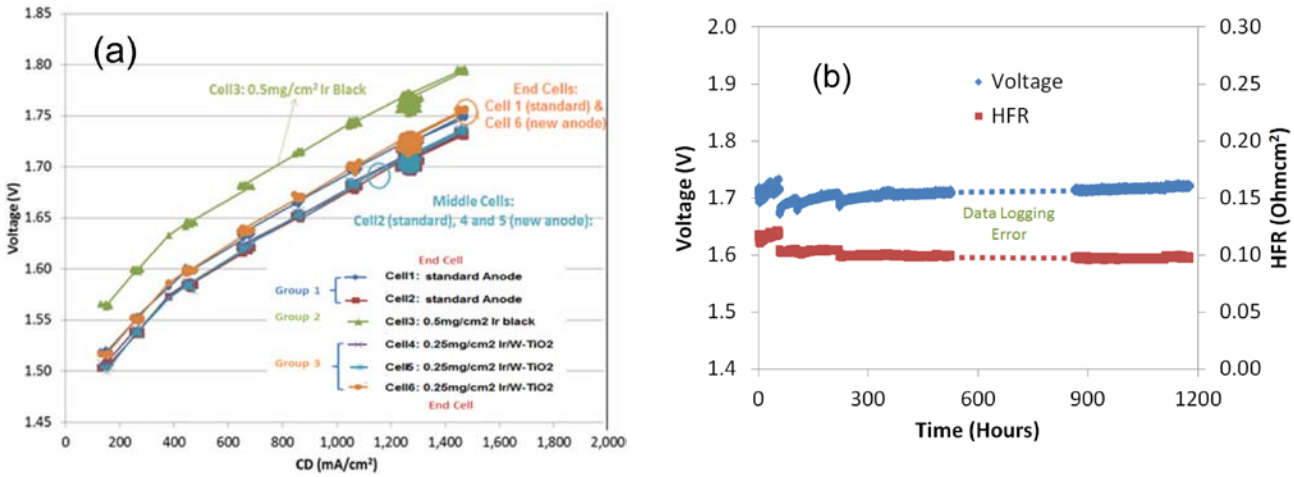

FIGURE 2. PEM electrolyzer performance and durability of Giner Ir/$W_xT_{1-x}O_2$ catalyst at 80°C. (a) PEM electrolyzer performance of a short stack of six cells with various anode catalysts. (b) 1,000-hour durability test at 1.5 A/cm^2. Membrane: Nafion® 115; cathode catalyst: Pt/C, Pt loading 0.4 mg/cm^2; anode catalyst: Ir/ $W_xT_{1-x}O_2$, Ir loading 0.4 mg/cm^2.

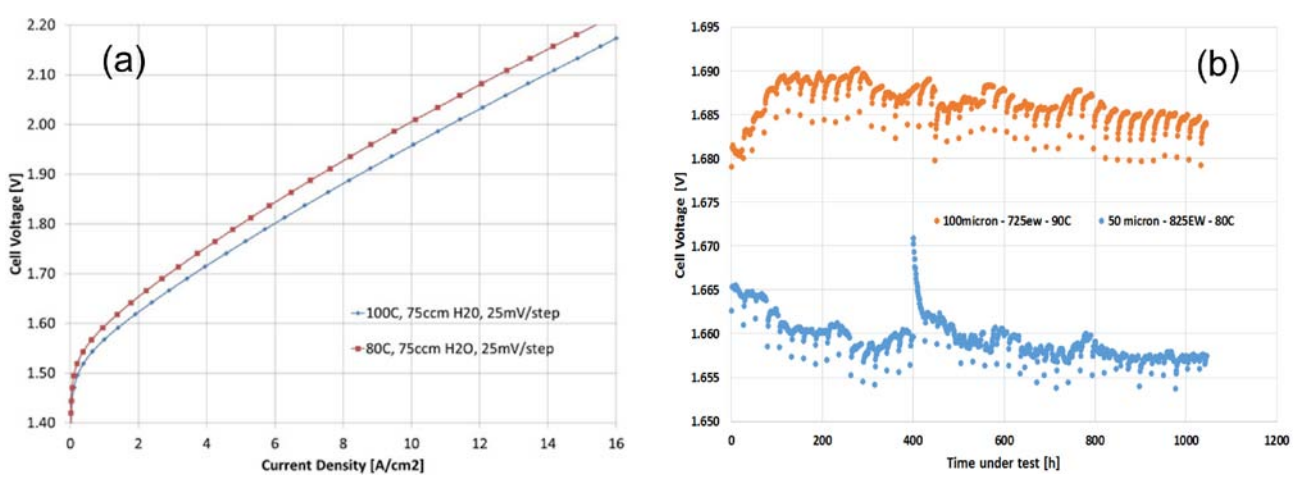

FIGURE 3. PEM electrolyzer performance and durability of 3M Ir/NSTF catalyst. (a) High current density operation of Ir/NSTF catalysts. (b) Durability of two 3M Ir/NSTF anode catalyst-based MEAs up to 1,500 hours. Cathode: 0.25 mg/cm^2. Pt Anode: 0.25 mg/cm^2 Ir. Test cycle: cycling from 1.4 V to 2.0 V, hold for 24 h at 1.5 A/cm^2.

hence cost, of PEM water electrolyzers. Durability testing of the Ir/NSTF was also conducted by 3M. Two MEAs were subjected to multiple hour long cycles of operation at 1.5 A/cm^2, one has a 100-µm thick membrane operated at 90°C; the other has 50-µm thick operated at 80°C. Both MEAs showed extremely stable performance over 1,500 hours of testing (Figure 3b).

NREL fabricated iridium nanotubes starting with various nanowire scaffolds. Iridium was deposited onto the nanowire surface using galvanic displacement. The galvanic displacement process occurs when the support material oxidizes and reduces iridium ions in solution to metallic iridium resulting in an iridium/iridium alloy coating on the support surface. During NREL's syntheses, the amount of iridium precursor supplied was varied to explore catalysts of various Ir loading and composition. After deposition, the nickel and cobalt nanowire supports were selectively exposed to acid leaching conditions to remove transition metals to various extents. The performance of select IrNi and IrCo nanowires evaluated by RDE are shown in Figure 4**.** The lower Ir content, the higher OER activity (Figure 4a). Mass activity improvements were found to be the result of both

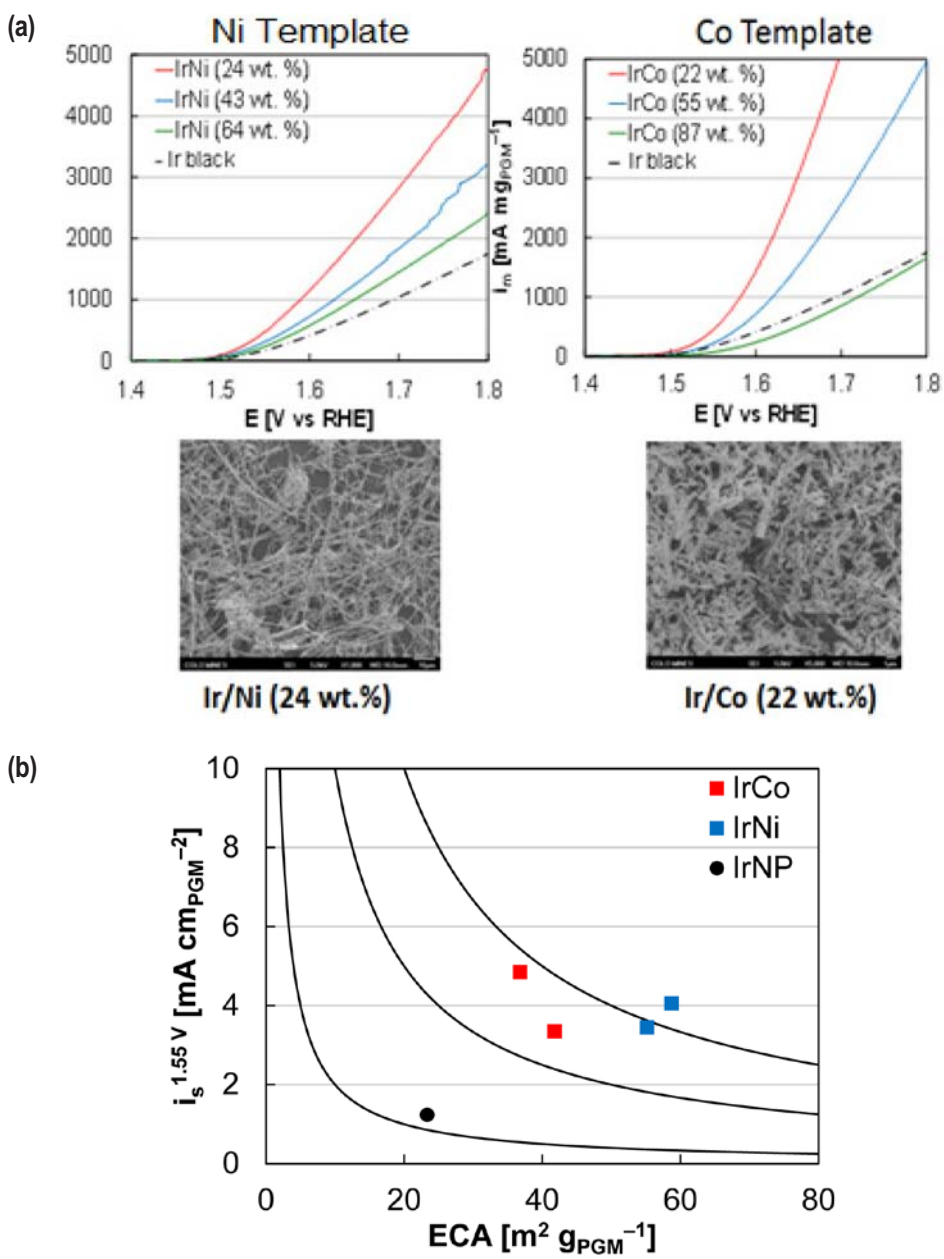

FIGURE 4. Catalytic activity of NREL IrNi and IrCo catalysts using RDE. (a) Ir/metal nanowires based on various templates. (b) ECSA and areal current density (i_s) of various batches of NREL's iridium-coated nanowires and nanotubes. The contour lines (right to left) are of constant mass OER activity of 200, 1,000, and 2,000 mA/mg Ir.

electrochemical surface area (ECSA) and specific activity (Figure 4b). The ECSA was measured by Hg under-potential deposition [2]. The contour lines in Figure 4b are of constant mass OER activity of 200, 1,000, and 2,000 mA/mg Ir, and highlight the approximately order-of-magnitude improvement in activity of both IrCo and IrNi nanowires compared to commercial Ir NP.

CONCLUSIONS AND FUTURE DIRECTIONS

Conclusions

- Ir-based OER catalysts for PEM electrolysis have been successfully synthesized
  - Giner: Ir/$W_xTi_{1-x}O_2$
  - 3M: Ir-NTSF
  - NREL: IrCo and IrNi nanowires
- Giner: Ir/ $W_xTi_{1-x}O_2$ catalyst-based MEA demonstrated excellent performance
  - A six-cell electrolyzer stack test: the catalyst matched Giner baseline but reduced Ir loading by 8x
  - Single cell test: successfully passed 1,000 h test with 20 mV voltage decay
- 3M: Durability test and mass production of Ir/NSTF catalysts
  - Enabled high current density (16 A/cm^2) at 0.25 mg/cm^2 Ir loading
  - Two MEAs passed 1,000 h test with negligible performance loss
- NREL: Activity and durability of Ir-metal nanowires investigated
  - RDE data shows that both IrCo and IrNi nanowires had ~10x mass activity compared to Ir nanoparticles

Future Directions

- Test Ir/$W_xTi_{1-x}O_2$ catalyst at high Ir loading (1–2 mg/cm^2) to study its effect on over-potential
- Test the catalyst durability of developed catalysts in a short stack under more harsh conditions and extended hours
- Select one category of catalyst with best durability for Giner sub-megawatt electrolyzer stack construction

FY 2015 PUBLICATIONS/PRESENTATIONS

1. Xu, H., B. Rasimick, A. Stocks, B. Pivovar, and K. Lewinski, "High-Performance, Long-Lifetime Catalysts for Proton Exchange Membrane Electrolysis," Progress Report, U.S. Department of Energy Phase II Grant No. DE-SC0007471, August 2014.

2. Xu, H., "Novel Oxygen Evolution Catalysts for Proton Exchange Membrane Water Electrolysis," presented in 224th meeting of ECS, Abstract #1239, Cancun, Mexico, October 2014.

3. Xu, H., "Invited talk: High-Performance and Long-Lifetime Oxygen Evolution Catalysts for PEM Water Electrolysis," presented in 225th meeting of ECS, Chicago, May 2015.

4. Xu, H., B. Rasimick, A. Stocks, B. Pivovar, and K. Lewinski, "High-Performance, Long-Lifetime Catalysts for PEM Electrolysis," final report, U.S. Department of Energy Phase II Grant No. DE-SC0007471, May 2015.

5. Xu, H., "High-Performance, Long-Lifetime Catalysts for Proton Exchange Membrane Electrolysis," presentation in DOE Hydrogen and Fuel Cell Merit Review Meeting, Washington, D.C., June 2015.

6. Shaun Alia, Shyam Kocha, Bryan Pivovar, "Establishing Baselines/Protocols Relevant for PEM Electrolysis," IEA PEM Electrolysis Workshop, Herten, Germany, April 20–21, 2015.

7. K.A. Lewinski and S.M. Luopa, "High Power Water Electrolysis as a New Paradigm for Operation of PEM Electrolyzer," L09: Oxygen or Hydrogen Evolution Catalysts for Water Electrolysis Session, #1948, 227th Meeting of the Electrochemical Society, Chicago, IL, May 24–28, 2015.

REFERENCES

1. Hamden, M., "PEM Electrolyzer Incorporating an Advanced Low Cost Membrane," Presentation in DOE 2012 H2 and Fuel Cells AMR meeting, http://www.hydrogen.energy.gov /pdfs/review12/ pd030_hamdan_2012_o.pdf (2012).

2. Kounaves, K.P., and Buffle, J. "Deposition and Stripping Properties of Mercury on Iridium Electrodes," *J. Electrochem. Soc.* 13, 2495-2498 (1986).

3. Xu, H., "High-Performance, Long-Lifetime Catalysts for Proton Exchange Membrane Electrolysis," Presentation in DOE Hydrogen and Fuel Cell Annual Merit Review Meeting, Washington, D.C., June 2014.

II.B.3 Low-Noble-Metal-Content Catalysts/Electrodes for Hydrogen Production by Water Electrolysis

Dr. Katherine Ayers
Proton Energy Systems d/b/a Proton OnSite
10 Technology Drive
Wallingford, CT 06492
Phone: (203) 678-2190
Email: kayers@protononsite.com

DOE Manager
David Peterson
Phone: (720) 356-1747
Email: David.Peterson@ee.doe.gov

Contract Number: DE-SC0008251

Subcontractor
Brookhaven National Laboratory (BNL), Upton, NY

Project Start Date: June 28, 2012 (Phase 1)
Project End Date: August 13, 2015 (with Phase 2 continuation)

Project Objectives

- Translate catalyst synthesis to a manufacturable process at Proton
- Develop a robust technique for manufacturable electrodes
- Demonstrate feasibility for 80% cost reduction in the anode catalyst
- Downselect promising anode electrode configurations to achieve >100 hours durability
- Achieve 500 hours of operation in production quality hardware using cost-reduced cathodes

Technical Barriers

This project addresses the following technical barrier from the Hydrogen Production section of the Fuel Cell Technologies Office Multi-Year Research, Development, and Demonstration (MYRDD) Plan:

(G) Capital Cost

Technical Targets

The table below shows the technical targets for distributed forecourt water electrolysis hydrogen production from the 2012 MYRDD Plan.

Characteristics	Units	2011 Status	2015 Target	2020 Target
Hydrogen Levelized Cost	$/kg	4.2	3.9	2.3
Electrolyzer System Capital Cost	$/kg $/kW	0.70 430	0.50 300	0.50 300
Stack Energy Efficiency	% (LHV) kWh/kg	74 45	76 44	77 43

**Note: Assumptions include a plant design capacity of 1,500 kg/day of hydrogen and that production has realized economies of scale.
LHV - lower heating value

Accomplishments

- Successfully scaled synthesis process by a factor of 10
- Showed >500 hours durability with ultra-low loaded Proton-made cathode
- Resolved early mass transport issues with deposited anode catalyst
- Demonstrated anode microporous layer does not impact cell resistance
- Demonstrated feasibility of >$100,000 savings in capital cost for megawatt-scale electrolysis

✧ ✧ ✧ ✧ ✧

INTRODUCTION

The economical use of hydrogen as a transportation and stationary power fuel remains a long-term Department of Energy (DOE) objective. Energy storage applications in Europe such as wind capture and improved biogas conversion efficiency are also driving significant interest in hydrogen production from renewable sources. New and efficient catalytic processes for hydrogen generation are therefore needed to achieve production targets for hydrogen cost. In the Phase 1 project, Proton Energy Systems (d/b/a Proton OnSite), in collaboration with Brookhaven National Laboratory (BNL), demonstrated feasibility for development of low-noble-metal-content catalysts/electrodes for proton exchange membrane (PEM) electrolyzers, through design and synthesis of core-shell nanocatalysts. In Phase 2, continued development of the anode formulation is being performed for reproducible and stable electrode fabrication, while technology transfer and scale-up from BNL to Proton is occurring for the cathode electrode fabrication. The Phase 2 project is strategically important because reduction of noble metal content is a significant opportunity for cost reduction to

address large-scale opportunities for hydrogen-based energy storage and hydrogen fueling.

APPROACH

The Phase 2 project continues maturation of the catalyst structures and electrode processing initiated in Phase 1, to develop a manufacturable electrode at relevant scale and ultra-low catalyst loadings. The overall technical approach includes development of the manufacturing process for the cathode electrode as well as cell stack validation for the alternative electrode configuration. In addition, for the anode, work focuses on continued optimization of catalyst application and gas diffusion layer (GDL) structure for reproducible and durable performance equal to or exceeding the current baseline. The impact of these advancements will be quantified using the H2A model.

General steps for the cathode include technology transfer of the catalyst synthesis techniques and electrode formulations to Proton, a study to determine the best method of manufacturing the electrodes proven at the bench scale, process scale-up, cell stack design adjustments to accommodate the new configuration, and validation. For the anode, based on the promising performance demonstrated in Phase 1, catalyst support structures for stability at >1.6 V/cell are investigated, and the catalyst composition will be refined for high activity. A study of anode GDLs with varying porosity vs. alternate methods of applying the catalyst to the GDL will also be performed, to synthesize an electrode with good catalyst distribution at the GDL surface while maintaining adequate water transport at the membrane surface.

RESULTS

After core-shell nanoparticles were synthesized at Proton based on the BNL process, Proton successfully scaled the process by an order of magnitude, resulting in relevant batch sizes for membrane electrode fabrication across Proton's platforms. The process involved additional safety reviews for dealing with the larger solvent volumes, and the batch had to be divided for the reducing process based on Proton's infrastructure limitations. While the synthesis was successful, difficulties managing the solvent quantities and reduction process point out the need for additional facilities considerations or partnership with a catalyst manufacturer with appropriate equipment. The catalyst was deposited on a gas diffusion layer at 1/10th of Proton's commercial baseline loadings and tested in Proton's cell hardware. Performance was equivalent to baseline, as shown in Figure 1. The electrode fabrication process was also scaled up to large active area (700 cm^2) and tested vs. the baseline process, with good durability and performance over 1,000 hours (Figure 2).

For the anode, work at BNL focused on determining whether core-shell catalysts could provide the same benefit as the work on the cathode. Ruthenium oxide and ruthenium-iridium core-shell particles were synthesized, characterized, and electrochemically tested. As expected, the ruthenium-containing compounds provided higher initial performance. Also as expected, the pure ruthenium oxide was not stable over several days of testing. However, unfortunately, the iridium cores did not result in improved stability of the ruthenium. Therefore, iridium-only catalysts were downselected for the remainder of the program, focusing on minimizing loading. A microporous layer (MPL) approach was taken, similar to the cathode, to provide a more continuous layer for catalyst deposition on the anode

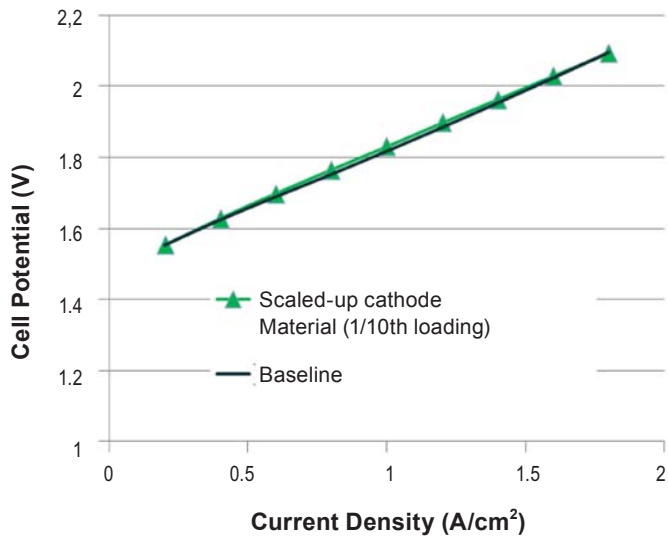

FIGURE 1. Performance data confirming scaled-up catalyst batch comparable to baseline, at 1/10th loading

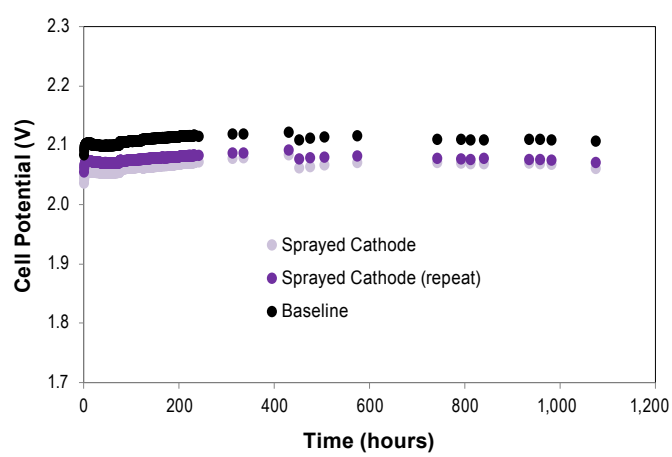

FIGURE 2. Durability performance and consistency for parts fabricated from large active area spray process

gas diffusion layer. Initially, mass transport limitations were observed, and optimization of the deposition layer had to be performed. Testing of just the GDL with an MPL against a traditional membrane electrode assembly (MEA) did not show mass transport issues, ruling out the MPL as the root cause of the issue. With adjustments in ink formulation and deposition parameters, improved performance was observed (Figure 3).

The advancements made throughout the project were combined together for a final demonstration. Anodes and cathodes with low catalyst loading were fabricated for multiple cells for Proton's 100-cm^2 active area configuration, and two cells were assembled with a baseline cell. The stack was tested at 400 psi and 1.8 A/cm^2. Performance is shown in Figure 4. While there was some variation in performance and a break-in period at the beginning, the performance stabilized after the first few hundred hours, and all three cells demonstrated stability with flat performance after the stabilization period. The variation in performance indicates that there is still optimization needed to achieve consistent electrodes, but the fact that one of the two low-loaded electrodes outperformed the baseline indicates promise for this approach with additional manufacturing development.

Based on the developments achieved over the course of the project, a cost analysis was performed for the alternate electrode configuration vs. Proton's current commercial fabrication processes. The analysis demonstrated that for megawatt-scale electrolysis, the catalyst and associated labor for the baseline deposition process represents over 25% of the stack cost. The advanced process and catalyst materials can provide over $100/kW savings, or roughly $0.12/kg H_2. This level of cost reduction provides a significant competitive advantage in the market, which is essential for the United States to compete in the emerging markets for energy storage.

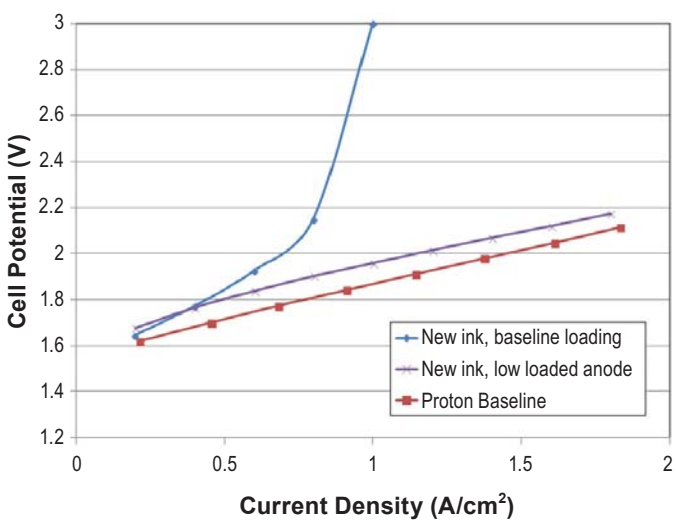

FIGURE 3. Polarization curves demonstrating resolution of anode mass transport issues

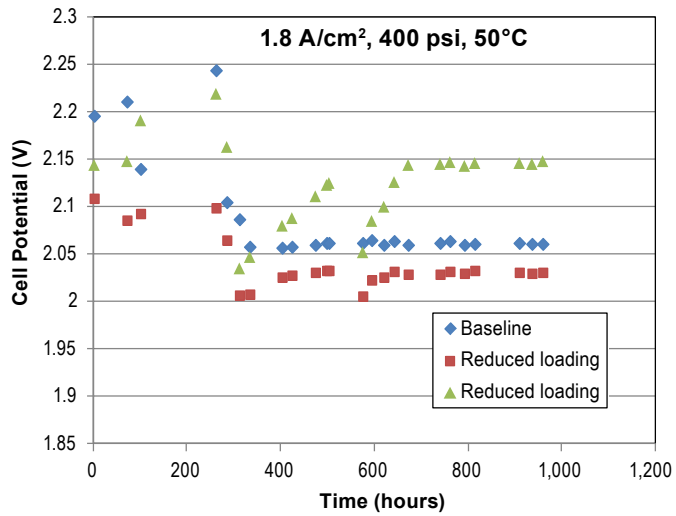

FIGURE 4. Anode and cathode performance with 90% cathode catalyst reduction and 75% anode catalyst reduction vs. baseline

CONCLUSIONS AND FUTURE DIRECTIONS

- Scale-up of core-shell synthesis and deposition process demonstrated for scales relevant to megawatt electrolysis for cathode
  - 10x catalyst batch size demonstrated
  - 90% reduction in catalyst loading
  - 7x increase in active area
- Downselected anode approach and demonstrated over 50% reduction in anode catalyst loading
  - Resolved mass transport issues at anode
  - MPL approach did not impact MEA performance
- Final demonstration completed for anode and cathode reductions combined
- Cost analysis shows $0.12/kg savings
  - Represents several million dollars in cost savings over first few years of megawatt product sales
- Continued investment in manufacturing and catalyst needed for commercialization of demonstrated advancements

FY 2015 PUBLICATIONS/PRESENTATIONS

1. 2015 DOE Annual Merit Review and Peer Evaluation Meeting presentation: pd098_ayers_2015_o.

2. Spring Electrochemical Society meeting, "Barriers to Commercial Deployment of Advanced PEM Electrolyzers."

II.B.4 High Temperature, High Pressure Electrolysis

Cortney Mittelsteadt (Primary Contact),
Jason Willey
Giner, Inc.
Giner Electrochemical Systems, LLC
89 Rumford Avenue
Newton, MA 02466
Phone: (781) 529-0529
Email: cmittelsteadt@ginerinc.com

DOE Manager
David Peterson
Phone: (720-356-1747)
Email: David.Peterson@ee.doe.gov

Contract Number: DE-SC0011310

Subcontractor
Prof. Judy Riffle, Virginia Polytechnic Institute and State University (Virginia Tech), Blacksburg, VA

Project Start Date: November 18, 2014
Project End Date: November 17, 2016

Overall Objectives

- Develop a polymer electrolyte membrane (PEM) with a high ratio of conductivity to permeability, which leads to an increase in efficiency
- Optimize lifetime of developed PEM using various methods
- Demonstrate improved lifetime and efficiency under high pressure (350 bar) operation

Fiscal Year (FY) 2015 Objectives

- Optimize crossover mitigation in nonperfluorinated membranes
- Optimize formulation of nonperfluorinated membranes for conductivity/permeability ratio and lifetime
- Demonstrate increased lifetime with medium pressure (70 bar) operation

Technical Barriers

This project addresses the following technical barriers from the Hydrogen Production section of the Fuel Cell Technologies Office Multi-Year Research, Development, and Demonstration Plan (MYRDDP):

(F) Capital Cost

(G) System Efficiency and Electricity Cost

(L) Operations and Maintenance

Technical Targets

Progress has been made in achieving the DOE targets listed in the MYRDDP. Table 1 lists the DOE's technical targets and where our research and development efforts stand to date.

TABLE 1. DOE Technical Targets and Giner, Inc. Status

Characteristic	Unit	2015 Target	2020 Target	Giner, Inc. Status
Electrolyzer System Capital Cost	$/kg $/kW	0.50 300	0.50 300	- 1,000
System Energy Efficiency	% (LHV) kWh/kg	72 46	75 44	- 45.5
Stack Energy Efficiency	% (LHV) kWh/kg	76 44	77 43	- 44.5

LHV - lower heating value

The goal of this project is to increase the efficiency of the PEM (electrolyzer stack and to improve durability of the membrane electrode assemblies [MEAs]), while providing hydrogen at a pressure of 350 bar. This project is still in the early stages. These goals would contribute significantly to reaching the 2020 DOE hydrogen production targets of:

- Hydrogen Levelized Cost: $4/kg H_2 (Dispensed)
- Stack Energy Efficiency: 43 kWh/kg H_2
- Electrolyzer System Capital Cost: $300/kW

FY 2015 Accomplishments

- Discovered, with Virginia Tech, novel, non-perfluorinated ionomer membranes that demonstrate conductivity to permeability ratios above two times that of Nafion®
- Designed and fabricated new hardware that will withstand the 350 bar differential operating pressure of the electrolyzer stack
- Demonstrated 1,000 h of stable electrolyzer performance at 1,000 psi and 95°C

✧ ✧ ✧ ✧ ✧

INTRODUCTION

Electrolysis of water is an important tool for energy storage in wind and solar applications. DOE has identified a need for electrolyzer efficiencies to reach 77% LHV by

2020. High pressure direct electrolysis is a desirable method for hydrogen generation and energy storage due to the reduced need for high pressure pumps and compressors. Direct electrolysis at elevated pressure permits hydrogen and/or oxygen tanks to be refilled directly, and reduces the overall mass, complexity, and cost of the electrolysis system. Efficiency can be increased by operation at a higher temperature, which increases both conductivity and oxygen evolution kinetics. However, this efficiency comes at the expense of higher permeability. Gas crossover (permeability) plays an increasingly significant role in performance as pressure rises, decreasing efficiency and accelerating membrane degradation while leading to potentially dangerous levels of hydrogen in oxygen and vice versa. Increasing membrane thickness or lowering cell operating temperature can decrease crossover, but also decreases efficiency. Given the permeability and conductivity at a given temperature, it is straightforward to optimize membrane thickness for efficiency. The key to making efficiency gains then is to increase the ratio of conductivity/permeability and operate at as high a temperature as possible without compromising the membrane. The overall objective for this DOE Small Business Innovation Research (SBIR) program is the development of a PEM with maximum conductivity/permeability ratio while simultaneously greatly reducing membrane degradation rates (2x and 10x improvement over Nafion®, respectively). Perfluorinated sulfonic acid- (PFSA) and hydrocarbon-based membranes generated with various additives, ionomer compositions and support structures were prepared and evaluated for conductivity and permeability as a function of temperature and water activity. The initial goal was to produce membranes with conductivity/permeability ratios greater than two with reference to Nafion®, and this goal has been achieved.

The optimized membranes developed under this work are currently being tested for durability and performance in Giner, Inc.'s high-pressure cell hardware at pressures up to 5,000 psi. Combinations of various additives are used to increase durability and reduce gas crossover in the MEA.

APPROACH

The general approach for this project is to test the conductivity/permeability ratio for both commercial and experimental membranes. Those membranes showing conductivity/permeability ratios more than twice that of Nafion® are tested for durability. The durability is then tested with unadulterated membrane, and with membrane that has additives to increase durability and to decrease gas crossover. The best performing of these membranes will be scaled up into a short stack build that will then be tested at high pressure and high temperature for performance and durability.

The initial stage of the project has been completed with several non-PFSA membranes showing promise. Testing is now focused on medium pressure testing for durability and performance.

RESULTS

The overall goal of the first phase of this project was to fabricate, test and select membranes that possess conductivity to permeability (C/P) ratios higher than that of Nafion®, to achieve the DOE goal of 76% LHV electrolyzer efficiency. A secondary goal was to ready a test station for testing membranes early in Phase II. Both of these goals were realized.

In total, 15 different ionomers were procured or fabricated and tested for conductivity and hydrogen permeability in Phase I. Excluding unmodified Nafion®, six were PFSA ionomers – three modified N1100 membranes and three low equivalent weight membranes. The remaining eight were hydrocarbon-based membranes made by Virginia Tech, our Phase I partner and Rensselaer Polytechnic Institute. Figure 1 shows the results of testing for the 15 membranes.

As can be seen in the figure, three hydrocarbon membranes exceed the Phase I goal of a ratio of two. These membranes will be included in the Phase II testing. One PFSA membrane tests close to the goal – the Solvay Aquivion 790 equivalent weight membrane with a C/P of 1.7. In the interests of keeping a PFSA membrane in the study, and with the hope that novel treatments can increase the C/P ratio significantly, the Solvay ionomer will be included in the durability testing.

Baseline durability testing has been completed on Nafion® and is moving to the hydrocarbon ionomers. The main marker for chemical degradation of Nafion® is fluoride. Giner measures fluoride in the cell exit water as a measure of membrane degradation. Figure 2 shows the typical durability test. Fluoride numbers for this test were below the detectable

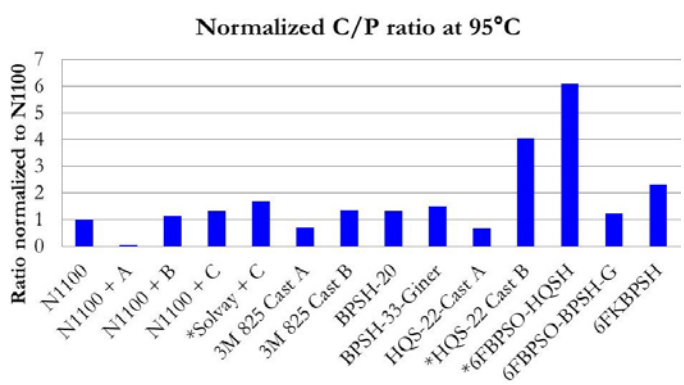

FIGURE 1. Conductivity, permeability and the C/P ratio for the membranes tested under the Phase I program. The go/no-go ratio is 2, and membranes above this ratio were moved on to the durability stage.

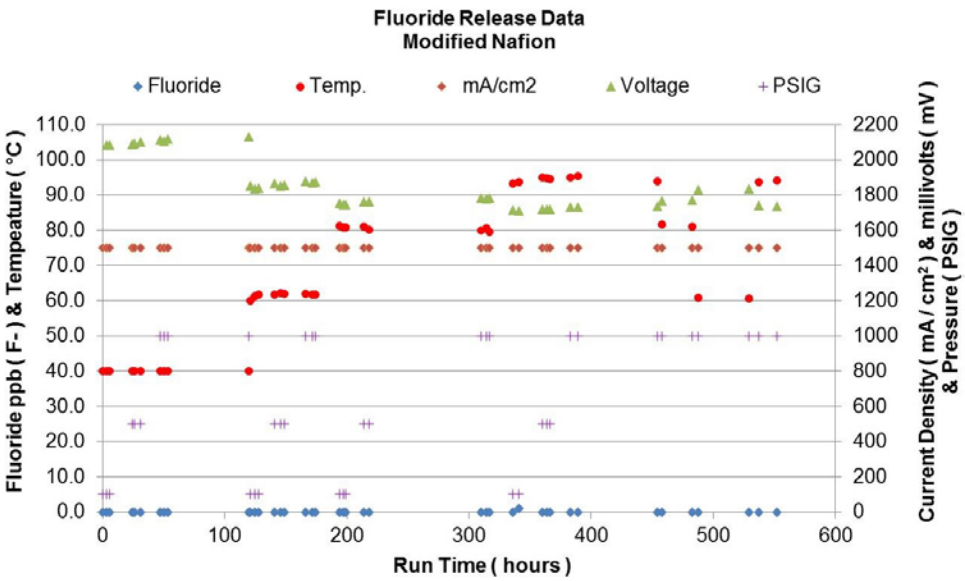

FIGURE 2. Various parameters measured during the durability test of a Nafion® membrane treated with a degradation mitigant

limit (~20 ppb) for the entire test, and voltage was stable at the various temperatures. These results suggest that chemical degradation was not an issue for this membrane with the degradation modification. Table 2 compares unmodified Nafion® N117 with Giner's modified N115, showing marked improvement in chemical durability with a thinner membrane at higher temperature and pressure.

TABLE 2. Comparison of Modified and As-Received Nafion®

Membrane	Pressure	Temperature	Stabilized	Estimated Lifetime (h)
N117	100 psi	80°C	None	10,000
N115	1,000 psi	95°C	Yes	>30,000

A new bipolar plate design was fabricated under this project capable of 350 psi operation without additional support. This design consists of two valve metal plates laser-welded together to provide a well-sealed flow path with low pressure drop for both the anode and cathode flows. The plates have been received and tested at pressures up to 70 bar with no overboard or cross-cell sealing issues. Testing up to 350 bar will be performed. Figure 3 shows an image of the 350 bar hardware.

CONCLUSIONS AND FUTURE DIRECTIONS

Although the project is still in early stages several conclusions can be drawn.

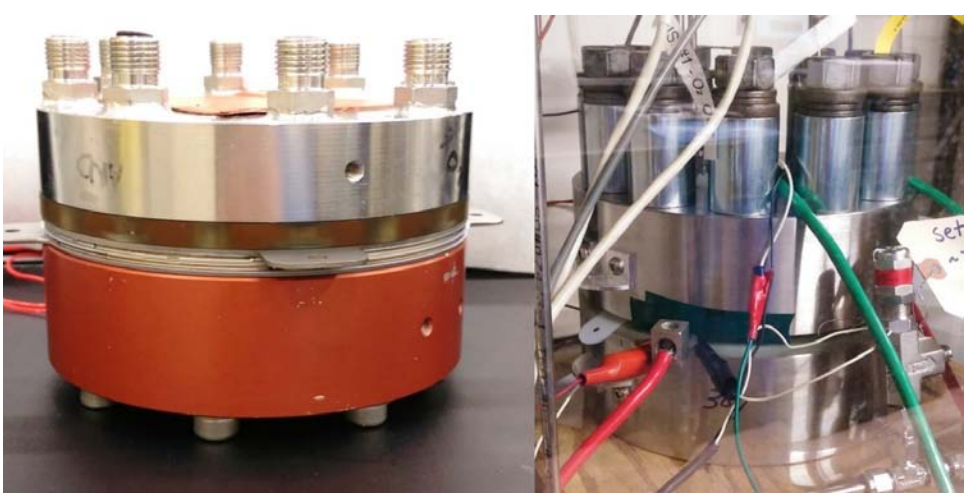

FIGURE 3. Fuel cell stack hardware designed to withstand 350 bar operational pressure

- Novel membranes have been discovered in this project with conductivity to permeability ratios much higher than that of Nafion®.
- Nafion® with Giner's degradation mitigant has shown no chemical degradation during operation up to 1,000 hours at 1,000 psi and 95°C.
- New high pressure bipolar plates have been designed and manufactured for operation in the high pressure test station.

Future work includes the following.

- Testing the novel membranes for performance and durability with and without Giner's additives for degradation and gas-crossover mitigation
- High pressure testing of membranes for performance and degradation
- Testing short-stack configuration of the best MEAs under high pressure conditions

FY 2015 PUBLICATIONS/PRESENTATIONS

1. C. Mittelsteadt. "PEM Electrolysis: Ready for Impact," ECS *Transactions*. Accepted.

2. C. Mittelsteadt. "PEM Electrolysis: Ready for Impact," 2015 ECS Fall Meeting, Invited.

3. C. Mittelsteadt, J Riffle, J.Willey, J. Rowlett, A. Daraei, J. McGrath, "Aromatic Block Copolymers for High Pressure Electrolysis," 2015 North American Membrane Society Meeting. Boston, June 2015.

II.C.1 High Efficiency Solar Thermochemical Reactor for Hydrogen Production

Anthony McDaniel
Sandia National Laboratories
MS9052
P.O. Box 969
Livermore, CA 94550
Phone: (925) 294-1440
Email: amcdani@sandia.gov

DOE Manager
Katie Randolph
Phone: (720) 356-1759
Email: Katie.Randolph@ee.doe.gov

Subcontractors:
- Profs. Ellen Stechel and Nathan Johnson, Arizona State University, Tempe, AZ
- Prof. Nathan Siegel, Bucknell University, Lewisburg, PA
- Prof. Ryan O'Hayre and Dr. Jianhua Tong, Colorado School of Mines, Golden, CO
- Prof. Christopher Wolverton, Northwestern University, Evanston, IL
- Prof. William Chueh, Stanford University, Stanford, CA

Project Start Date: October 1, 2014
Project End Date: September 30, 2016

Overall Objectives

- Verify the potential for solar thermochemical cycles for hydrogen production to be competitive in the long-term and by 2020, develop this technology to produce hydrogen with a projected cost of $3.00/gge (gasoline gallon equivalent) at the plant gate
- Develop a high-efficiency particle bed reactor for producing hydrogen via a thermochemical water-splitting cycle, and demonstrate eight continuous hours of operation on a solar simulator producing greater than 3 liters of hydrogen

Fiscal Year (FY) 2015 Objectives

- Discover and characterize suitable materials for two-step, non-volatile metal oxide thermochemical water-splitting cycles
- Design a particle receiver-reactor capable of continuous operation at 3 kW thermal input
- Develop a detailed unit operations model of a large scale single tower, multiple receiver solar thermochemical reactor

Technical Barriers

This project addresses the following technical barriers from the Hydrogen Production section of the Fuel Cell Technologies Office Multi-Year Research, Development, and Demonstration Plan:

(S) High-Temperature Robust Materials

(T) Coupling Concentrated Solar Energy and Thermochemical Cycles

(X) Chemical Reactor Development and Capital Costs

(AC) Solar Receiver and Reactor Interface Development

Technical Targets

This project is conducting fundamental studies on materials for use in concentrated solar power applications and designing reactor concepts that, when combined, will produce H_2 from thermochemical water-splitting (WS) cycles. Insights gained from these studies will be applied toward the design and optimization of a large-scale solar receiver and reactor that meets the following ultimate DOE hydrogen production targets:

- Hydrogen Cost: <$2/kg H_2
- Material of Reaction Cost: ≤$11,000/yr-TPD (metric tons per day) H_2
- Solar-to-Hydrogen (STH) Conversion Ratio: ≥26%
- 1-Sun Hydrogen Production Rate: $\geq 2.1\times10^{-6}$ kg/s m^2

FY 2015 Accomplishments

- Extended approach to material development by exploring several doped transition metal redox couples, streamlining screening experiments, and using first principles theory to inform discovery
- Used component-level modeling to establish design criteria for a 3 kW prototype reactor, developed conceptual layout of reactor, and derived hardware solutions for the solar-particle interface, pumping of reduction chambers, pressure separation, and particle flow
- Assembled and tested Olds Lift™ particle elevator, and qualified particle conveyance rates and vacuum separation

✧ ✧ ✧ ✧ ✧

INTRODUCTION

This research and development project is focused on the advancement of a technology that produces hydrogen at a cost that is competitive with fossil-based fuels for transportation. A two-step, solar-driven WS thermochemical cycle is theoretically capable of achieving a STH conversion ratio that exceeds the DOE target of 26% at a scale large enough to support an industrialized economy [1]. The challenge is to transition this technology from the laboratory to the marketplace and produce H_2 at a cost that meets or exceeds the DOE target of <$2/kg H_2.

Conceptually, heat derived from concentrated solar energy can be used to reduce a metal oxide at high temperature producing O_2 (step 1). The reduced metal oxide is then taken "off sun" and re-oxidized at lower temperature by exposure to H_2O, thus producing H_2 (step 2) and completing the cycle. Commercial success of solar thermochemical H_2 production is contingent upon developing suitable redox active materials and incorporating them into an efficient reactor. There are numerous material chemistries that have attributes suitable for inclusion in a thermochemical H_2 production system [2–4]. The challenge is to identify an optimally performing material. In addition, the development of redox material and reactor are not mutually exclusive, but must be conducted in parallel [5]. To maximize the probability of success, this project also addresses the reactor- and system-level challenges related to the design of an efficient particle-based reactor concept [6].

APPROACH

Thermochemical WS reactors are heat engines that convert concentrated solar energy (heat) to chemical work. Our approach is to discover materials to accomplish the WS chemistry and pair these materials with a novel cascading pressure receiver reactor (CPR2) that, when combined, can achieve an unprecedented STH conversion ratio. The material discovery work involves expanding our understanding of the underlying thermodynamics and kinetics in order to make performance improvements and/or formulate new, more redox-active compositions. Sandia's patented CPR2 technology is based on a moving bed of packed particles that embodies key design attributes essential for achieving high efficiency operation: (1) sensible heat recovery; (2) spatial separation of pressure, temperature, and reaction products; (3) continuous on sun operation; and (4) direct absorption of solar radiation by the redox-active material. Research efforts are focused on demonstrating this technology in a 3 kW-scale prototype.

RESULTS

Materials Research and Development Thrust

Sandia and collaborators synthesized and screened a select group of compounds for redox and WS activity. The synthesis effort was guided by experience gained through two years of investigating perovskite-type oxides for two-step thermochemical WS cycles. We also began two research initiatives, (1) application of first principles theory to inform the material discovery effort and (2) hypothesis testing of concepts for engineering the reduction entropy of WS materials (not discussed herein).

Seventy different compounds representing 14 perovskite families, and a LAMOX and a zircon-type crystal structure, were synthesized from 13 elements (Al, Ca, Ce, Fe, La, Mn, Mo, Nb, O, Sr, Ti, V, and Zr) in nine months of this project year. The $Ce^{3+/4+}$, $Fe^{3+/4+}$, $Mn^{3+/4+}$, $Mo^{3+/4+}$, $Ti^{3+/4+}$, and $V^{4+/5+}$ redox couples were explored. We adopted a more efficient primary screening methodology, called temperature programmed reaction (TPR), using a thermogravimetric analyzer (TGA) in order to keep pace with the synthesis activity. This approach measures oxygen evolution behavior during a single heat cycle and then infers WS candidacy from two figures of merit: (1) a redox capacity that exceeds CeO_2 (0.01 mol O/mol sample) and (2) an onset temperature for oxygen release (T_{OR}) between SLMA6464 (850°C) and CeO_2 (1220°C). While this method is currently deployed on a TGA, primary screening experiments can also run on conventional flow reactors if necessary to increase throughput.

Shown in Figure 1a are mass loss TPR profiles for representative materials from each group of the aforementioned compounds compared to CeO_2. From this data the T_{OR} can be derived, as shown in Figure 1b. The maximum reduction capacity is specified by the negative numbers inset to graph in Figure 1a, with more negative values indicating greater capacity. It is clear from this dataset that all compounds screened thus far have a greater redox capacity than CeO_2 under the conditions of this experiment. It is also clear that a few compounds, namely those with T_{OR} between SLMA6464 and CeO_2, are possible candidates for WS. We are most encouraged by COMP X, which is currently undergoing detailed analysis at Sandia's stagnation flow reactor (SFR) [7] facility.

While we have high confidence in our chemical intuition, the number of possible WS materials thought to exist within the perovskite family alone is extremely large. Therefore, we initiated a computational screening methodology, based on density functional theory (DFT), to inform the discovery effort. Two of the most challenging aspects of DFT are gaining confidence in the applicability of available pseudopotentials to our problem space (i.e., complex metal oxides are notoriously problematic), and fine tuning the numerical procedure. In an effort to validate theory, we

developed a model system by incremental B-site substitution of a $Sr(Mn_xCe_{1-x})O_3$ perovskite.

The data presented in Figures 2a and 2b show the effects of replacing Ce with Mn in $SrCeO_3$. In the base perovskite, Ce is trapped in the 4+ state making it extremely difficult to reduce. We have shown in the past that $SrMnO_3$ has very high redox capacity (i.e., large area under O_2 curve in Figure 2a), but does not split water (impossible to reoxidize with steam at ~800°C). When Mn and Ce mix on the B-site, the material splits water and has a greater redox capacity than CeO_2. We are currently conducting detailed electronic structure

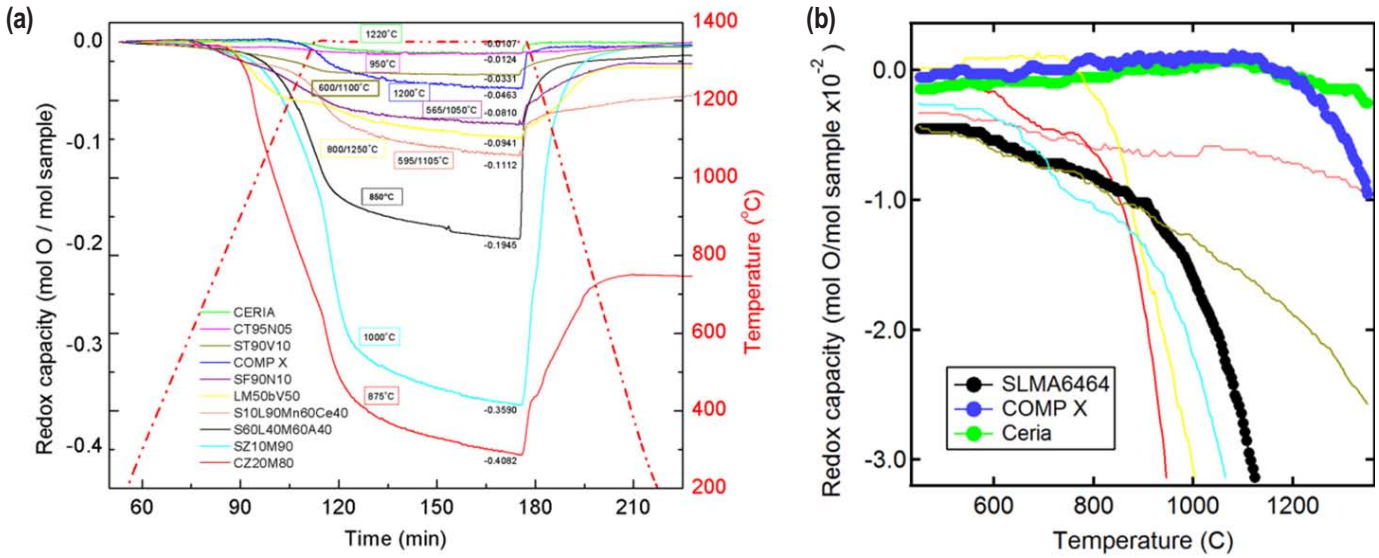

FIGURE 1. (a) Representative mass loss TPR screening results for 10 material formulations obtained using a TGA. Redox capacity is a measure of the mass-normalized moles of O_2 evolved from the sample during the course of heating from room temperature to 1,350°C at 20°C/min, and then dwelling at 1,350°C for 60 min. Temperature values outlined by colored framed boxes shown in graph are the T_{OR} values for each respective compound. (b) Onset temperature for O_2 evolution is derived from the TGA data for SLMA6464 (black), COMPOUND X (blue), and CeO_2 (green). T_{OR} between SLMA6464 and CeO_2 is one positive descriptor for commercially viable redox materials.

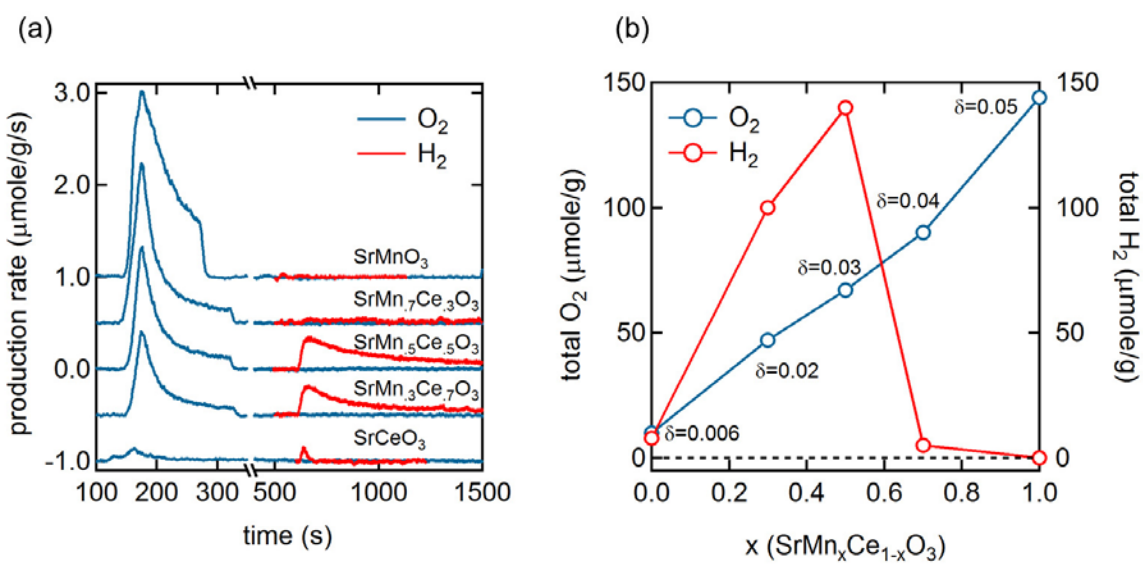

FIGURE 2. (a) O_2 and H_2 production rates for various $SrMn_xCe_{1-x}O_3$ perovskite formulations measured in Sandia's laser-heated SFR [7]. Thermal reduction is accomplished by heating at 10°C/s to a T_{RED} in the range 1,200–1,450°C. WS conditions were 25%vol H_2O in He at T_{OXD} in the range 850–1,000°C. The y-axis for each rate curve is offset for clarity. Note that the T_{RED} and T_{OXD} are not the same for all compositions. (b) Representation of the total amount of O_2 and H_2 formed during redox as a function of perovskite composition. The linear correlation with x is coincidental. The data in panels (a) and (b) demonstrates that WS chemistry can be activated/tuned by simple B-site substitution in the $SrCeO_3$ base perovskite. Understanding this behavior is key to developing optimal materials.

calculations on this system in an effort to validate our DFT approach, and to learn more about tuning perovskite WS activity from an atomistic perspective. Preliminary results of this analysis are encouraging.

CPR2 Design and Testing Thrust

By the conclusion of this project, this team will demonstrate continuous operation of a 3 kW prototype capable of producing >0.5 L/min H_2. In the first nine project months, design work steadily progressed from detailed specification of operating conditions to conceptual layouts of subcomponents, modeling of subcomponent behavior, and to fabrication and testing of certain hardware elements. Key design decisions for the CPR2 were derived during this process, the results of which are briefly summarized in Figure 3.

The solar receiver will consist of two reduction chambers (TR1, TR2) interfaced to pressure separation beds above and below (see Figure 3b). Particle flow will be controlled by gravity and actuation in the downward direction, and by an elevator in the upward direction. In TR1, heat enters through a window and raises the particle temperature to T_{TR} from ~800°C while partially reducing the oxide. In TR2, heat entering the chamber reduces the oxide to its maximum extent. O_2 is removed by pumping. The WS chamber exposes the reduced oxide to steam, in a countercurrent flow arrangement, to produce H_2 and reoxidize the oxide using a minimum amount of steam. Pressure separation along the flow path is accomplished by low gas permeability through the moving packed particle bed.

Next we describe a few main design challenges, and our solutions to them, associated with specific CPR2 elements.

1. Transferring heat to the oxide particles in TR1 and TR2 quickly and effectively. The small size of the CPR2 prohibits a falling particle approach because the freefall residence time is too short (<0.2 s). We note that this would not be a problem in a large scale system. The particles must therefore be exposed to radiation as a relatively slowly flowing bed, and the results of preliminary heat transfer experiments (see Figure 4a) indicate that the bed depth must be comparable to the particle dimensions. In addition to heat transfer into and within the bed, oxygen flow from a particle undergoing reduction must not be impeded as it makes its way out. To satisfy the above requirements, a thin layer of oxide will be moved through the irradiation zone on a horizontal ceramic plate. The plate will be actuated in a "stick slip" fashion at rates controlled by the operator.

2. Pumping oxygen from TR1 and TR2. Off-the-shelf roughing pumps, namely positive displacement pumps, are suitable but not ideal for the target pressures shown in Figure 3a because, under vacuum, they operate at

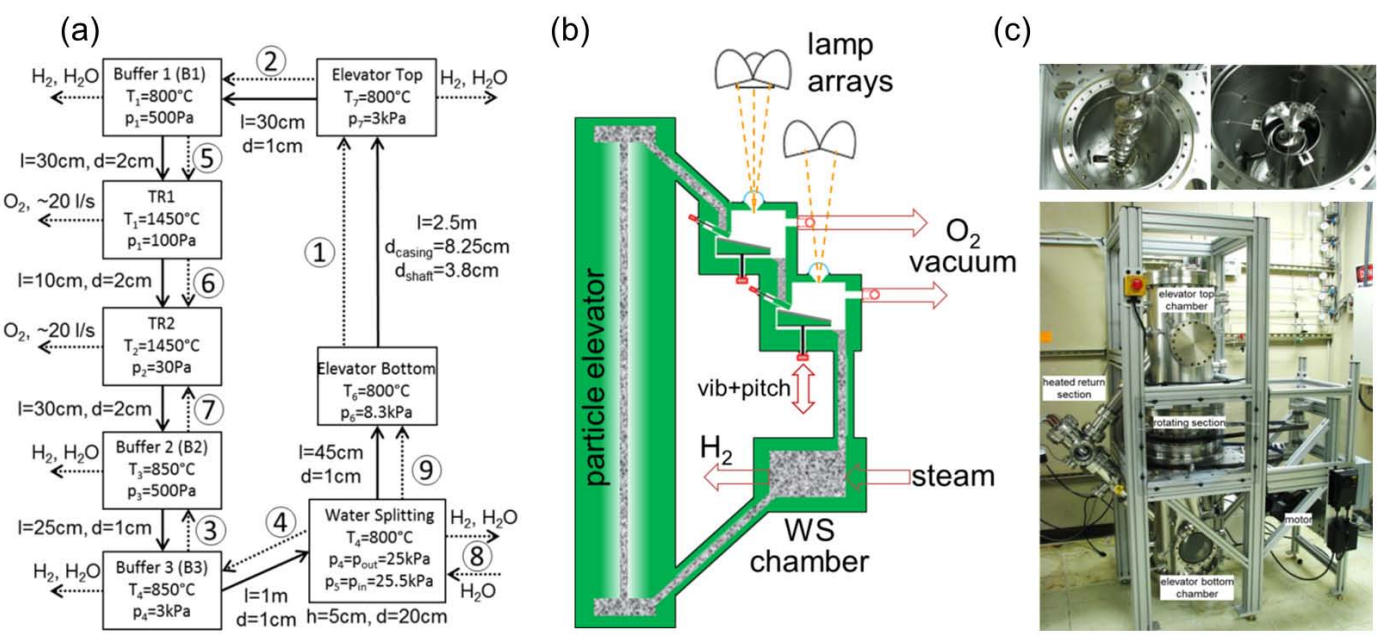

FIGURE 3. (a) CPR2 block diagram loosely resembles reactor geometry. Solid arrows indicate the direction of particle flow in a circular fashion throughout the reactor. Dashed arrows indicate gas flows, from higher to lower pressure elements, also labeled by circled numbers (1–9). Pressures shown are the result of detailed calculations, starting from the nominal input power, and a selection of pump size (pumping speed) for first thermal reduction chamber (TR1). The indicated dimensions (l = length, d = diameter) are those of the internal packed particle beds, not the physical dimensions of the exterior chambers and connecting elements. (b) A conceptual schematic of the CPR2 showing location of packed particle beds, solar lamp arrays, and main chambers. The pressure buffer chambers are not included in the drawing. (c) Picture of the particle elevator that will be incorporated into the CPR2. Top pictures show auger and casing elements as viewed from above.

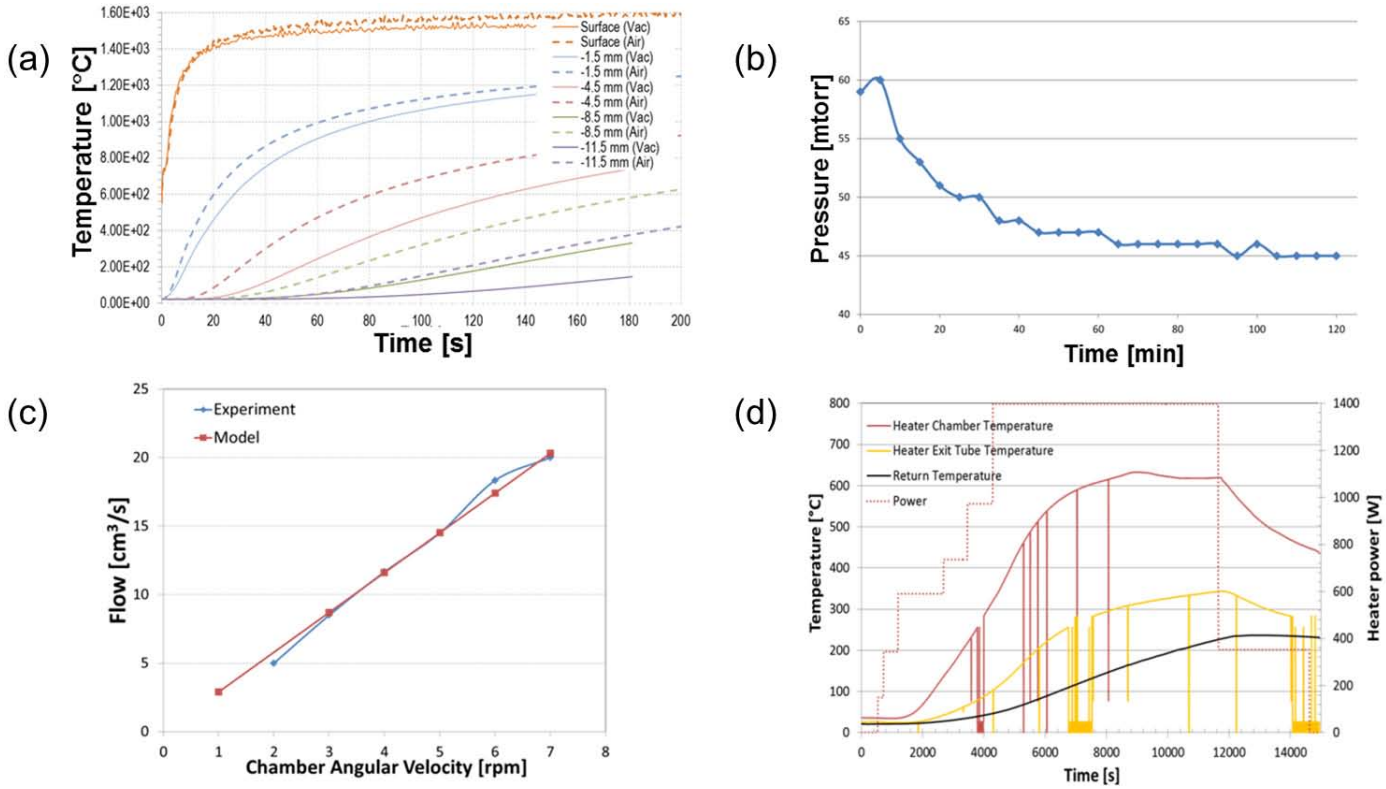

FIGURE 4. (a) Temperature measured in a stagnant bed of particles, as a function of time, during a heating test under solar simulated light in air and in rough vacuum. A pyrometer was used to measure surface temperature, thermocouples were used to measure temperature at indicated heights within the bed from 1.0–11.5 mm below the surface. The results indicate that vacuum and particle shading impede heat transfer to and within the bed. This must be accounted for in the CPR2 design (see text). (b) Pressure measured as a function of time during a room temperature test of the particle elevator pictured in Figure 3c. This result confirms rotary seal operation to be well within design specifications because 45 mtorr vacuum (~6 Pa) is 5x lower than CPR2 requirements (30 Pa). (c) Particle volumetric conveying rate measured as function of chamber angular velocity for particle elevator. Red line corresponds to a model with a conveying efficiency of 0.38. The conveying rate is well above the CPR2 design requirement even at low RPM. (d) Temperature and heater power measured as a function of time during high-temperature operation of the particle elevator at 25 Pa. The test lasted ~6 h, and achieved particle temperatures greater than 600°C. Spikes are due to intermittent gaps in data logging, not actual thermal fluctuations.

relatively low volumetric pumping speeds. Even though our novel cascading pressure design significantly reduces the pumping requirement, performance of existing small positive displacement pumps falls well outside the ideal for this application. Axial flow pumps that provide high flow speeds with modest initial compression are better matched to the CPR2, however, no suitably-sized axial flow pumps are available off the shelf. Therefore, the pumping speeds specified in Figure 3a are a result of compromises and will be accomplished using positive displacement pumps.

3. Ensuring sufficient steam flow throughout WS chamber. Steam must flow at ~0.3 L/s countercurrent to the oxide flow, while not inducing particle bed fluidization. This is a critical design feature of the CPR2, as the H_2O/H_2 ratio is vastly different between countercurrent and mixed flow, with the latter less efficient and requiring much more H_2O for reoxidation. The countercurrent, non-fluidized flow requirement is the main reason to use a large diameter, shallow bed (WS chamber dimensions shown in Figure 3a). Furthermore, for spherical particles, the ratio of the settling velocity to the minimum fluidization velocity is roughly 50. This ultimately constrains dimensions for all gas-flow chambers and connecting tubes.

4. Particle conveying and pressure separation. Moving particles under vacuum at high temperature is critical to the success of the CPR2. We are using a compact design called an Olds Lift™ to elevate oxidized particles exiting the WS chamber back up to TR1. This device, while inspired by a commercial system, was designed at Sandia to run under vacuum at high temperature. The data in Figures 4b and 4c show test results that confirm our custom built elevator can achieve the required vacuum operation and particle conveyance rate with considerable engineering margin. Preliminary flow test at high temperature, shown in Figure 4d, is also encouraging, especially since this test was conducted without thermal insulation in the elevator. In summary, conveying rates exceed CPR2 requirements by 10x, vacuum requirements by 5x, and we similarly expect

to meet or exceed thermal design requirements in the near future.

Thus far we have incorporated our extensive understanding of this process into the design of a 3 kW-scale reactor. When completed, the CPR2 will be used to evaluate all reactor functions, inclusive of continuous operation and hydrogen production under simulated solar radiation. Data collected from this instrument will be used to further refine reactor designs, and analytically up-scale Sandia's technology to a multi-MW centralized tower system.

CONCLUSIONS AND FUTURE DIRECTIONS

- Continue material discovery and optimization, develop thermodynamic and kinetic models of material performance as needed
- Produce ~100 kg of redox material for full scale CPR2 tests
- Fabricate components, assemble, and test CPR2 on a solar simulator and produce at least 3 liters of H_2 in eight continuous hours of operation
- Build systems models and conduct technoeconomic analysis of a 100 ton H_2/day plant

FY 2015 SELECTED PUBLICATIONS/ PRESENTATIONS

1. Stechel, E.B., Miller, J.E., "Concentrating Solar Thermochemical Fuels: Key Materials Issues for Commercial Viability and Scalability," In *20th International Conference on Solid State Ionics*; Materials Research Society: Keystone, CO, 2015.

2. Shanga, M., Tong, J., Sanders, M., McDaniel, A.H., O'Hayre, R., Chueh, W.C., "Screening Nonstoichiometric Perovskite Oxides for Solar Thermochemical Fuel Production," *submitted to Energy and Environmental Science* **2015**.

3. Muhich, C.L., Weston, K.C., Arifin, D., McDaniel, A.H., Musgrave, C.B., Weimer, A.W., "Extracting Kinetic Information from Complex Gas--Solid Reaction Data," *Industrial Engineering and Chemistry Research* **2015**, *54*, 4113–4122.

4. McDaniel, A., O'Hayre, R., Tong, J., Emery, A., Wolverton, C., "Optimizing Nonstoichiometric Perovskite Oxides for Solar Thermochemical Fuel Production," In *11th International Symposium on Ceramic Materials and Components for Energy and Environmental Applications*; American Ceramics Society: Vancouver, BC, Canada, 2015.

5. McDaniel, A., Ermanoski, I., "Benchmarking a Metal Oxide-Based Thermochemical Cycle for Solar Hydrogen Production," In *227th ECS Meeting*; The Electrochemical Society: Chicago, IL, 2015.

6. Lucero, B., Johnson, N., Stechel, E., McDaniel, A., Ermanoski, I., "Thermodynamic Systems-Level Analysis of Concentrating Solar Tower with Multiple Receivers and Metal Oxide Heat Transfer to Produce Pure Hydrogen," In *9th International Conference on Energy Sustainability*; American Society of Mechanical Engineers: San Diego, CA, 2015.

7. Ermanoski, I., "Maximizing Efficiency in Two-Step Solar-Thermochemical Fuel Production," *Energy Procedia* **2015**, *69*, 1731–1740.

8. Ermanoski, I., "Maximizing Efficiency in Two Step-Solar Thermochemical Fuel Production," In *9th International Conference on Energy Sustainability*; American Society of Mechanical Engineers: San Diego, CA, 2015.

9. Ermanoski, I., "Current and Future Status of Solar-Thermochemical Fuel Technology in the United States," *Journal of the Japan Institute of Energy* **2015**, *94* (3), 189–193.

10. Emery, A.A., Wolverton, C., "Discovery of Novel Perovskites for Solar Thermochemical Water Splitting from High-Throughput First-Principles Calculations," In *20th International Conference on Solid State Ionics*; Materials Research Society: Keystone, CO, 2015.

11. Barcellos, D., Tong, J., Sanders, M., McDaniel, A., O'Hayre, R., "Investigation on Nonstoichiometric Perovskite Oxides of $Sr_{1-x}La_xMn_{1-y}AlyO_3$ for Solar Thermochemical Hydrogen Production," In *20th International Conference on Solid State Ionics*; Materials Research Society: Keystone, CO, 2015.

12. Ermanoski, I., "Maximizing Efficiency in Two Step-Solar Thermochemical Fuel Production," In *SolarPaces*; Solar Power and Chemical Energy Systems managed under IEA: Beijing, China, 2014.

REFERENCES

1. N.P. Siegel, J.E. Miller, I. Ermanoski, R.B. Diver, and E.B. Stechel, *Ind. Eng. Chem. Res.*, **52**, 3276–3286 (2013).

2. W.C. Chueh and S.M. Haile, *Philos. Trans. R. Soc. Math. Phys. Eng. Sci.*, **368**, 3269–3294 (2010).

3. R.B. Diver, J.E. Miller, M.D. Allendorf, N.P. Siegel, and R.E. Hogan, *J. Sol. Energy Eng.*, **130**, 041001(1)–041001(8) (2008).

4. A.H. McDaniel, E.C. Miller, D. Arifin, A. Ambrosini, E.N. Coker, R.O'Hayre, W.C. Chueh, and J. Tong, *Energy Environ. Sci.*, **6**, 2424–2428 (2013).

5. J.E. Miller, A.H. McDaniel, and M.D. Allendorf, *Adv. Energy Mater.*, **4**, 1300469 (2014).

6. I. Ermanoski, N.P. Siegel, and E.B. Stechel, *J. Sol. Energy Eng.*, **135**, 031002 (2013).

7. J.R. Scheffe, A.H. McDaniel, M.D. Allendorf, and A.W. Weimer, *Energy Environ. Sci.*, **6**, 963 (2013).

II.C.2 Flowing Particle Bed Solarthermal Redox Process to Split Water

Alan W. Weimer (Primary Contact),
Charles Musgrave, Brian Ehrhart,
Ibraheam Al-Shankiti, Christopher Muhich,
Amanda Hoskins, Samantha Miller, Barbara Ward
University of Colorado Boulder
Campus Box 596
Boulder, CO 80309-0596
Phone: (303) 492-3759
Email: alan.weimer@colorado.edu

DOE Manager
Katie Randolph
Phone: (720) 356-1759
Email: Katie.Randolph@ee.doe.gov

Contract Number: DE-EE0006671

Subcontractor
National Renewable Energy Laboratory (NREL)
Golden, CO

Project Start Date: September 1, 2014
Project End Date: August 31, 2017

Overall Objectives

The University of Colorado's overall objective is to design and test individual components of a novel flowing particle solarthermal water splitting (STWS) system by optimizing active redox materials, reactor containment materials, and reactor design, with the ultimate goal of demonstrating our technology by producing three standard liters of hydrogen in eight hours on-sun in a prototype fluidized particle reactor.

Fiscal Year (FY) 2015 Objectives

- Demonstrate activity of initial formulation spray dried redox materials
- Finish construction and demonstrate operation of lab-scale flowing particle bed redox system
- Collaborate closely with National Science Foundation (NSF) materials discovery "sister" project to screen improved active materials
- Work with NREL to ready reactor for on-sun testing
- Design test system for reactor containment materials evaluation
- Update process model and Hydrogen Analysis (H2A) model to reflect experimental progress toward DOE goals

Technical Barriers

This project addresses the following technical barriers from the Hydrogen Production section of the Fuel Cell Technologies Office Multi-Year Research, Development, and Demonstration Plan:

(S) High-Temperature Robust Materials

(W) Materials and Catalysts Development

(X) Chemical Reactor Development and Capital Costs

Technical Targets

Using experimental results from our materials testing and thermodynamic modeling, a process model of a 50,000 kg H_2/day industrial-scale production plant, a detailed solar field model, and DOE's H2A techno-economic analysis program, our performance in the DOE technical target categories is projected, outlined in Table 1.

TABLE 1. Progress toward Meeting Technical Targets for Solar-Driven High-Temperature Thermochemical Hydrogen Production

Characteristics	Units	2015 Target	2020 Target	CU Boulder 2015 Status
Solar-Driven High-Temperature Thermochemical Cycle Hydrogen Cost	$/kg	14.80	3.70	14.67
Annual Reaction Material Cost per TPD H_2	$/yr-TPD H_2	1.47 M	89 K	62.7 K*
Solar to Hydrogen (STH) Energy Conversion Ratio	%	10	20	9.3
1-Sun Hydrogen Production Rate	kg/s per m^2	8.1×10^{-7}	1.6×10^{-6}	7.5×10^{-7}

*Assuming reaction material replacement lifetime of 1 year
TPD - Tonnes per day

FY 2015 Accomplishments

- The project manufactured and characterized spherical spray dried doped-hercynite active particles. Preliminary measurements suggest that spray dried active materials can produce >150 µmol H_2/g active material.
- Construction and start-up of lab-scale flowing particle redox test system capable of cycling >1 g spray dried active particles is nearly complete.
- The team completed an upgrade and successfully tested a laboratory test system to incorporate new, state-of-the-art mass spectrometers and more precise steam feeders.

- The scaled-up process model was expanded to include more detailed thermodynamic and kinetic models of active material performance and improved solar field and reactor design.
- The project team collaborated with NSF sister project to screen 1,678 of the 2,156 potential binary water splitting active materials in silico. Of those, 420 perovskites and 260 spinels were found to show potential for STWS.

✧ ✧ ✧ ✧ ✧

INTRODUCTION

In order to meet DOE targets for economical and efficient solarthermal hydrogen production at the commercial scale, advances in active redox materials and reactor fabrication materials need to be made. Ideal STWS materials have high H_2 production capacity, low thermal reduction temperatures, fast reaction kinetics, reduction enthalpies on the order of the water splitting enthalpy, are solid in both oxidized and reduced forms, operate isothermally or near-isothermally, and are highly stable over hundreds of thousands of cycles. We will develop new materials which possess the materials properties outlined above in conjunction with project collaborators. Initial materials development will be based on the doped-hercynite cycle (Red: $Co_{0.4}Fe_{0.6}Al_2O_4 \rightarrow Co_{0.4}Fe_{0.6}Al_2O_{4-\delta} + \delta/2\ O_2$) and perovskite structure (Red: $ABO_3 \rightarrow ABO_{3-\delta} + \delta/2\ O_2$) materials which have shown promise in reaching materials targets. The nature of efficient flowing particle reactors requires that the material is formed into particles that are robust, attrition resistant, and possessing of rapid heat and mass transfer properties. Therefore, we will develop particle formation procedures and formulations based on spray drying technology so that the particles are flowable, reactive, and robust. Additionally, we will evaluate reactor containment materials because the active redox materials must be compatible with the reactor materials of construction at the high temperatures at which water splitting occurs. In the end, we will produce reactor ready materials with demonstrated H_2 productivities to drive the field closer to meeting DOE's technical targets, as determined from our process model and techno-economic analysis.

APPROACH

A highly efficient STWS reactor must maximize heat flux to the reactive materials, and optimize mass transfer while minimizing sources of heat loss in a scalable and mechanically sound design. We are designing a novel beam-up, fluidized particle based reactor which maximizes heat flux to the reactor due to its beam-up configuration, and minimizes heat and mass transfer limitations due to the fluidized particles. The particles are moved through the reduction and oxidation zones by gravity and in entrained steam flow, respectively. The lack of moving parts at temperatures over 1,000°C greatly reduces the risk of critical reactor failure. The isothermal (or near-isothermal) nature of the reactor design minimizes the need to reheat material from the oxidation temperature to the reduction temperature found in many STWS designs. The reduction step will either be carried out at low pressure with vacuum pumping or using inert sweep gas to achieve the low O_2 partial pressures necessary for the reduction reaction.

In this project we will examine the individual components of the reactor system (kinetic and thermodynamic behavior of spray dried redox materials in a fluidized system, performance of coated reactor containment materials, effect of vacuum pumping vs. inert gas flow for O_2 removal following reduction, and solar concentration modeling) to determine their individual feasibilities and efficiencies. Using this information we will construct and operate a solar powered system producing three liters of H_2 in an eight-hour day. By the end of the project, we will have tested and modeled the individual portions of the reactor system and combined them into an overall system Aspen model which will be evaluated via technoeconomic analysis showing that we are capable of meeting the <$2/kg H_2 at 50,000 kg H_2/day ultimate project goals.

RESULTS

Progress on the development of active redox materials during this fiscal year has focused on thermodynamic modeling of hercynite materials, process efficiency calculations, synthesizing and characterizing preliminary spray dried particles, and building research systems. Generating spherical particles is important for promoting flowability and attrition resistance of the active materials, and having robust particles that do not degrade during fluidization is key to maintaining low active material replacement costs. Figure 1 shows scanning electron microscope images of spray dried hercynite particles. They appear spherical, with a particle size distribution around 10 µm. Spray dried particles have also been characterized using X-ray diffraction and elemental analysis to verify that they poses the desired crystal structure and stoichiometric composition. Spray dried particles are currently being tested for hydrogen production activity, and we are on track to meet our go/no-go target to produce more than 150 µmol H_2/g of active material by the end of September 2015.

Activity testing is also ongoing for new candidate active materials identified by our NSF STWS materials "sister" project. In order to make computational evaluations of candidate materials, a criteria based on the reaction thermodynamics was established to analyze the reaction mechanism and predict STWS behavior. The initial experimental work performed this year on spinel aluminate

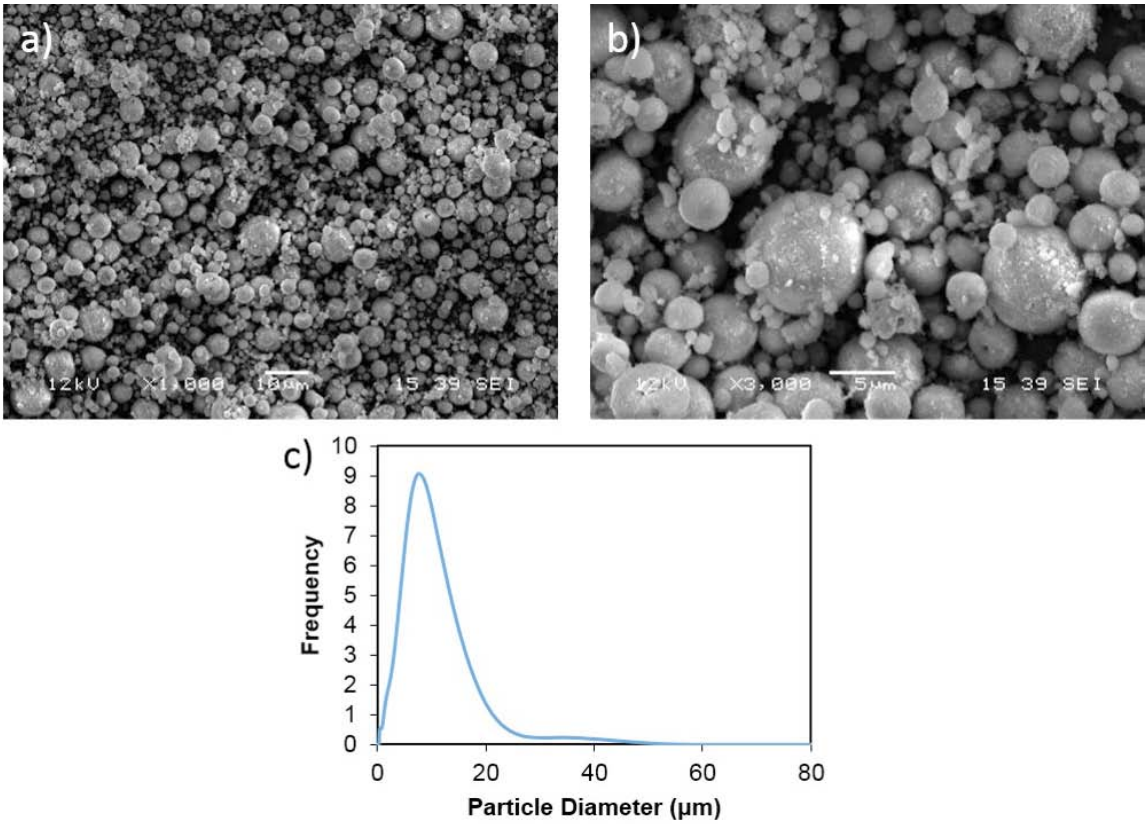

FIGURE 1. Scanning electron microscope images of preliminary spray dried hercynite particles at magnifications of (a) 1,000x and (b) 3,000x with (c) the particle size distribution shown

materials indicates that density functional theory can be used to accurately predict redox properties, and thus STWS behavior, of metal oxides based on their reduction enthalpies.

In addition to the thermodynamic modeling of active material behavior, a more general thermodynamic model for redox cycle efficiency has been developed this year. This model calculates heat requirements and benefits within the system and compares different operating conditions and assumptions. The model compares the chemical energy contained in a mole of hydrogen to the solar energy needed to make it; this ratio is the STH efficiency, or η_{STH}. The results of interest have been a comparison of vacuum and an inert sweep gas for the reduction reaction. The STH efficiency values have been calculated for both the vacuum pumping and recycled inert sweep gas cases, and the results are shown in Figure 2.

As can be seen, the efficiency values for vacuum pumping are drastically lower than for the recycled inert gas case. This is because the pump work increases exponentially at lower pressures, while simultaneously becoming exponentially less efficient at lower pressures. This means that the pump work increases dramatically at the pressure assumed in Figure 2 (10 Pa). By contrast, the recycled inert gas sweep looks promising, with optimal efficiency values of over 30%. This is consistent with work by others who have also suggested inert gas sweep [1].

The 2015 fiscal year was the start-up year for this three-year project, and has thus seen numerous improvements to our existing lab test system. We met our first quarter milestone of purchasing new, more precise steam feeders and upgraded quadrupole mass spectrometers for the four redox test systems dedicated to this project. The new equipment has been installed in the stagnation flow reactor, where it is producing improved quality mass spectrometer data during redox runs of manufactured spray dried hercynite particles.

Work is in progress to complete the construction of the electrically heated particle flow redox test system, which will enable us to test the fluidization and redox behavior of spray dried particles under various reactor configurations. This test stand will allow us to run the reduction reaction either at a reduced pressure, or with an inert sweep gas using a high temperature oxygen transport membrane, allowing for a direct theoretical/experimental comparison between these alternate O_2 removal processes. The power required to run the two electrical furnaces has been installed. A gas flow system with mass flow controllers, pressure controllers and pneumatic valves has been installed. Work is in progress to integrate the reactor system with the computer through

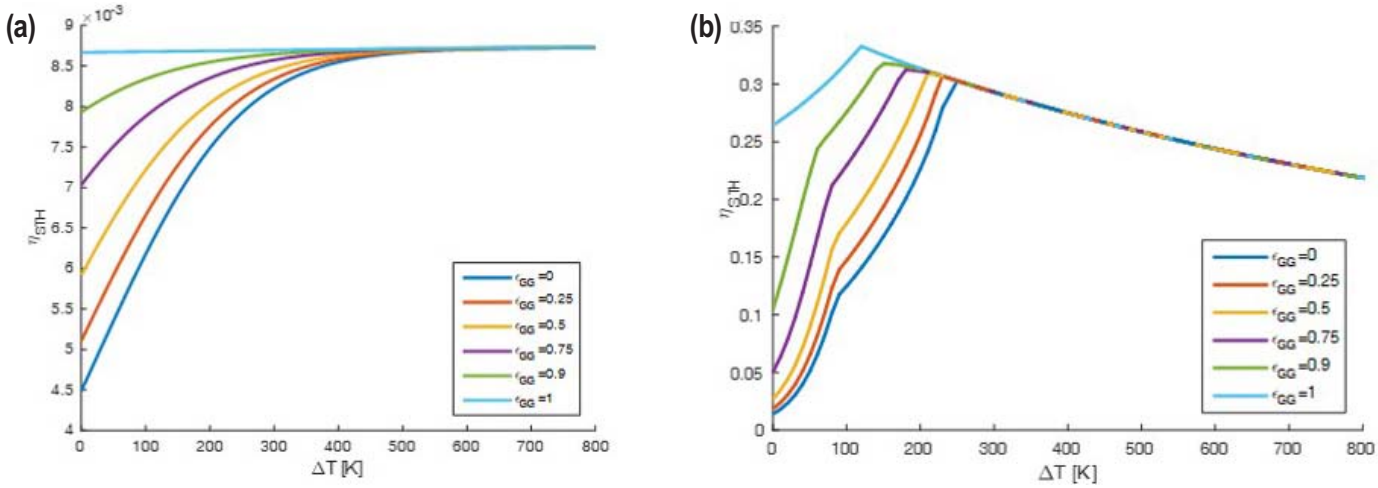

FIGURE 2. STH efficiency values for a system using ceria using (a) a vacuum pump and (b) a recycled inert sweep gas. Both sets of values are given for various ΔT values (difference between reduction and oxidation temperatures) and ε_{GG} values (gas heat recuperation effectiveness).

FIGURE 3. Photograph of the existing state of the flowing particle reactor test system

National Instruments data acquisition system (DAQ). The LabVIEW code to control and automate the reactor system has been completed and it will be tested once the interface between the DAQ system and equipment is finished. The current hood setup with mounted reactors, the gas flow system, the new downstream mass spectrometer, steam feeder, and vacuum pump is shown in Figure 3.

CONCLUSIONS AND FUTURE DIRECTIONS

- Preliminary spray dried redox particles are spherical and form material composition of interest. Research in the next year will focus on assessing and improving the activity and flowability of spray dried particles.
- Computational thermodynamic models can accurately predict H_2 production capacity of materials, which has been validated experimentally. The Musgrave group at the University of Colorado Boulder has been awarded an NSF grant to continue materials discovery screening using these computational techniques; and in the following year, we will conduct tests to experimentally validate the material models and identify new materials of interest.
- Reactor test system upgrades carried out this year will improve data collection in 2016.
- Thermodynamic efficiency calculations predict that reducing active materials in an inert gas sweep will achieve a higher STH efficiency than vacuum reduction.
- A flowing particle test system will allow for comparison of different system configurations and is on track for completion by September 2015. It will be used to compare the performance of vacuum and inert gas O_2 removal methods in the coming year.
- A focus on robust reactor containment materials will launch in FY 2016. We will be depositing alumina and mullite protective coatings on silicon carbide using atomic layer deposition (ALD) to assess the feasibility and reactivity of protective ALD coatings on potential reactor materials.
- In the next fiscal year, we will construct and demonstrate an on-sun redox fluidized bed test system at NREL's high flux solar furnace facility in order to begin assessing our technologies under concentrated sunlight.
- Experimental results will continue to be incorporated into our commercial scale process model and technoeconomic calculator to monitor the effects of

experimental progress on our progress toward overall efficiency and economic goals.

FY 2015 PUBLICATIONS/PRESENTATIONS

Publications

1. Muhich, Christopher L., Brian D. Ehrhart, Ibraheam Alshankiti, Barbara J. Ward, Charles B. Musgrave, and Alan W. Weimer. 2015. "A Review and Perspective of Efficient H_2 Generation via Solar Thermal Water Splitting." *Wiley Interdisciplinary Reviews: Energy and Environment*, doi: 10.1002/wene.174.

2. Muhich, Christopher L., Kayla C. Weston, Darwin Arifin, Anthony H. McDaniel, Charles B. Musgrave, and Alan W. Weimer. 2015. "Extracting Kinetic Information from Complex Gas-Solid Reaction Data." *ACS Industrial & Engineering Chemistry*, 54, 4113−4122.

Presentations

1. Brian D. Ehrhart, Christopher L. Muhich, Ibraheam Alshankiti, and Alan W. Weimer. 2014. "Solar Thermochemical Hydrogen Production Efficiency with Kinetic Limitations." Presented at American Institute of Chemical Engineers (AIChE) Annual Meeting, Atlanta, GA, November.

2. Christopher L. Muhich, Kayla Weston, Darwin Arifin, Anthony H. McDaniel, Eric Coker, Brian D. Ehrhart, Vanessa Witte, Charles B. Musgrave, and Alan W. Weimer. 2015. "The Mechanism of the Doped-Herycnite Cycle for Solar-thermal Water Splitting." Presented at ACS Spring Meeting, Denver, CO, March.

3. Christopher L. Muhich, Kayla Weston, Brian D. Ehrhart, Vanessa Witte, Darwin Arifin, Anthony H. McDaniel, Eric Coker, Charles B. Musgrave, and Alan W. Weimer. 2014. "The Chemistry and Thermodynamics of the Herycnite Cycle Solar-thermal Water Splitting Reaction." Presented at AIChE Annual Meeting, Atlanta, GA, November.

4. Christopher L. Muhich, Brian D. Ehrhart, Kayla Weston, Ibraheam Alshankiti, Darwin Arifin, Anthony H. McDaniel, Charles B. Musgrave, and Alan W. Weimer. 2014. "Extracting Kinetic Information from Complex Gas-solid Reaction Data: the Kinetics of Hercynite Materials for Solar Thermal CO_2 Splitting." Presented at AIChE Annual Meeting, Atlanta, GA, November.

5. Brian D. Ehrhart, Christopher L. Muhich, Ibraheam Alshankiti, and Alan W. Weimer. 2015. "Effect of Different Methods for Achieving Low Oxygen Partial Pressure on Solar Thermochemical Hydrogen Production Efficiency." Presented at American Society of Mechanical Engineers (ASME) Power & Energy 2015 – ASME 9th International Conference on Energy Sustainability.

6. Christopher L. Muhich, Brian D. Ehrhart, Ibraheam Al-Shankiti, Barbara J. Ward, Samantha L. Miller, Charles M. Musgrave, and Alan W. Weimer. 2015. "Needed Research Focus for Achieving Cost-effective and Reliable Solar-thermal Water Splitting." Presented by A.W. Weimer at the 227th Meeting of the Electrochemical Society, Chicago, IL, May 28.

7. Christopher L. Muhich, Brian D. Ehrhart, Ibraheam Al-Shankiti, Barbara J. Ward, Samantha L. Miller, Charles M. Musgrave, and Alan W. Weimer. 2015."Near-isothermal Doped-hercynite Redox Cycle for Solar-thermal Water Splitting." Presented by A.W. Weimer at the 227th Meeting of the Electrochemical Society, Chicago, IL, May 27.

REFERENCES

1. Krenzke, P.T. and J.H. Davidson. 2015. "On the Efficiency of Solar H_2 and CO Production via the Thermochemical Cerium Oxide Redox Cycle: The Option of Inert-Swept Reduction." *Energy & Fuels*. **29**(2): 1045-1054.

II.C.3 Electrolyzer Component Development for the HyS Thermochemical Cycle

William A. Summers (Primary Contact),
Héctor Colón-Mercado, Maximilian Gorensek,
Claudio Corgnale, Mark Elvington
Savannah River National Laboratory (SRNL)
SRS, Building 999-2W
Aiken, SC 29808
Phone: (803) 617-8590
Email: bill.summers@src.energy

DOE Manager
Eric Miller
Phone: (202) 287-5829
Email: Eric.Miller@ee.doe.gov

Subcontractor
Savannah River Consultants, Aiken, SC

Project Start Date: June 1, 2013
Project End Date: Project continuation and direction determined annually by DOE

Overall Objectives

- Develop highly efficient process designs for coupling the hybrid sulfur (HyS) thermochemical process with a concentrated solar energy system
- Demonstrate sulfur dioxide (SO_2)-depolarized electrolysis (SDE) using improved electrocatalysts and high temperature proton exchange membranes that permit high efficiency hydrogen production

Fiscal Year (FY) 2015 Objectives

- Identify and optimize design options for a solar-heated HyS process, including consideration of both thermal energy storage and chemical energy storage
- Perform system design and analysis, develop Aspen Plus™ process flowsheet models, material and energy balances and calculated plant performance and efficiency
- Estimate capital costs for a commercial plant and utilize the Hydrogen Analysis (H2A) tool to determine projected hydrogen production costs for various design and operating scenarios
- Construct and operate a pressurized button cell test facility (PBCTF) capable of testing advanced SDE designs at temperatures up to 120°C and pressures up to 5 bar
- Develop technical solutions to improving the performance, lifetime and cost effectiveness of the SDE, including identification of improved electrocatalysts and characterization of at least three candidate high temperature proton exchange membranes
- Demonstrate high temperature, high pressure SDE operation using advanced membranes with at least a 50 mV improvement over performance with the baseline Nafion® proton exchange membrane

Technical Barriers

This project addresses the following technical barriers from the Hydrogen Production section (3.1.5) of the Fuel Cell Technologies Office Multi-Year Research, Development, and Demonstration Plan:

(T) Coupling Concentrated Solar Energy and Thermochemical Cycles

(W) Materials and Catalyst Development

(X) Chemical Reactor Development and Capital Costs

(AB) Chemical and Thermal Storage

(AC) Solar Receiver and Reactor Interface Development

Technical Targets

This project is conducting system design studies and electrolyzer development and testing in order to improve the performance and lower the capital and operating costs for the HyS thermochemical cycle. Detailed flowsheet analysis and mass and energy balances are used to estimate potential overall system efficiency. Capital cost estimates used in the H2A analysis for hydrogen production costs are based on previous work funded by the DOE Office of Nuclear Energy combined with solar system cost estimates based on goals for the Office of Energy Efficiency & Renewable Energy Solar Program. Electrolyzer performance represents current low temperature (<90°C) operation; higher temperature electrolyzer operation is a goal of the program and is expected to significantly improve electrolyzer efficiency. Table 1 shows how this project contributes to the technical targets of the DOE Fuel Cell Technologies Office for solar-driven high temperature thermochemical hydrogen production.

FY 2015 Accomplishments

Accomplishments during the current project period include:

TABLE 1. Progress towards Meeting Technical Targets for Solar-Driven High Temperature Thermochemical Hydrogen Production

Characteristic	Units	2015 Target	2020 Target	SRNL Status (July 2015)	SRNL 2020 Projections
Solar-Driven Hydrogen Cost	$/kg	14.80	3.70	8.01	3.61
Solar-to-Hydrogen (STH) Energy Conversion Ratio	%	10	20	10.5	19.5
SDE Operating Temperature	°C	120	120	90	120
SDE Voltage at 500 mA/cm^2	mV	720	600	770	600

- Conducted flowsheet analyses and tradeoff studies to identify preferred solar-driven HyS system design configuration
- Completed full Aspen Plus™ flowsheet and overall process efficiency determination for baseline solar-driven HyS process design
- Constructed and commissioned new PBCTF to permit testing of membrane electrode assemblies (MEAs) using advanced high temperature membranes and improved electrocatalysts
- Redesigned and fabricated improved anode flow field for small-scale PBCTF to improve flow distribution and more closely match interdigitated design used in previous larger single cell test facility
- Characterized performance of baseline MEAs with Nafion® membranes
- Utilized DOE H2A tool to estimate hydrogen production cost for solar-driven HyS process for current status (2015) and projected calendar year 2020 conditions

✧ ✧ ✧ ✧ ✧

INTRODUCTION

Thermochemical water splitting processes produce hydrogen by using heat to drive a series of linked chemical reactions that result in water being split into separate hydrogen and oxygen streams with all the intermediate chemicals being recycled. Therefore, the inputs are simply water and heat, and the products are hydrogen and oxygen plus waste heat. Most thermochemical processes use relatively high temperature heat (in excess of 900°C), which can be generated by either high temperature nuclear reactors or concentrated solar energy.

The HyS process is one of the most advanced of the thermochemical water-splitting cycles; each of the major reaction steps has been experimentally validated and detailed system designs have been created. However, further process design work is necessary for use with solar energy, and key technical barriers remain to be overcome. HyS is the only practical two-step thermochemical cycle with all fluid reactants. In the first step sulfuric acid is thermally decomposed at high temperature (>800°C) to produce sulfur dioxide (SO_2) and oxygen. In the second step the SO_2 is used to depolarize the anode of a water electrolyzer, resulting in the production of hydrogen at the cathode and sulfuric acid (which is sent to the decomposer) at the anode. The overall reaction is the splitting of water into H_2 and O_2. The electrolyzer, known as the SDE, requires only about one-third as much electricity as a conventional water electrolyzer.

APPROACH

Much of the previous system design work on the HyS process was based on the use of heat from nuclear reactors, while the current work focuses on the use of solar energy. The key experimental work relates to development of the SDE. SRNL's approach is to build on prior experience gained through development of the nuclear-driven HyS process and to leverage in-house expertise in hydrogen technology and electrochemistry to verify and improve the SDE. The project is divided into two main tasks: (1) System Design and Analysis and (2) Electrolyzer Development and Testing. The goals of Task 1 are to utilize modelling and flowsheet analyses to develop efficient and cost effective HyS plant designs based on the use of concentrated solar power. Both direct and indirect solar heating of the high temperature acid decomposition step will be analyzed in addition to the use of both thermal energy storage and chemical energy storage. The focus of the research on the SDE is to improve performance by developing better electrocatalysts and increasing the cell's operating temperature from the 70–90°C range to 120–130°C. The higher temperature requires replacing the baseline Nafion® proton exchange membrane with new high temperature membranes. A new PBCTF will be built to permit the higher temperature testing and to facilitate rapid characterization of membrane candidates.

RESULTS

Several alternative configurations for the solar HyS flowsheet were studied. These included the following options:

- Gaseous-fed or liquid-fed electrolyzer
- Continuous or diurnal operation
- Thermal versus chemical energy storage
- Use of a secondary heat transfer fluid for the acid decomposer
- Integrated or separate operation of process sections (electrolysis and acid decomposition).

In addition, three different design options were selected for the solar receiver as follows:

- Falling particle receiver
  - Uses heated "sand" for thermal energy storage
  - Allows for continuous 24 h acid decomposition operation
- Cavity receiver with tubular heat exchanger
  - Secondary heat transfer fluid (e.g., He) heated in receiver
  - Daytime acid system operation combined with chemical energy storage
- Direct solar-heated acid vaporizer and decomposer
  - Daytime acid system operation combined with chemical energy storage.

The SO_2-depolarized electrolyzer can be operated with anode feed consisting of either vapor (SO_2 and H_2O) or liquid (SO_2 dissolved in sulfuric acid); both result in liquid H_2SO_4 anode product. Previous testing showed similar SDE performance for the two options, but they require different flowsheet designs to close the cycle and integrate the SDE with the solar acid decomposer. Extensive flowsheet analysis and trade studies were conducted to evaluate the two approaches, resulting in the conclusion that the liquid feed SDE approach is preferred.

An Aspen Plus™ flowsheet for the baseline system design using the Falling Particle Receiver, thermal energy storage and a liquid-fed electrolyzer was completed. Mass and energy balances were calculated and utilized to determine process efficiency. The overall STH conversion ratio for near-term design conditions was 10.5%; the 2020 STH was 19.5%. Efficiency assumptions are shown in Table 2. Additional improvements in the process flowsheet and the SDE performance are expected to result in the long-term STH exceeding the DOE goal of 20.0%. Hydrogen production cost estimates using the DOE H2A program resulted in near-term (2015) costs of $8.01 per kilogram and year 2020 costs of $3.61 per kilogram, exceeding DOE goals.

TABLE 2. Baseline Solar HyS Performance Summary

Plant Section	2015 Status	2020 Projections
Heliostat Field Efficiency	45%	55%
Solar Receiver Efficiency	85%	90%
Thermal Energy Storage Efficiency	95%	95%
Solar Electric Generation Efficiency	15%	22%
SDE Electrolyzer Voltage	770 mV	600 mV
Thermal Input to Acid Decomposition (from Aspen Plus™ Flowsheet)	477 kJ/mol	342 kJ/mol
Solar Input to Field for Heat	1,247 kJ/mol	691 kJ/mol
Solar Input for Electricity	1,049 kJ/mol	548 kJ/mol
Solar-to-Hydrogen Conversion Ratio	**10.5%**	**19.5%**

Accomplishments for Task 2, Electrolyzer Development and Testing, included the final assembly and commissioning of the PBCTF, fabrication and testing of MEAs, procurement of samples of several high temperature membranes, and redesign of the PBCTF electrolyzer, including a new flow field. Figure 1 shows the completed PBCTF. Membrane electrode assemblies for initial testing in the PBCTF were prepared using a Nafion® 115 proton exchange membrane,

FIGURE 1. Photograph of pressurized button cell test facility

with Tanaka Kikinzoku Kogyo Company (TKK) platinized carbon electrocatalyst for both the anode and cathode. These MEAs were used to determine the baseline SDE performance, with temperatures up to 90°C, the limit of both the Nafion® membrane and the current anolyte feed pump. A new anolyte pump, capable of operation up to 130°C and 10 bar, was received and will be installed for later high temperature cell testing.

Initial MEA testing indicated a problem with the introduction of anolyte feed (SO_2 saturated sulfuric acid) into the small (2 cm^2) circular button cell, resulting in a large pressure drop and poor flow distribution. Extensive SDE testing had been performed previously using larger (60 cm^2) rectangular MEAs with a linear interdigitated flow field. A new flow field was designed and fabricated for the PBCTF, resulting in improved performance similar to that of the larger, rectangular electrolysis cell. Test results are shown in Figure 2. The tests were performed in water and in 30 wt% sulfuric acid. The data was collected at temperatures between 60ºC and 90ºC. As it can be observed, the performance improves as a function of temperature. This result is expected since the kinetic overpotential loss is reduced as temperature (and the resulting reaction rate) is increased. This result is paramount in utilizing advanced high temperature membranes, since operating at elevated temperature necessitates the use of non-Nafion®-based proton exchange membranes. At temperatures above 80°C, Nafion® begins to dehydrate and its mechanical properties are reduced. This significantly lowers the ionic conductivity, rendering it impractical for efficient SDE use. Therefore, alternative high temperature membranes have been selected for potential application in the HyS electrolyzer. These membranes are required to have a combination of good chemical stability (resistant to H_2SO_4 corrosion), high ionic conductivity at high temperature (>120°C), and low SO_2 flux. Advanced membranes for testing include: sulfonated-diels-alder-poly-phenylene Sandia National Laboratories, sulfonated perfluorocyclobutyl aryl ether block copolymer (BPVE-6F, Clemson University), and a new generation of H_2SO_4-doped polybenzimidazole University of South Carolina and BASF. Future work will include testing these next generation MEAs at temperatures up to 130ºC.

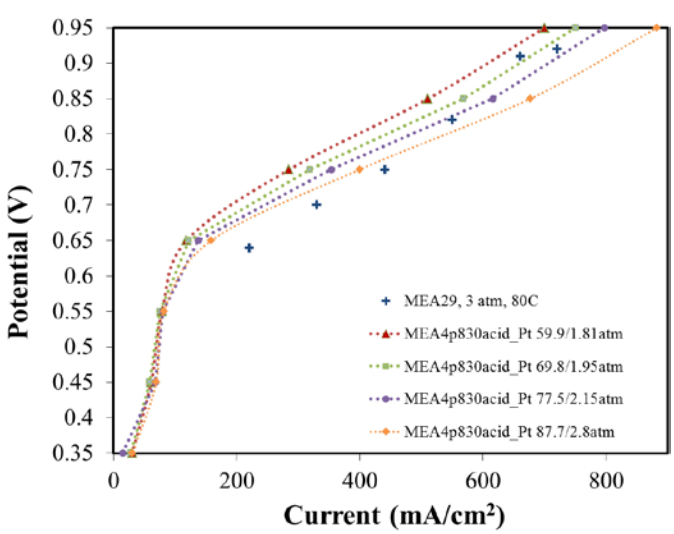

FIGURE 2. Electrolyzer performance for MEAs with Nafion® membranes in 30 wt% acid at various temperatures. MEA29 corresponds to previous large-scale test performance.

CONCLUSIONS AND FUTURE DIRECTIONS

Work this year has resulted in the following conclusions:

- The baseline solar HyS design meets DOE's goals for hydrogen production cost and solar-to-hydrogen conversion ratio.
- The baseline system design consists of the falling particle receiver, thermal energy storage, a liquid-fed SDE, and continuous (24/7) hydrogen production.
- The PBCTF with the modified flow field provides performance consistent with previous larger-scale tests and can be used to establish the baseline Nafion® performance.
- SDE performance improves with increasing temperature; new high temperature proton exchange membranes are necessary for tests above 90°C.

Future work will include the following:

- Completion of trade studies for the remaining receiver designs and process design options
- Updating of capital and operating costs for the baseline system design and preparation of a final hydrogen production cost estimate using the H2A program
- Modelling of the acid decomposition reactor based on the "bayonet" design concept
- Fabrication and testing of MEAs with at least three high temperature membranes and various electrocatalyst compositions in the PBCTF at 70–90°C
- Upgrading the PBCTF with the installation of the high temperature anolyte pump, followed by MEA testing at temperatures of 120–130°C
- Demonstration of MEA performance that exceeds the Nafion® baseline performance by ≥50 mV at a current density of 500 mA/cm^2.

FY 2015 PUBLICATIONS/PRESENTATIONS

1. William A. Summers, Maximilian Gorensek, and Hector Colon-Mercado, "Electrolyzer Component Development for the HyS Thermochemical Cycle, Project PD096," DOE EERE Fuel Cell Technologies Office, 2015 Annual Merit Review and Peer Evaluation, Arlington, VA, June 8–15, 2015.

II.C.4 High Efficiency Tandem Absorbers for Economical Solar Hydrogen Production

Todd G. Deutsch (Primary Contact), John A. Turner, James L. Young, Henning Döscher, Heli Wang
National Renewable Energy Laboratory
15013 Denver West Parkway
Golden, CO 80401
Phone: (303)275-3727
Email: Todd.Deutsch@nrel.gov

DOE Manager
David Peterson
Phone: (720) 356-1747
Email: David.Peterson@ee.doe.gov

Subcontractors
- University of Nevada Las Vegas, Las Vegas, NV (XGB-2-11673-01)
- University of Hawaii, Honolulu, HI (XGJ-5-52227-01)

Project Start Date: October 2014
Project End Date: Project continuation and direction determined annually by DOE

Overall Objectives

- Develop a semiconductor-based, solar-driven water splitting photoelectrochemical (PEC) device with greater than 20% solar-to-hydrogen (STH) efficiency and several thousand hours of stability under normal operating conditions
- Incorporate components that can be fabricated cost-effectively and are straightforward to scale up such that a plant scaled to 50,000 kg H_2 per day can achieve an estimated production cost of $1 to $2 per kilogram hydrogen using only sunlight and water as feedstocks
- Demonstrate a prototype photoreactor that produces 3 L of standard hydrogen within an 8-hour period under moderate solar concentration (~10x)

Fiscal Year (FY) 2015 Objectives

- Design tandem III-V semiconductor structures with lower bandgaps than $GaInP_2$/GaAs, 1.8 eV and 1.4 eV, respectively, that have the potential to push the boundaries on achievable STH efficiencies
- Demonstrate 15% STH at short circuit, establishing a new efficiency record
- Demonstrate surface modification for passivation against corrosion improves durability for lower bandgap III-V semiconductor electrodes at high current densities

Technical Barriers

This project addresses the following technical barriers from Section 3.1 (Hydrogen Production) of the Fuel Cell Technologies Office Multi-Year Research, Development, and Demonstration (MYRDD) Plan:

(AE) Materials Efficiency – Bulk and Interface

(AF) Materials Durability – Bulk and Interface

(AG) Integrated Device Configurations

(AI) Auxiliary Materials

Technical Targets

This project is a materials discovery investigation to identify a single semiconductor material that meets the technical targets for efficiency and stability. The 2015 technical targets from the MYRDD Plan PEC hydrogen production goals in Table 3.1.8.A are the following:

- 15% STH conversion efficiency
- 900-hour replacement lifetime (1/2 year at 20% capacity factor)
- $300/m^2 PEC electrode cost

FY 2015 Accomplishments

- We exceeded 400 hours of stability by testing a N_2^+ ion implanted and flash PtRu sputtered p-GaAs electrode for 468 hours at -15 mA/cm^2.
- We digested N_2^+ and PtRu sputtered GaAs and $GaInP_2$ samples in aqua regia and used inductively coupled plasma mass spectrometry to get quantitative data on loading and distribution. We discovered the distribution across the wafer surfaces is fairly uniform and the ion treatment is a significant source of PtRu. The total loading of PtRu nanoparticles, if they were compacted into a continuous thin film, is between 1–2 nm.
- Working with the University of Nevada, Las Vegas, one of our surface validation partners, we discovered more recently N_2^+ ion implanted and flash PtRu treated samples have less nitride incorporated and much greater PtRu loadings, which may be leading to less effective surface stabilization. We are amending treatment parameters to achieve surfaces with similar nitride and PtRu loadings to those found in our initial

samples, which had the greatest yield of stable electrodes to date.

- We worked with the Jaramillo group at Stanford to extend the durability of p-$GaInP_2$ coated with MoS_2 from a few hours to over 150 hours by changing deposition parameters.
- We designed and fabricated an electrochemical cell with short optical pathlength to minimize absorption of infrared photons by water.
- We collected our first results of a lowered bottom bandgap junction inverted metamorphic multijunction (IMM) cell and were able to generate a higher photocurrent density than $GaInP_2$/GaAs tandems. The voltage of the IMM cell was insufficient for unbiased water splitting, which we plan to address by incorporating a buried junction. This configuration with a buried junction should result in a new water splitting efficiency record.
- We filed a provisional patent on IMM cells for high efficiency water splitting.

✧ ✧ ✧ ✧ ✧

INTRODUCTION

Photoelectrolysis cells combine a light harvesting system and a water splitting system into a single, monolithic device. The catalyzed surface of a semiconductor is the light harvesting component as well as one part of the water splitting system with the balance consisting of a spatially separated counter electrode. Discovering a semiconductor system that can efficiently and sustainably collect solar energy and direct it towards the water splitting reaction could provide renewable and economically competitive fuel for the hydrogen economy.

The goal of this work is to develop a semiconductor material set or device configuration that (1) splits water into hydrogen and oxygen spontaneously upon illumination without an external bias, (2) has an STH efficiency of at least 15% with a clear pathway to exceed 20%, and (3) can ultimately be synthesized via high volume manufacturing techniques with a final hydrogen production cost below $2/kg.

APPROACH

All proven zero-bias PEC devices with STH over 1% rely on two, series-connected semiconductor junctions (tandem cell) to increase the majority-carrier potential at the counter electrode [1–4], providing sufficient potential difference, or photovoltage, for water splitting (Figure 1). Tandem devices also overcome the band alignment challenge common to PEC materials. For maximum efficiency, the currents in series-connected devices must be equal, creating the requirement of current matching. The maximum current generated by a semiconductor can be calculated by assuming unity quantum yield for every above-bandgap photon in the solar spectrum. Using the accepted lower heating value efficiency equation [5], 20% STH corresponds to a short circuit current density (J_{sc}) of 16.26 mA/cm^2 under AM1.5G (1 sun). The largest

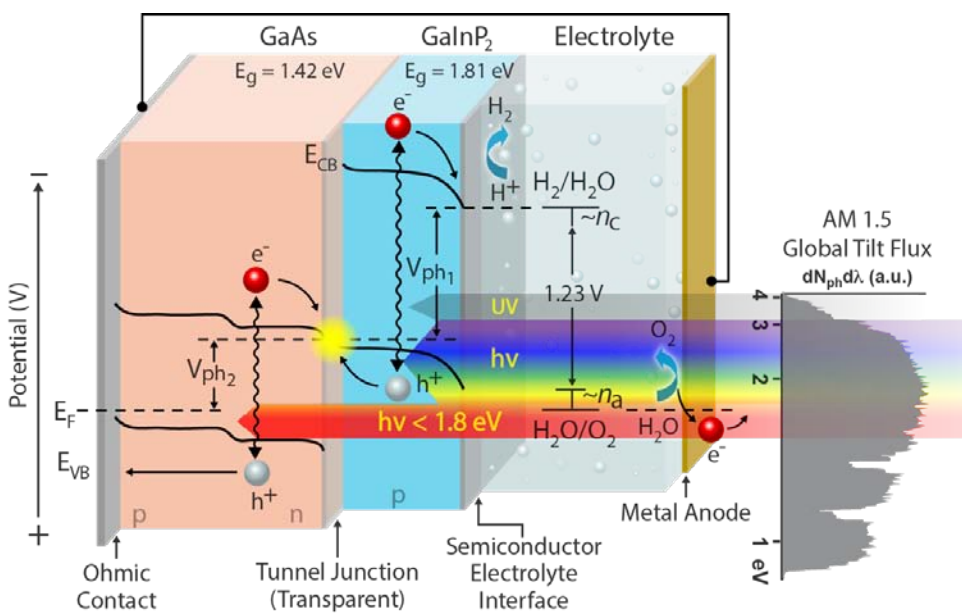

FIGURE 1. Energy-level diagram and spectral splitting of a tandem configuration photoelectrolysis cell. Photons with energies below the bandgap of the top junction pass through and generate an electron/hole pair in the bottom junction, which provides the holes with sufficient oxidative potential to perform water oxidation in this example.

bottom-cell bandgap that can be used and still achieve 20% STH is 1.41 eV. However, quantum yields are never 100% and semiconductors are not true step function devices. Therefore, to realistically achieve STH values in excess of 20%, we must use lower top-cell and bottom-cell bandgap combinations, which guides our selection of potential tandem materials. An additional variable that can be used to match the currents is the thickness of the top cell—a thinner cell will allow more photons through to the bottom cell. This gives us some additional flexibility in the bandgaps that we can use. The lower limit of useable bandgaps is ~0.8 eV [6], dictated by the penetration depth through water. We will focus on III-V semiconductors, which exhibit the highest conversion efficiencies among all photoabsorber materials, and design tandem junctions to maximize the spectrally split device current, while achieving sufficient voltage to drive the maximum current through the device. We plan to initially focus on conventional III-V metal organic vapor phase epitaxy to demonstrate maximum possible efficiencies and then port successful device structures to emerging synthesis techniques, such as spalling, epitaxial lift-off, or hydride vapor phase epitaxy, that have the potential to meet low cost absorber targets. We plan to improve the stability of III-V semiconductor water splitting electrodes by a variety of surface protecting modifications that include nitridation/sputtering, atomic layer deposition of oxides/nitrides, and thin coatings of MoS_2.

RESULTS

Over 400 Hours of Stability at Operating Conditions for Surface Protected p-GaAs

Our first attempt at achieving over 400 hours of durability on a nitrogen ion bombarded and PtRu sputtered p-GaAs electrode held at a constant (photo)current of -15 mA/cm^2 was unsuccessful. The applied bias was initially stable, but after 70 hours the bias gradually increased and the electrolyte yellowed. After about 170 hours, the semiconductor surface had a noticeable film and its ability to generate photocurrent under bias was greatly diminished. The performance of the semiconductor was restored by removing the film on its surface via sonication in methanol. We hypothesized the Triton X-100 surfactant was responsible for the yellowing and electrode fouling, which we confirmed experimentally by performing electrolysis on two platinum electrodes in an H-cell separated by a glass frit. Without surfactant, large bubbles build up on the semiconductor electrode surface and hasten degradation, so omitting it from durability electrolytes is not practical. We exceeded 400 hours of stability on p-GaAs operating at -15 mA/cm^2 by periodically stopping the experiment and replacing the electrolyte with fresh 3 M H_2SO_4 with 1 mM Triton X-100 either every day during weekdays or after 60 hours over weekends. The semiconductor electrode still exhibited fouling but it was not as severe as the uninterrupted 170-hour test described above. The electrolytes appeared yellow after only 24 hours of testing, after 60 hours the bubbles were noticeably larger and had a greater tendency to adhere to the sample surface than they did in a fresh solution. Without surfactant, a treated electrode failed in less than 24 hours.

The surface ion implantation and sputtering treatment shows the ability to protect the surface of p-GaAs for over 400 hours of operation (Figure 2) as demonstrated by a negligible loss in light-limited photocurrent magnitude. The illumination intensity from a 250 W tungsten light source was set using a silicon reference cell calibrated to AM1.5 G. One noticeable difference between pre and postdurability chopped light current density-voltage (J-V) curves is that the catalytic activity of the surface treatment appears to be lost during the durability testing. This is evidenced by the more negative onset of photocurrent for both the post 25-hour J-V and post 468-hour J-V. It is unclear whether this is due to the PtRu catalyst particles being deactivated by the cathodic fouling discussed above or due to physical detachment of the particles from the surface through etching or some other mechanism.

Demonstration of Novel III-V Structures for Improved Water Splitting Efficiency

We evaluated the first IMM cell designed for PEC water splitting. The new devices are described as "inverted"

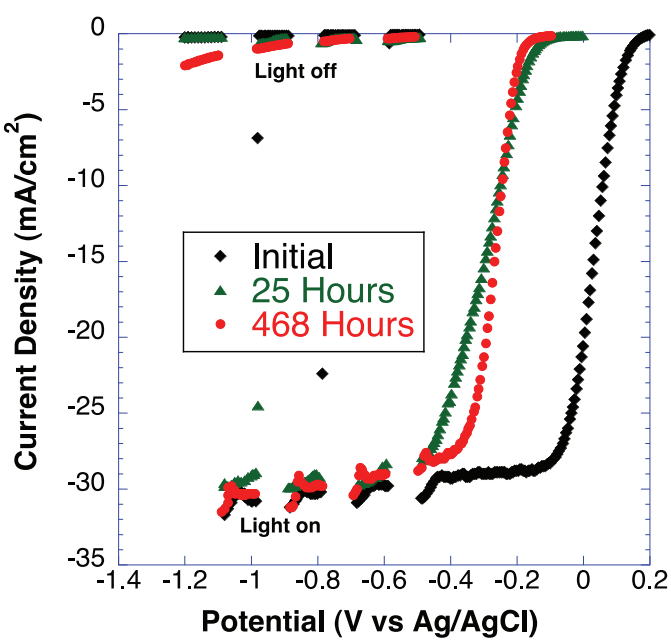

FIGURE 2. Chopped light J-V analysis in 3 M H_2SO_4 with 1 mM Triton X-100 before (black), after 25 hours (green), and after 468 hours (red) of galvanostatic testing at -15 mA/cm^2. Illumination was provided by a 250 W tungsten source set to AM1.5 G with a Si reference cell. The electrolyte was replaced every weekday to minimize fouling of the semiconductor by decomposed surfactant.

because the wider bandgap (top) junction, which is lattice-matched to the GaAs substrate, is grown first. A tunnel junction is then grown followed by a carefully engineered transparent buffer layer that grades the lattice constant to the lattice mismatched, "metamorphic" lower bandgap (bottom) junction. High quality multijunction structures can be realized because the transparent graded buffer layer moderates the strain induced by the lattice mismatch between the layers [7]. Additionally, the bandgaps of top and bottom absorbers are easily tailored by varying the III-V alloy compositions, allowing optimization of the device performance (current, voltage) with respect to water splitting requirements, with high precision. Our first modification to the $GaInP_2$/GaAs tandem aims to lower the bottom absorber bandgap, targeting 1.2 eV, by incorporating indium. This increases the overall fraction of the solar spectrum absorbed and makes the device, theoretically, top junction limited based on the current matching requirement (Figure 3).

The first characterization of the IMM cell was with incident photon-to-current efficiency, which revealed that the InGaAs cell was of high quality, and demonstrated values as good as GaAs, approaching the limit of reflection (~70% for our cell). We also took two-terminal J-V measurements, against a highly catalytic IrO_x anode, to determine the water splitting efficiency (Figure 4). Compared with the standard $GaInP_2$/GaAs tandem (green) line, the IMM cell (orange) exhibited an increased light-limited photocurrent density, but had a reduced onset voltage, making it unable to split water at zero bias. Our strategy to improve the onset is based on making a buried junction at the semiconductor surface. The black dashed line in Figure 4 had additional p-GaAs and i-$GaInP_2$ layers on the surface and demonstrates how this would lead to an improvement. These layers were included in the growth as etch-stop and window layers that are used for solid-state devices and were inadvertently left on after processing. Our hypothesis is that the i-$GaInP_2$ layer increased the voltage, but the p-GaAs layer acted as a filter and reduced the photocurrent of the device. We are currently testing various modifications of these layers, including thinning and entirely removing the p-GaAs layer, to determine the configuration that gives us the most voltage with minimal or no current loss. Improving the voltage (i.e., shifting the orange curve to the right) should allow us to exceed 15% STH, and set a new bar for unassisted photoelectrolysis efficiency. In order to surpass 20% STH, we will need to include an antireflective surface and possibly reduce the top bandgap from 1.8 eV to 1.7 eV. We are currently looking at both of these pathways to improving efficiency.

CONCLUSIONS AND FUTURE DIRECTIONS

- Surface passivation of III-Vs could provide sufficient durability to these high-efficiency materials to meet technical targets for efficiency and semiconductor absorber replacement schedule. We have exceeded 400 hours of stability at -15 mA/cm^2 with N_2^+ implantation and PtRu sputtering on GaAs and exceeded 150 hours of durability at -10 mA/cm^2 with MoS_2 films on $GaInP_2$. We plan to continue optimizing these surface modifications as well as exploring atomic layer deposition of thin oxide and nitride layers to demonstrate 900 hours of stability,

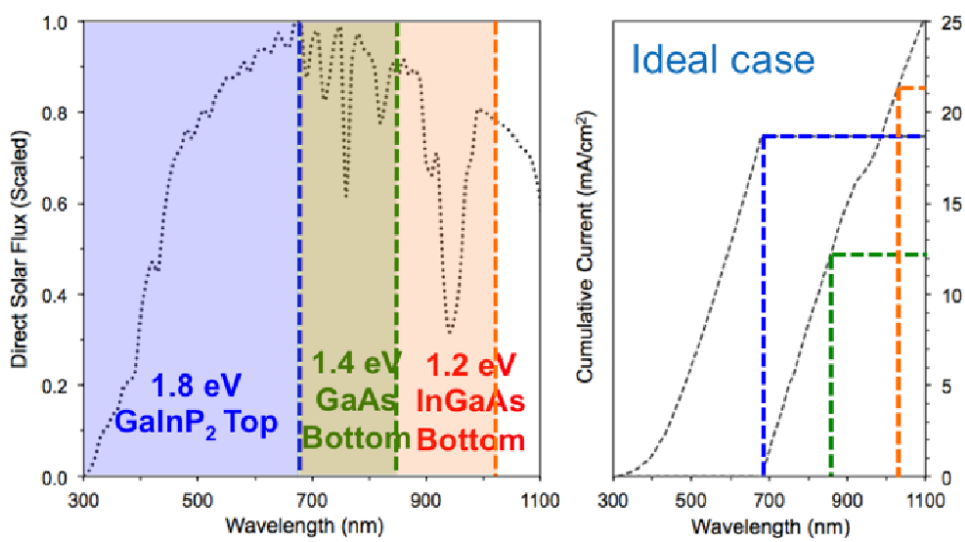

FIGURE 3. The portion of the direct solar spectrum that each semiconductor junction utilizes is depicted on the left. The right image depicts the integrated thermodynamic (no loss) limit of each junction and shows that using $GaInP_2$/GaAs will limit the overall current in these series connected tandems to about 12 mA/cm^2 due to the GaAs junction. Incorporating InGaAs will make the device top junction ($GaInP_2$) limited and increase the overall device current (and efficiency).

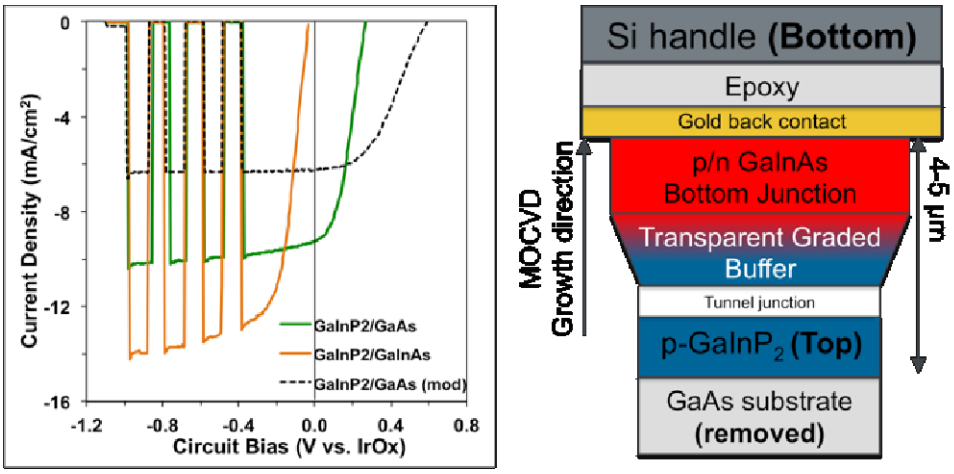

FIGURE 4. Current density vs. circuit bias for a standard tandem (green), an IMM tandem with a 1.2 eV bottom cell bandgap (orange), and a standard tandem with additional GaAs and $GaInP_2$ layers (black, dashed). These measurements were made in 3M H_2SO_4 with the surfactant Triton X-100 under AM1.5 G illumination. The cartoon on the right shows the layered structure of the IMM device.

which corresponds to a 6-month replacement schedule while operating at a 20% capacity factor.

- Lowering the bandgap of the bottom junction in a tandem device is a viable strategy to improving the photocurrent and exceeding 15% STH efficiency, assuming sufficient voltage can be maintained. In order to meet STH efficiency targets of 20% and beyond, antireflection strategies will have to be considered for the photoelectrode surface. We plan to investigate antireflection in parallel with lowered top and bottom bandgap IMM tandems.
- In order to meet PEC hydrogen production targets of <$2/kg, significant reductions in semiconductor synthesis costs must be realized in addition to improved efficiency and durability. We plan to synthesize, or obtain where necessary, semiconductor configurations that use alternative substrates, such as III-V(N) on Si, in addition to those that use synthesis techniques that re-use substrates (spalling, epitaxial lift-off) and evaluate their capacity to meet efficiency and stability targets. We also plan to model the viability of photoreactors that use higher optical concentrations as a possible way to make hydrogen cost less sensitive to those of the semiconductor absorber.

SPECIAL RECOGNITIONS & AWARDS/ PATENTS ISSUED

1. Pending Patent: "Stable Photoelectrode Surfaces and Methods," Publication number US20140332374A1.

FY 2015 PUBLICATIONS & PRESENTATIONS

1. "Enabling a Sustainable Energy Future Through Hydrogen," Science Undergraduate Laboratory Internship Seminar, Golden, CO. October 22, 2014. (Deutsch*) Invited*

2. "Semiconductor Materials for Photoelectrolysis: Requirements, Challenges and Opportunities," Colorado School of Mines MRS Chapter Seminar, Golden, CO. November 20, 2014. (Deutsch) *Invited*

3. "Photoluminescence Response of p-$GaInP_2$ Photocathodes to Vapor and Solution Ambient," American Vacuum Society, 61st Meeting, Baltimore, MD. November 10, 2014. (Young)

4. "Challenges in Photoelectrochemical Water Splitting," University of Arkansas, Little Rock, AR. December 8, 2014 (Turner) *Invited*

5. "Frontiers, Opportunities and Challenges for a Hydrogen Economy," TU Darmstadt, Darmstadt, Germany. February 24, 2015. (Turner) *Invited*

6. "Direct Conversion Photoelectrochemical Systems for Hydrogen Production from Sunlight and Water," Ovshinsky Award Session – A Legacy of Energy Technologies, 2015 American Physical Society March Meeting, San Antonio, TX. March 3, 2015. (Turner) *Invited*

7. "Challenges in photoelectrochemical water splitting materials," 249th American Chemical Society Meeting, Denver, CO. March 22, 2015. (Turner) *Invited*

8. "Solar Water Splitting and the Hydrogen Economy," ACS Committee on Science: Transitioning between Academic Research into Practical Use: Solar-Energy and Advanced Materials, 249th American Chemical Society Meeting, Denver, CO. March 23, 2015. (Turner) *Invited*

9. "Semiconductor materials for efficient photoelectrochemical water splitting: The PEC working Group," 249th American Chemical Society meeting, Denver, CO. March 23, 2015. (Wang) *Invited*

10. "High-Efficiency Tandem Absorbers for Economical Solar Hydrogen Production," RE3 Workshop, Louisville, KY. March 24, 2015. (Deutsch) *Invited*

11. "High-Efficiency Tandem Absorbers for Economical Solar Hydrogen Production," Materials Research Society Spring Meeting. San Francisco, CA. April 6, 2015. (Deutsch) *Invited*

12. "Sunlight Absorption in Aqueous Electrolytes and Inverted Metamorphic III-V Growth – a Pathway to Direct Solar Water Splitting with Highest Efficiencies," Materials Research Society Spring Meeting. San Francisco, CA. April 8, 2015. (Döscher)

13. "Developing a monolithic GaAs|GaAs tandem photovoltaic|p hotoelectrochemical device," Materials Research Society Spring Meeting. San Francisco, CA. April 9, 2015. (Young)

14. "Materials and Structures for Efficient Photoelectrochemical Water Splitting," Materials Research Society Spring Meeting. San Francisco, CA. April 10, 2015. (Wang)

15. "Tandem devices design for PEC water splitting: The impact of sunlight absorption in aqueous electrolytes and the role of inverted metamorphic III-V epitaxy," University of California-Davis, Davis, CA. April 13, 2015. (Döscher) *Invited*

16. "Direct solar water splitting at high efficiency: Impact of sunlight absorption in aqueous electrolytes and advanced III-V tandem design strategy," 1st International Solar Fuels Conference, Uppsala, Sweden. April 30, 2015. (Döscher)

17. "High-Efficiency Tandem Absorbers for Economical Solar Hydrogen Production," 227th Meeting of the Electrochemical Society, Chicago, IL. May 25, 2015. (Deutsch) *Invited*

18. "Materials for Efficient Photoelectrochemical Water Splitting: The PEC Working Group," 227th Meeting of the Electrochemical Society, Chicago, IL. May 25, 2015. (Wang)

19. "Hydrogen from Photoelectrochemical Water Splitting: What's it Gonna' Take?," 227th Meeting of the Electrochemical Society, Chicago, IL. May 25, 2015. (Turner) *Invited Plenary*

20. "Corrosion analysis of p-GaInP2 photocathodes: Comparison of oxygen and argon-sparged electrolyte," 227th Meeting of the Electrochemical Society, Chicago, IL. May 27, 2015. (Young)

21. "High-Efficiency Tandem Absorbers for Economical Solar Hydrogen Production," DOE Hydrogen and Fuel Cells Program Annual Merit Review, Washington, DC. June 11, 2015. (Deutsch)

22. "Tandem devices design for photoelectrochemical water splitting: The impact of sunlight absorption in aqueous electrolytes and the role of inverted metamorphic III-V epitaxy," TU Clausthal, Kolloquium, Clausthal-Zellerfeld, Germany. June 25, 2015. (Döscher) *Invited*

REFERENCES

1. Abdi, Fatwa F., Lihao Han, Arno H.M. Smets, Miro Zeman, Bernard Dam, and Roel van de Krol. 2013. "Efficient Solar Water Splitting by Enhanced Charge Separation in a Bismuth Vanadate-Silicon Tandem Photoelectrode." *Nature Communications* 4 (January). Nature Publishing Group: 2195. doi:10.1038/ncomms3195.

2. Brillet, Jeremie, Jun-Ho Yum, Maurin Cornuz, Takashi Hisatomi, Renata Solarska, Jan Augustynski, Michael Graetzel, and Kevin Sivula. 2012. "Highly Efficient Water Splitting by a Dual-Absorber Tandem Cell." *Nature Photonics* 6 (12). Nature Publishing Group: 824–28. doi:10.1038/nphoton.2012.265.

3. Kainthla, R.C., B. Zelenay, and J. O'M. Bockris. 1987. "Significant Efficiency Increase in Self-Driven Photoelectrochemical Cell for Water Photoelectrolysis." *Journal of The Electrochemical Society* 134 (4): 841. doi:10.1149/1.2100583.

4. Khaselev, O., and J.A. Turner. 1998. "A Monolithic Photovoltaic-Photoelectrochemical Device for Hydrogen Production via Water Splitting." Science (New York, N.Y.) 280 (5362): 425–27. http://www.ncbi.nlm.nih.gov/pubmed/9545218.

5. Chen, Zhebo, Thomas F. Jaramillo, Todd G. Deutsch, Alan Kleiman-shwarsctein, Arnold J. Forman, Nicolas Gaillard, Roxanne Garland, et al. 2010. "Accelerating Materials Development for Photoelectrochemical Hydrogen Production: Standards for Methods, Definitions, and Reporting Protocols." *Journal of Materials Research* 25 (1): 3–16. doi:10.1557/jmr.2010.0020.

6. Döscher, H., J.F. Geisz, T.G. Deutsch, and J.A. Turner. 2014. "Sunlight Absorption in Water – Efficiency and Design Implications for Photoelectrochemical Devices." *Energy & Environmental Science* 7 (9): 2951. doi:10.1039/C4EE01753F.

7. Geisz, J.F., D.J. Friedman, J.S. Ward, A. Duda, W.J. Olavarria, T.E. Moriarty, J.T. Kiehl, M.J. Romero, A.G. Norman, and K.M. Jones. 2008. "40.8% Efficient Inverted Triple-Junction Solar Cell With Two Independently Metamorphic Junctions." *Applied Physics Letters* 93 (12): 123505. doi:10.1063/1.2988497.

II.C.5 Wide Bandgap Chalcopyrite Photoelectrodes for Direct Water Splitting

Nicolas Gaillard
University of Hawaii (UH)
Hawaii Natural Energy Institute
2440 Campus Road, Box 368
Honolulu, HI 96822
Phone: (808) 956-2342
Email: ngaillar@hawaii.edu

DOE Manager
David Peterson
Phone: (720) 356-1747
Email: David.Peterson@ee.doe.gov

Contract Number: DE-EE0006670

Subcontractors
- University of Nevada, Las Vegas (UNLV), Las Vegas, NV
- Stanford University, Stanford, CA
- Lawrence Livermore National Laboratory, Livermore, CA
- National Renewable Energy Laboratory, Golden, CO

Project Start Date: October 1, 2014
Project End Date: September 30, 2017

Overall Objectives

In line with the Fuel Cell Technologies Office (FCTO) Multi-Year Research, Development, and Demonstration (MYRDD) plan, our project aims to identify suitable semiconducting materials for efficient and durable photoelectrochemical (PEC) hydrogen production at a cost of $2/kg or less. Specifically, our program aims to:

- Develop efficient copper chalcopyrite ($Cu(In,Ga)(S,Se)_2$)-based materials with ideal optoelectronic properties for PEC water splitting.
- Identify appropriate surface treatments to prevent photocorrosion, improve surface energetics and enhance hydrogen evolution reaction.
- Demonstrate 3 L of hydrogen produced in 8 hours using a copper chalcopyrite-based standalone PEC device.

Fiscal Year (FY) 2015 Objectives

- Identify photovoltaic (PV)-grade chalcopyrite alloys with controlled energetics and microstructure
- Model energetics at the absorber/"buffer" p-n junction interface
- Evaluate dichalcogenides (e.g., MoS_2 and WS_2) as both corrosion protective layer and hydrogen evolution reaction (HER) catalyst

Technical Barriers

This project addresses the following technical barriers from the Hydrogen Production section of the FCTO MYRDD plan:

(AE) Materials Efficiency

(AF) Materials Durability

(AG) Integrated Device Configuration

(AJ) Synthesis and Manufacturing

Technical Targets

This project aims to develop efficient and durable PEC devices using low cost semiconducting materials. Specifically, our program aims to modify the optoelectronic properties of the PV-grade copper chalcopyrite material class for PEC water splitting. Alongside, we are engineering new surface treatments to improve chalcopyrites' surface energetics, their catalysis toward HER as well as their resistance against photo-corrosion. The status of the UH's technical targets is documented in Table 1.

FY 2015 Accomplishments

Accomplishments during the current project period include:

- Successful synthesis of bandgap tunable $Cu(In,Ga)S_2$ and $CuGa(S,Se)_2$ thin films.
- Modeling of interface energetics formed by CdS or ZnS with various chalcopyrites.
- Improvement of $CuGaSe_2$ photoelectrodes durability using MoS_2 as a protective coating.
- Proof-of-principle experiments for in situ studies of the chalcopyrites/electrolyte interface.

✧ ✧ ✧ ✧ ✧

INTRODUCTION

The goals of this project are to (1) demonstrate PEC hydrogen production with a dual absorber system capable of generating at least 3 L of hydrogen in 8 hours and (2) to develop a standalone system with a solar-to-hydrogen (STH) conversion efficiency of 15% and operational life up to 2,000 hours.

APPROACH

The chalcopyrite material class, typically identified by its most popular *PV-grade* alloy $CuInGaSe_2$, provides

TABLE 1. Progress towards Meeting Technical Targets for Photoelectrochemical Hydrogen Production

Characteristics	Unit	2015 / Ultimate Targets	UH project status
Solar-to-Hydrogen Energy Conversion Ratio	%	15 / 25	4[a] to 10[b]
Capital Cost of Concentrator & PEC Receiver	$/m^2	200 / 63	270[c]
Photoelectrochemical Hydrogen Cost	$/kg	17.30 / 2.10	13.2[d]
Annual Electrode Cost per TPD H_2	$/yr-TPD H_2	2,000,000 / 14,000	1,500,000[d]
1-Sun Hydrogen Production Rate	kg/s per m^2	1.2 x 10^{-6} / 2.0 x 10^{-6}	3 x 10^{-7} to 1 x 10^{-6}

(a) achieved with coplanar structure
(b) anticipated based on photocurrent density measured on new Cu(In,Ga)(S,Se)$_2$ materials
(c) projected from technoeconomic analysis using known thin film PV manufacturing costs (CdTe by First Solar)
(d) using 4% STH efficiency, 15x concentration, 270 S/m^2 for PEC material replaced every 2 years
TPD - tonne per day

exceptionally good candidates for PEC water splitting. A key asset of this bandgap tunable, direct absorber, thin film semiconductor material is the outstanding photon-to-electron conversion efficiency, as demonstrated with $CuInGaSe_2$-based PV cells. An STH efficiency of 4% was achieved by our team in 2012 using a 1.6 eV bandgap $CuGaSe_2$ photocathode connected in series with three a-Si PV drivers (side-by-side architecture). The use of such coplanar architecture was dictated by the bandgaps of $CuGaSe_2$ that was too narrow for a "stacked" multi-junction integration. With wide bandgap chalcopyrites, we will be able to stack the PEC device over the PV driver and increase the STH efficiency.

RESULTS

PV-grade wide bandgap Cu(In,Ga)(S,Se)$_2$ absorbers. During this first year of our project, we have focused on the development of a baseline materials system to understand the basic properties and potential pitfalls of wide bandgap copper-chalcopyrites. Gallium-poor $CuInGaS_2$ thin films were fabricated using our two-step synthesis approach, in which a metal alloy with specific Cu, In and Ga composition is annealed under controlled sulfur atmosphere. Solar absorbers were then integrated as solar cells using a CdS layer to form a p-n junction, as well as resistive ZnO and conductive indium tin oxide transparent layers for electrical contact. Figure 1 presents the quantum efficiency (QE) measured on a gallium-poor $CuInGaS_2$ cell. At 550 nm, the conversion efficiency reaches a maximum of 68%. Then the QE drops suddenly, revealing possible recombination phenomena in the absorber. Eventually, the QE drops to zero at about 850 nm, a typical value for a Ga-poor $CuInGaS_2$ (1.53 eV bandgap). The photocurrent generated with such structure was 15 mA/cm^2. Our team is focusing now on widening the optical bandgap of $CuInGaS_2$ by increasing the gallium concentration, with a targeted bandgap of 1.8–2.0 eV.

Subsurface energetics improvement: theoretical modeling. The development of a functional PEC device relies on the ability to efficiently separate and transfer photo-

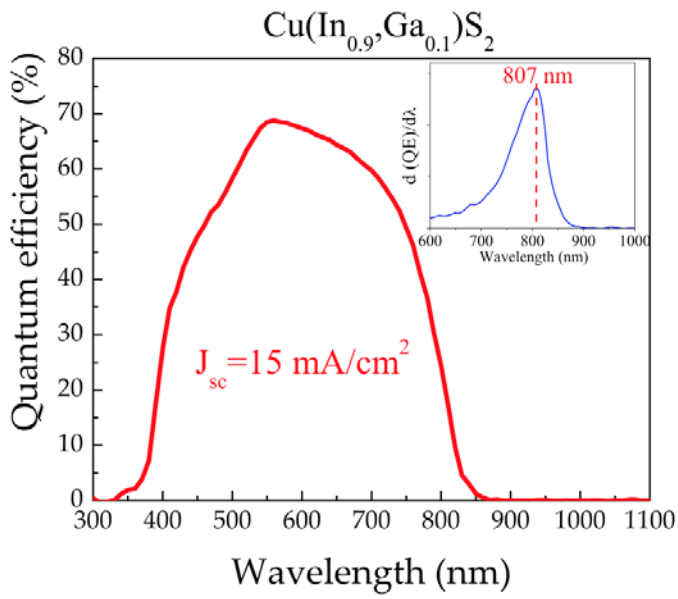

FIGURE 1. Quantum efficiency measured on $CuInGaS_2$-based solar cells

generated carriers to the catalytically active surface. Best performing Cu(In,Ga)Se_2-based devices typically employ CdS buffer layers due to a favorable conduction band offset. However, CdS does not form an ideal conduction band offset with wide bandgap sulfide alloys. This is illustrated in Figure 2, which shows the calculated band offsets of CdS relative to various chalcopyrites. While narrow bandgap $CuInSe_2$ and $CuInS_2$ have a moderate conduction band offset with CdS, a significant "cliff" is expected at the interface formed by intermediate bandgap $CuGaSe_2$ with CdS. A similar issue is likely to happen with wide bandgap $CuInGaS_2$ and CdS. Our results identify that the influence of Al incorporation, like Ga, is to primarily raise the conduction band of $CuInSe_2$ or $CuInS_2$. The degree that Al influences the conduction band position on an absolute energy scale and the resulting band offset with the buffer is expected to be more significant than for Ga, and offers alternative compositions

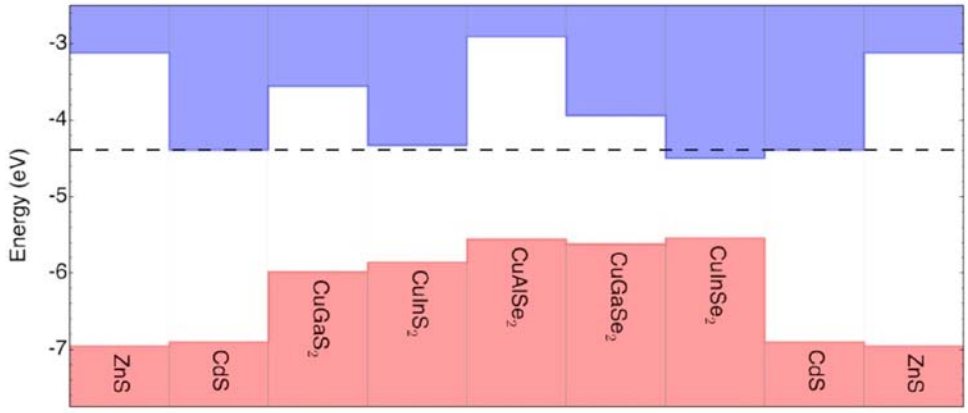

FIGURE 2. Calculated unstrained band offsets of CdS and ZnS with respect to various chalcopyrites

to $Cu(In,Ga)S_2$ alloys for targeting the desired 1.8–2.0 eV absorber bandgap of PEC materials.

Subsurface energetics improvement: advanced characterization. We utilized a suite of experimental techniques, both in the lab at UNLV and at Beamlines 8.0.1 and 9.3.1 at the Advanced Light Source (ALS), Lawrence Berkeley National Laboratory, to derive a comprehensive picture of surfaces and interfaces of the chalcopyrite-based PEC system. Experiments include in vacuo studies to investigate electronic structure properties and operando studies to gain insights into the chemical properties of electrolyte–solid interfaces. For example, we have used X-ray emission spectroscopy at the ALS to determine optimal film thickness for operando studies in our custom designed in situ cells. Furthermore, we have employed surface sensitive methods at UNLV to study a first sample set devoted to the optimization of sample handling procedures, film thicknesses, and detailed characterization parameters. As an example, Figure 3 shows the X-ray photoelectron spectroscopy survey spectra of a "bare" $Cu(In,Ga)S_2$ absorber and a "thick" CdS layer on top of a $Cu(In,Ga)S_2$ absorber. Next steps will include a detailed analysis and design of the next sample series for the in vacuo experiments at UNLV, as well as an experimental run at the ALS in September 2015, in which we will characterize the electrolyte–$Cu(In,Ga)S_2$ interface.

Surface catalysis and corrosion resistance. Cadmium sulfide (CdS) is a popular buffer layer material for forming a heterojunction in chalcopyrite materials but, like $CuGaSe_2$, is unstable in acid at the potentials of interest for hydrogen evolution. Protecting the CdS/$CuGaSe_2$ structure is important to achieve devices that can operate without degradation in an acidic electrolyte. Over the first year of the project, we have worked to engineer molybdenum disulfide (MoS_2) protective coatings to stabilize $CuGaSe_2$ absorbers in acid electrolyte. A 5-nm thick Mo metal layer was evaporated on the $CuGaSe_2$/CdS structure and then converted into MoS_2

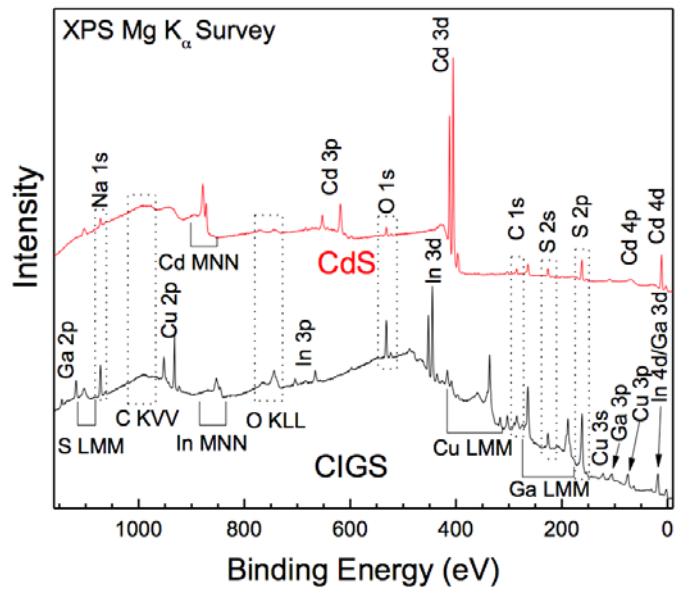

FIGURE 3. Mg Kα X-ray photoelectron spectroscopy (XPS) survey spectra of a "bare" $CuInGaS_2$ absorber and a CdS/CIGS interface sample

under H_2S atmosphere at 200°C. As shown in Figure 4, the electrodes with a MoS_2 protecting layer showed enhanced stability when compared with the unprotected CdS/$CuGaSe_2$ electrodes, though there is noticeable degradation from both the electrochemical measurements and X-ray photoelectron spectroscopy spectra. We hypothesized that the roughness of the $CuGaSe_2$ electrodes made complete protection by 5 nm evaporated films unfeasible and thicker films, which may protect the electrodes, would block too much of the incident light. We therefore turned to atomic layer deposition as a means to protect the electrodes. Initial tests demonstrated that atomic layer deposition is effective at coating WS_2 on rough $CuGaSe_2$.

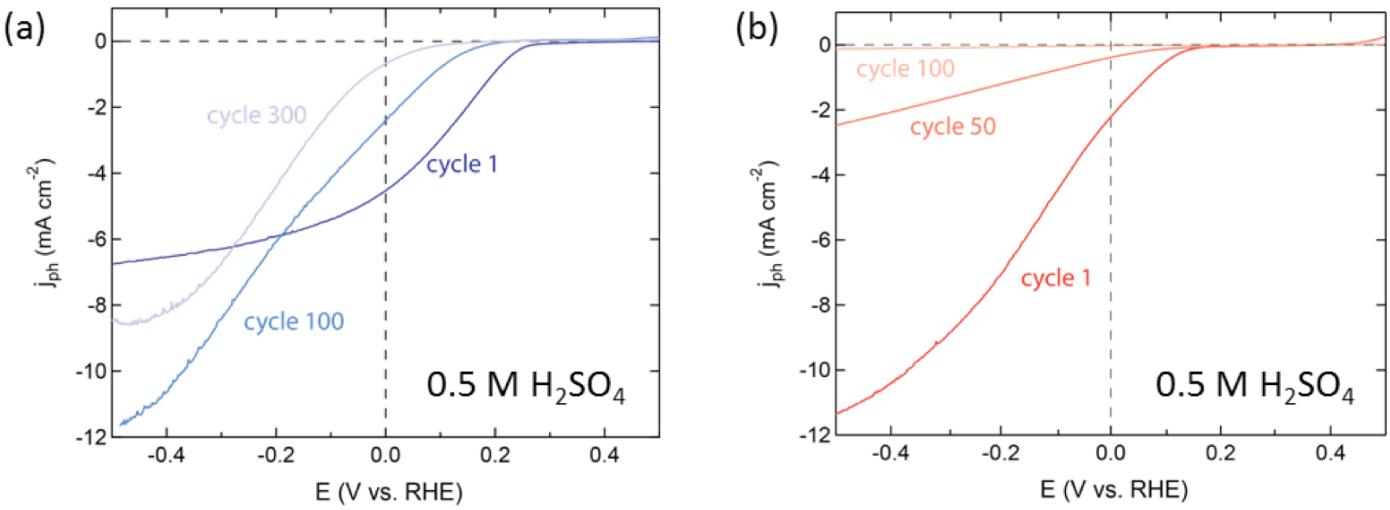

FIGURE 4. Photoelectrochemical activity and stability of (a) MoS_2/CdS/$CuGaSe_2$ electrodes and (b) CdS/$CuGaSe_2$ photoelectrodes in 0.5 M H_2SO_4

CONCLUSIONS AND FUTURE DIRECTIONS

- Cu(In,Ga)S_2 and CuGa(S,Se)$_2$ with controllable optoelectronic properties were successfully fabricated. In FY 2016, we will optimize our deposition processes to increase absorber efficiency.
- Cu(In,Ga)S_2-based solar cells with high open circuit potential (700 mV) have been achieved. In FY 2016, we will evaluate postdeposition treatments to passivate surface defects and develop alternative buffer layers to CdS.
- $CuGaSe_2$/CdS photocathode durability was enhanced with MoS_2. In FY 2016, highly conformal atomic layer deposition process will be improved to achieve pinhole-free MoS_2 layers.

FY 2015 PUBLICATIONS/PRESENTATIONS

1. Heli Wang, "Semiconductor Materials for Efficient Photoelectrochemical Water Splitting: The PEC Working Group," 249th ACS National Meeting, Denver, CO, March 22–26, 2015.

2. C. Heske, "Using Soft X-rays to Look into (Buried) Interfaces of Energy Conversion Devices," Chemical and Materials Engineering, University of Nevada, Reno, March 7, 2015 (invited).

3. N. Gaillard, "Wide Bandgap Chalcopyrite Photoelectrodes for Direct Solar Water Splitting," DOE Annual Merit Review Meeting, Arlington, VA, June 11, 2015 (invited).

4. N. Gaillard, A. Deangelis, M. Chong, and A. Zeng, "Development of Wide Bandgap Copper Chalcopyrite Thin Film Materials for Photoelectrochemical Hydrogen Production," Symposium J, MRS 2015 Spring Meeting, San Francisco (2015).

II.C.6 Accelerated Discovery of Advanced RedOx Materials for Solar Thermal Water Splitting to Produce Renewable Hydrogen

Christopher Muhich, Samantha Miller,
Ryan Trottier, Alan Weimer, and Charles Musgrave
(Primary Contact)
University of Colorado Boulder
Campus Box 596
Boulder, CO 80309-0596
Phone: (303) 735-0411
Email: charles.musgrave@colorado.edu

DOE Manager
Katie Randolph
Phone: (720) 356-1759
Email: Katie.Randolph@ee.doe.gov

Contract Number: NSF Grant No. 1433521

Project Start Date: October 1, 2014
Project End Date: September 30, 2017

Overall Objectives

- Develop a computationally accelerated and experimentally validated materials-by-design approach to design materials with optimum thermodynamic, mass transport, and kinetic properties for solar thermal water splitting (STWS) that can be tailored for materials discovery for other technologies
- Use our accelerated materials discovery approach to screen doped perovskite and spinel metal oxide materials for STWS and provide a rank-ordered list of promising redox active materials
- Address fundamental and broad materials chemistry questions in accomplishing Tasks 1 and 2
- In conjunction with DOE sister project (DE-EE0006671), test promising redox materials identified by our rapid screening process using a stagnation flow reactor (SFR) to validate screening methods

Fiscal Year (FY) 2015 Objectives

- Use density functional theory (DFT) to predict hydrogen production for metal aluminates through different mechanisms; experimentally test materials to establish mechanism for STWS redox reaction
- Develop and utilize a descriptor model [1] to predict the oxygen vacancy formation energy of binary perovskites
- Develop a computational materials screening approach for new materials based on thermodynamics of established mechanism
- Calculate potential energy surface for hydrogen production reaction on a model surface (hercynite)
- Initiate study of the sensitivity of metal oxide water splitting kinetics towards to composition

Technical Barriers

This project addresses the following technical barriers from the Hydrogen Production section of the Fuel Cell Technologies Office Multi-Year Research, Development, and Demonstration Plan:

(S) High-Temperature Robust Materials

(W) Materials and Catalyst Development

Technical Targets

This project involves conducting fundamental studies of novel perovskite and spinel redox active materials to identify those with high H_2 production capacities (>200 µmol $H_2/g_{material}$ /cycle), low thermal reduction temperatures (<1,400°C), fast kinetics, low cost, and enthalpies of reduction high enough to drive the water splitting reaction, but not so high as to be thermodynamically inefficient. Insights gained from these studies will be applied towards the design of a flowing particle solar water splitting system that meets the following DOE hydrogen production targets:

- Solar-Driven High-Temperature Thermochemical Cycle Hydrogen Cost: $2/kg
- Annual Reaction Material Cost: $11,000/yr-TPD (metric tons per day) H_2
- Solar to Hydrogen Energy Conversion Ratio: 26%

FY 2015 Accomplishments

- Predicted redox reaction mechanism and H_2 capacity of three metal aluminate materials using DFT calculations; experimentally validated computational results
- Identified a simple criteria and approach for assessing redox capabilities of new materials
- Used oxygen vacancy formation model to screen 1,078 binary perovskites and 590 binary spinels for STWS capabilities
- Characterized atomistic hydrogen formation reaction mechanism on hercynite surface

✧ ✧ ✧ ✧ ✧

INTRODUCTION

Two-step thermochemical redox processes based on metal oxide cycles are a promising route to efficiently capture and store solar energy because they have the potential to operate at high thermal efficiencies, are chemically simple, and require less land and water to operate than competing biomass, artificial photosynthesis and photovoltaic-driven electrolysis. In two-step metal-oxide-based STWS, a metal oxide is heated using concentrated solar thermal energy to a temperature at which it reduces, generating O_2. Subsequently, H_2O is introduced to the system as steam to re-oxidize the material to its initial state and generate H_2. Traditionally, two types of metal oxide redox chemistries are utilized in solar thermochemical H_2O splitting. The first prototypical chemistry utilizes a stoichiometric mechanism. Such materials undergo a phase change to produce a stoichiometric quantity of O_2. The vast majority of simple binary metal oxides previously examined for use as STWS materials have been examined under the assumption that they operate via this mechanism. The most studied of these are ZnO, SnO_2, and Fe_3O_4. While these materials theoretically exhibit high redox potential, in practice deactivation induced by irreversible processes such as sintering or the formation of liquid phases and metal vaporization lead to loss of active oxide. The second chemistry is based on the formation of oxygen vacancies in metal oxides during reduction, as shown in Equations 1 and 2, for which ceria is a representative example. Such redox materials are thermally reduced without undergoing a phase change, as the lattice is able to accommodate the strain induced by oxygen vacancy formation. These materials are thermally stable, although the extent of reduction, and hence H_2 production capacity per cycle, is small compared to other reducible oxides.

$$MO_x \rightarrow MO_{x-\delta} + \delta/2\ O_2 \quad (1)$$

$$MO_{x-\delta} + \delta\ H_2O \rightarrow MO_x + \delta\ H_2 \quad (2)$$

The ideal material for efficiently driving STWS has not yet been identified, although a large number of materials have been examined. To be a STWS material, a candidate material must undergo both reduction and water oxidation; to be a practical STWS material, it must reduce at temperatures which are achievable using concentrated sunlight and at which reactor containment materials do not degrade (<1,700°C). The assessment of STWS materials and cycles has generally been undertaken by one of two approaches: (1) evaluating a set of previously proposed water splitting cycles for their practical viability; (2) identifying novel materials from a broad set of candidates by predicting their ability to drive STWS. Because an optimal STWS material or cycle has not yet been identified, our focus is on the latter of these two approaches, which we call "STWS materials screening."

APPROACH

Our STWS materials screening approach to discover materials for an efficient cost effective H_2 production process involves using computational materials modeling based primarily on DFT quantum mechanical simulations to rapidly predict basic materials properties, which we use as descriptors within a model we will develop for predicting the redox properties of candidate materials. The computational screening will be used to guide an experimental effort to synthesize and validate promising redox materials identified by our rapid screening process.

Although in principle an ab initio approach could predict the redox properties of candidate metals oxides directly, the large number of possible materials (e.g., over 1.3 million possibilities just for earth abundant, non-radioactive, non-toxic, quaternary perovskites with the formula $A^1_{0.75}A^2_{0.25}B^1_{0.75}B^2_{0.25}O_3$), the properties of which are unknown a priori, makes this approach intractable. Thus, we are developing a computationally accelerated STWS material discovery and development method where DFT is used only to predict materials stability relative to melting and phase segregation and to predict basic materials properties. We are developing an advanced descriptor model informed by DFT calculated band gaps, materials heats of formation, and other fundamental properties to predict a material's redox thermodynamics and will apply this descriptor model to screen materials for STWS performance. Materials predicted to possess favorable thermodynamic properties for STWS will be analyzed for their kinetic properties for STWS using a novel descriptor method to quickly predict the kinetics of the rate-limiting step. At each stage of the screening process, the rigor and the associated computational costs of the methods will be increased, and materials not meeting material performance criteria, i.e., possessing a high likelihood of poor STWS performance, will be eliminated. Throughout this process, experiments will be carried out in conjunction with our DOE sister project led by Alan Weimer to validate the computational models, analyze stability and water spitting behavior, and inform the choice of performance criteria for material down-selection. This stage of computational "prototyping" will identify materials that are likely to have high H_2 production capacity (>200 µmol H_2/g/cycle), low thermal reduction temperature (<1,400°C), an enthalpy of reduction sufficiently high to drive the reactions at reasonable rates but not so high as to be thermodynamically inefficient (near the enthalpy of splitting water, 280 kJ/mol), and short reduction and oxidation times (<15 min).

RESULTS

During this fiscal year, active redox material development has focused on establishing and validating a screening criteria for metal oxide materials, using the

screening method to evaluate binary perovskites, and performing kinetics studies on a model surface. In order to assess new materials we first propose a two-step screening method then use this method to predict the redox reaction mechanism and H_2 production capacities for three aluminate materials, pure hercynite ($FeAl_2O_4$), cobalt aluminate ($CoAl_2O_4$), and doped-hercynite ($Co_xFe_{1-x}Al_2O_4$).

Since the enthalpies of both the reduction and oxidation steps together must be greater than the enthalpy of water splitting (Equation 3) and the oxidation of the material must be exothermic (to ensure a spontaneous oxidation reaction (since), the reduction enthalpy must be >286 kJ/mol. Therefore, 286 kJ/mol represents a minimum reduction enthalpy for STWS, and based on this requirement we can assess the viability of candidate STWS materials or reaction mechanisms by comparing their reduction enthalpies to the enthalpy required for water splitting, i.e., if the metal oxide reduction enthalpy is less than the water splitting enthalpy, the suggested material or reaction mechanism is unlikely to drive STWS without the input of external work.

$$\Delta H_{STWS} = \Delta H_{TR} + \Delta H_{OX} \geq 286\ kJ/mol \quad (3)$$

Although a reduced material may store sufficient energy to split water, this does not guarantee that it will do so after reduction at a reasonable operating temperature. As the reduction enthalpy of a particular material increases, the driving force for the water splitting reaction also increases, although the extent of reduction and the associated H_2 production capacity at a given reduction temperature decreases. Therefore, the extent of reduction, if any, must be determined at practical reduction temperatures. To do this, we proposed using a benchmark material to predict the H_2 production capacities of candidate materials. We used a method in which a material known to drive water splitting, even if very poorly, was chosen as a standard against which to compare readily obtainable reduction enthalpies of candidate materials within a similar STWS class, i.e., a similar crystal structure and reaction mechanism.

Thus, we assessed the water splitting ability of materials by a two-stage screening: first, we determined if the material or reaction pathway has sufficient energy to split water. If so, then we compared its ability to drive water splitting to previously characterized materials of a similar class as outlined in Equation 4.

$$r_{ben,can}(T) = \frac{e^{\left(\frac{-\Delta G_{can}}{RT}\right)}}{e^{\left(\frac{-\Delta G_{ben}}{RT}\right)}} \approx \frac{e^{\left(\frac{-\Delta H_{can}}{RT}\right)}}{e^{\left(\frac{-\Delta H_{ben}}{RT}\right)}} = e^{\left(\frac{-\Delta\Delta H_{can,ben}}{RT}\right)} \quad (4)$$

Two possible reactions mechanisms, a stoichiometric mechanism and an oxygen-vacancy mechanism, for three aluminates were examined using this screening method. In the stoichiometric reaction mechanism, the active material decomposes to a reduced phase to produce a stoichiometric quantity of O_2. In the O-vacancy reaction mechanism, materials produce oxygen vacancies within the lattice of the host material without it decomposing into a different phase; these vacancies are subsequently filled during oxidation by the O atoms of split H_2O molecules.

We calculated the reduction energy of the doped-hercynite ($Co_xFe_{1-x}Al_2O_4$) stoichiometric reaction to be 175 kJ/mol, indicating that the stoichiometric doped-hercynite cycle does not possess the reducing power to split water. For the O-vacancy mechanism, we calculated a reduction energy of 384–621 kJ/mol, where the wide range stems from the variation in local environments of the oxygen atom involved in the formation of an O-vacancy. This indicates that reduced $Co_{0.5}Fe_{0.5}Al_2O_4$ has sufficient energy to split water and suggests that the doped-hercynite cycle could operate via an O-vacancy mechanism. Furthermore, the energies of these different structures was calculated to determine the relative number of different sites within the material. Similar calculations were done using pure hercynite and cobalt aluminate and are summarized in Figure 1. This information was then used to predict a H_2 production capacity of 1:0.7:2x10^{-4} for $FeAl_2O_4$:$Co_{0.5}Fe_{0.5}Al_2O_4$:$CoAl_2O_4$ for the O-vacancy mechanism. Alternatively, if the enthalpic minimum for water splitting does not exist, Equation 4 predicts a relative production capacity of 1:0.012:0.004 for $CoAl_2O_4$:$Co_{0.5}Fe_{0.5}Al_2O_4$:$FeAl_2O_4$ for the stoichiometric mechanism.

These predicted H_2 capacities were then tested experimentally by cycling the materials near-isothermally between 1,500°C and 1,350°C in an SFR. The H_2 production ratios of the aluminates were found to be 1:0.6:0 for Fe Al_2O_4:$Co_{0.5}Fe_{0.5}Al_2O_4$:$CoAl_2O_4$. This agrees with the computationally predicted relative H_2 production capacities for the aluminates operating via an O-vacancy mechanism and suggests that the thermodynamic screening parameters for STWS viability and reaction mechanism are valid.

We used this screening criteria in conjunction with a predictive O-vacancy formation energy model [1] to screen 1,078 binary perovskites and 590 binary spinels. These materials have the general structure and are comprised of all combinations of the elements shown in Figure 2. The results of the screening are shown in Figure 3.

In addition to thermodynamic screening conducted during the past fiscal year, we performed theoretical kinetics studies to characterize the hydrogen formation reaction pathway on the hercynite, $FeAl_2O_4$, (100) surface. We considered the reaction starting from three possible initial states, (1) a defect free surface, (2) a surface oxygen vacancy coordinated to three aluminum and no iron atoms (referred to as O-Al3), and (3) a surface oxygen vacancy coordinated to two aluminum and one iron atom (O-FeAl2). We found that the O-FeAl2 surface was the thermodynamically most prevalent surface at operating conditions.

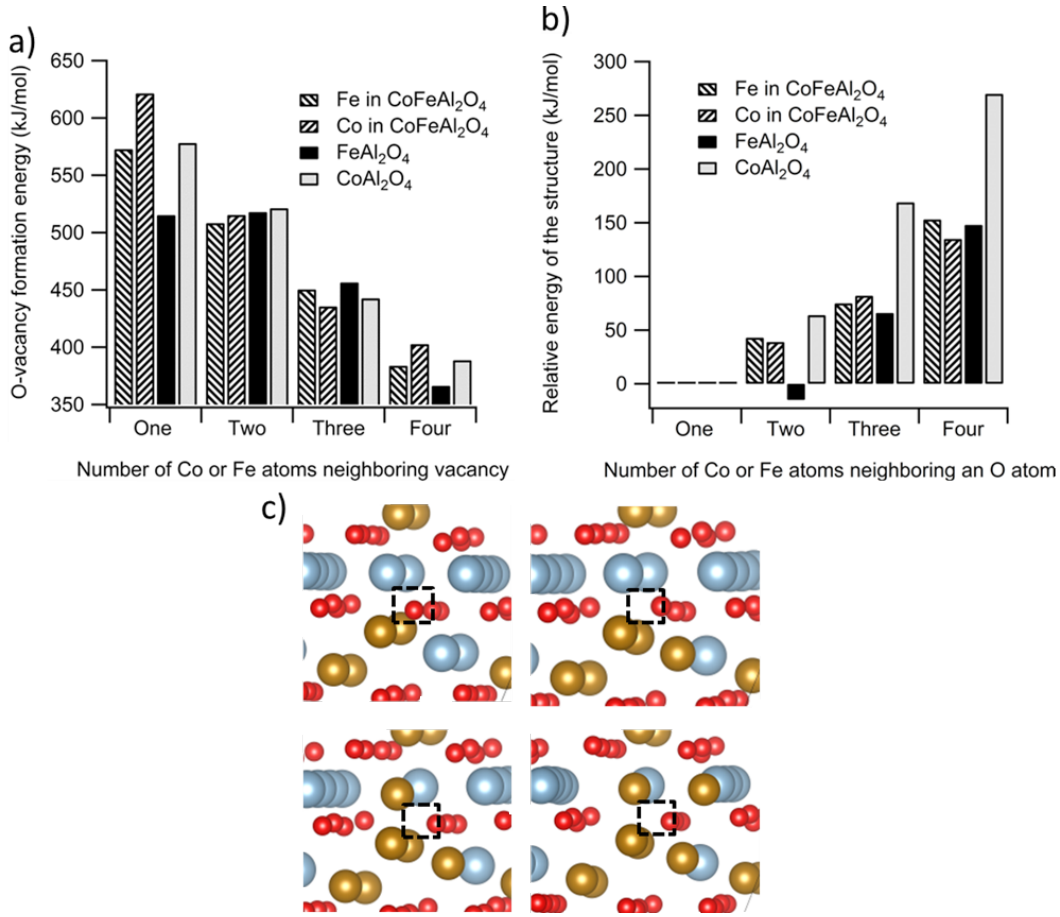

FIGURE 1. (a) Calculated O-vacancy formation energies at sites with varying numbers of Co or Fe nearest neighbors, and (b) the relative energies of exchanging cations to produce O sites with multiple Co or Fe nearest-neighbors. (c) The configurations of the ions in the $FeAl_2O_4$ spinel for an O-vacancy with one (top left), two (top right), three (bottom left), and four Fe neighbors (bottom right). The large blue, medium gold and small red spheres represent Al, Fe and O atoms, respectively and the black square indicates the location of an O-vacancy.

For this case, we have identified two kinetic pathways, which can be seen in Figure 4. In each of these pathways water dissociates into a hydroxide which occupies the oxygen vacancy. The destination of the remaining hydrogen atom differentiates these two kinetic pathways. Dissociation onto a nearby oxygen occurs in the "hydroxide pathway." This produces an intermediate with two protic hydrogens adsorbed to a defect free surface. These protic hydrogens then must pull electron density from the surface to produce H_2. For the hydroxide pathway the dissociation occurs with a lower barrier than the hydrogen formation. Along the "hydride pathway" the dissociated hydrogen adsorbs onto a nearby iron atom. When coordinated to the surface iron the hydrogen is hydridic, and the ensuing reaction between the oppositely charged hydrogens occurs with a lower activation barrier than in the hydroxide pathway.

For the defect free surface activation barriers were not considered. Without an oxygen vacancy to fill dissociation of water leaves an adsorbed oxygen on the surface. This final state lies higher in energy than the activation barriers for the oxygen vacancy case and thus its activation barrier must lie even higher and is thus unlikely to significantly contribute to the overall reaction. The O-Al3 case is currently neglected for a variety reasons. Primarily, it lies much higher in energy and, assuming a surface at equilibrium at a typical STWS temperature of 1,500°C, the O-FeAl2 vacancy would be more than 200 times more likely. Furthermore, because the vacancy lies far from the surface iron atoms, it can only react analogously to the previously discussed hydroxide pathway. After dissociation, no difference exists between these pathways and we have already determined that dissociation is not rate-limiting. As oxygen vacancy migration is studied it may become necessary to revisit this assumption.

CONCLUSIONS AND FUTURE DIRECTION

- Hercynite and doped hercynite redox reactions operate via an O-vacancy mechanism.

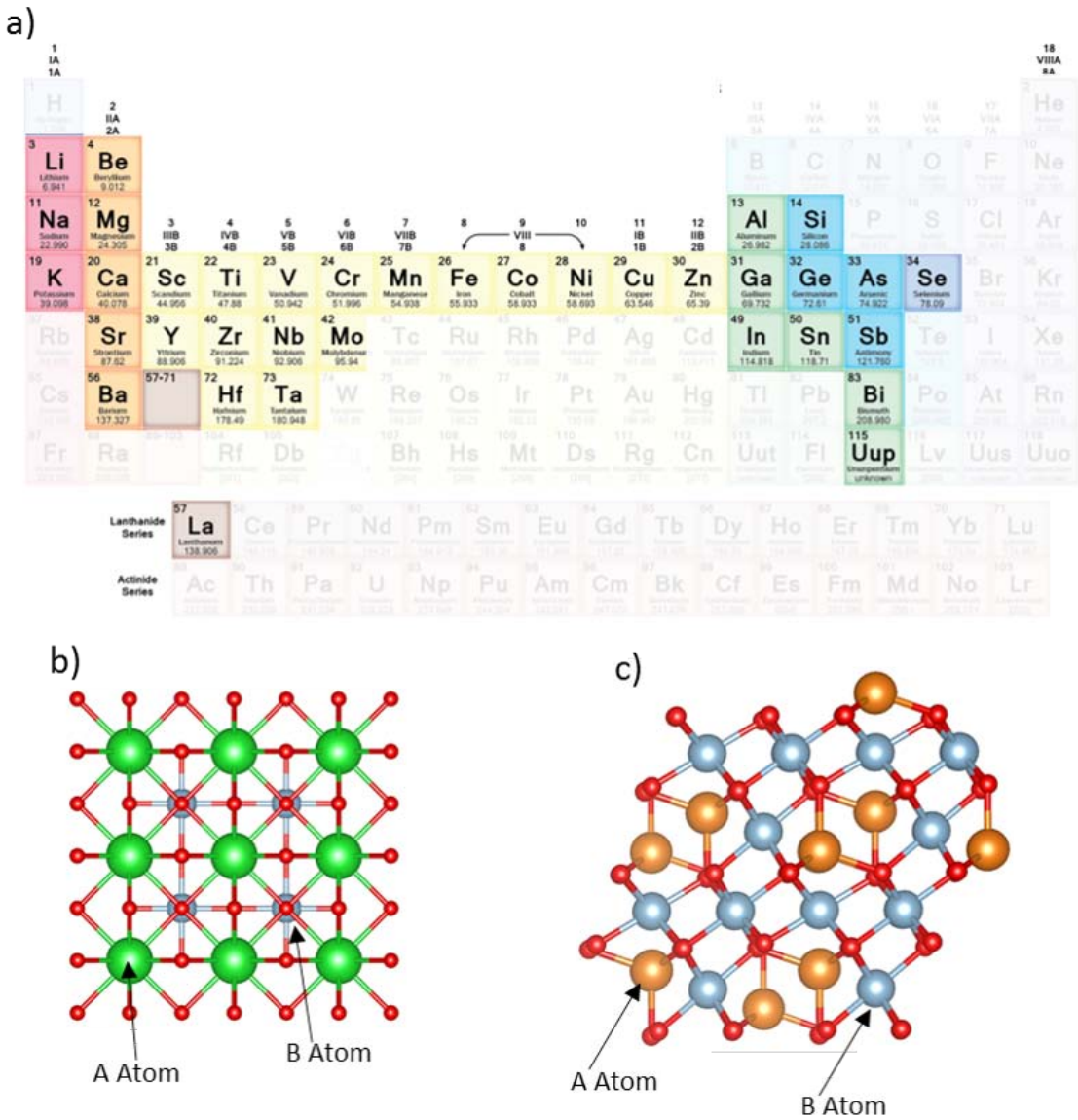

FIGURE 2. All earth abundant, non-radioactive, and non-toxic elements under consideration for forming perovskite and spinel materials.

- The two-step thermodynamic screening method can be used to accurately assess H_2 production capacities of new materials.
- An oxygen vacancy formation descriptor model was used to screen 1,078 binary perovskites and 590 binary spinels for STWS capabilities.
- Hydridic pathway for hydrogen production on a hercynite surface has a lower activation barrier than the hydroxide pathway.
- We will apply a computational approach for predicting water splitting abilities to doped perovskites and additional binary spinels.
- We will validate an oxygen vacancy formation energy model specifically for compounds of interest: perovskites and spinels.
- The project will extend the descriptor model of oxygen vacancy formation energy to systems with various spin and oxygen vacancy configurations, including "smart" scripts for automated searches.
- Important kinetic properties will be identified by substitution and removal of cations at and around the active site of reactive hercynite surface.
- We will extend results from hercynite studies to other potential STWS materials.
- We will characterize other reactions important to STWS, including oxygen vacancy formation and migration.

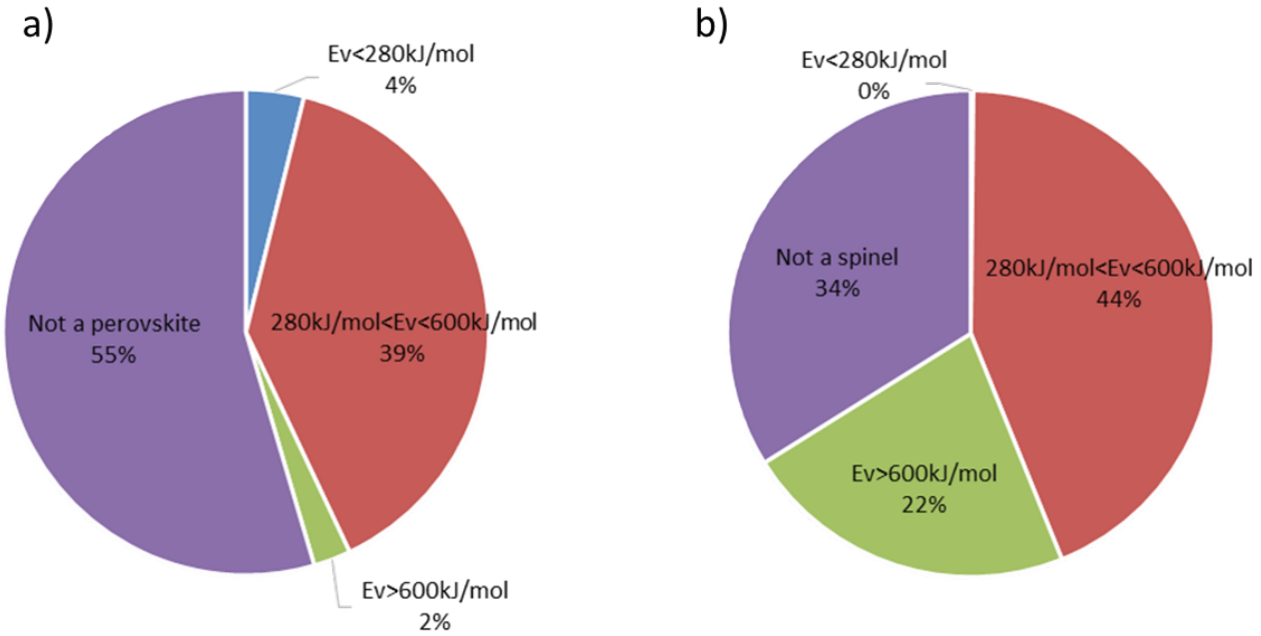

FIGURE 3. (a) Results from oxygen vacancy formation energy screening of 1078 binary perovskites. (b) Results from oxygen vacancy formation energy screening of 590 binary spinels.

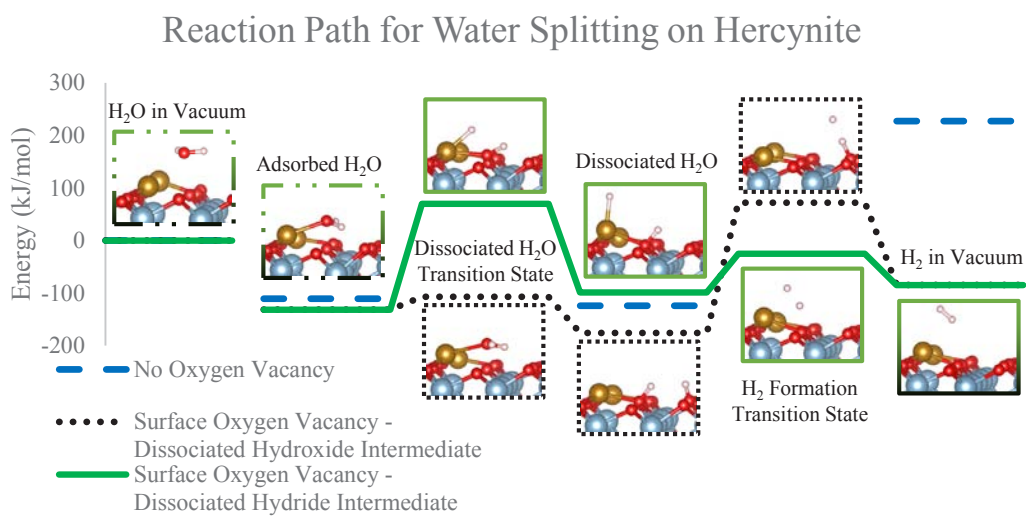

FIGURE 4. Kinetic pathways for hydrogen formation on hercynite. The surface without oxygen vacancies is show with a dashed blue, while the hydroxide and hydroxyl oxygen vacancy pathways are depicted as a dotted black line and green solid line respectively. States for which the transition state has not been identified have been left unconnected. Geometries for the oxygen vacancy pathways are depicted and formatted with borders matching the pathways as described above. Note that the first two states, H_2O in vacuum and adsorbed H_2O are identical and only shown once.

FY 2015 PUBLICATIONS/PRESENTATIONS

Publications

1. Muhich, C.L., B.D. Erhardt, I. Al Shakeri, B.J. Ward, C.B. Musgrave and A.W. Weimer, "A Review and Perspective of Efficient Hydrogen Generation via Solar Thermal Water Splitting," *WIREs Energy and Environment*, In Press, DOI: 10.1002/wene.174.

2. Muhich, C.L., K.C. Weston, D. Arifin, A.H. McDaniel, C.B. Musgrave, A.W. Weimer, "Extracting Kinetic Information from Complex Gas-solid Reaction Data," *Industrial and Engineering Chemistry Research*, 54 (16) 4113-4122 (2015). DOI: 10.1021/ie503894f.

Presentations

1. C. Muhich, B. Ehrhart, V. Witte, K. Weston, D. Arifin, A. McDaniel, E. Coker, C. Musgrave, and A. Weimer, "The Mechanism of Transition Metal Aluminates in Solar Thermal Water Splitting Reactions," presented at *The American Society of Mechanical Engineers Power and Energy Conference*, June 2015 (San Diego, CA).

2. C. Muhich, B. Ehrhart, I. Alshankiti, B. Ward, C. Musgrave, A. Weimer, "Near-Isothermal Doped-Hercynite Redox Cycle for Solar-Thermal Water Splitting," presented at *The 227th Electrochemical Society Meeting*, May 2015 (Chicago, IL).

3. C. Muhich, B. Ehrhardt, I. Al Shankiti, B. Ward, C. Musgrave, and A. Weimer, "Needed Research Focus for Achieving Cost-Effective and Reliable Solar-Thermal Water Splitting," presented at *The 227th Electrochemical Society Meeting*, May 2015 (Chicago, IL).

4. C. Muhich, K. Weston, D. Arifin, A. McDaniel, E. Coker, B. Ehrhart, V. Witte, C. Musgrave, A. Weimer, "The Mechanism of the Doped-Herycnite Cycle for Solar-thermal Water Splitting," presented at the *American Chemical Society Spring National Meeting*, March 2015 (Denver, CO).

5. A. Deml, R. O'Hayre, V. Stevanovic, A.M. Holder, C.B. Musgrave, "Material Descriptor of Oxygen Vacancy Formation Energies in Wide Band Gap Oxides," presented at the *American Chemical Society Spring National Meeting*, March 2015 (Denver, CO).

6. C. Muhich, A.W. Weimer, and C.B. Musgrave, "Rapid Computational Screening and Prototyping of Solar Thermal Water Splitting Materials," presented at *Department of Energy Fuel Cells Technology Office Webinar*, December 2014.

7. C. Muhich, K. Weston, B. Ehrhart, V. Witte, D. Arifin, A. McDaniel, E. Coker, C. Musgrave, A. Weimer, "The Chemistry and Thermodynamics of the Herycnite Cycle Solar-thermal Water Splitting Reaction," presented at *AIChE Annual Meeting*, November 2014 (Atlanta, GA).

8. C. Muhich, B. Ehrhart, K. Weston, I. Al-Shankiti, D. Arifin, A. McDaniel, C. Musgrave, A. Weimer, "Extracting Kinetic Information from Complex Gas-solid Reaction Data: the Kinetics of Hercynite Materials for Solar Thermal CO_2 Splitting," presented at *AIChE Annual Meeting*, November 2014 (Atlanta, GA).

REFERENCES

1. Deml, A.M., Holder, A.M., O'Hayre, R.P., Musgrave, C.B., Stevanovic, V., "Intrinsic Material Properties Dictating Oxygen Vacancy Formation Energetics in Metal Oxides," *The Journal of Physical Chemistry Letters*, 6 (2015): 1948-1953.

II.D.1 New Metal Oxides for Efficient Hydrogen Production via Solar Water Splitting

Yanfa Yan (Primary Contact), Corey Grice, Jie Ge, Tilak Poudel, Sofiya Didyuk, Feng Hong, Wan-Jian Yin, Xunming Deng
The University of Toledo
2600 Dorr Street
Toledo, OH 43606
Phone: (419) 530-5335
Email: yanfa.yan@utoledo.edu

DOE Manager
Eric Miller
Phone: (202) 287-5829
Email: Eric.Miller@ee.doe.gov

Contract Number: CBET-1433401

Project Start Date: September 1, 2014
Project End Date: August 31, 2017

Overall Objectives

The main objectives for this project have been focused into four specific categories which are designed to adhere to National Science Foundation and DOE's technological pathway to photoelectrochemical (PEC) production of renewable hydrogen fuel as well as disseminate knowledge and awareness of renewable energy principles and research.

- Design new metal oxides with physical, optical, chemical and electronic properties optimized for PEC hydrogen production
- Develop approaches for synthesizing designed metal oxides in bulk and thin film form with appropriate phase and grain/film structure for incorporation into PEC water-splitting devices
- Fabricate cells/systems using new metal oxides and characterize to determine overall PEC performance as well as fundamental junction, interface, and device properties and new metal oxide stability
- Instruction of post-doctoral researchers, graduate, and undergraduate students in principles and techniques relevant to renewable energy research and education/outreach activities for K-12 students and the general public regarding renewable energy awareness

Fiscal Year (FY) 2015 Objectives

- Development of design principles and performing density-functional calculations to identify appropriate novel metal oxide materials
- Synthesis of novel metal oxides in bulk and thin film forms
- Create necessary testing station(s) for PEC water-splitting performance evaluation and use to characterize small cells made from novel metal oxides

Technical Barriers

This project addresses the following technical barriers from the Photoelectrochemical Hydrogen Production section of the Fuel Cell Technologies Office Multi-Year Research, Development, and Demonstration Plan:

(AE) Materials Efficiency – Bulk and Interface

(AF) Materials Durability – Bulk and Interface

(AJ) Synthesis and Manufacturing

Technical Targets

This project is focused on identifying, designing, and synthesizing new semiconducting materials which may be successfully employed as light-absorbing materials that will drive the water-splitting reaction with a PEC water-splitting device. The insights and developments obtained from this work should prove useful towards meeting the following 2020 targets established by DOE for PEC hydrogen production in systems with solar concentration [1].

- PEC H_2 cost: \$5.70/kg
- Annual electrode cost tons per day (TPD) H_2: \$255,000/yr-TPD H_2
- Solar-to-hydrogen (STH) energy conversion ratio: 20%
- 1-Sun hydrogen production rate: 1.6×10^{-6} kg/s-m^2

FY 2015 Accomplishments

The accomplishments completed during the current reporting period are summarized below:

- The composition and crystal structure of a new metal oxide material, BBNO, was identified which could serve as a PEC photoanode. Density functional theory calculations suggest a direct bandgap of approximately 1.9 eV, which should be sufficient to drive a PEC reaction cell.

- Bulk BBNO material was successfully synthesized from a mixture of metal oxide precursor materials via solid-state reactions. This material showed coloration and X-ray diffraction patterns consistent with theoretical expectations for this material.
- Thin films of BBNO were successfully synthesized using multiple techniques (radio frequency [RF] sputtering, spin/dip coating), which can be incorporated into a photoelectrode.
- Initial PEC performance data was acquired for a BBNO photoanode which demonstrates over 100 $\mu A/cm^2$ photocurrent at a bias voltage of 1.0 V vs a Ag/AgCl reference electrode under 1-Sun illumination using sodium sulfite as the oxidation reagent, corresponding to an H_2 production rate of over 1.04×10^{-8} kg/s-m^2. Although this production rate is ~100x lower than the 2020 technical target, further optimization is expected to improve this performance measure. These initials tests have also shown that the oxide exhibits short-term stability (several hours) in aqueous electrolyte solutions.

✧ ✧ ✧ ✧ ✧

INTRODUCTION

Direct PEC water splitting has shown promise for producing hydrogen fuel in renewable and scalable manner [2,3], with technical/economic analysis showing that an STH energy conversion efficiency of at least 15% is necessary for economic viability [4]. It has been determined that a tandem device using two separate semiconducting absorbing layers (one n-type with negative charge carriers and one p-type with positive charge carriers), each with complimentary light absorption features, is needed to achieve this efficiency threshold [5–7]. While some of these types of devices have reached efficiencies of over 18% [8], a key problem is that most n-type materials, used in the photoanodes for O_2 generation in the PEC reactor, are not stable enough to sustain long-term operation at high efficiencies [9–15]. The most stable materials for O_2 producing photoanodes are metal oxides, although all of the metal oxides explored thus far [16,17] have underperformed due to inappropriate combinations of material properties such as optical bandgaps, light absorption coefficients, electrical conductivity, and carrier diffusion lengths. This project is intended to design, synthesize, and evaluate a new metal oxide photoanode material which will have a superior combination of materials properties that will permit high efficiency tandem PEC devices to be created that also demonstrate long-term stability.

APPROACH

The University of Toledo has identified several new metal oxide materials with the following desired combination of physical characteristics (1) direct optical bandgaps in the range of 1.6–1.8 eV for ideal PEC performance [7] and strong photon absorption, (2) low charge carrier effective masses, (3) low non-radiative recombination which results from material defects, (4) band edge energies which can drive O_2 evolution reactions, and (5) thermodynamic stability in oxidizing aqueous conditions. The design principles used to identify this metal oxide composition and microstructure were based upon theoretical material principles that predict higher rates of photogenerated charge carriers and transport within the material due to favorable combinations of electron bonding orbitals and crystal symmetry within the microstructure. The additional consideration of using elements that are earth-abundant and have relatively low toxicity was also included in the material design principles. The University of Toledo is able to leverage prior experience in materials synthesis and thin film deposition techniques used in the course of various thin film photovoltaic research efforts to fabricate these materials in both bulk powder and thin film forms. Thin films of these materials could then be deposited onto glass substrates with transparent conductive oxide coatings, or other suitable substrates, to create photoanode electrodes for additional performance evaluation and characterization. Information obtained from these initial photoanodes will guide further efforts towards adjusting the material synthesis and electrode fabrication techniques to optimize the PEC performance.

RESULTS

Using the design principles previously described, a number of metal oxides having either the perovskite or spinel crystal structures were identified that contain Sn, Sb, and/or Bi. The band structure for BBNO was calculated and is shown in Figure 1. The information contained in the band structure revealed an expected bandgap of 1.9 eV and electron transitions which should correspond to high optical absorption, thus increasing the likelihood of producing successful thin films for PEC photoelectrodes. Bulk powder synthesis was performed by annealing a stoichiometric mixture of oxide precursors in a closed crucible in air at temperatures between 600°C and 900°C for several hours. The resulting powder mixture had changed in color from light yellow to brown after annealing and X-ray diffraction patterns from the annealed powders revealed the presence of a single phase with perovskite structure consistent with that expected for BBNO, as shown in Figure 2. Closed crucibles were required during annealing at these temperatures to mitigate loss of Bi, the oxide of which has higher vapor pressure than the other two metal oxide precursors. Films were prepared from this annealed powder by creating a ball milled suspension

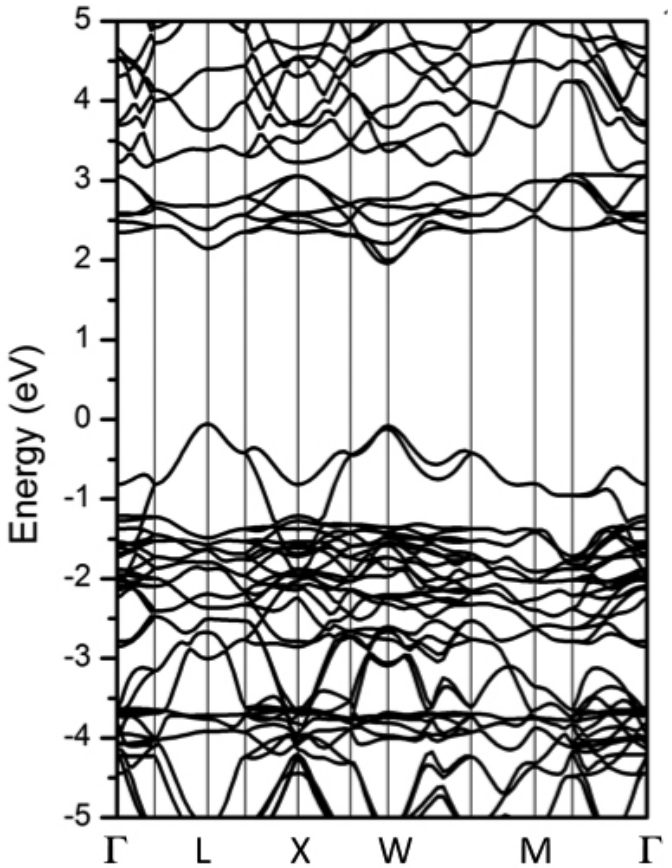

FIGURE 1. Calculated density functional theory band structure of BBNO

in solvents, such as acetone or ethanol, which was then applied to various substrates using dip coating or spin coating methods. The resulting films were several micrometers in thickness and had highly porous microstructures which were relatively unaffected by subsequent thermal processing (not shown). Alternatively, much thinner (<1 μm) films with more compact microstructures were obtained via two independent methods: RF sputtering and sol-gel reaction. Sputtered films were obtained from targets prepared in-house that were either mixed precursor powders (described earlier) or single phase annealed powder. A representative cross-sectional image of the RF sputtered films on a fluorine-doped tin oxide (FTO) coated glass substrate is shown in Figure 3. The sol-gel method involved dissolving metal oxide precursors, in a mixture of acetic acid, 2-methoxyethanol and pentane-2,4-dione. The resulting sol-gel was deposited via spin coating and annealed in air at temperatures between 500°C and 600°C for periods less than two hours. The film changed from light yellow to dark brown in color and was found to exhibit a band gap of nearly 1.9 eV, as expected. Preliminary evaluation for PEC photoanode activity was determined by illuminating films with a 300 W Xe arc lamp while immersed in solutions of 1 M sodium sulfite (after purging with nitrogen for over 30 minutes). It was found that the highly porous films drop spin/dip coating the ball milled powder suspension yielded almost no photocurrent, most likely due to poor electrical contact between individual grains and possibly high defect concentrations at the grain boundaries. The films deposited via RF sputtering and sol-gel spin coating

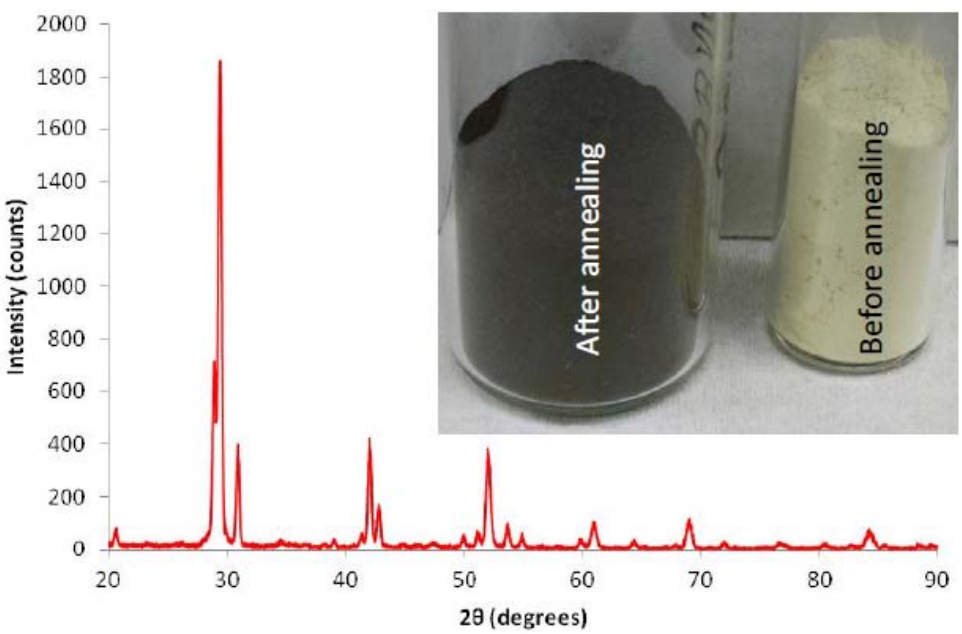

FIGURE 2. X-ray diffraction pattern for air annealed BBNO powder

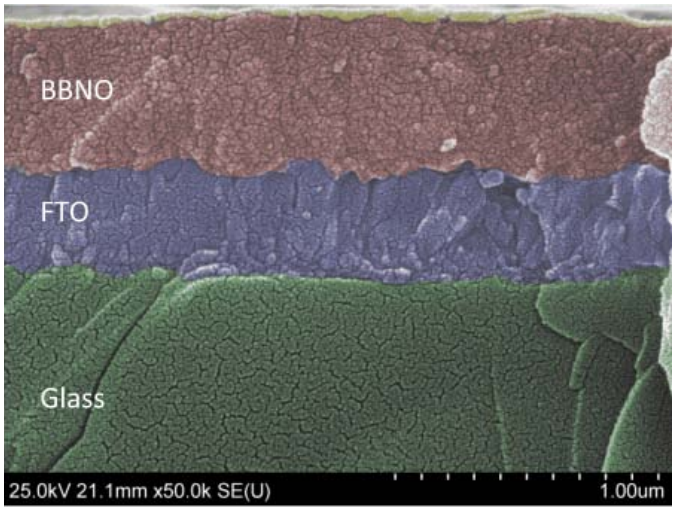

FIGURE 3. Cross-sectional scanning electron microscope image of RF sputtered BBNO film

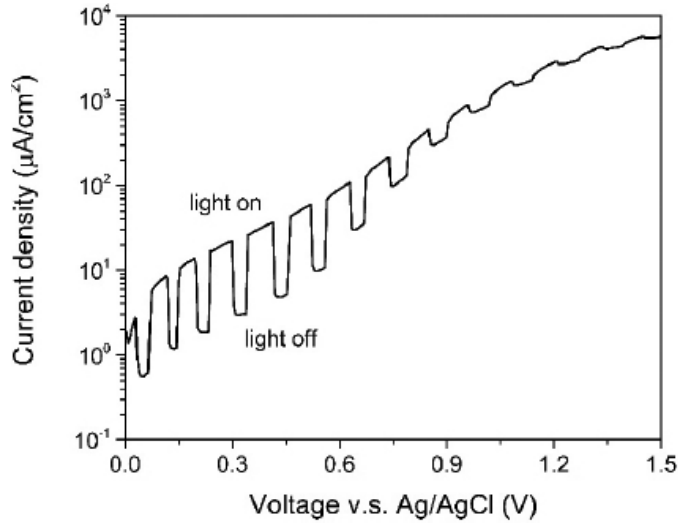

FIGURE 4. Preliminary J-V curve for BBON film photoanode prepared via sol-gel method

showed higher photocurrents, although these were only on the order of 100 μA/cm^2 at bias voltages near 1.0 V versus an Ag/AgCl reference electrode, as shown in Figure 4. Further characterization of the films from the photoanode samples revealed that they had p-type character, which was confirmed by both open-circuit photovoltage versus illumination intensity measurements and Mott-Schottky analysis using capacitance-voltage measurements (not shown here). The carrier concentrations of these films were on the order of 10^{16} cm^{-3} from the Mott-Schottky analysis. Investigations on manipulating the carrier type and concentration by varying the Bi:Nb ratios as well as incorporating dopant atoms such as Cl and F are underway but are still incomplete. Changing the carrier type is especially important since photoanodes operate most effectively when they have n-type character. Finally, all films appear to be stable in the aqueous electrolytes (without applied bias) for several hours without any visible signs of degradation. It was also discovered that the films are stable with the application of positive voltages (vs Ag/AgCl) up to the onset of O_2 evolution in the dark, while all films displayed degradation (in the form of brown-to-black color change and delamination) upon the application of negative bias beginning around -0.6 V (versus Ag/AgCl) and could be from reduction of the Bi and/or Nb cations. For photoanode applications, the negative bias potentials are unlikely to be experienced and should not be a significant concern.

The photocurrents observed are now about 100x lower than what is required for the technical targets, but adjustments to the material electronic characteristics (by altering carrier type/concentration), improving film interface quality, and application of suitable catalyst materials may possibly yield significant improvements. The initial observations for the film stability are encouraging for the ultimate lifetime requirements of a PEC water-splitting system.

CONCLUSIONS AND FUTURE DIRECTIONS

The conclusions obtained from the FY 2015 period are as follows:

- New metal oxide materials for PEC photoanodes were identified using well defined design principles, and the electronic band structure of one oxide, BBNO, was found to be a promising candidate for this application.
- BBNO was successfully synthesized in both bulk powder and thin film forms, the latter of which was successfully applied to FTO coated glass substrates to form PEC water-splitting photoanodes.
- Preliminary PEC photoanode performance and electrode stability was obtained for an aqueous solution with 1 M sodium sulfite oxidation reagent. While the observed photocurrent was much lower than the technical target, the film stability appears favorable for long term PEC operation.
- The observed conductivity of the BBNO films prepared is p-type with concentrations of approximately 10^{16} cm^{-3}, which is not ideal for photoanode operation.

Future work directions for the next reporting period include, but are not limited to:

- Exploring various changes to the material composition, such as adjusting the Bi:Nb ratio and incorporating dopants such as Cl and F, in order to change the conductivity to n-type.
- Investigating various interface treatments (such as oxygen plasma cleaning) to reduce the presence of defects (possible recombination centers) at the

metal oxide/substrate and metal oxide/electrolyte interfaces.

- Creation of nano-structured surfaces of the BBNO films which can increase the electrochemical surface area of the electrodes.
- Addition of water oxidation catalysts to metal oxide surface to reduce the reaction overpotentials.
- Synthesis and thin film fabrication of additional metal oxide materials suggested by the design principles but not yet explored.

FY 2015 PUBLICATIONS/PRESENTATIONS

1. Yanfa Yan, "Metal oxides for PEC water splitting," Invited talk at 227th ECS Meeting, Chicago, Illinois, 5/25/2015.

2. Yanfa Yan, "Band gap engineering of metal oxide for better water splitting," Invited talk at 2015 Spring MRS Meeting, San Francisco, 4/10/2015.

REFERENCES

1. http://energy.gov/sites/prod/files/2015/06/f23/fcto_myrdd_production.pdf

2. A. Bard and M.A. Fox, "Artificial photosynthesis: Solar splitting of water to hydrogen and oxygen," *Acc. Chem. Res.* **28**, 141 (1995).

3. J.A. Turner, "Sustainable hydrogen production," *Science* **305**, 972 (2004).

4. T. Hisatomi, J. Kubota, and K. Domen, "Recent advances in semiconductors for photocatalytic and photoelectrochemical water splitting," *Chem. Soc. Rev.* (2014). DOI: 10.1039/c3cs60378d.

5. R. Rocheleau and E. Miller, "Photoelectrochemical production of hydrogen: Engineering loss analysis," *Int. J. Hydrogen Energy* **22**, 771 (1997).

6. M. Hanna and A. Nozik, "Solar conversion efficiency of photovoltaic and photoelectrolysis cells with carrier multiplication absorbers," *J. Appl. Phys.* **100**, 074510 (2006).

7. S. Hu, C. Xiang, S. Haussener, A.D. Berger, and N.S. Lewis, "An analysis of the optimal band gaps of light absorbers in integrated tandem photoelectrochemical water-splitting systems," *Energy Environ. Sci*. **6**, 2984 (2013).

8. S. Licht, B. Wang, S. Mukerji, T. Soga, M. Umeno, and H. Tributsch, "Efficient Solar Water Splitting, Exemplified by RuO_2-Catalyzed AlGaAs/Si Photoelectrolysis," *J. Phys. Chem.* B **104**, 8920 (2000).

9. A.P. Goodey, S.M. Eichfeld, K.K. Lew, J.M. Redwing, T.E. Mallouk, "Silicon nanowire array photoelectrochemical cells," *J. Am. Chem. Soc.* **129**, 12344 (2007).

10. S.W. Boettcher, J.M. Spurgeon, M.C. Putnam, E.L. Warren, D.B. Turner-Evans, M.D. Kelzenberg, J.R. Maiolo, H.A. Atwater, and N.S. Lewis, "Energy-conversion properties of vapor-liquid-solid-grown Si wire-array photocathodes," *Science* **327**, 185 (2010).

11. S.W. Boettcher, E.L. Warren, M.C. Putnam, D.B. Turner-Evans, M.D. Kelzenberg, M.G. Walter, J.R. McKone, B.S. Brunschwig, H.A. Atwater, and N.S. Lewis, "Photoelectrochemical hydrogen evolution using Si microwire arrays," *J. Am. Chem. Soc.* **133**, 1216 (2011).

12. J.R. McKone, A.P. Pieterick, H.B. Gray, and N.S. Lewis, "Hydrogen evolution from P/Ru-coated p-type WSe_2 photocathodes," *J. Am. Chem. Soc.* **135**, 223 (2013).

13. H.C. Ye, H.S. Park, V.A. Akhavan, B.W. Goodfellow, M.G. Panthani, B.A. Korgel, and A.J. Bard, "Photoelectrochemica characterization of $CuInSe_2$ and $Cu(In_{1-x}Ga_x)Se_2$ thin film for solar cells," *J. Phys. Chem.* C **115**, 234 (2011).

14. P. Wang, T. Minegeshi, G.J. Ma, K. Takanabe, Y. Satou, S. Maekawa, Y. Kobori, J. Kubota, and K. Domen, "Photoelectrochemical conversion pf Toluene to Methyleyclohexane as an organic hybride by Cu_2ZnSnS_4-based photoelectrode assemblies," *J. Am. Chem. Soc.* **134**, 2469 (2012).

15. G.J. Ma, T. Minegishi, D. Yokoyama, J. Kubota, and K. Domen, "Photoelectrochemical hydrogen production on Cu_2ZnSnS_4/Mo-mesh thin-film electrodes prepared by electroplating," *Chem. Phys. Lett.* **501**, 619 (2011).

16. F.E. Osterloh, "Inorganic materials as catalysts for photochemical splitting of water," *Chem. Mater.* **20**, 35 (2008).

17. X. Chen, S. Shen, L. Guo, and S.S. Mao, "Semiconductor-based photocatalytic hydrogen generation," *Chem. Rev.* **110**, 6503 (2010).

II.D.2 Tunable Photoanode-Photocathode-Catalyst Interface Systems for Efficient Solar Water Splitting

G. Charles Dismukes (Primary Contact),
Martha Greenblatt, and Eric Garfunkel
Rutgers, the State University of New Jersey
610 Taylor Road
Piscataway, NJ 08854
Phone: (848) 445-1489
Email: dismukes@chem.rutgers.edu

DOE Manager
Erika Sutherland
Phone: (202) 586-3152
Email: Erika.Sutherland@ee.doe.gov

Contract Number
Research jointly funded by the National Science Foundation, Division of Chemical, Bioengineering, Environmental, and Transport Systems (CBET), and the U.S. Department of Energy, Office of Energy Efficiency and Renewable Energy, Fuel Cell Technologies Office, award number CBET-1433492

Project Start Date: September 1, 2014
Project End Date: August 31, 2017

Overall Objectives

- Design and construct a tandem configuration photoelectrochemical (PEC) cell by developing the knowledge base of a material's chemistry and semiconductor-catalyst interfaces (both photoanode and photocathode), which aim to attain or exceed the DOE benchmark of solar-to-hydrogen (STH) efficiency ≥10%
- Synthesize semiconductor light absorbers for the electrodes (photoanode and photocathode): investigate selected, phase-pure crystalline members of the perovskite oxynitride series $ABO_{3-x}N_x$ where A = alkaline earth or rare earth cations and B = Ti, V, Zr, Nb, or Ta
- Develop a robust and cost effective fabrication method for thin films of the above materials as light absorbers by pulsed laser deposition (PLD), atomic layer deposition (ALD), and/or spin-coated techniques in the second and third year
- Prepare Rutgers-patented oxygen evolution reaction (OER) catalyst (cubic-$LiCoO_2$) thin films on the light absorber using PLD or electrochemical deposition
- Produce stable interfaces between Ni_5P_4 (Rutgers-patented hydrogen evolution reaction [HER] catalyst) and various photocathodes (silicon and other low bandgap semiconductors) to achieve efficient electron capture for HER
- Engineer stable interfaces between Ni_5P_4 and alkaline exchange ionomers to achieve efficient hydroxide transport, slow charge recombination, and provide long-term stability
- Investigate two electrolyte systems for connecting the photoelectrodes: (1) aqueous alkaline electrolyte solution (pH 14) and (2) alkaline exchange membrane (AEM)

Fiscal Year (FY) 2015 Objectives

- Synthesize semiconductor light absorbers with shorter wavelength absorption ($\lambda \leq 2.1$ eV): select phase-pure crystalline members of the perovskite oxynitride series $ABO_{3-x}N_x$, where A = alkaline earth or rare earth and B = Ti, V, Zr, Nb, or Ta
- Investigate the appropriate band-gap and band-edge of selected light absorbers while preventing sub-bandgap absorption
- Prepare thin films of the OER catalyst, cubic $LiCoO_2$, on the photoanode
- Develop alkaline electrolytes compatible with both the OER and HER half-reactions

Technical Barriers

This project addresses the following technical barriers from the Manufacturing R&D section (3.5.5) of the Fuel Cell Technologies Office Multi-Year Research, Development, and Demonstration Plan:

(B) System Cost

(C) Efficiency

(D) Durability/Operability

Technical Targets

The goal of this project is to attain or exceed the DOE benchmark STH energy conversion ratio 10% (and 20% by 2020). The project is conducting work to characterize La-doped $SrNbO_2N$ and $SrTaO_2N$ as light absorbers on the photoanodes, and is optimizing the conditions for high quality thin film fabrication of those same light absorbers by PLD and other techniques. Knowledge from these studies will be applied towards tandem PEC devices that aim to meet the following DOE targets:

- STH energy conversion ratio: 20% (2020)

- PEC electrode cost: $300/m^2
- Electrode replacement lifetime: 0.5 year

FY 2015 Accomplishments

Photoabsorbers

- Improved nitridation conditions and thus materials properties using a KCl flux treatment
- Established the possibility to dope elements (La) into the Nb-based oxynitride(s)
- Prepared phase pure $SrTa(O,N)_3$
- Determined accurate bandgaps of three synthesized oxynitride light absorbers, $SrNbO_2N$, La_2O_3:$SrNbO_2N$, and $SrTaO_2N$, using ultraviolet–visible (UV-VIS) spectrometry with integrating sphere
- Scaled up the synthesis of $Sr_2Nb_2O_7$ and $Sr_2Ta_2O_7$ precursors for the PLD target (10 g) using a solid-state reaction
- Completed PLD instrument training and initiated first experiments that produced an oxide precursor thin film by the PLD method

Catalyst interfaces

- Produced a thin film of lithium cobalt oxide OER catalyst on conducting substrate by electrosynthetic method and characterized its composition by X-ray photoelectron spectroscopy

✧ ✧ ✧ ✧ ✧

INTRODUCTION

The ultimate goal of this project is to fabricate a PEC cell—in this case, a device that directly captures sunlight to aid in maximizing the electrolysis efficiency of decomposing water into fuel (hydrogen and oxygen). Current PEC devices suffer from low stability and efficiency; hence, this project aims to address both those needs by significantly increasing the solar-to-hydrogen conversion efficiency up to 10% while creating a stable device. To realize this goal, we will fabricate a tandem PEC—which is a system that uses two solar light absorbers (semiconductors)—in conjunction with OER and HER catalysts.

APPROACH

The Rutgers approach to increasing the STH efficiencies up to 10% has three strategies, The first strategy utilizes two light absorbers with different bandgaps in a tandem configuration each tuned to achieve optimal solar spectral coverage. Corrosion resistant metal oxides with wide bandgap are good candidates for the photoanode but inefficiently absorb sunlight. Spectral shifting to lower bandgap can be achieved by N doping, which increases the absorption and still preserves stability. Second, each absorber will have a built-in electric field (band-bending) achieved by doping to allow matching of valance (VB) and conduction (CB) band energy levels to the electrochemical required OER and HER potentials, respectively. Finally, to improve charge separation efficiency and lifetime, we will develop methods for creation of thin films of OER and HER catalysts recently developed at Rutgers which show significant promise in independent laboratory testing (Dr. Katherine Ayers, Proton OnSite). By coupling the photoanode to a low bandgap light absorber as photocathode and Rutgers' highly efficient catalysts, we expect to achieve a more cost effective PEC design.

RESULTS

Development of a semiconductor photoanode with durability, high carrier mobility, and appropriate optical bandgap and absorptivity is one of the keys for high STH efficiency PECs. The Rutgers team synthesized and characterized phase pure oxynitrides, $LaNbON_2$ and $SrNbO_2N$, which have relatively low bandgap (~1.8 eV) compared to other phase pure crystalline members in the perovskite oxynitride family. Solid-state synthesis using a KCl flux during the ammonia initiated nitridation step decreased the particle size while increasing particle uniformity. However, these light absorbers have sub-bandgap absorption in the near infrared (IR) range, which would limit performance of the longer wavelength active photocathode in the tandem device. This absorption is currently attributed to either Nb^{5+} reduction during high temperature ammonolysis or structure defects. The Rutgers team reassessed these photoanode light absorbers, and decided upon two different methods to overcome this limitation: (1) doping the *A* or *B* site on the Nb-based oxynitride, or (2) synthesizing different A/B members of crystalline oxynitrides, which have higher tolerance to unwanted reduction under the high temperature ammonolysis conditions.

1. For the Nb-based oxynitride, lanthanum was chosen to dope on to the *A*-site, because its higher oxidation state (3+ versus strontium's 2+) can suppress Nb^{4+}/Nb^{5+}mixed valency. A La-doped $Sr_2Nb_2O_7$ precursor was synthesized post solid-state reaction after achieving a phase pure $Sr_2Nb_2O_7$ oxide precursor. After ammonolysis, lanthanum doping on the $SrNbO_2N$ suppressed the near infrared (IR) absorption of the oxynitride (Figure 1). The expected stoichiometry of this product is La_2O_3:$SrNbO_2N$.
2. A Ta-based oxynitride, $SrTaO_2N$, was synthesized using a sol-gel method and its crystal structure was verified by powder X-ray diffraction (PXRD). The crystal

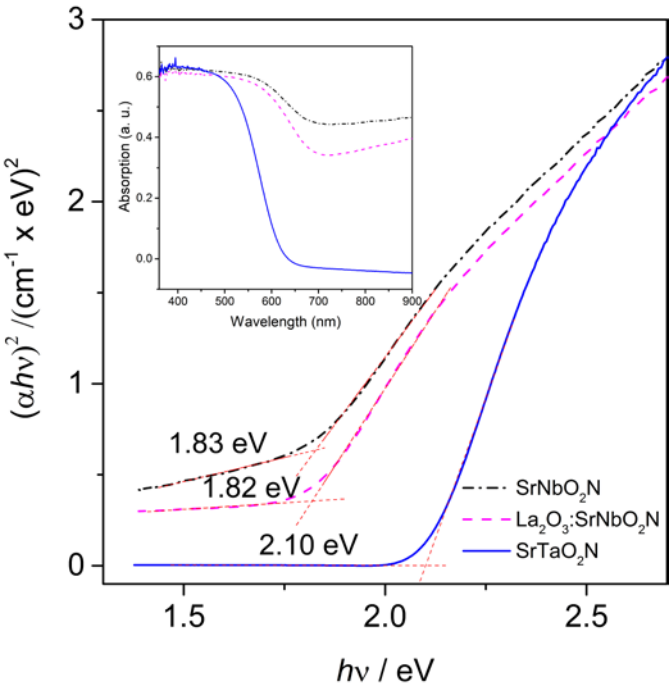

FIGURE 1. Tauc plot of $SrNbO_2N$, 5 mol% doped $SrNbO_2N$, and $SrTaO_2N$. Bandgap values of $SrNbO_2N$, 5 mol% doped $SrNbO_2N$, and $SrTaO_2N$ were obtained as 1.83 eV, 182 eV, and 2.10 eV, respectively (UV-VIS diffuse reflectance spectra).

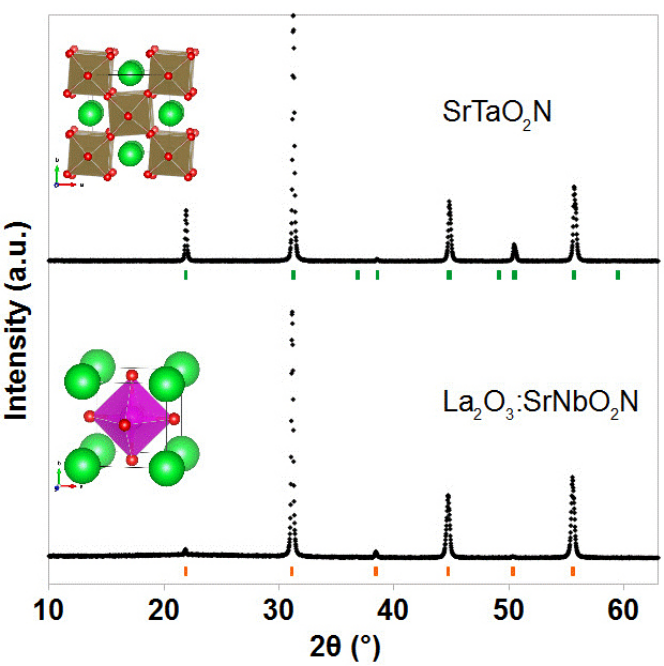

FIGURE 2. Laboratory X-ray powder diffraction for $SrTaO_2N$ (black dots; top) and La_2O_3 doped $SrNbO_2N$ (black dots, bottom) are matched to indexed peaks (green and orange ticks). Each structure (insets) contains Sr (green spheres), O/N (red), and a B-site cation (Nb = purple polyhedron, Ta = tan polyhedron).

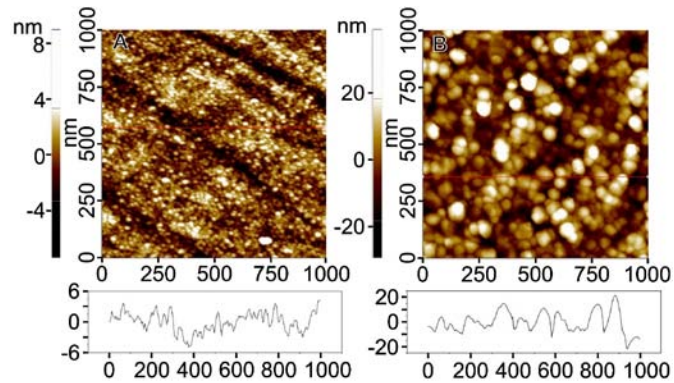

FIGURE 3. AFM image of (a) bare glassy carbon (GC) and (b) $Sr_2Nb_2O_7$ thin film deposited by PLD and line profile. Roughness of (a) and (b) are 1.3 nm and 7.8 nm, respectively.

structure and PXRD pattern are shown in Figure 2. Due to relativistic effects, tantalum (5+) is more redox stable than niobium (5+) and therefore $SrTaO_2N$ is not expected to form the Ta (4+) oxidation state and thus should not show sub band gap absorption in the IR range. The measured absorption spectrum of $SrTaO_2N$ confirmed this expectation of no IR absorption (Figure 1), while the bandgap was found to have a slightly higher threshold (2.1 eV).

Figure 1 compares the absorption spectra of all three synthesized materials: $SrNbO_2N$, La doped $SrNbO_2N$, and $SrTaO_2N$.

Homogeneous thin film light absorbers without defects are necessary to achieve high efficiency PEC devices. Thin film light absorbers can be deposited by the PLD method. In preparation for a high quality thin film, a robust and dense PLD target pellet is necessary for avoiding inhomogeneous and irreproducible films. High density, thick PLD targets of $Sr_2Nb_2O_7$ and $Sr_2Ta_2O_7$ were synthesized by solid-state reactions. Atomic force microscopy (AFM) confirmed the presence of a $Sr_2Nb_2O_7$ thin film and indicated the surface morphology (Figure 3).

Electrosynthesis of $LiCoO_2$ is a potentially rapid and cost effective technique to obtain conformal films on a conductive substrate of this OER catalyst. We have demonstrated synthesis of thin films of Li_xCoO_2 on glass carbon substrate and aim to extend this technique to a light absorbing film (photoanode) which has good electrical contact. Developing this technique was further investigated by X-ray photoelectron spectroscopy (XPS). Cobalt 2p XPS core level transitions reveal Co^{3+} and eliminates the presence of Co^{2+} on the electrodeposited film (Figure 4). Co^{2+} is not wanted here as it is more susceptible to dissolution during electrocatalysis and to corrosion in acid and base. This may explain why the electrodeposited film showed high stability during and following electrolysis.

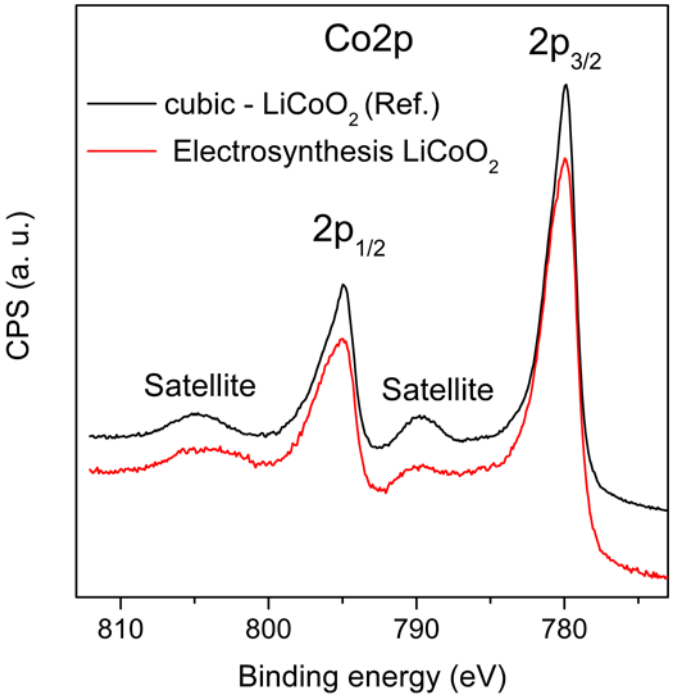

FIGURE 4. X-ray photoemission Co_{2p} spectra of cubic - $LiCoO_2$ and electrosynthesis $LiCoO_2$. $2p_{3/2}$ (780 eV) and satellite peaks (790 eV) are attributed to Co^{3+}.

CONCLUSIONS AND FUTURE DIRECTIONS

Conclusions derived from the work in FY 2015 include the following:

- Lanthanum (3+) doping of $SrNbO_2N$ suppresses near IR absorption, which benefits the optical performance of this material as photoanode.
- Synthesis of a light absorbing oxynitride, $SrTaO_2N$, was achieved with relatively low bandgap and no absorption in the near IR range.
- Thin film deposition of $Sr_2Nb_2O_7$ by the PLD method was achieved.
- An electrodeposited $LiCoO_2$ film was produced, and its CO^{3+} oxidation state and OER electrocatalytic activity were confirmed.

Future efforts toward FY 2015–2016 will include the following:

- Enhance carrier mobility in the photoanode perovskite absorber by choice doping
- Fabricate the OER-photoanode perovskite absorber interface
- Fabricate the interface of HER-photocathode pn-silicon absorber

FY 2015 PRESENTATIONS

1. Bin Liu, E. Garfunkel, M. Greenblatt, and G.C. Dismukes. Poster presented to the Metropolitan New York Catalysis Society annual meeting March 18 (1st place, graduate student award poster). "Perovskite-Related Oxynitrides as Photoanodes in Photoelectrochemical Cells."

2. S. Hwang, G. Gardner, E. Garfunkel, and G.C. Dismukes. Poster presented to the Metropolitan New York Catalysis Society annual meeting, March 18 "Selective Electrochemical Deposition of $LiCoO_2$ and Its Properties as an Electrocatalyst for Water Oxidation/Oxygen Evolution."

3. Bin Liu, E. Garfunkel, M. Greenblatt, and G.C. Dismukes. Poster presented to the 29th Annual Symposium of the Laboratory for Surface Modification (Rutgers), April 2. "Perovskite-Related Oxynitrides as Photoanodes in Photoelectrochemical Cells."

4. S. Hwang, G. Gardner, E. Garfunkel, and G.C. Dismukes. Poster presented to 29th Annual Symposium of the Laboratory for Surface Modification (Rutgers), April 2. "Selective Electrochemical Deposition of $LiCoO_2$ and Its Properties as an Electrocatalyst for Water Oxidation/Oxygen Evolution."

5. G.C. Dismukes, A. Laursen, B. Liu, K. Patraju, and M. Greenblatt (Rutgers). Oral presentation to the Electrochemical Society, Chicago, May 28 (Invited). Renewable Hydrogen Evolution on Nickel Phosphide Electrocatalysts: A Comparative Study of Efficiency and Tolerance to Corrosion."

6. G. Gardner, P. Smith, C. Kaplan, J.F. Al-Sharab, Y.B. Go, M. Greenblatt, and G.C. Dismukes. Oral presentation to the Electrochemical Society, Chicago, May 28. "Understanding the Influence of Structure on Activity and Stability in the Catalysis of the Oxygen Evolution Reaction (OER) Using Crystalline Oxides as a Platform."

7. G.C. Dismukes, E. Garfunkel, and M. Greenblatt. Poster presented at the DOE Hydrogen and Fuel Cell Program Annual Merit Review (June 9 2015). "Tunable Photoanode-Photocathode-Catalyst Interface Systems for Efficient Solar Water Splitting."

8. Graeme Gardner, Jafar Al-Sharab, Yong Bok Go, Martha Greenblatt, and G. Charles Dismukes, "Structural Basis for Differing Electrocatalytic Water Oxidation by the Cubic, Layered and Spinel Forms of Lithium Cobalt Oxides," manuscript in review.

II.E.1 Fermentation and Electrohydrogenic Approaches to Hydrogen Production

Pin-Ching Maness (Primary Contact),
Katherine Chou, and Lauren Magnusson
National Renewable Energy Laboratory (NREL)
15013 Denver West Parkway
Golden, CO 80401
Phone: (303) 384-6114
Email: pinching.maness@nrel.gov

DOE Manager
Katie Randolph
Phone: (720) 356-1759
Email: Katie.Randolph@ee.doe.gov

Subcontractor
Bruce Logan, Pennsylvania State University (PSU),
State College, PA

Start Date: October 1, 2004
Projected End Date: Project continuation and direction determined annually by DOE

Overall Objectives

- Optimize rates and yields of hydrogen production in a sequencing fed-batch bioreactor by varying hydraulic retention time and reactor volume replacement
- Optimize genetic tools to transform *Clostridium thermocellum* and obtain mutants lacking the targeted competing pathway to improve hydrogen molar yield
- Demonstrate hydrogen production from the NREL fermentation effluent to improve overall energy efficiency in hydrogen production from cellulosic biomass using a microbial electrolysis cell (MEC) reactor

Fiscal Year (FY) 2015 Objectives

- Optimize sequencing fed-batch parameters and convert corn stover lignocellulose to hydrogen by the cellulolytic bacterium *Clostridium thermocellum*; aimed to lower feedstock cost
- Use the genetic tools developed at NREL tailored for *C. thermocellum* and delete the ethanol and lactate competing pathway; aimed to improve hydrogen molar yield via fermentation
- Optimize a two-stage MEC to increase the removal of protein during treatment of fermentation effluent while maintaining hydrogen production rates with the overall aim of improving H_2 molar yield

Technical Barriers

This project supports research and development on DOE Technical Task 6, subtasks "Molecular and Systems Engineering for Dark Fermentative Hydrogen Production" and "Molecular and Systems Engineering for MEC," and it addresses barriers AX, AY, and AZ from the Hydrogen Production section of the Fuel Cell Technologies Office (FCTO) Multi-Year Research, Development, and Demonstration Plan.

(AX) Hydrogen Molar Yield

(AY) Feedstock Cost

(AZ) System Engineering

Technical Targets

TABLE 1. Progress toward Meeting DOE Technical Targets in Dark Fermentation

Characteristics	Units	Current Status	2015 Target	2020 Target
Yield of H_2 from glucose	mol H_2/mol glucose	2–3.2	4	6
Feedstock cost	¢/lb sugar	13.5	10	8
Duration of continuous production (fermentation)	Time	17 days	3 months	6 months
MEC cost of electrodes	$/m^2	2,400	300	50

Feedstock cost: The DOE Bioenergy Technologies Office is conducting research to meet its 2015 target of 10¢/lb biomass-derived glucose. NREL's approach is to use cellulolytic microbes to ferment cellulose and hemicellulose directly, which will result in lower feedstock costs.

FY 2015 Accomplishments

- Sequencing fed-batch reactor experiments were conducted and demonstrated that by using a hydraulic retention time (HRT) of 48 h and displacing 50% of the reactor liquid every 24 h, *C. thermocellum* converted corn stover lignocellulose (5 g/L loading based on cellulose content) to H_2 with a maximal rate of 1,373 mL $H_2/L_{reactor}$/d. The lignocellulose has undergone a new and milder pretreatment process via alkaline de-acetylation. *C. thermocellum* can hydrolyze the more recalcitrant de-acetylated substrate for H_2 production using its innate hydrolytic enzyme cocktails, a novel finding.

- A *C. thermocellum* mutant lacking the pyruvate-to-lactate electron-competing pathway has been generated yet with no change in total H_2 production albeit 24% more ethanol, suggesting the importance of deleting the ethanol-competing pathway, which is ongoing.
- A two-stage MEC treatment process was developed to increase the removal of protein from the fermentation effluent. Using a combined continuous flow (first stage) and batch-fed (second stage), the process achieved 93±3% chemical oxygen demand (COD) removal and 84±3% protein removal, respectively. The total hydrogen production rate of this combined treatment process was 0.3±0.1 L $H_2/L_{reactor}$/d. The first stage of the process achieved a hydrogen production rate of 2.1±0.4 L $H_2/L_{reactor}$/d.

✧ ✧ ✧ ✧ ✧

INTRODUCTION

Biomass-derived glucose feedstock is a major operating cost driver for economic hydrogen production via fermentation. DOE FCTO is taking advantage of the DOE Bioenergy Technology Office's (BETO) investment in developing less expensive glucose from biomass to meet its cost target of 10¢/lb by 2015. One alternative and viable approach to addressing the glucose feedstock technical barrier (Barrier AZ) is to use certain cellulose-degrading microbes that can ferment biomass-derived cellulose directly for hydrogen production. One such model microbe is the cellulose-degrading bacterium *Clostridium thermocellum*, which was reported to exhibit one of the highest growth rates using crystalline cellulose [1].

Another technical barrier to fermentation is the relatively low molar yield of hydrogen from glucose (mol H_2/mol sugar; Technical Barrier AX) using existing metabolic pathways in the cells. Biological pathways maximally yield 4 mol hydrogen per 1 mol glucose (the biological maximum) [2]. However, most laboratories have reported a molar yield of 2 or less [3,4]. Molecular engineering to block competing pathways is a viable option toward improving H_2 molar yield. This strategy had resulted in improved hydrogen molar yield in *Enterobacter aerogenes* [5].

A promising parallel approach to move past the biological fermentation limit has been developed by a team of scientists led by Bruce Logan at PSU. In the absence of O_2, and by adding a slight amount of negative potential (-250 mV) to the circuit, Logan's group has produced hydrogen from acetate (a fermentation byproduct) at a molar yield of 2.9–3.8 (versus a theoretical maximum of 4) in a modified microbial fuel cell (MFC) called an MEC [6]. It demonstrated for the first time a potential route for producing up to 8 moles of hydrogen per mole of acetate or potentially up to 12 moles of hydrogen per mole of glucose when coupled to a dark fermentation process. Indeed, in FY 2009 the team reported a combined molar yield of 9.95 when fermentation was coupled to an MEC in an integrated system [7]. Combining fermentation with MECs could therefore address Technical Barrier AX and improve the techno-economic feasibility of hydrogen production via fermentation.

APPROACH

NREL's approach to addressing feedstock cost is to optimize the performance of the cellulose-degrading bacterium *C. thermocellum* using corn stover lignocellulose as the feedstock. To achieve this goal, we are optimizing the various parameters in a sequencing fed-batch reactor to improve longevity, yield, and rate of H_2 production. To improve hydrogen molar yield, we are selectively blocking competing metabolic pathways in this organism via genetic methods. Through a subcontract, PSU is testing the performance of an MEC using both a synthetic effluent and the real waste stream from lignocellulosic fermentation generated at NREL.

RESULTS

Lignocellulose Fermentation

Lignocellulose is a solid substrate, and with continuous feeding the system will eventually suffer from clogging of feed lines and over-exhaustion of the feed pump. A more feasible strategy for lignocellulose fermentation is to feed the substrate at a predetermined interval instead of using continuous feeding. This strategy can be realized via the use of a sequencing fed-batch bioreactor. This method also simultaneously retains the acclimated microbes to increase rate of H_2 production. We carried out the experiment in a Sartorius bioreactor with a working volume of 2 L. The medium was continuously sparged with N_2 at a flow rate of 16 ccm and agitated at 100 rpm. We used HRT of 48 h, a liquid displacement of 50% working volume every 24 h, and seven cycles of carbon loadings at 5.0 g/L of lignocellulose (based on cellulose content). Corn stover was pretreated with a de-acetylation and mechanically refined (DMR) process that has less severity (using mild alkaline solution) hence better sugar recovery and less inhibitors generation. Biomass pretreated with the DMR process could therefore lower the biomass feedstock cost. The pretreated DMR lignocellulose material, kindly supplied by the NREL National Bioenergy Center, contained 42% glucan, 25% xylan and 16% lignin. Data from Figure 1 shows that a longer length of time is required to adapt the microbes to hydrolyze the more recalcitrant DMR biomass, which reached a maximal rate of H_2 production at the fifth cycle (fourth cycle upon DMR substrate loadings). The average H_2 production rate is 757 mL $H_2/L_{reactor}$/d (average of cycles 2–8), with a maximal rate at 1,373 mL/$L_{reactor}$/d (Cycle 5). This is the first report that

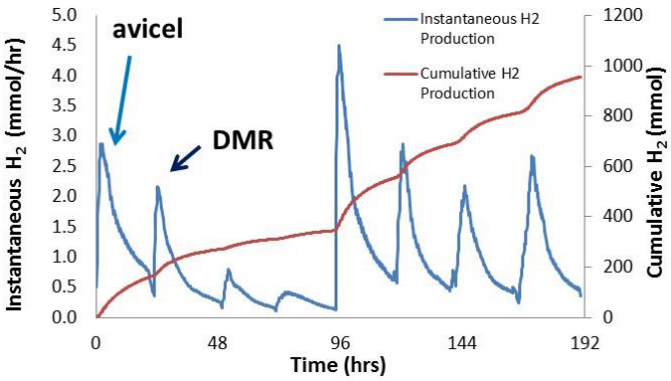

FIGURE 1. H_2 production from corn stover pretreated with a DMR process. Pure cellulose (avicel) was fed at Cycle 1 followed by seven cycles of DMR-biomass in a sequencing fed-batch bioreactor.

C. thermocellum or a cellulose-degrader can hydrolyze the more recalcitrant DMR biomass without adding expensive enzyme cocktail. Future work will devise strategy to shorten the lag time of *C. thermocellum* to start hydrolyzing the more recalcitrant DMR biomass.

Metabolic Engineering

The ultimate goal of this approach is to develop tools to inactivate genes encoding competing metabolic pathways, thus redirecting more cellular flux (i.e., electrons) to improve hydrogen molar yield. Transformation in *C. thermocellum* has been challenging, likely due to either an inefficiency of the plasmids used or an incompatibility of the DNA restriction system between the host and the plasmid [8]. To circumvent both challenges, we have redesigned a plasmid suited for genetic transformation in *C. thermocellum* strain DSM 1313 as the model cellulose-degrader. Following the protocols developed by Argyros et al. [9], we have created a mutant lacking the pyruvate-to-lactate pathway encoded by lactate dehydrogenase with the aim to redirecting more electrons toward H_2 production. The lactate pathway mutant yielded 24% more ethanol and with no change in total H_2 output, highlighting the importance of deleting the ethanol pathway. An effort to delete the ethanol pathway was initiated. We have obtained single colony on agar plate growing in the presence of the antibiotic marker, suggesting the deletion of the ethanol pathway-encoding gene. However, the single colony cannot be revived, likely due to metabolic or redox imbalance. Work is ongoing to devise new strategy for stable deletion of the ethanol pathway.

Two-Stage MEC Process for Increased Protein Removal

Previous research showed unexpected high concentrations of proteins in the fermentation effluent. To convert both acetate and protein to H_2, MEC anodes were conditioned separately to degrade acetate and protein (bovine serum albumin [BSA]) to achieve a goal of 80%) protein

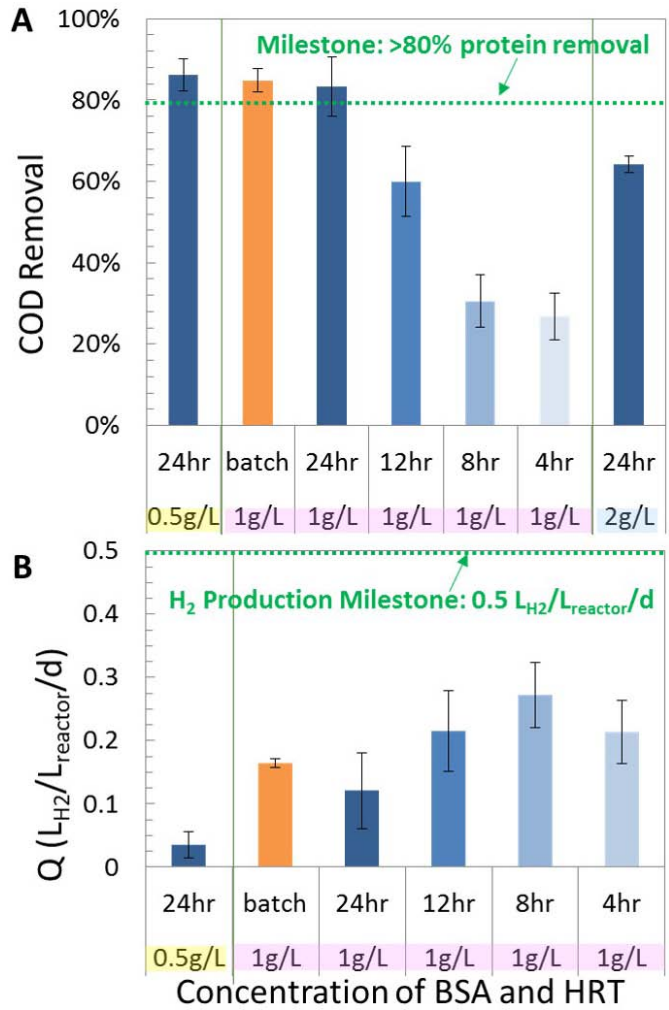

FIGURE 2. (A) Percent removal of protein (BSA) and (B) hydrogen production in MECs fed only BSA

removal with a H_2 production goal of 0.5 L $H_2/L_{reactor}$/d. COD removal decreased as the HRT in the anode chamber was decreased (Figure 2A). The MECs fed acetate achieved ≥80% COD removal at HRTs ≤12 h for all concentrations tested, and a H_2 production rate ≥0.5 L $H_2/L_{reactor}$/d was achieved at all HRTs tested in continuous flow mode. The highest H_2 production rate for the acetate-fed MECs was 2.5±0.3 L $H_2/L_{reactor}$/d at a 4 h HRT, but under these conditions there was <40% COD removal. In MECs treating acetate, a shorter HRT or higher substrate concentration led to increased H_2 production rates, but less COD removal. In BSA-fed MECs, increased protein removal did not result in improved current production (Figure 2B). Only MECs fed ≤1 g/L of BSA, and operated at a 24 h HRT or in fed-batch mode, achieved >80% COD removal, and none of the conditions tested achieved the target H_2 production rate, with the highest rate in the BSA fed MEC of 0.27±0.06 L $H_2/L_{reactor}$/d. When connected hydraulically in series, with the first MEC (acclimated to acetate) at an

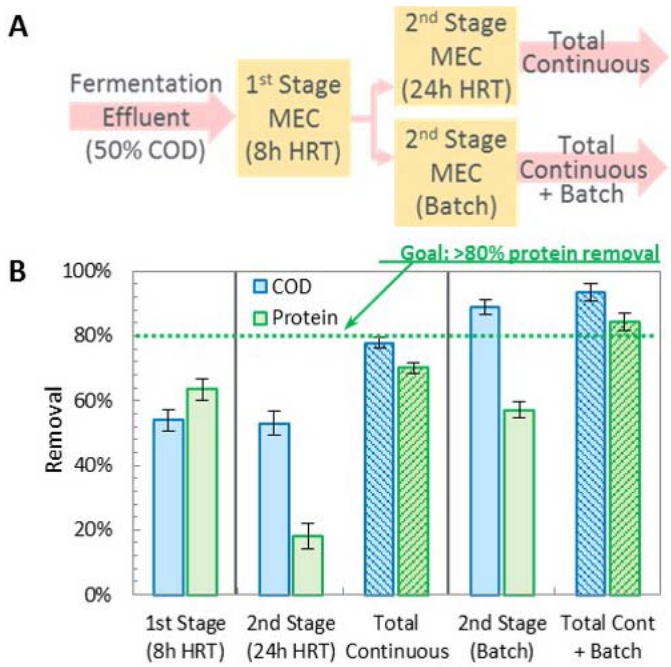

FIGURE 3. (A) Process diagram of effluent treatment stages and (B) COD and protein removal in each stage and for the combined process

8 h HRT to maximize H_2 production rates , and the second MEC (acclimated to BSA) operated at either a 24 h HRT or in batch mode, the two-stage process met the milestone of >80% protein removal (Figure 3). However, this process did not meet the goal of a H_2 production rate of 0.5 $L_{H2}/L_{reactor}/d$. The total H_2 production rate of the reactors combined in series was much lower than that of the first stage of the process (2.1±0.4 $L_{H2}/L_{reactor}/d$). The main reason for the limited H_2 production in the second stage MEC was a low COD concentration. With the effluent COD only 20% of the influent COD, there was insufficient organic matter to sustain high current densities by the anode biofilm. Going forward, we will focus on maximizing H_2 production rates.

Cathode Chamber Design

To increase the volumetric H_2 production rate, we investigated reducing the cathode chamber volume by decreasing the width to 0.7 cm. The volume was reduced to 28 mL (vs. 76 mL previously), for a total reactor volume reduction of 25% (final total volume of 144 mL). The catholyte used in these tests was 0.05 M phosphate buffer (5.6 min HRT), but more saline catholytes will be tested in the future as this can reduce reactor internal resistance. The resulting whole cell and anode potentials were similar to those measured in previous experiments with larger cathode chambers. Therefore, volumetric current density was greater than that of previous MECs with larger (76 – 163 mL) cathode chambers. The improved (reduced volume) MEC produced 1.4±0.2 L $H_2/L_{reactor}/d$ over more than three anode HRT cycles. Optimization will continue as higher salinity catholytes and various catholyte HRTs will be investigated.

CONCLUSIONS AND FUTURE DIRECTIONS

- Using corn stover lignocellulose pretreated via a DMR process (5 g/L based on cellulose content) as the substrate in a sequencing fed-batch reactor, an HRT of 48 h, and displacing 50% of the reactor liquid volume at 24 h intervals, we obtained an average rate of H_2 production at 757 mL/$L_{reactor}$/d, exceeding the benchmark value of the FY 2015 milestone using more recalcitrant substrate. We will optimize the feeding strategy aimed to decrease the H_2 production lag time.
- Following published protocols and using the NREL proprietary plasmid, we deleted the lactate dehydrogenase gene encoding the pyruvate-to-lactate pathway. Its phenotype of increasing ethanol production guided the design to delete the ethanol pathway. Work is ongoing toward generating mutants lacking both ethanol and lactate pathways and quantifying ethanol and H_2 production. The outcome should aid in future site-directed mutagenesis effort by deleting multiple competing pathways to improve hydrogen molar yield.
- There is a trade-off between maximum H_2 production rate and maximum COD and protein removals using a series of MECs for fermentation effluent treatment. The solution to this situation is to focus on maximizing H_2 production rate, and using a secondary process (no hydrogen gas production) to achieve overall COD removal..

In the future, we will operate the fed-batch bioreactor fermenting DMR-pretreated corn stover lignocellulose generated from a de-acetylated process. Due to its recalcitrance nature, we will feed DMR biomass in Cycle 1 to acclimate the microbes hence shortening the H_2 production lag phase. We will also test more frequent re-inoculations to decrease lag time. We will test a new mutagenesis approach via gene replacement to generate the ethanol-competing pathway mutant, determine ethanol and H_2 production profiles in the triple mutants with the outcomes guiding future mutagenesis effort to delete multiple competing pathways, aimed to improve hydrogen molar yield. We will continue to optimize the design of the cathode chamber with the aim of increasing the hydrogen production rate. In addition, we will evaluate combined aqueous/gas diffusion cathodes using electrochemical tests to determine if higher hydrogen production rates can be obtained by using a gas diffusion layer rather than an aqueous catholyte. As the cathode cost is impacted by the choice of the cathode catalyst, we will explore the use of non-precious metal cathode catalysts.

FY 2015 PUBLICATIONS/PRESENTATIONS

1. "Hydrogen metabolic network in *Clostridium thermocellum*." Oral presentation at the XIII International Clostridium Conference, September 19–21, 2014, Shanghai, China (Maness).

2. "Engineering *Clostridium thermocellum* for H_2 production." Oral presentation at the 249th American Chemical Society National Meeting & Exposition, March 22–24, 2015 (Chou).

3. Maness, P.C., and Logan, B. 2015. DOE Fuel Cell Technologies Office Annual Merit Review, June 11, 2015, Washington, DC. Presentation PD038.

4. Watson, V.J., and Logan, B. 2015. "Hydrogen production from continuous flow bioelectrochemical systems treating fermentation wastewater." DOE Fuel Cell Technologies Office Annual Merit Review Poster Session, June 9, 2015, Washington, DC. Poster Presentation PD122.

5. Watson, V.J., M.C. Hatzell, and B.E. Logan. 2015. "Hydrogen production from continuous flow, microbial reverse–electrodialysis electrolysis cells treating fermentation wastewater." *Biores. Technol*. 195: 51–56.

REFERENCES

1. Zhang, Y.P.; Lynd, L.R. (2005). "Cellulose utilization by *Clostridium thermocellum*: bioenergetics and hydrolysis product assimilation." *Proc. Natl. Acad. Sci. USA* **102**, 7321–7325.

2. Hawkes, F.R.; Dinsdale, R.; Hawkes, D.L.; Hussy, I. (2002). "Sustainable fermentative hydrogen production: challenges for process optimisation. *Intl. J. Hydrogen Energy* **27**, 1339–1347.

3. Logan, B.E.; Oh, S.E.; Kim, I.S.; Van Ginkel, S. (2002). "Biological hydrogen production measured in batch anaerobic respirometers." *Environ. Sci. Technol*. **36**, 2530–2535.

4. Van Ginkel, S.; Sung, S. (2001). "Biohydrogen production as a function of pH and substrate concentration." *Environ. Sci. Technol*. **35**, 4726–4730.

5. Rachman, M.A.; Furutani, Y.; Nakashimada, Y.; Kakizono, T.; Nishio, N. (1997). "Enhanced hydrogen production in altered mixed acid fermentation of glucose by *Enterobacter aerogenes*." *J. Ferm. Eng.* **83**, 358–363.

6. Cheng, S.; Logan, B.E. (2007). "Sustainable and efficient biohydrogen production via electrogenesis." *Proc. Natl. Acad. Sci. USA*. **104**, 18871–18873.

7. Lalaurette, E.; Thammannagowda, S.; Mohagheghi, A.; Maness, P.C.; Logan, B.E. (2009). "Hydrogen production from cellulose in a two-stage process combining fermentation and electrohydrogenesis." *Intl. J. Hydrogen Energy* **34**, 6201–6210.

8. Guss, A.; Olson, D.G.; Caiazza, N.C.; Lynd, L.R. (2012). "Dcm methylation is detrimental to plasmid transformation in *Clostridium thermocellum*." *Biotechnol. Biofuels* **5**, 30–41.

9. Argyros, D.; Tripathi, S.A.; Barrett, T.F.; Rogers, S.R.; Feinberg, L.F.; Olson, D.G.; Foden, J.M.; Miller, B.B.; Lynd, L.R.; Hogsett, D.A.; Caiazza, N.C. (2011). "High ethanol titers from cellulose by using metabolically engineered thermophilic anaerobic microbes." F *Appl. Environ. Microbiol.* **77**, 8288–8294.

II.E.2 Improving Cyanobacterial O_2-Tolerance Using CBS Hydrogenase for H_2 Production

Pin-Ching Maness (Primary Contact), Carrie Eckert, and Jianping Yu
National Renewable Energy Laboratory (NREL)
15013 Denver West Parkway
Golden, CO 80401
Phone: (303) 381-6114
Email: pinching.maness@nrel.gov

DOE Manager
Katie Randolph
Phone: (720) 356-1759
Email: Katie.Randolph@ee.doe.gov

Project Start Date: May 1, 2005
Project End Date: Continuation and direction determined annually by DOE

Overall Objectives

- Decipher the maturation machinery of the O_2-tolerant hydrogenase in *Rubrivivax gelatinosus* to transfer the correct number of genes to build a cyanobacterial recombinant
- Construct a cyanobacterial recombinant by expressing four hydrogenase genes and six maturation genes from *R. gelatinosus* for sustained H_2 production
- Demonstrate H_2 production in the cyanobacterial recombinant during photosynthesis for photolytic H_2 production

Fiscal Year (FY) 2015 Objectives

- Develop an O_2-tolerant cyanobacterial system for sustained and continuous light-driven H_2 production from water

Technical Barriers

This project addresses the following technical barrier from the Hydrogen Production section (3.1.4) of the Fuel Cell Technologies Office Multi-Year Research, Development, and Demonstration Plan

(AP) Oxygen Accumulation

TABLE 1. Technical Targets

Characteristics	Units	2011 Target	2015 Target	2020 Target	Ultimate Target
Duration of continuous H_2 production at full sunlight intensity	Time units	2 min	30 min	4 h	8 h

FY 2015 Accomplishments

- *Rubrivivax gelatinosus* CBS (hereafter CBS) contains two sets of maturation genes, *hyp1* and *hyp2* with unknown roles. We have generated CBS mutants lacking either or both *hyp1/hyp2*. Phenotypical analysis revealed that *hyp1* is essential for assembling the O_2-tolerant, H_2-evolving hydrogenase and *hyp2* is for the H_2-oxidizing uptake hydrogenase. The findings confirm that only *hyp1* genes (*hyp1FCDEAB*) will be genetically transferred into *Synechocystis* along with the hydrogenase genes to assemble the O_2-tolerant CBS hydrogenase.
- To ensure balanced protein expression between CBS and recombinant *Synechocystis*, we refactored the promoter/ribosome binding site (RBS) constructs and detected enhanced expression of most CBS proteins (CooLUH and HypBCE) in *Synechocystis* based on the available antibodies in hand. The outcomes serve as the first step toward active CBS hydrogenase activity in *Synechocystis*.

✧ ✧ ✧ ✧ ✧

INTRODUCTION

Photobiological processes are attractive routes to renewable H_2 production. With the input of solar energy, photosynthetic microbes such as cyanobacteria and green algae carry out oxygenic photosynthesis using solar energy to extract reducing equivalents (electrons) from water. The resulting reducing equivalents can be fed to a hydrogenase system yielding H_2. However, one major barrier is that most hydrogen-evolving hydrogenases are inhibited by O_2, which is an inherent byproduct of oxygenic photosynthesis. The rate and duration of H_2 production is thus limited. Certain photosynthetic bacteria are reported to have an O_2-tolerant, H_2-evolving hydrogenase, yet these microbes do not split water and require other more expensive feedstock.

To overcome these technical barriers, we propose to construct novel microbial hybrids by genetically

transferring O_2-tolerant hydrogenases from other bacteria into cyanobacteria. These hybrids will use the photosynthetic machinery of the cyanobacterial hosts to perform the water-oxidation reaction with the input of solar energy, and couple the resulting reducing equivalents to the O_2-tolerant bacterial hydrogenase, all within the same microbe. By overcoming the sensitivity of the hydrogenase enzyme to O_2, we address one of the key technological hurdles (Barrier AP) to cost-effective photobiological H_2 production, which currently limits the production of H_2 in photolytic systems.

APPROACH

Our goal is to construct a novel microbial recombinant, taking advantage of the most desirable properties of both cyanobacteria and other bacteria, to serve as the basis for technology to produce renewable H_2 from water and solar energy. To achieve this goal, we transfer known O_2-tolerant hydrogenase from CBS to the model cyanobacterium *Synechocystis* sp. PCC 6803.

RESULTS

Probing Hydrogenase Maturation Machinery in CBS

The overarching goal is to construct a cyanobacterial recombinant harboring the O_2-tolerant hydrogenase from CBS using *Synechocystis* sp. PCC 6803 as a model host for sustained photolytic H_2 production. A prerequisite for success is to gain better understanding of the CBS hydrogenase and especially its underlying maturation machinery to ensure transfer of the correct genes into *Synechocystis* to confer hydrogenase activity. CBS genome was sequenced and annotated in FY 2013 via collaboration with Michigan State University and Pacific Biosciences. Using the Basic Local Alignment Search Tool – Protein (BLASTP) tool, we uncovered in CBS genome a second set of hydrogenase maturation genes (*hyp2*), which is different from the set of hydrogenase maturation genes found earlier (*hyp1*). This raises the question as to which set of maturation genes is responsible for building an active CBS hydrogenase and hence needs to be co-transformed along with the CBS hydrogenase into *Synechocystis*. As such we conducted site-directed mutagenesis and obtained CBS mutants lacking either *hyp1* or *hyp2* or both. Genetic strategy and PCR verification of mutant generation are shown in Figure 1. Analysis of H_2 production, CO uptake, and H_2 uptake profiles in wild type and mutants revealed that *hyp1* genes are essential for assembly and maturation of the CBS O_2-tolerant hydrogenase. This finding thereby confirms that only *hyp1* (*hyp1FCDEAB*) will be co-transformed into *Synechocystis* along with the CBS hydrogenase structural genes (*cooLXUH*) to confer CBS hydrogenase activity.

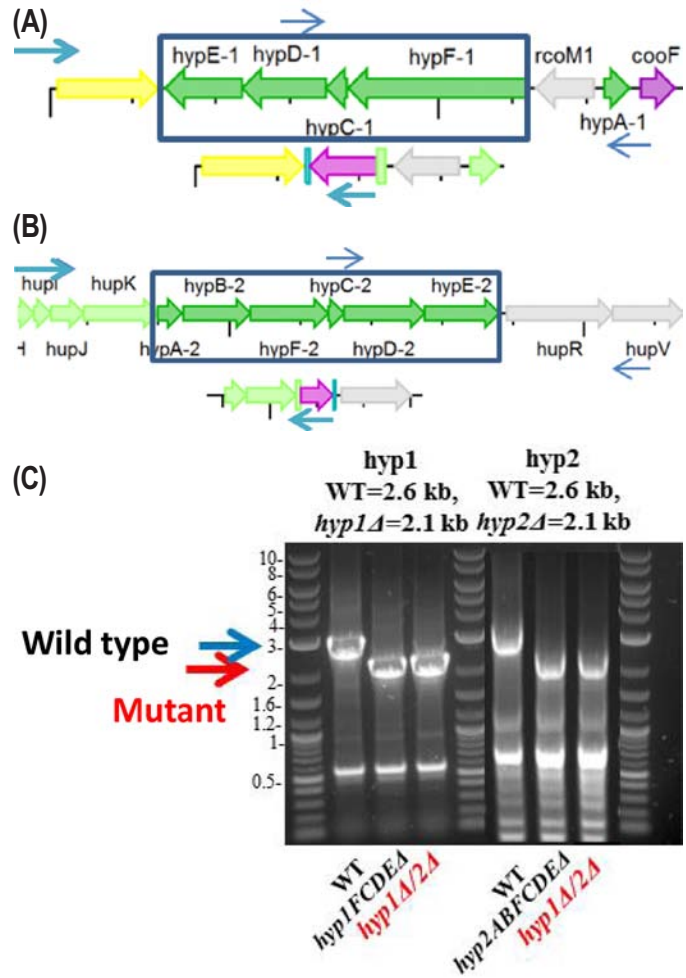

FIGURE 1. Genetic strategy for deletions of *hyp1* (A) and *hyp2* (B) in *Rubrivivax gelatinosus* CBS. Blue arrows denote 5-ft- and 3-ft-end primers for PCR verification; (C) PCR verification of *hyp1/hyp2* deletion mutant generation using primer set noted in (A) and (B).

Expression of the CBS Hydrogenase in *Synechocystis*

One strategy to increase H_2 production is to increase the amount of active CBS hydrogenase proteins expressed in *Synechocystis* by using stronger promoters (enhancing gene expression) and its cognate RBS (enhancing protein expression). We have acquired the antibodies to confirm the latter. In this new modular design, both *hyp1* genes and *cooLXUH* are driven by the stronger *Ptrc* promoter (as comparing to the *psbA* promoter) and Trc RBS known to enhance expression in *E. coli* and functional in cyanobacteria [1]. PCR data (not shown) confirmed the correct integration of both constructs in the neutral genome sites of *Synechocystis*. Based on protein western blots using the available antibodies in hand, we indeed detected enhanced expression of all the proteins (denoted by purple arrows) when comparing to the weaker *petE* and *psbA* promoters (Figure 2). Most protein levels are comparable to

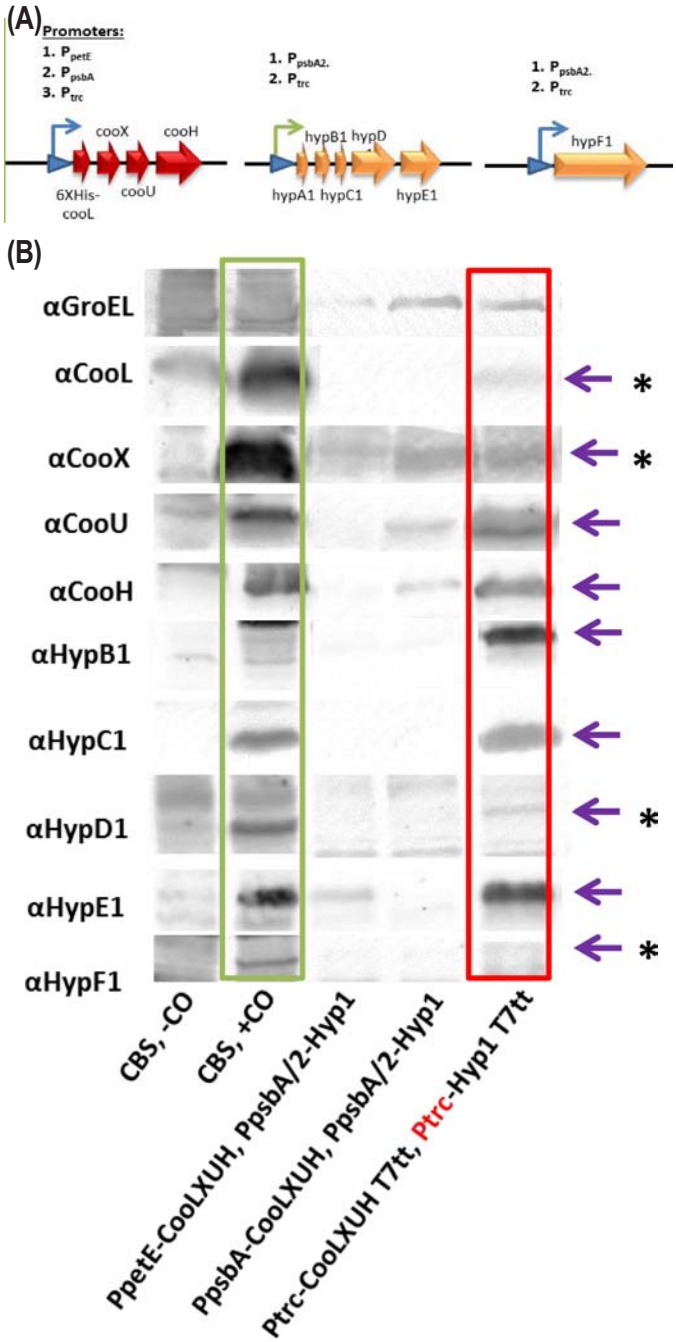

FIGURE 2. (A) Diagram illustrating promoters and tuning strategy for cloning into *Synechocystis*, and (B) balanced protein expression verified via protein western blots of various *Rubrivivax gelatinosus* CBS proteins expression levels in CBS native host and in recombinant *Synechocystis*, the latter driven by three different promoters.

those in native CBS (CO inducible) except those denoted with asterisks. The outcomes serve as the first step toward active CBS hydrogenase activity in *Synechocystis*. The recombinant *Synechocystis* however didn't display any in vitro hydrogenase activity when assayed using sodium dithionite as the reductant and methyl viologen as the mediator. Parallel transformation was also conducted in *E. coli* for troubleshooting. A culprit for the lack of activity could be the missing two subunits of CBS hydrogenase, CooM and CooK, both are membrane proteins and therefore more difficult for expression in foreign host. Work is ongoing for optimization and co-expression of *cooMK* in *Synechocystis* and in *E. coli* to afford hydrogenase activity.

CONCLUSIONS AND FUTURE DIRECTIONS

Conclusions

- CBS mutants analysis lacking either or both *hyp1/hyp2* revealed that only *hyp1* is essential for assembling the O_2-tolerant, H_2-evolving hydrogenase and that only *hyp1* genes (*hyp1FCDEAB*) will be genetically transferred into *Synechocystis* along with the hydrogenase genes to assemble the O_2-tolerant CBS hydrogenase.
- We refactored the promoter/RBS constructs and obtained a *Synechocystis* strain expressing all 10 CBS genes (*cooLXUH* and *hyp1FCDEAB*). We indeed detected enhanced expression of most CBS proteins in the *Synechocystis* recombinant. Yet the latter still lacks active hydrogenase activity.

Future Directions

- We will generate knockout mutant in CBS lacking *cooM*, *cooK*, or both to probe their functionality in assembling the active CBS hydrogenase activity.
- Optimize codons, build genetic constructs containing *cooM*, *cooK*, or both for expression in *Synechocystis* and in *E. coli* (for troubleshooting), and determine hydrogenase activity.

FY 2015 PUBLICATIONS/PRESENTATIONS

1. Wawrousek, K., S. Nobles, J. Korlach, J. chen, C. Eckert, J. Yu, and P.C. Maness. 2014. "Genome annotation provides insight into carbon monoxide and hydrogen metabolisms in *Rubrivivax gelatinosus*." PLoS One. DOI: 10.1371.

2. Eckert, C.E. "Improving cyanobacterial O_2-tolerance using CBS hydrogenase for hydrogen production." Poster presentation at the DOE Hydrogen and Fuel Cells Annual Merit Review, June 9, 2015, Washington, DC (PD095).

REFERENCE

1. Huang, H.-H., D. Camsund, P. Lindblad, and T. Heidorn. 2010. "Design and characterization of molecular biology tools for a synthetic biology approach towards developing cyanobacterial biotechnology." Nucleic Acids Res. 38: 2577–2593.

II.F.1 Monolithic Piston-Type Reactor for Hydrogen Production through Rapid Swing of Reforming/Combustion Reactions

Wei Liu[1] (Primary Contact), Yong Wang[2], Chris Bertole[3], Bang Xu[4]
[1]Pacific Northwest National Laboratory (PNNL)
Energy and Environment Directorate
902 Battelle Blvd.
Richland, WA 99352
Phone: 509-375-2524
Email: wei.liu@pnnl.gov
[2]Washington State University, Pullman, WA
[3]Cormetech Inc., Durham, NC
[4]Dason Technology Inc., Richland, WA

DOE Manager
Katie Randolph
Phone: (720) 356-1759
Email: Katie.Randolph@ee.doe.gov

Project Start Date: September 1, 2014
Project End Date: September 30, 2017

Overall Objectives

- Develop a compact reactor unit that can be readily transported and installed, and quickly turned around for distributed hydrogen production from biomass-derived liquids, as a pathway for reaching the DOE target of <$4/kg H_2
- Realize the unit-based scale of economy rather than the capacity-based scale of economy
- Develop an integrated, mobile test unit and demonstrate the critical technical performances

Fiscal Year (FY) 2015 Objectives

- Set up research agreements with collaborators
- Conduct process designs of the integrated reactor testing system and install the first version of the unit
- Develop low temperature steam reforming catalysts suitable for rapid reaction/regeneration cyclic operation
- Develop sorbent materials suitable for capturing CO_2 under steam reforming conditions
- Identify preparation methods to load the sorbent and catalyst materials into monolith structures

Technical Barriers

This project addresses the following technical barriers from the 3.1.5 (Distributed Hydrogen Production from Renewable Liquid Feedstocks) section of the Fuel Cell Technologies Office Multi-Year Research, Development, and Demonstration (MYRDD) Plan:

(A) Reformer Capital Cost and Efficiency

(B) Operations and Maintenance (O&M)

(C) Biomass Feedstock Issues

(D) Forecourt Footprint and Storage

(E) Control and Safety

Technical Targets

The main goal of this project is to develop a hydrogen production technology that enables utilization of low cost bio-derived liquids. Ethanol is valuable for liquid transportation fuel blend. It is clean and mass produced in the United States (U.S.) As shown in Table 1, its current cost is fairly high as a feedstock for hydrogen production. The other bio-derived liquids such as bio-oil are projected of much lower costs. But, there are no proven technologies for hydrogen production from this kind of feedstock. The compact reactor technologies will be developed to substantially lower the feedstock cost without significantly increasing the capital and operation costs.

TABLE 1. Progress towards Meeting Technical Targets for Distributed Bio-Derived Renewable Liquids

Characteristics	Units	2015–high-T ethanol reforming[a]	Present bio-oil reforming approach
Production unit capital cost contribution	$/kg	0.70	0.93
Feedstock cost contribution	$/kg	5.10[b]	2.07[c]
Production fixed O&M cost contribution	$/kg	0.10	0.42
Production of other variable O&M cost contribution	$/kg	0.10	0.37
Hydrogen levelized cost (production)	$/kg	5.90	3.81

[a]Values from Table 3.1.3 in MYRDD plan
[b]Ethanol cost = $2.15/gallon
[c]Bio-oil cost = $0.219/kg, ref: PNNL-23053, NREL/TP-5100-61178
T - temperature

FY 2015 Accomplishments

- A new CO_2 sorbent material system, made of inexpensive materials, is invented and demonstrated with superior performances for applications to CO_2 capture over a wide range of process conditions, such as 300–700°C. The sorbent shows rapid sorption kinetics, high working capacity and stability in repeated sorption/regeneration cycling tests in the presence of steam. These performance characteristics make it possible to integrate CO_2 capture with steam reforming reaction into one reactor vessel so that the hydrogen production process can be greatly simplified.
- A metal oxide composite catalyst, made of inexpensive materials, is identified to conduct bio-oil reforming reactions at much lower temperatures than what was typically used in the previous studies (600–800°C). Lowering the reforming temperature is beneficial to reducing the reactor vessel cost, increasing the thermal energy efficiency, and prolonging the catalyst lifetime.
- Preparation methods are identified to load the CO_2 sorbent and reforming catalyst materials into monolithic structures for development of compact monolith reactors.
- A once-through, small laboratory-bench reactor system has been built to evaluate sorbent and catalyst materials for respective sorption and reforming processes and to conduct quick tests of new reactor/process concepts.
- Designs for the integrated reactor system are done and major pieces of equipment are acquired to erect the first version of the reactor system, which enables process tests and development at much larger feed rates than the laboratory apparatus.

✧ ✧ ✧ ✧ ✧

INTRODUCTION

Biomass is a renewable resource and produced over a wide range of territories in the U.S. Some low cost processes can be used to convert biomass into liquids that are of high energy density and can be readily transported and stored. For example, bio-oils can be produced by pyrolysis and mixed oxygenates can be produced by hydrothermal deconstruction. These are attractive resource for distributed hydrogen production. The produced hydrogen or syngas can be used to generate electricity using fuel cells or gas turbines. Such a distributed power generation capability would help mitigate energy storage issues associated with other renewable energies such as solar and wind. Thus, distributed hydrogen production from biomass-derived feedstock is important to long term energy and environmental sustainability in the U.S.

However, there are no technologies available for economic conversion of the bio-liquids into hydrogen. Because of its complex compositions, almost all the catalysts reported so far for steam reforming of bio-oil showed rapid deactivation or limited lifetime. Even if the catalyst deactivation issue can be addressed, the conventional hydrogen production process involves a complex process diagram that can make the hydrogen production cost-prohibitive because of small process capacity for distributed production.

APPROACH

This project pursues several innovative approaches toward addressing critical problems associated with practical process development of distributed bio-oil reforming for H_2 production. First, low temperature reforming catalysts and rapid catalyst regeneration methods will be developed to address the catalyst deactivation issue. Second, novel sorbents will be developed for in situ capture of CO_2 produced during reforming to produce a H_2-rich stream in one step, eliminating the need for separate water-gas shift and reducing the hydrogen purification unit size. Third, monolithic modular-type reactors will be developed to minimize mass and heat transfer so that the reaction and regeneration (both the catalyst and sorbent) can be conducted via rapid cycling (in the order of minutes).

A project team of combinatory expertise and experiences is formed to achieve the project objectives, which include PNNL, Washington State University, Dason Technology, and Cormetech. The project team undertakes five major tasks, (i) monolith reactor technology development, (ii) model analysis and process design, (iii) development of monolith supports, (iv) catalyst characterization and development, and (v) reactor system tests and process development. Three major milestones will be achieved. The first-year milestone is about material innovations. The steam reforming catalyst and in situ CO_2 sorbent are developed that work effectively under the same reaction (~500°C) and regeneration (~700°C) conditions. Both high productivity and stability for rapid cyclic operation are the important performance criteria. The second-year milestone is mainly about monolithic reactor innovations. The optimum CO_2 sorbent and reforming catalyst materials will be integrated into monolith structures and demonstrated for one-step production of pure H_2. The sorption and reforming reaction processes need to be synchronized in one reactor vessel to achieve cyclic stability and high H_2 productivity. The third-year milestone is mainly about process innovations. The materials and monolith reactors will be demonstrated on an integrated reactor apparatus for long time stability, production >99% pure H_2, and ≥10 wt% H_2 yield at H_2 production capacity of about 2 kg/d.

RESULTS

To simplify the hydrogen production process (Figure 1), we want to integrate CO_2 sorption with steam reforming reaction into one reactor vessel. In this way, CO_2 is captured on metal oxide sorbents upon its formation from the reforming reaction so that pure or enriched H_2 gas is produced in one process step. The heat released from exothermic carbonation reactions can compensate the endothermic reforming reaction. Once the sorbent is saturated and/or the catalyst is deactivated, the reactor is switched to regeneration by air. During the regeneration, the endothermic carbonate decomposition can absorb the heat released from catalyst coke combustion. The regeneration is conducted at higher temperatures than the reforming reaction. Thus, the reactor provides thermal mass for subsequent reforming reaction. To realize this process design concept, we need to have a CO_2 sorbent that can work effectively under the reforming reaction. Both sorbent and catalyst need to be quickly regenerated by air calcination.

The literature reports and in-house studies [1-3] on CO_2 capture over a temperature range of 200–800°C have been reviewed. No existing sorbent materials were found suitable for the present application in terms of stability, kinetics, and capacity. Thus, a sorbent design model was proposed to guide preparation of a number of new sorbents. The sorbent materials were screened on thermogravimetric analyzer apparatus [4]. The promising candidates have been tested on a packed bed [5-6]. A novel sorbent system is found that provides high CO_2 working capacity over a range of CO_2 partial pressure, temperature, and steam partial pressure, which cover the likely operation windows of the bio-oil reforming. Rapid CO_2 sorption kinetics was observed under all the sorption conditions tested. As illustrated by the breakthrough curves in Figure 2, >95% CO_2 loading is completed within breakthrough time of 2 min. With dry feed gas (H_2/CO_2 = 2:1), the CO_2 loading tended to decrease with sorption/regeneration cycling. With wet feed gas of H_2O/dry gas = 1.0, the breakthrough curves for four sorption cycles completely overlapped. The results clearly show the positive effect of steam on the sorbent stability. The sorbent appears to be more stable in the presence of steam. Such performance characteristic is highly desirable for CO_2 capture applications under reforming conditions and for most practical applications as well, since the presence of steam is ubiquitous. The sorbent stability was assessed by conducting the sorption tests of the same bed for many cycles between 500°C sorption and 700°C regeneration. The CO_2 loading was stabilized at 19 wt% in the 17 cyclic testing. The rapid sorption kinetics and high working capacity are necessary to develop a compact reactor of high productivity.

The bio-oil reforming catalysis literature was reviewed and analyzed. No existing catalyst materials [7] were demonstrated to work under the presently desired conditions. The temperatures used in most vapor phase bio-oil reforming studies are higher than what is targeted for the present application (400–500°C). Lowering the reforming temperature is desired from points of views of achieving high

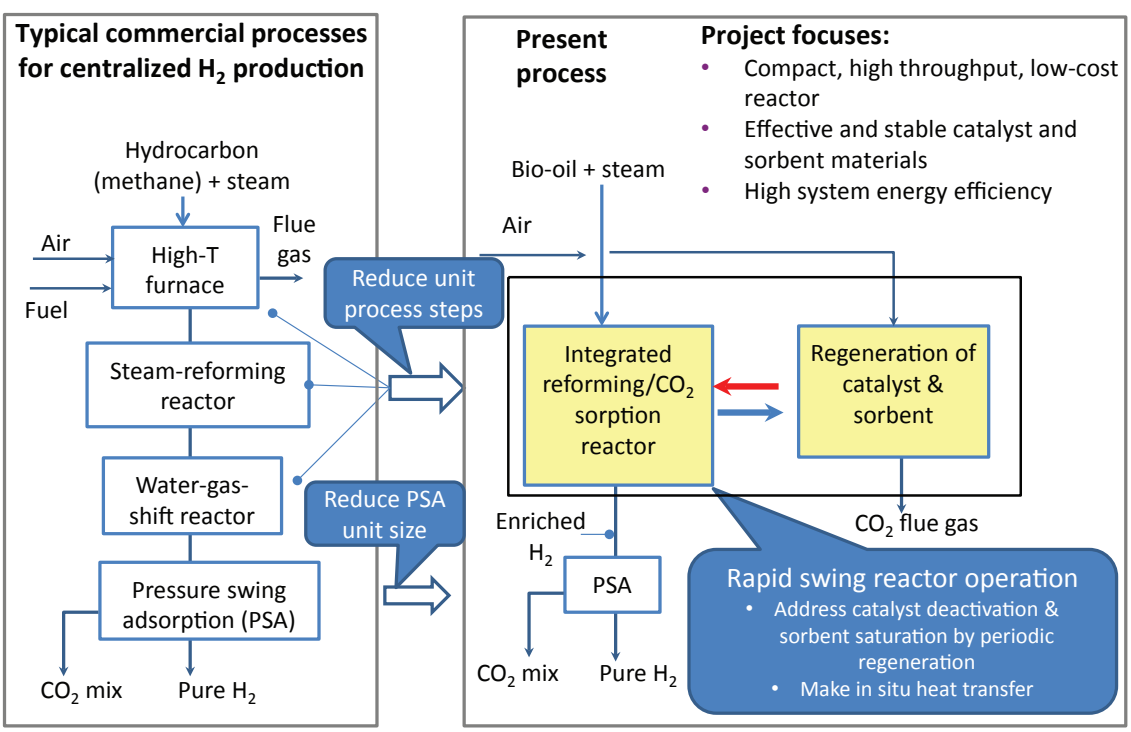

FIGURE 1. Process flow diagram of present hydrogen production technologies

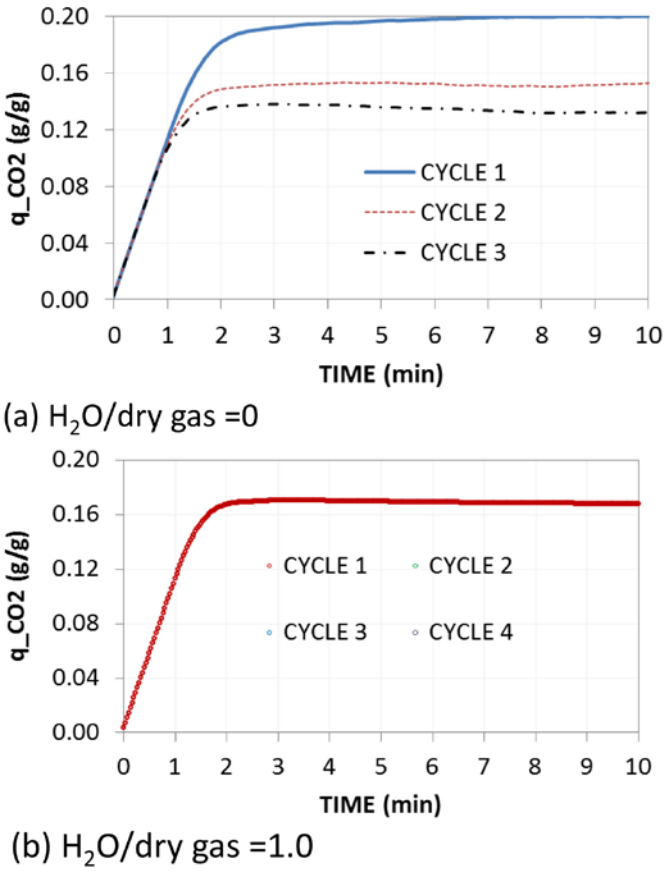

FIGURE 2. CO_2 sorption breakthrough curves of the packed sorbent bed with dry feed gas (a) and with wet feed gas (b) (sorption conditions: 500°C, 1.0 bar, gas hourly space velocity = 6,000 v/v/h based on standard dry gas flow rate, dry gas of H_2/CO_2 molar ratio = 2/1, wet gas of H_2O/dry gas molar ratio = 1/1; regeneration: 700°C, 1.0 bar, air purge)

thermal energy efficiency, reducing the reactor vessel cost, and prolonging catalyst lifetime. Almost all the catalysts deactivated or showed limited lifetime. Coking is the leading cause of catalyst deactivation. The information about catalyst regeneration and long term stability is missing. Thus, we conceived a new catalyst design model and formulated a number of new catalyst compositions, including zeolite-supported ones, zeolite/oxide composites, and metal oxide nano-composites [4]. The catalyst materials were screened by reforming reaction tests on a micro-reactor apparatus with phenol as a model feed. Preliminary tests of a few metal oxide composite catalysts were conducted with actual bio-oil reforming [5]. Both the model reaction and bio-oil reaction tests suggest that the M-Ce(D)-Al-O nano-composite is an active catalyst system for low temperature reforming reactions (400–500°C), where M = transition metal and D = dopant. Figure 3 shows that 70% conversion of phenol to gases and more than 80% of theoretical hydrogen yield was obtained with this composite catalyst at a high space velocity. This catalyst can be regenerated by air calcination. Further testing of this catalyst system with simulated bio-

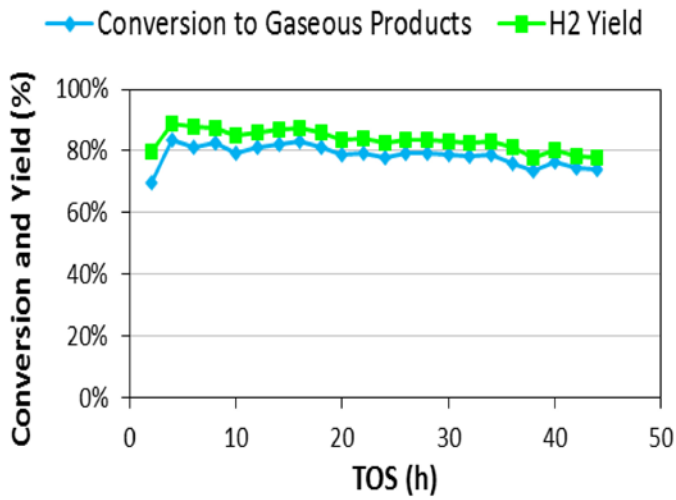

FIGURE 3. Variations of conversion and H_2 yield with time on stream (TOS) for steam reforming of phenol on a M-Ce(D)-Al-O oxide composite catalyst (reaction condition: catalyst loading = 600 mg, temperature = 500°C, steam/carbon ratio = 3.8, space velocity = 13,000 h^{-1})

oil is ongoing. We are planning to start with a preliminary mixture of 1:1:1:1 molar ratio of ethanol, acetic acid, acetone, and phenol and observe the effects of different reaction parameters such as temperature, partial pressure, and steam/carbon ratio. Then, we plan to add compounds into the feed which are more difficult to steam reform, such as glucose and furfural, in order to simulate more realistic bio-oil. After showing 80% H_2 yield, we will identify reaction conditions to achieve the project milestone of 0.6 kg H_2/h/kg. Catalyst productivity and stability will be demonstrated with more than 10 cycles of reforming/regeneration testing.

The monolith bed structures are pursued to develop a compact reactor for rapid reaction/regeneration swing operation. The monolithic structure enables the sorbent material to be fixed adjacent to the reforming reaction site so that rapid mass and heat transfer between the sorbent and reforming catalyst can be obtained. The straight flow channels of the monolith minimize the dead space and pressure drop so that the process streams can come in and out freely. In the first year, preparation methods for separate loading of sorbent and catalyst loading are identified. TiO_2 monoliths are used. For the sorbent loading, a sorbent material is prepared into slurry that is used to fill the alternate channels of the TiO_2 monolith. The results are illustrated with three monolith samples in Figure 4a. Almost all the channels in alternate rows are filled up for first and second samples. The results show the feasibility to load the sorbent material into the small monolith channels (~0.9 mm). However, the channel filling may not occur uniformly if the preparation procedures and conditions are not controlled well. As illustrated by the third sample, channel filling appeared randomly. The root causes for poor channel filling have been identified. We are in the process to standardize the channel

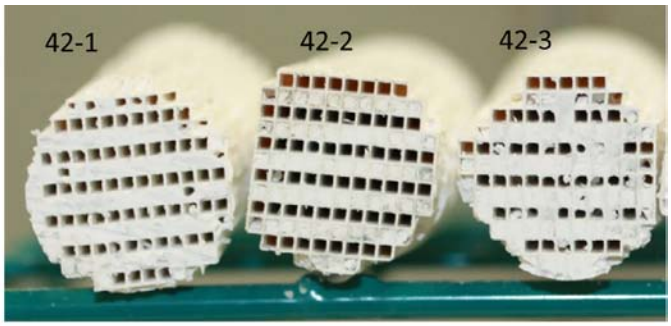

(a) Channel filling with CO_2 sorbent

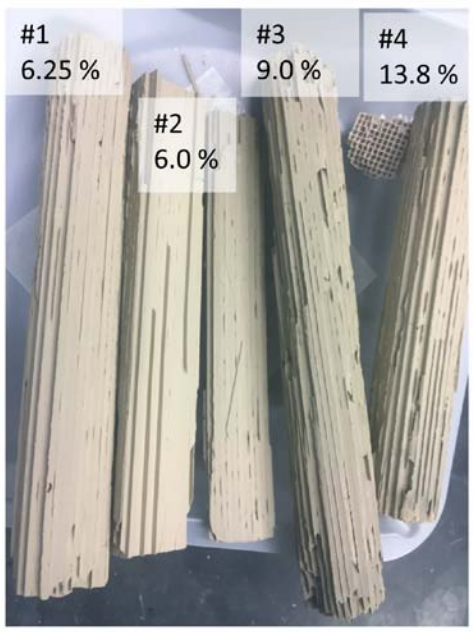

(b) Channel wall catalyzed with reforming catalyst

FIGURE 4. Monoliths loaded with CO_2 sorbent (a) and reforming catalyst (b)

filling process and produce consistent samples. For catalyst loading into the monolith structure, a simple impregnation method is identified. The salt solution containing the metal precursors is prepared and used to impregnate the pores on the channel wall. After the impregnation, the monolith is dried and calcined so that the metal precursor is converted into respective oxides and fixed on the channel wall. Figure 4b shows four monoliths of different loading levels of the M-Ce(D)-Al-O composite catalyst. The first and second samples were impregnated once, while the third and fourth monoliths were impregnated two and three times respectively. The catalyst loading increased with the times of impregnation. All the monoliths appear uniform in color, indicating uniformity of the catalyst distribution. The second monolith sample was cut open to reveal uniformity inside the channels and along the monolith length. Thus, an active reforming catalyst can be loaded into the monolith structure. The amount of catalyst loading required for actual reforming reactions will be determined by the reaction tests. If it is necessary to have high catalyst loading, channel coating may be used.

We found that it is very difficult to make uniform bio-oil flow distribution on the small-bench reactor apparatus because of the low flow rate and high oil viscosity. It is necessary to build a reactor system with adequate flow rates and length to conduct monolith reactor tests for bio-oil reforming reaction and CO_2 capture. Thus, an integrated reactor system has been designed. Major pieces of equipment, including reactor tubes and furnaces, steam generator and super heater, and flow distributor, have been acquired. The control system has also been designed. It is planned that first version of the reactor apparatus will be erected and debugged by end of FY 2015. The reactor provides 1 m x 2 cm reactor tubes that allow sorbent and catalyst loading in the order of 100 g levels with 0.5 kg/d hydrogen production capacity. The final version of the reactor system will be refined in the third year to have 5 cm reactor tubes for loading of 1.0 kg level of catalyst and sorbent materials with 2.5 kg/d of hydrogen production capacity.

CONCLUSIONS AND FUTURE DIRECTIONS

The following are main conclusions drawn from the project work done so far:

- Demonstrated a new CO_2 sorbent material system with rapid kinetics, high working capacity, and good stability for applications to capturing CO_2 under the steam reforming conditions.
- Identified a M-Ce(D)-Al-O metal oxide composite catalyst system to conduct steam reforming reactions at moderate temperatures (400–500°C) with high productivity. The catalyst can be regenerated by air calcination. Catalyst coking is very significant for bio-oil reforming. The catalyst regeneration by air calcination is essential.
- Identified preparation methods to fill up alternate monolith channels with the sorbent material and to fix the reforming catalyst inside the porous channel wall.
- Observed that the low flow rate of the small-scale reactor and the strong propensity of the bio-oil to charring/coking make uniform bio-oil flow distribution very difficult. It is critical to develop an effective flow distributor and necessary to build a reactor system with sufficiently high bio-oil feed rates.

The following are important future approaches toward making significant technology progress:

- Demonstrate targeted productivity and stability of the promising reforming catalyst through >10 rapid reaction/regeneration cycles with simulated bio-oil

- Validate the reforming catalyst performances with bio-oil reforming
- Scale up promising CO_2 sorbent and reforming catalyst preparation to 100 g level
- Deliver 2 cm diameter monolith samples loaded with the CO_2 sorbent and reforming catalysts for respective CO_2 sorption and reforming reaction tests in a monolith reactor tube
- Identify an effective bio-oil flow distributor for reaction tests on the integrated reactor apparatus
- Demonstrate the CO_2 sorption and reforming reaction performances in the monolith reactor with performances comparable or better than what are achieved on the small reactor apparatus
- Prepare 2 cm diameter monolith samples with both the CO_2 sorbent and reforming catalyst being incorporated
- Demonstrate the performances of monolith reactors for production of pure H_2 with in situ CO_2 capture, achieving the targeted productivity and stability
- Scale up the sorbent and catalyst preparation to 1 kg level
- Scale up the sorbent and catalyst loading into 5 cm diameter monolith modules
- Upgrade the integrated reactor system with 5 cm diameter reactors, bio-oil recycle, and post hydrogen purification
- Demonstrate the integrated reactor system performances for production of 2.5 kg H_2/d with >99% pure H_2, >80% hydrogen yield, and complete bio-oil conversion
- Conduct systematic evaluation of different bio-derived liquids on the reaction performances
- Conduct process designs and H2A analysis for 1,500 kg/d commercial-scale H_2 production units based on the research results achieved from this project
- Develop designs and plans for follow up field demonstration of the integrated reactor skid

SPECIAL RECOGNITIONS & AWARDS/ PATENTS ISSUED

1. W. Liu "An integrated reactor unit for H_2 production," provisional patent application (IP ID No. 30726-E).

FY 2015 PUBLICATIONS/PRESENTATIONS

1. W. Liu, "Monolithic Piston-Type Reactor for Hydrogen Production through Rapid Swing of Reforming/Combustion Reactions," presentation given at DOE/EERE HPTT Project Team Kick-off Meeting, NREL Golden, CO, August 25, 2014.

2. Wei Liu, Richard Zheng, Shari Li, Ken Rappé, David King, "Monolithic Piston-Type Reactor for Hydrogen Production through Rapid Swing of Reforming/Combustion Reactions," HPTT webinar, March 3, 2015.

3. W. Liu, "Monolithic Piston-Type Reactor for Hydrogen Production through Rapid Swing of Reforming/Combustion Reactions," presentation at AMR review, Washington DC., June 11, 2015.

REFERENCES

1. K. Zhang, et al., "Phase transfer-catalyzed fast CO_2 absorption by MgO-based absorbents with high cycling capacity," *Advanced Material Interface* 2014, 1400030.

2. K. Zhang, et al., "Roles of double salt formation and Na_2NO_3 in Na_2CO_3-promoted MgO absorbent for intermediate temperature CO_2 removal," *Int. J. of Green Gas Con.* 12 (2013) 351–358.

3. L. Li, et al., *Energy&Fuel*, 24 (2010) 3698-3703.

4. W. Liu, et al., "Monolithic Piston-Type Reactor for Hydrogen Production through Rapid Swing of Reforming/Combustion Reactions," FY15Q1 Quarterly Progress Report, January 31 2015.

5. W. Liu, et al., "Monolithic Piston-Type Reactor for Hydrogen Production through Rapid Swing of Reforming/Combustion Reactions," FY15Q2 Quarterly Progress Report, April 30, 2015.

6. W. Liu, et al., "Monolithic Piston-Type Reactor for Hydrogen Production through Rapid Swing of Reforming/Combustion Reactions," FY15Q3 Quarterly Progress Report, July 31, 2015.

7. S.A. Chattanathan, S. Adhikari, N. Abdoulmoumine, "A review on current status of hydrogen production from bio-oil, *Renewable and Sustainable Energy Reviews* 16 (2012) 2366– 2372.

II.F.2 Reformer-Electrolyzer-Purifier (REP) for Production of Hydrogen

Fred Jahnke (Primary Contact), Matt Lambrech, Pinakin Patel
FuelCell Energy, Inc. (FCE)
3 Great Pasture Rd.
Danbury, CT 06810
Phone: (203) 825-6108
Email: FJahnke@FCE.com

DOE Manager
David Peterson
Phone: (720) 356-1747
Email: David.Peterson@ee.doe.gov

Contract Number: DE-EE 0006669

Subcontractor
University of California, Irvine, Irvine, CA

Project Start Date: September 30, 2014
Project End Date: September 30, 2016

Overall Objectives

FCE's overall objectives are based on the Fuel Cell Technologies Office (FCTO) Multi-Year Research, Development, and Demonstration (MYRDD) Plan of 2015 to reduce the cost of hydrogen production to <$2.00/gge (<$4.00/gge delivered and dispensed). In addition, the technology used should minimize CO_2 emissions. To achieve this, FCE has the following key objectives.

- Construction and performance testing of a commercial scale reformer-electrolyzer-purifier (REP) unit
- Parameter optimization based on single cell testing and parametric study
- Long-term single cell testing to establish acceptable expected life
- Process and economics optimization
- Economic analysis to confirm cost of hydrogen

Fiscal Year (FY) 2015 Objectives

- Construction of single cell and test unit
- Parameter optimization on single cell based on single cell testing and parametric study
- Long-term single cell testing
- Process and economics optimization

Technical Barriers

This project addresses the following technical barriers from the Hydrogen Production section (3.1-23) of the FCTO MYRDD Plan.

(A) Reformer Capital Costs and Efficiency

(B) Operation and Maintenance (O&M)

(E) Control and Safety

(G) System Efficiency and Electricity Costs

(I) Grid Electricity Emissions (for Distribution)

Technical Targets

REP combines reforming and electrolysis into one unit. Therefore, the technical targets for hydrogen production from natural gas and from water electrolysis are both addressed by this program.

As you can see from Tables 1 and 2 where the expected REP performance has been added to MYRDD Plan targets below, the efficiency of the reformer and electrolyzer components is substantially higher than the target efficiencies. These higher efficiencies reduce operating costs sufficiently to offset the higher capital so that the total hydrogen cost target of $2.00/kg is still achieved. The higher efficiencies also have the advantage of reducing CO_2 and other emissions associated with typical hydrogen production from natural gas and electrolysis.

TABLE 1. Comparison to FCTO Technical Targets for Distributed Production of Hydrogen from Natural Gas (MYRDD Plan Table 3.1.2)

Characteristics	Units	2015 Target	REP Technology
Production Unit Energy Efficiency	% (LHV)	75.0	96.2
Production Unit Capital Cost (Uninstalled)	$ ($1,500 kg/day unit)	580,000	947,000
Total Hydrogen Cost	$/gge H_2	2.00	1.66

LHV – lower heating value; gge – gallon gas equivalent

TABLE 2. Comparison to FCTO Technical Targets for Distributed Water Electrolysis Hydrogen Production (MYRDD Plan Table 3.1.4)

Characteristics	Units	2017 Target	REP Technology
Hydrogen Cost	$/gge	<3.00	1.66
Electrolyzer Capital Cost	$/gge $/kW	0.30 125	Included above
Electrolyzer Energy Efficiency	% (LHV)	74	83.4

FY 2015 Accomplishments

Accomplishments during FY 2015 include the following.

- *Installed test unit.* Specified and purchased unit, installed unit on-site, shook down unit, reviewed safety of system, corrected flaws, started up the unit
- *Characterized cell performance based on single cell testing.* Varied operating conditions of the cell to determine the impact of all key operating parameters
- *Developed REP performance model.* Model very similar to one used for our commercial fuel cells; performed heat and material balances on single cell test operation to check accuracy of the model
- *Long-term testing of single cell.* Achieved 4,000 h of excellent operation
- Met all milestones
- Developed detailed configuration (process flow diagram [PFD]) which was used for estimating the cost of the system
- Rechecked the economics of the system using the updated costs developed based on the PFD
- Met go/no go requirements needed for approval to proceed to Phase 2
- Estimated performance for alternate feedstocks including syngas from biomass

✧ ✧ ✧ ✧ ✧

INTRODUCTION

The current conventional technology for production of hydrogen from natural gas suffers from excess CO_2 production due to incomplete conversion of methane and CO to hydrogen. The proposed technology would incorporate a high temperature electrochemical purification system to remove CO_2 from the reformed gas during the reforming process and drive the conversion of methane to H_2 and CO_2 to near completion, producing hydrogen from natural gas in a manner which approaches the theoretical minimum of CO_2 emissions.

The REP system incorporates components developed for FuelCell Energy's commercial molten carbonate fuel cell (MCFC) technology/Direct Fuel Cell (DFC®). When this technology is operated in purification mode as an electrolyzer, it will pump out almost all of the carbon from the system as CO_3^{2-}, leaving pure hydrogen from the reformed methane. In addition, the system efficiently produces additional hydrogen by dissociation of steam (electrolysis) in the pumping step. Thus, natural gas would provide about 80% of the hydrogen produced with the other 20% provided by the electrolysis reaction. The system appears to be highly attractive economically, and we are currently testing the system to confirm the performance is as expected.

APPROACH

Because the system will be based on our commercial DFC fuel-cell components, the emphasis of our work is to make sure that the system works as expected. Based on FuelCell Energy's long history of research and development, initial testing was done on a single 300 cm² cell. Experience has shown that this size cell provides a good reflection of the performance of our larger commercial scale cells. Testing of the large cells is included in Phase 2 of the program to insure there are no unexpected results from the flow distribution or the thermal distribution within the cells. The large cell testing will be based on a short stack of approximately 30 cells which we have found accurately reflects the performance of a commercial unit. In Phase 1, we are testing a single cell under various operating conditions to determine the impact on the cell performance. We are also doing long term testing to make sure that the cell has an adequate life and a reasonable performance degradation.

Based on the results of the testing, a detailed system configuration and performance has been simulated using CHEMCAD. The results of the simulation were then used in the Hydrogen Analysis (H2A) model to confirm the economic attractiveness of the system. Assuming the short stack testing is successful, we hope to follow that test with an additional program for a field demonstration of the technology.

RESULTS

The results to date have been excellent and the performance of the REP system is slightly better than the performance estimated for the proposal. Figure 1, which shows the voltage required to obtain various hydrogen purities, shows the data confirming the REP performance. Using the data from these tests and others, a detailed model was developed which allows us to accurately predict the REP performance for various configurations and feedstocks. Figure 2 shows how the model closely matches the observed data. This model has been used in our heat and material balance simulations to check the economics of the technology. Based on the detailed PFD developed, a heat and material balance was performed, equipment costs were estimated, and the results were analyzed using the DOE H2A model. As can be seen in Table 3, the cost of hydrogen meets the DOE target of $2/kg.

In addition to the performance of the system, we were also concerned about the life of the cell. To address this concern, a long-term test of a cell was performed. As shown

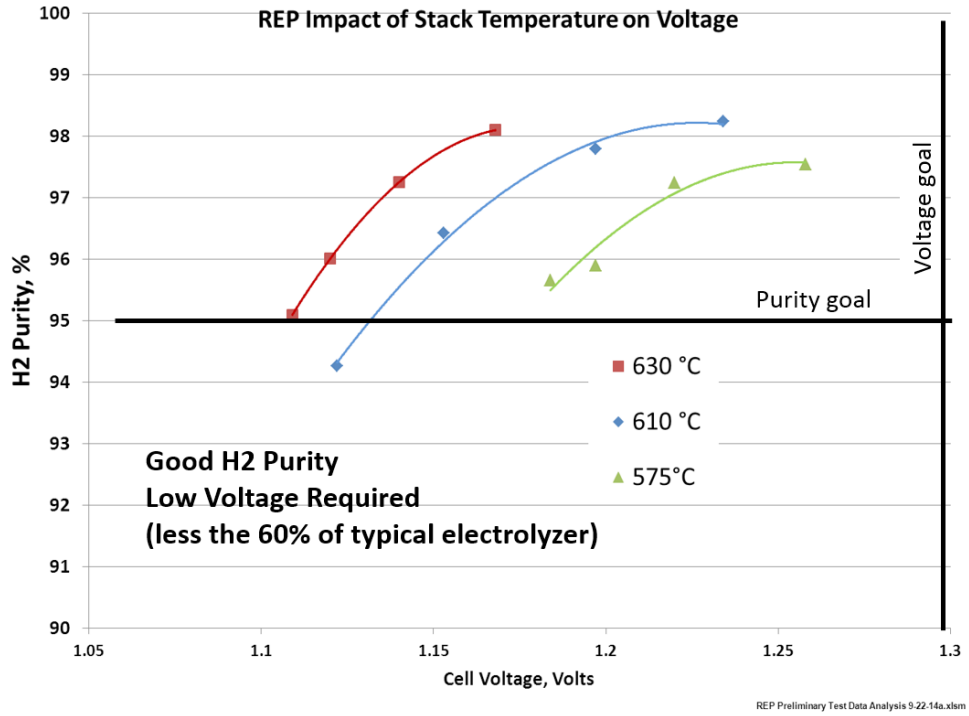

FIGURE 1. Performance of REP is attractive

$$E = E_T^o + \frac{RT}{2F}\ln\frac{\chi_{H_2}\chi_{O_2}^{1/2}\chi_{CO_2(c)}}{\chi_{H_2O}\chi_{CO_2(a)}} + \frac{RT}{4F}\ln P$$

Case	Model Voltage	Measured Voltage	Voltage Error
33.5A	1,159	1,170	0.9%
33.5A Low Air Flow	1,163	1,170	0.5%
37A	1,166	1,173	0.6%
37A Low T	1,209	1,220	0.9%
37A High T	1,149	1,140	-0.8%
40A	1,216	1,201	-1.3%
40A N2 Sweep	1,234	1,234	0.0%
40A No Cath Flow	1,271	1,333	4.3%
Average Error	0.07%		
Stnd Deviation	1.01%		

Error = (Meas V / Calc V) -1

REP Single Cell HMB Summary 10-1-14.xlsm

- Sophisticated Model developed for REP (adapted from MCFC fuel cell model with minor adjustments).
- Model closely matches test data.
- Model allows optimization of system operation and accurate heat and material balances.

V_1_	1142.6
E	1028.8
ηcathact_1_	-55.9
ηanact_1_	-28.9
ηconc_1_	-16.1
I * Zir	-40.0
ηnernst	27.1
E_1_	1.0287339
EoT_1_	1.0287607
F_1_	96485.3
i_1	-1582.1363
iL_1_	8000
iLk_1_	
iLkco2c_1_	11257.723
iLkco2c_1_	3958.1632
iLkh2oa_1_	N/A
iLkh2a_1_	8837.9536
iLkco2a_1_	N/A
ka_1_	3.10E-07
kc_1_	3.06E-09
kir_1_	2.15E-06
n_1_	2
nk_1_	
nko2c_1_	0.6
nkco2c_1_	0.4
nkh2a_1_	1
Pc_1_	1.0078587
Qa_1_	19.1
Qc_1_	61.67
Qir_1_	18.11
R_1_	0.0083145
Tc_1_	883.33333
Za_1_	1.826E-05
Zc_1_	3.532E-05
Zir_1_	2.531E-05
Xk_1_	
Xo2c_1_	0.2208908
Xco2c_1_	0.0327162
Xh2oa_1_	0.3637636
Xh2a_1_	0.5523721
Xco2a_1	0.0474421
Xo2cref_1	0.125
Xco2cref_1_	0.19
Xh2oaref_1_	0
Xh2aref_1_	0.5
Xco2aref_1_	0
DelGT_1_	-198520.57
ηact_1_	-0.0558881
ηact_1_	-0.0288915
ηconc_1_	-0.0161431
ηconco2c_1_	0.06575
ηconcco2c_1_	0.3362685
ηconch2oa_1_	0
ηconch2a_1_	0.0221303
ηconcco2a_1_	0
vk_1_	
vko2c_1_	0.5
vkco2c_1_	1
vkh2oa_1_	0
vkh2a_1_	1
vkco2a_1_	0
ηnernst	27.08542
Za_1_	182.6
Zc_1_	353.2
Zir_1_	253.1

FIGURE 2. Accurate model of REP was developed and validated

TABLE 3. H2A REP Economic Analysis for REP Integrated with a DFC® Fuel Cell System

Specific Item Cost Calculation		
Cost Component	**Cost Contribution ($/kg)**	**Percentage of H_2 Cost**
Capital Costs	$0.49	29.5%
Decommissioning Costs	$0.02	1.1%
Fixed O&M	$0.13	7.9%
Feedstock Costs	$1.01	60.7%
Other Raw Material Costs	$0.00	0.0%
Byproduct Credits	$0.00	0.0%
Other Variable Costs (including utilities)	$0.01	0.7%
Total	**$1.66**	

in Figure 3, 4,000 h of operation have been achieved with the voltage remaining well below the maximum target voltage.

We are currently looking at various configurations and feedstocks, performing heat and material balances for these cases and estimating the operating cost of hydrogen production for each case. The initial results from these studies are shown in Table 4. All of these cases show an attractive hydrogen production cost.

Note that the lowest marginal cost of hydrogen production is estimated for Case 4, a standalone REP system that incorporates an advanced configuration. We are currently preparing a patent application on this system. Although this is a good long-term case, the advanced system is more complicated and will require additional research funding before it can be demonstrated. We are also looking at additional cases, including cases involving CO_2 capture as well as power storage.

The system can use waste heat at various temperature levels to reduce fuel consumption and cost as can be seen in Case 3 which assumes low pressure steam at no cost is available to the process. Figure 4 shows the temperature level of heat that can be used and potential sources of that heat.

CONCLUSIONS AND FUTURE DIRECTIONS

The following conclusions were derived from the work in FY 2015.

- The REP system performs well.
- The economics of the REP system remain attractive after a detailed configuration and material balance were completed.
- The Phase 1 go/no go criteria have been met and we should proceed to Phase 2, construction of a commercial scale unit for testing.
- Not only does the REP system provide low cost hydrogen but it has the potential to be a good technology for excess electricity storage and CO_2 capture. These alternate

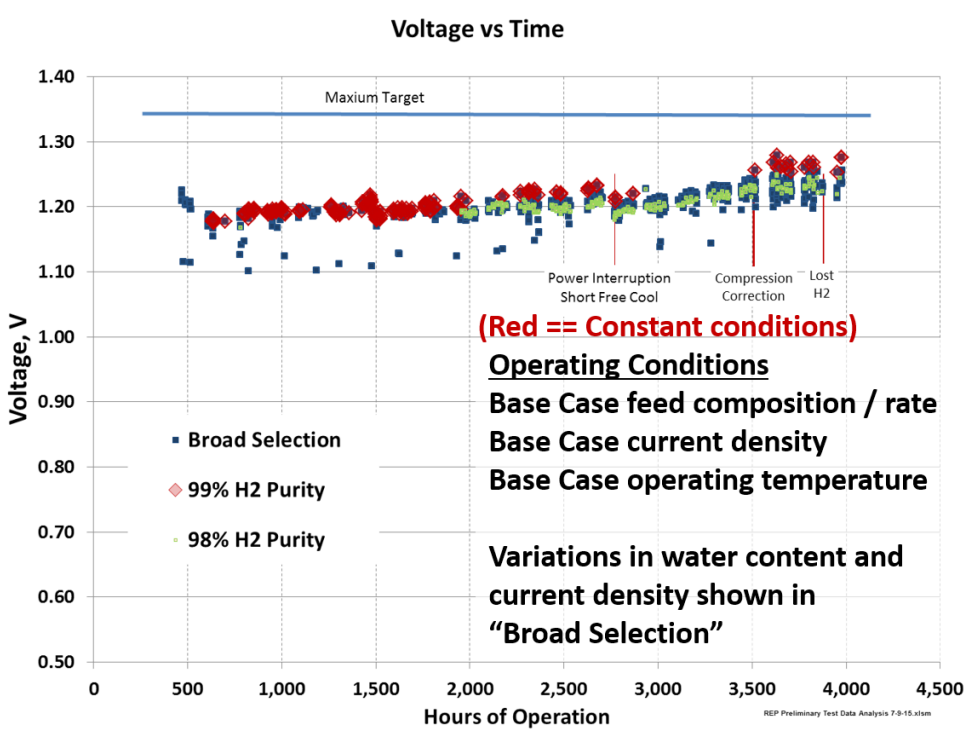

FIGURE 3. Long-term testing confirms acceptable cell life

TABLE 4. Configuration Analysis Based on Heat and Material Balances

Case	MMBtu NG /kg	kW NG /kW H_2	REP Power, kWh/kg	H2 Purity, %	Water, kg/kg	Operating Costs, $/kg*
1. Base Case– NG Feed Integrated with DFC®	0.069	0.62	7.915	97.0%	9.3	0.925
2. Standalone – NG for All Heat	0.114	1.02	7.216	98.1%	9.3	1.188
3. Standalone - External LP Steam	0.095	0.84	7.211	96.9%	9.3	1.058
4. Standalone - Advanced Cycle	-	-	-	-	-	0.488
5. Standalone - Syngas Feed	0.066	0.59	12.181	97.7%	8.7	1.529
6. Int with DFC - AE Pwr Storage	Future	-	-	-	-	-

* Assumes $6.77/MMBtu NG (LHV), $0.057/kWh power. Does not include capital and maintenance costs.
NG – natural gas; LP – low pressure; AE – anode exhaust (from DFC®); DFC® – FuelCell Energy commercial fuel cell

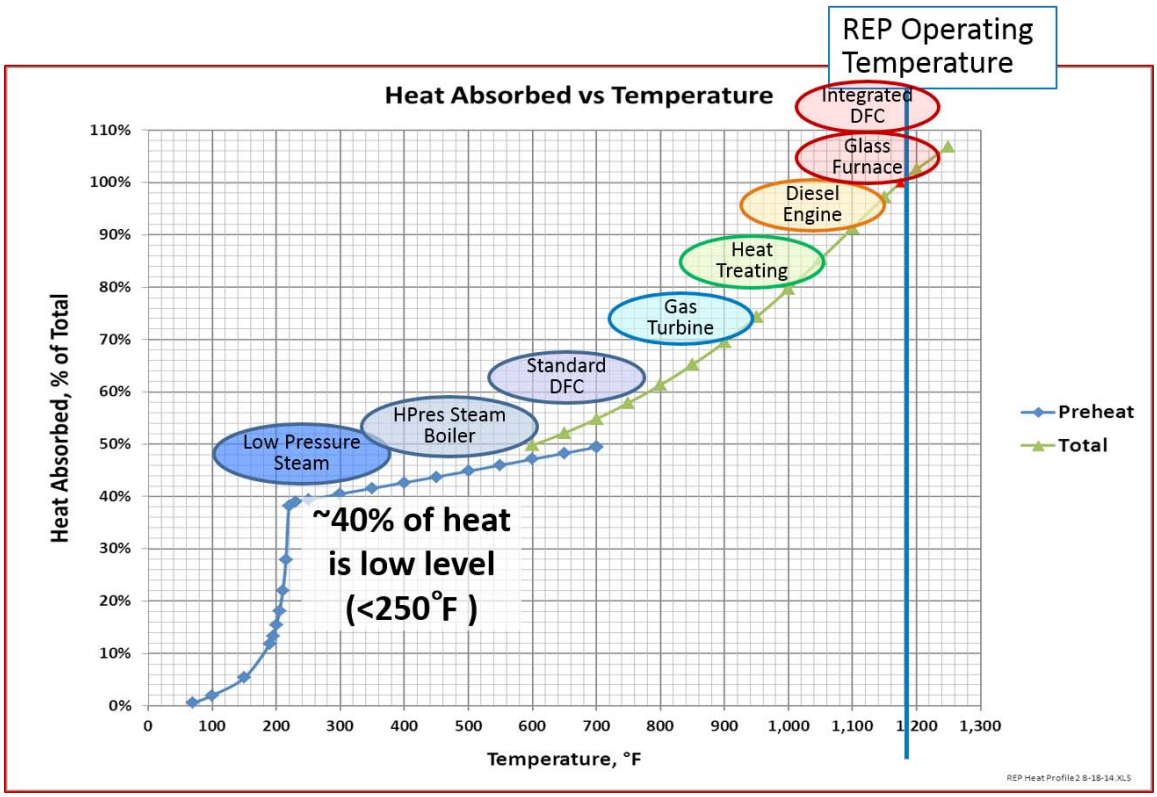

FIGURE 4. Multiple waste heat sources can improve efficiency and cost

uses should be explored further, and if found attractive, testing should be carried out to simulate the operating conditions for these applications also.

Future work in Phase 2 will comprise the following.

- Construction and testing of a commercial scale REP unit capable of around 100 kg/d of hydrogen production
- Continue long-term testing of single cell unit
- Test single cell under operating conditions for alternate configurations

SPECIAL RECOGNITIONS & AWARDS/ PATENTS ISSUED

1. A patent application for the process, including multiple configuration arrangements, was filed January 31, 2014, prior to start of program.

FY 2015 PUBLICATIONS/PRESENTATIONS

1. "Reformer-Electrolyzer-Purifier (REP) for Production of Hydrogen," 2015 AMR (Annual Merit Review), Washington,

DC, Fred Jahnke, FuelCell Energy, Inc. June 11, 2015, Project ID #:PD112.

2. "A Novel Hybrid Reformer-Electrolyzer-Purifier (REP) for Distributed Production of Low-Cost, Low Greenhouse Gas Hydrogen," review of project was given at the kick-off review meeting in Denver, August 26, 2014, for Hydrogen Production Technology Team Meeting.

III.0 Hydrogen Delivery Sub-Program Overview

INTRODUCTION

The Hydrogen Delivery sub-program addresses all hydrogen transmission and distribution activities from the point of production to the point of dispensing. Research and development (R&D) activities address challenges to the widespread commercialization of hydrogen technologies in the near term through development of tube trailer and liquid tanker technologies as well as forecourt compressors, dispensers, and bulk storage; and in the mid- to long-term through development of pipeline and advanced delivery technologies. Technoeconomic analysis is used by the sub-program to identify cost, performance, and market barriers to commercial deployment of hydrogen technologies, and to inform program planning and portfolio development.

GOAL

The goal of this program is to reduce the costs associated with delivering hydrogen to a point at which its use as an energy carrier in fuel cell applications is competitive with alternative transportation and power generation technologies.

OBJECTIVES

The objective of the Hydrogen Delivery sub-program is to reduce the cost of hydrogen dispensed at the pump to a cost that is competitive on a cents-per-mile basis with fuels used in competing vehicle technologies. Based on current analysis, this translates to a hydrogen threshold cost of <$4/kg (produced, delivered, and dispensed, but untaxed) by 2020[1], apportioned to <$2/kg for delivery and dispensing[2]. The program plans to meet these objectives by developing low-cost, efficient, and safe technologies to deliver hydrogen from the point of production to the point of use in both stationary fuel cells and fuel cell electric vehicles. This objective applies to all of the possible delivery pathways. Key objectives for specific delivery components include the following.

- **Tube Trailers:** Reduce the cost of compressed gas delivery via tube trailer by increasing vessel pressure and lowering trailer cost on a per-kilogram-of-hydrogen-transported basis
- **Pipeline Technology:** Develop mitigation strategies for combined material fatigue and hydrogen embrittlement in steel pipelines; advance the development and acceptance of alternative composite pipe materials that can reduce installed pipeline costs; and develop lower-cost, higher-reliability compression technology for hydrogen transmission by pipeline
- **Liquid Delivery:** Reduce the capital and operating costs of hydrogen liquefiers and bulk liquid storage vessels
- **Forecourt Technologies:**
  - Compression: Develop lower-cost, higher-reliability hydrogen compression technology for terminal and forecourt applications
  - Storage: Develop lower capital cost off-board bulk storage technology
  - Dispensers: Improve the cost and accuracy of 700 bar dispensers
- **Analysis:** Conduct comprehensive analyses on near- and longer-term hydrogen delivery options to identify the advantages of each and areas for potential improvement

FISCAL YEAR (FY) 2015 TECHNOLOGY STATUS AND ACCOMPLISHMENTS

In FY 2015, the Hydrogen Delivery sub-program kicked off several new projects, held two Funding Opportunity Announcements (FOAs), participated in one workshop, and saw significant progress in research, development, and demonstration (RD&D) activities of existing projects. Significant accomplishments included the following.

[1] Hydrogen Threshold Cost Calculation, Program Record (Office of Fuel Cell Technologies) 11007, U.S. Department of Energy, 2012, http://www.hydrogen.energy.gov/pdfs/11007_h2_threshold_costs.pdf

[2] Hydrogen Production and Delivery Cost Apportionment, Program Record (Office of Fuel Cell Technologies) 12001, U.S. Department of Energy, 2012

- Updates to the Multi-Year Research, Development, and Demonstration (MYRDD) Plan now detail the technical and economic status of delivery technologies as of FY 2015. The updated plan includes revised 2020 and ultimate targets for technologies in the three most mature delivery pathways: gaseous tube trailer, liquid tanker, and pipeline.
- Two new FOAs and one lab call focused on hydrogen pipelines, as well as compression and dispensing technologies. Selections are expected to be announced by the end of 2015.
- One workshop was held to foster collaboration between industry, government, and the international community to identify the current challenges and RD&D needs of forecourt technologies to reduce costs and improve system reliability.
- The Hydrogen Fueling Infrastructure Research and Station Technology (H2FIRST) project published a report in April of 2015 on fueling station designs and costs. The project is a collaboration between Sandia National Laboratories (SNL) and the National Renewable Energy Laboratory (NREL).

Workshops

The Third International Workshop on Hydrogen Infrastructure and Transportation, organized by NEDO (New Energy and Industrial Technology Development Organization) of Japan, NOW (National Organisation for Hydrogen and Fuel Cell Technology) of Germany, and the DOE and hosted by Technova, Inc., was held in June of 2015 in Tokyo. The workshop included members of industry, academia, and government from Japan, Germany, the European Union (EU), Scandinavian countries, and the United States. Key takeaways from the workshop are summarized in Table 1.

TABLE 1. Key Issues Discussed at Third International Workshop on Hydrogen Infrastructure and Transportation

Fueling	Germany has one operational device that validates station performance. The United States is expected to have such a device completed (Hydrogen Station Equipment Performance device, HySTEP) by the end of 2015.
Hydrogen Quality	The technical, cost, and time requirements of hydrogen quality monitoring remain common concerns. In the United States, water, carbon monoxide, hydrocarbons, and particulates are the primary contaminants of concern.
Metering	Japan and Germany are both considering interim regulations for station metering to allow the technology to evolve, similar to the approach that has been adopted in California. In FY 2015, the German Clean Energy Partnership will also validate a meter with an uncertainty of <1.5% at high pressures.
Hardware	The United States, Germany, and Norway all collect data on the failure rates and modes of station equipment. While compressors have shown significant improvement in the past year, fuel cooling requirements are now a concern. Germany and the EU's Joint Research Centre are studying the impacts of initial tank temperature on the need for pre-cooling.

Publications

In FY 2015, the H2FIRST project published a report that describes the designs and costs of hydrogen stations that are expected to be viable in the near term. The report includes detailed piping and instrumentation diagrams (P&IDs), bills of material, and layouts for five stations (Table 2). The report additionally describes the impact of several key variables (station utilization rate, capacity, number of hoses, and supply method) on capital costs, levelized costs of hydrogen, and station footprint. These analyses are used to provide recommendations for future research on station components, codes and standards, and business practices. The project completed much of its analysis using the Hydrogen Refueling Station Analysis Model (HRSAM), which was created at Argonne National Laboratory (ANL) in FY 2015. HRSAM allows a user to determine the levelized cost of hydrogen dispensing for a given fueling station design and projected utilization rate.

TABLE 2. Station Designs Detailed in H2FIRST Reference Station Design Report

Delivery Method	Daily Capacity (kg)	Target Market	Site Type	Installed Capital Cost ($K)	Fuel Cost ($/kg)
Gaseous	300	High Use	Gas station or greenfield	$1,265	$6.03
Gaseous	200	Low Use		$1,179	$5.83
Gaseous	100	Intermittent		$1,098	$13.28
Liquid	300	High Use	Greenfield	$2,007	[a]
Future Liquid	300	High Use		$1,551	$7.46

[a] This station type was not available in HRSAM as of this analysis and fuel cost could not be estimated. It has been included in the current version of the model.

Key conclusions from this report are as follows.

- Standardization of key station components (e.g., chillers and cryogenic pumps) would lower station costs by eliminating non-recurring engineering costs, driving manufacturing volume, and allowing interchangeability of parts.
- Liquid stations could benefit from the development of underground storage that lowers setback distances, as well as high pressure pumps and evaporators that eliminate the need for compressors and heat exchangers at high-use stations.
- Technically robust modeling of the setback distances necessary at liquid stations could significantly improve the viability of these stations, especially in urban settings.
- Business practices that could improve station viability include contracts with fleets of fuel cell vehicles, a reduction in the chilling at the station to enable customers to accept longer-duration fills for a lower cost, and the use of mobile refuelers to meet the rapidly changing demand in the near-term market.

FY 2015 Funding

The Fuel Cell Technologies Office (FCTO) Incubator FOA selections were announced in FY 2015, and the Hydrogen Delivery Technologies (DE-FOA-0000821) FOA selections are expected to be announced by the end of 2015. The Incubator FOA sought research on game-changing technologies that could reach FCTO targets but were under-represented in the program's MYRDD Plan targets and/or research portfolio. The Delivery Incubator Award selection was Gas Technology Institute for a feasibility analysis of thermal compression technologies that can pressurize hydrogen to 700 bar at hydrogen fueling stations in a cost-effective, reliable way.

During FY 2015, progress was made by existing projects in several key areas.

Tube Trailers and Bulk Storage

Significant cost reduction at the forecourt can be achieved through the use of high pressure tube trailers and low cost onsite storage. Increases in the capacity of high pressure tube trailers will lower the costs of delivery in the near term and improve station logistics. This year the following two projects have contributed to the cost reduction of the gaseous hydrogen delivery pathway.

- The TITAN™V XL40 trailer was developed and deployed in compressed natural gas service. These trailers can transport about 890 kg of hydrogen payload at 250 bar. Additionally, the liners in TITAN™ tanks were determined to be resilient to deep pressure cycles. The tanks were subject to rapid depressurization cycles after saturation with hydrogen to ensure that the liners would retain their integrity. (Hexagon Lincoln)
- A prototype 90 kg steel/concrete composite vessel (SCCV), which exceeded the DOE 2015 cost target for stationary storage, was built. The inner steel layer was certified by American Society of Mechanical Engineers (ASME) for 430-bar service after a burst test. The vessel is now being cycled in hydrogen to test its resistance to fatigue. (Oak Ridge National Laboratory [ORNL])

Pipeline Technologies

Pipelines are an attractive delivery pathway for large market scenarios. Advances in both pipeline compression and fiber reinforced polymer pipelines continue to improve the economics of the scenario, while work on hydrogen embrittlement of steel continues to improve the understanding of the performance of traditional pipeline materials for hydrogen pipeline transmission and distribution network.

- The inclusion of fiber-reinforced composite pipeline with a 50-year design life in the ASME B31.12 code was approved by the Code Committee and is now being considered by the Standards Committee. Burst testing and leak testing were completed on dry wrap thermoplastic piping with embedded monitoring and communication cables. The piping had a significantly greater burst strength than manufacturer specifications and an acceptable leak rate. (Savannah River National Laboratory)
- Fatigue analysis showed that, at modest stress ratios (R = 0.5), hydrogen pipeline thickness may not have to exceed that of a natural gas line to ensure 50-year life. The analysis was based on triplicate measurements of hydrogen assisted fatigue crack growth completed on X52 steel. Fatigue measurements were also completed on regions of friction stir welds in X52 steel. Additionally, data from FY 2014 measurements of hydrogen assisted fatigue crack

growth in the base metal, fusion zone, and heat-affected zones of girth welds in X65 pipeline steel were modified to account for crack closure effects. (SNL)

Forecourt Technologies

Forecourt technologies, in particular compression and onsite storage, are a key area of focus for the program. Efforts in this area aim to improve the reliability and reduce the cost of the technologies.

- A 30-cell, 82 cm^2 electrochemical hydrogen compressor stack has been demonstrated to compress 2 lb/d to 4,500 psig for over 200 h. The stack is utilizing cooling fins to improve its current density, and thereby lower capital cost. Additionally, a 185 cm^2 stack has now been compressing hydrogen to 3,000 psi for over 16,000 continuous hours, indicating strong reliability. The project is now concluding and will identify opportunities to transfer its technology to industry and government. (FuelCell Energy)
- HRSAM was developed and made publicly available. The model estimates the costs of station equipment based on recent vendor data and allows users to simulate gaseous stations, along with near-term and futuristic liquid stations. By the end of 2015, a modified version of the Hydrogen Delivery Scenario Analysis Model (HDSAM) will also be made publicly available. The model will incorporate recent cost data from vendors and from applications to the California Energy Commission and will include the ability to simulate varying annual station utilization rates, near-term and futuristic liquid hydrogen stations, and impacts of market penetration on component costs. (ANL)
- A novel dispensing hose material developed through a Small Business Innovation Research project was shown to meet cost and durability requirements, and a ceramer was developed to bind the material to nozzles. The hose material was tested for solvent resistance and abrasion resistance, and the ceramer was tested for compressive strength at a range of temperatures (-60°C–300°C) as well as shear strength. In the coming year, the hose durability, lifetime, and impact on hydrogen quality will be further characterized by measuring the pull-out strength of fittings crimped with the novel ceramer, hydrostatic strength, burst pressure in cyclic loading, and response to hydraulic pulse, as well as conducting dynamic mechanical analysis and evolved gas analysis. (NanoSonic)
- Pressure testing has been successfully completed on a prototype of a 765-liter, 875-bar cylinder being developed for forecourt storage of hydrogen. These cylinders are being developed by wrapping Type I vessels with high-strength steel wire. Finite element modeling has been completed to guide the design of future cylinders, and a significant literature review has been conducted to assess the impacts of hydrogen on fatigue crack growth at the conditions these vessels will experience (e.g., cycle frequency). The fracture analysis being completed aims to enable the vessels to be certified by the ASME Boiler and Pressure Vessel Code. In the coming year, an additional burst test will be completed on a short prototype, and equipment will be developed to enable wire-winding of the full-length vessels. (Wiretough)
- ORNL is optimizing the design of their 430-bar SCCV to enable low-cost 875-bar underground storage at stations. In FY 2015, high-strength steels and hydrogen permeation barrier materials with sufficient strength for use in these vessels have been identified. Additionally, an initial set of optimized vessel designs has been developed. In the coming year, the welding process for the high-strength steels will be assessed, the concrete reinforcement technology will be improved to lower cost, vessel design will be further optimized, and sensor technologies for the monitoring of vessel health will be evaluated. Vendor quotes will then be obtained for a prototype design. (ORNL)

BUDGET

The FY 2015 appropriation provided $20 million for the Hydrogen Production and Delivery program, with approximately $9.8 million provided for Delivery RD&D. The estimated budget breakdown for Delivery in FY 2015 and FY 2016 is shown in Figure 1. The budget request for Hydrogen Production and Delivery in FY 2015 is $23.6 million, with $11.6 million planned for Delivery RD&D, with an emphasis on improving reliability and reducing costs of near-term technologies, such as dispensers and forecourt storage, and developing technologies for longer-term pathways, such as liquefaction.

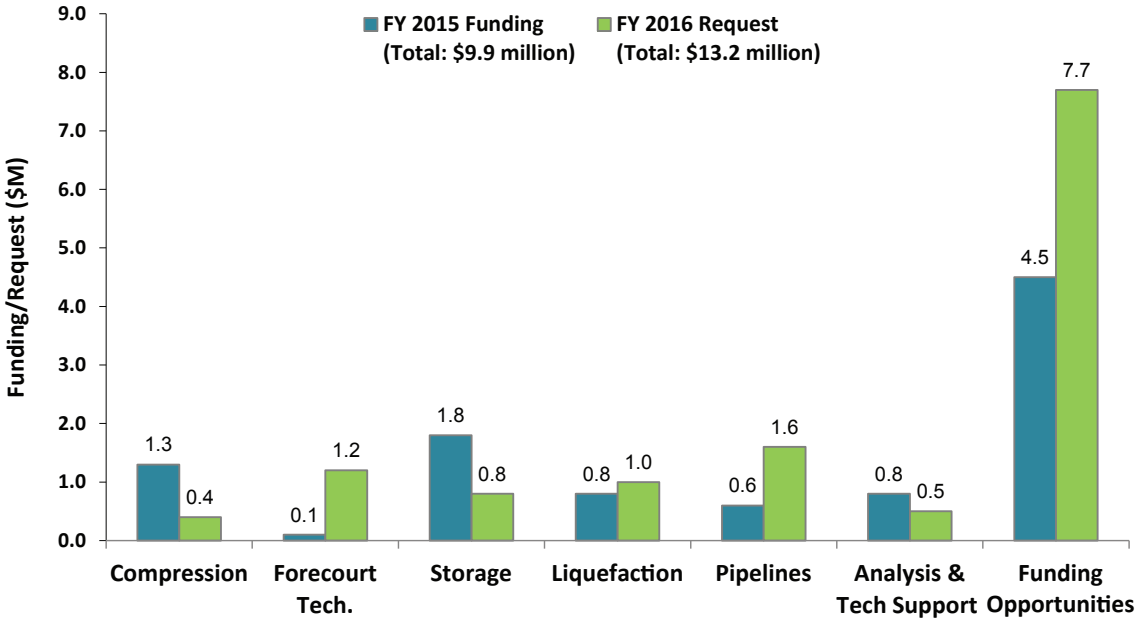

FIGURE 1. Hydrogen Delivery R&D Funding. Subject to appropriations, project go/no-go decisions, and competitive selections. Exact amounts will be determined based on research and development progress in each area and the relative merit and applicability of projects competitively selected through planned funding opportunity announcements.

FY 2016 PLANS

In FY 2016, the Hydrogen Delivery sub-program will focus on several key efforts, including the following.

1. Award and kick off a project to develop a low-cost hydrogen dispenser that can reliably complete communications-based fills with less than 4% error
2. Kick off two projects to develop higher efficiency hydrogen liquefaction technologies to achieve a figure of merit of 0.35 or better
3. Focus on lowering the cost of storage at the refueling station through the completion of two projects on stationary storage (ORNL and Wiretough)
4. Continue to address near-term forecourt R&D needs through the H2FIRST project, including analysis on the cost of onsite production and modular station designs (NREL and SNL)

Eric Miller
Hydrogen Production and Delivery Program Manager
Fuel Cell Technologies Office
Office of Energy Efficiency and Renewable Energy
U.S. Department of Energy
1000 Independence Ave., SW
Washington, D.C. 20585-0121
Phone: (202) 287-5829
Email: Eric.Miller@ee.doe.gov

III.1 Hydrogen Delivery Infrastructure Analysis

Amgad Elgowainy (Primary Contact) and Krishna Reddi
Argonne National Laboratory
9700 South Cass Avenue
Argonne, IL 60439
Phone: (630) 252-3074
Email: aelgowainy@anl.gov

DOE Manager
Erika Sutherland
Phone: (202) 586-3152
Email: Erika.Sutherland@ee.doe.gov

Project Start Date: October 2007
Project End Date: Project continuation and direction determined annually by DOE

Overall Objective

Evaluate hydrogen delivery and refueling concepts that can reduce hydrogen delivery cost towards meeting the delivery cost targets

Fiscal Year (FY) 2015 Objectives

- Develop and publish Hydrogen Refueling Station Analysis Model (HRSAM) with today's station configurations, utilization, and cost information
- Update and publish Hydrogen Delivery Scenario Analysis Model (HDSAM) with recent/current station configurations, market data, and cost information of delivery components for near-term and long-term markets

Technical Barriers

This project directly addresses Technical Barriers A, B, C, and E in the Hydrogen Delivery section of the Fuel Cell Technologies Office (FCTO) Multi-Year Research, Development, and Demonstration Plan (MYRDD).

(A) Lack of Hydrogen/Carrier and Infrastructure Options Analysis

(B) Reliability and Costs of Gaseous Hydrogen Compression

(C) Reliability and Costs of Liquid Hydrogen Pumping

(E) Gaseous Hydrogen Storage and Tube Trailer Delivery Costs

Technical Targets

- Develop HRSAM to evaluate alternative refueling station components for near-term/current market scenarios and component costs
- Update HDSAM with recent/current market data, component cost data for near-term and long-term markets (with varying market penetration), station configuration options, and utilization scenarios

Contribution to Achievement of DOE Hydrogen Delivery Milestones

This project contributes to the following DOE milestones from the Hydrogen Delivery section of the FCTO MYRDD Plan:

- Milestone 1.5: Coordinating with the H_2 Production and Storage sub-programs, identify optimized delivery pathways that meet a H_2 delivery and dispensing cost of <$2/gge for use in consumer vehicles. (4Q, 2020)
- Milestone 6.1: Define potential RD&D activities for other long-term market fueling/terminal needs. (4Q, 2015)
- Milestone 6.3: By 2020, reduce the cost of hydrogen delivery from the point of production to the point of use in consumer vehicles to <$2/gge of hydrogen for the gaseous delivery pathway. (4Q, 2020)

FY 2015 Accomplishments

- Developed and published the HRSAM
- Studied the impact of various parameters including station design capacity, utilization rate, and station configuration on the hydrogen refueling cost component
- Updated HDSAM with recent market data, cost indexes, and alternate liquid delivery station configurations, as well as projections of the cost reductions expected at different market penetrations

✧ ✧ ✧ ✧ ✧

INTRODUCTION

Initiated as part of the Hydrogen Analysis (H2A) project, HDSAM is an Excel-based tool that uses a design calculation approach to estimate the contribution of individual components of delivery infrastructure to hydrogen cost, energy use, and greenhouse gas emissions. The model

links individual components in a systematic market setting to develop capacity/flow parameters for a complete hydrogen delivery infrastructure. Using that systems-level perspective, HDSAM calculates the full, levelized cost (summed over all components) of hydrogen delivery, accounting for losses and tradeoffs among the various component costs. Users of HDSAM can specify the values of model inputs, or select the default inputs, which are based on data from literature, vendors, other stakeholders, or basic engineering calculations. The quality of the data and the direction of the analysis are vetted by partners at other national laboratories, independent consultants, and briefings to the Hydrogen Delivery Technical Team (HDTT). Argonne National Laboratory (ANL) also developed HRSAM, which calculates the cost of hydrogen refueling as a function of various fueling station capacity values and design configurations. HRSAM is an abbreviated version of HDSAM that focuses solely on near-term refueling station costs.

APPROACH

In this project, HDSAM was adapted to build HRSAM, a model that studies station economics, excluding all upstream costs (hydrogen production and delivery to the station). Cost formulas developed using current cost and design data of the refueling and delivery components have been embedded in the model. The station configurations represent the stations being installed in California today, and projected utilization rates are based on estimates from the California Air Resources Board. HRSAM outputs the annual and cumulative cash flows, total capital investment, cost of refueling per kilogram of hydrogen (which has an energy approximately equal to that in a gallon of gasoline), years required to break even on capital investment, and land area required by a given station. Figure 1 shows the inputs (can be user-specified or default values) and outputs of the HRSAM model.

The HDSAM model was also updated with recent market data, including key statistics of urban population, vehicle ownership rate, annual vehicle miles traveled, and average vehicle fuel economy, that enable calculations of market demand. Cost formulas for all dispensing equipment were also updated based on quotations received for today's technologies. Additionally, projections were made on the reductions in cost that can be expected in various market penetration scenarios due to learning, technology advancement, and economies of scale. The model was then updated to include these cost reduction factors as inputs. The model was also updated to include an option to define a utilization scenario for hydrogen refueling stations over the project period. Finally, the cost of refueling station precooling equipment was updated to simulate an advantageous configuration identified in a separate DOE-funded project (Hydrogen Fueling Station Pre-Cooling Analysis).

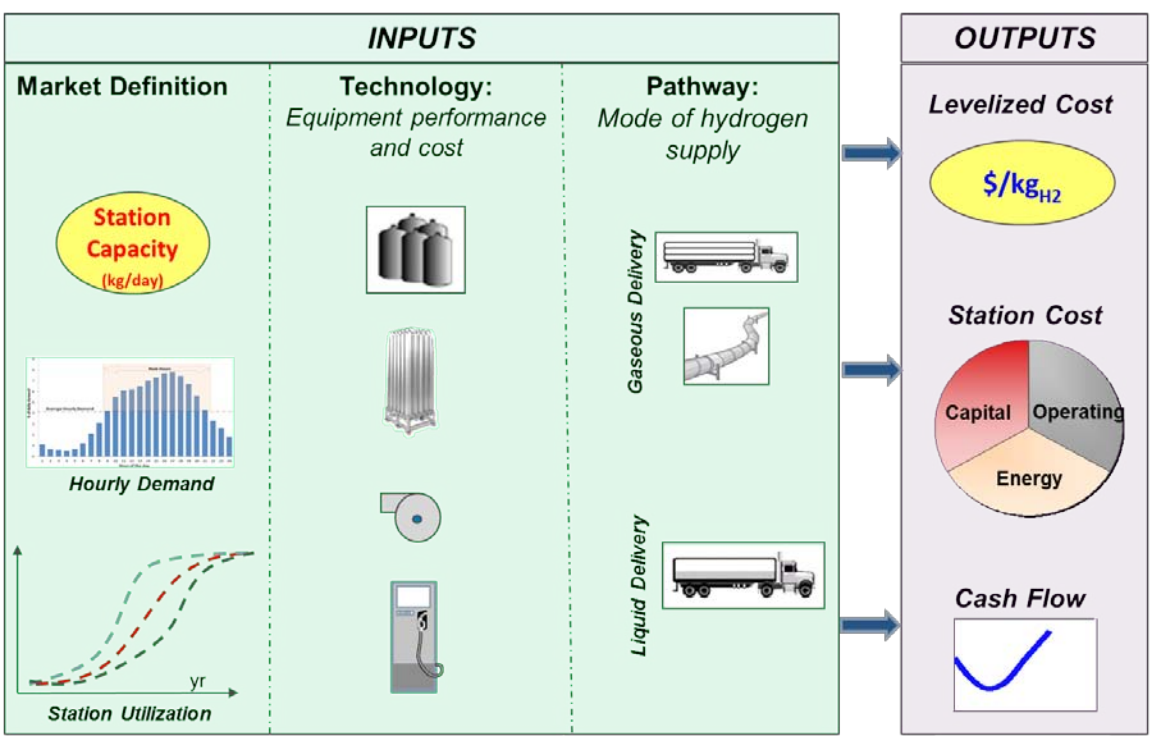

FIGURE 1. HRSAM overview

RESULTS

Hydrogen Refueling Station Analysis Model

HRSAM was developed to enable studies of the impact station design has on station economics. By ignoring the costs of hydrogen production and delivery to the station, HRSAM highlights the operating costs, capital costs, levelized costs, and cash flows of the refueling stations themselves. The model was used in the Hydrogen Fueling Infrastructure Research and Station Technology (H2FIRST) project's Reference Station Design Task to rapidly screen 160 station designs and identify the 15 with the most favorable economics. The model is also used for the generation of default inputs in Hydrogen Financial Analysis Scenario Tool (H2FAST), a model developed at the National Renewable Energy Laboratory in 2015. H2FAST is a web-based tool that provides detailed financial analyses of stations using an interface targeted for the financial community. Finally, HRSAM was used in 2015 by ANL to conduct several sensitivity analyses of the impacts of key variables on economics, as is discussed below.

Gaseous Compression vs. Liquid Pumping at Hydrogen Refueling Stations

At liquid hydrogen stations, gaseous cryo-compression is advantageous over liquid pumping when the station utilization is low (e.g., in early markets) or the capacity is small (even if utilization is high). Under-utilized hydrogen refueling stations with liquid pumping lose about 50 kg/day to boil-off because the pump and piping heat up when not being utilized. Additionally, if stations are small or under-utilized, the impact of boil-off loss on hydrogen cost becomes very large. On the contrary, liquid pumping may be beneficial over gaseous compression for stations with capacity greater than approximately 500 kg/day, as shown in Figure 2. The impact of overhead liquid boil-off losses on refueling cost becomes small when distributed over the much greater quantity of hydrogen dispensed at these large stations.

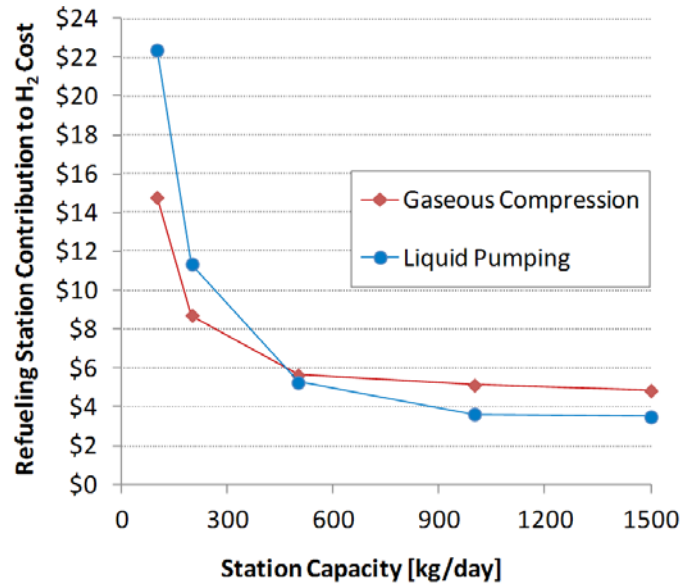

FIGURE 2. Refueling cost for various station capacities with gaseous compression and liquid pumping

Impact of Station Capacity and Utilization Ramp-Up Rate

As shown in Figure 3, large hydrogen refueling stations (HRSs), in spite of high capital investment, enable low refueling cost of hydrogen by taking advantage of the economies of scale. It is important to note, however, that

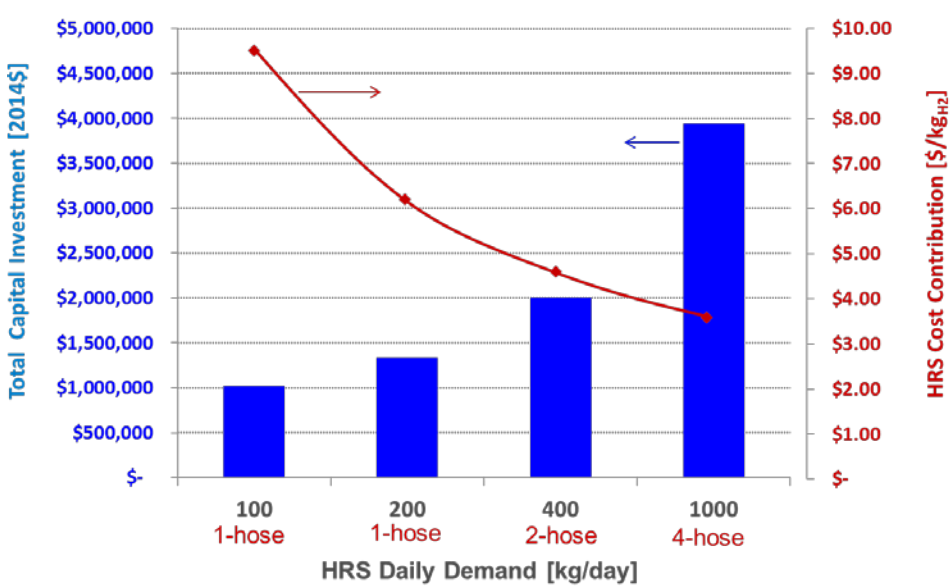

FIGURE 3. Station capital investment and cost contribution for different station capacities

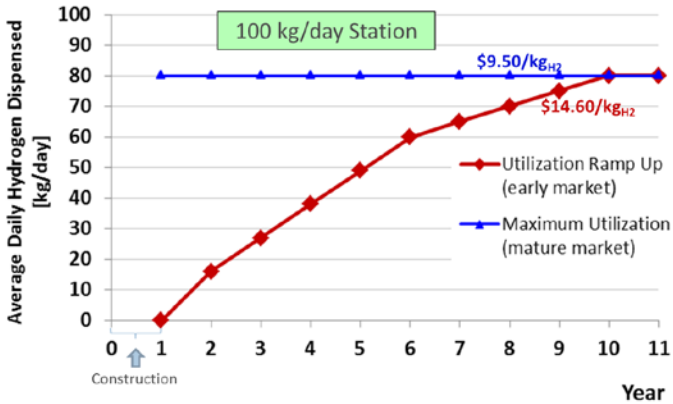

FIGURE 4. Impact of station utilization ramp-up on the refueling cost

this advantage diminishes when stations are under-utilized. Station utilization rate was identified as one of the most significant variables impacting dispensing cost. Figure 4 shows an example of a station utilization ramp-up scenario and the corresponding refueling cost for a 100 kg/d station.

CONCLUSIONS AND FUTURE DIRECTIONS

With liquid hydrogen supply, gaseous compression at the station is beneficial for early markets when the station utilization is low, and also for small stations irrespective of their utilization. On the other hand, liquid pumping is more advantageous for stations with large capacity and high utilization rates. The vehicle deployment rate significantly influences the success of hydrogen stations in the marketplace because the number of deployed vehicles is critical to the utilization of the station capacity, and therefore its economics. Under-utilization of station capital results in a significant increase in hydrogen refueling cost. For the remainder of FY 2015, efforts will be directed toward reviewing, documenting, and publishing the update of HDSAM.

As stations are deployed, HDSAM will continue to be updated with the most recent cost data and simulation of emerging technologies. The model will also continue to be used to evaluate refueling concepts and identify technology configurations with the potential to lower the cost or improve the performance of delivery technologies.

PUBLICATIONS

1. Reddi, K., Mintz, M., Elgowainy, A., Sutherland, E., "Challenges and opportunities of hydrogen delivery via pipeline, tube-trailer, liquid tanker and methanation-natural gas grid," Wiley (in press).

2. Reddi, K., Mintz, M., Elgowainy, A., Sutherland, E., "Building a hydrogen infrastructure in the United States," Compendium of Hydrogen Energy, Vol. 4 Hydrogen Use, Safety and the Hydrogen Economy, Woodhead Publishing, ISBN: 9781782423645.

3. Elgowainy, A., Reddi, K., Sutherland, E., and Joseck, F., 2014. Tube-trailer consolidation strategy for reducing hydrogen refueling station costs. *International Journal of Hydrogen Energy,* **39**(35), pp. 20197-20206.

4. Reddi, K., Elgowainy, A., and Sutherland, E., 2014. Hydrogen refueling station compression and storage optimization with tube-trailer deliveries. *International Journal of Hydrogen Energy,* **39**(33), pp. 19169-19181.

5. Pratt, J., Terlip, D., Ainscough, C., Kurtz, J., and Elgowainy, A., 2015. H2FIRST Reference Station Design Task Project Deliverable 2-2. Golden, CO: NREL/TP-5400-64107.

III.2 Vessel Design and Fabrication Technology for Stationary High-Pressure Hydrogen Storage

Zhili Feng (Primary Contact), Yanli Wang, Yong Chae Lim, Jian Chen and Lawrence Anovitz
Oak Ridge National Laboratory (ORNL)
1 Bethel Valley Rd., P.O. Box 2008, MS 6095
Oak Ridge, TN 37831
Phone: (865) 576-3797
Email: fengz@ornl.gov

DOE Manager
Erika Sutherland
Phone: (202) 586-3152
Email: Erika.Sutherland@ee.doe.gov

Subcontractors
- Global Engineering and Technology LLC, Camas, WA
- MegaStir Technologies LLC, Provo, UT
- Kobe Steel, LTD., Japan
- Hanson Pressure Pipe, Grand Prairie, TX
- Harris Thermal Transfer Products, Newberg, OR
- Temple University, Philadelphia, PA

Project Start Date: October 1, 2010
Project End Date: Project continuation and direction determined annually by DOE

Overall Objectives

- Address the significant safety and cost challenges in high-pressure stationary hydrogen storage technology
- Develop and demonstrate a novel steel/concrete composite vessel (SCCV) design and fabrication technology for stationary hydrogen storage systems

Fiscal Year (FY) 2015 Objectives

- Demonstrate and validate the entire SCCV design concept and manufacturability using today's industry-scale manufacturing technologies that are accepted by relevant code/standard requirements
- Complete an SCCV prototype mockup capable of storing 90 kg gaseous hydrogen at 430 bar, which captures all major features of SCCV design and manufacturing requirements
- Complete hydrostatic test at 616 bar (1.43 times the design pressure, 430 bar) of the mockup SCCV to demonstrate both the constructability and performance of the SCCV per American Society of Mechanical Engineers (ASME) boiler and pressure vessel (BPV) code requirement
- Complete the initial phase of long term testing of the prototype SCCV performance under cyclic high-pressure hydrogen loading, simulative of hydrogen charging and discharging cycles of hydrogen refueling stations, at one to two cycles per day from 100 bar to 430 bar

Technical Barriers

This project addresses the following technical barriers from the Hydrogen Delivery section (3.2) of the Fuel Cell Technologies Office Multi-Year Research, Development, and Demonstration (MYRDD) Plan (updated August 2015):

(E) Gaseous Hydrogen Storage and Tube Trailer Delivery Costs

Technical Targets

This project aims at developing and demonstrating SCCVs as low-cost, safe means of stationary storage for gaseous hydrogen storage. SCCVs are scalable to different pressures and capacities, and can therefore satisfy a variety of applications at hydrogen fueling stations, renewable energy hydrogen production sites, and other non-transport storage sites. As shown in Table 1, the current generation composite vessel made using the existing design and manufacturing technology exceeds the DOE cost targets in place when the project began [1].

TABLE 1. Progress Towards Meeting Technical Targets for Stationary Gaseous H_2 Storage Tanks (for Fueling Sites, Terminals, or Other Nontransport Storage Needs)

Pressure	DOE 2015 Status	Current SCCV (2015)	DOE 2020 Target
Low Pressure (160 bar) Purchased Capital Cost ($/kg of H_2 stored)	$850	$681	$500
Moderate Pressure (430 bar) Purchased Capital Cost ($/kg of H_2 stored)	$1,100	$713	$600
High Pressure (860 bar) Purchased Capital Cost ($/kg of H_2 stored)	N/A	$957	N/A
High Pressure (925 bar) Purchased Capital Cost ($/kg of H_2 stored)	$2,000	N/A	$600

Note: Cost analysis of SCCV was based on the pressure levels from a previous DOE MYRDD Plan.

FY 2015 Accomplishments

- Successfully passed a major milestone of the project: an SCCV mockup capable of storing 90 kg gaseous hydrogen at 430 bar has been designed, fabricated, and tested for hydrogen storage per relevant codes and standards
- Demonstrated and validated the SCCV operation and manufacturability using today's industry-scale manufacturing technologies that are accepted by relevant code/standard requirements
- Completed hydrostatic test at 616 bar (1.43 times the design pressure, 430 bar) of the mockup SCCV to validate both the constructability and performance of the SCCV per ASME BPV code requirement

✧ ✧ ✧ ✧ ✧

INTRODUCTION

Low-cost infrastructure, such as off-board bulk stationary hydrogen storage, is critical to successful market penetration of hydrogen-based transportation technologies. Stationary storage is needed in many locations ranging from hydrogen production plants to refueling stations. The design capacity and pressure of the stationary storage vessel are expected to vary considerably depending on the intended usage, the location, and other economic and logistic considerations. For example, storage vessels at a hydrogen refueling station may have higher pressures but smaller storage capacity when compared to those at a renewable energy hydrogen production site. Therefore, it is important to develop vessel designs that are scalable to different pressures and capacities. Moreover, since storage vessels provide the surge capacity to handle hourly, daily, and seasonal demand variations, they endure repeated charging/discharging cycles. Thus, the hydrogen embrittlement in structural materials, especially the accelerated crack growth due to fatigue cycling, needs to be mitigated to ensure the vessel safety. Safety and economics are two prevailing drivers behind the composite hydrogen storage technology.

In this project, ORNL leads a diverse multidisciplinary team consisting of industry and academia to develop and demonstrate an integrated design and fabrication technology for cost-effective high-pressure steel/concrete composite storage vessel that can meet different stationary hydrogen storage needs.

APPROACH

A novel SCCV has been specifically designed and engineered for stationary high-pressure gaseous hydrogen storage applications. SCCV has several inherent features aimed at solving the two critical limitations and challenges of today's high-pressure hydrogen storage vessels—the high capital cost and the safety concerns of hydrogen embrittlement (HE) of high-strength steel vessels.

The basic concept of SCCV is illustrated in Figure 1. SCCV comprises four major innovations: (1) flexible modular design that can be scaled to meet different pressure and capacity needs, as well as different manufacturing scenarios; (2) composite design that combines an inner steel vessel with a pre-stressed outer concrete reinforcement; (3) layered steel vessel wall and vent holes to solve the hydrogen embrittlement (HE) problem by design; and (4) integrated sensor system to monitor the structural integrity and operation status of the storage system. Together, these innovations make the SCCV cost-competitive and inherently safe for stationary high-pressure hydrogen storage services. The inner steel vessel is composed of multiple layers with strategically placed vent holes to prevent the intake and accumulation of hydrogen in the steel layers except the innermost layer. Since the innermost layer is the only one to face significant volumes of hydrogen, it is the only layer made of stainless steel. This layered design thereby minimizes steel vessel cost while ensuring resistance to HE. Furthermore, the novel steel/concrete composite vessel design allows for the stresses or the structural load from the high-pressure hydrogen to be shared between the inner steel vessel and the pre-stressed outer concrete reinforcement, thereby offering the flexibility to optimize the use of low-cost commodity materials (such as structural steels and concretes) and industry-accepted fabrication technologies for cost reduction. For example, the layered steel vessel technology is proven and accepted in industry standards and codes (e.g., ASME BPV code). Moreover, the layered steel vessel has potential for further cost reduction through advanced fabrication technologies, such as friction stir welding.

RESULTS

The primary focus in FY 2015 was to demonstrate and validate the entire SCCV design concept manufacturability and operation using today's industry-scale manufacturing technologies accepted by relevant code/standard requirements. This included the following major tasks: (1) complete the design, engineering, and construction of an SCCV prototype mockup capable of storing 90 kg gaseous hydrogen at 430 bar, which captures all major features of SCCV design and manufacturing requirements by April 30, 2015; (2) complete a hydrostatic test at 616 bar (1.43 times the design pressure, 430 bar) of the mockup SCCV to validate the performance of the SCCV per ASME BPV code requirement; and (3) complete the initial phase of long-term testing of the prototype SCCV performance under cyclic high-pressure hydrogen loading, simulative of the expected hydrogen charging and discharging cycles at hydrogen refueling stations, 1–2 cycles per day from 100 bar to 430 bar.

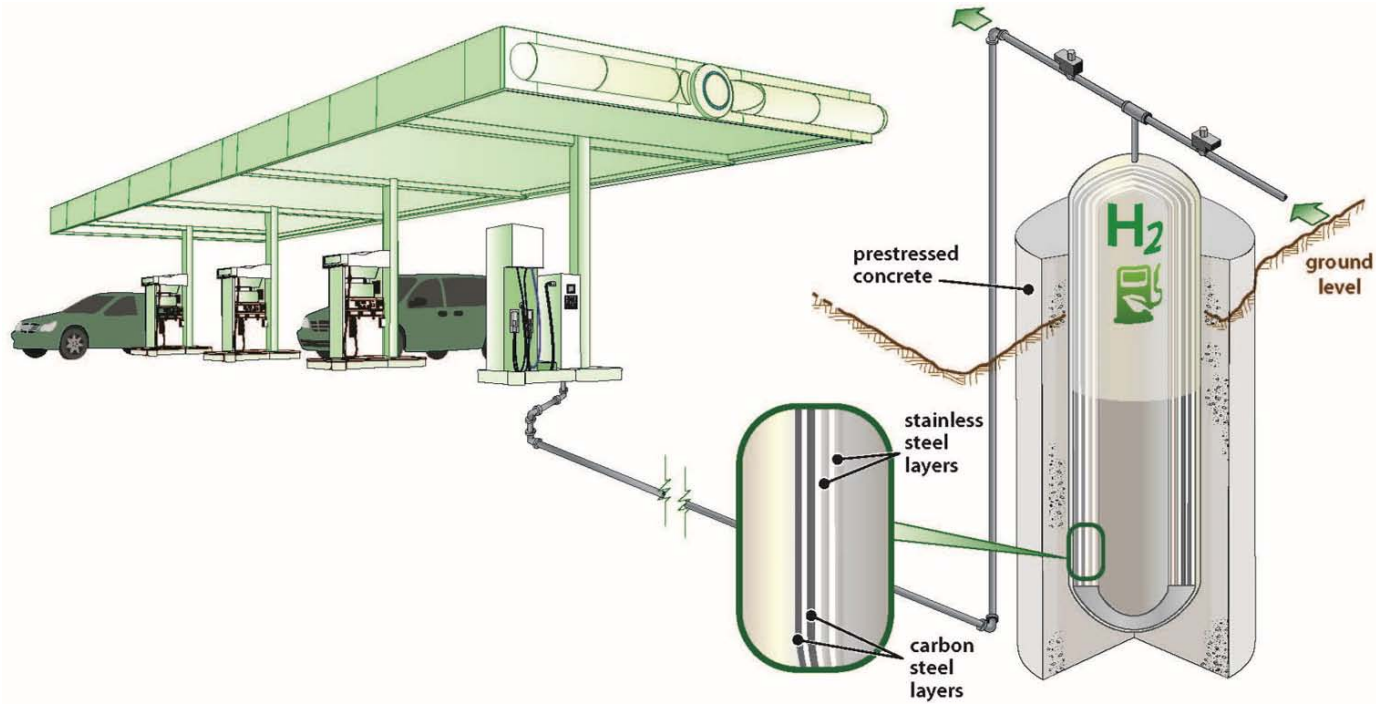

FIGURE 1. Schematic showing the design of a steel/concrete composite vessel comprising inner layered steel tanks and outer prestressed concrete confinement

Mockup SCCV Design and Engineering

A ¼ size mockup SCCV was designed, engineered, and constructed. Extensive finite element computations were carried out in the design and engineering of the mockup SCCV to realize the novel SCCV design concept while assuring relevant codes compliance and feasibility of fabrication using today's industry-scale manufacturing capability. Figure 2(a) shows the finite element model used in the design and engineering of the SCCV mockup. Figure 2(b) shows the hoop stress distribution in the concrete after pre-stress was applied, at operation pressure and at the hydrostatic test pressure. The calculation results are also given in Table 2. All stresses in different parts of the mockup are below the code allowable stress levels for these components during pre-stressing and at operation pressure of 6,250 psi (430 bar) and hydro-testing pressure of 8,940 psi (616 bar).

The mockup vessel has all the essential features and functionality of the full-size SCCV. It contains the inner steel vessel and the outer pre-stressed concrete reinforcement containment. The steel has a stainless steel inner layer as the hydrogen permeation barrier, hydrogen charging and discharging ports, and trunions for tank handling during the concrete construction and in-service installation. In addition, a manway on the top is added to the mockup vessel, as it is an essential feature in the construction, inspection, and repair of the full-size steel vessel.

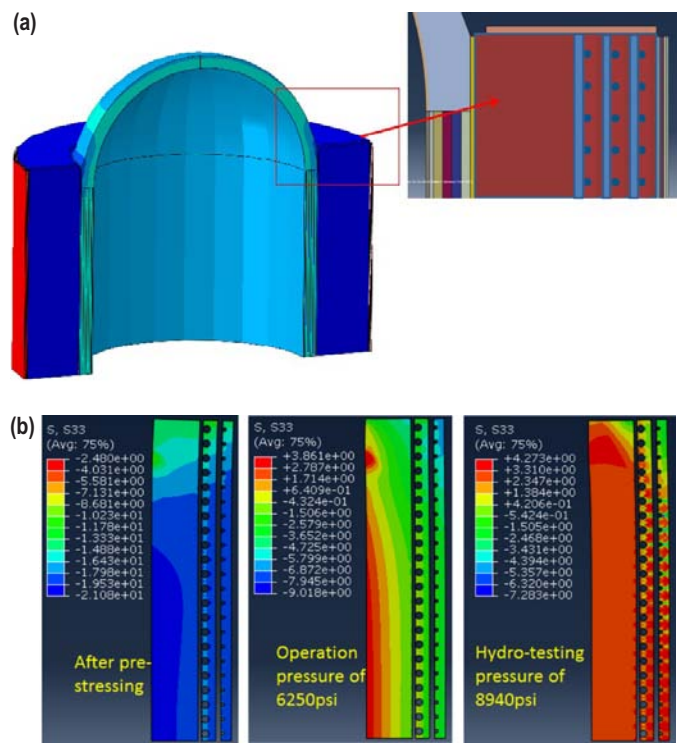

FIGURE 2. (a) Finite element model used to optimize the SCCV design; (b) Hoop stress distribution in the concrete after prestress applied, at operation pressure, and at the hydrostatic test pressure

TABLE 2. Hoop Stresses of the SCCV Steel Components (Code Allowable Stresses, σ_a, are in Parentheses)

Range of the Hoop Stresses		After prestressing, in ksi	6,250 psi operation pressure, in ksi	8,940 psi hydro-test pressure, in ksi
Inner steel vessel	Layered high strength steel shell (σ_a = 39.6 ksi)	-14 to -8	21 to 12	38 to 22
	Inner stainless liner (σ_a = 31 ksi, and -36 ksi for compression buckling)	-35.6 to -31.8	-1.5 to -9.1	7.8 to 0.5
Inner cage spiral rebar (σ_a = 32 ksi)		-15.6 to -10.8	1.4 to -3.0	9.5 to 0.7
Pre-stressing wire (σ_a = 227 ksi)		127 to 115	140 to 125	146 to 129

Mockup SCCV Construction

The inner steel vessel was constructed by Kobe Steel, per design specifications from the project. The inner steel vessel was built, inspected, and hydro-tested in accordance with the ASME BPV Code Section VIII Division 2 (2013 Edition) and was code-stamped for high-pressure services at 3,620 psi (without the pre-stressed concrete) before being shipped to add the pre-stressed concrete layer.

The outer concrete reinforcement was fabricated by Hanson Pressure Pipe. The concrete section is approximately 11 inches thick. It has three rebar cages, each consisting of vertical steel rebars and spiral steel rebars, as determined from the finite element modeling (FEM) analysis. These steel rebars were used to carry the tensile stresses from the service loading to prevent the concrete from cracking. In addition, a total of five layers of steel wire wrapping were used to pre-stress the concrete such that it is able to share 50% of the tension the vessel faces in service. Figure 3 shows the industry-scale wire wrapping process to apply the pre-stressing per SCCV design.

Mockup SCCV Testing

The completed SCCV mockup passed the hydrostatic test at 616 bar (8,940 psi), which is 1.43 times the 430 bar design pressure, thereby successfully validating both the constructability and performance of the SCCV per ASME BPV code requirement. An ASME certified inspector was on site during the hydrostatic test and certified that the entire hydrostatic test was in compliance with the ASME BPV testing requirement. The mockup was certified for pressure loading at the designed 430 bar (6,250 psi).

During both construction and testing of the mockup SCCV, strain gages and other sensors were strategically installed in various locations on the mockup to monitor and control the pre-stressing process of this first-of-its-kind SCCV design. The extensive use of the strain gages provided necessary experimental data to support and validate the design and engineering of SCCV. They also provided valuable insights to a number of variables in vessel manufacturing that influence the pre-stressing. These experiment data are critical for future technology transfer and commercialization of SCCV, especially related to key aspects in various stages of SCCV manufacturing. As one example, the strain variations during hydrostatic testing are presented in Figure 4. The actual strain gage readings during both pressurizing and depressurizing compared very well with the FEM design results. This validated our FEM-based design calculations. Furthermore, the strain gage readings confirmed that there was minimum relaxation of load carrying capacity

FIGURE 3. Wire wrapping during SCCV construction

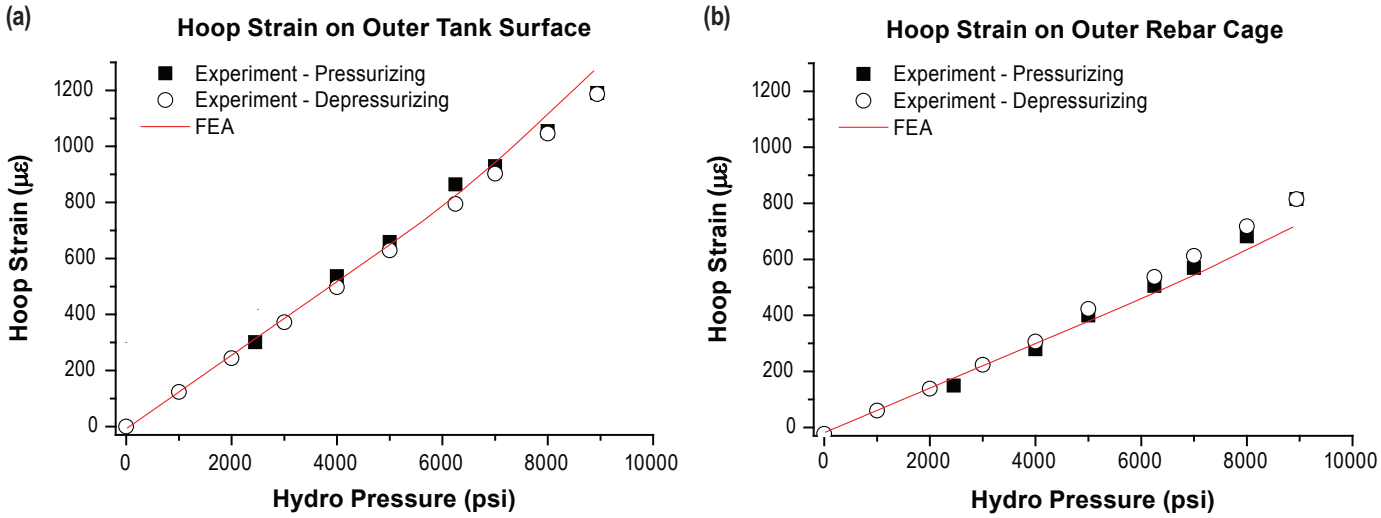

FIGURE 4. Comparison between experimentally measured and finite element analysis predicted strains during hydrostatic testing: (a) hoop strain on the outer surface of the steel vessel; (b) hoop strain on the outer rebar cage

of the vessel after the hydrostatic test. This is a critical experimental result that supports our design analysis and assumption that the concrete would sustain the peak tensile stress at code-required hydrostatic pressure level, which is 1.43 times the operating pressure, without damage.

CONCLUSIONS AND FUTURE DIRECTIONS

The project so far has achieved most of its major milestones and key project objectives:

- Demonstrated that the SCCV would meet or exceed the cost targets set forth in the DOE MYRDD Plan for all three different pressure levels for high-pressure gaseous hydrogen storage.
- Validated the technical basis for hydrogen mitigation by design through lab-scale experiments.
- Demonstrated the superior properties of multi-layer friction stir welds.
- Successfully designed, engineered, and constructed a mockup SCCV, which passed the hydrostatic testing, demonstrating and validating the entire SCCV design concept and manufacturability using today's industry-scale manufacturing technologies and relevant codes/standards.

Future planned activities include

- Completing the long-term testing of the mockup SCCV performance under cyclic hydrogen pressure loading, simulative of expected hydrogen charging and discharging cycles of hydrogen refueling stations, 1–2 cycles per day from 100 to 430 bar.
- Continuing with the lessons learnt in this project to further optimize all aspects of SCCV technology for additional major cost reduction in a follow-on project (Gen II SCCV).
- Technology commercialization.

FY 2015 PUBLICATIONS/PRESENTATIONS

1. Y.C. Lim, S. Sanderson, M. Mahoney, X. Yu, Y. Wang, and Z. Feng, 2014. "Characterization of Multilayered Multipass Friction Stir Weld on ASTM A572 G50 Steel," Welding Journal, vol. 93, 443-s.

REFERENCES

1. W. Zhang, F. Ren, Z. Feng, and J. Wang, "Manufacturing Cost Analysis of Novel Steel/Concrete Composite Vessel for Stationary Storage of High-Pressure Hydrogen," Oak Ridge National Laboratory Report, ORNL/TM-2013/113, Oak Ridge National Laboratory, Oak Ridge, TN, March 2013.

III.3 Hydrogen Embrittlement of Structural Steels

Brian Somerday (Primary Contact), Joe Ronevich
Sandia National Laboratories
P.O. Box 969
Livermore, CA 94550
Phone: (925) 294-3141
Email: bpsomer@sandia.gov

Sandia National Laboratories is a multi-program laboratory managed and operated by Sandia Corporation, a wholly owned subsidiary of Lockheed Martin Corporation, for the U.S. Department of Energy's National Nuclear Security Administration under contract DE-AC04-94AL85000

DOE Manager
Erika Sutherland
Phone: (202) 586-3152
Email: Erika.Sutherland@ee.doe.gov

Project Start Date: January 2007
Project End Date: Project continuation and direction determined annually by DOE

Overall Objectives

- Enable data-informed design safety factors for hydrogen pipelines, which impacts both reliability/integrity and cost
- Quantify fatigue crack growth aided by hydrogen embrittlement in pipeline steels, particularly for welds

Fiscal Year (FY) 2015 Objectives

- Complete triplicate measurements to establish reliable fatigue crack growth relationships for X52 friction stir weld (FSW) in 21 MPa hydrogen gas
- Complete fatigue tests on two model iron-carbon steels at two values of frequency and H_2 pressures in collaboration with International Institute for Carbon-Neutral Energy Research (I2CNER)

Technical Barriers

This project addresses the following technical barriers from the Hydrogen Delivery section of the Fuel Cell Technologies Office (FCTO) Multi-Year Research, Development, and Demonstration (MYRDD) Plan (Section 3.2.5):

(D) High As-Installed Cost of Pipelines

(K) Safety, Codes and Standards, Permitting

Technical Targets

This project impacts the following technical targets for hydrogen delivery components (Table 3.2.4 of the FCTO MYRDD Plan) related to pipelines for gaseous hydrogen delivery:

- Total capital investment: 695,000 $/mile (FY 2020)
- Transmission pressure: 100 bar (FY 2020)
- Lifetime: 50 years (FY 2020)

One salient safety and reliability issue for steel hydrogen pipelines is hydrogen embrittlement. For steel pipelines, the central unresolved issue is the pipeline performance under extensive pressure cycling. One of the objectives of this project is to enable safety assessments of steel hydrogen pipelines subjected to pressure cycling through the use of structural integrity models in design codes, e.g., American Society of Mechanical Engineers (ASME) B31.12. This structural integrity analysis can determine limits on design and operating parameters such as the allowable number of pressure cycles and pipeline wall thickness. Accurately specifying pipeline dimensions such as wall thickness also affects pipeline cost through the quantity of material required in the design.

FY 2015 Accomplishments

- Triplicate fatigue testing of X52 FSW pipe was completed in 21 MPa hydrogen gas at load ratio (R) of 0.5 and load-cycle frequency of 1 Hz. Three material regions were tested: base metal, center of FSW, and 15 mm off-center from weld.
- Submission of paper to *International Journal of Fatigue* on the effects of microstructure banding on hydrogen-accelerated fatigue crack growth in X65 base metal.
- Completed fatigue testing of fine- and coarse-grained Fe-C model steels at 10 Hz and R = 0.5 in 5.5 MPa and 34 MPa hydrogen gas.

✧ ✧ ✧ ✧ ✧

INTRODUCTION

Carbon-manganese steels are candidates for the structural materials in hydrogen gas pipelines; however, it is well known that these steels are susceptible to hydrogen embrittlement. Decades of research and industrial experience have established that hydrogen embrittlement compromises the structural integrity of steel components. This experience has also helped identify the failure modes that can operate

in hydrogen containment structures. As a result, there are tangible ideas for managing hydrogen embrittlement in steels and quantifying safety margins for steel hydrogen containment structures. Fatigue crack growth aided by hydrogen embrittlement is a well-established failure mode for steel hydrogen containment structures subjected to pressure cycling. This pressure cycling represents one of the key differences in operating conditions between current hydrogen pipelines and those anticipated in a hydrogen delivery infrastructure. The reliability/integrity of hydrogen pipelines in a delivery infrastructure will be assessed using structural integrity models along with measurements of relevant material properties. Such models are commonly used in design codes and standards (e.g., ASME B31.12) and could be enhanced through the derivation of physics-based relationships between fatigue crack growth rates and steel microstructure (in addition to cycle frequency, load ratios, and pressures). Enhancements of these models will increase confidence in their integrity, while also enabling higher-pressure, lower-cost pipelines.

APPROACH

The approach of this project is to apply the enabling capability in materials compatibility in high pressure hydrogen at SNL to measure the fatigue crack growth rates of technologically relevant pipeline steels in hydrogen gas. These properties must be measured for the base materials, but more importantly for the welds, which are likely to be most vulnerable to hydrogen embrittlement. Such measurements are necessary for enabling the application of structural integrity models in design codes. For example, the 2014 ASME B31.12 code for hydrogen pipelines includes a fracture mechanics-based integrity management option, which requires material property inputs such as the fatigue crack growth relationship in hydrogen gas.

Following the establishment of reliable fatigue crack growth relationships for pipeline steel base metal, weld heat-affected zone, and weld fusion zone in hydrogen gas, a secondary approach of this project is to apply analytical techniques such as electron microscopy to define the mechanisms of hydrogen embrittlement for the purpose of developing physics-based predictive models. Such predictive models can provide quantitative insight into the effects of environmental, material, and mechanical variables on hydrogen embrittlement. For example, quantifying the effect of microstructure on hydrogen-accelerated fatigue crack growth can aid in the qualification of line pipe steels and their welds for hydrogen service.

RESULTS

The fatigue crack growth rate (da/dN) versus stress-intensity factor range (ΔK) relationship is a necessary input to structural integrity models applied to steel hydrogen pipelines. One such integrity assessment methodology for steel hydrogen pipelines was recently published in the ASME B31.12 code. The measurement of fatigue crack growth relationships in this task supports the objective of establishing the reliability/integrity of steel hydrogen pipelines and informing appropriate design safety factors in future editions of hydrogen piping codes.

Low-strength line pipe steels such as X52, X60, and X65 were selected for this task because of their stakeholder-recognized relevance for hydrogen pipelines. Generally, lower-strength steels are selected for hydrogen pipelines since these steels are less susceptible to hydrogen embrittlement. Fatigue crack growth testing was previously performed on a gas metal arc welded X65 pipe and the results can be found in the FY 2014 annual report. For FY 2015, a section of X52 pipe containing a FSW was supplied by Oak Ridge National Laboratory for fatigue crack growth testing in hydrogen gas. Friction stir welds represent a lower cost welding technology as compared to conventional arc welding with consumables. A solid-state weld is fabricated by inserting a non-consumable welding tool into the steel and mechanically mixing the metal to form a permanent joint. For the supplied X52 pipe, the outside diameter was approximately 340 mm (13.4 in) with a nominal thickness of 6.35 mm (0.25 in). The pipe contains a friction stir weld in the circumferential direction and is shown in Figure 1. Single edge notched (ESE(T)) specimens

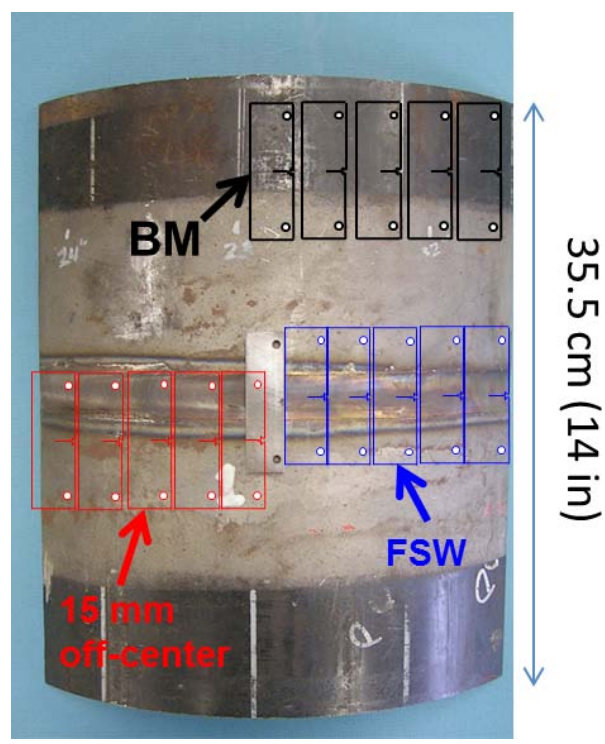

FIGURE 1. Image of the X52 friction stir welded steel pipe with ESE(T) specimens overlaid to show approximate location of specimen machining. Specimens removed from base metal (BM), center of FSW, and 15 mm off-center from FSW.

were extracted in the L-C orientation (wherein load is applied in the longitudinal direction and the crack propagates in the circumferential direction). Three material regions of the pipe were examined: base metal (BM), center of the FSW, and 15 mm off-center from the FSW. The three locations are shown in Figure 1. Figure 2 shows a macro-etch of the FSW. The dashed lines represent the crack planes of specimens tested in the center of the FSW (blue) and the 15 mm off-center position (red). Because specimens were extracted in the L-C orientation, the cracks propagated normal to the image plane in Figure 2. The 15 mm off-center location was chosen to evaluate effects of the welding process on the adjacent base metal (similar to the heat affected zone in studies on the X65 pipe from FY 2014). The location provided sufficient offset from the weld such that the entire crack plane would be contained within a more uniform microstructure, as observed macroscopically in Figure 2. This permitted easier analysis compared to having half of the crack plane located in the FSW and half in the BM.

The results of triplicate fatigue crack growth tests on the X52 friction stir welded pipe in 21 MPa hydrogen gas are shown in Figure 3. The da/dN vs ΔK relationship was measured following ASTM Standard E647 (as specified in ASME B31.12) at R = 0.5. Since the maximum pressure specified for hydrogen gas pipelines in the ASME B31.12 code is 3,000 psi (21 MPa), this upper-bound pressure was selected for the testing. The load-cycle frequency selected for the testing was 1 Hz, consistent with previous testing on line pipe steels and their welds in high pressure hydrogen gas. Fatigue crack growth relationships are plotted in Figure 3 for the three material regions (BM, FSW, and 15 mm off-center from FSW). For comparison, a single test was performed on the BM in air at a frequency of 10 Hz. All specimens tested in 21 MPa hydrogen gas exhibited accelerated fatigue crack growth rates (FCGR) as compared to the test in air and triplicate tests showed good repeatability. The FSW FCGR were slightly higher than the BM whereas the 15 mm off-center results were slightly lower than the BM. Fracture surfaces of select samples were examined in the scanning electron microscope (SEM) at a location corresponding to $\Delta K \sim 8.5$ MPa $m^{1/2}$. Similar fractions of intergranular fracture were observed on fracture surfaces of the BM and off-center specimens, consistent with other fatigue studies [1-4] of ferritic pipeline steels tested in hydrogen gas. However, the fracture surface of the FSW exhibited negligible intergranular fracture. Metallographic samples are under preparation to examine higher magnification SEM imaging of the three material regions examined to identify features in the microstructure that may contribute to the observed FCGR differences.

In collaboration with I2CNER, custom heats of two high-purity Fe-C materials were procured and delivered to Kyushu University (Fukuoka, Japan): a fine-grain-size (15 µm) heat and a coarse-grain-size (70 µm) heat. The goal was to assess the effects of grain size on the onset of hydrogen-accelerated fatigue crack growth. In FY 2014 tests were performed on the two Fe-C alloys at 10 Hz and R = 0.1 in 2.1 MPa H_2. In FY 2015, data from FY 2014 tests were re-analyzed to account for residual stresses, and tests were performed on the two alloys (fine and coarse grain) at a higher load ratio (R = 0.5), frequency = 10 Hz, and two gas pressures = 5.5 MPa (800 psi) and 34 MPa (5,000 psi). These pressures were selected to allow comparisons with data generated from the National Institute of Standards and Technology (NIST), as NIST has developed a phenomenological model based on test results at these two pressures. The preliminary results of the recent tests at higher R ratio are shown in Figure 4 for each alloy (coarse- and fine-grained) at the two gas pressures. Tests were performed in air for comparison. All tests performed

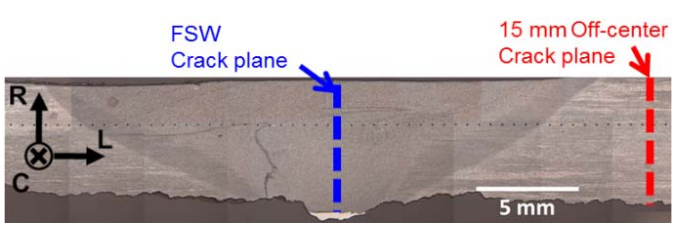

FIGURE 2. Optical image of friction stir welded region is shown with dashed lines representing the approximate location of specimen crack planes in the FSW and 15 mm off-center positions. Base metal samples were extracted more than 100 mm from the FSW.

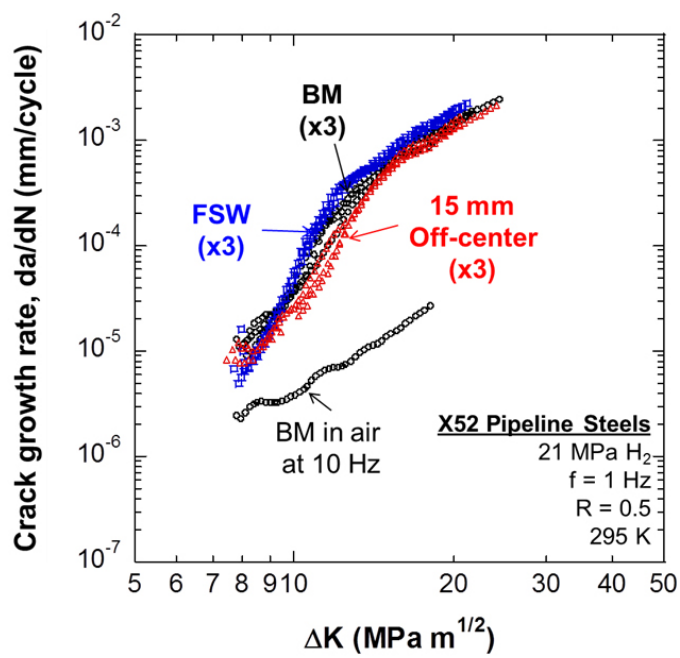

FIGURE 3. Fatigue crack growth relationships (da/dN vs ΔK) of X52 pipeline steel performed in 21 MPa hydrogen gas at R = 0.5 and frequency = 1 Hz. Three material regions were examined: base metal (BM), center of friction stir weld (FSW), and 15 mm off-center to the friction stir weld centerline. BM test in air at 10 Hz is shown for comparison.

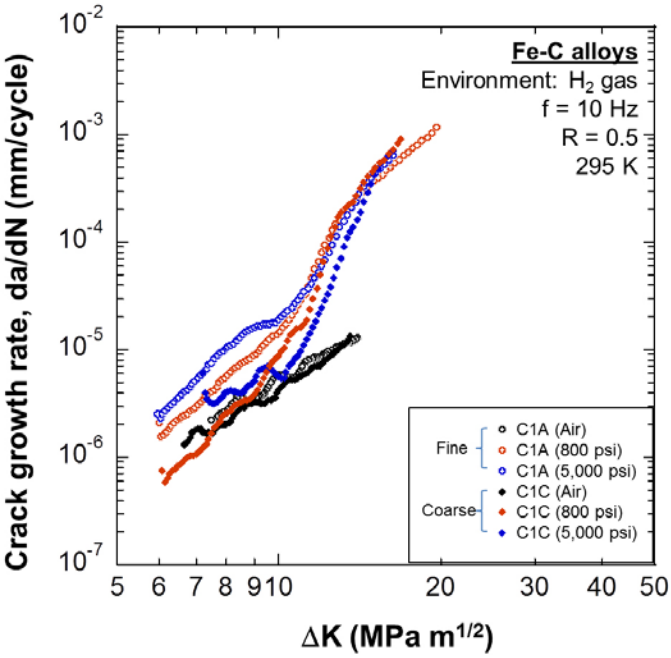

FIGURE 4. Fatigue crack growth relationships (da/dN vs. ΔK) for fine (C1A) and coarse (C1C) grained ferrite-pearlite alloys in 5.5 MPa and 34 MPa hydrogen gas as well as air. Tests were performed at 10 Hz and R = 0.5.

in hydrogen exhibited accelerated fatigue crack growth as compared to the tests in air. The C1A (fine grain) results exhibited greater FCGR when tested at 34 MPa pressure as compared to 5.5 MPa pressure. The C1C (coarse grain) material also exhibited accelerated fatigue crack growth; however, the onset of accelerated FCGR occurred at a lower ΔK for the lower pressure test (5.5 MPa) as compared to the test in 34 MPa hydrogen gas. This is contrary to what was expected as typically higher pressures result in earlier onset of hydrogen-accelerated FCG. Further testing is planned in the form of duplicates and at a lower frequency (1 Hz) to better define the trends.

CONCLUSIONS AND FUTURE DIRECTIONS

- Reliable da/dN vs. ΔK relationships were measured for the X52 friction stir welded (FSW) pipe in 3,000 psi (21 MPa) hydrogen gas. The FSW exhibited slightly greater crack growth rates as compared to the base metal and 15 mm off-center region. However, the results of the base metal indicate that X52 steel is capable of reliable operation in a 100-bar hydrogen pipeline with a thickness no greater than that required for natural gas service.
- Testing of model fine- and coarse-grained Fe-C alloys has commenced at higher R ratio (0.5) at two hydrogen gas pressures (5.5 MPa and 34 MPa) and load-cycle frequency = 10 Hz. Machining of additional specimens is in progress to complete this milestone.
- (Future) Complete manuscript for journal submission on fatigue crack growth testing of friction stir welded pipe in 21 MPa hydrogen gas.

FY 2015 PUBLICATIONS/PRESENTATIONS

1. J.A. Ronevich, B.P. Somerday, C.W. San Marchi, "Effects of Microstructure Banding on Hydrogen Assisted Fatigue Crack Growth in X65 Pipeline Steels." *International Journal of Fatigue,* submitted July 2015.

2. J. Ronevich and B. Somerday, "Assessing Gaseous Hydrogen Assisted Fatigue Crack Growth Susceptibility of Pipeline Steel Weld Fusion Zones and Heat Affected Zones." 15th International ASTM/ESIS Symposium on Fatigue and Fracture Mechanics in Anaheim, CA, May 20–22, 2015.

3. "Hydrogen Embrittlement of Pipeline Steels and Welds." Joe Ronevich and Brian Somerday, presented at ASME B.31.12 Committee Meeting, Atlanta, GA, USA, March 4, 2015.

4. "Hydrogen Embrittlement of Pipeline Steels in Base Metal and Welds," J. Ronevich and B. Somerday, Joint Delivery-Codes & Standards Tech Team Meeting, Sacramento, CA, January 2015.

REFERENCES

1. C. San Marchi, B.P. Somerday, K.A. Nibur, D.G. Stalheim, T. Boggess, and S. Jansto, "Fracture and Fatigue of Commercial Grade API Pipeline Steels in Gaseous Hydrogen," presented at the ASME 2010 Pressure Vessels & Piping Division, Bellevue, WA, USA, 2010.

2. B.P. Somerday, P. Sofronis, K.A. Nibur, C. San Marchi, and R. Kirchheim, "Elucidating the variables affecting accelerated fatigue crack growth of steels in hydrogen gas with low oxygen concentrations," *Acta Materialia,* vol. 61, pp. 6153–6170, 2013.

3. C. San Marchi, B.P. Somerday, K.A. Nibur, D.G. Stalheim, T. Boggess, and S. Jansto, "Fracture Resistance and Fatigue Crack Growth of X80 Pipeline Steel in Gaseous Hydrogen," presented at the ASME 2011 Pressure Vessels & Piping Division, Baltimore, MD, USA, 2011.

4. S. Suresh and R.O. Ritchie, "Mechanisitic dissimilarities between environmentally influenced fatigue-crack propagation at near-threshold and higher growth rates in lower strength steels," *Metal Science,* vol. 16, pp. 529–538, 1982.

III.4 Fiber Reinforced Composite Pipeline

George Rawls
Savannah River National Laboratory (SRNL)
Materials Science & Technology
773-41A/173
Aiken, SC 29808
Phone: (803) 725-5658
Email: george.rawls@srnl.doe.gov

DOE Manager
Erika Sutherland
Phone: (202) 586-3152
Email: Erika.Sutherland@ee.doe.gov

Project Start Date: October 1, 2006
Project End Date: October 1, 2016

Project Objectives

- Successfully adapt spoolable fiber reinforced polymer (FRP) composite pipeline currently used in the oil and natural gas industry for use in high-pressure hydrogen delivery systems and develop the data needed for codification of fiber reinforced composite piping into the American Society of Mechanical Engineers (ASME) B31.12 Hydrogen Piping Code

Fiscal Year (FY) 2015 Objectives

- Provide proposal for codification for FRP into the ASME B31.12 Hydrogen Piping Code
- Perform initial leak and burst testing on samples of dry wrap thermoplastic piping

Technical Barriers

This project addresses the following technical barriers from the Hydrogen Delivery section of the Fuel Cell Technologies Office Multi-Year Research, Development, and Demonstration Plan:

(D) High As-Installed Cost of Pipelines

(J) Hydrogen Leakage and Sensors

(K) Safety, Codes and Standards, Permitting

Technical Targets

This project is focused on the evaluation of FRP for hydrogen service applications. Assessment of the structural integrity of the FRP piping and the individual manufacturing components in hydrogen will be performed. Insights gained will support qualifications of these materials for hydrogen service including:

- Distribution pipeline lifetime: 50 years
- Distribution pipeline pressure: 100 bar
- Distribution pipeline leakage: 0.02%

FY 2015 Accomplishments

In FY 2015, the main activities at SRNL were to complete codification of FRP into the ASME B31.12 Hydrogen Piping Code and to provide initial burst and leak test data for dry wrap thermoplastic piping.

- The code case for inclusion of fiber reinforced plastic piping has been drafted and reviewed by FRP manufacturers.
- The code case has been approved by the B31.12 Hydrogen Piping Committee.
- Two burst tests were completed on dry-wrapped thermoplastic piping. The results of the burst tests showed acceptable design margins.
- Two leakage tests were completed on a crimped connector design used on thermoplastic piping. The results indicated that the connectors met the acceptance criteria. There were indications for high permeation rates from the leak testing.

✧ ✧ ✧ ✧ ✧

INTRODUCTION

The goal of the overall project is to successfully adapt spoolable FRP currently used in the oil industry for use in high-pressure hydrogen pipelines. The use of FRP materials for hydrogen service will rely on the demonstrated compatibility of these materials for pipeline service environments and operating conditions. The ability of the polymer piping to withstand degradation while in service and development of the tools and data required for life management are imperative for successful implementation of these materials for hydrogen pipelines.

APPROACH

To achieve the objective, an FRP life management plan was developed. The plan was a joint document developed by SRNL and the ASME to guide generation of a technical basis for safe use of FRP in delivery applications. The plan addresses the needed material evaluations and also focuses on the needed information for codification of FRP into the ASME B31 Code of Pressure Piping. The testing performed by SRNL has:

- Critically evaluated the current application of available FRP product standards through independent testing.
- Defined changes to the current FRP product standards to meet the ASME Code Methodology.
- Provided a body of data to support inclusion of FRP in the ASME B31.12 Hydrogen Piping Code.

The methodology being followed to address qualification of FRP for hydrogen is based on application of currently accepted industry standards for the FRP products. Independent testing has been performed to address any gaps in the existing qualification of FRP.

RESULTS

FRP Codification into ASME B31.12

During FY 2015 a code case providing the requirements for use of FRP in hydrogen service was completed. The code case was approved by the ASME B31.12 Hydrogen Piping Committee and Balloted to the ASME B31 standards committee. Additional comments have been received from the standards committee review. These comments have been incorporated in the code case, and it is moving through the approval process.

Thermoplastic Pipe Testing

Leak and burst testing was performed on two samples of dry wrap thermoplastic piping. The dry wrap thermoplastic piping is a relatively new concept for fiber reinforced pipe that is site manufactured in lengths up to two to three miles. The structural layer typically consists of an even number of helically wound tapes. There is no thermosetting resin within or between the various layers. The dry wrap allows for forming the piping into a compact shape that can easily be pulled through existing abandoned pipelines to ease installation in urban areas. The dry wrap thermoplastic piping will be included in the FRP codification proposal.

Two leak tests were performed in the dry wrapped thermoplastic pipe samples. The samples were formed into a compact C shape and re-rounded prior to testing. This forming process and shape are shown in Figure 1. The shape is formed into the piping to reduce the cross section to aide in pulling the pipe through existing piping. The test samples were C-formed and rerounded to ensure they would undergo the same loads as field installed piping.

Both tests were below the acceptable leak rate for a 25 minute test indicating no connector leakage. There were, however, indications of permeation following the connector leak test.

Following the leak tests, the samples were burst tested to evaluate their pressure design margins. The pressure design basis follows the American Society for Testing and Materials (ASTM) D2992 standard used for the thermosetting resin FRP. Two burst tests were performed in the dry-wrapped thermoplastic pipe samples. The burst test data are shown in Table 1. The rated pressure value includes a 0.67 hazardous gas service factor at 140°F service temperature. Burst pressures were above the manufacturer's acceptance limit of 3,538 psig, though burst testing used lower pressurization rates than specified by ASTM D1599.

TABLE 1. Burst Test Data for Dry Wrapped Thermoplastic Pipe

Test ID	Rated 50 Year Pressure (psig)	Burst Pressure (psig)
1	580	3,670
2	580	3,870

CONCLUSIONS AND FUTURE DIRECTIONS

Conclusions

- The code case for inclusion of fiber reinforced plastic piping has been drafted and reviewed by FRP manufacturers.

FIGURE 1. Forming process for C shape

- The code case has been approved by the B31.12 Hydrogen Piping Committee.
- The code case has been balloted to the B31 standards committee and additional comments have been incorporated.
- Two burst tests were completed on dry wrapped thermoplastic piping. The results of the burst tests showed acceptable design margins.
- Two leakage tests were completed on a crimped connector design used on thermoplastic piping. The results indicated that the connectors met the acceptance criteria. There were indications for high permeation rates from the leak testing.

Future Work

- Complete the FRP Codification into ASME B31.12.

FY 2015 PUBLICATIONS/PRESENTATIONS

1. Hydrogen Delivery Technology Team, Washington, DC, June 2014.

2. B31.12 Hydrogen Piping Committee Meeting, San Diego CA, September 2014.

3. B31.12 Hydrogen Piping Committee Meeting, Atlanta, GA, March 2015.

III.5 Development of High Pressure Hydrogen Storage Tank for Storage and Gaseous Truck Delivery

Don Baldwin
Hexagon Lincoln (formerly Lincoln Composites Inc.)
5117 N.W. 40th Street
Lincoln, NE 68524
Phone: (402) 470-5017
Email: don.baldwin@hexagonlincoln.com

DOE Manager
Erika Sutherland
Phone: (202) 586-3152
Email: Erika.Sutherland@ee.doe.gov

Contract Number: DE-FG36-08GO18062

Project Start Date: July 1, 2008
Project End Date: December 31, 2015

Overall Objectives

The objective of this project is to design and develop the most effective bulk hauling and storage solution for compressed hydrogen gas (CHG).

- Cost
- Safety
- Weight
- Volumetric efficiency

Fiscal Year (FY) 2015 Objectives

Project activity in 2015 is focused on the following.

- Continue to investigate cost improvements
- Improve performance and reliability of safety system(s) through evaluation and adoption of new technologies
- Increase volume/capacity per payload at operating pressure of 250 bar

Technical Barriers

This project addresses the following technical barriers from the Hydrogen Delivery section of the Fuel Cell Technologies Office Multi-Year Relearch, Development, and Demonstration Plan

(E) Gaseous Hydrogen Storage and Tube Trailer Delivery Costs

(I) Other Fueling Site/Terminal Operations

Technical Targets

This project has focused primarily on the design and qualification of a 3,600 psi pressure vessel and International Organization for Standardization (ISO) frame system to yield a combined storage capacity solution of approximately 34,000 L of water. The original scope of the project was to increase working pressure in the current design. Together with DOE, the project scope has been changed to work towards increasing available volume at the 3,600 psi working pressure. Further technical targets can be found in Table 1.

Accomplishments

- Successfully completed the design and qualification of a 3,600 psi pressure vessel (fourth quarter [4Q] 2009).
- Successfully completed the design and qualification of an ISO frame capable of holding four 3,600 psi pressure vessels with a combined capacity of 616 kg of hydrogen (third quarter [3Q] 2009).
- U.S. Department of Transportation (DOT) Special Permit (SP) 14951 issued to Hexagon Lincoln on February 22, 2012. SP 14951 authorizes the manufacture, making, sale, and use of TITAN™ modules in the United States.
- A trade study was performed in the first quarter [1Q] 2011; results indicated that CHG storage at 350 bar optimized hauling efficiency and system cost. However,

TABLE 1. Progress towards Meeting Technical Targets for Hydrogen Storage

Characteristic	Units	2010 Target	2015 Target	2020 Target	Status	Comments
Storage Costs	$/kg	$500/kg	$730/kg	$575	$800/kg	
Volumetric Capacity	kg/L	0.030 kg/L	>0.035 kg/L		0.018 kg/L	
Delivery Capacity, Trailer	kg	700 kg	700 kg	940 kg	720 kg	Titan5 Magnum trailer capacity is 800 kg Titan5 XL40 trailer capacity is 890 kg

development of a 350-bar system was not completed as part of this project due to insufficient market demand.

- Completed the design, manufacture and assembly of integrated TITAN™ 5 Magnum trailer system capable of storing ~800 kg H_2 at 3,600 psi. This new bulk hauling system was first deployed in compressed natural gas (CNG) service in 2013.
- Completed the design, manufacture and assembly of integrated TITAN™ 5 XL40 trailer system capable of storing ~890 kg H_2 at 3,600 psi. This new bulk hauling system was first deployed in CNG service in 2015.

✧ ✧ ✧ ✧ ✧

INTRODUCTION

Successful commercialization of hydrogen fuel cell vehicles will depend upon the creation of a hydrogen delivery infrastructure that provides the same level of safety, ease, and functionality as the existing gasoline and diesel fuel delivery infrastructure. Today, CHG is shipped in tube trailers at pressures up to 7,252 psi (about 500 bar). However, the capacity of these tube trailers results in high delivery costs. Hydrogen rail delivery is currently economically feasible only for cryogenic liquid hydrogen; almost no hydrogen is transported by rail. Reasons include the lack of timely scheduling and transport to avoid excessive hydrogen boil-off and the lack of rail cars capable of handling cryogenic liquid hydrogen. Hydrogen transport by barge faces similar issues in that few vessels are designed to handle the transport of hydrogen over inland waterways. The Hexagon Lincoln TITAN™ ISO-format module will enable low-cost transport of gaseous hydrogen by increasing the carrying capacity of 250-bar tube trailers.

APPROACH

In Phase 1 of this project, Hexagon Lincoln has designed and qualified a large composite pressure vessel and ISO frame that can be used for storage and transport of CHG over road, rail, or water.

The baseline composite vessel has a 250 bar (3,626 psi) service pressure, an outer diameter of 42.8 in and a length of 38.3 ft. The weight of this tank is approximately 2,485 kg. The internal volume is equal to 8,500 L water capacity and will contain 150 kg of CHG. The contained hydrogen will be approximately 6.0% of the tank weight (5.7% of the combined weight).

Four of these tanks are mounted in a custom-designed ISO frame, resulting in an assembly with a combined capacity of 600 kg of hydrogen. Installing the vessels into an ISO frame offers a benefit of having one solution for both transportable and stationary storage. This decreases research and development costs as well as the amount of infrastructure and equipment needed for both applications.

The large size of the vessel also offers benefits. A limited number of large tanks is easier to package into the container and requires fewer valves and fittings. This results in higher system reliability and lower system cost. The larger diameter also means thicker tank walls, which will make the vessel more robust and damage tolerant.

Phase 2 of the program was originally scoped to evaluate using the same approximate sized vessel(s) and ISO frame at elevated pressures. Trade studies performed in 2011 indicate optimization of hauling efficiency and system cost for CHG at 350 bar (5,076 psi). Due to differences in the compressibility of CHG and CNG, 350 bar operation is not an attractive option for CNG. The CHG market is difficult to forecast at this time and the cost to fully qualify a higher pressure module estimated at $5 million to complete. Based on insufficient CHG market definition to support a stand-alone business case for CHG, development of a 350 bar (5,076 psi) system has been placed on hold and will not be pursued under this project.

Consequently, it was determined that Hexagon Lincoln would work with our current 250 bar product and move forward with increasing the potential volume per load as well as improvements in safety. Increased volume has been achieved with the development of the TITAN™ 5 Magnum, an integrated trailer system with additional tankage. Other system improvements supported by the project include the evaluation, testing, and qualification of an improved emergency venting systems as well as development and installation of laboratory capabilities to evaluate the effects of hydrogen on liner materials.

RESULTS

Hexagon Lincoln completed qualification of the TITAN™ pressure vessel and ISO frame in 2009. The baseline 250 bar system shown in Figure 1 has an internal volume of 34,000 L water capacity and will contain 150 kg of CHG.

The initial Hexagon Lincoln TITAN™ 5 trailer prototype increased total payload capacity by 18% as compared with the baseline TITAN™ module. This new integrated trailer utilized the same four 40 ft TITAN™ cylinders with the addition of a single 30 ft TITAN™ tank placed lower in the assembly to utilize space between the frame rails of the trailer.

Lincoln Composites has continued the design and evaluation of a more robust emergency venting system utilizing memory metal as a trigger mechanism for depressurizing the tank in the case of a fire. This technology greatly reduces the cost of the system in both components and labor for assembly. The reduction of components in the

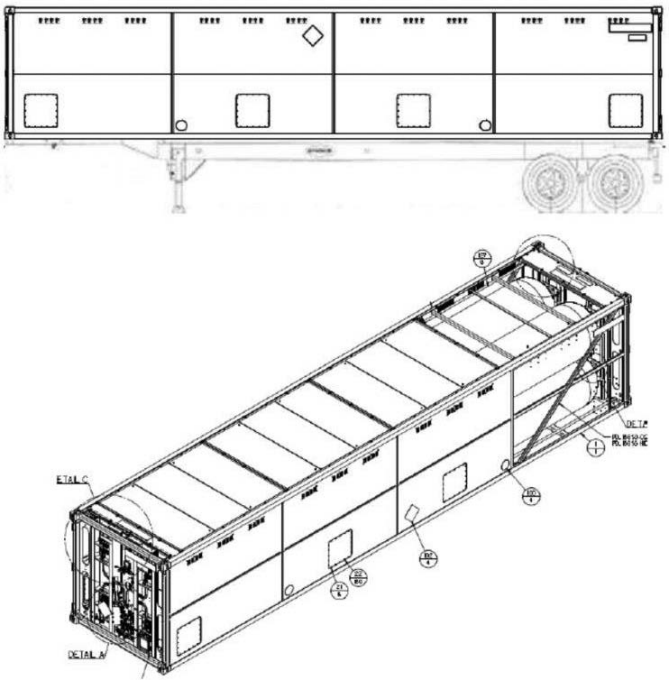

FIGURE 1. TITAN ISO-format module

system affects the potential number of failure modes that could occur and thus makes for a more reliable product.

The installation of a 100% hydrogen testing facility is complete. This laboratory will be used to fully investigate new materials with the potential to be integrated into liners. Specifically, these alternate materials will be qualified for their potential to reduce the permeation rates that are present in current Type 4 cylinders.

To further enhance system volume, the development/design of the TITAN™ 5 trailer systems was extended to the XL40 configuration with larger auxiliary tankage. This design utilizes four 38.5 ft and one 28.5 ft TITAN™ tanks with seven 26 in diameter tanks developed specifically for trailer installation. The new trailer is shown in Figure 2. This configuration has increased capacity by 44% when compared to the standard four cylinder TITAN™ module. This translates to an overall payload of 890 kg of hydrogen. This increase in capacity was achieved without increasing the loaded mass of the trailer because the trailer structure was designed and configured using high strength (100 ksi) steels. The TITAN™ 5 XL40 trailer system is currently deployed in CNG service in Central America.

The TITAN™ tanks were subject to rapid defueling events to assess their liners' potential for inward buckling or collapse. Testing involved defueling tanks from 250 bar to 25 bar within 25 min. The tests were performed once a week to allow for saturation of the liner prior to the defueling. The liner appeared to remain intact but will be further analyzed for localized deterioration in FY 2016.

FIGURE 2. TITAN™ 5 XL40 integrated trailer system

CONCLUSIONS AND FUTURE DIRECTIONS

- Proposed objectives for Phase 1 of this project were completed (4Q 2009). This includes successful qualification of a large 3,600 psi pressure vessel able to contain 8,500 L water capacity, and qualification of an ISO frame capable of holding four of these vessels with a combined capacity of 616 kg of hydrogen.
- DOT SP 14951 issued to Hexagon Lincoln on February 22, 2012. SP 14951 authorizes the manufacture, making, sale and use of TITAN™ modules in the United States.
- The TITAN™ 5 Magnum integrated trailer configuration has an increased capacity of 26% when compared to the standard four cylinder TITAN™ module. This translates to an overall payload of 775 kg of hydrogen.
- The TITAN™ 5 XL40 integrated trailer configuration has an increased capacity of 44% when compared to the standard four cylinder TITAN™ module. This translates to an overall payload of 890 kg of hydrogen.
- A program of deep cycle testing of TITAN™ pressure vessels with CHG was initiated in 1Q 2015 with completion in 3Q 2015. The goal of this demonstration is to characterize CHG-specific operating protocols for use of TITAN™ systems in CHG service at 250 bar.
- Hexagon Lincoln will prepare and submit an application for SP approval with DOT for the manufacture, making, sale, and use of TITAN™ 5 trailer systems in the United States Initial discussions with DOT indicate structural testing analogous to ISO 1496 will be required.

FY 2015 PUBLICATIONS/PRESENTATIONS

1. Quarterly Reports.

2. 2015 DOE Hydrogen Program Annual Merit Review, June 10, 2015.

III.6 Cryogenically Flexible, Low Permeability H_2 Delivery Hose

Jennifer Lalli (Primary Contact), William Harrison, Keith Hill, Vince Baranauskas, and Richard Claus
NanoSonic, Inc.
158 Wheatland Drive
Pembroke, VA 24136
Phone: (540) 626-6266
Email: jhlalli@nanosonic.com

DOE Manager
Erika Sutherland
Phone: (202) 586-3152
Email: Erika.Sutherland@ee.doe.gov

Contract Number: DE-SC0010162

Subcontractors
- National Renewable Energy Laboratory, Golden, CO
- Swagelok, Solon, OH
- New England Wire Technologies, Inc., Lisbon, NH

Project Start Date: July 28, 2014
Project End Date: August 27, 2016

Overall Objectives

NanoSonic's overall objectives for Hydrogen Dispenser Technologies mirror those of the Department of Energy Office of Energy Efficiency & Renewable Energy (DOE-EERE), Fuel Cell Technologies Office (FCTO), and Hydrogen Delivery Program to realize hydrogen as a safe, reliable, and cost competitive replacement for gasoline. Outcomes of this project will include:

- A highly durable hose that can reliably perform at 875 bar (for H70 service, 70 MPa delivery) and over a temperature range of -50°C to 90°C.
- A new class D hydrogen dispensing hose, for use on station side applications, that is chemically engineered to survive 51,240 fills (70 fills per day, 2 years) and meets the requirements outlined in American National Standards Institute/Canadian Standards Institute (ANSI/CSA) Hydrogen Gas Vehicle (HGV) 4.2-2013, with a dispenser compliant with Society of Automotive Engineers (SAE) Technical Information Report (TIR) J2601 and National Institute of Standards and Technology Handbook 44.
- A state-of-the-art hose based on a unique fiber reinforced, high performance, cryogenically flexible polymer to resist hydrogen embrittlement, survive the Joule-Thompson effect of thermal cycles, perform consistently at pressures greater than 875 bar, and endure mechanical wear and fatigue at the pump.
- An alternative to the singular German-made hydrogen dispenser hose that is currently qualified for H70 service, though it does not meet the service requirement of 25,550 fills/year, nor allow for a dispensed hydrogen cost of $4 per gallon of gasoline equivalent (gge).

Fiscal Year (FY) 2015 Objectives

- Quantify the burst strength of the new hydrogen hose
- Optimize the durability via pressure cycle testing
- Demonstrate environmental durability and delivery of fuel cell grade hydrogen with total impurities <100,000 ppb

Technical Barriers

This project addresses the following technical barrier from the Hydrogen Delivery section (3.2.5) of the FCTO Multi-Year Research, Development, and Demonstration Plan:

(I) Other Fueling Site/Termination Operations

Technical Targets

The goals of this project mirror those of the DOE-EERE to advance hydrogen delivery system technologies toward the DOE Hydrogen Delivery Program's 2017 delivery targets [1]. NanoSonic has increased the cryogenic flexibility of our hydrogen delivery hose by decreasing the glass transition temperature (T_g) to -65°C, and increasing upper thermal stability to 350°C (5% weight loss via thermogravimetric analysis (TGA). These modifications will enable a significantly wider service use temperature range than the competitor's hose with a service temperature range of -40°C to 65°C. Burst strength was increased from 2,000 psi to 9,000 psi during first quarter testing by crimping hose fittings in house. The burst strength will be increased in 2015 to 51,000 psi, four times the maximum allowing working pressure of 12,690 psi by a modification of the fiber–polymer interface design, and through the use of a fitting rated for >5,000 psi. Compression strength has been increased from 10 kN to >50 kN (>11,200 lb) through the use of a novel ceramer enhancement. Solvent and abrasion resistance are being tested per the targets outlined in ANSI/CSA HGV 4.2-2013, and evolved gas analysis and quality are being tested per the targets outlined in SAE J-2719 and International Organization for Standardization (ISO)/TS 14687-2. Current cost projections based on materials for 300 meters of hose are two times less than the competitor's price. Cost savings, normalized for lifetime, predict a 4x savings. NanoSonic's planned scale-up method predicts an

8x cost savings, assuming batch production of 600 m of hose and normalizing for the hose life.

The NanoSonic hose is being designed to meet or exceed the requirements of ANSI/CSA HGV 4.2-2012 for Class D hoses for 700-bar dispensing. Table 1 describes NanoSonic's hose performance.

TABLE 1. Technical Performance of Durable Hydrogen Hose for Fuel Cell Vehicles

Characteristic	Units	NanoSonic
T_g	°C	-60
Upper Service Temperature (Corresponding to Weight Loss of 5%)	°C	350
Burst Strength	psi	>9,000 (24,730 expected)
Cycle Pressure Test	cycles	in progress
Cost	$/m	<60

FY 2015 Accomplishments

- Developed low T_g (60°C) hose with an upper service thermal stability of 350°C that demonstrates ultra-low hydrogen permeance after 180° bending, three times in a -50°C chamber
- Fiber-reinforced hose has a predicted burst pressure of 1,705 bar
- Developed unique ceramer coupling agent for enhanced crimp survivability and increased compression strength, >11,200 psi
- Reduced cost to $60/m via scale-up
- Collaborating with gas distribution original equipment manufacturers, fittings manufacturers, national laboratories, and safety standards groups to qualify the hose and bring it to market for H70 service

✧ ✧ ✧ ✧ ✧

INTRODUCTION

NanoSonic is developing and manufacturing a cost effective new hose to offer reliable delivery of hydrogen for fuel cell vehicles as a safe, reliable, and cost competitive replacement for gasoline per the FCTO Hydrogen Delivery goals. This American-made hose will meet the DOE-EERE's FCTO technical targets to enable the hydrogen economy through enhanced safety and durability. There is a need for a highly durable hose that can reliably perform at 875 bar (for H70 service, 70 MPa delivery) and over a temperature range of -50°C to 90°C.

NanoSonic has worked during this DOE Small Business Innovation Research program to produce a new class D hydrogen dispensing hose, for use on station side applications. NanoSonic's hose was systematically and chemically engineered to survive 51,240 fills, or 70 fills per day for a period of at least two years. Our state-of-the-art hose is based on a unique fiber reinforced high performance, cryogenically flexible polymer to resist hydrogen embrittlement, survive the Joule-Thompson effect thermal cycles, perform consistently at pressures greater than 875 bar and endure mechanical wear and fatigue at the pump. Currently, there is only one hydrogen dispenser hose that is qualified for H70 service. This hose is not manufactured in the United States and does not meet the service requirement of 25,550 fills/yr or enable a dispensed hydrogen cost of $4/gge.

APPROACH

The new hydrogen hose involves an all polymer material approach in contrast to the currently qualified hose that utilizes steel as its reinforcing agent. The unique polymer fiber reinforcement design shall meet the current burst strength requirements, and surpass the durability of steel based hoses that are susceptible to weakening and catastrophic failure via hydrogen embrittlement. NanoSonic's state-of-the-art hose is based on a unique fiber reinforced high performance, cryogenically flexible polymer to resist hydrogen embrittlement, survive the Joule-Thompson effect thermal cycles, perform consistently at pressures greater than 875 bar (for H70 service, or 700 bar with a safety overpressure), and endure mechanical wear and fatigue at the pump. The polymer core is based on an ultra-low T_g backbone for cryogenic flexibility and modified for adhesion to the fiber reinforcing agents and ceramer inclusions for enhanced compression strength.

NanoSonic's manufacturing approach towards cost savings and enhanced durability is three-fold. First, a unique three-dimensional mold allows for tailored designs from the inner high pressure stable core to the fiber reinforced placement, and the outermost abrasion and solvent resistant jacket. Second, NanoSonic has two large-scale reactors that allow for the cost effective production of 55 gallon and 200 gallon drum batches of our nanocomposite resins. Finally, NanoSonic has invested in a crimper to integrate the end connection fittings directly onto our hoses. This design allows for enhanced adhesion and mechanical fit between the fitting and the hose. Crimping in house also yields a product with complete fit and finish for qualification and distribution.

RESULTS

NanoSonic's major focus during FY 2015 is on fittings' attachment to our hoses for hydrostatic strength and pressure cycle testing. The 2015 hoses are shown in Figure 1. Previously, NanoSonic delivered hoses to Swagelok for crimping. The low modulus hoses pulled out of the

fitting during hydrostatic strength tests at CSA Group per Section 2.4 in the hydraulic burst chamber, per the set up shown in Figure 2. The pressurization rate was set for 14,500 psi per minute. Failure pressure ranged between 200–2,100 psig, whereas the target value is four times (51,000 psi) the maximum allowable working pressure of 12,700 psi (875 bar) for H70 (70 MPa) service. Our Phase II fittings partner at Swagelok recommended that NanoSonic consider doing the fittings installation in house due to time constraints on their end. NanoSonic purchased a crimping machine from the recommended supplier. The crimper allows for installation of various dies for diameters down to 4 mm. NanoSonic owns crimping dies #12, 14, and 16 for an outer diameter crimping range of 12 mm to >19 mm.

NanoSonic purchased several types of materials to begin crimping with, including Swagelok fittings and carbon steel pipe. Our local distributor representative from Dibert Valve and Fittings recommended we begin with Swagelok compression tube fittings, end tub stub, and compressed natural gas hose ends with dimensions to accommodate our initial design. NanoSonic also purchased carbon steel pipe with similar dimensions as inexpensive option to begin with. Our partners at Swagelok conducted the initial crimping, and NanoSonic followed suit, though with our own crimp procedure, to yield a series of varied crimped dimensions, as shown in Table 2.

FIGURE 1. NanoSonic's hydrogen delivery hoses demonstrating cryogenic flexibility

Pull-out tests were conducted on NanoSonic's crimpled hoses using our benchtop loadframe. The texture analyzer has an upper load limit of 50 kg (110 lb). It was found that significant crimping results in increased stress on the low modulus polymer. In this case, the materials failed prior to pull-out. An optimized crimp could not be pulled from the hose just beyond the maximum force of the loadframe at 120 lb. NanoSonic also owns an Instron with an upper load limit of 50 kN, although the grips are not wide enough to accommodate the hoses. We have ordered two sets to allow for pull-out and pulley-style tensile testing.

NanoSonic developed a unique ceramer for use as an adhesive between the fitting and hose to offer additional

FIGURE 2. NanoSonic hose in hydrostatic burst strength test configuration

TABLE 2. Dimensions before and after Crimping

Crimper	Material	OD 1 (mm)	OD 2 (mm)	WT 1 (mm)	WT 2 (mm)	ID 1 (mm)	ID 2 (mm)
Swagelok	Swagelok SS	20	18	1.5	1.61	16.3	16.2
NanoSonic	Swagelok SS	20	16	1.5	1.64	16.3	13.6
NanoSonic	CS Pipe	22.3	15, 16, 17, 18, 19	3.1	3.2–4.7	16	8.9–6.7
NanoSonic	CS Pipe		19.4		3.5		12.4

SS – stainless steel; CS – carbon steel; ID – inside diameter; OD – outside diameter; WT – wall thickness

chemical strength beyond the mechanical strength of crimping alone. The adhesive-ceramer is a viable candidate as it also exhibits a wide service temperature range, with a low T_g of -60°C and exhibits 5% weight loss beyond 320°C.

Compression testing was conducted on NanoSonic's down-selected hose polymer and the proposed adhesive-ceramer material to establish feasibility for the high pressure testing. NanoSonic has designed a testing procedure in accordance with ASTM D 695: Standard Test Method for Compressive Properties of Rigid Plastics for materials greater than 3.2 mm thick. This testing was completed on NanoSonic's Instron load frame that has a 50 kN load cell, in conjunction with extensometer/compressometer. The exact cross-sectional area of all specimens was measured prior to testing, to ensure an accurate strength calculation. After the cross section of each specimen is measured, the samples are then be placed between two flat steel plates that are attached to the clamps of the Instron load frame. The cross-head is then moved at a constant rate of 1.3 mm/min until the compressive load begins to drop off. Three specimens for each sample set are tested. Data is given in Table 3, and materials are shown in Figure 3.

NanoSonic fabricated and delivered several hoses to Swagelok for fitting with end connectors. The down-selected prototype hydrogen dispensing hoses were of made using two different copolymers. These copolymer compositions are proprietary and the composition has proved to be influential on the flexibility and toughness of prototype hoses as well as the measured hydrogen permeability.

The hoses fitted with end connectors were 15 inches in length, as determined by the bend radii or as specified by the evaluating experiment scheduled at CSA laboratory. CSA was contracted to perform the two rounds of pressure evaluations on NanoSonic's high pressure hoses. The scheduled tests were (a) Hydrostatic Strength and (b) Pressure Cycle Test. The description of each test is described below.

A. Hydrostatic Strength (Section 2.4) of ANSI/CSA HGV 4.2-201 Standard for hoses for compressed hydrogen fuel stations, dispensers and vehicle fuel systems requires the following.

TABLE 3. Compression Testing on NanoSonic Hose and Adhesive with Ceramer

Material	Thickness (mm)	Displacement at Peak Load (mm)	Peak Load (kN)
Hose Control 1	6.14	-6.39	11.67
1-X % Ceramer	6.81	-6.87	22.02
1-Y % Ceramer	5.89	-5.97	2.73
1-Z % Ceramer	4.85	-4.86	23.54
Hose Control 2	5.43	-5.53	47.12
2-X % Ceramer	7.28	-6.89	52.50
2-Y % Ceramer	6.53	-5.86	51.38
2-Z % Ceramer	5.18	-3.85	52.50

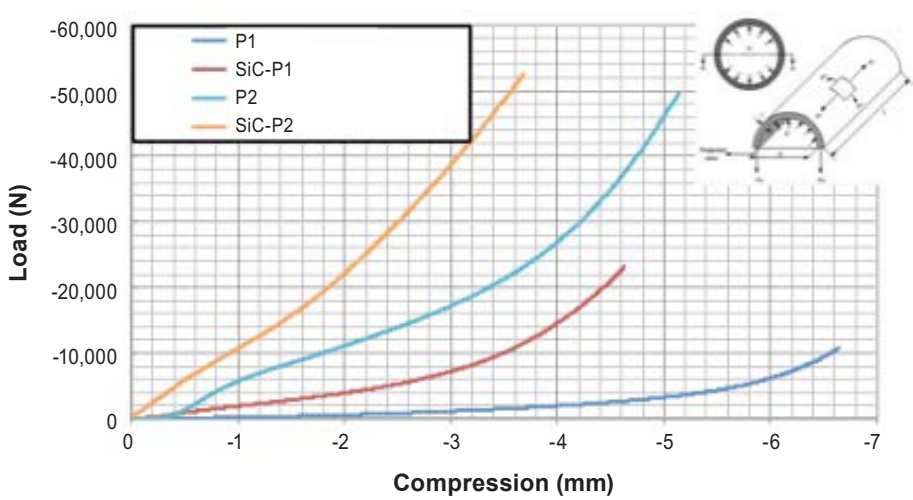

FIGURE 3. Compression strength for NanoSonic's ceramer enhanced hydrogen hoses

- A 1 min hold without burst or visible loss of fluid at a hydrostatic pressure of four times the manufacturer's specified MAWP
- Up to a 10,000 psi MAWP hose assembly
- Two production assembly samples of each model at 12-in length

B. Pressure Cycle Test (Section 2.17) of ANSI/CSA HGV 4.2-2013 Standard for hoses for compressed hydrogen fuel stations, dispensers, and vehicle fuel systems requires 50,000 cycles with maximum allowable working pressure (assuming 10,000 psi) at -40°C and 50,000 cycles with maximum allowable working pressure (assuming 10,000 psi) at 85°C, followed by compliance testing to Leakage (Section 2.2a) and Electrical Conductivity (Section 2.5). Two production assembly samples of each model hose length of "π(minimum bend radius) + 2(hose OD)" are required.

During the initial round of CSA testing, the outfitted hoses failed at the connector ends. The mode of failure was not rupture or bursting but slippage of the hose from the stainless steel hardware. There is no apparent damage to either the detached hose or the end connector. Post-test analysis of the hoses prompted discussions on how to prevent this failure mode in the future.

Crimping in house was conducted on the second set of hoses delivered to CSA for hydrostatic burst strength measurements. In this second set of tests, the hose burst strength was increased to >9,000 psi. A third set of hoses is under development with NanoSonic's ceramer technology, as the ceramer enables a significant increase in compression strength, as shown in Figure 4. NanoSonic is currently seeking fittings that exceed 5,000 psi to complement our new hoses.

CONCLUSIONS AND FUTURE DIRECTIONS

Conclusions derived from the work in FY 2015 are:

- NanoSonic is currently testing our hose with fittings against the Spir Star hose for hydrostatic burst strength and pressure cycling.

FIGURE 4. NanoSonic hydrogen hose with ceramer technology

- We will also be testing our hose against emerging potential commercial competitors, such as: Yokohama Rubber/Iwatani Industrial Gases, ContiTech, and Togawa Rubber. Yokohama's hose is rated for 70 MPa and the Togawa hose is rated for 35 MPa. There are few details given for ContiTech products.
- Environmental robustness and impact on fuel quality are being established through testing with CSA and the National Renewable Energy Laboratory.

FY 2015 PUBLICATIONS/PRESENTATIONS

1. Jennifer Lalli, "Cryogenically Flexible, Low Permeability H_2 Delivery Hose", *DOE Hydrogen and Fuel Cells Program and Vehicle Technologies Office Annual Merit Review and Peer Evaluation Meeting, 2015.*

III.7 Hydrogen Compression Application of the Linear Motor Reciprocating Compressor (LMRC)

Eugene L. Broerman (Primary Contact),
Norm Shade (ACI Services), Klaus Brun,
Jeffrey Bennett, Nathan Poerner, Diana Strickland,
Jerome Helffrich, Shane Coogan, Aaron Rimpel,
Pablo Bueno

Southwest Research Institute®
6220 Culebra Rd.
San Antonio, TX 78238
Phone: (210) 522-2555
Email: EBroerman@swri.org

DOE Manager

Erika Sutherland
Phone: (202) 586-3152
Email: Erika.Sutherland@ee.doe.gov

Contract Number: DE-EE0006666

Subcontractor

Norm Shade (contact), ACI Services, Cambridge, OH

Project Start Date: September 5, 2014
Project End Date: October 4, 2017

Overall Objectives

The primary project goal/objective is to demonstrate the linear motor reciprocating compressor (LMRC) by integrating individually developed technology readiness Level 4 or higher components and to demonstrate that the compressor has improved compression efficiency and a reduced capital and maintenance cost compared to conventional reciprocating compression technology. Another project goal is to meet the flow and pressure requirements in the Multi-Year Research, Development, and Demonstration (MYRDD) Plan tables. The success of these goals will be measured based on the metrics below.

- Improve isentropic efficiency above 73% by minimizing aerodynamic losses and using low-friction bearings (goal is above 95%)
- Reduce capital costs to half those of conventional reciprocating compressors by minimizing part count
- Reduce required maintenance by simplifying the compressor design to eliminate common wear items
- Design a system using the LMRC to compress hydrogen from 290 psia (20 bara) to 12,690 psia (875 bara) with flow rates greater than 22 lbm/h (10 kg/h)

Fiscal Year (FY) 2015 Objectives

The overall objective for FY 2015 was to perform the primary design steps needed to develop the LMRC to the stage at which detailed mechanical design is necessary. Design steps taken to develop the LMRC were as follows.

- Stage sizing: provide cylinder size for each stage and accompanying calculations
- Basic mechanical design: provide finite element analysis (FEA) results and analysis, basic structural design, and material selection
- Linear motor design: provide linear motor design, including required magnet size and configuration of windings
- Bearing and seal design and analysis: provide selected bearing and seal technology and supporting calculations
- Valve selection: provide the valve type/design that will be used for the proposed system
- Pulsation control design: provide pulsation control design and/or techniques such that the predicted piping system pulsations are at or below the amplitudes specified in the American Petroleum Institute (API) Standard 618
- Cooling system design: provide cooler sizes and cylinder cooling specifications (if needed)
- Materials and coatings selection: deliver material specifications and manufacturer availability
- Performance predictions and comparison: deliver performance predications and final computational fluid dynamics (CFD) calculations

Technical Barriers

This project addresses the following technical barriers from the Hydrogen Delivery section of the Fuel Cell Technologies Office MYRDD Plan:

(B) Reliability and Costs of Gaseous Hydrogen Compression

Technical Targets

During the proposal phase and kick-off of the project, the DOE technical targets were based on the 2012 MYRDD Plan. A 2015 MYRDD Plan was published recently. Table 1 compares the predicted characteristics of the LMRC design with 2015 targets from both MYRDD reports.

TABLE 1. Progress towards Meeting Technical Targets for Hydrogen Delivery with Small Compressors: Fueling Sites (~100 kg H_2/h peak flow)

Characteristic	Units	2015 Target per 2012 MYRDD / 2015 Target per 2015 MYRDD	LMRC 2015 Status (Predictions)
Reliability		Improved/NA	Improved
Availability	%	NA/70–90	TBD
Compressor Efficiency	Isentropic %	73%/NA	99% for Stage 1
Compressor Specific Energy	kWh/kg	100-bar pipeline delivery: NA/1.6 250-bar tube trailer delivery: NA/1.5	TBD
Losses	% of H_2 throughput	0.5%/0.5%	<0.4%
Uninstalled Capital Cost (based on 1,000 kg/day station, [~100 kg H_2/hr peak compressor flow])	$	400,000/NA (Two compressors at $200,000 each. Both at 50% throughput each, no backup) or $360,000/NA (one compressor, no backup)	TBD
Uninstalled Capital Cost (based on750 kg/day station, [~100 kgH_2/hr peak compressor flow])	$	100-bar pipeline delivery: NA/275,000 (Three compressors, no backup) 250-bar tube trailer delivery: NA/250,000 (One compressor, one backup)	TBD
Annual Maintenance	% of Installed Capital Cost	2.5%/8%	TBD
Outlet Pressure Capability	bar	860/950	875
Compression Power	kW	260 (20 bar at inlet)/NA	~20 per 10 kg/h (required for compression process—all 3 stages; 20 bar at inlet)
Contamination		Varies by design/NA	TBD
Lifetime	years	NA/–	TBD

NA – Not Applicable
TBD – To Be Determined

FY 2015 Accomplishments

Accomplishments during the current project period include:

- Compressor stage sizing identified the approximate sizes and forces/power that would be necessary for the H_2 compression process up to 875 bar. Based on the approximate size requirements, a three-dimensional (3D) model was developed that could be used to refine the design.
- FEA was used to determine the appropriate LMRC casing thickness and material type.
- A linear motor/actuator was designed to provide sufficient forces needed for the compression process.
- A high-pressure piston dynamic seal between the cylinder compression chamber and the magnets chamber was identified and analyzed. Predictions indicate a seal leak rate that is below the losses target of 0.5% of H_2 throughput identified in Table 1.
- Compressor valves were designed for the first stage LMRC.
- System pulsation characteristics were modeled, and predictions were found to be acceptable.
- System cooling was evaluated and modeled. Inter-stage cooler manufacturers were identified, and the LMRC internal cooling was designed to maintain the temperatures at adequately low levels for the various parts of the system.
- Appropriate system materials and coatings were identified based on the criteria of strength, hydrogen embrittlement characteristics, magnetic properties, coefficient of expansion, and Young's modulus.
- A performance prediction software package was developed to account for the unique motion of the compressor. Isentropic efficiency predictions indicate 99% efficiency for the first stage of compression.

✧ ✧ ✧ ✧ ✧

INTRODUCTION

Southwest Research Institute® (SwRI®) and ACI Services, Inc. (ACI) are developing an LMRC to meet the DOE goal of increasing the efficiency and reducing the cost of forecourt hydrogen compression. The proposed advanced compression system utilizes a novel and patented concept of driving a permanent magnet piston inside a hermetically sealed compressor cylinder through electromagnetic windings. The LMRC is an improvement over conventional reciprocating compressors as it minimizes the mechanical part count, reduces leakage paths, and is easily modularized for simple field installation (U.S. Patent 8,534,058) [1].

APPROACH

The LMRC is a novel concept compared to conventional reciprocating compression technology. The basic principles of reciprocating compressor design have shown that lower piston speeds and gas flow velocities are necessary to maintain isentropic efficiencies within five percentage points of the isentropic limit. In a low-speed reciprocating compressor, the piston imparts energy on a stationary gas resulting in minimal aerodynamic losses, especially when recirculation and friction losses are well controlled. Utilizing inter-stage cooling reduces the initial enthalpy of the gas per stage, which keeps the gas at a lower energy state and requires less compression power. The LMRC system uses these principles to keep parasitic losses minimized, using reduced piston speeds, low-pressure-drop contoured valves, and inter-stage cooling manifolds. Working at low reciprocating speeds of approximately 300 cycles per minute (CPM) (5 Hz), the LMRC is expected to meet an isentropic efficiency target of greater than 95% [2]. That efficiency can be compared with current state-of-the-art technology that typically has an efficiency of closer to 73%.

The compression system replaces the functions of an electric motor drive and reciprocating compressor with an integrated, linear, electrically actuated piston. It will have a magnetic piston within a cylinder and a gas compression chamber at each end of the piston. The compressor cylinder is comprised of an electromagnetic coil that is operable with the piston to convert an input of electrical power to a reciprocating movement of the piston. This uses the same technology seen in magnetic bearings in turbomachinery and does not require oil for lubrication. Since the driver and compressor are integrated into the same hermetically sealed component, there is a significant reduction in the number of parts and materials needed to construct this device. In addition, the simplicity of the design reduces required maintenance, minimizes seal leakages and wear, and allows for oil-free operation. As mentioned previously, the isentropic efficiency is improved with the LMRC design and mechanical losses are reduced by reducing secondary systems. This results in an increase in overall efficiency for the system.

RESULTS

The proposed process will follow a near isentropic thermodynamic path. To achieve this, the hydrogen will remain in the gas phase, and the system will include inter-stage cooling. The reciprocating motion of the piston is sufficient to compress the hydrogen gas to elevated pressures. The compression of the hydrogen from 290 psia (20 bara) to 12,690 psia (875 bara) will be accomplished through three stages of compression, as depicted in Figure 1. Using a speed range of 300–330 CPM and a compression ratio of

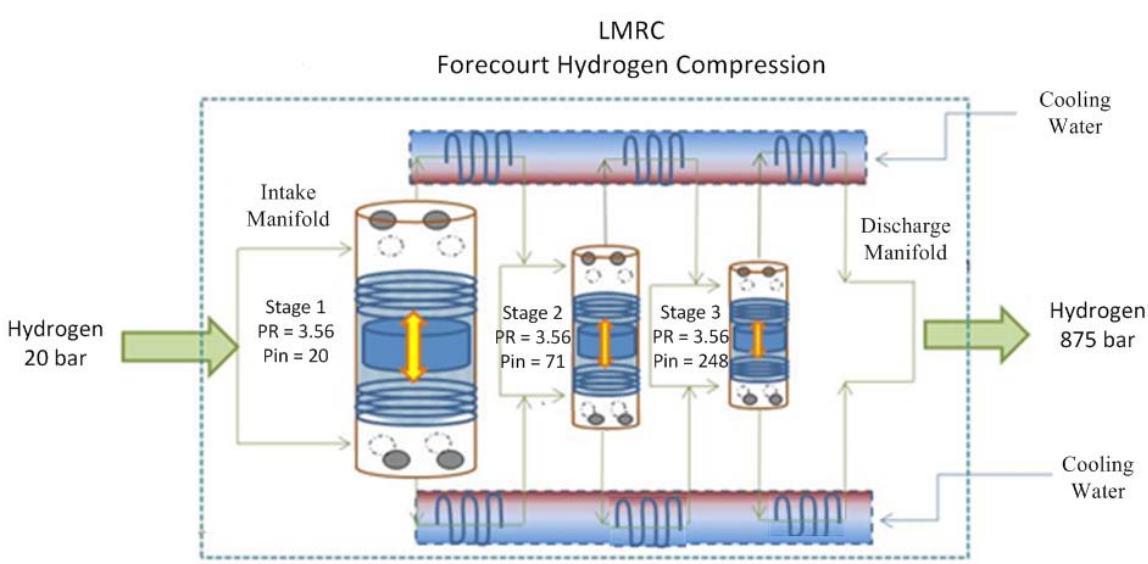

PR – pressure ratio; Pin – inlet pressure

FIGURE 1. LMRC three stage compression system concept with inter-stage cooling manifolds

approximately 3.6 for each stage, calculations indicate that the three stages of compression would be approximately 3.0-inch stroke and 2.6-inch bore, 1.5-inch bore, and 0.9-inch bore for stages one, two, and three, respectively. This stage sizing will allow the LMRC to meet the flow requirement of greater than or equal to 22 lbm/h (10 kg/h).

Basic mechanical design efforts have included LMRC 3D modeling and FEA. System modeling and FEA is in progress, and those tasks include modeling and analyses for each of the three stages of compression. Upon completion of the magnet and coil design, a 3D computer assisted design (CAD) model was developed for each of the three stages. A representative sample of the first-stage model is shown in Figure 2, and an expanded cross-section of one end of first stage is shown in Figure 3 with the significant components labeled. The structural design of the central casing was completed by performing an extensive finite element stress analysis with ANSYS 16.0 on the complete first and second stage pressure containment assemblies. Overall, the stress levels are acceptable. In addition to the structural design of the central casing, bolting design calculations were performed, piston shock absorbers were designed, a magnets assembly fixture is being designed, and a failure modes analysis was performed to thoroughly evaluate the LMRC mechanics.

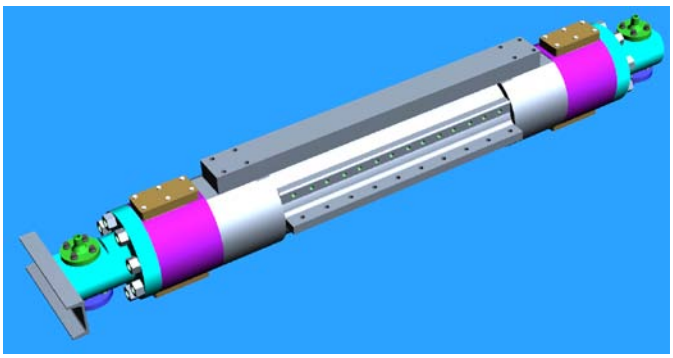

FIGURE 2. Representative screen shot of the first stage 3D CAD model

It was determined that no linear motor design existed that could be used for the LMRC; therefore, a linear motor/actuator was designed based on a traditional moving-magnet-type actuator. The design uses a stack of between seven and 10 actuators/coils (depending on the stage of the compressor) on a shaft. These coils can achieve the required actuation force while maintaining acceptable power dissipation per unit volume. The current-carrying coils are situated outside the pressure vessel where water cooling can easily be used to keep the coil temperatures within an acceptable range. A fully coupled dynamical model was developed that describes the piston action to better understand the linear motor dynamics and to feed critical system dynamic information to the system performance and controls model.

A high-pressure piston dynamic seal (polymeric seal on sapphire piston) between the cylinder compression chamber and the magnets chamber was identified by project partner, Thar Energy, for the LMRC system design. A leak rate analysis was performed on the seal that focused on bounding the leak rate and ensuring the leak rate is sufficiently small relative to its impact on machine performance. The analysis

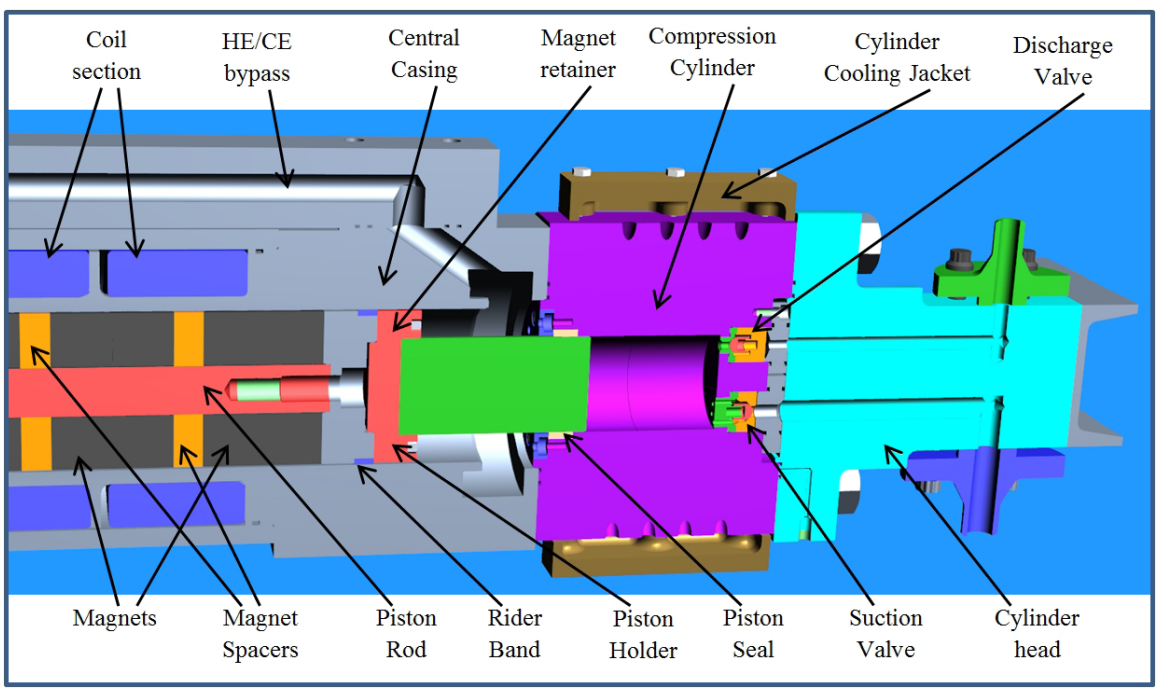

FIGURE 3. Cross-section of one identical end of the first stage LMRC

combined the static pressure load, assembly preload, and linear spring model to determine the likelihood of gap formation due to static loading only, and it was determined that the seals are adequate in terms of static-only conditions. Then dynamic loading was evaluated using the compressible Reynolds equation that governs fluid flow in thin films, and it was determined that the seal leak rate will be less than 0.4% of H_2 throughput per stage. In addition to the dynamic seal design, appropriate static seals were identified for the multiple areas of the LMRC where static sealing is necessary.

It was determined that no compressor valve manufacturers had existing valves or valve designs that could be used in the LMRC; therefore, valves are being designed. Utilizing a modified version of an internally developed valve design code and CFD modeling, initial valve designs conceptualized by ACI Services for each stage of compression are being optimized. First stage suction and discharge valves are designed, and second and third stage valve designs are in progress.

A pulsation analysis was performed to ensure that the inherent pulsating flow leaving the compressor does not cause any operational issues, such as high vibrations. Based on initial vessel sizing per API Standard 618 and a preliminary system layout as shown in Figure 4, SwRI utilized a proprietary acoustical simulation software, the Transient Analysis Pulsation Solver design tool (full Navier-Stokes solution in one-dimension which can be analyzed in the time or frequency domain), to perform the pulsation analysis for the LMRC piping system, and all pulsation amplitudes were predicted to be acceptable.

System inter-stage, first suction, and final discharge cooling requirements were identified, and cooler manufacturers were identified that could provide the necessary equipment. In addition to process gas cooling, the LMRC internal cooling was evaluated using a conjugate heat transfer analysis. Simulations were performed to predict steady-state temperatures and pressures, and system modifications were implemented to design the system such that each component will be maintained at acceptable temperature and pressure ranges during continuous operation.

The phenomenon of hydrogen embrittlement was one of the primary factors considered when determining the appropriate materials. Hydrogen embrittlement of high-strength NdFeB magnets is a severe problem if inadequate coatings are applied to the magnets. Appropriate system materials and coatings were identified based on the criteria of

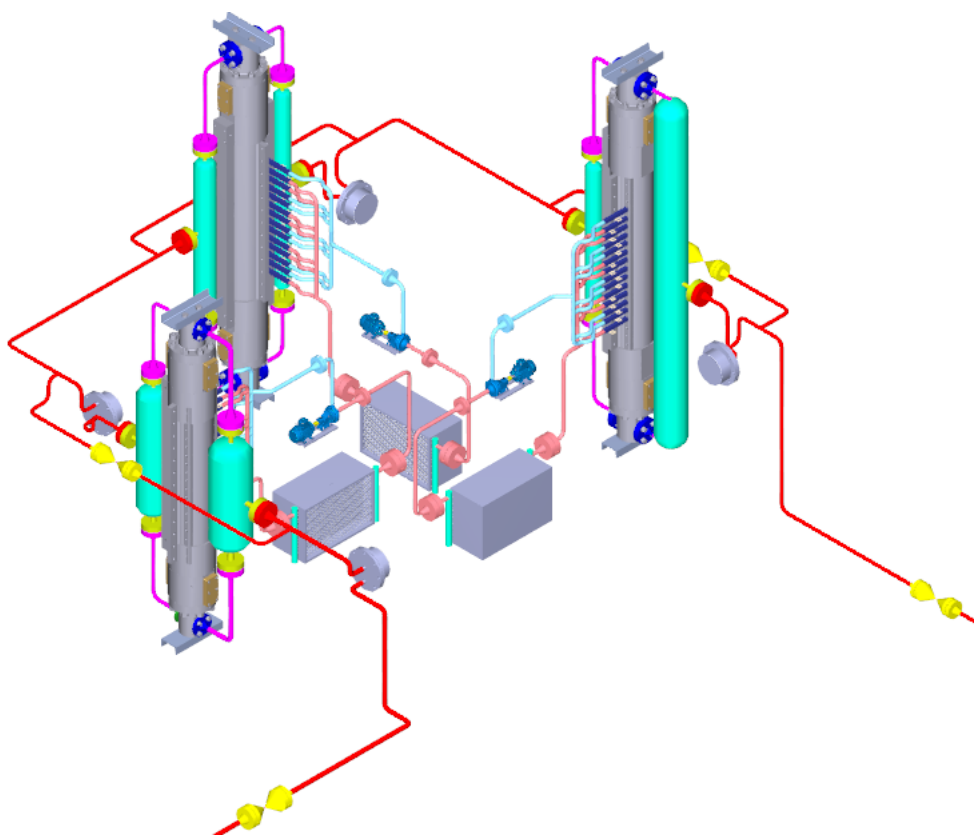

FIGURE 4. 3D model of LMRC piping system

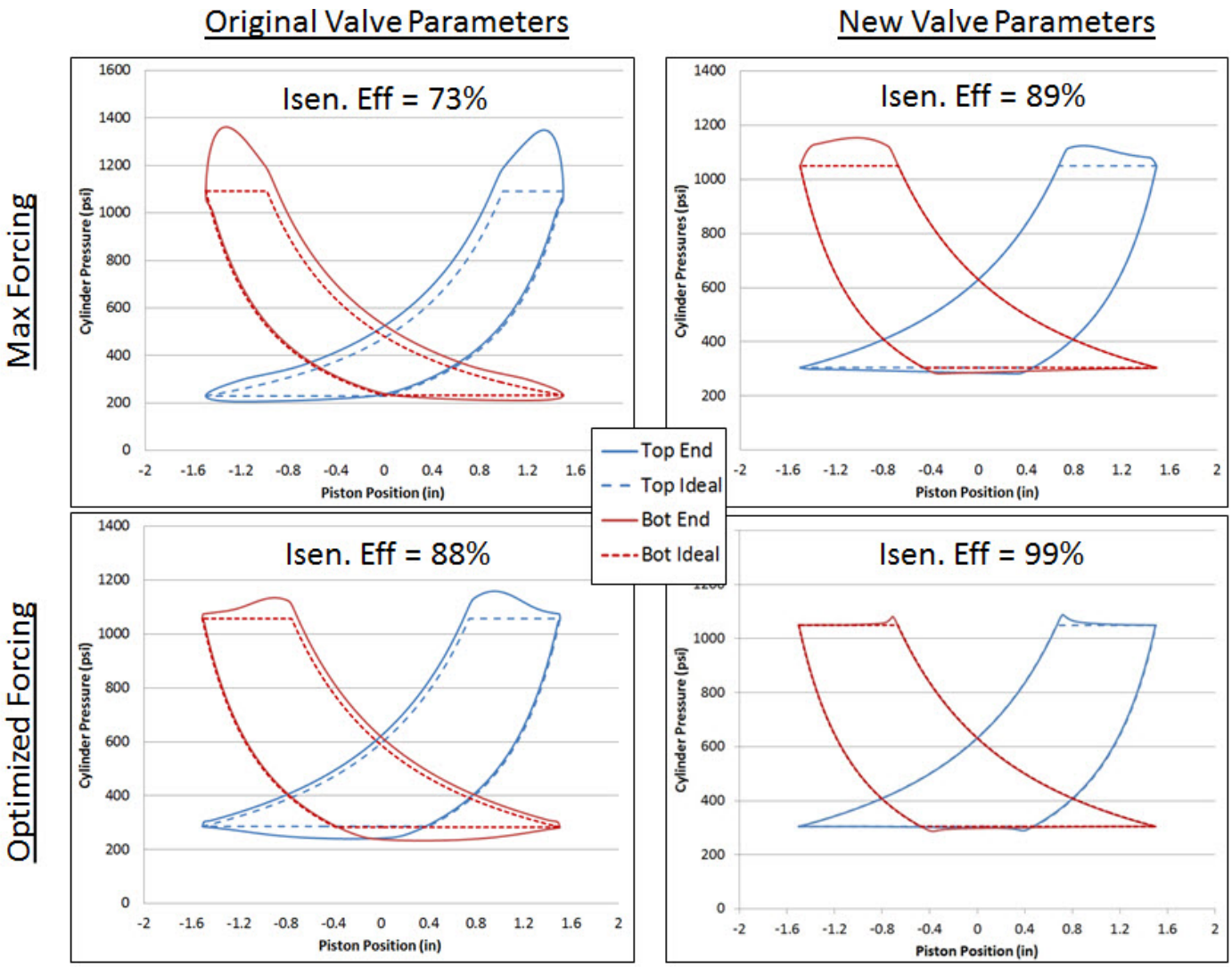

FIGURE 5. Predicted efficiencies

strength, hydrogen embrittlement characteristics, magnetic properties, coefficient of expansion, and young's modulus.

A system performance and controls model was developed to predict the compressor performance and to develop strategies for control of the compressor. This model was created as a software tool and incorporates the various compressor characteristics, such as the piston velocity and acceleration, valve losses, and magnet performance. The unique motion of the compressor emphasized the need for a unique performance prediction and controls simulation software package. Isentropic efficiency predictions indicate 99% efficiency for the first stage of compression after implementing an optimized control scheme. Predictions are depicted in Figure 5.

CONCLUSIONS AND FUTURE DIRECTIONS

Conclusions derived from the work conducted in FY 2015 are:

- Hydrogen embrittlement and powerful magnetic forces add a significant degree of difficulty to the design of a compressor system.
- The predicted leak rate of the selected dynamic seal is adequately low.
- Sufficient water cooling of the current-carrying coils, clearance volumes, bypass lines, optional recycle lines, and inter-stage gas cooling are predicted to maintain the LMRC system temperatures at acceptable levels.
- Valves and linear actuators that meet the criteria of the LMRC design are not readily available in industry; however, the project team is capable of designing and manufacturing sufficient components for the LMRC.

- It is predicted that highly efficient hydrogen compression is possible with an LMRC used for the compression process.

Future work in Project Year 2 (FY 2016) will include the following.

- Develop and check fabrication and manufacturing drawings; identify vendors and obtain quotes for the fabrication of the various components
- Estimate the cost of a full-scale version of the LMRC compressor based on supplier quotes for the bench-scale version; identify strategies to meet the capital and operating and maintenance targets in the MYRDD Plan for 2020
- Develop a test matrix for single-stage testing (low-pressure stage) and for testing the full compressor, design test fixtures and select instrumentation needed to test the compressor and measure the system performance, and develop a personnel and environmental safety plan for testing
- Fabricate and assemble the compressor and its supporting components
- Select and purchase hardware and fabricate the test stand
- Commission the test bench using nitrogen gas and following the plan previously defined.
- Complete testing of the LMRC system according to the defined test matrix with hydrogen
- Analyze the results from the single-stage (low-pressure stage) testing

FY 2015 PUBLICATIONS/PRESENTATIONS

1. Broerman, E., J. Bennett. "Hydrogen Compression Application of the Linear Motor Reciprocating Compressor (LMRC)," Joint Codes & Standards Tech Team (CSTT) and Hydrogen Delivery Tech Team (HDTT) Meeting, Sacramento, CA, January 21, 2015.

2. Broerman, E., J. Bennett, K. Brun, N. Shade, L. Chordia. "Designing a Linear Motor Recip Compressor to Achieve 12,700 psi Outlet Pressure," Abstract accepted and paper being reviewed by Gas Machinery Research Council (GMRC) for October 2015 GMC.

REFERENCES

1. U.S. Patent 8,534,058. Issued Sept. 17, 2013. "Energy Storage and Production Systems, Apparatus and Methods of Use Thereof," Patented in United States of America.

2. Deffenbaugh, D., et al., "Advanced Reciprocating Compression Technology," DOE Award No. DE-FC26-04NT42269, SwRI Contract No. 18.11052, December 2005.

III.8 Steel Concrete Composite Vessel for 875 Bar Stationary Hydrogen Storage

Zhili Feng (Primary Contact), Yanli Wang, and Yong Chae Lim
Oak Ridge National Laboratory (ORNL)
1 Bethel Valley Rd, PO Box 2008, MS 6095
Oak Ridge, TN 37831
Phone: (865) 576-3797
Email: fengz@ornl.gov

DOE Manager
Katie Randolph
Phone: (720) 356-1759
Email: Katie.Randolph@ee.doe.gov

Industry Partners and Subcontractors
- Air Liquide, Houston, TX
- AccerlorMittal, East Chicago, IN
- Bevilacqua Knight Inc., Sacramento, CA
- Global Engineering and Technology LLC, Camas, WA
- Hanson Pressure Pipe, Grand Prairie, TX
- LightSail, Berkeley, CA
- MegaStir Technologies LLC, Provo, UT
- POSCO, South Korea
- SustainX, Seabrook, NH
- Temple University, Philadelphia, PA
- WireTough Cylinders, Bristol, VA

Project Start Date: October 1, 2014
Project End Date: September 30, 2017

Overall Objectives

- Address the significant safety and cost challenges in high pressure stationary hydrogen storage system
- Develop and demonstrate the second generation (GEN II) steel/concrete composite vessel (SCCV) design and fabrication technology for stationary high pressure hydrogen storage at 875 bar
- Reduce the purchased capital cost of SCCV for forecourt hydrogen refueling station to \$800/kg H_2 at 875 bar in 2017 and meet all other DOE funding opportunity announcement (FOA) requirements including projected service life of at least 30 yr, scalability to 1,000 kg of storage, and versatility in meeting the scalability and footprint requirement of different forecourt hydrogen fueling stations

Fiscal Year (FY) 2015 Objectives

- Select three candidate high strength structural steels with 100–120 ksi yield strength suitable for the inner steel vessel
- Identify two alternative hydrogen permeation barrier materials; confirm at least one barrier material having no more than 10% notch strength reduction in 2,000 psi hydrogen and a hydrogen leak rate of less than 50 kg/yr (\$200/yr) for a reference 1,000 kg storage SCCV at 875 bar
- Identify alternative reinforcement technology with reduced cost over the reinforced concrete technology in first generation (GEN I) SCCV by 5%
- Identify options for SCCV design optimization for cost reduction with initial cost analysis

Technical Barriers

This project addresses the following technical barrier from the Hydrogen Delivery section in the Fuel Cell Technologies Office (FCTO) Multi-Year Research, Development, and Demonstration (MYRDD) Plan (updated August 2015):

(E) Gaseous Hydrogen Storage and Tube Trailer Delivery Costs

Technical Targets

This project aims at developing the ***second generation*** SCCV that will be more cost effective for forecourt hydrogen fueling station applications. Specific technical targets are as follows.

- Meet or exceed the cost targets (<\$1,000/kg H_2) stored at pressures of 875 bar or greater as specified in DOE DE-FOA-0000821 under which this project was awarded. Table 1 listed the FOA cost target and those from the most recent MYRDD plan (updated August 2015)
- Show compatibility of design materials with hydrogen and durability under pressure
- Meet all performance requirements included in the DOE FOA821 over a 30-year service life
- Construct and test a prototype system of sufficient size to adequately demonstrate the capability of the technology to be scaled to storage volumes of >1,000 kg H_2
- Scalability and footprint of the storage system for versatility in applications

TABLE 1. DOE MYRDD Technical Targets for Stationary Gaseous H_2 Storage Tanks, updated August 2015 (for Fueling Sites, Terminals, or Other Nontransport Storage Needs)

Pressure	DOE 2015 Status	GEN I SCCV (2015)	GEN II SCCV (2017)	DOE 2020 Target
Low Pressure (160 bar) Purchased Capital Cost ($/kg of H_2 stored)	$850	$681		$500
Moderate Pressure (430 bar) Purchased Capital Cost ($/kg of H_2 stored)	$1,100	$713		$600
High Pressure (875 bar) (FOA821) Purchased Capital Cost ($/kg of H_2 stored)	N/A	$957	$800	$1,000
High Pressure (925 bar) Purchased Capital Cost ($/kg of H_2 stored)	$2,000	N/A		$600

N/A – not applicable

FY 2015 Accomplishments

- Working with steelmaking partners (ArcelorMittal and POSCO), selected five candidate high strength structural steels with 100–120 ksi yield strength suitable for the inner steel vessel
- Identified and experimentally confirmed a new hydrogen permeation barrier material having 5.3% notch strength reduction in hydrogen and a leak rate of less than 1 kg/yr ($2/yr) for a reference 1,000 kg SCCV at 875 bar
- Identified two new wire wrapping technologies which would considerably simplify the vessel reinforcement construction with estimated cost reduction by more than 5% over the GEN I SCCV
- Through initial design optimization, identified a number of reference design options with estimated cost that is potentially below the targeted $800/kg H_2 using the same materials as in the GEN I SCCV mockup, and potentially below $600 (the 2020 target) using higher strength steels investigated in this project

✧ ✧ ✧ ✧ ✧

INTRODUCTION

In a previous DOE FCTO project, a novel SCCV technology, referred to as GEN I SCCV in this report, has been specifically developed and demonstrated for stationary high pressure gaseous hydrogen storage applications. The newly developed SCCV technology comprises four major innovations: (1) flexible and scalable modular design for different storage pressure and capacity needs, for cost optimization, and for system reliability and safety; (2) composite storage vessel design and construction with an inner steel vessel encased in a prestressed outer reinforcement; (3) the use of a hydrogen permeation barrier in a layered vessel structure and vent holes to solve the hydrogen embrittlement (HE) problem *by design*; and (4) integrated sensor system to monitor the structural integrity and operation status of the storage system. Together, these innovations form an integrated approach to make the SCCV cost competitive and inherently safe for stationary high pressure hydrogen storage services. The SCCV solved the two critical limitations and challenges of today's high pressure hydrogen storage vessels, the high capital cost and the safety concerns of HE of high strength steel vessels. The SCCV can be designed and constructed using mature and proven fabrication technologies acceptable by pertinent codes/standards. Therefore, while the concept of SCCV is new, SCCV technology as a whole is relatively mature. The SCCV technology is expected to be commercialized for hydrogen fueling station applications in 2–4 yr.

This project aims at developing GEN II SCCV that will be even more cost effective for forecourt hydrogen fueling station applications. An exceptionally strong team has been assembled that is best suited for R&D and commercialization of the GEN II SCCV. The technical expertise and research capabilities of the team are "vertically integrated" to cover all aspects of the SCCV technology development, from forecourt hydrogen station requirements, material selecting and development, high-pressure vessel design, engineering and construction, materials joining, high pressure hydrogen testing, cost modeling, as well as application specific knowledge required for the proposed work.

APPROACH

A systematic approach is employed to refine and optimize all major aspects of SCCV technology (design, engineering, materials and fabrication) to achieve the proposed GEN II SCCV cost target. A representative prototype mockup, capturing all major features of SCCV technology, will be fabricated and tested for hydrogen service at 875 bar to demonstrate the technical viability and cost effectiveness of the GEN II SCCV technology for forecourt high pressure hydrogen storage. R&D in this project will effectively utilize the knowledge obtained in developing the GEN I SCCV, including the identification of a number of R&D areas with potentials for considerable further cost reduction. Potential cost reduction estimates for the different areas are summarized in Table 2. These areas are briefly described below.

- Cost reduction by materials: High-pressure hydrogen vessels have in the past avoided the use of ultra-high-strength steels due to HE concerns. Our innovative layered vessel design minimizes vessel exposure to hydrogen, thereby eliminating the potential for HE.

Ultra-high-strength steels can therefore be used in the vessel. Increase in strength reduces the vessel wall thickness and the associated fabrication cost.

- Cost reduction by vessel design optimization: We will apply the cost analysis methodology developed previously to further optimize the SCCV design for cost reduction. Options to be investigated include (a) optimizing the shape and dimension of the SCCV, (b) replacing the stainless steel (SS) inner liner with low cost materials as hydrogen permeation barrier, and (c) optimizing the prestress level of the vessel. The design optimization will consider the limits and constraints of today's manufacturing technologies and availability of materials.
- Fabrication and sensor technologies: The following options will be investigated: (a) remote non-contact vessel inspection and remote repair welding technologies, (b) application of friction stir welding, and (c) new wire wrapping technologies for pre-stressing.

TABLE 2. Focused R&D Areas with Potentially Significant Cost Reductions (Reference Cost: DOE FOA Target $1,000 kg H_2 at 875 bar)

R&D Areas	Estimated Cost Reduction
Cost effective hydrogen permeation barrier	5%
Use of ultra-high-strength steels	15%
Cost effective prestressing technologies	5%
Friction stir welding scale up	10%
Novel sensor technologies	10%
Overall SCCV design optimization	15%
Total	60%

RESULTS

R&D in FY 2015 focused the following major milestones according to the project R&D plan.

Selection of Candidate Ultra-High-Strength Structural Steels

In the past, high pressure hydrogen vessels have avoided the use of ultra-high-strength steels due to HE concerns. The layered vessel design in SCCV eliminates HE by design. It therefore offers the opportunity to use ultra-high-strength steels for cost reduction through reduced wall thickness and the associated fabrication cost. This is an aspect that was unexplored in GEN I SCCV; steels used in the GEN I SCCV mockup were based on American Society of Mechanical Engineers (ASME) Boiler and Vessel Pressure Code (BVPC) approved steels for hydrogen services.

In this project, steels with yield strength level between 100 ksi and 120 ksi (690–830 MPa) were targeted. This represented an increase in strength of 35–60% over the SA-724B steel in GEN I SCCV.

We worked with our steelmaking team members (ArcelorMittal and POSCO, two largest steel producers in the world) to identify and select potentially qualified candidate steels. The selection of candidate steels was based on the consideration of their commercial viability (i.e., can be produced in commercial quantity), availability to the project, and meeting the cost reduction target of 15–30% from the current SCCV reference design through reduced wall thickness and the associated fabrication cost. Five candidate steels have been identified (Table 3). These steels will be down-selected based on further evaluation including weldability and weld properties of the steels, as planned.

TABLE 3. Mechanical Properties for Candidate Ultra-High-Strength Steels

	Candidate Steel A	Candidate Steel B	Candidate Steel C	Candidate Steel D	Candidate Steel E
σ_{ys}	100	120	Min. 100	101 ksi	127.6 ksi
σ_{ts}	100–130	--	Min. 115	113 ksi	142 ksi
Elongation	18%	--	16%	14%	<8%

Identification of Alternative Hydrogen Permeation Barrier Materials

GEN I SCCV design utilizes an austenitic SS liner to prevent hydrogen entering the subsequent high strength steel layers. However, austenitic SS is expensive. Cladding SS onto the layered steel vessel is also labor intensive and costly. The material and fabrication cost of the SS contribute to more than 10% of the total cost of the inner steel vessel for our reference GEN I SCCV design. For GEN II SCCV, low cost alternative materials were investigated as hydrogen permeation barrier.

The identification of hydrogen permeation barrier materials included extensive literature surveys of hydrogen permeability, diffusivity, and solubility for various potential materials. The leakage rate of each potential material was assessed based on the Fick's law for diffusion and the Sievert's law of hydrogen solubility as function of hydrogen pressure.

The leakage rate can be calculated following as:

$$Q = J \bullet A \bullet t$$

where Q is the leakage rate ($\frac{\text{kg}}{\text{year}}$), J the steady state flux of diffusion of hydrogen, A the surface area of pressure vessel, and t the time. In our analysis, a reference vessel containing 1,150 kg H_2 at 875 bar was assumed as shown in Figure 1. This reference vessel had a surface area of 65 m^2. The thickness of the hydrogen permeation barrier was assumed to be 6 mm. Hydrogen pressure of 875 bar was applied on one side of the hydrogen barrier layer, and 1 bar

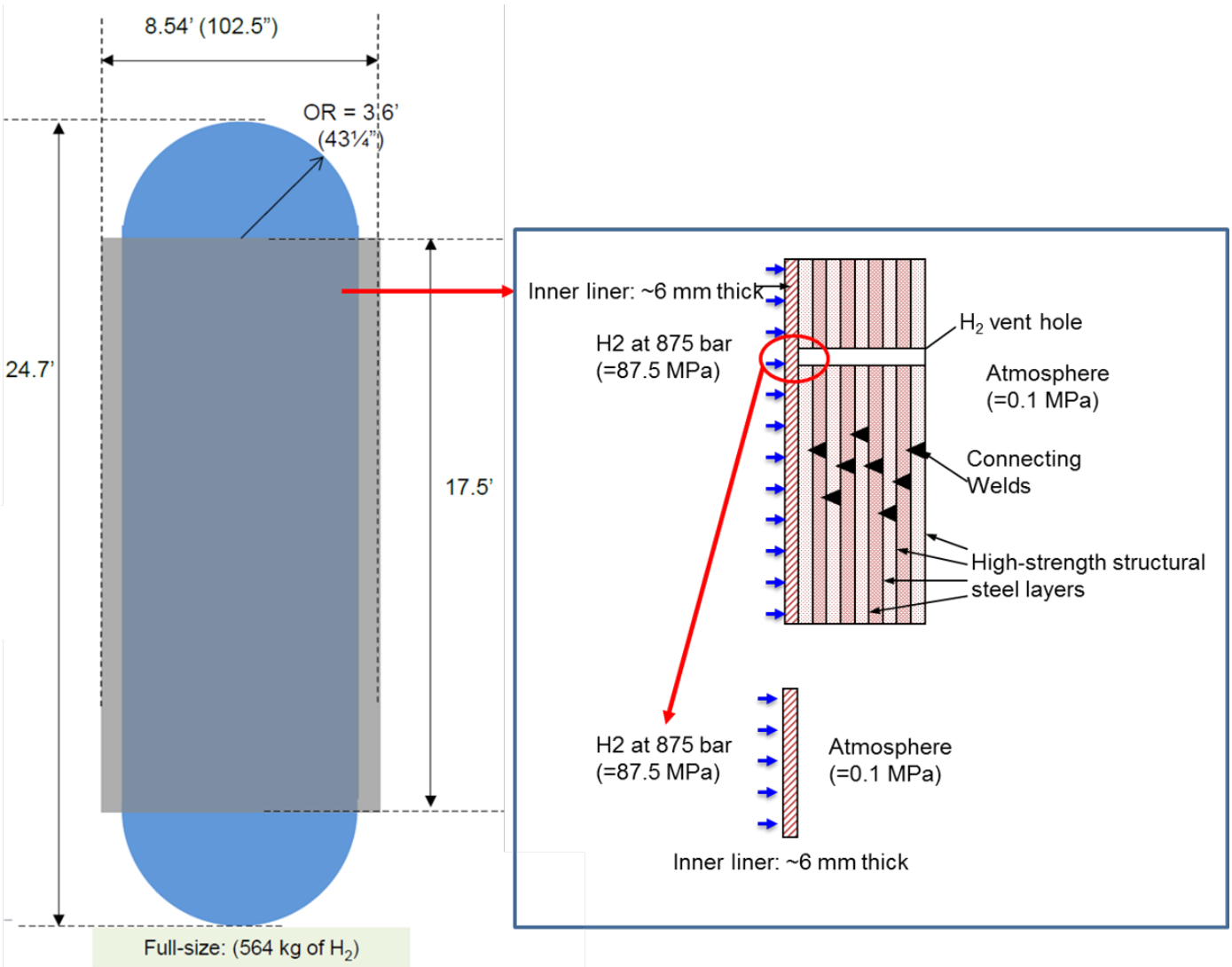

FIGURE 1. Schematics of the reference vessel containing 1,150 kg of H_2 at 875 bar for hydrogen permeation leak rate estimate. The dimensions are in feet.

was applied on the other side due to the presence of the vent holes.

The above leak rate analysis led to the identification of one low cost material with a leakage rate of 0.1–0.3 kg/yr, well below the target 50 kg/yr leak rate. (For reference, the stainless steel barrier has a leakage rate of approximately 1×10^{-5} kg/yr). The permeability of this material was experimentally measured at a test temperature up to 150°C. Calculations using the actual measurement data confirmed the above estimated leak rate. The newly identified material costs only a fraction of that of the stainless steel. Its use would also significantly reduce the fabrication cost compared to the current cladding process of stainless steel.

The low cost material identified above was also subjected to HE test. Notch tensile test in hydrogen at 2,000 psi confirmed that the material had an average of 5.3% reduction in notch tensile strength, suggesting excellent compatibility with hydrogen.

Two more materials are also identified as hydrogen permeation barrier. They are under further evaluation.

Design Optimization for Cost Reduction

A primary objective in this project is to develop a set of standard reference designs of different capacities that would meet the DOE cost target for refueling station. These reference designs would be systematically optimized for cost in this project. Such reference designs are intended for high volume off-the-shelf production with today's manufacturing capability of the project partners. It would minimize the capital investment and engineering cost by the manufacturers, which also eases the technology transfer and commercialization.

We have completed the initial, Level I, GEN II SCCV design optimization on five reference capacities (100, 200, 500 and 1,000 kg H_2 at 875 bar). As shown in Tables 4 and 5, this initial Level I design optimization suggested the possibility of meeting the \$800/kg H_2 cost target with steels available in the ASME BPVC. With the use of ultra-high-strength steels that are commercially available but not yet accepted by code, it is possible to reduce the cost of the vessel to a level of \$500/kg H_2.

The above initial GEN II SCCV designs will be used to guide the design optimization R&D in FY 2016. The designs and cost analysis will be further refined in FY 2016, with more detailed cost breakdown analysis for selected potentially low cost designs. Manufacturing capability constraints and fueling station requirements will need to be incorporated in the FY 2016 design optimization. It is expected that the final cost figures of the optimized designs would be different from the initial analysis performed in FY 2015.

TABLE 4. Initial Level I SCCV Design Optimization with Code Accepted Steels

(\$/kg H_2)	Tank capacity (kg)			
L/D ratio	**100**	**200**	**500**	**1,000**
1.67	982	959	945	936
5	816	801	765	745
10	756	747	715	697
40	750	762	674	670

L/D – Length to diameter ratio

TABLE 5. Initial Level I SCCV Design Optimization Using Ultra-High-Strength Steels with ASME BPVC Design Allowable of 50 ksi

	Tank capacity (\$/kg H_2)			
Aspect ratio	**100**	**200**	**500**	**1,000**
1.67	667	651	637	630
5	551	542	540	539
10	560	510	518	500
40	507	527	509	501

CONCLUSIONS AND FUTURE DIRECTIONS

The project so far has achieved all the major milestones planned for FY 2015.

- Identified five candidate high strength structural steels with 100–120 ksi yield strength suitable for the inner steel vessel
- Identified and experimentally confirmed a new hydrogen permeation barrier material that has estimated leak rate of less than 1 kg/yr (\$2/yr) for a reference 1,000 kg SCCV at 875 bar
- Identified two new wire wrapping technologies that may considerably simplify the vessel reinforcement construction
- Through initial design optimization, identified a number of reference design options with estimated cost that is potentially below the targeted \$800/kg H_2 using the same materials as in the GEN I SCCV mockup, and potentially below \$600 (the 2020 target) using higher strength steels investigated in this project

Future planned activities for FY 2016:

- Complete weldability evaluation and weld property testing of the new candidate high strength steels and down-select for inner steel vessel design and fabrication
- Complete the development of improved reinforcement technologies
- Complete the reference engineering and fabrication design of the reference designs that are optimized to meet the cost target
- Develop and demonstrate the remote sensor technology for vessel health monitoring and inspection

III.9 Low Cost Hydrogen Storage at 875 Bar Using Steel Liner and Steel Wire Wrap

Amit Prakash (Primary Contact) and Ashok Saxena
Wiretough Cylinders, LLC
14570 Industrial Park Rd., Suite C
Bristol, VA 24202
Phone: (276) 644-9120
Email: aprakash@wiretough.com; asaxena@wiretough.com

DOE Manager
Katie Randolph
Phone: (720) 356-1759
Email: Katie.Randolph@ee.doe.gov

Contract Number: DE-EE0006668

Subcontractors:
- Oak Ridge National Laboratory, Oak Ridge, TN
- N & R Engineering, Parma Heights, OH
- C P Industries, McKeesport, PA
- Ashok Saxena, Consultant, Fayetteville, AR
- Pressure Science Inc., Dallas, TX

Project Start Date: September 15, 2014
Project End Date: June 14, 2017

Overall Objectives

The goal of this project is to develop a pressure vessel to safely store hydrogen at 875 bar with a safety factor of 3 or higher that also meets the DOE storage tank cost target of <$1,000/kg hydrogen ($H_2$). The objectives are:

- To wire wrap a standard American Society of Mechanical Engineers (ASME) approved, 406-mm diameter and 9.14-m long cylinder with a capacity of 765 liters rated at a pressure of 460 bar to boost its pressure capacity to 875 bar while maintaining a safety factor of 3 on the burst pressure.
- To keep the cost of producing the storage tanks to less than $1,000/kg of stored H_2, maintain a design life of 30 years, and deliver hydrogen that meets the SAE J2719 hydrogen purity requirements.

Fiscal Year (FY) 2015 Objectives

- Develop an elastic-plastic finite element analysis model for analyzing stresses in wire wrapped high pressure storage tanks and evaluate/optimize design alternatives
- Procure 1,900-mm long and 408-mm diameter steel liners, wire wrap them, and demonstrate that the burst pressure exceeds three times the operating pressure of 875 bar
- Develop a fracture mechanics model to analyze the effects of high pressure H_2 on vessel properties to support ASME code analyses
- Initiate work on obtaining ASME code approval
- Develop specifications for a machine capable of wire wrapping full length (9.14-m long) steel liners

Technical Barriers

This project addresses the following technical barriers from the Hydrogen Delivery section of the Fuel Cell Technologies Office (FCTO) Multi-Year Research, Development, and Demonstration Plan:

(E) Gaseous Hydrogen Storage and Tube Trailer Delivery Costs

Technical Targets

This project's goals are to meet the 2020 targets for high-pressure hydrogen storage in the 2012 version of FCTO's Multi-Year Research, Development, and Demonstration Plan, as shown in Table 1.

TABLE 1. Wiretough's Progress towards Meeting Technical Targets for High Pressure H2 Ground Storage Systems

Characteristics	2020 Target	Wiretough
High Pressure (860 bar) Purchased Capital Cost ($/kg of H_2 stored)	1,000	On target to meet in 2017

FY 2015 Accomplishments

- Developed and validated an elastic-plastic finite element model for optimizing wire-wrapped pressure vessel design and evaluating design alternatives
- Modified the wire winding machines to accommodate 408-mm diameter liners with nominal wall thickness of 31.5 mm
- Procured four 1.9-m long metal liners and completed wire winding on two cylinders and burst testing on one cylinder
  - Second cylinder is currently being prepped for burst testing
  - Third liner is being used for material testing, and another is being used to optimize reinforcements in the transition regions between the cylinder body and the domes on the two ends

- Initiated ASME code approvals for wire-wrapped cylinders
- Completed literature review to assess susceptibility of SA 372 Class J steel liner to hydrogen assisted fatigue crack growth
- Developed a fracture mechanics model to assess integrity of high pressure (90 MPa) hydrogen storage vessel under cyclic loading

✧ ✧ ✧ ✧ ✧

INTRODUCTION

The DOE Fuel Cell Technologies Office within the Office of Energy Efficiency and Renewable Energy is supporting research and development (R&D) activities leading to the development of low cost, high pressure hydrogen storage systems for use in hydrogen refueling stations (forecourt). The goal of this project is to develop a pressure vessel to safely store 750 liters of gaseous hydrogen at 875 bar with a safety factor of 3 or higher that also meets the DOE storage tank cost target of <$1,000/kg H_2.

APPROACH

Type I metal cylinders (406-mm outer diameter) have been used for compressed natural gas (CNG) and hydrogen storage for several decades but are limited to pressures of 55 MPa for various technical reasons. Wiretough has a patent pending process to wrap these commercially available cylinders with ultra-high-strength steel wires (3 GPa in strength) to double the pressure capability of the cylinders, with a proven record of safely storing H_2. These wire-wrapped cylinders are further subjected to an autofrettage process in which they are subjected to pressures high enough to plastically deform the inner liner, but the wire jacket remains elastic. Upon release of the autofrettage pressure, the inner liner is left with high residual compressive hoop stresses. This process decreases the maximum tensile hoop stress in the liner under the operating pressure and can thus enhance the fatigue life of the vessel very significantly. In this project, this concept will first be demonstrated using short, 1.9-m long cylinders and then extended to 9.14-m long cylinders.

RESULTS

Four 1.9-m long (short) metal liners with outside diameter of 406 mm (16 in) and a nominal wall thickness of 31.75 mm (1.25 in) made from ASTM SA 372 Grade J Class 70 steel were produced by CP Industries and shipped to Wiretough's Bristol, VA, facility for wire wrapping, burst testing, and for characterizing material properties such as fatigue crack growth behavior in an H_2 environment. One of the metal liners was wrapped successfully and sent to Authorized Testing Inc., an independent test facility in Riverside, CA, for hydrostatic burst testing. Authorized Testing completed the test in which the internal pressure was raised to 262.7 MPa (38,100 psi) without any signs of failure; thus, the design met the factor of safety of 3 requirement on the burst pressure. Subsequent to pressure testing, a detailed destructive examination of the tested vessel was conducted, and no evidence of cracking was found (see Figure 1).

Finite element studies to support cylinder design, including establishing parameters such as autofrettage pressure, pre-tension in the wire during wrapping, and the optimum number of layers of wrapping, were successfully conducted to finalize those design details. Figure 2 shows the finite element model used in the analysis, the material properties used for the liner, and the wires. The figure also shows a table with the radial and hoop stresses predicted in the wall and the head regions of the liner at a pressure of 262 MPa (38,000 psi) and after release of the pressure. These results clearly show the high compressive hoop stresses locked in the liner wall after the pressure is released. The corresponding values of strains were compared with measured strains during the destructive testing of the tested cylinder, and very good agreement was found between the predicted and measured values of strains, validating the finite element model.

FIGURE 1. The condition of the liner after an attempted burst test during which the pressure was raised to 262.7 MPa (38,100 psi). Subsequently, the wires were cut to expose the surface of the cylinder. No visible sign of damage/cracking is seen anywhere on the liner walls.

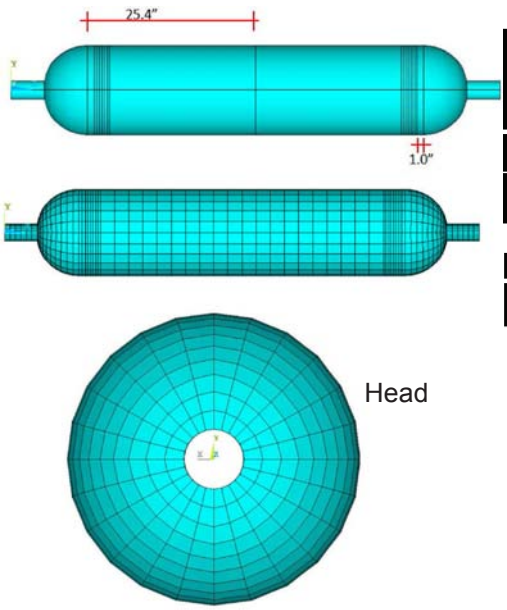

Stresses at a pressure of 38,000 psi

	Radial stress, (psi)	Hoop stress (psi)	Axial stress, (psi)	von Mises, (psi)
Head	28,075	111,590	87,361	113,510
Cylinder	2,214	127,760	62,050	112,600

Residual stresses after the pressure is released

Head	-899	-14,110	-2,238	13,163
Cylinder	-1,070	-61,752	-17,562	56,142

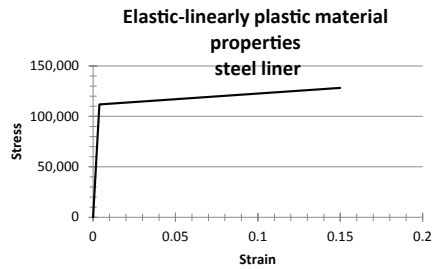

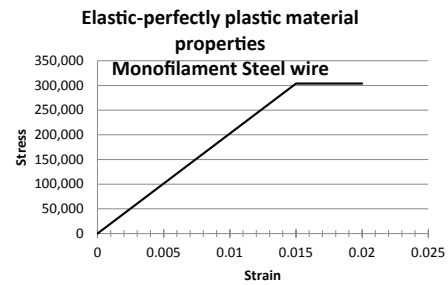

FIGURE 2. Finite element model for the cylinder body and the end caps also showing the material deformation model for the liner and the wires. The table in the figure presents values of hoop and radial stresses in the main liner body and dome in the hoop and radial directions at pressure and after the pressure has been removed.

A detailed literature survey was conducted to document the FCGR behavior and environment assisted crack growth behavior of SA 372 Grade J Class 70 steels in high pressure (100 MPa) hydrogen environment. This work has been conducted primarily at Sandia National Laboratories in the research group of Dr. Brian Somerday [1]. Figure 3a shows the fatigue crack growth behavior of SA 372 Grade J class 70 steel at a frequency of 1 Hz and a load ratio of 0.5 in 100 MPa hydrogen as compared to the behavior of similar steels in less demanding and innocuous environments. These results clearly demonstrate that high pressure hydrogen considerably accelerates the FCGRs (up to factor of 100) in these steels, so this degradation mechanism must be considered in the design of cylinders for H_2 storage. At stress intensity parameter values of less than 10 MPa(m)$^{1/2}$, it is observed that the effects of environment are not as significant. This provides guidance for the allowable design stress and inspection crack sizes.

The effects of high pressure hydrogen and load ratios on the FCGR behavior of SA 372 Grade J Class 70 steels at a frequency of 0.1 Hz were investigated [2] and are reported in Figure 3b. The average trend observed for a frequency of 1 Hz at R = 0.5 from Figure 3a was compared to the data at a frequency of 0.1 Hz in Figure 3b and was not found to differ significantly. The effect of frequency is thus minimal, as seen in the figure. Since ASME article KD-10 requires data to be generated at 0.1 Hz, the above result is significant for choosing conditions for generating additional data.

The load ratio, R, is an important variable in determining FCGR behavior, as demonstrated in Figure 3b. FCGRs are higher for R = 0.5 than for R = 0.2. For pressure vessels such as Wiretough's design that are subjected to autofrettage, the minimum stress will be compressive during a loading cycle. Thus, FCGR data are needed for R = -1.0 to -0.5 for estimating crack growth rates. Wiretough has placed a subcontract with a test laboratory very experienced in testing under hydrogen environment to characterize the effects of negative load ratios on the fatigue crack growth behavior in H_2 environment.

Figure 4 shows the environment-assisted crack growth rate data under high pressure hydrogen for SA 372 Grade J Class 70 steels [3]. The open symbols are from crack arrest tests in which the cracks are exposed to values of stress intensity parameter (K) that are higher than the threshold K under fixed displacement conditions, and then the K values corresponding to arrest are measured. These values are designated as $K_{th.a}$ and are about 65 MPa(m)$^{1/2}$ for these materials. The rising load tests yield lower threshold values of about 45 MPa(m)$^{1/2}$ for the same materials. The latter is more conservative and should be used as the maximum allowable K for this application. A fracture mechanics model has been developed to account for all these considerations in predicting the design life of the vessel.

Other progress includes preparing the specifications for a wire winding machine capable of wrapping 9.14-m long liners. This is now complete, and vendors are being identified

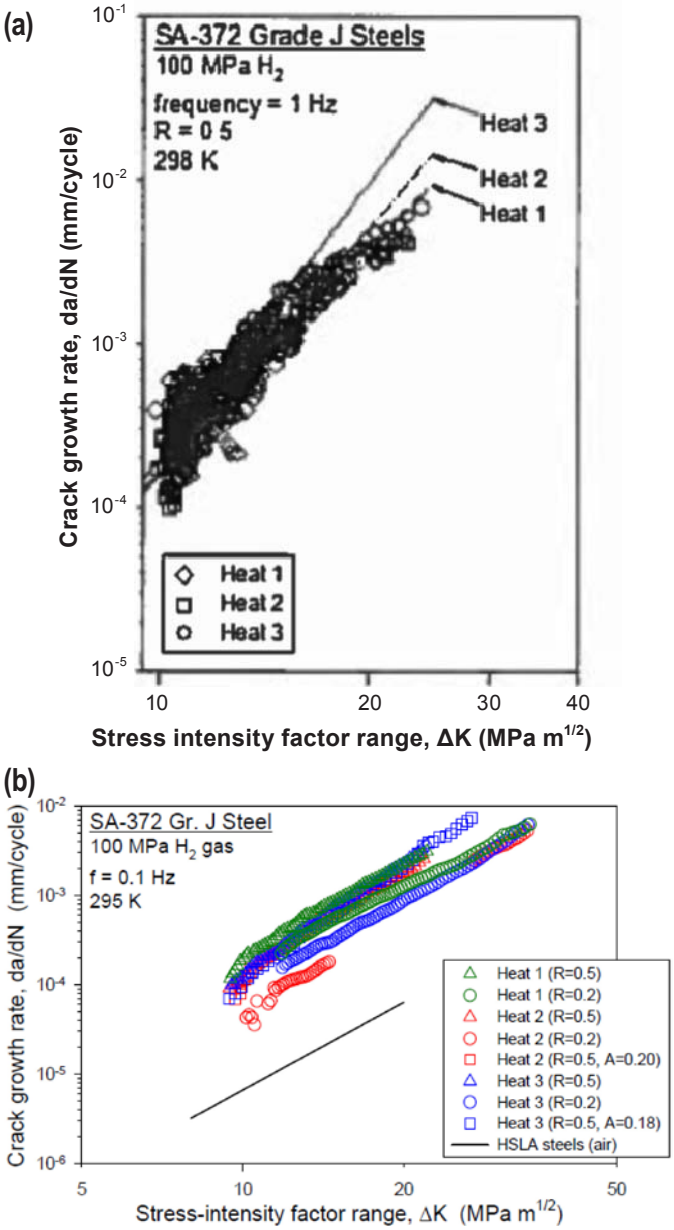

FIGURE 3. (a) FCGR behavior of SA 372 Grade J Class 70 steel under high pressure hydrogen (100 MPa) compared to the FCGR behavior of comparable steels under innocuous environments or lower hydrogen pressure (52 MPa) [1]. (b) FCGR behavior of A 372 Grade J Class 70 steels at a frequency of 0.1 Hz [2].

to produce and deliver the machine. The application for ASME code approval was also initiated.

CONCLUSIONS AND FUTURE DIRECTIONS

- The results produced during FY 2015 on this project appear promising for meeting the targets set by DOE as scheduled. All major milestones for Budget Period 1 are on target.

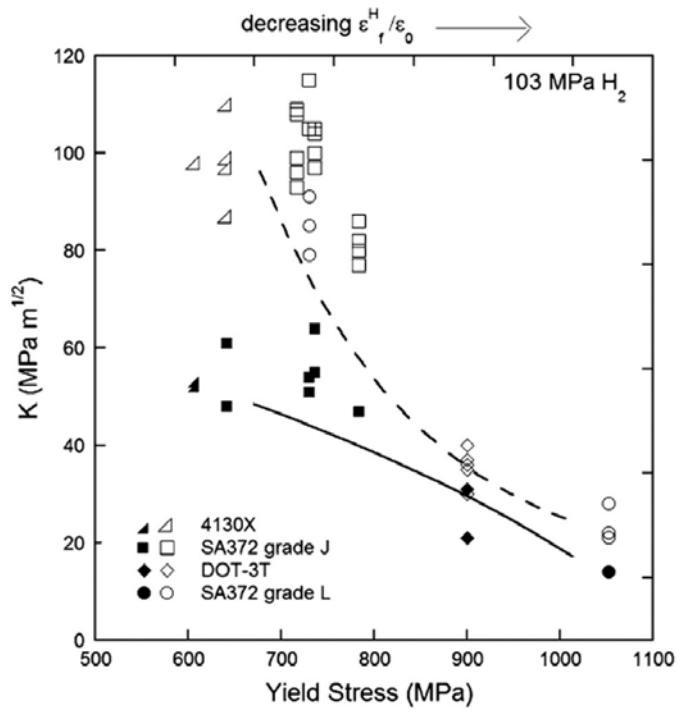

FIGURE 4. Effect of yield strength on the threshold value of K for environment assisted cracking in SA 372 Grade J Class 70 steels. Open symbols are from crack arrest tests, and the filled symbols are from rising load tests [3]. Since the rising load tests give lower values of threshold, those results are used in fracture mechanics calculations of fatigue crack growth life.

- There is a need to investigate the effects of hydrogen on FCGRs at negative load ratios to meet ASME requirements. This work, which will require six months for completion, was initiated in July of 2015.
- From the fracture mechanics model calculations it was determined that the nondestructive evaluations (NDEs) of the liners currently conducted by the suppliers are insufficient for high pressure H_2 storage tanks using thick wall liners. New NDE standards for this application are needed for ASME certifications of the design.
- The ASME code case application for non-hydrogen use of wire-wrapped cylinders of up to 750 liter capacity for pressure range up to 875 bar has been filed. The plan is to add storage of hydrogen to the application once the remaining crack growth data and inspection techniques are available.

SPECIAL RECOGNITIONS & AWARDS/ PATENTS ISSUED

1. Wiretough Cylinders, LLC was awarded a $2M grant over a two-year period beginning in mid-May of 2015 by the Tobacco Commission of the Commonwealth of Virginia to further develop technology for commercializing wire-wrapped ground storage tanks for CNG and H_2 storage applications.

FY 2015 PUBLICATIONS/PRESENTATIONS

1. A. Prakash and A. Saxena, "Light-weight Type II CNG Tank," DOE Project Kick-off Meeting, Oak Ridge National Laboratory, Oak Ridge, TN, August 13, 2014.

2. A. Prakash and W.H. Thomson, "Low Cost Hydrogen Storage at 875 Bar Using Steel Liner and Steel Wire Wrap," Hydrogen Delivery Tech Team Meeting, Southfield, Michigan, March 18, 2015.

3. A. Prakash and A. Saxena, "Low Cost Hydrogen Storage at 875 Bar Using Steel Liner and Steel Wire Wrap," DOE Annual Merit Review, Washington, DC, June 8–12, 2015.

REFERENCES

1. B.P. Somerday, K.A. Nibur, C. San Marchi, "Measurement of Fatigue Crack Growth Rates for Steels in Hydrogen Containment Components," Unpublished data reproduced with permission.

2. B.P. Somerday, C. San Marchi, Kevin Nibur, "Measurement of Fatigue Crack Growth Rates for SA372-Gr J Steel in 100 MPa Hydrogen Gas Following Article KD-10," Proceedings of the ASME 2013 Pressure Vessels and Piping Conference, PVP 2013, July 14–18, 2013, Paris, France. Reproduced with permission.

3. K.A. Nibur, B.P. Somerday, C. San Marchi, J.W. Foulk, M. Dadafarnia, P. Sofronis, Met Trans., Vol. 44A, 2013, pp. 248–269; reproduced with permission.

III.10 Electrochemical Hydrogen Compressor

Ludwig Lipp (Primary Contact), Pinakin Patel
FuelCell Energy, Inc. (FCE)
3 Great Pasture Road
Danbury, CT 06813
Phone: (203) 205-2492
Email: llipp@fce.com

DOE Manager
Erika Sutherland
Phone: (202) 586-3152
Email: Erika.Sutherland@ee.doe.gov

Contract Number: DE-EE0003727

Subcontractor
Sustainable Innovations, LLC, Glastonbury, CT

Start Date: July 15, 2010
End Date: July 14, 2015

Overall Objectives

- Demonstrate capability of electrochemical hydrogen compression (EHC) technology to meet the DOE targets for small compressors for refueling sites
- Quantify EHC cell performance and durability
- Reduce capital cost to demonstrate potential to meet DOE cost targets for hydrogen compression, storage and delivery

Fiscal Year (FY) 2015 Objectives

- Scale up the EHC stack height to increase hydrogen capacity
- Demonstrate taller stack performance stability at 3,000 psi for 1,000 hours
- Demonstrate long-term durability of EHC cells

Technical Barriers

This project addresses the following technical barrier from the Hydrogen Delivery section (3.2) of the Fuel Cell Technologies Office Multi-Year Research, Development and Demonstration Plan:

(B) Reliability and Costs of Gaseous Hydrogen Compression

Technical Targets

Technical targets for EHC are presented in Table 1.

TABLE 1. Progress Made Towards Meeting Technical Targets for Small Compressors for Fueling Sites [1]

Characteristic	Units	DOE 2015 Target	FCE Status
Reliability	-	Improved	20,000 h[§&]
Compressor Efficiency (Isentropic)	%	73%	75%[§#]
Losses (% of H_2 throughput)	%	0.5	1[§#]
Uninstalled Capital Cost	$	400,000	300,000 Projected for EHC Stack
Outlet Pressure Capability	bar	860	Up to 880*^
Contamination	-	Varies by Design	None

[§]For compression from 3 to 208 bar; ^3 bar inlet pressure; [&]0.1 kg H_2/d; [#]0.3 kg H_2/d; *<0.01 kg H_2/d

FY 2015 Accomplishments

- EHC Stack Scale-up: Scaled up stack height in 81 cm^2 design from five to 30 cells (Figure 1)
- EHC Cell Reproducibility: Reduced cell-to-cell variability by >70% in the past year (>90% in the program) (Figure 2)
- EHC Stack Pressure Capability: Increased stack hydrogen product pressure by 50% from 3,000 to 4,500 psi
- Stack Durability: Validated 4,500 psi product pressure in 30-cell stack for >1,500 hours, exceeding the program target by >50% (Figure 3)
- Cell Durability: Demonstrated 20,000 hours operation in larger area 185 cm^2 cell at >95% hydrogen recovery (Figure 4)

✧ ✧ ✧ ✧ ✧

INTRODUCTION

With the depletion of fossil fuel reserves and a global requirement for the development of a sustainable economy, hydrogen-based energy is becoming increasingly important. Production, purification and compression of hydrogen represent key technical challenges for the widespread commercialization of hydrogen fuel cell technologies. In the transportation sector, on-board storage of pure hydrogen is required at pressures up to 10,000 psi and compression of the hydrogen fuel up to 12,700 psi.

The level of maturity of current hydrogen compressor technology is not adequate to meet projected infrastructure demands. Existing compressors are inefficient and have

many moving parts, resulting in significant component wear and therefore excessive maintenance. New technologies that achieve higher operational efficiencies, are low in cost, safe and easy to operate are therefore required. This project addresses high-pressure hydrogen needs by developing a solid-state electrochemical hydrogen compressor.

APPROACH

The approach to address the program goals consists of the following major elements:

- Increase stack performance by improving reproducibility of cell performance during pressurized operation
- Reduce capital cost by increasing the hydrogen flux
- Reduce operating cost by improving membrane and electrode design
- Increase compressor capacity by increasing cell active area and stack height

To this end, the approach includes the design, fabrication and evaluation of improved cell architecture, and the development and demonstration of critical sealing technology to contain the high-pressure hydrogen within the EHC.

RESULTS

A major activity this year was to increase the EHC stack height to demonstrate the suitability of the architecture for building taller stacks with increased hydrogen flux. The 81 cm^2 cell design was improved to increase the manufacturing yields of key components and to reduce their cost. In addition, altered fabrication methods and procedures enabled fabrication of cell components with improved tolerances. New assembly equipment was put in place to enable stacking more than five to ten cells. New tooling and assembly fixturing was developed during attempts to increase stack height. Figure 1 shows successful implementation of these improvements in a 30-cell stack.

The stack was designed for a hydrogen product pressure of 4,500 psi, which is 50% higher than previous stacks. It was proof tested at 6,750 psi to ensure safety during operation. With this stack a new record was established in terms of the combination of taller stack (30 cells) and pressure capability (4,500 psi). After conditioning and parametric testing, the hydrogen product pressure was gradually increased to the design pressure of 4,500 psi. The cell-to-cell performance was over 70% lower compared to a stack tested during the previous FY, as shown in Figure 2. This performance is ascribed to the design and fabrication improvements described in the previous paragraph, as well as improved system controls enabled by a new test station developed for taller stack testing. Figure 2 also shows an improvement of >70% in cell-to-cell variation over the course of this program.

FIGURE 1. EHC 30-cell stack (81 cm^2 design)

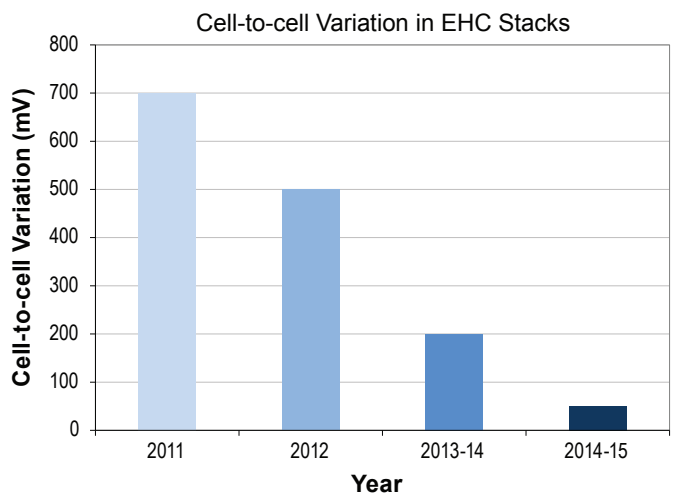

FIGURE 2. Cell-to-cell variability reduced by >70%

The 30-cell stack was endurance tested for 1,500 hours at 4,500 psi, as shown in Figure 3. The program milestone was to demonstrate 1,000 hours of performance stability in the 30-cell stack operating at 3,000 psi. Thus, the milestone was exceeded by 50% in both product pressure and duration.

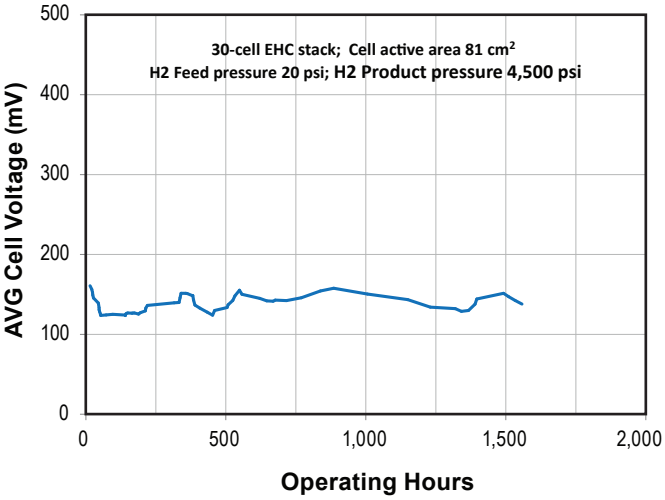

FIGURE 3. EHC 30-cell stack operation at 4,500 psi – milestone met

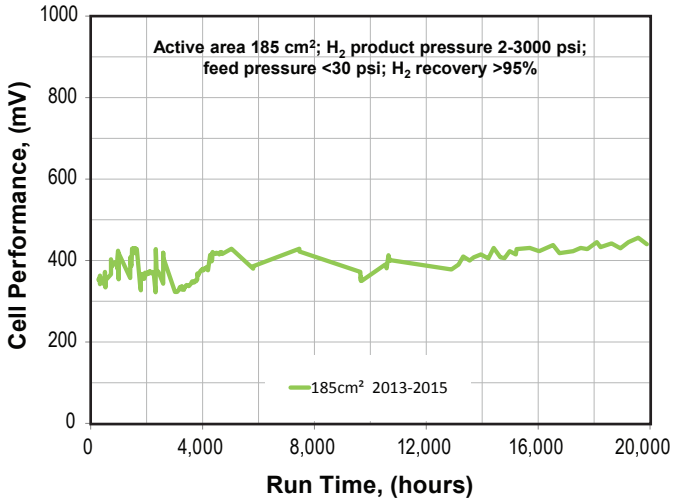

FIGURE 4. EHC 185 cm^2 single cell long-term operation at 2–3,000 psi

Over the total operating time of >4,000 hours, the stack was subjected to more than 20 pressure cycles from >3,000 psi to <30 psi. This cycling has not affected its performance, confirming the stack's robustness. Previously an EHC cell was cycled >1,000 times over that pressure range without adverse effects. The limited cycling data suggests that the pressure cycling capability was maintained in the stack scale-up to 30 cells.

Durability and reliability are significant barriers for mechanical compressors, and are major incentives for pursuing electrochemical compression. Therefore, continued emphasis was placed on endurance testing the EHC. A larger area EHC cell (185 cm^2 active area), fabricated and assembled in 2013, reached 20,000 hours of operation, compressing hydrogen from an inlet pressure of <30 psi to a product pressure of 2–3,000 psi at a hydrogen recovery rate of about 95%. As Figure 4 shows, cell performance has been quite stable, demonstrating long-term durability. This data is continued evidence of the robustness of the EHC cell architecture. Based on this data, durability well in excess of 40,000 hours is predicted. Therefore, EHC is expected to be able to meet the DOE target for high compressor reliability.

CONCLUSIONS AND FUTURE DIRECTIONS

The EHC stack height was increased from five to 30 cells. Simultaneously, the hydrogen product pressure was increased from 3,000 psi to 4,500 psi. Improvements in cell design, fabrication and assembly have resulted in a more than 70% reduction in cell-to-cell variability, resulting in improved operability. This improvement was demonstrated by running the 30-cell stack at 4,500 psi for more than 1,500 hours, with good performance stability. Durability of the scaled-up cell architecture has been demonstrated in a 20,000-hour test, confirming its robustness. The following summarizes critical performance parameters that were advanced during this reporting period:

Parameter	2014 Value	2015 Value
Number of cells in stack	5	30
EHC stack product pressure	3,000 psi	4,500 psi
Stack endurance at 4,500 psi	N/A	>1,500 hours
EHC cell endurance	10,900 hours	20,000 hours

N/A – not appliable

No additional work is planned under this project. Additional efforts are needed to further scale up the EHC stack to a building block size suitable for hydrogen refueling stations. Cost reduction opportunities include further advancing thermal management.

FY 2015 PUBLICATIONS/PRESENTATIONS

1. L. Lipp, "Electrochemical Hydrogen Compressor," 2015 DOE Hydrogen Program Merit Review and Peer Evaluation Meeting, Arlington, VA, June 8-12, 2015.

REFERENCES

1. DOE Office of Energy Efficiency and Renewable Energy (EERE) Fuel Cell Technologies Office Multi-Year Research, Development and Demonstration (MYRDD) Plan, Table 3.2.4 "Technical Targets for Hydrogen Delivery Components," section on Small Compressors, page 3.2-16.

III.11 Reference Station Design

Joe Pratt (Primary Contact)
Sandia National Laboratories
P.O. Box 969, MS-9052
Livermore, CA 94551
Phone: (925) 294-2133
Email: jwpratt@sandia.gov

Danny Terlip, Chris Ainscough, Jennifer Kurtz
National Renewable Energy Laboratory
Golden, CO 80401

Amgad Elgowainy
Argonne National Laboratory (ANL)
Lemont, IL 60439

DOE Manager
Erika Sutherland
Phone: (202) 586-3152
Email: Erika.Sutherland@ee.doe.gov

Project Start Date: March 1, 2014
Project End Date: March 1, 2015

Overall Objective

- Speed acceptance of near-term hydrogen infrastructure build-out by exploring the advantages and disadvantages of various station designs and propose near-term optima

Fiscal Year (FY) 2015 Objectives

- Provide a detailed view of how these stations fit in greenfield and existing sites in relation to the National Fire Protection Association 2 standard
- Help station developers quickly evaluate the suitability of their sites for a particular station type and capacity
- Provide station developers and local authorities a complete picture of the devices, components, and associated costs that make up a station
- Provide a tool that the H2USA financing and market support and acceleration working groups can use to develop station rollout scenarios
- Promote common component sizing and interchangeability

Technical Barriers

This project addresses the following technical barriers from the Hydrogen Delivery section of the Fuel Cell Technologies Office Multi-Year Research, Development, and Demonstration Plan:

(A) Lack of Hydrogen/Carrier and Infrastructure Options Analysis

(K) Safety, Codes and Standards, Permitting

Technical Targets

This project aimed to reduce the costs of near-term hydrogen fueling stations by describing cost-effective designs. The DOE 2020 cost target for hydrogen delivery and dispensing in a high-volume market (wherein costs decline due to economies of scale) is $2.00/gge for a fully utilized 1,000 kg/d station. The Reference Station Design task identified four station designs that leverage technologies available today and have a levelized cost of $5.80–$13.30/gge in today's market (assuming the costs of technologies today, and the utilization rates expected in California in the near term).

FY 2015 Accomplishments

- Primary Results
  - Screened 160 station designs that are possible in the near term, and selected five that are the most viable based on economics, technical feasibility, and market need
  - Produced spatial layouts, bills of materials, and piping and instrumentation diagrams for five station concepts that are viable in the near term
- Ancillary Results
  - Assessed several projections of annual fuel cell electric vehicle (FCEV) rollout in the near term
  - Assessed near-term hydrogen station rollout including number of stations, capacity, and overall utilization
  - Compiled current costs for all station components, and compared to default inputs in Hydrogen Refueling Station Analysis Model (HRSAM)
  - Assessed costs of 120 station permutations: capital cost and station contribution to cost of hydrogen, including effect of different utilization scenarios

✧ ✧ ✧ ✧ ✧

INTRODUCTION

The goal of the Hydrogen Fueling Infrastructure Research and Station Technology (H2FIRST) Reference Station Design Task is to accelerate acceptance of hydrogen infrastructure build-out by exploring the advantages and disadvantages of various station designs. These reference designs will help reduce the cost and speed the deployment of hydrogen stations by providing a common baseline with which to start a design. The designs enable quick assessment of the suitability of a particular site for a hydrogen station, and they drive interchangeability of parts and manufacturing scale by employing uniformly sized components. The station configurations evaluated were not all inclusive. It is not the intent to promote any specific station configuration or exclude any designs, but rather provide a rigorous analysis of a subset of likely near-term station configurations.

APPROACH

The H2FIRST team screened 160 possible station permutations using the Hydrogen Refueling Station Analysis Model developed by ANL. The team developed input parameters and station configurations with feedback from the H2USA Hydrogen Fueling Station Working Group (HFSWG), California Fuel Cell Partnership, California Air Resources Board (CARB), and industry. These station configurations were down selected by evaluating (1) the station contribution to the cost of hydrogen, (2) station capital cost, and (3) time to positive return on investment (ROI). An approximate seven-year ROI was used for all stations. The team then selected stations with the lower of the first two values. This narrowed the list to 15 stations. From this set, the team selected stations to meet projected near-term market needs based on the station classification system described by CARB: high-use commuter, low-use commuter, and intermittent use profiles. This selection narrowed the list to the final set of five stations. The team then developed detailed designs for those final four stations.

RESULTS

Estimated Near-Term Station Utilization

By estimating FCEV rollout scenarios and combining those with station build predictions, near-term network utilization was estimated and used as an input for cost modeling. For modeling purposes, it was assumed that the utilization rate of each individual station would be equivalent to that of the network.

Determined Station Parameters with Near-Term Ranges of Interest

Five parameters were chosen to describe the overall performance of a hydrogen fueling station: (1) design capacity, (2) peak performance, (3) number of hoses, (4) fill configuration, and (5) hydrogen delivery method. The H2FIRST team chose the selected parameters, definitions, and range values through detailed conversations with members of the H2USA HFSWG, DOE headquarters personnel, and ANL personnel in the spring of 2014, and vetted them with the entire H2USA HFSWG membership. Table 1 describes the parameters and ranges of interest chosen for near-term station designs.

TABLE 1. Performance Parameters and Values Used for Screening

Performance Parameter	Values Used for Screening
Design capacity (kg/d)	50, 100, 200, 300
Peak performance	2, 3, 4, 5, 6 consecutive fills per hose
Number of hoses	1, 2
Fill configuration	Cascade, booster compressor
Hydrogen delivery method	Gas (tube trailer), liquid trailer

Estimated Station Capital Cost and Station Contribution to the Cost of Hydrogen

The team used HRSAM to simulate 120 station concepts using the parameters, costs, and ranges defined earlier and the developed utilization and daily demand profiles. The team performed a comparative analysis to select the most cost-effective, near-term station designs for further analysis and design. Some high-level conclusions show the following.

- While the smallest capacity stations have the lowest capital cost, the levelized station contribution to the cost of hydrogen is the highest.
- For each station capacity (50, 100, 200, and 300 kg/d), the station concept that has the lowest capital cost also has the lowest levelized station contribution to the cost of hydrogen.
- The consecutive fill requirement has more of an impact on capital cost than on levelized station contribution to the cost of hydrogen.

In addition, all stations were resimulated using a constant 20% utilization for 10 years in order to compare the effect of low utilization on station economics and found that all station designs are nearly equally affected by the low utilization. In other words, there is no particular station design that is better than another in withstanding a lower-than-expected utilization.

Matched Economically Best-Performing Station Design Possibilities with Market Needs

Station performance parameters were mapped to station classifications as follows.

TABLE 2. Economically-viable station concepts determined by economic screening

Profile	Site Type	Delivery	Capacity (kg/d)	Consecutive Fills	Hoses	Station Contribution to Hydrogen Cost ($/kg)	Capital Cost (2009$)
High Use Commuter	Gas Station or Greenfield	Gaseous	300	6	1	$6.03	$1,251,270
High Use Commuter	Greenfield	Liquid	300	5	2	$7.46	$1,486,557
Low Use Commuter	Gas Station or Greenfield	Gaseous	200	3	1	$5.83	$1,207,663
Intermittent	Gas Station or Greenfield	Gaseous	100	2	1	$13.28	$954,799

- High use commuter: Greenfield or existing gasoline station, high daily capacity, multiple hoses, 5+ consecutive fills per hour per hose
- Low use commuter: Greenfield or existing gasoline station, compressed gas or liquid supply, medium daily capacity, single or multiple hoses, several consecutive fills per hour
- Intermittent: Greenfield, compressed gas supply, low daily capacity, single hose, ability to meet multiple consecutive fills per hour when called for

The most economically viable station concepts determined by economic screening was then selected to fulfill each of these three classifications as shown in Table 2.

Produced Full Station Designs

For each station identified in the above table, the team produced piping and instrumentation diagrams, corresponding component-level bills of materials with individual costs, and spatial layouts considering codified setback distances at both existing gasoline stations and Greenfield sites. (Note: the produced figures are too complex to be reproduced in the size of this report but are available online through the H2FIRST website: http://energy.gov/eere/fuelcells/h2first).

CONCLUSIONS AND FUTURE DIRECTIONS

This work presented the hydrogen community with a uniform, cost-optimal formula for designing and building hydrogen stations. The piping and instrumentation diagrams and bills of materials provided include a level of detail not previously reported publicly. Additionally, through this work the H2FIRST team has identified four primary areas where the design of stations and station networks can be further improved in the near term.

- Component technology: designs are needed for off-the-shelf chillers, cryogenic pumps, evaporators, high-capacity tube trailers, and underground storage.
- Station systems: work to reduce the need to chill hydrogen prior to dispensing, reduce boil off in liquid systems, and utilize more of the hydrogen in a gaseous tube trailer could all have significant impacts on the system cost.
- Codes and standards: this work reinforced the need to use science-based methods to reduce the setbacks required for liquid stations. These setbacks are one of the largest hurdles to the placement of high-capacity liquid hydrogen stations in dense urban areas (where the customer base will be the highest).
- Business practices: utilization is the most important variable to impact the financial viability of a station. To the extent that hydrogen station networks can be optimized to maximize utilization, more of those stations will be self-sustaining and profitable.

Future iterations of the reference station task would likely include the following.

- Assessment of technological and economic changes
- Re-evaluation of parameter ranges of interest to near-term stations
- Re-assessment of economic potential of new station concepts
  - On-site generation
  - Light-heavy-duty mixed stations
- Assisting assessment of economic impact of different business practices
- Production of new station designs that reflect these changes

FY 2015 PUBLICATIONS/PRESENTATIONS

1. D. Terlip, J. Pratt, A. Elgowainy, C. Ainscough, and J. Kurtz, "Reference Station Design," presented at the Interagency Working Group on Hydrogen and Fuel Cells, July 21, 2015.

2. D. Terlip, J. Pratt, A. Elgowainy, C. Ainscough, and J. Kurtz, "Reference Station Design," presented at the H2USA Hydrogen Fueling Station Working Group meeting, May 14, 2015.

3. J. Pratt, "How to Design a Hydrogen Station in Seven Easy Steps (and Why)," presented at Combustion Research Facility Research Highlights Series, April 2, 2015.

4. J. Pratt, D. Terlip, C. Ainscough, J. Kurtz, and A. Elgowainy, "H2FIRST Reference Station Design Task Project Deliverable 2-2," Technical Report NREL/TP-5400-64107 or SAND2015-2660R, April 2015.

5. D. Terlip, J. Pratt, A. Elgowainy, C. Ainscough, and J. Kurtz, "Reference Station Design," presented at the H2FIRST Spring Coordination Panel Meeting, March 18, 2015.

III.12 Hydrogen Fueling Station Precooling Analysis

Amgad Elgowainy (Primary Contact) and Krishna Reddi
Argonne National Laboratory
9700 South Cass Avenue
Argonne, IL 60439
Phone: (630) 252-3074
Email: aelgowainy@anl.gov

DOE Manager
Erika Sutherland
Phone: (202) 586-3152
Email: Erika.Sutherland@ee.doe.gov

Project Start Date: October 2014
Project End Date: Project continuation and direction determined annually by DOE

Overall Objectives

- Evaluate the cost and energy consumption of precooling system at hydrogen refueling stations, and identify strategies for precooling cost and energy reduction

Fiscal Year (FY) 2015 Objectives

- Evaluate theoretical precooling requirement at hydrogen refueling stations (HRS) with respect to Society of Automotive Engineers (SAE) J2601 refueling protocol
- Determine size of precooling equipment and heat exchanger (HX) with various refueling demands and frequencies
- Assess current precooling equipment design and cost and identify major drivers for precooling cost and energy consumption
- Analyze tradeoff between different design concepts

Technical Barriers

This project directly addresses Technical Barriers A, D, and E in the System Analysis section of the Fuel Cell Technologies Office (FCTO) Multi-Year Research, Development, and Demonstration (MYRDD) Plan. These barriers are:

(A) Future Market Behavior

(D) Insufficient Suite of Models and Tools

(E) Unplanned Studies and Analysis

Technical Targets

This project investigates the major drivers for precooling cost and energy consumption, including the impact of HRS utilization and frequency of fills, the impact of number of back-to-back fills, and the impact of SAE J2601 30-second window to reach precooling temperature.

Contribution to Achievement of DOE Systems Analysis Milestones

This project contributes to the following DOE milestone from the Systems Analysis section of the FCTO MYRDD Plan:

- Task 1.12: Complete an analysis of the hydrogen infrastructure and technical target progress for technology readiness. (4Q, 2015)
- Task 2.2: Annual model update and validation. (4Q, 2011 through 4Q, 2020)

FY 2015 Accomplishments

- Evaluated theoretical refrigeration capacity and precooling electricity consumption at hydrogen refueling stations (<1 kWh/kg$_{_H2}$)
- Developed a methodology to size precooling equipment and HX with respect to fill rate, number of back-to-back fills, and SAE J2601 30-second window
- Evaluated the tradeoff between on-demand cooling vs. large thermal mass heat HX
- Demonstrated the critical impact of HRS utilization on precooling energy consumption per kilogram of dispensed hydrogen
- Developed a formula for estimating cooling energy consumption kWh/kg$_{_H2}$

✧ ✧ ✧ ✧ ✧

INTRODUCTION

Reports from hydrogen refueling stations operating in Germany indicated that precooling electrical energy consumption exceeded 10 kWh/kg$_{_H2}$. Such energy consumption not only contributes more than \$1/kg$_{_H2}$ of operating cost, but also increases the greenhouse gas (GHG) emissions associated with hydrogen dispensing. Additionally, the precooling requirement at HRS to -40°C within 30 seconds according to the SAE J2601 fueling protocol requires an oversized refrigeration capacity and/

or heat exchanger thermal mass, resulting in significant capital cost of the precooling system. The station's precooling requirements depend on many operational and demand variables, including precooling temperature, fill rate, and fueling frequency.

There are several precooling system designs and configurations employed by various companies at HRS around the world. The variation of implementation of precooling systems at HRS reflect the fairly new application of such systems to hydrogen refueling and the recent approval of the SAE J2601 protocol. This project evaluates the different refrigeration concepts and designs at existing HRS through theoretical calculations grounded in physical laws of thermodynamics and heat transfer.

RESULTS

We used the theoretical laws of thermodynamics to calculate the cooling energy requirement for -40°C precooling and calculated the corresponding electrical energy consumption based on estimates of refrigeration system coefficient of performance (COP) at different ambient temperatures. Figure 1 shows that at 35°C ambient, the energy required for cooling is approximately 0.3 kWh/kg$_{H2}$. The corresponding electricity consumption is estimated at 0.4 kWh/kg$_{H2}$ assuming a conservative precooling system COP of 0.8 at 35°C. Figure 2 shows the calculated mass of aluminum HX block for various temperature increase between refueling of hydrogen vehicles assuming 5 kg of hydrogen to be dispensed in each fueling. The mass of the HX is approximately 1,500 kg when allowing 4°C HX

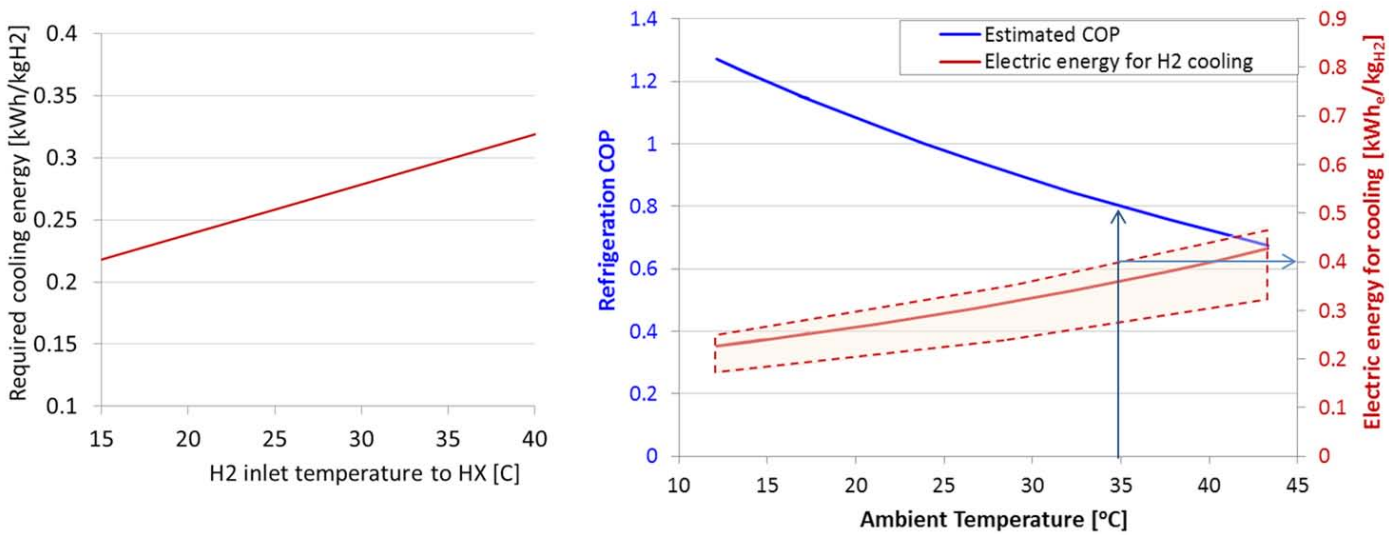

FIGURE 1. Cooling and electricity energy consumption at various ambient temperatures

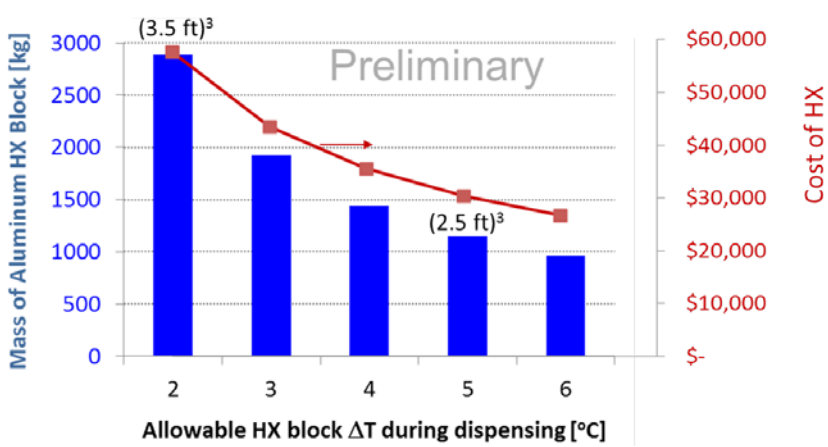

FIGURE 2. Impact of heat exchanger thermal mass on temperature change between fills

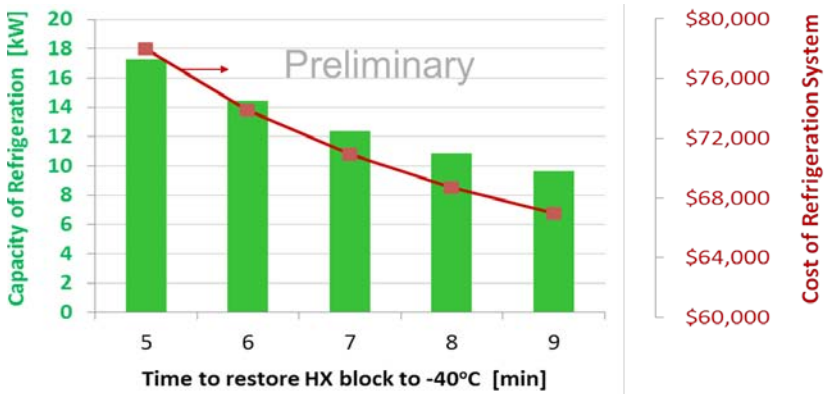

FIGURE 3. Refrigeration capacity requirement as a function of frequency of back-to-back fills

temperature rise with each fueling. A larger thermal mass of HX provides more reliable and near steady precooling at the dispenser during fueling.

Figure 3 shows the refrigeration capacity as a function of the time required to restore HX block to -40°C between back-to-back refueling. For a 5 kg_{H2} fill in 5 minutes (+2 minutes lingering), a cooling capacity of 12 kW (3.5 ton) is required. The time required to restore HX block to -40°C is an important parameter to satisfy the design requirement of fill rate and number of back-to-back fills.

Argonne collected precooling energy consumption requirement from several hydrogen refueling stations in California. The collected data averaged 54 kWh of precooling electricity consumption per day at 25°C ambient with no refueling events. The 54 kWh represents the overhead energy consumption to keep the HX cold at -40°C all the time in anticipation of possible refueling demand at any time during the day. Argonne proposed the following formula to calculate the precooling electricity consumption per kilogram of hydrogen dispensed based on the aforementioned calculation of precooling energy consumption and the collected data of overhead electricity use.

$$Cooling\ Electricity\ Consumption\ [kWh/kg_{H2}] \approx \frac{\left[0.3 + \frac{54}{Daily\ dispensed\ kg_{H2}}\right]}{System\ COP}$$

The formula shows that the precooling electricity consumption is a strong function of daily dispensed hydrogen. It is clear that when the average daily dispensed hydrogen is small (e.g., in the early phase of hydrogen vehicle deployment), the electricity consumption per kg of hydrogen can be significant as shown in Figure 4. The overhead electricity consumption diminishes in importance with average dispensed amount of greater than 100 kg/d.

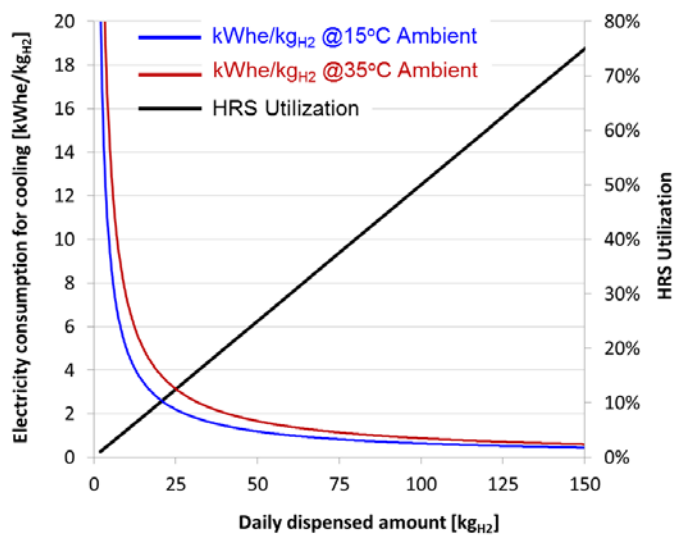

FIGURE 4. Electricity consumption for cooling H_2 as a function of refueling station utilization

CONCLUSIONS

The electrical energy required to precool the hydrogen at 35°C ambient is only about 0.3 kWh/kg_{H2}. However, modern-day stations additionally spend about 54 kWh keeping the heat exchanger at -40°C all day. The impact of this "overhead" on the levelized cost of hydrogen becomes significant when the daily dispensed amount is low, such as the case in early hydrogen vehicle markets. It is therefore important to report the daily dispensed amount along with the reporting of precooling electricity consumption per kg of dispensed hydrogen. When the daily demand of hydrogen exceeds 100 kg/d per hose, the precooling electricity consumption drops below 1 kWh/kg_{H2}.

III.13 700-Bar Hydrogen Dispenser Hose Reliability and Improvement

Kevin Harrison (Primary Contact), Owen Smith, Michael Peters, Krista Isham, Huyen Dinh, and Svitlana Pylypenko
National Renewable Energy Laboratory (NREL)
15013 Denver West Parkway
Golden, CO 80401-3305
Phone: (303) 384-7091
Email: Kevin.Harrison@nrel.gov

DOE Manager
Erika Sutherland
Phone: (202) 586-3152
Email: Erika.Sutherland@ee.doe.gov

Subcontractor
Marc Mann, Spectrum Automation Controls, Inc., Arvada, CO

Project Start Date: July 2013
Project End Date: Project continuation and direction determined annually by DOE

Overall Objectives

- Working closely with original equipment manufacturers (OEMs) (SpirStar, Yokohama Rubber) and groups developing advanced high pressure hydrogen hoses, NREL's hose reliability project aims to characterize and improve the reliability of 700-bar hydrogen refueling hose assemblies, and ultimately reduce the cost of dispensing hydrogen into fuel cell electric vehicles.
- We will design a fully automated test system that unifies the four stresses of pressure, temperature, time, and bending. The high cycling autonomous test apparatus will reveal the compounding impacts of high volume 700-bar fuel cell electric vehicle refueling that has yet to be experienced in today's low volume market. Testing includes pre- and post-cycling chemical and physical analysis of the inner hose liner to determine changes (if any) due to the stress of repeated fueling events.

Fiscal Year (FY) 2015 Objectives

- Begin operation of a test apparatus that unifies the stresses to which the hose is subjected during high volume back-to-back fueling events
  - The stresses include use of hydrogen gas, high pressure (up to 875 bar), low temperature (≥-40°C), 3–5 minute refueling time and automated mechanical bending and twisting of the hose assembly to simulate the refueling process.
  - SAE International technical specification J2601 pressure and temperature profiles for H70-T40 fills are simulated as closely as possible with the exception of total mass dispensed, which will be minimized via a tankless filling algorithm.
- Identify and perform dynamic mechanical analysis (DMA) tests to characterize pre-cycling and post-cycling structural and thermal viscoelastic properties in response to applied stress

Technical Barriers

This project is conducting applied research, development, and demonstration to reduce the cost of hydrogen delivery systems. This project addresses the following technical barriers from the Hydrogen Delivery section of the Fuel Cell Technologies Office Multi-Year Research, Development, and Demonstration Plan:

(I) Other Fueling Site/Terminal Operations

(J) Hydrogen Leakage and Sensors

Technical Targets

This project aims to generate data that will help OEMs and hose developers improve reliability and replacement intervals for high pressure gaseous hydrogen dispenser hoses. This data provided by this project will ultimately improve the robustness of hydrogen dispensers, thereby ensuring a positive customer fueling experience and lowering the cost of station maintenance.

- Target Hose Replacement Interval: 25,000 cycles or two years
- Target Cost of Hydrogen Delivery: <$4/gge by 2015, <$2/gge by 2020

FY 2015 Accomplishments

- Evaluated samples of polyoxymethylene hose liner using two different DMA approaches, time-temperature superpositioning (TTS) testing and torsion rheology testing
  - Torsion testing yielded meaningful characterization data on uncycled hose inner liner material from -60 to 50°C and will be added to the range of post-cycling chemical and physical testing.
- Designed and implemented improved safety systems in the high pressure test bays and hose test apparatus to enable autonomous hose testing in hydrogen
  - Facility upgrades include additional isolation valves, monitoring and feedback of facility

ventilation status, ultraviolet/infrared detection, video monitoring, and improved visual/audible alarming.
  - Safety measures implemented include a sampling system to rapidly detect hydrogen leaks at each crimp fitting, hose to nozzle, and hose to breakaway.
- Constructed and installed the high pressure, low temperature automated hose reliability test stand at the NREL-funded 700-bar Hydrogen Infrastructure Testing & Research Facility (HITRF) located at the Energy Systems Integration Facility (ESIF)
  - Developed and proved tankless algorithm to simulate SAE J2601 fueling protocol, while conserving mass dispensed

✧ ✧ ✧ ✧ ✧

INTRODUCTION

The hose reliability project aims to lower the capital and maintenance costs of hydrogen dispensers by benchmarking the performance of the current state-of-the-art. Results from this project will demonstrate hose performance in real-world conditions, increasing confidence in their use and giving manufacturers valuable performance data to guide improvements in hose reliability. Previous research at NREL has shown that about 13% of maintenance hours for hydrogen fueling infrastructure are associated with dispensers, with a significant amount attributed to hydrogen leaks or failed parts [1]. Improvement in the reliability of hoses would therefore significantly reduce station down time. Additionally, results on the material properties of today's hoses may facilitate the generation of new hose manufacturers. Only a small handful of companies manufacture hydrogen hoses worldwide today. An increase in the number of manufacturers could significantly advance the technology and lower its cost.

NREL is uniquely positioned to complete this project due to its ESIF. ESIF is a user facility with a broad array of capabilities in energy integration research, from materials testing to supercomputing. Fast and flexible swapping of research test articles is a hallmark of the facility. ESIF is utilized in DOE-funded projects, as well as in partnerships with industry to provide critical testing, validation, and refinement during product research and development. ESIF's high pressure hydrogen test bay (HPTB) integrates hydrogen production, compression, storage, dispensing and end use systems in a safe and controlled environment. The hose reliability test stand is housed in the HPTB due to its ability to test components under high pressure to failure while minimizing dangers to personnel or equipment.

APPROACH

This project aims to perform accelerated life testing using high pressure, low temperature hydrogen with ramp rates and fueling times that comply with SAE J2601 protocols. (Hydrogen stations being installed today for use by passenger vehicles are designed for compliance with SAE J2601.) This work is unique and goes beyond standard OEM testing in that it simultaneously stresses the hose assembly with realistic precooled fueling conditions closely following the SAE International technical specification SAE J2601 fueling protocol for H70-T40 fills. In addition, the project applies mechanical bending and twisting stress to the hose and nozzle assembly to simulate people refueling vehicles. Finally, the short time in between back-to-back fills, of a yet to be realized high volume hydrogen refueling market, will simulate a busy station where the dispensing equipment is kept cold and subjected to frequent decompression cycles. The only difference between the test plan and a high volume station is the mass dispensed per fill will be less than the 3–5 kg of a typical vehicle fill. To prevent overtaxing the production and compression capabilities of the HIRTF, the target mass dispensed per fill is 100–200 g. Back-to-back filling will maintain hose temperatures under the cold dispenser cases of SAE J2601. The performance of the hose will be monitored over time using a hydrogen sampling system attached to an outer protective sleeve near each flared crimp fitting to identify leaks as they occur.

The project also includes analysis of the physical and chemical property changes in the inner hose liner due to long duration cycling. Chemical tests previously identified and performed on pre-cycled specimens in FY 2014 include scanning electron microscopy to detect blistering due to hydrogen permeation and testing to characterize material degradation and compositional changes. Characterization testing included Fourier transform infrared spectroscopy, thermogravimetric analysis, differential scanning calorimeters, and X-ray spectroscopy. In FY 2015, DMA methods were investigated based on feedback received from industry experts and other stakeholders. As a result, TTS and torsion tests were performed on pre-cycled polyoxymethylene (POM) inner liner.

RESULTS

Automated Hose Reliability Test Stand

A new hose reliability test stand was developed to simulate SAE J2601 700-bar fills in a footprint small enough to fit in NREL's HPTB. The test stand closely mirrors an actual dispenser in its design and pressure ramping capabilities. A small six-axis robot was also installed and programmed to simulate human movement of the nozzle from 'dispenser' to one of two 'vehicle' receptacle positions. A hydrogen leak sampling system, using vacuum pumps

FIGURE 1. Completed hose test stand installed in HPTB

drawing air from chambers around each hose crimp fitting through a combustible gas detector, was installed to monitor for likely leak points. The completed hose test stand assembly is shown in Figure 1.

A tankless control algorithm was successfully developed using the interaction of an air-loaded pressure regulator on the dispenser side of the test apparatus and flow control valves on the vehicle side. The pressure ramp is controlled using a proportional, integral, and derivative (PID) method set to SAE J2601 average pressure ramp rates (APRR) and target pressures, similar to commercially available dispensers. Temperature control (-33°C to -40°C within 30 s of fueling, per SAE J2601 protocols) is achieved using an air operated valve that controls hydrogen flow. After this target temperature is attained, the air operated valve closes but flow continues through a bypass motorized needle valve at a rate just enough to maintain the temperature inside the hose. Good automated control of both pressure and temperature fills was demonstrated with nitrogen gas dispensed at 7.0 MPa (Figure 2). The tankless PID algorithm was successful in remaining within the SAE J2601 APRR and temperature tolerance bands for the duration of the fill except for a slight overshoot at the end. The total mass of nitrogen

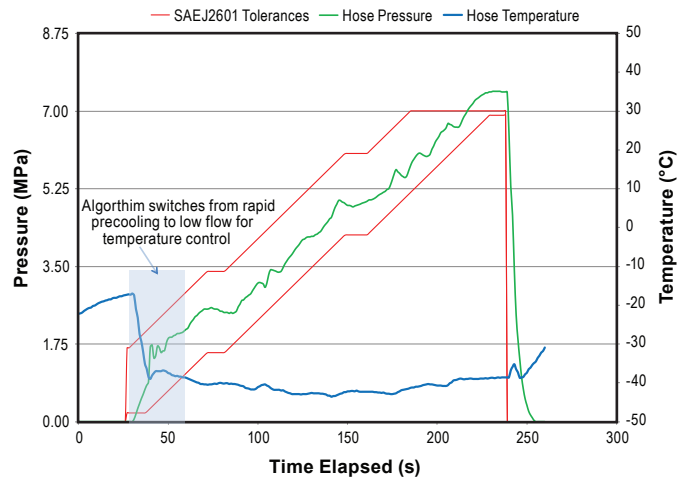

FIGURE 2. Preliminary pressure profile control with leak check holds, precooling, and temperature stabilization

dispensed during this fill was approximately 150 g. Nitrogen gas was used to develop the process to avoid unnecessarily wasting hydrogen. The control algorithm is being retuned for 70 MPa hydrogen gas and additional controls will be put in place to prevent overshoots.

Enhanced facility safety improvements were required by NREL's authority having jurisdiction causing some delays to full system operation. During this time, the team has worked to increase monitoring of potential leak points and enhance safety systems on the test apparatus. Safety systems now include hydrogen detectors, video camera feedback to the control room, automatic shut-off of the robotic arm in case of collision, and room ventilation monitoring.

Baseline (Pre-Cycled) Inner Hose Material DMA

Uncycled hose samples, supplied by SpirStar, were used to conduct DMA testing using two different methods. The TTS method involved cutting narrow strips of the cylindrical POM hose liner and placing it in a solids analyzer equipped with a three-point bending clamp. The sample was soaked in a nitrogen-purged forced convection oven from 30 to 100°C at a soak rate of 3 minutes for each 5°C step with frequency sweeps from 0.001 to 10 Hz. The TTS test results were affected by sample geometry and the semicrystalline nature of the POM nature, showing no usable time–temperature relationships. Analysis may be possible at low temperatures but useful only to predict short timescales or high frequencies. TTS DMA will therefore not be repeated for future pre-cycling or post-cycling characterization of the POM inner liner.

The data, shown in Figure 3, characterizes the transition in material structural rigidity and viscous response under applied stress and over the full temperature range possible in operation. Two separate cycled samples showed good

repeatability and clear relationships between the storage modulus and loss modulus. These relationships indicate that the hose material retains structural integrity from -60°C to 50°C. The torsion DMA tests will be repeated on the hose material after cycling to detect any shifts in the onset of glass transition or softening due to hydrogen permeation, mechanical fatigue, or other effects of the cycling.

The data, shown in Figure 3, characterizes the transition in material structural rigidity and viscous response under applied stress by measuring the ratio of the storage modulus and loss modulus over a full temperature range. Two separate cycled samples showed good repeatability and clear relationships between the two moduli, defining a stable region from -60°C to 50°C where the structural integrity is maintained. Post-cycled specimens undergoing torsion DMA tests will be able to show any shifts in the onset of either glass transition or softening caused by hydrogen permeation, mechanical fatigue, or other effects of the hose reliability test stand.

CONCLUSIONS AND FUTURE DIRECTIONS

- **Conclusion:** Completed design, development and fabrication of 700-bar hydrogen hose reliability test stand using a low volume (i.e., tankless) SAE J2601 filling algorithm to achieve realistic H70-T40 cooled fills while mechanically stressing and monitoring likely leak points of the hose assembly.
  - **Future:** The system will move quickly from attended to unattended mode of operation to accomplish high cycle counts of the first hose assembly until 25,000 cycles, excessive leak or hose failure.

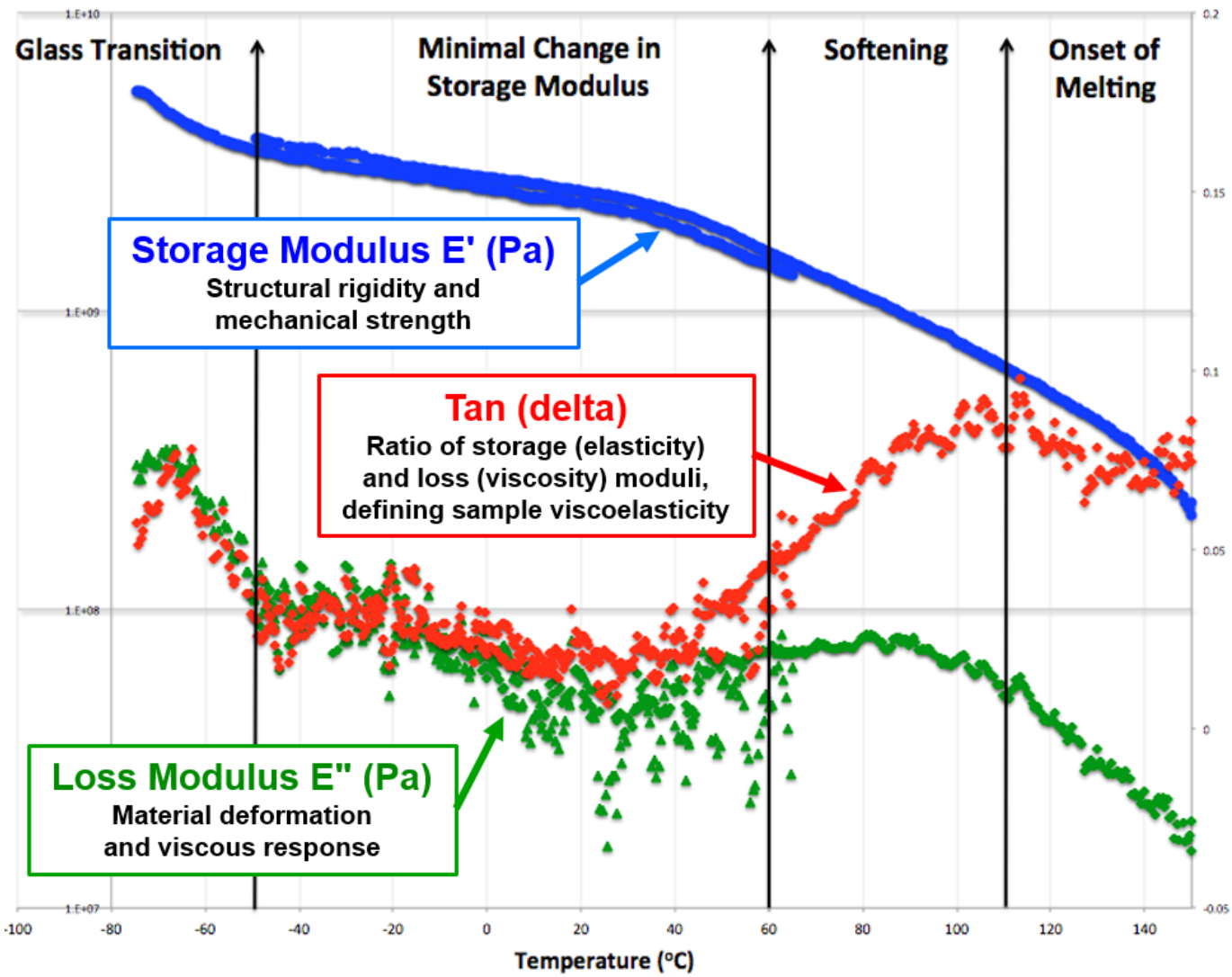

FIGURE 3. Torsion DMA results showing relationship between storage and loss moduli of two polyoxymethylene hose liner samples

  - **Future:** Methods to expedite warm-up rest periods between the 70 back-to-back fill sets will be developed. These periods are meant to introduce realistic thermal stressing that would be expected if the hose assembly were unused overnight.

- **Conclusion:** DMA, aimed at characterizing transitions in material structural rigidity between pre- and post-cycled hose material, was completed. Torsion DMA testing was selected for future testing because it showed stable and repeatable results in the region between -60°C and 50°C for the polyoxymethylene hose inner liner material before glass transition or softening occurred. TTS DMA test method will not be utilized in the future due to the inability to prepare a sample of the cylindrical hose liner in a way conducive for reliable data results.
  - **Future:** Perform post-cycling of hose assembly #1 using torsion DMA alongside suite of previously identified chemical analysis methods to reveal any changes in bulk material properties and elemental material composition.
- **Future:** Continue to work with industry partners like NanoSonic, SpirStar, and Yokohama Rubber. In FY 2016, NREL plans to test prototypes of hoses developed by NanoSonic through its Small Business Innovation Research Phase II project, "Cryogenically Flexible, Low Permeability Thoraeus Rubber™ Hydrogen Dispenser Hose."

FY 2015 PUBLICATIONS/PRESENTATIONS

1. 1-Page Fact Sheet - http://www.nrel.gov/docs/fy14osti/61091.pdf

2. YouTube Video - http://www.youtube.com/watch?v=Rbc7f01oP8kA

REFERENCES

1. Sprik, Sam, Jennifer Kurtz, Chris Ainscough, and Mike Peters. "Next Generation Hydrogen Station Composite Data Products - Data through Quarter 4 of 2014." Hydrogen Fueling Infrastructure Analysis. May 2015. http://www.nrel.gov/docs/fy15osti/64317.pdf.

III.14 Magnetocaloric Hydrogen Liquefaction

Jamie Holladay (Primary Contact), Jun Cui,
Kerry Meinhardt, Evgueni Polikarpov,
Ed Thomsen, John Barclay (EENW), Iver Anderson (Ames Laboratory)
Pacific Northwest National Laboratory (PNNL)
P.O. Box 999, MS: K1-90
Richland, WA 99352
Phone: (509) 371-6692
Email: Jamie.Holladay@pnnl.gov

DOE Manager
Erika Sutherland
Phone: (202) 586-3152
Email: Erika.Sutherland@ee.doe.gov

Subcontractor
Emerald Energy NW LLC (EENW), Redmond, WA

Project Start Date: October 1, 2015
Project End Date: September 30, 2018

Overall Objectives

- Quantify and incorporate novel configurations to achieve simpler, more efficient liquefier designs
- Identify, characterize, and fabricate magnetic materials in shapes suitable for high performance active magnetic regenerators (AMRs) from 280 K to 20 K
- Fabricate and characterize improved multi-layer magnetocaloric regenerator performance
- Design, fabricate, test, and demonstrate a lab-scale magnetocaloric hydrogen liquefier system
- Demonstrate a lab-scale hydrogen liquefier with a figure of merit (FOM) increase from 0.3 up to 0.5
- Perform technoeconomic analysis on a proposed full-scale (30 tons per day) system

Fiscal Year (FY) 2015 Objectives

- Obtain, refurbish, assemble, and successfully operate the first generation (GEN I) system
- Characterize the performance of the GEN I system using dual Gd regenerators by measuring the maximum temperature differential with heat sink temperature at ~285 K and no external load, with the heat sink temperature held constant at ~285 K, and measure cold temperature as a function of applied thermal load
- Demonstrate multi-layer operation and characterize the temperature distribution through the layered regenerator
- Design a second generation (GEN II) system to take advantage of new configurations and multi-layer design and incorporate several other lessons learned from GEN I operation

Technical Barriers

This project addresses the following technical delivery barrier from the Hydrogen Delivery section (3.2) of the Fuel Cell Technologies Office Multi-Year Research, Development, and Demonstration Plan:

(H) High-Cost and Low Efficiency of Hydrogen Liquefaction

Technical Targets

Conventional hydrogen liquefiers at any scale have a maximum FOM of ~0.35 due primarily to the intrinsic difficulty of rapid, efficient compression of either hydrogen or helium working gases (depending on the liquefier design). The novel approach of this magnetocaloric hydrogen liquefier (MCHL) project uses solid magnetic working refrigerants cycled in and out of high magnetic fields to execute an efficient active magnetic regenerative liquefaction cycle that avoids the use of gas compressors. Numerical simulation modeling of high performance MCHL designs indicates certain achievable designs have promise to simultaneously lower installed capital costs per unit capacity and to increase thermodynamic efficiency from an FOM of ~0.35 toward 0.5–0.6. Results from experimental prototypes should support the design and deployment of hydrogen liquefier plants that meet the DOE hydrogen production and delivery targets.

- Delivery cost of liquid hydrogen (LH_2) at <$2.00/kg
- $70 million capital cost for a turnkey plant with a capacity of 30,000 kg H_2/d
- Operational efficiency of a complete liquefier plant of 75% as defined by DOE and commensurate with a liquefier FOM of approximately 0.5–0.6

FY 2015 Accomplishments

- Successfully completed acquisition, refurbishment, assembly, and test of the GEN I prototype with the cooled solenoidal superconducting magnet, dual Gd magnetic regenerators, two electromechanical actuator drives, and the heat transfer fluid subsystems of our reciprocating active magnetic regenerative refrigerator MCHL prototype

- Mechanically and electrically integrated all eight subsystems of our first MCHL prototype into an operational system interfaced to the LabVIEW data acquisition and control program
- Experimentally demonstrated the first cooling curves of our MCHL and began to measure its performance under a variety of different operational parameters such as hot heat sink temperature, cycle frequency, magnetic field strength, heat transfer fluid flow rate, and cooling capability as a function of cold temperature; achieved maximum temperature span of approximately 317 K to 217 K (ΔT = 100 K) with a Gd at 3T net applied magnetic field change
- Demonstrated 40 W external cooling power with ~20 K approach temperature, a heat sink at ~286 K, a cold load temperature of ~266 K and using a Gd regenerator in a 3T field
- Demonstrated a novel configuration that increased the cooling power by 20% without changing the amount of magnetic material required
- Began to incorporate lessons learned from the first prototype into the design of the MCHL GEN II prototype with a rotary configuration with the objective to span from approximately 280 K to 20 K and produce LH_2 with an FOM of ~0.5

✧ ✧ ✧ ✧ ✧

INTRODUCTION

MCHL technology promises cost effective and efficient hydrogen liquefaction because it eliminates compressors, the largest source of inefficiency in the traditional Claude cycle liquefiers, and the need for liquid nitrogen to precool the hydrogen. The Claude cycle liquefier is the current industrial hydrogen liquefaction and uses a variety of processes with helium, hydrogen, or gas mixtures as coolant. The hydrogen feed to the process is first cooled by liquid nitrogen, and then further cooled in multistage heat exchangers where the cooling power is provided by turbo expanders. Liquefaction is finally accomplished by throttling in a Joule-Thomson valve. Conventional liquefier technology for hydrogen is limited to an FOM of ~0.35 for a large facility, and is typically less than 0.3 for a smaller facility.

The MCHL uses an AMR system which uses an alternating magnetic field and magnetocaloric materials to transfer heat between reservoirs. The magnetic material in a high performance regenerator is adiabatically placed in a high magnetic field. The conservation of total entropy in this adiabatic process requires the magnetic regenerators to increase in temperature to compensate for the increased order (lower entropy) among the material's magnetic moments. The increased thermal energy is transferred to a heat sink by the cold-to-hot flow of heat transfer fluid. After the cold-to-hot heat transfer fluid flow is completed, the magnetic material is adiabatically removed from the high magnetic field, resulting in a decreased regenerator temperature because order among the magnetic moments of the magnetic materials decreases. During a hot-to-cold flow of the heat transfer fluid at constant low magnetic field, the colder magnetic regenerator accepts heat from the thermal load from cooling the hydrogen process stream. The active magnetic regenerative cycle is repeated again at the operating frequency. The principle of operation is shown in Figure 1. The proposed MCHL project uses magnetocaloric refrigeration to achieve an efficient thermodynamic liquefaction cycle. Detailed modeling of the MCHL technology indicates it has the potential to simultaneously lower the installed capital costs per unit capacity, delivery cost, and to increase thermodynamic efficiency from an FOM of ~0.3 toward 0.5–0.6.

APPROACH

This project builds upon work first pioneered by Dr. John Barclay (partner). We utilized reciprocating dual regenerator design (GEN I) to evaluate magnetic materials and to better understand the temperature distribution in the regenerators. A simplified process flow diagram (PFD) of the GEN I unit and the schematic of the GEN I prototype are in Figures 2 and 3, respectively. The operation and experimental results from FY 2015 are located in the results section of this report. Based upon the results of GEN I, a GEN II MCHL design will be developed.

The GEN II will use a rotary regenerator design, which promises to balance the magnetic force for maximum work recovery. Its continuous magnetic material rotation becomes a constant magnetic flux device, which reduces induced flux jumps which occur in a persistent mode magnet during reciprocating motion of dual magnetic regenerators. The rotary MCHL is an advanced concept. In consideration of the likelihood of encountering unforeseeable technical challenges and due to limited resources and time, the development of a rotary MCHL will be divided into two phases. In Phase 1, a fully independent prototype (GEN II) will be designed, constructed and evaluated. GEN II will have only one superconducting (S/C) magnet subsystem, 4 K cryocooler, cold box, heat transfer gas circulator, data acquisition, integrated structures, and drive motors; but, it will incorporate the new novel configuration and have the capability to test several different magnetic wheels that are designed to operate over selected temperature ranges between 280 K and 20 K. A block diagram of the process flow for the rotary design is in Figure 4. For example, the regenerative wheel will be designed for 280–120 K which is the first stage of a multistage MCHL designed specifically to take advantage of the novel configuration. A complete liquefaction system will contain multiple stages, each with a wheel designed to operate over a specific temperature range.

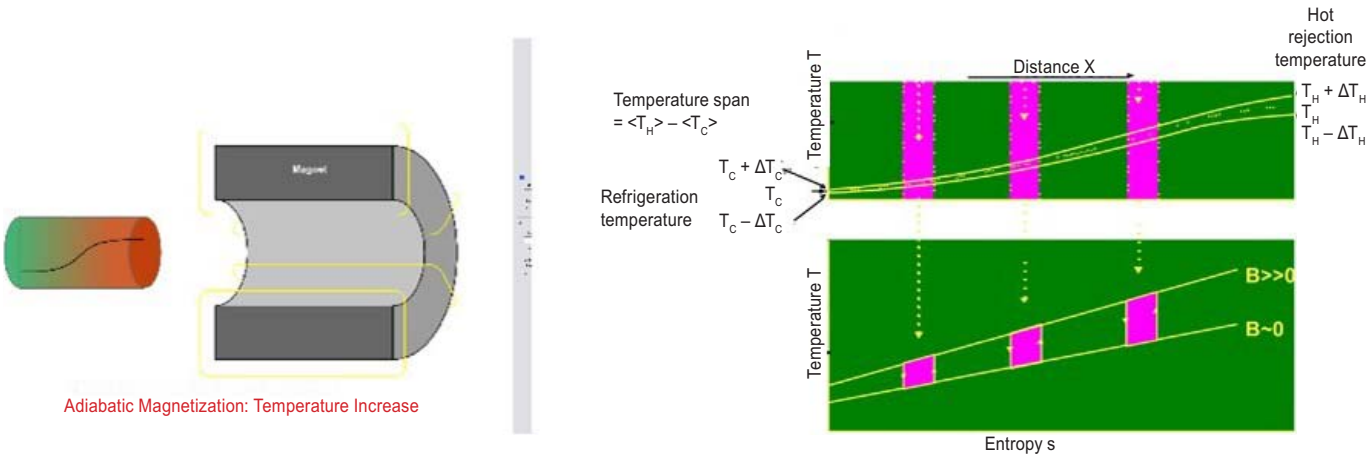

FIGURE 1. Active magnetic regenerative liquefier principle of operation

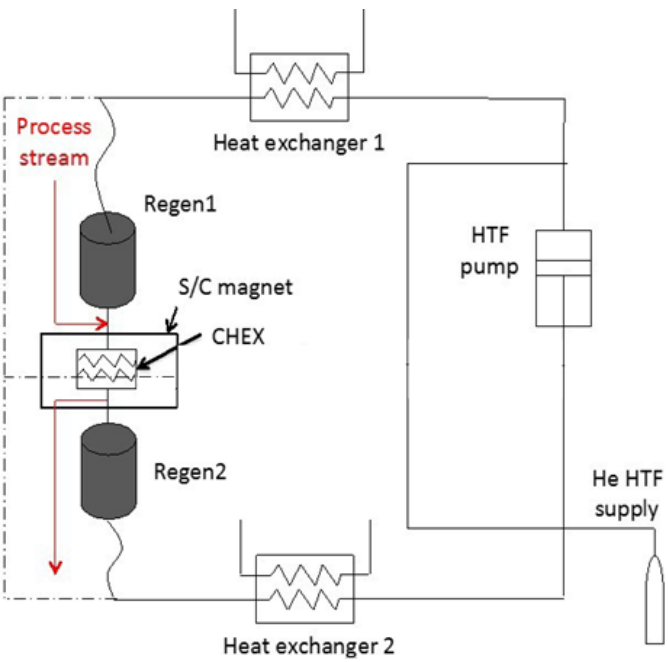

CHEX – cold heat exchanger; HTF – heat transfer fluid

FIGURE 2. Simplified PFD diagram of GEN I

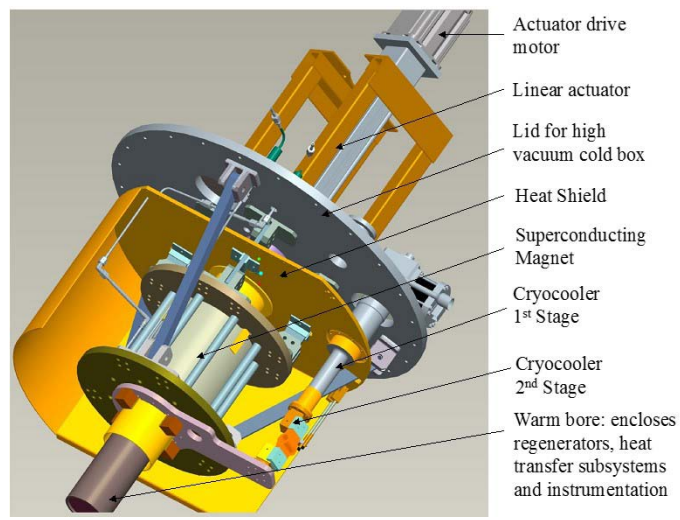

FIGURE 3. Schematic of the GEN-I prototype

Depending on the effectiveness of the new configuration innovations to be done in Phase I, a total of three to four stages may be required rather than six or more without the innovation. This approach will develop the necessary technical knowhow for the rotary system, including an arc shaped superconductor magnet, multilayered refrigerant wheels, fabrication of suitable refrigerant materials, and micro-channel heat exchangers. Phase II focuses on a multi-wheels system (third generation [GEN III]) capable of liquefying gaseous H_2 (GH_2) from 280 K. The key for a successful Phase II lies in the seamless integration of multiple wheels, magnets, and heat exchange subsystems, as well as successful preparation of refrigerant materials, which will require complete metallurgical understanding of 10–14 different rare earth metals and alloys. All lessons from GEN II will be incorporated into the design of GEN III, which will need multiple magnet subsystems, additional process and heat exchangers, and interconnections among the multiple refrigerant wheels to directly convert gaseous feedstock H_2 to LH_2. The GEN III prototype will be designed, constructed, commissioned, and evaluated. The results will provide a validated, realistic technical and economic assessment of the MCHL technology in general.

RESULTS

PNNL successfully received and installed the GEN I unit from Prometheus Energy Group Inc, with guidance from EENW. Updates to the system cooling, electronics, sensors,

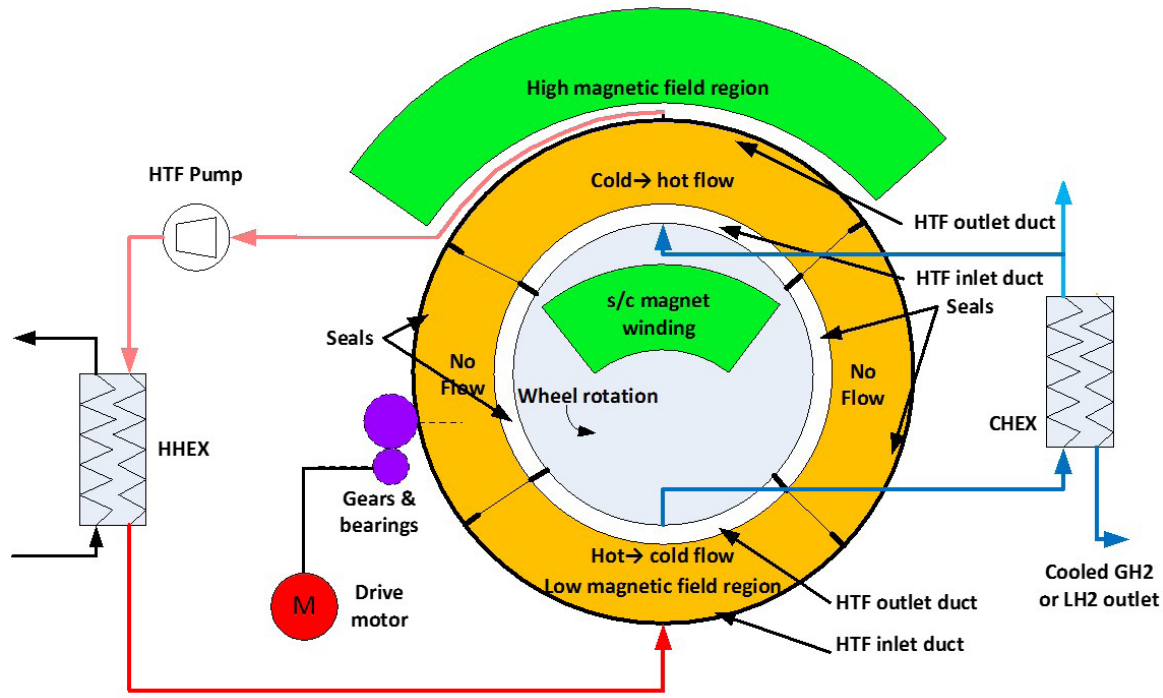

HHEX – hot heat exchanger

FIGURE 4. A block process flow diagram of the rotary magnetic wheel design

and controls were completed. The GEN I prototype used reciprocating dual magnetic regenerators in an AMR cycle (Figure 2). As indicated in an instance in the AMR cycle by the simplified PFD in Figure 3, the top regenerator is out of the high magnetic field and cooled by the magnetocaloric effect. When the bottom regenerator is in the high magnetic field, it is warmed by magnetocaloric effect. While the regenerators are stationary, helium gas at 200 psia from the double acting reciprocating piston pump flows through the chiller heat exchanger and into the top regenerator where it is cooled from ~T_{HOT} to ~T_{COLD}-ΔT_{COLD} as it flows into the CHEX. In the CHEX it picks up a thermal load from a process stream in a liquefier. The remaining portion of the cold helium gas picks up a thermal load in the CHEX and flows through the bottom regenerator where it is warmed to several degrees above T_{HOT} and returns to the helium pump. A programmable chiller is the thermal sink and cools the helium gas to a desired T_{HOT}. Once the flow segment of the AMR cycle in this snap shot is finished, the helium pump is stopped, Regen2 (bottom regenerator) is moved out of the magnetic field and Regen1 (top regenerator) is moved into the high magnetic field region by the drive actuator. After this magnetization/demagnetization segment of the cycle is completed, the helium flow is reversed and so on. A maximum cycle frequency in GEN I is about 0.5 Hz for all four steps in a complete AMR cycle. The dual regenerators are moved by a linear drive actuator in or out of the superconducting magnet along a programmable trapezoidal shaped motion vs. time curve. PNNL's first tests of GEN I were at 3T magnetic field with 1 kg of Gd spherical particles (~150 µm in diameter) in each dual regenerator. The cycle period was 4 s. The helium pump drive with a 20 cm maximum displacement The chiller kept the average temperature T_{HOT} at the warm end of each magnetic regenerator at ~285 K. With these conditions an average cold temperature measured in the CHEX with no external load (only parasitic heat load) was ~225 K. When T_{HOT} was increased to ~312 K, the maximum cold temperature was ~213 K, i.e., essentially 100 K. These temperature spans of 60 K and ~100 K with a single Gd refrigerant for these test parameters surpasses Prometheus's initial result and others in the literature [1].

The cooling power was assessed by applying varying external thermal loads to the CHEX and measuring the CHEX temperature up to 20 K of the T_{HOT}, i.e., 266 K. The load was applied via an installed heater which allowed accurate measurements. The maximum external load under these conditions was 40 W. The parasitic heat leak in this test configuration for GEN I is ~18 W.

We have developed a novel configuration for which we are in the process of submitting a patent application, so we cannot disclose the details. However, the results of the design increased the cooling power by 20% to ~48 W.

Finally, fabrication and tests with a two-layer magnetic material regenerator in the GEN I system were successfully

completed. The only quickly available suitable magnetic refrigerant as ~250 micron spheres we could obtain was $Gd_{0.74}Tb_{0.26}$. This homogeneous rare earth alloy has a Curie temperature of 274 K. We designed and fabricated a new monolithic, layered regenerator comprised of ~108 g of Gd spheres and ~107 g of $Gd_{0.74}Tb_{0.26}$ spheres. A dual regenerator of the same size (~215 g) of only Gd spheres was also fabricated into a monolithic regenerator to compare performance at the same conditions. These two regenerators were assembled into the dual AMR subsystem for GEN I with novel hermetic seals at 200 psia. These new regenerators each had five Type E micro-thermocouples embedded along the central axis of the regenerators to measure temperatures of the magnetic refrigerant and the helium heat transfer gas during the entire four-step AMR cycle. Three different experiments with the layered regenerator provided excellent results. For example, even though the mass of the new Gd and Gd/Tb regenerators was only 215 g each compared to ~1,050 g each for the original Gd regenerators, the temperature span obtained was 43 K with T_{HOT} ~286 K with three quarters of the helium heat transfer gas flow rate. The external load cooling power into the CHEX was ~28.4 W with T_{HOT} at ~285 K and T_{COLD} at ~265 K. (Please note that the parasitic heat leak was the same for the 215 g regenerator as the 1 kg regenerator.) This shows that our improved regenerator design with the layered regenerator operating provided 71% of the cooling power of the original Gd regenerators with only ~20% of the mass of magnetic refrigerant. The improvement in total cooling power due to the novel configuration was ~25% compared to without it. Perhaps the most important result was confirmation that the axial temperature profile from hot to cold in the layered regenerator is nonlinear (Figure 5). To our knowledge, this is the first time the nonlinearity of the temperature distribution has been measured.

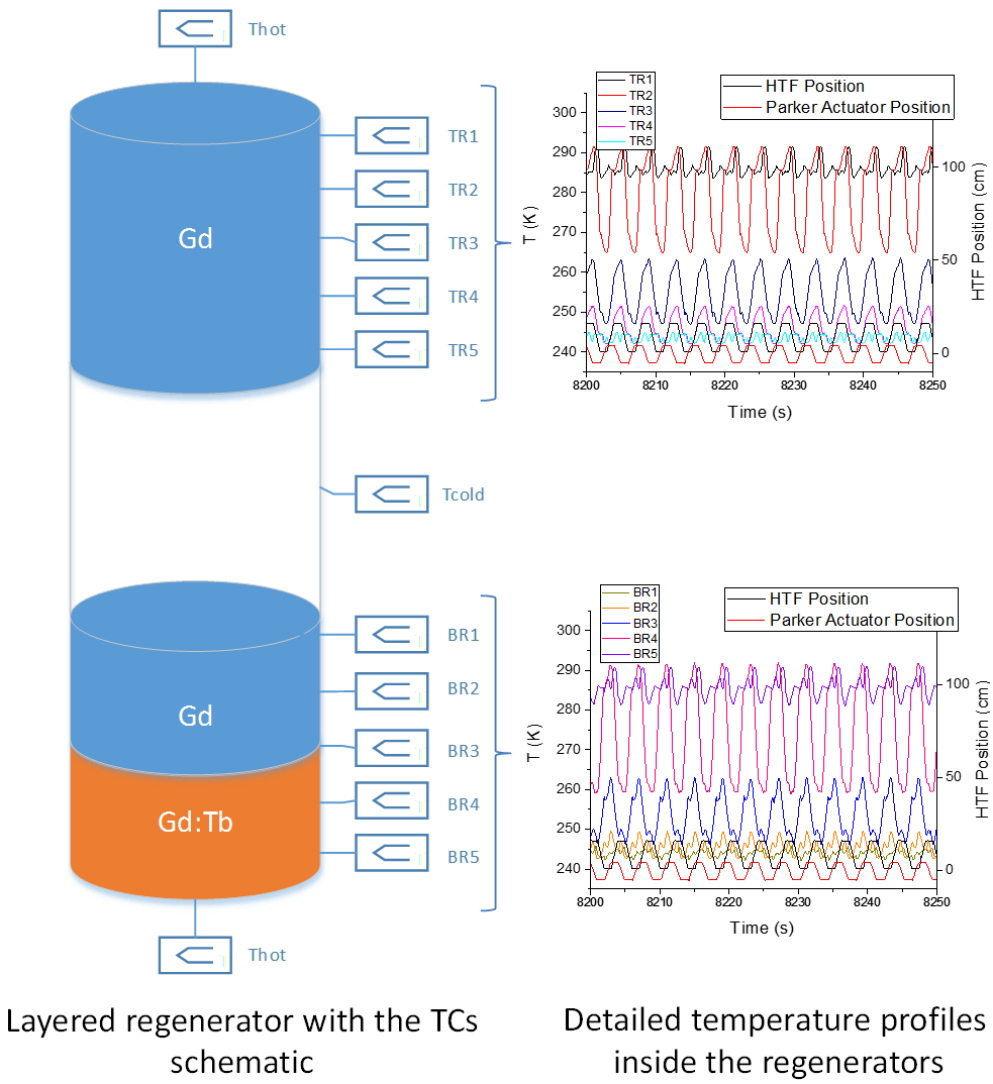

FIGURE 5. Dual regenerator with thermocouple (TC) locations and temperature profiles

CONCLUSIONS AND FUTURE DIRECTIONS

- Successful demonstration of the GEN I system showed the following.
  - A 100 K temperature span was demonstrated.
  - Cooling power of 40 W was demonstrated under optimum efficiency conditions.
  - A novel configuration was demonstrated with the potential of a 20% improvement in cooling power.
  - A multi-layer magnetic material regenerator was demonstrated.
- GEN II system preliminary design takes advantage of these discoveries and other lessons learned from GEN I.
  - It includes a rotary system to improve efficiency, decrease size, and enable other operational improvements.
- Techno-economic analysis is underway.

FY 2016 Work

- GEN I system
  - Magnetic refrigerants specified for GEN II preparation, characterization, and fabrication will be done to validate the performance of materials required for the GEN II system and to test potential new second order magnetic refrigerants provided by Ames.
- GEN II system prototype
  - Single wheel design
    - The rotary design will be proven out.
    - Seals are a major concern and will be an early focus area of the FY 2016 work.
  - A complete PFD and process and instrumentation diagram for each subsystem will be developed, components procured, and each subsystem completed.
- Magnetic materials
  - The shape and size of the magnetic material impacts the performance of the regenerator. Ames will provide tested magnetic refrigerants for this system.

REFERENCES

1. A. Tura, J. Roszmann, J. Dikeos, and A. Rowe, "Cryogenic AMR Test Apparatus," Advances in Cryogenic Engineering, 51, 985–992 (2006).

IV.0 Hydrogen Storage Sub-Program Overview

INTRODUCTION

The Hydrogen Storage sub-program supports research and development (R&D) of materials and technologies for compact, lightweight, and inexpensive storage of hydrogen for automotive, portable, and material handling equipment (MHE) applications. The Hydrogen Storage sub-program has developed a dual strategy, with a near-term focus on improving performance and lowering the cost of high-pressure compressed hydrogen storage systems and a long-term focus on developing advanced cold/cryo-compressed and materials-based low-pressure hydrogen storage system technologies.

In Fiscal Year (FY) 2015, the sub-program continued to focus on the development of lower cost precursors for high strength carbon fibers as well as alternative fiber and resins to lower the cost of composites used in high-pressure compressed hydrogen systems for ambient and sub-ambient conditions. The sub-program also continued efforts on materials-based system engineering for transportation applications and advanced material R&D efforts, including for metal hydrides and hydrogen sorbents.

GOAL

The sub-program's goal is to develop and demonstrate advanced hydrogen storage technologies to enable successful commercialization of fuel cell products in transportation, portable, and MHE applications.

OBJECTIVES

The Hydrogen Storage sub-program's objective is to develop technologies that provide sufficient onboard hydrogen storage to allow fuel cell devices to provide the performance and run-time demanded for the applications. For light-duty vehicles, this means providing a driving range of more than 300 mi (500 km) while meeting packaging, cost, safety, and performance requirements to be competitive with current vehicles. Although some fuel cell electric vehicles (FCEVs) have been demonstrated to travel more than 300 mi on a single fill using high-pressure tanks, this driving range must be achievable across the full range of vehicle models without compromising space, performance, or cost. The Hydrogen Storage sub-program has developed comprehensive sets of hydrogen storage performance targets for onboard automotive, portable power, and MHE applications. The targets can be found in the Multi-Year Research, Development, and Demonstration (MYRDD) Plan.

By 2020, the sub-program aims to develop and verify onboard automotive hydrogen storage systems achieving the following targets that will allow some hydrogen-fueled vehicle platforms to meet customer performance expectations.

- 1.8 kWh/kg system (5.5 wt%)
- 1.3 kWh/L system (0.040 kg H_2/L)
- $10/kWh ($333/kg stored hydrogen capacity)

To achieve widespread commercialization of hydrogen FCEVs across the full range of light-duty vehicle platforms, the sub-program has established the following onboard hydrogen storage targets to ultimately meet the needs for full fleet adoption.

- 2.5 kWh/kg system (7.5 wt%)
- 2.3 kWh/L system (0.070 kg H_2/L)
- $8/kWh ($266/kg stored hydrogen capacity)

Tables that include the complete sets of nearer-term and longer-term targets for onboard automotive, portable power, and MHE applications can be found in the MYRDD Plan.

FY 2015 TECHNOLOGY STATUS AND ACCOMPLISHMENTS

The status of the various storage technologies pursued is evaluated through techno-economic analyses within individual projects, but also through independent analyses carried out for the sub-program.

In the near term, automotive companies plan to commercialize FCEVs that use 700 bar compressed hydrogen storage systems onboard, with system cost being one of the most important challenges to commercialization. In fact, FCEVs have started to be offered this year in California by two automotive original equipment manufacturers (OEMs) for lease or commercial sale with 700 bar compressed hydrogen systems onboard the vehicle.

In FY 2015, the sub-program, working with automotive OEMs through the United States Driving Research and Innovation for Vehicle efficiency and Energy sustainability (U.S. DRIVE) Partnership, adjusted the onboard automotive hydrogen storage system cost targets to reflect advancement of technologies. In FY 2014, the cost target was $12/kWh of usable stored hydrogen to be reached by 2017. This target has now been changed to $10/kWh of usable stored hydrogen to be reached by 2020. The ultimate full fleet cost target remains unchanged at $8/kWh of usable stored hydrogen.

In FY 2015, Strategic Analysis Inc. (SA) updated the cost projections for 700 bar compressed hydrogen storage systems. The updated analysis projects a system cost $14.69/kWh, an overall cost reduction of approximately $2/kWh from the baseline cost of $16.76/kWh established in FY 2013. The analysis reflects recent technology advancements to reduce cost of carbon fiber precursor and resin and technology advancements through balance of plant (BOP) components integration. The analysis also includes changes in the tank design to better reflect commercially manufactured pressure vessels that result in increased projected costs. Specific changes to the 700 bar pressure vessel system cost include use of a low cost carbon fiber precursor based on high volume textile fiber processes developed by Oak Ridge National Laboratory (ORNL); BOP component revisions to reduce the number of fittings; and use of a low cost, low density resin identified by Pacific Northwest National Laboratory (PNNL). The analysis this year also explicitly accounted for cost increases associated with manufacturing design changes suggested by industry, including the removal of pre-woven endcaps and increased composite layer thickness to account for a more robust assessment of manufacturing variations. The relative cost impact of each component change is presented in Figure 1. The overall performance of the revised 700 bar compressed systems compared to the onboard storage targets is shown in Figure 2.

As a longer-term strategy, the Hydrogen Storage sub-program continues to pursue less mature hydrogen storage technologies that have the potential to satisfy all onboard hydrogen storage targets. These technologies include cold (sub-ambient temperatures as low as ~150–200 K) and cryo-compressed (temperatures <150 K) hydrogen and materials-based storage technologies. The materials-based efforts include total systems engineering and advanced hydrogen storage materials development. A major effort in materials-based system development the last several years has been through the Hydrogen Storage Engineering Center of Excellence (HSECoE).

The HSECoE is completing its Phase III activities in 2015, focusing on evaluation of two hydrogen adsorbent system designs that differ in heat exchanger concept, and completing the validation and posting of their complete system models for use by the research community. Updated spider charts, shown in Figures 3a–c, have been prepared for all three material types, indicating the current projected status of full scale systems compared against the DOE 2020 targets. The two prototype hydrogen adsorption systems have been built and are undergoing evaluation, primarily at Savannah River National Laboratory (SRNL), Oregon State University (OSU), and Université du Québec à Trois-Rivières (UQTR). One prototype (hexcell) uses a flow-through concept where excess hydrogen removes the heat of adsorption as it passes through the adsorbent that is packed within an aluminum hexagonal honeycomb structure. The second prototype uses a modular adsorption tank insert (MATI) microchannel heat exchanger that is cooled by flowing liquid nitrogen through it.

In the MATI concept, the adsorbent is compacted into densified pucks that are sandwiched between the MATI cooling plates, whereas, in the hexcell design, the adsorbent is packed as a powder within the hexagonal honeycomb structure. The effectiveness of the two heat exchange concepts will be evaluated, the performance compared with the modeled predictions, and the results used to improve and validate the system models. While the prototype testing focuses on removing/supplying the heat of hydrogen adsorption/desorption, PNNL and Hexagon Lincoln carried out efforts to evaluate the effectiveness of using liquid nitrogen to directly cool the vessel walls for fast fill capabilities. In their concept, the vessel includes an annular space around the outer surface of the pressure vessel containing the sorbent through which liquid nitrogen could flow.

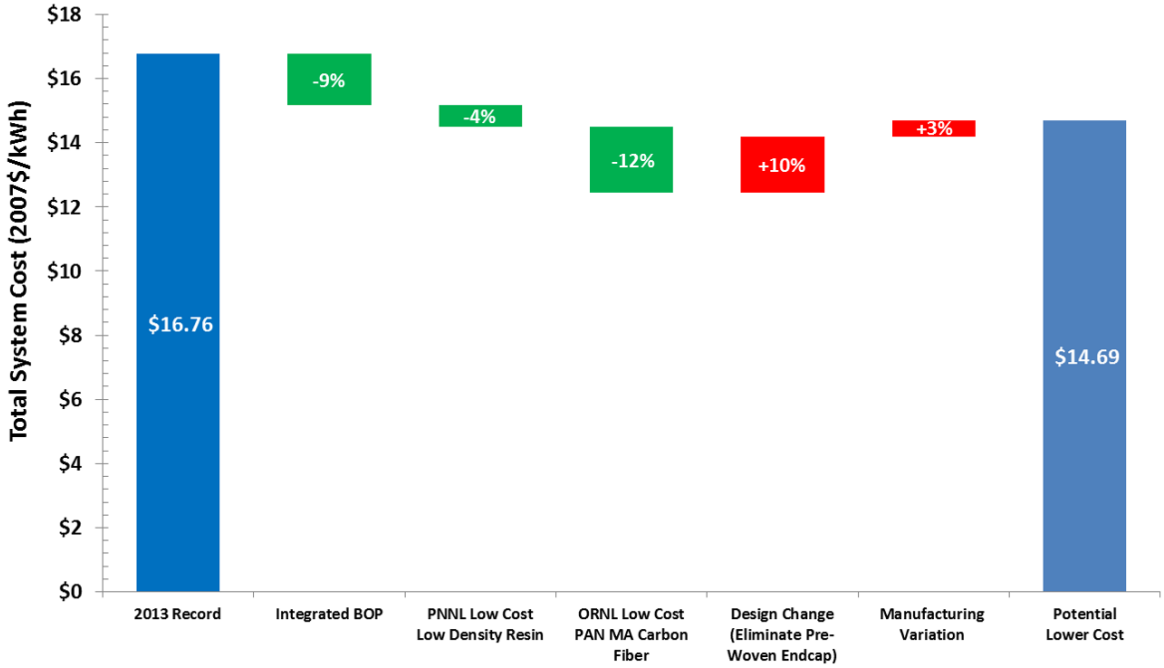

PAN MA – polyacrylonitrile with methyl acrylate

FIGURE 1. Revised projected costs for 700 bar compressed hydrogen storage systems for light-duty vehicles at 500,000 systems per year production, comparing approximate cost impacts of multiple simultaneous changes in carbon fiber pressure vessel systems between 2013 and 2015

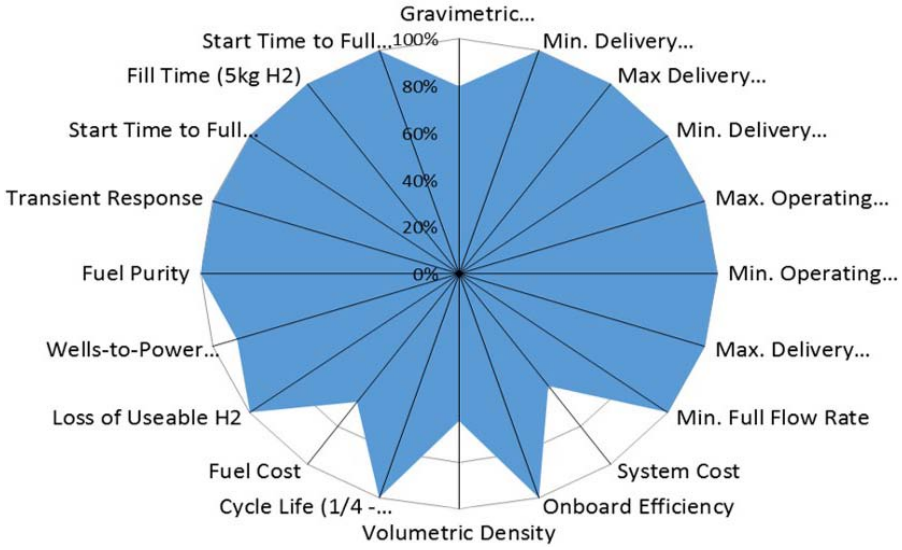

FIGURE 2. Spider chart comparing current projected performance of a state-of-the-art 700 bar compressed hydrogen storage system with 5.6 kg usable hydrogen storage with the 2020 onboard automotive targets

Results from sub-scale testing projected for a full scale vessel indicated that it could be cooled to the targeted temperature of 80 K in less than 3.5 min, meeting the fast fill requirements. National Renewable Energy Laboratory (NREL), working with the HSECoE partners, has posted framework models for all three material (metal hydride, chemical hydrogen, and sorbent) system types on the HSECoE.org website for use by the research community. One

improvement to these models in 2015 was the addition of a graphical user interface (GUI), making them more user friendly. The site also contains the metal hydride acceptability envelope and finite element models and the tank volume/cost estimator model.

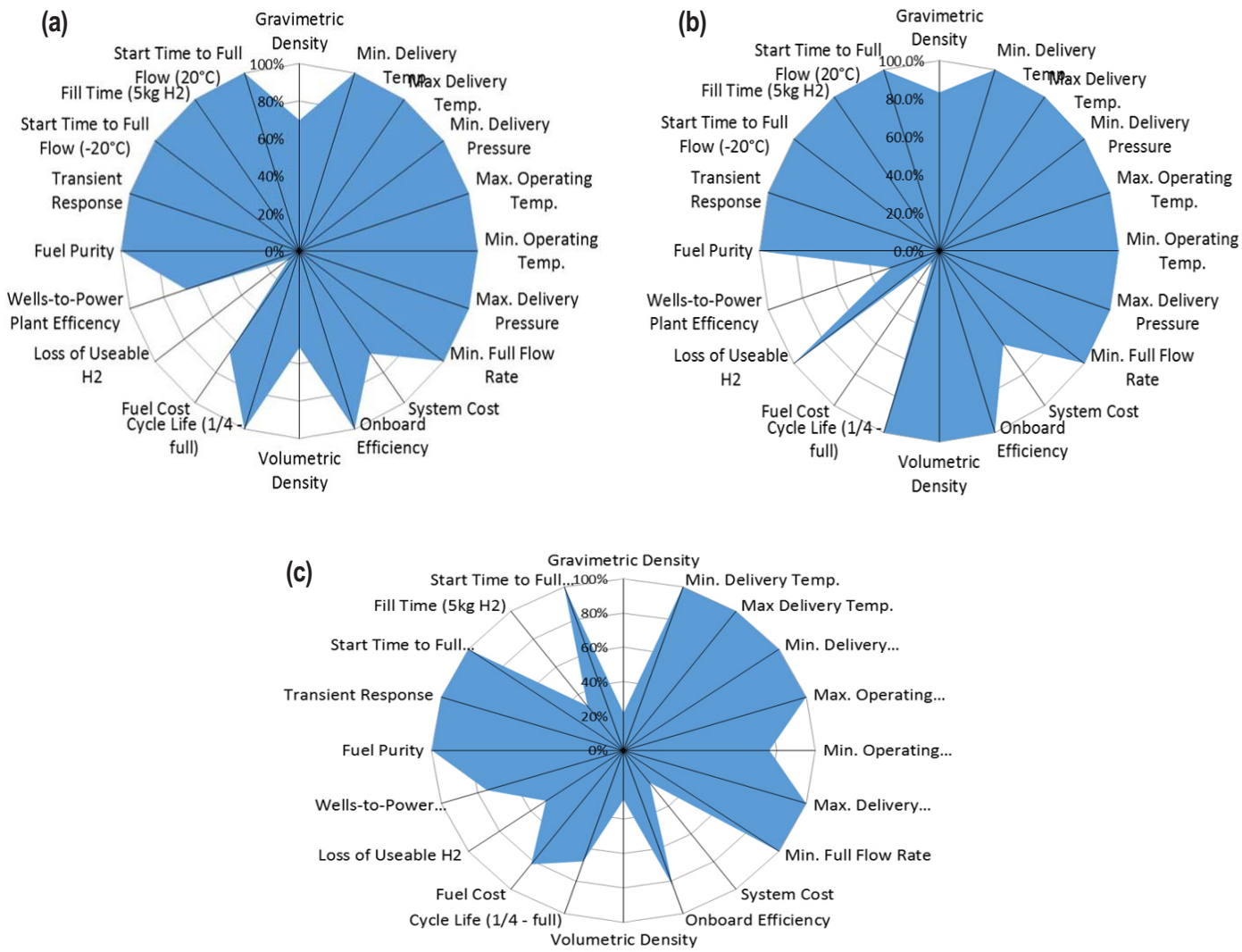

FIGURE 3. Projected status of full scale, 5.6 kg usable hydrogen systems versus the DOE 2020 onboard light-duty vehicle targets: (a) metal hydride system with $NaAlH_4$, (R&D terminated at end of Phase I); (b) chemical hydrogen storage system (50 wt% alane slurry) (R&D terminated at end of Phase II); (c) sorbent system with metal organic framework (MOF)-5 and flow-through hexcell heat exchanger design (status at end of Phase II, prototype testing continuing in Phase III)

Testing & Analysis

In FY 2015, the Hydrogen Storage sub-program continued carrying out techno-economic assessments of hydrogen storage technologies. Technical analysis and cost modeling of Type IV pressure vessel systems remained a critical focus during FY 2015, with detailed analyses to determine updated cost projections for the 700 bar system. Additionally, analyses were performed to reverse engineer chemical hydrogen storage material system performance to identify material property and well-to-tank (WTT) efficiency requirements to meet DOE system-level performance targets.

Specific accomplishments include the following.

- Updated analyses for the 700 bar compressed hydrogen storage system, resulting in a projected overall cost reduction of approximately $2/kWh (12%) from the 2013 baseline cost of $16.76/kWh (SA)

- Completed a Design for Manufacturing Assembly® analysis of two sorbent-based onboard hydrogen storage systems, the MATI and hexcell concepts as designed by the HSECoE (SA)
- Formulated system models and performed reverse engineering to determine material properties of chemical hydrogen storage materials needed to meet system targets, including WTT efficiency targets (Argonne National Laboratory [ANL])
- Conducted onboard cold gas (195 K and 400 bar) hydrogen storage system and related off-board WTT efficiency analyses; the results projected a ~30% increase in gravimetric capacity and a 13% decrease in off-board WTT efficiency over the baseline condition

Advanced Physical Storage

In FY 2015, the sub-program continued to reduce the cost of compressed hydrogen gas storage tanks, with efforts focused on low cost, high strength carbon fiber precursors, alternative fiber and resin, cold temperature operation, and advanced tank designs. Lightweight compressed gas storage vessels requiring a composite overwrap to contain hydrogen gas are considered the most likely near-term hydrogen storage solution for the initial commercialization of FCEVs, as well as for other early market applications. The carbon fiber composite used as overwraps can contribute as much as 75% or more to the overall cost of advanced Type IV tanks. The Hydrogen Storage sub-program supported efforts at ORNL to reduce the cost of polyacrylonitrile-based (PAN) fibers used as precursors to produce high strength carbon fibers. The ORNL efforts focused on advanced precursor materials and processing since precursors have been shown to contribute approximately 50% of the total cost of high strength carbon fibers. The team continued to investigate the development of melt-spinnable PAN precursors and processing techniques to replace the current more costly solution spinning methods. Additionally, a team led by PNNL focused on reducing the cost of a Type IV tank system by developing novel alternative resins and resin matrix modifications, modifying the carbon fiber surface to improve composite translational efficiency, developing methods for alternative fiber placement, and identifying enhanced operating conditions that demonstrate routes to increase carbon fiber usage efficiency.

In FY 2015, one new sub-program award was made.

- Center for Transportation and the Environment will work to develop advanced conformable 700 bar hydrogen storage systems that employ an over-braided, coiled pressure vessel that has the potential to surpass DOE system targets for specific energy (3.7 kWh/kg) and cost (<$10/kWh).

Specific accomplishments include the following.

- Developed alternative low cost and low density resin with equivalent or better performance than the currently used epoxy resin, resulting in a projected reduction in storage system cost (by SA) of $0.59/kWh compared to DOE's 2013 baseline (PNNL)
- Evaluated a graded construction approach utilizing thick wall effect and, evaluating various low cost fibers, identified Panex 35™ as a potential candidate fiber for the outer wrappings of the pressure vessels (Composite Technology Development)
- Produced a thick composite panel with less than 1% void volume through use of vacuum infusion of a low viscosity resin into dry-wound fiber forms (Materia)
- Initiated pilot scale production development of an ultra-high strength glass fiber (≥5,500 MPa) and evaluation of its performance in composites as a low cost alternative to carbon fiber in Type III and IV tanks (PPG Industries Inc.)
- Established a baseline for strain-hardened Type 316L stainless steel as a first step in an effort to identify alternative metal alloys that can be used as substitutes for materials of construction in balance of plant components for hydrogen applications, leading to lower costs and lower mass (Sandia National Laboratories)
- Initiated preliminary testing of the liquid hydrogen cryo-pump installation with 875 bar capability and installation of test facilities for extended cycle testing of high pressure cryo-compressed hydrogen storage systems (Lawrence Livermore National Laboratory [LLNL])

Advanced Materials Development

In FY 2015, the sub-program continued efforts in developing and improving hydrogen storage materials with potential to meet the 2020 onboard storage targets. In the area of metal hydrides, efforts emphasized material

discovery coupled with reducing desorption temperatures and improving kinetics. For hydrogen sorbents, efforts were focused on increasing the isosteric heat of adsorption mainly through inclusion of open metal centers or boron doping to increase the adsorbed capacity at higher temperatures, as well as on improving standard measurement practices for hydrogen capacity. Also in FY 2015, the Hydrogen Storage sub-program continued efforts to collect and disseminate materials data on advanced hydrogen storage materials that comprise the hydrogen storage materials database (http://hydrogenmaterialssearch.govtools.us/).

Four new awardees were selected in FY 2015.

- California Institute of Technology will develop high surface area adsorbents using graphene or exfoliated graphite to prepare materials with high volumetric capacity and gravimetric capacity of 11 wt% or higher.
- Texas A&M University will develop MOF sorbents with capacities that exceed the conventional storage limit per unit surface area of 1 wt% excess per 500 cc/g (the Chahine Rule) and improve system performance through enhanced thermal conductivity of sorbents/carbon composites.
- University of Michigan will investigate best-in-class sorbents that can simultaneously achieve higher volumetric and gravimetric density, identified through a computational survey of materials reported in the Cambridge Structural Database.
- Ames Laboratory will investigate silicon borohydrides and graphene composites as a way to develop low cost, reversible, high performance hydrogen storage materials; computational modeling will guide the experimental work in development of these materials.

Specific accomplishments include the following.

- Developed recommended volumetric capacity definitions and measurement protocols for hydrogen sorbent analyses to help the research community better report and understand its volumetric capacity material results and initiated dissemination of the protocols to the research community (NREL)
- Completed a comprehensive evaluation of the top performing MOFs for hydrogen storage, including Ni_2(*m*-dobdc), Co_2(*m*-dobdc), Ni_2(dobdc), Co_2(dobdc), and MOF-5. High-pressure isotherms were measured at 100°C, 75°C, 50°C, 25°C, 0°C, -25°C, -40°C, -50°C, and -75°C in order to determine the optimal temperature process to maximize total volumetric hydrogen usable capacity (Lawrence Berkeley National Laboratory [LBNL])
- Used high pressure neutron diffraction to determine the binding profile of hydrogen within MOF-5 at high pressures (up to 100 bar) and moderate temperature (77 K); this technique allows for the understanding of the density profile of hydrogen in the pores of MOFs and is currently being expanded for use with other MOF materials (LBNL)
- Developed a reverse pulsing technique to significantly reduce dendrite formation during electrochemical generation of alane and optimized the crystallization process for pure a-alane production (SRNL)
- Demonstrated formation of polymerized BH_x from $B_{10}H_{14}$ and hydrogen evolution from a reaction between BH_x and LiH (HRL Laboratories)
- Established initial modeling framework to predict phase fractions, accounting for (1) thermodynamics of interfaces, surfaces, and bulk; (2) elastic effects and mechanical stress/strain; and (3) phase nucleation/evolution and non-equilibrium (de)hydrogenation; completed initial calculations of thermodynamic parameters for bulk and surface MgB_2-$Mg(BH_4)_2$ (LLNL)

Engineering

In FY 2015, the HSECoE constructed two 2-L hexcell and MATI prototype sorbent systems and initiated evaluation of each. The MATI system was constructed and modeled by OSU, and evaluations are being carried out by SRNL. The hexcell system was constructed and is being evaluated by UQTR, with SRNL modeling the system. PNNL and Hexagon Lincoln carried out testing to evaluate the use of liquid nitrogen to quickly cool the vessel walls for fast refilling of the sorbent systems. Several HSECoE partners, such as NREL, United Technologies Research Center (UTRC), PNNL, OSU, and SRNL, were involved in continued efforts in developing and validating the complete system models integrated into a framework with vehicle and fuel cell level models. In FY 2015, significant efforts were also devoted to developing a GUI to make the models more user friendly. The models are posted on the models page of the HSECoE website (http://hsecoe.org/models.html), publically available for use by the hydrogen storage R&D community.

Specific accomplishments include the following.

- Completed assembly of a cryo-sorbent prototype test station (SRNL)
- Completed assembly and initiated evaluation testing of two sub-scale sorbent prototype systems (SRNL, OSU, UQTR)
- Evaluated alternative concepts for thermal conductivity enhancements (Ford, OSU)
- Evaluated use of liquid nitrogen to rapidly cool vessel walls to enable fast fill of hydrogen cryo-sorbent systems (PNNL, Hexagon Lincoln)
- Designed, built, and demonstrated an apparatus for and performed thermal conductivity measurements of hydrogen sorbent materials at hydrogen pressures up to 100 bar at liquid nitrogen temperatures; quantified the isotropic and anisotropic thermal conductivities for MOF-5 at elevated hydrogen pressures (LANL)
- Updated and posted HSECoE system models, including for 700 bar compressed storage systems, metal hydride systems, two chemical hydrogen storage systems, and adsorbent systems; completed sub-model validation, GUI improvements, and model parametrization (NREL, UTRC, PNNL, SRNL)

BUDGET

Of the FY 2016 budget request, $15.6 million is planned for hydrogen storage, consistent with $15.6 million from the FY 2015 congressional appropriation (Figure 4). In FY 2016, the Hydrogen Storage sub-program will continue to focus on nearer-term R&D to lower the cost of high pressure storage systems and longer-term technology development including cold/cryo-compressed hydrogen and materials-based storage technologies. The sub-program will also continue to carry out systems analyses. The sub-program plans to initiate new activities in these areas for onboard automotive applications.

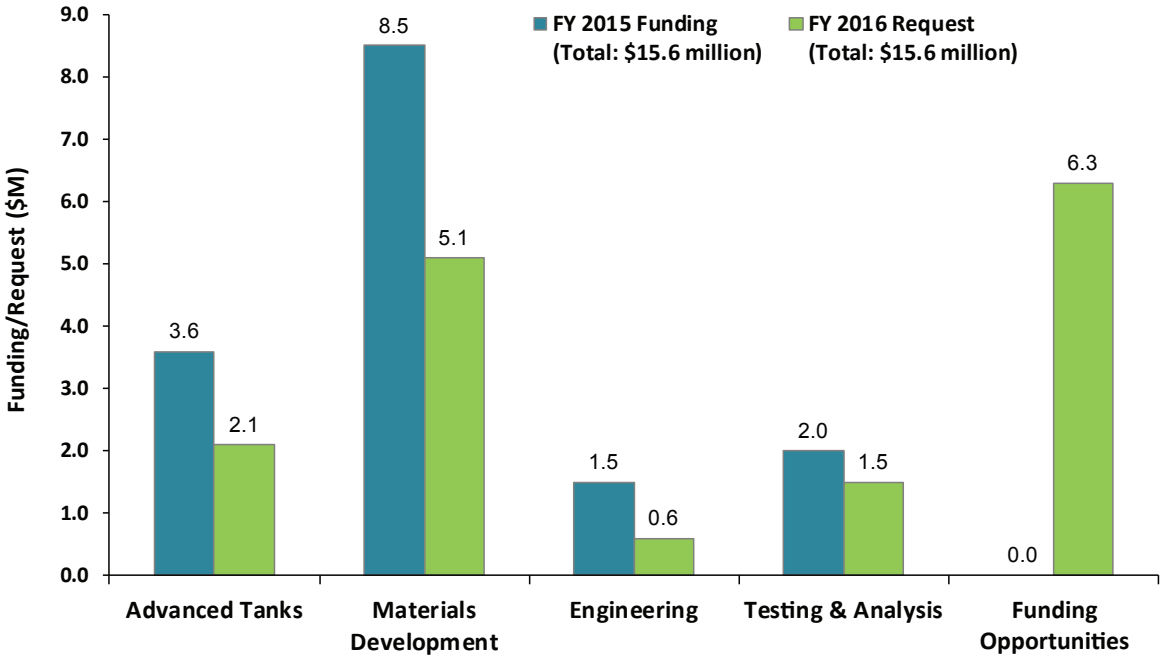

FIGURE 4. Hydrogen Storage R&D Funding. Subject to appropriations, project go/no-go decisions, and competitive selections. Exact amounts will be determined based on research and development progress in each area and the relative merit and applicability of projects competitively selected through planned funding opportunity announcements.

FY 2016 PLANS

The technology portfolio for the Hydrogen Storage sub-program emphasizes materials R&D to meet system targets for onboard automotive and non-automotive applications. The emphasis on developing lower cost physical storage technologies will continue and be coordinated with related activities through the Vehicle Technologies Office and Advanced Manufacturing Office (AMO) of the DOE Energy Efficiency and Renewable Energy Office. Specifically, the sub-program will coordinate with and leverage efforts through the recently established AMO-led Institute for Advanced Composite Manufacturing Innovation to develop approaches to low cost compressed gas storage systems manufacturing. System analysis will continue through efforts at ANL and SA. A new major thrust is planned for FY 2016 and includes a coordinated effort on development of advanced hydrogen storage materials with the requisite properties needed to enable a complete system to meet all of the onboard storage targets. The effort will involve a core national lab team that will carry out coordinated basic and applied research to further understanding of the interaction of hydrogen with storage materials; develop computational material design tools for developing materials with target properties; and work with individual research projects, competitively selected through future funding opportunity announcements, to design materials possessing characteristics needed to meet performance requirements.

Ned Stetson
Hydrogen Storage Program Manager
Fuel Cell Technologies Office
Office of Energy Efficiency and Renewable Energy
U.S. Department of Energy
1000 Independence Ave., SW
Washington, D.C. 20585-0121
Phone: (202) 586-9995
Email: Ned.Stetson@ee.doe.gov

IV.A.1 System Analysis of Physical and Materials-Based Hydrogen Storage

Rajesh K. Ahluwalia (Primary Contact), T.Q. Hua, J-K. Peng, and Hee Seok Roh
Argonne National Laboratory
9700 South Cass Avenue
Argonne, IL 60439
Phone: (630) 252-5979
Email: walia@anl.gov

DOE Manager
Grace Ordaz
Phone: (202) 586-8350
Email: Grace.Ordaz@ee.doe.gov

Start Date: October 1, 2004
Projected End Date: Project continuation and direction determined annually by DOE

Overall Objectives

- Model various developmental hydrogen storage systems
- Provide results to Hydrogen Storage Engineering Center of Excellence (HSECoE) for assessment of performance targets and goals
- Develop models to reverse engineer particular approaches
- Identify interface issues, opportunities, and data needs for technology development

Fiscal Year (FY) 2015 Objectives

- Performed ABAQUS analysis of improved Type 4 tank design that has the potential to reduce carbon fiber (CF) requirement
- Determine relationship between high-density polyethylene (HDPE) liner properties and liner failure at cryogenic temperatures to support cryo/cold H_2 storage
- Determined well-to-wheel energy consumption and fuel cost for cold hydrogen storage
- Establish chemical hydrogen material properties needed to satisfy onboard and off-board storage system targets

Technical Barriers

This project addresses the following technical barriers from the Hydrogen Storage section of the Fuel Cell Technologies Office Multi-Year Research, Development, and Demonstration Plan:

(A) System Weight and Volume

(B) System Cost

(C) Efficiency

(E) Charging/Discharging Rates

(J) Thermal Management

(K) System Life Cycle Assessments

Technical Targets

This project is conducting system level analyses to address the DOE 2017 technical targets for onboard hydrogen storage systems:

- System gravimetric capacity: 1.8 kWh/kg
- System volumetric capacity: 1.3 kWh/L
- Minimum H_2 delivery pressure: 5 bar
- Refueling rate: 1.5 kg/min
- Minimum full flow rate of H_2: 0.02 g/s/kW

FY 2015 Accomplishments

- ABAQUS analysis was conducted to determine HDPE liner behavior at cryogenic temperatures. The analysis predicted liner failure at -190°C for a liner with stiffness of 6 GPa and liner separation from the composite if tank pressure is below 3.2 MPa. ABAQUS analysis revealed high stress concentration at the liner/boss interface corners with peak stress approaching the liner tensile strength if the tank is kept at -190°C and 63 MPa internal pressure.
- Off-board analysis was performed for the cold gas storage option and determined that fuel cost is about 5% higher than baseline (700 bar compressed H_2) but onboard cost is ~20% lower. The well-to-wheel energy efficiency is about six percentage points lower than baseline.
- We formulated models and performed reverse engineering to determine thermodynamic properties of chemical hydrogen materials needed to meet onboard system and off-board well-to-engine efficiency targets.

✧ ✧ ✧ ✧ ✧

INTRODUCTION

Several different approaches are being pursued to develop onboard hydrogen storage systems with the goal of meeting the DOE targets for light duty vehicle applications. Each approach has unique characteristics, such as the thermal energy and temperature of charge and discharge, kinetics of the physical and chemical process steps involved, and requirements for the materials and energy interfaces between the storage system and the fuel supply system on the one hand and the fuel user on the other. Other storage system design and operating parameters influence the projected system costs as well. We are developing models to understand the characteristics of storage systems based on the various approaches and to evaluate their potential to meet the DOE targets for onboard applications, including the off-board targets for energy efficiency.

APPROACH

Our approach is to develop thermodynamic, kinetic, and engineering models of the various hydrogen storage systems being developed under DOE sponsorship. We then use these models to identify significant component and performance issues, and to assist DOE and its contractors in evaluating alternative system configurations and design, and operating parameters. We establish performance criteria that may be used, for example, in developing storage system cost models. We refine and validate the models as data become available from the various developers. We work with the Hydrogen Storage Systems Analysis Working Group to coordinate our research activities with other analysis projects to assure consistency and to avoid duplication. An important aspect of our work is to develop overall systems models that include the interfaces between hydrogen production and delivery, hydrogen storage, and the fuel cell.

RESULTS

Physical Storage

We conducted ABAQUS analysis of HDPE liner in Type 4 tanks for cold gas storage. We obtained the tensile stress strain data for HDPE from Pacific Northwest National Laboratory (PNNL) for two different temperatures, 25°C and -190°C [1]. The samples were prepared by injection, extrusion, or cut from a sheet. Two types of sheet samples were used, differing in the Young's modulus (2 GPa and 6 GPa). The data were fitted for input to ABAQUS for our analysis. We analyzed a typical Type 4 tank (length to diameter ratio = 3) which holds 5.6 kg recoverable hydrogen. The hoop and helical thicknesses of the carbon fiber composite were determined for nominal 500 bar storage pressure with a 2.25 safety factor. The HDPE liner is assumed to be 5 mm thick.

Figure 1 shows the calculated stresses in the liner with different Young's modulus. Initially the tank has an inner pressure of 2 MPa and is at room temperature. The small inner pressure does not cause the tank to deform; as a result the liner experiences a small compressive stress (black lines). As the tank cools down to -190°C, the inner pressure acts to oppose liner shrinkage causing the liner to be under tension. The axial and hoop tensile stresses (blue curves) are higher for the stiffer liner (6 GPa) but remain below the tensile strength. Increasing the inner pressure from 2 MPa to 63 MPa introduces compressive stress in the "soft" liner (E = 2 GPa). This is due to the larger deformation in the liner than the deformation of the tank in both the axial and

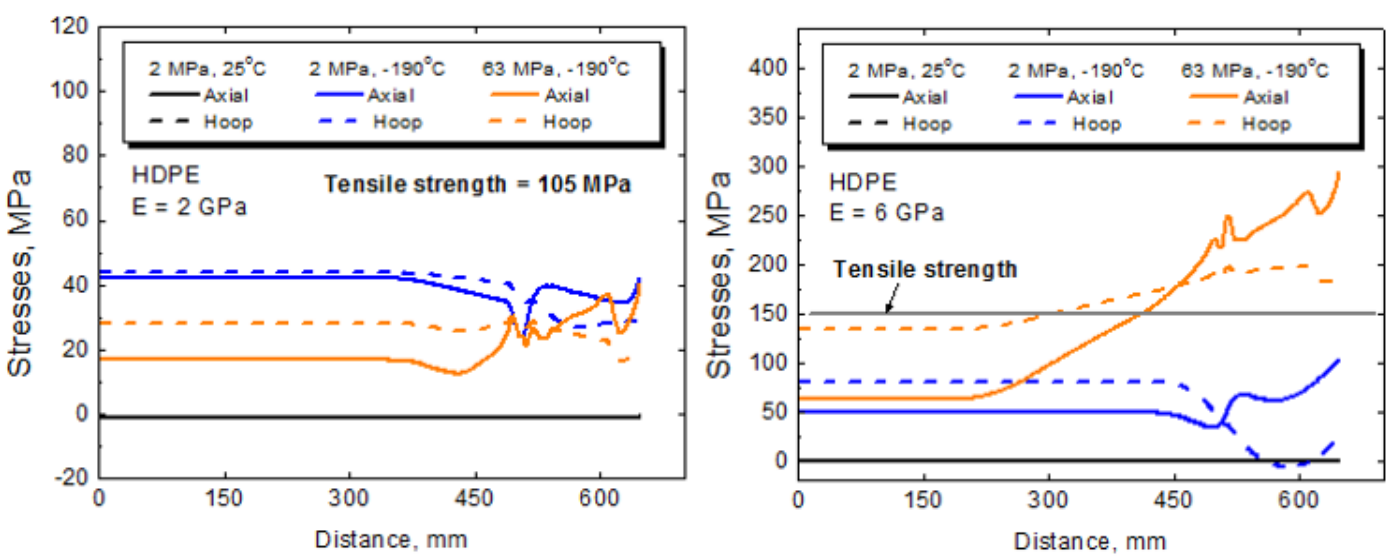

FIGURE 1. Axial and circumferential stresses in the HDPE liner for E = 2 and 6 GPa

hoop directions. The compressive stress has the net effect of reducing the tensile axial stress to 17 MPa and the hoop stress to 28 MPa. In the "stiff" liner (E = 6 GPa), increasing the inner pressure from 2 MPa to 63 MPa results in an increase in the tensile stress which exceeds the tensile strength of the liner. Under this scenario, liner failure is predicted.

Figure 2 shows that at -190°C, there is a minimum inner pressure needed to avoid liner separation as a result of the difference in the coefficients of thermal expansion (CTE) between liner and the composite. The gap can be as large as 6.4 mm in the dome and 2.8 mm in the cylinder if the tank is empty. The gap in the cylinder is eliminated and reduces to 1.3 mm in the dome if the tank has an inner pressure of 2 MPa. No gap exists when the pressure exceeds 3 MPa.

Additionally, ABAQUS simulations of the full-sized tank reveal high stress concentration region at the interface corners between the liner and the aluminum boss. At room temperature and inner pressure of 2 MPa, the peak stress at the interface is 1.9 MPa and increases 25-fold to 48 MPa when the tank is cooled to -190°C due to CTE mismatch between the HDPE liner and Al-6061 boss. The peak stress approaches the tensile strength of the liner (105 MPa) when the tank is further pressurized to 63 MPa at -190°C. For comparison, testing of two Type 4 tanks at liquid nitrogen (LN_2) temperature by Hexagon Lincoln showed that both tanks leaked at <28 MPa and cracks occurred at the liner–boss interface [2].

We analyzed an off-board delivery pathway for cold gas. Hydrogen is produced by steam methane reforming, transmitted via pipeline to the gas terminal at city gate. At the gas terminal, H_2 is compressed to 340 bar, then cooled to 83 K using LN_2 for storage in trailer tubes which are transported to the forecourt by tube trailers. Liquid nitrogen production plant is assumed to co-locate with the gas terminal. At the forecourt, the cold gas is compressed to 1.35x the nominal onboard storage pressure and stored in insulated Type 3 tube banks for cascade refueling. We conducted netting analysis (calibrated with ABAQUS model) to determine the weight, volume, and hydrogen capacity for the trailer tubes constrained by the International Organization for Standardization container dimensions and trailer payload for both baseline (700 bar, 300 K onboard) and cold gas storage (400 bar, 200 K onboard). Similar analysis was also carried out for the cascade storage tubes at the forecourt. As presented in Table 1, the amount of carbon fiber composite required for baseline is ~2.6x the requirement for cold gas. While the cost of CF is lower, the cold trailer tubes incur added cost for vacuum insulation. We estimated that the cold gas trailer tubes were ~38% lower in total cost due to the substantial reduction in CF requirement.

The off-board primary energy consumption for cold gas option is equivalent to ~ 60% of the lower heating value of hydrogen, and is ~73% higher than for baseline. The well-to-tank efficiency for cold gas storage was less than 50%, approximately six percentage points lower than baseline (Figure 3). The reduction is due primarily to the significant amount of electricity consumed to produce liquid nitrogen (7 kg LN_2/kg H_2) for cooling H_2 to 83 K at the gas terminal. We estimated that the off-board cost for cold gas is \$0.18–\$0.31/kg H_2 higher than baseline due to significantly higher costs at the gas terminal partially offset by lower costs at the forecourt and lower tube trailer costs.

Hydrogen Storage in Chemical Hydrogen Materials

We conducted a reverse engineering analysis to determine the minimal material requirements for a chemical hydrogen storage system to meet the DOE 2017 performance targets. Materials with negative free energy of decomposition (ΔG) are thermodynamically unstable at room temperature and are stabilized by extremely slow kinetics (e.g., alane, AB) or by other chemical means (addition of 3% NaOH to aqueous $NaBH_4$). Materials with positive ΔG (e.g., n-ethylcarbazole) are stable at room temperature. They can be decomposed at elevated temperatures or require a catalyst for sufficient kinetics at low temperatures. Results from our previous

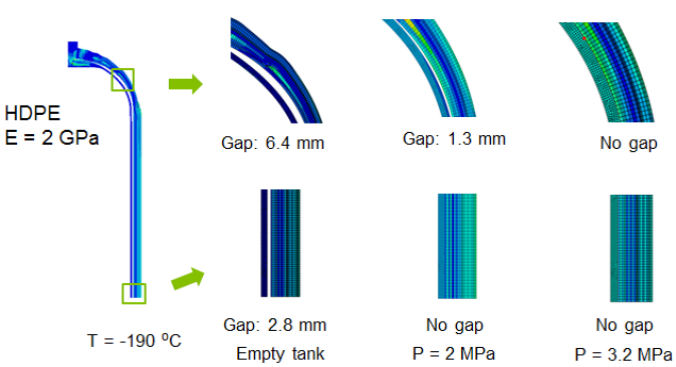

FIGURE 2. Gaps between the HDPE liner and the composite at -190°C

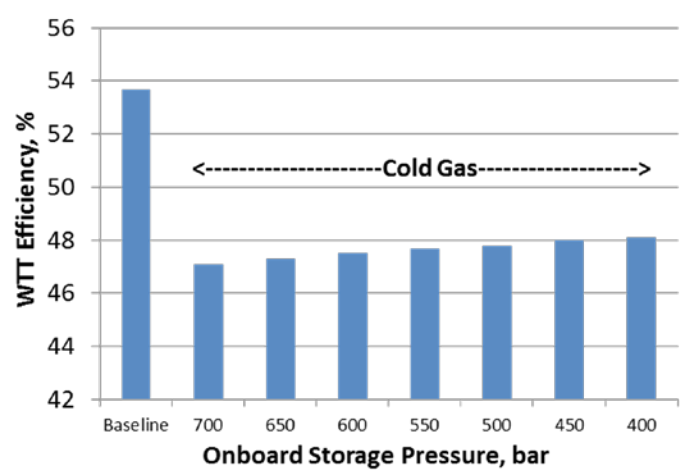

FIGURE 3. Well-to-tank (WTT) efficiency for ambient and cold gas storage

TABLE 1. Physical Parameters and CF Requirements for Storage Tubes

	Unit	Trailer Tube		Cascade Storage Tube	
		Baseline	Cold Gas	Baseline	Cold Gas
Type		4	3	3	3
Nominal Storage Pressure	bar	340	340	945	534
Minimum Pressure	bar	15	15	varies	varies
Nominal Storage Temperature	K	300	83	300	116
H_2 Stored	kg	116	137	46	45.3
H_2 Volume	m^3	5.1	2.25	0.96	0.77
Outside Length	m	12.1	11.1	5.8	5.1
Outside Diameter	m	0.79	0.56	0.58	0.51
Carbon Fiber Composite Weight	kg	1,148	425	712	278
Liner (Al or HDPE) Weight	kg	138	402	190	189
Shell Weight	kg	-	487	-	329
Total Tube Weight	kg	1,421	1,483	958	856

regeneration analyses for $NaBH_4$, AlH_3, AB, CBN, and LCH_2 were used to develop correlations between regeneration primary energy and free energy of decomposition. Three sets of correlations were obtained for low, medium, and high regeneration efficiencies. It was found that materials with large positive ΔG require elaborate regeneration processes with high demand for primary energy while materials with negative ΔG (rehydrogenation reaction is exothermic) or small positive ΔG require significantly less primary energy for regeneration. To achieve well-to-tank regeneration efficiencies of 50–60%, the free energy of decomposition should exceed 1.6 kJ/mol if ΔG(298 K) is positive and >-6.4 kJ/mol if ΔG(298 K) is negative. Over this narrow range of the desired ΔG(298 K) and for the expected material entropy in the range of 80–130 J/mol K, the enthalpy of reaction ΔH needs to be between 20 kJ/mol H_2 and 40 kJ/mol H_2, therefore exothermic materials are unsuitable. It was also noted that materials that decompose above the fuel cell system (FCS) coolant temperature (a burner is needed to provide the heat for decomposition) may not be acceptable since the onboard system efficiency is <70% for ΔH = 40 kJ/mol-H_2. It is desirable to have a class of materials that can decompose at 60–80°C using the FCS waste heat, mostly likely as a catalytic process in the reactor, otherwise the material would have short shelf life. Additionally, the desired decomposition kinetics should be independent of back pressure because the equilibrium hydrogen partial pressure at these conditions are too low, and as a result, the onboard buffer tank would have to be refueled with high pressure gaseous H_2 at the forecourt, a scenario that is unlikely to be acceptable.

Two onboard systems were analyzed, one with a burner and one without. The main system components include a volume exchange fuel tank, a hydrogen buffer tank for start-up and to accommodate fast transients, a reactor that operates at elevated pressure, reaction kinetics that are independent of back pressure, and heat exchangers (Figure 4). The fuel may be liquid, slurry, or in solution. For systems with a burner, a 50-kW microchannel HEX burner is used. For a reactor that operates at 150°C and ΔH = 40 kJ/mol H_2, the target usable gravimetric capacity of the material is 21 wt% H_2 with a volumetric capacity of 114 g H_2/L. The material capacity targets are strong functions of reactor temperature and ΔH. It was difficult to meet the 90% onboard system efficiency if a burner is needed. For systems without a burner, the reactor is thermally integrated with the FCS and provides an advantage of mitigating the FCS heat rejection problem. For a reactor that operates at 70–80°C with 100-bar back pressure, the target material capacity is 9.6 wt% H_2 with a material volumetric capacity of 68.5 g H_2/L. The baseline material targets for a system without a burner are summarized in Table 2.

CONCLUSIONS AND FUTURE DIRECTIONS

- The analysis results of HDPE liner behavior at cryogenic temperatures indicated that the tank fails at -190°C and 63 MPa internal pressure, and there is a minimum required internal pressure of 3 MPa to avoid liner separation at near LN_2 temperature. At -190°C, the peak stress at the liner/boss interface corners exceeds the tensile stress and could result in tank leakage
- The analysis results for cold gas storage showed that it has the potential to meet the gravimetric capacity target but is unlikely to meet the volumetric capacity target. The fuel cost is ~5% higher than baseline, off-

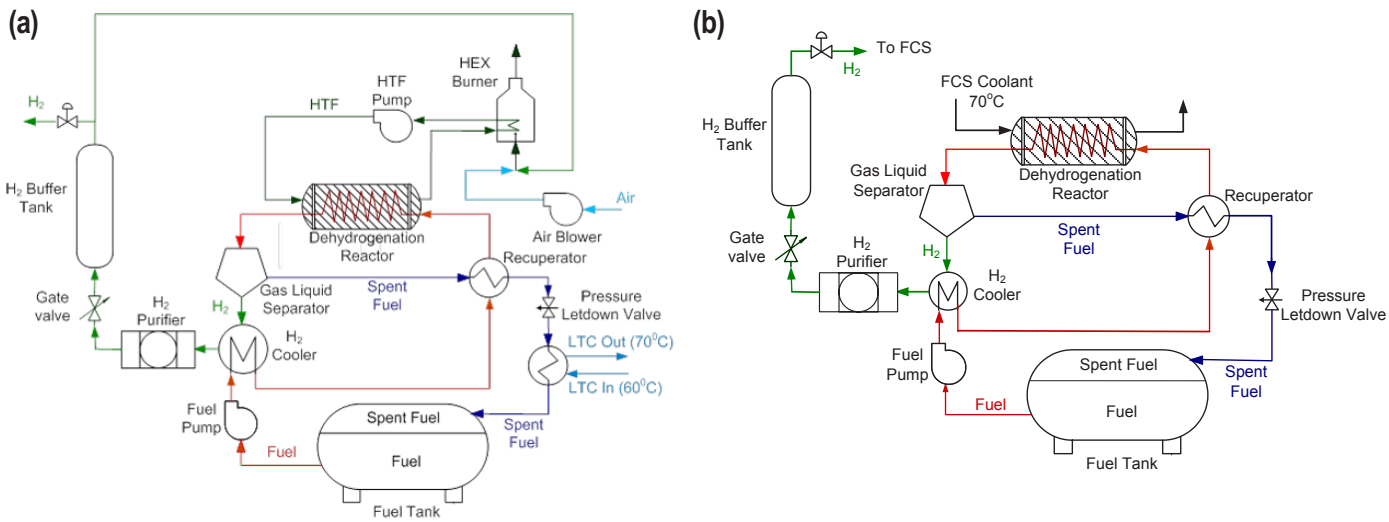

LTC – Low temperature coolant

FIGURE 4. Schematics of onboard system for chemical hydrogen storage material (a) with a burner and (b) without a burner

TABLE 2. Baseline Material Targets for a System with a Burner

		Units	Reference Values	Range of Values	Comments and Relevant Targets
Chemical Storage Material	Free Energy of Decomposition	kJ/mol	-1.6	-6.4 to 1.6	60% WTE efficiency
	Enthalpy of Decomposition	kJ/mol	40	20 to 40	90% on-board system efficiency
	Fuel Hydrogen Capacity	wt% H_2	TBD	TBD	5.5 wt% system gravimetric capacity
	Fuel Volumetric Capacity	g-H_2/L	TBD	TBD	40 g/L system volumetric capacity
	Decomposition Kinetcs		TBD	TBD	Avrami kinetics, 0.05 g/s/kg H_2 loss rate
Operating	Dehydrogenation Reactor	°C	150	150 - 250	1.6 g/s minimum full flow of H_2
Temperatures	Heat Transfer Fluid (HTF)	°C	200	200 - 300	
	Recuperator	°C	100	100 - 200	
Operating	Storage Pressure	bar	100	50 - 200	
Pressures	Minimum Delivery Pressure	bar	5		DOE target
H_2 Flow	Refueling Rate	kg/min	1.5		Not relevant for liquid fuels
Rates	Minimum Full Flow Rate	g/s	1.6		DOE target
Buffer H_2	Storage Pressure	bar	100	50 - 200	Start-up from -40°C
Storage	Buffer Storage Capacity	g-H_2	TBD	TBD	

WTE – Well-to-engine; TBD – to be determined

board cost for cold gas is \$0.18–\$0.31/kg H_2 higher, but onboard system cost is ~20% lower than baseline. The well-to-tank efficiency for cold gas is approximately six percentage points lower than baseline and is unlikely to meet DOE targets.

- The results from reverse engineering analysis of a chemical hydrogen material showed that to achieve well-to-tank regeneration efficiencies of 50–60%, the free energy of decomposition should exceed 1.6 kJ/mol if $\Delta G(298\ K)$ is positive and >-6.4 kJ/mol if $\Delta G(298\ K)$ is negative. Over this narrow range of the desired $\Delta G(298\ K)$ and for the expected material entropy in the range of 80–130 J/mol K, ΔH needs to be between 20 kJ/mol H_2 and 40 kJ/mol H_2; therefore, exothermic materials are unsuitable.
- In FY 2016, we will conduct ABAQUS simulations to determine the CF requirements for Type 4 700-bar hydrogen storage tanks incorporating recent improvements in liner design, hoop and helical winding methods, boss design, graded carbon fiber construction, alternate fibers, and alternate resins. We will use the model to perform sensitivity analysis with respect to fiber variability, tank length-to-diameter ratio, tank capacity, and on-board packaging restrictions.
- In FY 2016, we will determine the potential and attributes of unstable metal hydrides that can improve the performance of high pressure hydrogen storage tanks. We will conduct reverse engineering analysis to map the desired material physical, transport, thermodynamic ,and kinetic properties needed for the hybrid high pressure metal hydride tank system to approach the near term system cost and performance targets.
- In FY 2016, we will update the sorption model to analyze the performance of the best-of-class metal organic frameworks (e.g., M_2(m-dobdc), M = Mg, Mn, Fe, Co, Ni series of frameworks), developed at Lawrence Berkeley National Laboratory, in a representative on-board storage system under realistic operating conditions. Conduct system analyses to determine the resulting improvements in cost and performance relative to MOF-5 metal organic framework material that is considered the current standard.

FY 2015 PUBLICATIONS/PRESENTATIONS

1. R.K. Ahluwalia, J.K. Peng, and T.Q. Hua, "Bounding Material Properties for Automotive Storage of Hydrogen in Metal Hydrides for Low-Temperature Fuel Cells," International Journal of Hydrogen Energy, 39 (2014) 14874–14886.

2. R.K. Ahluwalia, J.K. Peng, and T.Q. Hua, "Sorbent Material Properties for On-board Hydrogen Storage for Automotive Fuel Cell Systems," International Journal of Hydrogen Energy, 40 (2015) 6373–6390.

3. R.K. Ahluwalia, J.K. Peng, and T.Q. Hua, "Cryo-compressed Hydrogen Storage," Book Chapter in Compendium of Hydrogen Energy, Elsevier, 2015.

4. R.K. Ahluwalia and T.Q. Hua, "Onboard Safety," Data, Facts and Figures on Fuel Cells, Detlef Stolten and Remzi Samsun (Editors), Wiley-VCH, 2015.

5. R.K. Ahluwalia and T.Q. Hua, "Pressurized System," Data, Facts and Figures on Fuel Cells, Detlef Stolten and Remzi Samsun (Editors), Wiley-VCH, 2015.

6. R.K. Ahluwalia, J.K. Peng, and T.Q. Hua, "Off-Board Considerations," DOE Materials-Based Hydrogen Storage Summit, Golden, CO, January 27, 2015.

7. R.K. Ahluwalia, T.Q. Hua, J.K. Peng, and H.S. Roh, "System Level Analysis of Hydrogen Storage Options," DOE Materials-Based Hydrogen Storage Summit PI Meeting, Golden, CO, January 28, 2015.

8. R.K. Ahluwalia, T.Q. Hua, J.K. Peng, and H.S. Roh, "System Level Analysis of Hydrogen Storage Options," Hydrogen Storage Tech Team Meeting, Southfield, MI, February 19, 2015.

REFERENCES

1. David Gotthold, PNNL, personal communication.

2. Norm Newhouse, "Development of Improved Composite Pressure Vessels for Hydrogen Storage," DOE Annual Merit Review, May 14, 2013.

IV.A.2 Hydrogen Storage Cost Analysis

Brian D. James (Primary Contact), Cassidy Houchins, Jennie M. Moton, Daniel D. DeSantis
Strategic Analysis, Inc. (SA)
4075 Wilson Blvd., Suite 200
Arlington, VA 22203
Phone: (703) 778-7114
Email: bjames@sainc.com

DOE Managers
Grace Ordaz
Phone: (202) 586-8350
Email: Grace.Ordaz@ee.doe.gov
Katie Randolph
Phone: (720) 356-1759
Email: Katie.Randolph@ee.doe.gov

Contract Number: DE-EE0005253

Project Start Date: September 30, 2012
Project End Date: September 29, 2016

Overall Objectives

- Identify and/or update the configuration and performance of a variety of H_2 storage systems for both vehicular and stationary applications
- Conduct rigorous cost estimates of multiple H_2 storage systems to reflect optimized components for the specific application and manufacturing processes at various rates of production
- Explore cost parameter sensitivity to gain understanding of system cost drivers and future pathways to lower system cost

Fiscal Year (FY) 2015 Objectives

- Update and expand the cost analysis of onboard hydrogen storage in pressurized carbon composite (fiber and resin) pressure vessels
- Incorporate reduced cost, integrated balance of plant (BOP) components into cost model
- Assess cost and performance impact of Pacific Northwest National Laboratory (PNNL) enhanced materials and design concepts for pressurized hydrogen storage
- Identify cost drivers and future pathways to lower cost
- Document all analysis results and assumptions
- Continue validation of cost savings from PNNL cold gas storage concept
- Prepare cost estimates of sorbent systems (both the HexCell and modular adsorption tank insert [MATI] concepts)

Technical Barriers

This project addresses the following technical barriers from the Hydrogen Storage section of the Fuel Cell Technologies Office Multi-Year Research, Development, and Demonstration Plan:

(B) System Cost

(H) Balance of Plant (BOP) Components

(K) System Life-Cycle Assessments

Technical Targets

This project conducts cost modeling to attain realistic, process-based system costs for a variety of H_2 storage systems. These values can inform future technical targets for system storage cost.

- System Storage Cost: <$12/kWh net (2017 target)

FY 2015 Accomplishments

- Updated the cost analysis of 700 bar Type IV compressed H_2 storage systems to reflect recent technological advances
  - Low cost, low density resin advances from PNNL
  - Carbon fiber cost reductions enabled by replacing a low volume precursor process with a high volume process used in the textile industry that was identified and adapted to high tensile strength carbon fiber by Oak Ridge National Laboratory (ORNL)
  - Completed analysis of an integrated pressure regulator block to reduce the cost of the BOP
  - Added explicit accounting for manufacturing and fiber variations into the cost model
  - Further refined assumptions and analysis based on expert feedback
  - Projected the cost of 700 bar Type IV compressed H_2 storage system to be $14.69/kWh at a manufacturing rate of 500,000 systems/year

- Completed a cost analysis of the MATI and HexCell sorbent H_2 storage systems (based on an Hydrogen Storage Engineering Center of Excellence [HSECoE] design and demonstrated in lab-scale systems[1])
  - Projected the cost of the MATI sorbent system to be $13.34/kWh at a manufacturing rate of 500,000 systems/year
  - Projected the cost of the HexCell sorbent system to be $12.79/kWh at a manufacturing rate of 500,000 systems/year
- Continued validation of the PNNL cold-gas H_2 storage system and confirmed cost savings made possible by the noncryogenic tank aspects

✧ ✧ ✧ ✧ ✧

INTRODUCTION

The Fuel Cell Technologies Office (FCTO) has identified H_2 storage as a key enabling technology for advancing H_2 and fuel cell technologies and has established goals of developing and demonstrating viable H_2 storage technologies for transportation and stationary applications. The cost assessment described in this report supports the overall FCTO goals by identifying the impact of components, performance levels, and manufacturing/assembly techniques on storage system cost at a variety of annual manufacturing rates. The results of this analysis enable the DOE to compare the cost impact of new components, etc., to the overall 2017 and ultimate DOE cost targets. The cost breakdown of the system components and manufacturing steps can then be used to guide future research and development decisions.

During 2015, the 700 bar type IV H_2 storage system analysis was updated based on advances made in materials and BOP components. In addition to the 700 bar Type IV compressed H_2 storage system analysis, two sorbent systems were analyzed: the MATI system and the HexCell systems. Both have been extensively studied by HSECOE.

APPROACH

A Design for Manufacturing and Assembly (DFMA®) style cost analysis methodology was used to assess the materials and manufacturing cost of hydrogen storage systems and components. Key system design parameters and engineering system diagrams describing system functionality and postulated manufacturing process flows were obtained from a combination of industry partners, Argonne National Laboratory (ANL), members of the HSECoE, and internal analysis. This data was used to develop a mechanical design of each component, including materials, scaling, and dimensions. Based on this design, the manufacturing process train was modeled to project the cost to manufacture each part. Cost was based on the capital cost of the manufacturing equipment, machine rate of the equipment, equipment tooling amortization, material costs, and other financial assumptions. Once the cost model was complete for the system design, sensitivity data for the modeled technology was obtained by varying key parameters. Results were shared with ANL, National Renewable Energy Laboratory (NREL), and industry partners to obtain feedback and further refine the model.

The analysis explicitly includes fixed factory expenses such as equipment depreciation, tooling amortization, utilities, and maintenance as well as variable direct costs such as materials and labor. However, because this analysis is intended to model manufacturing costs, a number of costs that usually contribute to the original equipment manufacturer price are explicitly not included in the modeling. These costs are excluded in this analysis: profit and markup, one-time costs such as nonrecurring research/design/engineering, and general expenses such as general and administrative costs, warranties, advertising, and sales taxes.

RESULTS

In FY 2015, SA updated the cost analyses for 700 bar Type IV H_2 storage systems to reflect recent materials and design advancements. Major changes to the 700 bar pressure vessel include use of a lower cost carbon fiber precursor based on high volume textile processing from ORNL, integration of BOP components to reduce the number of fittings, and use of a low cost, low density resin identified by PNNL. The analysis this year also explicitly accounted for costs associated with manufacturing design changes suggested by industry, including the removal of strips of carbon fiber composite used for local endcap reinforcement (referred to as doilies) and increased composite layer thickness to account for a more robust assessment of manufacturing variations. The relative impact of each component change computed versus the 2013 baseline system cost [1] is presented in the waterfall chart in Figure 1. Note that cost reductions in this figure are the result of single variable sensitivity analyses while the 2015 system cost is a result of the cumulative impact of all the changes. The waterfall chart is meant to capture qualitatively how the manufacturing cost was reduced from the 2013 baseline. To achieve this, the single variable changes reported in Figure 1 were scaled so that the relative percent adds up to the 12% reduction calculated for the 2015 tank. The assumptions used for each of the changes are described in further detail below.

In FY 2014 and FY 2015, SA examined the potential for compressed H_2 storage system cost reduction through use of

[1] Note that, whereas the 700 bar pressure vessels has been validated against commercially available compressed natural gas tanks, the sorbent systems represent lab-demonstrated technology and are therefore at a much lower technology readiness level and carry substantially increased performance and cost uncertainty.

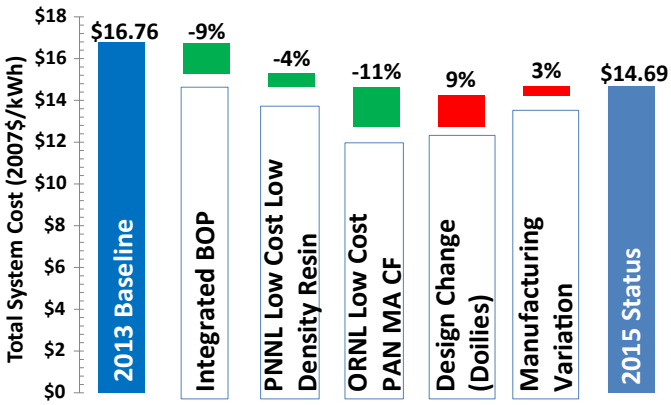

FIGURE 1. 700 bar Type IV pressure vessel storage system cost update for 2015 showing approximate cost impact of multiple simultaneous changes since 2013

a lower cost carbon fiber developed at ORNL. The ORNL developed carbon fiber is a replacement for the baseline Toray T-700S carbon fiber and is based on a polyacyrlonitrile with methacrylate (PAN-MA) precursor used in high volume textile manufacturing. ORNL identified significant cost savings enabled by switching to the PAN-MA precursor. Upon further analysis, SA applied factors to account for cost savings due to high volume carbon fiber manufacturing based on results from the Kline report [2] resulting in a total savings of 18.3% for PAN-MA over Toray T-700S carbon fiber.

System cost using the ORNL textile PAN-MA fiber is projected to be $15.03/kWh vs. $16.76/kWh for the 2013 baseline system using T-700S carbon fiber (both at 500,000 systems/year, in 2007$) or a reduction of $1.73/kWh. However, there is uncertainty in the ultimate tensile strength (UTS) which is the primary performance parameter for carbon fiber for pressure vessel applications. While only 653 KSI UTS was reported by ORNL in 2014, significantly higher performance has been observed in unpublished laboratory fabricated fibers. A preliminary tensile strength of 711 KSI was selected for the cost analysis to match the T-700 specification. When the upper limit of textile PAN-MA carbon fiber UTS is further documented and validated at production scale, the cost projections will be updated.

BOP improvements from last year were further refined by analysis of an integrated pressure regulator block. Component integration is a key cost reduction strategy and was suggested by the Storage Tech Team after a review of the number of fittings within the system. A DFMA® analysis was conducted based on a SS316 integrated pressure regulator block that is forged then machined with tight tolerances to allow proper fitting connections to components. O-rings provide a proper seal for attachment. Figure 2 shows a diagram of the integrated pressure regulator valve, bringing together six low pressure components (downstream of the pressure regulator). By combining the components into one unit, the integrated pressure regulator block body adds a component to the BOP list but reduces overall cost by eliminating piping and fittings. The combined cost reduction of the fitting component costs (2014) and the integrated pressure regulator (2015) is $1.34/kWh from the 2013 baseline tank at 500,000 systems per year. Further cost reductions are anticipated by replacing the SS316 with aluminum.

In FY 2015, SA worked with PNNL to assess their experimental efforts and to incorporate advances identified at PNNL into the baseline 700 bar storage system and cost model. A key element PNNL identified was to replace the epoxy resin used with carbon fiber to make carbon composite with a low cost, low density (vinyl ester) resin. The new resin reduced the total composite cost by lowering the total mass

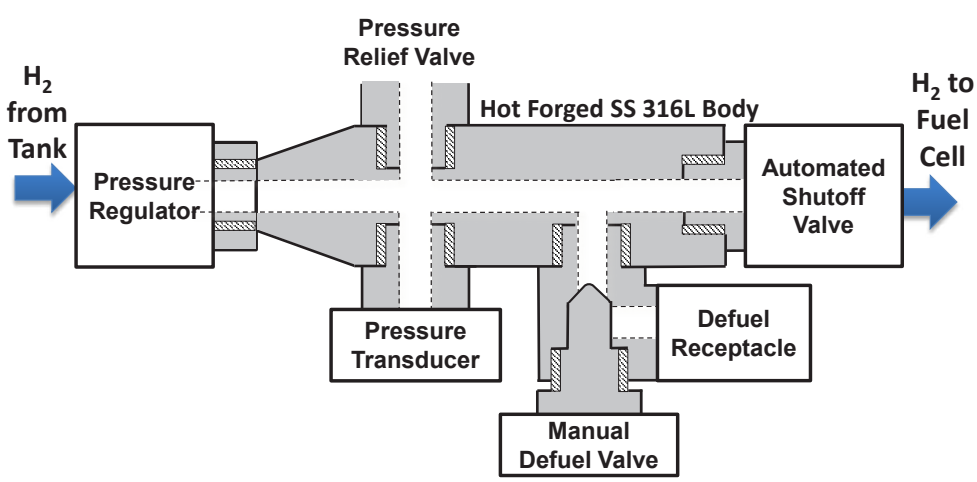

FIGURE 2. Cross-section of integrated pressure regulator block that combines six low pressure components

of resin required as well as using a less expensive resin. The total mass of composite required to meet the design bursts pressure was reduced by ~10% while the material cost of the resin was reduced by ~36%. This results in a reduction of $0.59/kWh over the 2013 baseline system at 500,000 systems per year.

Discussions with vessel manufacturers and ANL led to removal of the doilies previously used in the 2013 baseline tank system [1]. Analysis at ANL suggested that the 2013 baseline tank would require 102 kg composite, up from 91 kg, to meet the same burst pressure without doilies. This change results in an increase of $1.36/kWh from the 2013 baseline.

High volume manufacturing of composite pressure vessels with an extended service life requires some level of overdesign to ensure safety and statutory requirements. Consequently, vessels are designed with enhanced wall-thickness/burst-pressure to account for both fiber strength and manufacturing process variations in high volume manufacturing. Current design practice is based on a 3σ overdesign which is consistent with burst testing of every 200th tank. Based on conversations with tank manufacturers, typical coefficients of variation (COV) for manufacturing and fiber variation are around 3%. In previous analyses, ANL included a 10% increase in composite mass to account for variations in fiber strength: this is approximately equivalent to a 3σ overdesign and a fiber COV of 3.3%. In order to explicitly account for manufacturing variability and to be consistent with current manufacturing practices, a manufacturing COV of 3.3% was assumed for the 2015 tank. This results in a combined fiber and manufacturing overdesign of 14%. The cost impact relative to the 2013 baseline tank for including 3.3% manufacturing variation is $0.42/kWh. When all changes are applied to the model (the ORNL low cost carbon fiber, PNNL low cost resin, integrated BOP, design change, and manufacturing variation) the 2015 tank cost is $14.69/kWh or a reduction of $2.07/kWh from the 2013 baseline tank.

In addition to analyzing the high volume manufacturing cost of 700 bar pressure vessels, SA also conducted a DFMA® analysis of two sorbent based onboard H_2 storage systems: the MATI and HexCell concepts as conceptualized by the HSECoE. Both systems use a sorbent (modeled as MOF-5) to store gaseous H_2 at cryogenic temperatures. The MATI system uses liquid nitrogen (LN_2)-heated H_2 gas flowing through an internal heat exchanger to provide the heat of adsorption/desorption, whereas the HexCell system relies on conduction from a static heat exchange insert to transfer heat to the outer shell (which is jacketed by LN_2). The HexCell system manufacturing cost at 500,000 systems per year is $12.79/kWh while the MATI system cost is $13.34/kWh, as shown in Figure 3. The MATI system was anticipated to be more expensive than the HexCell system due to the greater mass of MOF-5 (41 kg/system at $8.44/kg [in 2007$ at 500,000 systems per year]) compressed into discs and a more

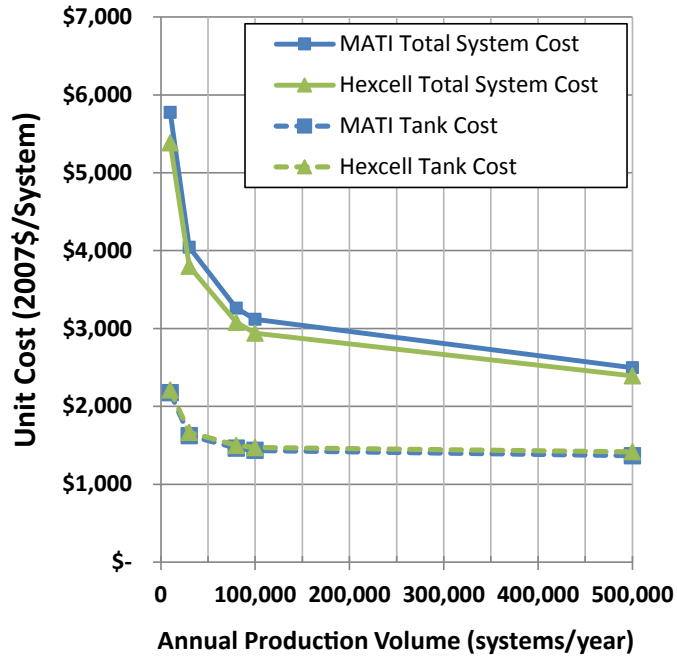

FIGURE 3. Total system and tank costs for both the HexCell and MATI sorbent systems at all manufacturing rates

extensive BOP. Figure 4 compares the breakdown in cost of the two systems at 500,000 systems per year. These cost results were vetted by HSECOE and the Hydrogen Storage Technical Team. Thus both systems are quite similar in cost, and slightly less than the 700 bar compressed pressure vessel system. Whereas the 700 bar pressure vessels have been validated against commercially available compressed natural gas tanks, the sorbent systems represent lab-demonstrated technology and are therefore at a much lower technology readiness level and carry substantially increased performance and cost uncertainty.

CONCLUSIONS AND FUTURE DIRECTIONS

Based on work completed this year the major conclusions are as follows:

- System cost for the single tank 700 bar pressure vessel system has come down by 12% over the 2013 baseline system (at 500,000 systems per year).
  - BOP costs were reduced by integrating components and reducing the total number of fittings leading to a cost reduction of ~9%.
  - Lower cost carbon fiber based on high volume textile processing replaced the conventional carbon fiber reducing the costs ~11%.
  - Low cost, low density resin resulted in a price reduction of ~4%.

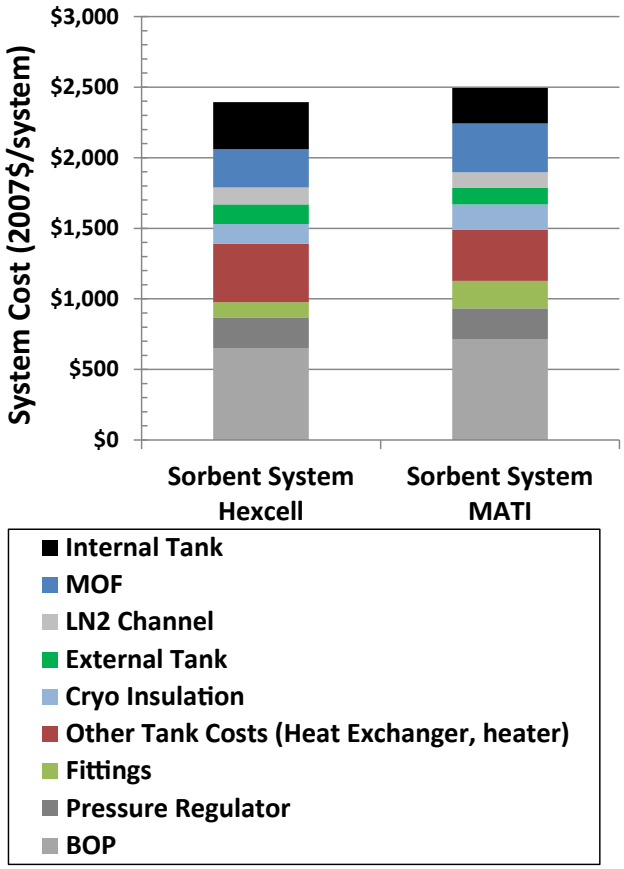

FIGURE 4. Breakdown in total system cost for both the HexCell and MATI sorbent systems

  - Tank design improvements and explicit accounting for manufacturing variation led to a cost increase of ~12%.

- Analyses of the MATI and HexCell sorbent-based onboard H_2 storage systems indicate system costs of ~$13/kWh (at 500,000 systems/year). This is slightly less than the cost of 700 bar compressed H_2 storage; however, there is greater uncertainty in the sorbent systems than for the pressure vessels.

Based on results from this year, SA plans to:

- Re-evaluate pressure vessel winding parameters to assess whether winding speed optimization can lead to lower cost.
- Investigate commercially available cryo-compressed liquid natural gas tanks as a validation case for analysis of the PNNL cyro-gas storage concept.
- As appropriate, track and model improvement from current DOE funded projects looking at lower cost materials, sorbents, and strategies to reduce carbon fiber usage.
- Evaluate alternative, lower cost material selections for the integrated BOP.

FY 2015 PUBLICATIONS/PRESENTATIONS

1. Brian D. James, Jennie A. Moton, Daniel A. DeSantis, "Hydrogen Storage System Cost: Status and Technical Challenges," Hydrogen Storage Summit (PI Workshop), National Renewable Energy Laboratory, Golden, CO, January 29, 2015.

2. Jennie A. Moton, Brian D. James, Daniel A. DeSantis, "Cost of On-Board Hydrogen Storage Systems: Status and Technical Challenges," Hydrogen Storage Technical Team Meeting, USCAR, Southfield, MI, February 19, 2015.

3. Brian D. James, "Hydrogen Storage Cost Analysis," 2015 DOE Hydrogen and Fuel Cells Program Review, Arlington, VA, June 9, 2015.

REFERENCES

1. Scott McWhorter and Grace Ordaz, "Onboard Type IV Compressed Hydrogen Storage Systems--Current Performance and Cost," DOE Program Record 13013 (2013) http://hydrogen.energy.gov/pdfs/13010_onboard_storage_performance_cost.pdf (accessed 14 August 2015).

2. "Cost Assessment of Pan-Based Precursor and Carbon Fiber," Kline and Company, Final Report: Automotive Composites Consortium, 27 November 2007.

IV.B.1 Hydrogen Storage Engineering Center of Excellence

Donald L. Anton (Primary Contact),
Theodore Motyka, Bruce J. Hardy,
David A. Tamburello, Claudio Corgnale, and
Martin Sulic
Savannah River National Laboratory (SRNL)
Bldg. 999-2W
Aiken, SC 29808
Phone: (803) 507-8551
Email: Donald.Anton@srnl.doe.gov

DOE Managers
Ned Stetson
Phone: (202) 586-9995
Email: Ned.Stetson@ee.doe.gov
Jesse Adams
Phone: (720) 356-1421
Email: Jesse.Adams@ee.doe.gov

Subcontractors
- Pacific Northwest National Laboratory (PNNL), Richland, WA
- United Technologies Research Center (UTRC), East Hartford, CT
- General Motors Company (GM), Warren, MI
- Ford Motor Company (FMC), Dearborn, MI
- National Renewable Energy Laboratory (NREL), Golden, CO
- Los Alamos National Laboratory (LANL), Los Almaos, NM
- Jet Propulsion Laboratory (JPL), Pasadena, CA
- University of Michigan (UM), Ann Arbor, MI
- California Institute of Technology (CalTech), Pasadena, CA
- Oregon State University (OSU), Corvallis, OR
- Hexagon Lincoln LLC, Lincoln, NE
- Université du Québec à Trois-Rivières (UQTR), Trois-Rivières, QC, Canada

Project Start Date: February 1, 2009
Project End Date: December 31, 2015

Overall Objectives

- Develop system models that will lend insight into overall fuel cycle efficiency
- Compile all relevant materials data for candidate storage media and define future data requirements
- Develop engineering and design models to further the understanding of onboard storage energy management requirements
- Develop innovative onboard system concepts for metal hydride, chemical hydrogen, and adsorption materials-based storage technologies
- Design components and experimental test fixtures to evaluate the innovative storage devices and subsystem design concepts, validate model predictions, and improve both component design and predictive capability
- Design, fabricate, test, and decommission the subscale prototype components and systems of each materials-based technology (adsorbents, metal hydrides, and chemical hydrogen storage materials)

Fiscal Year (FY) 2015 Objectives

- Coordination and facilitation of partner's activities
- Designed and fabricated a 2-L adsorbent subscale prototype utilizing a hexagonal aluminum honeycomb structure (HexCell) heat exchange system
- Completed validation of the hydrogen cryo-adsorbent test station
- Demonstrate performance of a flow through adsorbent subscale prototype system
- Demonstrate performance of a modular adsorbent tank insert (MATI) adsorbent subscale system

Technical Barriers

This project addresses the following technical barriers from the Hydrogen Storage section of the Hydrogen, Fuel Cells, and Infrastructure Technologies Program Multi-Year Research, Development, and Demonstration Plan:

(A) System Weight and Volume

(B) System Cost

(C) Efficiency

(D) Durability/Operability

(E) Charging/Discharging Rates

(G) Materials of Construction

(H) Balance of Plant Components

(J) Thermal Management

(K) System Life Cycle Assessments

(L) High Pressure Conformality

(P) Lack of Understanding of Hydrogen Physisorption and Chemisorption

(S) By-Product/Spent Material Removal

Technical Targets

The projected performance of the two adsorption systems, HexCell and MATI, being evaluated are given in Table 1 in comparison to the technical targets.

FY 2015 Accomplishments

- Completed assembly of the flow through subscale prototype system and began initial characterization experiments
- Completed validation of the hydrogen cryo-adsorbent test station for evaluating the performance of the 2-L MATI prototype
- Completed a slide package describing the adsorbent acceptability envelope and accompanying hydrogen storage applications for the DOE Materials-Based Hydrogen Storage Summit
- Completed assembly of MATI subscale prototype and completed charging and discharging characterization experiments

✧ ✧ ✧ ✧ ✧

INTRODUCTION

The Hydrogen Storage Engineering Center of Excellence (HSECoE) brings together all of the materials and hydrogen storage technology efforts to address onboard hydrogen storage in light-duty vehicle applications. The effort began with a heavy emphasis on modeling and data gathering to determine the state-of-the-art in hydrogen storage systems. This effort spanned the design space of vehicle requirements, power plant and balance of plant requirements, storage system components, and materials engineering efforts. These data and models will then be used to design components and subscale prototypes of hydrogen storage systems which will be evaluated and tested to determine the status of potential systems against the DOE 2020 and ultimate technical targets for hydrogen storage systems for light duty vehicles.

APPROACH

A team of leading North American national laboratories, universities, and industrial laboratories, each with a high degree of hydrogen storage engineering expertise cultivated through prior DOE, international, and/or privately sponsored programs has been assembled to study and analyze the engineering aspects of condensed phase hydrogen storage as applied to automotive applications. The technical activities of HSECoE are divided into three system architectures, adsorbent, chemical hydrogen, and metal hydride, matrixed with six technologies areas, performance analysis, integrated power plant/storage system analysis, materials operating requirements, transport phenomena, enabling technologies and subscale prototype construction, testing, and evaluation. The program is divided into three phases: Phase 1, System Requirements and Novel Concepts; Phase 2, Novel Concept Modeling Design and Evaluation; and Phase 3, Subscale System Design, Testing and Evaluation.

TABLE 1. System Status vs. Technical Targets for the Cryo-Adsorbent System

				HexCell		MATI	
		2020 Technical Targets	End of Phase 1	End of Phase 2	Projected End of Phase 3	End of Phase 2	Projected End of Phase 3
Gravimetric Density	*(kg H_2/kg sys)*	0.055	0.0312	0.0352	0.0384	0.0341	0.0385
Min. Delivery Temp.	*(°C)*	-40	-40	-40	-40	-40	-40
Max Delivery Temp.	*(°C)*	85	85	85	85	85	85
Min. Delivery Pressure	*(bar)*	5	5	5	5	5	5
Max. Operating Temp.	*(°C)*	60	60	60	60	60	60
Min. Operating Temp.	*(°C)*	-40	-40	-40	-40	-40	-40
Max. Delivery Pressure	*(bar)*	12	12	12	12	12	12
Min. Full Flow Rate	*([g/s]/kW)*	0.02	0.02	0.02	0.02	0.02	0.02
System Cost	*($/kWh net)*	$10	$18.30	$12.73	$14.79	$15.45	$16.32
Onboard Efficiency	*(%)*	90%	90%	90%	90%	97%	97%
Volumetric Density	*(kg H_2/liter)*	0.040	0.01938	0.01749	0.02059	0.02072	0.02363
Cycle Life (1/4 - full)	*(N)*	1500	1500	1500	1500	1500	1500
Fuel Cost	*($/gge)*	4	6.00	6.00	6.00	6.00	6.00
Loss of Useable H_2	*([g/hr]/kg H_2)*	0.05	0.4451	0.2670	0.8065	0.2670	0.6916
Wells-to-Power Plant Efficency	*(%)*	60%	40%	40%	40%	40%	40%
Fuel Purity	*(%)*	99.97%	99.99%	99.99%	99.99%	99.99%	99.99%
Transient Response	*(sec)*	0.75	0.75	0.75	0.75	0.75	0.75
Start Time to Full Flow (-20°C)	*(sec)*	15	15	15	15	15	15
Fill Time (5kg H_2)	*(min)*	3.3	3.3	3.3	3.3	3.3	3.3
Start Time to Full Flow (20°C)	*(sec)*	5	5	5	5	5	5

RESULTS

The 2-L HexCell prototype has been designed at SRNL and fabricated at UQTR. UQTR has been successful in sealing the domed 2-L vessel and have not had to switch to the new 2-L flanged vessel provided by Hexagon Lincoln. With the leak issue resolved, the following experimental efforts have been completed to date.

- Dead volume measurements with and without the HexCell internal heat exchanger structure within the 2-L vessel
- Room temperature isotherms for varying operating pressures in the fully instrumented 2-L prototype (powder MOF-5 [metal-organic framework] packed to a density of 160 kg/m^3)
- Initial isotherm measurements at 77 K for varying operating pressures; note that there have been some H_2 flow rate inconsistencies that UQTR is working to resolve

Much of the last year has been spent attempting to seal the 2-L vessels designed by Hexagon Lincoln. The newest vessel, a 2-L stainless steel flanged vessel, appears to have solved the leak issues that plagued the collared design. In addition, once a sealable vessel solution was built and in the hands of the team members, OSU has had several complications during the assembly and proof testing of the 2-L MATI prototype, including a cracked endcap and leaking through several thermocouple (TC) penetration locations. Thus, a six-month no-cost extension was requested and granted in order to complete the experimental phase of the project.

The 2-L MATI prototype was completed at OSU and shipped to SRNL on March 6, 2015. During shipping, significant damage to the system was identified, requiring full disassembly, re-instrumentation and reassembly. Images of the assembly process and the newly assembled prototype vessel are shown in Figure 1. The final 2-L MATI prototype assembly includes the following.

- 16 MOF-5 pucks
- 30 internal TCs
- One pressure transducer tap
- One gas inlet/outlet tap
- Two MATI pass-throughs

Once assembled, the prototype was pressure tested at room temperature up to 100 bar, and then in liquid nitrogen up to 100 bar as shown in Figure 2.

An acceptable leak rate is assumed to be no more than 0.100% of the full tank gas storage during an experimental run. Based on the initial models of the 2-L MATI prototype, 0.100% of the gas storage at 80 K and 100 bar (60 bar) is 0.0624 g (0.0510 g). Translating this into a drop in pressure, this corresponds to a maximum allowable pressure drop from 100 bar (60 bar) of 0.262 bar (0.147 bar). Assuming a 30 min drive cycle experiment, this corresponds to a leak rate of 0.0087 bar/min at 100 bar (0.0049 bar/min at 60 bar). The 2-L MATI prototype vessel as it is currently sealed has leak rates below 0.0033 bar/min, below the minimum acceptable rate.

Representative results from the desorption experiments from 60 bar to 1 bar while submerged in the liquid nitrogen (LN_2) bath are shown in Figure 3 for a gaseous nitrogen

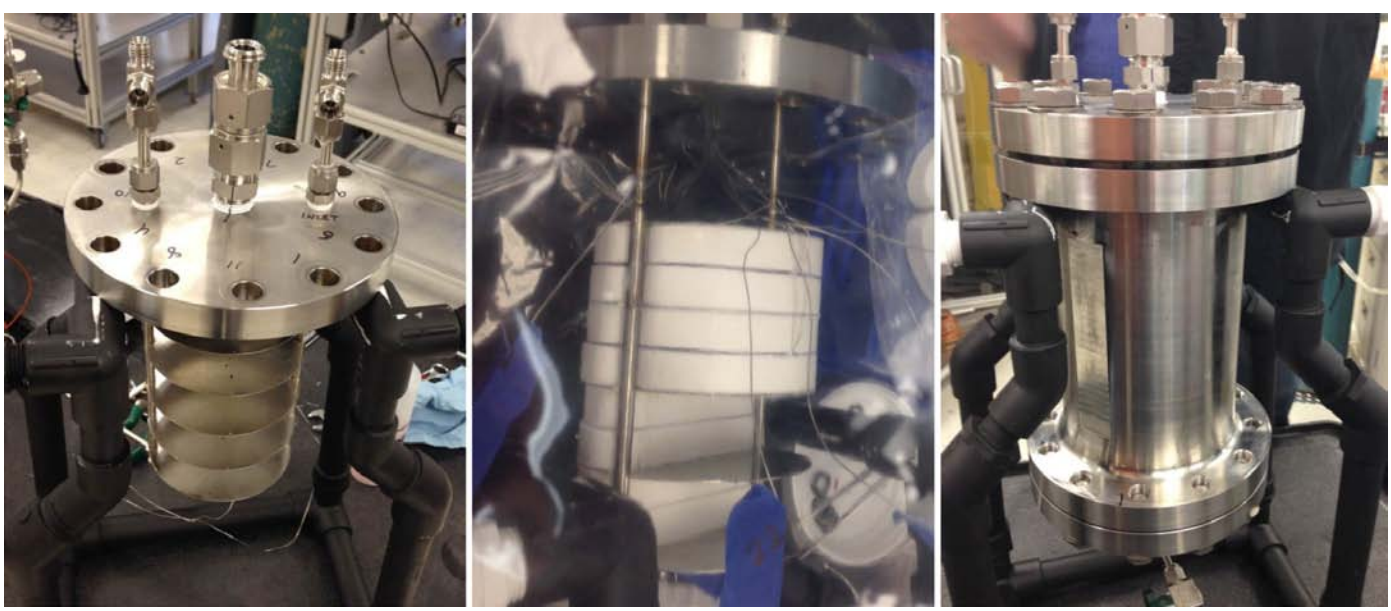

FIGURE 1. 2-L MATI prototype in various stages of assembly

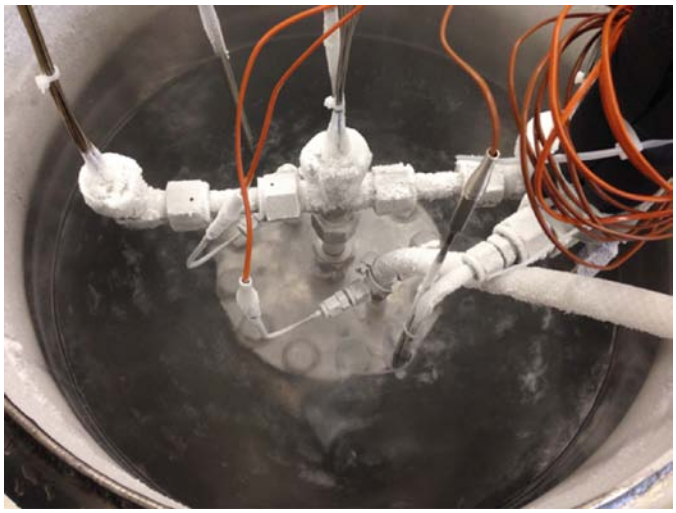

FIGURE 2. MATI prototype pressure test in liquid nitrogen

(GN_2) flow of 150 SLPM through the MATI. Due to cooling effects within the lines, the GN_2 enters the MATI at approximately 250 K, which is still more than enough heat to aid in desorption. Note that, even with the cooling effects of the LN_2 bath, the average puck temperature at 8 min is 150 K.

A MATI-only cool down experiment was also performed to cool the 2-L prototype assembly from room temperature without the aid of the LN_2 bath, with its results shown in Figure 4. The final length of LN_2 supply tubing would normally run through the LN_2 bath to maintain a near 80 K temperature prior to entering the MATI. Without the LN_2 bath, the LN_2 supply to the MATI remains >100 K at the MATI inlet. Even with this limitation, the average puck temperature drops from 285 K to 141 K after 6 min, 134 K after 9 min, and 129 K after 18 min. Thus, the MATI's design has shown to be quite capable of cooling the adsorbent pucks.

Several updates have been made to the adsorbent storage system to reflect the latest experimental data and detailed model simulations. Additional updates will be performed after the graphical user interface evaluation is complete and the Phase III results are available.

CONCLUSIONS AND FUTURE DIRECTIONS

Adsorbent system efforts are concentrated on Phase III prototype design, assembly, testing, and modeling, including test station design, construction, and capabilities verification. Two prototypes are being tested and modeled: (1) powder MOF-5 in a hexagonal heat exchanger (HexCell) that utilizes

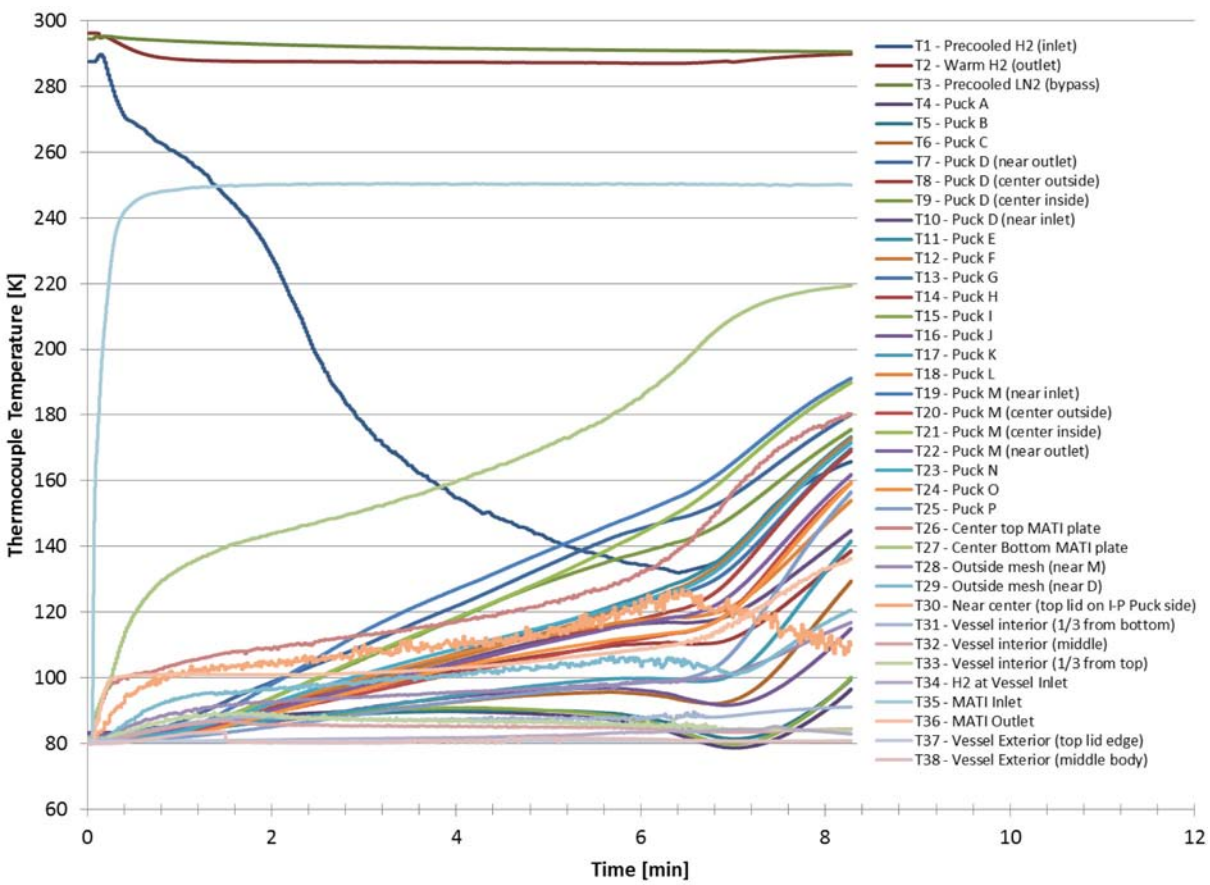

FIGURE 3. Temperature profiles for desorption of MATI system from 60 bar to 1 bar, initialized at 80 K, with a GN_2 flow at 150 SLPM

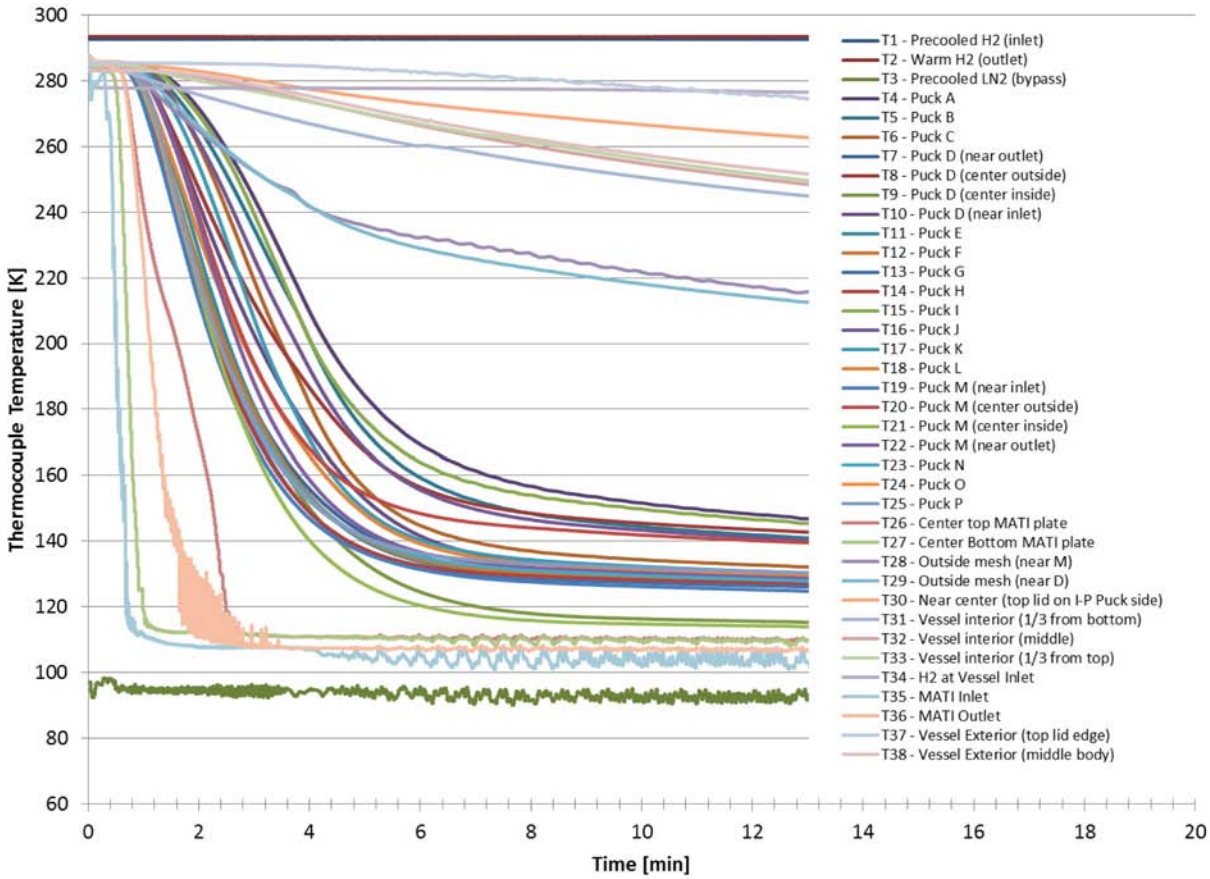

FIGURE 4. Temperature profiles for a closed-vessel cool down operation using only the MATI starting from room temperature

flow-through cooling during refueling and resistance heating during discharge is being tested at UQTR and modeled at SRNL, and (2) compacted MOF-5 in a MATI utilizing isolated LN_2 during refueling and isolated H_2 during discharge is being tested at SRNL and modeled at OSU. Initial tests on both systems have been concluded and both are working as anticipated, illustrating that adsorbent systems are capable of meeting many of the DOE technical targets for hydrogen storage.

Future technical work will include:

- Continue validation experiments on the 2-L MATI prototype assembly to include testing at pressures greater than 60 bar, cycling for a minimum of 50 cycles, and validation of thermal and mass flow models against experimental data
- Continued validation experiments on the 2-L HexCell prototype assembly to include cryogenic charging and discharging experiments, cycle testing to a minimum of 50 cycles, and validation of thermal and mass flow models against experimental data
- Update Simulink cryo-adsorbent system models to predict full-scale system performance

FY 2014/2015 PUBLICATIONS/ PRESENTATIONS BY SRNL/UQTR

1. Hardy, B., Corgnale, C., Tamburello, D., Anton, D. "Acceptability envelope for adsorption based hydrogen storage," Invited presentation at MCARE 2014, Clearwater (FL), USA.

2. C. Corgnale, B. Hardy, D. Tamburello, R. Chahine, and D. Anton, "Simulation of hydrogen adsorption systems adopting the flow through cooling concept," International Journal of Hydrogen Energy (2014), 39, 17083–17091.

FY 2014/2015 PATENTS BY SRNL/UQTR

1. Tamburello et al., Heat Transfer Unit Method for Prefabricated Vessel, 61/905,557, 12/12/2013.

IV.B.2 Ford/BASF SE/UM Activities in Support of the Hydrogen Storage Engineering Center of Excellence

Michael Veenstra (Primary Contact, Ford), Justin Purewal (Ford), Jun Yang (Ford), Chunchuan Xu (Ford), Donald Siegel (UM), Yang Ming (UM), Manuela Gaab (BASF SE), Lena Arnold (BASF SE), and Ulrich Müller (BASF SE)
Ford Motor Company
1201 Village Road
Dearborn, MI 48124
Phone: (313) 322-3148
Email: mveenstr@ford.com

DOE Managers
Jesse Adams
Phone: (720) 356-1421
Email: Jesse.Adams@ee.doe.gov
Ned Stetson
Phone: (202) 586-9995
Email: Ned.Stetson@ee.doe.gov

Contract Number: DE-FC36-GO19002

Subcontractors
- University of Michigan (UM), Ann Arbor, MI
- BASF SE, Ludwigshafen, Germany

Project Start Date: February 1, 2009
Project End Date: June 30, 2015

Overall Objective

This project addresses three of the key technical obstacles associated with the development of a viable hydrogen storage system for automotive applications.

- (Task 1) Create accurate system models that account for realistic interactions between the fuel system and the vehicle power plant
- (Task 2) Develop robust cost projections for various hydrogen storage system configurations
- (Task 3) Assess and optimize the effective engineering properties of framework-based hydrogen storage media (such as metal-organic frameworks [MOFs])

Fiscal Year (FY) 2015 Objectives

The project focus during FY 2015 was to complete the following objectives.

- Evaluate MOF-5 degradation beyond 300 cycles based on maximum allowable impurity levels as stated in SAE J2719 and report on the ability to mitigate to less than 10%
- Complete the failure mode and effects analysis (FMEA) associated with real-world operating conditions for a MOF-5-based system, for both HexCell and modular adsorbent tank insert (MATI) concepts based on the Phase 3 test results; report on the ability to reduce the risk priority numbers (RPN) from the Phase 2 peak/mean and identify key failure modes
- Update the cryo-adsorbent system model with Phase 3 performance data, integrate into the framework; document and release models to the public
- Explore approaches to optimize MOF-5 engineering properties, such as thermal conductivity and compaction effects

Technical Barriers

This project addresses the following technical barriers from the Hydrogen Storage section of the Fuel Cell Technologies Office Multi-Year Research, Development, and Demonstration Plan:

(A) System Weight and Volume

(B) System Cost

(C) Efficiency

(D) Durability/Operability

(E) Charging/Discharging Rates

(H) Balance of Plant (BOP)

(J) Thermal Management

Technical Targets

The outcomes of this project provide input to vehicle and system level models, cost projections, and also contribute to the assessment and optimization of materials properties. Insights gained from these studies are applied towards the engineering of hydrogen storage systems that attempt to meet the DOE 2020 and ultimate hydrogen storage targets, shown in Table 1. As a status based on the cooperative analysis within the Hydrogen Storage Engineering Center of Excellence (HSECoE), the current adsorbent systems are also shown in Table 1 based on powder and compacted MOF-5.

TABLE 1. Technical Targets and Current Adsorbent Systems

Storage Parameter	Units	DOE 2020 Target	DOE Ultimate Target	HexCell MOF-5 Powder	MATI MOF-5 Compact
System Gravimetric Capacity	$kg{\cdot}H_2/kg$	0.055	0.075	0.035	0.035
System Volumetric Capacity	$kg{\cdot}H_2/L$	0.040	0.070	0.0185	0.0213
Storage System Cost	$\$/kWh_{net}$	10	8	14.5	15.5
System Fill Time (for 5 kg H_2)	min	3.3	2.5	3–5	3–5
Minimum Full Flow Rate	(g/s)/kW	0.02	0.02	0.02	0.02
Min/Max Delivery Temperature	ºC	-40/85	-40/85	-40/85	-40/85
Min. Delivery Pressure (Fuel Cell)	atm	5	5	5	5

FY 2015 Accomplishments

- Completed impurity gas cycle tests that indicate low or no degradation from the exposure
- Updated FMEA action items and reduced the RPN from Phase 2 values
- Supported the Simulink framework release and model testing through development in the modeling group
- Coordinated adsorbent system design activities within the HSECoE as the System Architect
- Provided an original equipment manufacturer perspective and outlook for the development of the adsorbent system
- Demonstrated improvement in puck density results using filtering and other techniques
- Developed alternative materials and approaches to increase thermal conductivity beyond expanded natural graphite (ENG) mixtures

✧ ✧ ✧ ✧ ✧

INTRODUCTION

Widespread adoption of hydrogen as a vehicular fuel depends critically on the development of low cost, onboard hydrogen storage technologies capable of achieving high energy densities and fast kinetics for hydrogen uptake and release. Since present day technology based on compression and liquefaction is unlikely to attain established DOE targets, development of materials-based storage approaches has garnered increasing attention. To hasten development of these hydride materials, the DOE previously established three centers of excellence for materials-based hydrogen storage research. While the centers have made substantial progress in developing new storage materials, challenges associated with the engineering of the storage system around a candidate storage material have received much less attention.

APPROACH

Ford–UM–BASF is conducting a multi-faceted research project that addresses the key challenges associated with the development of materials-based hydrogen storage systems. As in previous years, we continue to be engaged in system modeling (Task 1), with the objective of a public release of the HSECoE Hydrogen Vehicle Simulation Model. Work also continues in the system cost analysis effort (Task 2). During the past year, a significant amount of effort has been focused on sorbent media (Task 3), with the primary goal of characterizing the "effective engineering properties" of MOFs in order to guide the development of optimal strategies for their use in an adsorbent system. In particular, we conducted impurity gas cycling degradation testing and refined the failure modes and effects analysis for the adsorbent storage system, and further explored approaches for optimization of MOF-5 adsorbent media using various novel compaction and thermal conductivity approaches. Additional details are provided in the following section.

RESULTS

Below is a description of our technical results for certain key accomplishments and how these results relate to achieving the DOE targets.

Impurity Gas Cycling Degradation Testing

The robustness of adsorbents with respect to repeated exposure to impurities in the hydrogen gas stream is an important performance metric for hydrogen storage applications. To meet the 2015 objective, we completed a comprehensive series of impurity-induced degradation tests using MOF-5 as the test material. We studied contaminant types and levels that were consistent with the SAE J2719 standard, using an extrinsic pressure cycling test method analogous to the actual operational cycles of a cryo-adsorption hydrogen storage system (see Figure 1). The objective required the MOF-5 capacity loss after 300 adsorption/desorption cycles with impure hydrogen gas to not degrade below 10%.

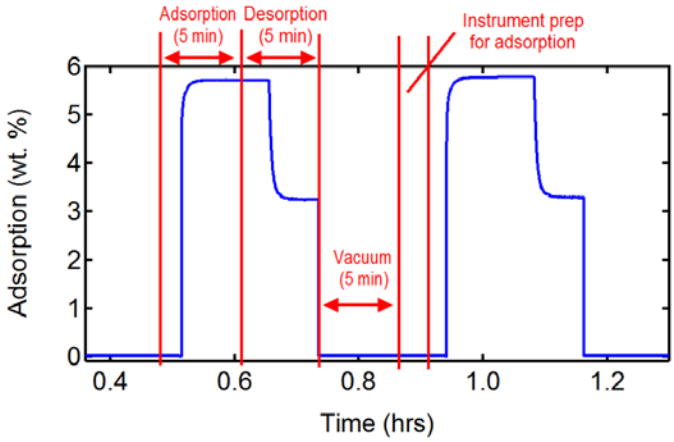

FIGURE 1. Test procedure used for pressure cycling of the impurity mixture test gas with a pressure swing during a single cycle depicted

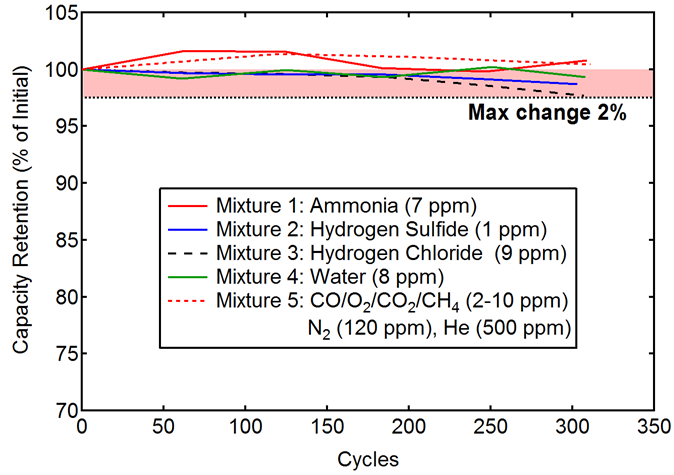

FIGURE 2. Summary of MOF-5 hydrogen storage capacity at 77 K during pressure cycling with impurity gas mixtures

Based on the SAE J2719 gas quality requirement for fueling stations, the following mixtures were independently cycled to analyze the effect of each impurity (1) ammonia (NH_3) at 7 ppm; (2) hydrogen sulfide (H_2S) at 1 ppm; (3) hydrogen chloride (HCl) at 9 ppm; (4) water (H_2O) at 8 ppm; and (5) carbon monoxide (CO) at 2 ppm, carbon dioxide (CO_2) at 6 ppm, methane (CH_4) at 8 ppm; oxygen (O_2) at 10 ppm, nitrogen (N_2) at 120 ppm, helium (He) at 500 ppm. The majority of these levels exceed the impurity limits defined in J2719 due to ability to qualify the concentration which results in a more stringent test of MOF-5 robustness. The impact on MOF-5 capacity was evaluated by measuring isotherms at 60 cycle increments until the test achieved 300 cycles with the impurity mixture. Figure 2 provides a summary of the hydrogen capacity measured during pressure cycling tests for all five impurity gas mixtures. The hydrogen capacity retention is shown in terms of the maximum excess adsorption at 77 K as a percentage of the initial capacity measured at the beginning of the cycle testing (i.e., capacity at cycle 0). For all five of the impurity gases tested, the capacity retention met the objective with a negligible change of only 2% after 300 cycles.

In addition, we also tested the practical consideration of the MOF being exposed to hydrogen fuel impurities for an extended period of time (1 week) and at higher storage temperature of 25°C. The test exposed MOF-5 powders under hydrogen gas with single impurity of 1 ppm H_2S and 8 ppm H_2O respectively with negligible change in the excess hydrogen adsorption isotherm, X-ray diffraction and Fourier transform infrared spectrum. We also further studied the impact of humid air exposure on MOF-5 properties and determined for humidity levels below ~50% threshold only minor degradation is observed for exposure times up to several hours, suggesting that MOF-5 is more stable than generally assumed under moderately humid conditions. In contrast, irreversible degradation occurs in a matter of minutes for exposures above the 50% threshold. In order to understand this mechanism, we used van der Waals-augmented density functional theory and transition state finding techniques to predict the thermodynamics and kinetics of water adsorption/insertion into the MOF-5 (see Figure 3). The calculations suggest that the thermodynamics of MOF hydrolysis are coverage dependent; water insertion into the framework becomes exothermic only after a sufficient number of H_2O molecules are adsorbed on a Zn-O cluster.

Failure Modes and Effects Analysis (FMEA)

As part of the 2015 objectives, the FMEA ratings were modified based on the HSECoE Phase 3 activities by the adsorbent team. Some of the key actions that facilitated the reduction in the RPN include the following.

- Completed testing to reduce occurrence ratings associated with hydrogen impurity concerns
- Assessed tank robustness with adsorbent material and cryogenic operating conditions
- Conducted thermal management evaluation testing to assess performance in adsorbent bed
- Performed system testing to assess material variability and effects of non-homogenous bed

The design verification plan updates from the key organizations involved in the testing—Université du Québec à Trois-Rivières, Oregon State University, Savannah River National Laboratory, United Technologies Research Center, Hexagon Lincoln, and Ford—were incorporated into the FMEA modified occurrence and detection ratings. The result achieved the 2015 objective by reducing the Phase 2 RPN mean from 513 to 288 and RPN mean from 157 to 114 based

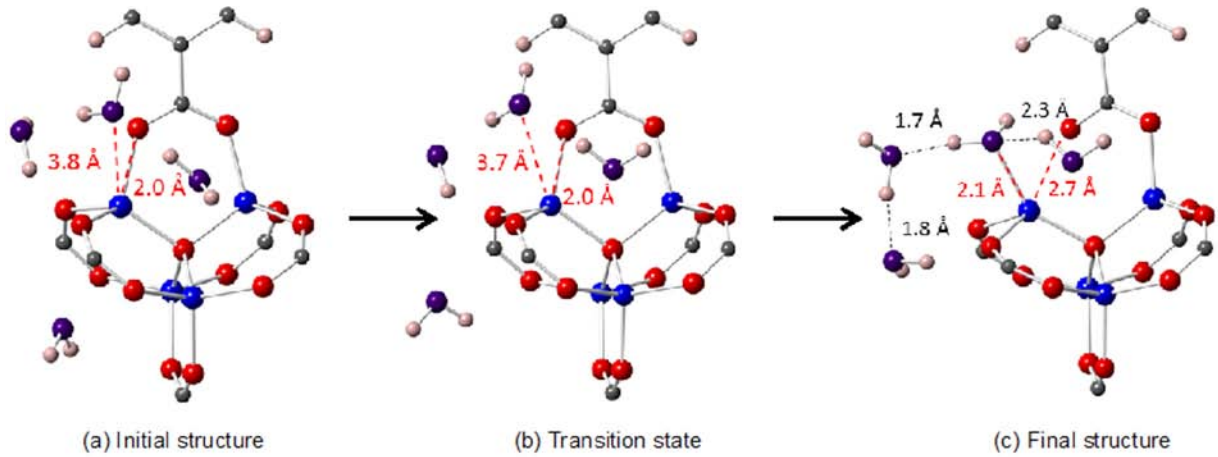

FIGURE 3. Water insertion process in MOF-5: (a) magnification of MOF-5 structure with 4 water molecules physically adsorbed near the Zn-O cluster; (b) transition state; (c) final MOF-5 structure containing a Zn-O bond broken via the insertion of a single water molecule

on the Phase 3 advancements of the original 109 potential failure modes identified by the team. The key outcome of the FMEA provides the potential top failure modes that should be considered in further research efforts for adsorbent storage systems. These top failure modes include: non-homogenous adsorbent bed, leaks at cold temperature, insulation performance, and degradation of the thermal management system over the system life.

Sorbent Media Optimization

The hydrogen storage media in the MATI system consists of densified "pucks" of MOF-5. These pucks have been compacted to a nominal density of 0.4 g/cc, which is two to three times the density of tapped powder. The best performance of these pucks will be achieved when the density variation is small. We utilized micro-computed tomography to characterize density variations (see Figure 4) and optimized the homogenous density of the puck with pre-meshed powders. The pucks had a diameter of 3 cm and height of 1 cm while mesh sized ranged from 2 mm to 0.8 mm.

ENG has been the additive included in MOF-5 compacts to enhance the thermal conduction. A potential drawback of ENG is the anisotropy of the heat conduction properties of MOF+ENG pucks formed by uniaxial compaction. As an alternative to ENG, we identified other thermal conductive additives such as graphene platelets which have a particle size that can completely coat the MOF-5 aggregates. The result was a formation of a continuous network of conductive carbon that improved the improved isotropic thermal conductivity in the axial direction by 62% in comparison to ENG at the same loading of 5%.

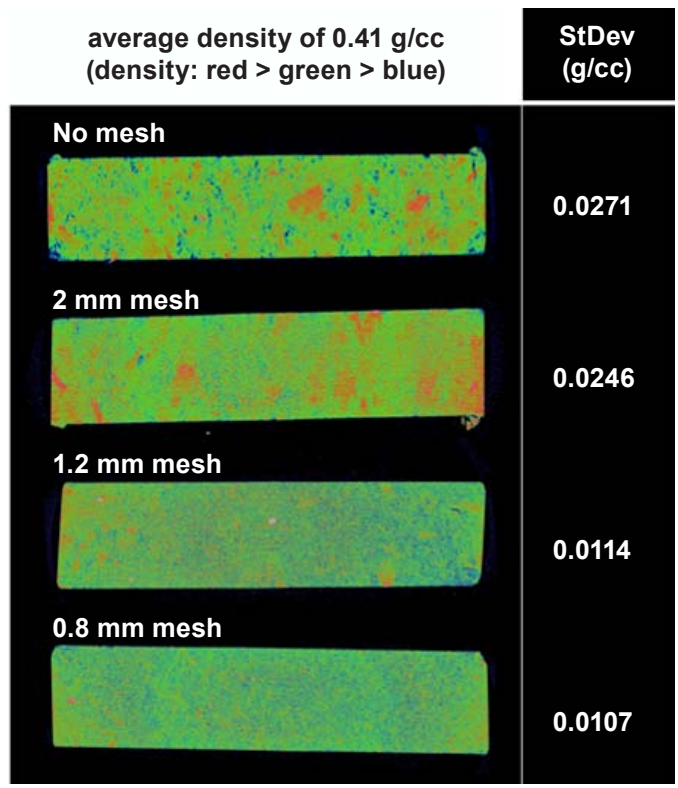

FIGURE 4. The micro CT images for pure MOF-5 pucks with pre-mesh powder prior to compaction along with standard deviation of density variation within the puck

CONCLUSIONS AND FUTURE DIRECTIONS

To ensure a successful conclusion of our HSECoE project, we plan to document our final results by completing the following publications:

- Stability of MOF-5 in a hydrogen gas environment with expected fueling station impurities
- Molecular scale water insertion mechanism in MOF-5
- Neutron and X-ray imaging studies of MOF-5 kinetics and tomography
- HSECoE Ford/UM/BASF final project report.

SPECIAL RECOGNITIONS & AWARDS/ PATENTS ISSUED

1. R. Blaser, M. Veenstra, and C. Xu, "Adsorbent material with anisotropic layering," U.S. Patent 9 006 137, April 14, 2015.

FY 2015 PUBLICATIONS/PRESENTATIONS

1. Y. Ming, H. Chi, R. Blaser, C. Xu, J. Yang, M. Veenstra, M. Gaab, U. Müller, C. Uher, D.J. Siegel, "Anisotropic Thermal Transport in MOF-5 Composites," International Journal of Heat and Mass Transfer, 82, 250 (2015). DOI: 10.1016/j.ijheatmasstransfer.2014.11.053.

2. Y. Ming, J. Purewal, J. Yang, C. Xu, R. Soltis, J. Warner, M. Veenstra, M. Gaab, U. Muller, and D.J. Siegel, "Kinetic Stability of MOF-5 in Humid Environments: Impact of Powder Densification, Humidity Level, and Exposure Time," Langmuir, 2015, 31 (17), pp. 4988–4995, DOI: 10.1021/acs.langmuir.5b00833.

3. M. Veenstra. "Onboard Automotive Targets: An OEM Perspective," DOE Materials-based Hydrogen Storage Summit, January 27, 2015.

4. D.J. Siegel. "Engineering and Adsorbent-based Hydrogen Storage System: What Have We Learned?" DOE Materials-based Hydrogen Storage Summit, January 27, 2015.

5. M. Veenstra, "Ford/BASF/UM Activities in Support of the Hydrogen Storage Engineering Center of Excellence," 2015 DOE Hydrogen Program Annual Merit Review Meeting, Washington, June 9, 2015.

IV.B.3 Microscale Enhancement of Heat and Mass Transfer for Hydrogen Energy Storage

Kevin Drost (Primary Contact), Goran Jovanovic, Vinod Narayanan, Brian Paul, Christopher Loeb, Mohammad Ghazvini, Agnieszka Truszkowska, and Hailei Wang
Oregon State University (OSU)
School of Mechanical, Industrial and Manufacturing Engineering
Rogers Hall
Corvallis, OR 97331
Phone: (541) 713-1344
Email: Kevin.Drost@oregonstate.edu

DOE Managers
Ned Stetson
Phone: (202) 586-9995
Email: Ned.Stetson@ee.doe.gov

Jesse Adams
Phone: (720) 356-1421
Email: Jesse.Adams@ee.doe.gov

Contract Number: DE-FC36-08GO19005

Project Start Date: February 1, 2009
Project End Date: June 30, 2015

Overall Objectives

Use microchannel processing techniques to:

- Demonstrate reduction in size and weight of hydrogen storage systems.
- Improve charge and discharge rates of hydrogen storage systems.
- Reduce size and weight and increase performance of thermal balance of plant components.

Fiscal Year (FY) 2015 Objectives

- Demonstrate 2-liter modular absorption tank insert (MATI)

Technical Barriers

This project addresses the following technical barriers from the Hydrogen Storage section (3.3.5) of the Fuel Cell Technologies Office Multi-Year Research, Development, and Demonstration Plan:

(A) System Weight and Volume

(E) Charging/Discharging Rates

(H) Balance of Plant (BOP) Components

Technical Targets

The Phase 3 technical targets for the Microscale Enhancement of Heat and Mass Transfer for Hydrogen Energy Storage project are shown in Table 1.

TABLE 1. Phase 3 Technical Targets

Characteristic	Units	2014 Smart Goals	Status
MATI Weight	kg	9.4	6.0
MATI Volume	liter	4.2	3.0

Accomplishments

Key developments and technical accomplishments for the reporting period are as follows:

- Completed assembly of three MATI prototypes and provided two to Savannah River National Laboratory (SRNL) for testing (Barriers A and E)
- Completed testing of conduction enhancement schemes for densified MOF-5 (metal organic framework) pucks (Barriers A and E)
- Initiated model validation development for the charge and discharge cycle for the 2-liter MATI to prototype (Barriers A and E)

✧ ✧ ✧ ✧ ✧

INTRODUCTION

Hydrogen storage involves coupled heat and mass transfer processes that are significantly impacted by the size, weight, cost, and performance of system components. Micro-technology devices that contain channels of 10–500 microns in characteristic length offer substantial heat and mass transfer enhancements by greatly increasing the surface-to-volume ratio and by reducing the distance that heat or molecules must traverse. These enhancements often result in a reduction in the size of energy and chemical systems by a factor of 5 to 10 compared to conventional designs, while attaining substantially higher heat and mass transfer efficiency. We are developing micro-technology-based advanced adsorption tank inserts (MATIs) for high media utilization and enhanced heat and mass transfer during charge and discharge of adsorbent hydrogen storage systems.

APPROACH

Our technical approach to meet Phase 3 goals is that for each high-priority component, we will use microchannel technology to reduce the relevant barriers to heat and mass transfer. Our approach involves (1) optimizing the performance of a single unit cell (i.e., an individual microchannel) and then "numbering up" using appropriate simulation tools that we then validate by experimental investigation; and (2) developing microlamination methods as a path to "numbering up" by low cost, high volume manufacturing.

RESULTS

In Phase 3, we are focused on the demonstration of one high-value application of microchannel technology: the MATI for cooling during charging, heating during discharging, and hydrogen distribution. The MATI concept integrates storage media, microchannel heat exchangers, and microchannel hydrogen distribution plates in such a way that allows convenient use of densified adsorption media with in-excess-of 94% of the tank volume being densified media. The concept separates the cooling process from the charging process, allowing flexibility in cooling strategies; in addition, the MATI can provide heating during discharge, avoiding the need to use electric energy for discharge heating. The full-sized MATI would consist of a number of cells, along with headers for cooling fluid and distributing hydrogen (see Figure 1).

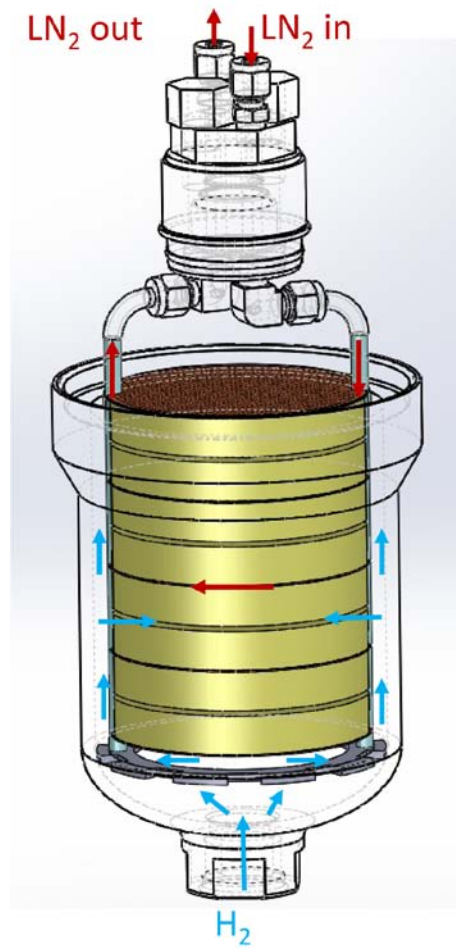

FIGURE 1. Two-liter prototype MATI design

At the end of Phase 2, the MATI was selected for inclusion in Phase 3 of the Hydrogen Storage Engineering Center of Excellence research scope. In Phase 3, we are engaged in demonstration of the MATI, specifically, in the design, assembly, and testing of a multi-cell MATI contained in a 2-liter pressure vessel. Testing will measure heat removal rates, hydrogen distribution, and durability. Two prototype MATIs have been supplied to SRNL for independent testing. Progress-to-date on the development of the microchannel-based tank insert includes the following:

- *Completed assembly of three MATI prototypes* – OSU has completed the assembly of three 2-liter MATI prototypes, including the insertion of MOF-5 pucks and sensors for testing. The MATI prototypes were fabricate in two processes. First, stainless steel lamina were chemically etched to form the flow paths and then diffusion bonded forming the cooling plate. Each cooling plate was pressure tested and tested for flow distribution. The cooling plates were then brazed to the distribution tubing, and the complete MATI was pressure tested. The assembly process for the test apparatus is shown in Figure 2. The MATI was first attached to the pressure vessel flange. Two half-pucks were slid in between two cooling plates, and the thermocouple leads were fed through one of the two 3/8" tubes on the flange and inserted into the bed. The assembly process was conducted inside a glove box in order to minimize the bed's exposure to air. Given the use of a glove box and the large number of thermocouples, the assembly process took a significant amount of time. One MATI is being used at OSU for conduction enhancement testing, and the remaining two MATIs have been shipped to SRNL for testing.
- *Completed testing of conduction enhancement schemes for densified MOF-5 pucks* – The time required to charge the MOF-5 with hydrogen can be significantly reduced if the conductivity of the densified MOF-5 pucks can be improved. OSU has conducted preliminary experimental investigations of five approaches to enhancement. These include the insertion of small aluminum pins into the puck and/or the mixing of high conductivity expanded natural graphite (ENG). In addition, unenhanced pucks were included for comparison. Each puck has two thermocouple holes in the same locations and depths of penetration for measuring bed temperature during absorption experiments. The OSU team submerged the

FIGURE 2. Various steps of assembly process and fully assembled flanged pressure vessel

MATI tank within a dewar filled with liquid nitrogen (LN_2) and modeled a charge cycle using nitrogen gas as a proxy for hydrogen. The absorption of nitrogen gas produced thermal energy that was removed from the puck to the liquid nitrogen cooling fluid in the cooling plates. By comparing the performance of enhanced pucks to the unenhanced puck, we were able to get an estimate of the value of the enhancement.

As shown in Figure 3, all of the conduction enhancements performed significantly better than the bare, unenhanced puck. The best performing enhancement (pins without any ENG) reached a steady-state temperature in 1,200 s, as compared to 2,700 s for the unenhanced puck. This is a significant improvement and suggests that puck conduction enhancement is both feasible and could lead to a significant improvement in the rate of charging and discharging of an adsorption bed formed from densified adsorbing material. We investigated a number of charging options, and the multiple experiments conducted during this quarter clearly demonstrated the benefit of conduction enhancement for current MATI design.

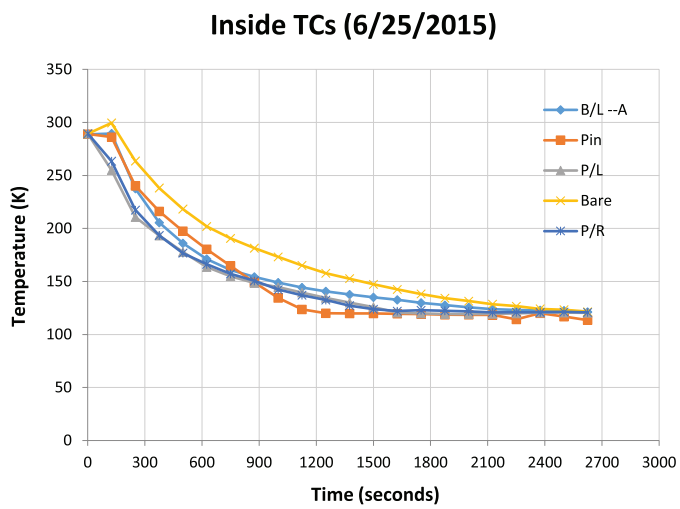

FIGURE 3. Bed temperature profiles for various conduction enhancements with submerged MATI tank

- *Initiated model validation for the charge and discharge cycle for the 2-liter MATI prototype* – Simulation models have been developed to model all relevant phenomena associated with the charging and discharging of the MATI. During Phase 2, the models were validated against the experimental results of our integrated testing. Overall, the average error between experiment and simulation results was between 4 and 5 percent, with the maximum error being between 8 and 9 percent. Based on these validation results, we were confident that we could accurately model the adsorption and desorption behavior of a single puck. However, to further improve our modeling capability, we worked with SRNL to incorporate several advanced features used by SRNL. With these modifications we have reduced the average error in our comparison with experimental data from 5.9 to 3.5 percent. We have completed the assembly of an eight-zone model (shown in Figure 4) that will model the complete MATI, including the pressure vessel during both the charge and discharge cycles. The eight-zone model simulated the various processes occurring in a single-unit cell. As data becomes available from the

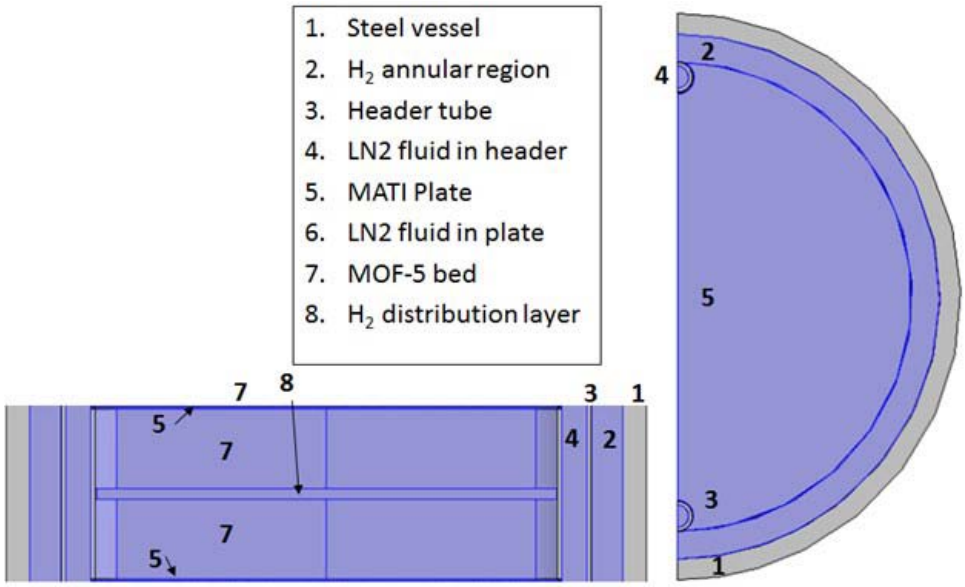

FIGURE 4. Eight-zone computational model for a MATI

SRNL comprehensive testing, we will use the eight-zone model for model validation and support of the experimental investigations being conducted at both OSU and SRNL.

CONCLUSIONS AND FUTURE DIRECTIONS

Key conclusions resulting from our research are as follows:

- The use of the MATI allows convenient use of densified adsorption media with in-excess-of 94% of the tank volume being densified media. The concept separates the cooling process from the charging process, allowing flexibility in cooling strategies, and the MATI can provide both cooling during charging and heating during discharge with a weight less than 9.5 kg for a hydrogen storage system containing 5.6 kg of hydrogen.
- The design of the 2-liter MATI has been completed, and three prototypes have been assembled and are being tested, demonstrating the technical feasibility of the concept.
- Testing at OSU has demonstrated the feasibility and impact of conduction enhancement of the MOF-5 pucks.
- The computational model has been validated with laboratory data and will be validated with prototype data being acquired by SRNL.

The next steps in our research are to complete the demonstration of the MATI, which includes comprehensive testing at SRNL, and to validate the model. The results of the project will be documented in a comprehensive project report that will include all OSU research activities associated with the Hydrogen Storage Engineering Center of Excellence.

IV.B.4 Advancement of Systems Designs and Key Engineering Technologies for Materials-Based Hydrogen Storage

Bart van Hassel (Primary Contact),
Jose Miguel Pasini, and Reddy Karra
United Technologies Research Center (UTRC)
411 Silver Lane
East Hartford, CT 06108
Phone: (860) 610-7701; Fax: (860) 610-7669
Email: vanhasba@utrc.utc.com

DOE Managers
Ned T. Stetson
Phone: (202) 586-9995
Email: Ned.Stetson@ee.doe.gov

Jesse Adams
Phone: (720) 356-1421
Email: Jesse.Adams@ee.doe.gov

Contract Number: DE-FC36-09GO19006

Project Start Date: February 1, 2009
Project End Date: June 30, 2015 (including 1 year no-cost extension)

Overall Objectives

UTRC's overall objectives mirror those of the Hydrogen Storage Engineering Center of Excellence (HSECoE) to advance hydrogen storage system technologies toward the DOE hydrogen program's 2020 storage targets. Outcomes of this project will include:

- A more detailed understanding of storage system requirements.
- Development of higher performance and enabling technologies such as novel approaches to heat exchange, on-board purification and compacted storage material structures.
- Component/system design optimization for prototype demonstration.

Fiscal Year (FY) 2015 Objectives

- Develop vehicle/power plant/storage system integrated system modeling elements to improve specification of storage system requirements and to predict performance for candidate designs
- Assess the viability of on-board purification for various storage material classes and purification approaches
- Collaborate closely with the HSECoE partners to advance materials-based hydrogen storage system technologies

Technical Barriers

This project addresses the following technical barriers from the Hydrogen Storage section (3.3.5) of the Fuel Cell Technologies Office Multi-Year Research, Development, and Demonstration Plan:

(A) System Weight and Volume

(D) Durability/Operability

(H) Balance of Plant (BOP) Components

Technical Targets

The goals of this project mirror those of the HSECoE to advance hydrogen storage system technologies toward the DOE hydrogen program's 2020 storage targets [1]. UTRC minimized the mass and cost of the particulate filtration system, which is part of the BOP of the cryo-adsorption system. The Simulink® framework enabled a comparison of all three materials-based hydrogen storage systems on a common basis by ensuring that each system provided 5.6 kg of usable H_2 to a common proton exchange membrane (PEM) fuel cell and light-duty vehicle model.

The status of UTRC's FY 2015 contributions to the technical targets is documented in Table 1.

TABLE 1. UTRC's Progress toward Meeting Technical Targets for Onboard H_2 Storage Systems

	Characteristic	Units	2020 Target	UTRC
Cryo-adsorbent H_2 storage system	H_2 Quality	% H_2	SAE J2719 and ISO/ PDTS 14687-2 (99.97% dry basis)	Meets

FY 2015 Accomplishments

Accomplishments during the current project period comprise:

- Collaborated with Savannah River National Laboratory on integrating the sorbent hydrogen storage system in the Simulink® framework.
- Implemented access to more model parameters internal to Pacific Northwest National Laboratory's chemical hydrogen storage system model in the Simulink® framework.

- Improved graphical user interface (GUI), operating manual and user-friendliness of the Simulink® framework.
- Developed a method to right-size the particulate filter area by considering the weight and cost of the particulate filter and the effect of pressure drop on hydrogen adsorption.
- Reached out to the hydrogen storage material development community at DOE's Materials-Based Hydrogen Storage Summit, Defining Pathways for Onboard Automotive Applications, Golden, Colorado, January 27–28, 2015, with presentations about the Simulink® framework and about niche application opportunities of hydrogen storage materials.

✧ ✧ ✧ ✧ ✧

INTRODUCTION

Physical storage of hydrogen through compressed gas and cryogenic liquid approaches is well established, but has drawbacks regarding weight, volume, cost, and efficiency, which motivate the development of alternative, low-pressure materials-based methods of hydrogen storage. Recent worldwide research efforts for improved storage materials have produced novel candidates and continue in the pursuit of materials with overall viability. While the characteristics of the storage materials are of primary importance, the additional system components required for the materials to function as desired can have a significant impact on the overall performance and cost. Definition, analysis and improvement of such systems components and architectures, both for specific materials and for generalized material classes, are important technical elements to advance in the development of superior methods of hydrogen storage.

APPROACH

UTRC's approach is to leverage in-house expertise in various engineering disciplines and prior experience with metal hydride system prototyping to advance materials-based H_2 storage for automotive applications. During the sixth year of the HSECoE project, UTRC continued the successful development of the Simulink® modeling framework for comparing H_2 storage systems on a common basis, which can now be downloaded from the National Renewable Energy Laboratory (NREL)-hosted website at www.hsecoe.org. UTRC also used the Darcy flow permeability values of the particulate filters (with and without an adsorbent filter cake), which it had measured in FY 2014, for right-sizing the filter area for a full-size H_2 storage system by considering the effect of pressure drop on the H_2 adsorption by the sorbent in the pressure vessel.

RESULTS

The Simulink® framework with a GUI was updated and disseminated on the web through NREL's website at www.hsecoe.org. It now contains models of the 350 bar and 700 bar compressed gas storage systems and the three models of the materials-based H_2 storage systems: ideal metal hydride, chemical hydrogen storage, and cryo-adsorption. Beta testing will continue in order to make the use of the storage system models more user-friendly to H_2 storage material developers and hydrogen storage program managers that are interested in determining how well a newly proposed material will meet the system level targets. A simplified view of the GUI of each of the materials-based H_2 storage systems is shown in Figure 1.

Figure 1a illustrates how the pressure in the ideal metal hydride system quickly drops to the equilibrium pressure of the metal hydride at the operating temperature of the tank. Figure 1b1 illustrates the high initial auxiliary power request of a chemical hydrogen storage system with a slurry of ammonia borane (AB). This initial auxiliary power is used to bring the reactor to the operating temperature that is required for the exothermic AB thermolysis. Figure 1b2 illustrates the auxiliary power request by the chemical hydrogen storage system with a slurry of aluminum hydride (alane). The endothermic release of H_2 requires constant power in order to maintain the reactor temperature. Figure 1c1 illustrates the thermal swing in a cryo-adsorption system with flow-through cooling. Heating the sorbent is used to reduce the heel of adsorbed H_2 in the tank and consumes auxiliary power. Figure 1c2 shows the drop in tank pressure in a cryo-adsorption system with the modular adsorption tank insert despite heating the adsorbent in a similar fashion as for the system in Figure 1c1. The simulation stops when the delivery pressure to the fuel cell drops below 5 bar. Each of the figures shows the material and system variables that are currently available to the user of the Simulink® framework. It has been proposed to greatly enhance the number of variables that can be varied in order to make the system simulation more useful to material developers.

The Simulink® framework is used to test whether the vehicle can follow pre-defined drive cycles by exercising the combined vehicle model, fuel cell model and H_2 storage systems. The model will control the power generation in order to reach the required speed within 2 mph and within 1 s of what is specified by the drive cycle, as shown in Figure 2. The user will be informed about any speed trace misses, which provides an opportunity to improve the characteristics of the specific H_2 storage system.

Figure 3 highlights the performance of the various H_2 storage systems in combination with the selected fuel cell system and light-duty vehicle characteristics. The shaded blue area illustrates a typical range of battery systems. DOE's 2020 target is clearly indicated with the red circle on the dark

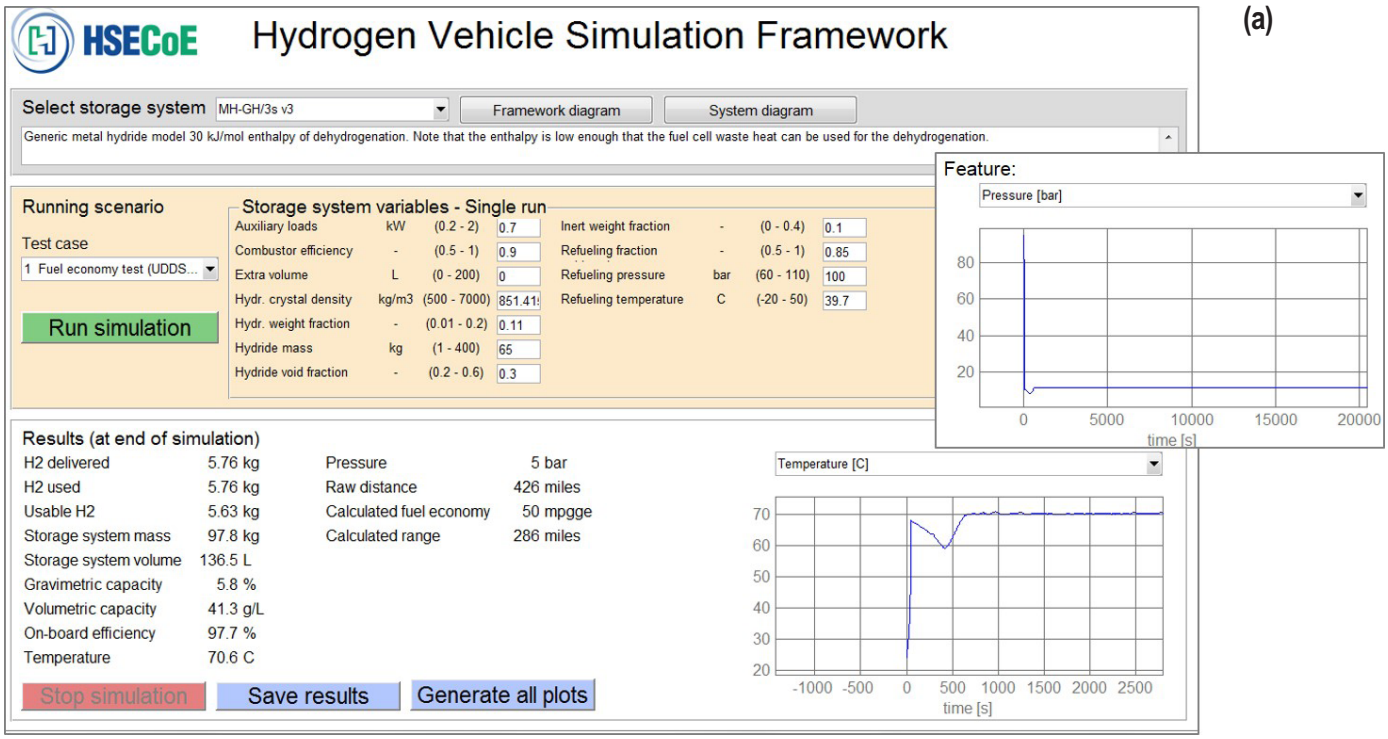

FIGURE 1a. GUI development for materials-based H_2 storage systems: ideal metal hydride system

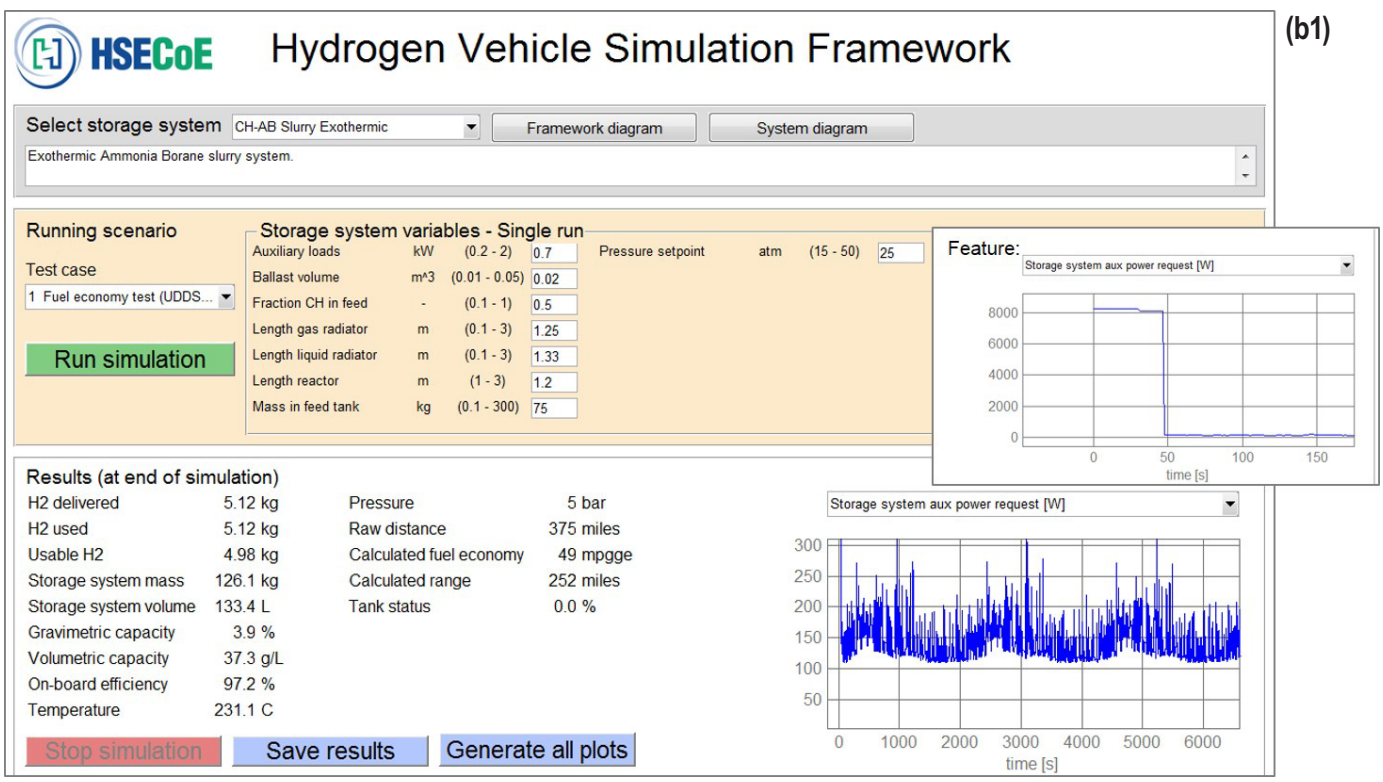

FIGURE 1b1. GUI development for materials-based H_2 storage systems: chemical H_2 storage: AB-slurry

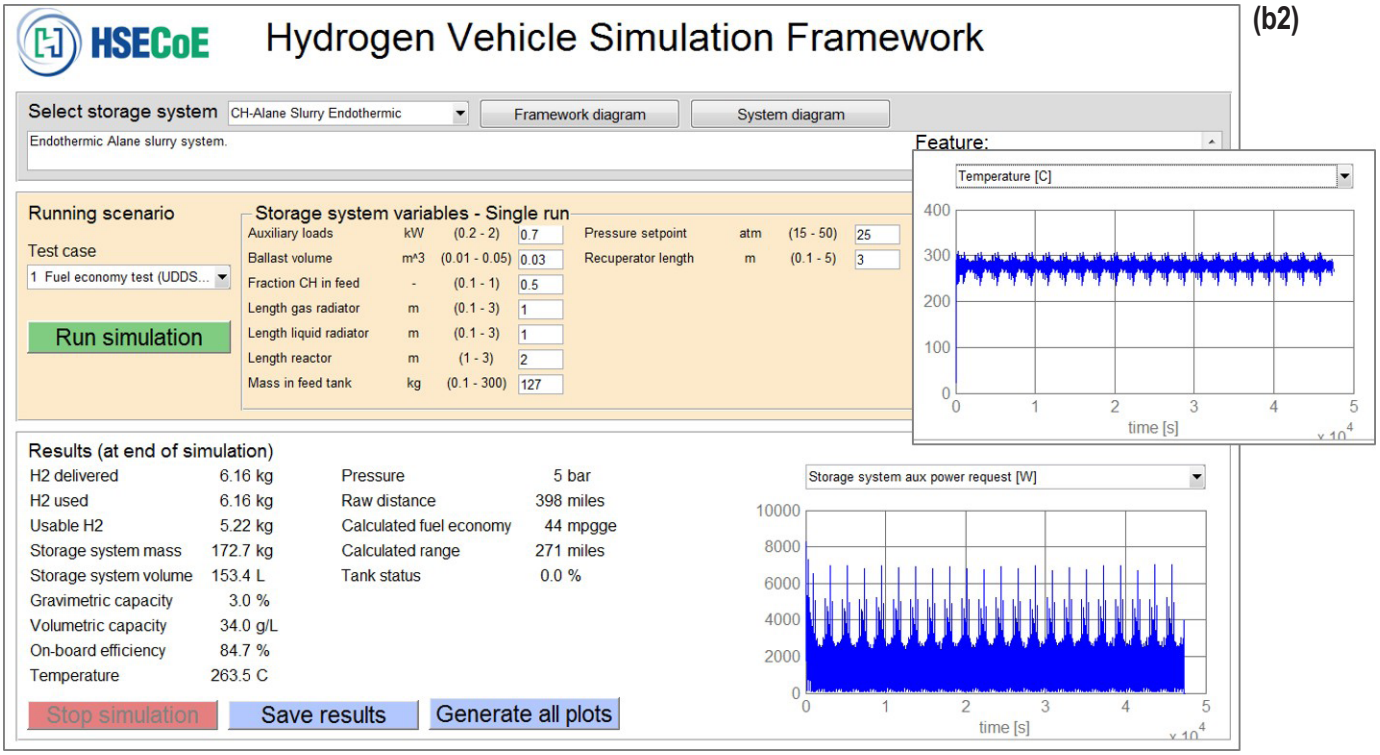

FIGURE 1b2. GUI development for materials-based H_2 storage systems: chemical H_2 storage: alane-slurry

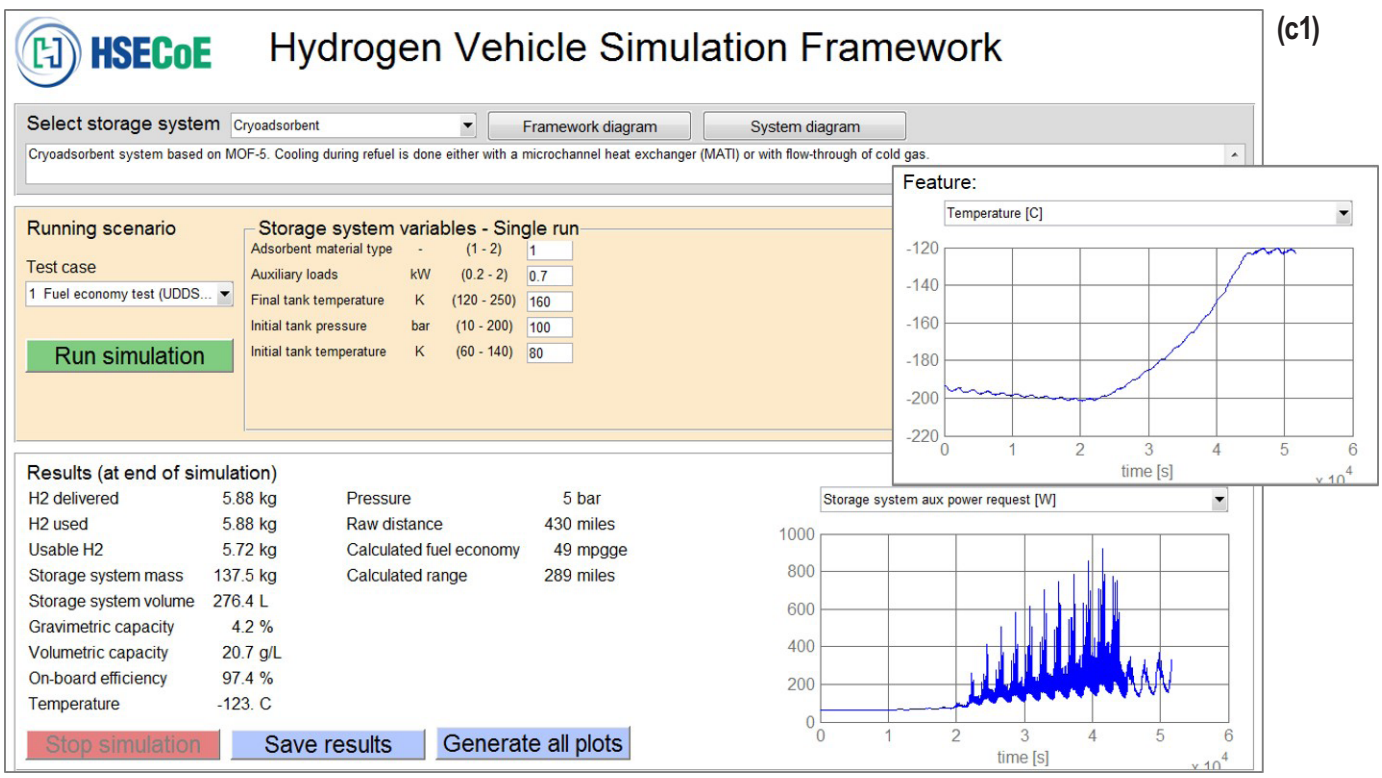

FIGURE 1c1. GUI development for materials-based H_2 storage systems: cryo-adsorption: flow-through-cooling

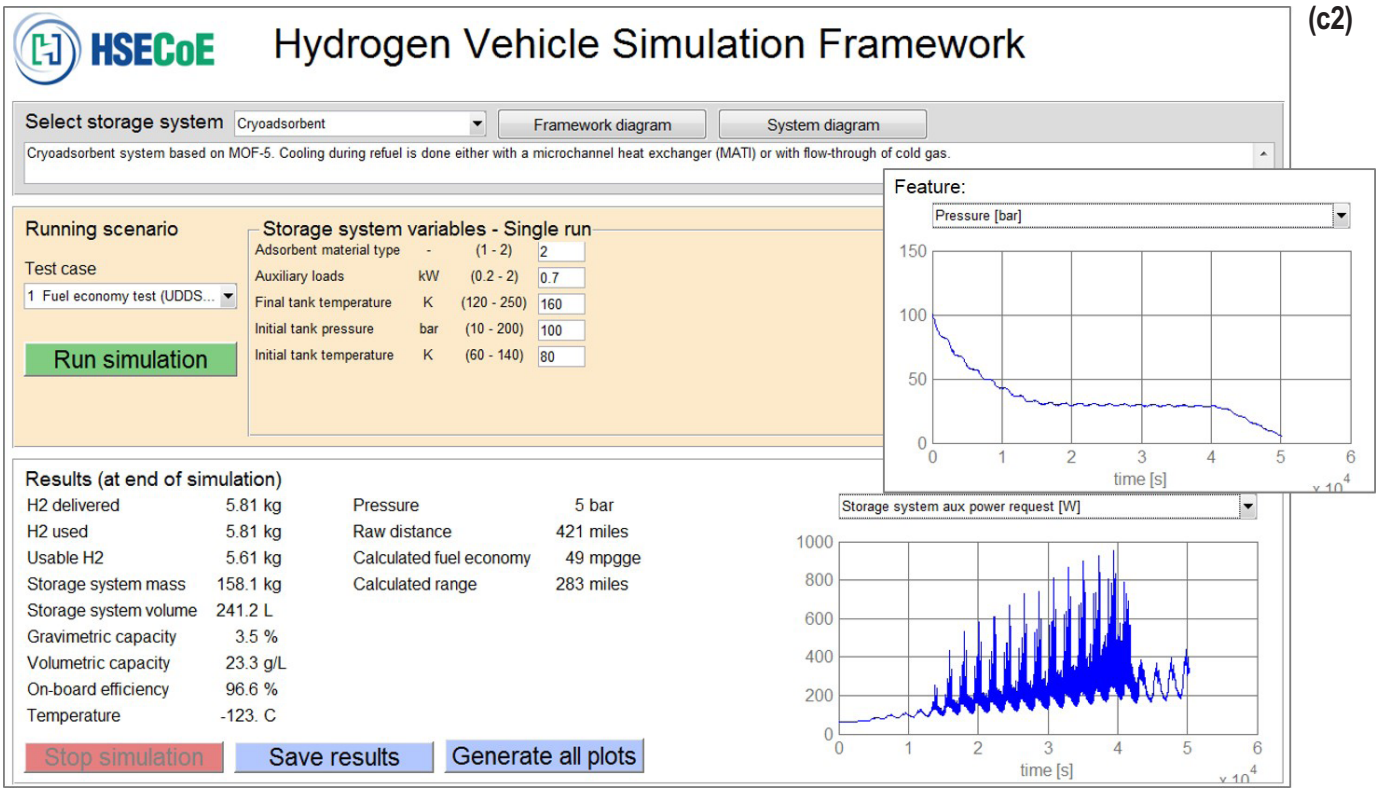

FIGURE 1c2. GUI development for materials-based H_2 storage systems: cryo-adsorption: modular adsorption tank insert

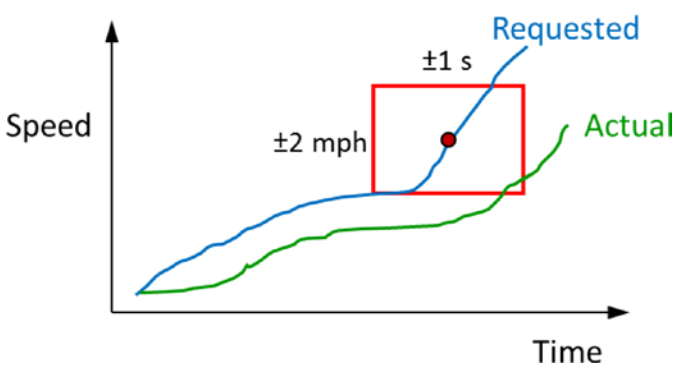

FIGURE 2. EPA trace (requested) and the actual speed trace as a function of time with the target box that will trigger alerts in the Simulink® framework in order to provide the designers an opportunity to improve their H_2 storage system (e.g., increase buffer size or install more H_2 storage material)

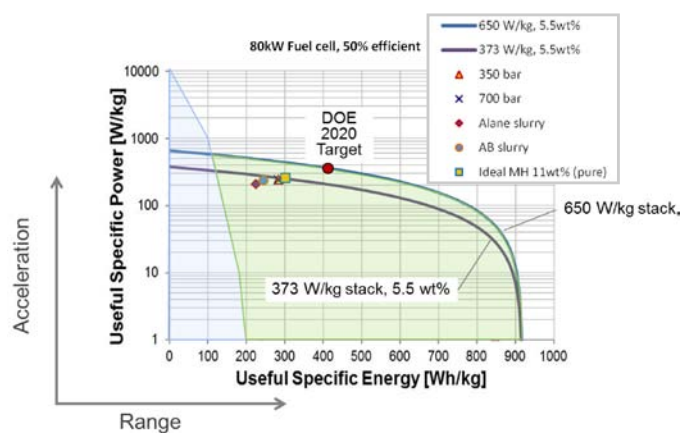

FIGURE 3. Location of the combined PEM fuel cell and H_2 storage systems within the HSECoE on a map of power density and energy density and in comparison to DOE's 2020 targets

blue line that bounds the achievable values of the specific power and specific energy of the combined fuel cell and H_2 storage system. The specific power of the current fuel cell system (373 W/kg) in the Simulink® framework model is considerably lower than the DOE target for such a fuel cell system (650 W/kg), and this lowers the achievable specific power towards the purple line. The ideal metal hydride model (yellow square) shows the achievable specific energy of the combined fuel cell plus H_2 storage system for an H_2 storage system with the targeted 5.5 wt% gravimetric capacity. The other H_2 storage systems are heavier than this ideal metal hydride model and this is reflected in the lower specific energy. A similar diagram could be drawn for the volumetric energy density, which would show the low volumetric energy density for the current adsorption-based H_2 storage systems.

A cryo-adsorption-based H_2 storage system requires a particulate filter in order to contain the adsorbent in the thermally insulated area of the pressure vessel and in order

to filter out any particulates from the H_2 gas that is sent to the PEM fuel cell to a particulate concentration <1,000 µg/m^3 while ensuring that any particulates will be smaller than 10 µm, per SAE J2719 guidelines. Particulate filters with such a performance were demonstrated in FY 2014. The Darcy permeability values with and without filter cake were also measured at that time. In FY 2015, UTRC used this data for developing a method to right-size the particulate filter area for DOE's light-duty automotive application. The flow of H_2 gas during fill and discharge causes a pressure drop across the particulate filter. This affects H_2 adsorption as the H_2 pressure downstream of the particulate filter will be less than the pressure that is available from the forecourt. It also affects H_2 desorption as the H_2 pressure upstream of the particulate filter will need to be higher than the minimum delivery pressure (i.e., 5 bar) to the fuel cell system. Both effects reduce the amount of usable H_2 gas from the H_2 storage system. This can be compensated for by installing more adsorbent in the cryo-adsorption vessel, as illustrated in Figure 4. Installing additional adsorbent increases the size of the pressure vessel and its weight. The weight penalty from installing more adsorbent and increasing the pressure vessel can be reduced by installing a larger particulate filter. The weight and cost of the particulate filter can be quite significant though. The combined effect is illustrated in Figure 5 for both the H_2 fill scenario (flow-through cooling) and for a H_2 discharge scenario near the tank empty condition. Table 2 shows the required particulate filtration areas for either minimizing system weight or system cost. An area of about 49 cm^2 of a filter media with a Darcy flow permeance of 1.72 x 10^{-13} m^2 (with filter cake) to 8.54 x 10^{-13} m^2 (without filter cake) appears to be a good compromise for the cryo-adsorption system when considering both the pressure drop during fill conditions and near the tank-empty condition.

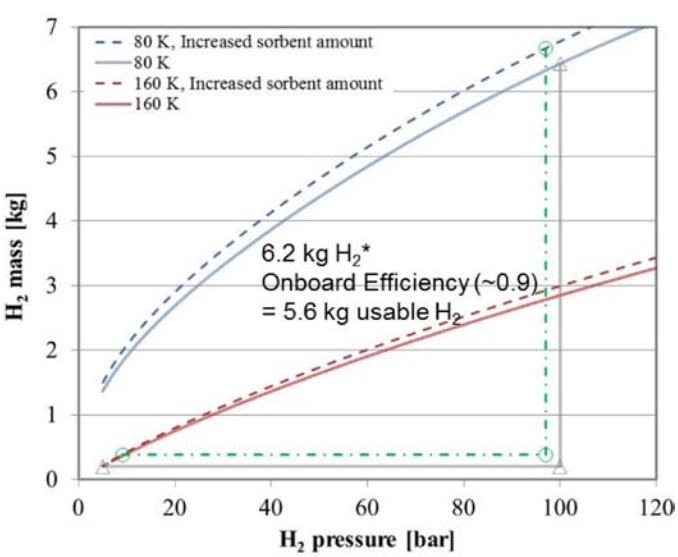

FIGURE 4. Particulate filter right-sizing method by taking into account the impact of pressure drop through the particulate filter during fill-conditions and near the empty-tank condition

CONCLUSIONS AND FUTURE DIRECTIONS

Conclusions derived from the work in FY 2015 are as follows:

- Users of the Simulink® modeling framework will benefit from having access to more H_2 storage material and H_2 storage system model parameters in the graphical user interface. This goes beyond the original objective of comparing each of the three materials-based H_2 storage systems on a common basis.
- There is an optimum particulate filter size for cryo-adsorption systems due to the effect of pressure drop across the filter on H_2 adsorption. The current high cost of particulate filters favors installing less filter area than what would be optimal for the overall weight of the H_2 storage system.

Phase 3 was completed on June 30, 2015.

FY 2015 PUBLICATIONS/PRESENTATIONS

1. Kriston P. Brooks, Troy A. Semelsberger, Kevin L. Simmons, and B.A. van Hassel, "Slurry-based chemical hydrogen storage systems for automotive fuel cell applications," Journal of Power Sources, 2014, 268, pp. 950 – 959.

2. Bart A. van Hassel, Randolph C. McGee, Allen Murray, and Shiling Zhang, "Engineering Technologies for Fluid Chemical Hydrogen Storage Systems," Invited Talk, 14th International Symposium on Metal-Hydrogen Systems: Fundamentals and Applications, Salford, Manchester, UK, July 20–25, 2014.

3. Bart A. van Hassel, Randolph C. McGee, Allen Murray, and Shiling Zhang, "Engineering Technologies for Fluid Chemical Hydrogen Storage Systems," 14th International Symposium on Metal-Hydrogen Systems: Fundamentals and Applications, Salford, Manchester, UK, July 20–25, 2014, Accepted by Journal of Alloys and Compounds.

4. B.A. van Hassel, Hydrogen Storage Systems for Mobile Applications, *IEA Task 32, Salford, Manchester, UK, July 25–26, 2014.*

5. Igor I. Fedchenia, Bart A. van Hassel, and Ron Brown, "Solution of Inverse Thermal Problem for Assessment of Thermal Parameters of Engineered H_2 Storage Materials," Inverse Problems in Science & Engineering, 2015, 23 (3), pp. 425-442.

6. Bart A. van Hassel, Jagadeswara R. Karra, Jose Santana, Salvatore Saita, Allen Murray, and Daniel Goberman, Richard Chahine, and Daniel Cossement, "Ammonia Sorbent Development for On-Board H_2 Purification," Separation and Purification Technology, 2015, 142, 215-226.

7. Bart A. van Hassel, Jagadeswara. R. Karra, David Gerlach, and Igor I. Fedchenia, "Dynamics of fixed-bed adsorption of ammonia on impregnated activated carbon for hydrogen purification," To be submitted to Separation and Purification Technology, In Preparation.

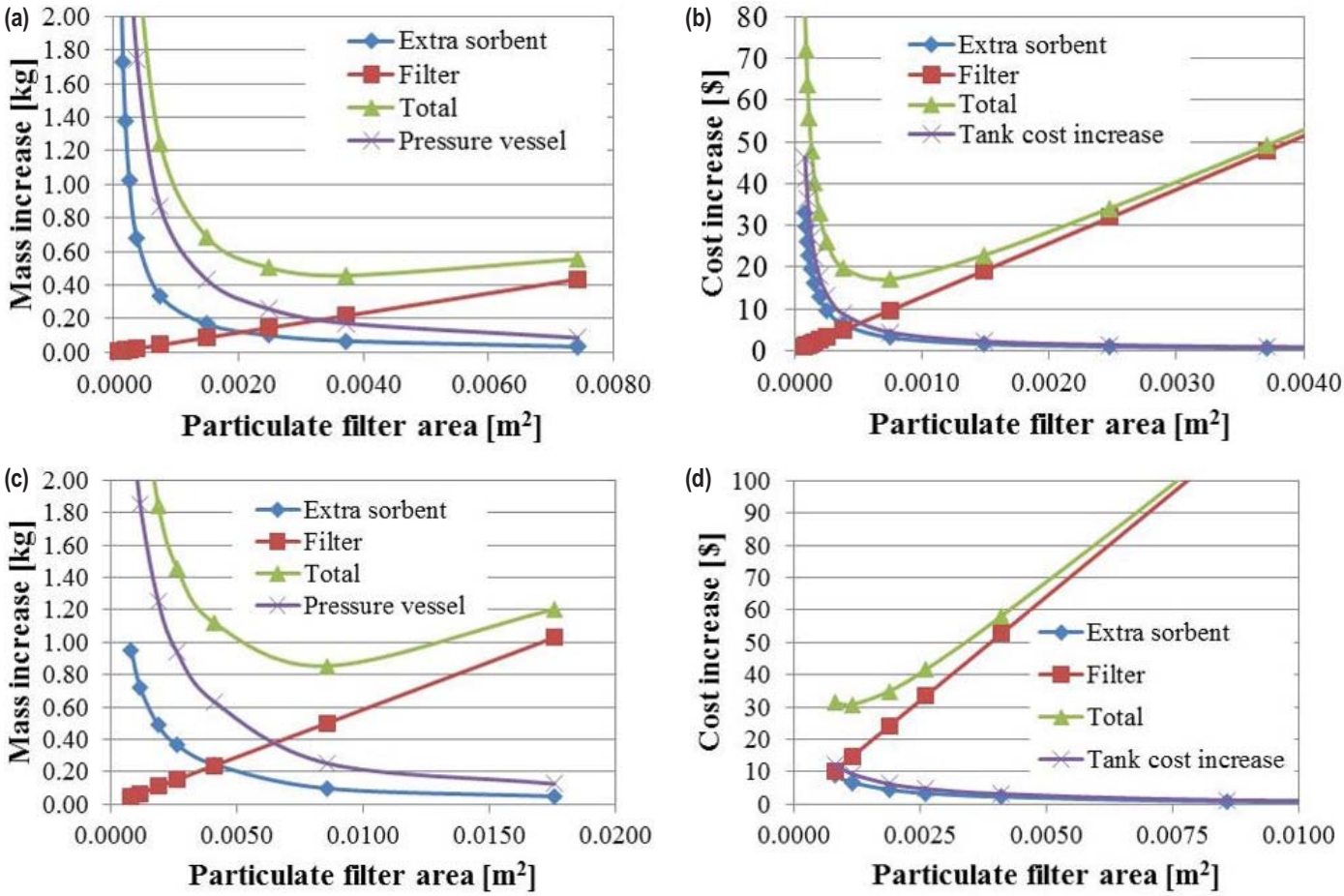

FIGURE 5. Impact of the particulate filter area and cost on the overall system while keeping the usable H_2 amount fixed at 5.6 kg

TABLE 2. Right-Sizing of Particulate Filter Area for Cryo-Adsorption System

Condition	Criterion	Area [cm²]	Pressure Drop [bar]	Total Weight Increase [kg]	Cost Increase [$]
Filling: 80 K, 100 bar, 0.060 kg-H_2/s, Filter permeability: 8.54 x 10^{-13} m²	Weight minimum	37	0.2	0.46	$49
	Cost minimum	7	1	1.25	$17
Near empty tank: 160 K, 5 bar, 0.016 kg-H_2/s, Filter permeability: 1.72 x 10^{-13} m²	Weight minimum	86	0.5	0.85	$122
	Cost minimum	12	3	2.64	$31

8. B.A. van Hassel, Hydrogen Storage Systems for Mobile Applications, *IEA Task 32, Chamonix, France, January 18–23, 2015.*

9. B.A. van Hassel, "Niche Application Opportunities," Invited Talk, DOE Materials-Based Hydrogen Storage Summit, Defining pathways for onboard automotive applications, Golden, CO, USA, *January 27-28, 2015.*

10. José Miguel Pasini, Jon Cosgrove, Matthew Thornton, Jeff Gonder, Kriston Brooks, David Tamburello, Michael Veenstra, "H_2 Models on the Web," Invited Talk, DOE Materials-Based Hydrogen Storage Summit, Defining pathways for onboard automotive applications, Golden, CO, USA, *January 27–28, 2015.*

11. Bart A. van Hassel and Jagadeswara R. Karra, Particulate Filtration for Sorbent-based H_2 Storage, Special Issue of Applied Physics A about H_2 Storage, Editor: Michael Hirscher.

12. B.A. van Hassel, "Niche Application Opportunities," Invited Talk, Gordon Research Conference, Hydrogen-Metal Systems, Fundamental Aspects of Hydrogen Interaction with Materials and Novel Energy Applications, July 12–17, 2015, Stonehill College, Easton, MA, USA.

REFERENCES

1. http://www1.eere.energy.gov/hydrogenandfuelcells/mypp/pdfs/storage.pdf

2. Information Report on the Development of a Hydrogen Quality Guideline for Fuel Cell Vehicles, SAE International Surface Vehicle Information Report, J2719 APR2008, Revised 2008-04.

IV.B.5 Systems Engineering of Chemical Hydrogen Storage and Cryo-Sorbent Storage, Pressure Vessel, and Balance of Plant for Onboard Hydrogen Storage

Kriston P. Brooks (Primary Contact),
Nicholas A. Klymyshyn, Kyle J. Alvine,
Mark R. Weimar
Pacific Northwest National Laboratory (PNNL)
P.O. Box 999/K6-28
Richland, WA 99352
Phone: (509) 372-4343
Email: Kriston.brooks@pnnl.gov

DOE Managers
Ned Stetson
Phone: (202) 586-9995
Email: Ned.Stetson@ee.doe.gov
Jesse Adams
Phone: (720) 356-1421
Email: Jesse.Adams@ee.doe.gov

Project Start Date: February 1, 2009
Project End Date: March 31, 2016

Overall Objectives

- Develop hydrogen storage systems that meet DOE 2020 targets for light duty vehicles based on adsorbents and chemical hydrogen storage (CHS) materials
- Identify, develop, and validate critical components of the chemical hydrogen and cryo-sorbent-based hydrogen storage systems
  - Address system performance, mass, volume, and cost
- Develop and validate models for a CHS system to further the understanding of onboard storage energy management requirements
  - Work with partners to integrate validated models into system framework that will lend insight into overall fuel cycle efficiency
- Mitigate materials incompatibility issues associated with hydrogen embrittlement, corrosion, and permeability through suitable materials selection for balance of plant (BOP) components

Fiscal Year (FY) 2015 Objectives

- Cryo-Adsorbent Hydrogen Storage Design
  - Develop and test prototype of the liquid nitrogen (LN_2) cooled-wall tank concept to increase refueling rate
  - Perform compressive tests of candidate polymer valve and seal materials under cryogenic temperatures with and without saturating the material with high-pressure hydrogen to evaluate each polymer's compatibility in cryo-adsorbent applications
  - Compare cost models for the two cryo-adsorption systems (hexagonal aluminum honeycomb [Hexcell] and modular adsorption tank insert [MATI]) to the Strategic Analysis' independent estimate and update costs to include BOP system upgrades
- Chemical Hydrogen Storage Design
  - Integrate storage system models for exothermic and endothermic systems into the vehicle framework and post the updated model on the Hydrogen Storage Engineering Center of Excellence (HSECoE) website to allow evaluation of other hydrogen storage materials

Technical Barriers

This project addressed the following technical barriers this last year for Hydrogen Storage from the Fuel Cell Technologies Office Multi-Year Research, Development, and Demonstration Plan:

(B) System Cost

(C) Efficiency

(E) Charging/Discharging Rates

(H) Balance of Plant (BOP) Components

(J) Thermal Management

Technical Targets

The current status of the cryo-sorption material systems versus the DOE Onboard Hydrogen Storage System Technical Targets addressed this fiscal year by PNNL is given in Table 1.

Fiscal Year (FY) 2015 Accomplishments

- Designed, fabricated, and tested LN_2 cooled-wall tank prototype. Compared the results of these prototype tests to the full-scale system and determined (1) that wall cooling to 90 K could be achieved in <3 minutes using 17.9 kg LN_2 and (2) the full scale system design was structurally and thermally sound.

TABLE 1. Cryo-Adsorbent Storage System Progress towards Meeting DOE Technical Targets

Target	Units	2020 DOE Goal	HSECoE Value
System Cost	$/kWh net	10	35 (Hexcell) 37 (MATI)
	$/kg H_2 stored	333	486 (Hexcell) 517 (MATI)
System Fill Time (5 kg)	min	3.3	2.7 (tank wall cooling only)
Operational Cycle Life	cycles	1,500	>1,000,000 (tank wall only)

- Updated cost models for the two cryo-adsorbent systems. This update included costs of the "consolidated valve block," a component of both systems in which multiple valves and instruments were incorporated into a single body. A cross comparison was made between the cost estimates made by PNNL and those produced by Strategic Analysis.
- Developed an approach to evaluating the hydrogen compatibility of polymers for cryo-adsorbent systems by analyzing the combined effects of high pressure H_2 (345 bar) and cryogenic temperatures (77 K).
- Updated the CHS system model, integrated into the framework and documented and released these models to the public on the HSECoE website (hsecoe.org).

✧ ✧ ✧ ✧ ✧

INTRODUCTION

Prior to HSECoE, multiple onboard vehicle-scale hydrogen storage demonstrations were performed. However, none of these demonstrations have simultaneously met all of the DOE hydrogen storage sub-program goals. Additionally, engineering of new cryo-adsorbent and CHS approaches is in its infancy, with ample opportunity to develop novel systems capable of reaching the DOE 2020 targets for light-duty vehicles. The goal of HSECoE, led by Savannah River National Laboratory (SRNL), is to develop and demonstrate low cost, high performing, onboard hydrogen storage through a fully integrated systems design and engineering approach. Toward this end, PNNL is working with HSECoE partners to design and evaluate systems based on slurry chemical and cryo-adsorbent hydrogen storage media.

APPROACH

As part of HSECoE, PNNL has actively contributed to the design and testing of hydrogen storage systems. As these designs are developed, efforts are made to address obstacles to meeting the DOE technical targets. For FY 2015, PNNL's primary responsibility was to address four issues for the cryo-adsorbent system: (1) rapid refueling, (2) system cost, (3) BOP mass and volume, and (4) hydrogen compatibility. The DOE technical targets require a cool down time of less than 3.3 minutes. One of the major needs is to cool the tank walls themselves. An approach to address this need was developed and a prototype system tested to validate the concept. This year's work also continued to refine the cost of the two cryo-adsorbent systems. Finally, the compatibility of the polymer materials that may be used within the BOP at low temperatures and high H_2 pressures was investigated.

As the systems are designed, HSECoE has developed models to describe the performance of these systems under a variety of drive cycle scenarios. In past years, PNNL work has focused on the development of the CHS models. The models that have been developed can be used to not only to predict the performance of current CHS materials such as ammonia borane (AB) and alane, but they can also help researchers predict the performance of yet-to-be-developed materials relative to DOE's technical targets for light-duty vehicles. This fiscal year, these models have been placed on the HSECoE website to allow their use by other researchers.

RESULTS

Liquid Nitrogen Cooled-Wall Tank Testing and Evaluation

During each refueling of cryo-adsorbent systems, the tank and its contents must be re-cooled from approximately 160 K to 80 K. This can be done by flowing cold hydrogen though the adsorbent in the tank in the case of the Hexcell system design, or LN_2 through the microchannels in the case of the MATI system design. Modeling of this process during refueling has demonstrated that while the adsorbent material can be cooled relatively easily using these approaches, the tank wall remains warm. To address this shortcoming, PNNL and Hexagon Lincoln have developed an LN_2 cooled-wall tank approach that utilizes the flow of LN_2 in an annulus between the tank and its insulation to cool the tank wall during refueling. This approach reduces the amount of excess hydrogen fuel required for the Hexcell design and the amount of LN_2 for the MATI design, saving on refueling time and cost.

To evaluate this concept, a 2-liter aluminum Type I tank was instrumented with thermocouples along its interior both axially and radially. This Type I tank was then installed inside of a dewar with a framework that centers it within the dewar cavity (see Figure 1). Insulation is inserted into the exit end of the dewar to allow ports for the flow of LN_2 and to minimize heat loss out of the dewar. Many access ports were designed into the test system and holes were bored through the insulation to provide flow paths for LN_2 and nitrogen steam.

Several different configurations were evaluated to speed the cooling process, including filling from the top, filling

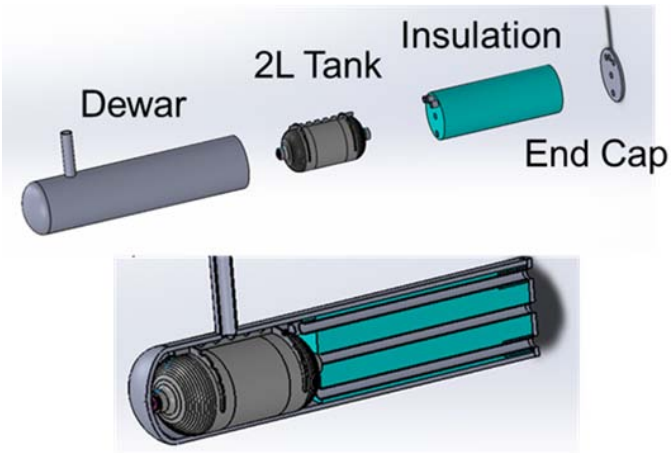

FIGURE 1. Design of the LN_2 cooled-wall tank 2-liter prototype system

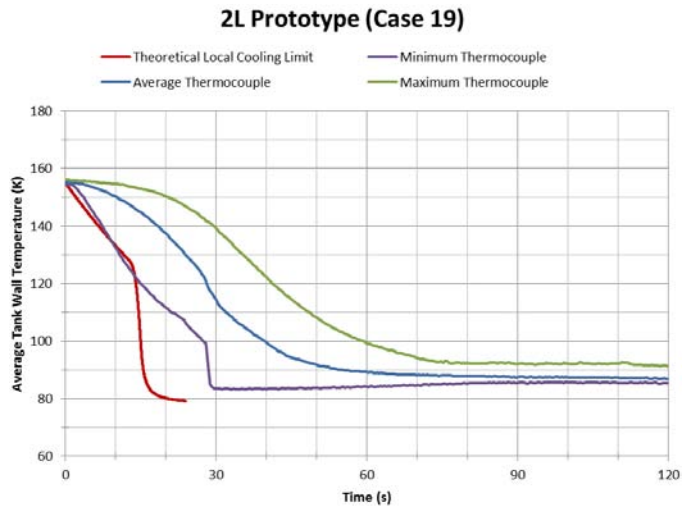

FIGURE 2. The fastest cooling results for the 2-liter prototype system compared to an ideal system

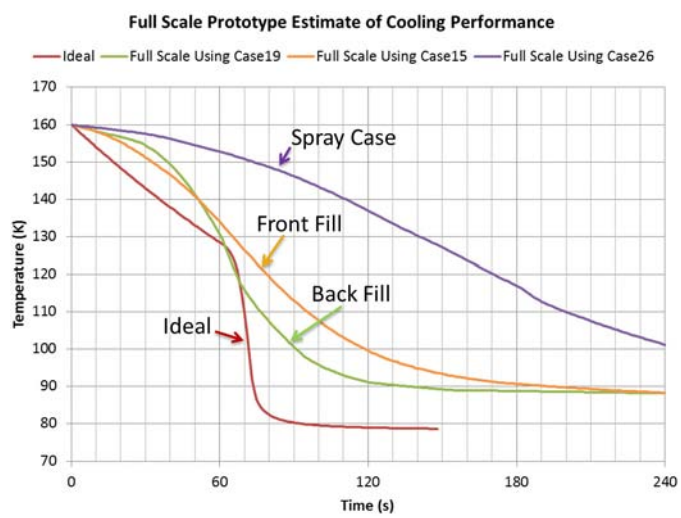

FIGURE 3. Estimated cool down times for a full scale LN_2 cooled-wall system using heat transfer values from the 2-liter prototype

from the side, and using a set of spray nozzles in an attempt to quickly cool the tank to the required temperature of 80 K. The best results were achieved with the highest flow rate of LN_2 and by filling the annulus from the rear of the dewar and exhausting the nitrogen gas product from the mouth of the dewar. Although the spray nozzles provided good coverage of the entire surface of the tank, due to its high pressure drop and the limited mass flow rate capacity of the LN_2 supply used in testing, the flow rate attainable was much less than other approaches. As a result, the cooling rate was not improved under test conditions.

The fastest cooling results were compared to modeling an ideal system assuming the tank was totally immersed in LN_2 and cooling is limited by the heat transfer between the LN_2 to the tank as shown in Figure 2. The plot shows that the minimum recorded temperatures match the full immersion cooling rates during the initial stages of cooling. It should be noted that the locations of minimum temperature change throughout the cool down process, which indicates a complex flow pattern of LN_2 within the dewar. Because of the complicated physical phenomenon within the dewar, this analysis is only concerned with the net cooling effect and the ability to recreate that effect in a full scale system.

Using the results of the prototype tests, predictions can be made for the cooling rate of the full-scale system with the same heat flux profiles witnessed in testing. A full scale system as defined by SRNL is an aluminum pressure vessel having a mass of 59.6 kg and having a surface area exposed to the LN_2 cavity of 26,500 cm^2. The results of this analysis are shown in Figure 3. The back fill curve cools the tank from 160 K to 90 K in about 130 seconds, which is well within the DOE target goal of a 3.3 minute refuel rate. However, the desired fully cold temperature is 80 K, which was not demonstrated to be achievable in testing. The 10 K difference in temperature is expected to be addressed via flow-through cooling on the adsorbent material inside the pressure vessel.

When determining the time required to cool the tank, the flow rate of LN_2 and the resulting amount of LN_2 loss must be considered. Higher flow rates will cool the tank more quickly but excess LN_2 will remain in the annulus after the tank has reached its setpoint temperature. Alternatively, the tank cooling can be slower but designed to reach its setpoint just as the ideal amount of LN_2 evaporates from the annulus. A balance between LN_2 flow rate and usage must be achieved. Table 2 makes performance projections for the full system based on these variables.

In addition to providing information necessary to project full scale system cooling performance, the 2-liter test data demonstrates that the cooling of the aluminum pressure vessel can be significantly non-uniform through time.

TABLE 2. Full System Performance Projections

LN_2 Mass Flow Rate (g/s)	LN_2 Mass Flow Duration (s)	Total LN_2 Delivered During Fill (kg)	Time to 90 K (s)	Temperature at 198 s (K)	LN_2 remaining at 198 s (kg)
188	102	19.2	132	81	1.56
188	93	17.5	144	84	0.52
188	88	16.5	161	89	0.19
150	117	17.5	157	85	0.64
125	140	17.5	172	86	0.74

While the aluminum wall eventually stabilizes to a uniform temperature, rapid localized cooling is apparent, which suggests that thermal stresses are present due to non-uniform thermal expansion of the structure. The thermal stresses were evaluated using a finite element model to determine if thermal fatigue was a problem for this design concept. The results of this modeling study found that localized cooling due to LN_2 boiling on the pressure vessel surface did not cause significant thermal stresses because the surface heat flux is naturally limited (by the Leidenfrost effect) and the thermal conductance of aluminum is so high that the temperature gradients that do occur are relatively gentle. As a result, the finite element study estimated a fatigue life of over 1,000,000 cycles for the full scale system.

Balance of Plant Polymer Compatibility for Cryo-Adsorbent System

The use of polymers is essential to providing adequate seals, pistons, and seats for the components used in the BOP. The compatibility of these polymers in the presence of low temperatures and high H_2 pressures was evaluated. Because PNNL does not currently have the ability to run in situ compression tests in the presence of hydrogen at cryogenic temperatures, an ex situ test was performed as follows. HDPE, PTFE, ECTFE, PCTFE, and PEEK polymer samples were exposed to 345 bar hydrogen for over 72 hours to allow adequate time for H_2 diffusion into the polymer. The H_2 pressure was quickly relieved and the samples were soaked in LN_2 until their temperature was equilibrated. A low temperature compression test was then run following ASTM D695 for rigid plastics.

Stress-strain and modulus curves of the different plastics under compression are shown in Figure 4. Both the hydrogen saturated and baseline tests showed the same qualitative behavior in the stress-strain curves and the failure mechanisms. An increase in the elastic modulus is observed for the hydrogen loaded samples for all materials by a statistically meaningful amount. Conversely, HDPE, PTFE, and ECTFE show a decrease in the yield stress with hydrogen compared to the baseline while there is no statistically significant change for PCTFE and PEEK. Based on these results, it appears that these materials are relatively compatible with a high pressure, low temperature H_2 environment.

Cost Analysis Update for Hexcell and MATI Systems

The cost analysis performed in previous years was updated for the Hexcell and MATI cryo-adsorbent systems. PNNL purchased a design for manufacturing code, Costimator®, that assisted in estimating the cost of those components that are not off the shelf but must be fabricated. The results of the cost analysis were compared to an independent cost study performed by Strategic Analysis. This comparison allowed differences to be addressed and result in improved estimates for both organizations. The results

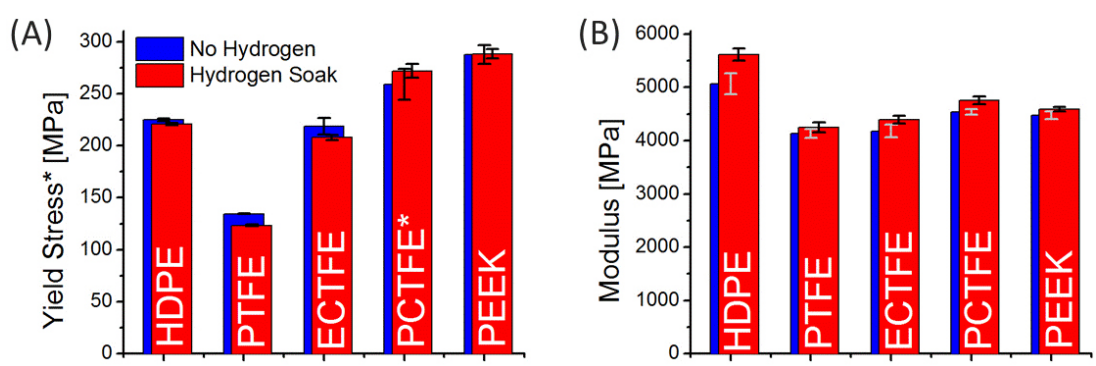

FIGURE 4. (a) Stress-strain and (b) modulus curves for various plastics under compression under LN_2 both with and without a hydrogen soak

of these studies are shown in Table 3. Although individual component costs varied, the overall system cost was consistent between the two organizations.

TABLE 3. Cost Comparison between Strategic Analysis and the HSECoE for Cryo-Adsorbent Systems Hexcell and MATI

Organization	Hexcell System	MATI System
HSECoE	$2,720	$2,897
Strategic Analysis	$2,580	$2,830

Chemical Hydrogen Storage Material Model Development

The CHS models were finalized and incorporated into the vehicle level model (i.e., framework). The graphical user interface allows users to select a representative exothermic CHS material (AB) or an endothermic CHS material (alane). Selected system sizing parameters can be adjusted and the model run to determine if the storage system can meet the four drive cycles available in the model. This newly updated framework with the CHS models and user's manual was uploaded onto HSECoE.org to make it available to the public. Material developers can now modify the thermodynamic and kinetic parameters of the current CHS material to evaluate their newly developed materials relative to the drive cycles with a simulated light-duty fuel cell vehicle.

CONCLUSIONS AND FUTURE DIRECTIONS

The conclusions of the FY 2015 work are as follows:

- Fabricated a 2-liter LN_2 cooled-wall tank prototype and tested it under a variety of conditions. Using the experimental data, the wall cool down time was estimated to be less than the 3.3 minutes required for the full-scale system by the DOE technical targets.
- The thermal mechanical fatigue analysis of the full-scale tank determined that the tank can be subject to over 1,000,000 fully reversing stress cycles to initiate a fatigue crack. This value is much greater than the 1,500 cycles required by the DOE technical targets.
- Polymer materials exposed to high pressure hydrogen followed by cryogenic compressive strength testing showed similar yield and modulus results to those not exposed to hydrogen, suggesting that they are hydrogen compatible under these conditions.
- Cost models developed by Strategic Analysis and HSECoE were compared and their differences reconciled, resulting in an improved cost analysis. The resulting system costs ($/kg H_2) are within 64–68% of the DOE technical targets.

The future direction of this work during FY 2016 is as follows:

- The cryo-adsorbent and CHS reports for HSECoE will be finalized and submitted to DOE.
- Support will continue for users of the vehicle level framework on the HSECoE website. PNNL will address questions and issues for the CHS models as well as develop a pre-processor that provides an estimate of the system sizing based on the material thermodynamic and kinetic parameters.

PATENTS

1. Newhouse, Norm, John Makinson, and Kevin Simmons, "Thermal Insulation Shell System for Composite Pressure Vessel," U.S. Provisional Patent Application No. 61/822,580, May 2013.

2. Brooks, Kriston P., Jamie Holladay, Kevin Simmons, "Combined on-board hydride slurry storage and reactor system and process for hydrogen-powered vehicles and devices," Patent # 8,889,097, November 18, 2014.

FY 2015 PUBLICATIONS/PRESENTATIONS

Publications

1. Brooks, Kriston P., Troy A. Semelsberger, Kevin L. Simmons, and Bart van Hassel, 2014, "Slurry-Based Chemical Hydrogen Storage Systems for Automotive Fuel Cell Applications," *Journal of Power Sources*, Vol. 268, 950–959.

2. Brooks, Kriston P., Richard P. Pires, Kevin L. Simmons, 2014, "Development and Validation of a Slurry Model for Chemical Hydrogen Storage in Fuel Cell Vehicle Applications," *Journal of Power Sources*, Vol. 271, 504–515.

3. Semelsberger, Troy A., Kriston P. Brooks, 2015, "Chemical Hydrogen Storage Material Property Guidelines for Automotive Applications," *Journal of Power Sources*, Vol. 279, 593–609.

4. Choi, Young Joon, Matthew Westman, Abhi Karkamkar, Jaehun Chun, and Ewa Rönnebro, "Synthesis and Engineering Materials Properties of Fluid Phase Chemical Hydrides for Automotive Applications," *Energy&Fuels*, submitted June 2015.

5. Westman, Matthew, Jaehun Chun, Young Joon Choi, and Ewa Rönnebro, "Scale-up of Fluid Phase Chemical Hydrogen Storage Materials and Materials Engineering Properties for Automotive Applications," *Energy&Fuels*, to be submitted, August 2015.

Presentations

1. Brooks, Kriston, Rich Pires, Matt Westman, Kevin Simmons, Troy Semelsberger, and Bart van Hassel, "Modeling and Experimental Validation in the Development of Chemical Hydrogen Storage Materials for Automotive Applications," 2014 Fuel Cell Seminar & Energy Exposition, Los Angeles, CA, November 12, 2014.

2. Brooks, Kriston, Rich Pires, Matt Westman, Kevin Simmons, Troy Semelsberger, and Bart van Hassel, "Modeling and Experimental Validation in the Development of Chemical Hydrogen Storage Materials for Automotive Applications," 2014 Annual Meeting AIChE, Atlanta, GA, November 16, 2014.

IV.B.6 System Design, Analysis, Modeling, and Media Engineering Properties for Hydrogen Energy Storage

Matthew Thornton (Primary Contact), Jeff Gonder, and Jonathon Cosgrove
National Renewable Energy Laboratory (NREL)
1617 Cole Boulevard
Golden, CO 80401
Phone: (303) 275-4273
Email: Matthew.Thornton@nrel.gov

DOE Managers
Ned Stetson
Phone: (202) 586-9995
Email: Ned.Stetson@ee.doe.gov
Jesse Adams
Phone: (720) 356-1421
Email: Jesse.Adams@ee.doe.gov

Project Start Date: February 2, 2009
Project End Date: September 30, 2015

Overall Objectives

- Perform vehicle-level modeling and simulations of various storage systems configurations
- Lead the storage system energy analysis and provide results
- Compile and obtain media engineering properties for adsorbent materials
- Coordinate the public access of select Hydrogen Storage Engineering Center of Excellence (HSECoE) models, including web posting documentation and tracking downloads and web activity

FY 2015 Objectives

- Coordinate the public access of select HSECoE models, including web posting documentation and tracking downloads and web activity
- Complete final report

Technical Barriers

This project addresses the following technical barriers from the Hydrogen Storage section of the Fuel Cell Technologies Program's Multi-Year Research, Development and Demonstration Plan:

(A) System Weight and Volume

(B) System Cost

(C) Efficiency

(E) Charging/Discharging Rates

(I) Dispensing Technology

(K) Systems Life-Cycle Assessments

Technical Targets

This project is conducting simulation and modeling studies of advanced onboard materials-based hydrogen storage technologies. Insights gleaned from these studies are being applied toward the design and synthesis of hydrogen storage vessels that meet the following DOE 2015 hydrogen storage for light-duty vehicle targets:

- Cost: to be determined
- Specific energy: 0.055 kg H_2/kg system
- Energy density: 0.040 kg H_2/L system
- Charging/discharging rates: 3.3 min
- Well to power plant efficiency: 60%

FY 2015 Accomplishments

- Updated and integrated several center storage system models with the molding framework and posted them on the web site portal
  - Included a 700 bar physical storage model, a metal hydride model two chemical hydride models and adsorbent system models
- Completed documentation updates for the posted models (including website text and downloadable user manual)
- Competed submodel validation, graphical user interface (GUI) improvement, model parametrization and simulation run time improvements
- Performed vehicle-level tradeoff analyses to better understand the impact of key engineering designs, for example, the tradeoff between mass, onboard hydrogen storage capacity, and vehicle range
- Completed final report

✧ ✧ ✧ ✧ ✧

INTRODUCTION

Overcoming challenges associated with onboard hydrogen storage is critical to the widespread adoption of hydrogen-fueled vehicles. The overarching challenge is

identifying a means to store enough hydrogen onboard to enable a driving range greater than 300 miles within vehicle-related packaging, cost, safety, and performance constraints. By means of systems analysis and modeling, hydrogen storage system requirements for light-duty vehicles can be assessed. With these findings and through collaboration with our HSECoE partners, optimal pathways for successful hydrogen storage system technology can be identified to enable future commercialization of hydrogen-fueled vehicles. At this stage of the project the focus of activities has moved from the model application and analysis to model validation and making select models developed under the HSECoE publicly available and accessible to other researcher.

APPROACH

An array of tools and experience at NREL are being used to meet the objectives of the HSECoE. Specifically, extensive knowledge of multiple vehicle simulations, well-to-wheels analysis, and optimization are being employed and integrated with fuel cell and material-based hydrogen storage system models developed by other HSECoE partners. This integrated model framework allows for the evaluation of various hydrogen storage options on a common basis. Engineering requirements are defined from these studies thus enabling the design of hydrogen storage vessels that could meet DOE performance and cost targets in a vehicle system context. The approach for FY 2015 is to complete updates, validation, troubleshooting, debugging, and documenting these framework and other models to that can be made accessible and use by other research organizations.

RESULTS

The following will provide results from work completed this year to support the HSECoE with a focus on the coordination of the public access of select HSECoE models, including web posting documentation and tracking downloads and web activity. In collaboration with several HSECoE partners, NREL worked on the validation, refinement, GUI improvements, troubleshooting, improving simulation run time, documentation of models selected for web posting and web activity monitoring/tracking and model download tracking. To date there have been 50 downloads of the tank volume/cost model, 31 downloads of the framework model, 17 downloads of the metal hydride (MH) finite element model and 13 down loads of the MH acceptability envelop.

Model validation work on the HSECoE MH stand lone acceptability envelope, MH finite element, the tank volume/cost models and the compressed gas, MH and chemical hydride (CH) framework models have been compete. Documentation and users guides for all of these HSECoE models have also been complete this year and all are currently or will soon be available via the HSECoE

FIGURE 1. HSECoE web home page

website (hsecoe.org). Figure 1, shows a screen caption of the current HSECoE home page which has direct links to the documentation, user guides and download area for all available models (Figure 2).

The following Table 1, shows all of the select HSECoE models that are available on the website.

TABLE 1. HSECoE Models Available on Web Portal and Model Posting Status

Model Name	HSECoE Lead	Status
MH Acceptability Envelop	SRNL	Complete
MH Finite Element Model	SRNL	Complete
Tank Volume/Cost Model	PNNL	Complete
MH Framework Model	UTRC/NREL	Complete
CH Framework Model	PNNL/UTRC/NREL	Complete
AD Framework Model	SRNL/UTRC/NREL	Complete

SRNL – Savannah River National Laboratory; PNNL – Pacific Northwest National Laboratory; UTRC – United Technologies Research Center; AD - adsorbent

In addition to the validation, documentation, user guide and posting activities this year efforts were also focused on the continued refinement of a GUI for the framework model in order to make the models more user friendly. In FY 2015 UTRC, NREL and other HSECoE partners teamed

FIGURE 2. HSECoE web models documentation and download page

on the GUI improvement effort. Figure 3 shows the current framework model GUI developed by UTRC. In this figure the model selection pull down menu, the parameter settings location and the model output and plot area. This specific storage system diagrams were also added to the GUI this year when available.

Now that several HSECoE models are available to a wider research audience via the HSECoE web page, the final task for this year has been to continue tracking and documenting website activity and model downloads. Figure 4 shows the latest web site activity over the last three months. As can be seen the site has received over 200 visitors since during this time and of those 66% were new visitors. The bounce rate, which indicates sessions under 10 seconds, is 19% which meant that 81% of the visitors stay longer than 10 seconds and stay over five minutes on average. The bounce rate last year was 53% and the session time was four minutes indicating that more users are staying at the site and saying for a longer time. Figure 5 shows the user flows for the site.

FUTURE DIRECTION

- Work with center partners to continue to update and improve center developed models available and accessible to the broader research and academic

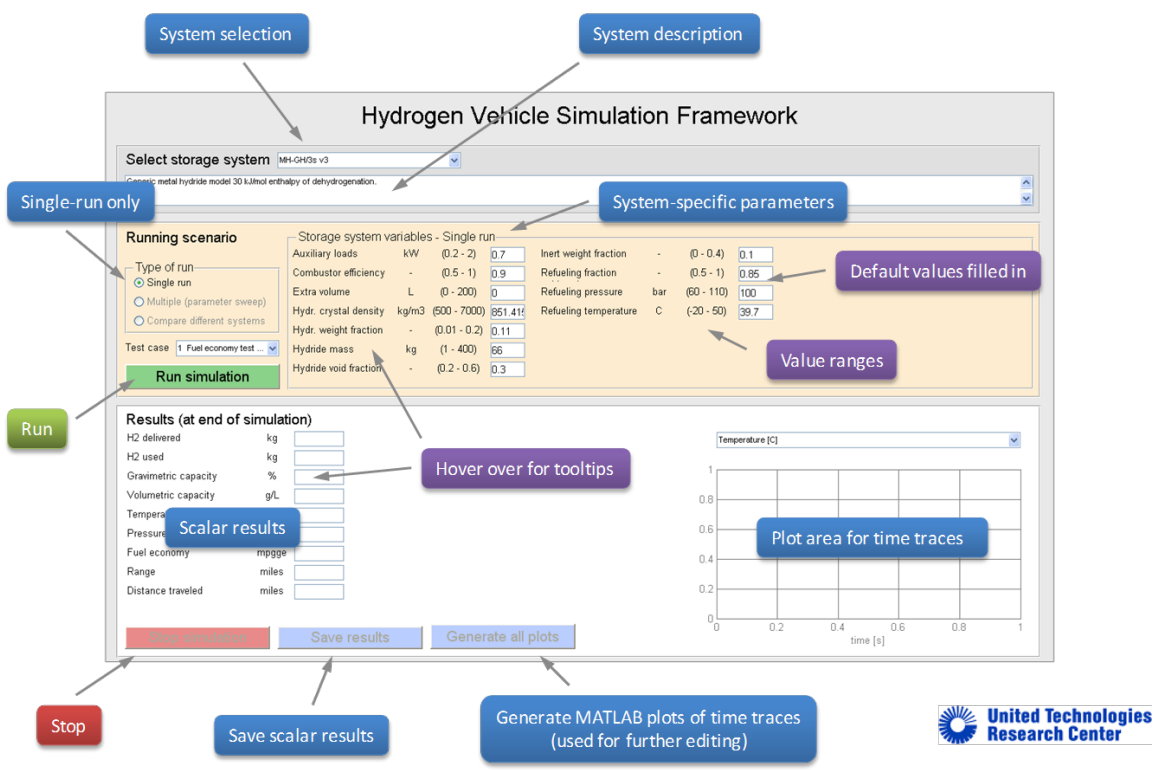

FIGURE 3. HSECoE framework model GUI

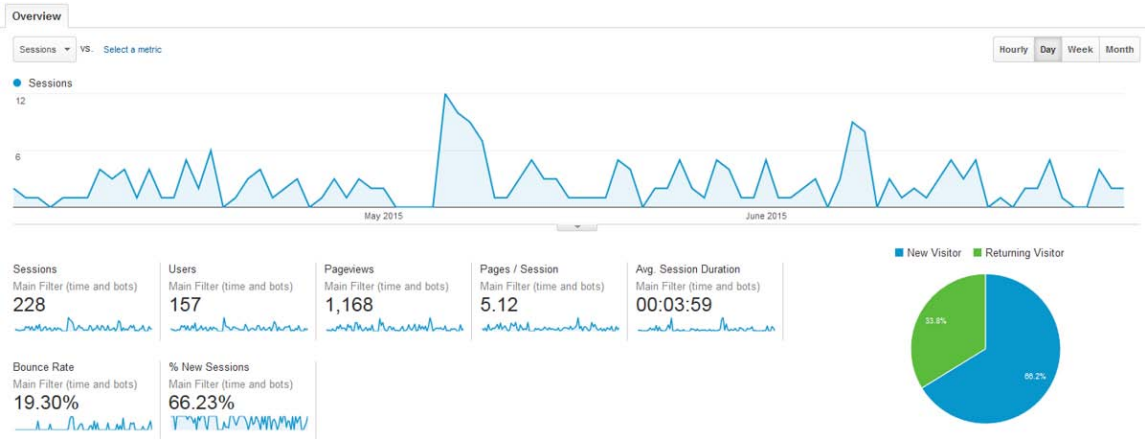

FIGURE 4. HSECoE web analytics: three-month site activity metrics

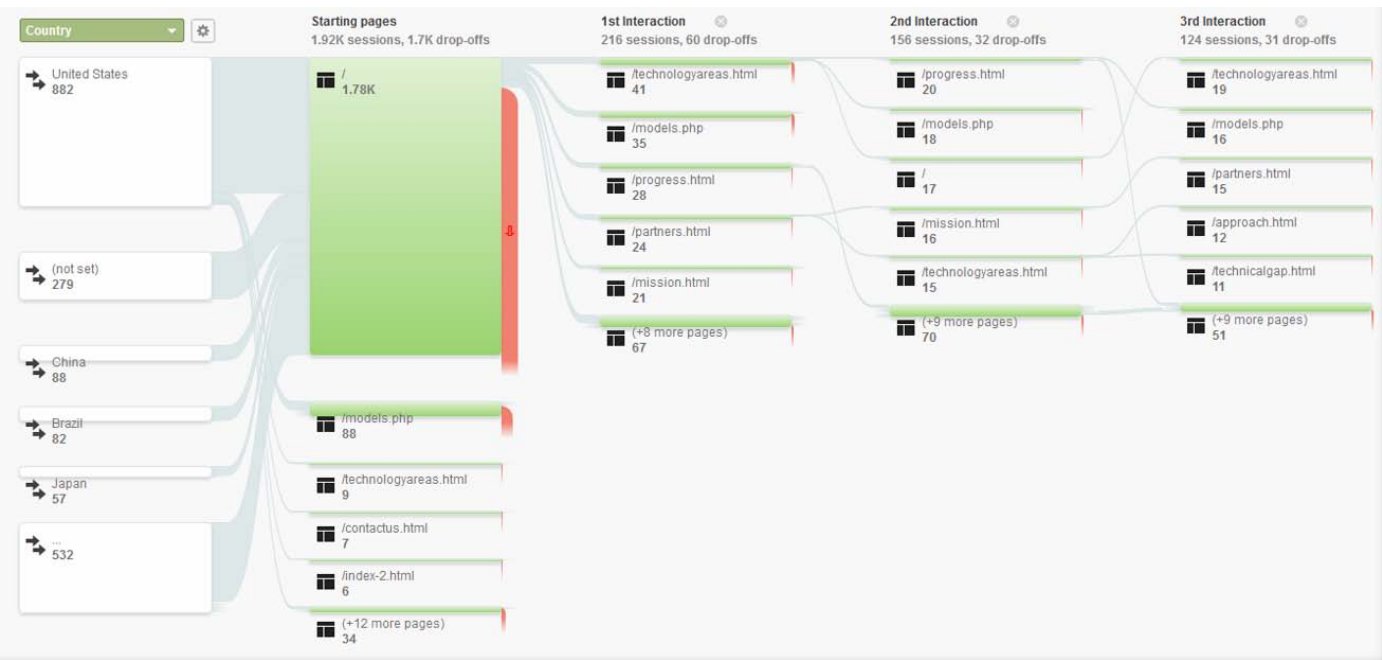

FIGURE 5. HSECoE web analytics: user flows

community through a controlled web based access portal and track downloads and website activity.

FY 2015 PUBLICATIONS/PRESENTATIONS

1. System Design, Analysis, Modeling, and Media Engineering Properties for Hydrogen Energy Storage, Matthew Thornton, DOE Annual Merit Review Meeting, June 9, 2015, Washington, D.C.

IV.B.7 Development of Improved Composite Pressure Vessels for Hydrogen Storage

Norman Newhouse (Primary Contact), Jon Knudsen
Hexagon Lincoln Inc. (formerly Lincoln Composites, Inc.)
5117 NW 40th Street
Lincoln, NE 68524
Phone: (402) 470-5035
Email: norman.newhouse@hexagonlincoln.com

DOE Managers
Jesse Adams
Phone: (720) 356-1421
Email: Jesse.Adams@ee.doe.gov
Ned Stetson
Phone: (202) 586-9995
Email: Ned.Stetson@ee.doe.gov

Contract Number: DE-FC36-09GO19004

Project Start Date: February 1, 2009
Project End Date: June 30, 2015 (Final report due September 30, 2015)

Overall Objectives

- Improve the performance characteristics, including weight, volumetric efficiency, and cost, of composite pressure vessels used to contain hydrogen in adsorbents
- Evaluate design, materials, or manufacturing process improvements necessary for containing adsorbents
- Demonstrate these improvements in prototype systems through fabrication, testing, and evaluation

Fiscal Year (FY) 2015 Objectives

- Manufacture prototype tanks and distribute to Hydrogen Storage Engineering Center of Excellence (HSECoE) partners for Phase 3 testing
- Demonstrate alternate tank designs with improved performance
- Demonstrate the use of liquid nitrogen to pre-cool the prototype tank and gather test data
- Design full-scale tanks based on testing of subscale designs

Technical Barriers

This project addresses the following technical barriers from the Hydrogen Storage section of the Fuel Cell Technologies Office Multi-Year Research, Development, and Demonstration Plan:

(A) System Weight and Volume

(B) System Cost

(G) Materials of Construction

Technical Targets

This project is conducting fundamental studies for the development of improved composite pressure vessels for hydrogen storage, and developing an optimized vessel for use by HSECoE partners in demonstrating a functioning vehicle storage system using adsorbent materials. The targets apply to the storage system, of which the vessel is a part. Insights gained from these studies will be applied toward the design and manufacturing of hydrogen storage vessels that meet the following DOE 2020 hydrogen storage targets:

- Gravimetric capacity: >5.5%
- Volumetric capacity: >0.040 kg H_2/L
- Storage system cost: <$10/kWh

FY 2015 Accomplishments

- The revised Phase 3 test vessel, of three-piece Type 1 construction, was designed as a right circular cylinder with flanged ends and end plates attached by bolts, having the same internal diameter as the Phase 2 vessel, but with simpler sealing mechanism and the ability to better compress the seals, so that there was no leakage at 100 bar and 80 K.
- Subscale Type 1, Type 3, and Type 4 tanks designed in the prior year have been manufactured and are being tested to evaluate further improvement possibilities in alternate designs.
- A Type 1 subscale tank was tested in a prototype liquid nitrogen cooling system, and data evaluation indicates the system can be used to fill a tank with the desired time.
- A Type 3 subscale tank was tested in the prototype liquid nitrogen cooling system. Full data evaluation has not been completed, but the data indicate the minimum temperature reached was higher than with the Type 1 tank, and there was an increased time to cool.
- Full-scale Type 1 and Type 4 tanks were designed based on testing conducted to date.

✧ ✧ ✧ ✧ ✧

INTRODUCTION

Hexagon Lincoln is conducting research to meet DOE 2020 hydrogen storage system goals by identifying appropriate materials and design approaches for the hydrogen container. The pressure vessels must continue to maintain durability, operability, and safety characteristics that already meet current industry guidelines. There is a continuation of work with HSECoE partners to identify pressure vessel characteristics and opportunities for performance improvement. Hexagon Lincoln is working to develop high-pressure vessels as are required to enable tank design approaches to meet weight and volume goals and to allow adsorbent materials that operate at cryogenic temperatures to operate efficiently.

APPROACH

Hexagon Lincoln established a baseline design for full-scale and test tanks using HSECoE team operating criteria as a means to compare and evaluate potential improvements in design, materials, and process to achieve cylinder performance improvements for weight, volume and cost. Hexagon Lincoln selected the most promising engineering concepts to meet go/no-go requirements for moving forward. The emphasis was on demonstrated technology to ensure ability of HSECoE partners to test their system components.

In Phase 3, operating conditions have been confirmed, and a reduced weight laboratory test vessel was designed and tested. This three-piece Type 1 tank was designed for safety and reusability, but problems developed with high-pressure sealing at cryogenic temperatures. A revised design was developed that addressed the sealing problem and allowed team partners to demonstrate their adsorbent systems. Studies are continuing to identify designs and materials that may result in lighter weight and/or less expensive tanks.

RESULTS

HSECoE partners confirmed operation at 100 bar service pressure, with an operating temperature range from 80 K to 160 K and a non operating limit of 373 K. A test vessel configuration with three-piece Type 1 construction, 2-L volume, and reduced wall thickness was also established to demonstrate component technology. Test vessels were designed, manufactured, tested, and distributed to HSECoE partners to facilitate Phase 3 testing of prototype components.

The Phase 3 Type 1 final test vessel was designed using 304 stainless steel (SS) and a three-piece construction (Figure 1). The three-piece construction allowed HSECoE partners to remove and replace components in the vessel between tests. This test vessel was intended to facilitate system testing by HSECoE partners and was not intended to be representative of production units. No leakage occurred after changing to this design.

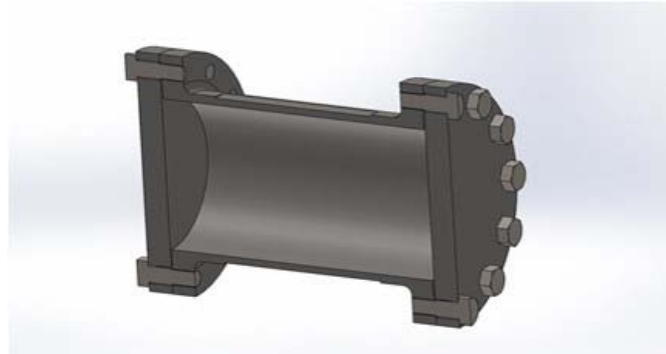

FIGURE 1. Phase 3 Type 1 test tank

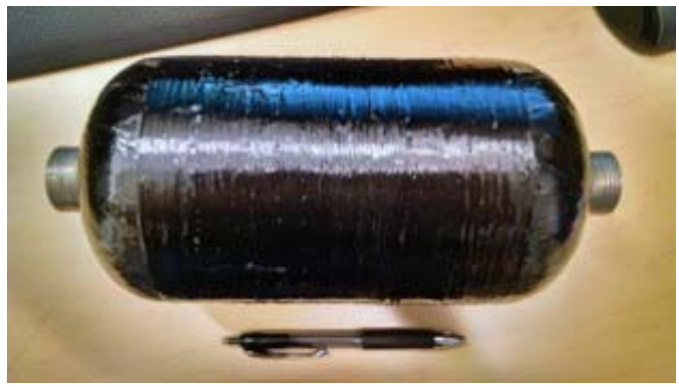

FIGURE 2. Type 3 tank

A Type 1 prototype tank and Type 3 prototype liner were manufactured in accordance with designs prepared during the prior year. The Type 3 tank (Figure 2) was burst at 318 bar (4,615 psi), well above the required burst pressure. The Type 1 tank was tested to 276 bar (4,000 psi). It did not burst at this pressure, but significant yielding had occurred, and the outer diameter had grown by about 10 mm (0.4 in).

Type 4 tanks have also been fabricated but have not yet been burst tested. A resin layer was used as a liner in these Type 4 tanks so that the tanks would not be affected by cryogenic temperatures, as was the prior high-density polyethylene liner. The first unit had a pronounced leakage rate, while the second unit had a low leakage/permeation rate, 1.2 cm^3/s at 4 bar (60 psi). The third unit had a leakage/permeation rate of only 0.001 cm^3/min at 4 bar (60 psi) and is undergoing additional testing.

Cooling studies were conducted with the prototype 2-L Type 1 tank to determine fill characteristics. Figure 3 shows sample data of wall temperature at various locations as a function of time with bottom fill. Data evaluation indicates the system can be used to fill a tank with the desired time.

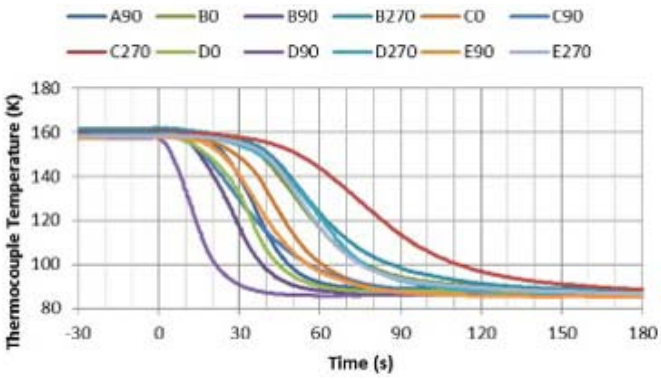

FIGURE 3. Wall temperature vs. time with bottom fill

Testing of a Type 3 tank, with carbon fiber reinforce, showed the minimum temperature reached was higher than with the Type 1 tank, and there was an increased time to cool, reflecting differences in thermal conductivity and heat capacity of the wall.

Full-scale Type 1 and Type 4 tanks were designed based on the prototype work done. The volume required to contain 5.6 kg usable hydrogen in MOF-5 (metal organic framework) adsorbent material, as reported during the 2015 DOE Annual Merit Review meeting, was about 300 L. Service pressure was 100 bar, and service temperatures were from 80 K to 160 K. Inner diameter was about 20 inches, and length about 65 inches. A Type 1 tank made of AA 6061-T6 would have a wall thickness of about 0.9 inch and would weigh about 390 pounds. This might decrease as elastic-plastic properties and cryogenic strength vs. room temperature properties and operating conditions are evaluated. A Type 4 tank made of carbon epoxy would be similar in size but would have a wall thickness of about 0.2 inch and weigh about 55 pounds. This might increase as damage tolerance is addressed.

CONCLUSIONS AND FUTURE DIRECTIONS

- A Type 1 tank met the pressure and temperature requirements for Phase 3 testing and component development and had the lowest program risk. A revised design would be required for production.
- Subscale one-piece Type 1, Type 3, and Type 4 tanks were fabricated to achieve higher performance than the three-piece Type 1 tank. Additional testing at room temperature and at 80 K is required to confirm suitability of the designs.
- A subscale tank was pre-cooled using prototype components. Data indicates desired filling rates could be met. Full-scale testing would also be desirable.
- Full-scale designs were completed based on testing of subscale components to date. These tanks are large compared with a passenger vehicle. Full-scale demonstration would be useful.
- Full-scale Type 1 and Type 4 designs were prepared. There is a need to improve volumetric efficiency of designs to be more usable on vehicles, and a need to optimize designs.

SPECIAL RECOGNITIONS & AWARDS/ PATENTS ISSUED

1. A patent application was filed on the concept for a thermal insulation shell system that would also allow cooling of the tank prior to refilling.

FY 2015 PUBLICATIONS/PRESENTATIONS

1. 2015 DOE Hydrogen Program Annual Merit Review, June 10, 2015.

IV.B.8 Chemical Hydride Rate Modeling, Validation, and System Demonstration

Troy A. Semelsberger (Primary Contact),
Dusan Spernjak, and Jose I. Tafoya
Los Alamos National Laboratory
MS J579, P.O. Box 1663
Los Alamos, NM 87545
Phone: (505) 665-4766
Email: troy@lanl.gov

DOE Managers
Ned Stetson
Phone: (202) 586-9995
Email: Ned.Stetson@ee.doe.gov
Jesse Adams
Phone: (720) 356-1421
Email: Jesse.Adams@ee.doe.gov

Project Start Date: February 2009
Project End Date: June 2015

Overall Objectives

- Develop an automotive chemical hydrogen storage system capable of meeting all of the 2020 DOE targets simultaneously
- Develop and validate chemical hydrogen storage system models
- Quantify viable chemical hydrogen storage material properties that will meet DOE 2020 technical targets with our current system
- Develop and demonstrate "advanced" (non-prototypical) engineering concepts

Fiscal Year (FY) 2015 Objectives

- Design, build, and demonstrate high-pressure, low-temperature thermal conductivity cell to measure thermal conductivities of MOF-5 (metal organic framework) compacts
- Quantify MOF-5 thermal conductivities as a function of hydrogen pressure (<100 bar) and temperature (-196°C)

Technical Barriers

This project addresses the following technical barriers from the Hydrogen Storage section of the Fuel Cell Technologies Office Multi-Year Research, Development, and Demonstration Plan:

(A) System Weight and Volume

(B) System Cost

(C) Efficiency

(D) Durability/Operability

(E) Charging/Discharging Rate

(F) Codes and Standards

(G) Materials of Construction

(H) Balance of Plant (BOP) Components

(J) Thermal Management

(K) System Life-Cycle Assessment

(R) By-Product/Spent Material Removal

Technical Targets

Our objectives in the last year of the Hydrogen Storage Engineering Center of Excellence were to design, build, and demonstrate a high-pressure, low-temperature thermal conductivity cell to measure the apparent thermal conductivity of engineered MOF-5 compacts under elevated hydrogen pressures (<100 bar) and low temperatures (-196°C to 18°C). There are no technical targets to which our work can be related; however, our work directly supports system modeling and validation of modular adsorption tank insert adsorbent systems.

Accomplishments

- Designed, built, and demonstrated the first thermal conductivity cell for measuring MOF-5 thermal conductivities at elevated hydrogen pressures (<100 bar) and liquid nitrogen temperatures
- Quantified MOF-5 isotropic and anisotropic thermal conductivities at elevated hydrogen pressures

✧ ✧ ✧ ✧ ✧

INTRODUCTION

Hydrogen storage systems based on adsorbents require accurate and reliable measurements of the overall or apparent thermal conductivities operating under realistic operating conditions (i.e., liquid nitrogen temperatures and hydrogen pressures of 100 bar) in order to design and implement the most efficient thermal management system while also minimizing the mass, volume, and cost. In addition, the

overall thermal conductivities must be measured in order to validate the system-level adsorbent models.

RESULTS

Isotropic Thermal Conductivity Measurements of Engineered MOF-5 Compacts

Shown in Figure 1 are the measured isotropic or bulk thermal conductivities of neat MOF-5 engineered compacts as a function of pressure (absolute) with helium and hydrogen. All measurements were performed at 16°C. The diameter and height of the engineered MOF-5 compacts were 5 cm and 1.5 cm, respectively. The density of MOF-5 compact was 0.4 g/mL. Ford Motor Company prepared the MOF-5 engineered compacts, and BASF provided the MOF-5 material. The sample did not contain any thermal conductivity enhancement additives (e.g., expanded natural graphite, ENG). The isotropic or bulk thermal conductivity of neat MOF-5 under vacuum (20 in Hg) was measured to be 0.133 W/m K. In both cases (hydrogen and helium), the apparent thermal conductivity increased with increasing pressure. The largest increase in the apparent thermal conductivity was observed for pressures up to around 30 bar. For pressures greater than 30 bar, the apparent thermal conductivity asymptoted to limiting values of 0.3 W/m K with helium and 0.33 W/m K with hydrogen. The differing apparent thermal conductivities of MOF-5 observed with hydrogen and helium can be attributed to the differing gas-phase thermal conductivities of hydrogen (0.1655 W/m K) and helium (0.1411 W/m K). The gas phase contribution to the increase in the apparent thermal conductivity is significant, with nearly a two-fold increase observed as compared to the thermal conductivity of evacuated neat MOF-5.

Anisotropic Thermal Conductivity Measurements of Engineered MOF-5 Compacts

Shown in Figure 2 are the measured anisotropic thermal conductivities of neat MOF-5 engineered compacts as a function of pressure (absolute) with helium at 16°C. All measurements were performed at 16°C. The samples are the same as those used for the isotropic measurements. The anisotropic measurements quantify the axial and radial contributions of the thermal conductivity. Analogous to the isotropic measurements, the axial and radial thermal conductivities are asymptotic with pressure. For pressures greater than 30 bar, the axial and radial thermal conductivities are insensitive to changes in pressure. The limiting values for the radial and axial thermal conductivities are 0.27 W/m K and 0.33 W/m K, respectively. The numbers above the data points in Figure 2 denote the order in which the measurements were made and indicate that there does not appear to be hysteresis. The dashed line in Figure 2 is the weighted contributions of the radial and axial thermal

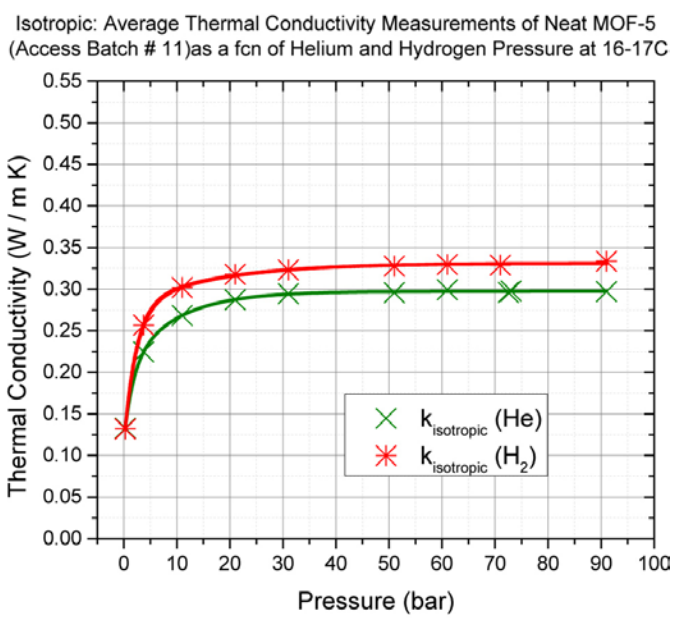

FIGURE 1. Isotropic (bulk) thermal conductivities of neat MOF-5 engineered compacts (diameter = 5 cm, height = 1.5 cm, ρ = 0.4 g/mL) as a function of pressure (absolute) and gas type at 16°C *(all samples were treated in an ultra-high-purity [UHP] N_2 purged oven at 160°C for a minimum of two days, followed by vacuum treatment for 12 hours; average standard deviations for isotropic and anisotropic measurements were ±0.0052 W/m K [helium, 137 measurements] and ±0.0033 W/m K [hydrogen, 104 measurements])*

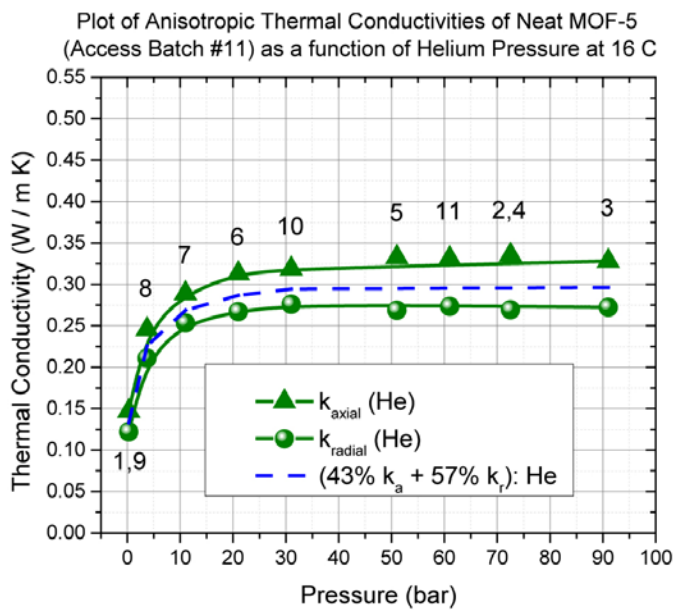

FIGURE 2. Anisotropic thermal conductivities of neat MOF-5 engineered compacts (diameter = 5 cm, height = 1.5 cm, ρ = 0.4 g/mL) as a function of pressure (absolute) with helium at 16°C *(all samples were treated in a UHP N_2 purged oven at 160°C for a minimum of two days, followed by vacuum treatment for 12 hours; average standard deviation for isotropic and anisotropic measurements was ±0.0052 W/m K [helium, 137 measurements])*

conductivities that equal the overall isotropic measurements. In other words, 57% of the isotropic measurement can be attributed to the radial contribution and 43% of the isotropic measurement can be attributed to the axial contribution. The overall trend of the anisotropic measurements agrees well with the isotropic measurements.

Shown in Figure 3 are the measured anisotropic thermal conductivities of neat MOF-5 engineered compacts as a function of pressure (absolute) with hydrogen at 16°C. All measurements were performed at 16°C. The samples are the same as those used for the isotropic measurements. The dashed line in Figure 3 is the weighted contributions of the radial and axial thermal conductivities that equal the overall

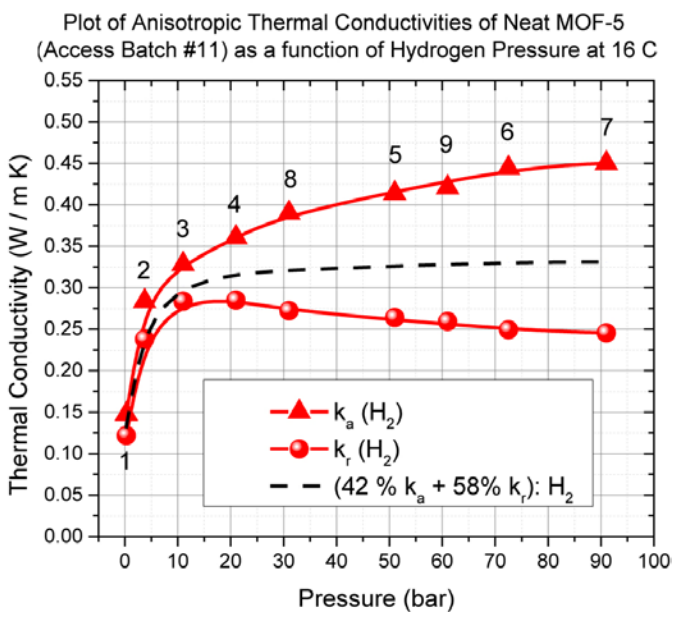

FIGURE 3. Anisotropic thermal conductivities of neat MOF-5 engineered compacts (diameter = 5 cm, height = 1.5 cm, ρ = 0.4 g/mL) as a function of pressure (absolute) with hydrogen at 16°C *(all samples were treated in a UHP N_2 purged oven at 160°C for a minimum of two days, followed by vacuum treatment for 12 hours; average standard deviation for isotropic and anisotropic measurements was ±0.0033 W/m K [hydrogen, 104 measurements])*

isotropic measurements. In other words, 58% of the isotropic measurement can be attributed to the radial contribution and 42% of the isotropic measurement can be attributed to the axial contribution. The anisotropic measurements quantify the axial and radial contributions of the thermal conductivity. Similar to the anisotropic measurements performed with helium, the radial thermal conductivity is less than the axial thermal conductivity. However, the axial and radial thermal conductivities do not follow the general asymptotic behavior observed in Figures 1 and 2. The axial thermal conductivity continues to increase beyond 30 bar and may begin to asymptote around 70–90 bar (~0.45 W/m K). The radial contribution is non-monotonic, exhibiting a maximum around 10–20 bar (0.28 W/m K). The radial contribution appears to asymptote around 70 bar (0.25 W/m K). The cause of this behavior is unknown, but we hypothesize that we are not correctly accounting for all the added hydrogen contributions associated with the hydrogen–MOF-5 composites. For example, the overall volumetric heat capacity of the hydrogen–MOF-5 composite is used to determine the radial and axial thermal conductivities. In turn, the volumetric heat capacity is dependent on the gas-phase hydrogen density, hydrogen heat capacity (which is a function of hydrogen ortho and para states, pressure and temperature) and the MOF-5 heat capacity and density. In short, there are a number of subtle contributions that need to be accounted for in order to obtain reliable thermal conductivity measurements—these contributions will be highlighted in a forthcoming publication.

CONCLUSIONS AND FUTURE DIRECTIONS

- Designed, built, and tested high-pressure (<100 bar), low-temperature (>-196°C) thermal conductivity cell
- Measured apparent thermal conductivities of neat MOF-5 samples exposed to hydrogen and helium pressures up to 90 bar at 16°C
- Finish thermal conductivity measurements at elevated hydrogen and helium pressures (<100 bar) at liquid nitrogen temperatures (-196°C)

IV.B.9 Testing, Modeling, and Evaluation of Innovative Hydrogen Storage System Designs

Mei Cai (Primary Contact), Jerome Ortmann
General Motors (GM) R&D Center
30500 Mound Road
Warren, MI 48090
Phone: (586) 596-4392
Email: mei.cai@gm.com

DOE Managers
Jesse Adams
Phone: (720) 356-1421
Email: Jesse.Adams@ee.doe.gov
Ned Stetson
Phone: (202) 586-9995
Email: Ned.Stetson@ee.doe.gov

Contract Number: DE-FC36-09GO19003

Project Start Date: February 1, 2009
Project End Date: June 30, 2015

Overall Objectives

- Develop and test system simulation models for on-board hydrogen storage systems using adsorbent materials, and determine system compliance with the DOE technical targets
- Design, build, and test an experimental vessel for validation of cryo-adsorption models and determine the fast fill and discharge dynamics of cryo-adsorbent storage systems

Fiscal Year (FY) 2015 Objectives

- Provide support to the modeling group by testing and evaluating new versions of the Framework model and any other models that are to be published on the web
- Participate in Phase III of the program as an original equipment manufacturer (OEM) consultant in face-to-face meetings and in teleconferences of the Coordinating Council, Adsorbent Team, and Modeling Team

Technical Barriers

This project addresses the following technical barriers from the Hydrogen Storage section of the Fuel Cell Technologies Office Multi-Year Research, Development, and Demonstration Plan:

(A) System Weight and Volume

(C) Efficiency

(E) Charging/Discharging Rates

(J) Thermal Management

Technical Targets

In this project, studies are being conducted to develop metal organic framework (MOF)-5 based storage media with optimized engineering properties. This material has the potential to meet the 2020 technical targets for onboard hydrogen storage shown in the following table:

Storage Parameter	2020 Target
System Gravimetric Capacity	0.055 (kg H_2/kg system)
System Volumetric Capacity	0.040 (kg H_2/L system)

FY 2015 Accomplishments

- GM's testing of the Vehicle Simulation Framework provided valuable feedback to the modeling team that led to improvements and refinements being made to the model.
- GM's testing of the "Tankinator" model provided useful input to Pacific Northwest National Laboratory (PNNL) before their release of the model on the web.

✧ ✧ ✧ ✧ ✧

INTRODUCTION

In Phases I and II as part of the Hydrogen Storage Engineering Center of Excellence (HSECoE), the GM team built hydrogen storage system models for sodium alanate, TiCrMn, and cryo-adsorbents that were subsequently tested in the Framework model. GM's role has changed in Phase III, as we have participated in the DOE HSECoE program as an OEM consultant and provided input to the construction of down-selected prototype tanks. GM contributed to the down selection of the HexCell and MATI heat exchange designs for subscale prototype adsorbent systems to be evaluated in Phase III. This selection was made by considering several factors, including the detailed model analyses with experimental validation, the overall system performance projections, the projected costs, and the future direction of adsorbent material research. As an OEM, we are in a unique position to help ensure that the selected designs are based on on-road demands of the fuel cell vehicles. As we transitioned to being an OEM consultant to the program, the deliverables for this phase have been redefined, particularly for our modeling related activities. GM will test and evaluate

the Framework model and any other models that are to be published on the web, and provide feedback regarding this testing in support of the modeling group.

APPROACH

The Vehicle Simulation Framework is a MATLAB/Simulink® model that enables users to perform driving simulations for a fuel cell vehicle with a variety of operating conditions and hydrogen storage system options. The Framework is designed so that the performance of different hydrogen storage systems may be compared on a single vehicle, keeping constant the vehicle-level and fuel cell system assumptions. The goal is to be able to separate the differences in performance that arise from the vehicle and fuel cell and those that arise from the storage system [1]. GM's test runs of the Framework were performed on an HP Z800 Workstation with 48 GB of RAM running the 64-bit version of Windows 7. The workstation had an Intel® Xeon® CPU (E5620) with two 2.40 GHz processors. Simulations were run with the 32-bit version of MATLAB® 8.3.0.532 (R2014a), although some were also run with the 64-bit version in order to compare execution times.

In addition to GM's beta testing of the Vehicle Simulation Framework, we evaluated another program that estimates the size and material composition of hydrogen storage tanks. PNNL has developed an Excel program that can be used to cross-compare various hydrogen storage pressure vessel types. The "Tankinator" model can estimate the mass, size, and material cost for cylindrical Type I, III, and IV hydrogen storage tanks [2]. It provides an estimate of basic tank geometry and composition from a limited number of geometric and temperature inputs. PNNL requested that GM perform an evaluation of the model and provide feedback before the model is placed on the HSECoE web site for distribution to the public.

RESULTS

Vehicle Simulation Framework Tests

Two chemical hydride storage systems were first included in the Framework in version v1.1rc5. The chemical hydrogen storage material system is selectable for either an exothermic or endothermic hydrogen release enthalphy. The exothermic and endothermic systems are represented by an ammonia borane slurry and an alane slurry, respectively [3]. The modeling team requested that GM perform Framework simulations using these two storage systems to determine if they run properly with MATLAB® R2014a. In particular, the team had determined that cold test case drive cycle simulations for both material systems had been having issues. Simulations for the alane slurry storage system were crashing after 140–170 seconds, and runs with ammonia borane slurry would hang up at completion before crashing. GM's test simulation using MATLAB® R2014a with the cold case drive cycle and the alane slurry storage system did not crash, but instead ran to completion (74,720.4 seconds). Likewise, a simulation with the ammonia borane slurry and the cold case also ran to completion, and the program ended normally without crashing. Detailed listings of all Simulink® preference settings were sent to the modeling team to help determine if something different in these particular settings was allowing the two cases to run successfully.

Version v1.1rc6 of the Framework contained several updates and was made available for testing. One key change made to this version was the setting of the maximum time step to 0.2 seconds. The value, dtmax, had been lowered to 0.2 seconds in order to avoid spurious trace miss errors and to address issues with the chemical hydride modules. The modeling team requested that GM perform Framework simulations using this version to test the model changes with MATLAB® R2014a. Test runs of the two latest Framework versions, v1.1rc5 and v1.1rc6, were performed for comparison of their performance and execution times. A selection of the simulation results for the two versions are shown in Tables 1 and 2. The default menu options were used for all simulations. Table 1 contains results for the metal hydride storage module. This module had been updated in version v1.1rc6 in order for the thermal conduction model to handle thicker walls. The execution times for v1.1rc6 increased substantially from version v1.1rc5. However, the metal hydride module is still one of the faster executing modules in the Framework. The driving times and, therefore, the distances traveled also are higher for v1.1rc6.

TABLE 1. Metal Hydride Storage Module Results for Both v1.1rc5 and v1.1rc6, Respectively

Drive Cycle	Elapsed Driving Time (s)	Distance Traveled (mi)	Execution Time (h:min)
Fuel Economy	49,649 / 50,926	414 / 424	5:0 / 17:23
Aggressive (US06)	21,400 / 22,442	286 / 299	4:0 / 8:22
Cold Cycle (FTP-75)	79,424 / 82,035	355 / 367	8:0 / 27:50
Hot Cycle (SC03)	57,446 / 59,952	343 / 358	8:0 / 20:04

FTP - Federal Test Procedure

TABLE 2. CH-AB Slurry Storage Module Results for v1.1rc5 and v1.1rc6, Respectively

Drive Cycle	Elapsed Driving Time (s)	Distance Traveled (mi)	Execution Time (h:min)
Fuel Economy	45,164 / 44,926	377 / 373	39:0 / 42:39
Aggressive (US06)	19,813 / 19,623	265 / 263	29:0 / 30:25
Cold Cycle (FTP-75)	72,032 / 71,568	324 / 319	46:0 / 1:00:08
Hot Cycle (SC03)	53,010 / 52,490	318 / 313	38:0 / 44:01

For some versions of MATLAB®, users of the chemical hydride storage modules were experiencing problems

in v1.1rc5, and simulations sometimes failed to run to completion. This problem did not occur in our simulations with MATLAB® R2014a, as can be seen in Table 2. Also, simulations using v1.1rc5 with the aggressive cycle were encountering "speed trace miss" messages on completion, including those that were run using MATLAB® R2014a. The new setting of the maximum time step to 0.2 seconds in version v1.1rc6 simulations was successful in preventing these messages from occurring. Execution times for v1.1rc6 (Table 2) showed modest increases for the chemical hydride-ammonia borane (CH-AB) slurry module simulations. These test results were a topic of discussion for the modeling group at subsequent teleconferences. Simulations with the two versions were obtaining somewhat different results for the distance traveled for cases being run with identical input parameters. For the metal hydride and compressed 350 bar storage modules the differences could be as high as 4.5%. For both of the chemical hydride modules, the differences were all below 2%. The differences in distance traveled were determined to be resulting from the change that had been made in the maximum allowable time step for the solver. The value had been lowered to 0.2 seconds in version v1.1rc6 in order to avoid spurious trace miss errors and to address issues with the chemical hydride modules. The modeling team made modifications to the Framework to verify that the model's computations were converging, and decided to use the 0.2 second time step value as a suitable choice to achieve both convergence and reasonable execution time.

Framework version v1.1rc8 was the first version of the Framework to feature the two cryo-adsorbent storage modules from Savanah River National Laboratory. Testing of these modules (MATI and Hex Cell) was performed. The MATI storage system was tested using lower final temperatures (140 K and 150 K) as well as for the default of 160 K. The module resizes the storage system to take into account the requested final tank temperature. For instance, the storage system mass and usable hydrogen are 158.1 and 5.58 kg, respectively, for the 160 K simulation, but they increase to 163.4 and 5.67 kg for the 140 K simulation. All simulations ran successfully to completion at these temperatures. Varying these and other options should prove to be instructive to end users of the Framework.

Tank Mass Estimator (Tankinator)

The Type I tank model can be used for any of four metals: 6061-T6 aluminum, 316 stainless steel, 4130 chromoly steel, and 4340 steel. The tank design must meet two criteria: a proof load of 1.5 times the operating pressure, under which the tank wall must not yield, and a burst load of 2.25 times the operating pressure, for which the tank must not exceed the peak von Mises stress. Initially, all four metals are compared using a thin wall stress relationship that calculates an estimate that is useful for low pressures. A thick-walled calculation is then performed for the chosen metal. Higher pressures and weak aluminum must be considered thick-walled even in the moderate pressure range. A series of three von Mises stress calculations are done to further refine the wall thickness. The design ratio, which is the calculated stress divided by the allowable stress limit, is used to correct the wall thickness estimate in these three iterative steps. The design ratio indicates how close the estimated wall thickness is to the ideal thickness and should converge to 1.0, otherwise additional refinements would be necessary [2].

For example, a case was run for a 6061-T6 aluminum tank with operating temperature of 22°C, pressure of 250 bar, inner radius of 22.5 cm, and inner length of 81 cm. The outer radius estimate undergoes the series of refinements from 26.53, 26.95, 27.05, to 27.08 cm, resulting in a final wall thickness estimate of 4.58 cm and a tank mass of 162.9 kg. A final design ratio of 1.001 and von Mises error of 0.14% confirm that the calculation has converged. Raw materials for the tank are estimated to be $725 based on 2007 commodity costs that are used for comparison purposes. Several other geometry, temperature, and pressure combinations were input for test runs, and the program always converged and obtained reasonable results. Suggestions for minor additions to the model's parameter descriptions were made to help clarify the use of the design ratios in refining the wall thickness estimates.

The Type III tank model is designed for cryogenic operating conditions. The tank is composed of an aluminum liner with a carbon fiber overwrap. The aluminum liner is sized to withstand 21% of the burst pressure, and the carbon fiber overwrap is sized to withstand the remaining 79% of the burst pressure. The thicknesses are calculated using the thin-walled pressure vessel hoop stress formula. Both low-bound and high-bound estimates are calculated. The low-bound value represents the best estimate value, and the high-bound value provides a conservative estimate that doesn't take credit for the support of the liner. This gives an idea of how large of a contribution the aluminum liner provides. As with the Type I tank model, testing was performed with a range of input parameters. Tank designs were calculated for an internal radius up to 30 cm and operating pressures as high as 300 bar, the limits suggested in the documentation. All results passed the built-in accuracy checks. The variations seen in the relative masses of the aluminum and carbon fiber composite were quite instructive, and they provided useful information for comparing tank designs.

The Type IV tank model is based on the assumption that the high-density polyethylene (HDPE) liner carries no load. However, the HDPE liner thickness is a required input parameter. The model description states that a thin-walled pressure vessel approximation is used; therefore, the estimates have a limited range of accuracy. As with the Type III model, this model provides fast, accurate estimates of the carbon fiber composite mass, thickness, and cost for comparison purposes.

CONCLUSIONS

- GM continued to participate in Phase III as an OEM consultant to the HSECoE team. GM contributed to the down selection of the HexCell and MATI heat exchange designs for subscale prototype adsorbent systems that were evaluated in Phase III.
- The Vehicle Simulation Framework has been thoroughly tested and will prove to be a valuable tool to the user community.

REFERENCES

1. H_2 Vehicle Simulation Framework: MODEL DESCRIPTION AND USER MANUAL, J.M. Pasini, J. Cosgrove.

2. PNNL Tank Mass Estimator for Cross Comparison of Type 1, Type 3, and Type 4 Pressure Vessels, Nicholas Klymyshyn, PNNL.

3. Slurry Model for Chemical Hydrogen Storage in Fuel Cell Vehicle Applications," Brooks, Kriston P., Richard P. Pires, and Kevin L. Simmons.

FY 2015 PUBLICATIONS/PRESENTATIONS

1. M. Cai, et al. (2015), Testing, Modeling, and Evaluation of Innovative Hydrogen Storage System Designs, presented at the 2015 DOE Hydrogen Program Annual Merit Review Meeting, Washington, D.C.

IV.C.1 Hydrogen Storage in Metal-Organic Frameworks

Jeffrey R. Long (Primary Contact),
Martin Head-Gordon
Lawrence Berkeley National Laboratory
1 Cyclotron Road
Berkeley, CA 95720
Phone: (510) 642-0860
Email: jrlong@berkeley.edu

DOE Manager
Jesse Adams
Phone: (720) 356-1421
Email: Jesse.Adams@ee.doe.gov

Subcontractors
- National Institute of Standards and Technology (NIST), Gaithersburg, MD (Craig Brown)
- General Motors Company (GM), Warren, MI (Anne Dailly)

Project Start Date: April 1, 2012
Project End Date: September 30, 2015

Overall Objectives

- Research and development of onboard systems that allow for a driving range greater than 300 miles
- Materials sought with the potential for meeting the DOE system targets of reversible uptake:
  - 2020 targets: 5.5% H_2 by mass, volumetric capacity of 40 g/L
  - "Ultimate full fleet" targets: 7.5% H_2 by mass, 70 g/L
- Synthesize new metal-organic frameworks (MOFs) capable of approaching the -20 kJ/mol adsorption enthalpy required for use as hydrogen storage materials operating under 100 bar at ambient temperatures

Fiscal Year (FY) 2015 Objectives

- Demonstration of a metal-organic framework with an initial H_2 adsorption enthalpy greater than the current record of 15.1 kJ/mol
- Synthesis of a metal-organic framework with reversible excess hydrogen uptake greater than 4.5 wt% at 298 K
- Demonstrate the use of quasielastic neutron scattering to help understand the roles of diffusion and entropy in H_2 binding to MOFs for the most interesting systems synthesized by Long
- Demonstrate the ability to determine H_2-metal interactions in realistic systems containing low-coordinate metal cations
- Pre-screen optimal metal-organic framework targets by identification of systems that produce an H_2 binding enthalpy greater than 20 kJ/mol

Technical Barriers

This project addresses the following technical barrier from the Hydrogen Storage section of the Fuel Cell Technologies Office Multi-Year Research, Development, and Demonstration Plan:

(A) System Weight and Volume

Technical Targets

Specific efforts are focused on the research and development of onboard systems that allow for a driving range greater than 300 miles. Materials are sought with the potential for meeting the 2020 DOE targets for reversible uptake and, subsequently, the "ultimate full fleet" targets (see Table 1).

TABLE 1. Progress towards Meeting Technical Targets for Onboard Hydrogen Storage for Light-Duty Vehicles

Storage Parameter	Units	2020 Target	Ultimate Target	2012 Status†	2013 Status†	2014 Status†	2015 Status†
System Gravimetric Capacity: Usable, Specific-Energy from H_2 (Net Useful Energy/Max System Mass)*	kWh/kg (kg H_2/kg System)	1.8 (0.055)	2.5 (0.075)	(0.016 kg H_2/kg Adsorbent)	(0.016 kg H_2/kg Adsorbent)	(0.016 kg H_2/kg Adsorbent)	(0.016 kg H_2/kg Adsorbent)
System Volumetric Capacity: Usable, Energy Density from H_2 (Net Useful Energy/Max System Volume)	kWh/L (kg H_2/L System)	1.3 (0.040)	2.3 (0.070)	(0.011 kg H_2/L Adsorbent)	(0.011 kg H_2/L Adsorbent)	(0.013 kg H_2/L Adsorbent)	(0.013 kg H_2/L Adsorbent)

* Generally the full mass (including hydrogen) is used; for systems that gain weight, the highest mass during discharge is used. All capacities are net useable capacity able to be delivered to the power plant. Capacities must be met at end of service life.
† Since the project deals with the development of storage materials, the performance status is given in terms of storage capacity for storage materials, not the whole storage system.

FY 2015 Accomplishments

- The metal-organic framework $Zr_6O_4(OH)_4(oxambpdc)_6$ (oxambpdc = 4,4'-oxalylbis(azanediyl)dibenzoic acid) was synthesized as an easily obtainable framework with a dianionic chelating ligand and subsequently metalated.
- An efficient synthetic route to the novel MOF cat-UIO-68 was developed, allowing for isolation of large quantities (multi-gram) of the material with a large measured Langmuir surface area of 4,025 m^2/g.
- A comprehensive evaluation of the top-performing metal-organic frameworks for H_2 storage was carried out, including Ni_2(*m*-dobdc), Co_2(*m*-dobdc), Ni_2(dobdc), Co_2(dobdc), and MOF-5. High-pressure isotherms were measured at 100, 75, 50, 25, 0, -25, -40, -50, and -75°C in order to determine the optimal temperature process to maximize total volumetric H_2 usable capacity.
- We measured a high H_2 binding enthalpy of 12.1 kJ/mol in the metal-organic framework $Cu[Ni(pdt)_2]$ (pdt = pyrazine-2,3-dithiolate), possibly suggesting the binding of two H_2 molecules to each metal center based on the optimal pore size.
- High-pressure neutron diffraction has been used to determine the binding profile of H_2 within MOF-5 at high pressures (up to 100 bar) and moderate temperature (77 K). This technique allows for the understanding of the density profile of H_2 in the pores of MOFs and is currently being expanded to use with other MOF materials.
- We synthesized a number of other ligands with chelating functionalities have been synthesized in order to attempt to bind extra-framework metal cations within the pores or MOFs and subsequently expose multiple sites per metal center for H_2 binding.
- First principles calculation was performed to determine optimal activation conditions for catecholate-based MOFs in order to maximize open-metal sites and enhance H_2 uptake.

✧ ✧ ✧ ✧ ✧

INTRODUCTION

MOFs are promising solid adsorbents for storage of H_2 at room temperature. They can be tailored to incorporate a large number of selected metal ions, thereby tuning the H_2 binding energy. The overall aim of the project is to synthesize new MOFs capable of achieving the 20 kJ/mol adsorption enthalpy and 40 g/L volumetric storage density required for use as hydrogen storage materials operating under 100 bar at ambient temperatures.

APPROACH

This research involves investigators with a range of capabilities—including synthesis and characterization of new materials, electronic structure calculations, neutron diffraction and scattering studies, and high-pressure gas sorption measurements. The team performs work in four areas.

- Task 1 Synthesis of metal-organic frameworks (Long-LBNL)
- Task 2 Characterization of framework–H_2 interactions (Brown-NIST)
- Task 3 First-principles calculations of hydrogen binding enthalpies (Head-Gordon-LBNL)
- Task 4 High-pressure H_2 adsorption measurements (Dailly-GM)

RESULTS

This past year, efforts have continued to focus on the development of metal-organic frameworks with ligands containing chelating functionalities that can bind non-structural metal cations, in an effort to obtain a material that can bind multiple H_2 molecules per metal center. Additionally, full characterization of high-pressure adsorption of H_2 in M_2(dobdc) (M = Co, Ni) and M_2(*m*-dobdc) (M = Co, Ni) at multiple temperatures has been undertaken to determine the optimal conditions for H_2 adsorption to maximize the total volumetric usable H_2 capacity in industrially relevant temperature-swing adsorption processes. Neutron diffraction measurements and first-principles electronic structure calculations have worked alongside our synthetic efforts to further understand H_2 interactions with new adsorbate materials and inform synthetic efforts to synthesize a new generation of MOF materials with enhanced H_2 storage properties.

Binding Multiple H_2 Molecules per Metal

One of the main thrusts of this research is to improve the volumetric capacity of metal-organic frameworks in order to make them viable H_2 storage materials in automotive applications. In order to do this, focus in this research has been on increasing the binding enthalpy of H_2 to at least 15.1 kJ/mol and increasing the density of strong H_2 binding sites (primarily at open-metal coordination sites) within the material. To that end, multiple synthetic targets have been achieved that are working toward achieving our ultimate goals of a binding enthalpy exceeding 15.1 kJ/mol and obtaining a material with a volumetric capacity of 40 g/L.

The most effective method we see as being viable for obtaining these high capacities is to significantly increase the number of strong binding sites available to H_2 within the pores of the framework, which have thus far been shown to be primarily open-metal coordination sites. The

strategy being pursued for this is to synthesize metal-organic frameworks with ligands that contain free chelating functionalities, which can post-synthetically bind metals that are subsequently desolvated, exposing multiple coordination sites for H_2 binding.

Multiple ligands have been synthesized for this purpose with various chelating functionalities, including catechols, oxamides, and bipyridines, among others. The two ligands seen in Figure 1a are able to form the UIO-68 structure type and be subsequently metalated with a variety of metal sources. In particular, the boc-protected catechol ligand is highly promising. The catechol provides charge balance for a M^{2+} cation at that site, potentially allowing for the removal of other ligands from the metal center. The synthetic route for the subsequent MOF, cat-UIO-68, is shown in Figure 1b. The key is formation of the framework with benzoate-capped pre-formed $Zr_6O_4(OH)_4$ clusters, rather than simply starting with $ZrCl_4$.

Following synthesis of the framework and solvent-exchanges, the boc protecting groups can be thermalized off, leaving a free catechol in the pores of the framework. Deprotection of the boc groups has been confirmed by infrared spectroscopy and structure determination is underway from powder diffraction data collected at the Advanced Photon Source at Argonne National Laboratory. This cat-UIO-68 MOF has been shown to have a very high surface area of 4,025 m^2/g. Metalation of this framework has been attempted with several metal sources, including $Zn(C_2H_5)_2$ and $Ni(allyl)_2$. Further studies are underway to optimize the metalation and desolvation of these materials

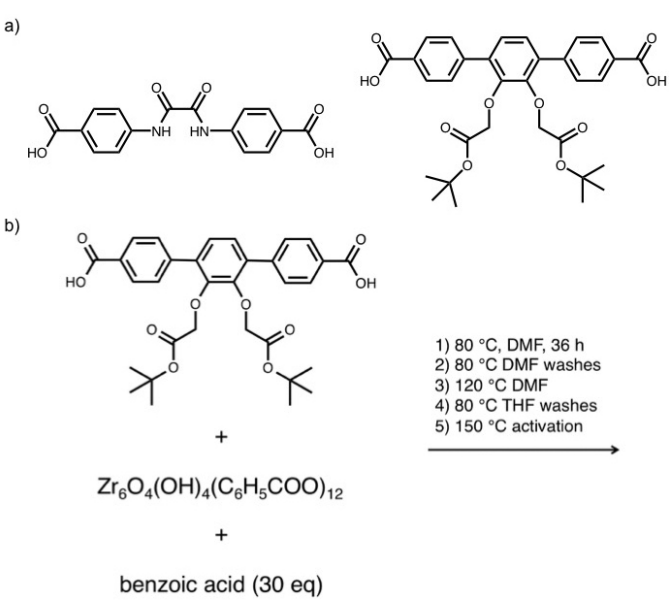

FIGURE 1. (a) The H_2(oxambpdc) (left) and boc-protected H_2(cat-bdc) (right) ligands. (b) The synthetic scheme for synthesizing the cat-UIO-68 MOF, including washes and thermalization of the boc protecting groups to expose free catechols in the pores of the framework.

to bind two H_2 molecules per metal center and ultimately produce a material that meets the volumetric storage targets set forth by DOE.

Determining the Optimal Conditions for H_2 Adsorption

Other efforts over the past year have focused on determining the optimal conditions for storing H_2 at relevant temperatures and pressures in known MOF materials. The previously reported M_2(*m*-dobdc) framework is particularly suitable for this study, as the Ni_2(*m*-dobdc) analog has among the highest known H_2 binding enthalpies of any MOF [1], leading to the expectation that this material will be particularly well-suited to storing large amounts of H_2.

In order to determine the best conditions and materials for storing H_2, top-quality samples (meaning those with Langmuir surfaces areas comparable to or exceeding those published in the literature) of several MOFs (Co_2(*m*-dobdc), Ni_2(*m*-dobdc), Co_2(dobdc), Ni_2(dobdc), and MOF-5) have been synthesized and tested for their high-pressure H_2 capacities at nine different temperatures: 100, 75, 50, 25, 0, -25, -40, -50, and -75°C. With such a wide sampling of temperatures, conclusions can be drawn about not only the ability of each material to store H_2 at a given temperature, but also how to optimize a temperature-swing process to maximize the usable H_2 stored in the system. Adsorption at 100 bar and desorption to a pressure of 5 bar are the DOE criteria for determining usable capacity, so all usable capacities were calculated between these two pressures in terms of the total volumetric capacity of the material.

The results for several of these materials can be seen in the isotherms in Figure 2. Ni_2(*m*-dobdc) is the top performing material as evaluated by multiple characteristics. It has a total usable capacity (the amount adsorbed between 100 bar and 5 bar) of 11.0 g/L at 25°C with no temperature swing process, which is superior to any other known MOF. Additionally, the usable capacity with a temperature swing from -40°C to 25°C is 18.2 g/L and from -75°C to 25°C is 23.0 g/L. These are each significantly higher than the usable capacities for all other measured materials. Table 2 presents a comparison of the total volumetric usable capacities for each material studied at relevant temperature swings.

TABLE 2. Total volumetric H_2 usable capacities for four MOF materials for various temperature swings (assuming single crystal density). All units are in g/L.

Swing	Ni_2(*m*-dobdc)	Co_2(*m*-dobdc)	Ni_2(dobdc)	Co_2(dobdc)
25°C, no swing	11.0	10.5	10.0	8.8
-75°C, no swing	19.0	18.2	18.4	16.5
-40 to 25°C	18.2	17.3	16.6	14.0
-75 to 25°C	23.0	21.9	21.4	18.3

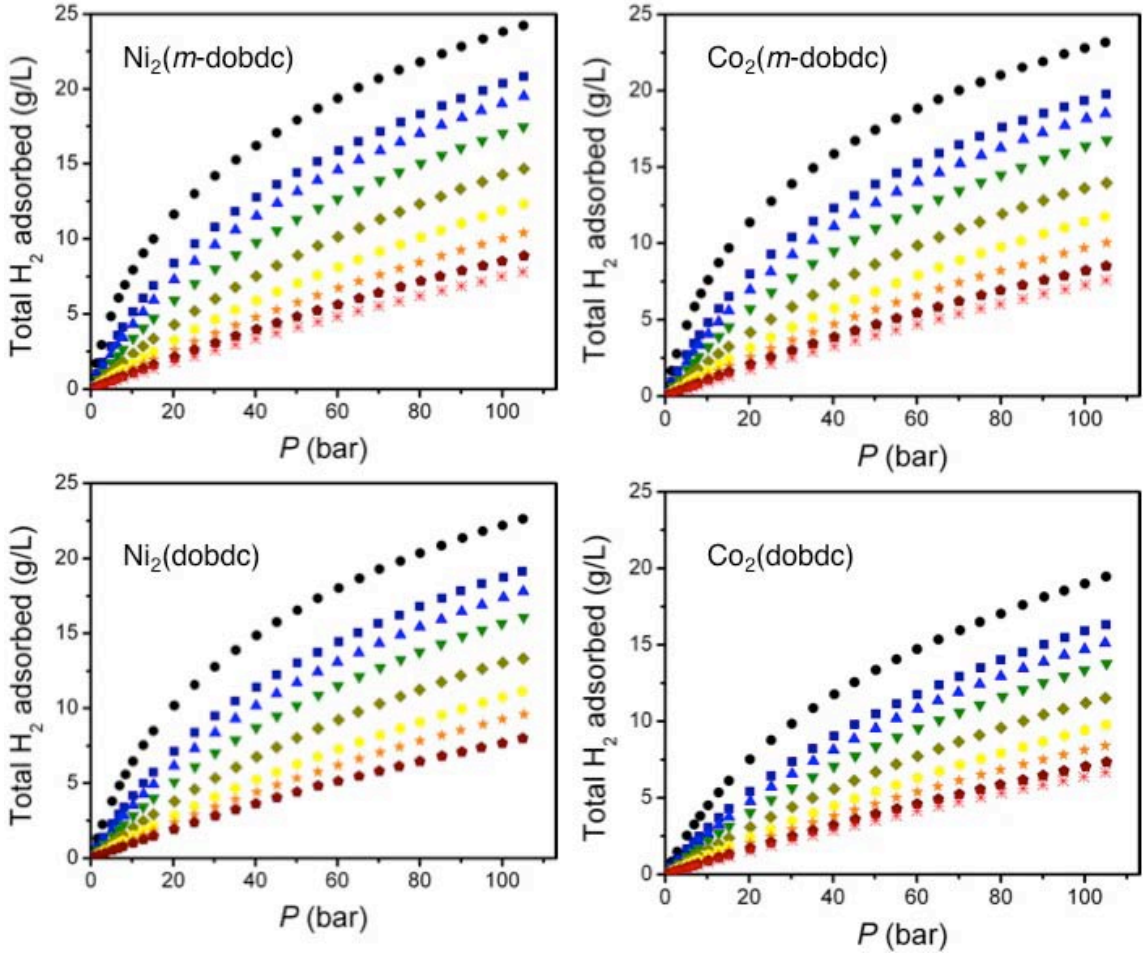

FIGURE 2. High-pressure H_2 isotherms for Ni_2(*m*-dobdc), Co_2(*m*-dobdc), Ni_2(dobdc), and Co_2(dobdc). The temperatures reported are -75°C (black circles), -50°C (navy squares), -40°C (blue triangles), -25°C (green downward-pointing triangles), 0°C (gold diamonds), 25°C (yellow circles), 50°C (orange stars), 75°C (dark red pentagons), and 100°C (red crosses). The capacity of each MOF at 100 bar decreases as temperature increases (assuming single crystal density).

First Principles Calculations

First principles electronic structure calculations were used in conjunction with experimental results to both explain the results seen from experimental studies and to inform future experimental targets. In order to devise successful hydrogen storage strategies, there is a need for a fundamental understanding of the weak and elusive physisorption interaction. We reported a range of calculations of the weak intermolecular interactions of adsorbed hydrogen molecules on MOF linkers by using cluster models.

Since physical interactions such as dispersion and polarization have a major contribution to attraction energy, we analyzed the adsorption interaction using energy decomposition analysis that distinguishes the contribution of the physical interactions from the charge-transfer "chemical" interaction [2]. Surprisingly, it is found that charge transfer from the adsorbent to the $\sigma^*(H_2)$ orbital is present in all studied complexes and can contribute up to approximately -2 kJ/mol to the interaction. When metal ions are present, donation from the $\sigma(H_2)$ to metal Rydberg-like orbital, along with the adsorbent to $\sigma^*(H_2)$ contribution, can contribute between -2 kJ/mol and -10 kJ/mol, depending on the coordination mode. To reach a sufficient adsorption enthalpy for practical usage, we find that the hydrogen molecule must be substantially polarized. Ultimately, the ability of the metalated linker to polarize the hydrogen molecule is highly dependent on the geometry of the metal ion coordination site, where a strong electrostatic dipole or quadrupole moment is required. MOFs containing metals bound to catechol functionalities were found to be superior to those containing metals bound in square planar and tetrahedral coordination modes. For example, an Al^{3+} bound to a catechol with a single F^- counterion was found to bind H_2 with a strength of about 20 kJ/mol, which is higher than any experimentally found binding enthalpy thus far. Thus, maximizing the number of available coordination sites on the metal cation is an important goal in order to allow for a maximum dipole moment and thus the strongest possible interaction with H_2.

Other work completed focused on the determination of an optimal method for desolvating metal cations bound post synthetically to the ligands in metal organic frameworks. This is the primary hurdle to obtaining low-coordinate metal cations in MOFs; the ability to desolvate the metal cation is of the utmost importance in exposing coordination sites that will serve as H_2 binding sites. To overcome this barrier, a series of stepwise solvent exchanges is proposed as a suitable route to exposing coordination sites. One potential route for this has been calculated and determined based on the ability of each solvent to penetrate the coordination sphere around the metal and displace the previously bound solvent molecule. Solvent substitution reactions are dynamic processes, involving the detachment of the previous solvent and its solvation in the new solvent and the attachment of the new solvent to the metal site. Thus, temperature is expected to play a significant role in the dynamics of the system and these dynamics must be appropriately modeled. Molecular dynamics simulations on large number of atoms/molecules are beyond the reach of accurate density functional theory, due to the heavy computational requirements for systems of these sizes. In light of this, we evaluated another method, the effective fragment potential (EFP) method, as a tool for carrying out calculations of solvent exchange. The EFP approach enables more direct construction of force fields without the need for extensive calibrations. Indeed, we were able to successfully use this approach to model the molecular dynamics of solvent exchange, for example in Figure 3 where we demonstrate that a single water molecule, marked by a red circle, is effectively replaced at the metal site by an acetone molecule, and propagated to the surface of the solvent droplet.

We further expanded the solvent-exchange methodology to examine experimentally relevant solvents that would be used in the metalation process of the MOF, and therefore eventually require removal to activate metal sites for H_2 uptake. Commonly used solvents, with an electron lone pair attached to the metal-coordinated atom, have an expected interaction energy (per solvent molecule) of about 100 kJ/mol with a catechol-Mg open-metal site and about 90 kJ/mol with a catechol-Ca open metal site. Given these large interaction energies, direct removal of these solvents from the open-metal site is not practical. Instead, these solvents may be substituted by other solvent molecules, such that each substitution step reduces the interaction of the solvent with the open-metal site. Computations enabled us to determine that an optimal sequence of solvent substitutions would be to use acetonitrile as a synthetic solvent, and to do successive exchanges with dichloroethane, ethylene, ethane, and methane, a sequence that would to successively minimize interaction energies at the metal site by approximately -15 kJ/mol. Ultimately, then, we have been able to use first principles calculations to support experimental efforts by determining optimal material activation conditions, which is essential in maximizing hydrogen uptake and meeting desired targets.

Neutron Diffraction Studies

The square-pore MOF $Cu[Ni(pdt)_2]^3$ (pdt^{2-} = pyrazine-2,3-dithiolate) shows potential for demonstrating the ability to bind two H_2 molecules to a single metal center (Figure 4). Data from H_2 isotherms indicated a strong H_2 binding enthalpy; thus, D_2-dosed samples were studied with neutron diffraction in order to determine the binding location of D_2 in the pores. Our efforts enabled the identification of the primary binding site being between the aromatic rings in the ligand, which is not what was expected. However, the diffraction data contained several peaks at low angles that could not be identified; we are working on determining the source of these peaks, but they are most likely due to an impurity in the bare material. Improved synthetic conditions have since produced a more pure material, which will again be studied using D_2-dosed neutron diffraction.

Another focus has been on the development of methods to understand H_2 adsorption at high pressures. Previously, we had conducted experiments on MOF-5 at high D_2 pressures to determine the binding profile of H_2 at high pressures in this material. Since then, this experiment has been conducted

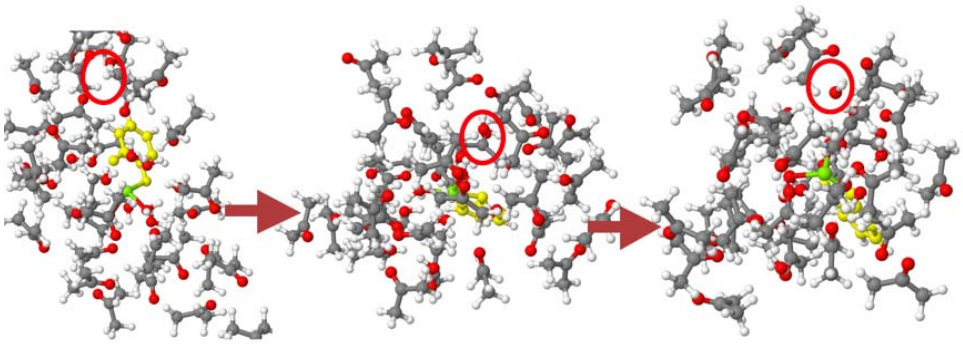

FIGURE 3. Evaluation of removal of water coordinating the metal site in catechol-Mg by acetone. The catechol molecule is in yellow and the metal ion is in green.

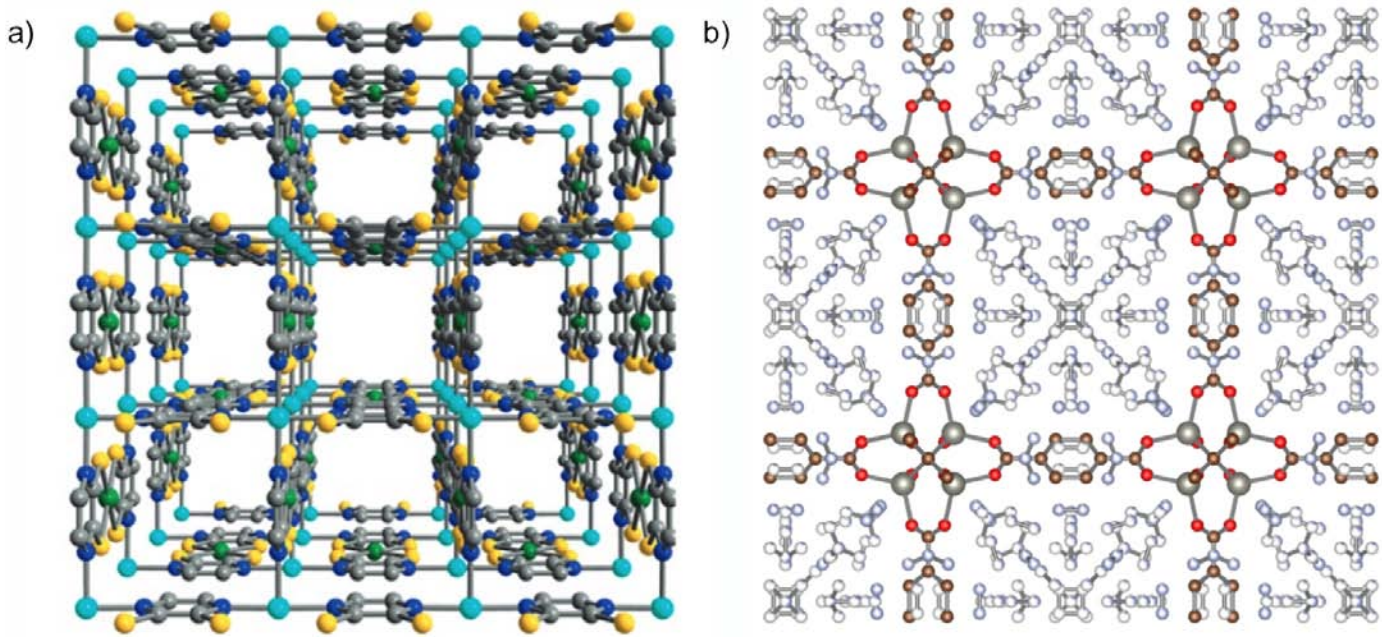

FIGURE 4. (a) The structure of $Cu[Ni(pdt)_2]$ showing the square channels and close Ni^{2+} to Ni^{2+} distances. (b) The structure of MOF-5 loaded with 100 torr N_2 at 77 K, showing the binding profile of N_2 within the pores.

with N_2 at similar conditions as the experiments done with D_2. We observed the N_2 molecules to be localized in specific locations in the pore, similar to what was observed for D_2, even when a nominal pressure of gas is present at the time of the data collection. The conditions used in this experiment mimic those in a standard surface area measurement and thus revealed that the simplified model of covering pores with a layer of N_2 molecules does not adequately describe adsorption of H_2 at the atomic level. These data confirm the validity of our method of solving high-pressure structures with D_2 and will aid in a rigorous understanding of gas interactions with open-metal sites in the framework, further informing the optimization of H_2 uptake in new materials.

CONCLUSIONS AND FUTURE DIRECTIONS

Overall, the work this year has been quite successful in working toward MOF materials that can store large amounts of H_2. The development of synthetic methods both for the boc-protected catechol ligand and the cat-UIO-68 MOF are crucial toward synthesizing MOFs with a high density of open-metal coordination sites, which is the most promising method moving forward for having a significant breakthrough in the total volumetric H_2 storage capacity of MOFs. Relatedly, a full evaluation of the current top H_2-storage MOF materials was undertaken to determine the conditions in a temperature-swing process that maximize the volumetric H_2 usable capacity. First principles electronic structure calculations and neutron diffraction experiments helped to direct synthetic efforts, as well as help determine where and how H_2 is binding within these frameworks.

Future work will primarily focus on obtaining materials that can bind non-structural metal cations that can subsequently be desolvated to expose multiple coordination sites for H_2 binding. This will be imperative in order to increase the volumetric capacity of these materials and reach the DOE targets. The following goals will be targeted in FY 2016.

- Further study the metalation of cat-UIO-68 in order to determine optimal metalation and desolvation conditions
- Test the metalated cat-UIO-68 for its H_2 storage properties
- Develop other ligands and MOFs for use in post-synthetic metalation
- Extend the high-pressure neutron diffraction experiments to other materials in order to understand the binding profile of H_2 in the pores of those MOFs
- Continue to optimize the solvent exchange cascade to fully desolvate metals bound to catechols in MOFs

SPECIAL RECOGNITIONS & AWARDS/ PATENTS ISSUED

1. Kapelewski, M.T.; Geier, S.J.; Long, J.R. "Metal-Organic Frameworks with a High Density of Highly Charged Exposed Metal Cation Sites." Submitted, patent pending.

FY 2015 PUBLICATIONS/PRESENTATIONS

Publications

1. Kapelewski, M.T.; Geier, S.J.; Hudson, M.R.; Stuck, D.; Mason, J.A.; Nelson, J.N.; Xiao, D.J.; Hulvey, Z.; Gilmour, E.; FitzGerald, S.A.; Head-Gordon, M.; Brown, C.M.; Long, J.R. "M_2(*m*-dobdc) (M = Mg, Mn, Fe, Co, Ni) Metal-Organic Frameworks Exhibiting Increased Charge Density and Enhanced H_2 Binding at the Open Metal Sites," *J. Am. Chem. Soc.* **2014**, *136*, 12119–12129.

2. Tsivion, E.; Long, J.R.; Head-Gordon, M. "Hydrogen Physisorption of Metal-Organic Framework Linkers and Metalated Linkers: A Computational Study of the Factors that Control Binding Strength," *J. Am. Chem. Soc.* **2014**, *136*, 17827–17835.

Presentations

1. Brown, C.M. Invited talk, Metal-Hydrides 2014, July 20, 2014, Manchester, U.K.

2. Brown, C.M. Invited talk, Chemistry Dept. Seminar, May 8, 2014, Drexel, PA, U.S.A.

3. Kapelewski, M.T.; Geier, S.J.; Hudson, M.R.; Stuck, D.; Mason, J.A.; Nelson, J.N.; Xiao, D.J.; Hulvey, Z.; Gilmour, E.; FitzGerald, S.A.; Head-Gordon, M.; Brown, C.M.; Long, J.R. "Structural Isomer of M_2(dobdc) with Increased Charge Density and Stronger H_2 Binding at the Open Metal Sites." 248th American Chemical Society National Meeting, San Francisco, CA: August 2014.

4. Jarad Mason. U.S. Car Hydrogen Storage Tech Team Presentation, Detroit, MI: September 2014.

REFERENCES

1. Kapelewski, M.T.; Geier, S.J.; Hudson, M.R.; Stuck, D.; Mason, J.A.; Nelson, J.N.; Xiao, D.J.; Hulvey, Z.; Gilmour, E.; FitzGerald, S.A.; Head-Gordon, M.; Brown, C.M.; Long, J.R. *J. Am. Chem. Soc.* **2014**, *136*, 12119–12129.

2. Tsivion, E.; Long, J.R.; Head-Gordon, M. *J. Am. Chem. Soc.* **2014**, *136*, 17827–17835.

IV.C.2 Hydrogen Sorbent Measurement Qualification and Characterization

Philip A. Parilla (Primary Contact),
Katherine Hurst, Michele Olsen, Thomas Gennett
National Renewable Energy Laboratory (NREL)
15013 Denver West Pkwy.
MS 3219
Golden, CO 80228
Phone: (303) 384-6506
Email: Philip.Parilla@nrel.gov

DOE Manager
Jesse Adams
Phone: (720) 356-1421
Email: Jesse.Adams@ee.doe.gov

Collaborators
- Karl Gross, H2 Technology Consulting LLC, Fremont, CA
- Jeff Long group, University of California, Berkeley, Berkeley, CA
- Joe Zhou group, Texas A&M University, College Station, TX
- Seth Cohen group, University of California, San Diego, San Diego, CA
- Hydrogen Storage Technical Team
- Troy Semelsberger, Los Alamos National Laboratory, Los Alamos, NM
- Craig Brown, National Institute of Standards and Technology, Gaithersburg, MD

Project Start Date: October 1, 2012
Project End Date: Project continuation and direction determined annually by DOE

Overall Objectives

- Provide validation measurements for the hydrogen capacity of storage materials
- Develop and disseminate measurement best practices and recommended protocols and data analysis procedures for hydrogen capacity measurements
- Assist research groups within the hydrogen storage community to perform robust and accurate measurements of hydrogen storage capacity
- Analyze for, identify, and recommend corrective actions for major sources of measurement error in volumetric and temperature programmed desorption (TPD) systems
- Develop an in situ thermal conductivity measurement capability for hydrogen storage materials with the ultimate goal of assisting materials-research groups to characterize and validate their thermal conductivity measurements

Fiscal Year (FY) 2015 Objectives

- Disseminate volumetric capacity protocols and recommendations for their implementation to the hydrogen storage community so that material properties can be reported in a uniform and unambiguous manner
  - Give input to and receive feedback from the Hydrogen Storage Technical Team on previously developed protocols and recommendations for determining and reporting on volumetric capacity for hydrogen storage materials
  - Submit a report that will be disseminated to the scientific community (pending at the time of this report)
- Develop an in situ thermal conductivity measurement capability for hydrogen storage materials for measurements from 77 K to 400 K and at ambient gas pressures up to 150 bar
  - Establish methodology for characterizing materials with different form factors
  - Design and integrate components for the measurement system
  - Validate measurement technique over entire temperature and pressure range
- Assist materials research groups to characterize and qualify their samples for hydrogen storage properties
  - Measure external samples at NREL to compare results with source group's and/or third party's results
  - Discover sources of measurement discrepancies and advise on corrective actions, if needed, for source group
- Analyze for, identify, and recommend corrective actions for major sources of measurement error in volumetric and TPD systems
  - Analyze realistic models for random and systematic errors
  - Identify the major error sources that will dominate the measurement
  - Recommend improved instrumentation and procedures to minimize such errors

Technical Barriers

This project addresses the following technical barriers from the Hydrogen Storage section of the Fuel Cell Technologies Office Multi-Year Research, Development, and Demonstration Plan:

(A) System Weight and Volume

(B) System Cost

(C) Efficiency

(E) Charging/Discharging Rates

(J) Thermal Management

(K) System Life-Cycle Assessments

(O) Lack of Understanding of Hydrogen Physisorption and Chemisorption

(P) Reproducibility of Performance

Technical Targets

This project supports the following overall DOE objective: "Capacity measurements for hydrogen-storage materials must be based on valid and accurate results to ensure proper identification of promising materials for DOE support." Insights gained from these studies will be applied toward the design and synthesis of hydrogen storage material systems that meet the 2020 DOE hydrogen storage targets:

- Cost: $10/kWh net
- Specific energy: 1.8 kWh/kg
- Energy density: 1.3 kWh/L

The specific technical objectives include:

- Disseminate measurements qualification and validation improvements to the hydrogen community
- Work with hydrogen storage material-synthesis researchers to measure, at least, two external samples.

FY 2015 Accomplishments

- Developed recommended volumetric capacity definitions and protocols that were thoroughly described in a report
  - Presented findings at the International Energy Agency-Hydrogen Implementing Agreement Task in Chamonix, France, January 2015
  - Presented findings before the Hydrogen Storage Technical Team, which subsequently provided feedback that was incorporated into the document
  - Will publish manuscript in a special edition for hydrogen storage in Applied Physics A
- Completed initial work for an in situ thermal conductivity measurement system for hydrogen storage materials
  - Developed thermal modeling and established the viability of the single-sided transient plane source technique for measuring the thermal conductivity
  - Designed two "plug-and-play" modules that will enable thermal conductivity measurements of samples with volumes ranging from 0.5–60 cm^3
  - Designed and assembled an instrument that includes temperature and pressure controls, capable of measuring the thermal conductivity of hydrogen sorption materials between 77 K and 400 K and at pressures up to 150 bar.
- Measured four external samples from outside laboratories, surpassing the milestone of measuring two external samples

✧ ✧ ✧ ✧ ✧

INTRODUCTION

The ultimate goal of the Hydrogen Storage sub-program is the development of hydrogen storage systems that meet or exceed the DOE's goals for onboard storage in hydrogen-powered vehicles. In order to develop new materials to meet these goals, it is extremely critical to accurately, uniformly, and precisely measure the materials' properties relevant to the specific goals; otherwise the metrics are meaningless and achieving of goals, uncertain. In particular, capacity measurements for hydrogen-storage materials must be based on valid and accurate results to ensure proper identification of promising materials for DOE support. This project focuses on maintaining a world-class measurement facility for determining hydrogen storage capacities of novel research materials, understanding the experimental issues, procedures, and analysis to ensure accurate measurements, and assisting the hydrogen storage community in performing and understanding these measurements. NREL's main focus is on the manometric measurement technique; this technique is also known as the volumetric and Sieverts technique.

Another important aspect for hydrogen storage systems is the thermal conductivity of the storage material used in the system because it impacts the design of heat exchangers necessary for temperature control during charging and discharging of the hydrogen. Low thermal conductivity (TC) materials require additives such as graphite and/or macroscopic heat transfer enhancing structures such as fins in the storage vessel. Furthermore, the TC of these materials depends on both temperature and the hydrogen gas pressure. To design proper thermal management for a given material, therefore, requires knowledge of the TC under the expected

operating conditions. For hydrogen sorption materials, the required temperatures may be as low as 77 K and pressures easily reaching 150 bar. An apparatus that can measure materials over the desired temperature and pressure range is not commercially available and requires customization.

APPROACH

NREL continues with a multiyear intensive effort to improve measurement quality and accuracy, understand the sources of and correct for measurement error, work with external groups to provide measurements and verify results, and collaborate with the hydrogen community to improve measurements. NREL had previously managed the "Best Practices" Project to disseminate recommended practices and procedures [1]. The approach for measurement quality and accuracy can be divided into three components (1) work with external groups to measure samples and to examine their measurement techniques and procedures; (2) analyze for, identify, and recommend corrective actions for major sources of measurement error in manometric systems; and (3) develop standardized procedures and protocols so that data and results are reported in a uniform manner to allow direct comparison of material performance. In this fiscal year, NREL has further developed definitions and implementations for determining volumetric capacity of hydrogen storage materials and has focused on producing a document describing these definitions and protocols with extensive input from the hydrogen storage community.

For a TC apparatus, measurements must be performed over a wide range of temperatures and pressures and capable of measuring small samples with different form factors such as pucks and powders. To facilitate facile throughput of sample measurements, it is desirable that these measurements be done quickly. We surveyed both steady-state and transient techniques, and identified the transient plane source technique as meeting these requirements. In its traditional application, a combined heater/sensor is sandwiched between two identical samples of the material under test. At time $t = 0$, constant power is applied to the heater, and the temperature change of the sensor as a function of time is fit to a model to obtain the TC and diffusivity of the material. The requirement of two samples with a minimum volume of ~0.5 cm^3 can be prohibitive to materials research groups developing novel materials. To limit the quantities needed, we endeavored to develop a single-sided technique in which the sensor is placed between the sample under test and a sample of a material with known (and reasonably insulating) thermal properties. While this technique is incorporated into some commercial instruments, the technique is not published in the literature. To understand the impact of the reference material, we developed a thermal model of the technique. Because the model requires experimental validation, the TC apparatus will allow for both single-sided and traditional, double-sided transient plane source (TPS) measurements.

With respect to working with external groups, NREL actively seeks out collaborations for comparison studies, helps with DOE projects to ensure robust measurements, and tests very promising results for verification. Additionally, NREL works with external groups to discover sources of measurement discrepancies and provides advice on corrective actions, if needed. This work entails sending standardized samples to external labs to test instrumentation and experimental procedures, examining data and data analysis protocols to discover possible avenues to improve measurement techniques, and making recommendations to labs for improvements.

RESULTS

1. Continued to develop recommended volumetric capacity (VC) definitions and protocols and incorporate them into a report with input from the hydrogen storage community. VC determinations ultimately involve a separate accounting of hydrogen in a storage vessel or system and a separate accounting of quantifying the volume of said vessel or system and dividing the former by the latter. Different accountings for hydrogen and volumes define different figures of merit (FOMs) and depending on the goals of the project with corresponding emphasis of different merits, the best FOM to use to quantify those merits will change with the emphasis. Seven FOMs have been described and are recommended in the report that has been invited to be published in a special issue on hydrogen storage in Applied Physics A.
2. We developed a thermal model of the TPS techniques using COMSOL Multiphysics. With this model, we were able to simulate the single-sided TPS technique using the thermal properties of various real and fictitious materials. The fictitious materials allowed the thermal conductivity or diffusivity to be held fixed to determine the impact of the other parameters on the temperature increase at the sensor. In this way, the basic dependencies on the parameters were identified. Figure 1a shows a cross-sectional view of the modeled temperature profile within two dissimilar materials. Figure 1b shows the modeled temperature increase at the sensor as a function of time for single-sided TPS measurements with various sample materials (see legend in Figure 1c) and the reference material is polymethyl methacrylate (PMMA). Figure 1c shows the scaled simulated temperature increase as a function of a proposed time scaling that approaches a universal curve for all the simulated materials. Using this proposed scaling, we expect to be able to measure both the TC and thermal diffusivity of unknown materials, and the model will be experimentally validated.

   For the overall TC apparatus, we have customized commercial instruments to achieve the required pressure

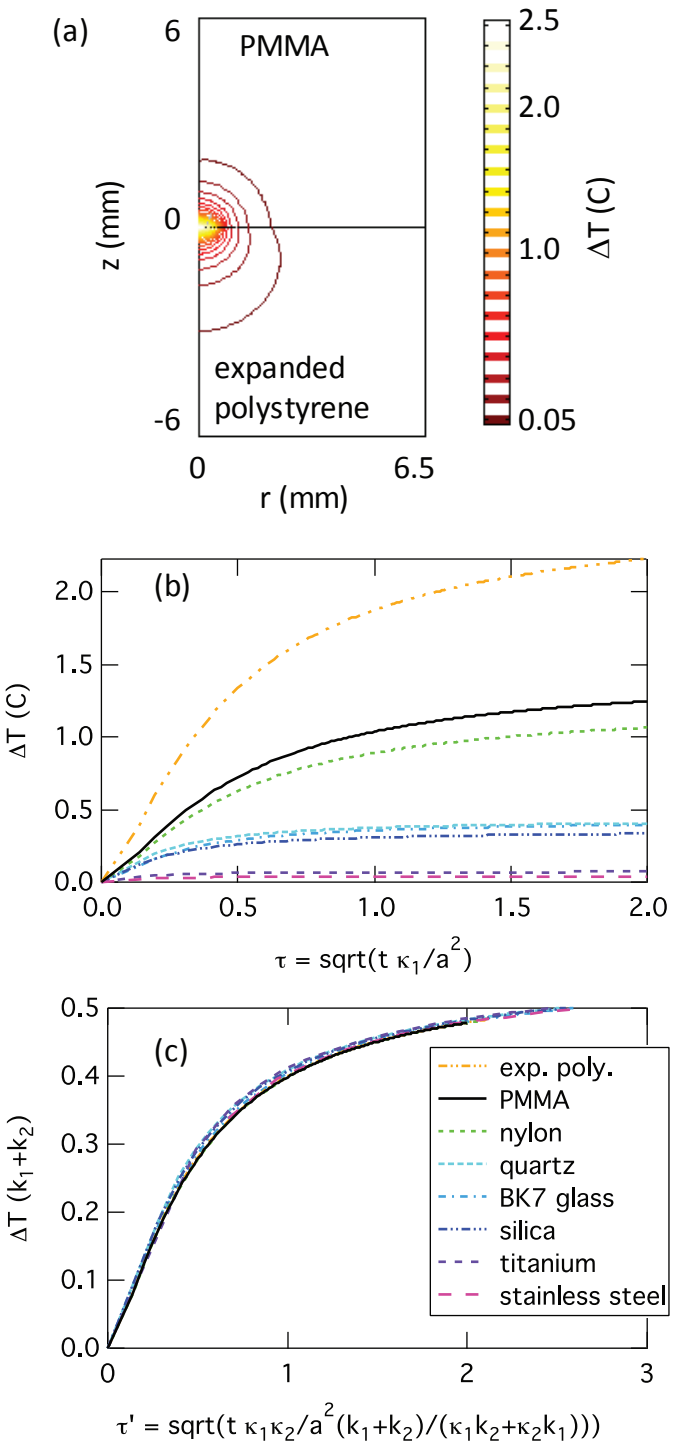

FIGURE 1. Thermal modeling of single-sided TPS measurements: (a) simulated temperature profile within two dissimilar materials, (b) temperature increase at the sensor as a function of time for a variety of materials, and (c) proposed scaling to extract thermal properties from single-sided TPS measurements

and temperature range. It consists of a cryostat from Advanced Research Systems that has a temperature range between 2 K and 400 K, and has been customized to include a high-pressure hydrogen inlet. There is also a customized pressure vessel from Parr Instruments with the necessary gas port and electrical feed-throughs for the TC measurement. To measure a sample, the sensor and sample are mounted inside the pressure vessel, and as shown in Figure 2a, the vessel is mounted on the cold head of the cryostat, the radiation shield (lower left) is mounted around the pressure vessel, and the entire system is enclosed within the vacuum shroud of the cryostat. We are designing several measurement "modules" that are plug-and-play sensor and sample holders for mounting samples with different form factors within the pressure vessel. Figure 2b shows the design of a module for measuring 13-mm diameter pucks with the single-sided TPS technique.

3. Measured four external samples from outside laboratories. This number surpasses the milestone of measuring two external samples. Each sample typically undergoes approximately nine measurements using different techniques in the course of a typical analysis. Techniques include multiple pressure-composition-temperature (PCT) isotherms, Brunauer-Emmett-Teller isotherm for surface-area analysis, TPD during degas, TPD after PCT, density and cycle-life PCT. Sample material types have included high-surface-area carbons with and without catalysts, BC_x (a boron substituted carbon material formed by the pyrolization of triethylborane) with and without catalysts, and metal organic frameworks (MOFs) with and without catalysts. Data from these external samples are considered proprietary.

4. Continued to develop realistic models for the data analysis for manometric systems, both for isothermal and non-isothermal conditions. The importance of using realistic models should not be underestimated. Volumetric mass-balance models in the scientific literature, although ideally correct, typically do not account for real-world measurement situations. Most volumetric systems contain many more moles in the gas phase than the moles sorbed onto the sample, thus requiring very accurate mass-balance accounting. We have concluded that the most dominant errors are still systematic errors! The main sources of systematic error are improper "null" calibration, inadequate data analysis models (mass-balance models), ignorance of the large error associated with non-uniform temperature fluctuations, and importance of having adequate sample mass and inexperience leading to undeserved trust in results (black-box syndrome).

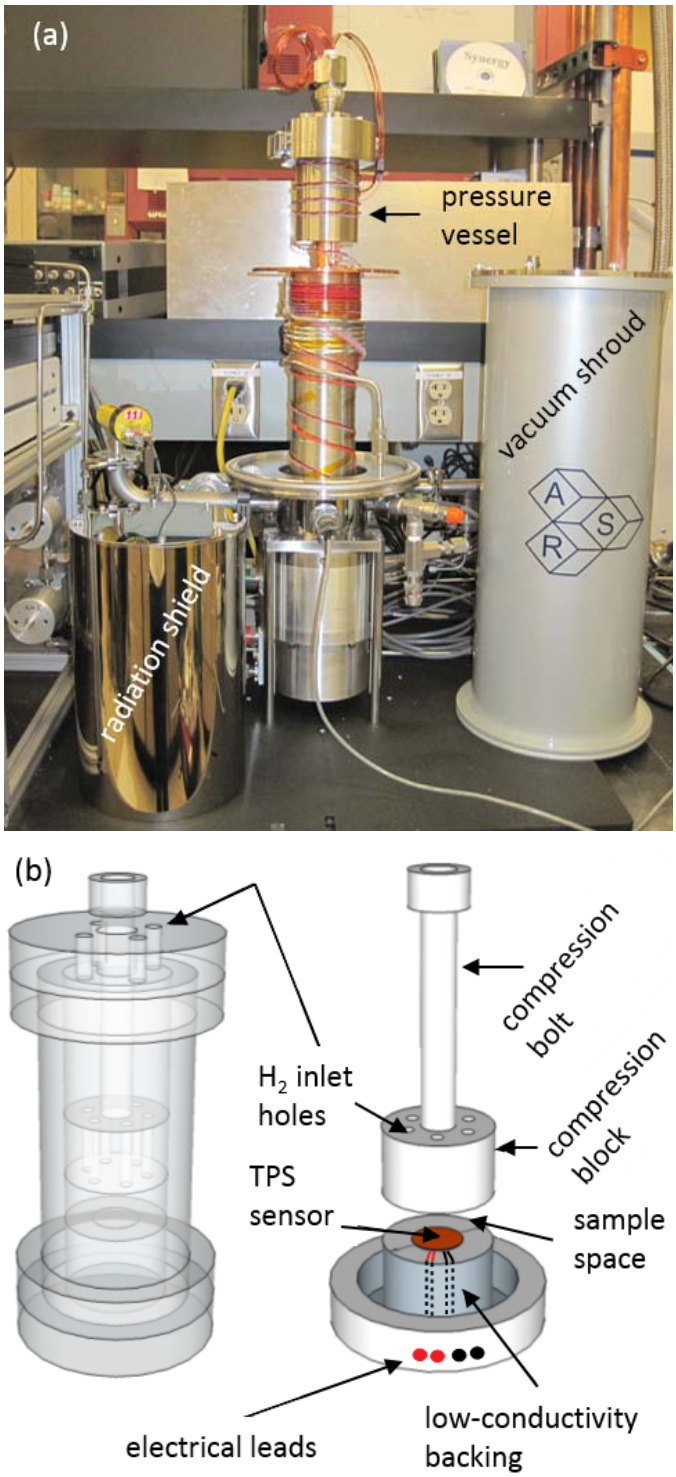

FIGURE 2. Thermal conductivity apparatus: (a) photo showing the components of the measurement apparatus and (b) schematic of a single-sided TPS measurement module

CONCLUSIONS AND FUTURE DIRECTIONS

- Efforts have continued to develop recommended volumetric capacity definitions and protocols, and these were thoroughly described in a report that will be published in a manuscript in a special edition for hydrogen storage in Applied Physics A.
- The hydrogen-storage community will benefit from these efforts to ensure accurate capacity measurements. Increased quality-control efforts will ensure that the proper emphasis will be placed on new hydrogen-storage materials. Recommendations addressing these issues have been made to improve measurement quality.
- We have designed and built an apparatus to measure the thermal conductivity of hydrogen storage materials over the temperature range of 77–400 K and with hydrogen over pressures up to 150 bar. The thermal conductivity apparatus is capable of measuring both pucks and powders with volumes as small as 0.5 cm^3. The validation of the apparatus will begin with measurements of known materials (i.e., silica or nylon) with thermal properties similar to typical hydrogen sorption materials, as well as measurements of MOF-5 samples characterized by the Hydrogen Storage Engineering Center of Excellence. Once validated, this apparatus will be used to characterize new and existing hydrogen storage materials developed by NREL and external groups.
- The hydrogen-storage community will continue to benefit from validation efforts in the future and help ensure high quality research. NREL will continue to assist in these efforts and provide expertise for the hydrogen-storage community. NREL will expand its measurement capabilities to include variable-temperature PCT measurements. With modification to one of NREL's PCT systems and the design and construction of a cryocooler addition, NREL will be able to perform measurements between 40 K and 330 K and pressures above 160 bar. This capability will provide the opportunity to determine the energetics associated with hydrogen sorption.

FY 2015 PUBLICATIONS/PRESENTATIONS

1. Invited Paper: "*Recommended Volumetric Capacity Definitions and Protocols for Accurate, Standardized and Unambiguous Metrics for Hydrogen Storage Materials,*" P.A. Parilla, K. Gross, K.E. Hurst, T. Gennett in preparation for Appl. Phys. A.

2. Invited Paper: "*An International Multi-Laboratory Investigation of Hydrogen Sorbent Materials,*" K.E. Hurst, T. Gennett, P.A. Parilla, in preparation for Appl. Phys. A.

3. Invited Talk: "*Proposed Standard Methodologies for Hydrogen Storage Measurements on Sorbents,*" K.E. Hurst, P.A. Parilla, M. Olsen, T. Gennett, Task 32 IEA HIA Expert Meeting, January 19, 2015, Chamonix, France.

4. Talk: "*Protocols and Conventions for Volumetric Capacity Determination,*" P.A. Parilla, presentation to the Hydrogen Storage Tech Team, September 18, 2014.

5. Talk: "*Hydrogen Sorbent Measurement Qualification and Characterization,*" P.A. Parilla, DOE Materials-Based Hydrogen Storage Summit, Golden, CO January, 2015.

6. Poster: "*Hydrogen Sorbent Measurement Qualification and Characterization,*" June 2015, 2015 U.S. DOE Hydrogen and Fuel Cells Program Annual Merit Review and Peer Evaluation Meeting – P.A. Parilla.

7. Poster. "*Hydrogen Sorbent Measurement Qualification and Characterization,*" July 2015, 2015 Gordon Research Conference, Hydrogen Metal Systems, Stonehill College, Easton, MA – T. Gennett.

REFERENCES

1. http://www1.eere.energy.gov/hydrogenandfuelcells/pdfs/best_practices_hydrogen_storage.pdf

IV.C.3 Neutron Characterization in Support of the DOE Hydrogen Storage Sub-Program

Terrence J. Udovic (Primary Contact),
Craig M. Brown, Dan A. Neumann
National Institute of Standards and Technology (NIST)
NIST Center for Neutron Research
100 Bureau Dr., MS 6102
Gaithersburg, MD 20899-6102
Phone: (301) 975-6241
Email: udovic@nist.gov

DOE Managers
Channing Ahn
Phone: (202) 586-9490
Email: Channing.Ahn@ee.doe.gov

Ned Stetson
Phone: (202) 586-9995
Email: Ned.Stetson@ee.doe.gov

Project Start Date: October 2010
Project End Date: Project continuation and direction determined annually by DOE

Overall Objectives

- Support the DOE-EERE-funded hydrogen-storage projects by providing timely, comprehensive characterization of materials and storage systems using state-of-the-art neutron methods
- Direct partner synthesis efforts based on the understanding gained through the use of these methods
- Demonstrate the fundamental characteristics of useful hydrogen-storage materials

Fiscal Year (FY) 2015 Objectives

- Investigate structural and dynamical properties of alkali (*A*) and alkaline-earth (*Ae*) metal decahydro-*closo*-decaborates $A_2B_{10}H_{10}$ and $AeB_{10}H_{10}$
- Start characterization work on new hydrogenated metal silicides ($M_x[SiH_3]_y$)
- Start characterization work on hydrogenated/dehydrogenated Li_3N in nanoporous carbon, hydrogenated metal borides, and decaborane-based materials

Technical Barriers

This project addresses the following technical barriers from the Hydrogen Storage section of the Fuel Cell Technologies Office Multi-Year Research, Development, and Demonstration Plan:

(A) System Weight and Volume

(O) Lack of Understanding of Hydrogen Physisorption and Chemisorption

Technical Targets

NIST provides important materials metrologies for DOE-EERE-funded projects using neutron scattering measurements to understand and characterize hydrogen-substrate interactions of interest in a variety of materials ranging from H_2 adsorbed in nanoporous materials to hydrogen chemically bonded in complex hydride materials. Insights gained from these studies will be applied toward the design and synthesis of hydrogen storage materials that meet the following DOE 2020 storage targets:

- Specific energy: 1.8 kWh/kg
- Energy density: 1.3 kWh/L
- Cost: $10/kWh

FY 2015 Accomplishments

- Manuscript published on kinetic trapping of D_2 in MIL-53(Al)
- Two manuscripts published on the effects of partial halide anion substitution on BH_4^- reorientational motion in $NaBH_4$
- Manuscript published on the structural properties of modified $A_2B_{12}H_{12}$ compounds
- Manuscript published on the room-temperature $Li_2B_{10}H_{10}$ structure and thermal behavior
- Manuscript published on the correct room-temperature monoclinic $Na_2B_{10}H_{10}$ structure
- Manuscript published on the high-temperature disordered structure and conductivity of $Na_2B_{10}H_{10}$

✧ ✧ ✧ ✧ ✧

INTRODUCTION

To obtain the DOE levels of hydrogen storage in a timely manner, it is imperative that trial-and-error testing

of materials be avoided. Thus, the focus must be upon the rational design of new systems. From a thorough understanding of the physics and chemistry that governs the hydrogen-substrate interactions, we will be able to make a more concerted effort to push the frontiers of new materials. The key to improving materials is a detailed understanding of the atomic-scale locations of the hydrogen and determining how it gets there and how it gets out. Neutron scattering is perhaps the premier technique for studying hydrogen, and the NIST Center for Neutron Research is currently the leading facility in the U.S. for studying these materials.

APPROACH

NIST provides important materials characterization for DOE-funded hydrogen storage projects using neutron-scattering measurements to probe the amount, location, bonding states, dynamics, and morphological aspects of (1) molecular hydrogen in carbon-based materials such as polymers, metal organic frameworks (MOFs), and carbonaceous materials such as carbon nanohorns; and (2) atomic hydrogen in a variety of complex hydride materials including those containing boron and nitrogen, as well as their intermediates and by-products. NIST works directly with DOE and other partners that produce novel hydrogen-storage materials to analyze the most promising samples and to help determine and resolve the fundamental issues that need to be addressed.

RESULTS

In collaboration with University of Maryland and the Université de Picardie Jules Verne, we investigated the spectroscopic and dynamical properties of various alkali-metal silanides $MSiH_3$ (M=K, Rb, Cs), which store hydrogen reversibly through an $MSi/MSiH_3$ equilibrium, yielding a 0.1 MPa H_2 equilibrium pressure at ~410 K. Hence, these materials, comprised of M^+ cations and SiH_3^- anions, are potentially promising for hydrogen storage applications. They typically undergo order-disorder phase transitions by ~325 K. Agreement between neutron vibrational spectroscopy (NVS) and density functional theory (DFT) phonon calculations corroborated the ordered β-$MSiH_3$ structures determined by diffraction methods. Neutron-elastic-scattering fixed-window scans (FWSs) indicated that the pyramidal SiH_3^- anions attain high orientational mobilities (>>10^{10} H jumps/s) that increase with cation size. Complementary quasielastic neutron scattering (QENS) data for $CsSiH_3$ confirmed a change to a more three-dimensional SiH_3^- reorientation mechanism upon transformation to the disordered cubic α-phase.

In collaboration with University of Maryland, HRL Laboratories, University of Missouri-St. Louis, and University of Utah, we started NVS measurements to assist in determining the chemical nature of thermally treated decaborane $B_{10}H_{14}$. We successfully established the baseline spectroscopic signature for $B_{10}H_{14}$ (Figure 1) to be used later for comparison with polymerized versions after thermal treatments and potential lithiation. The neutron vibrational spectrum of $^{11}B_{10}H_{14}$ is in good agreement with the DFT phonon calculations. Neutron prompt-gamma activation analysis is currently being used to obtain accurate B/H ratios in different thermally treated samples of $B_{10}H_{14}$.

In collaboration with Sandia National Laboratories (SNL), Lawrence Livermore National Laboratory, and Mahidol University, Bangkok, we spectroscopically characterized the (de)hydrogenation of Li_3N in nanoporous carbon. NVS measurements associated with (de)hydrogenated nanoconfined Li_3N after five desorption/absorption cycles compared to reference spectra (Figure 2) indicated that relatively little H exists in the dehydrogenated state, whereas both $LiNH_2$ and LiH are present in the hydrogenated state, with no obvious presence of the Li_2NH intermediate phase. The lack of Li_2NH suggests a change in the expected reaction pathway.

In collaboration with University of Maryland and SNL, we investigated the structural behavior of $Li_2B_{10}H_{10}$, another stable compound within the technologically relevant Li-B-H phase diagram. Based on X-ray powder diffraction and neutron powder diffraction (NPD), DFT calculations, and NVS, $Li_2B_{10}H_{10}$ was found to exhibit atypical hexagonal symmetry (Figure 3) to best stabilize the ionic packing of the relatively small Li^+ cations and large ellipsoidal $B_{10}H_{10}^{2-}$ anions [1]. Differential scanning calorimetry (DSC) and neutron-elastic-scattering FWSs suggested that $Li_2B_{10}H_{10}$ completes an order-disorder phase transition by ~680 K, similar to $Li_2B_{12}H_{12}$, concomitant with

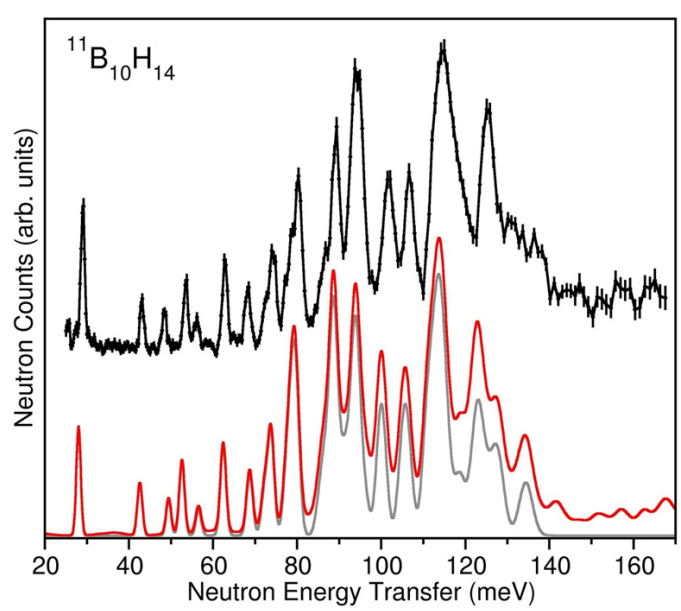

FIGURE 1. The neutron vibrational (NV) spectrum at 4 K of $^{11}B_{10}H_{14}$ (black) with the DFT-simulated 1-phonon (gray) and 1+2-phonon (red) spectra

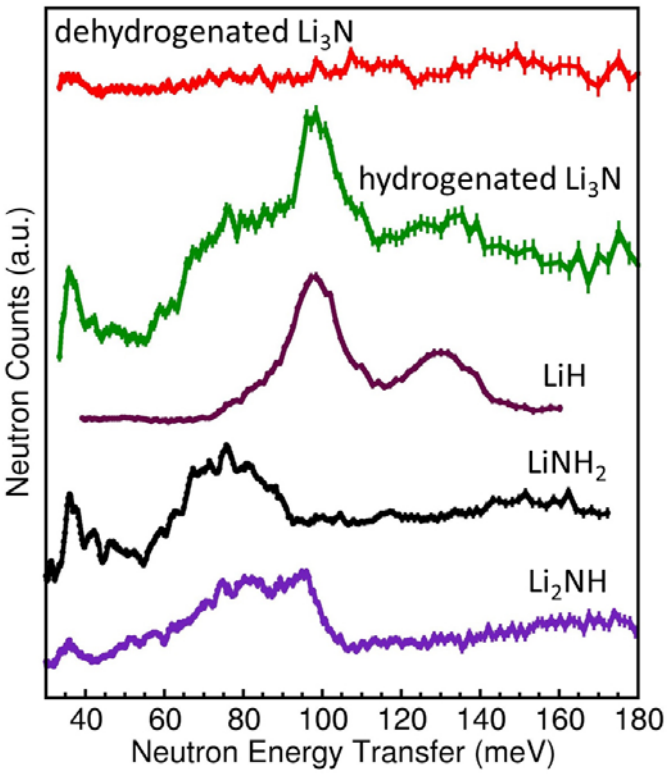

FIGURE 2. The NV spectra at 4 K associated with (de)hydrogenated Li_3N confined in nanoporous carbon after five desorption/absorption cycles, compared to reference spectra

enhanced anion orientational mobility. These results provide valuable structural information pertinent to understanding the potential role that $Li_2B_{10}H_{10}$ plays during $LiBH_4$ (de) hydrogenation.

In collaboration with University of Maryland, SNL, Institute of Metal Physics Ekaterinburg, and Tohoku University, we also investigated the structural behavior of $Na_2B_{10}H_{10}$. A modified structure [2] for monoclinic $Na_2B_{10}H_{10}$ with less-distorted and differently oriented $B_{10}H_{10}^{2-}$ anions than the previously published structure [3] (Figure 4) was determined from NPD measurements of $Na_2{}^{11}B_{10}D_{10}$ in conjunction with DFT computations. Compared to the previous structure, it is found to be lower in energy, exhibits more reasonable Na-H distances, and yields simulated phonon densities of states in better agreement with NVS data for both $Na_2{}^{11}B_{10}H_{10}$ and $Na_2{}^{11}B_{10}D_{10}$. Via a combination of DSC, NPD, QENS, nuclear magnetic resonance spectroscopy and ac impedance measurements, [4] $Na_2B_{10}H_{10}$ was found to form a disordered, face-centered-cubic phase above ~360 K, with a vacancy-rich Na^+ cation sublattice within the interstitial network formed by highly orientationally mobile anions. This liquid-like cation sublattice exhibits impressive superionic conductivity (e.g., $\sigma \approx 0.01$ S cm^{-1} at 383 K) to substantially lower temperatures than for $Na_2B_{12}H_{12}$.

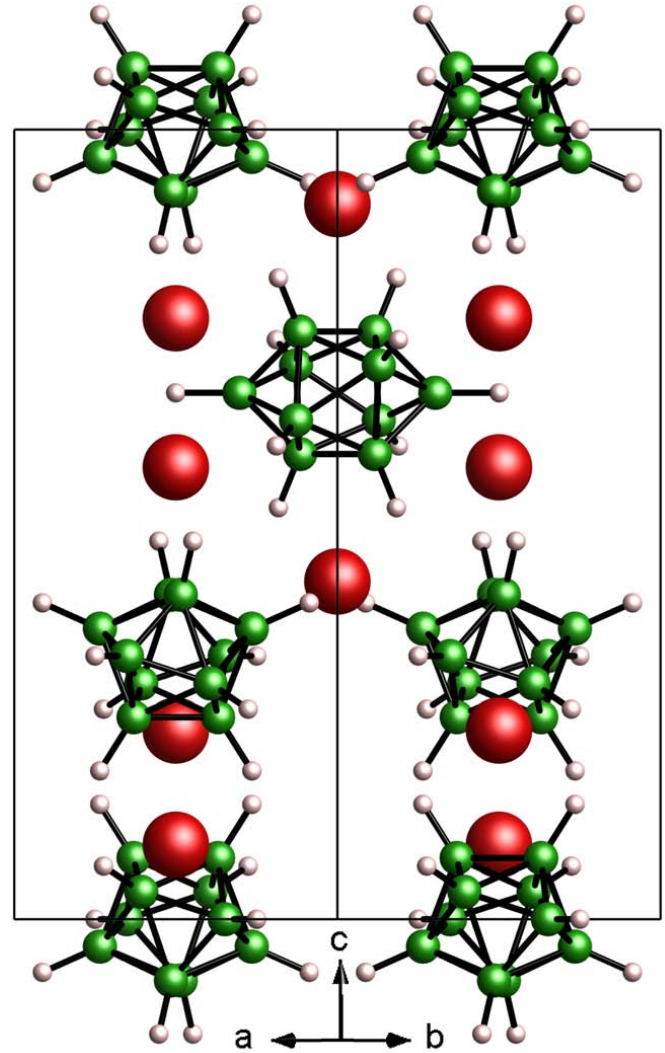

FIGURE 3. The structure of $Li_2B_{10}H_{10}$, with hexagonal $P6_4$ 22 symmetry; red, green, and white spheres denote Li, B, and H atoms, respectively

CONCLUSIONS AND FUTURE DIRECTIONS

- Neutron methods have provided crucial, non-destructive characterization tools for the DOE Hydrogen Storage Sub-Program.
- Agreement between NVS and DFT corroborates β-$MSiH_3$ structures determined by diffraction methods.
- FWS/QENS data for $CsSiH_3$ corroborate the change to a more 3D SiH_3^- reorientation mechanism upon transformation to the disordered cubic α-phase.
- We successfully established the baseline spectroscopic signature for $B_{10}H_{14}$ to be used later for comparison with polymerized versions after thermal treatments and lithiation.

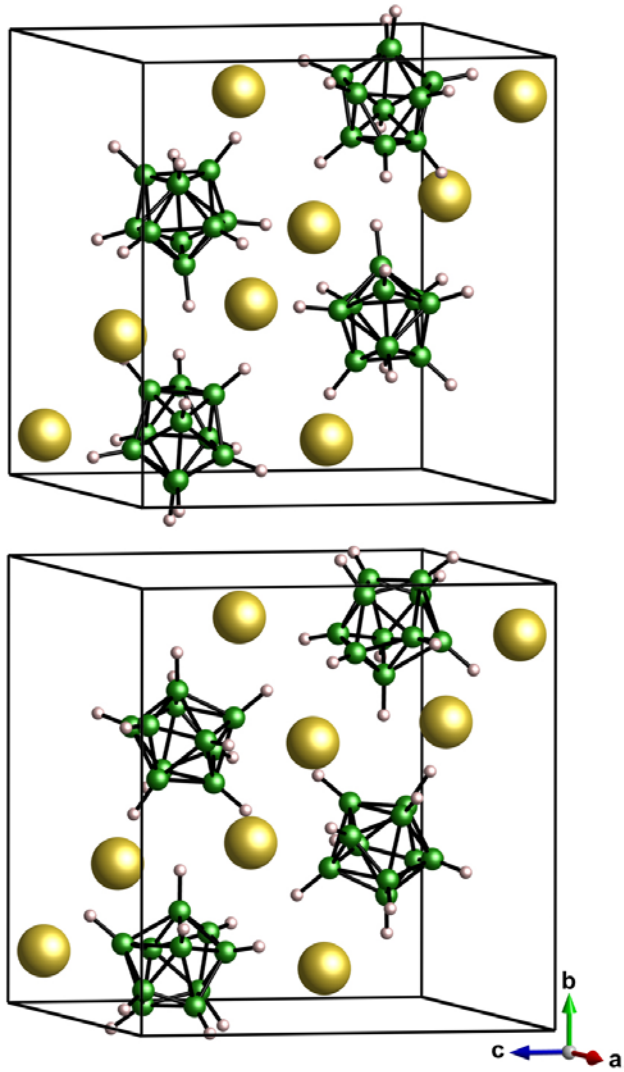

FIGURE 4. The corrected ($P2_1/n$) monoclinic $Na_2B_{10}H_{10}$ crystal structure (top) compared to the published structure (bottom); yellow, green, and white spheres denote Na, B, and H atoms, respectively

- NVS confirms that both $LiNH_2$ and LiH are hydrogenation products from carbon-nanoconfined Li_3N, with no obvious presence of Li_2NH.
- $Li_2B_{10}H_{10}$ was found to exhibit hexagonal symmetry to best stabilize the ionic packing of the relatively small Li^+ cations and large ellipsoidal $B_{10}H_{10}^{2-}$ anions.
- $Li_2B_{10}H_{10}$ completes an order-disorder phase transition by ~680 K concomitant with enhanced anion orientational mobility.
- Using neutron scattering methods in conjunction with DFT, we have corrected structural errors in the previously published, monoclinic ordered $Na_2B_{10}H_{10}$ structure.
- An improvement over $Na_2B_{12}H_{12}$, $Na_2B_{10}H_{10}$ exhibits dramatic superionicity above its ~360 K phase transition, aided by the large mobile anions and the appearance of cation vacancies.
- We will continue characterization work on hydrogenated metal borides and decaborane-based materials.
- We will start characterization work on mixed alkali metal silanides.
- We will continue to perform neutron based structural and spectroscopic characterizations of new materials in conjunction with the needs of the DOE-funded projects, including novel bulk and nanoconfined complex hydride materials.

FY 2015 PUBLICATIONS/PRESENTATIONS

1. R.A. Pollock, J.-H. Her, C.M. Brown, Y. Liu, and A. Dailly, "Kinetic Trapping of D_2 in MIL-53(Al) Observed Using Neutron Scattering," J. Phys. Chem C 118, 18197 (2014).

2. T.J. Udovic, M. Matsuo, W.S. Tang, H. Wu, V. Stavila, A.V. Soloninin, R.V. Skoryunov, O.A. Babanova, A.V. Skripov, J.J. Rush, A. Unemoto, H. Takamura, and S. Orimo, "Exceptional Superionic Conductivity in Disordered Sodium Decahydro-*closo*-decaborate," Adv. Mater. 26, 7622 (2014).

3. R.V. Skoryunov, O.A. Babanova, A.V. Soloninin, A.V. Skripov, N. Verdal, and T.J. Udovic, "Effects of Partial Halide Anion Substitution on Reorientational Motion in $NaBH_4$: a Nuclear Magnetic Resonance Study," J. Alloys Compds. 636, 293 (2015).

4. H. Wu, W.S. Tang, V. Stavila, W. Zhou, J.J. Rush, and T.J. Udovic, "The Structural Behavior of $Li_2B_{10}H_{10}$," J. Phys. Chem. C 119, 6481 (2015).

5. H. Wu, W.S. Tang, W. Zhou, V. Stavila, J.J. Rush, and T.J. Udovic, "The Structure of Monoclinic $Na_2B_{10}H_{10}$: A Combined Diffraction, Spectroscopy, and Theoretical Approach," CrystEngComm 17, 3533 (2015).

6. N. Verdal, T.J. Udovic, J.J. Rush, and A.V. Skripov, "Quasielastic Neutron Scattering Study of Tetrahydroborate Anion Dynamical Perturbations in Sodium Borohydride due to Partial Halide Anion Substitution," J. Alloys Compds. (in press). doi:10.1016/j.jallcom.2014.12.070.

7. W.S. Tang, T.J. Udovic, and V. Stavila, "Altering the Structural Properties of $A_2B_{12}H_{12}$ Compounds via Cation and Anion Modifications," J. Alloys Compds. (in press). doi:10.1016/j.jallcom.2015.01.061.

8. A. Unemoto, T. Ikeshoji, S. Yasaku, M. Matsuo, V. Stavila, T.J. Udovic, and S. Orimo, "Stable Interface Formation between TiS_2 and $LiBH_4$ in Bulk-Type All-Solid-State Lithium Batteries," Chem. Mater. (in press). doi: 10.1021/acs.chemmater.5b02110.

9. W.S. Tang, H. Wu, W. Zhou, T.J. Udovic, N. Verdal, J.J. Rush, A.V. Skripov, V. Stavila, M. Matsuo, and S. Orimo, "Investigations on Hydroborate-based Compounds as Fast-ion Conductors," Neutron Day: Symposium on Exploring Structure and Dynamics in Hard Matter with Neutrons, University of Maryland, College Park, MD, Oct. 2014.

10. H. Wu, "Neutron Studies in Complex Metal Hydrides," Neutron Day: Symposium on Exploring Structure and Dynamics in Hard Matter with Neutrons, University of Maryland, College Park, MD, Oct. 2014.

11. C.M. Brown, "Structural Studies of Small Molecules in MOFs," Telluride SRC Workshop, Telluride, CO, Jun. 2015.

12. S. Orimo, "Complex Hydrides: A New Series of Solid-State Electrolytes for Battery Devices," Hydrogen-Metal Systems Gordon Research Conference, Stonehill College, Easton, MA, Jul. 2015.

13. A.V. Skripov, "NMR Approach to Study Atomic Jump Motion in Complex Hydrides," Hydrogen-Metal Systems Gordon Research Conference, Stonehill College, Easton, MA, Jul. 2015.

14. W.S. Tang, M. Matsuo, H. Wu, W. Zhou, V. Stavila, T.J. Udovic, J.J. Rush, and S. Orimo, "Understanding Complex Hydride Materials as Fast-Ion Conductors," Hydrogen-Metal Systems Gordon Research Conference, Stonehill College, Easton, MA, Jul. 2015.

REFERENCES

1. H. Wu *et al.*, J. Phys. Chem. C **119**, 6481 (2015).

2. H. Wu *et al.*, CrystEngComm **17**, 3533 (2015).

3. K. Hofmann and B. Albert, Z. Kristallogr. **220**, 142 (2005).

4. T.J. Udovic *et al.*, Adv. Mater. **26**, 7622 (2014).

IV.C.4 High-Capacity Hydrogen Storage Systems via Mechanochemistry

Vitalij K. Pecharsky (Primary Contact),
Duane D. Johnson, Marek Pruski, Shalabh Gupta
Ames Laboratory
Iowa State University
253 Spedding Hall
Ames, IA 50011-3020
Phone: (515) 294-8220
Email: vitkp@ameslab.gov

DOE Manager
Ned Stetson
Phone: (202) 586-9995
Email: Ned.Stetson@ee.doe.gov

Subcontractor
Eric Majzoub
M 305, University of Missouri
St. Louis, MO 63121-4400
Phone: (314) 516-5779

Project Start Date: August 1, 2015
Project End Date: July 30, 2018

Overall Objectives

The proposed research seeks to discover and develop hydrogen storage materials that are constituted largely from highly abundant and low cost elements, such as silicon and boron. The specific objectives of this project are two-fold.

- Identify computationally and synthesize hitherto unknown high-capacity Si-based borohydrides (Si-BHs) possessing gravimetric hydrogen density of 12–14 wt%, and decomposition enthalpies of 25–35 kJ/mol-H_2, such that hydrogen desorption occurs at the operating temperature (~80–100°C) of the proton exchange membrane (PEM) fuel cell
- Develop simple and scalable strategies to form two-dimensional (2D) graphene/hydride composites that will directly address the (re)-dehydrogenation kinetic issues that often plague the performance of high capacity borohydrides and other known complex metal hydrides

The successful completion of this project would provide a hydrogen storage material with kinetic and thermodynamic properties tailored appropriately to supply high-purity hydrogen to a PEM fuel cell, satisfying one of the most important goals of the DOE and the Fuel Cell Technologies Office and the Hydrogen Storage Program.

Fiscal Year (FY) 2015 Objectives

- We will initiate studies on computational identification of novel hypersalts of Si-based borohydrides of the type $(A/AE)_xSi_y(BH_4)_z$, in which A and AE represent light/early alkali and alkaline earth metals, respectively. Validated computational methods such as prototype electrostatic ground states (PEGS) [1] will be used to guide synthesis and save experimental time by avoiding attempted synthesis of clearly unstable compounds. The focus will be to identify candidates for hypersalts of silicon borohydride that provide finite-temperature enthalpies within 27 ± 10 kJ/mol-H_2. The new Si-based borohydrides will possess hydrogen contents of at least 11 wt% and volumetric capacity in excess of 130 g H_2/L. For example, in the simplest case of x = y = 1, the composition will be $(A/AE)Si(BH_4)_{5/6}$.
- During FY 2015 we will also initiate experiments to synthesize the most promising Si-based borohydrides identified computationally. Mechanochemical reactions involving metathesis will be performed on those systems that have positive enthalpies for desorption. Preliminary characterization of the newly synthesized borohydrides will be performed by X-ray diffraction and gas-volumetric techniques.

Technical Barriers

This project addresses the following technical barriers from the Hydrogen Storage section (3.3) of the Fuel Cell Technologies Office Multi-Year Research, Development, and Demonstration Plan:

(A) System Weight and Volume

(B) System Cost

(D) Durability/Operability

(O) Lack of Understanding of Hydrogen Physisorption and Chemisorption

Technical Targets

The project addresses lack of suitable materials impeding implementation of materials-based onboard hydrogen storage systems. Successful completion would provide a hydrogen storage material with high gravimetric and volumetric capacity, and kinetics and thermodynamics suitable to supply high-purity hydrogen to a PEM fuel cell. The new materials identified and synthesized as an outcome of this project will achieve or exceed the DOE targets as presented in Table 1.

TABLE 1. Hydrogen Storage Parameters of Novel Si-Based Borohydrides Targeted in This Project and Comparison with DOE Ultimate Targets

Storage Parameters	DOE Technical Targets*	Our Targets**
Gravimetric capacity (kg H_2/kg)	0.075	>0.100
Volumetric capacity (kg H_2/L)	0.070	>0.130

*Ultimate (2020) system level targets, **material basis

INTRODUCTION

Hydrogen has unequivocally been identified as a sustainable fuel for the next generation energy needs that offers tremendous potential to reduce our dependence on fossil fuels, and thereby mitigates our carbon footprint caused by their use. However, since hydrogen is an energy carrier and not the primary energy source, energy must first be invested to produce it. Moreover, the produced hydrogen must be stored and distributed to the point of end use in an efficient and safe manner. This has proved to be a major roadblock in the implementation of hydrogen fuel cell technologies, and a challenging technological caveat to overcome.

For most energy applications, hydrogen has been traditionally stored and transported as a compressed or liquefied gas. The potential safety risks and economical drawbacks associated with these forms of hydrogen storage (H-storage) are well recognized. In this regard, materials-based H-storage, in which hydrogen is either physically or chemically bound in a light weight solid, has emerged as the cutting-edge solution to the H-storage problem. Although a large number of such hydrogen rich compounds have been discovered and synthesized over the last decade, their utility for H-storage and delivery is limited either by their unfavorable thermodynamics or/and poor kinetics of hydrogen release and subsequent uptake [2]. The H-storage problem is compounded by the fact that only a few candidate hydrides with useful gravimetric density have enthalpies of dehydrogenation in the range of -25 kJ/mol-H_2 to -30 kJ/mol-H_2 that is required to achieve 1–10 bar H_2 equilibrium pressure at the working temperature of a PEM fuel cell. Discovery of novel functional solids that combine high gravimetric hydrogen content (>11 wt%) and the desired thermodynamic properties is thus challenging. A commercially viable material must also be inexpensive and easily produced on a mass scale. This project adopts a comprehensive and rational approach based on experiments guided by theory for (1) design and synthesis of hitherto unknown silicon (Si)-based borohydrides and (2) formulation of carbon/hydride nano-composites based on graphene-derived, 2D carbon allotropes. Both of these classes of materials will be experimentally accessed via a highly versatile and sustainable, green, and energy-efficient mechanochemical process that potentially offers a cost effective solution for large scale production of advanced functional materials.

APPROACH

A combined theoretical and experimental approach will be adopted for rapid down-selection of stable candidates in the novel multi-cation Si-borohydride hypersalt and/or ammoniated systems of the type Alkaline/Alkaline earth-Si-(BH_4) followed by their synthesis and performance evaluation. Highly efficient and validated computer codes based on density functional theory (DFT) and crystal structure searching methods will lead to quick and precise identification of promising Si-borohydrides based on their calculated thermodynamic properties. These short-listed candidate Si-borohydrides will then be synthesized via a mechanochemical route by utilizing well known double-exchange or metathesis reactions, followed by their comprehensive characterization and hydrogen sorption properties. The as-synthesized Si-borohydrides will be further processed mechanochemically to obtain graphene/borohydride nano-composites with the aim of improving/tuning the hydrogen desorption kinetics and reversibility. The fabrication of graphene/hydride composites will also be extended to other high hydrogen capacity hydrides, such as $LiAlH_4$, $LiBH_4$ and $Mg(BH_4)_2$ that are currently being actively investigated.

RESULTS

Preliminary computational studies using prototype electrostatic ground state methods have identified high symmetry structures for $Si(BH_4)_4$ and $NaSi(BH_4)_5$. Both, $Si(BH_4)_4$ and $NaSi(BH_4)_5$ are found to crystallize with tetragonal structures in the space group (121) and (82), respectively. The ground state structures of these two compounds are presented in Figures 1a and 1b.

Furthermore, formation energies were calculated for several hypothetical hypersalt structures using the density functional theory including zero point energy. The calculated hypersalt structures were found to be increasingly stable with the size of the cation as presented in Table 2.

CONCLUSIONS AND FUTURE DIRECTIONS

Because decomposition temperature of borohydrides scale well with the cation Pauling electronegativity (χ_P), it is estimated that for metal borohydrides to be potentially suitable for H-storage applications, the cation χ_P must fall within the range of 1.2–1.5 [3]. Notwithstanding such a prediction, silicon has χ_P of 1.9, which is higher than the prescribed window. Nevertheless, preliminarily calculations

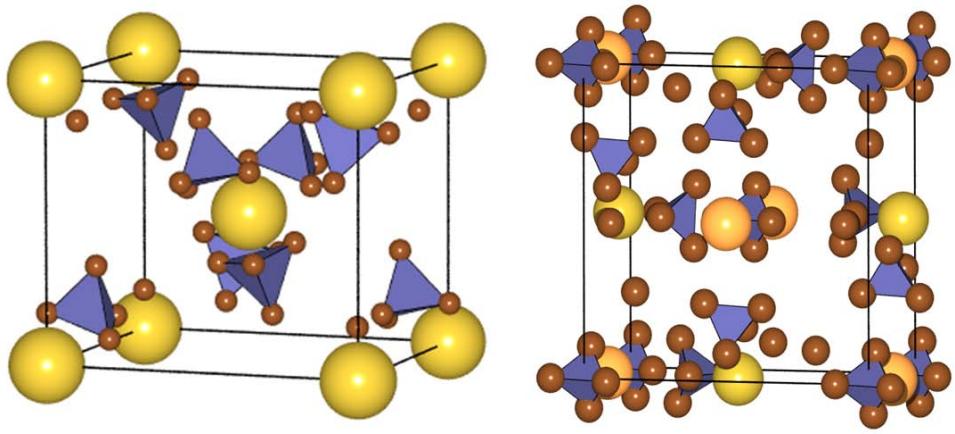

(a) $Si(BH_4)_4$ (b) $NaSi(BH_4)_5$

FIGURE 1. Ground state structures of (a) $Si(BH_4)_4$ and (b) $NaSi(BH_4)_5$ calculated by prototype electrostatic ground state method. The yellow, orange, and brown spheres represent silicon, sodium, and hydrogen, respectively. The hydrogen tetrahedras (lilac) are centered by boron atoms.

TABLE 2. Formation Energies of Si-Based Hypersalt Structures Calculated via DFT Indicate That Stability Increases with Increasing Cation Size

Compound	Formation Energy $\Delta E_f°$ [kJ/mol]
$Si(BH_4)_4$	↓ Increasing Stability
$LiSi(BH_4)_5$	
$NaSi(BH_4)_5$	
$KSi(BH_4)_5$	

indicate that silicon-borohydrides hypersalts are increasingly stabilized with increasing the size of the cation.

Future work will focus of identifying stable borohydride hypersalts, and the synthetic attempts will target hypersalts that shows negative formation enthalpies. In the upcoming Phases 1–3 of this project the following tasks will be undertaken.

- Computational screening and synthesis of novel silicon-based borohydrides via hypersalt stabilization
- Screening candidate Si^{4+} and Si^{2+} hypersalt compounds using PEGS
- Synthesis of Si-based borohydrides with monovalent, double-cation monovalent alkali metals or divalent alkaline earth metals
- First principles thermodynamics calculations for graphene/hydride composites
- Synthesis and physiochemical characterization of $LiAlH_4/Mg(BH_4)_2$/ Si-borohydrides-graphene composites
- Nuclear magnetic resonance characterization of Si-based borohydrides and graphene-hydride composites
- Thermal and mechanochemical reversibility of Si-borohydride salts
- Purification and characterization of newly synthesized Si-borohydride salts
- Optimization of kinetics in the Si-borohydride hypersalts synthesized and characterized in Phases 1 and 2
- Computational optimization of kinetics in Si-based borohydride hypersalts
- Optimization of kinetics in graphene/hydride composites

FY 2015 PUBLICATIONS/PRESENTATIONS

1. A poster entitled "High-capacity Hydrogen Storage Materials via Mechanochemistry," was presented during the kick-off meeting at the Annual Merit Review meeting, 2015 in Crystal City, VA.

REFERENCES

1. E. Majzoub & V. Ozolins, Phys. Rev. B, 2008, 77, 104115.

2. L.E. Klebanoff, J.O. Keller, Int. J. Hydrogen Energy 2013, 38, 4533.

3. Y. Nakamori, et al., Phys. Rev. B, 2006, 74, 45126.

IV.C.5 Electrochemical Reversible Formation of α-Alane

Ragaiy Zidan (Primary Contact), Joe Teprovich, Patrick Ward, Scott Greenway
Savannah River National Laboratory
999-2W Room 121
Savannah River Site
Aiken, SC 29808
Phone: (803) 646-8876
Email: ragaiy.zidan@srnl.doe.gov

DOE Manager
Ned Stetson
Phone: (202) 586-9995
Email: Ned.Stetson@ee.doe.gov

Project Start Date: October 1, 2011
Project End Date: Project continuation and direction determined annually by DOE

Overall and Fiscal Year (FY) 2015 Objectives

- Develop methods of α-aluminum hydride (α-alane or α-AlH_3) production and regeneration that lower the cost of α-alane production to less than $10/kg
- Demonstrate and characterize alane production system that lowers the cost of α-alane production with the lowest possible capital and operating costs
- Identify and quantify fundamental properties of α-alane production chemistry and physics that will lead to improved design and modeling of systems for α-alane production and use

Technical Barriers

This project addresses the following technical barriers from the Hydrogen Storage section of the Fuel Cell Technologies Office Multi-Year Research, Development, and Demonstration Plan:

(A) System Weight and Volume

(B) System Cost

(C) Efficiency

(Q) Regeneration Processes

Technical Targets

In this project studies are being conducted to lower cost and improve efficiency of the electrochemical method to form α-AlH_3. This material has the potential to meet long-term and near-term targets for various applications such as portable power [1,2]. The research performed as part of this contract is equally applicable to both areas.

- By 2015, develop and verify a single-use hydrogen storage system for portable power applications achieving 0.7 kWh/kg system (2.0 wt% H_2) and 1.0 kWh/L system (0.03 kg H_2/L) at a cost of $0.09/Wh net ($3/g hydrogen stored)
- By 2020, develop and verify a single-use hydrogen storage system for portable power applications achieving 1.3 kWh/kg system (4.0 wt.% H_2) and 1.7 kWh/L system (0.05 kgH_2/L) at a cost of $0.03/kWh net ($1.0/g hydrogen stored).

FY 2015 Accomplishments

- Developed reverse pulsing technique capable of significant reduction of dendrites formed during the electrochemical generation of α-alane etherate
- Investigated the use of spent α-alane for the production of aluminum electrodes
- Optimized crystallization process to produce pure α-alane with particle sizes >4 µm

✧ ✧ ✧ ✧ ✧

INTRODUCTION

DOE is supporting research to demonstrate viable materials for on-board hydrogen storage. Aluminum hydride (alane - AlH_3), having a gravimetric capacity of 10 wt% and volumetric capacity of 149 g H_2/L and a desorption temperature of ~60–175°C (depending on particle size and the addition of catalysts), has the potential to meet the 2015 and 2020 DOE system-level targets for portable power applications, as well as the requirements for other hydrogen storage applications. The main barrier for using alane as a hydrogen storage material is the high material cost and unfavorable thermodynamics towards (re)hydrogenation. Zidan et al. [3] were the first to show a reversible cycle utilizing electrochemistry and direct hydrogenation, where gram quantities of alane were produced, isolated, and characterized. This regeneration method is based on a complete cycle that uses electrolysis and catalytic hydrogenation of spent Al(s). This cycle avoids the impractical high pressure needed to form α-AlH_3 and the chemical reaction route of α-AlH_3 that leads to the formation of alkali halide salts, such as LiCl or NaCl, that become a thermodynamic sink because of their stability.

During FY 2015, research was continued to demonstrate methods that will improve the generation of alane. This work

was performed in collaboration with Ardica Technologies and focused on increasing the efficiency and reducing the costs of the manufacturing unit operations including the following key steps: (1) electrochemical alane etherate production, (2) crystallization of the alane etherate to α-alane, and (3) stabilization of the α-alane. This research is paving a path forward for the large scale continuous production of lower cost α-alane for portable power and transportation applications.

APPROACH

The electrochemical generation of α-alane has been shown [3,4] to be capable of generating high purity material using methods that can be developed into a fueling cycle for hydrogen vehicles, portable power systems, or other applications. This research has demonstrated methods to enhance the practicality of utilizing the electrochemical method for the large scale production of alane etherate as well as the crystallization of the etherate to stable crystals of α-alane. By reinvestigating the Dow method for alane crystallization, conditions required to produce large crystals of pure α-alane have been determined. The understanding of this process has provided direction to a path utilizing cheaper and less hazardous crystallizing solvents under reasonable conditions. Improvements to the electrochemical cell voltages patterns have also resulted in a method to nearly eliminate the dendrite formation that limits the time for which an electrochemical process can run continuously without interruptions.

RESULTS

The electrochemical generation of alane etherate has been improved by utilization of a reverse pulse technique where the voltage is briefly reversed to reduce Li_3AlH_6 (dendrite material) back into $LiAlH_4$ (electrolyte). While this method reduces the overall amount of time that alane is being produced, the production rates can still be increased due to the ability to have the electrodes in closer proximity without shorting the electrochemical cell. The reserve pulsing timing sequence demonstrating the best results for this particular electrochemical cell and the electrodes are shown in Figure 1. In the figure, dendrites formation, which is a consequence of evaporating solvent, can be observed at the top of the electrode (anode). The dendrites cannot be converted back to $LiAlH_4$ unless they are submerged in the solvent. This effect can easily be accounted for by insulating the electrode at the surface of the electrolyte solution.

The use of spent alane in electrode production was also investigated. It was found that spent alane pellets pressed at 4 tons could be used as electrodes, but did not perform as well as commercial aluminum electrodes. Scanning electrode microscopy (SEM) images revealed that this was controlled by the contact resistance between the particles within the

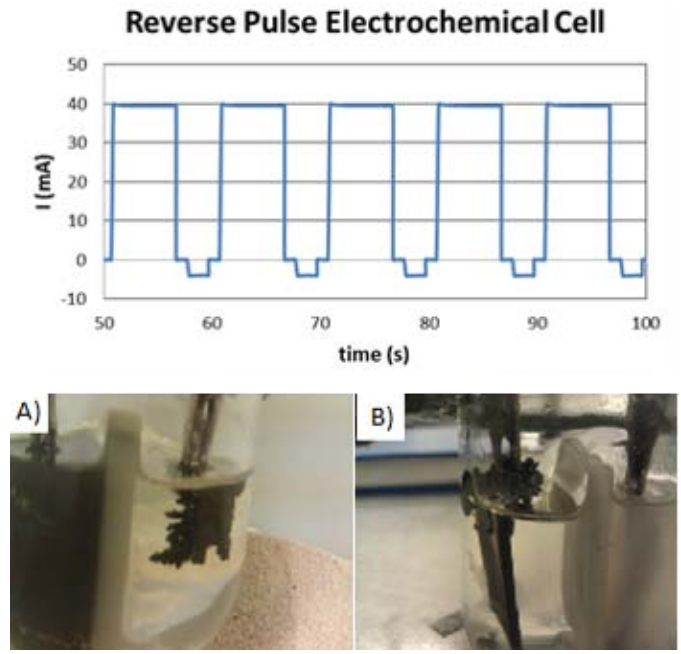

FIGURE 1. Plot of the current vs. time for the reverse pulsing technique used for dendrite formation reduction: (A) anode without reverse pulsing technique and (B) anode with reverse pulsing technique

pressed pellets. This hypothesis was evidenced by charging observed in cracks and certain regions of the pellets as shown in Figure 2. Furthermore, the spent alane pellets were brittle compared to the malleable commercial aluminum electrodes. SEM images of the inside of a spent alane pellet displayed an array of particles sandwiched together that cause the higher electrical resistance observed and the brittle nature of the pellets. Our observations conclude that spent alane pellets may be used as electrode, but optimal electrode design would require pressing pellets and much higher pressures or melting the spent alane to produce aluminum electrodes.

In order to produce stable, high-capacity α-alane, crystallization techniques based on the Dow method were explored. The most significant parameters for crystallization were determined to be solvent removal rate, temperature, and time. These parameters must be meticulously controlled to achieve pure α-alane with particle sizes above 4 μm. Of those factors the ether removal rate was determined to be the most influential for α-alane phase formation. Figure 3 displays the X-ray diffraction (XRD) patterns and SEM images for two crystallizations that were carried out under the same conditions with the exception of ether removal rate. Figures 3B and 3D show that alpha prime is primarily formed when the rate of ether removal is very slow. Figures 3A and 3C show that pure α-alane can be formed when the rate of ether removal is higher; however, the optimum rate of ether removal is highly dependent on thermal control and crystallizer vessel design and is currently a point of emphasis for our studies. Thermogravimetric analysis/

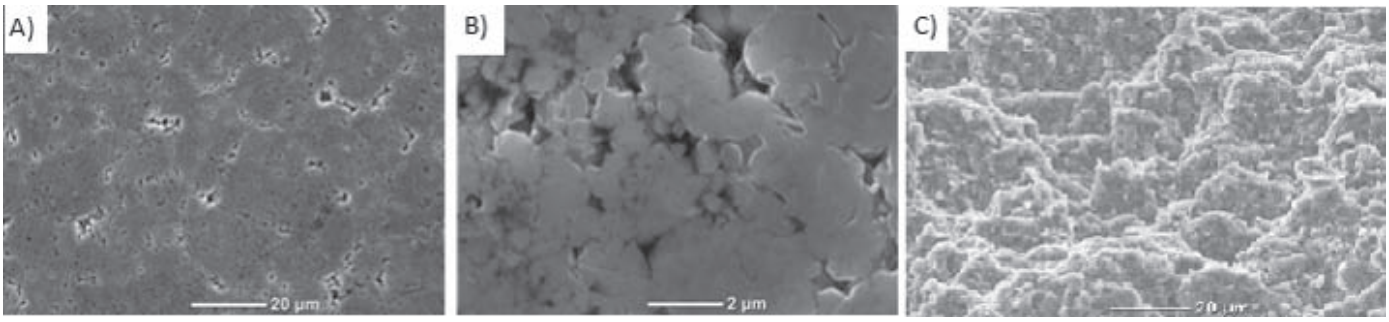

FIGURE 2. (A) SEM image of the surface of a spent alane pellet pressed at 4 tons, (B) increased magnification of the same spent alane pellet, and (C) SEM image of the inside of a broken spent alane pellet

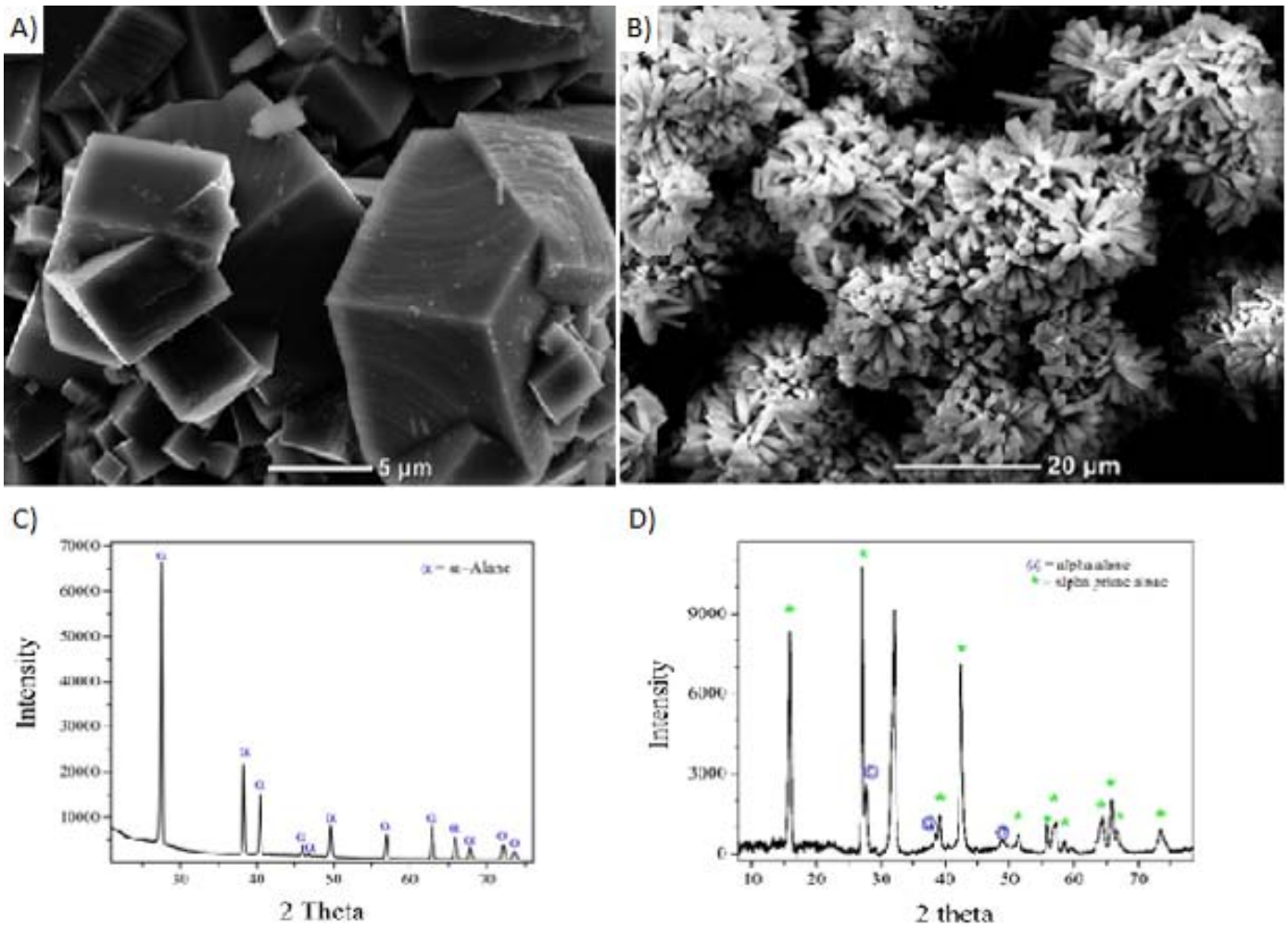

FIGURE 3. (A) SEM image of alpha-alane crystals, (B) SEM image of alpha prime crystals, (C) XRD pattern of pure alpha alane, and D) XRD pattern of alpha prime alane with trace alpha alane

residual gas analysis (TGA/RGA) results (Figure 4) from the pure α-alane show that this material contains >9 wt% H_2. Also, XRD results confirm the absence of any aluminum in the final product. Altogether, this work provides important information required for the production of stable α-alane.

CONCLUSIONS AND FUTURE DIRECTIONS

The following conclusions were drawn:

- Further work on the crystallization is required to make large-scale, continuous production practical.

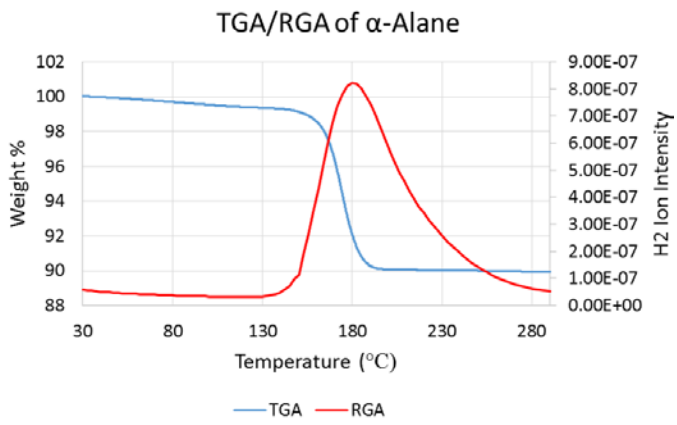

FIGURE 4. TGA/RGA of α-alane displaying >9 wt% H_2

- Increasing the current of the electrochemical cell is one of the last critical issues related to alane adduction production.

Future work includes the following:

- Investigate additives and other solvents that may increase the conductivity of the electrochemical cell for increasing alane adduct production rates.
- Develop recycling techniques for the crystallization process including the use of removed ether for the final product wash and the recovery of toluene, $LiBH_4$, and $LiAlH_4$ for subsequent crystallizations.
- Investigate alternative crystallization pathways that may be suitable for the crystallization of other adducts of alane.
- Develop ambient pressure toluene crystallization technique to reduce the overall cost of alane crystallization.

SPECIAL RECOGNITIONS & AWARDS/ PATENTS ISSUED

1. Ragaiy Zidan, Douglas A. Knight, Long V. Dinh; Novel Methods for Synthesizing Alane without the Formation of Adducts and Free of Halides US20120141363 February 2013.

2. Ragaiy Zidan; Electrochemical Process and Production of Novel Complex Hydrides US8,470,156B2 June 2013.

FY 2015 PUBLICATIONS/PRESENTATIONS

1. Patrick Ward, Joseph Teprovich, Scott Greenway, Ragaiy Zidan. Current Progress in the Low-cost Production of Alane. Gordon Research Conference Metal-Hydrogen Systems. July 2015.

2. Ragaiy Zidan (PI), Joseph Teprovich, Patrick Ward, Ted Motyka, Scott McWhorter, Scott Greenway, Héctor R. Colón-Mercado. Tech to Market Presentation 2015.

3. Ragaiy Zidan. Reversible Formation of Alane. Department of Energy Annual Merit Review 2015.

REFERENCES

1. Teprovich, J.A., T. Motyka, and R. Zidan, International Journal of Hydrogen Energy, 2012. **37**(2): p. 1594–1603.

2. Graetz, J. and J.J. Reilly, J. Phys. Chem. B, 2005. **109**(47): p. 22181–22185.

3. Zidan, R., et al., Chemical Communications, 2009(25): p. 3717–3719.

4. Martinez-Rodriguez, M.J., et al., Appl. Phys. A-Mater. Sci. Process., 2012. **106**(3): p. 545–550.

IV.C.6 Low-Cost α-Alane for Hydrogen Storage

Richard Martin
Ardica Technologies, Inc.
2325 3rd Street, Suite 424
San Francisco, CA 94107
Phone: (412) 445-8612
Email: dmartin@ardica.com

DOE Manager
Katie Randolph
Phone: (720) 356-1759
Email: Katie.Randolph@ee.doe.gov

Contract Number: DE-EE0006629

Subcontractor
SRI International, Menlo Park, CA

Project Start Date: July 15, 2014
Project End Date: July 14, 2017

Overall Objectives

The overall objective of this project is to reduce the production cost of α-alane (AlH_3) to meet the DOE 2015 and 2020 hydrogen storage system cost targets for portable low and medium power applications. This will enable broader applications in consumer electronics (smart phones, tablets, laptops…), back-up power, unmanned aerial vehicles, forklifts, and vehicles.

Fiscal Year (FY) 2015 Objectives

- Complete preliminary process and economic models
- Develop baseline performance of electrochemical process
- Set up fluidized bed reactor and establish test operations

Technical Barriers

This project addresses the following technical barriers from the Hydrogen Storage section of the Fuel Cell Technologies Office Multi-Year Research, Development, and Demonstration Plan:

(A) System Weight and Volume

(B) System Cost

(C) Efficiency

(J) Thermal Management

(K) System Life-Cycle Assessments

(Q) Regeneration Processes

Technical Targets

The objective of this project is to reduce the production cost of α-alane by developing, demonstrating, and performing an economic analysis of an electrochemical process to synthesize α-alane. The reduced production cost will enable alane-based hydrogen storage to achieve the DOE portable power cost target of <$1/g H_2 stored.

FY 2015 Accomplishments

- Preliminary process and economic models were developed for the electrochemical route for the synthesis of α-alane.
- Evaluation of the electrochemical cell reported by Zidan et al. [1], for the electrochemical synthesis of α-alane.
- Candidate materials for the anodic current collector and current collector designs were evaluated. Stainless steel was determined to be the most optimal of the materials tested.
- Particles of aluminum of various sizes were evaluated in the anodic compartment. The consumption of the particles to produce alane was verified. Cell current and resistance were comparable to that observed for a slab aluminum electrode.
- Alane production was verified by the isolation of N-ethylmorpholine and triethylene diamine alane adducts from the electrochemical cell.
- Strategies were developed to mitigate the cathodic production of dendritic material (Li_3AlH_6 + Al).
- Preliminary design of a fluidized bed was developed.

✧ ✧ ✧ ✧ ✧

INTRODUCTION

This project is developing improvements to the Savannah River National Laboratory (SRNL) lab-scale electrochemical synthesis of alane and Ardica-SRI chemical downstream processes that are necessary to meet DOE cost metrics and transition alane synthesis to large scale production. These modifications are focused on critical cost-saving design improvements to the electrochemical cell.

The use of a fluidized bed reactor will replace the sheet aluminum electrodes of the current SRNL process with a bed of conductive aluminum particles maintained in a state

of agitation by a flowing electrolyte and/or a fluidizing gas. Electrical contact with these particles is maintained through a sheet current collector, and the high surface area of these particles will ensure efficiency of reaction. In our approach, spent alane particles can be provided directly to the reactor. This avoids the costs required to convert spent alane into sheet or rod form for use in other electrochemical reactor designs or the need for costly disposal.

APPROACH

To develop synthesis technology to reduce the cost of α-alane to <$4/kg, the approach is to transition a bench-scale electrochemical route to alane to an electrochemical process that will be more conducive and economical for large scale alane production (Figure 1). Specifically, we propose a process that uses spent fuel as a starting material in a continuous synthesis/regeneration of alane from less costly elemental aluminum and hydrogen. This technique could greatly reduce fuel costs and accelerate the commercial acceptance of alane-based fuel cell technology. The long-term goal of the project is to reduce the cost of the initial alane charge to $4/kg and the recycling cost to $2/kg. This reduction in fuel costs translates to storage system costs of <$1 per g H_2, achieving the DOE hydrogen storage system metrics for 2015 and 2020.

RESULTS

- Preliminary process and economic models were completed. The alane production cost is estimated to be <$250/kg alane. The economic model shows an estimated storage system cost of <$6.7/g H_2 for medium power applications (Table 1).
- A baseline was determined for performance of the electrochemical process. The performance of the electrochemical cell is such that sufficient alane is produced from aluminum rather than $NaAlH_4$ to meet the cost target in Task 1.1.
- A fluidized bed reactor was set up and is operational (Figure 2). When a sheet aluminum anode is replaced with a fluidized particulate aluminum anode, the increase in cell resistance is to be not more than twice the value of the sheet electrode (Figure 3).
- The identification of process unit operations was included in the Phase 1 process design and economic analysis. The alane product is an amine adduct of alane from the non-fluidized cell.
- The economic model shows an estimated storage system cost of <$3.3/g H_2 for medium power applications.

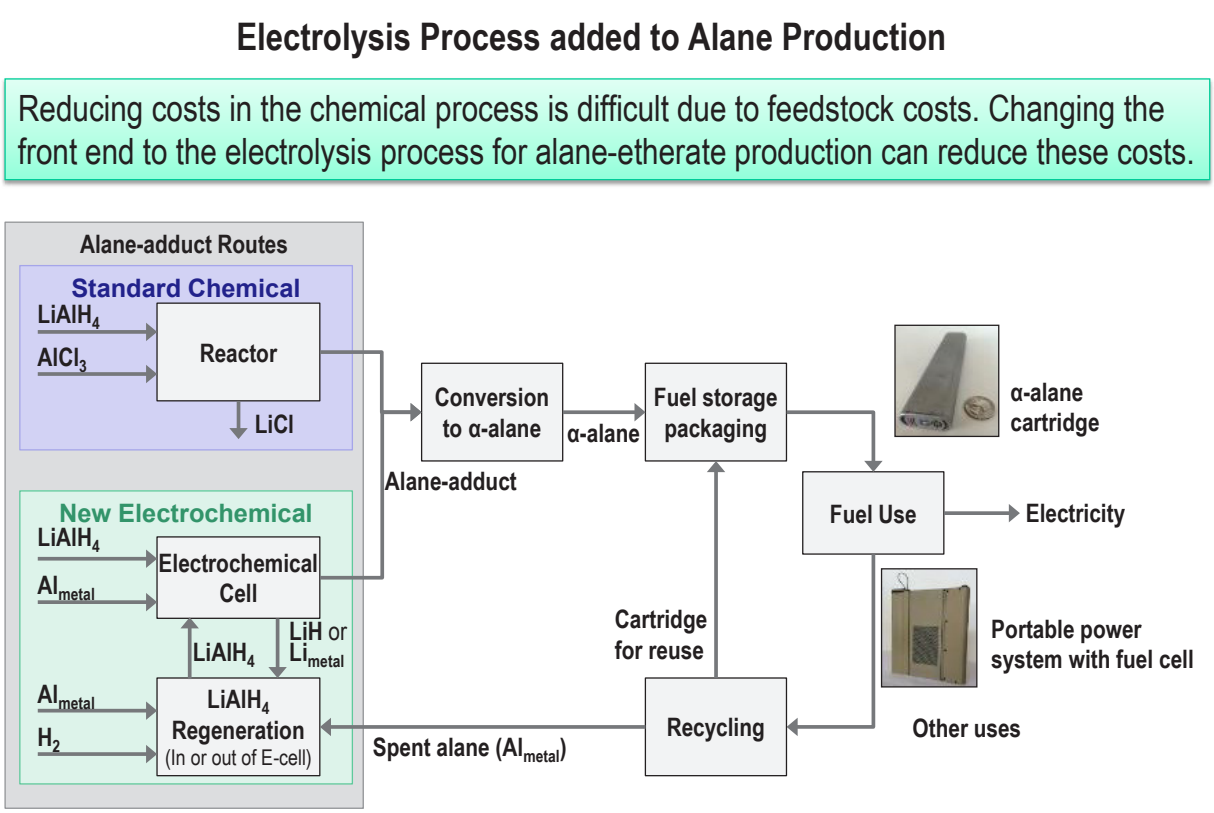

FIGURE 1. Electrolysis process added to alane production

TABLE 1. Progress towards Meeting Technical Targets for Hydrogen Storage
Note: Chemical and electrochemical route productions costs are for a 320 Mton/yr process.

Storage System Costs			Current Cost	Chemical Route	Electrochemical Route: Improved Anode	Electrochemical Route: Cathode Recycle	Electrochemical Route: Optimized Process
			Pilot Plant	Commercial Scale	(20% AlH_3 from Al)	(25% AlH_3 from Al, $LiAlH_4$ regenerated)	(25% from Al, $LiAlH_4$ recycle/ regeneration)
Fuel		$/kg alane	3,500	112	87	55	34
Cartridge components		$/kg alane	79	79	79	79	79
Total		$/kg alane	3,579	191	166	134	113
Storage System Cost		$/g H_2	40	2.15	1.87	1.51	1.27
DOE Metrics		$/g H_2		Target Met?			
Low Power	2015	3	N	Y	Y	Y	Y
	2020	1	N	N	N	N	N
Medium Power	2015	6.7	N	Y	Y	Y	Y
	2020	3.3	N	N	N	Y	Y

Aluminum Particle Fluidized Bed

Background

$$3\ LiAlH_4 + Al_{metal} \rightarrow 4\ AlH_3 + 3\ Li^+ + 3\ e^-$$

(Anode reaction)

- Electrochemical process developed by Ragaiy Zidan at SRNL
- Uses $NaAlH_4$ or $LiAlH_4$ electrolyte, Pt cathode, and Al anode

Proposed Fluidized Bed Reactor

- Fluidized bed of conductive particles act as electrodes, ideally both anode and cathode
- High surface to volume enhance kinetics enabling high current and throughput. Potential for continuous process.
- Direct regeneration of spent alane fuel now feasible

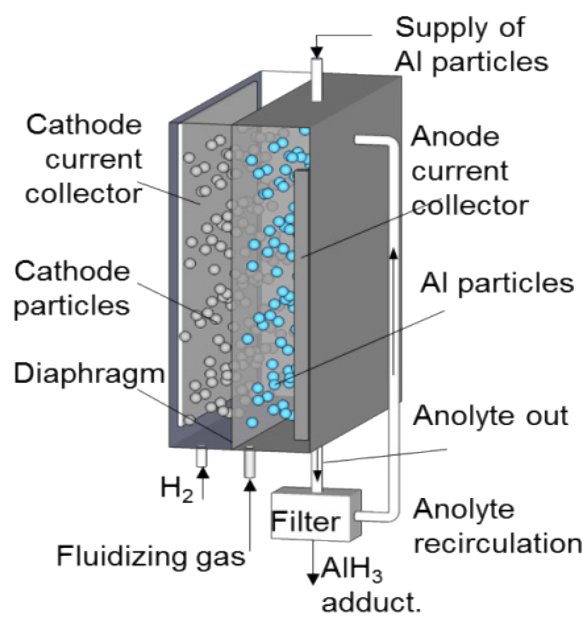

FIGURE 2. Aluminum particle fluidized bed

- We demonstrated a gravimetric capacity of >0.7 kWh/kg and a volumetric capacity of >1.0 kWh/L, achieving the 2015 performance metrics.

CONCLUSIONS AND FUTURE DIRECTIONS

- The project will construct a fluidized or moving bed for the anode that optimizes electrode kinetics, enables high-current, and hence high-throughput, operation. (2015–2017)
- A cathode compartment based on lithium battery technology that prevents dendritic (Li_3AlH_6 + Al) material at the cathode will be constructed, which directly addresses conservation of $MAlH_4$ (M= Li or Na) and reduces cost. (2016–2017)

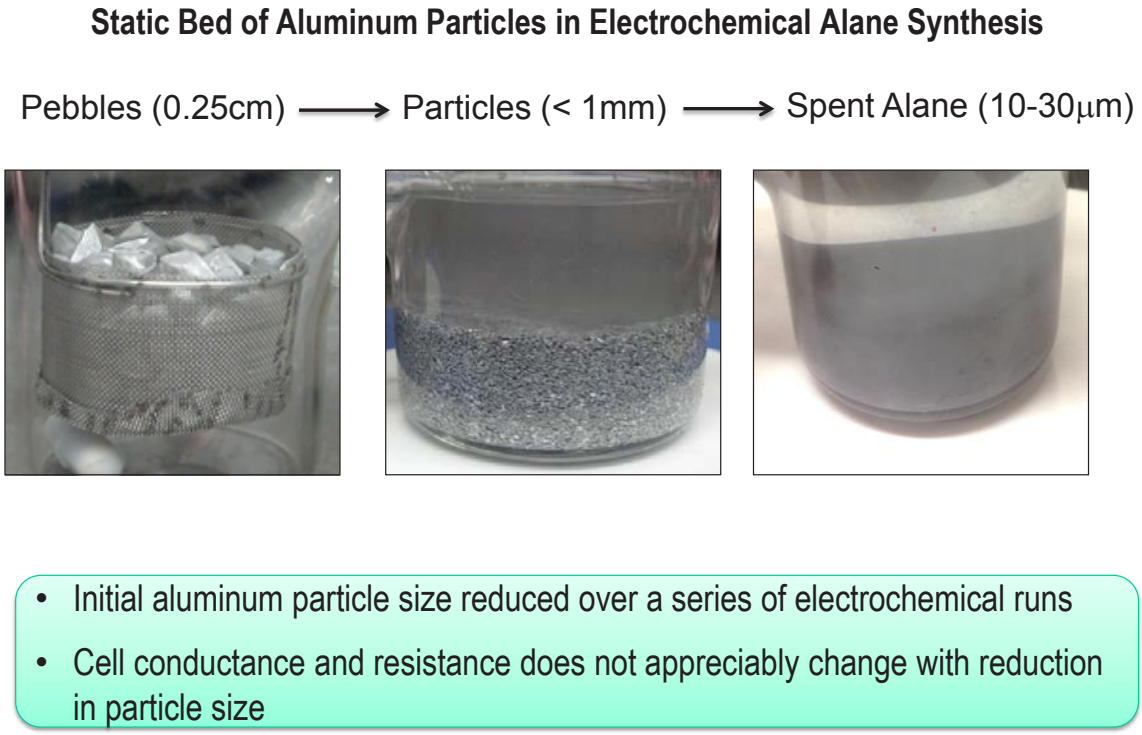

FIGURE 3. Static bed of aluminum particles in electrochemical alane synthesis

- Electrolytes compatible with the deposition of lithium or lithium hydride in the cathodic cell compartment will be optimized. A structural membrane permeable to lithium ion and impermeable to tetrahydroaluminate will be implemented. (2015–2016)
- The project will optimize deposition of lithium or sodium or metal hydrides at high activity and yield for further reaction and regeneration of lithium or sodium aluminum hydride. Cathodic bed particles for deposition of these materials will be fluidized. (2016–2017)
- Conductivity of $LiAlH_4$/ether electrolyte will be improved to enhance electrical energy efficiency of alane production. Additives and supporting electrolytes will be utilized. (2015–2017)
- The project will optimize the process for complete separation of alane adduct from the concentrated electrolyte and optimize thermal conversion to α-alane. (2015–2017)

SPECIAL RECOGNITIONS & AWARDS/ PATENTS ISSUED

1. Mark Petrie was recognized by SRI International for his work on alane and other energetics by selection as an SEI Fellow.

REFERENCES

1. Zidan, R., et al., Electrochemical reversible formation of alane, DOE FY 2013 Annual Progress Report (2013).

IV.C.7 Novel Carbon(C)-Boron(B)-Nitrogen(N)-Containing H_2 Storage Materials

Shih-Yuan Liu (Primary Contact), Frank Tsung
Boston College
Department of Chemistry
2609 Beacon Street
Chestnut Hill, MA 02467
Phone: (617) 552-8543
Email: shihyuan.liu@bc.edu

Tom Autrey, Abhi Karkamkar, Mark Bowden, Sean Whittemore, Kriston Brooks
Pacific Northwest National Laboratory, Richland, WA

David Dixon
The University of Alabama, Tuscaloosa, AL

Paul Osenar, Jim Sisco
Protonex Technology Corporation, Southborough, MA

DOE Manager
Grace Ordaz
Phone: (202) 586-8350
Email: Grace.Ordaz@ee.doe.gov

Contract Number: DE-EE0005658

Project Start Date: March 5, 2012
Project End Date: August 14, 2015

Overall Objectives

- Develop new carbon-boron-nitrogen (CBN)-based chemical hydrogen storage materials that have the potential to meet the DOE technical targets for vehicular and non-automotive applications

Fiscal Year (FY) 2015 Objectives

- Synthesize a liquid CBN hydrogen storage material with thermal stability that satisfies DOE specifications (no spontaneous decomposition below 60°C)
- Develop a catalytic system for H_2 release from the carbonaceous component of CBN materials
- Continue computational and experimental studies of the mechanism of H_2 release from CBN materials

Technical Barriers

This project addresses the following technical barriers from the Hydrogen Storage section of the Fuel Cell Technologies Office Multi-Year Research, Development, and Demonstration Plan:

(A) System Weight and Volume

(C) Efficiency

(E) Charging/Discharging Rates

Technical Targets

This project is developing and characterizing new CBN materials for hydrogen storage. Insights gained from these studies will be applied toward the design and synthesis of hydrogen storage materials that meet the following DOE 2020 hydrogen storage system targets:

- Specific energy: 1.8 kWh/kg (5.5 wt%)
- Energy density: 1.3 kWh/L (4.0 vol%)

FY 2015 Accomplishments

- Measured the kinetics of the release of the first equivalent of H_2 from Compound B using ReactIR; the reaction order, activation energy, pre-exponential factor, and enthalpy and entropy of activation were all experimentally determined to corroborate the results of computational modeling of the BN dehydrogenation process
- Applied density functional theory calculations to develop a mechanism for the initial H_2 release from B consistent with the above kinetic data; such mechanistic understanding will aid in identifying the geometric and electronic elements which govern the thermal stability of CBN materials
- Measured the kinetics of the release of two equivalents of H_2 from Compound J using a gas burette; the activation energy and pre-exponential factor for each loss of H_2 was estimated based on these results and used in subsequent COMSOL modeling (*vide infra*)
- Achieved dehydrogenation from the carbonaceous component of a CBN material using a Pd/C catalyst in a gas flow micro-reactor to facilitate reaction kinetics analysis
- Experimentally determined the activation energy, pre-exponential factor, and enthalpy and entropy of activation for carbonaceous dehydrogenation for comparison with all-carbon analogues and use in COMSOL modeling (*vide infra*)
- Applied combined experimental and computational results for both BN and CC dehydrogenation to modeling a coupled exothermic-endothermic H_2 release system in a theoretical reactor using COMSOL to assess the benefits of such coupling

- Developed new approaches to predict melting points and stabilities (resonance stabilization energies) to more efficiently identify new molecular structures for stable liquid CBN materials

✧ ✧ ✧ ✧ ✧

INTRODUCTION

Approaches to store H_2 in chemical bonds provide a means for attaining high energy densities. Molecular complexes containing protic and hydridic hydrogen such as ammonia borane (AB) provide between 8 wt% to 16 wt% H_2 at acceptable temperatures in a kinetically controlled decomposition. AB shows promise to meet a number of important technological targets such as high volumetric and gravimetric density of H_2, fast kinetics, thermal stability, facile synthesis at large scale and safe handling under atmospheric conditions. Some of the challenges involving AB include volatile impurities (e.g., ammonia, diborane, borazine) and the economics of spent fuel regeneration [1–4].

This project is developing hydrogen storage materials that contain the element carbon in addition to boron and nitrogen. The inclusion of carbon can be advantageous for developing chemical H_2 storage materials that are structurally well defined (thus have good potential to be liquid phase to use current infrastructure), exhibit thermodynamic properties conducive to reversibility, and demonstrate good storage capacities.

APPROACH

This project will develop new CBN H_2 storage materials that have the potential to meet the DOE targets for motive and non-motive applications. Specifically, we will be focusing on three basic systems (1) liquid phase systems that release H_2 in a well defined and high yield fashion, minimizing the formation of NH_3 and $B_3N_3H_6$; (2) reversible storage systems that could potentially be regenerated onboard; and (3) high H_2-content storage systems that can be used in slurries and regenerated off-board (Figure 1). Computational chemistry studies will help direct our research. Finally, we will demonstrate the developed material as a fuel in a fuel cell device. These new materials will be prepared and characterized by our interdisciplinary team comprised of Boston College, The University of Alabama, Pacific Northwest National Laboratory, and Protonex Technology Corporation (Southborough, Massachusetts, a small business fuel cell manufacturer).

RESULTS

Mechanistic Studies of Compound B BN-Hydrogen Release

A kinetics analysis of the thermal decomposition of Compound B in tetraglyme was performed using ReactIR. Specifically, the evolution of the first equivalent of H_2 from B was measured by monitoring the disappearance of a peak unique to the starting material at 1,600 cm^{-1}.

The reaction order of the initial loss of H_2 from B was determined by the initial rates method; by varying the initial concentration of B between 0.56 M and 1.28 M, the

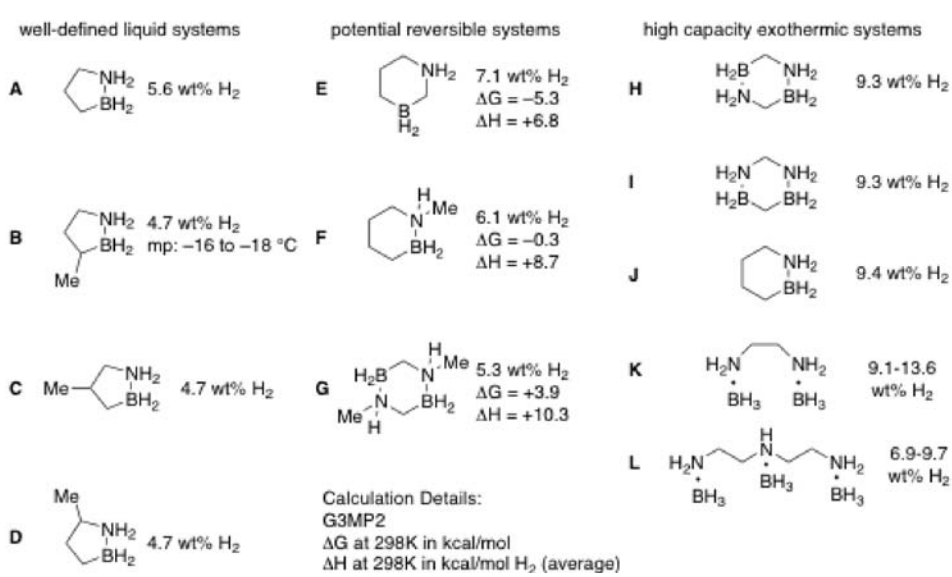

FIGURE 1. Selected synthetic targets and their potential storage capacities and predicted thermodynamic parameters

reaction was found to be second order in B. The temperature of the reaction was also varied between 100°C and 160°C to perform Arrhenius and Eyring analyses. The former yielded an activation energy (E_a) of 15.7 kcal-mol^{-1} and a pre-exponential factor (A) of 4.98 x 10^5 M^{-1}-s^{-1}, while the latter revealed an enthalpy of activation ($\Delta H^{\ddagger}$) of +14.9 kcal-mol^{-1} and an entropy of activation ($\Delta S^{\ddagger}$) of –35.0 cal-mol^{-1}-K^{-1}.

The mechanism of the thermal decomposition of B was also explored computationally at the B3LYP/DZVP2 level of density functional theory followed by higher level correlated molecular orbital theory calculations. To simplify the calculations, the de-methyl form of B, i.e., Compound A, was used for the actual modeling. Evidence of a bimolecular process (*vide supra*) directed investigation toward a system involving two molecules of A wherein one is ring-opened (A') through heterolytic dissociation of the B–N bond (Figure 2). Interaction between the BH_2 units of A and A' results in formation of a complex (AA') 16.9 kcal-mol^{-1} lower in energy than the separated species. The lowest energy transition state (TS1) for loss of H_2 from AA' involves the BH_2 unit of A transferring a hydride to the BH_2 group of A', while a proton from the NH_2 group of A interacts with another hydride of the A' BH_2 to form H_2. The barrier to this transition state from AA' was calculated as 23.0 kcal-mol^{-1}, significantly less than that required for unimolecular decomposition from the separate species (TSuni, 35.2 kcal-mol^{-1}). These results are highly reminiscent of those previously reported by Dixon for the BH_3-catalyzed decomposition of ammonia borane [5].

Kinetic Studies of Compound J BN-Hydrogen Release

A kinetic analysis of the loss of two equivalents of H_2 from Compound J catalyzed by Pd/C at 80°C, 100°C, and 120°C was performed using a gas burette. The measured rates of H_2 evolution were treated as originating from a pair of first-order reactions occurring in series and were fitted to an appropriate theoretical model. From this model, the activation energy and pre-exponential factor for release of the first and second equivalents of H_2 were estimated as 19.0 kcal-mol^{-1} and 8.04 x 10^8 s^{-1} and 39.7 kcal-mol^{-1} and 3.53 x 10^{19} s^{-1}, respectively.

Dehydrogenation of the Carbonaceous Component of a BN-Heterocycle

The acceptorless dehydrogenation of the carbonaceous component of a model BN-heterocycle, 1,2-dimethyl-1,2-BN-cyclohexene (X), was achieved using a Pd/C catalyst in a gas-flow micro-reactor. In-line quantitative mass spectrometry showed the reaction proceeded to consistently generate H_2 and the aromatized product X' in a 2:1 ratio, in accordance with the expected stoichiometry for complete CC dehydrogenation (Figure 3). Varying the reaction temperature from 170°C to 190°C enabled Arrhenius and Eyring analyses; for comparison, these analyses were also performed for the dehydrogenation of the related all-carbon species cyclohexene and cyclohexane. As shown in Table 1, the E_a and $\Delta H^{\ddagger}$ values for dehydrogenation of X are similar to those of cyclohexene,

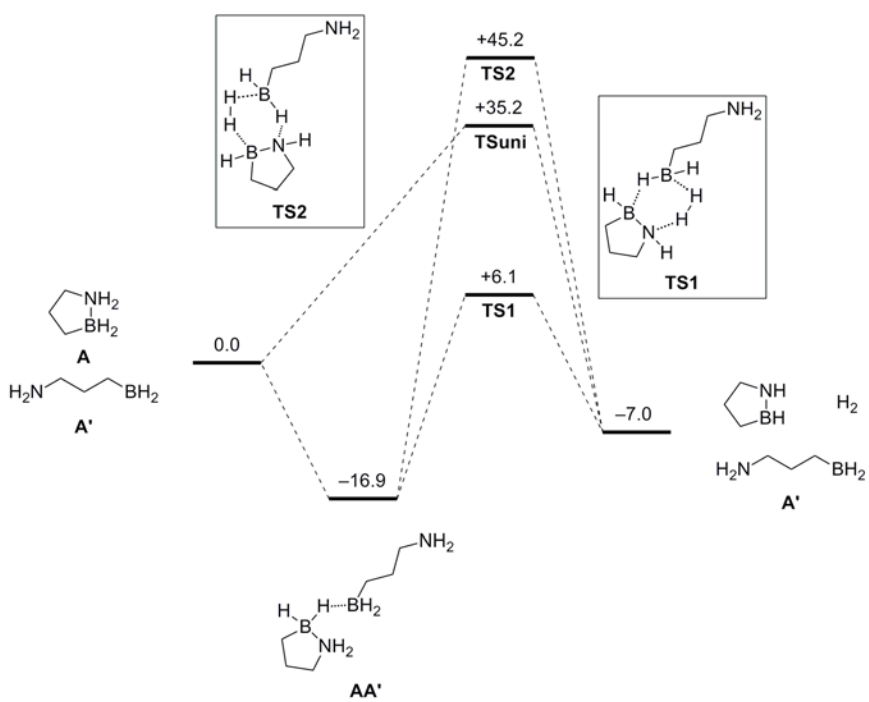

FIGURE 2. Potential energy surface in kcal•mol^{-1} (B3LYP/DZVP2, 298 K) for a bimolecular mechanism of elimination of first equivalent of H_2 from A

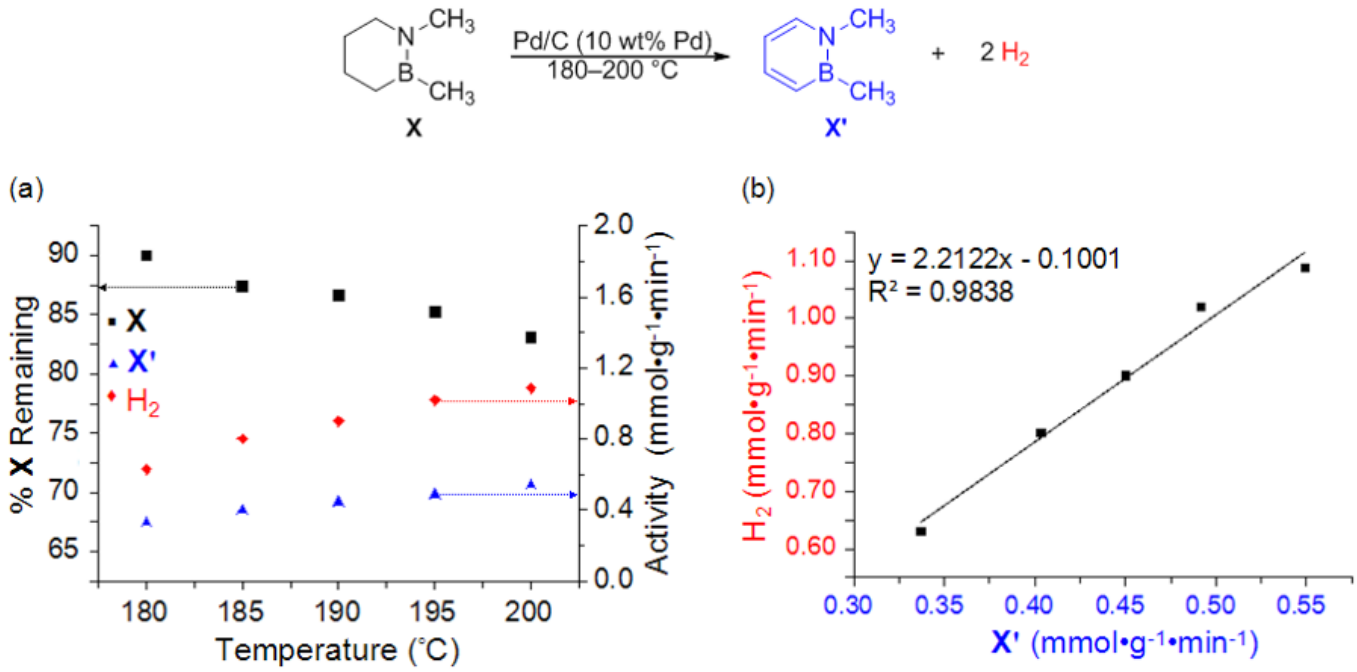

FIGURE 3. (a) Percent unreacted X (left) and rates of H_2 and X' formation normalized by mass catalyst (right); (b) comparison of H_2 and X' evolution rates

TABLE 1. Measured Activation Parameters for Dehydrogenation of X, Cyclohexane, and Cyclohexene

Reaction[a]	E_a (kcal mol^{-1})	$\log_{10}(A)$	$\Delta H^{\ddagger}$ (kcal mol^{-1})	$\Delta S^{\ddagger}$ (cal mol^{-1} K^{-1})
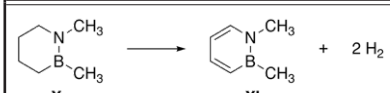	+10.3±0.3	2.2±0.2	+9.4±0.3	–51.6±1.0
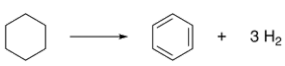	+12.9±0.1	3.1±0.4	+12.0±0.1	–47.0±1.8
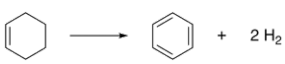	+10.9±0.2	5.6±0.2	+10.2±0.2	–35.5±1.0

[a] Conditions: 50 mL/min Ar carrier gas, 10 wt% Pd/C; substrate injection rates (mmol-s^{-1}): X (1.04×10^{-4}), cyclohexane (1.03×10^{-4}), cyclohexene (1.10×10^{-4}); hydrogen evolution rates measured at 5°C increments over temperature range indicated: X (170–190°C), cyclohexane (170–190°C), cyclohexene (70–110°C). All reactions repeated in triplicate.

and lower than those of cyclohexane by approximately 2.6 kcal-mol^{-1}. Conversely,the pre-exponential factor ($\log_{10}(A)$) for X is lower than that of either cyclohexene or cyclohexane and the $\Delta S^{\ddagger}$ value is also more negative; this is indicative of a more entropically demanding rate-determining step for the dehydrogenation of X compared to that of the all-carbon compounds.

Modeling Coupled Exothermic-Endothermic Hydrogen Release

The experimentally derived kinetic parameters for BN dehydrogenation of J and CC dehydrogenation of X (*vide supra*) were combined with computationally derived enthalpies of reaction for both processes to facilitate COMSOL Multiphysics® modeling of potentially coupled exothermic-endothermic H_2 release from a single CBN material (Figure 4). The reaction was modeled in the liquid phase in a plug flow reactor and accounted for heat and mass transfer with both axial and radial heat conductance. As shown in Table 2, the model predicted that maximum conversion resulting from BN (100%) and CC (39%) dehydrogenation occurred within the first 4% of the length of the reactor. Additionally, in the absence of endothermic CC dehydrogenation, the maximum reactor temperature was significantly higher than in the combined exothermic-endothermic case (364°C vs. 292°C,

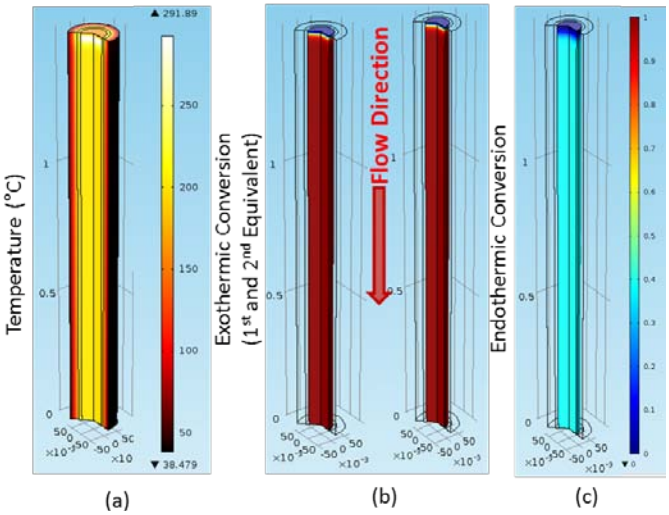

FIGURE 4. Temperature (a), exothermic reaction conversion (b), and endothermic reaction conversion (c) estimates from the COMSOL model for the coupled exothermic-endothermic dehydrogenation of a single CBN material

TABLE 2. Modeling Results of Thermodynamically Coupled Reactions of a Single CBN Material

Active Reactions	Exothermic Conversion	Endothermic Conversion	Maximum Reactor Temperature
Exothermic and Endothermic	100%	39%	292°C
Exothermic only	100%	–	364°C
Endothermic only	–	5.6%	160°C
Exothermic and Endothermic w/o equilibrium constraints	100%	74%	292°C

respectively). Conversely, in the absence of exothermic BN dehydrogenation, the maximum reactor temperature was significantly lower (160°C), and also conversion from CC dehydrogenation was greatly reduced (5.6%). By eliminating the equilibrium constraints of the reversible CC dehydrogenation reaction, the endothermic conversion can be nearly doubled in the coupled reactions. This result indicates that most of the limitations of reaction coupling of these materials result from the reaction equilibrium rather than balancing the reaction heat and kinetics.

CONCLUSIONS

This year we performed kinetics analyses of the initial H_2 release from B, the release of two equivalents H_2 from J, and the dehydrogenation of the carbonaceous component of X. The results obtained from the study of B aided in the development of a plausible mechanism for the reaction using electronic structure calculations. The kinetic parameters determined for J and X were used in the COMSOL modeling of coupled exothermic-endothermic H_2 release from a single CBN material. The end of FY 2015 marks the conclusion of this project.

FY 2015 PUBLICATIONS/PRESENTATIONS

1. G. Chen, L.N. Zakharov, M.E. Bowden, A.J. Karkamkar, S.M. Whittemore, E.B. Garner III, T.C. Mikulas, D.A. Dixon, T. Autrey, S-Y. Liu. "Bis-BN Cyclohexane: A Remarkably Kinetically Stable Chemical Hydrogen Storage Material," *J. Am. Chem. Soc.* **2015,** *137,* 134.

2. S.G. Kukolich, M. Sun, A.M. Daly, W. Luo, L.N. Zacharov, S.-Y. Liu. "Identification and Characterization of 1,2-BN Cyclohexene Using Microwave Spectroscopy," *Chem. Phys. Lett.* **2015**, *639*, 88–92.

3. "Novel Carbon(C)-Boron(B)-Nitrogen(N)-Containing H_2 Storage Materials," Washington DC, DOE Annual Merit Review, June 10, 2015.

4. Mark Bowden, Tom Autrey, Shih-Yuan Liu, Sean Whittemore, Kriston Brooks, "Liquid Carbon-Boron-Nitrogen (CBN) Hydrogen Storage Materials," presented at the January 2015 Expert Meeting of Task 32 IEA Hydrogen Implementation Agreement, January 18–22, 2015, Chamonix, France.

REFERENCES

1. S. McWhorter, C. Read, G. Ordaz, N. Stetson. "Materials-Based Hydrogen Storage: Attributes for Near-Term, Early Market PEM Fuel Cells," *Current Opin. Sol. State Mat. Sci.* **2011**, *15*, 29.

2. A. Staubitz, A.P. Robertson, I. Manners. "Ammonia-borane and related compounds as dihydrogen sources," *Chem. Rev.* **2010**, *110*, 4079.

3. C.L. Aardahl, D. Rassat. "Overview of systems considerations for on-board chemical hydrogen storage," *Int. J. Hydrogen Energy* **2009**, *34*, 6676.

4. A.D. Sutton, A.K. Burrell, D.A. Dixon, E.B. Garner III, J.C. Gordon, T. Nakagawa, K.C. Ott, J.P. Robinson, M. Vasiliu. "Regeneration of Ammonia Borane Spent Fuel by Direct Reaction with Hydrazine and Liquid Ammonia," *Science* **2011**, *331*, 1426.

5. M.T. Nguyen, V.S. Nguyen, M.H. Matus, G. Gopakumar, D.A. Dixon. "Molecular Mechanism for H_2 Release from BH_3NH_3, Including the Catalytic Role of the Lewis Acid BH_3," *J. Phys. Chem. A* **2007**, *111*, 679.

IV.C.8 Boron-Based Hydrogen Storage: Ternary Borides and Beyond

John J. Vajo (Primary Contact), Jason Graetz, Vitalie Stavila, Lennie Klebanoff, Eric Majzoub
HRL Laboratories, LLC
3011 Malibu Canyon Road
Malibu, CA 90265
Phone: (310) 317-5745
Email: jjvajo@hrl.com

DOE Manager
Katie Randolph
Phone: (720) 356-1759
Email: Katie.Randolph@ee.doe.gov

Contract Number: DE-EE0006630

Subcontractors
- Sandia National Laboratories, Livermore, CA
- University of Missouri, St. Louis, MO

Project Start Date: August 1, 2014
Project End Date: January 31, 2016

Overall Objectives

Improve the hydrogen cycling kinetics of high capacity boron-based hydrogen storage materials

- Eliminating multiple-phase reaction barriers using ternary borides and mixed-metal borohydrides that maintain single phases during cycling
- Minimizing boron atom rearrangement using borane substrates that cycle hydrogen by reacting with lithium hydride while preserving the boron-boron bond framework

Fiscal Year (FY) 2015 Objectives

- Synthesize single-phase Mg/transition metal ternary boride and mixed-metal borohydride with potential hydrogen content of 11 wt%
- Demonstrate example of reversible borane/lithium hydride reaction with measureable (>0.1 wt%) hydrogen release
- Calculate stability of Mg-based ternary borides and mixed-metal borohydride with potential hydrogen contents of >10 wt%
- Calculate energetics of Li/H exchange reactions with model borane substrates

Technical Barriers

This project addresses the following technical barriers from the Hydrogen Storage section of the Fuel Cell Technologies Office Multi-Year Research, Development, and Demonstration Plan:

(A) System Weight and Volume

(C) Efficiency

(E) Charging and Discharging Rates

Technical Targets

This project is conducting initial studies of hydrogen storage in ternary borides/mixed-metal borohydrides and lithiated boranes. Results of these studies will be applied toward developing hydrogen storage materials that meet the following DOE hydrogen storage system targets.

- Specific energy: 5.5 wt% H_2
- Energy density: 40 g-H_2 /L

FY 2015 Accomplishments

- Calculation of stable Mg-based ternary borides with Mn, Fe, and Co
- Synthesis of single-phase Mg/Mn (1:1, 3:1, and 9:1) ternary borides
- Demonstration of ~1 wt% H_2 cycling in Mg-Mn ternary boride
- Common scheme synthesis of Mg and Mn borohydrides
- Calculation of Li/H exchange energies and influence of heteroatom dopants
- Formation of polymerized borane BH_x from $B_{10}H_{14}$
- Demonstration of hydrogen evolution from reaction of BH_x with LiH

✧ ✧ ✧ ✧ ✧

INTRODUCTION

Many boron based hydrogen storage materials have been identified with high capacities and thermodynamics that can be tailored. However, the kinetics of hydrogen exchange in these materials are too slow for practical applications. In part, the kinetic limitations originate from the multiple phases that are typically involved and/or from the extensive rearrangement of the boron atom framework over the dehydrogenation/rehydrogenation cycle. To address these

issues, this project is exploring two classes of boron-based hydrogen storage materials. The first is ternary (or possibly higher order) metal borides that reversibly hydrogenate to single-phase mixed-metal borohydrides. By reducing the number of phases to a single dehydrogenated phase (the ternary boride) and a single hydrogenated phase (the mixed-metal borohydride), the kinetic barriers associated with phase nucleation and diffusion of heavy atoms should be minimized thus improving the kinetics. In addition, use of multiple metals of varying electronegativity permits tuning of the exchange thermodynamics. The second class of materials termed "lithiated boranes" reversibly release hydrogen from boranes (B_nH_x) by reaction with LiH to form B_nLi_x while preserving the underlying boron atom framework (B_n). By preserving this framework, the kinetic barriers associated with boron atom rearrangement are avoided. If possible, this reaction would constitute a new class of hydrogen storage materials.

APPROACH

Work in this project involves parallel experimental efforts for both classes of materials approached from the hydrogenated and the dehydrogenated states. Thus, ternary borides will be synthesized from the elements or the corresponding binary borides. After characterization to determine that the desired ternary boride is single-phase and stable, the hydrogenation behavior will be studied. Similarly, from the hydrogenated state, mixed-metal borohydrides will be synthesized directly or from the pure metal borohydrides. Dehydrogenation of these materials will then be studied. For reaction of boranes with lithium hydride, a variety of possible borane substrates will initially be screened. These range from molecular to polymeric and nanoparticle, and extended Li-B alloys representing the dehydrogenated state. Selected boranes will then be mixed with lithium hydride and their hydrogen cycling behavior studied. Together with this experimental effort, a computational effort will guide material choices. Computations will be used to screen the stability of possible ternary borides and mixed-metal borohydrides. Calculations will also be performed to access the energetics of Li/H exchange in reaction of LiH with model borane compounds.

RESULTS

Initial work on the ternary borides began by considering ternary borides of Mg with the first row transition metals (TM). Figure 1 shows predicted reaction energies (ΔE) for the formation of Mg/TM ternary borides with the compositions of $MgTMB_4$ and Mg_2TMB_6, according to the reactions

$$MgB_2 + TMB_2 \rightarrow MgTMB_4$$

and

$$2MgB_2 + TMB_2 \rightarrow Mg_2TMB_6$$

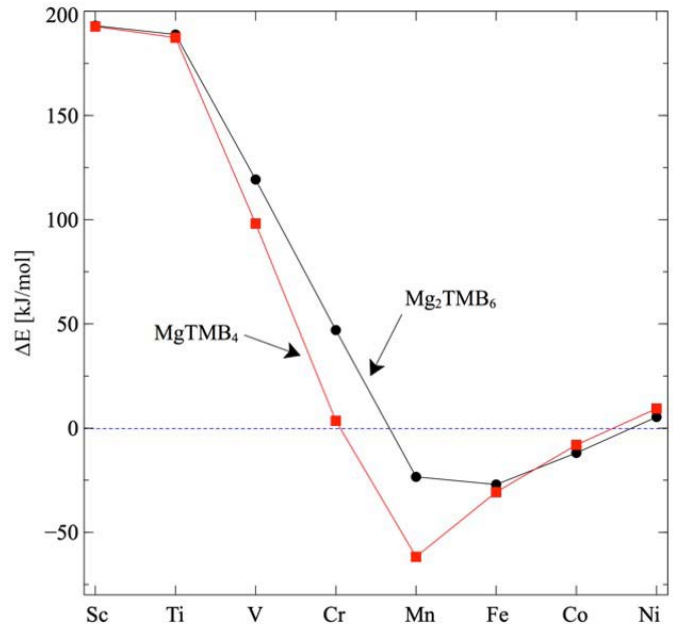

FIGURE 1. Predicted stability of ternary borides. Reaction energies for the formation of $MgTMB_4$ and Mg_2TMB_6 from the binary borides calculated using density functional theory at 0 K including zero point energies (ZPE) with known experimental structures, such as Pbam, as prototypes.

The binary borides TMB_2 do not form for TM = Fe, Co, and Ni. Thus, for these reactions B + TMB was substituted for TMB_2. If fully hydrogenated to the mixed-metal borohydrides, all of these compositions would have capacities of >11 wt% hydrogen enabling meeting the DOE system target. The reaction energy is predicted to be >0 kJ/mol for TM = Sc, Ti, V, indicating that these borides may be unstable and could phase separate into the binary borides during hydrogen cycling. In contrast, for TM = Mn, Fe, and Co, the predicted energy is negative indicating that these compounds are stable. Compositions with Mg:TM ratios of 1:1 are predicted to be more stable than for ratios of 2:1. For TM = Cr and Ni, the predicted energy is approximately thermo-neutral.

Based in part on the calculations described above, synthesis of $Mg_xMn_{1-x}B_2$ for x = 0.5, 0.75, and 0.9 was performed by high-energy mechanical milling of the binary borides, MgB_2 and MnB_2. The results for x = 0.5 (Mg:TM ratio of 1:1) are shown using X-ray diffraction in Figure 2. The diffraction pattern for the milled sample shows the same symmetry as MgB_2 suggesting a single phase was in fact synthesized, exclusive of small peaks associated with a Mn_3B_4 impurity in the MnB_2 starting material. The diffraction angles are intermediate between those for MgB_2 and MnB_2. This also suggests a single phase with an intermediate unit cell size. In addition, energy dispersive X-ray analysis showed a uniform distribution of Mg and Mn.

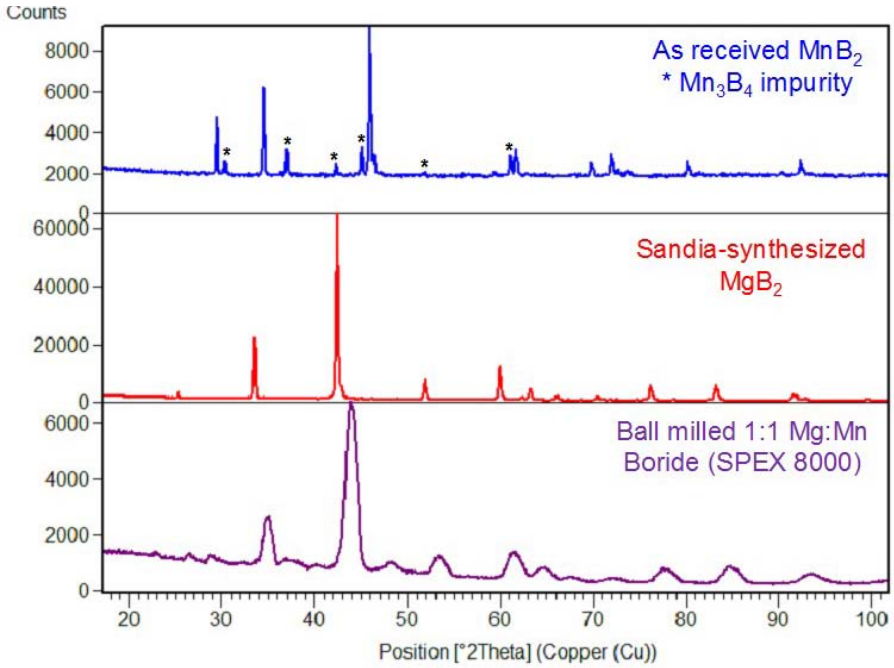

FIGURE 2. Synthesis of $Mg_{0.5}Mn_{0.5}B_2$ ternary boride. (top panel) X-ray diffraction patterns for commercial MnB_2 with Mn_3B_4 impurity; (middle panel) MgB_2 synthesized at Sandia National Laboratories; and (bottom panel) ternary boride from 1:1 mixture of MgB_2 and MnB_2 after mechanical milling (SPEX 8000) for 16 h.

Finally, the peaks are broadened indicating a nanocrystalline phase resulting from the milling.

For a similarly synthesized sample with a composition of $Mg_{0.75}Mn_{0.25}B_2$, the hydrogen cycling behavior was studied. After hydrogenation in 150 bar H_2 at 380°C for 38 h, the uptake was estimated to be 1.2 wt% H_2. Infrared spectroscopy indicated that borohydride anions $[BH_4]^-$ were formed, although the composition of the hydrogenated phase is still being investigated. Following hydrogenation, hydrogen desorption began upon heating to 225°C with 0.8 wt% H_2 desorbed up to 400°C. While this capacity is small, under the same conditions little detectable hydrogen cycling (~0.07 wt%) and borohydride formation occurred for pure MgB_2. This comparison illustrates a beneficial effect of using the ternary borides. In this case the Mn may have acted as a catalyst promoting dissociative hydrogen adsorption.

Reversible reaction of a borane substrate with lithium hydride to evolve hydrogen and form a lithiated borane has not, to our knowledge, been reported. Thus the energetics of such reactions are not known. To assess whether such reactions could have energies suitable for practical hydrogen storage, calculations were performed for Li/H exchange from LiH in a series of small molecular boranes. Initial calculations assumed gas phase boranes for simplicity. The results are shown in Figure 3. The predicted energies are highly endothermic, >100 kJ/mol-H_2. However, the energies decrease drastically with framework size indicating more favorable energies for larger solid polymeric boranes.

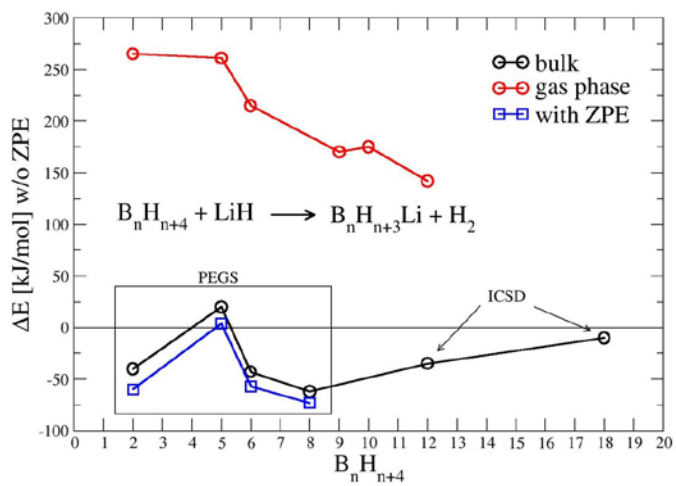

FIGURE 3. Energies for Li/H exchange reactions. Comparison of first principles gas-phase calculations (top circles, red) with bulk density functional theory calculations (bottom circles, black) including ZPE (squares, blue) all at T = 0 K. As indicated, bulk calculations using prototype electrostatic ground state structures for n = 2, 5, 6 and 8 and inorganic crystal structure database structures for n = 12 and 18.

Subsequently, calculations for solid-state clusters of selected boranes were also performed. As also shown in Figure 3, these calculations give much lower predominately exothermic energies that may increase with framework size. As expected, solid-state energies differ significantly from gas-phase

energies for small frameworks. However, they appear to converge for larger frameworks, suggesting an exchange energy of ± 25 kJ/mol-H_2 for boranes B_nH_x with n >20. While this current uncertainly is large, the results suggest that a reversible reaction is feasible. Additional calculations performed have focused on how heteroatom doping, for example with C, N, O, or Cl alters the exchange energy.

Initial experiment work to demonstrate a reversible lithiated borane hydrogen storage reaction utilized commercially available molecular substrates $B_{10}H_{14}$ and $C_2B_{10}H_{12}$. While reactions with LiH were seen, the volatile nature of these substrates made them impractical for hydrogen storage and lab-scale Sieverts apparatus measurements. To eliminate the issue of volatility, $B_{10}H_{14}$ was thermally polymerized by extended (days) heating at temperatures of 200°C to 300°C. The resulting borane was found to have a composition, by both weight loss measurements and neutron prompt gamma ray activation analysis (conducted at the National Institute of Standards and Technology), of BH_x with x = ~0.6 to 0.7. After polymerization the resulting BH_x material was milled with LiH at a B:Li ratio of 1:1. The first cycle dehydrogenation of a sample polymerized at 250°C for 2 days is shown in Figure 4. A small (~0.5 wt%) but significant hydrogen desorption occurs from ~100°C to 200°C. This dehydrogenation appears to be associated with reaction with LiH because a control sample similarly prepared but not milled with LiH showed desorption beginning at higher temperatures with much less hydrogen evolved (~0.1 wt%). Thus far, this hydrogen desorption has not been reversible and differential scanning calorimetry measurements indicated that the reaction is exothermic. At higher temperatures (350°C to 400°C) reversible cycling of ~1 wt% H_2 occurred; however, this hydrogen appeared to be associated with the formation of $LiBH_4$. Study of this reaction is continuing and modified polymerization routes that incorporate heteroatoms are being considered.

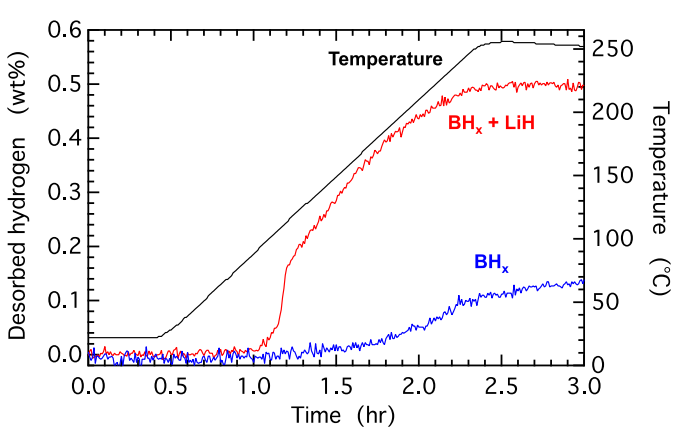

FIGURE 4. Dehydrogenation in polymerized borane/lithium hydride reaction. As labeled: temperature ramp (black) and desorbed hydrogen from polymerized borane BH_x + LiH (red) and polymerized borane BH_x without LiH (blue).

SUMMARY AND FUTURE DIRECTIONS

Stable Mg/TM ternary borides were predicted computationally and a stable single-phase Mg/Mn material was achieved experimentally. The Mg/Mn boride showed significant enhancements for hydrogen uptake (~1 wt% for the conditions of the experiment) and borohydride formation when compared to pure MgB_2. Polymerized $B_{10}H_{14}$ was identified as a nonvolatile substrate for Li/H reaction with LiH. Additives could be incorporated into the boron framework during polymerization enabling versatile modification by heteroatom doping. A low temperature (100°C to 200°C) Li/H exchange (hydrogen evolution) reaction of polymerized borane with LiH was identified, although thus far the reaction was not reversible. Calculations were performed to determine the energetics of exchange. An initial estimate, limited by the complexity of crystalline molecular boranes, of ±25 kJ/mol-H_2 was found indicating that a practical reversible reaction may be possible.

Future work will include:

- Calculations of ternary borides with lower TM ratios in the solid solubility range in order to optimize potential hydrogen capacity.
- Synthesis and characterization of Mg/Fe and Mn/Co ternary borides with a wide range of compositions.
- Synthesis and hydrogen cycling behavior of mixed-metal borohydrides.
- Optimization of borane polymerization to achieve reversible hydrogen cycling with LiH.
- Evaluation of hydrogenated boron nanoparticles for Li/H exchange.
- Refinement of the predicted energies for Li/H exchange.

FY 2015 PUBLICATIONS/PRESENTATIONS

1. "Boron-Based hydrogen Storage: Ternary Borides and Beyond," Presentation to the Hydrogen Storage Tech Team, Southfield, MI, January, 2015.

2. "Boron-Based hydrogen Storage: Ternary Borides and Beyond," Presentation at the Hydrogen Storage PI Meeting, Golden, CO, January, 2015.

3. "Boron-Based hydrogen Storage: Ternary Borides and Beyond," Presentation at the 2015 DOE Fuel Cell Technologies Program Annual Merit review, Crystal City, Virginia, June 2015.

IV.C.9 Improving the Kinetics and Thermodynamics of $Mg(BH_4)_2$ for Hydrogen Storage

Brandon Wood (Primary Contact),
Lennie Klebanoff, Vitalie Stavila, Tae Wook Heo,
Keith Ray, Jonathan Lee, Hui-Chia Yu,
Katsuyo Thornton
Lawrence Livermore National Laboratory (LLNL)
7000 East Ave., L-413
Livermore, CA 94550
Phone: (925) 422-8391
Email: brandonwood@llnl.gov

DOE Manager
Jesse Adams
Phone: (720) 356-1421
Email: Jesse.Adams@ee.doe.gov

Subcontractors
- Sandia National Laboratories, Livermore, CA
- University of Michigan, Ann Arbor, MI

Project Start Date: August 1, 2014
Project End Date: August 31, 2017

Overall Objectives

- Combine theory, synthesis, and characterization across multiple scales to understand the intrinsic kinetic and thermodynamic limitations in $MgB_2/Mg(BH_4)_2$
- Construct and apply a flexible, validated, multiscale theoretical framework for modeling (de)hydrogenation kinetics of the Mg-B-H system and related metal hydrides
- Devise strategies for improving kinetics and thermodynamics through nanostructuring and doping

Fiscal Year (FY) 2015 Objectives

- Synthesize and characterize high-purity MgB_2 and $Mg(BH_4)_2$ materials
- Measure hydrogenation kinetics of bulk MgB_2 and examine phase composition
- Establish and calibrate initial modeling framework and test computational feasibility

Technical Barriers

This project addresses the following technical barriers from the Hydrogen Storage section of the Fuel Cell Technologies Office Multi-Year Research, Development, and Demonstration Plan:

(O) Lack of Understanding of Hydrogen Physisorption and Chemisorption

(A) System Weight and Volume

(E) Charging/Discharging Rates

Technical Targets

This project is conducting fundamental studies of hydrogenation and dehydrogenation of nanoscale $Mg(BH_4)_2$-based materials using a combined theory/experiment approach. Insights will be applied toward the design and synthesis of hydrogen storage materials that meet the following DOE hydrogen storage targets:

- Specific energy: 1.8 kWh/kg
- Energy density: 1.3 kWh/L
- Minimum delivery pressure: 5 bar
- Minimum delivery temperature: 85°C
- System fill time: 1.5 kg H_2/min

FY 2015 Accomplishments

- Synthesized high-purity MgB_2 and $Mg(BH_4)_2$ materials
- Performed measurements of bulk MgB_2 hydrogenation kinetics
- Performed nuclear magnetic resonance (NMR) and X-ray absorption (XAS)/X-ray emission (XES) of pristine and partially hydrogenated bulk MgB_2
- Established initial modeling framework to predict phase fractions, accounting for (1) thermodynamics of interfaces, surfaces, and bulk; (2) elastic effects and mechanical stress/strain; and (3) phase nucleation/evolution and non-equilibrium (de)hydrogenation
- Completed initial calculations of thermodynamic parameters for bulk and surface MgB_2-$Mg(BH_4)_2$
- Tested computational feasibility of phase fraction prediction code on Li-N-H system to successfully explain observed changes in reaction pathways with nanoconfinement

✧ ✧ ✧ ✧ ✧

INTRODUCTION

$Mg(BH_4)_2$ is one of very few metal hydride candidates that lie close to the "viability window" of capacity (14.9 wt% H) and desorption enthalpy (ΔH_{des}) required to satisfy the 2020 and ultimate DOE hydrogen storage targets [1–2]. However, $Mg(BH_4)_2$ suffers from extremely poor kinetics whose origin is not well understood. If the kinetic limitations could be removed and the effective ΔH_{des} slightly improved, then facile hydrogen uptake and release could be attained, and a complex metal hydride-based system could achieve long-term targets. Prior work points to particle size reduction and doping with additives as viable and cost effective improvement strategies [3]. However, it is difficult to fully leverage these without comprehending how, why, and under what conditions these improvements are observed. This project applies multiscale theoretical and experimental tools to develop a fundamental understanding of kinetic and thermodynamic limitations in the Mg-B-H hydrogen storage system, and to devise specific strategies for optimizing its performance under cycling conditions.

APPROACH

This project aims to establish a closely coupled theory/characterization/synthesis approach to understand the roles of nanostructuring and doping in the Mg-B-H system, and apply it to devise possible strategies for improving kinetics and thermodynamics. We focus on three objectives, (1) determining whether chemical, phase nucleation, or transport processes are rate limiting; (2) understanding the origin of the kinetic/thermodynamic changes upon nanosizing/doping; and (3) devising and implementing rational modifications for improvement of H_2 storage properties. Our modeling effort relies on the application of a multiscale framework that combines atomistic density functional theory (DFT) for predictive chemistry and thermodynamics with continuum phase-field modeling (PFM) for describing phase nucleation/growth and non-equilibrium transport kinetics. The predictions are informed and validated by controlled synthesis of size-selected nanoparticles free from binders and nanoscaffolds that may otherwise burden the system with unacceptably high gravimetric penalties. To better understand the kinetic pathways and processes, we apply gravimetric and thermochemical analysis, and utilize in situ and ex situ microscopic and spectroscopic characterization to derive chemical and phase compositions.

RESULTS

Experimental: To provide the large amount of high-quality $Mg(BH_4)_2$ and MgB_2 needed for the bulk hydrogenation kinetic and reaction pathway measurements, we developed synthetic methods for isolating phase-pure $Mg(BH_4)_2$ and MgB_2 with purities exceeding that available from commercial sources. $Mg(BH_4)_2$ was synthesized using a wet-chemistry approach involving the reaction of dibutylmagnesium with borane-dimethylsulfide (BH_3-SMe_2) in a heptane/toluene solution to form a dimethylsulfide adduct of magnesium borohydride, $Mg(BH_4)_2(SMe_2)_2$, which was converted to γ-$Mg(BH_4)_2$ by mild heating at 80°C in vacuum. MgB_2 was synthesized by reacting excess Mg with boron upon heating. X-ray diffraction (XRD) patterns confirming the high quality of our as-synthesized materials are shown in Figure 1, alongside patterns for the

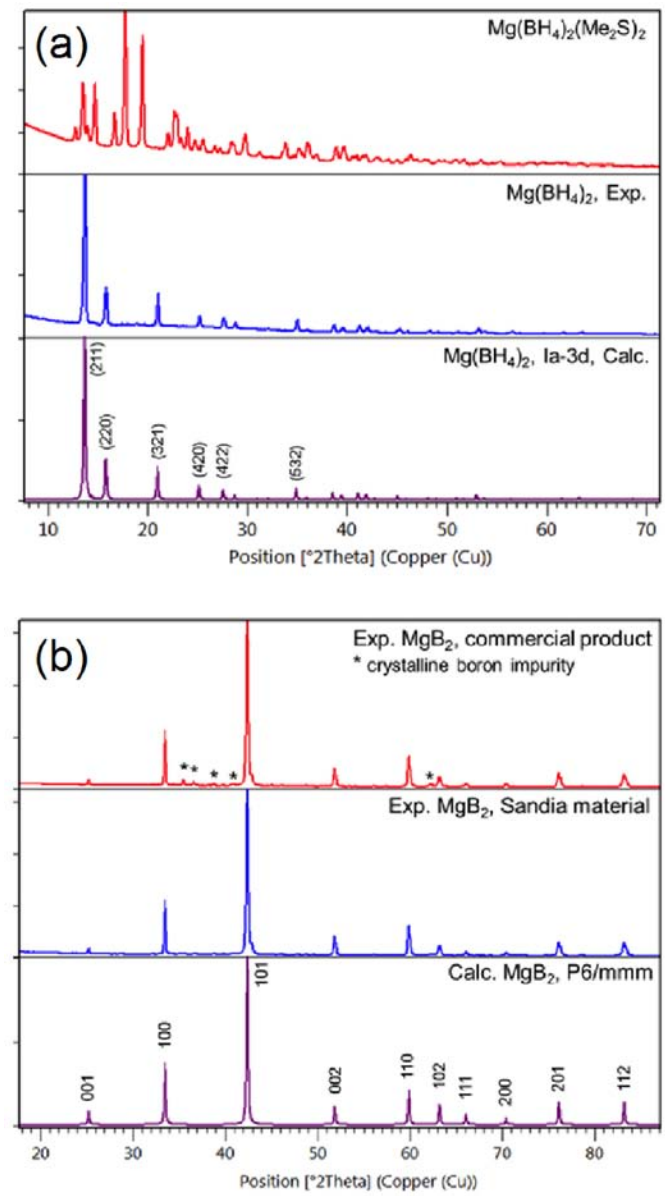

FIGURE 1. Synthesis of MgB_2 and $Mg(BH_4)_2$ (a) XRD patterns of as-synthesized $Mg(BH4)_2(SMe_2)_2$ and low temperature $Mg(BH_4)_2$ and a comparison with the calculated pattern for γ-$Mg(BH_4)_2$ (b) XRD pattern of high-purity MgB_2 synthesized at Sandia, compared with commercial MgB_2 and the calculated MgB_2 pattern

$Mg(BH_4)_2(SMe_2)_2$ precursor and commercial MgB_2 (found to contain significant crystalline boron impurities).

$Mg(BH_4)_2$ can be converted almost entirely to MgB_2 upon heating in vacuum up to 550°C, which involves several steps featuring formation of polyborate intermediates (e.g., $Mg(B_3H_8)$ and $MgB_{12}H_{12}$) alongside MgH_2 and Mg metal [4-9]. It has been further demonstrated that $Mg(BH_4)_2$ can be produced in good yield when MgB_2 is heated at 390–440°C and 70–90 MPa hydrogen pressure. However, in contrast to dehydrogenation, the composition and sequence of intermediates formed during MgB_2 rehydriding are poorly established. Such characterization is vital to understanding the hydrogenation pathway and the factors that control its kinetics. Accordingly, we collected hydrogenation data for bulk MgB_2 in a Seivert's instrument at several temperatures and at two different pressures (Figure 2). At 105 bar hydrogen pressure (Figure 2a), the uptake shows two distinct kinetic regions with ~0.02 wt%/h and 0.002 wt%/h hydrogenation kinetics (based on 105 bar hydrogen pressure and 380°C). The variable temperature (Figure 2b) studies allow a measurement of the activation energy (E_a) for hydrogenation within each of the identified kinetic regimes. Preliminary E_a values are 113 kJ/mol for the faster initial step and 191 kJ/mol for the slower second step. These numbers will be compared with theoretical estimates to identify the different rate limiting mechanisms.

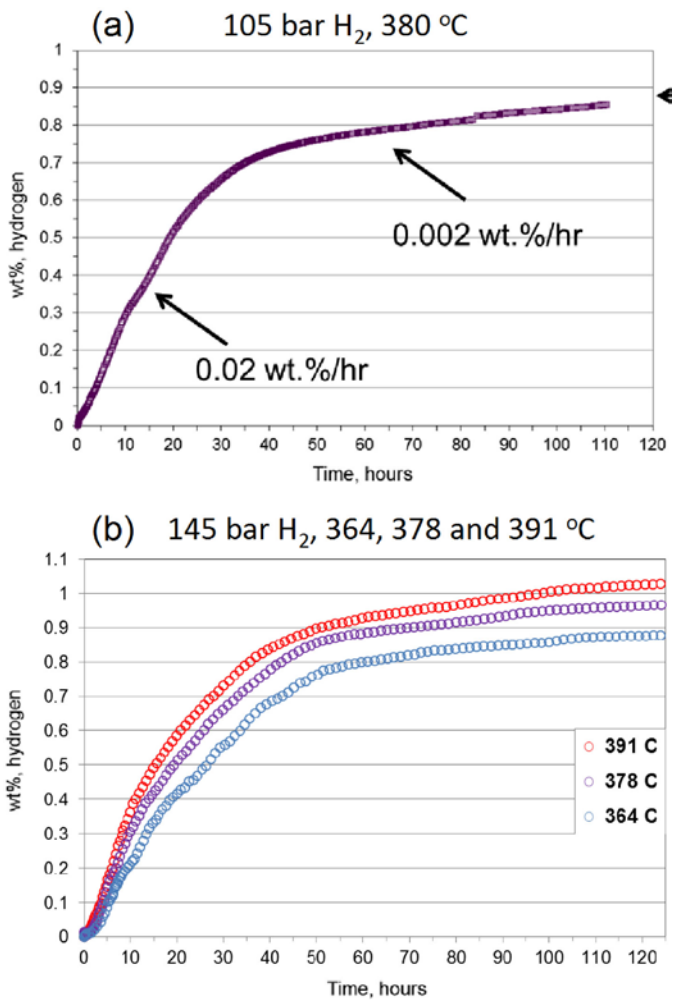

FIGURE 2. Hydrogenation kinetics of bulk MgB_2 (a) Hydrogenation at 105 bar of hydrogen at 380°C, highlighting two distinct kinetic regions with ~0.02 wt%/h and 0.002 wt%/h hydrogenation kinetics (b) Hydrogenation of bulk MgB_2 at 145 bar at 364°C, 378°C, and 391°C

Since intermediates may be present in amorphous phases or solid solutions, their identification requires methodologies beyond XRD that are chemically sensitive. Toward this end, we have collected XAS and XES spectroscopic data for MgB_2, $MgB_{12}H_{12}$, $Mg(BH_4)_2$, and samples at intermediate hydrogenation stages using the Lawrence Berkeley National Laboratory Advanced Light Source synchrotron. The XES data, along with appropriate reference spectra, are presented in Figure 3a. For these spectra, a B 1 s (K edge) core electron is ejected, and the resulting radiative decay of valence electrons into the core hole is measured as a function of emitted photon energy (specifically, we probe the *p*-component of the valence density of states due to dipole selection rules). The XES and XAS data are compared with theoretical simulations of some of the spectra in Figure 3a using the method described by Prendergast, et al. [10] (relative peak positions are typically reproduced better than amplitudes). In the experimental XES spectrum for MgB_2, there exists a main peak near 184 eV with a shoulder extending to 185.5 eV, as well as a poorly resolved shoulder at ~181 eV. All of these features also appear in the simulated spectra. In the experimental XES spectrum for pure $Mg(BH_4)_2$, we notice a wide peak centered around 181.0 eV as well as a smaller feature at around 193.5 eV. The simulated spectra reproduce the positions of both features well, confirming identification of these peaks. There is however a peak in the $Mg(BH_4)_2$ experimental spectrum at 184 eV which seems not to have a theory counterpart. This discrepancy is under examination. The $MgB_{12}H_{12}$ XES spectrum has a peak at 184 eV and a distinct shoulder at 187.5 eV. Calculated spectra for $MgB_{12}H_{12}$ are in progress, but the 187.5 eV peak, having no correspondence in the spectra of the other species, is useful in identifying $MgB_{12}H_{12}$ among the possible hydrogenation intermediates. B_2O_3 exhibits an XES spectrum similar to $Mg(BH_4)_2$, preventing unequivocal identification of oxidation based on XES alone; however, the XAS results (not shown here) do not exhibit features that are consistent with significant oxidation. Similar analyses of other potential reaction intermediates are underway, including simulations of spectra arising from different local coordinations and off-stoichiometric hydrogen compositions.

While analysis of the data is still in progress, some general conclusions can be drawn from the XES data in Figure 3. MgB_2 + H (1.2%, 391°C) and MgB_2 + H (0.8%, 380°C) exhibit spectra similar to as-prepared MgB_2, suggesting these samples at the early stages

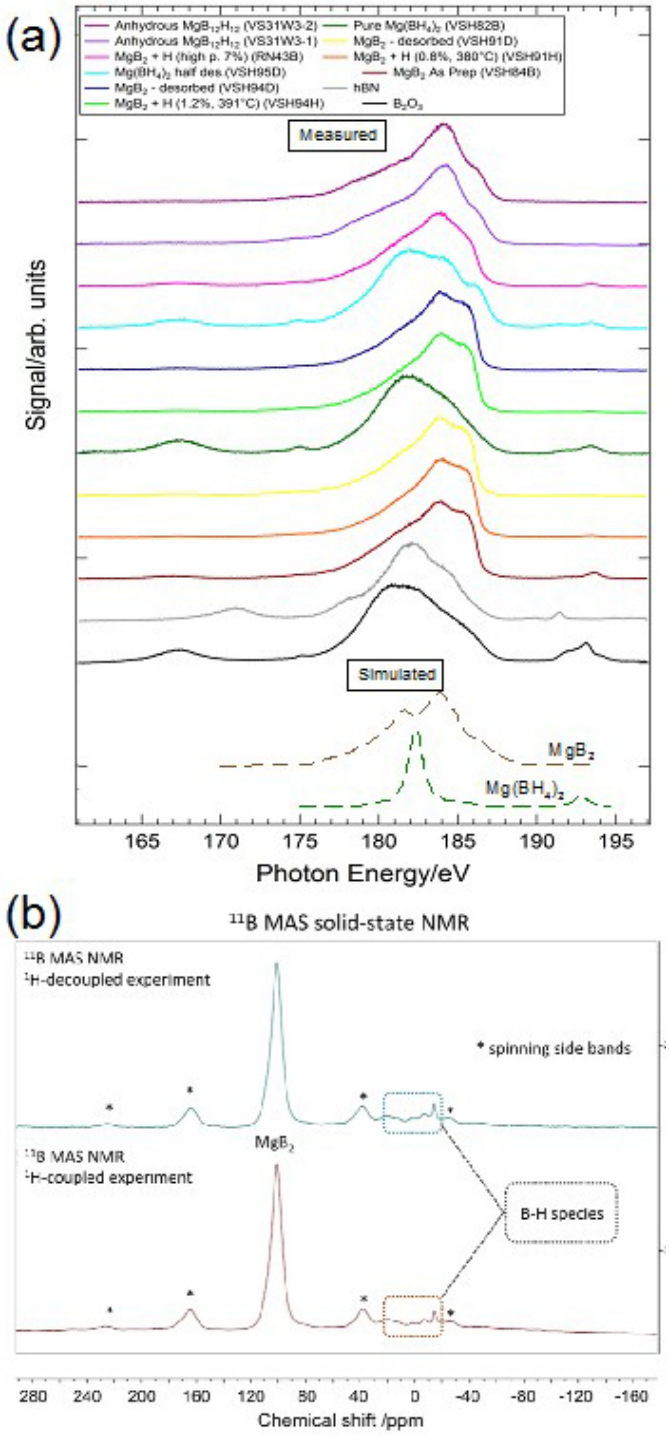

FIGURE 3. Spectroscopic characterization (a) Measured X-ray B K-edge XES spectra of anhydrous $MgB_{12}H_{12}$, pure $Mg(BH_4)_2$, MgB_2 produced by desorption, MgB_2 + H (high p. 7%), MgB_2 + H (0.8%, 380°C), $Mg(BH_4)_2$ half desorbed, MgB_2 as prepared, MgB_2 + H (1.2%, 391°C), hexagonal BN, and B_2O_3 samples, compared with theoretically simulated spectra for MgB_2 and $Mg(BH_4)_2$ (b) ^{11}B MAS spectra for a partially hydrogenated MgB_2 sample with 0.8 wt% H obtained from hydrogenation of MgB_2 at 364°C

of hydrogenation are retaining much of their original chemistry. The XES spectra for the half-desorbed (VSH95D) and half-hydrogenated (RN43B) $Mg(BH_4)_2$ are very different, indicating different pathways for desorption and hydrogenation. The half-desorbed sample looks like a mixture of the phase-pure $Mg(BH_4)_2$ and $MgB_{12}H_{12}$ spectra, whereas the half-hydrogenated sample more closely resembles the MgB_2 spectrum with little evidence for the formation of $MgB_{12}H_{12}$ or $Mg(BH_4)_2$. One feature of note in the XAS spectrum of partially hydrogenated MgB_2 is that the more bulk-sensitive (~100 nm) fluorescence yield shows very similar characteristics as the more surface-sensitive electron yield measurement (~1 nm sensitivity, not shown), which suggests that boron is being hydrogenated throughout the sample rather than just at the surface. Accordingly, hydrogen transport into the sample may not be as difficult as has generally been envisioned.

To gain further chemical sensitivity as a companion to the XAS/XES data, we also collaborated with Pacific Northwest National Laboratory to perform NMR measurements on our sample sets. The ^{11}B magic angle spinning (MAS) NMR spectra (Figure 3b) shows a spectrum of MgB_2 hydrogenated with 0.8 wt% H at 364°C. The results indicate that MgB_2 is the major species present (peak at ~100 ppm), however small amounts of B-H species are observed as well between -2 and -18 ppm. Although the identity of these species remains to be established, it is clear that at least some boron atoms in MgB_2 react with H_2 to form B-H bonds. Interestingly, no peaks from BH_4^- anions could be detected, suggesting the absence of $Mg(BH_4)_2$ material. This is consistent with the XES observations.

Theoretical: Significant progress was made in developing and parameterizing our software codes for predicting the thermodynamic and kinetic evolution of metal hydrides during (de)hydrogenation. Existing codes were adapted to account for thermodynamic hydrogenation conditions of temperature and partial pressure, and a formalism was included for studying the coexistence of multiple phases, including reaction intermediates. Two codes are being developed, (1) a code for predicting thermodynamic phase fractions of mixed-phase systems within a given microstructure, and (2) a code for predicting phase evolution kinetics using a PFM formalism. Both are intended to go beyond idealized descriptions based on bulk enthalpies alone and instead consider the complexities associated with surfaces and interfaces.

Our first code relies on DFT-computed bulk, surface, and interface energies, as well as zero-point and vibrational entropic contributions, to predict thermodynamic phase fractions based on an input microstructure. To account for microstructure-associated effects that are neglected in typical phase diagrams, we include penalties associated with the presence of surfaces and internal phase boundaries, as well as entropic contributions associated with phase

coexistence (assuming ideal mixing). Currently, only core-shell microstructures are implemented, although the framework is extensible. Pending delineation of the phase microstructure of the Mg-B-H system, this code was tested on the $Li_3N/LiNH_2$+2LiH system, which exhibits many properties in common with $MgB_2/Mg(BH_4)_2$ but has few intermediates and a core-shell phase microstructure that can be readily assumed from available literature data (Figure 4a). As a validating case, we focused on predicting two peculiar behaviors associated with nanosizing that were found in extensive (de)hydrogenation data collected previously by our Sandia partners: first, a transition from the low-pressure α-Li_3N phase to a high-pressure β-Li_3N phase; and second, a conversion from a two step reaction to a single-step reaction that eliminates the otherwise stable Li_2NH intermediate, resulting in dramatically improved kinetics and reversibility. Our computational framework was able to properly predict the α-Li_3N/β-Li_3N phase stability reversal for particles smaller than 7.1 nm diameter, driven by a larger surface energy penalty for α-Li_3N. On the other hand, the single step reaction cannot be explained by considering surface energies alone. Instead, by estimating interface energies within the assumed phase microstructure using an established empirical procedure [11], our framework predicts near-complete elimination of the ordinarily stable Li_2NH intermediate once the size is reduced beyond ~5 nm (Figure 4b–d). This further validates the predictive capability of the code and provides a concrete explanation for the experimentally

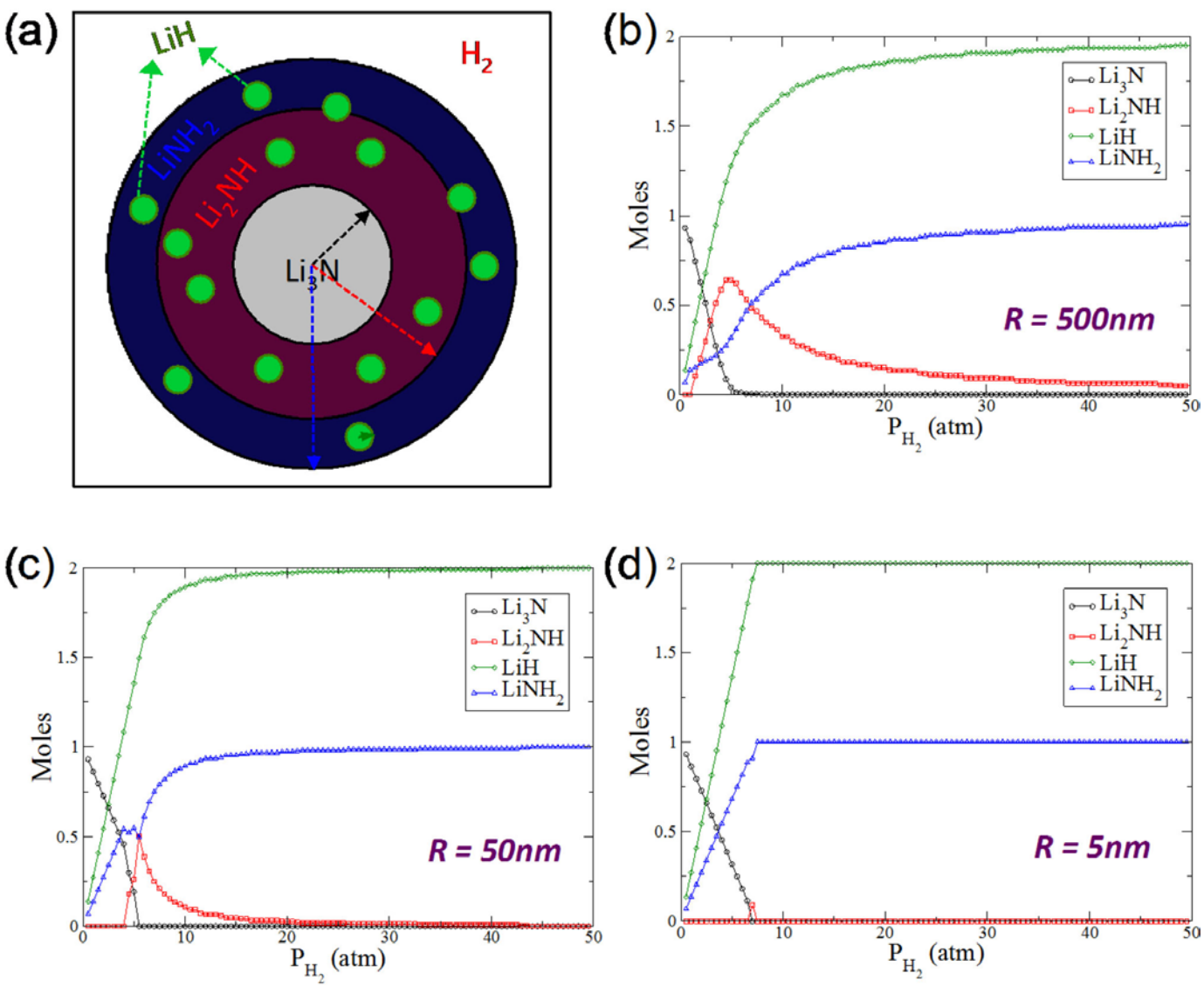

FIGURE 4. Predicted phase fractions in metal hydride nanoparticles (a) Core-shell model of the Li-N-H hydrogen storage system under hydrogenation conditions (b-d) Equilibrium phase fractions of Li_3N, Li_2NH, LiH, and $LiNH_2$ during hydrogenation for (a) 500 nm, (b) 50 nm, and (c) 5 nm radius particles. The smallest particles show essentially no evidence of stable Li_2NH intermediate formation (red)

observed single-step decomposition reaction. We emphasize that the disappearance of the intermediate results directly from the penalty associated with the formation of interfaces *within* the particle, which become increasingly larger contributions as the particle size is reduced. The possibility of using interfaces and phase microstructure to drive reaction pathways and kinetics is very compelling, and will be a key ingredient in our $Mg(BH_4)_2$ study. The results of this joint theory-experiment study have recently been submitted for publication [12].

Having established the predictive capability of the phase fraction code, we are currently obtaining the necessary parameters for application to the Mg-B-H system once the phase microstructure can be confirmed. In addition to previously calculated bulk enthalpies [4,7,9], we have computed the DFT energies for the low-index surfaces of MgB_2 and $Mg(BH_4)_2$, as shown in Table 1. We considered only (100) surfaces for $Mg(BH_4)_2$ because it neatly cleaves the large-scale arrangement of Mg atoms. The (100) surface of MgB_2 is the most stable, although (110) and (101) have surface energies that are within 20% of (100). $Mg(BH_4)_2$ has much lower surface energy, which could have important consequences for phase stabilities of nanostructured Mg-B-H systems. We are currently computing similar quantities for the possible intermediate phases, as well as elastic moduli for each phase that can be used to estimate contributions to interfacial energies arising from lattice mismatch at internal phase boundaries.

TABLE 1. DFT-computed surface energies (J/m^2) of low-index surfaces of $MgB_2/Mg(BH_4)_2$

Surface	MgB_2	$Mg(BH_4)_2$
(100)	1.92	0.32
(001)	2.72	--
(110)	2.24	--
(101)	2.24	--
(111)	2.56	--

The second code in our suite is designed to predict the kinetics of phase evolution, which will be an increasingly important effort in future project years. We are currently implementing formalisms for kinetic contributions arising from chemomechanical gradients based on differences in elastic moduli, non-equilibrium mass transport of hydrogen and metal cations, and phase nucleation barriers. These functionalities will be tested in the coming months. Explicit modeling of surface hydrogen dissociation and association will be performed via subcontract with the University of Michigan; this feature will be important for considering the effects of catalytic additives. Early versions of the PFM code using sample parameters have already been benchmarked on the high performance computing resources at LLNL. Both spherical and plate-shaped geometries were tested to ensure robustness against particle morphology. We were able to simulate the phase evolution upon 50% (de)hydrogenation of a model ~100 nm particle using an allocation of 160 central processing unit cores, running for one week of continuous processing time (~25,600 core-hours). We expect that further optimization may be possible. Corresponding parameters are currently being computed for the Mg-B-H using DFT and ab initio molecular dynamics.

CONCLUSIONS AND FUTURE DIRECTIONS

- Hydrogenation of MgB_2 evidences two distinct kinetic regimes. XAS/XES and NMR can uniquely identify BH_x chemical species at partial hydrogenation stages, and suggest that dehydrogenation and hydrogenation occur via different pathways.
- Phase fraction prediction code reproduces known reaction pathways in a complex metal hydride system. Early learning on the metal hydride system demonstrates the need to consider interfaces and suggests the possibility of morphological/microstructural engineering as a strategy for kinetic improvement.
- *Future direction:* Collect XAS/XES and Fourier transform infrared data and simulate corresponding theoretical spectra for additional samples of Mg-B-H at varying stages of (de)hydrogenation to get information on local chemical environments.
- *Future direction:* Establish the nanoparticle synthesis laboratory to begin the synthesis of MgB_2 and $Mg(BH_4)_2$ nanoparticles with controlled sizes.
- *Future direction*: Calculate remaining thermodynamic parameters for MgB_2, $Mg(BH_4)_2$, and $MgB_{12}H_{12}$ bulk, surfaces, and interfaces, comparing against literature values to benchmark chosen parameters. Perform ab initio molecular dynamics of MgB_2, $Mg(BH_4)_2$, and key intermediates and surfaces for extraction of transport coefficients and anharmonic contributions to entropy.
- *Future direction*: Implement additional physical ingredients in our kinetics code, including a new modeling framework for chemical reaction kinetics on surfaces (clean or oxidized).

FY 2015 PUBLICATIONS/PRESENTATIONS

1. Wood, B.C. et al., "Improving the kinetics and thermodynamics of $Mg(BH_4)_2$ for hydrogen storage." *U.S. DOE Hydrogen and Fuel Cells Program Annual Merit Review*, Washington, D.C., June 2015.

2. Stavila, V., N. Poonyayant, T.-W. Heo, K. Ray, T.J. Udovic, N. Angboonpong, P. Pakawatpanurut, L.E. Klebanoff, B.C. Wood, "Nanostructuring: A Route for Enhancing Reversibility in Metal Hydrides?" *Gordon Conference on Hydrogen-Metal Systems*, Easton, MA, July 2015.

3. Wood, B.C., V. Stavila, N. Poonyayant, T.-W. Heo, K. Ray, L.E. Klebanoff, T.J. Udovic, J. Lee, N. Angboonpong, and P. Pakawatpanurut, "Nanointerface-driven reversible hydrogen storage in the nanoconfined Li-N-H system." *Submitted* (2015).

REFERENCES

1. Klebanoff, L. E., and J.O. Keller, "5 Years of Hydrogen Storage Research in the US DOE Metal Hydride Center of Excellence (MHCoE)," *Int. J. Hydr. Energy* 38 (2013): 4533-4576.

2. Pasini, J.M., C. Corgnale, B.A. van Hassel, T. Motyka, S. Kumar, and K.L. Simmons, "Metal Hydride Material Requirements for Automotive Hydrogen Storage Systems," *Int. J. Hydr. Energy* 38 (2013): 9755-9765.

3. Fichtner, M., Z. Zhao-Karger, J. Hu, A. Roth, and P. Weidler, "The Kinetic Properties of $Mg(BH_4)_2$ Infiltrated in Activated Carbon," *Nanotechnology* 20 (2009): 204029.

4. Zhang, Y., E. Majzoub, V. Ozoliņš, and C. Wolverton, "Theoretical Prediction of Metastable Intermediates in the Decomposition of $Mg(BH_4)_2$," *J. Phys. Chem. C* 116 (2012): 10522-10528.

5. Chong, M., A. Karkamkar, T. Autrey, S. Orimo, S. Jalisatgi, and C.M. Jensen, "Reversible Dehydrogenation of Magnesium Borohydride to Magnesium Triborane in the Solid State Under Moderate Conditions." *Chem. Commun.* 47 (2011): 1330-1332.

6. Hwang, S.-J., R.C. Bowman, J.W. Reiter, J. Rijssenbeek, G.L. Soloveichik, J.-C. Zhao, H. Kabbour, and C.C. Ahn. "NMR Confirmation for Formation of $[B_{12}H_{12}]^{2-}$ Complexes during Hydrogen Desorption from Metal Borohydrides." *J. Phys. Chem. C* 112 (2008): 3164-3169.

7. Ozolins, V., E.H. Majzoub, and C. Wolverton, "First-Principles Prediction of Thermodynamically Reversible Hydrogen Storage Reactions in the Li-Mg-Ca-BH System," *J. Am. Chem. Soc.* 131 (2008): 230-237.

8. Soloveichik, G.L., Y. Gao, J. Rijssenbeek, M. Andrus, S. Kniajanski, R.C. Bowman, S.-J. Hwang, and J.-C. Zhao, "Magnesium Borohydride as a Hydrogen Storage Material: Properties and Dehydrogenation Pathway of Unsolvated $Mg(BH_4)_2$," *Int. J. Hydr. Energy* 34 (2009): 916-928.

9. Zhang, Y., E. Majzoub, V. Ozoliņš, and C. Wolverton, "Theoretical Prediction of Different Decomposition Paths for $Ca(BH_4)_2$ and $Mg(BH_4)_2$," *Phys. Rev. B* 82 (2010): 174107.

10. Prendergast, D., and G. Galli, "X-ray absorption spectra of water from first principles calculations," *Phys. Rev. Lett.* 96 (2006): 215502.

11. Porter, D.A., and K.E. Easterling, *Phase Transformations in Metals and Alloys.* 2nd ed.; Chapman & Hall: London, UK (1992).

12. Wood, B.C., V. Stavila, N. Poonyayant, T.-W. Heo, K. Ray, L.E. Klebanoff, T.J. Udovic, J. Lee, N. Angboonpong, and P. Pakawatpanurut, "Nanointerface-Driven Reversible Hydrogen Storage in the Nanoconfined Li-N-H System," *submitted* (2015).

IV.D.1 Innovative Development, Selection, and Testing to Reduce Cost and Weight of Materials for BOP Components

Chris San Marchi (Primary Contact),
Jonathan Zimmerman
Sandia National Laboratories
7011 East Avenue
Livermore, CA 94550
Phone: (925) 294-4880
Email: cwsanma@sandia.gov

DOE Managers
Ned Stetson
Phone: (202) 586-9995
Email: Ned.Stetson@ee.doe.gov
Grace Ordaz
Phone: (202) 586-8350
Email: Grace.Ordaz@ee.doe.gov

Subcontractor
Hy-Performance Materials Testing LLC, Bend, OR

Project Start Date: July 15, 2014
Project End Date: September 30, 2017

Overall Objectives

- Reduce weight of structural materials for balance of plants (BOP) components by 50%
- Reduce cost of structural materials for BOP components by 35%
- Expand the scope of materials of construction for BOP components
- Identify simplified testing procedures to enable materials qualification

Fiscal Year (FY) 2015 Objectives

- Quantify fatigue life of baseline Type 316L austenitic stainless steel with internal hydrogen
- Develop framework to assess the stacking fault energy (SFE) of austenitic stainless steels with compositions that are consistent with technologically relevant alloys (e.g., Fe-(15-25Cr)-(2-20)Ni-(2-20)Mn)
- Establish a robust computational method for compositional and configurational variations in multi-component alloys (i.e., quantify the effects of randomly distributed elements on results of simulation with a relatively small number of atoms)
- Compare the fatigue response of baseline stainless steel in different environments (internal and external hydrogen) to establish the dependence on environment, including pressure

Technical Barriers

This project addresses the following technical barriers from Hydrogen Storage section of the Fuel Cell Technologies Office (FCTO) Multi-Year Research, Development, and Demonstration Plan:

(A) System Weight and Volume

(B) System Cost

(H) Balance of Plant (BOP) Components

Technical Targets

No specific technical targets have been set. This project is a basic study of materials of construction for BOP with the goals of identifying lower cost alternatives to the baseline of annealed Type 316L that can be implemented in lighter weight designs (i.e., high strength materials). The project targets are:

- Reduce weight of structural materials for BOP components by 50%
- Reduce cost of structural materials for BOP components by 35%

FY 2015 Accomplishments

- Fatigue life data for strain-hardened Type 316L stainless steel have been compared in gaseous (external) hydrogen at moderate-pressure (10 MPa), high-pressure (103 MPa) and with internal hydrogen
- For baseline material, the less expensive testing with internal hydrogen represents fatigue performance measured in moderate-pressure and high-pressure external hydrogen
- Simulation framework for predicting stacking fault energy has been demonstrated for pure nickel

✧ ✧ ✧ ✧ ✧

INTRODUCTION

The primary objective of this effort is to identify alloys to replace Type 316/316L in hydrogen service for BOP applications onboard fuel cell electric vehicles (FCEVs).

Type 316/316L austenitic stainless steels are used extensively in hydrogen systems for their resistance to hydrogen embrittlement, which is attributed to the relatively high nickel content of Type 316/316L alloys. Nickel content, however, drives the cost of austenitic stainless steels, thus Type 316/316L alloys impose a cost premium compared to similar alloys with lower nickel content. Since the cost of BOP components is a large fraction of the cost of hydrogen fuel systems (even dominating the cost at low production volumes [1]), alternative materials are desired. In addition, Type 316/316L alloys are relatively low strength, thus high-pressure components tend to be heavy to accommodate the stresses associated with the pressure loads. Higher strength materials will reduce weight of the components (an added benefit for onboard components) and contribute to lower cost since less material is needed. However, engineering data to justify selection of lower cost and higher strength alloys for high-pressure hydrogen service are currently unavailable. Moreover, alloy design could enable low cost solutions to the specific needs of onboard hydrogen storage.

APPROACH

The objective of this project is addressed from two perspectives: (1) experimental evaluation of commercial alloys, (2) computational materials discovery of new alloys. In the first case, fatigue properties in hydrogen environments will be evaluated for low cost, high strength alloys and compared to the benchmark of annealed Type 316/316L. The use of fatigue stress as a performance based metric will be used for comparison with the goal of achieving 35% reduction of cost and 50% reduction of weight. The experimental activity does not seek to identify materials that are immune to hydrogen embrittlement. Rather, a comprehensive test program seeks appropriate trade-offs between materials cost and performance, such that hydrogen embrittlement can be effectively managed in design. In order to provide performance data, testing must be conducted at temperature consistent the temperature of maximum embrittlement for these alloys, which is reported to be in the range of 200–220 K from tensile testing; the effect of hydrogen on fatigue as a function of temperature has not been reported. The tasks in this project are organized to provide a methodical approach to effectively reach the proposed targets. An additional goal of the experimental activity is to demonstrate a straightforward, simplified methodology by which materials may be qualified for safe hydrogen service, including the use of internal hydrogen (saturation of the material with hydrogen by thermal precharging) as a robust substitute for testing in gaseous hydrogen.

The goal of the computational discovery activity, like the experimental activity, is to identify low-Ni content (and thus lower cost) stainless steel alloys to be used in BOP components that are compatible for hydrogen service. To achieve this goal from a computational perspective, a quantum based materials exploration and design (QMED) framework is being developed—one that combines sophisticated optimization and uncertainty quantification with ab initio calculations. This framework will be used to create a comprehensive database and materials design relations that identify stainless steel alloys that optimize stacking fault energy (indicative of hydrogen embrittlement resistance) with reduced Ni content. This effort represents a new initiative in the FCTO research portfolio to use computational materials science coupled with high performance computing to identify and evaluate low cost stainless steels that are tailored for hydrogen embrittlement resistance. This innovative approach will provide the DOE and United States industry a framework and computational tools to efficiently and effectively explore the design space for next generation materials used in fuel cell technologies.

RESULTS

Experimental Evaluation of Commercial Alloys

Fatigue life measurements of strain hardened Type 316L have been performed in gaseous hydrogen at moderate pressure of 10 MPa (1.5 ksi) by Hy-Performance Materials Testing and at high pressure of 103 MPa (15 ksi) by Sandia National Laboratories. The fatigue-life data for these two conditions are shown in Figure 1 along with data for the as-received (AR) material in air (AR, reference condition) and material with internal hydrogen (hydrogen precharged [PC]). Also shown in Figure 1 is a power-law fit to the data measured on the AR material (dashed black line). The relative variability in the data is represented by 95% confidence limits on the fit, shown by the red dashed lines in this figure.

The presence of external hydrogen reduces the fatigue life of strain-hardened Type 316L. The measured fatigue life in external hydrogen at pressure of 10 MPa and 103 MPa appear to overlay (Figure 1). This observation suggests that tests may not need to be performed at high pressure. While testing in external hydrogen indicated a clear decrease in performance for the strain-hardened Type 316L, testing the steel with internal hydrogen (PC) had no measurable effect on the fatigue life (Figure 1); since the stress-life data of the hydrogen-precharged Type 316L are within the confidence limits of the fit to the AR data. However, it is important to consider the 10–15% increase in yield strength typically observed in stainless steels with internal hydrogen. Figure 2 shows the same data with the fatigue stress amplitude normalized by the yield strength. When normalized, the fatigue-life data for internal hydrogen (PC) converge with the data for external hydrogen (both pressures). This is an important finding since it suggests that internal hydrogen can be a substitute for testing in high-pressure external hydrogen. More data is needed to determine if these observations can be extended to low temperature and with other materials (such as XM-11). Preliminary data (not shown here) suggest that

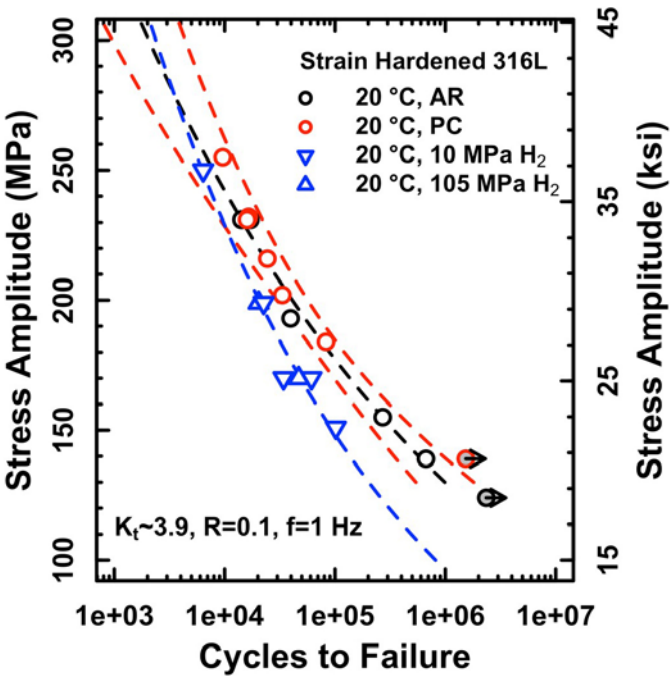

FIGURE 1. Stress-life fatigue curves of high-strength Type 316L austenitic stainless steel at 20°C (293 K), notched specimens ($K_t \approx 3.9$), loaded in tension-tension (R = 0.1): AR material, hydrogen-precharged condition, as well as in external gaseous hydrogen at pressure of 10 MPa and 103 MPa. The lines on the plots represent power-law fit to the data for the AR condition (black) and tests in external hydrogen (blue). The red curves represent 95% confidence limits for the AR data. Shaded symbol with arrows represent samples that did not fail.

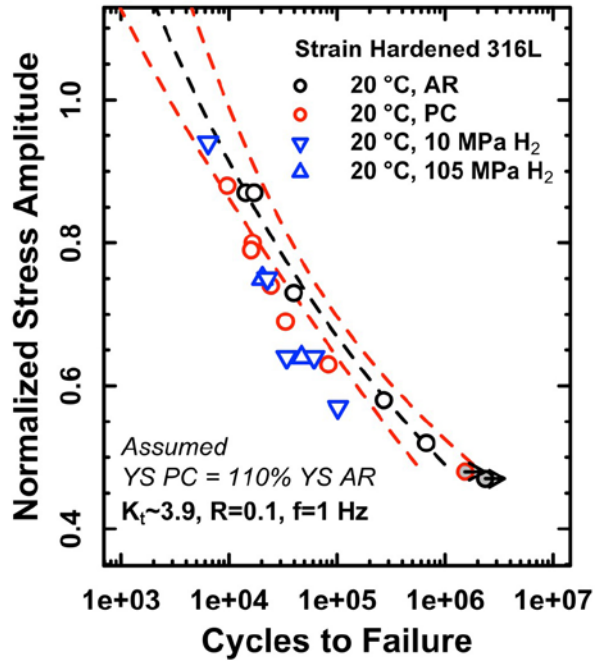

FIGURE 2. Stress-life curves normalized by yield strength (same data as Figure 1)

the same trends can be applied to strain-hardened Type 316L at low temperature and to Type XM-11 at room temperature. Testing is underway to substantiate these preliminary data and observations.

Computational Materials Discovery

The literature is unclear on the correlation between intrinsic properties such as SFE and the effects of hydrogen. As low SFE is known to correlate with propensity for both planar slip of dislocations (as opposed to cross-slip), as well as martensite formation, this suggests that hydrogen's effect on SFE might preferentially favor specific deformation mechanisms and mechanical behavior that imply resistance to the effects of hydrogen.

The SFE for ternary stainless steel alloys using large supercells (450 atoms) have been calculated from first principles (within density functional theory). We considered a perfect lattice and a lattice with three stacking faults. The initial composition considered was 66% Fe, 14% Cr, and 20% Ni. No temperature effects were included and the paramagnetic phase (that sets in experimentally above the transition temperature) was constrained by imposing zero total magnetic moment. The initial spin configuration was modeled by a random distribution of local magnetic moments on the Fe sublattice. Two different exchange-correlation functionals, GGA and GGA+U have been considered. In both cases the convergence of the total energy is very slow, taking thousands of iterations for each spin configuration and resulting in several days of computation time using several hundred processors. Furthermore, variations in initial spin configuration lead to different converged states. Within GGA+U, the SFE of the Fe-Cr-Ni alloy was found to range from 150 mJ/m^2 to 500 mJ/m^2 depending on the spin configuration. An alternative, indirect approach is also being pursued to calculate SFE using smaller supercells within the axial interaction model (used by Vitos, et al. [2,3]). Within this model, SFE can be estimated using calculated energies from hexagonal close-packing (hcp), double hcp and face-centered cubic lattice structures.

We have refined our sampling approach to assess the influence of atom configuration (for a given target composition) on SFE. We changed our approach from a space-filling approach based on a location-level view (i.e., determining the element that would populate each specific site) to one that employs perturbations that preserve sample properties and has a configuration-level view with respect to each element. For example, if the material composition is 66% Fe, 23% Cr, 11% Ni, we enumerate all of the possible Cr location combinations and all of the possible Ni location combinations. We then sample various Cr and Ni combinations and fill in the remaining locations with Fe. Testing is still underway, but preliminary results indicate that we can maintain space-filling properties, meet target

composition, and reduce the occurrence of duplicates to a manageable level.

To verify the predictive capability, SFE of commercial alloys and experimental alloys is being measured. SFE is very difficult to measure; high fidelity measurements require advanced high resolution imaging such as transmission electron microscopy (TEM). Specimens of annealed Type XM-11 austenitic stainless steels and experimental high manganese-aluminum austenitic stainless steels are being evaluated. Our TEM observations of the Mn-Al stainless alloy shows deformation structures characteristic of planar slip, although the alloy was designed to mitigate planar slip. Systemic diffraction contrast imaging and analyses are being used to glean information concerning the defect arrangements and their relationship with respect to other features in the microstructure. Our goal is to determine whether the planar slip in this material is due to low SFE, second phase particles, or other aspects of the microstructure. Diffraction contrast images of dislocations of Type XM-11 commercial alloy and the experimental Mn-Al stainless alloy are provided in Figure 3.

CONCLUSIONS AND FUTURE DIRECTIONS

- Testing of the baseline Type 316L shows that consistent fatigue results can be extracted from testing with internal and external hydrogen environments; additionally, for external hydrogen, fatigue life testing appears insensitive to pressure in the range of 10 MPa to 100 MPa
- Test methods must be verified at low temperature and for alloys that display greater effects of hydrogen
  - Preliminary results at low temperature are in qualitative agreement with tests at room temperature for Type 316L
  - Preliminary results from Type XM-11 suggest the test method can be applied to alloys that are more susceptible to hydrogen, but lower cost
- Two commercial, technologically relevant alloys have been selected for fatigue evaluation: Type XM-11 and Nitronic 60
- The computational framework for predicting SFE is being optimized to enhance the efficiency of evaluating commercial austenitic stainless steels and technologically relevant experimental alloys

SPECIAL RECOGNITIONS & AWARDS/ PATENTS ISSUED

1. C. San Marchi, Certificate of Recognition for Technical Committee Service, Materials and Fabrication, American Society of Mechanical Engineers, Pressure Vessels and Piping Division, 2015, presented at the ASME 2015 Pressure Vessels & Piping Division Conference, Boston, MA, 22 July 2015.

a.

b.

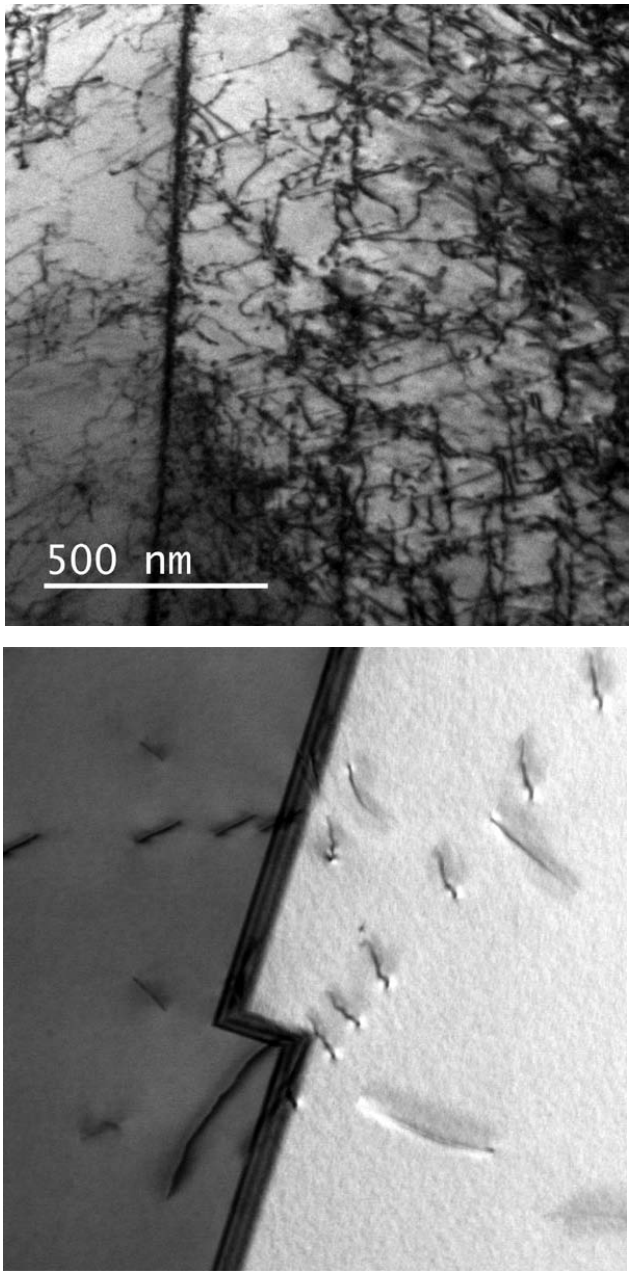

FIGURE 3. Diffraction contract images of dislocations in (a) experimental Mn-Al austenitic stainless steel, and (b) commercial Type XM-11 austenitic stainless steel

FY 2015 PUBLICATIONS/PRESENTATIONS

1. C. San Marchi, J.A. Zimmerman, K. Thuermer, X. Tang, S. Kernion, K.A. Nibur, "Stress-based fatigue performance of austenitic stainless steel in hydrogen environments," (PVP2015-45421), *Proceedings of the ASME 2015 Pressure Vessels & Piping Division Conference*, Boston MA, 19-23 July 2015.

2. C. San Marchi (presenter), "Hydrogen Energy Research at Sandia," (SAND2014-19188 PE), presented at SAE H_2 Compatibility Workshop, 9 March 2015.

3. C. San Marchi (presenter), "Innovative Development, Selection and Testing of Materials to Reduce Cost and Weight of BOP Components," (SAND2015-1912 O), in-person presentation at Swagelok Company, 11 March 2015.

REFERENCES

1. DOE Fuel Cell Technologies Office Record # 13010.

2. L. Vitos, J-O. Nilsson, B. Johansson. Acta Materialia 54 (2006) 3821–3826.

3. L. Vitos, P.A. Korzhavyi, B. Johansson. Phys Rev Lett 96 (2006) 117210.

IV.D.2 Thermomechanical Cycling of Thin Liner High Fiber Fraction Cryogenic Pressure Vessels Rapidly Refueled by LH_2 Pump to 700 bar

Salvador M. Aceves (Primary Contact),
Gene D. Berry, Guillaume Petitpas, Vernon Switzer
Lawrence Livermore National Laboratory (LLNL)
7000 East Avenue
Livermore, CA 94550
Phone: (925) 422-0864
Email: aceves6@llnl.gov

DOE Managers
Ned Stetson
Phone: (202) 586-9995
Email: Ned.Stetson@ee.doe.gov
Jesse Adams
Phone: (720) 356-1421
Email: Jesse.Adams@ee.doe.gov

Subcontractors
- Spencer Composites Corporation, Sacramento, CA
- Linde LLC, Hayward, CA

Project Start Date: January 2014
Project End Date: January 2017

Overall Objectives

- Develop ultra-light cryogenic pressure vessels with 12 in diameter and 700 bar rating
- Optimize metallic liner thickness, composite fiber fraction and ultra-thin vacuum jacket
- Quantify liquid hydrogen (LH_2) pump durability over 6,000 refuelings to 700 bar
- Demonstrate full scale system density of 50 g H_2/L_{system} and 9 wt% H_2, and a cycle life of at least 1,500 refills

Fiscal Year (FY) 2015 Objectives

- Submit safety plan for cryogenic H_2 cycling facility rated for 5 kg H_2 prototype vessels and obtain DOE/LLNL approval
- Fabricate 700 bar 163 L system using commercial vessel to test insulation and supports
- Complete civil construction of H_2 test facility
- Design and fabricate initial full scale (63.5 L) prototype 700 bar pressure vessel with a high ratio between inner and outer volume (80+% volumetric efficiency)
- Demonstrate 1,600 bar cryogenic (LN_2) strength of initial prototype (2.28 safety factor)

Technical Barriers

This project addresses the following technical barriers from the Hydrogen Storage section (3.3.5) of the Fuel Cell Technologies Office Multi-Year Research, Development, and Demonstration Plan:

(A) System Weight and Volume

(D) Durability/Operability

(N) Hydrogen Venting

Technical Targets

This project specifically addresses three technical targets for onboard hydrogen storage in light duty fuel cell vehicles: system gravimetric capacity, system volumetric capacity, and operational cycle life. Previous projects on the development of the cryogenic high pressure storage technology achieved peak gravimetric and volumetric capacities of 0.074 kg H_2/kg system and 0.045 kg H_2/L system, respectively, using a 4,000 psi, 151 L (10.7 kg H_2 capacity), 25-in internal diameter, aluminum lined pressure vessel [1]. This current project aims at exploring designs with a 700 bar (10,000 psi) operating pressure, 63.5-L internal volume (5.6 kg H_2 capacity), 12-in internal diameter and a non-Al liner. FY 2015 efforts at designing, fabricating, and cryogenically strength testing pressure vessels produced a 63.5 L, non-Al liner Type III pressure vessel with 81% volume efficiency and 32 kg mass for 700 bar operating pressure, performance that would enable to meet our projected target of 0.090 kg H_2/kg system and 0.050 kg H_2/L system. Those projected performances will be demonstrated with a full size insulated system at the end of this project. Theoretical design calculations have also shown that this pressure vessel would have an operational life of at least 1,500 cycles. This cycle life will be experimentally tested through up to four full size prototype vessels in FY 2016. Table 1 summarizes our projected performance towards the three main technical targets addressed in this project.

FY 2015 Accomplishments

- Sought and obtained LLNL safety approval of 65 bar containment for transient H_2 peak pressure and dynamic vessel wall loading of 2.5–5 kg H_2 over the full pressure and temperature range
- Completed civil site construction and control room installation for cryogenic H_2 cycling facility using 875 bar LH_2 pump

TABLE 1. Progress towards Meeting Technical Targets for Onboard Hydrogen Storage for Light Duty Fuel Cell Vehicles

Storage Parameter	Units	2020	Ultimate	Projected
System Gravimetric Capacity	kg H_2/kg system	0.055	0.075	0.090
System Volumetric Capacity	kg H_2/L system	0.040	0.070	0.050
Durability/Operability Operational Cycle Life	Cycles	1,500	1,500	1,500

- Designed and fabricated a 63.5 L thin lined carbon fiber overwrapped prototype vessel rated to 700 bar with 81% volumetric efficiency
- Demonstrated cryogenic strength of prototype vessel to 1,560 bar

✧ ✧ ✧ ✧ ✧

INTRODUCTION

Storing cryogenic H_2 in a pressurized, insulated system has many benefits in terms of safety, volumetric and gravimetric densities and ownership cost that have been studied and demonstrated by LLNL [2,3] and external parties [4-7]. High utilization (>1,500 kg H_2/d) commercial scale fueling stations will likely require the use of liquid H_2 by means of a fast, energy efficient LH_2 pump. Until now, the development of cryogenic pressure vessels by LLNL has used "off the shelf" pressure vessels with an aluminum liner, a maximum operating pressure limited to 350 bar with large capacity (151 L, equivalent to 10.7 kg H_2) and large diameter (25 in). We believe that system densities (both volumetric and gravimetric), cycle life and manufacturability could be improved by developing pressure vessels specifically tailored towards cryogenic utilization, even at a 5.6 kg H_2 scale, by exploring: thin liner design (especially important for 12 in diameter), non-Al liner materials, high fiber fraction for the composite overwrap, 700 bar operating pressure and ultra-thin vacuum jacket designs.

APPROACH

Within the project, we are designing, manufacturing and cryogenically pressure testing full scale (65 L) 700 bar pressure vessels with a thin (<2 mm), non-Al liner and high fiber fraction. Our primary goal is to assess the *cryogenic* strength of these prototype composite vessels after 1,500 thermomechanical H_2 cycles, while secondary objectives will be accomplished in parallel to (1) measure LH_2 pump performance at 700 bar after 6,000 refuelings (~24 tonnes of LH_2), (2) demonstrate lightweight vacuum jackets for cryogenic H_2 pressure vessels, and (3) design and fabricate an experimental cryogenic H_2 storage system with 5.6 kg H_2 capacity.

In order to achieve the thermomechanical cycling, a LH_2 testing facility will be constructed next to the existing 875 bar LH_2 pump, capable of rapidly cycling full scale (63.5 L) non-certified cryogenic pressure vessels up to 700 bar and performing strength testing of those vessels up to 160 K, 1,300 bar. One to two vessels could be cycled at the same time in this single-manned, remotely operated facility that would also include a vent stack and a 40 kW heat exchanger.

RESULTS

The time period (July 2014 to July 2015) covered by this report focused on five tasks.

Development of Thin-Lined, High Fiber Fraction Vessels

Following the room temperature tensile testing done in FY 2014, ring burst tests, cryogenic tensile test, and pipe welding test completed the small-scale testing for the development of thin-lined high fiber fraction vessels. A design study was then carried out, including liner fatigue and finite element analyses.

The ring burst test procedure was used to evaluate liner buckling after autofrettage, where a liner "ring" (about 1.5 in wide) is overwrapped with a thin carbon fiber ring and then pressurized. This test enables to experimentally determine the minimum thickness the liner can have before it buckles. Thicknesses between 1.3 mm and 1.8 mm were shown to be sufficient for our conditions. Preliminary off-site cryogenic tensile strain testing was then conducted. This mechanical testing was necessary to determine basic variations of the properties of the liner material at cryogenic temperatures, such as Young modulus, elastic strain and tensile (ultimate) strength. It was observed that both the Young modulus and the elastic strain increase with decreasing temperatures. Also, the ultimate strength varied from 80 ksi at room temperature to almost 200 ksi at cryogenic LN_2 temperature. The results from the weld quality testing, tensile tests and ring burst tests showed that the selected material would perform as required.

A design study concerning the construction of the thin lined filament wound composite prototype pressure vessel was then carried out. The pressure vessel was designed based on the American Society of Mechanical Engineers

(ASME) Boiler and Pressure Vessel Code, Section X for Class III vessels with non-load sharing liners for gaseous hydrogen stationary service. A finite element analysis was also performed. The composite design was developed based on netting analysis and a helical-to-hoop fiber stress ratio of 75%. The hoop plies were consolidated into four groups to limit the number of elements required to uniquely model the helical and hoop layers. The dome shape for this pressure vessel was developed using geodesic-isotensoid theory. A winding table was generated.

Safety Analysis and Approval of 2.8 m^3, 65 bar Vessel for Containment of Non-Certified Pressure Vessels during Pressurization and Cycling

Following the safety plan submitted to DOE in June 2014 and a visit from the DOE H_2 Safety Panel in August 2014, it was decided by DOE management that authorization for the design and operation of the containment of non-certified pressure vessels under cycling and strength testing conditions should ultimately be granted by LLNL's pressure safety committee. Internal reviews were performed with pressure and containment experts leading to the ultimate approval of the operation as initially proposed.

Civil Construction of the H_2 Vessel Test Facility

Civil construction of the H_2 vessel test facility started in early FY 2015, and was completed in February 2015. It consisted of the construction of several concrete pads next to the existing LH_2 pump to accommodate a 100 psi air compressor, a control room, support racks for cryogenic high pressure H_2 lines, instrumentation and control air, and a 30 ft by 30 ft pad where the H_2 equipment (containment vessels, vent stacks, heat exchanger) will be installed. Figure 1 is a picture of the completed civil construction together with markers showing the future location of the main H_2 components.

Manufacture and Cryogenic Strength Test of the First Thin-Lined, Full Scale (63.5 L), 700 bar Pressure Vessel Prototype

The first thin-lined full scale 700 bar prototype vessel was fabricated by Spencer Composites then delivered to LLNL for cryogenic strength testing. Based on weight and geometrical measurements, we estimated that the vessel had 81% volumetric efficiency (ratio between inner and outer volume). The vessel was installed in an unmanned pressure test cell and initially filled with liquid N_2 at atmospheric pressure. It was then pressurized with room temperature N_2. Given the difficulty of maintaining a reasonable pressurization rate, the vessel underwent rather large pressure spikes (see Figure 2) before bursting at 1,560 bar and at an estimated temperature of 150 K. Based on the analysis of these results, DOE agreed to validate this go/no-go milestone.

Assembly of the H_2 Vessel Test Facility

Assembly of the test facility started after passing the first go/no-go milestone (previous task) and included instrumentation (pressure transducers, temperature sensors, vacuum transducer, H_2 sensor), air controlled valves (rated for cryogenic H_2 up to 30,000 psi), lines and fittings (rated for cryogenic H_2 up to 20,000 psi), vent stacks, 40 kW heat exchanger, and the containment vessel (Figure 3).

We anticipate completing construction of the H_2 test facility (without the heat exchanger, scheduled to arrive during the fall) by the end of FY 2015 allowing the beginning of prototype vessel cycle testing by that time.

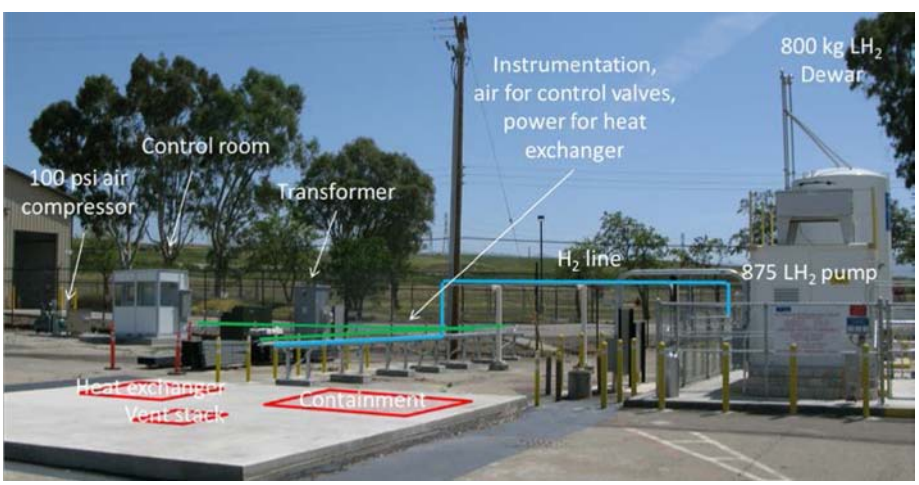

FIGURE 1. Completed site construction of the future H_2 test facility. Future locations of the main components (heat exchanger, vent stack, containment vessel and H_2 line) are shown.

CONCLUSIONS AND FUTURE DIRECTIONS

Small scale tests (welded/non-welded, LN_2/room temperature tension tests, and ring tension tests) were first carried out to determine the behavior of candidate liner metals for the prototype vessels. This was followed by a finite element analysis based on the geometrical and cycling requirements for the thin lined, carbon fiber overwrapped prototype pressure vessel, to help determine winding patterns. The first full scale prototype was then fabricated by Spencer Composites Corporation, and tested at LLNL. We successfully completed the cryogenic strength test of 63.5 L prototype with 81% volumetric efficiency burst at 1,560 bar, which represented the first go/no-go milestone for this project. In parallel, we completed the civil site construction and control room installation for the H_2 test facility. LLNL safety approval for simultaneous testing of multiple vessels within the containment vessel was also received.

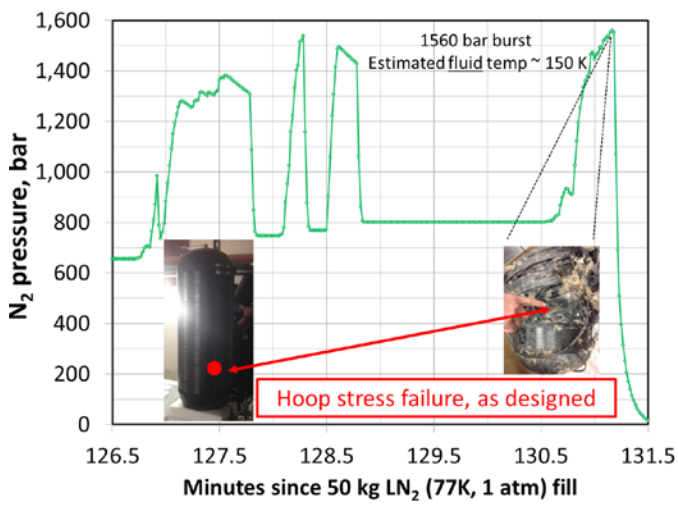

FIGURE 2. Cryogenic strength test of 63.5 L prototype with 81% volumetric efficiency burst at 1,560 bar

Future directions include the following:

- Fabricate two 63.5 L prototype vessels for cycle and subsequent strength testing
- Complete assembly and commissioning of H_2 test facility
- Cycle test two prototype vessels 1,500 times each with cryogenic H_2 followed by a strength test; a successful pressure test of either prototype with 80% volumetric

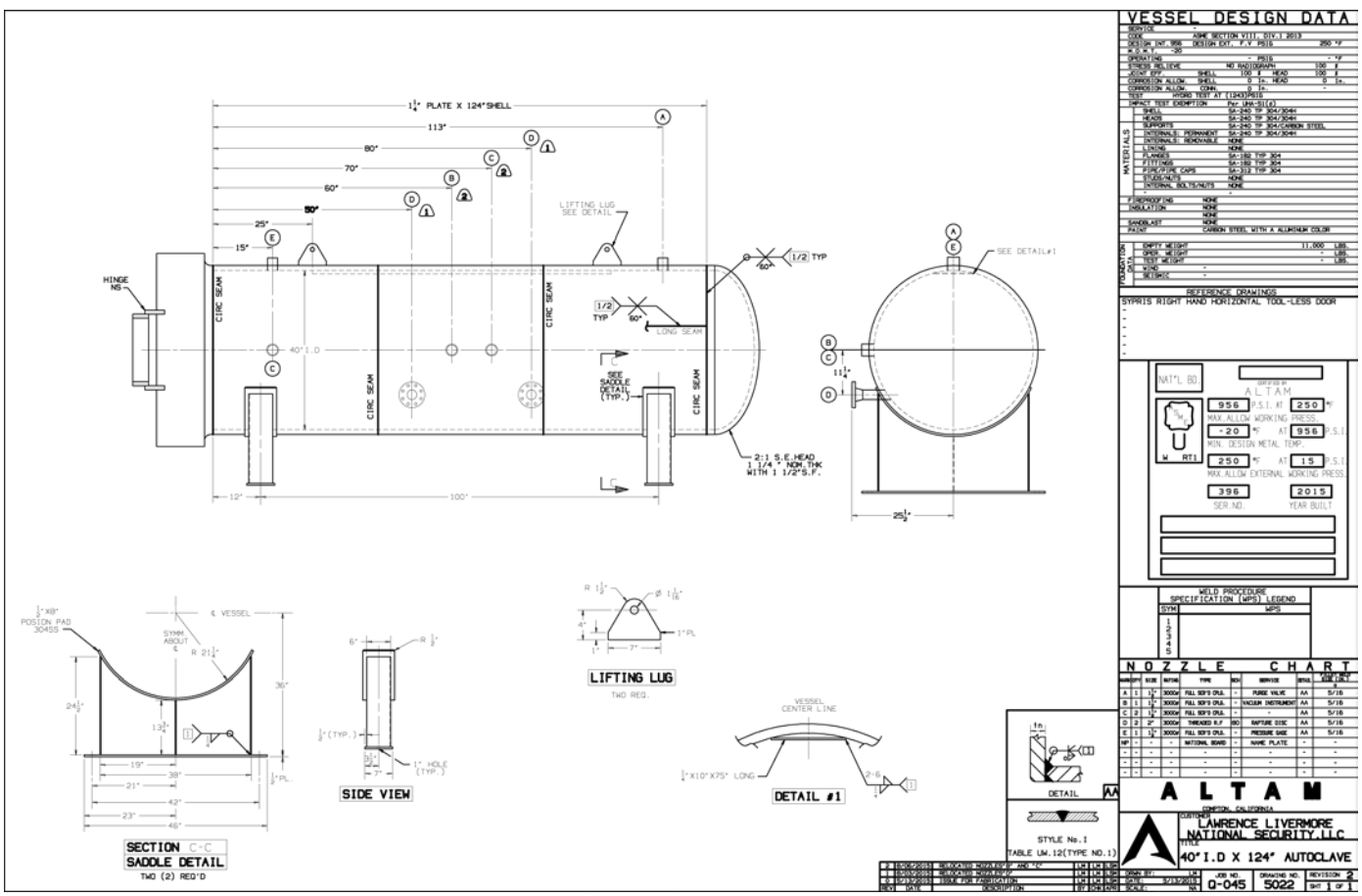

FIGURE 3. ASME certified 65 bar containment vessel design. A hinged-door will be installed on the left hand side.

efficiency when refueled at 72 g H_2/L density from the LH_2 pump will complete the second go-no go milestone

SPECIAL RECOGNITIONS & AWARDS/ PATENTS ISSUED

1. Threaded Insert for Compact Cryogenic-Capable Pressure Vessels, Francisco J. Espinosa-Loza, Timothy O. Ross, Vernon A. Switzer, Salvador M. Aceves, Nicholas J. Killingsworth, Elias Ledesma-Orozco, US Patent 9,057,483 B2, June 16, 2015.

FY 2015 PUBLICATIONS/PRESENTATIONS

1. A. Weisberg, S.M. Aceves, "The potential of dry winding for rapid, inexpensive manufacture of composite overwrapped pressure vessels," International Journal of Hydrogen Energy, Volume 40, pp. 4207-4211, 2015.

2. Salvador M. Aceves, Francisco Espinosa-Loza, John W. Elmer, Robert Huber, "Comparison of Cu, Ti and Ta Interlayer Explosively Fabricated Aluminum to Stainless Steel Transition Joints for Cryogenic Pressurized Hydrogen Storage," International Journal of Hydrogen Energy, Volume 40, pp. 1490-1503, 2015.

REFERENCES

1. Aceves S.M., Espinosa-Loza F., Ledesma-Orozco E., Ross T.O., Weisberg A.H., Brunner T.C., et al., "High-density automotive hydrogen storage with cryogenic capable pressure vessels." International Journal of Hydrogen Energy 2010;35:1219–26. doi:10.1016/j.ijhydene.2009.11.069.

2. Petitpas G, Aceves S.M., "Modeling of Sudden Hydrogen Expansion from Cryogenic Pressure Vessel Failure." International Conference on Hydrogen Safety, San Francisco: 2011.

3. Aceves S.M., Petitpas G., Espinosa-Loza F., Matthews M.J., Ledesma-Orozco E. "Safe, long range, inexpensive and rapidly refuelable hydrogen vehicles with cryogenic pressure vessels." International Journal of Hydrogen Energy 2013;38:2480–9. doi:10.1016/j.ijhydene.2012.11.123.

4. Kircher O., Greim G., Burtscher J., Brunner T. "Validation of cryo-compressed hydrogen storage (cch2)–a probabilistic approach." Proceeding of the International Conference on Hydrogen Safety, San Francisco: 2011.

5. Paster M.D., Ahluwalia R.K., Berry G., Elgowainy A., Lasher S., McKenney K., et al. "Hydrogen storage technology options for fuel cell vehicles: Well-to-wheel costs, energy efficiencies, and greenhouse gas emissions." International Journal of Hydrogen Energy 2011;36:14534–51. doi:10.1016/j.ijhydene.2011.07.056.

6. Ahluwalia R.K., Hua T.Q., Peng J-K., Lasher S., McKenney K., Sinha J., et al. "Technical assessment of cryo-compressed hydrogen storage tank systems for automotive applications." International Journal of Hydrogen Energy 2010;35:4171–84. doi:10.1016/j.ijhydene.2010.02.074.

7. Ahluwalia R.K., Hua T.Q., Peng J-K., Roh H.S., Bailey J., Kumar R. "System Level Analysis of Hydrogen Storage Options," DOE Annual Merit Review, Washington DC: 2012.

IV.D.3 Enhanced Materials and Design Parameters for Reducing the Cost of Hydrogen Storage Tanks

David W. Gotthold (Primary Contact)
Pacific Northwest National Laboratory (PNNL)
PO Box 999, MSIN
Richland, WA 99352
Phone: (509) 375-2073
Email: David.Gotthold@pnnl.gov

DOE Manager
Grace Ordaz
Phone: (202) 586-8350
Email: Grace.Ordaz@ee.doe.gov

Subcontractors
- Hexagon Lincoln, Lincoln, NE
- Ford Motor Company, Dearborn, MI
- Toray Composites America, Decatur, AL
- AOC, LLC, Collierville, TN

Project Start Date: January 18, 2012
Project End Date: June 30, 2016

Overall Objectives

- Reduce carbon fiber (CF) usage and hydrogen tank cost through a series of combined material and design approaches for a cumulative 37% cost savings
- Reduce tank cost by reducing composite mass through (1) resin matrix modifications and alternatives, (2) CF surface properties that increase load translational efficiency, (3) alternate CF placement and materials, and (4) enhanced operating conditions to increase the energy density vs. pressure
- Demonstrate the combined costs reductions through modeling, materials, and burst testing

Fiscal Year (FY) 2015 Objectives

- Fabricate set of six test tanks for each identified design improvement: (1) resin matrix modifications and alternatives, (2) CF surface properties that increase load translational efficiency, and (3) alternate CF placement and materials.
- Complete burst testing of all tank sets to validate design improvements
- Develop scalable process for resin modification with nanoparticulates and evaluate performance with test tanks

Technical Barriers

This project addresses the following technical barriers from the Manufacturing R&D section of the Fuel Cell Technologies Office Multi-Year Research, Development, and Demonstration (MYRDD) Plan:

(A) System Weight and Volume

(B) System Cost

(G) Materials of Construction

(J) Thermal Management

(L) Lack of Tank Performance Data and Understanding of Failure Mechanisms

Technical Targets

This project contributes to achieving the following DOE milestone from the Manufacturing R&D section of the Fuel Cell Technologies Office MYRDD Plan:

- By 2020, the project will develop and verify onboard automotive hydrogen storage systems achieving 1.8 kWh/kg system (5.5 wt% hydrogen) and 1.3 kWh/L system (0.040 kg hydrogen/L) at a cost of $10/kWh ($333/kg $H_{2\ stored}$). Progress toward targets shown in Table 1.

TABLE 1. Progress toward Meeting Technical System Targets for Onboard Hydrogen Storage for Light-Duty Fuel Cell Vehicles

Storage Parameter	Units	2020 Targets	PNNL 2015 Status
System Gravimetric Capacity	kg H_2/kg system	0.055	0.051
System Volumetric Capacity	kg H_2/L system	0.040	0.027
Storage System Cost	$/kWh net	10	15.37

FY 2015 Accomplishments

- Low cost resin alternative developed and tested with equivalent or better performance than existing epoxy resin that, based on analysis by Strategic Analysis, will reduce the storage system cost by $0.59/kWh compared to DOE's 2013 baseline
- Optimized nanoparticulate materials and processing selected and scaled to tens of gallons of modified resin to enable production of 70l batches of modified resins. The modified resins did not show increases in burst pressure and caused increased manufacturing variations

- Alternate winding patterns tested, improved high shear failure model developed that more accurately represents high shear layers and determined that existing winding pattern is near optimal for the selected tank dimensions and manufacturing processes
- Eleven sets of six tanks built and burst tested to evaluate previous theoretical design improvements with statistically significant sample sizes

✧ ✧ ✧ ✧ ✧

INTRODUCTION

The goal of this research is to reduce the cost of compressed hydrogen storage vessels by at least 37% from the current high volume projections of $17/kWh to $11/kWh for commercialization in early market and light duty hydrogen fuel cell vehicles. The cost and performance baseline comparisons are the current 70 MPa Type-IV pressure vessel (high strength, standard modulus carbon fiber in an epoxy matrix filament wound on a high density polyethylene liner). The high strength carbon fiber composite can account for nearly 70%–80% of the overall tank costs. Therefore, our research objective is to reduce carbon fiber usage and associated tank cost through a series of combined material and design improvements that are estimated to total nearly 37% of the project initial baseline tank cost. The project has identified through modeling a series of material design optimizations and experiments that achieve the cost savings goal. It is probable that these cost savings, combined with future reductions in CF cost could lead to the 50% cost reduction toward the ultimate DOE target.

APPROACH

The project takes a holistic approach to improve performance by lowering the required gas pressure at lower operating temperature, refining the tank composite design with local reinforcement and hybrid layups, plus increasing the composite translation efficiency with material modifications at the composite constituent level. The project team includes industry experts in each of the following focus areas of improvement: enhanced operating conditions to improve energy density/pressure ratios, load translational efficiency improvements by CF surface modification, resin matrix modifications and alternatives, and alternate fiber placement and materials. We expect these savings approaches to be compatible and additive.

RESULTS

The key work for FY 2015 was to validate the previously identified design and material improvements by fabricating and burst testing a set of six tanks with each design modification. In total 66 tanks were made and burst tested and the results are summarized in Table 2.

Improved and Modified Resins

Based on work in FY 2014, a low cost modifed vinyl ester resin was developed based on a commercially standard T015 vinyl ester resin. The new resin, XR-4079, was modified to have a reduced tackiness and optimized viscosity for nanoparticle integration. Tanks were made with both standard 24k tow carbon fiber with epoxy sizing and with 12k

TABLE 2. Summary of measured tank data for the 35.4 L test tanks. The burst data is all measured relative to the baseline tank. The rightmost column is the estimated total tank masses for a full-size 145 L tank.

				Estimated Tank Masses at 100% Burst					Tank Volume 35.4L	Tank Volume 145L
		Actual Relative to Baseline		Estimated Mass** at 100% Burst	Carbon Fiber, kg	Resin kg	Liner & Bosses kg	Total Mass kg	Total Composite @ 1 Test Tank	Total Composite @ 1 Fullscale Tank
Description		Mass	Burst							
	Baseline	100.0%	100.0%	100.0%	18.0	8.4	6.8	33.2	26.4	108.1
Low cost Resins										
	Baseline + Resin 1 Substitution	95.3%	100.0%	95.3%	18.0	6.9	6.8	31.6	24.8	101.7
	Baseline+Resin1+12kT700+Alt. Sizing	93.2%	101.2%	92.3%	17.7	6.1	6.8	30.7	23.9	97.7
Modified Resins										
	Baseline + Resin 1 + Nano Mod 1	96.1%	87.4%	107.0%	20.5	8.2	6.8	35.5	28.7	117.7
	Baseline + Resin 1 + Nano Mod 2	95.8%	89.9%	104.3%	20.0	7.8	6.8	34.6	27.8	113.9
Fiber Winding Patterns										
	Sorted HAHs, Interspersed with LAH	95.0%	91.0%	102.4%	18.5	8.7	6.8	34.0	27.2	111.4
	Sorted HAHs, No Interspersion	88.0%	83.0%	101.8%	18.4	8.6	6.8	33.8	27.0	110.6
	Baseline with 1 Adj Removed	96.0%	95.0%	100.0%	17.9	8.4	6.8	33.2	26.4	108.1
	Baseline with 2 Adj Removed	91.0%	88.0%	100.6%	18.1	8.5	6.8	33.4	26.6	109.0
Alternate Fibers										
	Baseline with T720 Substitution	96.2%	104.0%	93.3%	17.3	6.9	6.8	31.0	24.2	99.0
	Baseline with T800 Substitution	98.7%	112.6%	89.9%	15.9	7.1	6.8	29.9	23.1	94.5

tow carbon with sizing optimized for vinyl ester resins. Both fibers showed reduced mass compared to the baseline tanks.

For tanks made with the standard 24k tow T700 carbon fibers, the average burst pressure for these tanks was exactly the same as the baseline tank. The reduction in mass was due to the reduced viscosity of the resin leading to a high CF volume fraction in the final tank. This is reflected in the same CF mass (18 kg) as the baseline tank, and the reduced resin mass (6.9 kg vs. 8.4 kg). A full scale tank would weigh 101.7 kg vs. 108.1 kg for a baseline epoxy tank.

For the tanks made with the 12k T700 fiber with a sizing optimized for vinyl ester resins, the measured burst pressure was improved by 1.2% over the baseline tank due to improve adhesion between the resin matrix and the fibers. The improved performance is visible in the burst tank shown in Figure 1, where the broomstraw-like appearance is an indication of improved energy transfer. This improved burst pressure means that the carbon fiber content can be reduced from 18 kg to 17.7 kg and still achieve the same burst pressure as the baseline tank. When combined with the reduced resin cost (~50% of standard epoxy resins), this will lead to a 5%–7% cost reduction in the full sized tanks.

Alternative fiber placement

Despite initially promising model predictions, fiber placement resulted in lower burst pressures. Extensive work was done to understand the mismatch between the modeled and measured burst pressures for the alternate winding patterns. Hexagon Lincoln reviewed a range of different failure models and observed that burst performance correlated well with the Yamada-Sun combined stress (or strain) failure criteria [1]. The Yamada-Sun model combines both the uniaxial and shear stresses (or strains) to better predict failure when there is a high shear component.

$$\left[\frac{\sigma_1}{X_1}\right]^2 + \left[\frac{\tau_{12}}{S_{12}}\right]^2 = 1$$

FIGURE 1. Image of burst tank made with vinyl ester resin

The equation accounts for both the uniaxial stress (σ_1) and shear stress (τ_{12}) and scales both to the corresponding uniaxial failure strength (X_1) and shear failure strength (S_{12}). The Yamada-Sun failure criteria can also be expressed in terms of the ratios of the applied uniaxial and shear strains to the corresponding failure strains. With this new model, shown in Figure 2, we can now accurately predict failures for designs with higher interlaminar shear. However, this new understanding implies that the current designs are near at least a local optimum, as the most load is taken up by the purely tensile carbon fiber, not the lower strength matrix needed for shear. At this point, we continue to review the model to see if there are significant improvements to be made, but the likelihood of significant improvement is reduced.

Alternative fibers, T720 and T800, were also made into tanks to evaluate opportunities for fiber strength optimization. While significant weight reductions were observed—6.7% for the T720 and 10.1% for the T800 fibers—the increased cost of these fibers outweighs the potential savings from mass reductions.

Enhanced Operating Conditions

Initial materials testing has been initiated to validate the feasibility of low temperature gas storage. Initial tests have been completed for standard high density polyethylene (HDPE) at dry-ice temperatures. For the purposes of testing the HDPE, button head dog-bone type tensile samples were fabricated from standard HDPE rod stock. Samples were cooled for at least two hours in crushed dry-ice to ensure cold temperature saturation at -78.5°C. The dwell time was determined by monitoring a similar HDPE sample with a thermocouple implanted inside it.

The tensile tests clearly showed increased modulus and ultimate tensile strength (UTS) for the HDPE with decreasing temperature at both dry-ice and liquid nitrogen (LN_2) temperatures. No significant changes in ductility were observed within this temperature range. For example, the UTS was nearly 50% higher at dry-ice temperatures and 70% higher at LN_2 temperatures relative to room temperature. Likewise, the modulus was increased by 60% and 125% for dry-ice and LN_2 temperatures respectively as compared to room temperature. Elongation of at least 20% was observed at all temperatures.

CONCLUSIONS AND FUTURE DIRECTIONS

Research during FY 2015 has demonstrated the challenges between modeling and full scale test data, with better than expected results for the alternative resins, and worse than expected for the nanoparticle modified and alternate winding patterns.

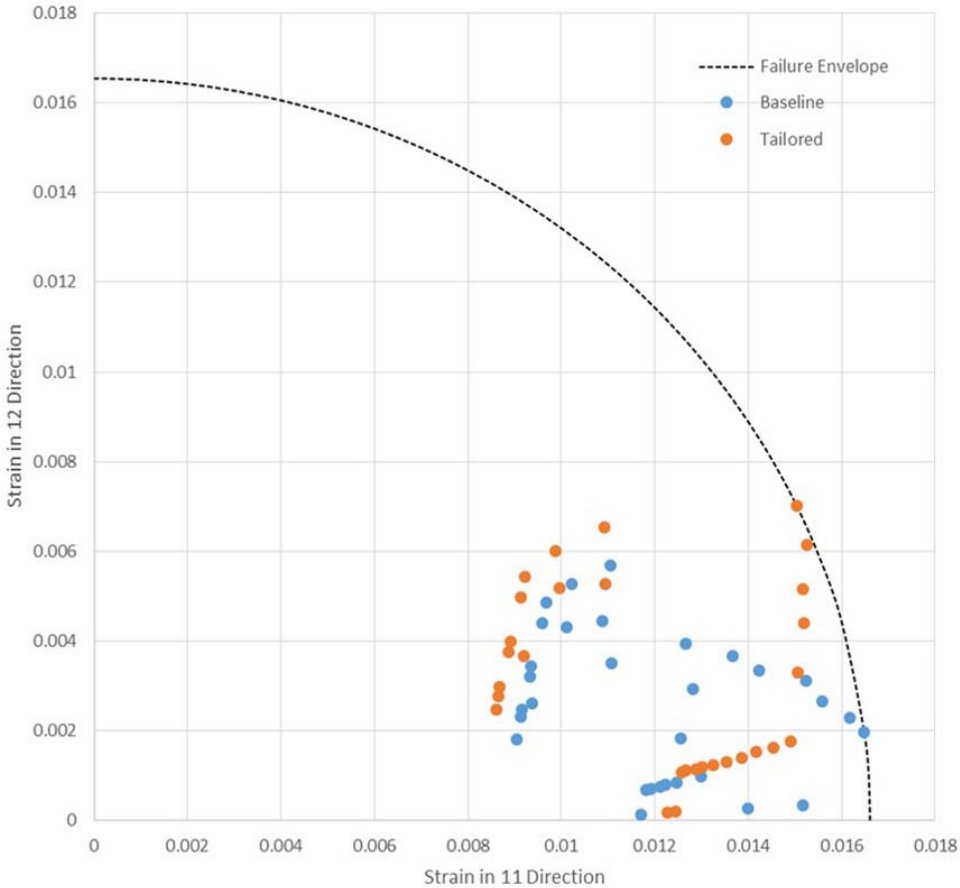

FIGURE 2. Tensile and shear strains for discrete lamina in both the baseline and tailored tank designs. The arc is the Yamada-Sun combine tensile-shear failure criteria, while the standard failure criteria only considers tensile strain (x-axis).

FY 2016 Future Work

- Fabricate and fatigue test impact damaged tanks to further validate the performance of the new vinyl ester resin for potential commercial usage
- Perform mechanical properties tests at low temperature enhanced operating conditions for key materials, including stability of all key structural materials and performance of insulation
- Coordinate vehicle-level enhanced operating conditions with the infrastructure and delivery model developed by Argonne National Laboratory
- Report project results of modeling, material testing, and tank fabrication and burst testing

FY 2015 PUBLICATIONS/PRESENTATIONS

1. D.W. Gotthold et al. 2015. "Enhanced Materials and Design Parameters for Reducing the Cost of Hydrogen Storage Tanks." Project ID# ST101. DOE Fuel Cells Office Annual Merit Review, June 8–12, 2015, Washington, DC. Pacific Northwest National Laboratory, Richland, WA.

REFERENCES

1. Yamada, S.E. and C.T. Sun, "Analysis of Laminate Strength and Its Distribution." Journal of Composite Materials, 1978. **12**(JUL): p. 275–284.

IV.D.4 Next Generation Hydrogen Storage Vessels Enabled by Carbon Fiber Infusion with a Low Viscosity, High Toughness System

Brian Edgecombe
Materia, Inc.
60 N. San Gabriel Blvd.
Pasadena, CA 91107
Phone: (626) 584-8400, Ext. 210
Email: bedgecombe@materia-inc.com

DOE Manager
Grace Ordaz
Phone: (202) 586-8350
Email: Grace.Ordaz@ee.doe.gov

Contract Number: DE-EE0006625

Subcontractors
- Montana State University (MSU), Bozeman, MT
- Spencer Composites Corporation, Sacramento, CA

Project Start Date: August 5, 2014
Project End Date: August 30, 2016

Overall Objectives

The project is focused on supporting the key DOE metrics for a 700-bar, Type IV tank by meeting the following objectives:

- Reduce the carbon fiber (CF) composite content by 35%
- Demonstrate cost of composite materials of $6.5/kWh; this component cost is an important element of the DOE 2020 system cost target of $10/kWh
- Demonstrate industry standard performance (burst strength of 1,575 bar and 90,000 cycle life)

Fiscal Year (FY) 2015 Objectives

- Select resin formulation compatible with process
- Demonstrate infusion on triaxial wound CF plates
- Evaluate static properties and void content on test plates
- Prepare and burst small tanks via infusion process
- Quantify effect of resin toughness and voids on mechanical performance of composites

Technical Barriers

This project addresses the following technical barriers from the Hydrogen Storage section of the Fuel Cell Technologies Office Multi-Year Research, Development, and Demonstration Plan:

(A) System Weight and Volume

(B) System Cost

(D) Durability/Operability

(G) Materials of Construction

Technical Targets

The project is focused on the technical targets highlighted in Table 1 related to the gravimetric and cost metrics of onboard automotive hydrogen storage systems. Since a significant portion of the cost is directly from the CF composite overwrap, the project aims to reduce the amount of composite necessary to meet the tank specifications. During FY 2015 the project has met important milestones. However, we are not yet able to estimate the gravimetric and cost values.

TABLE 1. Progress towards Technical Targets for Onboard Automotive Hydrogen Storage System

Characteristic	Units	2020 Target	FY 2015 Status
Gravimetric	kWh/kg system	1.8	TBD
System Cost	$/kWh at 500,000 units per year	10	TBD

TBD – to be determined

FY 2015 Accomplishments

- Demonstrated the ability to make composite-overwrap pressure vessels (COPVs) and lab-scale prototypes with the less conventional vacuum infusion process
- Achieved burst strength above design pressure (>1,575 bar) for a vacuum-infused COPV (small-scale prototype)
- Prepared thick plate infusion (32 mm) with low void content (<0.5 vol%)
- Completed evaluation of static properties and void content on test plates
- Optimized the processing of COPVs via novel vacuum infusion to obtain low-void composites (<0.1 vol%)
- Started fatigue/cycle testing on composite specimens with high and low void content to elucidate the relationship between void content and composite performance

✧ ✧ ✧ ✧ ✧

INTRODUCTION

The Office of Energy Efficiency & Renewable Energy has established aggressive performance targets for Type IV hydrogen storage vessels for Year 2020. Current designs and materials of construction for COPVs within the industry do not reach the performance targets as shown by the base case published by Ahluwalia from Argonne National Laboratory. The specialty chemical producer, Materia, has developed a novel composite resin system, Proxima®, with ultra-low viscosity (<15 cP) which enables vacuum infusion processing for thick CF composite components. The use of this process with Proxima circumvents some challenges inherent with traditional wet filament winding such as the presence of voids and dry spots. Although the concept of infusing dry filament wound structures has been mentioned in the open literature, the small inter fiber gaps associated with high performance CF composites results in considerable significant processing difficulties. Therefore, the commercial application of this approach appears to be limited which may be related to traditional resins possessing viscosities >200 cP.

In addition to reducing void content, Proxima-based composites have significantly improved fracture toughness and fatigue performance over currently employed composites for hydrogen storage tanks. The project seeks to leverage this new combination of tough resin and new process to produce composite overwrap with better performance, especially in fatigue and damage tolerance testing. These high performing composites will enable the reduction of the quantity of CF composite overwrap which alone can account for over 75% of the storage tank system cost. The tank manufacturing costs for this new process is expected to similar to current manufacturing costs with wet-winding. By reducing the CF composite content in COPVs by 35%, the project aims to reduce the cost and weight of COPVs and contribute to meeting the DOE 2020 cost target of $10/kWh.

APPROACH

Since the project requires expertise in a variety of fields, the project team includes Spencer Composites Corporation to lead the specialized filament winding effort and MSU to evaluate composite materials and also use finite element analysis (FEA) models to anticipate problem areas in tanks designs. Materia is leveraging its experience in infusion process optimization with low viscosity resin (<15 cP) to demonstrate a series of prototype parts including tanks and model flat plates of filament wound composites. In order to manage the risks associated with a new resin and a new process for COPVs, the project activities were divided into the following stages and associated objectives.

- Process optimization: demonstrate infusion feasibility with CF (high-thickness plates)
- COPV design: develop preliminary designs for COPVs using FEA models and materials data (static and fatigue)
- Processing optimization with COPVs: extend processing technique to small COPV prototypes
- Design optimization: quantify relationship between void defects and composite performance
- Scale-up of process: demonstrate and refine process and design with full-scale COPVs to maximum cost effectiveness of performance

In particular, the project team wanted to deploy sufficient resources during FY 2015 on the significant challenge of conducting vacuum infusion to produce high-quality COPVs.

RESULTS

The start of FY 2015 coincided with the ramp-up of this new project with its initial focus on the qualification of a resin formulation for the challenging processing conditions. In vacuum infusion, the rate of resin infusion is dominated by viscosity. Therefore, a modification was made to an existing a resin formulation to allow for the minimum in viscosity (<15 cP) for >4 h. Using traditional viscosity measurement techniques, the work time and viscosity was demonstrated to meet the preliminary targets. To ensure that the modifications of resin formulation did not adversely affect the mechanical performance of the resin, unreinforced resin castings were prepared and tested with success.

With a resin formulation appropriate for the application, processing studies were conducted using high-thickness, flat-plate CF laminates from unidirectional CF fabrics based on Toray T700 fiber. These fabrics are notorious for their low permeability during vacuum infusion processing. Therefore, these experiments provided a fast, low cost manner to provide feedback on the processing during vacuum infusion. The project team demonstrated the ability to produce low-void laminates (<0.5 vol%) with 32-mm thickness with infusion processing times under 2 h. This result was considered an important part of de-risking the key step of infusion of small scale COPVs.

Given the achievement of high quality flat CF composite plates, the processing efforts of the project team moved the focus to small scale COPVs. The infusion studies were conducted on Type III tanks with aluminum liners, 6-in. diameter by 18-in. length in order to speed development. By working with filament winding experts, a winding strategy was selected to achieve >1,575 bar burst strength and the design was validated by the production and testing of wet-wound epoxy tanks. As expected the dry-wound COPVs presented a series of challenges for the team. By optimizing the infusion ports, port placement, process aids and bagging techniques, steady progress was made in improvements until

FIGURE 1. Fully infused small-scale (7.5 liter) COPV

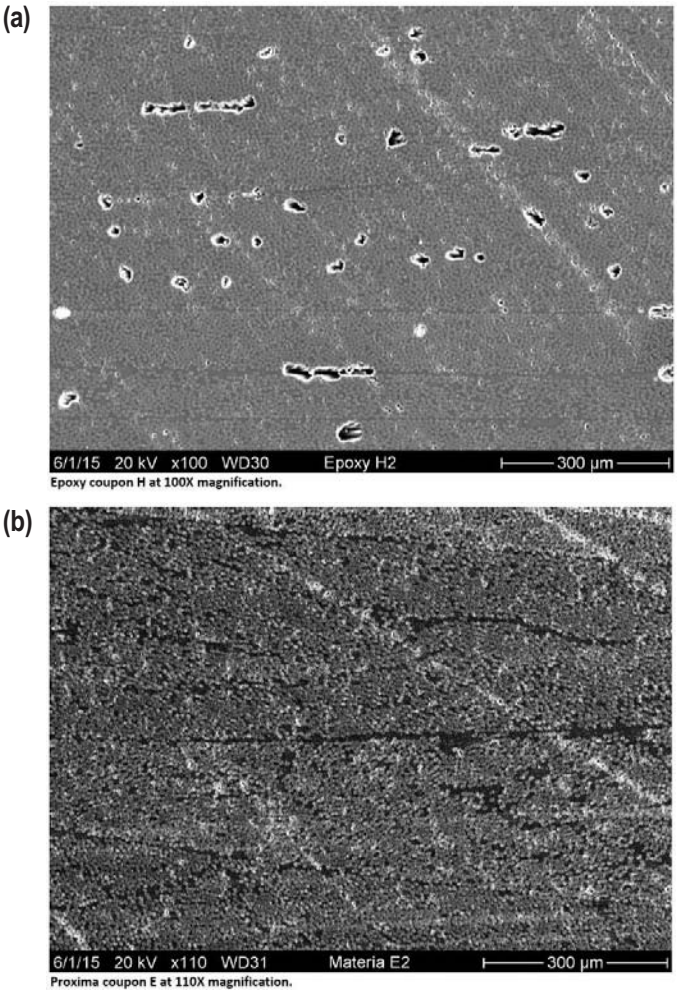

FIGURE 2. (a) Cross-section of wet-wound epoxy tank with voids (3% to 9% voids across seven regions); (b) Cross-section of infused Proxima tank with no voids

low-void tanks were obtained and repeated. A fully infused Proxima-based tank is shown in Figure 1. Some Proxima tanks were cut and compared for void content to analogous wet-wound epoxy tanks (as a reference). In Figure 2, representative images are shown of the void-containing epoxy tank wall and the low-void Proxima wall.

Although the void content was on target, some visible fiber buckling was observed from the process which had a negative effect on burst strength. In Table 1, burst strength values are compared of three infused Proxima tanks and wet wound epoxy tanks. Since burst strength is known to be sensitive to fiber bending, the first set of Proxima tanks did not reach the target of >1,575 bar and failures appeared to be starting from areas of wrinkles. However, the team is optimistic that significant improvements can be attained by reduction of fiber buckling. Several causes are under investigation, including the winding tension (lower than the epoxy control) and the crimping effect of the current design of infusion ports. Recently, working with a supplier, we were able to confirm that dry-winding can be conducted at the higher levels of tension shown in Table 1 without significant damage of fiber.

TABLE 1. Comparison of Epoxy COPVs with Proxima COPVs

COPV type	Winding Tension (lb)	Burst Strength (bar)	Comment
Epoxy controls (wet-wound)	8–11	1,822 (avg)	Failed near cylinder
Proxima (infused N3)	3–5	853	Failed near wrinkles
Proxima (infused, N5)	3–5	744	Failed near wrinkles
Proxima (infused, N4)	5–8	1,408	Failed near wrinkles
Proxima (infused)	8–10	TBD	In progress
Proxima (infused)	10–12	TBD	In progress
Proxima (infused)	12–14	1,688	Failed near dome transition

In order to support the experimental work at Materia, MSU has developed an infusion model which can be used to predict the flow front of the resin during the infusion process. Refinements of the model will be conducted based on development of permeability data of the dry-fiber. For the full scale prototypes, a preliminary design has been evaluated by Spencer and MSU, and planning has started to validate the assumptions in the model.

CONCLUSIONS AND FUTURE DIRECTIONS

From the current results of the project, the team has derived the following conclusions.

- Preparation of COPVs with <1% void content using vacuum infusion of dry filament wound form is viable, but requires further process optimization.
- Process configurations which eliminate fiber buckling upon application of vacuum appear to be an important consideration.

- Current FEA modeling approaches are useful for estimated static performance, but fatigue results will require extensive testing.

The following activities will be the area of focus in the future.

- Refine full-scale tank design and verify compatibility of vacuum infusion with Type IV polymer liners.
- Develop further fatigue data on plates and small-scale tanks in order to validate the ability to reduce the amount of carbon fiber.
- Develop cost estimates of tanks based on new designs and processes.

IV.D.5 Melt Processable PAN Precursor for High Strength, Low Cost Carbon Fibers (Phase II)

Felix L. Paulauskas (Primary Investigator),
Bob Norris (Primary Contact), Ken Yarborough, and Fue Xiong
Oak Ridge National Laboratory (ORNL)
MS 6053
Oak Ridge, TN 37831-6053
Phone: (865) 576-1179
Email: norrisrejr@ornl.gov

DOE Manager
Grace Ordaz
Phone: (202) 586-8350
Email: Grace.Ordaz@ee.doe.gov

Subcontractors
- Donald G. Baird, Judy Riffle, Jianhua Huang
  Virginia Polytechnic Institute and State University (Virginia Tech), Blacksburg, VA

Project Start Date: October 2013
Project End Date: Project continuation and direction determined annually by DOE

Overall Objectives

- Demonstrate means to achieve cost reduction of ≥25% in manufacture of carbon fiber meeting properties of industry baseline carbon fiber utilized in fabrication of composite vessels for hydrogen storage
- Develop and demonstrate new chemistry and spinning techniques and assess capability for advanced conversion technologies to meet needs in reducing carbon fiber manufacturing costs for fiber meeting program performance goals

Fiscal Year (FY) 2015 Objectives

- Complete extruder installation and checkout and any required modifications necessary to begin melt spinning precursor samples meeting progressively greater properties as evidenced by testing of converted carbon fiber. As scale-up from bench scale experiments utilizing a capillary rheometer does not entail just making larger quantities of precursor dope, it was anticipated that this would be completed in early FY 2015, but acknowledged it could take longer.
- Utilizing integrated effort of formulation and processing team members, down-select appropriate chemistry including polyacrylonitrile co-polymerized with methyl acrylate (PAN-MA) constituent levels and molecular weight of this recipe to allow spinning precursor that can be fully processed through conversion while not necessarily meeting ultimate project performance goals. With baselines established, optimum chemistry will be developed in iterations moving towards these ultimate objectives.
- Establish better and more precise stretching tools to facilitate low temperature drawing immediately after spinning and conversion trials with precursors to minimize time required in developing and demonstrating appropriate conversion protocol for producing carbon fiber.

Technical Barriers

High strength carbon fibers account for approximately 65% of the cost of the high pressure storage tanks. This project addresses the following technical barriers from the Hydrogen Storage section of the Fuel Cell Technologies Program Multi-Year Research, Development, and Demonstration Plan:

(A) System Weight and Volume

(B) System Cost

(D) Durability/Operatability

(G) Materials of Construction

High strength carbon fiber enables the manufacture of durable, lightweight, compressed hydrogen storage vessels for use in high pressure storage. Unfortunately, current high strength carbon fiber products are far too expensive to meet DOE goals for storage system costs.

Technical Targets

Working targets are approximate equivalence with Toray T-700 at substantially reduced production costs:

- 700 ksi ultimate tensile strength
- 33 Msi tensile modulus
- Production cost reduction of at least 25% versus baseline

Accomplishments

- Extruder installation and checkout were completed and a number of modifications were implemented in order to enable melt spinning of PAN precursor. Related spinning equipment such as spinnerets with larger hole

numbers, spin packs, and larger pressure chamber have been completed and installed. Initial attempts to directly feed PAN powder were met with significant difficulties; these difficulties were overcome by developing a simplified process for pelletizing the material for near-term trials. At the time of this report, fiber has been produced with the modified spinning system but the quality of this fiber is not sufficient for proceeding with conversion trials.

- Chemistry, spinning, and conversion teams collaborated to establish a baseline PAN dope recipe and a contract put in place to procure adequate quantities of a specific PAN-MA blend at a specific molecular weight for initial studies.
- Processes for producing and characterizing specific formulations of PAN and MA along with the effectiveness of various pasticizer approaches in suppressing the melt temperature to acceptable processing temperatures below the cross-linking temperatures have been established.
- Better and more precise stretching tools to (1) facilitate low temperature drawing immediately after spinning, and (2) enhance molecular orientation in conversion trials have been designed, built, and delivered. These tools will serve to more systematically minimize time required in developing and demonstrating appropriate conversion protocol for producing carbon fiber.

✧ ✧ ✧ ✧ ✧

INTRODUCTION

High strength carbon fiber enables the manufacture of durable, lightweight, compressed hydrogen storage vessels for use in high pressure storage. Unfortunately, current high strength carbon fiber products are too expensive to meet DOE goals for storage system costs. Developing and demonstrating a melt-spun PAN approach to producing precursor for carbon fiber will provide a more cost-effective route to achieving performance necessary for high pressure gas storage. Melt spinning removes significant costs in handling and recovering solvents involved in solution spinning as well as eliminating a significant bottleneck in production rates required by the time, space, and energy utilized in the solvent recovery steps. Although somewhat similar processes have been demonstrated in the past, no PAN-based carbon fiber is produced currently utilizing this approach due to specific materials employed in the previously demonstrated process and lack of investment from industry to revisit and revamp that process. It is anticipated that the melt-spinning approach could save 25% of cost involved in producing carbon fiber for high pressure gas storage systems and that additional savings may be possible in combination with ORNL advanced conversion approaches. It is also projected that the melt spinning process would be more attractive for PAN fiber production in the United States, possibly helping to revitalize some of the acrylic fiber business lost due to environmental concerns.

A major milestone was achieved during latter portions of Phase I with demonstration of carbon fiber properties exceeding the go/no-go point established at 15 Msi modulus and 150 ksi strength. Properties meeting follow-on milestone levels up to 25 Msi modulus and 250 ksi strength were also achieved. These properties were achieved with melt spun PAN produced at Virginia Tech and utilizing conversion protocol developed by ORNL in earlier work. The conversion protocol consists of a number of steps in simulating oxidation with DSC testing and then preliminary tensioning experiments in batch mode utilizing the customized ORNL precursor evaluation system. Small tows as spun at Virginia Tech were combined at ORNL to obtain a tow with ample number of filaments (~100) to enable progressive tensioning during multiple oxidative stabilization steps and specific shrinkage management in low and high temperature carbonization. During the last year, Phase I has been completed and activities in Phase II are now underway with resumption of the broader approach evaluating new chemical formulations, advanced spinning techniques, and novel conversion processes.

APPROACH

This project is structured into tasks focused on precursor development and conversion process improvements. Development and demonstration of melt-spinnable PAN is the project's primary precursor option. If successful, melt spinning is projected to be significantly less costly than wet spinning with capability to produce high quality, relatively defect-free precursor. This requires concurrent activities in both development of melt-stable PAN copolymer and blends as well as the processes necessary to successfully spin the formulations into filamentary tows. Melt processing of PAN is a difficult issue, although Virginia Tech and others have made modest progress over the last decade [2-6]. One of the principal problems is that polyacrylonitrile degrades (cross-links) even without main chain scission or weight loss, and this essentially precludes melt processing. Reactions of the side groups have been discussed in many reports [7-10]. These degradative reactions can take place both in an intra-molecular manner, but also via intermolecular branching and gelation, which quickly alters the capacity for these materials to be melt fabricated. At 200–220°C, the material can quickly increase in viscosity, thus rendering an intractable material in a very short time. Ideally, one would like to maintain constant viscosity for a required period, and practical considerations suggest that this should be at least 30 minutes or longer.

The following have been identified as key elements of the project approach:

- Melt-spun precursors are being formulated for evaluation with the goal of developing a palletized form for later melt-spinning. The optimum formulation of polyacrylonitrile, methyl acrylate and a ter-monomer will be determined based upon small scale spinning trials.
- Methods for handling, melting and spinning the polymer developed in Task 1 above are being developed to produce precursor fiber for the oxidative stabilization and carbonization conversion processes. Critical will be development of the spinning process including temperature, speed, pressure and draw profiles.
- Processing of the new polymer into finished carbon fiber will be necessary beginning with conventional processes. By applying conventional processes a good estimate of the cost benefit of the change in precursor alone will be obtainable and the technology will be developed to allow for introduction of the precursor into current commercial processing lines.
- Processing of the new polymer into finished carbon fiber using the alternative manufacturing processes will be assessed. By applying the alternative processes the synergistic cost savings of a less expensive precursor along with less expensive processing technologies will be obtainable.

RESULTS

During this period, the project team has accomplishments in completing appropriate upgrades and implementing/demonstrating the capabilities required to produce adequate quality and quantities of precursor fiber necessary to establish stable, continuous conversion processes. Although the team continues to utilize lower cost and no longer critical quantities of polyacrylonitrile co-polymerized with vinyl acetate (PAN-VA) formulations employed to demonstrate basic feasibility in Phase I for equipment checkout and technique development, the developmental focus has been fully transitioned to PAN-MA formulations projected to be necessary to achieve both economic and performance goals. The synthesis efforts at Virginia Tech have focused on the preparation of ranges of AN content poly(acrylonitrile-*co*-methyl acrylate) materials for small scale spinning trials. The parameters to be controlled in the synthesis are the molecular weight and molecular weight distribution, and the acrylonitrile content. All of these parameters, in conjunction with the plasticizer type and content and spinning parameters will determine the spinnability of a particular composition. The current objectives are to provide trial materials with approximately 95 wt% acrylonitrile and 5 wt% methyl acrylate although the team has selected somewhat lower levels for establishing project baselines. The materials are being screened in the modified capillary rheometer spinning apparatus using plasticizers such as water and acetonitrile to determine the spinnability.

Formulation Development

Recent formulation work has been focused on characterization of copolymer compositions, thermal properties of the copolymers in the presence of water and ethylene carbonate, and melt viscosities conducted under pressure to accommodate low-boiling plasticizers in the potential spinning compositions. PAN is typically spun from solutions of dipolar aprotic solvents because it has a melting point that is above the onset of cyclization (cross-linking), and therefore cannot be melt-processed without special conditions as sought after in this research. Comonomers, particularly vinyl acetate or methyl acrylate, can be introduced that disrupt intermolecular interactions among the polar nitrile groups and the polymer backbone. Randomly spaced comonomers can increase the distance between pendent nitriles and interrupt the sequences of nitriles. Plasticizers such as water, acetonitrile, and ethylene or propylene carbonate can likely reduce both t_g and t_m relative to the dry copolymers. Thus, the short-term objectives in this phase of the research include determination of thermal and rheological properties of polyacrylonitrile copolymers, and thermal and rheological effects of adding plasticizers to the formulations.

A sample of PAN-MA copolymer from a commercial producer that has a composition of 96 mol% of acrylonitrile and 4 mol% of methyl acrylate has been utilized for sensitivity studies. This corresponds to 93 wt% acrylonitrile and 7 wt% methyl acrylate. It has a weight average molecular weight of approximately 220,000 g/mol. It is anticipated that these copolymer properties may lead to the high strength carbon fibers that will be optimum for reinforcing the composites to be used for hydrogen storage. For comparisons, the project team has synthesized a series of copolymers with PAN-MA compositions. It is anticipated that copolymers with higher acrylonitrile compositions may lead to improved properties in the converted carbon fibers, but that melt-spinning will be more challenging as the acrylonitrile content is increased.

A PAN-MA copolymer that contained 94 mol% of acrylonitrile and 6 mol% of methyl acrylate (i.e., 91 wt% acrylonitrile and 9 wt% of methyl acrylate) was blended with an excess of water, dried down to approximately 20 or 50 wt% of water in the blend, then cold-pressed into pellets. The weight average molecular weight of this copolymer is approximately 130,000 g/mol. The thermogravimetric analysis (TGA) weight loss profiles of that copolymer and a blend of the copolymer with nominally 20 and 50 wt% of water are depicted in Figure 1. One can observe evaporation of the water at ~100°C in approximately the expected amounts, then a weight loss at about 300°C, likely corresponding to loss of some of the comonomer

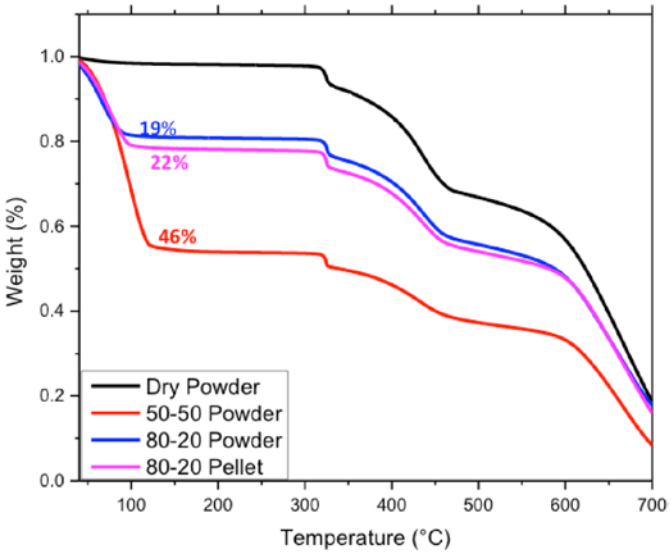

FIGURE 1. Weight loss profiles for PAN-MA with 94 mol% acrylonitrile and 6 mol% methyl acrylate

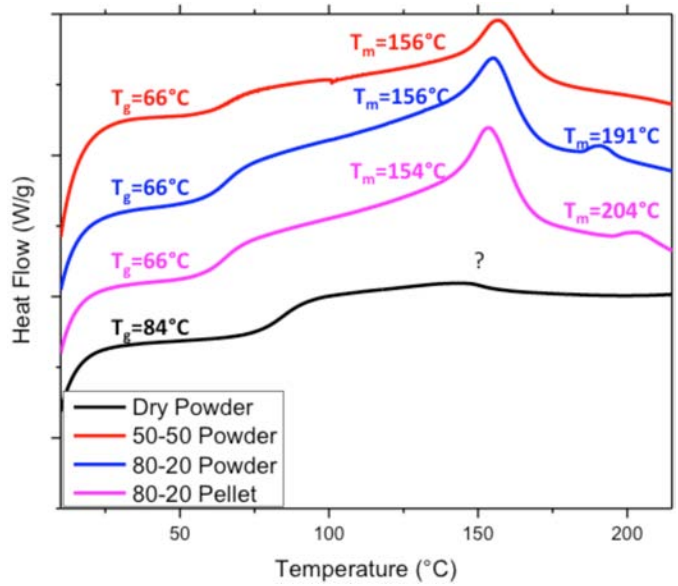

FIGURE 2. Thermal properties of PAN-MA with 94 mol% acrylonitrile and 6 mol% methyl acrylate and blends of that copolymer with water

residues. The amount of weight loss at 300°C is lower in this copolymer relative to the PAN-VA copolymer depicted in Figure 2, and this is likely due to the smaller amount of comonomer in this copolymer relative to that in the PAN-VA. Isothermal TGA scans of these two materials at 325°C show that the time required for the weight loss around 300°C is about 36 minutes for the PAN-MA and 49 minutes for the PAN-VA.

Differential scanning calorimetry (DSC) thermograms of these blends are shown in Figure 2. The dry copolymer has a t_g of 84°C that is depressed to about 66°C in both blends. All of the blends have a broad t_m region that peaks at approximately 155°C but that extends to approximately 175°C. The similarity of the transitions suggests that all of the blends have the maximum amount of water absorbed into the copolymer. It may be noteworthy, however, that the blends with 20 wt% of water show a second small melting endotherm at about 190–200°C that is absent in the blend with 50 wt% of water. It is encouraging that the melting endotherms of these blends are very similar to those observed for the PAN-VA blend. Viscosity profiles as a function of time will be important as a future comparison.

Work with a PAN-VA copolymer blend that contained 20 wt% of water has a maximum temperature in the melting endotherm range of about 180°C. This blend has a melt viscosity of 1,400–1,500 Pa·s at a shear rate of 72 s^{-1} and the viscosity at this temperature is stable over at least 40 minutes. This suggests that the blend may be spinnable from the melt under pressure. A polymer spinning aid formulation for the PAN-VA that contains the copolymer, a small amount of water, and ethylene carbonate as a plasticizer has a lower melting point by about 20°C than blends of this copolymer with water. This, or a similar composition, may serve as a valuable processing aid for both start-up and clean-up of a melt-spinning operation for PAN-VA. Blends of PAN-MA copolymers will require more investigation to evaluate and identify properties relative to the PAN-VA copolymers.

Spinning Process Development

Significant upgrades have been integrated to the extrusion system during the current reporting period. In addition to modifications to the extruder itself as described below, other key changes include (1) a much larger spin pack was designed, fabricated, sealed, and installed; (2) a larger spinneret was designed and procured; and (3) a larger pressure chamber and winder system was integrated. Even though the project focus has moved from PAN-VA to PAN-MA chemistry, the team decided to utilize older PAN-VA materials to work through feeding and initial spinning problems in order to conserve the more valuable PAN-MA materials for critical work in meeting targeted spun and converted fiber properties. Most spinning extruders are fed via pellets typically compounded by a preparatory melt extrusion process. Since thermal history of PAN dope is critical to not cross-linking the material, it had been hoped that this preparatory pelletization process might be avoided entirely which would both minimize cross-linking and provide additional cost-savings by eliminating a production step. Problems were encountered in getting powder to feed as the tackiness of the moist powder (moisture is required for plasticization) has resulted in nonuniform feed rates. The relatively open feed and extrusion process has also evolved significant portions of the moisture incorporated for plasticization resulting in materials also sticking once they are actually in the extruder.

Although it has not been concluded that the powder feed approach will not work (in fact there is some indication that BASF had some success in their work), the team concluded that it was more important to switch to a pelletizing approach in the near-term. It was thought that a commercial pasta extruder with an electronic cutting knife that could be used with the extruder to cut the strands into pellets at the desired length might be used for this purpose, but testing was not successful. Further more detailed discussion with persons having experience in this area led to consideration of a commercial meat grinder. The grinder as shown in Figure 3 was obtained and after a number of trials, success in making pellets at low temperature with hole diameters of 1/8 in was achieved as shown in Figure 4.

Utilizing the pellets as shown above, trial extrusion was run successfully using PAN-VA pellets plasticized with 20% water. For the first time, steady melt pressure and continuous PAN extrusion were achieved as shown in Figure 5. The efforts to purge PAN-VA out of the extruder/die with polypropylene failed. The screw had to be removed from the extruder for cleaning. Degraded PAN (dark brown in color) was still found on the screw.

Unfortunately most of the spinning trials have been unsuccessful in getting the PAN completely through and ejected from the extruder system. When the system is disassembled, degradation of PAN has been observed in essentially all extrusion experiments as evidenced by significant portions of darkened polymer representative of degradation through excessive cross-linking deposited in the screw chamber as well as frequently in other locations. The degradation is assumed to be a function of time and temperature exposure of the polymer. A contributing factor is believed due to the loss of water (plasticizer) at various places in the extrusion system. An early culprit was moisture leakage through the open hopper. After the hopper was sealed and pressurized, it was apparent that sealing the hopper only was not enough to prevent the PAN from degrading. The plasticization moisture appeared to now be leaking through the gap between the screw and the barrel resulting in significant degraded deposits on the screw as shown in Figure 6. After evaluation of several approaches to mitigate leaking, the spinning team chose to cut a small groove and install an O-ring on the root part of the screw to seal the gap (see Figure 7). The extruder has been tested under static and dynamic conditions and is now airtight.

Near the end of this reporting period, the team did generate PAN fibers using the 397-hole spinneret for the first time and wound them on a bobbin (see Figures 8 and 9). The polymer pellets used were PAN-VA copolymer containing

FIGURE 3. The LEM Products 12# meat grinder in the spinning laboratory

(a)

(b)

FIGURE 4. Wet PAN strands made with a meat grinder (a) and dried PAN pellets (b)

FIGURE 5. Fiber spinning using PAN pellets without the pressure chamber

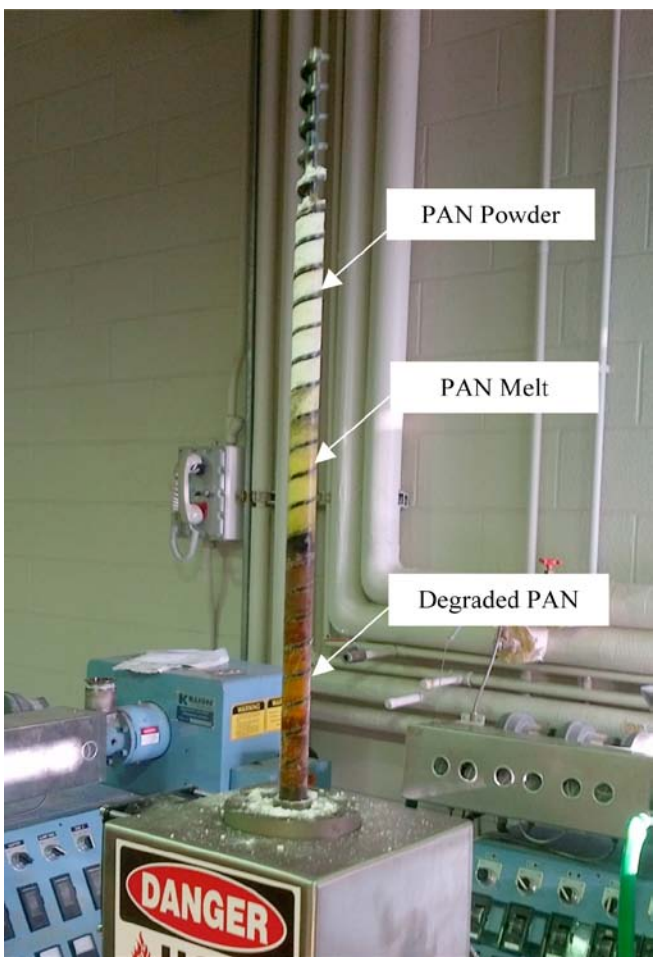

FIGURE 6. Polymer residual on the screw after trial extrusion

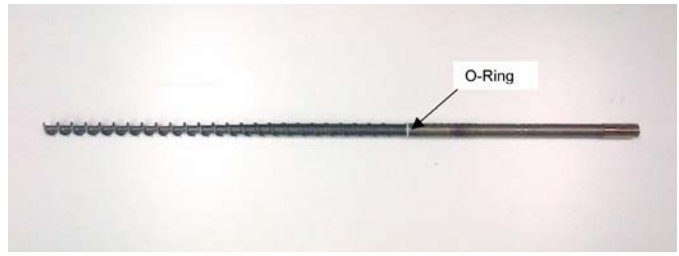

FIGURE 7. Modification of the screw by cutting a groove and installing an O-ring to provide an airtight dynamic seal between the screw and the barrel

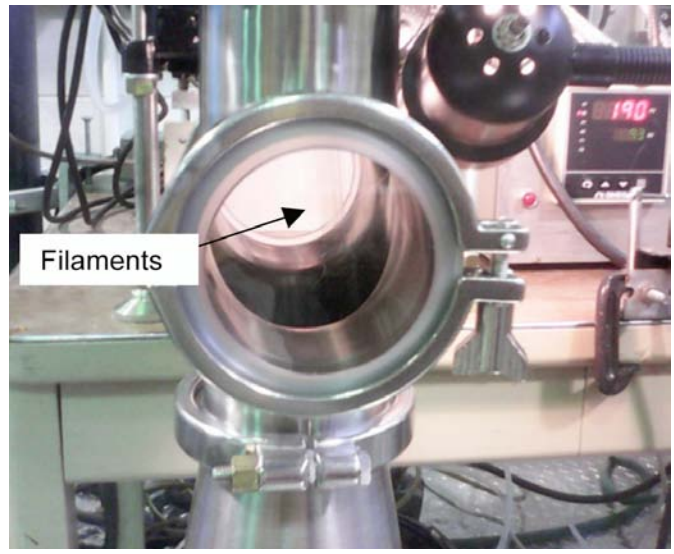

FIGURE 8. Melt-spinning of PAN fibers is in progress; the filaments could be seen through the sight window of the pressure chamber

FIGURE 9. PAN filaments generated from 397-hole spinneret; the diameter of each filament is about 35 microns

20 wt% of water. The spinning temperature was about 190°C. The fiber tow is estimated to contain hundreds of filaments at about 30 meters in length. The diameter of each filament is about 35 microns. While the fibers did not look good and were difficult to despool (could not find the fiber end), it is an important achievement in the research efforts.

It was noted that this spinning trial lasted about 20 minutes or so before it had to be stopped due to high torque on the screw/motor. This was again apparently caused by degradation of PAN based on the observation on the residual polymers inside the spin pack. Although the quality of this precursor material was not sufficient to conduct conversion trials, the team does feel it is close to that key milestone.

Carbon Fiber Conversion Development

The conversion team technically supported other efforts as described above as well as bringing additional technical resources to the team having past experience in hands-on spinning of similar materials and contracted with an outside support to custom formulate and manufacture PAN dope to project team specifications. The team also designed and procured a steam draw system as shown in Figure 10 and a linear stretcher as shown in Figure 11. These equipment capabilities will facilitate development and demonstration of optimized conversion recipes for producing carbon fiber from the melt spun precursor.

FIGURE 10. Steam draw unit for precursor fiber

FIGURE 11. Linear stretcher for conversion processes

CONCLUSIONS AND FUTURE DIRECTIONS

Significant progress has been made in demonstrating and improving melt spinning processes and producing precursor fiber in sufficient quality and minimum quantity to begin carbon fiber conversion investigations. Mechanical properties of the earlier melt spun precursor fiber are comparable to commercially produced fibers. Initial conversion protocols have been developed and demonstrated indicating that we are indeed taking an effective approach and making progress towards project goals.

Near-term objectives are for Virginia Tech to produce longer and more uniform tows that are then drawn in a secondary step as previously described. ORNL will characterize fiber and conduct more extensive conversion trials on precursor filaments generated using its precursor evaluation system. Working on the precursor chemistry necessary to enhance baseline properties and move towards the ultimate goals of 33 Msi modulus and 700 ksi strength has been resumed and is making progress. Equipment necessary to scale the spinning processes up so that the team can work with larger tow sizes and more continuous tows in further enhancing the conversion processes and providing feedback to the chemistry and fiber forming development has either been obtained or is on order. The filaments at various steps of the conversion process will be fully characterized and the data used to commence optimization of precursor chemistry and the filament generation process. In order to fully address application requirements, the team will also need to evaluate and implement appropriate post treatment operations including surface treatment and sizing for the fiber. Plans are also in place to evaluate whether advanced plasma-based conversion processes (oxidative stabilization and carbonization) under development at ORNL are appropriate for these fibers in reducing costs while meeting performance goals. As the technology is being successfully demonstrated at the Carbon Fiber Technology Facility in Oak Ridge, ORNL will concentrate on the commercialization strategy for technology transfer and implementation.

FY 2015 PUBLICATIONS/PRESENTATIONS

1. Bob Norris and Felix Paulauskas, "Melt Processable PAN Precursor for High Strength, Low-Cost Carbon Fibers," presentation at Hydrogen Storage Tech Team Meeting, March 19, 2015.

2. Felix L. Paulauskas and Bob Norris, "Melt Processable PAN Precursor for High Strength, Low-Cost Carbon Fibers," presentation at 2015 DOE Hydrogen Program and Vehicle Technologies Annual Merit Review and Peer Evaluation Meeting, June 10, 2015.

REFERENCES

1. Hydrogen, Fuel Cells and Infrastructure Technologies Program Multi-Year Research, Development and Demonstration Plan Planned program activities for 2005–2015, October 2007 update.

2. Wiles, K.B., V.A. Bhanu, A.J. Pasquale, T.E. Long, and J.E. McGrath, Journal of Polymer Science: Part A: Polymer Chemistry, Vol. 42, 2994–3001 (2004).

3. Bhanu, V.A. P. Rangarajan, K. Wiles, M. Bortner, S. Sankarapandian, D. Godshall, T.E. Glass, A.K. Banthia, J. Yang, G. Wilkes, D. Baird, and J.E. McGrath, Polymer, 43, 4841–4850, (2002).

4. Godshall, D., P. Rangarajan, D.G. Baird, G.L. Wilkes, V.A. Bhanu, and J.E. McGrath, "Polymer 44 (2003), 4221–4228.

5. Rangarajan, P., V.A. Bhanu, D. Godshall, G.L. Wilkes, J.E. McGrath, and D.G. Baird, Polymer 43, 2699–2709 (2002).

6. Bortner, Michael J., Vinayak Bhanu, James E. McGrath, and Donald G. Baird, Journal of Applied Polymer Science, 93(6), 2856–2865 (2004).

7. Peng, Fred M., "Acrylonitrile Polymers," in Mark, Herman F.; Bikales, Norbert M.; Overberger, Charles G.; Menges, Georg; Editors. Encyclopedia of Polymer Science and Engineering, Vol. 1: A to Amorphous Polymers. (1986), 843 pp, pages 426–470, and references therein.

8. Back, Hartwig, C, and Knorr, Raymond S. "Acrylic Fibers," in Mark, Herman F.; Bikales, Norbert M.; Overberger, Charles G.; Menges, Georg; Editors. Encyclopedia of Polymer Science and Engineering, Vol. 1: A to Amorphous Polymers. (1986), 843 pp, pages 334–388, and references therein.

9. Capone, Gary J.; Masson, James C. Fibers, acrylic. Kirk-Othmer Encyclopedia of Chemical Technology (5th Edition) (2005), 11 188–224

10. Frushour, Bruce G.; Knorr, Raymond S. Acrylic fibers. International Fiber Science and Technology Series (2007), 16 (Handbook of Fiber Chemistry (3rd Edition)), 811–973.

IV.D.6 Achieving Hydrogen Storage Goals through High-Strength Fiber Glass

Hong Li (Primary Contact), Brian Kornish, Norman Newhouse, Kenneth Johnson
PPG Industries, Inc.
400 Guys Run Road
Cheswick, PA 15024
Phone: (412) 820-8132
Email: hli@ppg.com

DOE Manager
Grace Ordaz
Phone: (202) 586-8350
Email: Grace.Ordaz@ee.doe.gov

Contract Number: DE-EE0006626

Subcontractors
- Hexagon Lincoln, Lincoln, NE
- Pacific Northwest National Laboratory (PNNL), Richland, WA

Project Start Date: September 1, 2014
Project End Date: August 30, 2016

Overall Objectives

Our objective is to demonstrate a Type IV composite overwrapped pressure vessel reinforced exclusively with glass fiber. We expect to achieve this goal with the following:

- Develop a new glass fiber with strength exceeding T-700 at less than half its cost
- Demonstrate a novel glass fiber manufacturing process
- Conduct composite validation laboratory tests to determine the safety factor for the tank made by using new high strength glass fiber
- Build cost models to demonstrate the new tank will reduce the composite contribution to system cost by nearly 50% with minimal impact on tank weight and capacity compared to tanks made with T-700 carbon fiber.

Fiscal Year (FY) 2015 Objectives

- Develop two candidate high-strength glass fibers that offer pristine tensile strength greater than 5,000 MPa
- Identify two candidate sizing chemistries to be used for coupling with specific epoxy resin currently used for the hydrogen storage tank
- Perform bushing runs to produce high-strength glass fibers of the two candidate compositions with two pre-selected sizing chemistries
- Build vessels using both high-strength fibers and reference E-glass fibers (as a control) for mechanical tests compared with performance of the vessels made from T-700 carbon fibers
- Demonstrate throughput enhancement of the proposed new high-temperature glass melting platform

Technical Barriers

This project addresses the following technical barriers from the Hydrogen Storage section (3.3.5) of the Fuel Cell Technologies Office (FCTO) Multi-Year Research, Development, and Demonstration Plan:

(B) System Cost

Technical Targets

The project is to demonstrate the technical and commercial feasibility of using high strength fibers to match with the tensile strength of T-700 carbon fibers at about 50% of the cost. At the completion of the project, experimental results and modeling output will enable us to benchmark with key parameters shown in Tables 1 and 2. The actual targets for our project, as written in our proposal, are detailed in the Introduction section of this report.

TABLE 1. Technical System Targets: Onboard Hydrogen Storage for Light-Duty Fuel Cell Vehicles [1]

Storage Parameter	Units	2020	Ultimate	Project towards targets (2015)
System Gravimetric Capacity	kWh/kg	1.8	2.5	TBD
System Volumetric Capacity	kWh/L	1.3	2.3	TBD
Storage System Cost	$/kWh net $/kg H_2 stored	10 333	8 266	TBD TBD

TBD – to be determined

TABLE 2. Projected Performance of Hydrogen Storage Systems [1] [a]

Hydrogen Storage System	Gravimetric (kWh/kg sys)	Volumetric (kWh/L sys)	Cost ($/kWh; projected to 500,000 units/yr)	Project towards targets (2015)
700-bar compressed (Type IV) [b]	1.7	0.9	19	TBD

[a] Assumes a storage capacity of 5.6 kg of usable hydrogen
[b] Based on Argonne National Laboratory performance and TIAX cost projections

FY 2015 Accomplishments

During the first phase of our project in FY 2015, the team has successfully completed the following objectives:

- Developed two new high-strength glass fiber chemistries with their pristine tensile strength close or slightly higher than T-700 carbon fibers
- Successfully produced glass cullets of the two fiber glass chemistries for the planned fiber production
- Identified two fiber glass sizing chemistries for use
- Built all of the required E-glass reference vessels and started testing the vessels
- Built environmentally controlled stress corrosion test apparatus after a thorough evaluation of grips
- Completed design of the new high-temperature glass melting vessel for demonstration; the system installation is scheduled.

✧ ✧ ✧ ✧ ✧

INTRODUCTION

This project addresses the FCTO's intermediate 2017 goals for onboard hydrogen storage for light-duty fuel cell vehicles. Specifically, we target a fiber cost less than $6/lb, a composite contribution to system cost of less than $6/kWh, a volumetric capacity of 0.86 kWh/L (26 g/L), and a gravimetric capacity of 1.3 kWh/kg (4 wt%), while minimizing increases in tank mass compared to T-700 carbon fiber vessels. The project tasks are organized to continually decrease project risk, moving from a Technology Readiness Level of 4 to 6.

APPROACH

To begin, we develop fibers at the bench and characterize stress rupture at the fiber level. We then develop a pilot version of our new glass manufacturing process to produce the high-strength fibers, and we ended Year 1 with test data from prototype tanks built from up to four new fiber samples, i.e., fiber chemistry and sizing chemistry in combination.

In Year 2, we will optimize the best performing fiber and the production process, characterize stress rupture at the composite level, and investigate alternate tank designs. We will end the project with a prototype tank built according to a design tailored to the properties of the new glass that can be tested against a wide range of industry testing.

RESULTS

The development of new high-strength fibers, shown in Table 3, can address DOE's technical barrier in the system cost reduction described earlier.

Successful glass cullet production of both high-strength fiber compositions, using conventional combustion technology, was another important milestone that demonstrated that both high-strength glass fibers can be produced at large scale using improved commercial glass melting technology that can adequately reduce production costs towards the DOE target.

Although there are still some challenges for the fiber forming process, our initial production of fibers using a small scale pilot platform will successfully demonstrate the technical feasibility of the fiber drawing processes close to existing commercial fiber forming process.

TABLE 3. High-Strength Glass Fiber Properties

ID	Chemistry A	Chemistry B
ρ (g/cm^3)	2.64	2.63
E (GPa)	91.8	92.6
s_f (MPa)	5243	5583
ε (%)	5.7	6.0

Note 1: ρ – average fiber density; E – average pristine fiber Young's modulus by sonic method; s_f – average pristine fiber strength; ε – average pristine fiber failure strain

Production of high strength fibers has been delayed against the original plan due to equipment issues. Currently we have identified a new solution that will enable us to draw fibers with good stability at appropriate temperatures without introducing a busing control problem.

One of the fiber sizing chemistries has been tested by Hexagon Lincoln using our reference E-glass roving packages; the vessel quality, i.e., uniformity of strand distribution and level of broken filaments, through the fiber winding process is satisfactory compared with standard commercial fiber glass wound composite vessels. During the composite vessel winding process, we also obtained data to determine translation losses (about 10%) in terms of the vessel burst strength between using large direct draw product without assembling and using assembled roving from small packages.

Stress rupture test apparatus with temperature and humidity controls has been built at PNNL (Figures 1a, 1b). The set up and design have been validated by testing our reference fibers, INNOFIBER® CR 2026 fiber glass, as illustrated in Figure 2. The section of final grips (Figure 3)

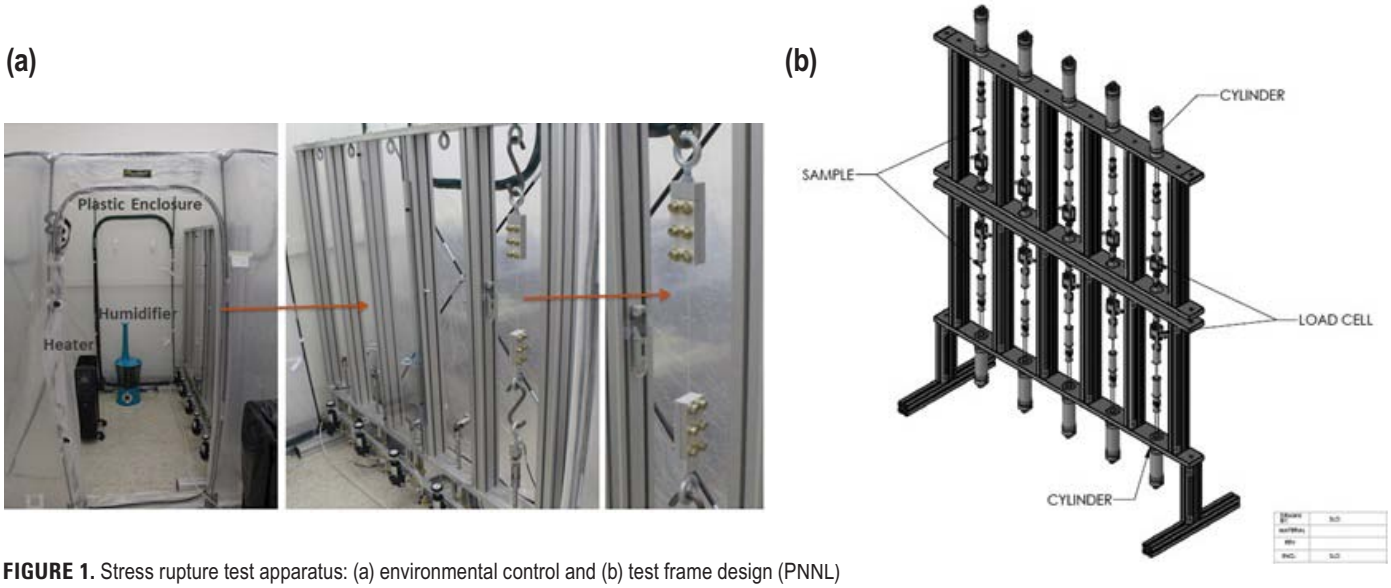

FIGURE 1. Stress rupture test apparatus: (a) environmental control and (b) test frame design (PNNL)

BareFiber PNNL Custom Grip	Average	Stdev	Min	Max
Peak Load (LbF)	270.64	9.87	251.0476	282.2207
Extension (mm)	8.30	2.80	8.1159	10.1112
Elongation at Break (%)	6.14	0.41	5.4106	6.7408

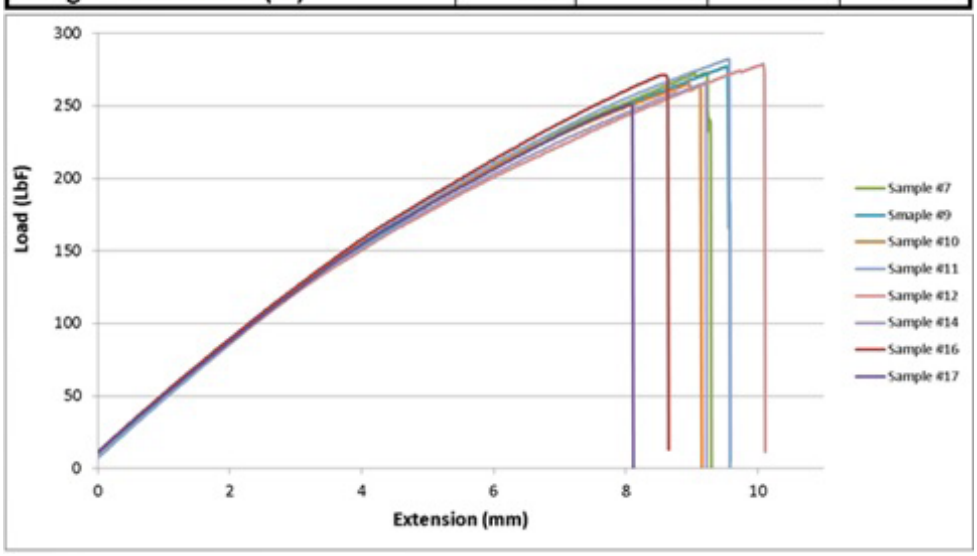

FIGURE 2. Example of stress rupture tests using INNOFIBER® CR 2026 glass fiber as control

was made based on evaluations of sample tap geometry and different types of commercial grips.

CONCLUSIONS AND FUTURE DIRECTIONS

The project has developed two new high-strength fiber glass chemistries with some positive confirmation from the glass melting and limited fiber forming process. The challenging part in the short term is to produce a sufficient amount of fiber packages for composite tank testing as well as stress corrosion or stress rupture tests. For the long term, the key is to reduce translation loss of fibers through each step of fiber forming and package drying processes. In FY 2016, we plan to complete all new high-strength fiber making, composite vessel tests, and fiber stress corrosion tests. The new results will enable us to achieve:

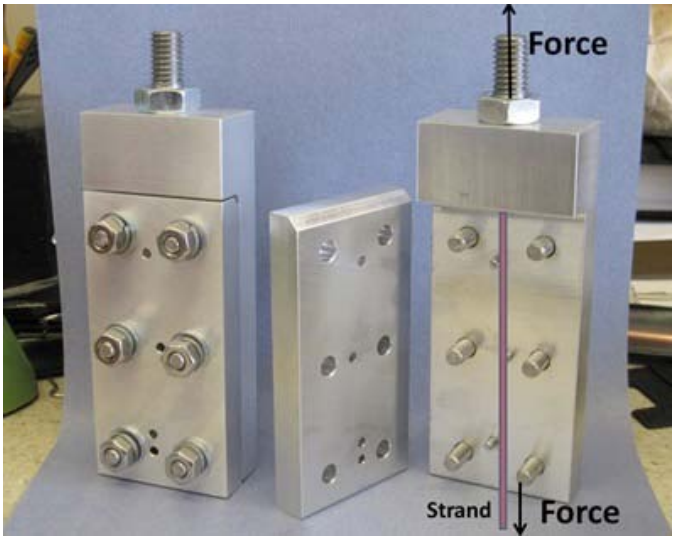

FIGURE 3. Grips selected for the stress rupture test

- Model-based cost prediction on high-strength fiber glass cost contribution to the system cost.
- Feasibility of high strength fiber replacing T-700 carbon fiber for hydrogen storage tank.

FY 2015 PUBLICATIONS/PRESENTATIONS

1. H. Li, Achieving Hydrogen Storage Goals through High-Strength Fiber Glass, at the Hydrogen Material Workshop and PI Meeting in Golden, CO, on January 29, 2015.

2. H. Li, Achieving Hydrogen Storage Goals through High-Strength Fiber Glass, at U.S. DRIVE Technical Meetings in Detroit, MI, on March 19, 2015.

3. H. Li, Achieving Hydrogen Storage Goals through High-Strength Fiber Glass, at 2015 U.S. DOE Fuel Cell Technologies and Vehicle Technologies Annual Merit Review and Peer Evaluation Meeting, Washington, DC, June 8–12, 2015.

REFERENCES

1. http://energy.gov/eere/fuelcells/downloads/fuel-cell-technologies-office-multi-year-research-development-and-22

IV.D.7 Optimizing the Cost and Performance of Composite Cylinders for H_2 Storage Using a Graded Construction

Andrea E. Haight
Composite Technology Development, Inc. (CTD)
2600 Campus Drive, Suite D
Lafayette, CO 80026
Phone: (303) 664-0394
Email: andrea.haight@ctd-materials.com

DOE Manager
Ned Stetson
Phone: (202) 586-9995
Email: Ned.Stetson@ee.doe.gov

Contract Number: DE-SC0009449

Subcontractor
Adherent Technologies, Inc., Albuquerque, NM

Project Start Date: February 19, 2013
Project End Date: May 14, 2016

Overall Objectives

- Develop a 700 bar Type IV graded composite structure pressure vessel design incorporating low cost carbon fiber
- Optimize composite performance of low cost fibers
- Demonstrate the performance of a graded composite structure pressure vessel

Fiscal Year (FY) 2015 Objectives

- Optimize fiber property translation in filament wound composites utilizing 50,000 low cost carbon fiber tows
- Optimize design models utilizing experimental data to generate design for subsequent prototype construction
- Conduct preliminary cost analysis showing the potential cost savings realized through use of low cost carbon fiber

Technical Barriers

This project addresses the following technical barriers from the Hydrogen Storage section (3.3.5) of the Fuel Cell Technologies Office Multi-Year Research, Development, and Demonstration Plan:

(A) System Weight and Volume

(B) System Cost

Technical Targets

The overall goal of this program is to address the high cost of physical hydrogen storage in Type IV composite overwrapped pressure vessels (COPV) with an overall cost reduction target of 25%. The cost of these COPV is currently driven by the high cost of carbon fiber; this program aims to replace 40–60% of the high cost fiber with a low cost carbon fiber to achieve the cost reduction target.

A combination of finite element analysis (FEA) driven composite design, experimental data, prototype construction, testing, and cost analysis will be used to demonstrate the approach.

Fiscal Year (FY) 2015 Accomplishments

Accomplishments during the current project period include the following:

- Demonstration of high fiber property translation in composites that are filament wound using large tows of a commercial low cost carbon fiber
- Refinement of COPV designs based on experimental data obtained from low cost carbon fiber composite panels
- Preliminary cost modeling, based on refined designs, shows potential cost savings as high as 30% depending upon relative costs of Toray T700S and low cost carbon fiber candidates

✧ ✧ ✧ ✧ ✧

INTRODUCTION

The challenges associated with bringing reasonably priced hydrogen fuel cell electric vehicles to market are numerous. One significant challenge is reducing the cost for on-board hydrogen storage tanks while continuing to provide a driving range of greater than 300 miles. COPV have been designed and qualified for this application. However, these tanks are extremely expensive as currently manufactured, due in large part to the high strength carbon fibers used (e.g., Toray's T700S). The cost of carbon fiber alone can constitute as much as 75% of the total cost of the vessel [1].

DOE's near-term goal is to reduce the cost of COPV for high pressure hydrogen storage by 25%. CTD believes that this can be achieved by constructing the structural shell using a graded composite in which a portion of the expensive, high performance fiber is replaced with lower

cost carbon fibers based on common textile fibers. Since the projected cost for these newer fibers is significantly lower than that for carbon fibers produced from higher grade precursors, their utilization in a significant portion of the mass of the composite material in the vessel will translate to a corresponding reduction in the cost of the raw materials for the vessel, thereby meeting DOE's target for cost reduction.

APPROACH

In this effort, CTD is investigating the use of a graded composite tank structure, in which a portion of the high cost T700S carbon fiber is replaced by lower cost fibers, such as the low cost carbon fibers being developed at Oak Ridge National Laboratory (ORNL) with DOE funding. The reduced strain requirements for the composite through the thickness of the pressure vessel enables the use of lower cost, lower performing fibers for a substantial portion of the composite structure. A design has been developed based on targeted low cost fiber properties that would allow for replacement of a large fraction of the costly T700S fiber with a less expensive option.

Work during FY 2015 focused on gathering experimental data from commercial lower cost fibers with properties equivalent to those expected from newer textile-based fibers. These data were then used to refine the design and cost models for the program. Suitable low cost fiber options from ORNL were not available during this period.

RESULTS

One key factor for success in the application of low cost fibers to pressure vessels is fiber property translation, defined by rather than defined as how close the mechanical properties (strength, modulus, and strain) of the composite are to those of the reinforcing fiber itself. Fiber property translation in excess of 85% will likely be required if low cost fibers are to be used in any portion of the pressure vessel construction. Factors affecting fiber property translation include: fiber wetting, fiber consolidation, tow spreading, and resin cure conditions. Tow spreading is particularly challenging for low cost fibers where large tows (>50,000) are typical. Significant effort in FY 2015 was directed toward achieving high fiber property translation for large tows.

The initial large tow handling work was conducted using two commercial fibers, including Zoltek's Panex® 35 50,000 tow fiber. Both commercial fibers were selected because they had strength, modulus, and strain values that are very similar to those projected for the ORNL textile PAN-based low cost fiber candidates. Panex® 35 was also used during the Phase I effort and thus allowed for a direct comparison back to the previously acquired data relative to the reported translation values.

It was believed that to improve the translation numbers from the Phase I study and to provide consistent data across different test plates, it would be necessary to spread the 50,000 tow fiber to a larger width as it traversed the wetting mandrel. Thus, the fibers would achieve a better impregnation of the resin prior to being applied to the mandrel, as well as offering the potential to more thoroughly align the individual fibers within the tow. This improves fiber translation properties. To spread the fiber to a wider width, CTD evaluated effects of the fiber tension, span between the roll tensioner and the first roller, location, number and rotation of spreading rollers, as well as contact area with the spreading rollers.

Using the same resin system as was employed in Phase I, CTD manufactured five different test plates and created 30 different tensile test samples to observe if improved translation numbers could be obtained during Phase I. The average fiber property translation values for the five tested samples of each individual test plates are shown in Figure 1; a line corresponding to the data obtained in Phase I is included for reference.

A comparison of the Phase I and Phase II translation data is provided in Table 1.

TABLE 1. Improvement in Panex® 35 Average Fiber Property Translation

	Phase I	Phase II
Strain	78%	89.2%
Strength	65%	73.8%
Modulus	91%	91.5%

While the modulus translation remained relatively unchanged, an increase in the average strain and strength numbers of 14% and 13.5%, respectively, was achieved relative to Phase I, indicating that we have refined our process enough to greatly increase the translation numbers for the Panex® 35 fiber. Achieving this level of fiber property translation is critical for the success of the graded structure design for 700 bar tanks.

Finite Element Modeling

A typical 700 bar composite pressure vessel requires a thick composite shell, in which there is a significant grading in the longitudinal (fiber direction) strain from the inside to the outside of the vessel wall (Figure 2). A COPV has been designed to the following dimensions, based on the use of Toray T700 high strength carbon fiber. The outer diameter of the pressure vessel was restrained in size to 500 mm (20 in) nominal because of the available space inside the automobile. The tank had the following dimensions:

- Inside diameter = 17.5 in
- Cylinder length = 27.5 in
- Thickness in the cylindrical section = 1.32 in

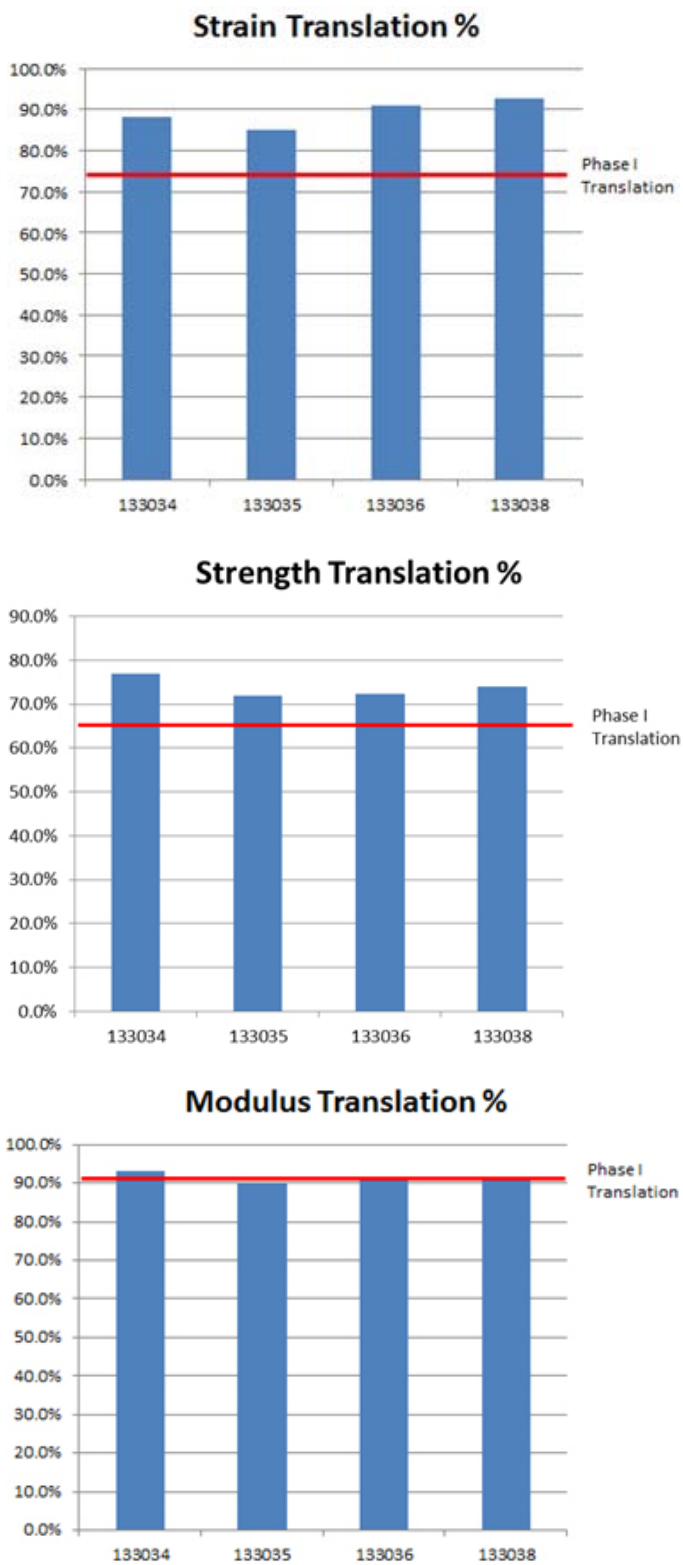

FIGURE 1. Average fiber property translation data (%) for Panex® 35 panels; five specimens each from four manufactured panels

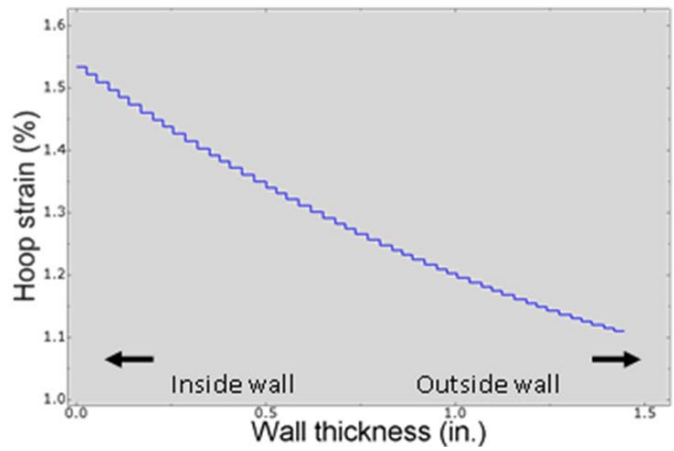

FIGURE 2. Distribution of hoop strain in composite wall of a 20-inch-diameter Type IV vessel designed for 700 bar operating pressure

- Length of the tank = 41 in

Since the outer layers are strained less than the inner fibers, the outer fibers can be replaced with fibers with lower strain capability and lower strengths (and lower cost) as long as the strain levels are maintained at acceptable levels (<1.8% for T700S carbon fiber and <1.5% for textile PAN fibers). Material properties of Toray T700S and Panex® 35 composites fabricated and evaluated by CTD (Table 2) were used in the finite element models (Figure 3) to determine how much of the Toray T700 fiber could be substituted with a lower cost variant.

TABLE 2. Material Properties of T700S Fiber Composite and Panex® 35 Fiber Composite

Property	T700S Composite	Panex® 35 Composite
Bandwidth (in)	1.69	1.69
Hoop Thickness (in)	0.027	0.027
Helical Thickness (in)	0.0164	0.0164
Longitudinal Elastic Modulus, E_1 (Msi)	18.5	19.05
Transverse Elastic Modulus, E_2 (Msi)	1.3	1.01
Poisson Ratio, ν_{12}	.28	.28
Shear Modulus, G_{12} (Msi)	0.5	0.5
Failure Strain in Fiber Direction (%)	1.8	1.34

Several analyses were conducted in order to find the amount of each material necessary to meet the design criteria. The analysis runs were used to vary the content of high strength Toray T700S fibers and Panex® 35 fibers. The layup sequence that was used was the same layup sequence used for the Phase I design; however, the number of layers of Panex® 35 fibers was varied as needed.

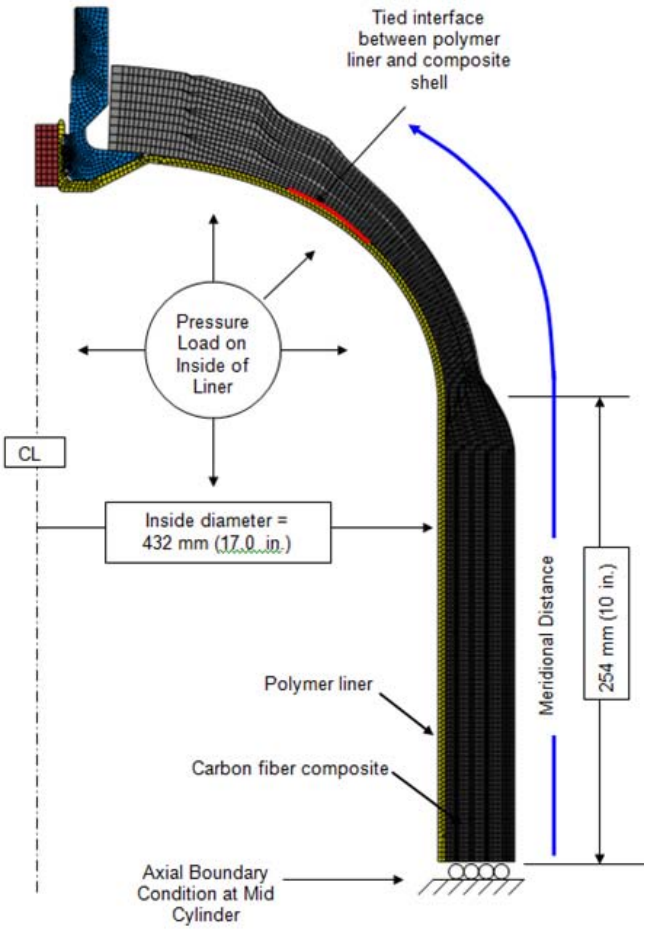

FIGURE 3. Finite element model of the COPV

The strain criteria were met in all layers consisting of Toray T700S carbon fiber regardless of composition. Figure 4 shows the hoop strain for the maximum allowable fraction of Panex® 35 fiber in the pressure vessel construction. This fraction is substantial and, should the fiber cost be low enough, would result in a significant cost savings.

Cost Analysis

As the first step in creating a cost analysis, a flow chart of the manufacturing process was generated. This allows the identification of any minor or major changes in the process flow that might result from using multiple carbon fiber types in COPV construction.

The only real changes in the process occur when purchasing two different fibers and having to change from one fiber to the next in the manufacturing process. The changes to procurement of the fibers are minimal and, other than the fiber cost, the largest change comes from any additional labor hours added to the process due to fiber change out.

A subsequent cost analysis was then used evaluate potential cost savings that might be realized by manufacturing a portion of the tank with a low cost fiber.

Results of the cost analyses conducted to date are provided in Figure 5. Included in Figure 5 are three charts: one chart shows the weight of fiber used to make each tank, and the other two charts show the estimated cost savings for the two different graded structures (50/50 vs. 60/40) utilizing three different cost parameters for the T700 and the low cost fiber.

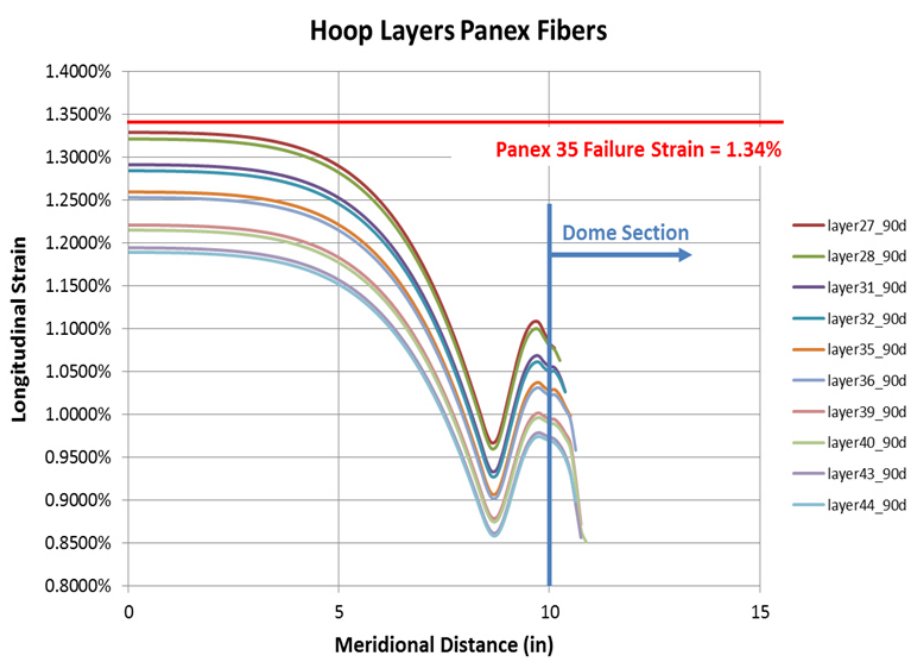

FIGURE 4. Hoop strain in Panex® fibers at the design burst pressure of 23,852 psi

T700 Price Range = $13 - $20
Low Cost Fiber Price Range = $7 - $12

These calculations come from a composite that has 50% fiber volume

50% T700 Toray/50% Low Cost Fiber				
		Low Cost Fiber ($/lb)		
		$ 7.00	$10.00	$12.00
T700 Toray ($/lb)	$13.00	20.4%	9.1%	1.6%
	$15.00	24.3%	14.5%	7.9%
	$20.00	30.6%	23.2%	18.3%

Weight of Fiber				
Percent	T700 lb	T700 kg	LC Fiber lb	LC Fiber kg
60/40	58.0	26.36	38.8	17.64
50/50	48.4	22.00	48.4	22.00
100	96.8	44.00		

60% T700 Toray/40% Low Cost Fiber				
		Low Cost Fiber ($/lb)		
		$ 7.00	$10.00	$12.00
T700 Toray ($/lb)	$13.00	15.9%	6.9%	0.8%
	$15.00	19.1%	11.2%	6.0%
	$20.00	24.3%	18.3%	14.4%

FIGURE 5. Results of cost analysis for two graded structure cases; potential cost savings are expressed as a percentage reduction over the 100% Toray T700 case

This cost analysis shows that the cost savings of a graded tank are between 0.8% and 30.6% depending on the price of T700 and the second fiber. This clearly demonstrates that there is potential for significant cost savings arising from the use of low cost carbon fiber, particularly if a cost on the order of $7.00/lb can be realized.

CONCLUSIONS AND FUTURE DIRECTIONS

Based on the results achieved during FY 2015, CTD will proceed with the construction and testing of a sub-scale prototype hydrogen storage tank based on the graded composite approach during FY 2016.

Additional work will be conducted in evaluating low cost carbon fiber options as provided by ORNL. Mechanical properties of unidirectional panels will be evaluated as was done for the commercial low cost fibers in FY 2015. The resulting data will be used in the finite element models to determine the amount of low cost fiber that can be used in a 700 bar hydrogen storage vessel. This composition, along with cost data provided by ORNL for the textile PAN-based carbon fiber options, will then be used in the cost model to predict the potential cost savings that may be realized through the use of graded composite structures in these pressure vessels.

REFERENCES

1. Fuel Cell Technologies Office Multi-Year Research, Development, and Demonstration Plan, Section 3.3 – Hydrogen Storage, updated May 2015.

IV.E.1 Complex Hydrides – A New Frontier for Future Energy Applications

Principal Investigator: Vitalij K. Pecharsky

Organization: Ames Laboratory

Program Scope

Every energy-related application of hydrogen (H_2) requires safe and efficient storage. H_2 can be stored as a compressed gas, a cryogenic liquid, or in an H-rich solid. The first two approaches require substantial energy for compression or liquefaction, and, therefore, entail multiple containment, safety, and economical issues. Conversely, H-rich solids are believed to be the best medium to store high-purity H_2 required for fuel cells. Solid hydrides ensure high volumetric density of the fuel because in many of them the volumetric density of H_2 at ambient conditions is nearly twice that of a cryogenic liquid at 20 K, reaching 120 g H_2/l. The specific objectives of this project are to address issues that will advance basic science of complex hydrides and open up possibilities for their future use by drawing on the experience and expertise of principal investigators in materials science, physics and chemistry of complex hydrides, X-ray diffraction, high-resolution solid-state nuclear magnetic resonance (NMR), electron microscopy, and first-principles theory and modeling.

FY 2014 Highlights

A successful strategy for the solvent-free, room temperature mechanochemical synthesis of alane (AlH_3) via a solid state metathesis reaction of LiH and $AlCl_3$ has been developed. Alane, one of the forefront materials for practical solid-state hydrogen storage, has a hydrogen capacity of 10% by weight and gives up hydrogen in a single step at the temperature that is close to the operating temperature of hydrogen fuel cells. Prior to this work, realizing the enormous potential of alane has been frustrated by the lack of a straightforward method for its synthesis. The novelty of the process is the addition of $AlCl_3$ to the reaction mixture in three steps, hence completely suppressing parasitic side reactions that lead to a nearly complete loss of hydrogen from the system. By adding $AlCl_3$ to LiH in three steps and applying gas pressure, quantitative yield of AlH_3 – an important energetic material – has been achieved. X-ray diffraction, solid state NMR, and temperature programmed desorption analyses importantly established the mechanism of mechanochemical transformation: $3LiH + AlCl_3 \rightarrow 3LiCl + AlH_3$. This quick and efficient production method meets DOE requirements for hydrogen storage applications pending development of an economical large-scale synthesis process.

IV.E.2 Elucidation of Hydrogen Interaction Mechanisms with Metal-Doped Carbon Nanostructures

Principal Investigator: Ragaiy Zidan

Organization: Savannah River National Laboratory

Program Scope

This program supports the Office of Basic Energy Sciences (BES) mission through the development of a basic understanding of the formation and the physicochemical properties of carbon nanostructures, formed by the interaction of doped carbon nanomaterials with hydrides and/or hydrogen gas. For many years extensive work has been conducted on hydrogen interaction with metals and alloys forming hydrides. The research work on metal hydrides involved a significant number of studies and characterization efforts, where chemical, electronic, optical, and magnetic properties were determined. Our work continues to focus on a unique class of materials—metal-doped carbon nanostructures—and the interaction of these materials with hydrogen. Our work will continue to focus on understanding the formation of these materials and on investigating their chemical, electronic, optical, and magnetic properties when reacted with hydrogen. Previous work in our group through BES programs has led to advances in control over a material's properties at the electronic, molecular, and atomic level, which serve as the foundation of new energy technologies and can support other aspects of DOE missions. Our group has observed related properties in the materials such as hydrogen storage and luminescence with potential applications in clean energy and energy storage. However, developing customizable functional materials requires relating the microstructure of the materials to their physical properties. Our research activities will be aimed at developing and characterizing a novel class of hydride materials based on metal-carbon nanostructures. The current work will investigate different carbon materials utilizing their structure as building blocks for achieving unique properties based on zero, one, and two dimension structures such as fullerenes, carbon nanotubes, and graphene, respectively.

FY 2014 Highlights

Theoretical calculations (Prof. Jena, Virginia Commonwealth University) reveal that a new class of highly electronegative species can be created when a central metal atom is surrounded by superhalogen moieties. Building on this knowledge, we were able to synthesize and characterize a stable hyperhalogen salt, $K[Al(BH_4)_4]$, whose anion, $Al(BH_4)_{4-}$, has an extremely high electron affinity. Unlike the few hypersalts synthesized so far, this new salt is stable at temperatures of up to 154°C. Besides providing a new functional material, the work validates the use of computational studies for rational design of new compounds based on superhalogens and hyperhalogens. Building on our previous study of ionic mobility in a $LiBH_4$-C_{60} system, a series of electrochemical measurements was performed to quantify the lithium ionic mobility in the material under various conditions. This study also demonstrated that the material can be used as a solid electrolyte in an all solid-state lithium ion battery. Theoretical calculations by Prof. Jena's group indicated that the Li^+BH_{4-} bonding is perturbed in the presence of C_{60} resulting in a highly mobile Li ion due to the C_{60}-BH_{4-} interaction. This suggests a nanoionic mechanism is responsible for the enhanced Li ion mobility due to the formation of new interfaces at the nanoscale favoring the production of charge carriers. Further laser-desorption/ionization time-of-flight mass spectrometry analysis of a sodium intercalated fullerene (Na_xC_{60}) in the hydrogenated state provided the first spectroscopic evidence for the formation of $C_{60}H_{60}$ among other highly hydrogenated fullerenes ($C_{60}H_{>36}$). This finding was also confirmed through deuteration of the same material to form $C_{60}D_{60}$. Current efforts in this system are focusing on the isolation of the $C_{60}H_{60}$ from the other fullerenes for further analysis and characterization. Our current work is aimed at understanding how hydrogen interaction with C_{60} and other carbon nanomaterials can potentially lend itself to other energy storage systems and energy conversion devices.

IV.E.3 Activation of Hydrogen under Ambient Conditions by Main Group Molecules

Principal Investigator: Philip Power

Organization: University of California, Davis

Program Scope

The main theme of this project is the investigation of the reactions of small, important molecules such as hydrogen, olefins, alkanes, amines, isocyanides, carbon monoxide, carbon dioxide, and related species, with main group element compounds. The reactivity of the compounds arises from the presence of both occupied and unoccupied frontier orbitals, which are separated by modest energies of four electron volts or less. The reactions generally occur by a synergic route that involves a push-pull redistribution of electron density that facilitates bond making and breaking. The conditions for reaction reversibility are determined by the energy and symmetry of the molecular energy levels in the compounds, which can be manipulated by changing the electronic and steric properties of the substituents. In principle, the information from these studies can be used to design inexpensive catalysts for fundamental organometallic reactions based on earth-abundant elements, rather than on rare and expensive noble metals. The major focus is on compounds of the elements silicon and aluminum, which are the second and third most abundant elements in the earth's crust. Unfortunately, there are few stable low-coordinate silicon and aluminum compounds with suitable frontier orbital properties for reversible small molecule binding. A program is underway to synthesize low-valent and/or small molecular clusters of these elements with reactive exposed atoms. In the clusters, the coordination of their constituent elements can resemble that of the surfaces of the pure elements, which generally possess highly reactive surface atoms that interact readily with small molecules. The clusters also offer multiple coordination sites for synergistic reactions.

FY 2014 Highlights

Over the past year, work has concerned a variety of topics relevant to the project's theme. The first reversible complexation of ethylene by a silylene under ambient conditions was studied and the energetics of the reaction were determined. It was shown that the silylene also reacted readily with a variety of substituted alkynes, but not with substituted alkenes, except for conjugated alkenes. A diarylgermylene was shown to react reversibly with white phosphorus at room temperature. A cage germanium-phosphorus compound was formed and characterized spectroscopically and structurally. Photolysis in toluene resulted in regeneration of the germylene and phosphorus. It was shown that the reaction cycle could be repeated up to ten times with little decomposition. In addition, diarylgermylene or stannylene was shown to insert readily into a phosphorus-hydrogen bond of phosphine to generate primary phosphide products. In anticipation of their use as synthons, four bulky primary organoalanes were synthesized and characterized. They were shown to react with ammonia and phosphine to give primary amido alanes or cages with aluminum-phosphorus frameworks. The primary alanes were also reacted with alkenes and alkynes. The latter readily underwent a cis-addition to the Al-H moiety under mild conditions. The ready addition to both terminal olefins and alkynes was attributed to the bulky aluminum substituent, which generated high concentrations of the more reactive unassociated alane. An inverse relationship between the size of the alane substituent and reactivity was established experimentally. The reaction of methylisocyanide with a diarylgermylene afforded isocyanide coupling/oligomerization through carbon-carbon bond formation. Investigation of the reaction mechanism showed that the initial step involved isocyanide complexation, followed by sequential migratory insertion into the germanium-carbon bond and subsequent carbon-hydrogen bond activation.

IV.E.4 Elucidation of Hydride Interaction Mechanisms with Carbon Nanostructures and the Formation of Novel Nanocomposites

Principal Investigator: Puru Jena

Organization: Virginia Commonwealth University

Program Scope

The objectives of this project are to provide, by working closely with experimentalists, a fundamental understanding of the structure-property relationships of a novel class of highly electronegative clusters in the gas phase, study their interaction with support and counter ions, and explore their potential as building blocks of materials with tailored properties. The project deals with four inter-related thematic areas of bare and supported clusters with rather uncommon properties. (1) Using first principles theory, we design new, highly electronegative clusters whose electron affinities far exceed that of chlorine and validate their properties by working closely with experimentalists. These species, called superhalogens and hyperhalogens, usually consist of a metal atom at the core surrounded by halogen or oxygen atoms. Our goal is to create superhalogens and hyperhalogens without a metal, halogen, or oxygen atom by tailoring their size and composition and to push their electron affinities to values even higher than that currently known. (2) By suitably identifying counter ions, we explore the ability of their corresponding salts to store hydrogen. (3) Superhalogens with magnetic moments are designed using transition metal atoms as key components. Their magnetic coupling is then studied by assembling them on graphene and noble metal substrates. (4) Using electronegative species as building blocks, we explore the potential of multifunctional nanoparticles with Janus anisotropy for application in light harvesting. The computations are carried out using multiscale theoretical approach based on density functional theory (DFT) with hybrid and generalized gradient approximation based exchange-correlation functionals. When needed, quantum chemical methods such as Moller-Plesset perturbation theory and coupled cluster CCSD(T) (coupled cluster single double [triple]) are used to test the accuracy of the DFT-based results.

FY 2014 Highlights

Publications

Thirty papers were published in peer reviewed journals. Space does not permit to list all. Following is a reduced list:

1. Chen, H., Kong, X., Zheng, W., Yao, J., Kandalam, A.K., and Jena, P.: "Anomalous Property of $Ag(BO_2)_2$ Hyperhalogen: Does Spin-Orbit Coupling Matter?" Chem. Phys. Chem. 14, 3303(2013).

2. Knight, D.A., Zidan, R., Lascola, R., Mohtadi, R., Ling, C., Sivasubramaniam, P.K., Kaduk, J.A., Hwang, S.-J., Samanta, D., and Jena, P.: "Stabilization of Hydrogen Rich, Yet Highly Pyrophoric $Al(BH_4)_3$ via the Synthesis of the Hypersalt $K[Al(BH_4)_4]$," J. Phys. Chem. C 117, 19905 (2013).

3. Kan, M., Zhou, J., Sun, Q., Kawazoe, Y., and Jena, P.: "Intrinsic Ferromagnetism in MnO_2 Monolayer," J. Phys. Chem. Letters 4, 3382 (2013).

4. Zhang, S., Wang, Q., Chen, X., and Jena, P.: "Stable Metallic 3D Metallic Phase of Carbon with Interlocking Hexagons," Proc. Nat. Acad. Sci. 110, 18809 (2013).

5. Zhang, S., Wang, Q., Kawazoe, Y., and Jena, P.: "Three Dimensional Metallic Boron Nitride," J. Am. Chem. Soc. 135, 18216 (2013).

6. Wang, H., Zhang, X., Jae Ko, Y., Grubisic, A., Li, X., Gantefoer, G., Schnoeckel, H., Eichhorn, B.W., Lee, M.S., Jena, P., Kandalam, A.K., Kiran, B., and Bowen, K.H.: "Aluminum Zintl Anion Moieties within Sodium Aluminum Clusters," J. Chem. Phys. 140, 054301 (2014).

7. Tao, K., Sun, Q., Wang, Q., Stepanyuk, V., and Jena, P.: "Self-consistent Determination of Hubbard U for Explaining the Anomalous Magnetism of Gd_{13} Cluster," Phys. Rev. B 89, 085103 (2014).

8. Child, B., Gronett, S., and Jena, P.: "Aromatic Superhalogens," Chemistry- A European Journal 20, 4736 (2014).

9. Giri, S., Moore, C.H., Mcleskey, J.T., and Jena, P.: "Origin of Red-shift in the Photo Absorption Peak in MEH-PPV Polymer," J. Phys. Chem. C 118, 13444 (2014).

10. Awnehss, A., Behera, S., El-Kaderi, H., and Jena, P.: "New Insights into Carbon Dioxide Interactions with Benzimidazole-linked Polymers," Chem. Comm. 50, 3571 (2014).

11. Eleven invited talks were delivered at conferences and academic institutes. One student was awarded a PhD.

V.0 Fuel Cells Sub-Program Overview

INTRODUCTION

The Fuel Cells sub-program supports research, development, and demonstration of fuel cell technologies for transportation applications, as well as stationary and early market applications, with a primary focus on reducing cost and improving durability. Efforts include research and development (R&D) of fuel cell stack components, system balance of plant components, and subsystems, as well as system integration. The sub-program seeks a balanced, comprehensive approach to fuel cells for near-, mid-, and longer-term applications. The development of fuel cells for transportation applications is a primary goal due to the nation's requirements for significantly reduced energy and petroleum consumption and the subsequent increase of available high-efficiency fuel cell electric vehicles (FCEVs). Stationary applications for fuel cells include distributed power generation, including combined heat and power (CHP) for residential and commercial applications. Early market and near-term market applications for fuel cells include backup power, auxiliary power units, and specialty applications such as material handling equipment. The existing market traction that fuel cell technologies have achieved in these applications provides support for adoption of FCEVs in the transportation sector. The sub-program's R&D portfolio is primarily focused on polymer electrolyte membrane (PEM) fuel cells but also includes longer-term technologies, such as alkaline fuel cells and higher temperature fuel cells like molten carbonate fuel cells (MCFCs) for stationary applications.

The sub-program's fuel cell tasks in the Fuel Cell Technologies Office Multi-Year Research, Development, and Demonstration Plan are organized around development of components, stacks, subsystems, and systems; supporting analysis; and testing, technical assessment, and characterization activities.

GOAL

The sub-program's goal is to advance fuel cell technologies with a focus on transportation, as well as enabling stationary and early market applications.

OBJECTIVES[1]

The sub-program's key objectives include the following.

- Develop a 65% peak efficient, direct-hydrogen fuel cell power system for transportation, with 5,000-hour durability, that can be mass produced at a cost of $30/kW ($40/kW by 2020)
- Develop distributed generation and micro-CHP fuel cell systems (5 kW) operating on natural gas or liquid petroleum gas that achieve 45% electrical efficiency and 60,000-hour durability at an equipment cost of $1,500/kW by 2020
- Develop medium-scale CHP fuel cell systems (100 kW–3 MW) by 2020 that achieve 50% electrical efficiency, 90% CHP efficiency, and 80,000-hour durability at a cost of $1,500/kW for operation on natural gas and $2,100/kW when configured for operation on biogas

FY 2015 TECHNOLOGY STATUS AND ACCOMPLISHMENTS

Reducing cost and improving durability while maintaining performance continues to be the key challenge facing fuel cell technologies. Reduction in platinum group metal (PGM) loading and increase in membrane electrode assembly (MEA) areal power density are required to reduce material costs. Current state-of-the-art MEAs with very low cathode PGM loading experience higher than expected reduction in performance when operating at high power (e.g., near the rated power point), but significant progress has been made in FY 2015 to address this performance loss. Commercial fuel cells are expected to use PGM-based catalysts in the near term, but in the long term, developing PGM-free fuel cells would reduce cost and improve competitiveness with incumbent and alternative technologies. Advances in FY 2015 have brought non-PGM catalysts significantly closer to parity with conventional PGM-based catalysts. Major advances in FY 2015 were also made in development of durable, high performance membranes that will allow fuel cells to operate for longer periods of time under harsh conditions.

[1] Note: Targets and milestones were recently revised; therefore, individual project progress reports may reference prior targets.

One of the most important metrics is the projected high-volume manufacturing cost for automotive fuel cells, which the sub-program tracks on an annual basis. This year, the cost of an 80-kW_{net} automotive PEM fuel cell system based on next-generation laboratory technology and operating on direct hydrogen was projected to be \$53/kW_{net} when manufactured at a volume of 500,000 units/year. For comparison, the expected cost of automotive PEM fuel cell systems that are based on current technology and planned for commercialization in the 2016 timeframe is approximately \$280/kW when manufactured at a volume of 20,000 units/year.

The 2015 cost estimate was based on Argonne National Laboratory's projected stack performance for a de-alloyed $PtNi_3$ catalyst (d-PtNi), a change from the nanostructured thin film (NSTF) cathode catalyst selected for last year's analysis. With this change as well as other modifications incorporated into modeling, including a decrease in the cell active-to-total-area ratio, a re-examination of machinery size and procedures utilized at low production volumes, and improved estimates of air humidifier system size, the net change in system cost from 2014 to 2015 was approximately \$2/kW. Practically, the use of the d-PtNi catalyst permits the use of relatively less expensive catalyst application processes and offers a higher likelihood of achieving DOE catalyst lifetime targets. The results of the current year's cost analysis are compared to previous years in Figure 1.

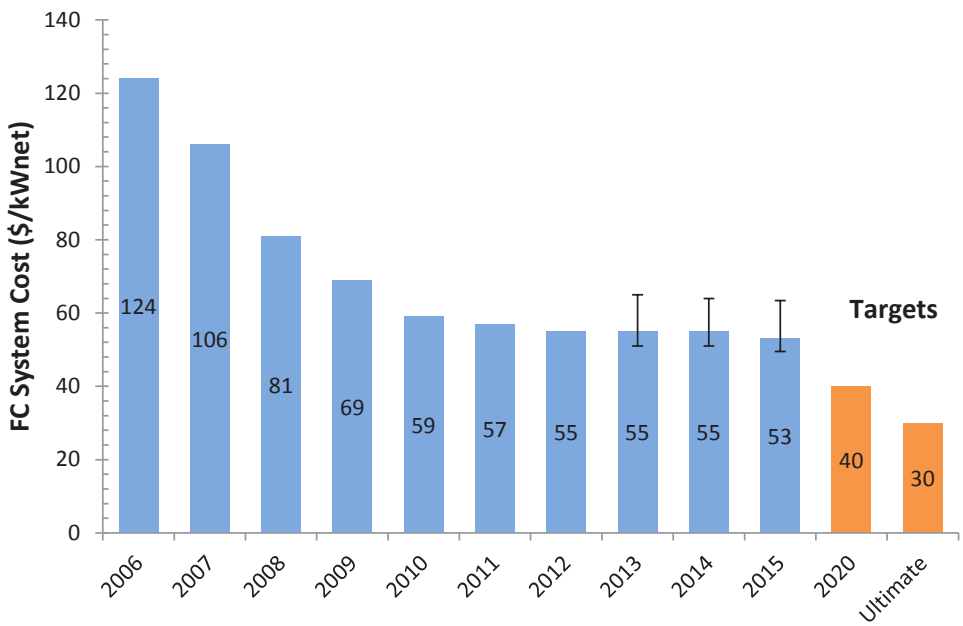

FIGURE 1. Modeled cost of an 80-kW_{net} PEM fuel cell (FC) system based on projection to high-volume manufacturing (500,000 units/year).

To enable vehicle commercialization, the sub-program is targeting a cost reduction to \$40/kW by 2020. Long-term competitiveness with alternative powertrains is expected to require further cost reduction to \$30/kW, which represents the sub-program's ultimate cost target.

Several new R&D projects were awarded in FY 2015 to explore innovative, off-roadmap ideas that could have a major impact on fuel cell cost, performance, and durability. New approaches being explored through these initiatives include the use of high temperature MEAs for liquid fuel utilization; development of advanced catalysts and MEAs for reversible alkaline membrane fuel cells; development of non-PGM hydrogen oxidation catalysts for alkaline membrane fuel cells; development of anion-exchange membranes for redox flow batteries; and development of non-PGM cathode catalysts for high temperature MEAs.

Performance and durability remain as major technical barriers to fuel cell commercialization. A new initiative announced in FY 2015, Fuel Cell Performance and Durability (FC-PAD), will directly address these topics through an R&D consortium led by a team of national laboratories. This core lab team will work with competitively selected industry and academic partners to advance the science and engineering of fuel cells, with a particular focus on development of durable, high performance electrodes.

Examples of R&D advancements achieved in FY 2015 are described below, including major improvements in fuel cell catalysts, membranes, and MEAs.

Catalysts

Several approaches to developing non-precious oxygen reduction catalysts were pursued in FY 2015, resulting in improvements in fuel cell activity measured at 0.9 V on pure oxygen and at 0.8 V measured on air. Current densities of 14–24 mA/cm^2 and 90–110 mA/cm^2 were achieved in the 0.9 V and 0.8 V testing, respectively, representing an improvement from 9–15 mA/cm^2 and 25–75 mA/cm^2 in FY 2014. The FY 2015 performance measurements indicate good progress toward achieving the targeted performance levels of 44 mA/cm^2 at 0.9 V and 300 mA/cm^2 at 0.8 V (which are equivalent to DOE targets for platinum-based catalysts). Catalysts investigated in FY 2015 were based on metal atoms or particles (typically iron) coordinated in a carbon-nitrogen matrix structure, including iron incorporated in metal organic framework structures and iron incorporated in a matrix of pyrolyzed cyanamide and polyaniline (CM-PANI-Fe-C) (Figure 2). Durability studies of these materials are underway, but the CM-PANI-Fe-C catalyst has already demonstrated high stability in ex situ testing, surviving 30,000 cycles from 0.2–1.0 V with only 30 mV decline in half-wave potential. (Los Alamos National Laboratory [LANL], Argonne National Laboratory, and Northeastern University)

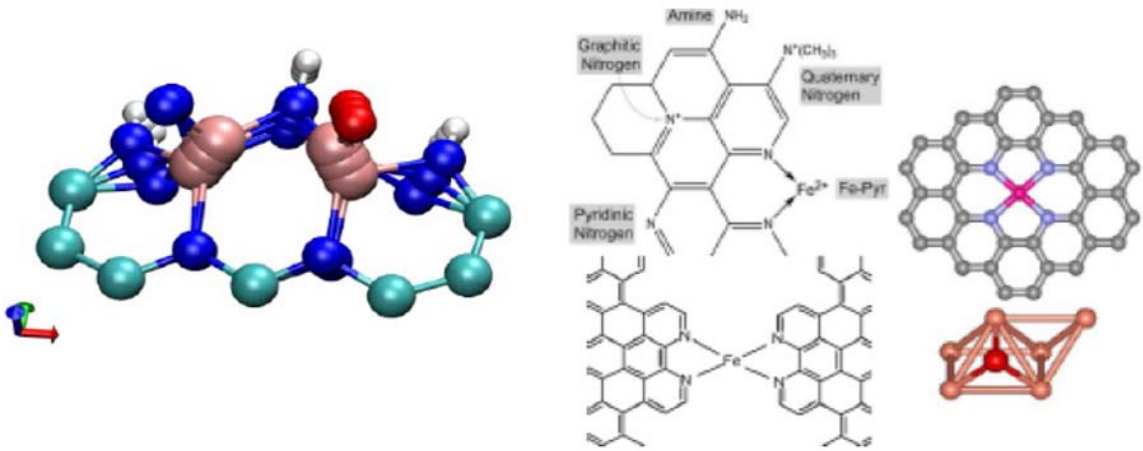

FIGURE 2. Left: Model active site in a CM-PANI-Fe-C catalyst. Right: Proposed structure of an iron metal organic framework catalyst.

Electrolytes

Improved nanofiber-supported fuel cell membranes containing multi-acid side chain ionomers were developed in FY 2015 (Figure 3). These membranes meet DOE durability targets and have better performance under hot and dry conditions than state-of-the-art conventional membranes. The new membranes, which combine low equivalent weight (EW) ionomers with electrospun nanofiber supports and chemical stabilizers, are promising candidates to improve fuel cell performance robustness and decrease humidification requirements. The inclusion of multiple acid sites on each side chain enables the new ionomer to have the high conductivity of a low-EW ionomer while retaining the good mechanical properties of a high-EW ionomer. Up to four acid groups were incorporated into each side chain, leading to unprecedented levels of conductivity in a stable perfluorinated ionomer. Mechanical testing of the electrospun membrane supports indicated that they already have strength similar to conventional expanded polytetrafluoroethylene supports, but further work is ongoing to achieve even higher strength. (3M)

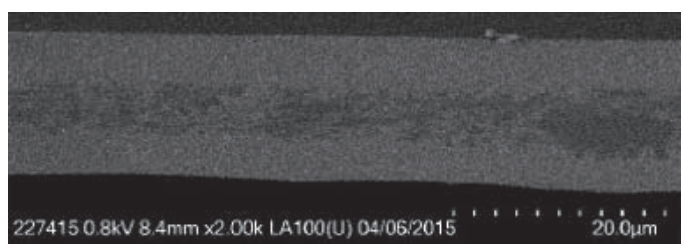

FIGURE 3. Cross-section of an advanced composite membrane showing an internal nanofiber-based support layer surrounded by a multi-acid side chain ionomer.

An improved electrolyte matrix for MCFCs with increased porosity and improved pore size distribution was developed in FY 2015. The new matrix has porosity more than 20% higher than the baseline matrix, enabling a higher electrolyte concentration with lower ohmic resistance. The new matrix has a narrower pore size distribution (Figure 4), with the fraction of undesirable large pores (larger than 0.2 µm) decreased by more than 30% in a cell that was verified over a 2,000-hour test. A 25% increase in mechanical strength of the matrix was also demonstrated. These improvements are part of a "smart" matrix development project that is expected to increase rated stack power by more than 20% while doubling stack lifetime. Successful achievement of these goals, which will be verified through accelerated testing of a full-area 30 kW demonstration stack, will enable larger scale deployment of MCFCs for distributed generation and CHP applications. (FuelCell Energy)

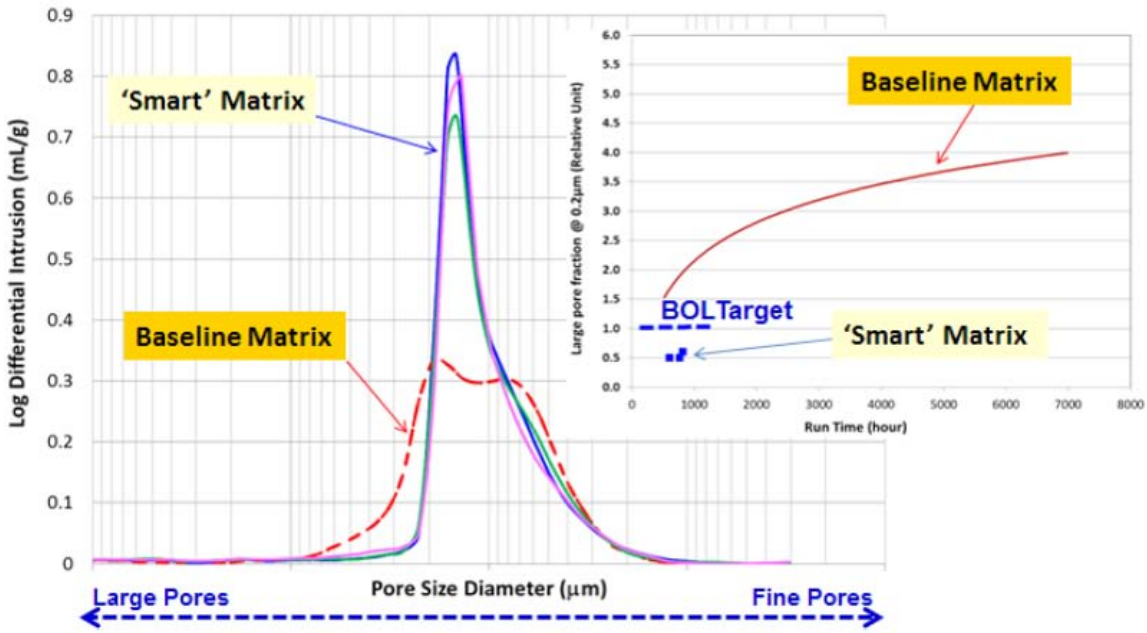

BOL – beginning of life

FIGURE 4. A new MCFC electrolyte matrix developed in FY 2015 has improved pore size distribution, enabling higher performance and longer lifetime.

Membrane Electrode Assembly Integration

Improved integration of fuel cell components based on NSTF catalysts into high performance MEAs enabled a substantial increase in performance in FY 2015. Power output per gram of PGM at rated power increased to 6.5 kW/g_{PGM} (improved from 2.8 kW/g_{PGM} in 2008 and 6.2 kW/g_{PGM} in FY 2014) under conditions that satisfy the DOE heat rejection target (Figure 5). The performance of this MEA at 0.8 V surpassed the DOE target of 300 mA/cm^2, while the performance at rated power of 855 mW/cm^2 fell just short of the DOE target of 1,000 mW/cm^2. The inclusion of a platinum nanoparticle-based cathode interlayer in this MEA represents a major improvement in enabling higher operation robustness and tolerance to non-ideal operating conditions. Development of a new ionomer

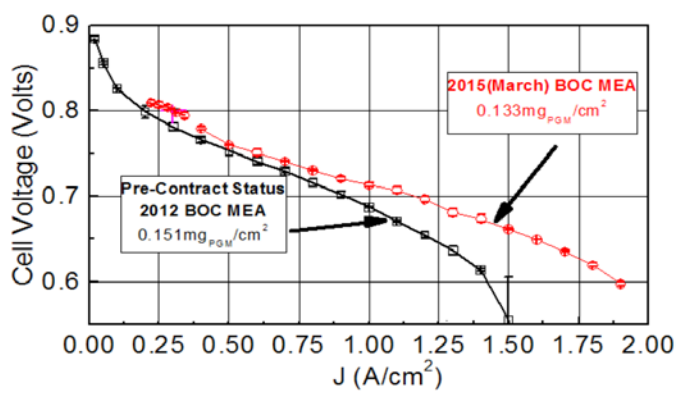

FIGURE 5. Reduction in PGM loading and improvement in MEA performance have enabled performance levels as high as 6.5 kW/g_{PGM} in NSTF-based MEAs.

membrane that reduces the extent of catalyst poisoning by ionomer degradation products also led to a 30% decrease in rated power degradation versus the 2014 baseline. (3M)

A new fuel cell fabrication method was developed in FY 2015 in which the fuel cell cathode has higher performance with lower platinum catalyst loading. This improvement was enabled by incorporating carbon nanotubes covered by a thin layer of Nafion® into the cathode, thereby providing a continuous pathway for transport of protons between the fuel cell membrane and the catalyst particles. Inclusion of this continuous pathway enables the use of thinner coatings of Nafion® on the platinum catalyst particles, making the particles more accessible to reactant oxygen and improving performance. Fuel cells containing these engineered cathodes had performance similar to state-of-the-art commercial fuel cells despite having a lower surface area of platinum. (LANL)

Improved Characterization Techniques

Development of improved visualization techniques has enabled physical mapping of fuel cell structures with unprecedented resolution. High spatial resolution images of fluorine distribution obtained through energy dispersive spectroscopy (Figure 6) have enabled mapping of ionomer content across an entire 5-µm cathode catalyst layer, data that is helping modelers to better understand electrode structure and resulting transport properties. (Oak Ridge National Laboratory)

Similarly, high resolution cryo-electron tomography (Figure 7) has enabled visualization of the heterogeneous domain structure of ionomer membranes, enabling better understanding of transport within the membrane and at interfaces. (Lawrence Berkeley National Laboratory)

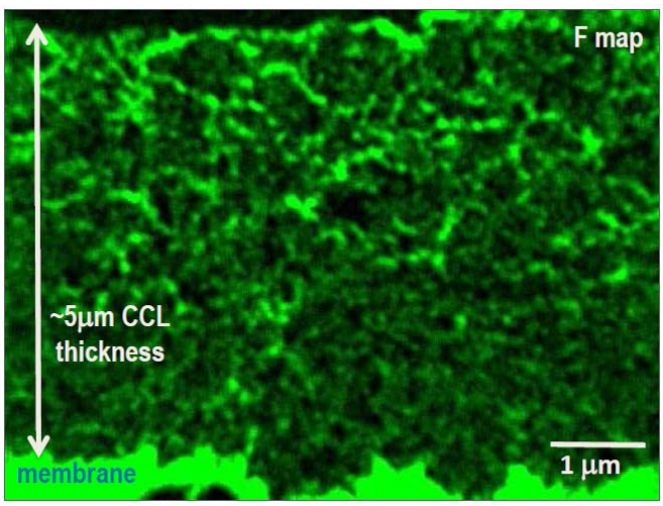

FIGURE 6. Ionomer distribution (fluorine X-ray map) across full thickness of 5-µm cathode catalyst layer.

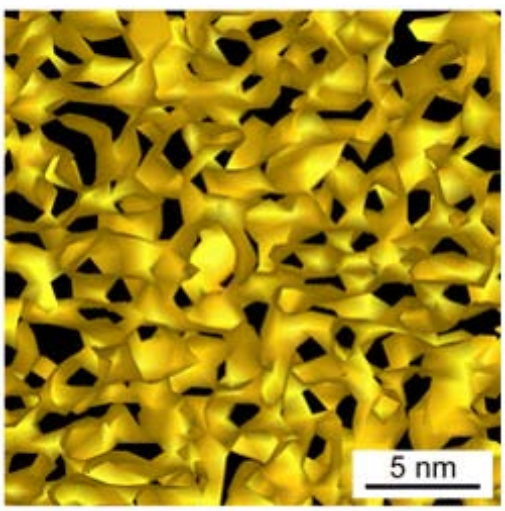

FIGURE 7. Cryo-electron tomography of hydrated Nafion® reveals a connected locally-flat network.

BUDGET

The FY 2016 budget request calls for $36 million for the Fuel Cells sub-program, which is a slight increase from the FY 2015 appropriation.

Figure 8 shows the budget breakdown by R&D area for FY 2015 and the FY 2016 budget request. The sub-program continues to focus on reducing costs and improving durability with an emphasis on fuel cell stack components. New projects were initiated in FY 2015 for R&D on several advanced off-roadmap concepts, and a new lab-led consortium tasked with coordinating and harmonizing fuel cell performance and durability R&D was selected. In FY 2016, the sub-program plans to issue funding opportunity announcements for awards funded in FY 2016.

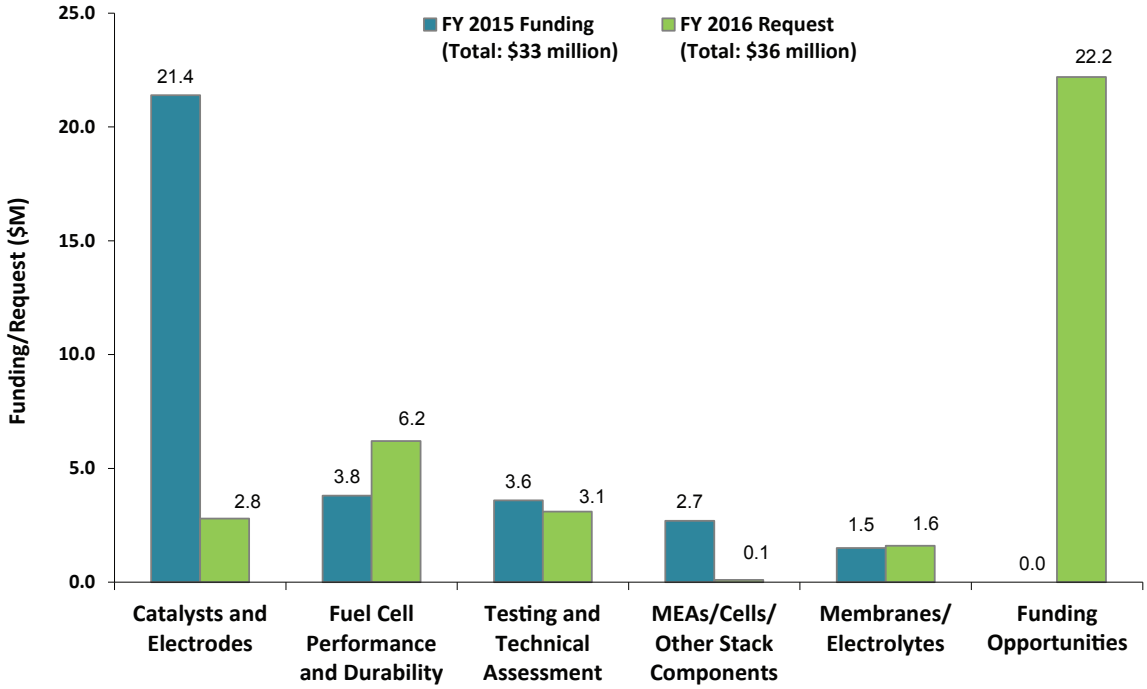

FIGURE 8. Fuel Cell R&D Funding. Subject to appropriations, project go/no-go decisions, and competitive selections. Exact amounts will be determined based on research and development progress in each area and the relative merit and applicability of projects competitively selected through planned funding opportunity announcements.

FY 2016 PLANS

In FY 2016, the Fuel Cells sub-program will continue R&D efforts on fuel cells and fuel cell systems for diverse applications, using a variety of technologies (including PEM and alkaline membrane fuel cells) and a range of fuels (including hydrogen, natural gas, and liquid fuels). Support will continue for R&D that addresses critical issues with electrolytes, catalysts, electrodes, and modes of operation, with an emphasis on cost reduction and durability improvement. The sub-program will also continue its emphasis on science and engineering with a focus on component integration at the cell level. Ongoing support of modeling will guide component R&D, benchmarking complete systems before they are built and enabling exploration of alternate system components and configurations. Cost analysis efforts include studies of fuel cells for transportation applications as well as distributed power generation systems (including CHP) and systems for early markets; further detailed results of these analyses are expected in FY 2016. Updates to target values will be released in a revision of the Multi-Year Research, Development, and Demonstration Plan, which is scheduled for release in FY 2016.

Dimitrios Papageorgopoulos
Fuel Cells Program Manager
Fuel Cell Technologies Office
Office of Energy Efficiency and Renewable Energy
U.S. Department of Energy
1000 Independence Ave., SW
Washington, D.C. 20585-0121
Phone: (202) 586-5463
Email: Dimitrios.Papageorgopoulos@ee.doe.gov

V.A.1 Extended, Continuous Pt Nanostructures in Thick, Dispersed Electrodes

Bryan Pivovar (Primary Contact), Shaun Alia, KC Neyerlin, Katherine Hurst, Jason Zack, Clay Macomber, Shyam Kocha
National Renewable Energy Laboratory
15013 Denver West Parkway
Golden, CO 80401
Phone: (303) 275-3809
Email: Bryan.Pivovar@nrel.gov

DOE Manager
David Peterson
Phone: (720) 356-1747
Email: David.Peterson@ee.doe.gov

Subcontractors
- Yushan Yan (PI), Jarrid Wittkopf
  University of Delaware, Newark, DE
- Svitlana Pylypenko, Dave Diercks, Ami Neyerlin, Jeremy Leong
  Colorado School of Mines (CSM), Golden, CO

Project Start Date: July 20, 2009
Project End Date: Sept 30, 2015

Overall Objectives

- Increasing mass activity and durability of Pt-based electrocatalysts through the implementation of high-surface area extended surface electrocatalysts
- Optimize fuel cell performance of extended surface electrocatalysts
- Demonstrate DOE 2020 target performance and durability in fuel cell tests

Fiscal Year (FY) 2015 Objectives

- Using pre-leaching on top performing novel electrocatalysts to reduce transition metal dissolution impact on durability, demonstrate a mass activity of 880 mA mg Pt^{-1} at 0.9 V (2x DOE 2020 target) and less than a 5% loss after durability testing (30,000 cycles, mass activity) in rotating disk electrode (RDE) tests with a total transition metal dissolution of less than 1% of initial catalyst mass (current high performance materials experience dissolution rates up to 7% mass under these conditions)
- Aligned with DOE's 2020 targets
  - 1,000 mW/cm^2 at rated power and less than 40% loss in catalytic activity
  - Develop membrane electrode assemblies (MEAs) with 100% improvement in initial mass activity when compared to baseline Pt/C catalysts at rated power (5 A/mgPt at 0.75 V infrared [IR] corrected) using novel electrocatalysts
  - Demonstrate less than 40% loss of mass activity at rated power (0.75 V IR free) 80°C, 100% relative humidity (RH) after 30,000 potential cycles between 0.6 and 1.0 V at 500 mV/s

Technical Barriers

This project addresses the following technical barriers from the Fuel Cells section (3.4.4) of the Fuel Cell Technologies Office Multi-Year Research, Development, and Demonstration (MYRDD) Plan:

(A) Durability (of catalysts and membrane electrode assemblies)

(B) Cost (of catalysts and membrane electrode assemblies)

(C) Performance (of catalysts and membrane electrode assemblies)

(D) Start-up and Shut-down Time and Energy/Transient Operation

Technical Targets

This project synthesizes novel extended thin film electrocatalyst structures (ETFECS) and incorporates these catalysts into electrodes with and without carbon blacks for further study. The project has targets outlined in the MYRDD Plan for both electrocatalysts for transportation applications (Table 3.4.13) and MEAs (Table 3.4.14). The specific targets and status of highest relevance are presented in Table 1.

TABLE 1. Technical Targets for Electrocatalysts for Transportation Applications

Characteristic	Units	2017/2020 Targets	Status
Mass activity (150 kPa H_2/O_2 80°C, 100% RH)	A/mg-Pt @ 900 mV	0.44/0.44	0.45
Electro catalyst support stability	% mass activity loss	<10/<10	<10*
Loss in initial catalytic activity	% mass activity loss	<40/<40	<10*

*measured in RDE, following 30,000 cycles between 0.6 V and 1 V

FY 2015 Accomplishments

- The project has demonstrated extended surface catalysts with remarkably high surface area and specific activity that offer the potential to dramatically decrease required Pt loadings through exceptionally high mass activities (>2,500 mA/mg Pt).
- These materials have also demonstrated good durability under select (potential cycling, both RDE and MEA) conditions, including dramatically reduced transition metal dissolution rates.
- The project has advanced the performance of these materials in MEAs and demonstrated the need for further understanding and development in these areas.

✧ ✧ ✧ ✧ ✧

INTRODUCTION

Conventional nanoparticle Pt/C electrocatalysts (2–5 nm) used in automotive fuel cells appear to have plateaued in terms of electrochemical area and catalytic activity. ETFECS offer the possibility of higher specific activities, comparable to that of bulk poly-Pt. ETFECS materials formed by direct deposition traditionally exhibit lower electrochemical surface areas ([ECAs], and lower mass activities); synthesis by galvanic displacement, however, has in cases allowed for a thrifting of the noble metal layer, and for ECAs comparable to conventional nanoparticle catalysts. This year we have for the first time demonstrated materials that not only greatly exceed the 2020 mass activity target, but also demonstrate exceptional durability when exposed to acid and potential cycling.

APPROACH

Our overall approach is towards developing extended surface Pt catalysts with high mass activity and durability, and incorporating these structures into robust, high efficiency MEAs. This approach has focused on the synthesis of novel ETFECS formed by spontaneous galvanic displacement, specifically with Ni and Co templates. These materials have demonstrated high specific activity and durability, as well as surfaces areas significantly larger than traditionally found in extended surface Pt catalysts (3M [1], others [2]). In our most recent work, we have optimized post-synthesis processing parameters including annealing conditions in different environments and acid leading in order to both improve catalyst performance and durability.

RESULTS

We have completed detailed studies focused on post-processing of PtNi nanowires (NWs) to increase durability while still retaining performance. We have conducted post-processing of PtNi NWs synthesized via galvanic displacement through annealing under reducing and/or oxidizing conditions as well as acid leaching. We have optimized each one of these processes independently and arrived at optimized conditions for all three combined processes. Figure 1a shows the mass and specific activity of PtNi NWs for samples following annealing under oxidizing conditions. These samples had been previously annealed under reducing conditions and acid leached. The peak performance for these samples occurred at 10.7% Pt, >2,500 mA/mg Pt (>5x improvement in mass activity in rotating disc electrode studies, compared to DOE 2020 MEA target). These samples also exhibited exceptionally high

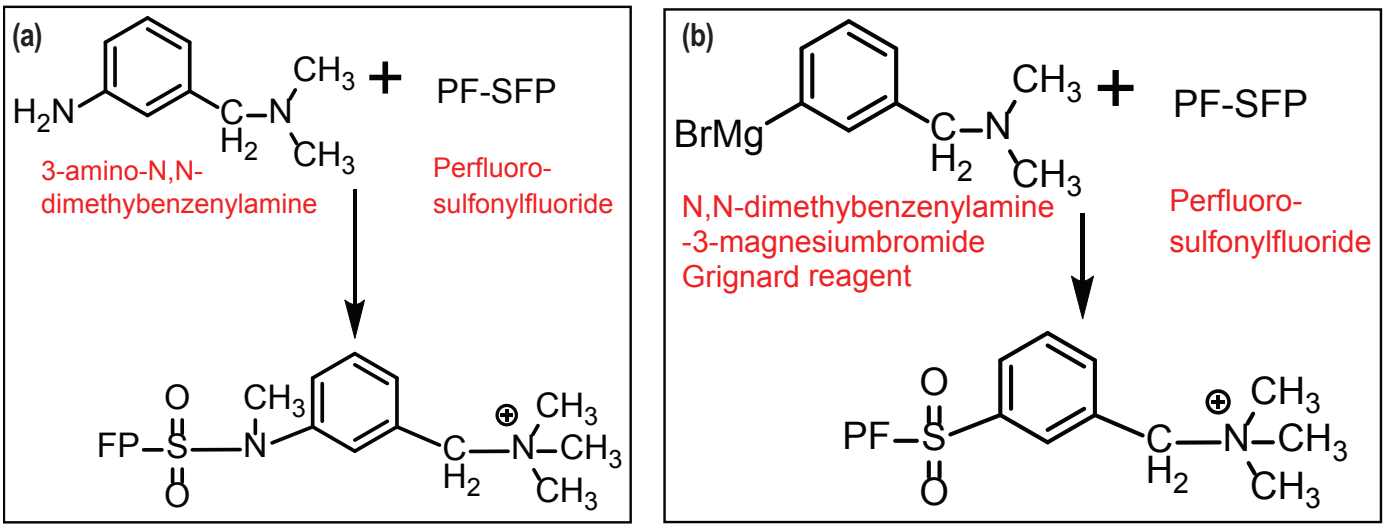

FIGURE 1. (a) Specific and mass activity of PtNWs after annealing under reducing conditions, acid leaching and annealing under oxidizing conditions; (b) Pt and Ni dissolution rates upon exposure to acid and post-potential cycling of samples shown in Figure 1a

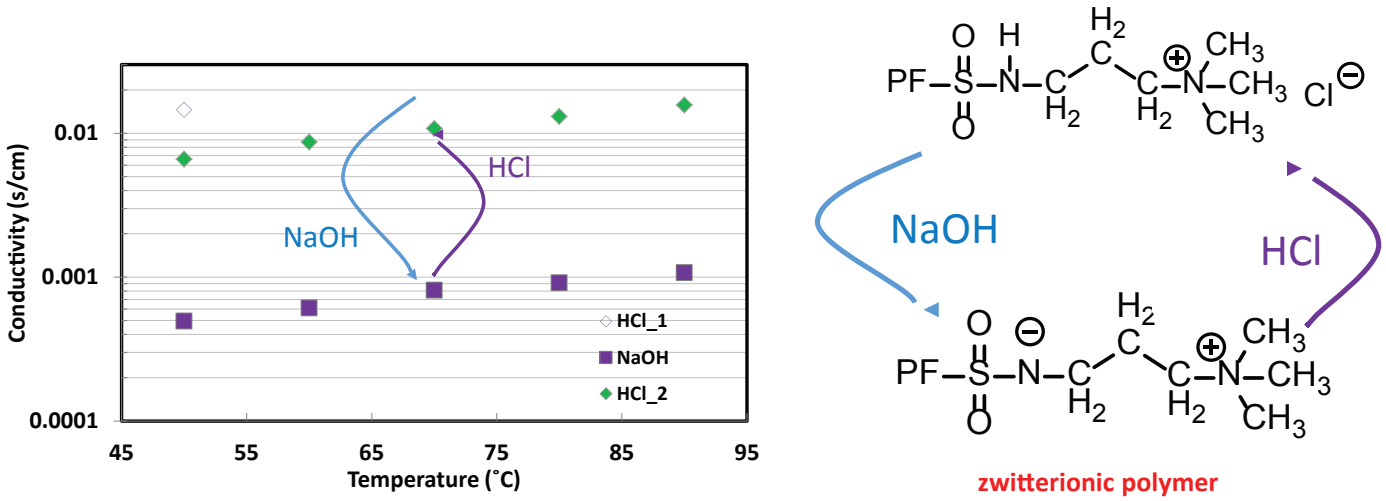

FIGURE 2. Summary of high ECA PtNi NWs before and after potential cycling (30,000 cycles, 0.6 V to 1 V) compared to baseline Pt/C (solid line denotes DOE 2020 MEA target)

durability to Ni dissolution (Figure 1b) following exposure to acid (break-in) and 30,000 potential cycles between 0.6 V and 1.0 V. Through the optimized post-processing conditions we were able to both make highly active samples and highly durable samples, advancing the performance of our materials relative to those reported in FY 2014, particularly in the area of durability/transition metal dissolution. Figure 2 provides a summary of the performance of our top performing catalysts (all with initial electrochemical surface areas >80 m^2/g Pt). The arrows in Figure 2 denote performance following potential cycling (30,000 cycles between 0.6 V and 1 V in RDE studies). While earlier samples with high performance showed poor stability, the optimized materials maintained their high performance post-cycling. These results were exceptionally promising, however, our attempts to scale up synthesis batch size resulted in losses in performance (~25%) and batch to batch reproducibility concerns that remain as on-going issues.

In order to address scale up and reproducibility issues, we applied atomic layer deposition (ALD) as a potential route to reproducing the performance of galvanically displaced samples with a potentially more reproducible method, lower cost, and amenable to large scale manufacture. Preliminary results (shown in Figure 3) based on post-synthesis annealing demonstrated that high ECA could be obtained by this route, as samples annealed to 250°C exhibited ECAs ~95 m^2/g Pt. Specific activity of these ALD samples has not reached the level of galvanically displaced samples, but remains an area of potential interest.

PtNi NWs were also fabricated into electrodes of MEAs to gauge fuel cell performance and durability. The unique density and dispersion characteristics of PtNi NWs render them difficult to effectively process into high performance MEAs. In previous work we had shown MEA performance

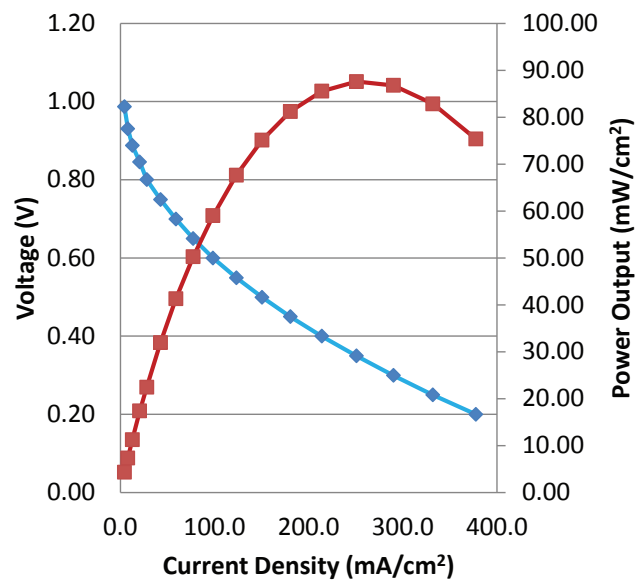

FIGURE 3. Electrochemical properties of PtNiNWs synthesized via atomic layer deposition following annealing in a reducing atmosphere as a function of reducing temperature

improvements through the incorporation of carbon into electrodes or through improved dispersion preparation. For the first time our team applied impedance and limiting current measurements to these systems in order to assess performance losses attributed to mass transport and protonic resistance in the electrode layer. We also demonstrated significantly improved durability of these materials when compared to traditional Pt/C materials when tested in the carbon corrosion region (potential cycling between 1 V and 1.5 V), Figure 4. While both samples showed similar initial performance, the PtNi NW sample showed negligible

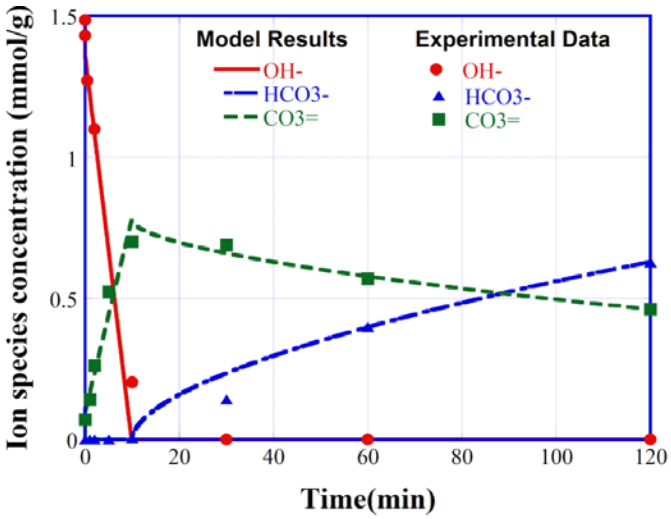

FIGURE 4. Fuel cell polarization curves of PtNWs compared to Pt/C baseline material before and after potential cycling

degradation after being subject to 6,000 potential cycles; in contrast, Pt/C showed significant performance loss after only 1,000 cycles.

CONCLUSIONS AND FUTURE DIRECTIONS

The project has synthesized many novel catalysts using materials, geometries, and approaches not previously demonstrated. We improved upon the durability of Pt Ni nanowires reported in FY 2014, decreasing Ni metal dissolution rates to obtain highly durable, high performing samples. Our efforts going forward will seek to further increase the catalyst activity and optimize MEA performance in order to maintain RDE activity in fuel cell tests by focusing on the following.

- Electrocatalyst synthesis focus on reproducibility/increased batch size
  - Galvanic displacement to produce materials of target performance in increased quantity
  - Further post-processing studies of ALD synthesized materials, use of rotary ALD system to improve intra- and inter-batch reproducibility
- Electrode structure/fuel cell studies
  - Optimization of electrode structure/fuel cell performance using ETFECS with a focus on catalyst ink dispersions and composition
  - Isolation of overpotential losses in MEA electrodes made with ETFECS materials (deconvolution of mass transfer, ohmic, and kinetic losses)
  - Durability studies to quantify performance loss with a specific emphasis on transition metal leaching

FY 2015 PUBLICATIONS/PRESENTATIONS

1. Shaun M. Alia, Svitlana Pylypenko, K.C. Neyerlin, Shyam S. Kocha, and Bryan S. Pivovar, "Nickel Nanowire Oxidation and Its Effect on Platinum Galvanic Displacement and Methanol Oxidation," ECS Trans. 2014 64(3): 89–95; doi:10.1149/06403.0089ecst.

2. Jeremy Leong, Abbas Ebnonnasir, Maxwell C. Schulze, Matthew B. Strand, Chilan Ngo, David Maloney, Sarah L. Frisco, Huyen N. Dinh, Bryan Pivovar, George Gilmer, Suneel Kodambaka, Cristian V. Ciobanu, and Ryan M. Richards, "Shape-directional growth of Pt and Pd nanoparticles," Nanoscale, 2014.

3. S.M. Alia, Y. Yan, B.S. Pivovar, "Galvanic Displacement as a Route to Highly Active and Durable, Extended Surface Electrocatalysts," Catalysis Science and Technology, 2014, 4 (10), 3589–3600.

4. Leong, G.J.; Schulze, M.C.; Strand, M.B.; Maloney, D.; Frisco, S.L.; Dinh, H.N.; Pivovar, B.; Richards, R.M., "Shape-directed Platinum Nanoparticle Synthesis: Nanoscale Design of Novel Catalysts," Applied Organometallic Chemistry, 28, 1–17, 2014.

5. Shaun M. Alia, Svitlana Pylypenko, Arrelaine Dameron, K.C. Neyerlin, Shyam S. Kocha, and Bryan S. Pivovar, "Oxidation of Platinum Nickel Nanowires to Improve Durability of Oxygen-Reducing Electrocatalysts," submitted.

6. Pivovar, B. (Aug., 2014). "Fuel Cell and Electrolysis Activities at the National Renewable Energy Lab," Presented at MRES, Northeastern University, August 21, 2014.

7. Pivovar, B. (Nov., 2014). "Fuel Cell R&D focused on Alkaline Membranes and Advanced Catalysis at the National Renewable Energy Lab," Presented at Wuhan University, Wuhan, China, November 12, 2014.

8. Pivovar, B. (Nov., 2014). "Fuel Cell R&D focused on Alkaline Membranes and Advanced Catalysis at the National Renewable Energy Lab," Presented at Dalian Institute of Chemical Physics, Dalian, China, Nov. 13, 2014.

9. Pivovar, B. (March, 2015). "Past, Current, and Future Research in Polymer Electrolyte Fuel Cells," Presented at University of Colorado – Denver, Denver, CO, March 6, 2015.

10. Pivovar, B. (April, 2015). "Past, Current, and Future Research in Polymer Electrolyte Fuel Cells," Presented at University of Wyoming, Laramie, WY, April 2, 2015.

11. Pivovar, B. (April 2014). "Past, Current, and Future Research in Polymer Electrolyte Fuel Cells," Presented at Purdue University, West Lafayette, IN, April 3, 2014.

REFERENCES

1. http://www.hydrogen.energy.gov/pdfs/review08/fc_1_debe.pdf.

2. Z. Chen, W. Li, M. Waje, Y.S. Yan, *Angew. Chem. Int. Ed.* 2007, 46:4060–4063.

V.A.2 Nanosegregated Cathode Alloy Catalysts with Ultra-Low Platinum Loading

Vojislav R. Stamenkovic (Primary Contact) and Nenad M. Markovic
Argonne National Laboratory
Argonne, IL 60439
Phone: (630) 252-8946
Email: vrstamenkovic@anl.gov

DOE Manager
Nancy Garland
Phone: 202-586-5673
Email: Nancy.Garland@ee.doe.gov

Subcontractors
- Karren More, Oak Ridge National Laboratory, Oak Ridge, TN
- Deborah Myers, Argonne National Laboratory, Argonne, IL

Project Start Date: September 2009
Project End Date: September 2015

Overall Objectives

- Establish the parameters that control kinetics of the oxygen reduction reaction on multimetallic PtM (M = Co, Ni, Fe, and Ti) and PtM_1N_2 (M_1 =Co/Ni; N_2 = TM) alloys
- Develop highly efficient, durable, nanosegregated Pt-skin PtM and PtM_1N_2 catalysts with ultra-low Pt content
- Develop highly active and durable Au/PtM_3 nanoparticles (NPs) with ultra-low Pt content
- Find relationships between activity/stability of well characterized bulk alloys and NPs
- Develop novel chemical and physical methods for synthesis of monodispersed PtM and PtM_1N_2 alloy NPs and thin metal films
- Resolve electronic/atomic structure and segregation profile of PtM and PtM_1N_2 systems
- Resolve composition effects of PtM and PtM_1N_2 systems
- Demonstrate mass activity and stability improvement of PtM and PtM_1N_2 alloy NPs in rotating disk electrodes (RDEs) and membrane electrode assemblies (MEAs)
- Use computational tools as the basis to form any predictive ability in making binary and ternary systems with desirable reactivity and durability properties
- Develop and synthesize highly active and durable practical catalysts with ultra-low content of precious metals

Fiscal Year (FY) 2015 Objectives

- Development of synthesis routes to produce larger volumes of catalysts in a single batch
- Synthesis and characterization of the most active and durable Pt-alloy NPs with controlled size, compositional profile, and Pt-skin surface
- Electrochemical characterization of the nanosegregated catalysts by RDE
- Reproducibility of performance for large scale batches of highly active catalysts
- Integration of highly active catalyst into MEA, fabrication and characterization

Technical Barriers

This project addresses the following technical barriers from the Fuel Cells section (3.4.5) of the Fuel Cell Technologies Office (FCTO) Multi-Year Research, Development, and Demonstration Plan of 2012:

(A) Durability

(B) Cost

(C) Performance

Technical Targets

This project is conducting research related to Pt-based binary PtM (M= Ni, Co, Fe, Cr, V, and Ti), ternary PtM_1N_2 (NM = Fe, Co, and/or Ni) and core/shell Au/Pt_3M multimetallic NPs for the oxygen reduction reaction. The design and synthesis of highly efficient, durable, nanosegregated Pt-skin catalysts with ultra-low Pt content are targeted to meet or exceed the DOE 2015 targets shown in Table 1.

TABLE 1. Progress towards Meeting DOE 2015 Technical Targets for Electrocatalysts

	Unit	2015 DOE Targets	Project Status
PGM Total Loading	mg_{PGM}/cm^2	0.200	0.035
Mass Activity	A/mg_{Pt} @ 900 mV	0.44	0.76
Specific Activity	$\mu A/cm^2_{Pt}$ @ 900 mV	720	2,600

PGM – precious group metal

FY 2015 Accomplishments

- Synthesized novel bi/multi-metallic NPs with controlled size and composition by colloidal organic solvothermal approach
- Increased the amount of a single batch for synthesis of highly active nanoframe catalyst from 5 mg to 30 mg per batch
- Established a relationship between the mass of single batch and performance
- Established structure–composition–function relationship for a novel class of core/interlayer/bimetallic shell NPs
- Optimized the thickness of the subsurface Au-interlayer in the Ni-core/Au-interlayer/NiPt-shell NPs for the maximal catalytic activity, superior durability, and minimal loading of PGMs
- Verified 20,000 cycle activity/durability performance for core-interlayer/shell NPs
- Employed nanoframe catalyst in MEA
- Established structural properties of nanoframes in MEA before and after testing
- Established compositional properties of nanoframes in MEA before and after testing
- Evaluated catalyst/ionomer ratio for nanoframe particles in MEA suspension
- Established oxygen reduction reaction (ORR) performance for nanoframes by RDE and MEA for the ORR
- Implemented ionic-liquid approach into the nanoframe catalyst and performed detailed structural and electrochemical evaluations by high resolution transmission electron microscopy (HR-TEM) and MEA
- Achieved three-fold improvement in specific activity and two-fold improvement in mass activity vs. 2015 DOE technical targets for PtNi nanoframe catalyst in MEA

✧ ✧ ✧ ✧ ✧

INTRODUCTION

In the quest to make the polymer electrolyte membrane fuel cells a competitive force, one of the major challenges is to reduce the significant overpotential for the ORR and minimize dissolution of the cathode catalysts. Here, we report progress for FY 2015 in experimental studies to address the importance of alloying Pt with 3d metals in order to form catalytically active materials with so-called *nanosegregated profile* [1]. In our previous work we have identified that the nanosegregated surfaces are superior in both exceptional catalytic activity for the ORR and improved stability of Pt surface atoms, which make them capable to address DOE technical targets for application of fuel cells in transportation.

APPROACH

In order to address the challenges that are listed as the DOE targets for FCTO, we rely on our materials-by-design approach [1-11]. This approach involves five major steps: (i) advanced chemical and physical methods for synthesis of novel nano/mesoscale materials, which enables control of material size, composition, morphology and structure; (ii) characterization of atomic and electronic properties by ex situ and in situ surface specific tools and theoretical methods; (iii) resolving the surface electronic and crystal structures at atomic/molecular level that govern efficient kinetics of the ORR; (iv) synthesis/fabrication (scale-up) of the highly efficient practical catalysts, which are guided by the fundamental understanding of structure-function relationships; and (v) electrochemical evaluation of catalyst properties by RDE and MEA.

RESULTS

Non-PGM Core/Au-Interlayer/with Pt-Based Overlayers

These unique nanostructures were introduced last year through a synthesis that produced an intentional concentration profile that warrants catalytic performance of Pt-bimetallic alloys with substantially improved durability due to presence of subsurface Au atoms. The initial step in synthesis was to produce monodisperse Ni particles with narrow size distribution of 3.1 nm ($\sigma < 5\%$) Ni NPs and to coat them with optimized quantity of Au, forming an intermediate Ni@Au core/shell nanostructure. The final step in chemical synthesis was to deposit a desirably thick PtNi shell of approximately 1 nm. Ni@Au@PtNi nanoparticles with a diameter of 5.0 nm ($\sigma = 6\%$) were formed and characterized to confirm compositional profile and reveal electrochemical properties. The scanning transmission electron microscopy analysis showed that after exposure to 0.1 M $HClO_4$ electrolyte, the core/shell structure and the Ni core are preserved, while the line-scan of energy dispersive X-ray spectroscopy depicts the formation of the Pt-skeleton surface due to dissolution of surface Ni atoms that are present on the as-prepared NP surfaces. Electrochemical evaluation after 10,000 potential cycles between 0.6 V and 1.1 V vs. reference hydrogen electrode (RHE) showed a negligible loss in activity of the NPs with core/interlayer/shell structures (Figure 1). Our initial report on the role of subsurface Au explained that placement of Au atoms with higher redox potential in the near-surface region lowers the probability for both Ni and Pt dissolution through the hindered place-

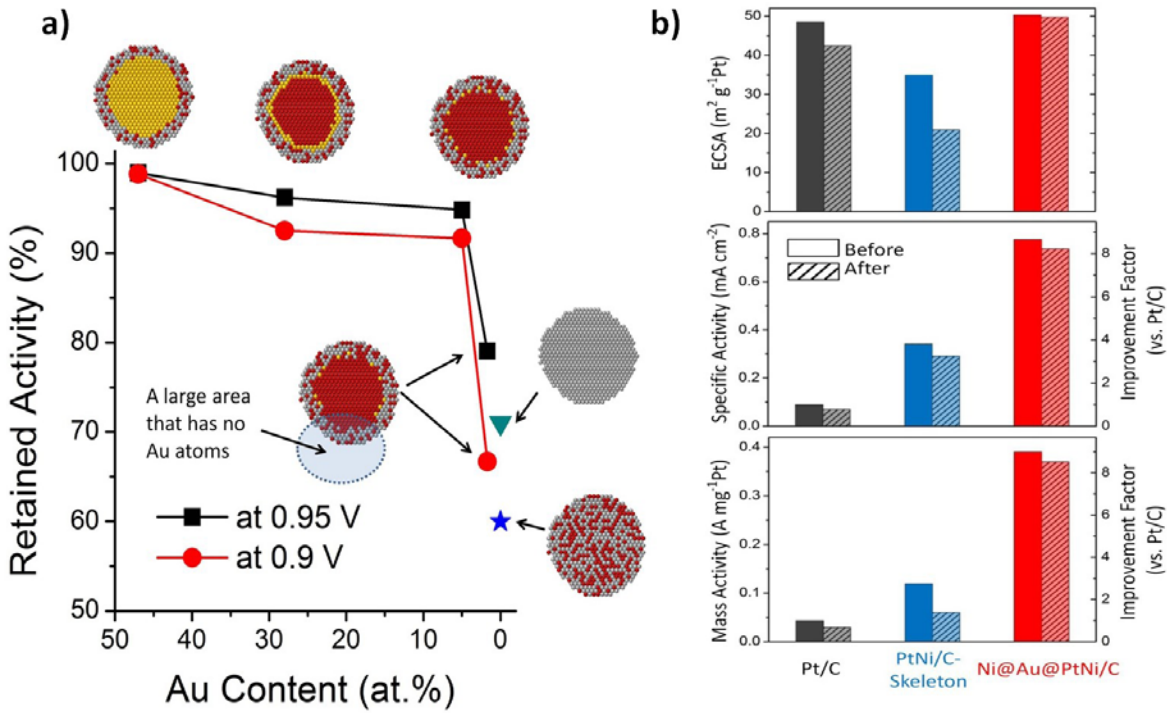

FIGURE 1. Core/interlayer/shell NPs. a) Retained activity after 10,000 potential cycles between 0.6 V and 1.1 V for NPs with different content of Au. b) Electrochemical evaluations by RDE of Ni@Au@NiPt/C, PtNi/C, and Pt/C before and after potential cycling.

exchange mechanism. Moreover, we found that minimal amount of subsurface Au could be around 5 at%, which is close to 0.25 ML, in order to induce high durability in designated potential region. The specific and mass activity enhancement of Ni@Au@PtNi/C is over eight-fold versus the Pt/C and outperforms multilayered Pt-skin PtNi/C [8] due to the replacement of expensive Pt by Ni in the core. Structural characterization of Pt/C, PtNi-Skeleton/C, and Ni@Au@PtNi/C nanoparticles before and after 10,000 cycles revealed that the size of Pt and PtNi NP was significantly changed, while the size and shape of Ni@Au@PtNi was not affected, demonstrating high durability of this system.

In the most recent period, we extended our focus on the possibility to further enhance catalytic activity by achieving a favorable nanosegregated subsurface concentration profile with Pt-skin as the topmost surface layer. Our initial attempts to induce Pt-skin formation by thermal annealing were spoiled due to the strong tendency of Au to segregate over Pt in a given multimetallic system. For that reason, we have changed the strategy by introducing another component in the system that might prevent Au from migrating to the surface. Initial results obtained with sputtered thin films are shown in Figure 2, which illustrates the effect of thermal annealing and confirms feasibility of Pt-skin formation over PtNi shell for the systems that contain subsurface Au. Such fine tuning of the near surface composition profile allows synergy between maximal utilization of precious metals and maximal catalytic and durability performance.

Synthesis Scale-up of the PtNi Nanoframe Catalyst

Nanoframe Pt_3Ni catalyst exhibits 16-fold improvement in specific activity for the ORR at 0.95 V vs. commercial Pt/C electrocatalyst. The open architecture of the Pt_3Ni nanoframes enables access of reactants to both the internal and external surfaces and leads to 22-fold enhancement in the mass activity vs. Pt/C in RDE measurements. The mass activity at 0.9 V was measured to be 5.7 A mg^{-1} Pt and is over one order of magnitude higher than 0.44 A mg^{-1} Pt, the DOE 2017 target, which makes the Pt_3Ni nanoframes the most efficient electrocatalyst for the ORR [12]. In addition, nanoframes exhibited remarkable durability due to the nanosegregated composition profile that has at least two atomic layer thick Pt surface. Our initial synthesis effort was focused to produce quantities that would be sufficient for RDE evaluations, which was in the order of 5 mg of catalyst per single batch. Considering that MEA evaluation was our main target, we have optimized synthesis protocol to produce higher amounts of nanoframes. Figure 3 displays the outcome of our efforts expressed as performance measured for different batch quantities over a wide time frame. As of now, we managed to establish a synthesis protocol that yields about 30 mg of catalyst with performances that match the lower quantities reported last year. From Figure 3, it is

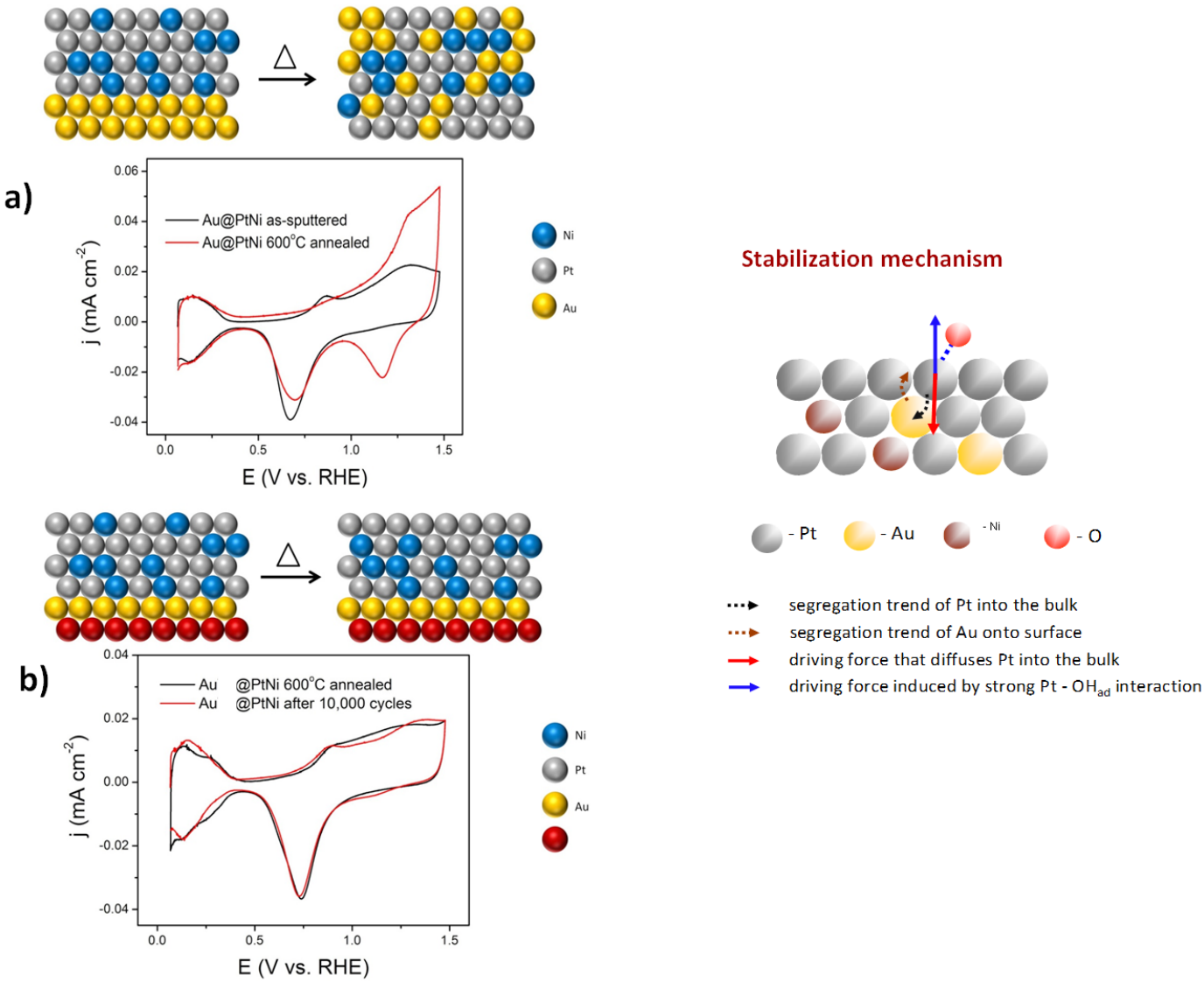

FIGURE 2. RDE characterization of sputtered thin films with distinct segregation profiles. a) Typical cyclic voltammetry after thermal annealing that shows redox Au peaks confirming the existence of surface Au atoms that lowers the number of Pt active sites atoms and specific activity for the ORR. b) Altered core composition prevents segregation of Au atoms after thermal annealing and allows Pt-skin formation with superior specific activity.

apparent that higher amounts of catalyst produced under laboratory conditions did coincide with the same structural, and hence catalytic, properties. For that reason we optimized the synthesis protocol for amounts lower than 30 mg of catalyst per single batch.

MEA Evaluation of PtNi Nanoframe Catalyst

A number of nanoframe catalyst evaluations were carried out in 5 cm^2 MEAs. The results for the best performing MEAs are shown in Figure 4, and they are compared to an MEA with a commercial Tanaka Kikinzoku Kogyo (TKK) 20 wt% Pt/C catalyst on the cathode. The same loading of the catalyst was applied for the results shown below. The MEAs were fabricated by the decal method with the ionomer and membrane in the proton form and hot-pressing of the decals to the membrane at 130ºC. The ionomer to carbon ratio was set to 0.8, and it is important to emphasize that the ionomer was found to be detrimental to the activity of this catalyst in RDE testing. Below is the summary of the MEA characteristics.

- Cathode: PtNi nanoframe, 0.0346 mg-Pt/cm^2
- Cathode electrochemically active surface area (ECSA): 49 cm^2 H_{upd}
- Cathode ionomer to carbon ratio: 0.8
- Anode: 0.2 mg-Pt/cm^2 TKK 46 wt% Pt/HSC
- Nafion® XL membrane

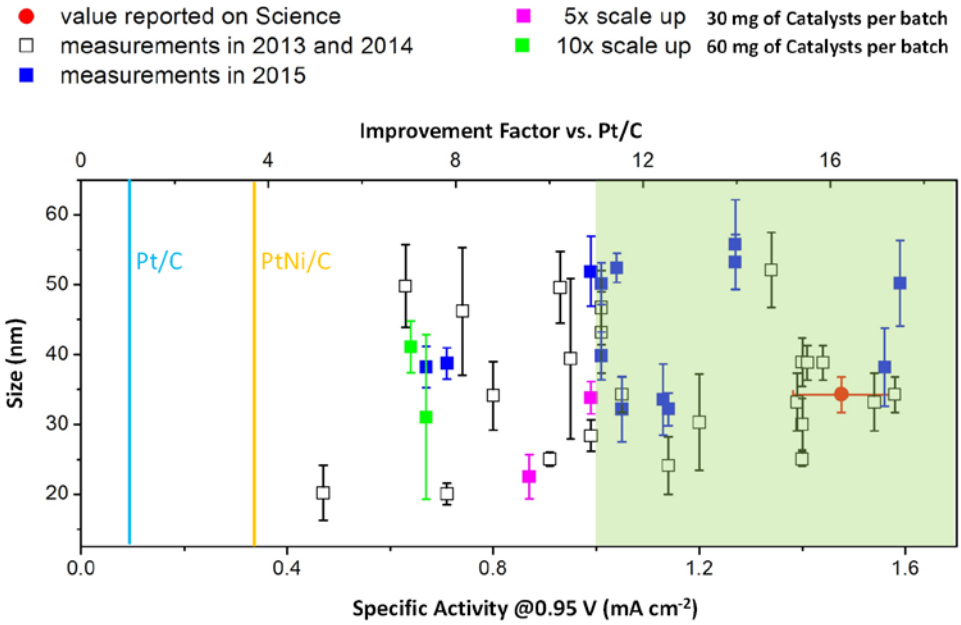

FIGURE 3. Scale-up synthesis of Pt_3Ni nanoframes: variation in performance of Pt_3Ni nanoframe catalyst for different batches of catalysts.

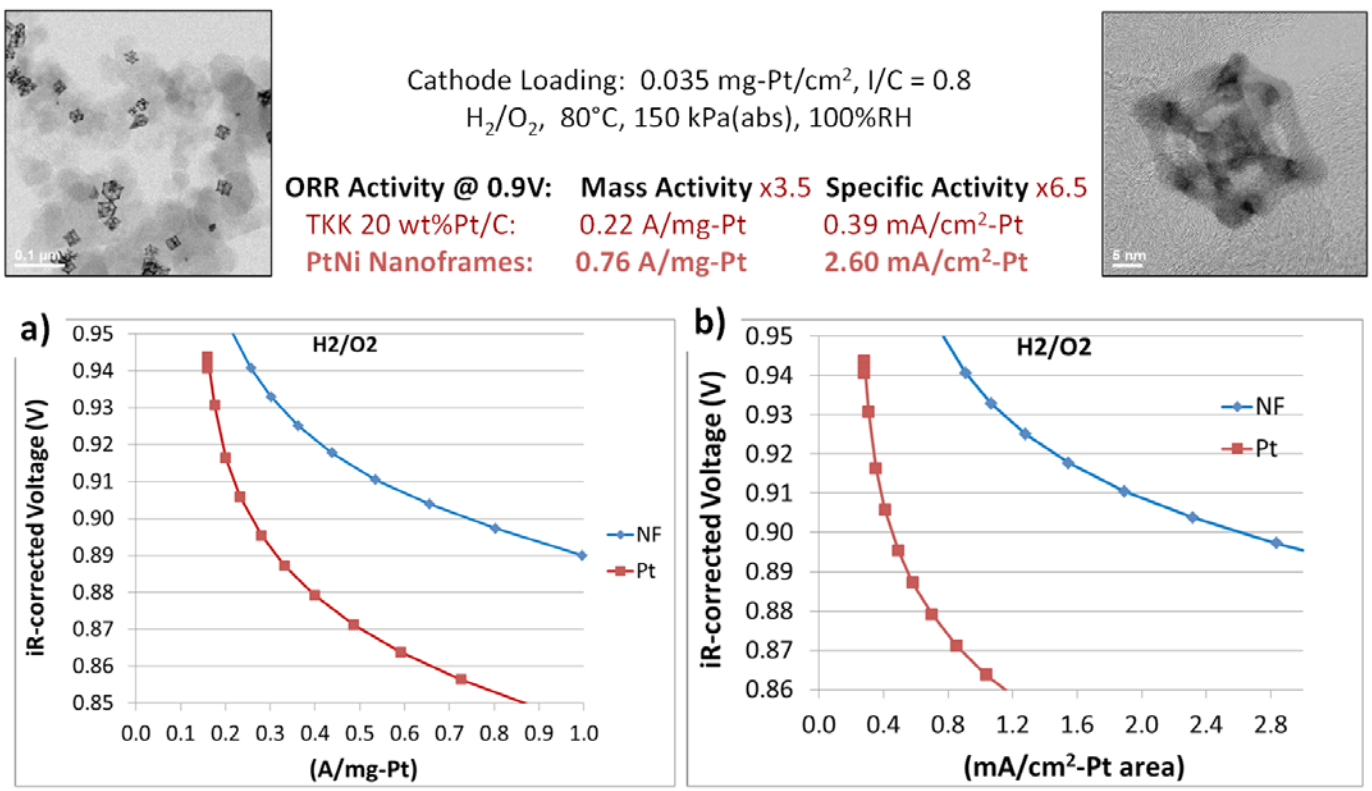

RH – relative humidity

FIGURE 4. MEA evaluation of Pt_3Ni nanoframe catalyst: hydrogen-oxygen polarization curves from 5 cm^2 MEA obtained for PtNi nanoframes and Pt/C TKK catalysts. Note that the Pt loading is approximately three times lower than the DOE technical target yet the performance surpasses the DOE technical target for both mass activity (~two-fold) and specific activity (three-fold).

- Gas diffusion layer: Sigracet 25 BC

The MEAs were tested at temperatures ranging from room temperature to 80ºC, with 150 kPa(abs) humidified hydrogen on the anode at 1 L/min and with 150 kPa(abs) humidified oxygen or air on the cathode, with a relative humidity of 100%. The hydrogen-oxygen mass activity results are provided for the MEAs with nanoframe cathode catalyst and the TKK Pt/C cathode catalyst.

The ECSA based on H_{upd} charge from the RDE results is approximately 60 m^2/g Pt, while the H_{upd} based ECSA in MEA was found to be 49 m^2/g Pt.

The hydrogen-oxygen performance showed specific activity at 0.9 $V_{iR\text{-}corr.}$ of 2,600 μA/cm^2 and mass activity of 0.76 A/mg Pt. Improved utilization of the PtNi nanoframes through optimization of the ionomer-carbon ratio allowed the PtNi nanoframe MEAs to surpass the DOE MEA performance targets by almost a factor of two, while specific activity was improved by factor of three. For comparison, the TKK Pt/C catalyst showed specific and mass activities at 0.9 $V_{iR\text{-}corr.}$ of 326 μA/cm^2 and 0.24 mA/mg Pt.

The hydrogen-air performance for these two MEAs is shown in Figure 2. The performance of the nanoframe MEA surpasses that of the TKK Pt/C MEA. The current density at 0.8 V is 115 mA/cm^2. Given that the cathode catalyst loading in the nanoframe MEA was one third that of the DOE target cathode loading of 0.1 mg Pt/cm^2 (assuming an anode loading of 0.025 mg Pt/cm^2), an MEA with a nanoframe catalyst loading of 0.1 mg Pt/cm^2 is expected to surpass the DOE target of 300 mA/cm^2 at 0.8 V.

CONCLUSIONS AND FUTURE DIRECTIONS

- Different classes of materials have been synthesized in the form of NPs, nanowires, and nanoframes and these materials have been characterized by transmission electron microscopy, high resolution scanning electron microscopy, in situ HR-TEM, X-ray diffraction, RDE, and MEA.
- Specific activity for the ORR measured in RDE of Pt-alloy vs. Pt/C electrocatalysts can be improved by 20-fold for nanoframes and mesostructured thin films (MSTF), 10-fold for core/shell NPs and seven-fold for nanowires.
- Mass activities improvements for the ORR measured in RDE vs. Pt/C are 36-fold for nanoframes, seven-fold for core/shell, six-fold for MSTF and four-fold for nanowires (RDE in 0.1 M $HClO_4$ at 0.95 V vs. RHE).
- Stability of nanoframes, MSTF, core/shell NPs and nanowires can be substantially improved compared to Pt/C.
- Two-fold power of annealing facilitates the formation of an energetically more favorable surface state rich in (111) facets and distinct oscillatory segregation profile in core/shell NPs, nanowires, MSTF and nanoframes.
- Nanoframes are the first nanoscale catalyst with ORR bulk single crystal activity.
- Specific and mass activities of nanoframe catalysts measured in MEA surpass the 2015 DOE Technical Target by ~three-fold and two-fold, respectively.

This project is officially over in FY 2015; however, the performance of nanostructured catalysts in MEA will remain in focus in the next funding cycle.

SPECIAL RECOGNITIONS & AWARDS/ PATENTS ISSUED

1. C. Chen, Y. Kang, N.M. Markovic, G. Somorjai, Peidong Yang and V.R. Stamenkovic, Patent Pending, "Highly Crystalline Pt_3Ni Nanoframes with Three-Dimensional Electrocatalytic Surfaces."

2. R&D 100 Award Finalist Berkeley-Argonne Lab Nanoframe catalysts P. Yang and V. Stamenkovic.

FY 2015 PUBLICATIONS/PRESENTATIONS

1. Joshua Snyder, Yijin Kang, Dongguo Li, N. Markovic, and V. Stamenkovic, "Electrocatalysts with Tailored Properties," 226th Electrochemical Society Meeting, October 2014, Cancun, Mexico.

2. Joshua Snyder, Yijin Kang, Dongguo Li, Dusan Strmcnik, N. Markovic, and V. Stamenkovic, "Novel Pathways for Improving the ORR Rate," (KEY NOTE LECTURE), 226th Electrochemical Society Meeting, October 2014, Cancun, Mexico.

3. Y. Kang, N.M. Markovic, and V. Stamenkovic, "Electrochemical Energy Conversion," (KEY NOTE LECTURE), International Conference on Electrochemical Science, October–November 2014, Shanghai, China.

4. Y. Kang, J. Snyder, D. Li, K. More, N.M. Markovic, and V.R. Stamenkovic, **"**Multimetallic Core/Interlayer/Shell Nanostructures as Advanced Electrocatalysts," Nano Letters, 14(2014)6361–6367.

REFERENCES

1. V. Stamenkovic, B. Fowler, B.S. Mun, G. Wang, P.N. Ross, C. Lucas, and N.M. Markovic, "Improved Oxygen Reduction Activity on Pt_3Ni(111) via Increased Surface Site Availability," *Science.*, 315 (2007) 493–497.

2. V. Stamenkovic and N.M. Markovic, "Electrocatalysis on Model Metallic and Bimetallic Single Crystal Surfaces, Model Systems in Catalysis: from Single Crystals and Size Selected Clusters," Ed. Robert M. Rioux, Harvard University, USA; Publisher: Elsevier Science, The Netherlands, *2009.*

3. K.J.J. Mayrhofer, B.B. Blizanac, M. Arenz, V. Stamenkovic, P.N. Ross, and N.M. Markovic, "The Impact of Geometric and Surface Electronic Properties of Ptcatalysts on the Particle Size Effect in Electrocatalysis," *J. Phys. Chem, B*, 109 (2005) 14433–14440.

4. C. Wang, D. van der Vliet, K.C. Chang, H. You, D. Strmcnik, J.A. Schlueter, N.M. Markovic, V.R. Stamenkovic, "Monodisperse Pt_3Co Nanoparticles as a Catalyst for the Oxygen Reduction Reaction: Size Dependent Activity," *J. Phys. Chem. C.,* 113 (2009)19365.

5. C. Wang, D. van der Vliet, K.C. Chang, N.M. Markovic, V.R. Stamenkovic, "Monodisperse Pt_3Co Nanoparticles as Electrocatlyst: the Effect of Particle Size and Pretreatment on Electrocatalytic Reduction of Oxygen," *Phys.Chem.Chem.Phys*., 12 (2010)6933–6939.

6. V. Stamenkovic, B.S. Mun, M. Arenz, K.J.J. Mayrhofer, C. Lucas, G. Wang, P.N. Ross, and N.M. Markovic, "Trends in Electrocatalysis on Extended and Nanoscale Pt-bimetallic Alloy Surfaces," *Nature Materials.*, 6 (2007) 241–247.

7. C. Wang, D. van der Vliet, K.L. More, N.J. Zaluzec, S. Peng, S. Sun, H. Daimon, G. Wang, J. Greeley, J. Pearson, A.P. Paulikas, G. Karapetrov, D. Strmcnik, N.M. Markovic, V.R. Stamenkovic, "Multimetallic Au/$FePt_3$ Nanoparticles as Highly Durable Electrocatalysts," *Nano Letters*, 11 (2011)919–928.

8. C. Wang, M. Chi, D. Li, D. Strmcnik, D. van der Vliet, G. Wang, V. Komanicky, K-C. Chang, A.P. Paulikas, D. Tripkovic, J. Pearson, K.L. More, N.M. Markovic, and V.R. Stamenkovic, "Design and Synthesis of Bimetallic Electrocatalyst with Multilayered Pt-Skin Surfaces," *Journal of American Chemical Society*, 133 (2011)14396.

9. C. Wang, M. Chi, D. Li, D. van der Vliet, G. Wang, Q. Lin, J.F. Mitchell, K.L. More, N.M. Markovic, V.R. Stamenkovic, "Synthesis of Homogeneous Pt-Bimetallic Nanoparticles as Highly Efficient Electrocatalysts," *ACS Catalysis*, 1 (2011)1355.

10. D. van der Vliet, C. Wang, M.K. Debe, R.T. Atanasoski, N.M. Markovic, V.R. Stamenkovic, "Platinum Alloy Nanostructured Thin Film Catalysts for the Oxygen Reduction Reaction," *Electrochimica Acta*, 56,24 (2011)8695.

11. D. van der Vliet, C. Wang, D. Tripkovic, D. Strmcnik, X.F. Zhang, M.K. Debe, R.T. Atanasoski, N.M. Markovic, V.R. Stamenkovic, "Mesostructured Thin Films as Electrocatalysts with Tunable Composition and Surface Morphology," *Nature Materials*, 11(2012)1051.

12. C. Chen, Y. Kang, J. Snyder, M. Mavrikakis, Y. Li, N.M. Markovic, G. Omorjai, Peidong Yang, V.R. Stamenkovic, "Highly Crystalline Multimetallic Nanoframes with Three-Dimensional Electrocatalytic Surfaces," *Science*, 343(2014)1339–1343.

V.A.3 Contiguous Platinum Monolayer Oxygen Reduction Electrocatalysts on High-Stability, Low-Cost Supports

Radoslav Adzic (Primary Contact), Jia Wang, Miomir Vukmirovic, Kotaro Sasaki
Brookhaven National Laboratory (BNL), Bldg. 555
Upton, NY 11973-5000
Phone: (631) 344-4522
Email: adzic@bnl.gov

DOE Manager
Nancy Garland
Phone: (202) 586-5673
Email: Nancy.Garland@ee.doe.gov

Project Start Date: July 1, 2009
Project End Date: Project continuation and direction determined annually by DOE

Overall Objectives

- Synthesizing high-performance Pt monolayer (ML) electrocatalysts on stable, inexpensive metal or alloy nanoparticles for the oxygen reduction reaction (ORR) at fuel cell cathodes
- Increasing activity and stability of the Pt ML shell and stability of supporting cores while reducing noble metal contents

Fiscal Year (FY) 2015 Objectives

- To increase activity and stability of Pt monolayer catalysts to meet the DOE technical targets for 2020 through the following:
  - Electrodeposition of inexpensive refractory metal alloy nanoparticles on gas diffusion layers (GDLs) to fabricate the electrodes of 5 cm^2, 25 cm^2, and 50 cm^2 and perform membrane electrode assembly (MEA) tests at BNL and General Motors (GM)
  - Further developing the nitriding method of core (PdNi) stabilization; the stabilization method involving the addition of Au to nanoparticle cores will also be developed
  - Demonstrating suitability of graphene as support for Pt ML catalysts

Technical Barriers

This project addresses the following technical barriers from the Fuel Cells section of the Fuel Cell Technologies Office Multi-Year Research, Development, and Demonstration Plan:

(A) Durability

(B) Cost

(C) Performance

Technical Targets

We are focusing on simplifying the synthetic processes to obtain better catalyst activity, higher Pt utilization, lower content of precious group metals (PGMs), and simpler MEA fabrication (see Table 1).

TABLE 1. Progress toward Meeting DOE Fuel Cell Electrocatalysts Technical Target

	DOE 2020 Targets	Pt_{ML}/Pd/WNi/GDL 80°C, H_2/O_2, 150 kPa	Pt_{ML}/Pd/WNi/GDL 80°C, H_2/O_2, 300 kPa
PGM total loading, mg_{PGM}/cm^2	<0.125	0.07 mg_{PGM}/cm^2 at the cathode	0.07 mg_{PGM}/cm^2 at the cathode
Loss in performance at 0.8 A/cm^2	<30 mV	19 mV after 34,000 AST	7 mV after 34,000 AST
Loss in performance at 1.5 A/cm^2	<30 mV	22 mV after 34,000 AST	19 mV after 34,000 AST
Mass activity at 900 $mV_{iR\ free}$, A/mg_{PGM}	>0.44	0.37	0.46

AST – accelerated stress test

FY 2015 Accomplishments

- The stabilization method involving nitride-stabilized non-noble core components was developed. Pt_{ML} on nitride-stabilized PdNi core catalysts exhibited excellent properties.
- Electrodeposition of dendritic nanostructured cores was demonstrated to be a promising strategy for improving the MEA's performance under H_2/air feed at low or no back pressure and at high current densities.
- Using Au to stabilize various cores: Pt_{ML} on Au-modified W compounds showed no change of activity in the accelerated stability test of 30,000 potential cycles.
- Pt ML on Pd core on reduced graphene oxide (rGO) proved to be an excellent catalyst.
- Atomic level control of metal deposition using cation adsorption/reduction/atom displacement was shown to be possible with rGO.

- MEA with rGO was found to have promising properties: Pd content is reduced by 50% in comparison with the Pt/Pd/C catalyst, while stability and activity are enhanced.
- A very small increase in the ORR kinetics was demonstrated for adsorbed fluorinated short-chain molecules at small coverages likely as a consequence of surface hydrophobization and easier O_2 adsorption.

✧ ✧ ✧ ✧ ✧

INTRODUCTION

Further improvements of oxygen reduction electrocatalysts are necessary to overcome the remaining technological difficulties that hinder automotive applications of fuel cells. Our research was focused on reducing Pt or PGM contents in our electrocatalysts while increasing their stability and activity. Optimizing the properties of supporting cores such as the composition, size and shape makes possible further improvements of the Pt monolayer catalysts.

APPROACH

We are improving Pt ML catalysts using novel core compositions and new synthetic methods including:

- Nitriding non-noble metal core components for increased stability.
- Electrodeposition of cores (refractory metal alloys) to optimize their composition and maximize catalyst utilization.
- Synthesis of ordered intermetallic compounds with high activity without Pt.
- Reactive spray deposition method of the synthesis of novel low cost cores.
- Pulse—potential deposition of cores on GDL carbon used to obtain nanoparticles with narrow size distribution and 100% Pt utilizations.
- Using graphene and reduced graphene oxide as supports.

RESULTS

We describe four results illustrating the new methods developed in FY 2015 for improving Pt ML catalysts for the ORR.

Electrodeposition of WNi and MEA Tests of Pt/Pd/WNi/C

Further studies of electrodeposition of PtML/Pd/WNi/C cores were focused on MEA stability tests. Polarization curves from a 5 cm^2 MEA with loading of 0.07 mgPGM/cm^2 were determined. After co-deposition of W and Ni, replacing the top layers of Ni by Pd, and placing a Pt ML by galvanic exchange of a Cu ML, we achieved low PGM loading and high Pt utilization. The data surpassed the DOE targets for mass activity and loss in performance at higher back pressure. The performance in air needs to be further improved (Table 1, Figure 1).

We used the electrodeposition method to make dendritic nanostructured cores, which is a promising strategy for improving the MEA performance at low or no back pressure and at high current density in H_2/air feed. The results illustrating these possibilities are shown in Figure 2.

Nitride-Stabilized Pt-M Core-Shell Catalysts in Acid Media

We developed highly active and stable oxygen reduction catalysts by depositing Pt monolayers on a nitrided PdNi alloy core (Figure 3). The prepared Pt_{ML}PdNiN/C catalyst retains 89% of the initial electrochemical surface area after 50,000 cycles between potentials of 0.6 V and 1.0 V. Nanoparticles consisting of $Pd_{50}Ni_{50}$/C were calcinated in N_2 at 250°C for 1 h and in NH_3 at 510°C for 2 h. Scanning transmission electron microscopy/electron energy loss spectroscopy (STEM/EELS) show that Pd atoms segregate on the surface. X-ray absorption spectroscopy shows a decrease in Ni bonding due to the formation of Ni nitride. The experimental data and the density functional theory (DFT) calculations indicate that the nitride cores improve the

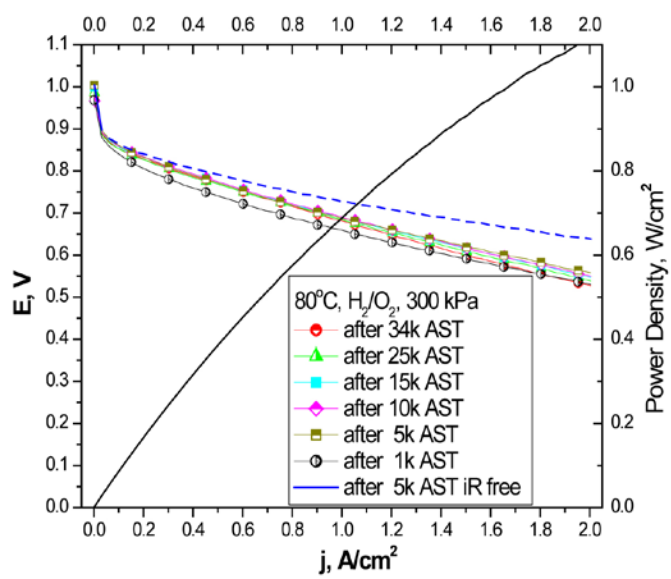

FIGURE 1. Polarization curves from a 5 cm^2 MEA with loading of 0.07 mg_{PGM}/cm^2 Pt_{ML}/Pd/WNi/GDL catalyst on the cathode obtained by co-deposition of WNi , replacing top layers of Ni by Pd and placing a Pt ML by galvanic exchange of a Cu ML. TKK Pt catalysts (0.05 mg_{Pt}/cm^2) on anode and Nafion® HP membrane are used. A negligible loss in activity occurs after 34,000 potential cycles.

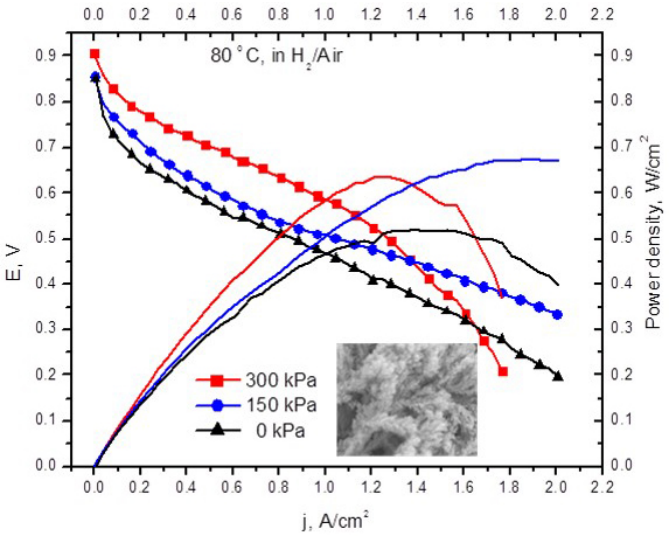

FIGURE 2. MEA polarization curve with H_2/air feed at three different back pressures in the cathode obtained by electrodeposition of Pd dendrites to increase a three-dimensional (3D) porosity and mass transfer at low gas pressure; insert shows Pd dendritic deposit.

performance of the Pt shell by inducing both the geometric and electronic effects. Pd content is reduced by 50% in comparison with the Pt/Pd/C catalyst, while stability and activity are enhanced.

Graphene as Support for Pt Monolayer Catalysts

We synthesized Pt ML on Au core on rGO catalysts that verifies the possibility of using graphene as a support. Au nanoparticles were deposited on reduced graphene oxide using the Pb^{2+} cation adsorption/reduction/Pb^0 atom displacement method. Highly crystalline Au nanoparticles having a narrow size distribution have been obtained. The activity and stability of this catalyst is excellent which demonstrates that graphene can be an excellent support for Pt ML catalysts (Figure 4).

CONCLUSIONS AND FUTURE DIRECTIONS

Further improvements of Pt ML catalysts have been achieved by the development of four methodologies (three discussed in some detail here) that reduced the Pd content in cores by 50%, increased catalyst stability, and improved syntheses efficiency. Electrodeposition methodology was improved and its use was expanded to dendritic growth of cores to form 3D porosity that facilitates a better performance with air, lower pressure, and operation at high current density ranges. The other two successful methodologies for improving activity and stability of these catalysts include nitriding of non-noble metal cores constituents and using Au as a Pt ML support on graphene and promoting the formation of ordered intermetallic compounds. The latter can act as catalyst without Pt or serve as high stability core for a Pt ML.

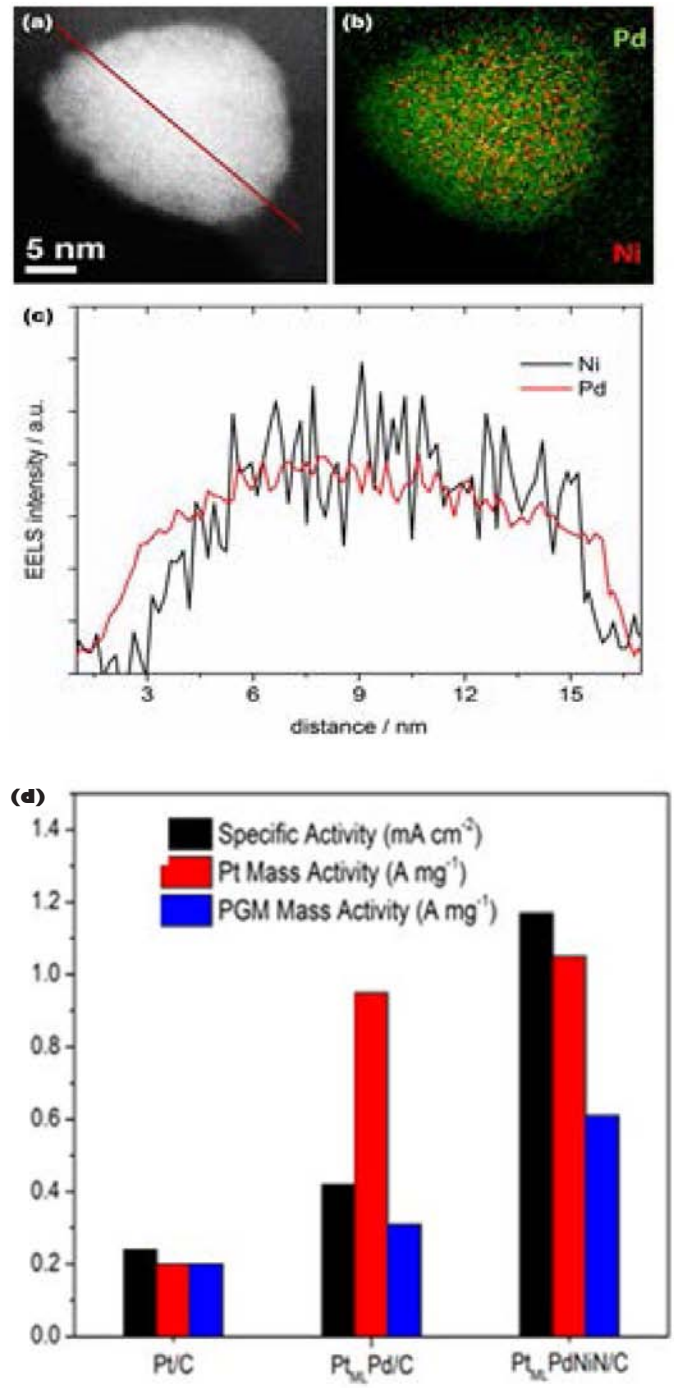

FIGURE 3. Nitride-stabilized Pt/PdNi/C core-shell catalyst; (a) high-angle annular dark-field-STEM image of PdNiN core-shell nanoparticle; (b) two dimensional EELS mapping of Ni L signal (red) and Pd M signal (green); (c) EELS line scan profile for Pd M-edge and Ni L-edge along the scanned line indicated in (a); (d) specific and mass activities for the commercial Pt/C, Pt_{ML}Pd/C and Pt_{ML}PdNiN/C catalysts at 0.9 V (RHE).

Future work will focus on:

- MEA and stack tests in 50 cm^2 electrodes will be performed at BNL and GM with Pt ML on graphene-

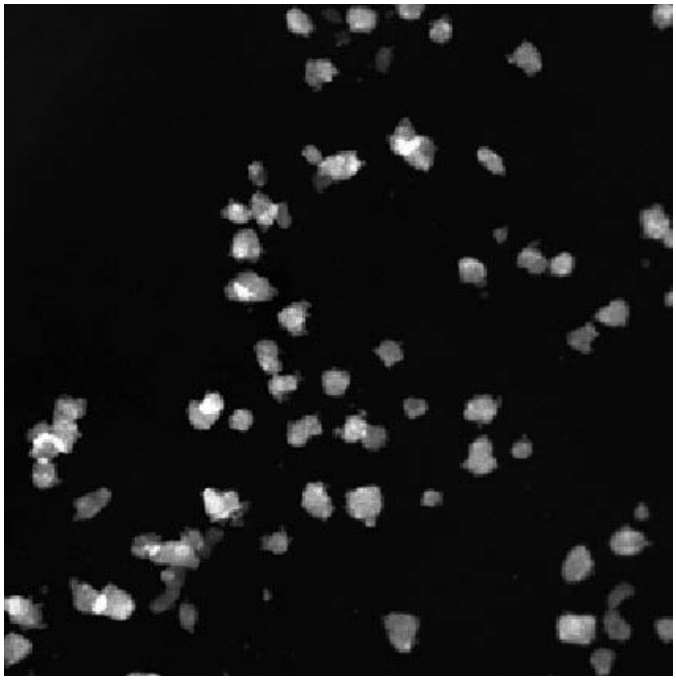

FIGURE 4. Pt deposited on Au nanoparticles on graphene using Cu UPD technique

supported cores and on nitride- and Au-stabilized non-noble and refractory metal alloy cores.

Novel strategies to synthesize high performance Pt monolayer electrocatalysts include:

- Electrodeposition from non-aqueous solvents to obtain new classes of cores.
- High pressure nitridation performed in a new tube reactor at temperatures up to 1,100°C in a NH_3 gas at pressures up to 10 MPa to generate various types of nitride nanoparticles with refractory metals such as Ti, V, Nb, Ta, and W to enhance the stability and activity of Pt shells.
- Reactive spray deposition technology as another method to obtain cores unattainable thus far with conventional syntheses.
- Onion-structured nanoparticles with new cores of multiple metal layers to tune Pt monolayer properties and shift E° closer to 1.23 V. Supporting DFT calculations have been completed.
- Searching for new ordered intermetallic compounds for Pt-free catalysts and supporting cores for Pt monolayers.
- Using a layer of Au to modify refractory metals and alloys. Some refractory metals and alloys could serve as highly corrosion-resistant cores but we found they need an Au interlayer to preclude too large negative shifting of the *d*-band center of surface Pt atoms. A Pt ML on Au-W compounds (patent pending) already shows enhanced ORR performance with no degradation in 30,000 cycles.

SPECIAL RECOGNITIONS & AWARDS/ PATENTS ISSUED

1. R. Adzic, S. Bliznakov, and M. Vukmirovic, U.S. Patent: Core-Shell Fuel Cell Electrodes, US2015/0017565 A1, Jan. 15, 2015.

2. Jia X. Wang, Radoslav R. Adzic, "Underpotential deposition-mediated layer-by-layer growth of thin films," U.S. Patent 9034165 B2, May 19, 2015.

3. R.R. Adzic, J. Zhang, K. Sasaki, "Method and Electrochemical Cell for Synthesis and Treatment of Metal Monolayer Electrocatalysts, Metal, Carbon, and Oxide," U.S. Patent No. 9,017,530.

4. K. Sasaki, W.F. Chen, J.T. Muckerman, R.R. Adzic, "Molybdenum and Tungsten Nanostructures and Methods for Making and Using Same," U.S. Patent No. 8,927,453.

5. Kurian Kuttiyiel, Kotaro Sasaki, Radoslav Adzic, "Nitride Stabilized Core-Shell Nanoparticles," U.S. Patent -20150147682, 05/28/2015.

FY 2015 PUBLICATIONS/PRESENTATIONS

1. Kurian A Kuttiyiel, YongMan Choi, Sun-Mi Hwang, Gu-Gon Park, Tae-Hyun Yang, Dong Su, Kotaro Sasaki, Ping Liu, Radoslav R. Adzic, "Enhancement of the oxygen reduction on nitride stabilized Pt-M (M= Fe, Co, and Ni) core-shell nanoparticle electrocatalysts," *Nano Energy*, 2015, 13, 442–449.

2. Jue Hu, Kurian A Kuttiyiel, Kotaro Sasaki, Dong Su, Tae-Hyun Yang, Gu-Gon Park, Chengxu Zhang, Guangyu Chen, Radoslav R. Adzic, "Pt Monolayer Shell on Nitrided Alloy Core—A Path to Highly Stable Oxygen Reduction Catalyst," *Catalysts*, 2015, 5, 1321–1332.

3. Y. Li, K.A. Kuttiyiel, L. Wu, Y. Zhu, E. Fujita, K. Sasaki, R.R. Adzic, "Cobalt Manganese Oxynitride Nanocatalysts on Graphene as Oxygen Reduction and Evolution Bifunctional Catalysts," *Journal of American Chemical Society*, submitted.

4. J. Hu, K.A. Kuttiyiel, K. Sasaki, D. Su, G.-G. Park, C. Zhang, G. Chen, R.R. Adzic, "Pt Monolayer Shell on Nitride Alloy Core—A Path to Highly Stable Oxygen Reduction Catalyst," *Catalysts*, accepted.

5. H. Liu, W. An, Y. Li, A. Frenkel, K. Sasaki, C. Koenigsmann, D. Su, R. Anderson, R.M. Crooks, R.R. Adzic, P. Liu, S.S. Wong, "Combining Theory and Experiment to Deduce the Active Structure Geometry of Ultrathin Nanowires Analyzed In Situ for the Oxygen Reduction Reaction," *Journal of American Chemical Society*, submitted.

6. K.A. Kuttiyiel, Y.M. Choi, S.-M. Hwang, G.-G. Park, T.-H. Yang, D. Su, K. Sasaki, P. Liu, R.R. Adzic, "Enhancement of the oxygen reduction on nitride stabilized Pt-M (M=Fe, Co, and Ni) core-shell nanoparticle electrocatalysts," *Nano Energy* (2015) 13, 442–449.

7. S. Bliznakov, M. Vukmirovic, R. Adzic, in "Atomically-Precise Methods for Synthesis of Solid Catalysts," S. Hermans and T. Visart de Bocarme, Editors, p. 144, The Royal Society of Chemistry Book Chapter, *RCS Catalysis* Series No. 22, (2015).

8. K. Sasaki, N. Marinkovic, "X-ray Absorption Spectroscopic Characterization of Nanomaterial Catalysts in Electrochemistry and Fuel Cells," submitted to the 5th volume of SPRINGER book series on "Characterization Tools for Nanoscience & Nanotechnology," submitted.

PRESENTATIONS

1. X. Wang, P. He, Y. Zhang, and S. Ye, "Can CO-tolerant Anodes be Economically Viable for PEMFC Applications with Reformates?" J Electrochemical Society Meeting, Cancun, Mexico, October 8, 2014.

2. Kurian Kuttiyiel, "Enhancement of the ORR on Nitride Stabilized Pt-M (M = Fe, Co & Ni) Core-Shell Electrocatalysts," 227th Electrochemical Society Meeting, Chicago, IL, USA (May 2015).

V.A.4 Synthesis and Characterization of Mixed-Conducting Corrosion Resistant Oxide Supports

Vijay K. Ramani (Primary Contact),
Jai Prakash (Co-PI)
Illinois Institute of Technology (IIT)
10 W 33rd Street 127 PH
Chicago, IL 60616
Phone: (312) 567-3064
Email: ramani@iit.edu

DOE Manager
Jacob Spendelow
Email: Spendelow@lanl.gov

Contract Number: DE-EE0000461

Subcontractor
Nissan Technical Center, North America (NTCNA), Farmington Hills, MI

Project Start Date: September 1, 2010
Project End Date: January 31, 2015

Overall Objectives

This project addresses the following targets from the Fuel Cells section (Table 3.14.12) of the DOE Fuel Cell Technologies Office Multi-Year Research, Development, and Demonstration Plan:

- <40% electrochemical area (ECA) loss in electrocatalysts using the synthesized supports tested per the General Motors (GM) protocol
- <30 mV electrocatalyst support loss in the synthesized supports after 100 h at 1.2 mV; tested using the GM protocol

Fiscal Year (FY) 2015 Objectives

- Evaluate the suitability of titanium dioxide-ruthenium dioxide (RTO), and indium tin oxide (ITO) as conducting catalyst supports for proton exchange membrane fuel cells (PEMFCs)
- Optimize the Pt deposition method on the above catalyst supports to improve PEMFC performance and durability
- Demonstrate the performance and durability (under start-stop and load cycling protocols) of Pt deposited on RTO and ITO in a PEMFC

Technical Barriers

This project addresses the following technical barrier from the Fuel Cells section of the DOE Fuel Cell Technologies Office Multi-Year Research, Development, and Demonstration Plan:

(A) Durability

Technical Targets

See the targets listed under overall objectives.

This project is conducting fundamental studies of RTO and ITO supports and catalyzed supports. A brief list of our current status is listed below:

- Initial oxygen reduction reaction (ORR) mass activity: 40% Pt/RTO: 0.160 A/mg Pt; 40% Pt/ITO: 0.160 A/mg Pt
- Loss of initial electrochemical active surface area (ECSA) activity after 10,000 cycles (load cycling protocol): 40% Pt/RTO: 34%; 40% Pt/ITO: <40% (measured in a rotating disk electrode [RDE] set-up)
- Cell voltage loss at 1 A/cm^2 after 10,000 cycles (load cycling protocol): 40% Pt/RTO: 6%; 40% Pt/ITO: Never measured (Pt/ITO not stable under fuel cell operating conditions)

FY 2015 Accomplishments

- We have found that the fuel cell performance of Pt/ITO was much lower than Pt/C or Pt/RTO despite the similar ORR activities found in RDE experiments. RDE stability experiments done following DOE stability protocols also revealed exceptional stability for the ITO support.
- X-ray photoelectron spectroscopy (XPS) was employed to investigate the changes occurring in Pt/ITO during PEMFC operation, and revealed the formation of indium hydroxides, which we found to be the reason for the lower performance (loss of electronic conductivity).
- NTCNA has synthesized 10% Pt/RTO catalyst with better Pt particle dispersion, ECA, and mass activity than 40% Pt/RTO catalyst due to better Pt utilization.
- NTCNA estimated, using a model, that a more appropriate ionomer/support (I/S) weight ratio of 0.3 should be employed for 10 wt% Pt/RTO to match the ionomer film coverage in 30% Pt/GKB (graphitized Ketjenblack®). Experimental results corroborated the calculations.

✧ ✧ ✧ ✧ ✧

INTRODUCTION

Carbon black, which is currently used as support material for the Pt in the polymer electrolyte fuel cell (PEFC) electrocatalyst can undergo corrosion under fuel cell operational conditions [1]:

$C + 2H_2O \rightarrow CO_2 + 4H^+ + 4e^-$ $E_o^0 = 0.207$ V vs. standard hydrogen electrode (SHE)

This is a thermodynamically favorable reaction, but it is very slow under normal operating conditions. However, the reaction can be accelerated during voltage spikes (as high as 1.5 V) occurring during start-stop and fuel starvation [2,3]. The irreversible carbon corrosion leads to the aggregation of Pt resulting in an irreversible loss of the electrochemical active surface area (ECSA) and ORR mass activity that significantly reduce fuel cell performance. To overcome these obstacles, it is necessary to replace the carbon with high electronic conductivity, high surface area and porous support, with high corrosion resistance.

APPROACH

We have explored selected mixed metal oxide supports, namely RTO and tin doped ITO. Each support (RTO and ITO) was evaluated for electrochemical stability using the start-stop transient protocol (start-stop protocol: triangular wave from 1 to 1.5 V at 0.5 V/s for 10,000 cycles). Pt was deposited on stable supports and the resultant catalyst stability evaluated using start-stop protocol and load cycling protocol (rectangular wave between 0.6 V and 0.95 V with a hold of 3 s at each potential for 10,000 cycles). Membrane electrode assemblies (MEAs) were made and tested in a PEMFC to evaluate fuel cell performance for each catalyst.

RESULTS

We have already reported (in previous annual reports) on our excellent results (RDE and MEA) with Pt/RTO and will not repeat these here. We focus here on the work we have done on Pt/ITO, and on further optimization of Pt/RTO.

Fuel Cell Performance for Pt/ITO

The start-stop cycling durability test was performed to determine changes between the beginning of life (BoL) and end of life (EoL) performance of Pt/ITO, and the results are shown in Figure 1a. The ink formulation that was used was the same as for the Pt/RTO samples in order to make a direct comparison with the MEA results of Pt/RTO (an I/S mass ratio of 0.9 was used). The Pt/ITO ink was successfully sprayed onto SGL 25 BCH gas diffusion layers, and four 25 cm^2 MEAs were made using established protocols at

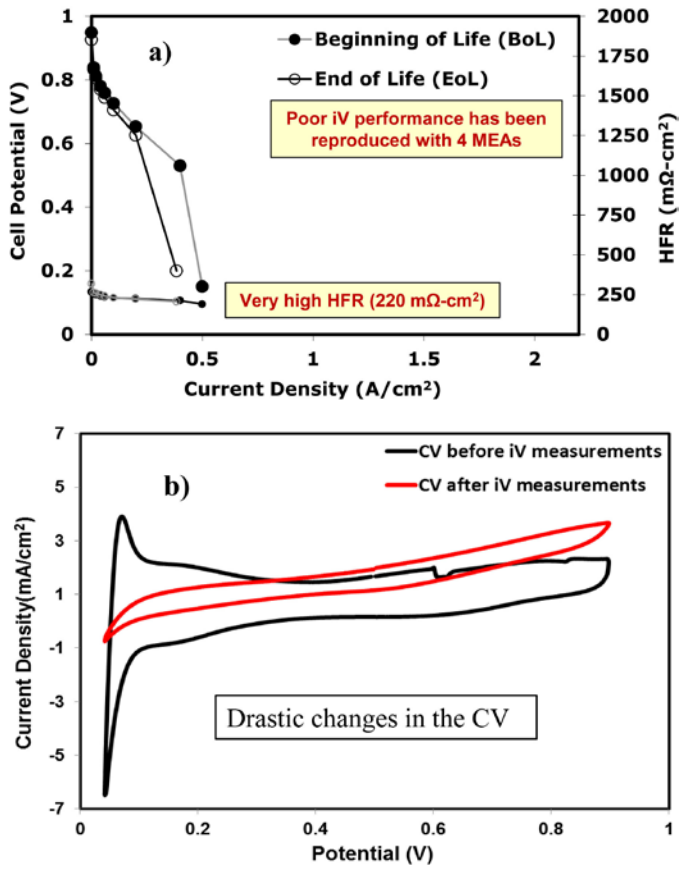

FIGURE 1. (a) MEA iV performance of Pt/ITO vs. Pt/C under oxygen operation; (b) CV plots of Pt/ITO before and after iV measurements. Cell conditions: H_2/O_2, 80°C, 100% relative humidity, 1 bar_g backpressure; Pt loading: 0.35 mg/cm^2.

NTCNA. The EoL performance does not appear to be significantly different than the BoL curve, indicating that the ITO support may be able to maintain its properties at its BoL state through 1,000 potential cycles from 1.0–1.5 V during the start-stop cycling. However, more importantly, we have also constantly observed (in several similar tests) that 40% Pt/ITO performs very poorly during PEMFC testing.

The high frequency resistance (HFR) was very high (220 mΩ-cm^2, normally at ~60 mΩ-cm^2), during all the testing, suggesting some conductivity problems with the ITO support. Furthermore, as can be seen in Figure 1b, drastic changes in the cyclic voltammograms (CV) profile (loss of H_{upd} features and resistive behavior) was observed after minimal operation in fuel cell mode, suggesting changes in the chemical composition of the ITO support. It is possible that hydroxyl species may have formed on the ITO surface under fuel cell operating conditions during the iV curve measurements. This would explain the increase in ohmic resistance observed during MEA operation, and will be analyzed in more detail in the next section.

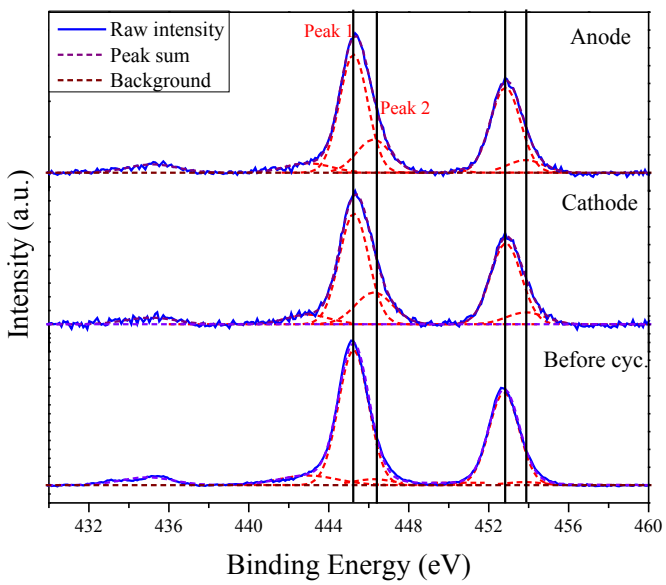

FIGURE 2. XPS fitting results for Indium $3d_{5/2}$ before and after PEMFC performance testing (40% Pt/ITO used in the anode and cathode). Peak 1 (445 eV) was assigned to In^{3+} in the oxide (ITO); Peak 2 (446 eV) was assigned to In^{3+} adjacent to hydroxide species.

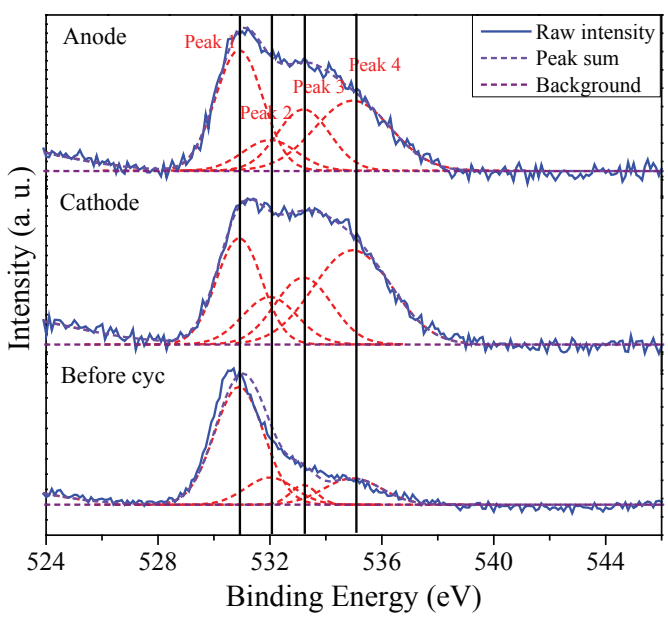

FIGURE 3. XPS fitting results for oxygen 1 s before and after PEMFC performance testing (40% Pt/ITO used in the anode and cathode). Peak 1 (530 eV) was assigned to oxide in ITO. Peak 2 (531 eV) was assigned to oxide that is adjacent to an oxygen vacancy; Peak 3 (532 eV) was assigned to hydroxides; Peak 4 was included to account for impurities.

XPS Analysis of Pt/ITO Before and After PEMFC Tests

The In 3d and O1s XPS spectra of 40% Pt/ITO before and after being used in a PEMFC are shown in Figures 2 and 3. The In 3d spectrum showed the presence of a doublet peak. The In $3d_{5/2}$ and In $3d_{3/2}$ peaks were positioned at approximately 445 eV and 453 eV and had asymmetric shapes. The position of the In $3d_{5/2}$ peak revealed that indium was mainly in its oxide form (In^{3+}). The shift of In $3d_{5/2}$ and In $3d_{3/2}$ peaks after the catalyst was used in a PEMFC, towards higher binding energies, was a consequence of the formation of surface hydroxides and oxyhydroxides; the presence of hydroxide makes the In $3d_{5/2}$ peak shift to approx. 446 eV [4]. The peak relative areas represent the surface concentration of each species. Fitting results showed clearly that before fuel cell operation, In^{3+} was almost entirely in the oxide form in the catalyst and that minimal indium hydroxide was present (approximately 5%). After fuel cell operation, the anode and cathode catalysts (40% Pt/ITO) were recovered and similar XPS analysis was performed. Figure 2 compares XPS fitting results for 40% Pt/ITO before testing, and at the anode and cathode after fuel cell operation (In $3d_{5/2}$). Fitting results showed the presence of a peak at ~446 eV, initially assigned to In^{3+} adjacent to hydroxides, which increased after the catalyst was used in the PEMFC. According to the fitting results, hydroxide moieties on the surface of ITO increased from approximately 5%, before the catalyst was used, to 25% of the total amount of indium, once the catalyst was evaluated in the PEMFC (see Figure 2). We suspect that the presence of surface hydroxides increases the electrode resistivity (as seen in Figure 1) affecting fuel cell performance. Figure 3 shows the XPS fitting results for oxygen 1 s in 40% Pt/ITO before and after being used as catalyst in the PEMFC. We found that ITO initially contained almost 100% oxide-like species, but after the catalyst was used in the fuel cell, the surface hydroxides increased to approximately 30%. The results were in agreement with the conclusions obtained from Indium 3d peak fitting.

Pt Loading on RTO and the Appropriate Ionomer Content of the Pt/RTO

In our work we also optimized the Pt loading on RTO and the ionomer content in the Pt/RTO catalyst layer. Our calculations showed that the target Pt loading for Pt/RTO should be 10 wt% to match the Pt particle density of 30% found in Pt/GKB. 30% Pt/GKB would be a good comparison for Pt/RTO since both GKB and RTO have low surface areas and microporosity. We have also calculated that to match the ionomer film coverage in 30% $Pt/GKB_{150m2/g}$ electrode (I/S weight ratio of 1.3), an I/S weight ratio of 0.3 should be used for 10 wt% Pt on $RTO_{39\ m2/g}$.

As shown in Figure 4, the ECA for the 10% Pt/RTO sample was 45 m^2/g, higher than the value obtained for 40% Pt/RTO (at only 26 m^2/g). This indicates that the dispersion of Pt on the low surface area RTO support is better for the 10% sample such that more Pt active area is exposed and accessible. This is supported by the MEA PEMFC polarization curves in H_2/air (as shown in Figure 4a) where the 10% Pt/RTO catalyst had a higher mass activity than the

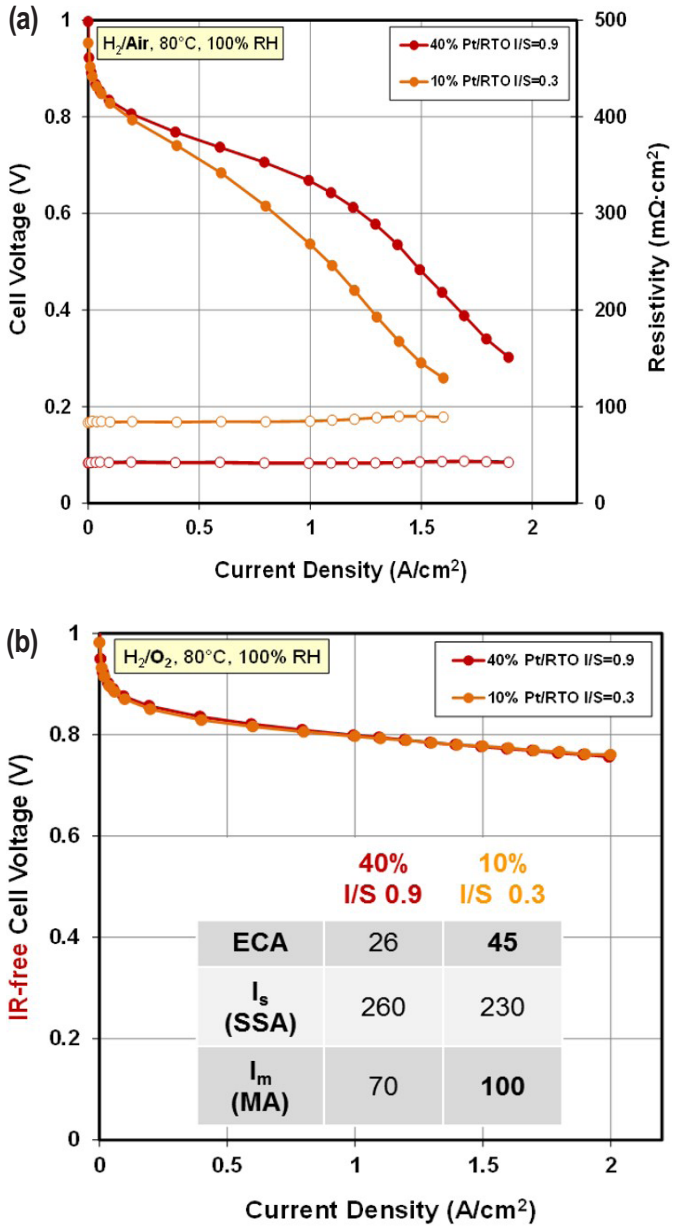

FIGURE 4. H_2/air and H_2/O_2 iV performance of 10% Pt/RTO vs. 40% Pt/RTO. The 10% Pt/RTO MEA had lower iV performance due to ohmic losses (poor electronic conductivity).

40% sample. The HFR was also significantly higher for the 10% Pt/RTO. We have determined that the increase in HFR is not due to the decrease in ionomer content since several previous MEA tests has showed that decreasing the ionomer content does not lead to such drastic increases in HFR. Furthermore, the 10% Pt/RTO catalyst regardless of I/S ratio shows an HFR of around 100 mΩ-cm^2, about twice as high as the typical HFR of ~55 mΩ-cm^2. RTO is a mixed metal oxide consisting of RuO_2 and TiO_2 phases, and if a significant fraction of Pt particles are anchored on the TiO_2 phase, they could become electronically isolated.

CONCLUSIONS

- The fuel cell performance of 40% Pt/ITO catalyst was much lower than Pt/C and Pt/RTO despite the similar ORR activities found in RDE experiments. XPS revealed the formation of indium hydroxide leading to support degradation (and loss of electronic conductivity) during fuel cell operation.
- NTCNA synthesized 10% Pt/RTO catalyst, which showed better Pt particle dispersion (transmission electron microscopy), ECA and mass activity than the originally reported 40% Pt/RTO catalyst, demonstrating better Pt utilization.
- NTCNA estimated by using a model that a more appropriate I/S weight ratio of 0.3 should be employed for 10 wt% Pt on RTO to match the ionomer film coverage in 30% Pt/GKB.

FY 2015 PUBLICATIONS/PRESENTATIONS

1. G. Wang, E. Niangar, K. Huang, D. Atienza, A. Kumar , N. Dale , K. Oshihara , and V. Ramani, *ECS Trans* (2015).

REFERENCES

1. N. Takeuchi; T.F. Fuller, *J. Electrochem. Soc.*, **155** (2008) B770–B775.

2. L. Reiser, L. Bregoli, T.W. Patterson, J. S. Yi, J.D. Yang, M.L. Perry, T.D. Jarvi, Electrochem. *Solid-State Lett.* **8** (2005) A273–A276.

3. H. Tang, Z. Qi, M. Ramani, J.F. Elter, *J. Power Sources* **158** (2006) 1306–1312.

4. C. Donley, D. Dunphy, D. Paine, C. Carter, K. Nebesny, P. Lee, D. Alloway, N.R. Armstrong, *Langmuir* **18** (2001) 450–457.

V.A.5 Development of Novel Non-PGM Electrocatalysts for Proton Exchange Membrane Fuel Cell Applications

Sanjeev Mukerjee (Primary Contact)
Department of Chemistry and Chemical Biology
Northeastern University (NEU)
Boston, MA 02115
Phone: (617) 373-2382
Email: S.mukerjee@neu.edu

DOE Managers
Donna Lee Ho
Phone: (202) 586-8000
Email: Donna.Ho@ee.doe.gov
David Peterson
Phone: (720) 356-1747
Email: David.Peterson@ee.doe.gov

Contract Number: DE-EE0000459

Subcontractors
- University of New Mexico (UNM), Albuquerque, NM (Prof. Plamen Atanassov)
- Michigan State University (MSU), East Lansing, MI (Prof. Scott Barton)
- Nissan Technical Center, North America (NTCNA), Detroit, MI (Dr. Nilesh Dale)
- Pajarito Powder, LLC (PPC), Albuquerque, NM (Dr. Bar Halevi)

Project Start Date: August 1, 2010
Project End Date: July 31, 2015

Overall Objectives and Objectives for Fiscal Year (FY) 2014-2015

The objective of this project is to design non-platinum group metal (non-PGM)-based catalysts and supporting gas transport layers, and optimize both the interfacial reaction zone between the electrode and membrane as well as the underlying gas diffusion medium to meet and exceed DOE goals for application in solid polymer electrolyte fuel cells. This project is focused on materials development and is assisted by employing advanced analytical tools, computation, and testing to improve overall design by gaining a critical understanding of the the electrocatalysis pathway in these novel structures. The principle target for the reporting FY was to take the project beyond the first phase, where the project's go/no-go milestone of 100 mA/cm^2 at 0.8 V (internal resistance-free, iR-free) at 80°C, in pure H_2/O_2, and with 1.5 bar total pressure was met. For this reporting period, the principle objectives were to (a) transition the project from hydrogen/oxygen to hydrogen/air with a slated target of 30 mA/cm^2 at 0.8 V, 2.5 bar total pressure and (b) reach an end-of-project target of 1 A/cm^2 at 0.4 V (same total pressure), both under 100% relative humidity. On a quarterly timeline basis, the target for scale-up was to achieve 50 g batch size by the fourth quarter FY 2014 and 100 g batch size at the end of the program (second quarter FY 2015). Both of these scale-up targets had a quality control milestone of less than 5% variation of activity as measured with hydrogen/air (2.5 bar total pressure) at 0.8 V. In addition, the project aimed to arrive at a unified understanding of the nature of active sites in these catalysts as well as some preliminary understanding of the mechanistic pathway.

Technical Barriers

This project addresses the following technical barriers from the Fuel Cells section of the Fuel Cell Technologies Office Multi-Year Research, Development and Demonstration Plan:

(A) Durability (increase the durability/stability of catalysts with cycling)

(B) Cost (eliminate precious metal loading of catalysts)

(C) Performance (increase the specific and mass activities of catalysts)

Technical Targets

The technical targets for this project are listed in Table 1.

FY 2015 Accomplishments

Since achieving our go/no go decision target (July 2013), our down-selected catalysts were obtained from University of New Mexico and were referred to as UNM-CTS (mechano-chemical approach using water insoluble nicarbazin) catalysts. In order to transition to areal performance in air, several blends of the down-selected catalysts were made by combining them with a previously developed catalyst from UNM referred to as UNM-CBDZ (prepared using a nonmetal chelating approach using carbendazim material). As per our milestones for areal activity in hydrogen/air (Table 1), we have successfully surpassed the low current density target (30 mA/cm^2 at 0.8 V). Our current state-of-the-art for high current density performance stands at 1,050 mA/cm^2 using the above-mentioned blends. These results correspond to a 200 g batch size well in excess of the end of the program metrics. In addition, emerging catalysts prepared using an iron-encapsulated metal organic framework (MOF) chemistry approach referred to as NEU-Fe-MOF (from Northeastern

TABLE 1. Progress towards Meeting Technical Targets for Non-PGM Electrocatalysts for Transportation Applications

Characteristic	Units	2015 Target	NEU 2015 Status
Specific Activity @ 80°C, 1.5 bar total pressure, H_2/O_2, 100% relative humidity (RH) 2013 Go/No-Go Target	A/cm^3 A/cm^2	Volumetric activity of 300 A/cm^3 -0.8 V (iR-free) projected from ~10 mA/cm^2 Un-projected volumetric activity (no target set) 100 mA/cm^2 (iR-free)	400 A/cm^3 95 A/cm^3 100 mA/cm^2
Specific Activity @ 80°C, 2.5 bar total pressure, H_2/Air, 100% RH 2014 Target	A/cm^2	Areal activity of 30 mA/cm^2 @ 0.8 V Areal activity of 1 A/cm^2 @ 0.4 V	100 mA/cm^2 1,050 mA/cm^2
Scale-Up of Catalyst Batch Size Intra and Inter Batch Variability	g %	50 g & trajectory to 100 g 5% variation for both inter and intra batch	Target successfully met Target successfully met
Durability at 80°C Cycling: Catalyst Durability	% loss of activity	5%	<1%
Durability at 80°C Cycling: Carbon Corrosion Durability	% loss of activity	10%	<50% Partially recoverable

University) show great promise for an alternative approach. Preliminary measurements indicate that this material has the potential to meet both the low and high current density areal activity targets in air. Our initial report (the last annual report) showed this data using small batch synthesis (a batch size of less than 1 g). Current efforts include developing approaches for scaling up the synthesis using low cost precursors, and these have achieved 30 g batch size levels. While the low current density performance is well in excess of 30 mA/cm^2 (100 mA/cm^2 at 0.8 $V_{non\ IR\text{-}corrected}$), the high current density target is still a challenge with the current state-of-the-art exhibiting 750 mA/cm^2 at 0.4 $V_{non\ IR\text{-}corrected}$) short of the targeted 1 A/cm^2.

Our current efforts towards scale-up performed by PPC are on target based on the timelines for the slated milestones. At the end of the second quarter, in the second phase of this project, we successfully demonstrated less than 5% variability in performance in the low current density target potential (0.8 V) and approximately 5% variability at the higher current density (0.6 V). These variabilities reflect both inter and intra batch measurements. These data are based exclusively on areal activity measurements made using single cell data in air as per this project's slated operating conditions (2.5 bar total pressure in air, 100% humidification at 80°C).

Durability measurements conducted on the down-selected UNM-Fe-CTS (Fe-organic charge transfer salt based on nicarbazin) catalysts shows excellent tolerance to catalysts stability tests (based on Nissan protocol, similar to DOE protocol). Carbon corrosion testing that involved load cycling to 1.5 V vs. the reference hydrogen electrode, however, indicated significant losses; these results were similar to losses seen with a PGM cathode.

The understanding of the nature of the active site was significantly advanced in this reporting period with the identification of a dual site mechanism wherein the N_{2+2} site was responsible for the initial adsorption and reduction of oxygen to peroxide moieties followed by a second cascade step of further reduction of the peroxide in surrounding Fe-N_2 sites. This description of the mechanism was supported with in situ X-ray absorption spectroscopy (XAS) and targeted electrochemical probe measurements.

✧ ✧ ✧ ✧ ✧

INTRODUCTION

Recent reports [1–3] have clearly demonstrated the significant advancements made in enabling good oxygen reduction activity with iron-based non-PGM catalysts. These so called Fe-N_x-based systems have evolved over several decades of intense work leading up to the current state-of-the-art, reported recently [1,4]. This report provides for the first time a comprehensive view of (a) the gains in oxygen reduction reaction (ORR) activity derived from materials prepared using current state-of-the-art materials developed by two different university groups (NEU and UNM) and the successful scale-up of these by a startup company, PPC; (b) the successful transition from previous operations in oxygen to air (MSU, NEU, and PPC); (c) excellent durability in terms of catalyst stability (*vide* DOE and Nissan protocols) (UNM and NTCNA); and (d) a detailed understanding of the nature of active sites and electrocatalytic pathways as distinct from the parallel pathway in alkaline electrolytes (UNM and NEU).

APPROACH

The approach adopted in this reporting period involved blends of materials derived using two separate approaches: a UNM group's silica templating methodology referred to as UNM-CTS and a UNM-CBDZ approach. The former (UNM-CTS) was derived using the mechano-chemical approach of ball milling an organic charge transfer salt (nicarbazin) in the presence of Fe salt and the latter using an aqueous formulation of a non-chelating material, carbendazim, with Fe salt, and both were supported on

silica followed by several pyrolysis and etching steps. Typical blends comprised of a 1:1 mixture. The Northeastern University approach involved a one pot synthesis of an MOF material referred to as ZIF-8 that encapsulated a chelated metal salt.

These materials were tested in single cells (5 cm^2) using a commercial anode electrode (Alfa Aesar) with a 0.1 mg/cm^2 Pt loading. The typical cathode loading was 3 mg/cm^2 and the membrane used was a Nafion® 211, with 50% Nafion® loading at the cathode. Tests were conducted under steady-state potentiostatic conditions with each point measured for a minimum of 60 s. In this annual report all reported tests were conducted at PPC, using scaled-up batches of 50 g and above for the UNM-CTS approach and 30 g for the NEU-MOF approach. Common test protocols were replicated at NTCNA and NEU. Durability measurements were performed using two well-established protocols (catalyst durability) and carbon corrosion tests (both are DOE protocols). Investigation of the nature of active sites and ORR electrocatalysis steps as measured using in situ synchrotron spectroscopy at the Fe-K edge were performed under actual cell operando conditions.

RESULTS

PPC has scaled up formulations of both the UNM sample and the NEU-developed approach and also modified the UNM catalyst for improved performance. Brief descriptions of the approaches employed for both catalysts are given in the approach section. The UMN catalyst was reformulated to (a) improve mass transport to meet the areal activity target in hydrogen/air as well as (b) provide higher durability under the two above-mentioned (see Approach section) DOE mandated protocols. The chemically intensive approach for scale-up involved several key steps requiring optimization. The initial scale-up effort was focused on a 10–20 g batch [1], with the goal that the methods developed could be applied for synthesizing between 30 g and 50 g, with a long-term goal of 100 g batches.

Demonstration of progress towards 100 g per batch synthesis of the original Fe-CTS catalyst involved pre-treatment of precursors to reduce and eliminate residual precursor and batch consistency effects on manufacturing. As mentioned above the milestone is to meet the hydrogen/air areal performance target of 30 mA/cm^2 at 0.8 V and 1,000 mA/cm^2 at 0.4 V in 2.5 bar air and 80°C at 100% humidification.

Progress towards 100 g batches was established through use of larger volume processing equipment, processing vessel materials changes, and tuning of processing parameters such as the pyrolysis temperature trajectory, etching times and agitations, and mixing times and intensity. In this way, 200 g batches have been prepared.

A brief summary illustrating these developments is presented showing a nearly 80% improvement in performance in air (compared to previous reporting period) with 70 mA/cm^2 at 0.8 V and 1,000 mA/cm^2 at 0.8 V achieved using 3 mg/cm^2 loading gas diffusion electrodes. Figure 1a shows two separate blend formulations, Gen 1 and Gen 2, made using variations in silica templates. Comparison of Gen 2 (100% CTS batch) and Gen 2A (CTS/CBDZ blend with variation of silica template show remarkable inter batch reproducibility in hydrogen/air performance in accordance to this project's targeted operating conditions. The low current density target of 30 mA/cm^2 at 0.8 V (uncorrected) has been met and exceeded with current state-of-the-art performance at 70 mA/cm^2 current density. The higher current density target of 1 A/cm^2 at 0.4 V (infrared [IR]-corrected) (second quarter, FY 2015) has nearly been met with current activity at 0.92 A/cm^2 (uncorrected) and 1.05 A/cm^2 (IR-corrected). These performance figures are better delineated in the corresponding Tafel (semi-log plot) shown in Figure 1a. Both of these results are reported without any IR correction.

A brief introduction to the NEU catalyst synthesis methodology is reported in Figure 2a, wherein an iron-based non-PGM ORR electrocatalyst utilizes an MOF-based support that hosts a chelated iron complex within its pores. The MOF support was chosen in order to take advantage of the porosity and high surface area, key variables known to improve the catalytic activity and mass transport. A one pot encapsulation procedure developed by NEU uses a zinc MOF (ZIF-8 MOF) synthesized in the presence of chelated iron (or Co) precursors. The final product was dried in a vacuum oven for four hours at 70°C and then further treated by either one or two heat treatments in argon at 1,050°C and ammonia at 950°C, respectively. Preliminary rotating disc electrode (RDE) analysis shown in Figure 2b shows performance exceeding that of platinum in alkaline electrolyte (0.1 M KOH) and a half wave potential difference of 70 mV compared to platinum in acidic pH (0.1 M $HClO_4$). Non-iron-containing MOF shows, in comparison, 400 mV over-voltage indicating predominant peroxide generation. Preliminary fuel cell measurements made using hydrogen/oxygen (1.5 bar total pressure), 80°C, and 100% humidification indicated performance in excess of DOE Phase 1 target of 100 mA/cm^2 at 0.8 V (IR-corrected) with current state-of-the-art at 170 mA/cm^2. More importantly, the hydrogen/air performance meets both the low 0.8 V (IR-uncorrected) and high current density 0.4 V (IR-uncorrected) values with current state of the art at 75 mA/cm^2 (at 0.8 V) and 1 A/cm^2 (at 0.4 V).

After a lengthy analysis, PPC identified unique processing equipment and supplies needed for the technology transfer and scale-up. Once in place, lengthy visits by PPC personnel to NEU led to creation of standard operating procedures, and critical points of manufacturing were

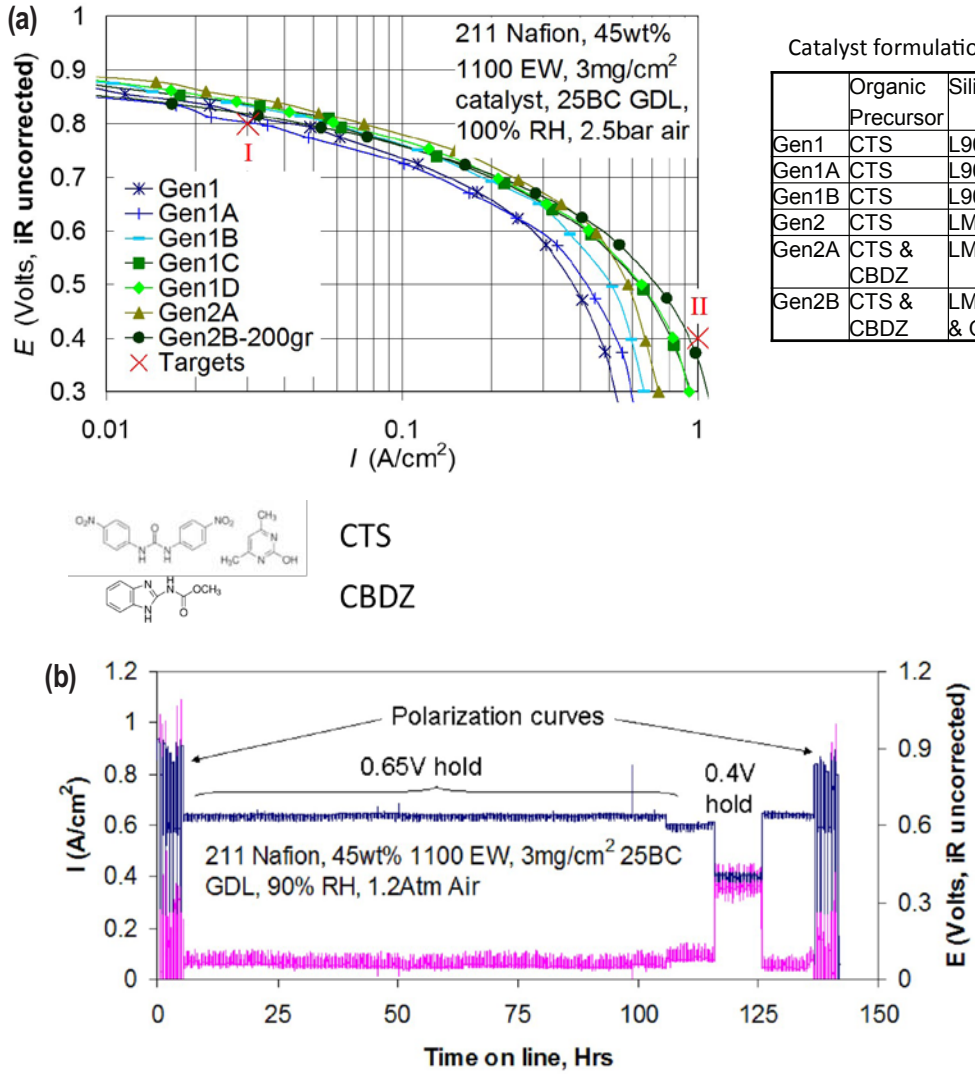

Catalyst formulations

	Organic Precursor	Silica
Gen1	CTS	L90
Gen1A	CTS	L90
Gen1B	CTS	L90
Gen2	CTS	LM150
Gen2A	CTS & CBDZ	LM150
Gen2B	CTS & CBDZ	LM150 & OX50

FIGURE 1. Areal activity measured using 5 cm^2 single cells using H_2/air (2.5 bar total pressure), 80°C, 100% humidity using 3 mg/cm^2 non-PGM catalyst loading at the cathode and anode comprising of a commercially obtained Pt/C catalyst (JM Hispec 2000, 0.1 mg/cm^2 Pt loading on SGL substrate). The non-PGM catalyst depicted was comprised of both a pure UNM-CTS (Gen 1) and a formulation (1:1) of UNM-CTS and UNM-CBDZ using different formulations of silica support (resultant pore formation). Here, the batch sizes used were in excess of 50 g. (a) Tafel slope exhibiting performance meeting this project's milestones for both low and high current density operation, including a 200 g batch. (b) 0.65 V potentiostatic hold test for the 200 g batch, exhibiting excellent stability over 100 h.

determined to be (1) making the MOF, (2) mixing the MOF and precursors, and (3) pyrolysis both in inert and reactive atmospheres. To establish calibration points of processing equipment a series of materials at the different stages of manufacturing identified have been sent to project partners (NEU and NTCNA) and are being characterized to determine points of congruency in the processing. This procedure allowed baseline levels and sensitivity of processing variables for the key processing steps to be established and used during scale-up.

Scale-up required modification of the both the recipe and procedure used in the key MOF-forming step. First, switching from a small shaker-type mill to a larger planetary ball mill lead to a tendency for powder clumping that is inherent with powder milling. When simply applying NEU's procedure with a planetary ball mill, the resulting MOF powder included clumps, and the resultant material had a lower surface area than what is required for producing good catalysts. Clumping increased with 10, 20, and 50x batch sizes. Numerous iterations of precursor pretreatments, sequence of addition, and even material ratios were attempted unsuccessfully. Methods were found in the literature and with NEU's assistance, a formulation that decreased clump formation was successfully achieved even when applied at 50x scale, producing good quality MOF as determined by X-ray diffraction (XRD), Brunauer-Emmett-

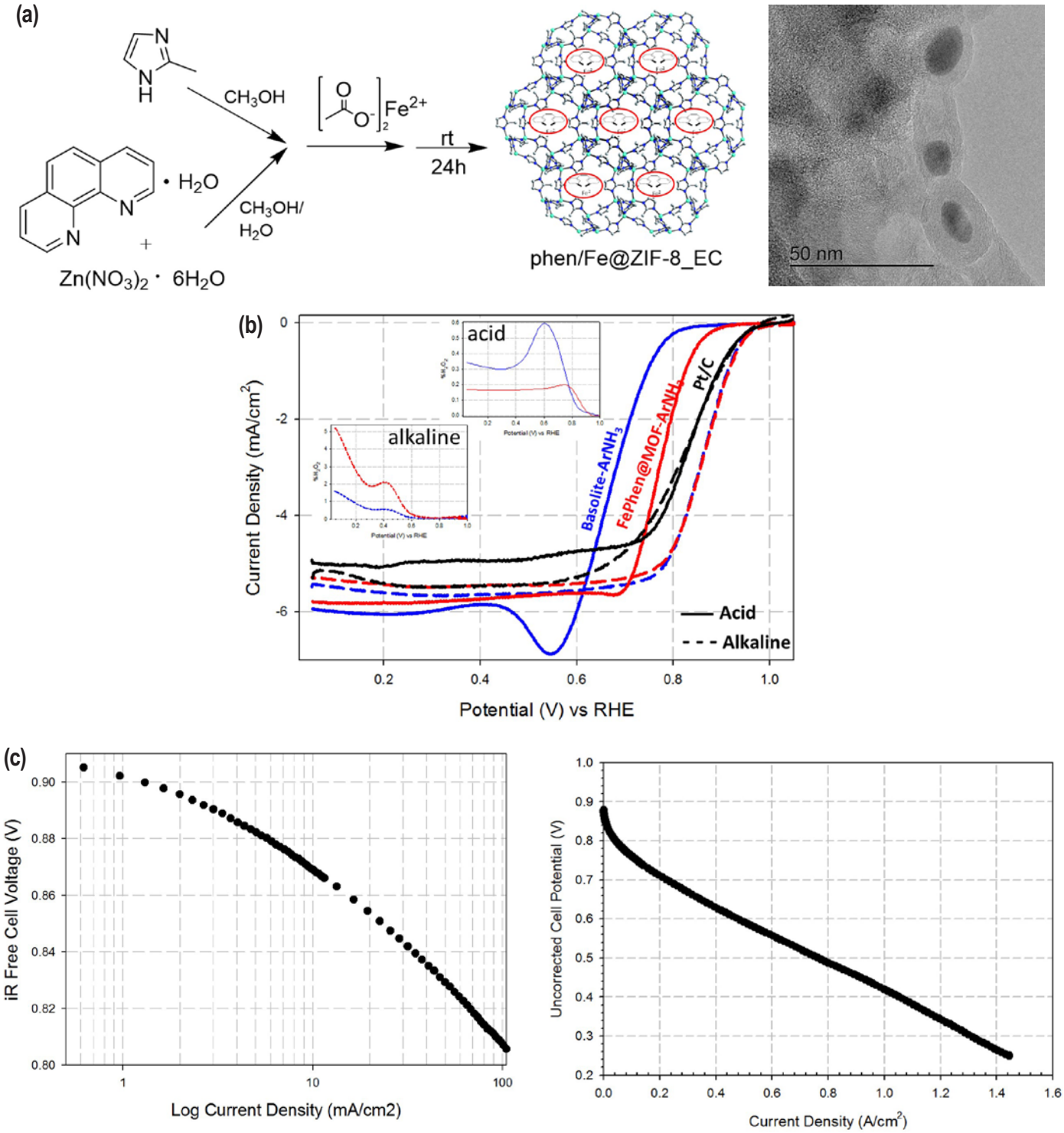

FIGURE 2. (a) Schematic showing the one pot synthetic approach for NEU MOF-based iron encapsulated catalysts. Scanning electron microscope micrograph shows encapsulation and carbon fiber formation. (b) RDE comparison with Pt/C (Tanaka 30% Pt/C) in both acid and alkaline pH (0.1 M KOH and $HClO_4$). Also plotted is a non-iron-containing catalyst referred to as Basolite. (c) Tafel plot for single cell data (5 cm^2) in H_2/O_2 with 1.5 bar total pressure, 100% RH, 80°C. Also shown is the corresponding linear polarization data (IR-uncorrected) in H_2/air showing the concomitant low and high current density performances under 2.5 bar total pressure.

Teller surface areas at different processing steps, and final catalyst performance. Figure 3a shows the XRD patterns of commercial ZIF-8 MOF, as well as the time trajectory of MOF phase evolution at various milling times, and the final 50x batches used for making the excellent performance MOF-based catalyst shown in Figure 3b. Figure 3b shows the performance of scaled-MOF based catalysts, and improvement in both performance and scale to a final catalyst made at 50x scale (30+ g per batch) with performance after being on-line for more than two hours of more than 100 mA/cm^2 at 0.8 V, and 800 mA at 0.4 V in 2.5 bar air.

Iron speciation in the Fe-CTS and Fe8AA catalysts was characterized with Fe Mössbauer spectroscopy [5,6] together with in situ XAS (Figure 4). Two iron species (D1 and D2) were identified in the Fe8AA catalyst that resulted in the appearance of two doublets (Figure 1a). D1 and D2 can be assigned to a four-fold nitrogen or nitrogen–carbon coordination of Fe^{II} in low-spin (LS) and medium-spin state (MS), respectively [5,7]. Consistently, the Fourier transform of the sole extended X-ray absorption fine structure (EXAFS) peak around 1.5 Å (without phase-correction) is assigned to the Fe-N_4 moieties based on EXAFS fitting results. D1 and D2 are the subject of ongoing research related to the exact site structure and to the integration of FeN_4 or FeN_2C_2 moieties that can be viewed either as defect sites within a graphene layer (edge defects) or as a structure bridging two graphene zigzag-or armchair-edges [5,6]. The observed ORR activity has been widely linked to either or both of the D1 and D2 species. In addition to the two doublets (D1 and D2), three more iron species were identified in the Fe-CTS catalyst resulting in a singlet, and two sextets (Figure 1c). The singlet is assigned to either γ-Fe or super paramagnetic iron nanoparticles [5] while the sextet's parameters match those of α-Fe and iron carbide [5,7]. The coexistence of the Fe-N species and metallic iron nanoparticles (NPs) under reactive conditions in acid are in good agreement with in situ XAS results, the two FT-EXAFS peaks around 1.5 and 2.1 Å are ascribed to the Fe-N scattering and Fe-Fe scattering within pure iron NPs and/or iron carbides, respectively. The long-term existence of metallic iron species in an acidic environment strongly suggests that they are fully wrapped in graphitic layers. These metallic iron species were previously believed to be inactive due to their lack of exposure to the electrochemical environment. However, recently published research by various groups has shown that the nitrogen-doped carbon encapsulating these metallic iron species are highly ORR active [1,8,9]. Therefore, the control over the content in the final products after high-temperature treatment as shown here has enormous consequences on elucidating the fundamental synthesis/morphology/activity correlations for non-PGM catalysts.

CONCLUSIONS

- Catalyst blends (1:1) prepared by PPC using 50+ g batch sizes with University of New Mexico catalysts, UNM-CTS and UNM-CBDZ, show inter- and intra-batch variations below 5%. They also meet and exceed the low current density areal activity target in hydrogen/air (2.5 bar total pressure, 80°C, 100% RH). High current density is currently at 920 mA/cm^2 at 0.4 V. A separate MOF-based approach from NEU shows excellent areal activity under these performance metrics exceeding the low current density benchmark and meeting the high current density target. This approach has been scaled up to 30 g batches.
- Detailed durability studies reported earlier on the UNM catalysts measured by NTCNA indicate excellent tolerance to catalyst stability tests, and relatively poor resistance to carbon corrosion test protocols; the

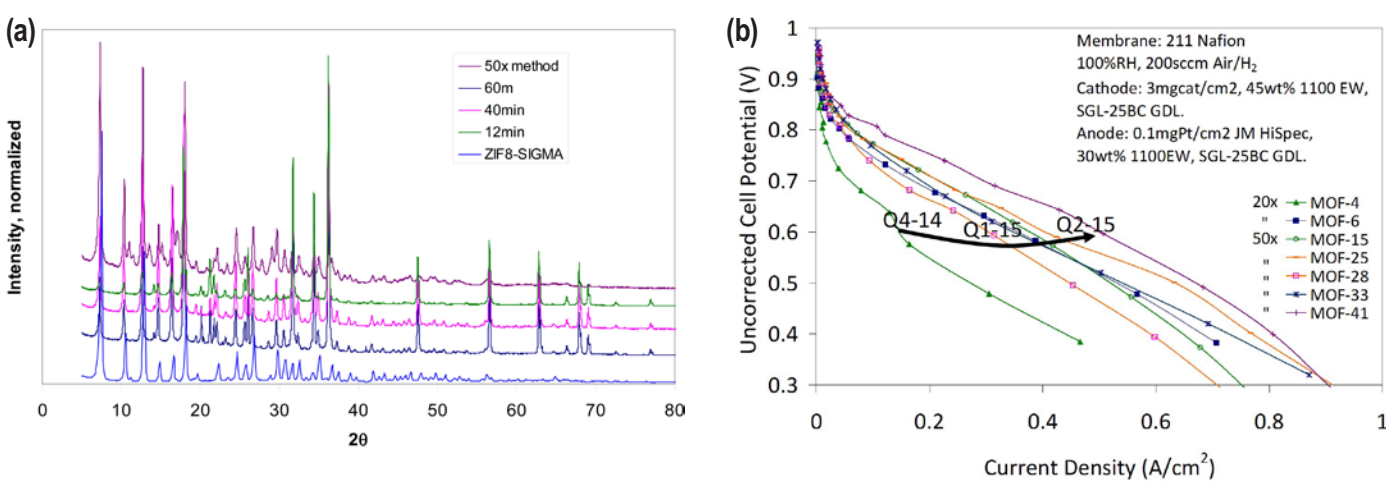

FIGURE 3. (a) Time evolution of XRD patterns measured at different time intervals of precursor ball milling of MOF Fe-chelates exhibiting the evolution of MOF structure as a result of reactive ball milling. (b) Evolution of areal activity as a function of scale-up efforts measured in H_2/air, 80°C, 100% RH, 2.5 bar pressure using 3 mg/cm^2 cathode MOF derived catalyst and standard 0.1 mg/cm^2 Pt/C anode.

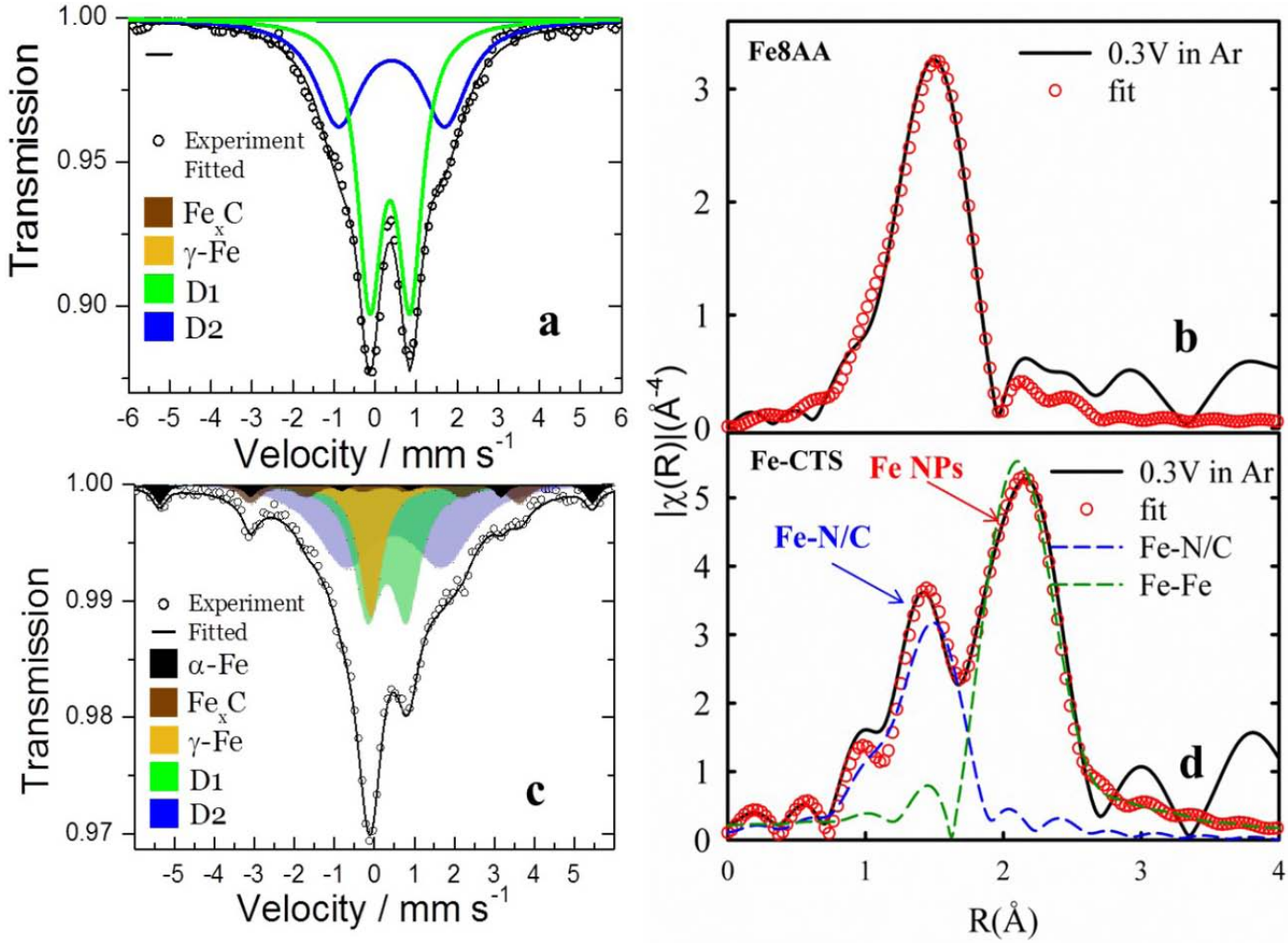

FIGURE 4 (a-d). Mossbauer spectra collected [5,7] for UNM catalysts, FeAA8Pyr (Fe-Amino-antipyrene) and Fe-CTS (Fe-organic charge transfer salt based on nicarbazin) in consonance with in situ synchrotron XAS in terms of Fe K edge Fourier transform of the EXAFS showing remarkable congruence on identification of the relative presence of Fe-N and Fe-NPS moieties.

latter, however, is on par with those observed for PGM catalysts.

- Switching behavior involving the transition metal as identified using Mossbuer spectroscopy [5,6], and in situ XAS indicates the central role it plays in determining the activity of ORR.

FUTURE DIRECTIONS

- The principle focus of the group will be to meet the high current density areal activity target at 0.4 V (IR-uncorrected) using both UNM and NEU blend formulations.
- We will optimize scale-up and MEA fabrication for MOF based catalysts from NEU.
- NTCNA will perform testing to validate durability under DOE protocols.
- We will further test the validity of the proposed mechanism using the final set of in situ and operando synchrotron XAS data in conjunction with density functional theory calculations. In addition, we will use the in situ spectroscopy to probe degradation pathways.

FY 2014-2015 PUBLICATIONS/REFERENCES

1. Ganesan, S., Leonard, N., and Barton, S.C. Impact of transition metal on nitrogen retention and activity of iron–nitrogen–carbon oxygen reduction catalysts. *Physical Chemistry Chemical Physics* 16, 4576–4585 (2014).

2. Leonard, N.D., and Barton, S.C. Analysis of Adsorption Effects on a Metal-Nitrogen-Carbon Catalyst Using a Rotating Ring-Disk Study. *Journal of The Electrochemical Society* 161, H3100–H3105 (2015).

3. Robson, M.H., Artyushkova, K., Patterson, W., Atanassov, P., and Hibbs, M.R. Non-platinum Carbon-Supported Oxygen Reduction Catalyst Ink Evaluation Based on Poly (sulfone) and Poly (phenylene)-Derived Ionomers in Alkaline Media. *Electrocatalysis* 5, 148–158 (2014).

4. Serov, A., Artyushkova, K., Andersen, N.I., Stariha, S., and Atanassov, P. Original Mechanochemical Synthesis of Non-Platinum Group Metals Oxygen Reduction Reaction Catalysts Assisted by Sacrificial Support Method. *Electrochimica Acta* (2015).

5. Serov, A., Artyushkova, K., and Atanassov, P. Fe-N-C Oxygen Reduction Fuel Cell Catalyst Derived from Carbendazim: Synthesis, Structure, and Reactivity. *Advanced Energy Materials* 4 (2014).

6. Tylus, U. *et al.* Elucidating Oxygen Reduction Active Sites in Pyrolyzed Metal–Nitrogen Coordinated Non-Precious-Metal Electrocatalyst Systems. *The Journal of Physical Chemistry C* 118, 8999–9008 (2014).

7. Serov, A., Tylus, U., Artyushkova, K., Mukerjee, S., and Atanassov, P. Mechanistic studies of oxygen reduction on Fe-PEI derived non-PGM electrocatalysts. *Applied Catalysis B: Environmental* 150, 179–186 (2014).

8. Strickland, K., Miner, E., Jia, Q., Tylus, U., Ramaswamy, N., Liang, W., Sougrati, M.T., Jouen, F., and Mukerjee, S., 'Metal Nx Free Electrocatalyst with High Activity for Oxygen Reduction Reaction,' Nature Comm., 6, 7343 (2015).

9. Nano-strcutured non-platinum catalysts for automotive fuel cell applications, A. Serov, K. Artyushkova, E. Niangar, C. Wang, N. Dale, F. Jaouen, M-T. Sougrati, Q. Jia, S. Mukerjee, and P. Atanassov, Nano-Energy, 16, 293 (2015).

REFERENCES

1. Strickland, K. *et al.* Highly active oxygen reduction non-platinum group metal electrocatalyst without direct metal-nitrogen coordination. *Nat. Commun.,* **6,** 7343 (2015).

2. Wu, G., More, K.L., Johnston, C.M., and Zelenay, P. High-performance electrocatalysts for oxygen reduction derived from polyaniline, iron, and cobalt. *Science* **332,** 443–447 (2011).

3. Jaouen, F. *et al.* Recent advances in non-precious metal catalysis for oxygen-reduction reaction in polymer electrolyte fuel cells. *Energy Environ. Sci.* **4,** 114–130 (2011).

4. Chung, H.T., Won, J.H., and Zelenay, P. Active and stable carbon nanotube/nanoparticle composite electrocatalyst for oxygen reduction. *Nat. Commun.* **4,** 1922 (2013).

5. Kramm, U.I., Lefèvre, M., Larouche, N., Schmeißer, D., and Dodelet, J.-P. Correlations between mass activity and physicochemical properties of Fe/N/C catalysts for the ORR in PEM fuel cell via 57Fe Mößbauer spectroscopy and other techniques. *J. Am. Chem. Soc.* (2013).

6. Kramm, U.I. *et al.* Structure of the catalytic sites in Fe/N/C-catalysts for O_2-reduction in PEM fuel cells. *Phys. Chem. Chem. Phys.* **14,** 11673–11688 (2012).

7. Ramaswamy, N., Tylus, U., Jia, Q., and Mukerjee, S. Activity descriptor identification for oxygen reduction on nonprecious electrocatalysts: Linking surface science to coordination chemistry. *J. Am. Chem. Soc.* **135,** 15443–15449 (2013).

8. Deng, D. *et al.* Iron Encapsulated within Pod-like Carbon Nanotubes for Oxygen Reduction Reaction. *Angew. Chem. Int. Ed.* **52,** 371–375 (2013).

9. Hu, Y. *et al.* Hollow Spheres of Iron Carbide Nanoparticles Encased in Graphitic Layers as Oxygen Reduction Catalysts. *Angew. Chem. Int. Ed.* **53,** 3675–3679 (2014).

V.A.6 Development of Ultra-Low Platinum Alloy Cathode Catalysts for PEM Fuel Cells

Branko N. Popov
University of South Carolina
301 Main Street
Columbia, SC 29208
Phone: (803) 777-7314; Fax: (803) 777-8265
Email: popov@cec.sc.edu

DOE Manager
Donna Ho
Phone: (202) 586-8000
Email: Donna.Ho@ee.doe.gov

Technical Advisor
Thomas Benjamin
Phone: (630) 252-1632
Email: benjamin@anl.gov

Contract Number: DE-EE0000460

Project Start Date: September 1, 2010
Project End Date: December 31, 2015

Overall Objectives

- Develop a unique hybrid cathode catalyst (HCC) through the interaction of a highly active and stable compressive Pt-lattice catalyst (Pt*) with an activated carbon composite support (A-CCS) having high activity for the oxygen reduction reaction (ORR)
- Enhance the activity of HCC by increasing the synergistic effect of catalytic active sites present on the supports and those on the Pt* catalyst
- Specific objectives are to:
  - Perform optimization studies to develop a catalyst support with high kinetic activity and stability.
  - Estimate the role of Brunauer-Emmett-Teller (BET) surface area, porosity, pore size and distribution, and hydrophilic/hydrophobic properties on the support stability.
  - Synthesize a low-platinum group metal (PGM) cathode catalyst for automotive application by decreasing the PGM loading while simultaneously increasing the catalytic activity and stability of both A-CCS and Pt*.
  - Develop low-cost procedures to synthesize A-CCS and Pt*/A-CCS.

Specific Objectives for Fiscal Year (FY) 2015

- Development of an A-CCS with desired BET surface area, porosity, pore-size distribution, and hydrophilic/hydrophobic properties
- Synthesis and performance evaluation of Pt^*/A-CCS catalyst using optimized A-CCS
  - Initial mass activity under H_2-O_2
  - Initial high current density performance under H_2-air
  - Catalyst durability under 0.6–1.0 V potential cycling experimental conditions
  - Support stability under 1.0–1.5 V potential cycling experimental conditions

Technical Barriers

This project addresses the following technical barriers from the Fuel Cells section of the Fuel Cell Technologies Office Multi-Year Research, Development, and Demonstration Plan:

(A) Durability

(B) Cost

(C) Performance

Technical Targets

In this project, studies are being conducted to develop highly active and stable ultra-low Pt loading cathode catalysts for proton exchange membrane (PEM) fuel cells. In FY 2015, a Pt*/A-CCS catalyst was synthesized using procedures developed at the University of South Carolina (USC). Our results showed that the Pt*/A-CCS catalyst has the potential to meet the 2017 DOE technical targets for electrocatalysts for automotive applications as shown in Table 1.

FY 2015 Accomplishments

The following results were accomplished for the Pt*/A-CCS catalyst:

- Achieved an initial mass activity of 0.41 A/mg_{PGM} and loss of mass activity of 46% after 30,000 cycles (0.6–1.0 V)
- Measured a potential loss of 35 mV (iR-free) at 0.8 A/cm^2 after 30,000 cycles (0.6–1.0 V)
- Accomplished 25% ECSA loss after 30,000 cycles (0.6–1.0 V)

TABLE 1. Progress towards Meeting Technical Targets for Electrocatalysts for Automotive Applications

Characteristic	Units	2017 DOE Targets	FY 2015 Status at USC (Pt*/A-CCS)
PGM total content	g/kW (rated)	0.125	0.19
PGM total loading	mg_{PGM}/cm^2	0.125	0.2
Mass activity (H_2/O_2 (2/9.5 stoic.) 80 °C, 100% RH, 150 kPa_{abs}.)	A/mg_{Pt} @ 0.9 $V_{iR\text{-}free}$	0.44	0.41
Catalyst durability (30,000 cycles, 0.6–1.0 V, 50 mV/s, 80 °C, H_2/N_2, 100% RH, no back press.)	% mass activity (MA) loss % ECSA loss mV loss @ 0.8 A/cm^2	≤40% ≤40% ≤30 mV @ 0.8 A/cm^2	46% loss (MA) 25% loss (ECSA) 35 mV loss (H_2-air)
Support stability (5,000 cycles, 1.0–1.5 V, 500 mV/s, 80 °C, H_2/N_2, 100% RH, no back press.)	% mass activity (MA) loss % ECSA loss mV loss @ 1.5 A/cm^2	≤40% ≤40% ≤30 mV @ 1.5 A/cm^2	53% loss (MA) 24% loss (ECSA) 10 mV gain (H_2-air)

RH - relative humidity; ECSA - electrochemical active surface area

- Pt*/A-CCS showed excellent support stability after 5,000 cycles (0.6–1.0 V)
  - Potential gain of ~10 mV (cell potential) was accomplished at 1.5 A/cm^2 after 5,000 cycles
- Accomplished 53% mass activity loss and 24% ECSA loss after 5,000 cycles (1.0–1.5 V)
- Accomplished (rated) initial power density of 0.19 g_{PGM}/kW

✧ ✧ ✧ ✧ ✧

INTRODUCTION

Novel methodologies were developed at USC to synthesize catalytically active and highly stable carbon-based supports [1–19]. Pt/A-CCS and Pt*/A-CCS catalysts with enhanced ORR kinetics were developed that showed higher performance than commercial Pt/C at low loadings (≤0.1 mg/cm^2) [17–19]. In FY 2015, a Pt*/A-CCS catalyst with high activity towards ORR was synthesized and its support stability (1.0–1.5 V potential cycling, 5,000 cycles) and catalyst durability (0.6–1.0 V potential cycling, 30,000 cycles) were evaluated.

APPROACH

The HCC technology developed at USC is based on a two-step patented process to synthesize highly active and stable ultra-low-PGM HCC. The research at USC was aimed at developing catalytically active and stable supports to sustain load cycling and startup/shutdown conditions. In the first step, the following major constraints directed our development of cathode catalyst supports: (1) the support should be chemically and electrochemically stable at high potentials, low pH, and high temperature; and (2) the support should have an onset potential and kinetic activity for ORR similar to that of the platinum catalyst. To accomplish these requirements, an A-CCS was synthesized with optimized (1) BET surface area, porosity, pore size, and pore size distribution; (2) hydrophilic/hydrophobic ratio; (3) structural properties (amorphous/crystalline ratio); (4) number of catalytic active sites through metal catalyzed pyrolysis; (5) Pt/Pt*-support interaction by inclusion of active surface functional groups; and (6) with cobalt incorporated into its structure, necessary for the formation of Pt*.

In the second step, a compressive Pt-lattice catalyst (Pt*) was synthesized through a USC-developed annealing procedure that controls the particle size during annealing. Monolayers of Pt* were formed by diffusing Co atoms present in the support into Pt which is deposited on the A-CCS. A mathematical model developed at USC was used to optimize the Co diffusion time, annealing temperature, and Pt/Co stoichiometric ratio.

RESULTS

Synthesis, support stability, and catalyst durability of the Pt/A-CCS catalyst were reported in the FY 2014 annual report. In FY 2015, the A-CCS with optimized physical properties was used for the synthesis of Pt*/A-CCS to meet the DOE 2017 technical targets for electrocatalysts and catalyst support. Initially, Pt/A-CCS was prepared by depositing Pt nanoparticles on A-CCS using a modified polyol reduction procedure developed at USC [17–19]. Then, a Pt*/A-CCS catalyst having a particle size distribution of 4–5 nm was synthesized through the controlled annealing of the Pt/A-CCS catalyst. The novel annealing procedure developed at USC inhibited the Pt particle growth at high temperature. The compressive Pt-lattice is formed by the diffusion of cobalt, which is present in the A-CCS, into Pt during the annealing process. The support stability and catalyst durability of the Pt*/A-CCS catalysts were evaluated

using 1.0–1.5 V potential cycling and 0.6–1.0 V potential cycling protocols, respectively.

Figure 1 shows the initial mass activity and stability of mass activity after 30,000 potential cycles (0.6–1.0 V) for the 30% Pt*/A-CCS catalyst. At 0.9 $V_{iR\text{-}free}$, the catalyst showed an initial mass activity of 0.41 A/mg_{Pt} and 46% loss after 30,000 cycles. The commercial 30% Pt/C catalyst showed a 68% loss (Table 2) after 30,000 cycles. The ECSA loss for the Pt*/A-CCS catalyst is 25% (decreased from 24.1 m^2/g_{Pt} to 18 m^2/g_{Pt}) while the commercial 30% Pt/C catalyst showed an 80% loss after 30,000 cycles.

The H_2-air fuel cell performance of the 30% Pt*/A-CCS catalyst subjected to 0.6–1.0 V potential cycles (30,000 cycles) is shown in Figure 2A (iR-corrected cell voltage vs. current) and Figure 2B (cell voltage vs. current). In H_2-air, the fuel cell exhibited an initial current density of 1.55 A/cm^2 at 0.6 $V_{iR\text{-}free}$ with a rated power density of 0.19 g_{PGM}/kW. The catalyst showed 35 mV (iR-free) loss and 32 mV (cell voltage) loss at 0.8 A/cm^2 after 30,000 cycles (0.6–1.0 V). The commercial Pt/C catalyst showed no activity at 0.8 A/cm^2 after 30,000 potential cycles between 0.6 V and 1.0 V. The catalyst durability results of the 30% Pt*/A-CCS and commercial Pt/C catalysts are compared in Table 2.

Figure 3A (iR-corrected cell voltage vs. current) and Figure 3B (cell voltage vs. current) show the H_2-air fuel cell performance of 30% Pt*/A-CCS catalyst subjected to 1.0–1.5 V potential cycles (5,000 cycles). The 30% Pt*/A-CCS catalyst exhibited an initial mass activity of 0.41 A/mg_{Pt} and 53% loss after 5,000 cycles. The H_2-air fuel cell performance showed an initial current density of 1.4 A/cm^2 at 0.6 $V_{iR\text{-}free}$ and 1.45 A/cm^2 after 5,000 cycles. The catalyst showed 10 mV gain (iR-free) and 29 mV gain (cell voltage) at 1.5 A/cm^2 after 5,000 cycles (1.0–1.5 V). The ECSA loss is 24% (decreased from 21 m^2/g_{Pt} to 16 m^2/g_{Pt}). The commercial

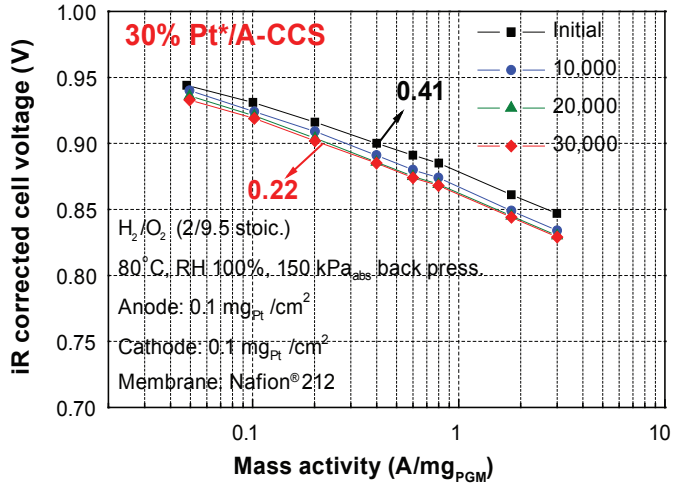

FIGURE 1. Stability of mass activity of Pt*/A-CCS catalyst subjected to 30,000 potential cycles between 0.6 V and 1.0 V at 50 mV/s. The catalyst loading is 0.1 mg_{PGM}/cm^2 on both the anode and cathode electrodes. The fuel cell operating conditions are: H_2/O_2 (2/9.5 stoic.), 80°C, 100% relative humidity (RH), 150 kPa_{abs} back pressure. Nafion® NRE 212 membrane is used as the electrolyte.

Pt/C catalyst showed very high mass activity loss (74%), 92% ECSA loss, and no activity at 1.5 A/cm^2 after 5,000 potential cycles between 1.0 V and 1.5 V. The support stability test results for the 30% Pt*/A-CCS and commercial Pt/C catalysts are summarized in Table 2. According to Reiser et al. [20], the cathode interfacial potential difference can reach ~1.5 V due to the H_2-air front in the anode compartment during startup/shutdown and carbon corrosion is an inevitable parasitic reaction at these high potentials. However, the 1.0–1.5 V potential cycling experimental results of the 30% Pt*/A-CCS catalyst show that the USC-developed A-CCS

TABLE 2. Summary of Support Stability Test (5,000 Potential Cycles between 1.0 V and 1.5 V) and Catalyst Durability Test (30,000 Potential Cycles between 0.6 V and 1.0 V) for Pt*/A-CCS and Commercial Pt/C Catalysts

Catalyst/Test	Particle Size (nm)	Mass Activity (A/mg_{Pt})		ECSA (m^2/g_{Pt})		Cell Voltage Loss (mV)	
		Initial	Final	Initial	Final	ΔV_{Cell}	$\Delta V_{iR\text{-}free}$
Pt*/A-CCC Support Stability	4~5	**0.41**	**0.19** (53% loss) (5,000 cycles)	21	16 (24% loss) (5,000 cycles)	0 (29 mV gain) at 1.5 A/cm^2 (5,000 cycles)	0 (10 mV gain) at 1.5 A/cm^2 (5,000 cycles)
Catalyst Durability	4~5	**0.41**	**0.22** (46% loss) (30,000 cycles)	24	18 (25% loss) (30,000 cycles)	32 at 0.8 A/cm^2 (30,000 cycles)	35 at 0.8 A/cm^2 (30,000 cycles)
Commercial Pt/C Support Stability	2.2	**0.18**	0.047 (74% loss) (5,000 cycles)	68	5.4 (92% loss) (5,000 cycles)	No activity (5,000 cycles)	No activity (5,000 cycles)
Catalyst Durability	2.2	**0.18**	0.057 (68% loss) (30,000 cycles)	68	13.6 (80% loss) (30,000 cycles)	No activity (30,000 cycles)	No activity (30,000 cycles)

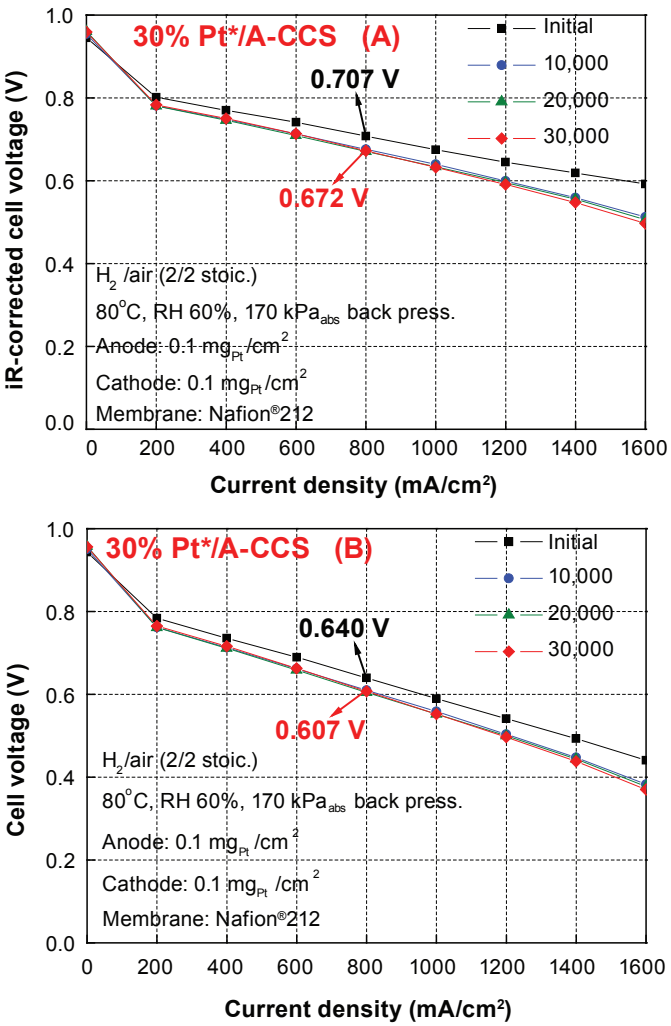

FIGURE 2. Comparison of H_2-air fuel cell performance of 30% Pt*/A-CCS catalyst subjected to 30,000 potential cycles between 0.6 V and 1.0 V at 50 mV/s. (A) iR-corrected cell voltage vs. current and (B) cell voltage vs. current. The catalyst loading is 0.1 mg_{PGM}/cm^2 on both the anode and cathode electrodes. The fuel cell operating conditions are: H_2-air (2/2 stoic.), 80°C, 60% RH, 170 kPa_{abs} back pressure. Nafion® NRE 212 membrane is used as the electrolyte.

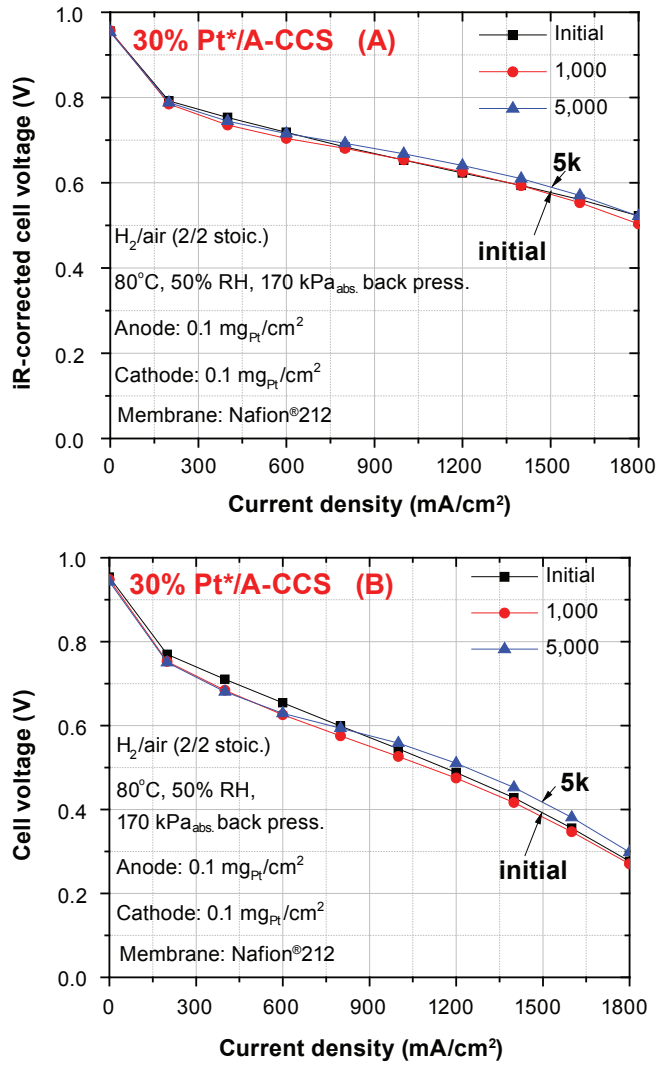

FIGURE 3. Comparison of H_2-air fuel cell performance of 30% Pt*/A-CCS catalyst subjected to 5,000 potential cycles between 1.0 V and 1.5 V at 500 mV/s. (A) iR-corrected cell voltage vs. current and (B) cell voltage vs. current. The catalyst loading is 0.1 mg_{PGM}/cm^2 on both the anode and cathode electrodes. The fuel cell operating conditions are: H_2/air (2/2 stoic.), 80°C, 50% RH, 170 kPa_{abs} back pressure. Nafion® NRE 212 membrane is used as the electrolyte.

support is highly stable at high potentials when compared to the carbon support used in commercial Pt/C catalyst. For the first time, by developing a breakthrough stable carbon-based composite at the Center for Electrochemical Engineering at USC, we have shown excellent support stability under 1.0–1.5 V potential cycling conditions for the Pt*/A-CCS catalyst.

CONCLUSIONS AND FUTURE DIRECTIONS

Conclusions for Pt*/A-CCS Catalyst

- Accomplished initial mass activity of 0.41 A/mg_{PGM} and loss of mass activity of 46% after 30,000 cycles (0.6–1.0 V)
- Accomplished potential loss of 35 mV (iR-free) and 32 mV (cell voltage) loss at 0.8 A/cm^2 after 30,000 cycles (0.6–1.0 V)
- Accomplished 25% ECSA loss after 30,000 cycles (0.6–1.0 V)
- The Pt*/A-CCS showed excellent support stability after 5,000 cycles (1.0–1.5 V)
  - Potential gain of ~10 mV (iR-corrected cell voltage) was accomplished at 1.5 A/cm^2 after 5,000 cycles

- Accomplished 53% mass activity loss and 24% ECSA loss after 5,000 cycles (1.0–1.5 V)
- Accomplished (rated) initial power density of 0.19 g_{PGM}/kW

Future Anticipated Accomplishments

- Our studies showed the formation of an ordered tetragonal Pt-Co phase, while the disorder to ordered Pt-Co phase ratio increased with increasing pyrolysis temperature. The catalyst performance was found to depend on the disordered/ordered Pt-Co structures (Pt*/A-CCS).
  - Detailed studies will be carried out to optimize the performance of Pt*/A-CCS with the structural properties of Co-doped Pt.
  - Structure-property performance relationships will be evaluated for different Pt-Co ratios which result in structures with different degrees of formation of compressive Pt-lattice structure.
  - A mathematical model developed at USC will be used to optimize the ratio of ordered and disordered Pt-Co phases.
- Further studies will be carried out to increase the H_2-air fuel cell performance of the Pt*/A-CCS catalyst by controlling the hydrophilic/hydrophobic properties of A-CCS. The goal is to eliminate the eventual flooding of the support during 1.0–1.5 V cycling.
- The catalyst which best achieves the 2017 DOE technical targets for electrocatalysts and catalyst supports will be selected.
- Reproducibility studies of the selected catalyst in 25 cm^2 and 50 cm^2 MEAs will be conducted.
- High-volume production procedures for the A-CCS support and Pt*/A-CCS catalyst will be optimized.
- Cost reduction will be achieved by:
  - Further decreasing the PGM loading.
  - Developing cost-effective synthesis procedures that eliminate the chemical leaching process during Pt*/A-CCS synthesis.
  - Optimizing of the Pt/Co ratio and decreasing the annealing temperature and reaction time.

Deliverables

1. Supply of 25 and 50 cm^2 MEAs for independent evaluation at NREL by the end of December 2015.

FY 2015 PUBLICATIONS

1. Wonsuk Jung, Tianyuan Xie, Taekeun Kim, Prabhu Ganesan, Branko N. Popov, "Highly Active and Durable Co-Doped Pt/CCC Cathode Catalyst for Polymer Electrolyte Membrane Fuel Cells," *Electrochim. Acta*, **167**, (2015) 1–12.

2. T. Kim, T. Xie, W.S. Jung, F. Gadala-Maria, P. Ganesan, B.N. Popov, "Development of Catalytically Active and Highly Stable Catalyst Supports for Polymer Electrolyte Membrane Fuel Cells," *J. Power Sources*, **273**, (2015) 761–774.

3. T. Xie, W.S. Jung, T. Kim, P. Ganesan, B.N. Popov, "Development of Highly Active and Durable Hybrid Cathode Catalysts for Polymer Electrolyte Membrane Fuel Cells," *J. Electrochem. Soc.*, **161** (2014) F1489–F1501.

REFERENCES

1. N.P. Subramanian, S.P. Kumaraguru, H.R. Colon-Mercado, H. Kim, B.N. Popov, T. Black, and D.A. Chen, "Studies on Co-Based Catalysts Supported on Modified Carbon Substrates for PEMFC Cathodes," *J. Power Sources*, **157** (2006) 56–63.

2. R.A. Sidik, A.B. Anderson, N.P. Subramanian, S.P. Kumaraguru, and B.N. Popov, "O_2 Reduction on Graphite and Nitrogen-Doped Graphite: Experiment and Theory," *J. Phys. Chem. B*, **110** (2006) 1787–1793.

3. X. Li, H.R. Colon-Mercado, G. Wu, J.-W. Lee, B.N. Popov, "Development of Method for Synthesis of Pt-Co Cathode Catalysts for PEM Fuel Cells," *Electrochem. Solid-State Lett.*, **10** (2007) B201–B205.

4. Nallathambi, Vijayadurga; Lee, Jong-Won; Kumaraguru, Swaminatha P.; Wu, Gang; Popov, Branko N., "Development of high performance carbon composite catalyst for oxygen reduction reaction in PEM Proton Exchange Membrane fuel cells," *J. Power Sources*, **183** (2008) 34–42.

5. Subramanian, Nalini P.; Li, Xuguang; Nallathambi, Vijayadurda; Kumaraguru, Swaminatha P.; Colon-Mercado, Hector; Wu, Gang; Lee, Jong-Won; Popov, Branko N., "Nitrogen-modified carbon-based catalysts for oxygen reduction reaction in polymer electrolyte membrane fuel cells," *J. Power Sources*, **188** (2009) 38–44.

6. Liu, Gang; Li, Xuguang; Ganesan, Prabhu; Popov, Branko N., "Development of non-precious metal oxygen-reduction catalysts for PEM fuel cells based on N-doped ordered porous carbon," *Appl. Catal. B: Environmental,* **93** (2009) 156–165.

7. Li, Xuguang; Park, Sehkyu; Popov, Branko N., "Highly stable Pt and PtPd hybrid catalysts supported on a nitrogen-modified carbon composite for fuel cell application," *J. Power Sources*, **195** (2010) 445–452.

8. Liu, Gang; Li, Xuguang; Ganesan, Prabhu; Popov, Branko N., "Studies of oxygen reduction reaction active sites and stability of nitrogen-modified carbon composite catalysts for PEM fuel cells," *Electrochim. Acta*, **55** (2010) 2853–2858.

9. Xuguang Li, Gang Liu, Branko N. Popov, "Activity and stability of non-precious metal catalysts for oxygen reduction in acid and alkaline electrolytes," *J. Power Sources*, **195** (2010) 6373–6378.

10. B.N. Popov, X. Li, and J.W. Lee, "Power source research at USC: Development of advanced electrocatalysts for polymer electrolyte membrane fuel cells," *Int. J. Hyd. Energy*, **36** (2011) 1794–1802.

11. Xuguang Li, Branko N. Popov, Takeo Kawahara, Hiroyuki Yanagi, "Non-precious metal catalysts synthesized from precursors of carbon, nitrogen, and transition metal for oxygen reduction in alkaline fuel cells," *J. Power Sources*, 196 (2011), 1717–1722.

12. Gang Liu, Xuguang Li, Jong-Won Lee, and Branko Popov, "A Review of the Development of Nitrogen Modified Carbon-based Catalyst for Oxygen Reduction at USC," *Catalysis Science & Technology,* 1, (2011) 207–217.

13. Branko N. Popov, Tianyuan Xie, Taekeun Kim, Won Suk Jung, Joseph C. Rotchford, Akos Kriston, and Prabhu Ganesan, "Development of Ultra-Low Loading Pt Alloy Cathode Catalyst for PEM Fuel Cells," *ECS Trans*., **58** (2013) 761–778.

14. Ákos Kriston, Tianyuan Xie, David Gamliel, Prabhu Ganesan, Branko N. Popov, "Effect of Ultra-Low Pt Loading on Mass Activity of PEM Fuel Cells," *J. Power Sources*, **243** (2013) 958–963.

15. Ákos Kriston, Tianyuan Xie, Prabhu Ganesan, Branko N. Popov, "Effect of Pt Loading on Mass and Specific Activity in PEM Fuel Cells," *J. Electrochem. Soc*., **160** (2013) F406–F412.

16. Ákos Kriston, Tianyuan Xie, and Branko N. Popov, "Impact of Ultra-low Platinum Loading on Mass Activity and Mass Transport in H_2-Oxygen and H_2-Air PEM Fuel Cells," *Electrochim. Acta*, **121** (2014) 116–127.

17. Wonsuk Jung, Tianyuan Xie, Taekeun Kim, Prabhu Ganesan, Branko N. Popov, "Highly Active and Durable Co-Doped Pt/CCC Cathode Catalyst for Polymer Electrolyte Membrane Fuel Cells," *Electrochim. Acta*, **167**, (2015) 1–12.

18. T. Kim, T. Xie, W.S. Jung, F. Gadala-Maria, P. Ganesan, B.N. Popov, "Development of Catalytically Active and Highly Stable Catalyst Supports for Polymer Electrolyte Membrane Fuel Cells," *J. Power Sources*, **273**, (2015) 761–774.

19. T. Xie, W.S. Jung, T. Kim, P. Ganesan, B.N. Popov, "Development of Highly Active and Durable Hybrid Cathode Catalysts for Polymer Electrolyte Membrane Fuel Cells," *J. Electrochem. Soc*., **161** (2014) F1489–F1501.

20. C.A. Reiser, L. Bregoli, T.W. Patterson, J.S. Yi, J.D. Yang, M.L. Perry, T.D. Jarvi, "A Reverse-Current Decay Mechanism of Fuel Cells," *Electrochem. Solid-State Lett*. **8** (2005) A273–A276.

V.A.7 Non-Precious Metal Fuel Cell Cathodes: Catalyst Development and Electrode Structure Design

Piotr Zelenay (Primary Contact), H. Chung, U. Martinez, E. Holby, U. Tylus, G. Purdy
Materials Physics and Applications Division
Los Alamos National Laboratory (LANL)
Los Alamos, NM 87545
Phone: (505) 667-0197, Fax: (505) 665-4292
Email: zelenay@lanl.gov

DOE Manager
Nancy Garland
Phone: (202) 586-5673
Email: Nancy.Garland@ee.doe.gov

Subcontractors
- J. Ziegelbauer (PI), General Motors, Warren, MI
- M. Odgaard (PI), D. Schlueter, IRD Fuel Cells, Albuquerque, NM
- S. Litster (PI), S.K. Babu, Carnegie Mellon University (CMU), Pittsburgh, PA
- M. Neidig (PI), J. Kehl, J. Kneebone, University of Rochester, Rochester, NY
- Z. Chen (PI), D. Higgins, G. Jiang, M.-H. Seo, University of Waterloo, Waterloo, Canada
- K.L More (PI), D. Cullen, Oak Ridge National Laboratory (ORNL), Oak Ridge, TN

Project Start Date: April 1, 2013
Project End Date: March 31, 2016

Overall Objectives

- Advance non-platinum group metal (PGM) cathode technology through the development of new materials and implementation of novel electrode concepts resulting in:
  - High oxygen reduction reaction (ORR) activity, viable for practical automotive systems
  - Improved catalyst durability
  - High ionic/electronic conductivity within the catalyst layer
  - Adequate oxygen mass transport and effective removal of the water product

Fiscal Year (FY) 2015 Objectives

- Optimize multiple nitrogen precursor synthesis approach for the development of advanced Fe-N-C catalysts
- Develop non-PGM cathode model based on microstructurally-consistent agglomerate parameters from nano-X-ray tomography (XRT) and electron microscopy
- Combine theoretical density functional theory (DFT) modeling with surface probe approaches, nuclear resonance vibrational spectroscopy (NRVS) and Δμ-X-ray absorption spectroscopy (XAS), for the identification of Fe-N_x active sites
- Large-scale membrane electrode assembly (MEA) fabrication (50 cm^2) in industry environment

Technical Barriers

This project addresses the following technical barriers from the Fuel Cells section (3.4.5) of the Fuel Cell Technologies Office Multi-Year Research, Development, and Demonstration (MYRDD) Plan [1]:

(A) Durability (catalysts, electrode layers)

(B) Cost (catalyst, MEAs)

(C) Performance (catalysts, electrodes, MEAs)

Technical Targets

Non-PGM fuel cell cathode catalyst research in this project focuses on the DOE technical targets outlined in Table 3.4.13 in the Fuel Cells section (3.4.4) of the MYRDD Plan [1]. The ultimate technical targets of the project are:

- Catalyst activity in H_2/O_2 MEA at 0.044 A cm^{-2} (80°C): ≥0.87 V (*iR*-free)
- Four-electron selectivity (rotating ring-disk electrode [RRDE]): ≥99% (H_2O_2 ≤1%)
- MEA maximum power density at 80°C: ≥1.0 W cm^{-2}
- Performance loss at 0.80 A cm^{-2} after 30,000 cycles in N_2: ≤30 mV

TABLE 1. Progress towards Meeting Technical Targets for Electrocatalysts for Transportation Applications

Characteristic	Unit	Targets (CWG Proposed)		2015 Status
		2020	Ultimate	
Voltage at 0.044 A/cm^{2*}	$V_{iR\text{-free}}$	0.87	0.90	0.86

* Test at 80°C H_2/O_2 in MEA; fully humidified with total outlet pressure of 150 kPa (abs); anode stoichiometry 2; cathode stoichiometry 9.5 [2].
CWG – Catalysis Working Group

FY 2015 Accomplishments

- An advanced cyanamide-polyaniline (CM-PANI)-Fe-C catalyst with favorable micro- and meso-structure was synthesized via the novel multiple nitrogen precursor approach. The catalyst was tested in H_2/O_2 MEA (80°C) reaching a catalyst activity of 0.86 V (*iR*-free) at 0.044 A cm^{-2}, only 0.01 V from the 2020 target (as proposed by DOE Catalysis Working Group).
- Promising initial activity was obtained from a Fe-free catalyst (CM-PANI-Co-C) in rotating disk electrode (RDE) ($E_{½}$ of 0.74 V) and fuel cell testing (with relatively low loading, 2.0 mg cm^{-2}).
- Combination of DFT modeling, NRVS, and Δμ-XAS studies points to the presence of surface active Fe-N_x sites.
- A microstructurally consistent fuel cell model was validated against experimental H_2–air fuel cell data with varying Nafion® loading.

✧ ✧ ✧ ✧ ✧

INTRODUCTION

Cost studies estimate that Pt-based catalysts involve almost half of the entire polymer electrolyte fuel cell (PEFC) stack cost and as much as 20% of the overall system cost [3]. Since Pt is a precious metal, its cost will not benefit from economies of scale and is subject to volatile price fluctuations and monopolized global distributions. Reducing, or ideally replacing, expensive Pt and/or Pt-alloy catalysts in PEFC systems is highly desirable and has been a major focus of research and development efforts in fuel cell electrocatalysis. Owing to the inherently sluggish ORR occurring at the fuel cell cathode, higher Pt content is required at the cathode than at the anode. Successful development of non-PGM catalysts for ORR would provide the most significant economic advantage in PEFC systems. However, hindering the successful elimination of Pt cathode catalysts in PEFC systems is the lack of non-PGM catalysts that can provide sufficiently high ORR activity and, especially, the durability under the conditions of fuel cell cathode operation.

APPROACH

In this research project, we intend to accomplish major advancements in non-PGM cathode technology through the development and implementation of novel materials and concepts. Our catalyst development effort has concentrated on novel synthesis methods, including high temperature catalyst synthesis using multiple nitrogen-containing precursors, advanced carbon supports, and in an earlier stage of the project, non-pyrolyzed phthalocyanine-derived catalysts, as well as metal-free catalysts based on nitrogen-doped carbon nanostructures. Comprehensive testing of materials, including initial performance screening by in situ electrochemical techniques and ex situ characterization to assess catalyst activity and durability, identify catalytic sites and validate fuel cell performance of the most promising materials, represents a substantial fraction of the efforts.

The use of non-PGM ORR catalysts results in cathodes with increased thickness compared to that of Pt-based cathodes. Thus, significant effort is required to address the resulting electrode design challenges. Key issues include oxygen mass transport, proton conductivity and prevention of catalyst layer flooding. Our research has focused on the validation of existing General Motors electrode model for non-PGM electrodes and parameter approximation using in situ microstructured electrode scaffold (MES) diagnostics. Electrode optimization is based on the insight obtained from the modeling, nanoscale XRT imaging, and advanced microscopy analysis. In parallel to the catalyst and electrode development components of this project, MEA fabrication, optimization and scale-up are being performed to obtain a 50 cm^2 (or larger, if needed) MEA with the best performing materials for independent testing and evaluation at a DOE-approved facility.

RESULTS

Achieved fuel cell voltage of 0.86 V (iR-free) at 0.044 A cm^{-2} in H_2/O_2 fuel cell testing. An advanced non-PGM catalyst developed according to LANL's dual nitrogen precursor approach was synthesized, optimized, and tested for fuel cell performance. A fuel cell operating with advanced CM-PANI-Fe-C catalyst achieved a voltage of 0.86 V (*iR*-free) at 0.044 A cm^{-2} in H_2/O_2 MEA testing at 80°C (Figure 1a). This fuel cell voltage is only 0.01 V below the 2020 target voltage of 0.87 V (see Table 1 above). Further, the advanced CM-PANI-Fe-C catalyst demonstrated superior durability with potential loss at $E_{½}$ ~30 mV after 30,000 cycles between 0.2 V and 1.0 V in N_2-saturated electrolyte. This durability was accompanied by less than 2% H_2O_2 yield in the entire ORR potential range (Figure 1b). These results achieve and exceed the June 2015 durability and selectivity targets.

DFT modeling of most active reported structure to date, $FeCoN_5(OH)$, based on thermodynamic stability arguments. Calculation of active site structures was performed using thermodynamic limiting potential, U_L, with a computational hydrogen electrode and DFT of ORR intermediate binding energies. In the developed model, *OH ligand spontaneously formed in water-bearing environments, modifying the active site structure and thus improving predicted ORR activity. Higher limiting potentials were obtained from bi-metallic sites. U_L for $Fe_2N_5(OH)$ was calculated to be 0.72 V while a mixed-metal active site structure, $FeCoN_5(OH)$, resulted in

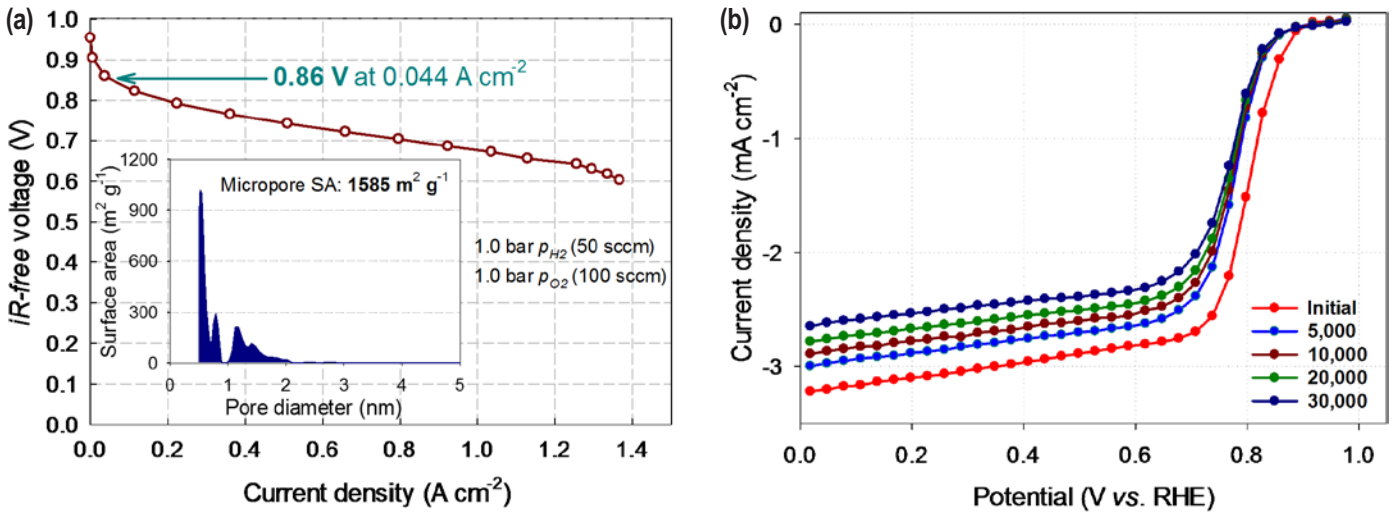

FIGURE 1. (a) Fuel cell performance of advanced CM-PANI-Fe-C non-PGM catalyst demonstrating fuel cell voltage of 0.86 V (*iR*-free) at 0.044 A cm^{-2} in H_2-O_2. Inset: Pore size distribution data for catalyst tested. Anode: 0.2 mg_{Pt} cm^{-2} Pt/C H_2, 50 sccm, 1.0 bar H_2 partial pressure; cathode: ~4.0 mg cm^{-2} air, 100 sccm, 1.0 bar air partial pressure; membrane: Nafion® 117; cell size: 5 cm^2. (b) RDE durability cycling of advanced CM-PANI-Fe-C catalyst demonstrating potential loss ~30 mV $E_{½}$ after 30,000 cycles in N_2-saturated electrolyte. Inset: cyclic voltammogram showing no surface area change after durability cycling. RRDE: 0.5 M H_2SO_4; 900 rpm; 25ºC; Hg/$HgSO_4$ (0.5 M H_2SO_4) reference electrode; graphite counter electrode; steady-state potential program: 30 mV steps, 30 s/step; cyclic voltammetry: 0.5 M H_2SO_4; 0 rpm; 25ºC; N_2-saturated solution; 20 mV/s. Durability cycling: 0.2–1.0 V; N_2-saturated solution; 200 mV/s.

the most active structure reported to date from computational studies: 0.80 V.

Validation of surface-probe XAS approach with theoretical modeling for identification of active site structures. In situ surface-sensitive XAS/Δμ-X-ray absorption near edge spectroscopy (XANES) analytical technique was utilized to monitor changes in Fe-N_x-O species while under fuel cell and RDE operation. Experimental Δμ results obtained are in good agreement with theoretical DFT-derived model structures: Fe_2N_6, FeN_4, and FeN_5 (Figure 2a). Monitoring of Δμ changes after potential cycling under inert (N_2) and reaction (air) conditions indicates that Fe-N_x centers are likely responsible for ORR activity (Figure 2b).

Separate mapping of catalyst and Nafion® distribution and validation of fuel cell cathode model. The advanced non-PGM catalysts prepared from multiple nitrogen precursors were integrated into electrodes containing Nafion® ionomer and studied using nano-XRT for the development of microstructurally-consistent cathode model (Figure 3a). Staining of Nafion® with Cs^+ allowed for the identification of the distribution of the ionomer layer in thick cathodes to separately map catalyst (Zernike phase contrast) and Nafion®

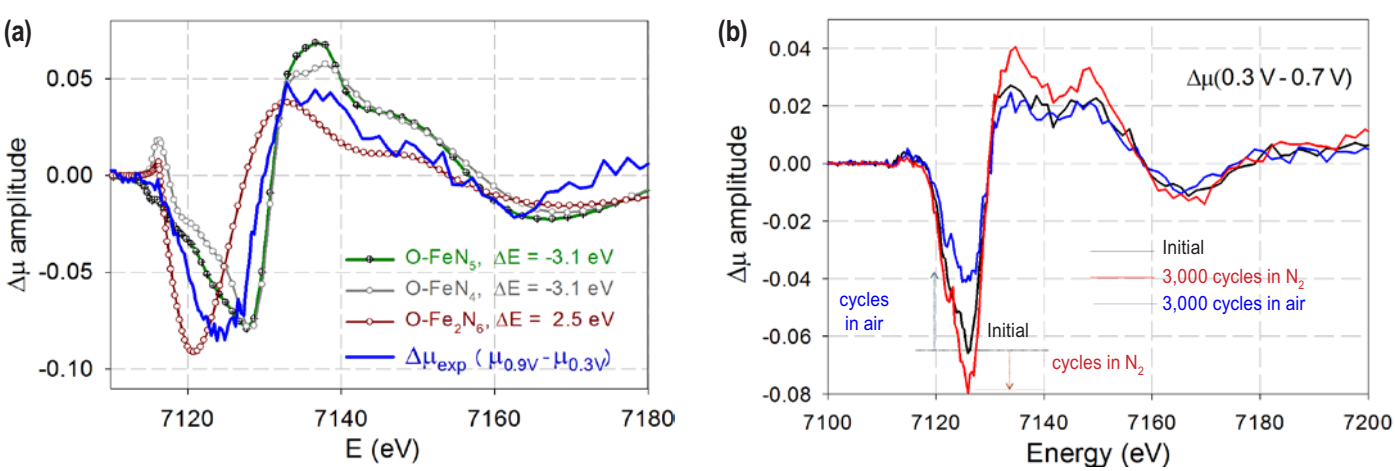

FIGURE 2. (a) Experimental Δμ data showing good agreement with theoretical DFT-derived Fe-N_x structures: FeN_5, FeN_4, Fe_2N_6. (b) Experimental Δμ data as a function of cycling suggesting Fe-N_x centers are likely responsible for ORR activity. Cycling: 3,000 cycles, H_2/N_2 and H_2/air.

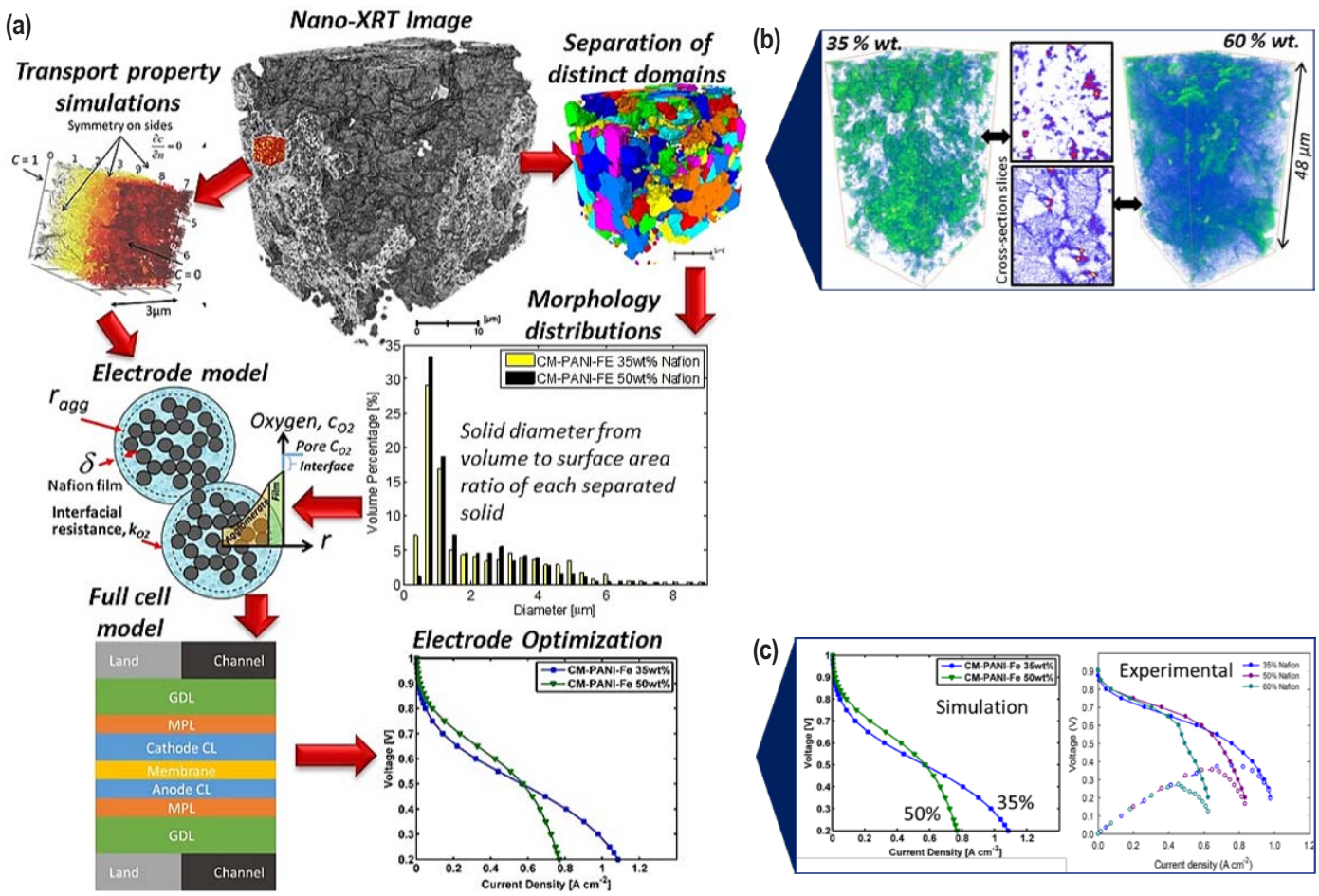

FIGURE 3. (a) Microstructurally consistent model framework showing the process involved in the development of a cathode model based on morphological property distribution inputs and transport property simulations. (b) 3D Nafion® density maps obtained from Cs^+ staining of Nafion® for two different loadings, 35 wt% and 60 wt%. (c) Simulated and experimental H_2–air fuel cell polarization plots validating cathode model obtained from morphological parameters observed and calculated from nano-XRT for various Nafion® loadings.

(absorption contrast) at up to 50 nm resolution (Figure 3b). At a lower Nafion® loading (35 wt%), the ionomer forms clumps with low infiltration into the dense pores of the catalyst. While at higher Nafion® loadings (50–60 wt%), infiltrated ionomer forms thick films on the surface.

A cathode model was developed based on microstructurally consistent morphological properties obtained from nano-XRT imaging along with transport property simulations. This model was validated against H_2–air fuel cell experiments at varying Nafion® loading (Figure 3c). A key finding of the two-phase model is a notable performance improvement obtained by mitigation of liquid water flooding of thicker electrodes. Results suggest that carbon agglomerate size distribution has a significant impact on fuel cell performance, proving predictions from single diameter model insufficient. The combination of mapping of catalyst-Nafion® distribution along with fuel cell performance at varying ionomer loading suggests that an optimal dispersion of ionomer within carbon-rich catalyst in the cathode is an essential strategy for increasing catalyst utilization, thereby significantly improving catalyst performance.

Microstructured Electrode Scaffold (MES) for direct ORR and conductivity measurements. Figure 4a displays the MES schematic used for direct conductivity measurement during PEFC operation. The local ORR rate and potential distribution of Nafion® were measured as a function of distance from the membrane for three different relative humidity (RH) conditions: 50%, 80%, 140%. An RH of 50% showed limited proton transport with the ORR primarily occurring near the proton exchange membrane. On the other hand, 140% RH showed increased proton conductivity as a result of water production. Further, a large *iR*-drop due to water accumulation gave rise to the second ohmic slope, evident in catalyst-coated membrane (CCM) studies with high Nafion® loading and consistent with modeling studies. ORR at 140% RH occurs mainly near the gas diffusion layer (Figure 4b).

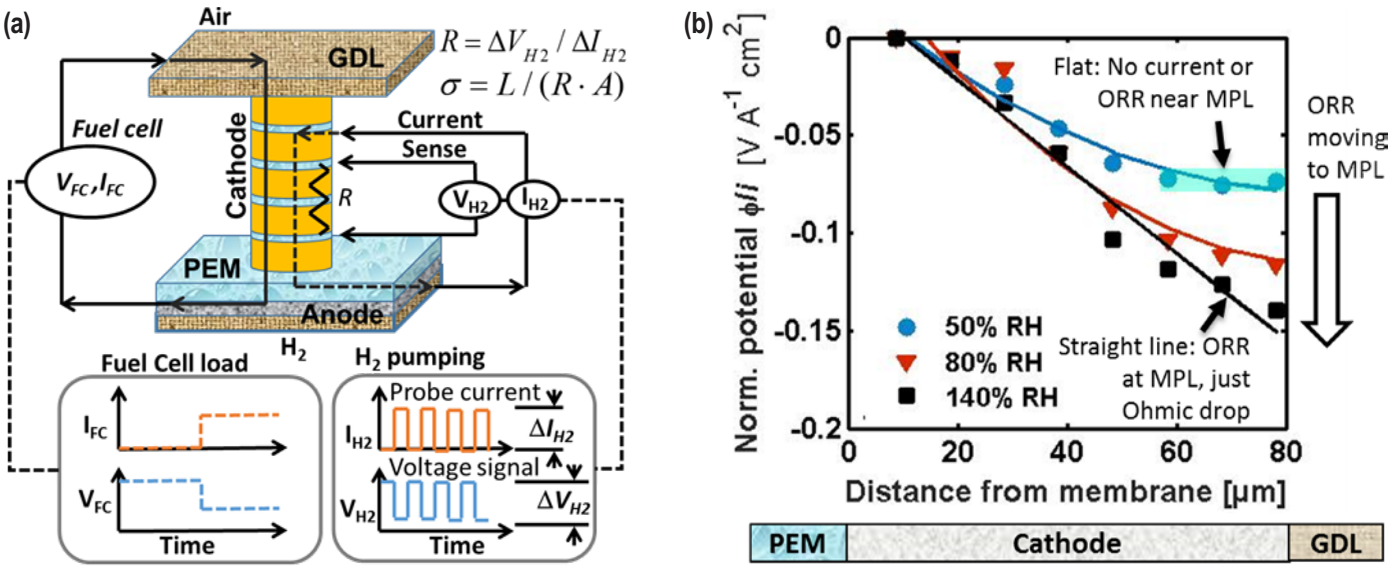

FIGURE 4. (a) Schematic of MES used for direct conductivity measurement during PEFC operation. (b) Potential distribution of Nafion® as a function of distance from membrane for three different RH conditions: 50%, 80%, 140%. An RH of 50% shows limited proton transport, while 140% RH shows increased proton conductivity as a result of water production. The large *iR*-drop observed for 140% RH is due to water accumulation giving rise to the second Ohmic slope and validating the model.

Electron microscopy analysis of state-of-the-art LANL catalysts and electrodes. Advanced scanning electron microscopy, transmission electron microscopy, and scanning transmission electron microscopy were performed to study the advanced CM-PANI-Fe-C catalyst material in order to provide insight into the structure of high-performance catalysts with favorable micro- and meso-porosity. Figure 5 shows the CM-PANI-Fe-C morphology consisting of fibrous carbonaceous agglomerates (randomly oriented, intertwined graphitic domains) and layered graphene sheets. Presence of graphene sheets are mostly associated with Fe/FeS particles. Annular dark-field-STEM imaging in combination with high resolution electron energy loss spectroscopy analysis was used to identify the presence of Fe atoms dispersed on the surface of few-layer graphene sheets. These Fe atoms were highly mobile under the electron beam.

CONCLUSIONS

- Continued development of the high surface area multiple nitrogen precursor CM-PANI-Fe-C catalyst led to notable improvement in H_2–air performance resulting in a fuel cell voltage of 0.86 V obtained at 0.044 A cm^{-2} (nearing the proposed 2020 target of 0.87 V).
- ORR selectivity and durability targets for June 2015 were achieved and exceeded with advanced CM-PANI-Fe-C catalyst:
  - Potential loss of ~30 mV at $E_{½}$ after 30,000 cycles between 0.2 V and 1.0 V.
  - H_2O_2 yield of less than 2% across the entire potential range.
- Theoretical DFT modeling studies found that multi-metal Fe_2N_5 sites are likely the key moiety, in agreement with NRVS-$NO_{(g)}$ and XAS/Δμ-XANES probing.
- A cathode model was developed using morphological property distribution inputs from nano-XRT imaging and transport property simulations. The model was validated against experimental H_2–air fuel cell studies with different Nafion® loadings.

FUTURE DIRECTIONS

- Catalyst Development:
  - Completion of remaining activity/durability catalyst performance targets
  - Enhancement of the ORR activity of Fe-free catalysts
  - Further development of two-nitrogen precursor catalysts, focusing on activity and durability
- Active Site and Durability Studies:
  - In situ XAS studies in combination with DFT-FEFF calculations for active site determination
  - Completion of the Mössbauer study of active sites using molecular probes
  - Determination of corrosion rate measurements; comparison with Pt/C catalysts
- Electrode Design and Modeling:

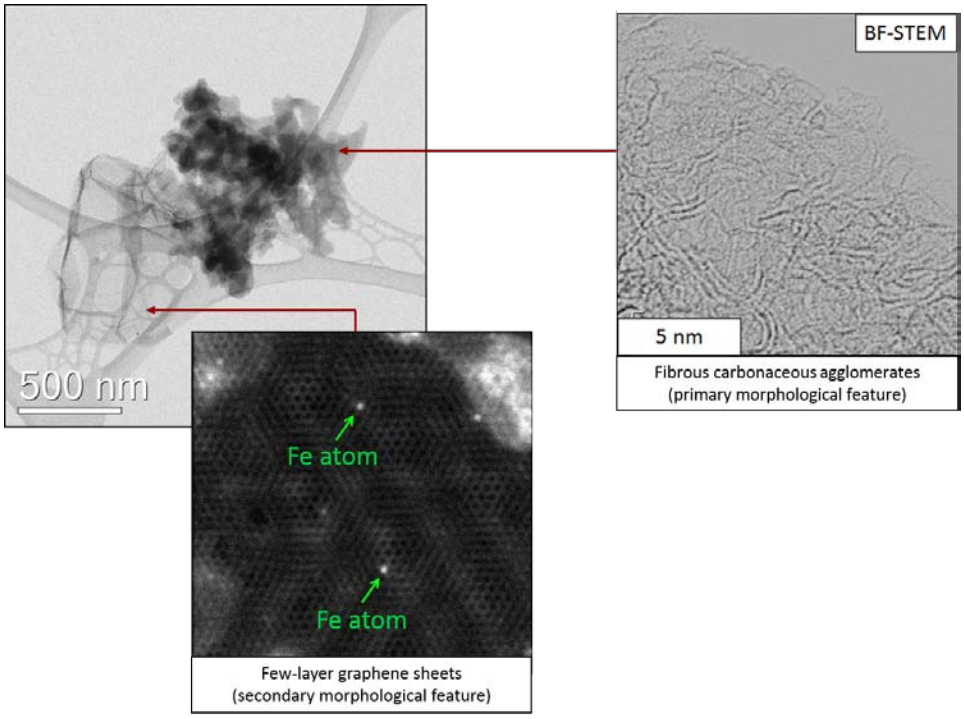

FIGURE 5. Microscopy studies for advanced CM-PANI-Fe-C catalyst showing two morphological features. The primary feature consists of fibrous carbonaceous agglomerates which are randomly oriented and have an intertwined graphitic domain. The secondary morphological feature consists of few-layer graphene sheets with associated Fe/FeS particles and Fe atoms dispersed atop graphene.

  - Electrode structure and modeling analysis of scaled IRD and General Motors electrodes using nano-XRT
  - Detailed modeling of MES system for model improvement; parametric studies of electrode formulation by MES
- MEA Optimization and Fabrication:
  - Completion of electrode optimization study
  - Optimization of the first generation spray-coated MEAs
  - Fabrication and testing of 50 cm^2 MEAs

SPECIAL RECOGNITIONS & AWARDS/ PATENTS ISSUED

1. Piotr Zelenay awarded Los Alamos National Laboratory Fellows Prize "for longstanding contributions to the understanding of non-precious metal electrocatalysts for fuel cells," February 2015.

2. Piotr Zelenay awarded Fellowship of the Electrochemical Society "for major contributions in the development of materials and concepts for polymer electrolyte fuel cells," October 2014.

FY 2015 PUBLICATIONS

1. H.T. Chung and P. Zelenay, "A Simple Synthesis of Nitrogen-Doped Carbon Micro- and Nanotubes," *Chem. Comm*., DOI: 10.1039/C5CC04621A (2015).

2. Q. Jia, N. Ramaswamy, H. Hafiz, U. Tylus, K. Strickland, G. Wu, B. Barbiellini, A. Bansil, E.F. Holby, P. Zelenay, and S. Mukerjee, "Dynamic Nature of Active Sites in Iron-based Catalysts during Electrocatalysis," *Nat. Chem*. submitted.

3. U. Martinez, G.M. Purdy, E.F. Holby, K. Artyushkova, J.H. Dumont, A. Singh, N.H. Mack, P. Atanassov, D.A. Cullen, K.L. Moore, M. Chhowalla, P. Zelenay, A.M. Dattelbaum, A.D. Mohite, and G. Gupta, "Critical Role of the Removal of Intercalated Water for Electrocatalytically Active Graphitic Systems," *Nat. Chem*., submitted.

4. L. Chen, G. Wu, E.F. Holby, P. Zelenay, W. Tao, and Q. Kang, "Lattice Boltzmann Investigation of Reactive Transport in Cathode Catalyst Layers of Proton Exchange Membrane Fuel Cells," *Electrochim. Acta*, **158**, 175–186 (2015).

5. D. Higgins, F. Hassan, M. Seo, J. Choi, A. Hoque, D. Lee, and Z. Chen, "Shape-Controlled Octahedral Cobalt Disulfide Nanoparticles Supported on Nitrogen and Sulfur-Doped Graphene/ Carbon Nanotube Composites for Oxygen Reduction in Acidic Electrolyte," *J. Mat. Chem. A* **3**, 6340–6350 (2015).

6. E.F. Holby, G. Wu, P. Zelenay, and C.D. Taylor, "Structure of Fe-N_x-C defects in Oxygen Reduction Reaction Catalysts from First Principles Modeling," *J. Phys. Chem. C*, **118** (26) 14388–14393 (2014).

7. S. Komini Babu, H. Chung, G. Wu, P. Zelenay, and S. Litster, "Modeling Hierarchical Non-Precious Metal Catalyst Cathodes for PEFCs Using Multi-Scale X-ray CT Imaging," *ECS Trans.*, **64** (3), 281–192 (2014).

8. U. Martinez, T.L. Williamson, K. Artyushkova, N.H. Mack, G.M. Purdy, J.H. Dumont, D. Kelly, W. Gao, A. M. Dattelbaum, A. Mohite, G. Gupta, and P. Zelenay, "Thin-Film Non-Precious Metal Model Catalysts for Oxygen Reduction Reaction," *ECS Trans.*, **64** (3), 293–301 (2014).

9. Q. Li, G. Wu, N.H. Mack, H.T. Chung, P. Xu, H.-L. Wang, S. Ma, and P. Zelenay, "Phosphate-Tolerant Oxygen Reduction Catalysts," *ACS Catal.*, **4** (9), 3193–3200 (2014).

10. P. Zelenay, H.T. Chung, E.F. Holby, C.D. Taylor, and G. Wu, "Carbon Composite Non-Precious Metal Catalysts for Oxygen Reduction in Electrochemical Energy Conversion," *Prepr. Pap.-Am. Chem. Soc., Div. Fuel Chem.*, accepted (2014).

11. R. Mukundan, D. Spernjak, G. Wu, D. Hussey, D. Jacobson, A. Steinbach, R. Borup, and P. Zelenay, "Visualizing Water in Non-Precious Metal Catalyst-based Polymer Electrolyte Fuel Cells Using Neutron Imaging," *Prepr. Pap.-Am. Chem. Soc., Div. Energy Fuels*, accepted, (2014).

12. E.T. Holby, G. Wu, P. Zelenay, and C.D. Taylor, "Structure of Fe-N_x-C Defects in Oxygen Reduction Reaction Catalysts from First Principles Modeling," *J. Phys. Chem. C*, **118**, 14388–14393 (2014).

13. H.T. Chung, G. Wu, Q. Li, and P. Zelenay, "Role of Two Carbon Phases in Oxygen Reduction Reaction on the Co-PPy-C Catalyst," *Int. J. Hydrogen Energy*, **39**, 15887–15893 (2014).

14. D.C. Higgins, G. Wu, H.T Chung, U. Martinez, S. Ma, Z. Chen, and P. Zelenay, "Manganese-Based Non-Precious Metal Catalysts for Oxygen Reduction in Acidic Media," *ECS Trans.*, **61** (31) 35–42 (2014).

15. M. Seo, D. Higgins, G. Jiang, S. Choi, B. Han, and Z. Chen, "Theoretical Insight into Highly Durable Iron Phthalocyanine Derived Non-Precious Catalysts for Oxygen Reduction Reactions," *J. Mat. Chem. A* **2**, 19707–19616 (2014).

16. P. Zamani, D. Higgins, F. Hassan, G. Jiang, J. Wu, S. Abureden, and Z. Chen, "Electrospun Iron–Polyaniline–Polyacrylonitrile Derived Nanofibers as Non–Precious Oxygen Reduction Reaction Catalysts for PEM Fuel Cells," *Electrochim. Acta*, **139**, 111–116 (2014).

FY 2015 PRESENTATIONS

1. S. Litster, "Fuel cell and battery electrodes: Advanced characterization and new electrode concepts," University of Victoria, Victoria, Canada, June 29 (2015) – *invited lecture*.

2. S. Litster, "Nano-scale X-ray computed tomography applied to fuel cell and battery electrode characterization and optimization," Naval Research Laboratory, Washington, DC, June 11 (2015) – *invited lecture*.

3. D. Higgins, H. Chung, U. Tylus, Z. Chen, and P. Zelenay, "Combined Nitrogen Precursor Approach to Develop Cobalt-Based Non-Precious Catalysts for Polymer Electrolyte Fuel Cell Cathodes," 227th Meeting of the Electrochemical Society, Chicago, Illinois, USA, May 24–28 (2015).

4. J.H. Dumont, U. Martinez, A. Mohite, G.M. Purdy, A.M. Dattelbaum, P. Atanassov, and P. Zelenay, G. Gupta, "Graphene Oxide Based Non Precious Metal Catalysts for Oxygen Reduction Reaction in Alkaline Media," 227th Meeting of the Electrochemical Society, Chicago, Illinois, USA, May 24–28 (2015).

5. H. Chung, D. Higgins, D. Kim, G. Wu, U. Tylus, K. More, D. Cullen, P. Zelenay, "An Approach for Highly Porous Non-Precious Metal Catalyst Synthesis for Polymer Electrolyte Fuel Cell Cathodes," 227th Meeting of the Electrochemical Society, Chicago, Illinois, USA, May 24–28 (2015).

6. U. Martinez, T. Williamson, K. Artyushkova, M. Hoffbauer, G. Purdy, J. Dumont, A. Dattelbaum, A. Mohite, G. Gupta, and P. Zelenay, "Model Non-Precious Metal Catalysts for Oxygen Reduction Reaction: A Bottom-up Approach," 227th Meeting of the Electrochemical Society, Chicago, Illinois, USA, May 24–28 (2015).

7. U. Tylus, H. Chung, D. Higgins, D. Myers, D. Nordlund, C. Segre, and P. Zelenay, "Study of Non-PGM ORR Catalyst Degradation Using Synchrotron Techniques," 227th Meeting of the Electrochemical Society, Chicago, Illinois, USA, May 24–28 (2015).

8. S. Litster, "Nano-scale X-ray computed tomography applied to fuel cell and battery electrode characterization and optimization," National Institute of Advanced Industrial Science and Technology (AIST) Kansai, Osaka, Japan, May 12 (2015) – *invited lecture*.

9. S. Litster, "Nano-scale X-ray computed tomography applied to fuel cell and battery electrode characterization and optimization," Chemical Engineering, Kyoto University, Kyoto, Japan, May 11 (2015) – *invited lecture*.

10. H. Chung, E. Holby, U. Martinez, G. Purdy, J. Dumont, U. Tylus, D. Higgins, G. Gupta, A. Dattelbaum, Z. Chen, and P. Zelenay, "Oxygen Reduction Electrocatalysts for Fuel Cell Applications," Materials Research Society Meeting & Exhibit, San Francisco, California, April 6–10 (2015) – *invited lecture*.

11. P. Zelenay, "A Few Highlights from Fuel Cell Electrocatalysis Research at Los Alamos," CARISMA 2014 - International Fuel Cell Conference, Cape Town, South Africa, December 1–3 (2014) – *invited lecture*.

12. G. Wu, H.T. Chung, E.F. Holby, and P. Zelenay, "Oxygen Reduction on Non-Precious Metal Fuel Cell Catalysts," Henan Normal University, Xinxiang, China, November 5 (2014) – *invited plenary lecture*.

13. P. Zelenay, "Electrocatalysts for Fuel Cell Applications," International Conference on Energy Science and Technology (EEST2014), Shanghai, China, November 1–3 (2014) – *invited plenary lecture*.

14. E.F. Holby, C.D. Taylor, and P. Zelenay, "Modeling Non-Precious Metal Catalyst Structures for Oxygen Reduction," International Symposium on Electrocatalysis: Explorations of the

Volcano Landscape, Whistler, British Columbia, Canada, October 26–29 (2014).

15. P. Zelenay, "Oxygen Reduction on Non-Precious Metal Electrocatalysts: Accomplishments and Challenges," International Symposium on Electrocatalysis: Explorations of the Volcano Landscape, Whistler, British Columbia, Canada, October 26–29 (2014) – *invited keynote lecture.*

16. U. Martinez, E.F. Holby, G.M. Purdy, G. Gupta, A. Mohite, G. Wu, H.T. Chung, A.M. Dattelbaum, and P. Zelenay, "Model Systems and Modeling of Non-precious Metal Oxygen Reduction Catalysts," 226th Meeting of the Electrochemical Society, Cancun, Mexico, October 5–10 (2014) – *invited lecture.*

17. U. Martinez, T.L. Williamson, G.M. Purdy, J.H. Dumont, N.H. Mack, A.M. Dattelbaum, A. Mohite, G. Gupta, and P. Zelenay, "Thin-Film Non-Precious Metal Model Catalysts for Oxygen Reduction Reaction," 226th Meeting of the Electrochemical Society, Cancun, Mexico, October 5–10 (2014).

18. S.K. Babu, H.T. Chung, G. Wu, P. Zelenay, and S. Litster, "Modeling Hierarchical Non-Precious Metal Catalyst Cathodes for PEFCs using Multi-Scale X-ray CT Imaging Data," 226th Meeting of the Electrochemical Society, Cancun, Mexico, October 5–10 (2014).

19. U. Martinez, A. Mohite, G. M. Purdy, A. M. Dattelbaum, P. Zelenay, and G. Gupta, "Highly Tunable and Ordered Graphene-Oxide-Based Materials for Energy Applications," 226th Meeting of the Electrochemical Society, Cancun, Mexico, October 5–10 (2014).

20. P. Zelenay, "Non-Precious Metal Electrocatalysts: Accomplishments and Challenges," "226th Meeting of the Electrochemical Society, Cancun, Mexico, October 5–10 (2014) – *invited lecture*.

21. R. Borup, R. Mukundan, D. Spernjak, G. Wu, A. Steinbach, P. Zelenay, D. Hussey, and D. Jacobson, "Neutron Imaging to Optimize PEM Fuel Cells Performance," 10th World Conference on Neutron Radiography (WCNR-10), Grindelwald, Switzerland, October 5–10 (2014).

22. P. Zelenay, "Oxygen Reduction on Non-Precious Metal Fuel Cell Electrocatalysts," Department of Chemistry, University of Indiana, Bloomington, Indiana, September 23 (2014) – *invited lecture.*

23. P. Zelenay, H.T. Chung, E.F. Holby, C.D. Taylor, and G. Wu, "Carbon Composite Non-Precious Metal Catalysts for Oxygen Reduction in Electrochemical Energy Conversion," 248th American Chemical Society Meeting and Exposition, San Francisco, California, August 10–14 (2014).

24. R. Mukundan, D. Spernjak, G. Wu, D. Hussey, D. Jacobson, A. Steinbach, R. Borup and P. Zelenay, "Visualizing Water in Non-Precious Metal Catalyst-based Polymer Electrolyte Fuel Cells Using Neutron Imaging," 248th American Chemical Society Meeting and Exposition, San Francisco, California, August 10–14 (2014). (invited lecture).

25. S. Komini Babu, H.T. Chung, G. Wu, P. Zelenay, and S. Litster, "Modeling Hierarchical Non-Precious Metal Catalyst Cathodes for PEFCs using Multi-Scale X-Ray CT Imaging," Gordon Research Conference on Fuel Cells, Smithfield, Rhode Island, August 3–8 (2014) –*received the best student poster award.*

26. P. Zelenay, "A Few Highlights from Fuel Cell Electrocatalysis Research at Los Alamos," International Symposium on Clean Energy from Ethanol, ISCEE 2014, Rzeszow, Poland, July 28–31 (2014) – *invited keynote lecture.*

27. P. Zelenay, "Modern Fuel Cell Electrocatalysis," AGH University of Technology, Krakow, Poland, July 23 (2014) – *invited lecture*.

28. P. Zelenay, "Electrocatalysis in Fuel Cells," Industrial Chemistry Research Institute, Warsaw, Poland, July 22 (2014) – *invited lecture.*

REFERENCES

1. *Multi-Year Research, Development and Demonstration Plan: Section 3.4 Fuel Cells*, Fuel Cell Technologies Office, 2011. http://www1.eere.energy.gov/hydrogenandfuelcells/mypp/pdfs/fuel_cells.pdf

2. H. Gasteiger et al., *Appl. Catal. B-Environ.*, **56**, 9–35, 2005.

3. B. James et al., DTI, Inc., 2010 DOE Hydrogen Program Review, Washington, DC, June 9, 2010.

V.A.8 High-Throughput Synthesis, ORR Activity Modeling, and Testing of non-PGM PEMFC Cathode Catalysts

Deborah J. Myers (Primary Contact),
Xiaoping Wang, Sheldon Lee, Magali Ferrandon,
Nancy N. Kariuki, and Theodore Krause
Argonne National Laboratory (ANL)
9700 S. Cass Avenue
Lemont, IL 60439
Phone: (630) 252-4261
Email: dmyers@anl.gov

DOE Manager
Dimitrios Papageorgopolous
Phone: (202) 586-5463
Email: Dimitrios.Papageorgopoulos@ee.doe.gov

Collaborators
Piotr Zelenay, Hoon Chung, Ulises Martinez, Edward Holby, and Samrat Choudhury, Los Alamos National Laboratory (LANL), Los Alamos, NM

Project Start Date: August 14, 2014
Project End Date: September 30, 2015

Overall Objectives

- Accelerate the development of high activity and stable non-platinum group metal (PGM) cathode catalysts for proton exchange membrane fuel cells (PEMFCs)
- Develop tools for the rapid synthesis, fabrication, composition characterization, and activity and durability screening of non-PGM PEMFC cathode catalysts
- Identify a non-PGM cathode catalyst and synthesis conditions for catalysts in the polyaniline-Fe,(Co)-carbon (PANI-Fe,(Co)-C) class with higher oxygen reduction reaction (ORR) activity than the current best-in-class of PANI-Fe-C pyrolyzed at 900°C
- Achieve a current density of >200 mA/cm^2 at 0.8 $V_{iR\text{-}free}$ for a fuel cell with a PANI-Fe,(Co)-C cathode catalyst

Fiscal Year (FY) 2015 Objectives

- One year project. See Overall Objectives.

Technical Barriers

This project addresses the following technical barriers from the Fuel Cell section of the Fuel Cell Technologies Office (FCTO) Multi-Year Research, Development, and Demonstration (MYRDD) Plan:

(A) Durability

(B) Cost

(C) Performance

Technical Targets

The DOE technical targets relating to this project are shown in Table 1.

TABLE 1. Technical Targets from FCTO MYRDD Plan

Barrier	Target
C. Performance	Catalyst activity in H_2/O_2 at 0.044 A cm^{-2} (80°C): ≥0.87 V (iR-free)
B. Cost	<\$7/kW$_e$ MEA cost target
A. Durability	<40% performance loss at 0.80 A cm^{-2} after 30,000 accelerated stress test cycles in nitrogen

MEA – membrane electrode assembly

FY 2015 Accomplishments

- Developed a high-throughput (HT) method for synthesizing and characterizing high surface area (HSA) non-PGM ORR catalysts
- Applied a commercial combinatorial method/cell, a multi-electrode channel flow double electrode (m-CFDE) cell, to screening the ORR activity of HSA catalysts simultaneously; the ORR activity trends from the m-CFDE cell for the HT-synthesized catalysts were identical to those from rotating disk electrode (RDE) tests of large, single batches of catalysts, validating the HT methods.
- Designed, built, and utilized an m-CFDE cell which has improved performance and ease of use compared to the commercial m-CFDE
- Achieved ORR half-wave potential agreements between m-CFDE and RDE results of 9 mV for commercial Pt/C and 80 mV for PANI-Fe$_4$Co-C catalyst
- Identified a PANI-Fe,Co-C catalyst with higher ORR activity than the previous best catalyst in this class (PANI-Fe-C, pyrolyzed at 900°C) and synthesized sufficient quantities of this catalyst for MEA tests
- Developed a density functional theory (DFT) model to screen non-PGM ORR activity and stability, screened 22 possible sites, and down-selected the eight most probable sites based on activity

✧ ✧ ✧ ✧ ✧

INTRODUCTION

The goal of this project was to accelerate the development of high activity and stable non-PGM cathode catalysts for PEMFCs. The means for achieving this overall goal and a secondary goal of the project was to develop generally applicable methods for the rapid throughput synthesis of non-PGM catalysts and the rapid throughput screening of ORR activity of catalysts in an aqueous environment. The non-PGM catalyst class studied was the iron and iron-cobalt-containing materials derived from a composite of the metal salts, polyaniline (carbon, nitrogen-containing polymer), and HSA carbon. This class of material was first discovered in the LANL-led project entitled "Advanced Cathode Catalysts" [1]. In that project, it was determined that variables such as metal, polymer, and carbon content, as well as the temperature and atmosphere in which the composites are pyrolyzed, are important in determining the activity and activity stability of the resulting catalysts. Changing these variables and testing their effects on the resulting catalyst properties is a very time consuming process and only a limited portion of the composite composition and temperature space have been explored.

Another aspect of the project was the development of computational means for determining the energetically most favored active sites in Fe,Co-carbon-nitrogen catalysts by calculating formation energies and computationally screening the ORR activity of potential activity sites.

APPROACH

The overall approach of the project was to develop and utilize the capability for HT synthesis and ORR activity testing of non-PGM PEMFC cathode catalysts, with a specific application of the approach to rapidly explore the compositional and temperature space for the PANI-Fe,Co-C class of catalysts. This approach involved the rapid throughput (1) synthesis of the precursor composites; (2) pyrolysis of catalyst precursors in a multi-sample tube furnace; (3) physical and chemical characterization of catalysts using multi-sample, automated X-ray diffraction (XRD) and X-ray fluorescence (XRF); and (4) screening of the catalysts' ORR and ORR activity stability in a hydrodynamic aqueous cell. The approach also included determining the validity of the combinatorial hydrodynamic aqueous cell using RDE, developing the capability for high-throughput screening of possible Fe-N-C active site moieties for activity and stability using DFT-based descriptors, and scaling up the best base metal-PANI-C catalyst for MEA fabrication and testing. The computational aspect of this project also involved calculating the formation energies of potential sites collected from the literature and calculating a structure predominance diagram as a function of N and Fe/Co chemical potentials (representing varied synthesis conditions).

RESULTS

The synthesis of PANI-Fe,Co-C non-PGM PEMFC cathode catalysts involves the following steps: (1) polymerizing aniline in the presence of dissolved cobalt and iron and HSA carbon, (2) driving off the solvent, (3) grinding the precipitate, (4) pyrolyzing the precipitate in an inert atmosphere at temperatures between 800°C and 1,000°C, (5) acid treating the powder at an elevated temperature, (6) removing the acid from the powder, and (7) pyrolyzing the powder at the same temperature as the first pyrolysis [1]. In this project, the single batch, single composition procedure developed by Zelenay et al. [1] was adapted into an HT fabrication process, where feasible. Methods were developed and utilized for synthesizing the PANI-Fe,Co-C composite catalyst precursor with nine different Fe to Co ratios using a robotic platform (CM3, FreeSlate Inc.) and for pyrolyzing, acid treating, and rinsing these samples in an HT manner. For example, the acid treatment was performed using a multi-port reflux system and the catalysts powders were separated from the supernatant acid using a multi-sample centrifuge rather than filtering. The samples were pyrolyzed at five temperatures between 800°C and 1,000°C to yield 45 different catalysts. The phase compositions of the catalysts were determined by a multi-sample HT XRD after the first pyrolysis step and after the second pyrolysis step. The Fe and Co weight percentages in the catalysts after the second pyrolysis were also determined by XRF.

The ORR activities of these catalysts were screened in a high throughput fashion using two multi-electrode channel flow double electrode cells, one purchased from Eiwa Corporation and the other designed and built at ANL. Both of these cells allow ORR activity testing of four catalyst samples simultaneously in a hydrodynamic aqueous environment with operating principles similar to those of RDE. The "double electrode" refers to an upstream glassy carbon electrode on which catalyst-ionomer inks are deposited and a downstream Pt electrode on which reaction products (e.g., peroxide) can be detected similar to the ring electrode in rotating ring disc electrode measurements. Figure 1 shows pictures of the Eiwa and ANL cells. The most significant difference between the two cells is that the Eiwa cell's electrodes are permanently imbedded in the bottom plate of the cell, whereas in the ANL cell each set of glassy carbon-platinum electrodes is mounted in a removal electrode "plug." The removable plugs facilitate the quick changing of the catalyst on the glassy carbon electrode and also replacement of damaged electrodes.

The validity of the two cells in providing data similar or equivalent to that obtained using RDE was first tested using a commercial Pt/C catalyst which was extensively tested in the project FC111 "Best Practices and Benchmark Activities for ORR Measurements by the Rotating Disk Electrode Technique" [2]. As shown in Figure 2, the half-

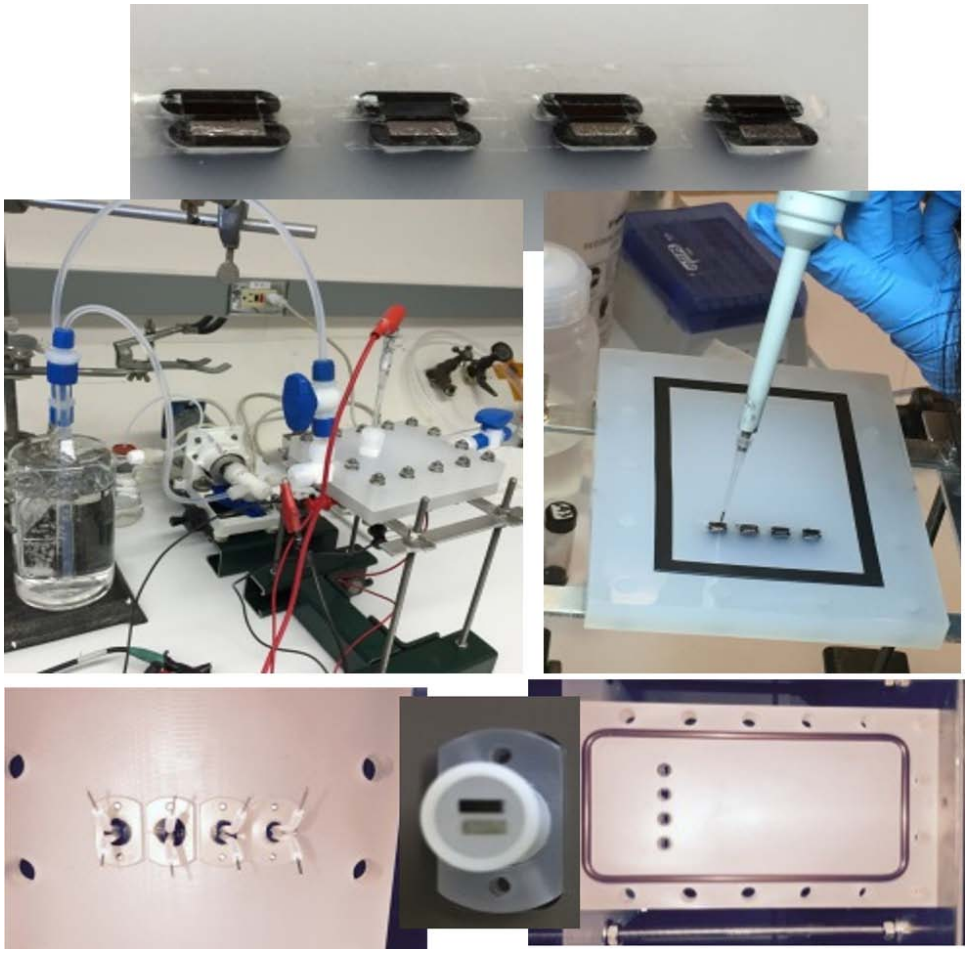

FIGURE 1. Pictures of the Eiwa m-CFDE, cell showing the glassy carbon and platinum electrodes imbedded in the cell wall, and of the ANL m-CFDE showing the electrodes imbedded in removal "plugs"

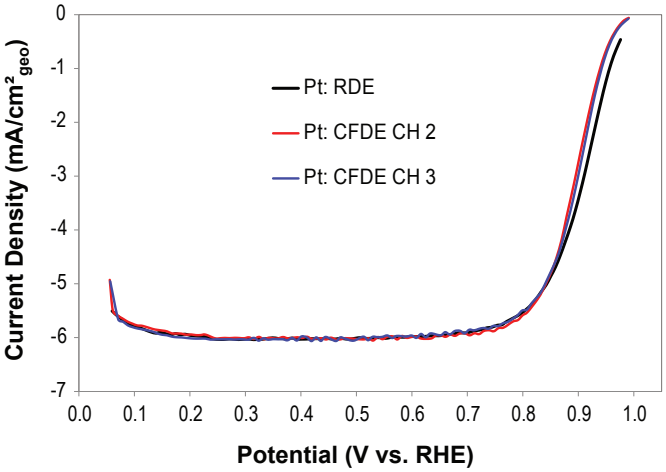

RHE – Reference hydrogen electrode

FIGURE 2. ORR voltammograms for a Tanaka Pt/C catalyst in 0.1 M $HClO_4$ electrolyte using RDE (from FC111 project) and using the ANL m-CFDE cell (two m-CFDE electrodes shown for comparison)

wave potentials for the ORR, a comparative measure of ORR activity when using identical Pt loadings (18 µg/cm^2), agree within 9 mV when comparing the ANL RDE results from FC111 [2] and the m-CFDE (ANL-built cell) results for the same catalyst.

Select results from the ORR activity screening of the 45 PANI-Fe,Co-C catalysts using the m-CFDE are shown in Figure 3. The m-CFDE screening of the PANI-Fe-C HT-produced catalysts showed the same activity trends with pyrolysis temperature as the single large batch-RDE results from LANL [1], validating both the HT synthesis method and the m-CFDE screening technique. The most active catalyst for ORR in these screening was found to be the PANI-Fe_4Co-C catalyst pyrolyzed at 800°C. This catalyst composition was scaled up and the effect of total metal loading on the support was determined. The highest ORR activity of this class was found for the material that had a total metal molar loading that was half that of the standard metal loading. The RDE and m-CFDE results for this catalyst at a loading of 0.6 mg/cm^2 are also compared in Figure 3.

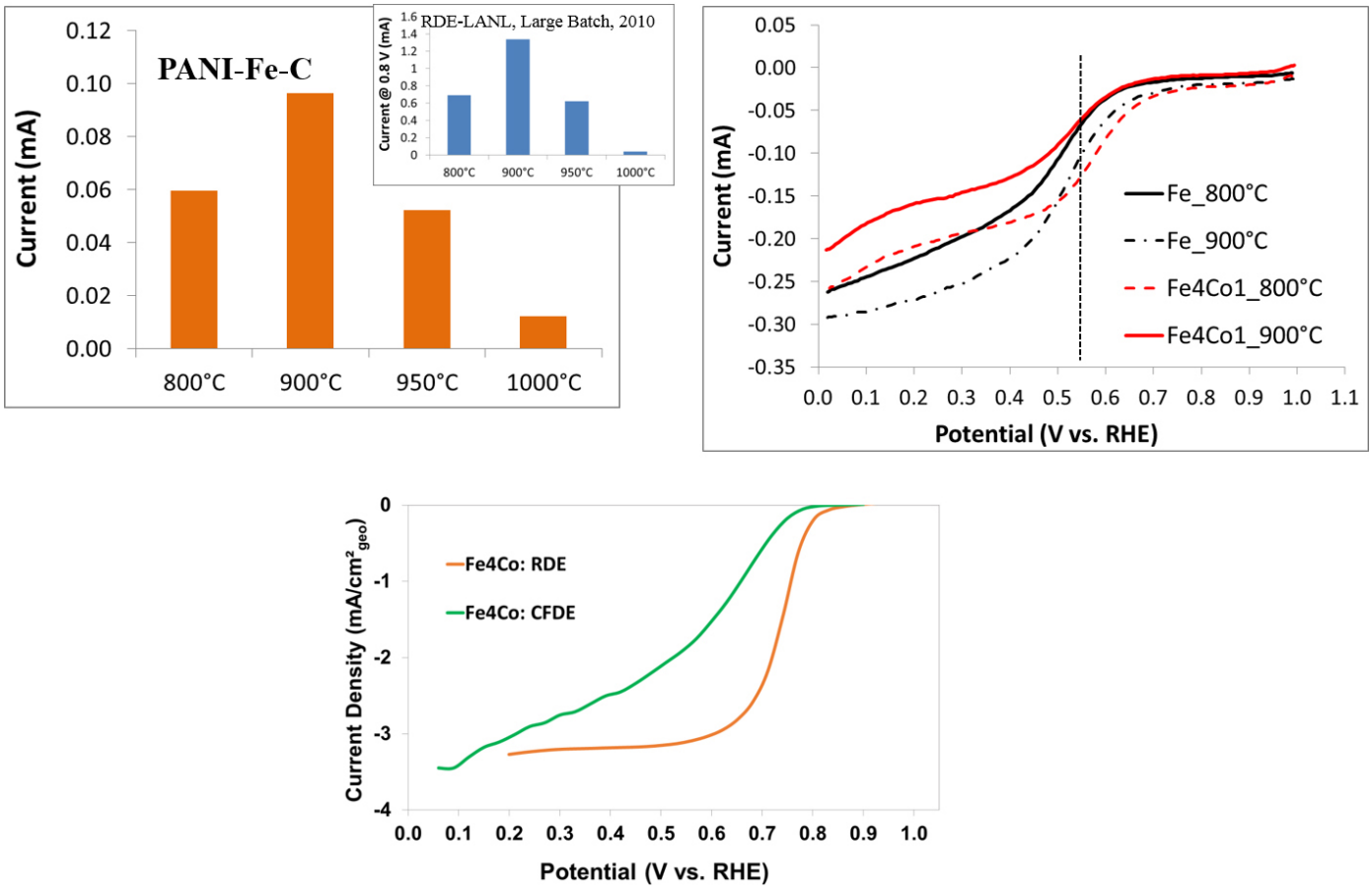

FIGURE 3. Select results from the ORR activity screening of the 45 PANI-Fe,Co-C catalysts using the m-CFDE, comparison of m-CFDE ORR activity trends with pyrolysis temperature for HT PANI-Fe-C with RDE activity trends for LANL's large batch PANI-Fe-C; comparison of m-CFDE and RDE results for HT PANI-Fe_4Co-C

This comparison shows that while the m-CFDE is able to screen relative ORR activity of non-PGM at these high loadings, further work is necessary to determine absolute half-wave potentials for non-PGM catalysts with high loadings on the glassy carbon m-CFDE electrode.

In the computational modeling aspect of the project at LANL, 22 initial structures were considered and eight were down-selected based on the activity descriptor, OH* binding energy. Full ORR reaction pathways have been calculated, using DFT, on the down-selected catalyst structures (Figure 4) developing the first ORR catalyst/activity library for iron-carbon-nitrogen ORR catalysts. Of these structures, the Fe_2N_5(*OH) structure on the zig-zag edge has the highest calculated thermodynamic limiting potential, U_1 (0.76 V vs. computational hydrogen electrode, [CHE]). This value serves as the ORR activity figure of merit and a higher value represents a higher calculated ORR activity. This value of 0.76 V vs. CHE is the highest calculated Fe-based ORR activity value to date (though still below that calculated for a Fe/Co structure). This suggests that selection of ligand species and geometry is a valuable tool in optimizing future

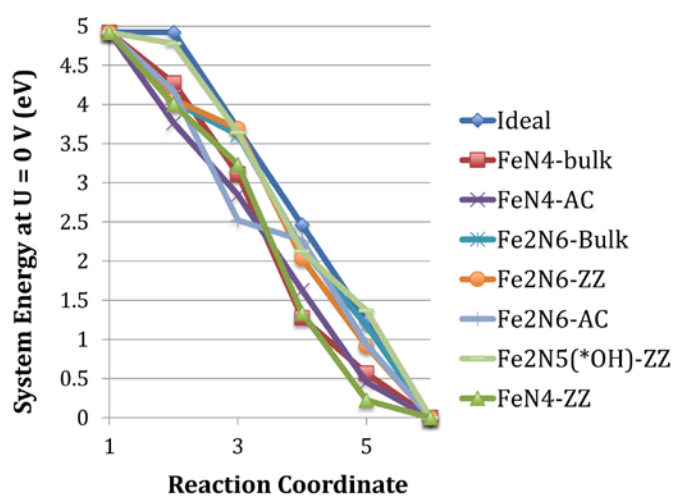

FIGURE 4. ORR reaction pathway on Fe_xN_y-C active site structures from DFT. Reaction coordinates are: (1) * + $4H^+$ + $4e^-$ + O_2, (2) *OO + $4H^+$ + $4e^-$, (3) *OOH + $3H^+$ + $3e^-$, (4) *O + $2H^+$ + $2e^-$ +H_2O, (5) *OH + H^+ + e^- + H_2O, (6) * + $2H_2O$ *represents the active site structure with or without adsorbate. Fe2N5-bulk is not included as *OO and *OOH were found to not bind to this structure.

non-PGM ORR catalyst structures. Additionally, the FeN_4 and Fe_2N_6 structures show that host C material (zig-zag [ZZ] edge, arm-chair [AC] edge, or bulk graphene) can also significantly modify the ORR reaction pathway.

CONCLUSIONS AND FUTURE DIRECTIONS

Conclusions

- Non-PGM catalysts can be synthesized and characterized using an HT approach.
- A PANI-Fe_4Co catalyst pyrolyzed at 800ºC can potentially have a higher ORR activity than the highest activity PANI-Fe,Co-C catalyst known to date.
- A combinatorial technique for screening the ORR activity of catalysts in an aqueous environment, the m-CFDE technique, can achieve half-wave potentials approaching those of RDE and can provide relative ORR activity of non-PGM catalysts.

Future Directions

- RDE screening of select HT PANI-Fe,Co-C samples, in addition to the PANI-Fe_4Co-C samples, to further validate m-CFDE and HT synthesis approach
- Fabrication, performance testing, and durability testing of MEAs containing the PANI-Fe_4Co-C catalyst fabricated using the HT approach
- Correlation of ORR activity trends with phase composition and metal content of numerous HT PANI-Fe,Co-C samples
- Diagnosis of sources of half-wave discrepancy between RDE and m-CFDE results for non-PGM catalysts (i.e., for thick electrocatalyst layers)
- Development of techniques for HT/robotic deposition of catalyst-ionomer inks on the m-CFDE glassy carbon electrodes
- Code development for automation of catalyst active site screening using a DFT Monte Carlo search program
- Development of HT, fully-automated non-PGM-based MEA electrode fabrication

FY 2015 PUBLICATIONS/PRESENTATIONS

1. Holby, E.F. and Taylor, C.D. "Activity of N-coordinated multi-metal-atom active site structures for Pt-free oxygen reduction reaction catalysis: Role of *OH ligands." Sci. Rep. 5, (2015).

REFERENCES

1. Zelenay, P., FC-003, "Advanced Cathode Catalysts," 2007-2011.

2. Kocha, S., FC-111, "Best Practices and Benchmark Activities for ORR Measurements by the Rotating Disk Electrode Technique," 2014.

V.A.9 Non-Platinum Group Metal OER/ORR Catalysts for Alkaline Membrane Fuel Cells and Electrolyzers

Nemanja Danilovic (Primary Contact),
Katherine Ayers
Proton Energy Systems d/b/a Proton OnSite
10 Technology Drive
Wallingford, CT 06492
Phone: (203) 678-2154
E-mail: ndanilovic@protononsite.com

DOE Manager
Jacob Spendelow
Email: Spendelow@lanl.gov

Contract Number: DE-SC0013179

Subcontractor
Professor Charles Dismukes, Rutgers University,
New Brunswick, NJ

Project Start Date: February 17, 2015
Project End Date: November 16, 2015

Overall and Fiscal Year (FY) 2015 Objectives

- Produce 2–10 gram quantities of the cubic phase of lithium cobalt oxide ($LiCoO_2$) and A site derivatives of $LiCoO_2$ (A = Li^+, Mg^{2+}, Zn^{2+}) while preserving particle size, composition purity, and surface structural integrity
- Synthesize O site imide (NH) derivatives of the cubic phase of $LiCoO_2$, $LiCoO_x(NH)_{2-x}$ and screen for enhanced oxygen reduction reaction (ORR) activity
- Optimize ionic and electronic conductivity as well as water transport through modification of flow field geometries and degree of hydrophobicity
- Develop manufacturing methods to combine catalysts and ionomers with an alkaline exchange membrane
- Benchmark oxygen evolution reaction (OER) catalysts in membrane electrode configurations as single cell stacks

Technical Barriers

This project addresses the following technical barrier from the Hydrogen Production and Fuel Cells sections of the Fuel Cell Technologies Office Multi-Year Research, Development, and Demonstration (MYRDD) Plan:

(G) Capital Cost (Electrolyzer + Fuel Cell)

Technical Targets

See Table 1.

FY 2015 Accomplishments

- Synthesis, performance and reproducibility at 5 grams verified for $LiCoO_2$
- Synthesized and characterized multiple A and B-site doped $ABCoO_2$ (A=Mg, Zn; B=Mn) by rotating disk electrode studies
- Defined flowfield geometry, fabricated hardware and optimized wet proofing for oxygen electrode
- Obtained baseline performance in fuel cell and electrolysis mode for anion exchange membrane (AEM)-based unitized regenerative fuel cells (URFCs)
- Obtained preliminary fuel cell and electrolysis data for $LiCoO_2$ with 1,300-hour stability test completed in electrolysis mode

✧ ✧ ✧ ✧ ✧

INTRODUCTION

Two key cost issues represent barriers to implementation of regenerative fuel cells for energy applications. First, the platinum group metal (PGM) catalysts typically used for polymer electrolyte membrane based systems are scarce and expensive. Second, the stack is still a significant cost component of both the electrolyzer and fuel cell subsystems, as discussed at a 2011 Department of Energy workshop on reversible fuel cells. AEMs and ionomers have been gaining stability through significant research and development by multiple groups, and have shown enough feasibility to generate interest in integrating them into devices. At the same time, the alkaline chemistry opens up a wider range of stable materials, including non-noble metals. The end goal of this work is to enable a PGM-free reversible fuel cell, also known as a URFC, based on AEM materials.

The URFC configuration combines the functionality of an electrolyzer and fuel cell stack in one integrated unit. As fuel cell developments have been leveraged in electrolysis cells, there now exists a pathway to design of efficient, durable URFCs compatible with both modes of operation. In addition to enabling catalysts containing nickel, iron, and cobalt that have activity for water splitting and stability in alkaline environments, the AEM cell also eliminates the need for expensive flow field materials such as titanium for

TABLE 1. Technical Targets - Portable Power Fuel Cell Systems and Distributed Forecourt Water Electrolysis Hydrogen Production from the 2012 MYRRD Plan

Table 3.4.7.a Technical Targets: Portable Power Fuel Cell Systems (<2 Watt)[a]				
Characteristic	Units	2011 Status	2013 Targets	2015 Targets
Specific power[b]	W/kg	5	8	10
Power density[b]	W/L	7	10	13
Specific energy[b,c]	Wh/kg	110	200	230
Energy density[b,c]	Wh/L	150	250	300
Cost[d]	$/system	150	130	70
Durability[e,f]	hours	1,500	3,000	5,000
Mean time between failures[f,g]	hours	500	1,500	5,000

Table 3.1.4 Technical Targets: Distributed Forecourt Water Electrolysis Hydrogen Production [a, b, c, l]				
Characteristics	Units	2011 Status	2015 Target	2020 Target
Hydrogen Levelized Cost [d] (Production Only)	$/kg	4.20 [d]	3.90 [d]	2.30 [d]
Electrolyzer System Capital Cost	$/kg $/kW	0.70 430 [e, f]	0.50 300 [f]	0.50 300 [f]
System Energy Efficiency [g]	% (LHV)	67	72	75
	kWh/kg	50	46	44
Stack Energy Efficiency [h]	% (LHV)	74	76	77
	kWh/kg	45	44	43
Electricity Price	$/kWh	From AEO 2009 [i]	From AEO 2009 [i]	0.037 [j]

gge – gasoline gallon equivalent; LHV – lower heating value
Note: Estimates are based on H2A v2.1, for electrolysis only (compression-storage-delivery not included). Model assumes $0.05/kWh.
Electrolyzer cost based on 1500 kg/day capacity, 500 units/year. Efficiency based on system projections and demonstrated stack efficiency of 74% LHV efficiency.

the high potential oxygen electrode, allowing substitution with stainless steel or nickel. Proton Energy Systems d/b/a Proton OnSite (Proton) will leverage experience in water management and URFC design, with catalyst synthesis and characterization expertise at Rutgers University, to focus on a bifunctional oxygen electrode in Phase I, to demonstrate a catalyst and flow field configuration that enable efficient operation for both OER and ORR.

APPROACH

In this project, Proton is focusing on cell design and electrode testing while Rutgers develops a new class of bifunctional OER-ORR catalysts based on modified cubic-$LiCoO_2$. The project focuses on three developments: (1) modification of catalysts that have been shown to provide good OER activity in AEM systems for application to ORR, (2) processing and assembly to stabilize the electrode structure, and (3) changes in cell design to improve water transport in the cell. Rutgers will tune the activity and stability of the catalyst through metal substitution, and doping of the oxide with nitrides or imides. Proton will leverage recent developments in ink deposition and gas diffusion layer formulation to improve overall cell stability. Treating the oxygen electrode to wick the water away from the electrode is likely to improve stability, while making the hydrogen electrode more hydrophilic may be beneficial to fuel cell performance based on our previous Advanced Research Projects Agency-Energy program.

RESULTS

Rutgers synthesized well-defined non-PGM catalysts based on $LiCoO_2$ and lithium manganese oxide ($LiMn_2O_4$) families using sol gel methods. This synthetic approach yielded high phase purity and high surface area as verified by X-ray diffraction and scanning electron microscopy. The ORR and OER activity was tuned by substitution of the cobalt sites with manganese, making compounds with the general formula $LiMn_{2-x}Co_xO_4$ ($0 < x < 1.5$). Cyclic

voltammetry showed that adding manganese enhanced ORR activity, but pure $LiMn_2O_4$ loses OER activity. A reasonable balance could be obtained by partial substitution (Figure 1).

Promising compounds were then delivered to Proton for testing. Electrolysis screening was performed first, using either deionized water or potassium carbonate. Improved performance was demonstrated for the Rutgers catalyst vs. previously tested catalysts. A durability test was then performed, using stainless steel flow fields and gas diffusion layers on the oxygen side and carbon on the hydrogen side. Potassium carbonate was used and electrolyte was fed to the anode. Over 1,200 hours of operation were demonstrated as shown in Figure 2.

Fuel cell testing was then performed using platinum-platinum cells to examine the impact of the flow field geometry. The anode was underhumidified to prevent flooding while the cathode was overhumidified to lessen dryout. Serpentine and straight channel configurations with and without wetproofing on the hydrogen electrode were compared, with serpentine channels on both electrodes demonstrating the best performance (Figure 3).

Cyclic voltammetry data demonstrated that the $LiCoO_2$ meets technical targets for OER and ORR. However, OER performance was more affected by testing in fuel cell mode first than ORR performance was impacted by testing first in electrolysis mode. Full cell data also showed better OER performance before fuel cell testing, but the difference was not nearly as large, only resulting in about 50 mV loss at 0.4 A/cm^2 (Figure 4). Fuel cell performance was significantly lower than the optimized platinum data in Figure 3 and slightly lower than the worst platinum data. Additional optimization of the water transport is expected to significantly improve the fuel cell performance, based on the Rutgers data.

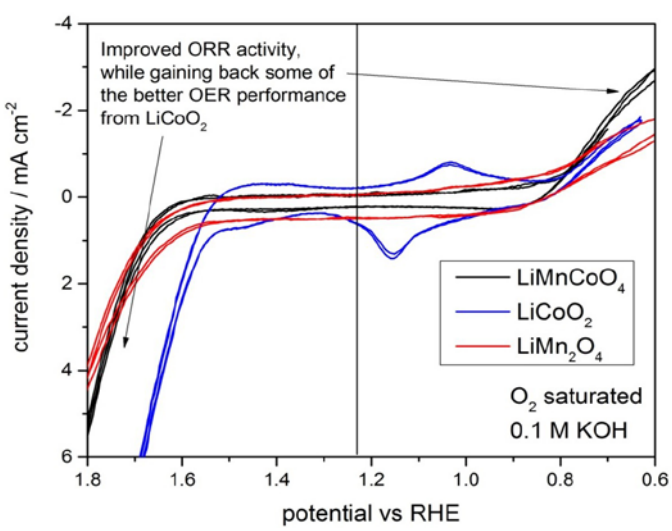

FIGURE 1. Cyclic voltammetry of lithium cobalt manganese oxide compounds

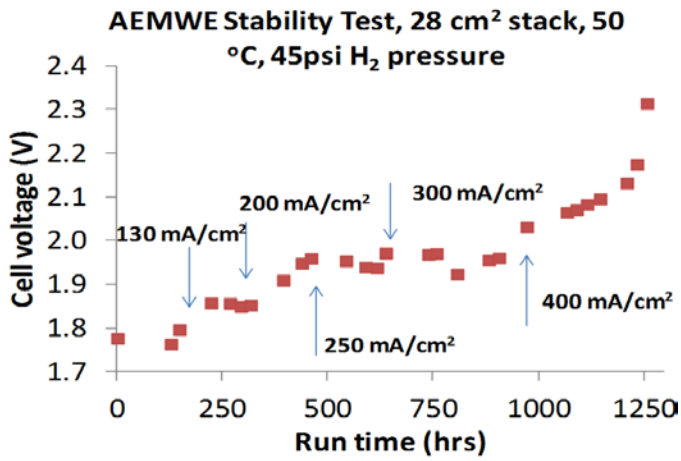

FIGURE 2. Durability and rate capability testing for lithium cobalt oxide (AEMWE = anion exchange membrane water electrolysis)

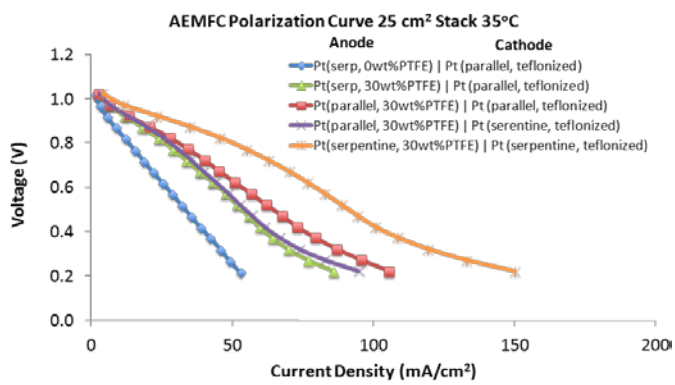

FIGURE 3. Fuel cell performance vs. flow field and gas diffusion layer configuration (AEMFC = anion exchange membrane fuel cell; PTFE = polytetrafluoroethylene)

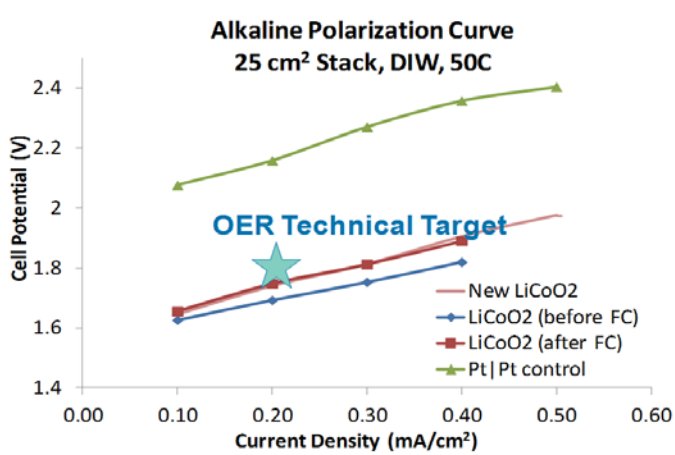

FIGURE 4. Electrolysis testing before and after fuel cell testing (DIW = deionized water)

CONCLUSIONS AND FUTURE DIRECTIONS

- Concluded that $LiCoO_2$ shows good promise for OER/ORR in bench screening, but in cell water management may not be ideal
- Evaluate impact of improved hydrogen catalyst structure and water transport improvements on ORR performance
- Promote configuration to 28 cm^2 retest with $LiCoO_2$ anode
- Conduct 10 cycles using new cathode, $LiCoO_2$ anode
- Continue to evaluate anion and cation dopants on ORR/OER activity

V.A.10 Non-Precious Metal Bi-Functional Catalysts

Paul Matter (Primary Contact), Minette Ocampo, Michael Beachy, and Chris Holt
pH Matter, LLC
1275 Kinnear Rd.
Columbus, OH 43212
Phone: (614) 484-5038
Email: info@phmatter.com

DOE Manager
Jacob Spendelow
Email: Spendelow@lanl.gov

Contract Number: DE-SC0013111

Project Start Date: February 18, 2015
Project End Date: November 17, 2015

Overall Objectives

- Prepare and characterize a matrix of catalysts and membrane electrode assemblies (MEAs) for use in reversible anion exchange membrane (AEM) fuel cell systems
- Demonstrate a bi-functional gas diffusion electrode (GDE) that meets project targets (350 mW/cm^2, <10% degradation over hundreds of cycles)
- Perform economic analysis on reversible AEM fuel cell system following published guidelines for candidate grid load leveling technologies [1]

Fiscal Year (FY) 2015 Objectives

- Prepare and characterize a matrix of catalysts and MEAs for use in reversible AEM fuel cell systems
- Demonstrate a bi-functional GDE that meets project targets (350 mW/cm^2, <10% degradation over hundreds of cycles)
- Perform economic analysis on reversible AEM fuel cell system following published guidelines for candidate grid load leveling technologies [1]

Technical Barriers

This project addresses the following technical barriers from the Fuel Cells section of the Fuel Cell Technologies Office Multi-Year Research, Development, and Demonstration Plan, with respect to alkaline fuel cells for energy storage:

(A) Durability: increase the durability/stability of catalysts

(B) Cost: development of low-cost non-precious group metal (PGM) catalysts for reversible anion-exchange membrane fuel cells (oxygen reduction and oxygen evolution)

(C) Performance: integrate catalysts with membranes and GDLs into MEAs that operate at high power and efficiency

Technical Targets

This Phase I small business innovation research (SBIR) project is developing new catalyst materials for reversible alkaline fuel cells. The materials being developed address the following technical requirements for regenerative energy storage applications:

- Hundreds of cycles with less than 10% voltage loss
- Power density competitive with PGM catalysts (>350 mW/cm^2 at 0.8 V vs. reversible hydrogen electrode [RHE])

FY 2015 Accomplishments

By the midpoint of this nine-month Phase I SBIR, the following work related to the technical objectives has been accomplished:

- Used rotating disk electrode (RDE) set-up to test an array of catalysts for the oxygen reduction reaction (ORR) and oxygen evolution reaction (OER), and durability for cycling between the two reactions. Identified several compositions with excellent stability (<10 mV potential loss after 100 cycles), and with over-potentials competitive with state-of-the-art precious metal catalysts.
- Prepared a matrix of gas diffusion electrodes that incorporated down-selected catalysts. In half-cell testing, demonstrated stable current density exceeding 450 mA/cm^2 at 0.8 V vs. RHE when operating in pure oxygen at 70°C.
- In half-cell testing, demonstrated GDE with no degradation after 50 cycles between projected ORR and OER voltages at room temperature, and current density of 40 mA/cm^2.
- Built an economic model demonstrating that if technical targets can be achieved at the stack scale, then a reversible alkaline membrane fuel cell would be cost-competitive with compressed air energy storage and pumped hydro energy storage approaches. Unlike these low cost energy storage approaches, the fuel cell system would not be subject to geological restrictions. The projected delivered electricity would

cost <$0.14/kWh using the assumptions developed by Steward et al. [1].

✧ ✧ ✧ ✧ ✧

INTRODUCTION

Low temperature fuel cells, such as proton exchange membrane (PEM) and alkaline fuel cells, offer an efficient and clean means of energy conversion of hydrogen to electricity. However, PEM fuel cells typically require platinum in the cathode to operate at high power density and high efficiency, which hurts the economics for this technology. Platinum is used as an electro-catalyst for ORR; the cathode side half reaction is shown below for acidic and alkaline electrolytes, respectively:

1. Oxygen Reduction Reaction (acid) $O_2 + 4\,H^+ + 4\,e^- \rightarrow 2\,H_2O$
2. Oxygen Reduction Reaction (alkaline) $O_2 + 2\,H_2O + 4\,e^- \rightarrow 4\,OH^-$

The slow kinetics in the cathode is one of the largest sources of inefficiency in fuel cells, thus high platinum catalyst loadings are needed to prevent even more voltage losses (or over-potential). At commercial scale, precious metals in the cathodes of PEM fuel cells would comprise a significant portion of the entire stack cost [1,2]. Additionally, Pt-based ORR catalysts can degrade quickly under fuel cell operating conditions, such as frequent load cycling.

More recently, there has been renewed interest in alkaline fuel cells for stationary applications. Development of commercial AEMs is helping to alleviate system-level problems with alkaline fuel cells, such as pressure balance and carbonate precipitation. Further, recent published results at Los Alamos National Laboratory have shown that alkaline fuel cells could potentially operate at high efficiency with non-platinum catalysts [3]. Alkaline fuel cells are of particular interest for energy storage applications that do not have size constraints, such as grid load leveling. The fuel cells could potentially be operated in a reversible manner, allowing renewable energy to be stored in the form of hydrogen. This would be particularly valuable when coupled with renewable energy generation (wind or solar) to provide energy storage and load leveling. However, when operating in regeneration mode, cathode degradation is even more pronounced for conventional catalysts because of the high voltages required for OER, the reverse of Reactions 1 or 2 above. Consequently, in existing reversible systems, a separate precious metal electrode is typically used for oxygen evolution, adding to the already high system cost. If a low-cost bi-functional cathode could be developed for reversible fuel cells, it would be a key breakthrough in the commercial viability of such systems [5]. In this project, pH Matter, LLC, is developing and demonstrating a low cost, non-precious metal, bi-functional cathode for use in reversible alkaline fuel cell systems.

APPROACH

The overall objective of the proposed project is to develop and demonstrate a bi-functional cathode that meets DOE targets for reversible fuel cells for use in stationary energy storage. In the project, researchers at pH Matter will synthesize several variations of novel catalysts, and a matrix of GDEs based on these materials. The materials and GDEs will be fully characterized and tested under bi-functional conditions to determine what properties are important for performance and stability. This information will be used to prepare a second iteration of more optimized GDEs, which will be incorporated into MEAs. The materials in the MEAs will be subjected to longer-term tests in order to demonstrate their capacities to function as next generation non-precious-metal catalysts for reversible fuel cell cathodes. The project will establish a foundation for future work, where larger reversible fuel cells based on the novel cathodes will be further optimized and demonstrated over longer times and in fuel cell stacks. Additionally, an economic model of the reversible fuel cell system is being built to provide input to design and operating condition decisions, and to verify advantages of the system approach compared to available technologies. The proposed Phase I work is intended to demonstrate the feasibility of the novel catalysts to enable a reversible fuel cell system with economic advantages compared to existing technologies.

RESULTS

The Phase I project first began with synthesis of a matrix of novel non-precious metal catalysts. The materials were tested for ORR and OER cycling in a conventional thin-film RDE set-up operating in 1.0 M KOH. The test cell was jacketed with an oil bath for temperature control. Samples were subjected to 100 cycles, typically from 1.2 V to 0.75 V and 1.2 V to 1.5 V vs RHE at room temperature, 50°C, and 70°C. Differences were observed in initial activity and stability. The least stable samples degraded more rapidly at 70°C. Figure 1 shows the ORR current for a carbon-based catalyst doped with nitrogen and phosphorus that demonstrated high performance (exceeded the take-off current of commercial 20 wt% platinum on VULCAN® carbon), and was stable over 100 cycles. This result is significant with respect to the objectives because it demonstrates catalyst stability when cycled to OER voltages, and intrinsic performance that is competitive with state-of-the-art precious metal catalysts. The particular sample shown in Figure 1 was down-selected for most of the GDE testing.

GDEs were made using a screen-printing method. Various catalysts, catalyst loadings, ionomers and/or binders, ink compositions, and electrode substrates were examined.

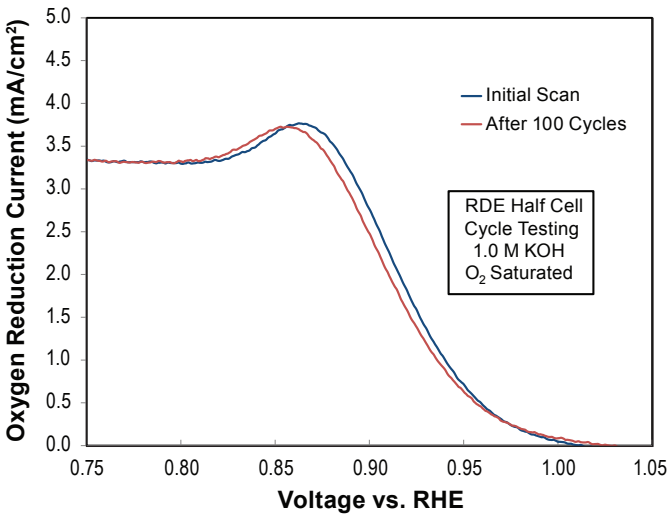

FIGURE 1. Oxygen reduction current of non-precious metal catalyst before and after 100 cycles during RDE testing in oxygen saturated 1 M KOH at room temperature from 0.75 V to 1.45 V vs. RHE

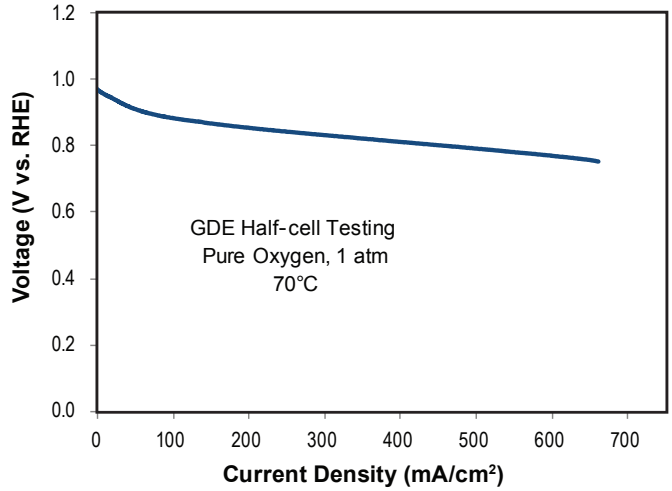

FIGURE 2. Current-voltage curve obtained in half-cell GDE testing of non-precious metal catalyst at 70°C in pure oxygen; aqueous 5 M KOH fed to the counter electrode chamber

Testing was conducted with both aqueous electrolyte, and AEMs in an in-house constructed stainless steel half-cell set-up. Initial tests focused on ORR performance. For the grid load-leveling application, it is expected that current density will be highest (by a factor of 5–6) during periodic cell discharges (ORR operation) compared to OER operation. Testing for the ORR performance demonstrated that optimal GDEs could produce high current density at 70°C in pure oxygen, as shown in Figure 2. Over 450 mA/cm^2 was obtained at 0.8 V vs RHE. This result is significant, as it demonstrates the novel catalyst can produce sufficient current at low enough over-potential to meet operating targets.

Half-cell GDE testing also examined cycling between ORR and OER conditions. For these tests at room temperature, cycles were conducted at 40 mA/cm^2, with the direction of the current being reversed every 10 minutes. Some GDE configurations showed excellent stability for ORR and OER during these tests in up to 50 cycles. Figure 3 shows the half-cell cycle test for the standard material using an ionomer and AEM, and operating in pure oxygen (note that four of the cycles were removed due to data collection errors). Work remains in the second half of Phase I to demonstrate stability under conditions that are optimal for ORR performance (i.e., optimized GDE composition and higher temperatures) and in full-cell configurations.

In the first half of the project, an economic model was built to project electricity costs for energy stored with a regenerative alkaline fuel cell system. The guidelines for the model and assumptions generally followed those used by Steward et al. [1], but assumed a reversible alkaline fuel cell stack that could operate at Phase I targets. The model demonstrated that if technical targets can be achieved at the stack scale, then a reversible alkaline membrane fuel cell would be cost-competitive with compressed air energy storage and pumped hydro energy storage approaches. However, unlike these approaches, fuel cell systems would not be subject to geologic restrictions. The projected delivered electricity would cost less than $0.14/kWh. The model was also used to run sensitivity of the electricity cost to a number of factors, particularly those that have yet to be demonstrated. The sensitivity analysis found that competitive economic performance will be dependent on stack lifetime greater than four years, and achieving roundtrip efficiency higher than 42%.

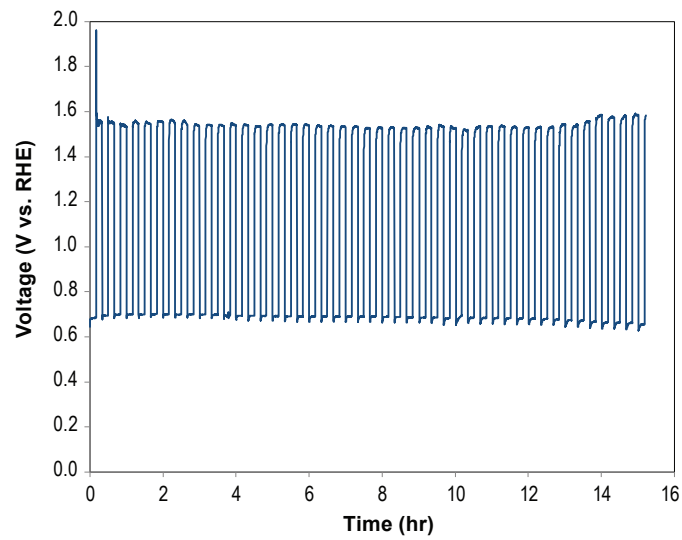

FIGURE 3. Cycle testing obtained in half-cell GDE testing at room temperature for non-precious metal catalyst in pure oxygen; aqueous 2 M KOH fed to the counter electrode chamber

CONCLUSIONS AND FUTURE DIRECTIONS

The following conclusions can be drawn from work completed to this point:

- The novel non-precious metal catalysts being developed on this project show performance comparable to precious metal ORR catalysts, and good stability during cycling from ORR to OER voltages.
- The performance of GDEs optimized for ORR performance would enable DOE targets to be achieved for power density and efficiency for AEM fuel cells.
- The cycling stability for 50 cycles has been demonstrated with GDEs that are not optimized for ORR performance.
- The economic modeling suggests that the reversible AEM fuel cell concept would be an excellent energy storage option for grid load leveling if performance targets can be achieved at the stack and system level.

Future work in the remainder of the Phase I project and in Phase II will include:

- Demonstration of cycling stability at higher ORR performance conditions.
- Demonstration of bi-functional electrode performance in full cell configurations.
- Update of economic model based on demonstrated performance.
- Demonstration of the technology is a prototype energy storage system.

FY 2015 PUBLICATIONS/PRESENTATIONS

1. Matter, Paul H., Minette Ocampo, Michael Beachy, and Chris Holt, "Non-Precious Metal Bi-Functional Catalysts." *DOE Hydrogen and Fuel Cells Program Annual Merit Review and Peer Evaluation* (2015), June 8, 2015, Arlington, VA.

REFERENCES

1. Steward, D., G. Saur, M. Penev, and T. Ramsden, "Lifecycle Cost Analysis of Hydrogen Versus Other Technologies for Electrical Energy Storage," NREL Report NREL/TP-560-46719 (2009). Accessed July 23, 2015. http://www.nrel.gov/docs/fy10osti/46719.pdf

2. James, Brian D., Jennie M. Moton, and Whitney G. Colella, "Mass Production Cost Estimation of Direct H_2 PEM Fuel Cell Systems for Transportation Applications: 2013 Update," Accessed July 23, 2015. http://energy.gov/sites/prod/files/2014/11/f19/fcto_sa_2013_pemfc_transportation_cost_analysis.pdf

3. Chung, H.T., J.H. Won, and P. Zelenay, "Active and stable carbon nanotube/nanoparticle composite electrocatalyst for oxygen reduction," *Nature Communications* 4 (2013). Accessed July 23, 2015. doi: 10.1038/ncomms2944.

4. Remick, R.J., and D. Wheeler, "Reversible Fuel Cells Workshop Summary Report," Accessed July 23, 2015. http://www1.eere.energy.gov/hydrogenandfuelcells/pdfs/rev_fc_wkshp_report.pdf

V.B.1 New Fuel Cell Membranes with Improved Durability and Performance

Michael Yandrasits (Primary Contact)
3M Company
3M Center, Building 201-1W-28
St. Paul, MN 55144
Phone: (651) 736-5719
Email: mayandrasits@mmm.com

DOE Managers
Jacob Spendelow
Phone: (202) 586-4796
Email: Jacob.Spendelow@ee.doe.gov

Greg Kleen
Phone: (720) 356-1747
Email: Gregory.Kleen@ee.doe.gov

Contract Number: DE-EE0006362

Subcontractors:
- General Motors Fuel Cell Activities, Pontiac, MI – Craig Gittleman
- Vanderbilt University, Nashville, TN – Peter Pintaro

Project Start Date: October 1, 2013
Project End Date: September 30, 2016

Overall Objectives

- This project seeks to meet all of the DOE Fuel Cell Technologies Office (FCTO) Multi-Year Research, Development, and Demonstration (MYRDD) Plan membrane performance, durability, and cost targets simultaneously with a single membrane.
- Membranes will be based on multi-acid side chain (MASC) ionomers.
- Electrospun nanofiber structures will be developed to reinforce membranes.
- Peroxide scavenging additives will be used to enhance chemical stability.
- New membranes will have improved mechanical properties, low area specific resistance, and excellent chemical stability compared to current state of the art.
- Experimental membranes will be integrated into membrane electrode assemblies and evaluated in single fuel cells and finally fuel cell stacks.

Fiscal Year (FY) 2015 Objectives

- Produce a supported membrane based on 3M's MASC polymer technology to meet project milestone 4 targets for durability and performance
- Meet project milestone 5 to demonstrate ionomer proton conductivity at 80°C and 40% relative humidity of 0.1 S/cm using ionomers containing more than two acid groups per side chain
- Produce larger scale quantities (1–5 kg) of perfluoroimide acid (PFIA) ionomer
- Develop new nanofibers and nanofiber supported composite membranes
- Investigate surface treatments for nanofiber supports

Technical Barriers

This project addresses the following technical barriers from the Fuel Cells section of the Fuel Cell Technologies Office MYRDD Plan:

(A) Durability

(B) Cost

(C) Performance

Technical Targets

Technical targets for the PFIA-based project milestone 4 membrane are shown in Table 1 along with the comparative data for a perfluorosulfonic acid (PFSA) control. Both membranes contain a nanofiber support material and peroxide stabilizing additives.

FY 2015 Accomplishments

- Go/no-go milestone 4 consisting of both performance and durability targets was met with a 14 micron membrane made with lab-scale PFIA ionomer and experimental nanofibers.
- Perfluoro ionene chain extended (PFICE) ionomers with two, three, or four acid groups per side chain have shown exceptional proton conductivity with PFICE-4 meeting the conductivity target for project milestone 5.
- One pilot-scale run of PFIA ionomer has been completed.
- A simple model based on nanofiber and ionomer properties has been developed that predicts membrane swell after boiling in water.

TABLE 1. Technical Targets for PFIA-Based Membranes

Characteristic	Units	2017 & 2020 Targets	725 EW-S (14 µm)	Project milestone 4 PFIA-S (14 µm)
Maximum oxygen cross-over	mA/cm^2	2	n/a	n/a
Maximum hydrogen cross-over	mA/cm^2	2	1.1	1.4
Area specific proton resistance at:				
120°C, P_{H2O} = 40 kPa	Ohm cm^2	0.02	0.153	0.072
80°C, P_{H2O} = 25 kPa	Ohm cm^2	0.02	0.040	0.027
30°C, P_{H2O} = 4 kPa	Ohm cm^2	0.03	0.028	0.027
-20°C	Ohm cm^2	0.2	n/a	n/a
Minimum electrical resistance	Ohm cm^2	1,000	5,600[a]	5,700[a]
Cost	$/$m^2$	20	n/a	n/a
Durability				
Mechanical	Cycles with <10 sccm crossover hours	20,000	>20,000	>23,000
Chemical	hr	>500	894	742

[a]Data provided by GM
sccm: standard cubic centimeter per minute
S: Siemens

- Blister test data has shown that experimental nanofibers developed in this project have similar strength properties as expanded polytetrafluoroethylene (ePTFE).
- Surface treatments for nanofiber have been investigated.
- Lab membranes made by electrospinning a support fiber and an ionomer fiber simultaneously followed by pressing ionomer fibers into continuous phase.

✧ ✧ ✧ ✧ ✧

INTRODUCTION

Membrane resistance remains a challenge for automotive applications where fuel cells are operated under hot or dry conditions. The focus of this program is to reduce this resistance while maintaining good durability and acceptable cost. Increasing the number of proton charge carriers through increased acid content of the membrane is one way to reduce membrane resistance. Unfortunately membranes based on PFSA polymers become water soluble when the acid content exceeds about 1.4 mmol/g or an equivalent weight (EW) of about 700 g/mol. By using MASC polymers, we are able to increase proton conductivity and lower membrane resistance while retaining a water insoluble polymer. However, membranes made using these polymers typically fall short of durability targets thereby requiring a mechanical support. Electrospun nanofibers offer one way to provide support resulting in durable membranes. It is the goal of this program to develop new ionomers and new nanofiber supports in order to meet all of the DOE targets for resistance, durability, and cost in a single membrane.

APPROACH

The new materials part of this project include both ionomer and nanofiber support development. Ionomers are based on 3M PFSA backbone polymer where the side chain is extended to include one, two, or three imide groups and terminated with the traditional sulfonic acid (Figure 1). 3M's PFIA polymer is the case where n = 1 and the PFICE polymers describe the more general case where n = 1, 2, or 3. For this class of materials, the nitrogen proton is highly acidic and functions as a proton charge carrier while the number of tetrafluoroethylene units in the backbone remain high, preventing the polymer from dissolving in water.

Electrospun nanofiber development is shared between the labs at 3M and Vanderbilt University. Nanofiber materials developed at 3M can be used in a traditional cast

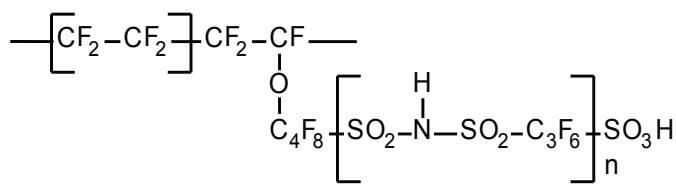

FIGURE 1. Chemical structure for 3M's PFICE polymers. The number of imide containing repeat units is designated by n where the special case of n = 1 is PFIA.

and fill process to make a composite membrane where Vanderbilt is pursuing membrane fabrication methods based on electrospinning both a support fiber and an ionomer fiber. This dual fiber approach allows the ionomer fibers to be pressed into a continuous matrix while leaving the reinforcing support fibers intact. A wide range of fiber distribution throughout the membrane are possible with this method.

Experimental membranes are characterized at Vanderbilt, 3M, and General Motors (GM) with 3M and GM performing most of the fuel cell testing. Final stack testing will be competed in the GM labs.

RESULTS

This last year we successfully passed our project's first go/no-go milestone 4, using lab-made PFIA ionomer and experimental nanofiber support materials. This milestone required that the performance of the new membrane exceed that of a similar thickness state-of-the-art 3M 725 EW-based membrane and pass the chemical (open-circuit voltage) and the mechanical (relative humidity [RH] cycle) accelerated stress tests. Table 1 shows that the durability target has been met and that we have improved upon the resistance values but still fall short of the DOE established targets.

A pilot-scale batch of PFIA was completed this last year in order to supply material for membrane development. This batch was determined to have an equivalent weight of about 660 g/mol by titration and will be used as one of the ionomer options for the next project's go/no-go milestone 8 requiring that all of the DOE targets be meet with a single membrane. See Table 2 for in-plane swell and solubility values.

Laboratory quantities of the PFICE polymer have been made and tested for conductivity, swell, and water solubility. Table 2 shows the expected equivalent weight and the titrated values for a series of polymers made from the same, 700 EW, backbone polymer.

As expected, these polymers had very high swell but were largely insoluble in water. The conductivity of the unsupported membrane, however, was measured to be very high at all humidities, and the PFICE-4 met the project milestone 5 target of 0.1 S/cm^3 at 80°C and 40% RH (Figure 2).

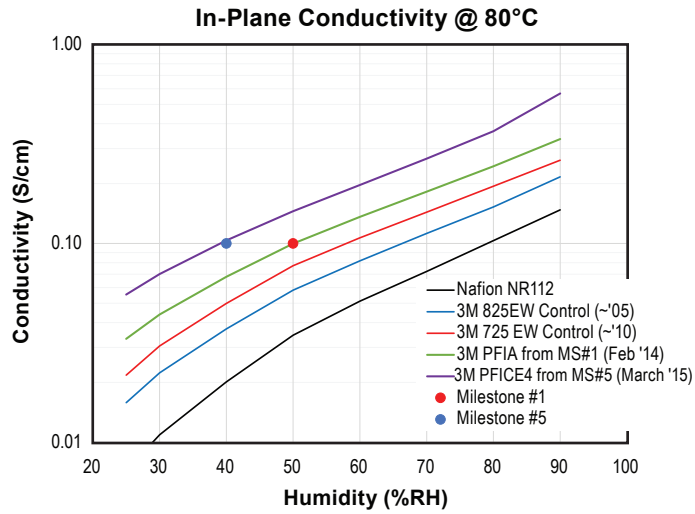

FIGURE 2. In-plane proton conductivity for PFIA and PFICE-4 (4 acid groups per side chain) at 80°C as a function of relative humidity. 3M's 825 and 725 EW membranes along with Nafion® 112 are shown for reference.

Controlling in-plane swell of these membranes is an important function of the nanofiber support material. A method of predicting the swell of a composite membrane (ε_c) was developed based on a rule of mixing approach using the modulus of the supporting nanofiber (E_s), the fiber fraction (f), the modulus of the unsupported swollen ionomer (E_i) and the swell of the ionomer (ε_i).

$$\varepsilon_c = \frac{E_i * (1-f) * \varepsilon_i}{E_i * (1-f) + E_s * f} \quad (1)$$

This analysis was applied to a variety of experimental support materials and an ePTFE support and shown in Figure 3. By plotting swell versus the product of the fiber modulus and fraction, in other words a stiffness factor, we can estimate the swell for new nanofiber candidates at a variety of fiber fractions.

The supports developed under this program have also been evaluated for strength using GM's blister test method [1,2]. A series of membranes were made with a variety of fiber fractions using a fluoropolymer nanofiber (FC1) or a comparative ePTFE support. The normalized pressure

TABLE 2. Swell, Solubility, EW, and Titrated Values for a Series of PFIA-Based Polymers

Ionomer	Starting polymer EW	Number of Imides (n)	Theoretical EW (g/mol)	Titrated EW (g/mol)	In-plane Swell after Boing in Water (%)	Water Solubility (%)
Pilot-Scale PFIA	825	1	560	660	48	4.8
PFICE-2	700	1	501	534	95	9.2
PFICE-3	700	2	431	475	113	10.2
PFICE-4	700	3	397	438	204	14

needed to burst the membrane is plotted versus fiber fraction for two different blister fill rates (Figure 4). In the case of the rapid fill rate (200 s) the burst strength is higher for the more compliant ePFTE but at slower fill rate (2,000 s) there is no difference in strength between the FC1 nanofiber and the ePTFE comparison. It is our belief that the longer fill times are more relevant for predicating membrane durability in a fuel cell.

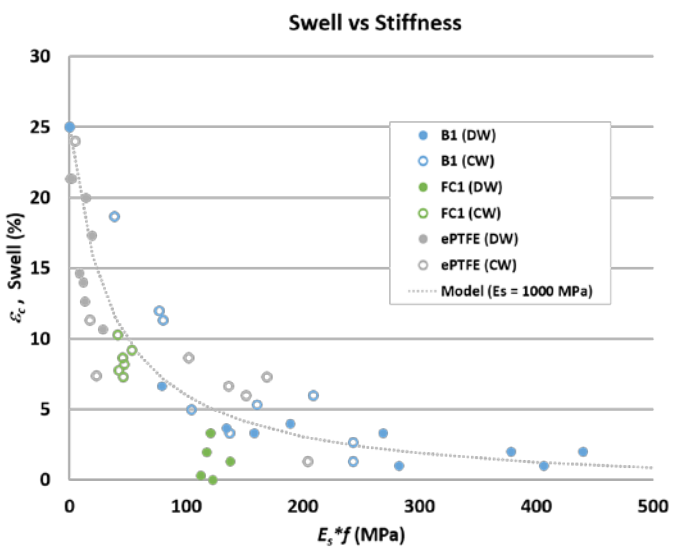

FIGURE 3. Swell versus the product of fiber modulus (*Es*) and fiber fraction (*f*). Symbols represent measured data points and the dotted line represents the values predicted by the rule of mixing model.

Work at Vanderbilt University focused on developing new nanofiber systems, multiple fiber composites, and fibers made from ionomer and inter polymer blends. Also investigated was the used of plasma treating fibers in an effort to improve the fiber-ionomer interface. To date surface treatments have not resulted in improved membrane properties.

CONCLUSIONS AND FUTURE DIRECTIONS

Conclusions from FY 2015:

- PFIA-based membranes have very high proton conductivity values. However, the 14 micron supported membrane used in project milestone 4 still does not meet the DOE's targets for area specific resistance.
- Experimental PFICE ionomers have exceptional proton conductivity while remaining largely insoluble in water.
- Characterization of membrane swell and blister strength as a function of fiber and ionomer properties can provide guidance for developing new nanofiber supports and subsequent membranes.

Future work for FY 2016:

- Pilot-scale PFIA ionomer will be used to fabricate membrane for the project's next go/no-go milestone 8. A target thickness of 10 microns has been selected in order to meet the area specific resistance targets set out by the DOE FCTO MYRDD Plan.

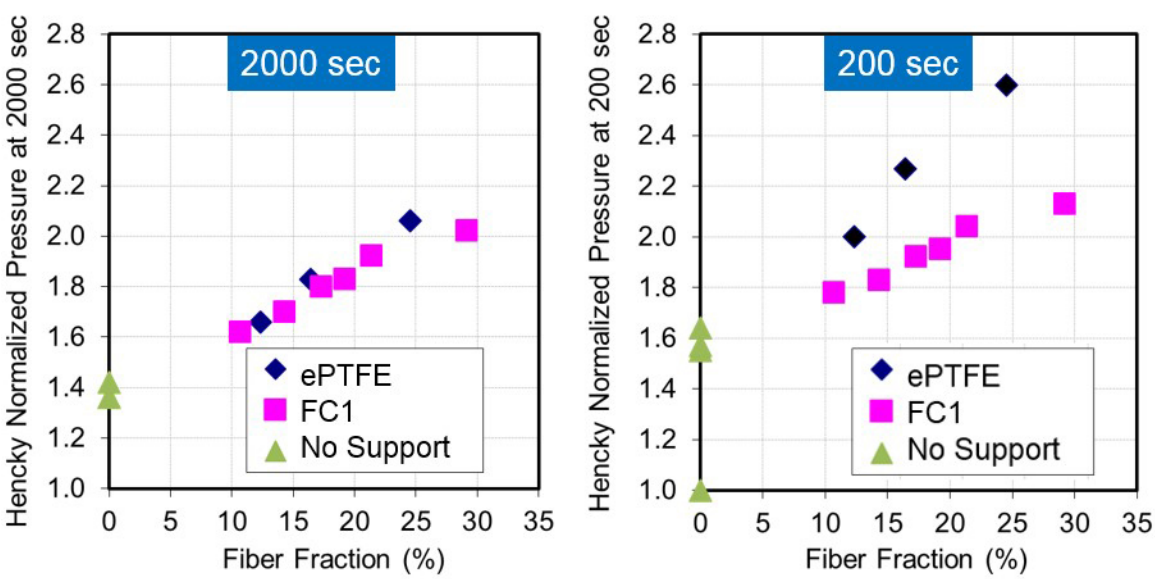

FIGURE 4. Hencky normalized pressure at burst for membranes made with experimental nanofiber supports, FC1 (■), ePTFE (♦) or no support (▲). Data on the right represents fast fill rates (200 seconds) and the graph on the right represents slow fill rates (2,000 seconds).

- Sufficient quantities of the project milestone 8 membrane will be fabricated for single cell durability testing and, ultimately, stack testing at GM.
- Postmortem analysis will begin to better understand degradation mechanisms for the PFIA and PFICE systems.

FY 2015 PUBLICATIONS/PRESENTATIONS

1. USCAR Fuel Cell Tech Team Presentation; "New Fuel Cell Membranes with Improved Durability and Performance," August 13, 2014, Southfield, MI.

2. "V.C.1 New Fuel Cell Membranes with Improved Durability and Performance," 2014 DOE Hydrogen and Fuel Cells Annual Progress Report.

3. "Electrospinning PFSA + PVDF Nanofibers for Fuel Cell Membrane Fabrication," R. Wycisk, J.W. Park, D. Powers, and P.N Pintauro, 226th meeting of the Electrochemical Society, October 8, 2014, Cancun, Mexico.

4. Project Review Meeting with DOE Staff on November 4, 2014, St. Paul, MN.

5. Peter N. Pintauro, Ryszard Wycisk, and Jun Woo Park, "New Membrane Morphologies for PEM Fuel Cells," American Institute of Chemical Engineers Annual Meeting, Atlanta, GA, November 2014 (invited talk).

6. "Engineering a Proton Exchange Membrane for Automotive Fuel Cell Applications," Craig Gittleman, Advances in Polymers for Fuel Cells and Energy Devices Asilomar Conference Grounds Pacific Grove, California, February 8, 2015.

7. M. Yandrasits, "New Fuel Cell Membranes with Improved Durability and Performance," FC109 at DOE's Annual Merit Review in Washington, DC, on June 9, 2015 http://www.hydrogen.energy.gov/annual_review15_fuelcells.html#membranes.

REFERENCES

1. Li, Y., Grohs, J., Pestrak, M.T., Dillard, D.A., Case, S.W., Ellis, M.W., Lai, Y.H., Gittleman, C.S., and Miller, D.P., "Fatigue and Creep to Leaking Tests of Proton Exchange Membrane Using Pressure-Loaded Blisters," *J. Power Sources,* Vol 194, pp. 873–879, 2009.

2. Dillard, D.A., Li, Y., Grohs, J., Case, S.W., Ellis, M.W., Lai, Y.H., Budinski, M.K., and Gittleman, C.S., "On the Use of Pressure-Loaded Blister Tests to Characterize the Strength and Durability of Proton Exchange Membranes." *Journal of Fuel Cell Science and Technology*, Vol 6 (3), pp. 031014-1 – 031014-8, 2009.

V.B.2 Advanced Hybrid Membranes for Next Generation PEMFC Automotive Applications

Andrew M. Herring (Primary Contact)
Mei-Chen Kuo, James L. Horan, Andrew R. Motz, Terra Dunham
Colorado School of Mines
1500 Illinois Street
Golden, CO 80401
Phone: (303) 384-2082
Email: aherring@mines.edu

DOE Manager
Greg Kleen
Phone: (720) 356-1672
Email: Gregory.Kleen@ee.doe.gov

Technical Advisor
John Kopasz
Phone: (630) 252-7531
Email: Kopasz@anl.gov

Contract Number: DE-EE0006363TDD

Subcontractors
- Bryan Pivovar, National Renewable Energy Laboratory, Golden, CO
- Nilesh Dale, Nissan Technical Center North America, Farmington Hills, MI
- Steven Hamrock, 3M Company, Fuel Cell Components Group, St. Paul, MN

Project Start Date: October 1, 2013
Project End Date: September 30, 2016

Overall Objectives

- Fabricate a low cost, high performance polymer electrolyte membrane (PEM) that operates at the temperature of an automotive fuel cell stack and requires no system inlet humidification
- Optimize the membrane to meet durability, cross-over, and electrical resistance targets
- Incorporate the membrane into a 50 cm^2 membrane electrode assembly (MEA)

Fiscal Year (FY) 2015 Objectives

- Show that thin heteropoly acid (HPA) films can be fabricated and have a low area specific resistance at the temperature of an automotive fuel cell stack, whilst also functioning as an electrical resistor
- Increase HPA loading and organization for maximum proton conduction in two different perfluorinated polymer systems
- Begin the development of electrodes specifically for these membranes so that MEA testing can begin

Technical Barriers

This project addresses the following technical barriers from the Fuel Cells section of the Fuel Cell Technologies Office Multi-Year Research, Development, and Demonstration Plan:

(A) Durability

(B) Cost

(C) Performance

Technical Targets

The technical targets are shown in Table 1

TABLE 1. Progress towards Meeting Technical Targets for Membranes for Transportation Applications

Polymer System	DOE ASR Target 2017 Ω cm^2	ASR Result June 2015 Ω cm^2	Thickness µm	Conditions
System I TFVE-HPA	0.02	0.04	16	80°C 95%RH
System II FC-2178-HPA	0.02	0.01–0.02	10–20	>70°C 95% RH

ASR – area specific resistance; RH – relative humidity;
TFVE – trifluorovinyl ether

FY 2015 Accomplishments

- Analyzed the reaction mechanism of the polymerization of trifluorovinyl ether (TFVE) and showed that the growing polymer chain must rotate; this analysis led to a solvent mediated improvement in the synthesis
- Redesigned the synthesis of the FC-2178-HPA material to increase efficiency and yield moving the polymer platform closer to the DOE cost target of <$20 m^2
- Showed that the FC-2178-HPA material could be fabricated into films with thickness <20 µm, ASR of <0.02 Ω cm^2 and an electronic resistance of >1,000 Ω cm^2

✧ ✧ ✧ ✧ ✧

INTRODUCTION

The objective of this project is to fabricate a low cost high performance hybrid inorganic/polymer membrane that has a proton ASR <0.02 ohm cm^2 at the operating temperature of an automotive fuel cell stack (95–120°C) at water partial pressures from 40–80 kPa with good mechanical and chemical durability. Additionally the membrane will be optimized for low hydrogen and oxygen crossover with high electrical ASR at all temperatures and adequate proton ASR at lower temperatures. We also seek to gain valuable insights into rapid proton transport at the lower limit of proton hydration. Additional research will be performed to incorporate the membrane into a 50 cm^2 MEA.

The materials at the start of this project are at a technology readiness level (TRL) of 2, as we have shown that they have proton conductivity under high and dry conditions, but we have not yet consistently shown that they will function in an operational fuel cell. At the project's end the materials will be at a TRL of 4 and will be integrated into an MEA, demonstrating that they can function with electrodes as a single fuel cell. This work will enable hydrogen-powered fuel cells as it will negate the need for costly and bulky external humidification unit operations in the fuel cell system. Additionally excess water will not be an issue for freeze or fuel cell reactant supply. The project is addressing the 2017 DOE technical targets for membranes for transportation applications.

APPROACH

In past funding from the Department of Energy and National Science Foundation (NSF) we have developed completely new ionomer systems based on incorporation of inorganic super acids into polymer systems that have high proton conductivity under conditions of low humidity, higher temperature operation, high oxidative stability, and little swelling when wet. This project will perform the work to optimize the proton conductivity and mechanical properties in these materials to produce a robust thin film for polymer electrolyte membrane fuel cells (PEMFCs). The technical concept is to use functionalized inorganic super acids, which require little water to achieve high proton conductivity, as the protogenic group covalently attached to a polymer backbone optimized for all other functions of the membrane.

Many composite inorganic/polymer films have been fabricated, but unless the inorganic particles have dimensions on the nano-scale, there is no advantage as the improvement to film properties occurs at the particle polymer interface. The limit of this approach is to use molecules with high acidity as the highly activating functionalities, but to do this we must immobilize them, control the morphology of the proton conducting channel, and fabricate an amorphous material. The two moieties that have received the most attention and appear to greatly enhance proton transport are HPAs and zirconyl phosphonates (ZrPs). In previous work, we demonstrated these materials as composite membranes [1-3], but the inorganic super acid in the membrane was not immobilized. Here, we continue our work to fabricate true hybrid materials where the inorganic super acid is incorporated as a functionalized monomer [4-6]. At the beginning of the project these materials were not yet fuel cell ready, as the syntheses were inefficient and there were no methods of processing the polymers into thin proton conductive films. In this project, we will overcome all of these disadvantages with an innovative approach to amorphous materials to produce high proton conductivity and all other properties desired of a PEM.

RESULTS

Work was performed on two polymer systems that have both shown promising proton conductivities under automotive fuel cell operating conditions. We stopped work on the zirconyl phosphonate system described in last year's report, as we were unable to make the material stable to boiling water despite its high proton conductivity. Progress towards making fuel cell ready membranes for the two remaining systems is described below.

The thermal polymerization of TFVE-derived HPA monomers proved to be very challenging. Many different approaches were investigated, including replicating the heating steps of the base polymerization. To further investigate this system a computational study was initiated. The results from this study are shown in Figure 1, which shows the minimum energy pathway. The mechanism necessitates that the growing polymer chain rotate 180°. Clearly to achieve this the viscosity of the polymerizing system must be reduced. We, therefore, started using a solvent, ethylene glycol, and rigorously excluded oxygen from the reaction vessel. The ^{19}F nuclear magnetic resonance (NMR) is shown in Figure 2. The large central peak is attributed to the desired perfluorocyclobutane moiety that is the result of the polymerization of the TFVE groups. Clearly very few end groups remain and an analysis of the spectrum

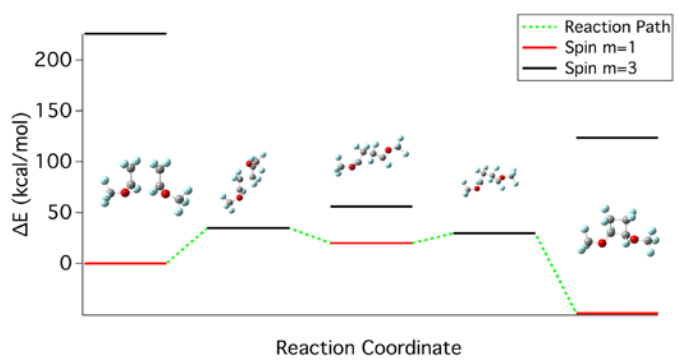

FIGURE 1. Computational study of TFVE monomer polymerization

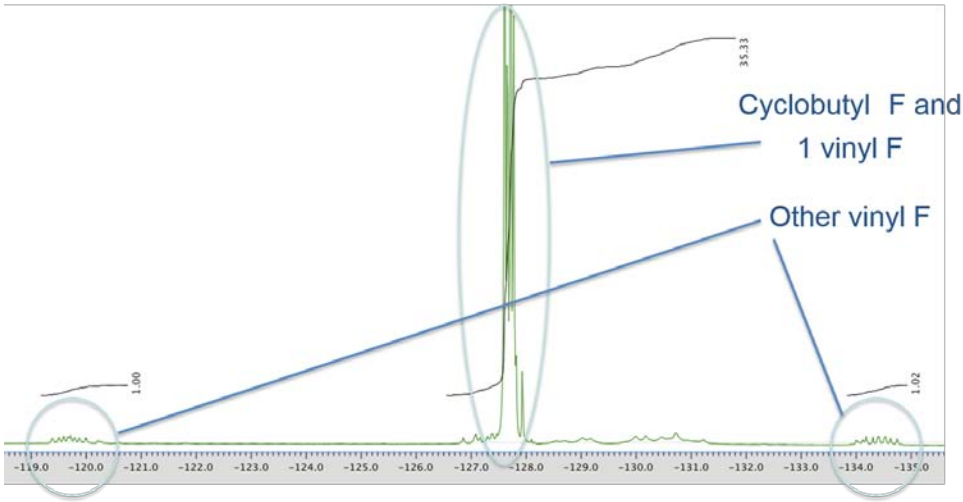

FIGURE 2. ^{19}F NMR of the high MW TFVE-HPA polymer

gives a molecular weight (MW) of 21,500 g mol^{-1}. While this result was very encouraging, we have, to date, been unable to make films from this material. We do feel that due to its very high proton conductivity, it will have utility as an ionomer in the electrode catalysts layer.

The original synthesis of the FC-2178-HPA polymer involved too many manipulations and isolations of the polymer that resulted in poor yields and a very inefficient time-consuming synthesis. In order to fix these issues a convergent synthesis was developed in which more of the key steps where performed on a small molecule precursor. The steps were all standardized and improved to maximize yield and purity. A new method was developed to control the ion exchange capacity, and methods were developed to improve the cross-linking in the membrane. All these improvements have allowed the scale up and synthesis of large area materials for testing by our partners. The materials now have consistently high proton conductivities. Freestanding thick films can be readily made with σ >0.1 S cm^{-1} at temperatures above 60°C and 95% RH. Data for one such film with a thickness of 176 μm is shown in Figure 3. It has been challenging so far to make this material free standing and so it must be supported. The ASR data of another sample as a 12 μm thin film supported on Kapton® is shown in Figure 4. The ASR can clearly be seen to be <0.02 Ω cm^2 above 70°C at 95% RH.

A sample of the polymer with a 15 wt% loading of HPA was sent to Nissan USA for baseline testing. From previous work with our Generation I materials we know that >50 wt% of HPA is necessary to achieve a phase-separated film with adequate proton conductivity. Nevertheless, Nissan USA was able to demonstrate that an MEA could be constructed and tested in fuel cell hardware. Both hydrogen and oxygen crossover were shown to be very low in this film; however, this result could be due to low loading of HPA. It is still a very encouraging result that indicates some of the advantages of this system that hopefully will be propagated into the films with practical proton conductivities.

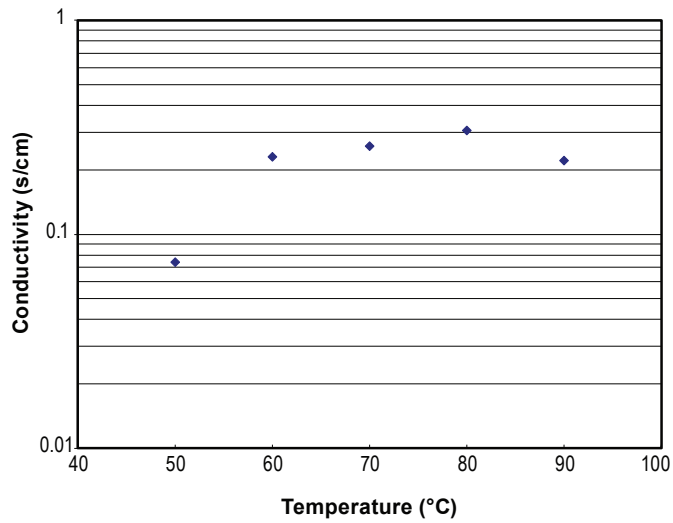

FIGURE 3. Proton conductivity as a function of temperature for a 176 μm FC-2173-HPA polymer at 95% RH

CONCLUSIONS AND FUTURE DIRECTIONS

- Understood how to polymerize TFVE-HPA polymers and demonstrated that high MW materials could be achieved
- Improved the synthesis of the FC-2178-HPA system and showed that films could be produced with high proton conductivity and thin films with low ASR
- Continue to improve the fabrication of thin TFVE-HPA polymers or FC-2178-HPA materials with higher HPA

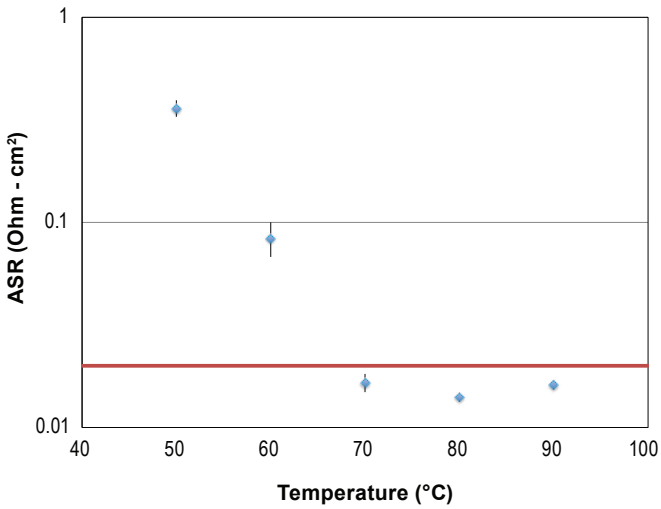

FIGURE 4. ASR of a 12 μm FC-2173-HPA polymer at 95% RH

loadings and incorporate into MEAs for testing and optimization with our partners

SPECIAL RECOGNITIONS & AWARDS/ PATENTS ISSUED

1. "Acidic Ion Exchange Membrane And Method For Making And Using The Same." Gregory J. Schlichting, and Andrew M. Herring, US patent application 13/052,968, March 21, 2011.
US patent 8,906,270 issued December 9, 2014

FY 2015 PUBLICATIONS/PRESENTATIONS

1. "Advanced Hybrid Membranes for Next Generation PEMFC Automotive Applications."

2. A.M. Herring, J.L. Horan, M.-C. Kuo, and A.R. Motz, oral presentation, presented at CARISMA 2014, Cape Town, South Africa, December 2014.

3. "Synthesis and characterization of water stable, silicotungstic acid functionalized perfluorocyclobutyl polymer electrolyte." A.M. Herring, J.L. Horan, M.-C. Kuo, and A.R. Motz, poster presentation, presented at 249th ACS Meeting, Denver, CO, March 2015.

4. "Synthesis and Characterization of Water Stable, Silicotungstic Acid Functionalized Perfluorocyclobutyl Polymer Electrolyte," Andrew R. Motz, Mei-Chen Kuo and Andrew M. Herring, poster presentation, 20th International Conference on Solid State Ionics, Keystone, CO, June 2015.

REFERENCES

1. Haugen, G.; Meng, F.; Aieta, N.; Horan, J.; Kuo, M.; Frey, M.; Hamrock, S.; Herring, A. *Electrochemical and Solid State Letters* **2007**, *10*, B51.

2. Malers, J.; Sweikart, M.; Horan, J.; Turner, J.; Herring, A. *Journal of Power Sources* **2007**, *172*, 83.

3. Meng, F.; Aieta, N.; Dec, S.; Horan, J.; Williamson, D.; Frey, M.; Pham, P.; Turner, J.; Yandrasits, M.; Hamrock, S.; Herring, A. *Electrochimica Acta* **2007**, *53*, 1372.

4. Horan, J.; Genupur, A.; Ren, H.; Sikora, B.; Kuo, M.; Meng, F.; Dec, S.; Haugen, G.; Yandrasits, M.; Hamrock, S.; Frey, M.; Herring, A. *ChemSusChem* **2009**, *2*, 226.

5. Schlichting, G.J.; Horan, J.L.; Jessop, J.D.; Nelson, S.E.; Seifert, S.; Yang, Y.; Herring, A.M. *Macromolecules* **2012**, *45*, 3874.

6. Horan, J.L.; Lingutla, A.; Ren, H.; Kuo, M.-C.; Sachdeva, S.; Yang, Y.; Seifert, S.; Greenlee, L.F.; Yandrasits, M.A.; Hamrock, S.J.; Frey, M.H.; Herring, A.M. *The Journal of Physical Chemistry C* **2014**, *118*, 135.

V.C.1 High Performance, Durable, Low Cost Membrane Electrode Assemblies for Transportation Applications

Andrew Steinbach (Primary Contact),
Dennis van der Vliet, Cemal Duru, Andrei Komlev,
Darren Miller, Amy Hester, Mike Yandrasits,
Andrew Haug, John Abulu, and Matthew Pejsa
3M Company, Fuel Cell Components Program
3M Center, Building 201-2N-19
St. Paul, MN 55144-1000
Phone: (651) 737-0103
Email: ajsteinbach2@mmm.com

DOE Managers
Dimitrios Papageorgopoulos
Phone: (202) 586-5463
Email: Dimitrios.Papageorgopoulos@ee.doe.gov
Gregory Kleen
Phone: (720) 356-1672
Email: Gregory.Kleen@ee.doe.gov

Contract Number: DE-EE0005667

Subcontractors
- Johns Hopkins University, Baltimore, MD
- Michigan Technological University (MTU), Houghton, MI
- Lawrence Berkeley National Laboratory (LBNL), Berkeley, CA
- General Motors Co., Pontiac, MI
- Argonne National Laboratory, Argonne, IL (collaborator)
- Los Alamos National Laboratory, Los Alamos, NM

Project Start Date: September 1, 2012
Project End Date: February 29, 2016

Overall Objectives

- Demonstrate a durable, low-cost, and high performance membrane electrode assembly for transportation applications, characterized by:
  - Total platinum (Pt) group metal loadings of ≤0.125 mg/cm^2 of membrane electrode assembly (MEA) area
  - Performance at rated power of ≥1,000 mW/cm^2
  - Performance at ¼ power (0.8 V) of ≥0.3 A/cm^2
  - Durability of ≥5,000 hours under cycling conditions
  - Q/ΔT of ≤1.45 kW/°C
  - Cost of $5–9/kW, projected at high volume
- Improve operational robustness to allow achievement of transient response, cold-startup, and freeze-startup system targets

Fiscal Year (FY) 2015 Objectives

- Improve operational robustness via material optimization, characterization, and modeling
- Optimize post-processing of 3M Pt_3Ni_7/NSTF oxygen reduction reaction (ORR) cathode electrodes for improved MEA activity, durability, and rated-power capability
- Integrate ultra-low platinum group metal (PGM) nanostructured thin film (NSTF) anode catalysts, NSTF cathode catalysts, and next-generation supported 3M polymer electrolyte membranes (PEMs) for improved MEA performance, durability, and cost
- Identify key factors influencing NSTF MEA durability, with a primary focus on maintenance of rated power performance

Technical Barriers

This project addresses the following technical barriers from the Fuel Cells section of the Fuel Cell Technologies Office Multi-Year Research, Development, and Demonstration Plan:

(A) Durability

(B) Cost

(C) Performance

Technical Targets

This project is focused on development of a durable, high performance, low cost, and robust MEA for transportation applications. Table 1 lists current project status against the DOE technical targets for MEAs (Table 3.4.14) and a subset of electrocatalyst targets (Table 3.4.13) from the 2012 Multi-Year Research, Development and Demonstration Plan. The project status values are provided by results from the 2015 (March) Best of Class (BOC) MEA, tested in duplicate and described at the bottom of Table 1. This MEA has achieved the DOE 2020 Q/ΔT and performance at 0.8 V characteristics, and is within 15% of the performance at rated power and 7% of the PGM total loading characteristics. Durability with cycling status under the prescribed protocol is not available, but the MEA does pass the DOE membrane chemical durability test.

TABLE 1. Status against Technical Targets

Characteristic	Units	2020 Targets	3M 2015 Status*
Q/ΔT	kW/°C	1.45	1.45
Cost	$/kW	7	5 (PGM only @ $35/$g_{Pt}$)
Durability with cycling	hours	5,000	NA
Performance @ 0.8 V	mA/cm^2	300	304
Performance @ rated power	mW/cm^2	1,000	855
PGM total content (both electrodes)	g/kW (rated)	0.125	0.155
PGM total loading	mg PGM/cm^2 electrode area	0.125	0.133

*3M Status with 2015 (March) Best of Class MEA: 0.015 mg_{PGM}/cm^2 PtCoMn/NSTF anode electrode, 0.102 mg_{PGM}/cm^2 Pt_3Ni_7(TREATED)/NSTF + 0.015 mg_{PGM}/cm^2 Pt/C interlayer cathode electrode, 14 µ 725EW 3M supported PEM, 3M "X2"/2979 Anode/Cathode GDLs, Optimized Flow Fields.
90°C, 150 kPa hydrogen/air (outlet), 2.0/2.5 hydrogen/air Stoichiometry
84°C Dewpoints (J > 0.4 A/cm^2), 68°C Dewpoints (J < 0.4 A/cm^2)
Rated power defined at 0.692 V.
NA – not applicable; GDL – gas diffusion layer

FY 2015 Accomplishments

- Cathode catalyst dealloying method validated in continuous pilot production trials. Trial-to-trial reproducibility was established and 50' continuous roll-good was generated.
- Cathode interlayer with high durability developed that maintains improved NSTF MEA operational robustness and performance after the DOE Support cycle accelerated stress test (AST) and through most of the DOE Electrocatalyst cycle AST.
- MTU's GDL Pore Network Model and LBNL's MEA Continuum models were successfully integrated. The combined model accurately predicts performance temperature sensitivity of NSTF MEAs with different anode gas diffusion layers.
- The 2015 (March) BOC MEA was integrated with improved performance, cost, and operational robustness over 2014 status.
- 3M validated that rated power degradation of NSTF MEAs is caused by perfluorosulfonic acid (PFSA) PEM decomposition. An improved PEM was developed that decreased rated power degradation 30% compared to baseline.

✧ ✧ ✧ ✧ ✧

INTRODUCTION

While significant progress has been made, state-of-the-art polymer electrolyte membrane fuel cell MEAs utilized in today's prototype automotive traction fuel cell systems continue to suffer from significant limitations due to high cost, insufficient durability, and low robustness to off-nominal operating conditions. State-of-the art MEAs based on conventional carbon-supported platinum nanoparticle catalysts currently incorporate precious metal loadings that are significantly above those needed to achieve MEA cost targets; performance, durability, and/or robustness decrease significantly as loadings are reduced. This project focuses on integration of 3M's state-of-the-art NSTF anode and cathode catalysts with 3M's state-of-the-art PEMs, advanced and low-cost GDLs, and robustness-enhancing interfacial layers. At significantly lower precious metal content, the NSTF catalyst technology platform has several significant demonstrated benefits in performance, durability, and cost over conventional catalysts.

APPROACH

This project optimizes integration of advanced anode and cathode catalysts with next generation PFSA PEMs, gas diffusion media, and flow fields for best overall MEA performance, durability, robustness, and cost by using a combined experimental and modeling approach.

RESULTS

We previously reported an improved chemical dealloying method developed at Johns Hopkins University that resulted in a ca. 20% increase in hydrogen/air limiting current density of Pt_3Ni_7/NSTF cathodes over the pre-project baseline dealloying method [1]. Work this year has focused on process development to optimize dealloying conditions to maximize performance and enable continuous roll processing. Figure 1A shows that after batch dealloying, the platinum mole fraction increases substantially, which depends upon dealloying time and temperature. Resultant MEA mass activity and hydrogen/air performance also vary strongly with treatment conditions, and peak hydrogen/air performance and mass activity occur at ca. 40–42 at% Pt. Dealloyed catalyst generated in continuous process trials showed good agreement between target and actual catalyst composition and very good trial-trial reproducibility (Figure 1B), and hydrogen/air performance was substantially improved over non-dealloyed (Figure 1C).

Historically, one challenge of NSTF MEA integration into automotive stacks has been its higher performance sensitivity to operating conditions than traditional thick dispersed electrode MEAs, especially at cool and wet conditions applicable to automotive startup. In previous work, we had shown that variation of the anode GDL backing can have an extraordinarily large positive influence [2], but the mechanism was unclear. Last year, we reported that spatial variation in anode GDL backing carbon paper density was a key material factor enabling improved low

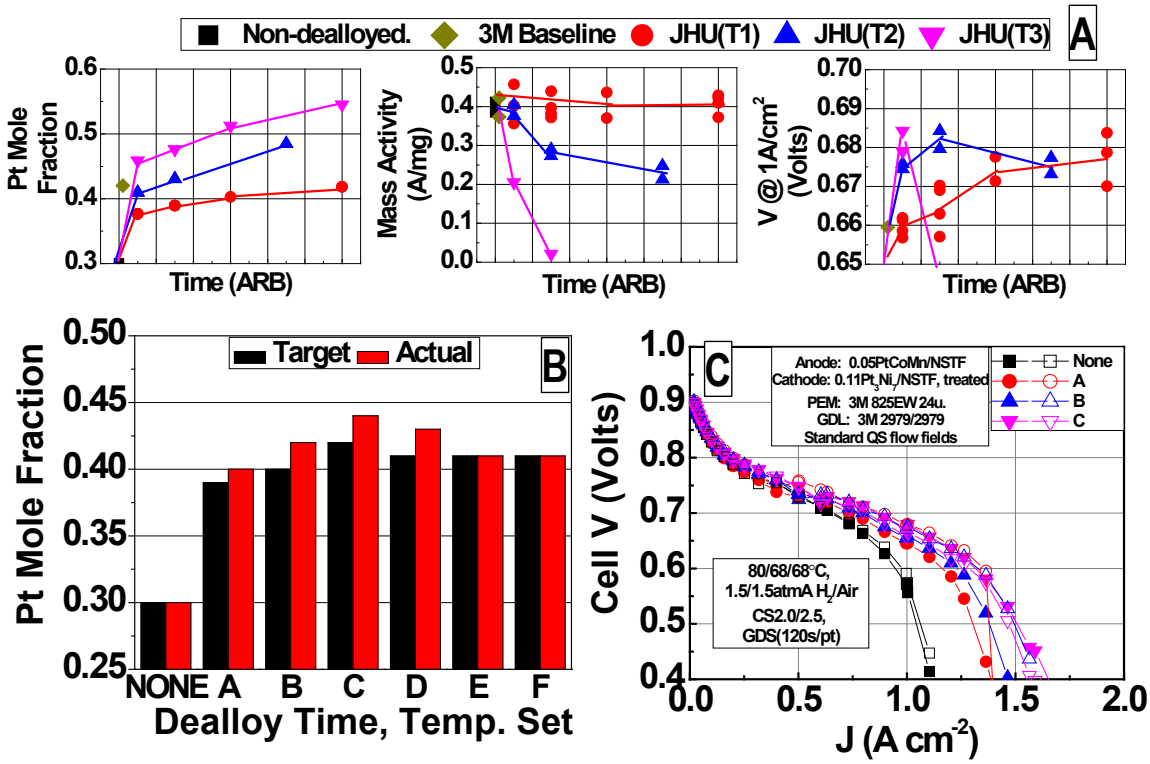

FIGURE 1. Cathode activity, hydrogen/air performance and composition vs. batch dealloy process conditions (A). Continuous dealloying process control (B) and resultant hydrogen/air performance (C).

temperature performance of NSTF MEAs [1]. These so-called "banded" GDLs enabled higher anode liquid water removal rates in MEAs, reducing cathode flooding. Pore network modeling at MTU suggested possibly higher gas and liquid permeability due to preferential liquid water transport in low density regions. This year, X-ray computed tomography studies at LBNL confirmed that as liquid pressure increases, liquid water preferentially fills low density regions while maintaining reduced saturation in the high density region (Figure 2A). Additionally, significant work focused on integration of MTU's pore network models of 3M GDLs with LBNL's continuum MEA model, and the resultant combined model accurately predicts NSTF MEA performance sensitivity to temperature with two anode GDL types (Figure 2B).

In addition to the improvements demonstrated with the anode GDL, we have previously shown that integration of a cathode interlayer (low-loaded Pt/C electrode between NSTF cathode and GDL) substantially improves NSTF MEA's ability to withstand load transients (step increases in current density to 1 A/cm^2) under condensing conditions [1]. One concern with the approach is that conventional dispersed Pt/C electrocatalysts may not be sufficiently durable due to well-known degradation modes such as platinum agglomeration and dissolution and carbon corrosion. This year, we have optimized the cathode interlayer for improved durability while maintaining improved operational robustness demonstrated previously [1]. Figure 3 shows that when an NSTF MEA with the improved interlayer was evaluated under the DOE Support Cycle AST, hydrogen/air performance at rated power improved substantially, mass activity and specific area losses were modest, steady state performance at low temperatures improved substantially, and load transient performance was largely maintained.

MEA integration work this year has focused on incorporation of several improved components towards improved performance, cost, and operational robustness. Figure 4A compares the hydrogen/air performance of the 2015 (March) BOC MEA to the pre-project 2012 BOC MEA. The 2015 BOC MEA incorporates many improved components over 2012 status, including a reduced PGM anode, improved performance, reduced-PGM dealloyed PtNi/NSTF cathode, a higher conductivity mechanically-stabilized 3M PFSA PEM, an optimized anode gas diffusion layer and a cathode interlayer that enable improved operational robustness, and optimized flow fields. The 2015 BOC has substantially improved performance and reduced PGM loading, resulting in a 48% increase in specific power at the DOE Q/ΔT heat rejection target of 1.45 kW/°C. Figure 4B shows that the operational robustness of the 2015 BOC MEA is substantially improved over 2013 status, where the stable operating temperature window for 1 A/cm^2 operation was increased from 70–80°C to 40–80°C and is within 10°C of targets.

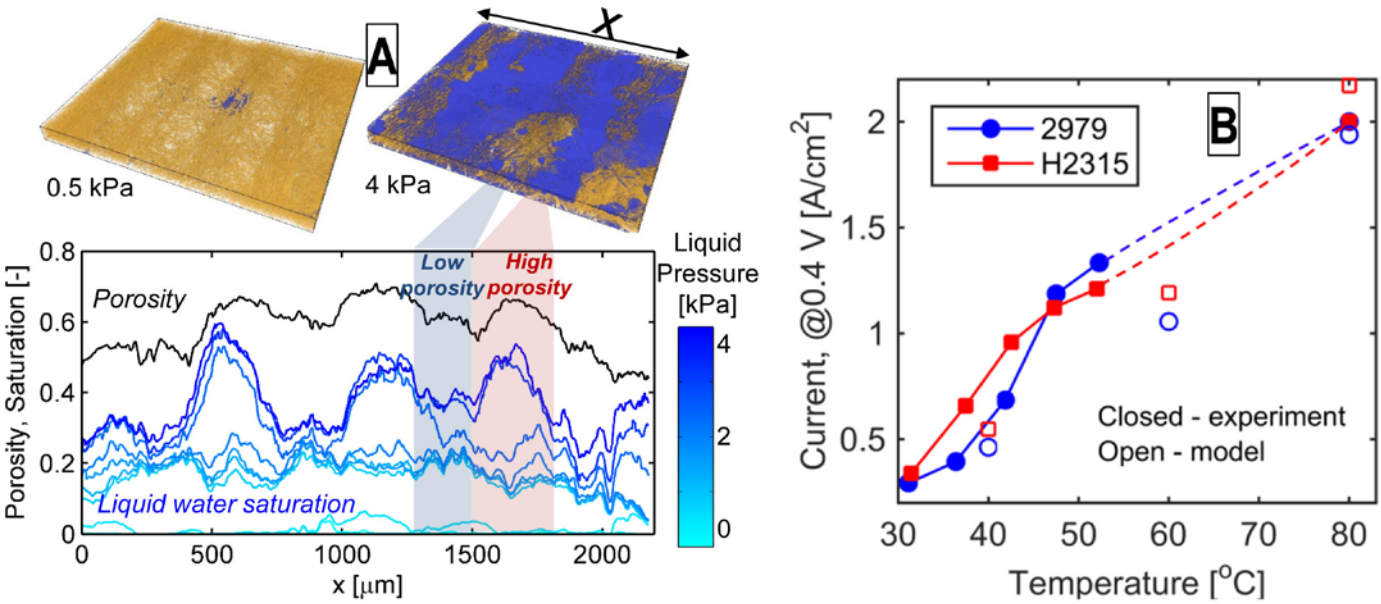

FIGURE 2. X-Ray computed tomography analysis of spatial water saturation in anode GDL (A). Integrated MTU-LBNL model prediction of NSTF MEA temperature sensitivity with two anode GDLs (B).

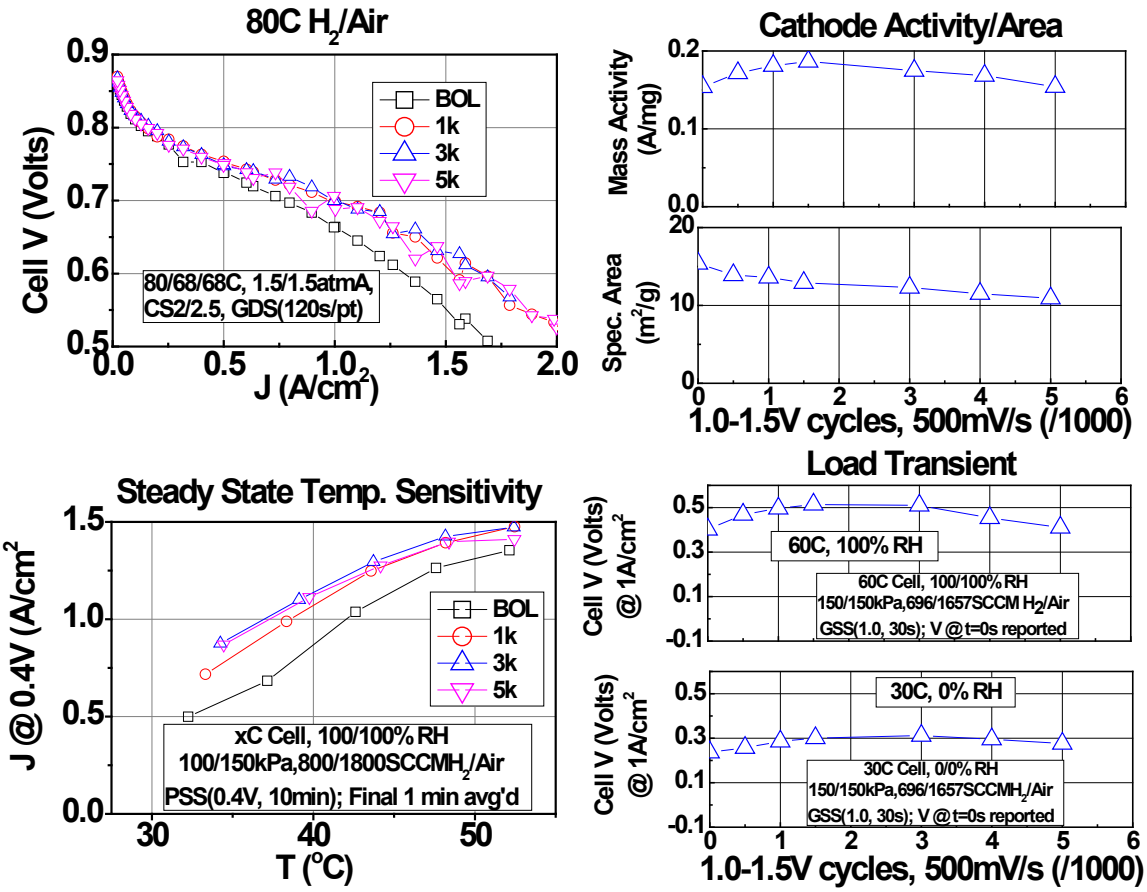

FIGURE 3. Evolution of hydrogen/air performance, cathode activity, and operational robustness of NSTF MEA with cathode interlayer during the DOE Support Cycle AST.

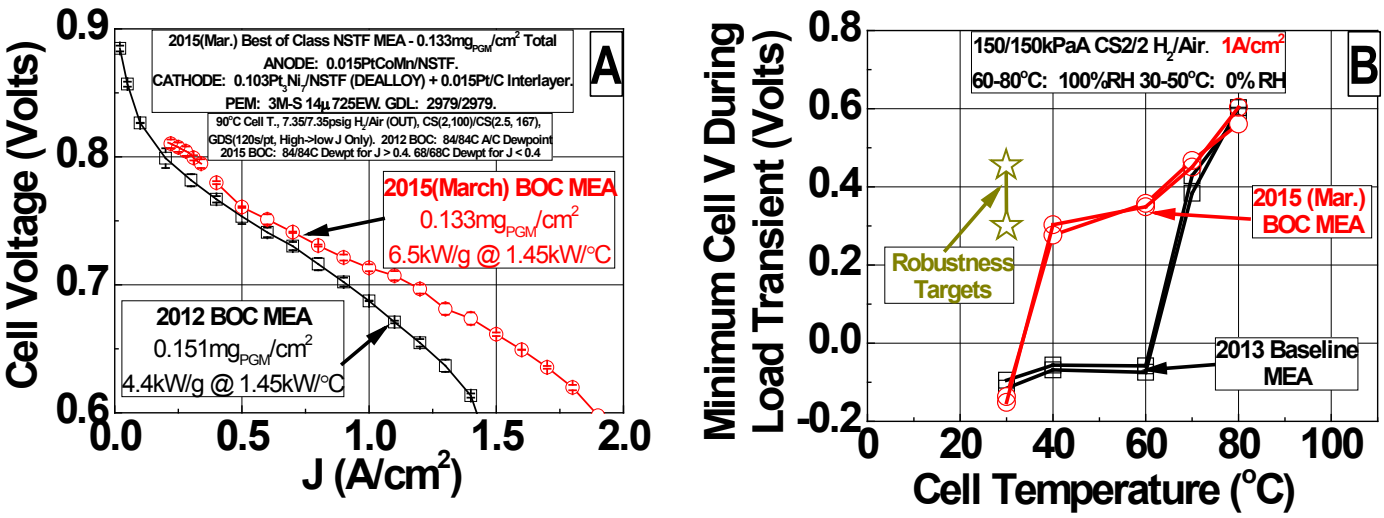

FIGURE 4. 3M NSTF 2015 (March) Best of Class MEA Hydrogen/air performance (A) and operational robustness (B).

Work has continued this year to understand the factors influencing rated power durability of NSTF MEAs, and work has been initiated to improve the durability. Last year, we reported key results and our assessment that rated power degradation was correlated to the loss of ORR absolute activity due to the irreversible adsorption of one or more unidentified PFSA PEM decomposition products [1]. This year, experiments were conducted to validate this hypothesis and to analyze the relationship between performance loss and PEM decomposition. Figure 5A shows that when baseline PtCoMn/NSTF MEAs are held at 90°C cell temperature at different fixed cell voltages, the performance loss rate increases over 3x as cell voltage is decreased from 0.90 to 0.30 V and F^- emission rates increase substantially. We have previously shown that NSTF MEA performance loss at both low and high current density appears to be explained entirely by absolute ORR activity loss [1] and this was found to also be the case here (Figure 5B). The ORR activity loss in this testing was determined to be due to two factors: loss of cathode surface area as a function of test time and loss of cathode specific activity due to PEM decomposition as determined by cumulative F^- generation (Figure 5C). Based on this work, a new experimental 3M PEM was developed that reduced the voltage decay rate by 30% and substantially reduced ORR activity losses (Figure 6).

CONCLUSIONS AND FUTURE DIRECTIONS

Significant progress has been made towards improvement of NSTF MEA performance, cost and operational robustness, and all relevant DOE 2020 targets have been reached or substantially approached. Durability of rated power remains a primary concern, but the confirmed hypothesis linking NSTF MEA rated power loss to PFSA PEM decomposition has provided clear directions towards improvement, including development of novel PEMs and integration of NSTF cathodes with higher surface area and activity. Primary future directions for the current project include:

- 2015 (March) BOC MEA evaluation in short stacks for performance and operational robustness.
- Development of material and operational mitigation approaches to reduce rated-power degradation.

FY 2015 PUBLICATIONS/PRESENTATIONS

1. A. Kusoglu, C. Blake, F. Allen, A. Crothers, A.Z. Weber, *Understanding Conduction and Structure in PFSA Membranes*, 17th Solid State Protonic Conductors, Seoul, Korea, September 14–19, 2014.

2. A.J. Steinbach, project presentation to USCAR Fuel Cell Tech Team, October 15, 2014, Southfield, MI.

3. V. Konduru, E.F. Medici, and J.S. Allen, *Modeling Thermal Transport in Heterogeneous Porous Media of PEM Fuel Cells Using Pore Network Model,* Trans. of the 226th Electrochemical Society Meeting, October 2014, Cancun, Mexico.

4. A.J. Steinbach and D. van der Vliet, project presentation to DOE, November 4, 2014, St. Paul, MN.

5. I.V. Zenyuk, A. Santamaria, P.K. Das, A. Steinbach, R. Mukundan, R.L. Borup, A.Z. Weber, *Water Management with Thin-Film Catalyst Layers*, CARISMA, South Africa, Dec. 1, 2014.

6. I.V. Zenyuk, D.Y. Parkinson, G. Hwang, A.Z. Weber, *Understanding Water Transport in Compressed Gas Diffusion Layers of Polymer-Electrolyte Fuel Cells Using X-ray Computed Tomography*, 2015 MRS Spring Meeting & Exhibit, April 9, 2015.

7. D.A. Cullen, M. Lopez-Haro, P. Bayle-Guillemaud, L. Guetaz, M.K. Debe, and A.J. Steinbach, *Linking Morphology with Activity in Novel PtNi Nanostructured Thin Film Catalysts*, J. Mat. Chem. A **3** 11660, 2015.

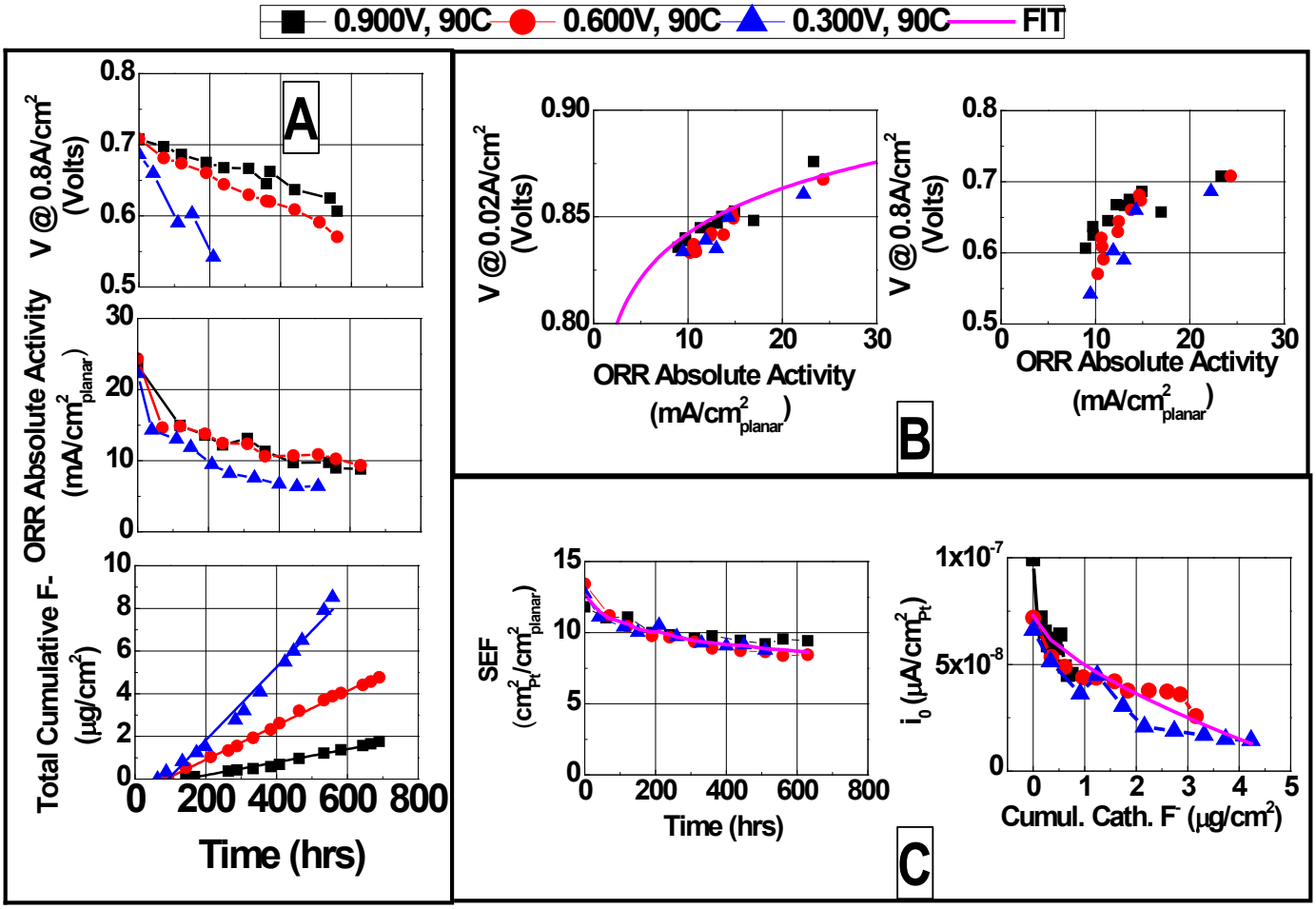

FIGURE 5. Cell voltage, cathode absolute ORR activity, and cumulative F^- emission over time vs. cell voltage (A). Hydrogen/air performance loss due to ORR activity loss (B). ORR activity losses due to cathode surface area loss and specific activity loss (C).

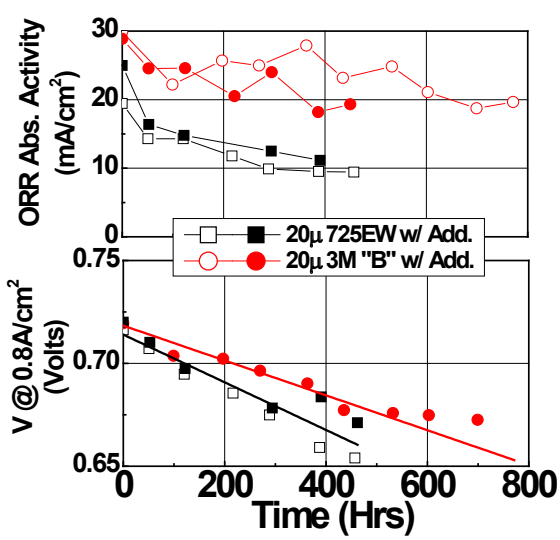

FIGURE 6. Improved ORR activity retention and 30% decrease in cell voltage loss rate with improved experimental 3M PEM "B".

8. I. Zenyuk, E.F. Médici, J.S. Allen, and A.Z. Weber, *Coupling Continuum and Pore Network Models in Polymer Electrolyte Fuel Cells,* 7th International Conference on Porous Media, May 2015, Padova, Italy.

9. V. Konduru, J.S. Allen, J. Pharaoh, *Multiscale modeling of water transport in porous transport layers (PTL) of PEM fuel cells using combined pore network and finite volume modeling,* 7th International Conference on Porous Media, May 2015, Padova, Italy.

10. A.J. Steinbach, *High Performance, Durable, Low Cost Membrane Electrode Assemblies for Transportation Applications*, Presentation FC104, 2015 DOE Annual Merit Review, Washington, DC, June 2015.

11. A.J. Steinbach, *High Performance, Durable, Low Cost Membrane Electrode Assemblies for Transportation Applications*, IEA Annex 34 - Fuel Cells for Transportation, June 24, 2015, Jülich, Germany.

12. R.K. Ahluwalia, X. Wang, and A.J. Steinbach, *Performance of Advanced Automotive Fuel Cell Systems with Heat Rejection Constraint*, J. Power Sources, 2015, submitted.

13. A.J. Steinbach and D. van der Vliet, project presentation to DOE, July 16, 2015, St. Paul, MN.

14. I.V. Zenyuk, E.F. Médici, J.S. Allen, and A.Z. Weber, "Coupling Continuum and Pore- Network Models in Polymer-Electrolyte Fuel Cells," European Fuel Cell 2015 – Piero Lunghi Conference, Naples, December 16–18, 2015.

V.C.2 Rationally Designed Catalyst Layers for PEMFC Performance Optimization

Deborah J. Myers (Primary Contact),
Nancy N. Kariuki, Rajesh Ahluwalia,
Xiaohua Wang, and Jui-Kun Peng
Argonne National Laboratory
9700 S. Cass Avenue
Lemont, Illinois 60439
Phone: (630) 252-4261
Email: dmyers@anl.gov

DOE Manager
Nancy Garland
Phone: (202)586-5673
Email: Nancy.Garland@ee.doe.gov

Subcontractors:
- Johnson Matthey Fuel Cells, Sonning Common, United Kingdom
- Jonathan Sharman, Alex Martinez, Dash Fongalland, Brian Theobald, L. Smith, D. Ozkaya, M. Gutierrez, Graham Hards, and Willie Hall, United Technologies Research Center, East Hartford, CT
- Zhiwei Yang and Michael Perry,University of Texas at Austin, Austin, TX
- Paulo Ferreira, Kang Yu, Somaye Rasouli, and Andres Godoy, Indiana University Purdue University Indianapolis, Indianapolis, IN
- Jian Xie, Le Xin, Zhefei Li, Yadong Liu, Yuan Zhou, and Fan Yang

Project Start Date: May 1, 2013
Project End Date: April 30, 2016

Overall Objectives

- To realize the oxygen reduction reaction (ORR) mass activity benefits of advanced platinum-based cathode electrocatalysts in membrane electrode assemblies (MEAs) and stacks operating at high current densities and on air and at low platinum group metal (PGM) loading (≤0.1 mgPt/cm² on cathode)
- To determine the source(s) of performance limitations of de-alloyed PtNi-containing membrane-electrode assemblies at high current densities (>1 A/cm^2) when operating on air
- To design and develop an electrode layer composition and/or structure, based on in-cell diagnostics, advanced characterization, and performance modeling to exceed the technical targets for MEAs for transportation applications
- To develop the catalyst support morphology, surface functionality, and/or catalyst ink composition to optimize the performance of the cathode, guided by modeling

Fiscal Year (FY) 2015 Objectives

- Synthesize d-PtNi catalyst with functionalized proton-conducting carbon support and determine performance of this functionalized catalyst/support in MEAs
- Fabricate and test MEAs with alternative cathode catalyst layer ionomer to carbon ratio, with alternative solvent in catalyst-ionomer inks, and with post-MEA-fabrication treatment toward the goal of improving the high current density air performance
- Improve high current density air performance of an MEA containing the dealloyed PtNi-based cathode catalyst by ≥115 mA/cm² at 0.675 V/cell to achieve ≥850 mW/cm^2 at rated power, toward the DOE 2020 target of 1,000 mW/cm² at rated power

Technical Barriers

This project addresses the following technical barriers from the Fuel Cells section of the Fuel Cell Technologies Office Multi-Year Research, Development, and Demonstration Plan:

(C) Performance

(B) Cost

(A) Durability

Technical Targets

The technical targets for this project are listed in Table 1.

FY 2015 Accomplishments

- Determined effect of increased ionomer content on An-Pt/C and d-PtNi/C catalyst layer structure and performance
- Determined effect of organic versus aqueous solvent in inks on An-Pt/C and d-PtNi/C performance
- Determined agglomerate structure of An-Pt/C and d-PtNi/C inks and dry inks/electrode layers
- Determined extent of Ni lost from d-PtNi catalyst during ink preparation, MEA fabrication, and testing and impact of Ni^{2+} in ionomer on cathode resistance and ionomer oxygen permeability

TABLE 1. Progress towards Meeting Technical Targets for Electrocatalysts and MEAs for Transportation Applications

Characteristic	Units	DOE 2020 Electrocatalyst and MEA Targets	Project Status (50 cm^2 cell, differential conditions)
Mass activity	A/mg_{PGM} @ 0.9 $mV_{iR\text{-}free}$	≥0.44	0.57
Specific activity	$\mu A/cm^2_{PGM}$ @ 0.9 $mV_{iR\text{-}free}$	≥720	986
PGM total loading	$mg\text{-}PGM/cm^2_{geo}$	≤0.125	0.092, cathode
MEA performance	mA/cm^2_{geo} @ 800 mV	≥300	347
MEA performance	mW/cm^2_{geo} @ 675 mV	≥1000	827

- Increased hydrogen/air current density by 90 mA/cm^2 to 1,225 mA/cm^2 and power density by 89 W/cm^2 to 827 mW/cm^2 at 0.675 V of a d-PtNi-containing MEA through a combination of increase of ionomer content in the cathode catalyst layer (CCL) and acid-washing of the catalyst-coated membrane (CCM)

✧ ✧ ✧ ✧ ✧

INTRODUCTION CCL

One of the major cost contributors to a polymer electrolyte membrane fuel cell (PEMFC) is the electrocatalyst [1]. The high cost of the cathode electrocatalyst results from the high loadings of catalyst necessary to overcome the limitations of low ORR activity, low utilization of PGM, and loss of activity with operating time. Alloying platinum with base metals (e.g., cobalt, iron, and nickel) is well known to improve its intrinsic ORR activity [2]. While ORR activities exceeding the DOE 2020 targets (>0.44 A/mg PGM and 720 $\mu A/cm^2$ @ 900 mV) have been demonstrated for high surface area carbon supported platinum alloy and core-shell nanoparticle catalysts in aqueous cell rotating disk electrode (RDE) tests and in MEAs [3], some as high as 5.75 A/mg-Pt in RDE tests [4], the full performance of cathode catalyst layers based on these promising catalysts has yet to be achieved in MEAs, especially at the low cathode platinum loadings necessary to achieve the DOE MEA PGM loading target (≤0.125 $mg\text{-}Pt/cm^2$) and when operating at realistic current densities on air rather than oxygen. There are several possible reasons the full potentials of these advanced catalysts have not been realized in MEAs operating on air and at current densities >1 A/cm^2 arising from the complex requirements for full utilization of the electrocatalytic sites and for adequate reactant transport in the MEA cathode layer. Fulfillment of these requirements at high current densities in an MEA cathode relies on optimization of the electrode composition and structure to balance the structure of the proton-conducting phase, the electron-conducting phase, and the distribution and size of pores for reactant/product diffusion. This optimization is a lengthy, trial-and-error process and has taken several years for the traditional platinum-only cathode layers. The goal of this project is to optimize the electrode layer composition, structure, and materials properties of cathodes based on advanced alloy catalysts so their intrinsically high performance for the ORR can be translated into performances at high current densities and on air that exceed simultaneously the DOE performance, durability, and cost targets for PEMFCs for automotive applications.

APPROACH

The overall approach of the project is to:

- Determine the properties of advanced alloy-based catalysts and/or cathode catalyst layers that limit the high current density/air performance using:
  - In-cell diagnostics of d-PtNi versus high surface area platinum and platinum of comparable electrochemically active surface area (ECSA).
  - A suite of in situ and ex situ techniques, such as transmission electron microscopy (TEM), cryogenic TEM, dynamic light scattering, ultra-small angle X-ray scattering (USAXS), X-ray absorption spectroscopy, and porosimetry.
- Design the catalyst layer composition and structure and support functionality to mitigate the performance limitations, guided by computational modeling.
  - Study the dispersion of d-PtNi/C catalyst aggregates and the ionomer particles in liquid media and in electrodes and compare them to Pt/C-based inks and electrodes
  - Develop an ink composition and/or ink processing (e.g., solvent removal process) that result in optimum agglomerate structure in d-PtNi/C-based electrode
  - Develop the catalyst support surface functionality to increase the performance of the catalyst and cathode to decouple proton conductivity from ionomer content

The catalyst selected for this project is high surface area carbon supported dealloyed PtNi nanoparticles (d-PtNi), which was developed by Johnson Matthey Fuel Cells within the General Motors-led project [5]. The catalyst precursor is comprised of 5.4 nm mean diameter $PtNi_3$ alloy particles deposited on Ketjen black carbon via a commercially-scalable method followed by annealing to drive alloy formation. The resulting catalyst precursor is "dealloyed" via an acid treatment step to leach Ni to form a catalyst with an approximate composition of Pt_3Ni_2 with a Pt loading on the carbon support of approximately 30 wt%. As shown in Table 1, the ORR mass activity of this catalyst in an MEA exceeds the DOE 2020 target [5], the kinetic stability of this catalyst can exceed the DOE 2020 target.

RESULTS

The effects of ionomer to carbon ratio and organic versus aqueous solvents in the ionomer-catalyst inks on agglomerate structure in inks, agglomerate structure in electrodes, and cathode catalyst layer performance under a variety of oxygen partial pressures and relative humidities were determined for the d-PtNi/C catalyst and, for comparison, for a Pt/C catalyst with a particle size distribution comparable to that of the d-PtNi/C (An-Pt/C). The following summarizes the results of these characterization and performance studies:

Increased ionomer content (I/C ratio) in the catalyst-ionomer inks:

- Enhances the MEA performance under dry and wet conditions, except for d-PtNi/C at 100% relative humidity (RH) where it increased mass transport on air (Figure 1).
- Increases breakup of carbon agglomerates, increasing fraction of small agglomerates (70–100 nm) as determined by dynamic light scattering of dilute inks and USAXS of the as-prepared ionomer-carbon inks (Figure 2).
- Decreases catalyst layer pore volume fraction and permeability, as determined by porosimetry.

Organic solvent vs. aqueous solvent in catalyst-ionomer inks:

- Increases breakup of carbon agglomerates, increasing fraction of small agglomerates (70–100 nm) (Figure 2).
- Increases porosity and permeability of resulting catalyst layer.
- Increases amount of ionomer not associated with catalyst/carbon and decreases size of ionomer rods.
- Decreases amount and effect of Ni^{2+} in the "free" ionomer (Figure 3).

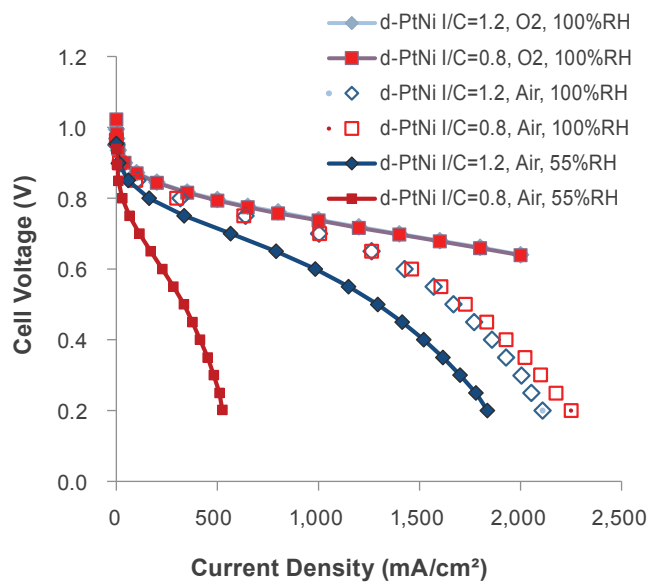

FIGURE 1. Hydrogen-oxygen and hydrogen-air polarization curves for MEAs with ~0.1 mg-Pt/cm^2 loading of d-PtNi/C with I/C ratios in the CCL of 0.8 or 1.2. Cell conditions: 80°C, 150 kPa (abs.), high and fixed flow for differential conditions (3 slpm O_2 or air).

- Primarily enhances cathode performance at high and low RH. Extent of effect is pO_2 dependent.

d-PtNi/C vs. An-Pt/C:

- Inks have larger agglomerates and less agglomerate breakup.
- Inks have more "free" ionomer not associated with catalyst/carbon, for I/C of 0.8.
- "Free" ionomer in inks has rod-like structure in solvent and diameter of rods is larger for free ionomer in d-PtNi/C inks than in An-Pt/C inks.
- Reactant transport to d-PtNi/C at 100% RH is linked to low absolute catalyst ECSA (same as for An-Pt/C). At low RH additional mass transport losses are observed that are unique to d-PtNi/C.
- Ni^{2+} is leached from d-PtNi into ionomer during ink preparation and MEA fabrication (Figure 2).
- Ni^{2+} in ionomer decreases oxygen permeability and decreases catalyst layer ionic conductivity, as determined by RDE-ORR diffusion-limited current measurements and by in-cell electrochemical impedance spectroscopy measurements.
- Acid-washing CCM improves mass transport in d-PtNi/C catalyst layer, improving hydrogen–air performance at 0.675 V by 90 mA/cm^2 to 1,225 mA/cm^2 and greatly improving low RH performance (Figure 4).

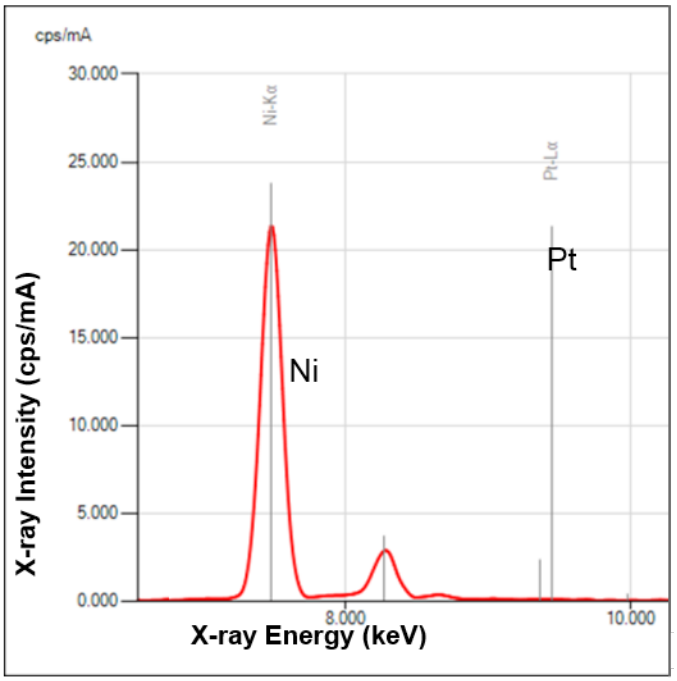

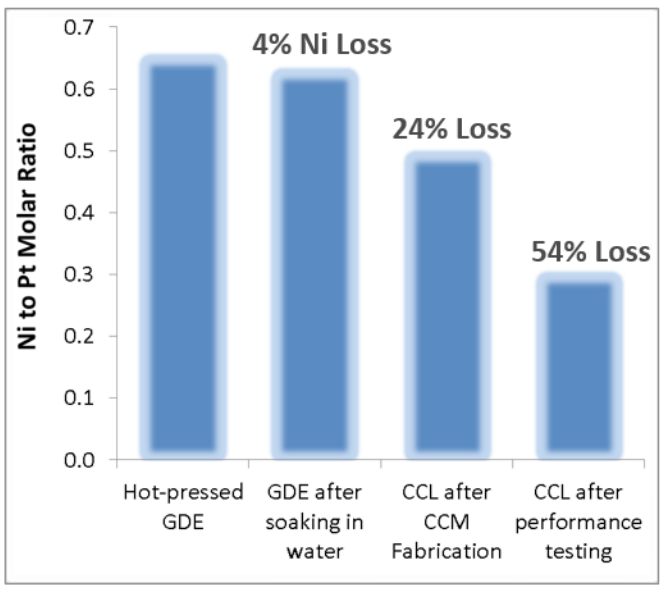

GDE: Gas Diffusion Electrode
CCL: Cathode Catalyst Layer
CCM: Catalyst Coated Membrane

FIGURE 2. (Top) XRF of dried supernatant from d-PtNi/C-ionomer-solvent organic ink showing that Ni^{2+} has leached into the ionomer-solvent. The ratio of the Ni to S XRF peak areas was 16 for the aqueous ink and 2.7 for the organic ink showing that the organic ink leaches less Ni^{2+} from the d-PtNi/C catalyst. (Bottom) XRF of d-PtNi/C electrode layers at various stages of MEA fabrication and testing illustrating that Ni is removed from the cathode at all stages.

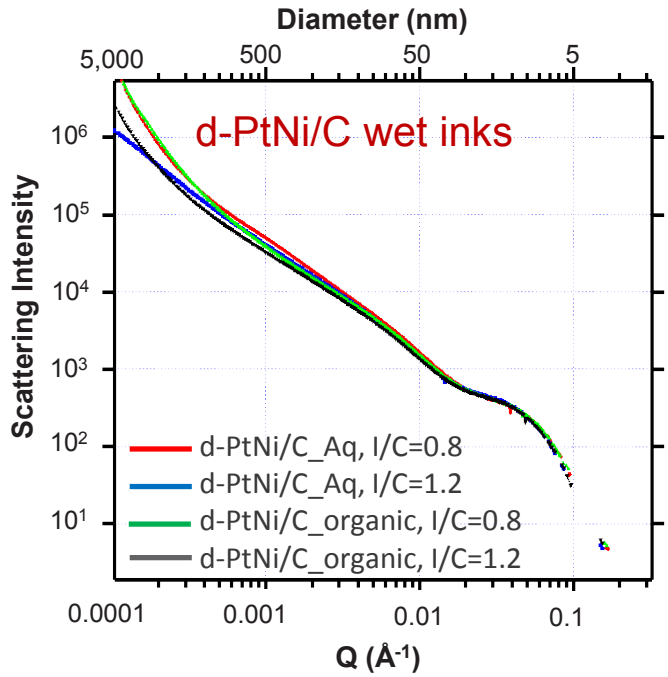

FIGURE 3. USAXS curves of as prepared d-PtNi/C inks made with aqueous or organic solvents and with I/C ratios of 0.8 or 1.2, illustrating that increased ionomer content and use of organic solvent versus aqueous solvent decreases the sizes of agglomerates in the inks.

CONCLUSIONS AND FUTURE DIRECTIONS

Conclusions

- Issues with the d-PtNi/C-containing catalyst are drop-off in performance at >1 A/cm^2 (i.e., not maintaining mass activity benefit relative to high-surface-area Pt/C) under high and intermediate humidity conditions and a severe drop-off at low RHs, due to:
  - Mass transport to low loadings of large particles.
    - Can be mitigated with smaller particles that are greater than approximately 4 nm to ensure stability against dissolution-related ECSA loss
  - Sensitivity to low humidity conditions unique to d-PtNi/C (i.e., not observed with comparably-sized Pt/C).
    - Can be partially mitigated with increased ionomer content and organic solvents that improve dispersion of d-PtNi/C particles, and can be greatly improved with acid treatment of CCM
- Results thus far indicate that Ni^{2+} in the ionomer, leached during ink and CCM fabrication, is altering the agglomerate structure of the CCL and also altering the oxygen permeability of the ionomer phase, decreasing mass transport, especially at low RH.
  - More aggressive leaching of Ni^{2+} prior to ink synthesis and CCM fabrication can improve d-PtNi/C cathode performance, especially under dry conditions.

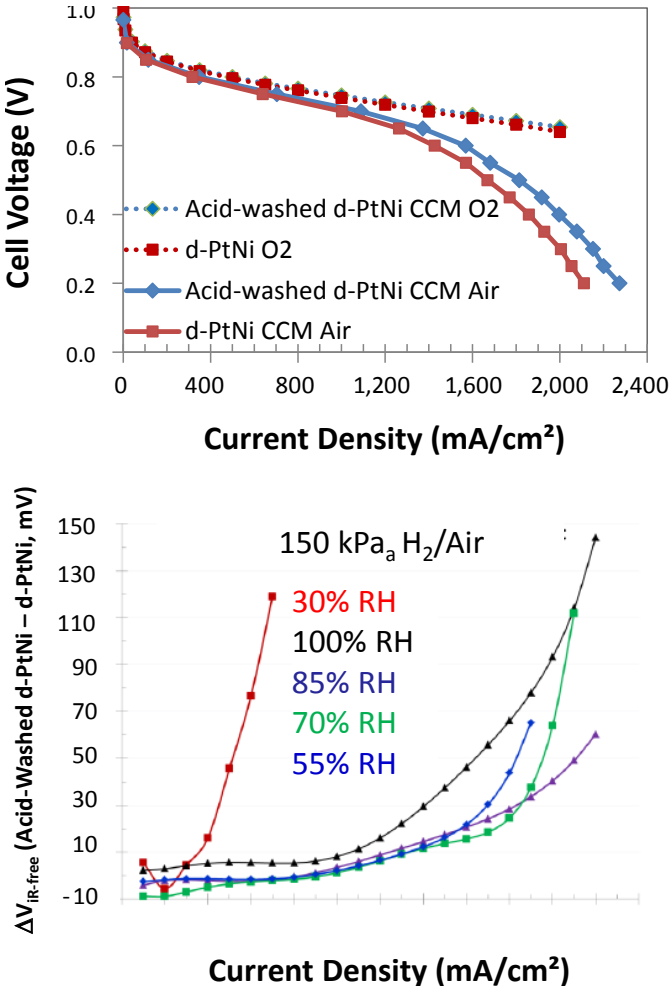

FIGURE 4. Hydrogen-oxygen and hydrogen-air polarization curves (top, 150 kPa_a,100% RH) and the difference between the polarization curves (bottom, air, RH dependence) of as-fabricated and acid-treated MEAs with ~0.1 mg-Pt/cm^2 loading of d-PtNi/C, I/C ratio of 1.2, and using an aqueous ink to fabricate the CCL.

- Functionalization of carbon support with -SO_3H groups improves low RH performance, but decreases catalyst mass activity.

Future Directions

- Conduct acid-treatment and performance testing of a CCM containing a d-PtNi-based cathode made with organic solvent to achieve ≥850 mW/cm^2 at 0.675 V
- Perform USAXS tomography for spatial distribution of agglomerates in catalyst layers, coupled with TEM for ionomer imaging
- Perform nano x-ray tomography for spatial distribution of pore and agglomerates in catalyst layers
- Continue analysis of electrochemical impedance spectroscopy data for proton conductivity of all electrode layer compositions and electrode loss breakdown
- Take solid state cell measurements of permeability of oxygen through ionomer and impact of Ni^{2+} on permeability/solubility
- Complete transport model of electrode layer using imaging results
- Determine causes of loss of mass activity of d-PtNi/C upon functionalization of carbon and develop solutions to mitigate activity loss
- Fabricate and test of CCMs and stack using ink compositions and catalyst and CCM treatments that result in the best overall hydrogen-air performance as a function of RH (40 to 100% RH)

FY 2015 PUBLICATIONS/PRESENTATIONS

1. Perry, Mike L., "Characterization of Polymer Electrolyte Fuel Cells with Ultra-Low Catalyst Loadings," Abstract 1081, Invited Presentation, 226th Electrochemical Society Meeting, October 5–10, 2014.

2. Yang, Zhiwei, and Perry, Mike, "Performance of Advanced Pt-Ni Alloy Catalysts in Polymer-Electrolyte Fuel Cells", Abstract 1020, 226th Electrochemical Society Meeting, October 5–10, 2014.

3. Li, Zhe-Fei; Zhang, Hangyu; Yang, Fan; Stanciu, Lia; Xie, Jian, "Pt Catalysts Supported on Polybenzimidazole-Grafted Graphene for PEMFCs," Abstract 1210, 226th Electrochemical Society Meeting, October 5–9, 2014.

4. Myers, Deborah; Kariuki, Nancy; Hammons, Joshua; Ahluwalia, Rajesh; Xiaohua; Peng, Jui-Kun; Fongalland, Dharshini, "Dealloyed Pt-Ni Polymer Electrolyte Fuel Cell Cathodes: Effects of Catalyst-Ionomer Ink Composition on Structure and Performance," Abstract 1555, 227th Electrochemical Society Meeting, May 24–28, 2015.

5. Xin, Le; Yang, Fan; Li, Zhe-Fei; Sun, Chengjun; Stanciu, Lia; Xie, Jian, "Stability Enhancement of the Interaction between Pt Nanoparticles and Carbon Supports through Carbon Surface Functionalization," Abstract 1557, 227th Electrochemical Society Meeting, May 24–28, 2015.

6. Li, Zhe-Fei; Xin, Le; Yang, Fan; Xie, Jian, "High-Performance Pt Catalysts Supported on Polybenzimidazole-Grafted XC72 for PEMFCs," Abstract 1558, 227th Electrochemical Society Meeting, May 24–28, 2015.

7. Wang, Xiaohua; Peng, Jui-kun; Ahluwalia, Rajesh; Myers, Debbie; and Yang, Zhiwei, "Mass Transfer Overpotentials in Dispersed Pt/C and De-alloyed PtNi/C Polymer Electrolyte Fuel Cell Cathodes," Abstract 1666, 227th Electrochemical Society Meeting, May 24–28, 2015.

8. Li, Zhe-Fei; Zhang, Hangyu; Yang, Fan; Stanciu, Lia; Xie, Jian, "Pt Catalysts Supported on Polybenzimidazole-Grafted Graphene for PEMFCs Catalyst Supports," ECS Trans. 2014 64(3): 131–136.

REFERENCES

1. James, Brian D., "Fuel Cell Vehicle and Bus Cost Analysis," 2015 DOE Hydrogen and Fuel Cells Program Review, Arlington, VA, June 8–12, 2015.

2. (a) Gasteiger, H.A.; Kocha, S.S.; Sompalli, B.; Wagner, F.T., "Activity benchmarks and requirements for Pt, Pt-alloy, and non-Pt oxygen reduction catalysts for PEMFCs." Appl Catal B-Environ., 2005, 56 (1-2), 9–35; (b) Thompsett, D., Pt Alloys as Oxygen Reduction Catalysts. In Handbook of Fuel Cells: Fundamentals, Technology and Applications; Vol. 3, Vielstich, W.; Lamm, A.; Gasteiger, H.A., Eds. John Wiley & Sons: Chichester, 2003; p. 467.

3. (a) Zhang, J.; Lima, F.H.B.; Shao, M.H.; Sasaki, K.; Wang, J.X.; Hanson, J.; Adzic, R.R., "Platinum monolayer on non-noble metal-noble metal core-shell nanoparticle electrocatalysts for O_2 reduction," J Phys Chem B 2005, 109 (48), 22701–22704; (b) Wang, C.; van der Vilet, D.; Chang, K.C.; You, H.D.; Strmcnik, D.; Schlueter, J.A.; Markovic, N.M.; Stamenkovic, V.R., "Monodisperse Pt_3Co Nanoparticles as a Catalyst for the Oxygen Reduction Reaction: Size-Dependent Activity," J Phys Chem C 2009, 113 (45), 19365–19368; (c) Wang, C.; Wang, G.F.; van der Vliet, D.; Chang, K.C.; Markovic, N.M.; Stamenkovic, V.R., "Monodisperse Pt_3Co nanoparticles as electrocatalyst: the effects of particle size and pretreatment on electrocatalytic reduction of oxygen," Phys Chem Chem Phys 2010, 12 (26), 6933–6939; (d) Markovic, N.; Stamenkovic, V., "Nanosegregated Cathode Alloy Catalysts with Ultra-Low Platinum Loading." DOE Fuel Cell Technologies Annual Report 2014; (e) Mani, P.; Srivastava, R.; Strasser, P., "Dealloyed Pt-Cu core-shell nanoparticle electrocatalysts for use in PEM fuel cell cathodes," J Phys Chem C 2008, 112 (7), 2770–2778.

4. (a) Markovic, N.; Stamenkovic, V., "Nanosegregated Cathode Alloy Catalysts with Ultra-Low Platinum Loading," DOE Hydrogen Program Annual Report 2013; (b) Chen, C.; Kang, Y.; Huo, Z.; Zhu, Z.; Huang, W.; Xin, H.L.; Snyder, J.D.; Li, D.; Herron, J.A.; Mavrikakis, M.; Chi, M.; More, K.L.; Li, Y.; Markovic, N.M.; Somorjai, G.A.; Yang, P.; Stamenkovic, V.R. "Highly Crystalline Multimetallic Nanoframes with Three-Dimensional Electrocatalytic Surfaces," Science 2014, 343 (6177), 1339–1343.

5. Kongkanand, A., "High-Activity Dealloyed Catalysts," 2014 DOE Hydrogen and Fuel Cells Program Review, Washington, D.C., June 16–20, 2014.

V.C.3 Novel Structured Metal Bipolar Plates for Low Cost Manufacturing

Conghua "CH" Wang
TreadStone Technologies, Inc.
201 Washington Road
Princeton, NJ 08543
Phone: (609) 734-3071
Email: cwang@TreadStone-Technologies.com

DOE Manager
Jacob Spendelow
Email: Spendelow@lanl.gov

Contract Number: DE-SC0009215

Partner
University of Hawaii, Honolulu, HI

Project Start Date: July 1, 2014
Project End Date: July 1, 2016

Overall Objectives

The technical objective of the Phase II project is to optimize the electrically conductive titanium oxide coating technology that has been developed in the Phase I project, and to demonstrate its performance in an automobile short stack. The objective is to optimize the technology for the full size, high volume production using industrially available physical vapor deposition (PVD) production systems. It will include the titanium alloy target material optimization, PVD process development for the uniform coating, and if it is necessary, a post deposition reactive ion etching (RIE) process to obtain the desired surface composition and microstructure.

Fiscal Year (FY) 2015 Objectives

Task 1: The objective of this task is to identify the best composition of titanium alloy target as the coating material for proton exchange membrane fuel cell applications. The PVD and wet chemical etching process that was developed in the Phase I project will be used in this task for the titanium alloy composition optimization.

Task 2: The objective of the PVD process development is to obtain a uniform Ti alloy thin film (~0.1 μm thick) coating without the wet etching process. The deposition condition will be optimized to avoid or minimize the composition segregation of the Ti alloy coating. Alternatively, if it is difficult to eliminate the composition segregation, plasma non-reactive ion (argon) etching or RIE will be used to obtain the uniform thin film layer of Ti alloy on the stainless steel (SS) substrate. The plasma etching process can precisely control the etching depth and can be easily integrated with the deposition process in the low cost, high volume production system.

Task 3: The objective of this task is to demonstrate full size bipolar plates and conduct the test of the coated stainless steel metal plates in an automotive short stack (20 cells). The stack test will focus on the prestamped plates and TreadStone will apply the nanostructured conductive titanium oxide coating on the stamped plate (poststamping coating).

Technical Barriers

This project addresses the following technical barriers from the Fuel Cells section of the Fuel Cell Technologies Office Multi-Year Research, Development, and Demonstration Plan.

(A) Durability

(B) Cost

(C) Performance

Technical Targets

The targets of the technology development include the following.

- Low electrical contact resistance with gas diffusion layer (<5 mΩ cm)
- Low corrosion resistance: <1 $\mu A/cm^2$
- Low cost: $3/kW by 2017
- Low cost coolant side coating for low contact resistance (<2 mΩ cm) of cathode and anode plates
- Capable of roll to roll coating and postcoating stamping

FY 2015 Accomplishments

In Task 1, we have identified the Ti alloy target materials that have low electrical contact resistance and exceptional corrosion resistance in accelerated stress tests. It was found that the electrical contact resistance and durability of both Ti-Ta and Ti-Nb coated stainless steel can meet DOE's targets. We also finished an 1,100-hour durability test of Ti-Nb coated SS plates in a single cell performance test. There was no degradation of the plates after the test. In Task 2, we have we have compared the properties of direct current magnetron sputtering and cathodic arc deposition processes. It was found that the coating deposited by sputtering has lower electrical resistance and higher durability after a chemical etching treatment. More investigations have also been conducted in

the dry etching process for surface layer modification. It has demonstrated the feasibility of using dry etching for coating surface modification. Ford Motor Company evaluated the performance of the Ti-Nb coated SS plate. Ford duplicated TreadStone's results and agreed to provide a stack for the durability demonstration in an automobile fuel cell stack of Task 3. The detailed stack testing plan was determined and TreadStone is in the process of finishing the coating of the plates provided by Ford for the stack durability test.

✧ ✧ ✧ ✧ ✧

INTRODUCTION

The thrust of the proposed work is to use the nanostructured, electrically conductive titanium oxide layer grown on the titanium alloy surface to protect SS metal plates from corrosion. This technology will go beyond TreadStone's current gold-dot technical solution to meet the latest metal plate technical requirements, which are aimed at cost reduction and performance improvements to guarantee lifetime performance of fuel cell vehicles.

APPROACH

The scope of the Phase II project is focused on the titanium alloy target material development, PVD process development for the titanium alloy surface coating layer deposition. The electrically conductive titanium oxide coating will be grown by thermal oxidization under controlled conditions. The surface layer composition and microstructure will be determined. The coated stainless steel plates will be tested by ex situ evaluation and in situ tests using small (16 cm^2) single cells (Task 1 and 2), and full size, short (20 cells) stack (Task 3) under automobile dynamic driving conditions.

RESULTS

Task 1

In Phase I of the project, we tested the Ti-Nb alloy target with an Nb concentration of 3 at%, 5 at%, and 7 at%. It was found that the Ti-Nb alloy with 3% Nb (Ti-3Nb) has the lowest resistance. It was verified by the phase diagram of Ti-Nb that Ti-Nb will be in single α-phase with the Nb concentration below 2 at%. At higher concentration, a high Nb content ß-phase (up to 40 at% of Nb) will show up. The surface oxide layer on this ß-phase may have a high electrical resistance.

In order to avoid the high Nb content ß-phase in the Ti alloy coating layer, we prepared two types of Ti alloy target with lower (2 at%) dopant element concentration, which are 2 at% Nb (Ti-2Nb) and 2 at% Ta (Ti-2Ta), respectively. These targets were used for the Ti alloy coating on SS foil, using the PVD process. The electrical contact resistance (in the form of through plate resistance, TPR) was measured. The TPR of the as coated SS foil using a sputtering process was very high (300–700 mΩ cm^2, comparing with the target of <10 mΩ cm^2). Surface chemistry analysis indicted that the composition of the bulk of the coating layer is same as the target material, but the surface layer (~10 nm deep) is pure Ti without Nb or Ta alloy element. The reason for this composition segregation on the surface during sputtering process is unknown.

The surface pure Ti layer was removed by a wet chemical etching process using 3% hydrogen fluoride (HF) solution, the same way as that in Phase I of the project, then thermally oxidized in air to obtain a more stable surface oxide layer. The coated SS foil was first evaluated by potentiodynamic and potentiostatic corrosion tests in pH 3 H_2SO_4 + 0.1 ppm HF solution at 80°C. Figure 1 shows the potentiodynamic curves of Ti2Nb and Ti2Ta coated stainless steel (Ti2Nb-SS, Ti2Ta-SS, respectively) with the scanning rate of 10 mV/min. It was found that both Ti2Nb and Ti2Ta coated SS had low corrosion current. The typical transpassivation corrosion peak of stainless steel between 0.8–0.9 V_{NHE} (0.6–0.7 $V_{Ag/AgCl}$) almost disappeared, which indicates that the Ti alloy coating can effectively protect the SS substrate. The corrosion current of Ti2Ta coated SS is much lower than that of Ti2Nb coated SS, which could indicate that the Ti2Ta-SS has a better corrosion resistance than that of Ti2Nb-SS.

The curves of the potentiostatic test of Ti2Nb-SS and Ti2Ta-SS are shown in Figure 2. It shows that the corrosion

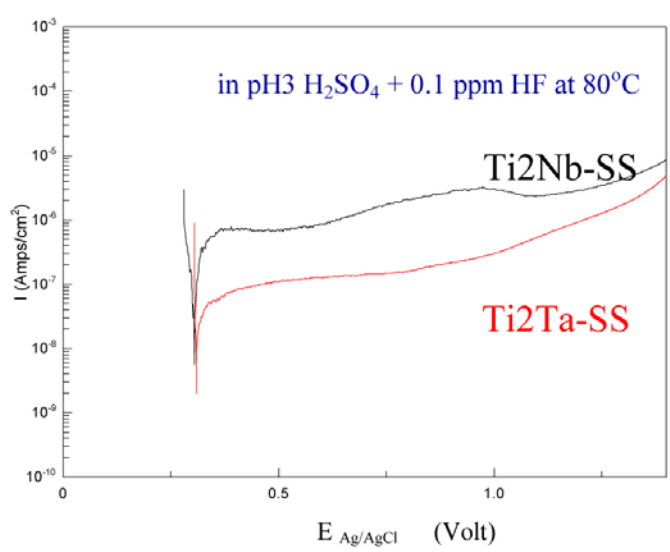

FIGURE 1. Potentiodynamic curves of Ti2Nb-SS and Ti2Ta-SS with the scan rate of 10 mV/min

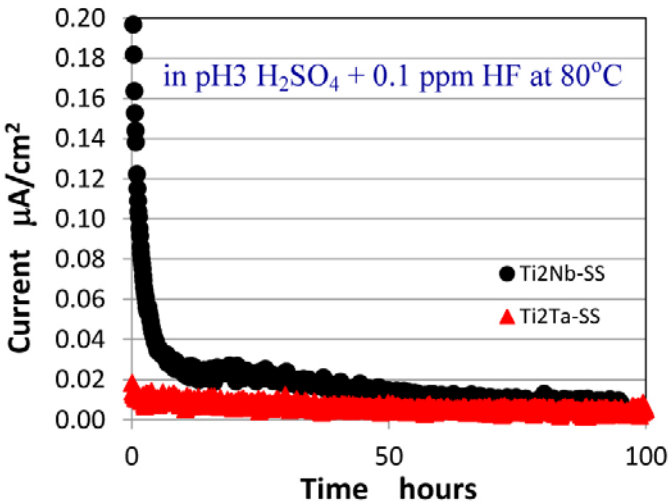

FIGURE 2. Potentiostatic curves of Ti2Nb-SS and Ti2Ta-SS under the polarization of potential of 0.8 V_{NHE}

current of both Ti2Nb-SS and Ti2Ta-SS are very low (<0.2 µA/cm^2) which easily meet the target defined by DOE (<1 µA/cm^2). As with the potentiodynamic test, Ti2Ta-SS has a lower corrosion current than that of Ti2Nb-SS.

The electrical properties of Ti2Ta-SS and Ti2Nb-SS were compared by the TPR measurement with the plate in contact with TGP-H-060 Toray Paper. The TPRs of the Ti-2Nb and Ti-2Ta coated SS are lower than that of Ti-3Nb coated SS developed in Phase I of the project. The TPR difference between Ti-2Nb and Ti-3Nb is more significant after 1.6 V_{NHE} corrosion test in pH 3 H_2SO_4 - 0.1 ppm HF solutions at 80°C. As shown in Figure 2, Ti-2Nb coated SS has a lower resistance after the test despite the much longer corrosion time (24 hours) than that of Ti-3Nb (6 hours).

It was found in Phase I that the thermally oxidized Ti alloy coated SS has much better stability under the high potential corrosion conditions for proton exchange membrane fuel cells, despite the fact that the thermally oxide plates have higher electrical resistance. The higher stability of the oxidized coating may lead to the potential benefit that the thermally oxidized plate resistance at the end of life is lower than that of nonoxidized plates. Therefore, this process is continually used in this phase of the project. The thermal oxidization of the coated SS increases TPR compared to the etched plates. But the increase of Ti-2Nb coated SS is much smaller than that of Ti-3Nb coated SS. The corrosion stability of Ti-2Nb coated and oxidized SS was evaluated with the electrochemical corrosion test at 0.8 V_{NHE}, 1.6 V_{NHE} and 2.0 V_{NHE} in pH 3 H_2SO_4 - 0.1 ppm HF solutions at 80°C for 24–100 hours. It was found that the thermally oxidized Ti-2Nb coated SS is very stable. It did not have a TPR increase after those corrosion tests (within measurement error). In comparison, Ti-3Nb coated SS had shown a TPR increase after 0.8 V and 1.6 V corrosion tests as reported in Phase I of the project. The hypothesis is that the high Nb content ß-phase is left on the surface after etching process will grow a high Nb content surface oxide layer. This oxide surface layer may have high electrical resistance and the resistance will keep increasing during corrosion due to the thickness increase of the oxide surface layer. On the other hand, the elimination of the ß-phase in Ti-2Nb successfully avoids this issue.

The Ti2Nb alloy coated stainless steel plates were further evaluated in a single cell durability test. The cell hardware was from Fuel Cell Technologies, with 16 cm^2 active area and serpentine flow field design. The cell was tested around 30°C at constant current (maintain the cell voltage between 0.70 V and 0.75 V). The total test time was 1,100 hours. The surface contact resistance of the plate was measured with TGP-H-060 Toray Paper before and after the single cell durability test. Figure 3 shows the cell voltage curve during the test and Figure 4 shows the comparison of the electrical contact resistance of the cathode and anode plates before and after the single cell test. It shows that the surface contact resistance of the plates (with flow field channels) is below 4 mΩ cm^2 at 150 psi, which meets DOE's target (<10 mΩ cm^2). After the 1,100-hour test in single cell, there was no contact resistance increase.

Task 2

In this period, we have evaluated the Ti alloy coating using sputtering and cathodic arc deposition process. The TPR of as coated SS foils was measured. It was found that between the as coated stainless steel plate, sputtering coated

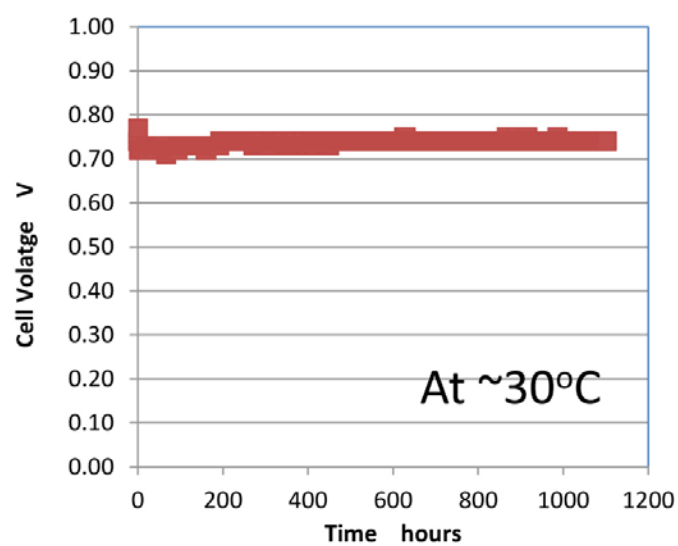

FIGURE 3. Comparison of TPR of Ti-2Nb, Ti-2Ta, and Ti-3Nb coated stainless steel foil

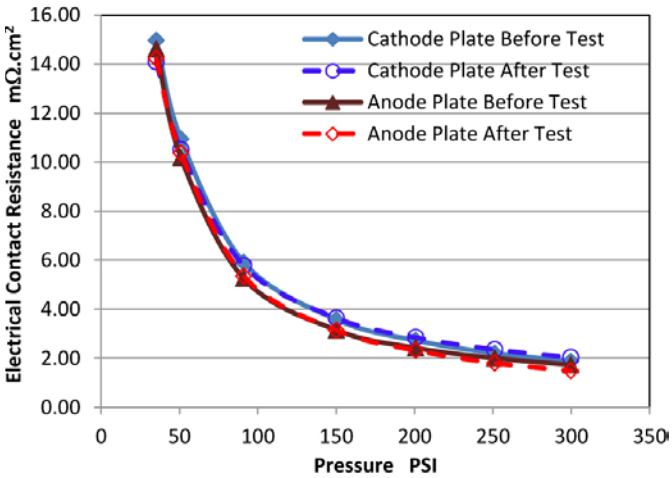

FIGURE 4. Comparison of TPR of Ti-2Nb and Ti-3Nb coated stainless steel foil after corrosion test at 1.6 V_{NHE}

TABLE 1. TPR (mΩ cm^2) Comparison of As-Coated SS with Ti-2Nb Alloy Using Sputtering and Cathode Arc Methods

Pressure PSI	35	51	91	150	201	250	300
Sputtering	1,037.33	806.95	633.21	479.48	399.86	329.19	274.14
Cathodic Arc	38.74	27.22	14.35	8.36	6.12	4.81	4.02

SS has much higher TPR than that of cathodic arc coated SS, as shown in Table 1.

On the other hand, sputtering can deposit a very thin coating layer and has a high target utilization rate for low cost production. Cathodic arc coated surface is very rough, with many micron-scale particles on the surface. The surface chemistry analysis by X-ray photoelectron spectroscopy indicates that the surface layer of SP-Ti2Nb-SS does not contain niobium, but the surface layer composition of cathodic arc coated Ti2Nb-SS (CA-Ti2Nb-SS) is the same as the target material (2 at% of Nb in Ti).

Despite the lower TPR of the as-coated cathodic arc coated Ti2Nb-SS, its TPR will increase after the corrosion test due to the continuous growth of the titanium oxide surface layer. The through plate resistance after 2 V_{NHE} 24-hour corrosion is near 50 mΩ cm^2, which does not meet DOE's target. Thermal oxidization can stabilize the surface oxide layer, but the TPR of a CA-Ti2Nb-SS plate is 33 mΩ cm^2 at 150 psi, that does not meet DOE's target. Wet etching of CA-Ti2Nb-SS could reduce the TPR, but the TPR of a thermally oxidized plate (23.8 mΩ cm^2) still can't meet the requirement. In addition, the TPR will keep increasing after the corrosion test (to 30.3 mΩ cm^2 after 0.8 V_{NHE} 70 hours). The reason for the higher TPR and unsatisfied stability of cathodic arc deposited coating is not clear, further development is needed to invest the feasibility of using cathodic arc as the coating method. At this stage of the project, we will focus on sputtering deposition despite the surface composition segregation issue.

It was found that the surface layer composition of the sputtered Ti-2Nb coating is pure Ti. Nb only exists in the subsurface layer (below 10 nm from the surface). A chemical etching step is necessary to obtain the Ti alloy on the coating surface. In this project, different etching methods have been evaluated, including wet etching using diluted HF solution, and vacuum etching (dry etching) using various chemicals. Dry etching uses fluorine or chlorine containing compounds that can react with titanium in a vacuum. Because of the high vapor pressure of titanium fluoride and titanium chloride, the reaction product can be continually removed from the plate surface and maintain the continuing etching process. This process has been readily used in the semiconductor industry. Compared to wet etching, dry etching is more controllable to remove very thin layer (nanometers). In addition, dry etching has the advantage to be easily integrated with the PVD process as a one-pass coating/surface treatment process for low cost manufacturing.

We evaluated three dry etching processes. One uses XeF_2 vapor; the second uses HF-H_2O vapor at low vacuum. The third uses plasma reactive ion etching using CF_4. Vapor etching has the advantage of low capital cost but may have the challenge of the uniform etching of large size plate in high volume production because of mass transport limitations. On the other hand, plasma etching generates the reactive species between electrodes. It is easier to achieve uniform etching with the planar electrode reactors.

The TPRs of XeF_2 (with Ar as carrier gas), HF-H_2O vapor and CF_4 plasma etched Ti-2Nb coated SS plates are shown in Figure 5. It was found that all three methods can effective reduce the TPR of Ti-2Nb coated SS plates. This experiment shows the feasibility of postdeposition surface

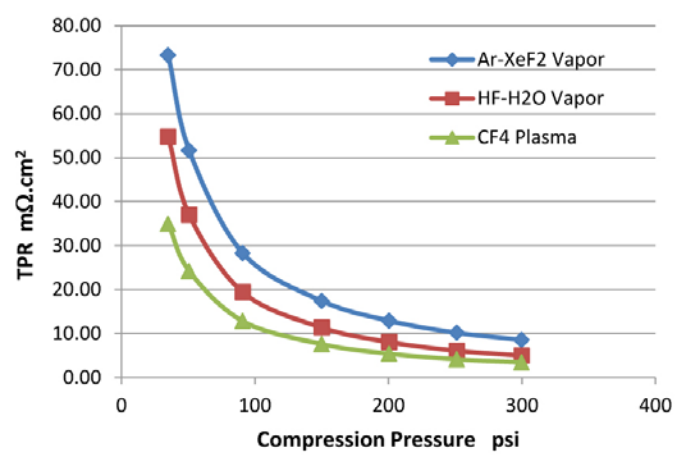

FIGURE 5. Comparison of TPR of Ti-2Nb coated dry etched using different processes

modification using the dry etching process. Although its TPR is not as low as the as wet etched Ti-2Nb coated SS, the resistance can still meet the application requirements (<10 mΩ cm^2) using HF vapor and plasma etching processes. Further corrosion resistant tests of these coated materials will be conducted in the following months of the project.

It was found that XeF_2, HF vapor etching and plasma enhanced RIE can effectively remove titanium alloy. However, it was found that the etching rate for Ti is much higher than that of Nb and Ta. The Nb and Ta concentration of the dry etched surface layer is very sensitive to the etching condition, and difficult to control. We have detected the Nb concentration up to 20–50% on the dry etched surface. The electrical contact resistance of such high alloy content surface is too high for proton exchange membrane fuel cell applications.

Another phenomenon we have observed in dry etching is the impurity enrichment on the surface. The typical metallic impurity in titanium is iron. Because of the low vapor pressure of iron fluorite and chloride, iron cannot be removed in dry etching. Other minor impurities may have the same issue in the dry etching process. Figure 6 is a scanning electron microscope (SEM) picture of a plasma RIE treated Ti2Nb coated SS surface. It clearly shows the grain boundary of the Ti2Nb coating layer. At higher magnification, it seems that the grain boundary stands out of the grain surface. The hypothesis is that the etching rate of the grain boundary is slower than that of the grain because of the enrichment of iron and other impurities with low etching rates. The stand-out grain boundary may have a negative impact to the surface charge of the plate with the gas diffusion layer.

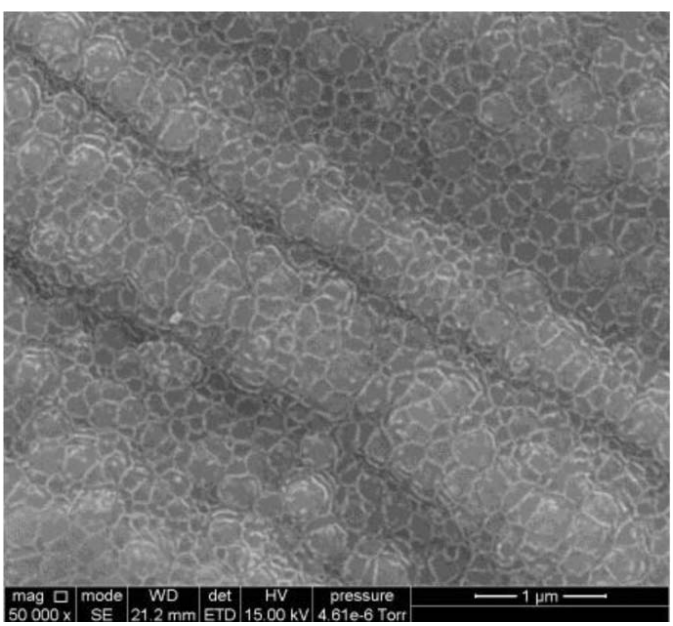

FIGURE 6. SEM picture of RIE treated surface of Ti-2Nb coated stainless steel

Task 3

After demonstrating the superior stability and low electrical resistance of the coated stainless steel plates, we sent the Ti2Nb alloy coated SS samples to Ford for their evaluation. After ex situ corrosion and electrical contact resistance tests, they were satisfied with the performance of TreadStone's coating and agreed to provide metal plates and membrane electrode assemblies (MEAs) for the stack durability test for the project. The plate will use Ford's standard design, instead of the latest high performance flow field design to protect their intellectual properties. However, Ford only has a limited amount of MEAs for this plate design and it is difficult to obtain new MEAs from their supplier, W.L. Gore. So, Ford recommended the following adjustments in the stack test plan.

- Test a 10-cell short stack, with power of 2–2.5 kW.
- Ford will assemble the stack, conduct the initial performance test (~100 hours) before it ships to the University of Hawaii.
- The University of Hawaii will conduct a 1,500–2,000-hour test, depending on the MEA degradation rate. No plates will be taken out during the test.
- Testing protocol is the combined public drive cycles, e.g., Environmental Protection Agency (city and highway) and New European Drive Cycle.
- The stack will be sent back to Ford for inspection after the 1,500–2,000-hour test.
- If the performance is satisfactory and Ford still has available MEAs, the stack may be assembled again with new MEAs for the second 1,500–2,000-hour test.

Ford sent 20 pieces of formed bipolar plates to TreadStone for coating in June 2015. However, we experienced issues in the Ti-2Nb alloy sputtering with our PVD partner in June and July. The coated SS plates are more difficult to etch compared with the plates coated in the early part of the project, and the finished plates have high resistance. TreadStone processed over ten batches of Ti alloy coated SS through the project before processing the bipolar plates from Ford. All of these batches were processed between October and April; the humidity was low in the northeastern United States and none of those batches had etching problems. We learned from the PVD partner that their system took a longer time to reach the desired vacuum for the process in the latest batches in June and July. The hypothesis is that high humidity in the summer has an impact on the coating properties. There is a coating on the inner wall of the vacuum chamber in the PVD system. It may absorb moisture from air during the loading/unloading period, then it may slowly release water vapor during the Ti alloy deposition process and lead to the high oxygen content in the alloy coating. The etching behavior of the high oxygen

content Ti alloy layer could be different from the normal coating because of the big difference of the etching rate of titanium metal and titanium oxide.

Due to the limitation of its system, TreadStone decided to wait to resume plate coating until September/October, when humidity is lower in the Northeast.

CONCLUSIONS AND FUTURE DIRECTIONS

The stable performance of the Ti-2Nb and Ti-2Ta coated stainless steel at high potential (1.6 V_{NHE} and 2.0 V_{NHE}) is very significant for the practical application in proton exchange membrane fuel cells. It means that this coating has the capability to withhold the high potential transient conditions, which is the key barrier for precious metal free coating technologies, such as nitride and graphite coatings.

The dry etching process can be used to optimize the surface chemistry composition. But it has to be carefully controlled so that only a very thin (nanometers) layer is removed to avoid too high an Nb or Ta concentration and minimize the impurity enrichment on the Ti alloy surface.

V.C.4 Advanced Ionomers and MEAs for Alkaline Membrane Fuel Cells

Bryan Pivovar (Primary Contact), Matt Sturgeon, Zbyslaw Owczarczyk, Hai Long
National Renewable Energy Laboratory (NREL)
15013 Denver West Parkway
Golden, CO 80401
Phone: (303) 275-3809
Email: Bryan.Pivovar@nrel.gov

DOE Manager
Dave Peterson
Phone: (720) 356-1747
Email: david.peterson@ee.doe.gov

Subcontractors
- Shimshon Gottesfeld (PI), Dario Dekel
  CellEra, Inc., Caesarea, Israel
- Mike Yandrasits (PI), Krzysztof Lewinski, Steve Hamrock
  3M, St. Paul, MN
- Andy Herring (PI), Mei-chen Kuo, Zachary Page-Belknap
  Colorado School of Mines (CSM), Golden, CO

Project Start Date: April 22, 2013
Project End Date: December 31, 2015

Overall Objectives

- Synthesize novel perfluoro (PF) anion exchange membranes (AEMs) with high temperature stability and high water permeability
- Employ high performance PF AEM materials in electrodes and as membranes in alkaline membrane fuel cells

Fiscal Year (FY) 2015 Objectives

- Produce at least two square meters of novel PF AEM membranes for systematic studies of properties including mechanical and chemical stability
- Demonstrate membrane electrode assemblies (MEA) performance >350 mW/cm^2 employing novel PF AEMs in CO_2 free environments

Technical Barriers

This project addresses the following technical barriers from the Fuel Cells section (3.4.4) of the Fuel Cell Technologies Program's Multi-Year Research, Development, and Demonstration (MYRDD) Plan:

(A) Durability (of membranes and membrane electrode assemblies)

(B) Cost (of membranes and membrane electrode assemblies)

(C) Performance (of membranes and membrane electrode assemblies)

Technical Targets

This project will synthesize novel PF AEMs and ionomers and incorporate these MEAs for fuel cell testing. The project generally supports targets outlined in the MYRDD Plan in application specific areas (portable, stationary, transportation). However, as alkaline membrane fuel cells are at an earlier stage of development, specific target tables have not yet been developed. There are two tasks in the Technical Plan of the MYRDD Plan for alkaline membranes, this project seeks to address both.

TABLE 1. Tasks Addressed from the Technical Plan of the MYRDD Plan for Alkaline Membranes

	Task
1.4	Demonstrate an anion-exchange membrane that retains 99% of original ion exchange capacity for 1,000 hours in hydroxide form at T > 80°C. (2Q 2013)
3.8	Demonstrate anion-exchange membrane technologies in MEA/single cells with non-PGM catalysts that maintain performance higher than 350 mW/cm^2 for 2,000 hours at T > 80°C. (4Q, 2016)

PGM—precious group metals

FY 2015 Accomplishments

- The project has explored multiple PF AEM chemistries for amide and aryl/alkyl linkages (Grignard).
- We have improved our polymer synthesis and membrane casting.
- We have isolated zwitterionic polymers from amide linkages as a key limiting factor for polymer electrolyte performance and have developed methylation strategies to mitigate.
- We have further investigated novel Grignard chemistry, and have shown perfluoro sulfonyl fluoride precursor (PF-SFP) solubility and Grignard viability in hydrofluoro ethers (HFEs).
- We have developed and applied models to evaluate carbonate uptake/poisoning in alkaline membrane fuel cells (AMFCs).
- We have synthesized significant quantities of methylated polymers (>100 g) and supplied to 3M for dispersion preparation and membrane casting.
- We have obtained initial fuel cell performances ~100 mW/cm^2 with novel PF AEM-based fuel cells.

INTRODUCTION

AMFCs are of interest primarily because they enable the use of non-Pt catalysts, the primary cost/supply limitation of proton exchange membrane fuel cells. AMFCs, therefore, offer the potential of greatly decreased polymer electrolyte fuel cell cost. Operating AMFCs under ambient conditions where carbon dioxide is present remains a challenge due to carbonate formation. An approach that has shown promise for carbon dioxide tolerance is increased operating temperature. Unfortunately, the stability of the cation side chains on the membrane polymer and water management within the membrane both become more difficult as temperature rises.

The use of perflourinated ionomers, similar to those used in proton exchange membrane systems, with tethered hydroxide conduction cation head groups should help improve water transport properties and offer exceptional chemical durability of the backbone. The significant advances demonstrated in AMFC systems have been accomplished primarily through improving water management and the bonding between membrane and electrode. Both issues can be tackled much more effectively when employing PF AEMs and ionomers. The project consists of three sub-tasks: (1) synthesis of novel perfluorinated alkaline ionomers (NREL, CSM, 3M); (2) developing membranes and dispersions (3M, NREL); and (3) MEA fabrication and fuel cell testing (CellEra, 3M, NREL).

APPROACH

The team will focus on achieving higher temperature, higher power density AMFC operation through implementation of novel alkaline PF membranes and ionomeric dispersions. The PF materials proposed are expected to enhance water transport capabilities and electrode performance/durability significantly, thereby enabling higher temperature and power density operation. The combination of high current density and operating temperature will improve the ability of these devices to tolerate ambient CO_2 and potentially enabling complete tolerance to these conditions. Starting with the sulfonyl fluoride form of current PF ionomers we have identified, and in several cases verified, the ability to convert commercially available precursors into anion exchange polymers and membranes. The synthesized PF ionomers have been cast into membranes, made into polymeric dispersions, and characterized in fuel cell tests.

RESULTS

While PF chemistry improves PF sulfonic acidity, the strongly electron withdrawing PF backbone creates challenges for anion exchange membranes. From the readily available PF-SFP, different strategies can be employed to tether cations to the PF-SFP. We have focused on two, an amide linkage and an aryl/alkyl linkage employing Grignard reagents, shown in Figure 1. As of the 2014 Annual Merit Review, we had synthesized many grams of amide linked polymer, cast films and shown good water uptake and conductivity in halide salt form membranes [1]. Early polymers were difficult to dissolve and cast into high quality films, however, improved synthesis resulted in better solutions and pilot scale casting. Testing of these early membranes resulted in poor hydroxide conductivity, but reasonably high halide ion conductivity that was recoverable following ion exchange, shown in Figure 2. This behavior was unexpected due to the higher mobility of hydroxide than chloride in aqueous media. The unexpected behavior has been attributed to a weakly acidic proton on the sulfonamide

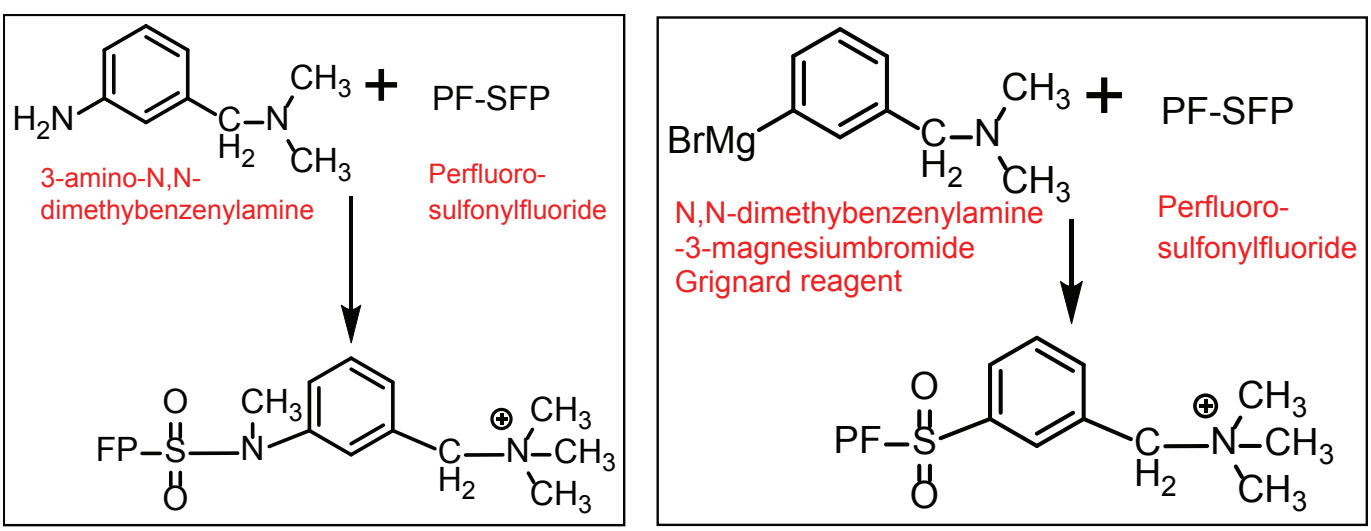

FIGURE 1. Strategies for attaching cationic groups to PF-SFP through amide (left) and Grignard chemistries

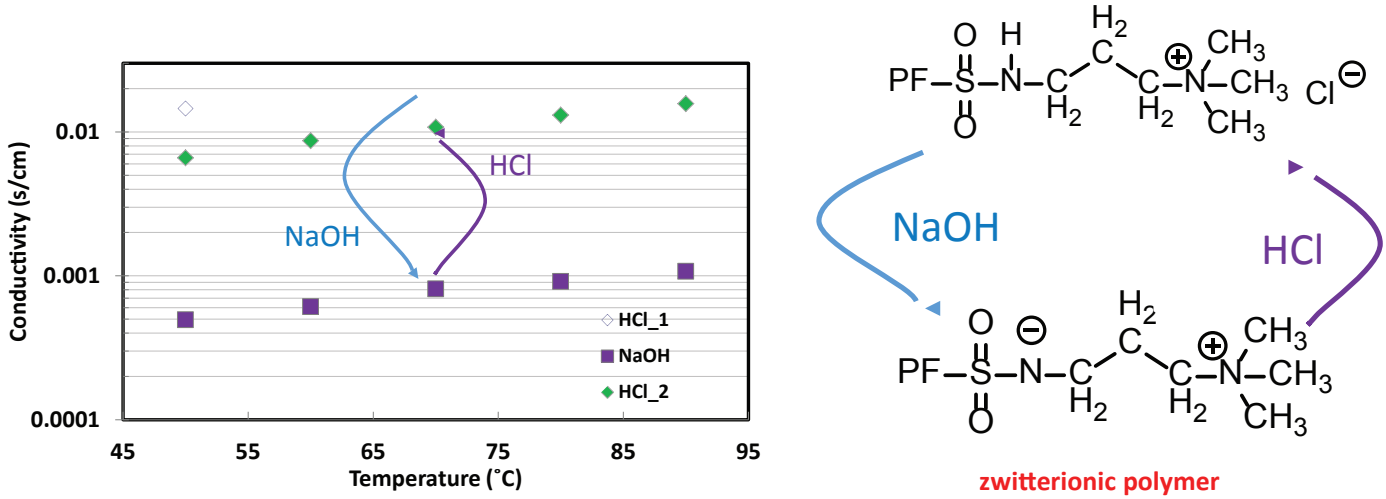

FIGURE 2. Conductivity of amide linked PF AEMs for samples in chloride form, hydroxide form, and chloride form again (left); Schematic representation of chemical structures and ion exchange that led to low conductivity zwitterionic polymers in the hydroxide form and high conductivity chloride ion form polymers (right)

linkage that forms a zwitterionic polymer upon exposure to base, also shown in Figure 2. As target polymers depend on having free hydroxide available and the zwitterionic nature of the polymer was unacceptable for required fuel cell performance, we set about modifying our chemical synthesis approaches to either replace this acidic proton through substitution or remove it entirely by exploring synthesis strategies beyond sulfonamide linkages.

While other non-amide-based synthesis routes have been explored, initial results have shown promise through methylation of the sulfonamide linkage. Through a modified chemical synthesis approach, we have confirmed methylation of the sulfonamide linkage and high hydroxide conductivities of PF AEMs. Membranes cast from these modified synthesis conditions have resulted in liquid equilibrated conductivities of ~17 mS/cm in the chloride form and ~55 mS/cm in the hydroxide form and have maintained similar conductivities when exchanged between chloride and hydroxide form at room temperature. These materials have been processed into MEAs and tested in fuel cells. Figure 3 shows a polarization curve of the methylated, amide-linked PF AEM materials at 60°C under H_2/O_2, fully humidified conditions. The sample shows good open circuit voltage but high ohmic resistance and poor high current density performance. The sample shown was prepared by applying the electrodes directly to the gas diffusion layer, but alternate fabrication routes (direct painting, decal transfer) showed similar performances. The high resistance of the cells (>0.4 ohm/cm^2) and the relatively poor durability are current areas of focus. A key concern for the non-amide-based synthesis route is solubility of polymers. We have introduced HFEs and demonstrated the ability to both improve solubility and perform select target chemistries using HFEs.

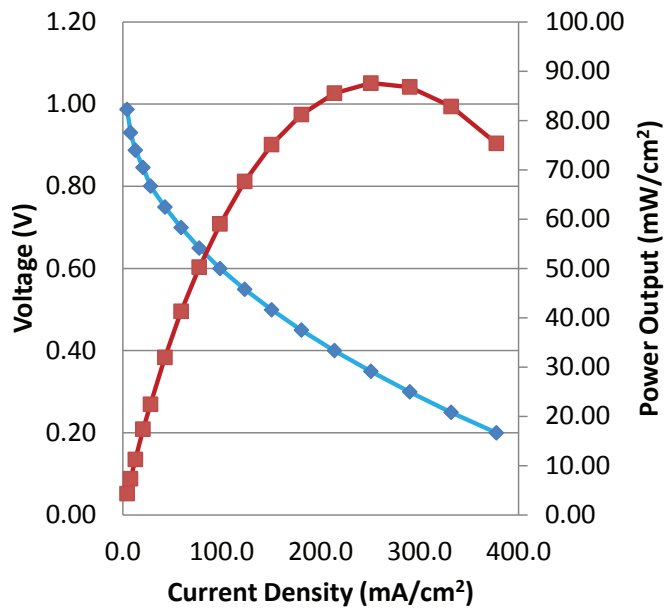

FIGURE 3. AMFC performance of methylated, amide-linked PF AEM

Carbonate formation is a known source of performance loss for hydroxide conducting fuel cells. Scrubbing CO_2 from air has been employed as a mitigation technique, but self-purge has also been promoted as a viable approach to prevent carbonate related losses. Fundamentally, the carbonate/bicarbonate/hydroxide equilibrium is poorly understood. In order to address the concern presented by carbonate poisoning and the limits of the self-purge approach, we have developed a carbonate uptake model that can be employed with a fuel cell model to determine boundary conditions that impact AMFC performance. Figure 4 shows model

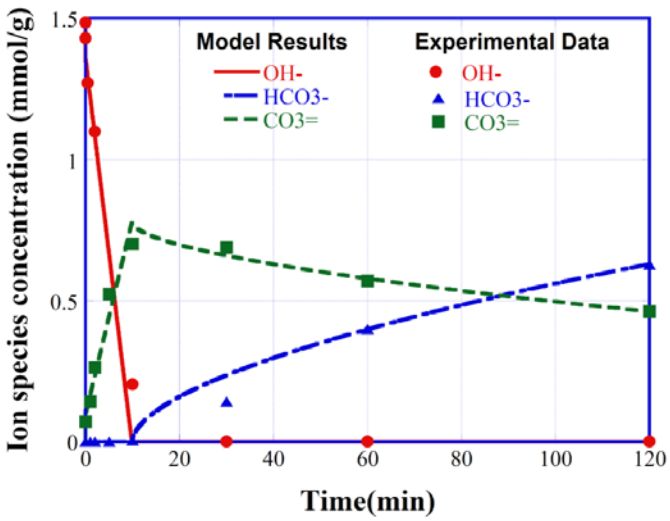

FIGURE 4. Modeling of carbonate formation and equilibrium in AEMs, experimental data from Yangai, et al. [2]

results at room temperature with experimental data for carbonate uptake from the literature [2]. The results show good agreement with experiment and can be used to explore parametric studies to determine the impact of carbonate formation in AMFC systems.

CONCLUSIONS AND FUTURE DIRECTIONS

The project has demonstrated multiple PF AEM chemistries. We have determined that initial amide linked materials were zwitterionic in nature and therefore did not possess required conductivity in the hydroxide form. We improved methylation strategies and now have polymer membranes in hand for further studies. We have determined that HFEs are good solvents under specific conditions for the PF-SFP materials. This has allowed additional chemistries to be probed in a known solvent for the PF-SFP materials. Polymers/membranes have been characterized using a variety of techniques including infrared, nuclear magnetic resonance, thermal gravimetric analysis, differential scanning calorimetry, conductivity, and water uptake.

- Membrane Synthesis
  - Improved methylation/secondary amine tethering for non-protic sulfonamide linkage
  - Grignard (or related) chemistry in HFEs
- Characterization
  - Continued characterization along the lines of that currently on-going
- Modeling
  - Parametric studies looking at temperature, membrane thickness, and CO_2 concentration
- Dispersion Preparation, Membrane Casting, MEA Fabrication/Fuel Cell Testing
  - Continued testing with current and next generation materials
  - Focus on improved electrode fabrication and high cell resistance

FY 2015 PUBLICATIONS/PRESENTATIONS

1. Pivovar, B. (Nov., 2014). "Fuel Cell R&D focused on Alkaline Membranes and Advanced Catalysis at the National Renewable Energy Lab," Presented at Wuhan University, Wuhan, China, Nov. 12, 2014.

2. Pivovar, B. (Nov., 2014). "Fuel Cell R&D focused on Alkaline Membranes and Advanced Catalysis at the National Renewable Energy Lab," Presented at Dalian Institute of Chemical Physics, Dalian, China, Nov. 13, 2014.

3. Pivovar, B. (March, 2015). "Past, Current, and Future Research in Polymer Electrolyte Fuel Cells," Presented at University of Colorado – Denver, Denver, CO, March 6, 2015.

4. Pivovar, B. (April, 2015). "Past, Current, and Future Research in Polymer Electrolyte Fuel Cells," Presented at University of Wyoming, Laramie, WY, April 2, 2015.

REFERENCES

1. B. Pivovar, 2014 AMR, "Advanced Ionomers & MEAs for Alkaline Membrane Fuel Cells," http://www.hydrogen.energy.gov/pdfs/review15/fc108_pivovar_2015_o.pdf.

2. Yanagi, H. and K. Fukuta, ECS Transactions, 2008. 16(2): p. 257-262.

V.D.1 Roots Air Management System with Integrated Expander

Dale Stretch (Primary Contact), Brad Wright
Eaton Corporation
W126N7250 Flint Drive
Menomonee Falls, WI 53051-4404
DUNS: 360921261
Phone: (248) 226-6799
Email: DaleAStretch@Eaton.com

DOE Manager
Jason Marcinkoski
Phone: (202) 586-7466
Email: Jason.Marcinkoski@ee.doe.gov

Contract Number: DE-EE0005665

Subcontractors
- Ballard Power Systems, Burnaby, BC
- Kettering University, Flint, MI
- Electricore, Inc., Valencia, CA

Project Start Date: July 5, 2012
Project End Date: December 31, 2015

Overall Objectives

- Primary Objectives
  - 62/64% (baseline 2011) > 65/70% (target 2017) Compressor/expander efficiency at 25% of full flow
  - 80% (baseline 2011) > 90% (target 2017) Combined motor/motor controller efficiency full flow
  - 11.0/17.3 kW (baseline 2011) < 8/14 kW (target 2017) Compressor/expander input power at 100% of full flow
- Secondary Objectives
  - Meeting all 2017 project target objectives in Table 1
  - Conduct a cost reduction analysis to identify areas for additional possible cost reductions

A fully tested and validated technology readiness level (TRL) 7 air management system hardware capable of meeting the 2017 project targets in Table 1 will be delivered at the conclusion of this project.

Fiscal Year (FY) 2015 Objectives

- Complete plastic expander rotors development and final assessment of Eaton's all plastic expander
- Complete performance and validation testing on the complete air system per predefined test plan approved by DOE
- Baseline Ballard HD7 fuel cell as benchmark for assessing Eaton's Air Management System
- Assess the performance capability of Eaton's Air Management System on Ballard HD7 fuel cell per predefined test plan approved by the DOE
- Provide system test data for Argonne National Laboratory for model development and verification
- Document Eaton's Air Management System performance capability in test report

Technical Barriers

This project addresses the following technical barriers from the Fuel Cells section of the Fuel Cell Technologies Office Multi-Year Research, Development, and Demonstration Plan:

(B) Cost: Reduce by ~50%

(C) Performance
- Reduce power by ~30%
- Motor Efficiency: Increase by ~40%
- Compressor Efficiency: Increase by ~5%
- Expander Efficiency: Increase by ~9%

Technical Targets

At the conclusion of this project, a fully tested and validated TRL 6 air management system hardware capable of meeting the 2017 project targets in Table 1 will be delivered.

FY 2015 Accomplishments

- End of Period 2 Conclusions
  - Delivered final prototype of the compressor/expander assembly with integrated motor
  - Delivered compressor/expander validation test report which included expander, motor and compressor, wet and dry maps, system maps, and acceleration and acoustic noise test results
  - Successfully demonstrated twisted plastic rotors in compressor and expander environment
  - Worked on developing a high compression ratio (3.0) roots compressor with minimal efficiency losses using low thermal growth material; fabrication process prevented complete evaluation; many

TABLE 1. 2015 and 2017 Project Targets

Characteristic	Units	Current Status	Project Target 2015	DOE Target 2017
Input power[a] at full flow[b] (with expander/without expander)	kWe	9.9/13.8	8/14	8/14
Combined motor & motor controller efficiency at full flow[b]	%	90	90	90
Compressor/expander efficiency at full flow (C/E only)[b]	%	68/64	75/75	75/80
Input power at 25% flow[c] (with expander/without expander)	kWe	1.3/1.7	1.0/2.0	1.0/2.0
Combined motor & motor controller efficiency at 25% flow[c]	%	70	80	80
Compressor / expander efficiency at 25% flow[c]	%	61/70	65/70	65/70
Input power at idled (with/without expander)	We	TBD/270	200/200	200/200
Combined motor/motor controller efficiency at idle[d]	%	TBD	?	70
Compressor/expander efficiency at idle[d]	%	TBD	60/60	60/60
Turndown ratio (max/min flow rate)		20	20	20
Noise at maximum flow (excluding air flow noise at air inlet and exhaust)	dB(A) at 1 meter	65 (with enclosure & suppression)	65 (with enclosure & suppression)	65
Transient time for 10–90% of maximum airflow	sec	1	1	1
System volume[e]	liters	15	15	15
System weight[e]	kg	16	15	15
System cost[f]	$	TBD	500	500

[a] Electrical input power to motor controller when bench testing fully integrated system. Fully integrated system includes control system electronics, air filter, and any additional air flow that may be used for cooling.
[b] Compressor: 92 g/s flow rate, 2.5 bar (absolute) discharge pressure; 40°C, 25% RH inlet conditions. Expander: 88 g/s flow rate, 2.2 bar (absolute) inlet pressure, 70°C, 100% RH inlet conditions
[c] Compressor: 23 g/s flow rate, minimum 1.5 bar (absolute) discharge pressure; 40°C, 25% RH inlet conditions. Expander: 23 g/s flow rate, 1.4 bar (absolute) inlet pressure, 70°C, 100% RH inlet conditions
[d] Compressor: 4.6 g/s flow rate, minimum 1.2 bar (absolute) discharge pressure; 40°C, 25% RH inlet conditions. Expander: 4.6 g/s flow rate, < compressor discharge pressure, 70°C, 20% RH inlet conditions
[e] Weight and volume include the motor, motor controller and system enclosure.
[f] Cost target based on a manufacturing volume of 500,000 units per year
[g] DTI cost model of the Honeywell 100,000 rpm machine, 2.5 bar (absolute), 92 g/s, dry air, 40°C: $960 including markup. TIAX, LLC 2009 estimate of Honeywell technology (compressor, expander, motor, motor controller) presented at 2010 Annual Merit Review and Peer Evaluation: $790 including 15% markup.
RH—relative humidity; TBD - to be determined

lessons learned on how to fabricate correctly; second attempt will have a much higher level of success

- Beginning of Period 3 Conclusions
  - Built and tested two sets of Eaton's Air Management Systems for Ballard testing
  - Experimented with injecting water at the compressor inlet Eaton's Air Management System as a potential replacement to the fuel cell humidifier
  - Baselined the HD7 system using the existing air system for comparison to Eaton's Air Management System

✧ ✧ ✧ ✧ ✧

INTRODUCTION

Proton exchange membrane (PEM) fuel cells remain an emerging technology in the vehicle market with several cost and reliability challenges that must be overcome in order to increase market penetration and acceptance. Some of the major technological barriers that must be overcome include DOE's identification of the lack of a cost effective, reliable, and efficient air supply system that meets the operational requirements of a pressurized PEM 80-kW fuel cell. This project will leverage roots blower advancements and develop and demonstrate an efficient and low cost fuel cell air management system. Eaton will build upon our newly developed P-Series roots blower and shift the peak efficiency, making it ideal for use on an 80 kW PEM module. Advantages to this solution include the following.

- Lower speed of the roots blower eliminates complex air bearings present on other systems
- Broad efficiency map of roots systems provide an overall higher drive cycle fuel economy
- Core roots machine technology has been developed and validated for other transportation applications

Eaton will modify its novel R340 Twin Vortices Series (TVS) roots-type supercharger for this application. The TVS delivers more power and better fuel economy in a smaller package as compared to other supercharger technologies. By properly matching the helix angle with the rotor's physical aspect ratio, the supercharger's peak efficiency can be moved to the operating range where it is most beneficial for the application. The compressor will be designed to meet the 92 g/s flow at a pressure ratio of 2.5, similar in design to the R-Series 340. A net shape plastic expander housing with integrated motor and compressor will significantly reduce the cost of the system.

APPROACH

The approach will be to leverage recent advancements to, and further development of, roots compressor and expander technology by leveraging the broad efficiency map of Eaton's TVS compressor to improve the overall fuel cell drive cycle fuel economy. In Period 1, the project will optimize the expander and compressor individually at the specified requirements, with an integrated expander, compressor and motor concept as the final deliverable. The primary goal is to meet the power and efficiency objectives. The secondary objective is to reduce subsystem cost by keeping part count low by developing a net shape plastic expander housing and rotor. This work will be supplemented with computational fluid dynamics analysis to help optimize the expander and compressor performance and system analysis which will help optimize the integrated system.

Period 2 will finalize the integrated concept, then build and test the integrated system and individual subsystems. The last phase, Period 3, will be to incorporate the Roots Air Management System (AMS) with integrated expander into a hydrogen fuel cell application. This will include designing, building, and testing the complete system.

RESULTS

In the first half of 2014 the team designed and built the finalized compressor/expander air system concept. The remainder of 2014 validated the hardware through a series of tests. The test plan consisted of seven different performance tests conducted on the AMS with two of the tests run on Eaton's relative humidity dynamometer. The performance tests are as follows:

- Expander Component Test
- Motor Component Test
- Compressor Component Test
- Expander + Motor Sub-System Testing
- Dynamometer + Motor + Compressor Full-System Testing
- Noise Testing on Full-System
- Transient Time Testing on Full-System

Table 2 summarizes how Eaton's AMS (Eaton Test Results) has met the project target objectives laid out by DOE at the beginning of the project. The table presents all the criteria given in DOE's Table 1. The objective barriers (second to last column of data) are the percent improvements requested by DOE ([2015 Target – 2011 Baseline]/2011 Baseline). The barriers the Eaton AMS achieved (last column) are the percent improvements Eaton actually achieved with the AMS ([Eaton Test Results – 2011 Baseline]/2011 Baseline). The achieved numbers presents how well Eaton's AMS has improved on the 2011 air system. These values can be compared to the DOE objectives to see how well the Eaton system has improved its air management system technology.

The following conclusions can be drawn from the testing of Eaton's AMS (Table 2).

- Although the 100% and idle compressor power have not achieved the targeted value, there have been improvements compared to the 2011 numbers.
- The low and mid-range power numbers have improved significantly in comparison to the 2011 numbers with the 25% flow point exceeding the target amount.
- The roots expander published efficiencies are lower than centrifugal expander efficiencies. This is partially attributed to the way roots efficiency is measured compared to centrifugals. The roots compressor efficiency calculation incorporates shaft power whereas the centrifugal does not.
- Motor efficiencies for the roots application have exceeded the 100% flow target value but have fallen short of the 25% flow and idle target values.
- Costing has made some improvement towards the target value. It was noticed by the study that most of the product cost resides in the motor and controller. These two products are outside Eaton's control since Eaton purchases these parts.

Expander Plastic Rotor

In Period 1 of this project, straight plastic rotors were successfully tested. In Period 2, helical plastic rotors were designed, built, and tested. Molds were made for both right and left hand rotors. After molding, the rotors were finish coated to reduce rotor-to-rotor and rotor-to-housing clearances. Figure 1 shows the finished rotors and a full plastic expander assembly. The expander was tested without failure to a pressurized or 1.5 bar and rotational speed of 12,000 rpm.

TABLE 2. 2011 to 2015 Goals and Achievements

Flow	Characteristic	Units	Baseline 2011	2015 Project Target		Eaton Test Results	Barriers Objective vs. 2011 Baseline	
				Lower	Upper			
100% (see notes a & b)	Input power with expander	kWe	11.0		8.0	12.1	-27%	10%
	Input power without expander	kWe	17.3		14.0	15.5	-19%	-10.4%
	Combined motor & motor controller efficiency	%	80.0	90.0		95.0	12%	19%
	Compressor efficiency	%	71.0	75.0		57.5	5.6%	-19%
	Expander efficiency	%	73.0	75.0		59.0	9.6%	-19%
25% (see notes c)	Input power with expander	kWe	2.3		1.0	1.6	-57%	-30%
	Input power without expander	kWe	3.3		2.0	1.9	-39%	-42%
	Combined motor & motor controller efficiency	%	57.0	80.0		75.0	40%	32%
	Compressor efficiency	%	62.0	65.0		58.5	4.8%	-5.6%
	Expander efficiency	%	64.0	70.0		44.5	9.4%	-30%
Idle (see notes d)	Input power (1.2 Pressure Ratio) with expander	kWe	600.0		200.0	300.0	-67%	-50%
	Input power (1.2 Pressure Ratio) without expander	kWe	765.0		200.0	300.0	-74%	-61%
	Combined motor / motor controller efficiency	%	35.0	70.0		40.0	100%	14%
	Compressor efficiency	%	61.0	60.0		34.1	-1.6%	-44%
	Expander efficiency	%	59.0	60.0		0.0	1.7%	-100%
n/a (see notes e, f & g)	Turndown ratio (max/min flow rate)	none	20.0	20.0		130.0	0.0%	550%
	Noise at maximum flow dB(A)	dB(A)	n/a		65.0	95.6	n/a	n/a
	Transient time for 10 - 90% of maximum airflow	sec	1.0		1.0	1.0	0.0%	0%
	System volume	liters	15.0		15.0	12.0	0.0%	-20%
	System weight	kg	22.0		15.0	23.5	-32%	6.8%
	System cost	$	960.0		500.0	815.0	-48%	-15%

For a-g flow notes, see Table 1

FIGURE 1. Expander plastic rotors and assembly

Compressor/Expander Validation Testing On Ballard Stack—Baseline Testing

The HD7 system was tested using the existing production air system. The load profile used was a combination of down-polarizations, up-polarizations, constant current operation, and several cycles of the "Whistler Drive Cycle," which is a dynamic load profile taken from field data. The entire baseline test lasted for approximately three days. During testing, a data acquisition system logged process parameters internal to the module. These include stack specific parameters, including voltage and current, as well as air system specific parameters, including flows, temperatures and pressures measured throughout the air system. This test will be the basis for comparison to the Eaton's AMS.

CONCLUSIONS AND FUTURE DIRECTIONS

- End of Period 2 Conclusions
  - Delivered final prototype of the compressor/expander assembly with integrated motor and validation test report
  - Successfully demonstrated twisted plastic rotors in compressor and expander environment
  - Successfully demonstrated that roots compressor value was advanced from baseline
  - Successfully demonstrated that roots compressor + expander value is on par or slightly better than baseline, depending on duty cycle
  - Demonstrated that the use of plastic for most of the components has potential to improve roots expander value for customers
- Beginning of Period 3 Conclusions
  - Delivered two working sets of Eaton's Air Management Systems for Ballard testing
  - Baselined the HD7 system using the existing air system for comparison to Eaton's Air Management System
- Future Directions
  - Complete the performance and validation testing on Ballard's HD7 fuel cell

- Compressor/expander validation testing On Ballard Stack
- Durability test as per test plan

– Document Eaton's Air Management System performance capability in test report

– Complete all objectives and milestones by the end of Period 3

FY 2015 PUBLICATIONS/PRESENTATIONS

Presentations

1. Stretch, Dale, "Roots Air Management System with Integrated Expander," 2015 DOE Hydrogen and Fuel Cells Program and Vehicle Technologies Program Annual Merit Review and Peer Evaluation Meeting, June 10, 2015.

2. Stretch, Dale, "Roots Air Management System with Integrated Expander," U.S. DRIVE Technical Meetings, Fuel Cell Tech Team (FCTT), February 11, 2015.

V.E.1. Durability Improvements through Degradation Mechanism Studies

Rod Borup[1] (Primary Contact),
Rangachary Mukundan[1], Dusan Spernjak[1],
Andrew Baker[1], Roger Lujan[1], David Langlois[1],
Rajesh Ahluwalia[2], Dennis. D. Papadias[2],
Adam Weber[3], Ahmet Kusoglu[3], Shouwen Shi[3],
Karren More[4], Steve Grot[5]
[1]Los Alamos National Laboratory (LANL)
MS D429, P.O. Box 1663
Los Alamos, NM 87545
Phone: (505) 667-2823
Email: Borup@lanl.gov

DOE Manager
Nancy Garland
Phone: (202) 586-5673
Email: Nancy.Garland@ee.doe.gov

Subcontractors & Collaborators
[2] Argonne National Laboratory, Argonne, IL
[3] Lawrence Berkeley National Laboratory, Berkeley, CA
[4] Oak Ridge National Laboratory, Oak Ridge, TN
[5] Ion Power, New Castle, DE

Project Start Date: October 1, 2009
Project End Date: Project continuation and direction determined by DOE

Overall Objectives

- Identify and quantify degradation mechanisms
  - Components, component interfaces, component interactions, and degradation mechanisms
  - Discern impact of electrode structure on durability and performance
- Develop advanced in situ and ex situ characterization techniques, accelerated stress test (AST) protocols
- Develop models related to degradation mechanisms
- Explore non-system related mitigation methods

Fiscal Year (FY) 2015 Objectives

- Catalyst layer morphology effect on durability (carbon corrosion during drive cycle)
- Membrane structural changes and cerium migration/stabilization
  - Changes in properties including: crystallinity, water up-take, transport, mechanical strength, swelling, crack propagation
  - AST validation and new AST protocol development
  - Metal bipolar plates
  - Reversible degradation, transport (gas diffusion layer effects), shut-down/start-up (SD/SU)
  - Durability evaluation of Pt alloys, effect of Pt and alloy migration on membrane durability/performance

Technical Barriers

This project addresses the following technical barriers from the Fuel Cells section of the Fuel Cell Technologies Office Multi-Year Research, Development, and Demonstration Plan:

(A) Durability

(B) Cost

Technical Targets

- Transportation Durability: 5,000 hours (with cycling)
  - Estimated Start/Stop Cycles: 17,000
  - Estimated Frozen Cycles: 1,650
  - Estimated Load Cycles: 1,200,000
- Stationary Durability: 40,000 hours
- Transportation Survivability: -40°C
- Transportation Cost: $30/kWe

FY 2015 Accomplishments

- Measurement of carbon corrosion during drive cycle operation
- Modeling of the measured carbon corrosion
- Measurement of membrane structural changes
- In situ and ex situ measurements of cerium migration
- Development of new ASTs
  - Combined chemical/mechanical AST with a better representation of membrane failure in the field
  - Catalyst AST and acceleration factor comparison with drive cycle tests
- Measurement of metal bipolar plate corrosion and effect on membrane durability

✧ ✧ ✧ ✧ ✧

INTRODUCTION

The durability of polymer electrolyte membrane (PEM) fuel cells is a major barrier to the commercialization of these systems for stationary and transportation power applications. By investigating cell component degradation modes and defining the fundamental degradation mechanisms of components and component interactions, new materials can be designed to improve durability. To achieve a deeper understanding of PEM fuel cell durability and component degradation mechanisms, we utilize a multi-institutional and multi-disciplinary team with significant experience investigating these phenomena.

APPROACH

Our approach to understanding durability and degradation mechanisms within fuel cells is structured in three areas: fuel cell testing (life testing, ASTs, and ex situ aging), characterization of component properties as a function of aging time, and modeling (component aging and integrated degradation modeling). The modeling studies tie together what is learned during component characterization and allow better interpretation of the fuel cell studies. This approach enables an increased understanding of fuel cell degradation and development of materials to overcome durability limitations in fuel cell systems. This work is also being coordinated with other funded projects examining durability through the DOE Durability Working Group.

RESULTS

Carbon Corrosion at Normal Operating Fuel Cell Potentials

Corrosion of the carbon electrocatalyst support is one of the major contributors to degradation which leads to changes in the catalyst layer structure and reduces its activity. During FY 2015, we measured and quantified carbon corrosion during the drive cycle operation recommended by the Fuel Cell Tech Team (FCTT). We also evaluated the effect of varying the upper and lower potential limits used during drive cycle operation on the carbon corrosion rate.

A series of carbon corrosion spikes during potential cycling of a high-surface area carbon support (E-type carbon) are shown in Figure 1a where the upper potential was varied from 0.95 V to 0.60 V while the lower potential was kept constant at 0.40 V. Figure 1b illustrates the cathode carbon corrosion rate during the same FCTT drive cycle where

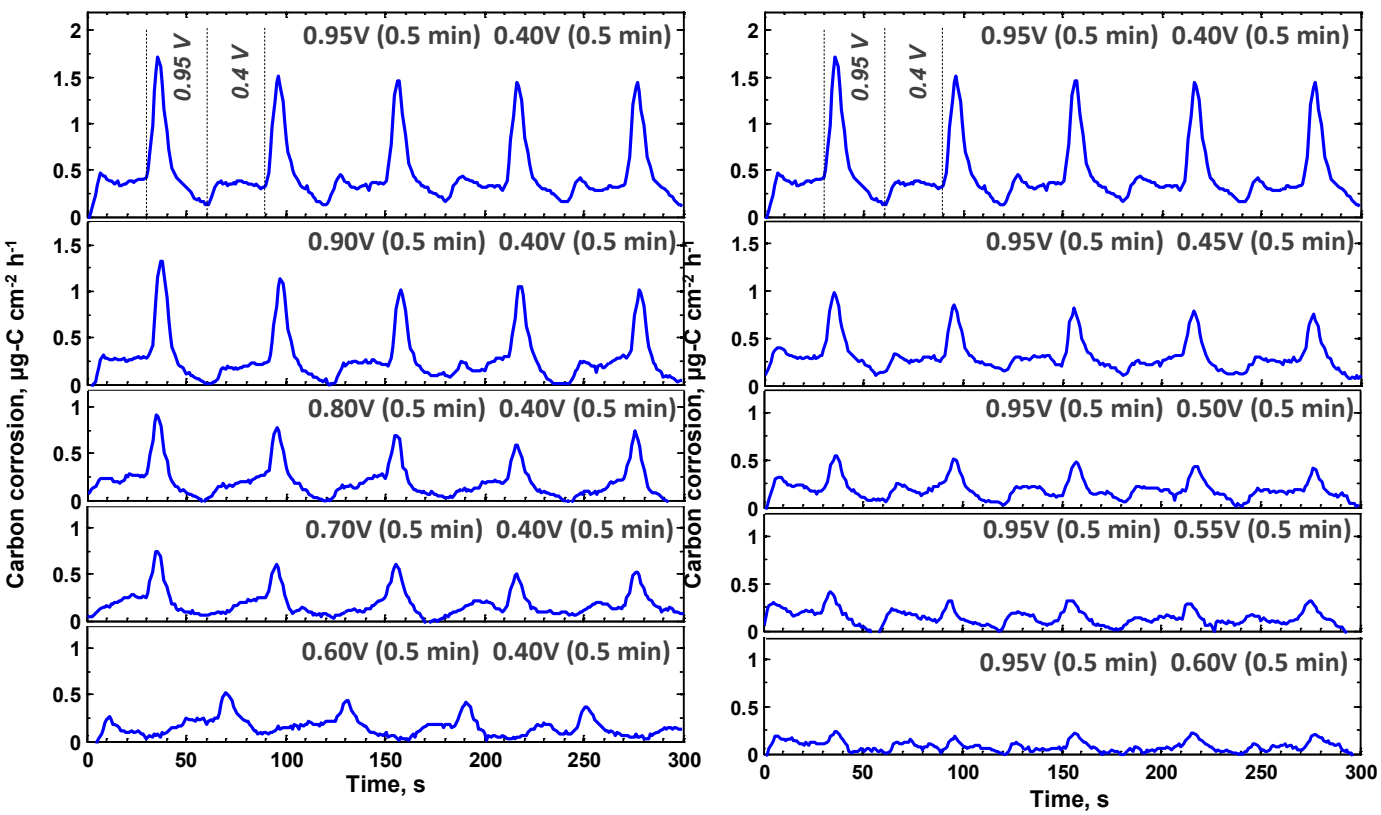

FIGURE 1. Carbon dioxide emissions from the fuel cell cathode for E-type support carbon during potential cycling operation for (a) varying upper potential limits (0.95 V, 0.90 V, 0.80 V, 0.70 V, 0.60 V) and constant lower potential of 0.4 V and (b) varying lower potential limits (0.40 V, 0.45 V, 0.50 V, 0.55 V, 0.60 V) and constant upper potential of 0.95 V. Operation at 80°C and 100% relative humidity (RH). Figure 1 has 0.5 min hold times at both upper and lower potential.

the lower potential was varied from 0.40 V to 0.60 V while keeping the upper potential constant at 0.95 V.

Sharp spikes in the carbon corrosion rate are observed during a step increase in cell potential during the simulated drive cycle operation, with the magnitude of the spikes decreasing as the upper cell potential is reduced from 0.95 V to 0.60 V. The peak in CO_2 evolution occurs when the cell potential increases from high power operation to low power operation near open circuit voltage (OCV). This correlates with the observation of CO_2 evolution during cyclic voltammograms (CVs), which occurs during the positive sweep at ~0.55 V to 0.60 V. The evolution of this CO_2 peak suggests that oxygen is adsorbed onto the carbon and/or CO is formed on the Pt surface.

The carbon corrosion rate at the upper cell potential (0.95 V) decreases with time at potential, indicating formation of passivating carbon surface oxides; this is indicated by the lower CO_2 evolution during longer durations at the higher potentials. The corrosion rate at lower cell potentials does not decrease with time, consistent with the absense of the oxide passivation layer at the lower potentials. Furthermore, a non-zero corrosion rate is also observed at low cell potentials (0.4 V).

For fixed upper cell potential (0.95 V), the magnitude of spikes decreases as the lower cell potential is raised from 0.4 V to 0.6 V (see Figure 1b). This reducing trend in carbon corrosion as the gap between upper and lower potential is reduced is similar to what was observed in Figure 1a, where the upper potential was reduced. This suggests that the corrosion rate strongly depends on the amplitude of the square potential cycle, not as much on the potential limits in this potential range. Keeping the carbon either in the oxidized or reduced states results both result in lower corrosion rates.

Catalyst support carbon corrosion occurs under normal fuel cell operating conditions and is exacerbated by the voltage cycling inherent in automotive drive cycle operation. Carbon corrosion was measured during the drive cycle measurements for all three types of carbon, with the relative carbon corrosion rates of high surface area > VULCAN® > graphitized. All types of carbon show a similar trend in reduction of carbon corrosion as the potential gap between upper and lower potential is reduced.

The amount of carbon corrosion is greater during drive cycle voltage cycling than at constant potential operation. The potential gap between upper and lower potentials appears to be more important than the absolute operating potentials in the normal operating potential regime (0.40 V to 0.95 V), as changes in the measured carbon corrosion are similar when the upper potential was lower compared to raising the lower potential. Catalyst layer thinning was observed during the simulated drive cycle operation, which had an associated decrease in catalyst layer porosity. This catalyst layer thinning is not due solely to carbon corrosion, although carbon corrosion likely plays a role; much of this thinning must be from compaction of the material in the catalyst layer. The decrease in catalyst layer porosity leads to additional performance losses due to mass transport losses.

Cerium Migration in Polymer Electrolyte Membranes

Cerium ions enhance the durability of PEM fuel cell components by rapidly and reversibly scavenging degrading radical species which are generated during operation. However, during cell assembly, conditioning, and discharge, these ions migrate between the membrane and the catalyst layers of the membrane electrode assembly (MEA) [1,2]. Cerium migration in PEMs was induced through ex situ experiments and monitored during cell assembly and operation at OCV.

When a 1.5 V potential was applied across a 12.5 mm wide window cell, cerium migrated steadily towards the lower potential over 140.5 hours (Figure 2a). Plotting the change of mean peak location with time yields a migration rate of 0.09 mm/h. Based on these results, potential differences generated during fuel cell operation can cause cerium ions to migrate towards the lower potential. After 140.5 hours at 1.5 V, the potential difference was removed and the membrane was dried in air at room temperature for 24 hours. Figure 2b reveals that the cerium ions did not equilibrate across the cell after 24 hours of drying at 0 V at room temperature and ambient RH. This result suggests that at ambient temperature and RH, cerium ion diffusion is slow relative to its potential-driven mobility.

During long-term, 100% RH operation at OCV, water content gradients generate in-plane cerium concentration variations. At OCV, cerium washout at 30% RH was greater than at 100% RH, presumably due to increased membrane degradation. Side chain attacks may cause the detachment of sulfonic acid groups, which contain exchanged cerium cations. However, cerium washout reduced total MEA cerium inventory by only a projected 1.5% after 5,000 hours of low RH OCV operation. Results demonstrate rapid cerium movement within in the MEA due to electronic potentials and protonic currents, as well as diffusion due to heat and hydration.

Membrane Accelerated Stress Testing

The development of ASTs is a critical step in the evaluation and improvement of PEM fuel cell durability. The availability of validated component ASTs can lead to the accelerated development of materials with improved durability. However, the ASTs must faithfully reproduce the degradation mechanisms of interest while attempting to accelerate the degradation rates, without introducing new degradation modes. Furthermore, the acceleration factors need to be determined accurately with respect to the intended application, to provide manufacturers with a valuable tool

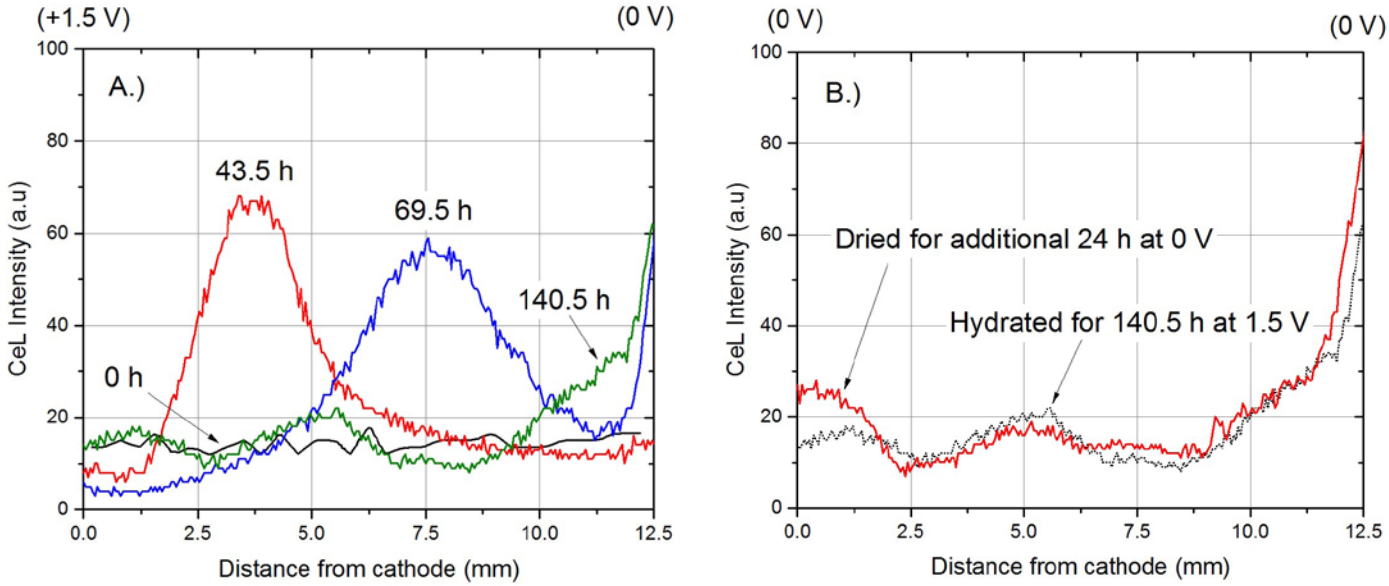

FIGURE 2. Cerium concentration measured over time via X-ray fluorescence in ex situ tests in hydrated Nafion XL® membranes at (a) 1.5 V and (b) 0 V

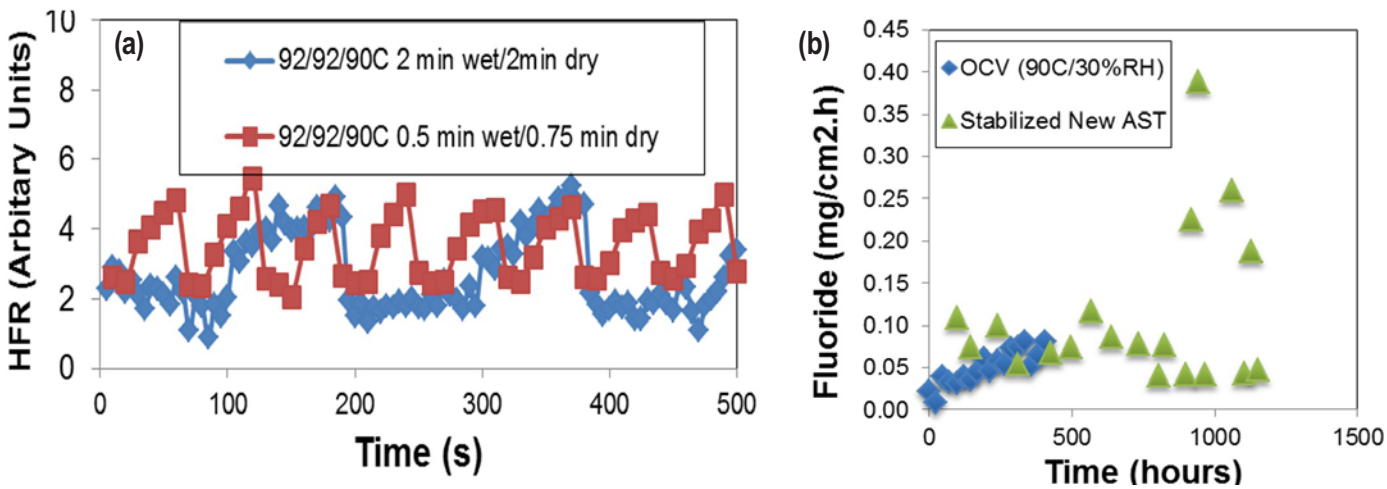

FIGURE 3. (a) High-frequency-resistance measurements during RH cycling comparing 2 minute wet/dry holds and 0.5 min wet/0.75 min dry hold times and (b) a comparison of fluoride emission rate during RH cycling at OCV (new AST) versus OCV hold at constant 30% RH

that enables informed decision making regarding cost, performance, and durability.

The FCTT has two recommended ASTs for membranes, with one focusing on chemical degradation (OCV hold at 90°C and 30% RH) and another focusing on mechanical degradation (RH cycling in air). Our previous results have indicated that both ASTs are not representative of membrane failure in the field [3]. During FY 2015, we developed a new AST that combines mechanical and chemical degradation and is more representative of field failure. This AST consists of cycling the RH between saturated and dry conditions in a H_2/air atmosphere at 90°C. The duration of the wet and dry cycles are 30 s and 45 s, respectively and results in similar high frequency resistance values as the FCTT recommended 2 minute wet/dry cycles (Figure 3a). The fluoride release rate observed during this AST using DuPont XL® membranes, illustrated in Figure 3b, is comparable to the chemical AST and significantly higher than in the mechanical AST. A baseline MEA using an unstabilized membrane sample fails at ≈1,500–2,000 cycles, while a stabilized DuPont XL® MEA fails at ≈25,000–30,000 cycles (625 hours). Moreover the failure is primarily due to mechanical failure with some global thinning (chemical degradation) observed during the long term. This AST better reproduces drive cycle failure

and is a significant acceleration over the drive cycle and other membrane ASTs.

Catalyst Accelerated Stress Testing

The FCTT has recommended potential cycling from 0.6 V to 1.0 V at 50 mV/s as the electrocatalyst AST. This potential cycling is performed at 80°C in 100% RH with H_2 (anode) and N_2 (cathode) and results in Pt particle growth and loss in electrochemical surface area (ECSA). This loss in ECSA and associated performance loss correlates well to the degradation observed in the field and during simulated drive cycle operation. Figure 4 compares the degradation observed during this AST (old AST) to that observed during the wet portion of the FCTT Drive Cycle (current cycling from 0.02 A/cm^2 to 1.2 A/cm^2 at 80°C and saturated conditions). It is seen that this AST has a 5X acceleration factor for three different MEAs that were evaluated. In order to further accelerate this AST, we modified the triangle wave to a square wave and lowered the upper potential to 0.95 V. This new AST consisted of a square wave with upper and lower potentials of 0.95 V and 0.6 V with 3 seconds duration, and was based on literature reports [4], although a lower upper potential was used to lessen carbon corrosion. This new AST (Figure 4) demonstrated a 100X acceleration factor compared to the drive cycle which is a 20 time improvement over the old AST. Moreover, this new AST retained the Pt growth mechanism while minimizing carbon corrosion.

CONCLUSIONS

We have measured and quantified carbon corrosion during drive cycle operation and studied the effect of varying the upper and lower potential limits used in the drive cycle. Carbon corrosion is observed during the normal operating cycle potentials, although it's significantly less than corrosion induced by start/stop cycles.

Cerium migration in PEMs was induced through ex situ experiments and monitored during cell assembly and operation at OCV. Results demonstrate rapid cerium movement in the MEA due to electronic potentials and protonic currents, as well as diffusion due to heat and hydration.

New ASTs were developed for membranes and catalyst testing. These ASTs have higher acceleration factors and better represent failures observed during drive cycle testing than the current FCTT recommended ASTs.

FUTURE DIRECTIONS

- Ionomer/electrode stability and structural changes
  - Characterize and model performance losses (kinetic and mass transfer) in low-loaded MEAs
    - Effect of ionomer durability in ultra low-loaded catalyst layers
    - Chemical degradation of ionomer (increased radicals)
- Durability of catalysts
  - Alloy catalyst materials
    - Stability of PtCo/C or de-alloyed PtNi/C catalysts in CV, rotating disc electrode and aqueous dissolution apparatus
    - Effect of transitional metals (from alloys)
  - Support stability
    - Quantitative relationship between carbon corrosion and resulting changes in cathode catalyst layer structure (Pt/pore distributions, Pt utilization, ECSA)

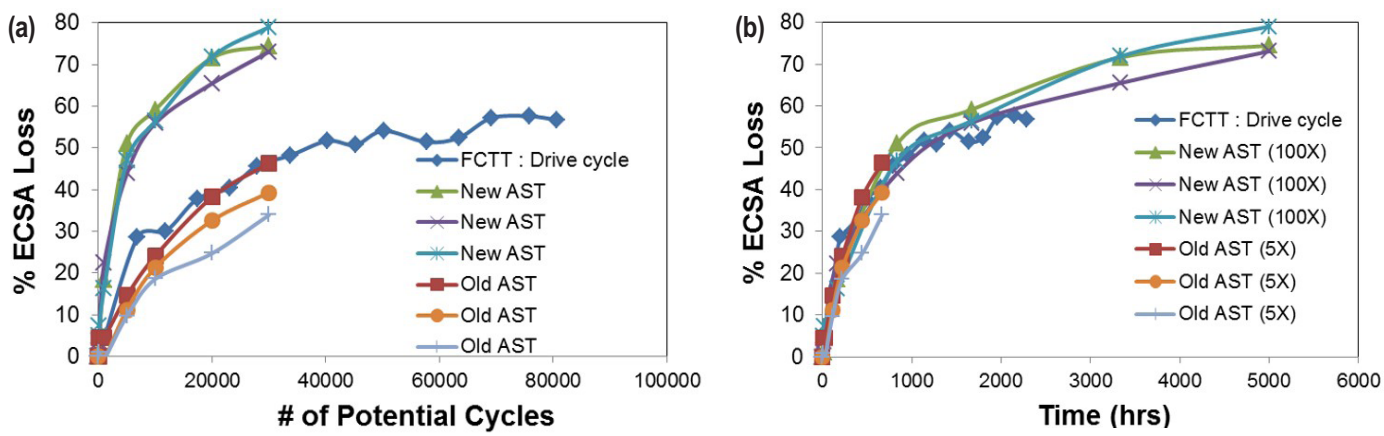

FIGURE 4. Comparison of the degradation rate (ECSA loss) observed during a FCTT drive cycle and two different catalyst ASTs as a function of (a) number of potential cycles and (b) time. Old AST: 0.6 V to 1.0 V @ 50mV/s @ 80°C and 100% RH. New AST: Square ware 0.6 V (3 s), 0.95 V (3 s) @ 80°C and 100% RH.

    - Correlate catalyst and support durability
- Accelerated stress testing and protocol development
  - Finalize combined chemical/mechanical AST protocol
    - Compare fast RH cycling with water concentration cycling by induced current profiles
  - Metal bipolar plate in situ AST durability protocol
  - Freeze tolerance MEA protocol
- Benchmark durability status
  - State-of-art catalyst/MEAs in DOE/FCTT durability protocol
  - Un-mitigated SD/SU
  - Metal bipolar plates
  - Durability comparison of ultra-low loadings
- Bipolar plate durability
  - Corrosion of advanced bipolar plate materials
  - Transport of dissolved cations through catalyst ionomer and membrane
  - In situ protocol for AST testing of metal bipolar plates
- Membrane structural/chemical degradation and radical scavenger effect
  - Structural/chemical changes to membranes
    - Including the effect of RH and temperature, and flow rate
    - Crystallinity changes and crystallinity effect on proton and water transport and gas crossover
  - Mechanistic modeling of chemical degradation including effect of ceria
    - Fatigue crack-growth model for interfacial cracks and multiple defects
    - Effect of loading conditions, cell and membrane design
    - Validation with experimental AST data and canning electron microscopy of failed membranes
  - Combined crossover/pinhole model with chemical-degradation effects
    - Cerium/radical scavenger migration
    - Model ceria/cation migration in the membrane with reaction terms
    - Measurement of cerium dissolution and migration
    - Concentration profile (in situ mapping) during fuel cell operation in both x-y and z directions
      - Define driving forces behind cerium migration (RH, current, potential)
- Mitigation
  - Cerium stabilization and localization
  - Cerium encapsulation and time-release
  - Model mitigation strategies

REFERENCES

1. F.D. Coms, H. Liu, and J.E. Owejan, *ECS Trans.*, 16, 1735–1747 (2008).

2. S.M. Stewart, D. Spernjak, R.L. Borup, A. Datye, and F. Garzon, *ECS Lett.*, 3, F19–F22 (2014).

3. R. Mukundan et al., *ECS Trans.*, V. 50 No. 2, 1003 (2013).

4. A. Ohma, K. Whinohara, A. Liyama, T. Yoshida, and A. Daimaru, *ECS Trans.*, V. 41 No. 1, 775 (2011).

SPECIAL RECOGNITIONS & AWARDS/ PATENTS ISSUED

1. ***Rod Borup (LANL)*** 2015 Research Award by Energy Technology Division of the Electrochemical Society (ECS).

2. ***Adam Weber (LBNL)*** 2014 Charles W. Tobias Award, 2014 Kavli Fellow of the National Academy Sciences Award.

FY 2015 PUBLICATIONS/PRESENTATIONS

1. Papadias, Dionissios D.; Ahluwalia, Rajesh K.; Thomson, Jeffery K.; Meyer, Harry M.; Brady, Michael P.; Wang, Heli; Turner, John A.; Mukundan, Rangachary; Borup, Rod, "Degradation of SS316L bipolar plates in simulated fuel cell environment: Corrosion rate, barrier film formation kinetics and contact resistance," Journal of the Electrochemical Society (2014), 161(3), F291–F304.

2. Ahluwalia, Rajesh K.; Arisetty, Srikanth; Peng, Jui-Kun; Subbaraman, Ram; Wang, Xiaoping; Kariuki, Nancy; Myers, Deborah J.; Mukundan, Rangachary; Borup, Rodney; Polevaya, Olga, "Dynamics of particle growth and electrochemical surface area loss due to platinum dissolution," Journal of Power Sources (2015), 273, 1237–1249.

3. Dillet, J.; Spernjak, D.; Lamibrac, A.; Maranzana, G.; Mukundan, R.; Fairweather, J.; Didierjean, S.; Borup, R.L.; Lottin, O., "Impact of flow rates and electrode specifications on degradations during repeated startups and shutdowns in polymer-

electrolyte membrane fuel cells," Journal of Power Sources (2014), 250, 68–79.

4. Stewart, S. Michael; Spernjak, Dusan; Borup, Rodney; Datye, Abhaya; Garzon, Fernando, "Cerium migration through hydrogen fuel cells during accelerated stress testing," ECS Electrochemistry Letters (2014), 3(4),F19–F22.

5. Weber, Adam Z.; Borup, Rodney L.; Darling, Robert M.; Das, Prodip K.; Dursch, Thomas J.; Gu, Wenbin; Harvey, David; Kusoglu, Ahmet; Litster, Shawn; Mench, Matthew M., et al., "A critical review of modeling transport phenomena in polymer-electrolyte fuel cells," Journal of the Electrochemical Society (2014), 161(12), F1254–F1299, 46 pp.

6. Rangachary Mukundan, Rod Borup, John Davey, Roger Lujan, Dennis Torraco, David Langlois, Fernando Garzon, Dusan Spernjak, Joe Fairweather, Adam Weber, Karren More, Paul Beattie, and Steve Grot, "Accelerated Testing Validation," DOE Fuel Cell Technologies Office, FY 2014 Annual Report.

7. Rod Borup, Rangachary Mukundan, Dusan Spernjak, Roger Lujan, D. Langlois, Fernando Garzon, S. Michael Stewart, Rajesh Ahluwalia, Xiaohua Wang, Adam Weber, Ahmet Kusoglu, Karren More, Steve Grot, "Durability Improvements Through Degradation Mechanism Studies," DOE Fuel Cell Technologies Office, FY 2014 Annual Report.

8. A. Kusoglu and A.Z. Weber, "A Mechanistic Model for Pinhole Growth in Fuel-Cell Membranes during Cyclic Loads," Journal of The Electrochemical Society, 161, E3311 (2014).

9. Shouwen Shi, Thomas J. Dursch, Colin Blake, Rangachary Mukundan, Rodney L. Borup, Adam Z. Weber, and Ahmet Kusoglu, "Impact of Hygrothermal Ageing on Structure/Function Relationship of Perfluorosulfonic-acid Membrane," *submitted to Journal of Polymer Science.*

10. Rodney L. Borup, D.D. Papadias, Rangachary Mukundan, Dusan Spernjak, David Langlois, R. Ahluwalia, Karren More, and Steve Grot, "Carbon Corrosion in PEM Fuel Cells during Drive Cycle Operation," submitted to JECS Trans.

12. A.M. Baker, D. Torraco, E.J Judge, D. Spernjak, R. Mukundan, R.L. Borup, S.G Advani, and A.K. Prasad, "Cerium Migration during PEM Fuel Cell Assembly and Operation," submitted to ECS Transactions.

Presentations

1. A. Kusoglu, A.Z. Weber, "Synergistic Chemical/Mechanical Degradation of Polymer-Electrolyte Membranes," MRS Meeting, San Francisco, CA. April 2015.

2. A. Kusoglu, M. Tesfaye, S. Shi, W. Tong, A.Z. Weber, "Impact of Ageing on Properties of PFSA Ionomers," APS Meeting, San Antonio, TX. March 2015.

3. S. Shi. M. Tesfaye, A.Z. Weber, A. Kusoglu, "Understanding Ionomers: Impact of Ageing and Related Factors on Structure-Function Relationships Across Length Scales," Advances in Materials for PEMFC Systems, Pacific Grove, CA. February 2015 (poster).

4. A. Kusoglu, "Mechanical Aspects of Membrane Durability in PEM Fuel Cells" State-of-the-Art Tutorial on Durability in Low Temperature Fuel Cells," (Invited) Electrochemical Society (ECS) Spring Meeting, Orlando, FL. May 2014.

5. Borup, Rodney L., Rangachary Mukundan, Yu Seung Kim, Dusan Spernjak, David Langlois, Karren More, R. Ahluwalia, S. Arisetty, G. Maranzana, J. Dillet and O. Lottin, "PEM Fuel Cell MEA Degradation During Drive Cycle Operation," (Invited) Spring ECS May 2014.

6. Borup, Rodney L., Rangachary Mukundan, Dusan Spernjak, David Langlois, Dennis Torraco, Karren More, R. Ahluwalia, S. Arisetty Laure Guetaz, "Electrocatalyst Layer Degradation of PEM Fuel Cells," (Invited), Fall ECS October 2014.

7. R.L. Borup, R. Mukundan, J. Fairweather, Dusan Spernjak, D. Langlois, K. Rau, K.L. More, G. Maranzana, A. Lamibrac, J. Dillet, S. Didierjean, O. Lottin, L. Guetaz, R. Ahluwalia, and S. Arisetty, "PEM Fuel Cell Electrode Layer Degradation," (Invited: Energy Technology Division Award Presentation), Spring ECS May 2015.

8. R. Mukundan and R.L. Borup, "Diagnostic Methods Utilized in Accelerated Stress Testing of Polymer Electrolyte Membrane Fuel Cells," (Invited), Spring ECS May 2015.

9. R.L. Borup, "Very Brief Account from Electrocatalysis-Relevant Discussion at Durability Working Group in Chicago Last December," DOE Catalyst Working Group Meeting, Jan. 2015.

10. R.L. Borup, "Durability-related Freeze Protocol," DOE Durability Working Group Meeting, Dec. 2014.

11. M.P. Rodgers, L.J. Bonville, R. Mukundan, R. Borup, S. Knights, R. Ahluwalia, P. Beattie, R.P. Brooker, N. Mohajeri, H.R. Kunz, D.K. Slattery, J.M. Fenton, "Perfluorinated Sulfonic Acid Membrane and Membrane Electrode Assembly Degradation Correlating Accelerated Stress Testing and Lifetime Testing," (Invited), Spring ECS May 2014.

12. Rangachary Mukundan, Paul Beattie, John Davey, David Langlois, Dusan Spernjak, Joe Fairweather, Dennis Torraco, Fernando Garzon, Adam Z Weber, Karren More, and Rodney L. Borup, "Durability of PEM Fuel Cells and the Relevance of Accelerated Stress Tests," (Invited), Spring ECS May 2014.

13. R.L. Borup, F.H. Garzon, R. Mukundan, D. Spernjak, J. Fairweather, M. Stewart, J. Davey, K. Rau, R. Lujan, D. Langlois, D. Torraco, R. Ahluwalia, S. Arisetty, A. Weber, A. Kusoglu, K. Clark, K. More, S. Grot, D. Jacobson, and D. Hussey, "PEM Fuel Cell Component Durability: Electrode Morphology Changes," Fuel Cells 2014 Science & Technology, Grove Fuel Cell Event, Amsterdam, April 2014.

14. R.L. Borup, "PEM Fuel Cells: Design and Durability at the Microstructural Level," Materials Capability Review: 2014 Materials for the Future, Los Alamos, 2014.

15. R.L. Borup, "PEM Fuel Cells for Transportation: Design and Durability at the Microstructural Level," (Invited), 226th ECS Meeting, Cancun, October 2014.

16. R.L. Borup, "Metal Bipolar Plate Degradation Mechanisms and AST Development," DOE 2014 Durability Working Group Meeting, Dec. 2014.

V.E.2 Fuel-Cell Fundamentals at Low and Subzero Temperatures

Adam Z. Weber
Lawrence Berkeley National Laboratory
1 Cyclotron Rd., MS 70-108B
Berkeley, CA 94720
Phone: (510) 486-6308
Email: azweber@lbl.gov

DOE Manager
Donna Ho
Phone: (202) 586-8000
Email: Donna.Ho@ee.doe.gov

Subcontractors
- Los Alamos National Laboratory (LANL), Los Alamos, NM
- United Technologies Research Center (UTRC), East Hartford, CT
- 3M Company, St. Paul, MN

Project Start Date: September 21, 2009
Project End Date: Project continuation and direction determined annually by DOE

Overall Objectives

- Fundamentally understand transport phenomena and water and thermal management at low and subzero temperatures
- Examine water (liquid and ice) management with thin-film catalyst layers (CLs), such as 3M's nanostructured thin film (NSTF) CLs
- Develop diagnostic methods for critical properties for operation with liquid water
- Elucidate the associated degradation mechanisms due to subzero operation and enable mitigation strategies to be developed

Fiscal Year (FY) 2015 Objectives

- Use validated mathematical model to explore water-out-the-anode scheme for NSTF CLs
- Measure water content and resistance of traditional CLs
- Examine materials properties for low equivalent weight (EW) ionomer membranes and thin films
- Explore water distributions for and impacts of various gas diffusion layers (GDLs) and microporous layers (MPLs)

Technical Barriers

This project addresses the following technical barriers from the Fuel Cells section of the Fuel Cell Technologies Office Multi-Year Research, Development, and Demonstration Plan:

(A) Durability

(C) Performance
- Cell Issues
- Stack Water Management
- System Thermal and Water Management
- System Start-up and Shut-down Time and Energy/Transient Operation

Technical Targets

This project is conducting fundamental investigations into fuel cell operation at low and subzero temperatures. The knowledge gained will enable various metrics to be met or exceeded. These include those related to durability, performance, and cost. Specially,

- Durability
  - 5,000 h (automotive) and 40,000 h (stationary)
  - Thermal cycling ability with liquid water
- Performance
  - Unassisted start from -40°C
  - Cold start to 50% power in 30 seconds and with 5 MJ or less energy
  - Efficiency of 65% and 55% for 25% and 100% rated power, respectively
  - Stack power density of 2 kW/kg
  - Platinum group metal loading of 0.2 g/kW
- Cost: $\$15/kW_e$

FY 2015 Accomplishments

- Combined modeling and experiment to understand low-temperature performance of NSTF showing how the critical factor is removing liquid water through the anode
- Examined transient operation showing how the membrane properties and GDL interface are the most sensitive parameters for water-out-of-the-anode scheme

- Increased water out the anode lowers cathode flooding and is driven by morphological features that decrease GDL surface adhesion force
- Developed along-the-channel model to correlate spatially varying results
- Investigated water movement and existence in diffusion media including under compression where water-imbibition front and CL water content were imaged
- Examined operation of novel MPLs containing hydrophilic additives
- Investigated traditional CL resistance and importance of ionomer mass-transport resistance at low catalyst loadings

✧ ✧ ✧ ✧ ✧

INTRODUCTION

Polymer-electrolyte fuel cells experience a range of different operating conditions. As part of that range, they are expected to be able to survive and start at low and subzero temperatures. Under these conditions, there is a large amount of liquid and perhaps frozen water. Thus, water and thermal management become critical to understanding and eventually optimizing operation at these conditions. Similarly, durability aspects due to freezing and low temperatures are somewhat unknown and need further study in order to identify mechanisms and mitigation strategies. In addition, it is known that thin-film CLs, such as NSTF developed by 3M, have issues with large amounts of liquid water due to their thinness. These layers provide routes towards meeting the DOE cost targets due to their high catalytic activities. This project directly focuses on the above aspects of operation at lower temperatures with both NSTF and traditional CLs with the goal that improved understanding will allow for the DOE targets to be met with regard to cold start, survivability, performance, and cost.

APPROACH

The overall approach is to use a synergistic combination of cell, stack, and component diagnostic studies with advanced mathematical modeling at various locations (national laboratories, industry, and academia). Ex situ diagnostics are used to quantify transport properties and to delineate phenomena that are used in the modeling. The two-dimensional (2D) cell model is developed and validated by comparison of measured in situ cell performance in both single cells under a variety of cell assemblies and architectures in order to highlight specific controlling phenomena. To explore controlling phenomena and the impact of various layers, a systematic investigation at the component scale is accomplished, including the development of a suite of advanced ex situ diagnostics that measure and evaluate the various critical material properties and transport-related phenomena.

RESULTS

As fuel cells operate at low and subzero conditions, liquid water and water management become more important. Thus, there is a need to study properties of the porous fuel cell layers in the presence of liquid water. It is also expected that this problem is exacerbated in thin-film CLs such as NSTF CLs as shown previously with single cell, low-temperature operation. To improve performance, it is thought that one needs to reduce the amount of water within the thin-film cathode, and thus increase it out of the anode as was shown previously. This year, the 2D model was used to examine the impact of the water-out-the-anode scheme. As shown in Figure 1a, the model correctly predicts this trend by changing the liquid water pressure boundary condition (Figure 1c). The change in condition is related to the adhesion force and droplet detachment values that we measure. Figure 1b shows the impact of GDL permeability, which is not a strong impact compared to the pressure (Figure 1c), highlighting that interfacial phenomena are key in determining water removal impacts.

The above analysis is for a NSTF cell, but, in practice, platinum on carbon (Pt/C) CLs are traditionally used that are thicker, thus minimizing the impact of water flooding. However, to reach such thicknesses, these electrodes contain ionomer that provides proton conduction throughout the layer. To explore impacts of this ionomer, various diagnostic tests were conducted. Using a hydrogen pump setup, we were able to measure both the CL and dry GDL and MPL resistances to gas transport. As shown in Figure 2, the CL resistance dominates, even though the test uses hydrogen and does not generate water. Furthermore, this resistance increased with lower Pt loadings, which is consistent with previous reported observations and shows a key limiting factor in decreasing catalyst loading. Currently we are working to explore these resistances by measuring gas permeation coefficients in the ionomer thin-film and correlating them to the structure of the film such that ways can be found to minimize its effect.

It is important as well to visualize water to understand where it exists and thus improve models as well as elucidate governing phenomena. Figure 3 shows two such visualizations. In the top figure, high-resolution neutron imaging was used to visualize the water content of cells with thick CLs in order to collect enough data points. As seen, the cathode CL behaves quite differently than the anode one. Furthermore, the impact of phase-change-induced flow is clearly seen in that the water content decreases in the cathode and increases at the cathode GDL boundary as a function of increasing temperature due to the temperature gradient across the GDL. In the bottom figure, X-ray computed

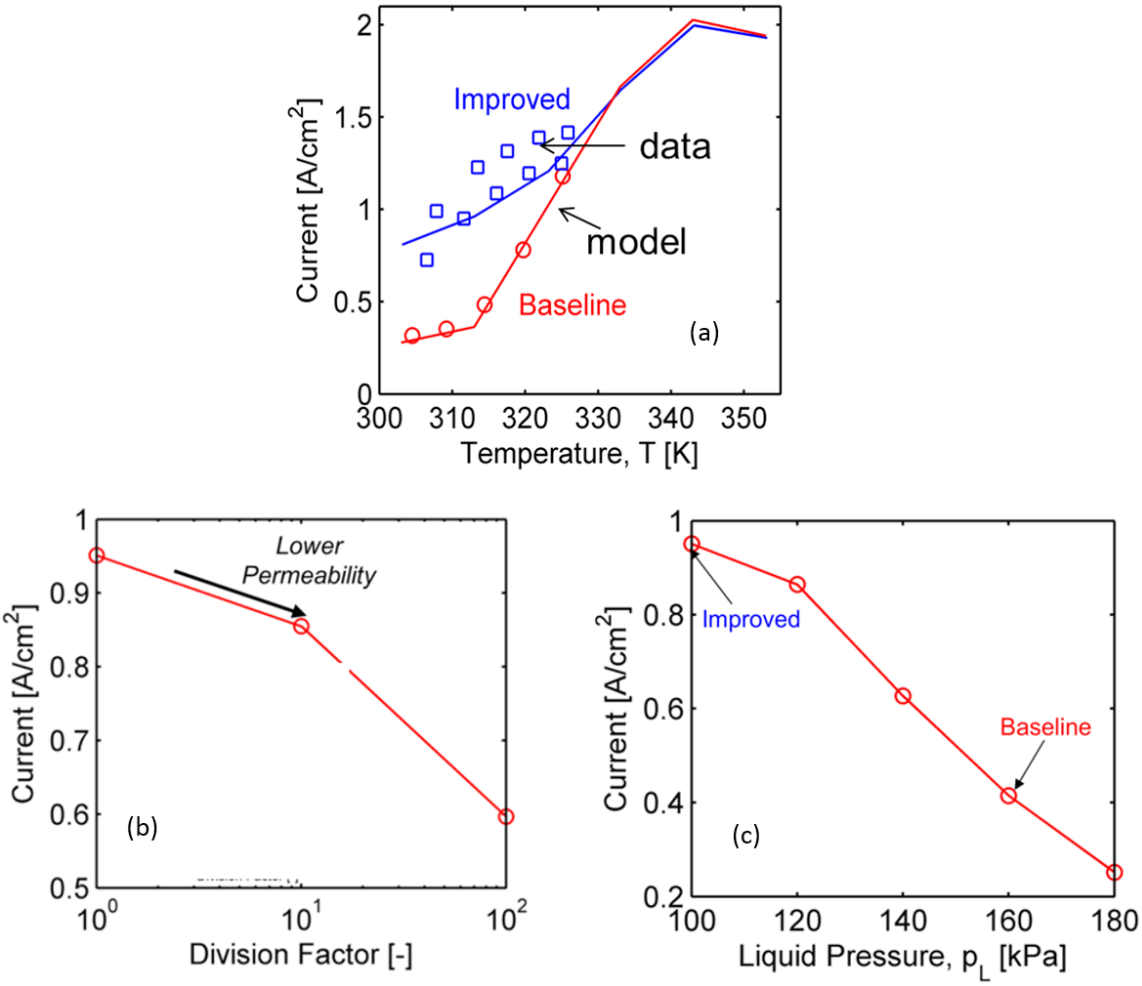

FIGURE 1. (a) Cell voltage (at 0.25 A/cm^2) as a function of temperature with 100% relative humidity feeds at 150 kPa for an NSTF cell with a baseline or improved anode GDL including both data (points) and 2D model results (lines). Sensitivity study for (b) GDL permeability and (c) GDL/channel liquid pressure boundary condition on cell voltage at 40°C and 0.25 A/cm^2.

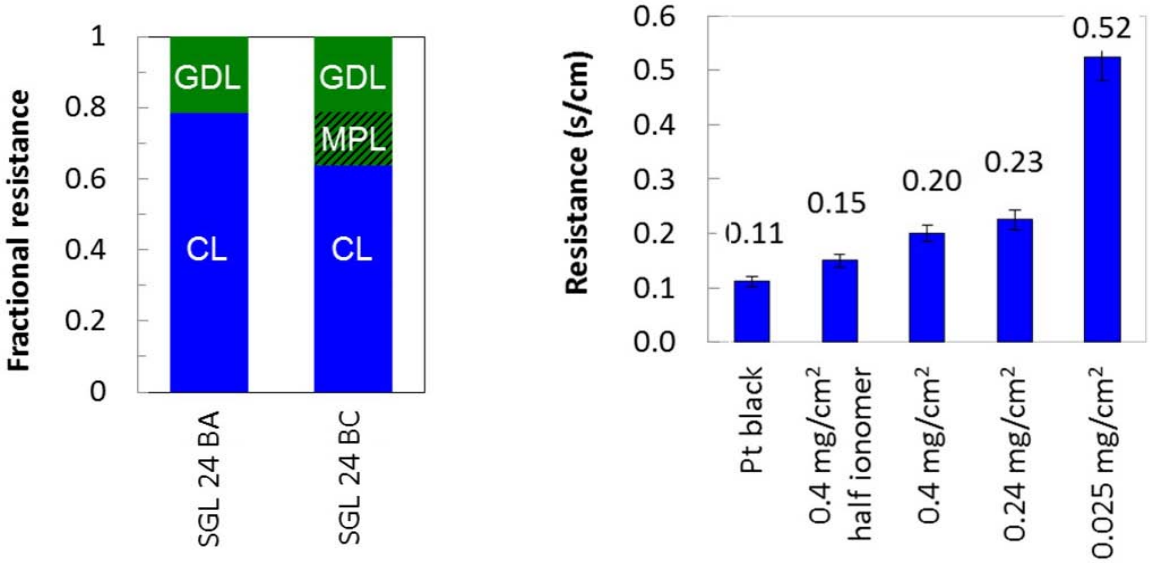

FIGURE 2. Normalized gas-phase effective resistance as measured by hydrogen pump limiting current for GDL, MPL, and traditional Pt/C catalyst layer. Measured transport resistance as a function of catalyst-layer type and loading.

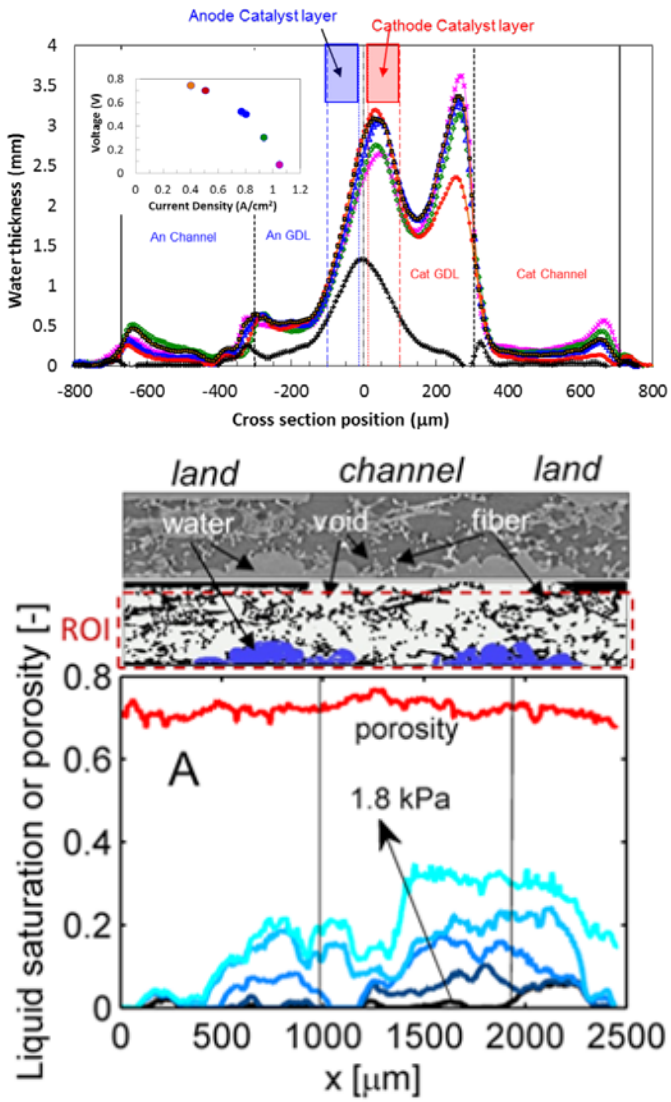

FIGURE 3. (top) Water thickness from neutron imaging with thick catalyst layers at 80°C; the inset shows the polarization performance. (bottom) Liquid saturation of a GDL as measured by X-ray computed tomography showing the water saturation in-plane as a function of inlet pressure from 0 to breakthrough.

tomography at the Advanced Light Source was used to ascertain the position and structure of water imbibition into the GDL. It is clearly seen that water exists as a front partway through the GDL but then capillary fingering occurs. Thus, models that use volume-averaged quantities such as saturation will not be accurate since they cannot capture the stochastic nature of water percolation.

CONCLUSIONS AND FUTURE DIRECTIONS

The project focus this year was on developing and utilizing diagnostic methods for fuel cell components at low temperatures to elucidate routes for performance improvement. Such activities also include incorporating the experimental observations into a transient performance model that can describe the observed changes. Several novel methods were developed and measurements for membranes, GDLs, and CL ionomer were made. The results allow for a better understanding of liquid formation and movement within the cell, as well as limitations due to ionomer films at low catalyst loadings. In addition, single-cell testing of cells containing traditional CLs was accomplished including segmented cells with transient data, adiabatic cells, and thick CLs for neutron imaging.

Future work is summarized as follows:

- Cell Performance
  - Run cool and cold starts using adiabatic cell hardware (UTRC)
  - Examine possible interlayers and multilayer electrodes
  - Run NSTF and Gore cells with different diffusion media and operating conditions (LANL)
  - Perform imaging: segmented cell and NIST imaging including thick CLs
- Component Characterization
  - Measure transport resistance, especially for low Pt loadings
  - Measurement of key GDL properties, including PSD, liquid-water pathways, and adhesion force, for new GDLs
  - Measure transport properties of ionomer films, especially low EW ones
  - Characterize reinforced membranes
- Modeling
  - Exercise model to determine critical properties and guide material development and provide design targets
  - Incorporate more advanced interfacial and kinetic models
  - Examine pore-scale models and new GDL model possibilities
- Understand and increase the operating window with thin-film CLs
  - Focus on solutions and strategies derived from the integrated model and cell and component studies
- Solicit input and advice from original equipment manufacturers and material companies on cell performance

SPECIAL RECOGNITIONS & AWARDS/ PATENTS ISSUED

1. Adam Z. Weber, Charles W. Tobias Award of the Electrochemical Society.

2. Adam Z Weber, Kavli Fellow, of the National Academy of Sciences.

FY 2015 PUBLICATIONS

1. Ahmet Kusoglu, Douglas Kushner, Devproshad K. Paul, Kunal Karan, Michael A. Hickner, and Adam Z. Weber, 'Impact of Substrate and Processing on Confinement of Nafion® Thin Films,' *Advanced Functional Materials*, **24** (30), 4763–4774 (2014).

2. Anthony D. Santamaria, Prodip K. Das, James C. MacDonald, and Adam Z. Weber, 'Liquid-Water Interactions with Gas-Diffusion-Layer Surfaces,' *J. Electrochem. Soc*., **161** (12), F1184–F1193 (2014).

3. Adam Z. Weber, Rodney L. Borup, Robert M. Darling, Prodip K. Das, Thomas J. Dursch, Wenbin Gu, David Harvey, Ahmet Kusoglu, Shawn Litster, Matthew Mench, Rangachary Mukundan, Jon P. Owejan, Jon Pharoah, Marc Secanell, and Iryna Zenyuk, 'A Critical Review of Modeling Transport Phenomena in Polymer-Electrolyte Fuel Cells,' *J. Electrochem. Soc*., **161** (12), F1254–F1299 (2014).

4. Adam Z. Weber and Ahmet Kusoglu, 'Unexplained transport resistances for low-loaded fuel-cell catalyst layers,' *J. Materials Chemistry A*, **2** (42), 17207–17211 (2014). *(highlight)*

5. Frances I. Allen, Luis R. Comolli, Ahmet Kusoglu, Miguel A. Modestino, Andrew M. Minor, and Adam Z. Weber, 'Morphology of Hydrated As-Cast Nafion® Revealed through Cryo Electron Tomography,' *ACS Macro Letters*, **4**, 1–5 (2015). (*Cover, ACS Editors Choice article*)

6. Iryna V. Zenyuk, Dilworth Y. Parkinson, Gisuk Hwang, and Adam Z.Weber, 'Probing water distribution in compressed fuel-cell gas-diffusion layers using X-ray computed tomography,' *Electrochemistry Communications*, **53**, 24–28 (2015).

7. Pablo A. García-Salaberri, Gisuk Hwang, Marcos Vera, Adam Z. Weber, and Jeffrey T. Gostick, 'Effective diffusivity in partially-saturated carbon-fiber gas diffusion layers: Effect of through-plane saturation distribution,' *International Journal of Heat and Mass Transfer*, **86**, 319–333 (2015).

FY 2015 PRESENTATIONS

1. Adam Weber, "Understanding Transport in Fuel-Cell Ionomer," Chemical Engineering Colloquium, Colorado School of Mines (invited).

2. I.V. Zenyuk, D.Y. Parkinson, G. Hwang, A.Z. Weber "Understanding Water Transport in Compressed Gas Diffusion Layers of Polymer-Electrolyte Fuel Cells Using X-ray Computed Tomography," 2015 MRS Spring Meeting & Exhibit, 2015.

3. A.Z. Weber, A. Kusoglu, A. Hexemer, "Structure of Nafion® Thin Films on Gold." APS Meeting, San Antonio, 2015.

4. A. Kusoglu, A.Z. Weber, "Structure/Property Relationship of PFSA in Thin Film regime," SSPC17, Seoul, 2014.

5. A.Z. Weber, A. Kusoglu, S. Shi, M. Tesfaye, "Understanding ionomer thin films," ACS Meeting, Denver, 2015.

6. A. Kusoglu, A.Z. Weber, "Structure-Function Relationship of PFSA Thin Films," ISPE14 Meeting, Australia, 2014.

7. P.A. García-Salaberri, J.T. Gostick, G. Hwang, M. Vera, A.Z. Weber, "Pore-Scale Calculations of Effective Diffusivity in Partially-Saturated GDLs: Application to PEFC Continuum Models," MODVAL 12, Germany, 2015.

8. M. Tesfaye, A. Kusoglu, B.D. McCloskey, A.Z. Weber, "Impact of Structure on Transport Properties of Bulk and Thin-film Ionomers," Advances in Fuel Cells, Asilomar, 2015.

9. A. Kusoglu, A. Crothers, A.Z. Weber, "Understanding and Modeling Water Transport in Proton-Exchange Membranes," ISE Meeting, Lausanne, 2014.

10. P.K. Das, A.Z. Weber, "Role of GDL Surface Wettability and Operating Conditions in Liquid-Water Removal from NSTF Catalyst Layers," IMECE, 2014.

11. A. Kusoglu, A.Z. Weber, "Study of PFSA Ionomers using X-Ray Scattering Techniques," ACS Meeting, San Francisco, 2014 (invited).

12. T.J. Dursch, G.J. Trigub, R. Lujan, R. Mukundan, C.J. Radke, A.Z. Weber, "Ice-Crystallization Kinetics During Fuel-Cell Cold-Start," ECS Meeting, Orlando, 2014 (award talk).

13. A.Z. Weber, "Understanding Transport Phenomena in Polymer-Electrolyte Fuel Cells," ECS meeting, Cancun, 2014 (award talk).

14. D.L. Jacobson, D. O'Kelly, D.S. Hussey, D. Spernjak, A.Z. Weber, R. Mukundan, J. Fairweather, J.S. Spendelow, and R.L. Borup, "Using neutron radiography to accurately quantify the through-plane water content of a proton-exchange membrane," ACNS, 2014.

15. M.L. Perry, "Characterization of Polymer Electrolyte Fuel Cells with Ultra-Low Catalyst Loadings," ECS Meeting, Cancun, 2014 (invited).

16. A. Weber, "Understanding Transport in Fuel-Cell Ionomer," Chemical Engineering Colloquium, Tufts University, 2014 (invited).

17. I.V. Zenyuk, A. Santamaria, P.K. Das, A. Steinbach, R. Mukundan, R.L. Borup, A.Z. Weber, "Water Management with Thin-Film Catalyst Layers," CARISMA, South Africa, 2014.

18. A. Kusoglu, A.Z. Weber, "Critical role of the interface in controlling transport in PFSA membranes," ACS Meeting, San Francisco, 2014.

V.E.3 Effect of System Contaminants on PEMFC Performance and Durability

Huyen N. Dinh (Primary Contact), Guido Bender, Clay Macomber, Heli Wang
National Renewable Energy Laboratory (NREL)
15013 Denver West Parkway
Golden, CO 80401-3305
Phone: (303) 275-3605
Email: Huyen.Dinh@nrel.gov

DOE Manager
David Peterson
Phone: (720) 356-1747
Email: David.Peterson@ee.doe.gov

Partners
- CRADA: Paul T. Yu and Balsu Lakshmanan, General Motors LLC (GM), Honeoye Falls, NY
- John Weidner, University of South Carolina, Columbia, SC
- Ryan Richards and Jason Christ, Colorado School of Mines, Golden, CO

Project Start Date: October 1, 2013
Project End Date: Project continuation and direction determined annually by DOE

Overall Objectives

Our overall objective is to decrease the cost associated with balance of plant (BOP) materials in polymer electrolyte membrane fuel cell (PEMFC) systems without compromising function, fuel cell performance, or durability.

Our specific project objectives are to:

- Understand the severity of relevant BOP materials on fuel cell performance.
- Identify and quantify contaminants derived from BOP materials.
- Understand fundamental contamination mechanisms and recoverability of BOP materials.
- Guide system developers on future material selection.
- Be a resource to the fuel cell community.

Fiscal Year (FY) 2015 Objectives

- Determine the effect of leaching conditions on contaminant concentration
- Develop gas chromatography mass spectrometry (GCMS) method to identify and quantify organic contaminants
- Investigate fundamental mechanisms of contamination and recoverability using organic and anion model compounds

Technical Barriers

This project addresses the following technical barriers from the Fuel Cells section (3.4.4) of the Fuel Cell Technologies Office's Multi-Year Research, Development, and Demonstration Plan:

(A) Durability

(B) Cost

Technical Targets

This project focuses on quantifying the impact of system contaminants on fuel cell performance and durability. Insights gained from these studies will increase performance and durability by limiting contamination-related losses and decreasing overall fuel cell system costs by lowering BOP material costs. Proper selection of BOP materials will help meet the following DOE 2020 targets:

- Cost: $30/kW for transportation; $1,000–1,700/kW for stationary
- Lifetime: 5,000 hours for transportation; 60,000 hours for stationary (2–10 kW)

FY 2015 Accomplishments

- We expanded the set of leaching conditions (time, temperature, surface area/water ratio) and determined that plastic material type and time significantly impacted leachate concentration. Hence, BOP material selection and the material's exposure time to water are important considerations for fuel cell systems and operations.
- Three methods to quantify organic concentrations in leachates were explored. GCMS-flame ionization detector (FID) yielded the best trade-off between sensitivity and reproducible data. The ranges of caprolactam (<10 ppm) and aniline (<20 ppm) concentrations found in polyamide material leachates provided important guidance on selecting concentrations to be used in infusion experiments.
- More trace organic species were identified via solid phase micro-extraction GCMS, suggesting

BOP leachates comprise complicated mixtures of organics.

- We determined that low BOP leachate concentrations, caprolactam, and mixtures of caprolactam and sulfate had an impact on fuel cell performance, including Pt adsorption and membrane and catalyst ionomer poisoning.
- Multiple techniques (cyclic voltammetry, electrochemical quartz crystal microbalance, and oxygen reduction reaction [ORR]) were performed to understand the role of functional groups and fluorocarbon chain length on Pt adsorption and ORR activity.
- The NREL website (www.nrel.gov/hydrogen/contaminants.html) and interactive material data tool (www.nrel.gov/hydrogen/system_contaminants_data) were enhanced by updating the list of NREL publications and presentations and adding contaminants-related publications from the Naval Research Lab. This website serves as a resource for the fuel cell community.

✧ ✧ ✧ ✧ ✧

INTRODUCTION

Cost and durability issues of PEMFC systems are challenging for the fuel cell industry. The current status of fuel cell system cost is $55/kW, much lower than $124/kW in 2006, but still higher than the ultimate target of $40/kW [1]. As fuel cell systems become more commercially competitive, the impact of contaminants derived from fuel cell system component materials becomes more important. Such contaminants—from structural materials, lubricants, greases, adhesives, sealants, and hoses—have been shown to affect the performance and durability of fuel cell systems. Lowering the cost of PEMFC system components requires understanding of the materials used in these components as well as the contaminants derived from them. Unfortunately, there are many possible contamination sources from system components [2-12]. Currently deployed, high-cost, limited-production systems use expensive materials for system components. In order to make fuel cell systems commercially competitive, the cost of BOP components must be lowered without sacrificing performance and durability. Fuel cell durability requirements limit the performance loss attributable to contaminants to at most a few millivolts over the required lifetimes (thousands of hours), which means system contaminants must have a near-zero impact.

As catalyst loadings decrease and membranes are made thinner (both are current trends in automotive fuel cell research and development), fuel cell operation becomes even more susceptible to contaminants. In consumer automotive markets, low-cost materials are usually required, but lower cost typically implies higher contamination potential. The results of this project will provide the information necessary to help the fuel cell industry make informed decisions regarding the cost of specific materials versus the potential contaminant impact on fuel cell performance and durability. The project will also identify the impact of different operating conditions on contaminant concentrations, quantify and identify the contaminants in leachate solutions, and enhance understanding of the impact of selected model compounds on fuel cell performance.

APPROACH

Our goal is to provide an increased understanding of fuel cell system contaminants and to help guide the implementation and, where necessary, development of system materials to support fuel cell commercialization. While much attention has been paid to air and fuel contaminants, system contaminants have received limited public attention and very little research has been publicly reported [2-9]. Our approach aims to quantify leachate concentrations and determine the effect of leaching parameters on material leaching concentration, determine the fuel cell performance impact of lower leachate concentrations, perform mechanistic studies on organic and ionic model compounds derived from structural plastics to understand the effect of individual compounds and mixtures of compounds on fuel cell performance, and disseminate information about material contamination potential that would benefit the fuel cell industry in making cost-benefit analyses for system components. To date, fuel cell system BOP materials are based upon existing automotive material sets. These materials often contain additives and processing aids that may be detrimental to fuel cell performance and durability. The BOP materials selected for this study were generally developed for other applications. Leachate solutions were created from BOP materials to identify compounds that leach out of them. The leachates, individual compounds and compound combinations were studied to understand the effect of BOP materials and specific functional groups on the fuel cell.

RESULTS

One of this year's accomplishments was updating NREL's contaminants website with related publications and presentations from NREL as well as the Naval Research Lab. This publicly accessible website serves as a resource for the fuel cell community—it has a material database of about 60 commercially available BOP materials (structural components, hoses, and assembly aids such as seals, gaskets, and adhesives) and their contamination potential and impact on fuel cell performance. The NREL material screening data tool was designed to be interactive, easy to use, and informative to the fuel cell community [2].

In addition, we expanded the conditions for extracting contaminants from plastics: time (10–1,000 h), temperature (50–90°C), and plastic surface area/water ratio (SA/vol = 1.5–3 cm^2/mL), as outlined in Table 1. The effects of these leaching conditions and the plastic material type on the leaching index (LI), which is the sum of the total organic carbon (TOC, ppm) and solution conductivity (µS/cm), are shown in Figure 1. As expected, the less expensive polyamide (PA) material leached out more contaminants (higher LI) than the polyphthalamide (PPA) material. Furthermore, longer time, higher temperature, and higher SA/vol ratio resulted in more contaminants extracted. Statistical analysis showed that the three major leaching parameters affecting contaminant concentration are: plastic material type, time, and the interaction between time and material type. Hence, BOP material selection and the material's exposure time to liquid water are very important considerations for fuel cell systems design and operations.

One focus this year was to develop a GCMS method to quantify the concentration of organic contaminants in material leachates. To accomplish this, we explored three GCMS methods: total ion count-single ion monitoring, thermal conductivity detector, and FID. GCMS-FID yielded the best trade-off between sensitivity and reproducibility. The results for the eleven leachate solutions (Table 1) are summarized in Figure 2. The caprolactam and aniline concentrations in the PA leachates were below 10 ppm and 20 ppm, respectively. In contrast, the PPA leachate solutions were relatively clean with caprolactam and aniline concentrations of 1 ppm or below the detection limit of the GCMS method. The quantification of caprolactam and aniline, two major organic species identified in structural plastic leachates, provided important guidance on selecting concentrations for fuel cell infusion experiments.

Leachates typically contain a variety of contaminants, including organics, inorganics, anions, and cations. These species can adsorb onto Pt catalyst surface and/or affect membrane/catalyst ionomer conductivity. We studied the impact of mixtures, as produced from the leaching of PA and PPA materials (Figure 3a), as well as the impact of individual model compounds (caprolactam and sulfate anion, Figure 3b). Both caprolactam and sulfate anion were found in the leachate solutions, and hence they were chosen for the model compound study.

Figure 3a shows that the PA leachate, which has more organic and ionic contaminants (Table 1), resulted in a higher fuel cell performance loss (ΔV_1) than the cleaner PPA leachate. Also, the PA leachate showed incomplete self-induced recovery (ΔV_2) while full recovery was observed

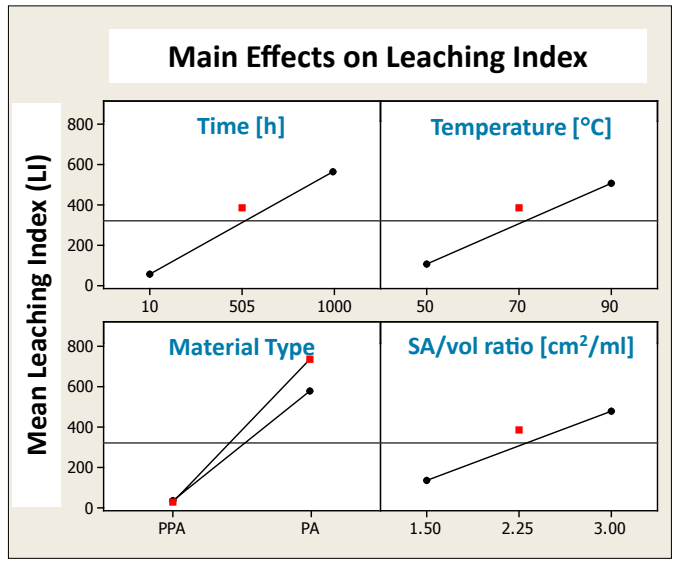

FIGURE 1. Effects of material type and leaching conditions (time, temperature, and surface area to volume ratio) on the solution LI (conductivity + total organic carbon). Leachates and analysis provided by GM.

TABLE 1. Different Leaching Conditions Used to Extract Contaminants from the PPA and PA Material, as well as the Sample Number and the Measured TOC and Solution Conductivity of These Leachate Solutions

	Plastic	Temp. [°C]	Time [h]	SA/Vol Ratio [cm^2/ml]	Sample #	TOC [ppm]	Solution Conductivity [µS/cm]
1	PPA	50	10	1.5	W-81	0.6	3
2	PPA	50	1000	3	W-82	4.7	12
3	PPA	90	10	3	W-83	6.9	7
4	PPA	90	1000	1.5	W-84	47	55
5	PA	50	10	3	W-85	50	19
6	PA	50	1000	1.5	W-86	246	78
7	PA	90	10	1.5	W-87	84	23
8	PA	90	1000	3	W-88	1422	391
9	PA	90	1000	1.5	W-89	983	221
10	PA	70	505	2.3	W-90	585	154
11	PPA	70	505	2.3	W-91	13	18

Structural materials: PA = polyamide (BASF Ultramid PA – A3HG6)
PPA = polyphthalamide (Solvay Amodel PPA–HFZ–1133)

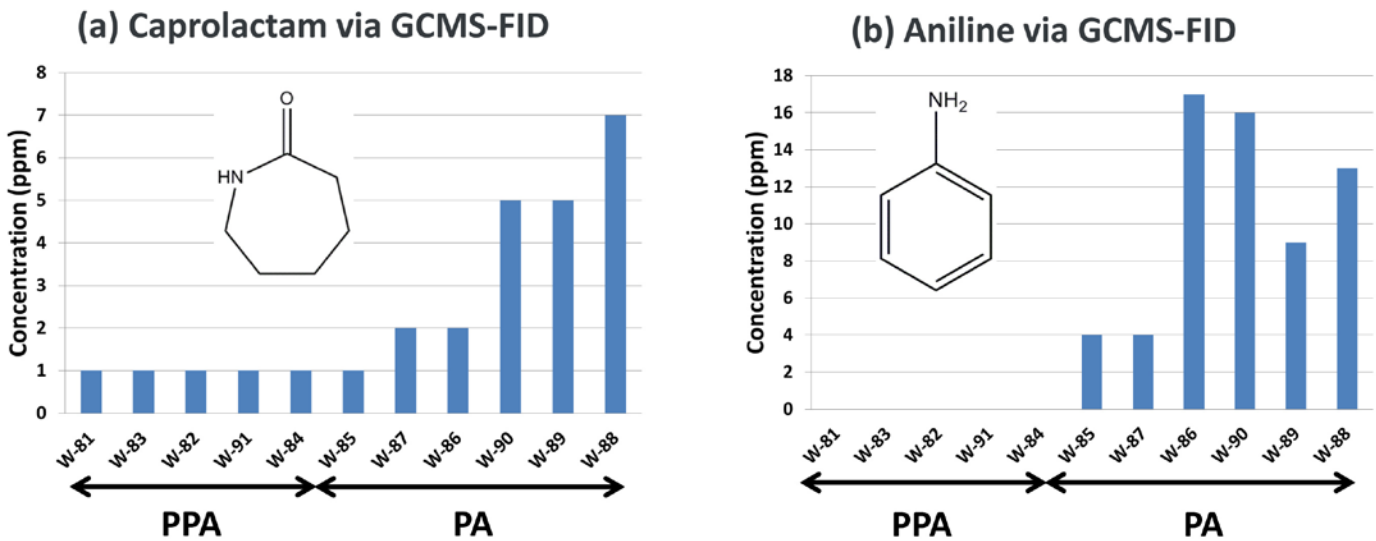

FIGURE 2. Concentration of caprolactam and aniline in the different PPA and PA leachates, as quantified by GCMS-FID method developed at NREL. PPA material leachates are relatively clean compared to PA material leachates.

for the PPA leachate. When 1 mM caprolactam was infused into the fuel cell cathode (Figure 3b, green curve), a relatively high fuel cell performance loss (ΔV_1 = 100 mV) and incomplete self-induced recovery (ΔV_2 = 30 mV) were observed. Surprisingly, no fuel cell performance loss was measured for the infusion of 10 mM sulfate anion at 0.2 A/cm^2 (Figure 3b, blue curve). This may be due to the Donnan exclusion effect and/or non-adsorption of sulfate onto Pt oxide. When a mixture of 1 mM caprolactam and 10 mM sulfate was infused into the fuel cell cathode (Figure 3b,

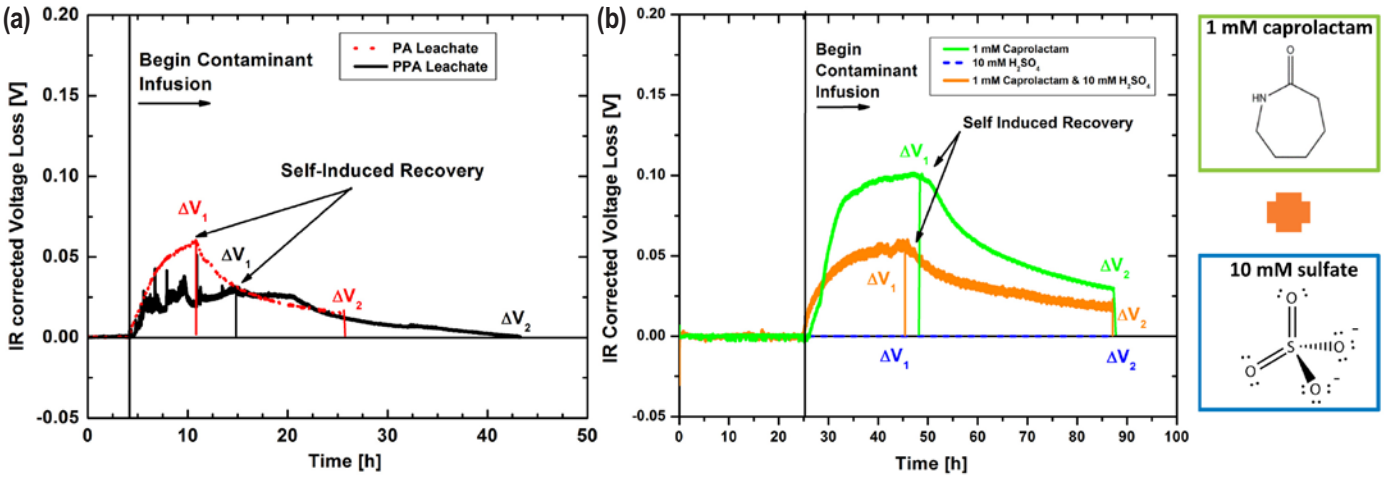

PA	ΔV_1 = 55 mV	ΔV_2 = 16 mV
PPA	ΔV_1 = 23 mV	ΔV_2 = 0 mV

1 mM caprolactam	ΔV_1 = 100 mV	ΔV_2 = 30 mV
1 mM caprolactam & 10 mM sulfate mixture	ΔV_1 = 60 mV	ΔV_2 = 17 mV
10 mM sulfate	ΔV_1 = 0 mV	ΔV_2 = 0 mV

FIGURE 3. (a) In situ fuel cell voltage loss due to contaminants (ΔV_1) derived from the PPA (black) and PA (red) materials. (b) The effect of individual model compounds: caprolactam (green), sulfate anion (blue), and mixtures of caprolactam and sulfate anion on the in situ fuel cell voltage loss due to contaminants (ΔV_1) and self-induced recovery (ΔV_2). Standard operating conditions (SOC): 80°C, 32/32% inlet relative humidity, 0.2 A/cm^2, H_2/air stoic = 2/2; 150/150 kPa, cathode Pt loading = 0.4 mg/cm^2.

orange curve), a lower fuel cell voltage loss was measured (ΔV_1 = 60 mV) compared to the caprolactam alone. This indicates that there is an interaction between caprolactam and sulfate, which is currently being investigated. Incomplete self-induced recovery was also observed for this mixture. Other supporting data (not shown) indicates that caprolactam had an impact on membrane conductivity, poisoned Pt sites to some extent, blocked Pt oxide formation, and decreased oxygen reduction reaction mass activity.

Model compound studies are important because they provide a more in-depth understanding of the contamination and recovery mechanisms of specific contaminants, identify the contaminant(s) that may have contributed to the overall fuel cell performance loss, and provide insights about the potential interaction(s) of different contaminants. Furthermore, results from the model compound studies contribute to the general understanding of compound-specific contaminants, based on their chemical structure, rather than specific plastic materials. This helps with BOP material selection and design for fuel cell systems.

CONCLUSIONS AND FUTURE DIRECTIONS

- We updated the list of NREL publications and presentations and added contaminants-related publications from the Naval Research Lab on the NREL project website.
- We determined that plastic material type and leaching time significantly impacted leachate concentration. Hence, BOP material selection and the material's exposure time to water are important considerations for fuel cell systems and operations.
- We developed a method to quantify organic concentrations in leachates. GCMS-FID yielded the best trade-off between sensitivity and reproducible data. The ranges of caprolactam (<10 ppm) and aniline (<20 ppm) concentrations found in polyamide material leachates provided important guidance on selecting concentration to be used in infusion experiments.
- We determined that low BOP leachate concentrations, caprolactam, and mixtures of caprolactam and sulfate had an impact on fuel cell performance, including Pt adsorption and membrane and catalyst ionomer poisoning.
- We will perform ex situ mechanistic studies on individual and mixtures of model compounds to understand interaction between different species in leachate solutions and their effect on fuel cell performance.
- We will develop analytical methods to identify and quantify volatile species, if any exist, derived from structural materials.
- We will study the effect of contaminants on low loading Pt/C catalyst (0.1 mg Pt/cm^2) and advanced catalysts (e.g., Pt alloys/C).
- We will develop an understanding of the impact of contaminants on catalyst ionomers.
- We will study the effect of non-sulfonated perfluorinated membrane degradation products on fuel cell performance.
- We will disseminate project information via the NREL website, publications, reports, and presentations.

FY 2015 PUBLICATIONS/PRESENTATIONS

1. Jason M. Christ, K.C. Neyerlin, Ryan Richards, and Huyen N. Dinh, "Concentration Effects of Polymer Electrolyte Membrane Degradation Products on Oxygen Reduction Activity for Three Platinum Catalysts," *J. Electrochem. Soc.* **161** (14) F1360–F1365 (2014).

2. Jason M. Christ, K.C. Neyerlin, Heli Wang, Ryan Richards, and Huyen N. Dinh, "Impact of Polymer Electrolyte Membrane Degradation Products on Oxygen Reduction Activity for Platinum Electrocatalysts," *J. Electrochem. Soc.* **161** (14) F1481–F1488 (2014).

3. James Waldecker, "System Contaminant Library Published," Fuel Cell Tech Team Accomplishment Report, 2014 U.S. DRIVE Highlight.

4. Huyen N. Dinh, "Making Fuel Cells Cleaner, Better, and Cheaper," NREL R&D Technical Highlight (2015).

5. Hyun-Seok Cho, Mayukhee Das, Heli Wang, Huyen N. Dinh, and J.W. Van Zee, "The Contamination Mechanism and Behavior of Amide Bond Containing Organic Contaminant on PEMFC," *J. Electrochem. Soc.* **162** (4) F427–F435 (2015).

6. Huyen N. Dinh, "Effect of System Contaminants on PEMFC Performance and Durability," Section V.B.1. *2014 DOE Hydrogen and Fuel Cells Program Annual Progress Report*, pp. V128–V132.

7. Jason M. Christ, K.C. Neyerlin, Ryan Richards, and Huyen N. Dinh, "Adsorption Characteristics of Polymer Electrolyte Membrane Chemical Degradation Products and Their Impact on Oxygen Reduction Reaction Activity for Platinum Catalysts," American Chemical Society Meeting, San Francisco, CA, August 2014.

8. Huyen N. Dinh, Jason M. Christ, Clay Macomber, Charles Staub, Guido Bender, and Heli Wang, "Effect of System Contaminants on PEMFC Performance and Durability," Project update to DOE, NREL, Golden, CO, September 24, 2014.

9. Jason Christ, Charles Staub, K.C. Neyerlin, Ryan Richards, and Huyen N. Dinh, "Effect of Organic Model Compound Contaminants on Platinum Catalysts," 226th Electrochemical Society Meeting, Cancun, Mexico, October 9, 2014.

10. Huyen N. Dinh, Jason Christ, Clay Macomber, Guido Bender, Charles Staub, and Paul Yu, "Effect of System Contaminants on PEMFC Performance and Durability," Fuel Cell Tech Team Meeting, Southfield, MI, February 11, 2015.

11. Charles Staub, Jason Christ, Guido Bender, Clay Macomber, Heli Wang, and Huyen N. Dinh, "Multiple Advance Diagnostics to Probe the Effect of Balance of Plant Materials on Fuel Cell Performance," Abstract #1599, 227th Electrochemical Society Meeting, Chicago, IL, May 2015.

12. Huyen N. Dinh, "Effect of System Contaminants on PEMFC Performance and Durability," DOE Fuel Cell Technologies Office Annual Merit Review, Washington, DC, June 2015.

REFERENCES

1. J. Spendelow and J. Marcinkoski, "Fuel Cell System Cost – 2013", DOE Fuel Cell Technologies Office Record #14012, http://hydrogen.energy.gov/pdfs/14012_fuel_cell_system_cost_2013.pdf, June 13, 2014.

2. Huyen N. Dinh, "An Overview of NREL's Online Data Tool for Fuel Cell System-Derived Contaminants," DOE Fuel Cell Technologies Office Webinar, http://energy.gov/sites/prod/files/2014/06/f16/webinarslides_fuel_cell_contaminants_052714.pdf, May 27, 2014.

3. Huyen N. Dinh, "Effect of System Contaminants on PEMFC Performance and Durability," Section V.E.1. *2013 DOE Hydrogen and Fuel Cells Program Annual Progress Report*, pp. V129–V134.

4. Huyen N. Dinh, "Effect of System Contaminants on PEMFC Performance and Durability," Section V.B.1. *2012 DOE Hydrogen and Fuel Cells Program Annual Progress Report*, pp. V57–V62.

5. Huyen N. Dinh, "Effect of System Contaminants on PEMFC Performance and Durability," Section V.B.1. *2011 DOE Hydrogen and Fuel Cells Program Annual Progress Report*, pp. 640–643.

6. Huyen N. Dinh, "Effect of System Contaminants on PEMFC Performance and Durability," Section V.C.4. *2010 DOE Hydrogen and Fuel Cells Program Annual Progress Report*, pp. 737–740.

7. G.A. James, et. al., "Prevention of Membrane Contamination in Electrochemical Fuel Cells," U.S. Patent Application US2005089746A.

8. R. Moses, "Materials Effects on Fuel Cell Performance," National Research Council Canada Institute for Fuel Cell Innovation, International Fuel Cell Testing Workshop, September 20–21, 2006.

9. K. O'Leary, B. Lakshmanan, and M. Budinski, "Methodologies for Evaluating Automotive PEM Fuel Cell System Contaminants," Canada-USA PEM Network Research Workshop, February 16, 2009.

10. D. Gerard, "Materials and Materials Challenges for Advanced Automotive Technologies Being Developed to Reduce Global Petroleum Consumption," 2007 Materials Science and Technology (Invited), Detroit, MI, September 16–20, 2007.

11. D.A. Masten and A.B. Bosco, *Handbook of Fuel Cells,* ed. W. Vielstich, et al. (Wiley, 2003), Vol. 4, Chapter 53, p. 714.

12. Q. Guo, R. Pollard, J. Ruby, T. Bendon, P. Graney, and J. Elter, *ECS Trans*., Vol. 5(1), p. 187 (2007).

V.E.4 The Effect of Airborne Contaminants on Fuel Cell Performance and Durability

Jean St-Pierre (Primary Contact), Yunfeng Zhai, Junjie Ge, Tatyana Reshetenko, Michael Angelo, Jing Qi, Trent Molter[1], Leonard Bonville[1], Ugur Pasaogullari[1], Ozan Ozdemir[1], Md Aman Uddin[1], Jaehyung Park[1], Selvarani Ganesan[1], William Collins[2], Tommy Cheng[3]
Hawaii Natural Energy Institute
1680 East-West Road
Honolulu, HI 96822
Phone: (808) 956-3909
Email: jsp7@hawaii.edu

DOE Manager
Nancy Garland
Phone: (202) 586-5673
Email: Nancy.Garland@ee.doe.gov

Contract Number: DE-EE0000467

Subcontractors
[1] University of Connecticut, Storrs, CT
[2] WPCSOL, East Windsor, CT
[3] Ballard Power Systems, Burnaby, BC, Canada

Project Start Date: April 1, 2010
Project End Date: December 31, 2015

Overall Objectives

- Identify and mitigate the adverse effects of airborne contaminants on fuel cell system performance and durability
- Provide contaminants and tolerance limits for filter specifications (preventive measure)
- Identify fuel cell stack's material, design, operation, or maintenance changes to remove contaminant species and recover performance (recovery measure)

Fiscal Year (FY) 2015 Objectives

- Demonstrate successful mitigation of the impact of the four most important airborne contaminants

Technical Barriers

This project addresses the following technical barriers from the Fuel Cells section of the Fuel Cell Technologies Office Multi-Year Research, Development, and Demonstration Plan:

(A) Durability

(B) Cost

(C) Performance

Technical Targets

The following 2020 technical targets for automotive applications, 80 kW_e (net) integrated transportation fuel cell power systems operating on direct hydrogen, are considered:

- Durability: 5,000 hours in automotive drive cycle
- Cost: \$40/kW_e
- Performance: 60% energy efficiency at 25% of rated power

The effects of specific airborne contaminants are studied, including a commercially relevant low cathode catalyst loading, and the resulting information will be used to impact both preventive measures and recovery procedures:

- Airborne contaminant tolerance limits to support the development of filtering system component specifications and ensure negligible fuel cell performance losses
- Fuel cell stack material, design, operation, or maintenance changes to recover performance losses derived from contamination mechanisms

FY 2015 Accomplishments

- Assessed the impact of acetonitrile and Ca^{2+}, which led to larger peroxide production rates in ex situ rotating ring disc electrode tests by up to 1,300%, on membrane degradation during long duration fuel cell tests and found a decrease in exhaust water fluoride concentration of 67% for acetonitrile
- Defined the partial effectiveness of two in situ recovery procedures to reverse the effects of Ca^{2+} contamination (cell performance loss, salt deposition): (1) operation at a low cell voltage and (2) acid solutions without or with isopropanol
- Determined the impact of four cleansers diluted by a factor of 20 on fuel cell performance

✧ ✧ ✧ ✧ ✧

INTRODUCTION

The composition of atmospheric air cannot be controlled and typically includes other gases including many volatile

organic compounds, as well as ions entrained in liquid water and encountered as droplets in the form of rain, mist, etc., especially near marine environments. Materials require cleansers to remove oils and dirt introduced by fuel cell manufacturing and assembly operations. Specific types of air contaminants and cleansers may cause deleterious effects which include decreased cell performance and durability [1,2] of proton exchange membrane fuel cells. Numerous air contaminants and cleansers have not yet been tested in fuel cells and consequently their effects as well as recovery methods are unknown [2,3]. Furthermore, prevention is difficult to achieve because tolerance limits are also missing in most cases [2]. This increases the risk of failure for fuel cell systems and thus jeopardizes their introduction into the market.

Airborne contaminants and foreign ions have previously been selected using a cost effective two tiered approach combining qualitative and quantitative criteria [3]. Automotive fuel cells are used under a wide range of operating conditions resulting from changes in power demands (drive cycle). Temperature and current density impact fuel cell contamination the most [4]. The effect of contaminant concentration is also particularly important. Contaminant threshold concentrations for predetermined fuel cell performance losses were determined [5] to facilitate the definition of air filtering system tolerances (prevention). Subsequently, contamination mechanisms were investigated using a variety of ex situ and in situ characterization techniques [6] to facilitate the development of performance recovery procedures. The series of ex situ tests aimed at isolating the kinetic contribution (rotating ring disc electrode) revealed much larger peroxide production rates, an oxygen reduction side reaction, in the presence of organic or cationic contaminants [7-10]. The membrane is more susceptible to degradation in the presence of peroxide [11,12]. It was deemed important to expose fuel cells to contaminants for a long period to confirm the peroxide impact on membrane degradation because the ex situ test is performed at a significantly lower temperature of 30°C in comparison to 80°C in an application and with a liquid electrolyte contacting the catalyst thin film. Although fuel cells contaminated with iron [13] and sulfur dioxide [14] have shown elevated levels of fluoride in the exhaust water, a product of membrane degradation, these indirect measurements were not corroborated with membrane/electrode assembly material characterizations including membrane thickness and conductivity, and catalyst active surface. Although cation contamination data have revealed that the mechanism proceeds with an ion exchange step with the membrane proton [15-17], the evaluation of in situ recovery strategies that take advantage of that knowledge has not previously been attempted. The effectiveness of two cation contamination recovery methods was therefore investigated. Finally, cleansers were classified and selected for fuel cell screening tests because that contaminant class has not been previously explored.

APPROACH

The contaminant pool was previously reduced to one cation (Ca^{2+}) and seven organic species (acetonitrile, acetylene, bromomethane, isopropanol, methyl methacrylate, naphthalene, propene) for detailed mechanistic studies [6]. For the long-term duration contamination tests, one contaminant was selected from each of these contaminant classes. The choice of the cation was straightforward whereas acetonitrile was chosen because it had a larger effect than five of the other six organic species according to one of the two quantitative down-selection criteria [3] and is the only organic species that impacted ohmic losses mostly associated with the membrane. As focus was given to membrane degradation, diagnostics included in situ membrane resistivity (impedance spectroscopy, milliohmmeter), and fuel cell exhaust water analyses for fluoride (ion chromatography, ion selective electrode). Destructive tests were also considered at the end of the long duration test to measure the membrane and catalyst layer thicknesses by scanning electron microscopy.

Two in situ contamination recovery methods were investigated. A high current density, low cell voltage was used to assist foreign cation removal from the membrane by the high rate of water production at the cathode and the displacement of the foreign cations towards the cathode due to the predominant electric field effect [18,19]. Ion exchange was also used by circulating acid solutions in the cathode compartment. Only the acid solution approach was evaluated for the removal of salt deposits from the flow field channels and the gas diffusion layer after the cell was contaminated in situ. Both methods were assessed for their effectiveness on cell performance recovery after a controlled ex situ contamination step to avoid salt precipitation. The presence of salt was ascertained visually (photography, scanning electron microscopy) and spectroscopically (energy dispersive X-ray spectroscopy). Salt removal was also ascertained by measuring the membrane ion exchange capacity and the gas diffusion layer contact angle.

Cleansers were selected on the basis of prior suggestions provided by industry. The fuel cell injection method is based on the cleanser boiling point. The cleanser is evaporated for a liquid with a boiling point below 20°C whereas it is injected as a mist above that temperature. The cleanser is diluted by a factor of 20 which is the leftover concentration estimated on the basis of two rinses. The cleanser is initially injected in the cathode compartment. If the cleanser has no effect on fuel cell performance, it is re-tested by injection on the anode side. Focus is given to the cell performance loss resulting from the cleanser injection for screening and selection purposes.

RESULTS

Figure 1 illustrates the ion chromatography results of outlet water samples collected during the 1,000-hour long-term test with 5 ppm acetonitrile. The presence of acetonitrile decreases the fluoride concentration in water samples. In particular, it is noted that after the contaminant is introduced, the fluoride concentration decreases whereas after the contaminant injection is interrupted, the fluoride concentration increases. The average fluoride concentration is respectively 0.15 mg L^{-1} and 0.05 mg L^{-1} during the recovery and contamination period corresponding to a 67% decrease during the contamination period. It is hypothesized that acetonitrile acts as a scavenger for the radicals and/or peroxide generated at the cathode. The present results contrast with iron [13] and sulfur dioxide [14] data which demonstrated an increase rather than a decrease in fluoride concentration. Therefore, the scavenging effect is contaminant specific and needs to be ascertained for each contaminant. Membrane resistances and catalyst layer and membrane thicknesses after the recovery period were not affected by the long term exposure to acetonitrile and support the acetonitrile as scavenger hypothesis.

The long duration test for Ca^{2+} was prematurely interrupted after more than 350 h of contamination due to salt deposits blocking the gas diffusion layer and the flow field channels. The membrane resistance obtained by impedance spectroscopy did not significantly change but the cathode catalyst layer became thinner (more than a 50% reduction in thickness). However, the ion selective electrode fluoride measurements were inconclusive as values were below the detection level. Samples will be re-analyzed by ion chromatography. Platinum dissolution which could negligibly contribute to a thinner catalyst layer (presumably, the carbon support network remains intact) was discounted because its concentration in water samples was not affected (inductively coupled plasma mass spectrometry) and the platinum signal although spread over a shorter distance was more intense (energy dispersive X-ray spectroscopy). The possibility remains that carbon corrosion might be partly responsible for the thinner cathode catalyst layer in addition to membrane degradation but a specific test is needed to discriminate between these two possibilities (for example, an increase in air outlet carbon dioxide concentration, a product of carbon corrosion).

The in situ circulation of an acid solution to recover performance losses sustained during Ca^{2+} contamination was only partly effective. The most direct evidence is depicted in Figure 2 with a catalyst coated membrane ion exchange capacity after recovery still lower than the value for a fresh sample by about 30%. The reason for this incomplete recovery which is significantly smaller than the extent that can be achieved by applying the method ex situ to a catalyst coated membrane, has not been clarified. It is likely related to the gas diffusion layer acting as a barrier. Ion exchange can only take place if there is a direct contact between the acid solution and the ionomer as revealed by ex situ contamination tests and immersing the catalyst coated membrane in the solution with and without a gas diffusion layer. The addition of isopropanol as surface active agent (a relatively benign contaminant [3]) did not improve the performance recovery. Sophisticated methods will be required to verify the contact between the acid solution and the ionomer, and improve the performance recovery. Cell operation at a high current density, low cell voltage was ineffective in recovering any cell performance losses due to calcium contamination even after ~40 h of operation under these conditions.

The in situ acid solution flush was largely effective in removing salt deposits on the cathode flow field channels and gas diffusion layer (Figure 3a). However, the cell

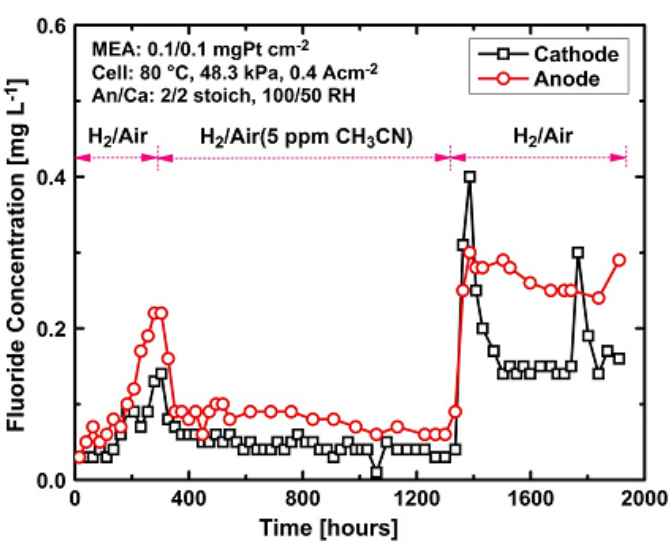

FIGURE 1. Fluoride concentration in liquid water samples extracted from fuel cell cathode and anode outlet streams as a function of time before, during and after an exposure to 5 ppm acetonitrile in air

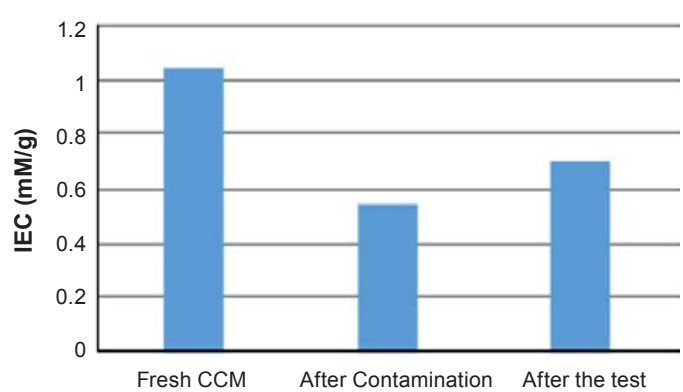

FIGURE 2. Catalyst coated membrane ion exchange capacity before, after contamination with Ca^{2+} and after recovery procedures

performance was only recovered in the mass transfer regime (Figure 3b). This observation is consistent with the extent of recovery achieved by contaminating the membrane electrode assembly ex situ (no salt deposits) and suggests that the presence of salt deposits has a smaller effect on cell performance than if the foreign cation penetrates the ionomer/membrane. A membrane electrode assembly cross section obtained after the test was completed confirms that the in situ acid solution flush is only partly effective as salt deposits of calcium sulfate are still present throughout the gas diffusion layer (Figure 3c, left image). This statement is confirmed by energy dispersive X-ray spectroscopy maps for sulfur (Figure 3c, center image) and calcium (Figure 3c, right image). The use of isopropanol did not improve the situation, concurring with the in situ observation that performance recovery is not improved with the addition of isopropanol. The impact of operating conditions on the salt dissolution rate may play a role and therefore they should be investigated.

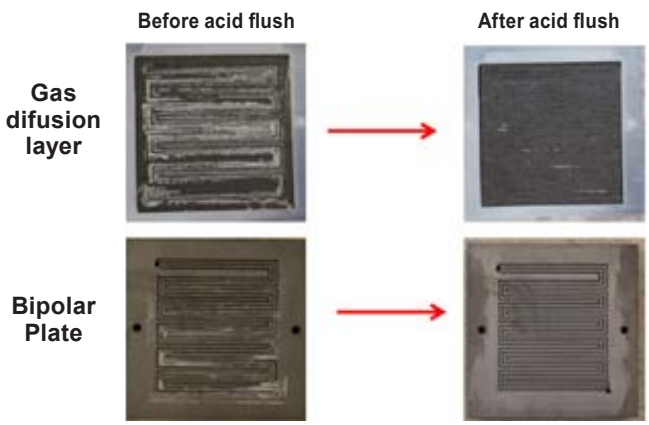

FIGURE 3A. Calcium salt deposit extent on the cathode gas diffusion layer and bipolar plate before and after in situ cleaning with an acid solution circulated in the cathode compartment

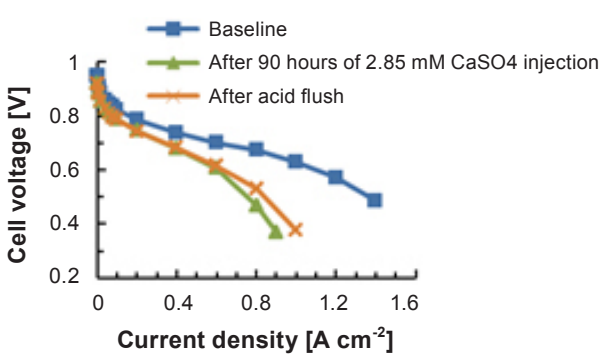

FIGURE 3B. Polarization curves obtained before and after in situ calcium contamination and after in situ recovery by circulating an acid solution in the cathode compartment

The project scope was expanded with the objective to screen a number of cleansers and determine their impact on fuel cell performance. The results related to four different cleansers were documented. The major components of Cleanser B include triethanolamine, ethoxylated alcohol and propylene glycol butyl ether. Figure 4 illustrates Cleanser B results. A large performance loss >0.2 V is observed over a period of approximately 10 h. This loss was partially recovered with a cell voltage gain >0.1 V. Results for all four cleansers already justify the need for this study. In each case, a significant loss in performance was noted.

CONCLUSIONS AND FUTURE DIRECTIONS

- Acetonitrile appears to scavenge the peroxide produced at the cathode or its decomposition products (radicals).
- The circulation of acid solutions in the cathode compartment was partly effective to recover both

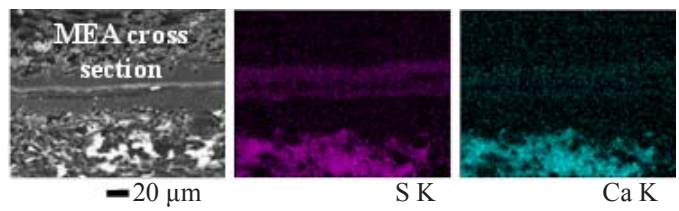

FIGURE 3C. Scanning electron microcopy image of the gas diffusion layer contaminated in situ with calcium after recovery with an acid solution (left) and corresponding sulfur S (center) and calcium Ca (right) maps obtained by energy dispersive X-ray spectroscopy; the cathode corresponds to the lower half of the image

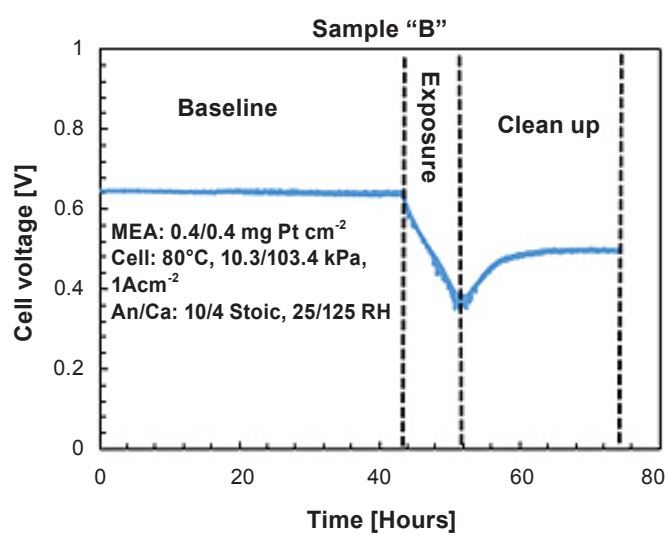

FIGURE 4. Voltage transient recorded during Cleanser B evaluation

performance loss and removing salt deposits resulting from Ca^{2+} contamination.

- Cell operation at a high current density, low cell voltage was ineffective to recover performance losses resulting from Ca^{2+} contamination.
- The four cleansers tested all lead to a loss in performance of at least 0.1 V when they were injected with a dilution factor of 20.
- Water samples obtained during Ca^{2+} contamination will be re-analyzed to ascertain the impact on membrane degradation (fluoride concentration).
- The long duration, low loading membrane electrode assembly contamination test (0.1 mg Pt cm^{-2}) will be initiated with a mixture of organic contaminants using lower concentrations than those previously used during this program (moving towards practical operating conditions).
- Recovery procedure tests for bromomethane, an organic contaminant characterized by a slow and incomplete recovery in comparison to the other six studied species from that group, will be initiated.
- Bromomethane contamination tests with metallic bipolar plates will be completed to assess the existence of interactions (bromine promotes corrosion).
- We will continue to analyze, summarize, and disseminate the large fuel cell contamination database.

FY 2015 PUBLICATIONS/PRESENTATIONS

1. Y. Zhai, O. Baturina, D. Ramaker, E. Farquhar, J. St-Pierre, K. Swider-Lyons, *J. Phys. Chem,* **119** (2015) 20328.

2. M.A. Uddin, J. Qi, X. Wang, U. Pasaogullari, L.J. Bonville, *Int. J. Hydrogen Energy,* **40** (2015) 13099.

3. M.A. Uddin, X. Wang, J. Qi, M.O. Ozdemir, U. Pasaogullari, L. Bonville, T. Molter, *J. Electrochem. Soc.*, **162** (2015) F373.

4. M.A. Uddin, X. Wang, J. Park, U. Pasaogullari, L. Bonville, *J. Power Sources*, **296** (2015) 64.

5. T.V. Reshetenko, J. St-Pierre, *J. Power Sources*, **293** (2015) 929.

6. T.V. Reshetenko, J. St-Pierre, *J. Power Sources*, **287** (2015) 401.

7. J. Qi, X. Wang, M.O. Ozdemir, M.A. Uddin, L. Bonville, U. Pasaogullari, T. Molter, *J. Power Sources*, **286** (2015) 18.

8. Y. Zhai, J. St-Pierre, *J. Power Sources*, **279** (2015) 165.

9. S. Ganesan, M.A. Uddin, J. Park, U. Pasaogullari, L.J. Bonville, T. Molter, "Impact of Cationic Impurities on Low-Pt Loading PEFC Cathodes," *Electrochem. Soc. Trans.*, accepted.

10. M.A. Uddin, J. Park, S. Ganesan, U. Pasaogullari, L.J. Bonville, T. Molter, "A Cationic Contamination in PEFC Cathode: A Cause and Effect Study," *Electrochem. Soc. Trans.*, accepted.

11. J. Park, M.A. Uddin, S. Ganesan, U. Pasaogullari, L.J. Bonville, "Effects on Wetting Agents in Cationic Contamination and Mitigation in PEFCs," *Electrochem. Soc. Trans.*, accepted.

12. M.A. Uddin, U. Pasaogullari, T. Molter, *Electrochem. Soc. Trans.*, **64**(3) (2014) 705.

13. M.A. Uddin, J. Park, X. Wang, J. Qi, U. Pasaogullari, L.J. Bonville, T. Molter, *Electrochem. Soc. Trans.*, **64**(3) (2014) 537.

14. M.A. Uddin, J. Park, U. Pasaogullari, L.J. Bonville, ECS Conference on Electrochemical Energy Conversion and Storage with SOFC-XIV poster presentation, abstract 647.

15. J. Park, M.A. Uddin, S. Ganesan, U. Pasaogullari, L.J. Bonville, ECS Conference on Electrochemical Energy Conversion and Storage with SOFC-XIV oral presentation, abstract 614.

16. J. St-Pierre, United States Department of Energy 2015 Annual Merit Review meeting oral presentation, project ID # FC065.

17. J. Park, M.A. Uddin, S. Ganesan, U. Pasaogullari, L.J. Bonville, 227th Electrochemical Society meeting poster presentation, abstract 1592.

18. M.A. Uddin, J. Park, S. Ganesan, U. Pasaogullari, L.J. Bonville, T. Molter, 227th Electrochemical Society meeting oral presentation, abstract 1549.

19. S. Ganesan, M.A. Uddin, J. Park, U. Pasaogullari, L.J. Bonville, T. Molter, 227th Electrochemical Society meeting oral presentation, abstract 1548.

20. W. Collins, SAE International meeting oral presentation, March 10, 2015.

21. J. St-Pierre, U.S. DRIVE Fuel Cell Tech Team meeting oral presentation, January 14, 2015.

22. T.V. Reshetenko, J. St-Pierre, 2014 Fuel Cell Seminar and Energy Exposition meeting oral presentation, abstract 56.

23. Y. Zhai, J. St-Pierre, J. Ge, 226th Electrochemical Society meeting oral presentation, abstract 1271.

24. Y. Zhai, O. Baturina, D.E. Ramaker, J. St-Pierre, K.E. Swider-Lyons, 226th Electrochemical Society meeting oral presentation, abstract 1268.

25. M.A. Uddin, J. Park, X. Wang, J. Qi, U. Pasaogullari, L.J. Bonville, T. Molter, 226th Electrochemical Society meeting oral presentation, abstract 1229.

26. M.A. Uddin, U. Pasaogullari, T. Molter, 226th Electrochemical Society meeting oral presentation, abstract 1033.

REFERENCES

1. J. St-Pierre, "Air Impurities," in *Polymer Electrolyte Fuel Cell Durability*, Edited by F.N. Büchi, M. Inaba, T.J. Schmidt, Springer, 2009, p. 289.

2. J. St-Pierre, M. Angelo, K. Bethune, J. Ge, S. Higgins, T. Reshetenko, M. Virji, Y. Zhai, *Electrochem. Soc. Trans.*, **61** (23) (2014) 1.

3. J. St-Pierre, Y. Zhai, M.S. Angelo, *J. Electrochem. Soc.*, **161** (2014) F280 and **162** (2015) X7.

4. J. St-Pierre, Y. Zhai, M. Angelo, *Int. J. Hydrogen Energy*, **37** (2012) 6784.

5. J. St-Pierre, Y. Zhai, J. Ge, M. Angelo, T. Reshetenko, T. Molter, L. Bonville, U. Pasaogullari, W. Collins, S. Wessel, DOE Hydrogen and Fuel Cells Program, FY 2013 Annual Progress Report, p. V-3.

6. J. St-Pierre, United States Department of Energy 2015 Annual Merit Review meeting oral presentation, June 10, 2015.

7. J. Ge, J. St-Pierre, Y. Zhai, *Electrochim. Acta*, **133** (2014) 65.

8. J. Ge, J. St-Pierre, Y. Zhai, *Electrochim. Acta*, **134** (2014) 272.

9. J. Ge, J. St-Pierre, Y. Zhai, *Electrochim. Acta*, **138** (2014) 437.

10. J. Ge, J. St-Pierre, Y. Zhai, *Int. J. Hydrogen Energy*, **39** (2014) 18351.

11. W. Liu, K. Ruth, G. Rusch, *J. New Mater. Electrochem. Syst*., **4** (2001) 227.

12. A. Bosnjakovic, S. Schlick, *J. Phys. Chem. B*, **108** (2004) 4332.

13. A. Pozio, R.F. Silva, M. De Francesco, L. Giorgi, *Electrochim. Acta*, **48** (2003) 1543.

14. Y. Zhai, K. Bethune, G. Bender, R. Rocheleau, *J. Electrochem. Soc.*, **159** (2012) B524.

15. M.F. Serincan, U. Pasaogullari, T. Molter, *Int. J. Hydrogen Energy*, **35** (2010) 5539.

16. J. St-Pierre, *J. Power Sources*, **196** (2011) 6274.

17. J. St-Pierre, *Int. J. Hydrogen Energy*, **36** (2011) 5527.

18. A.Z. Weber, C. Delacourt, *Fuel Cells*, **8** (2008) 459.

19. B.L. Kienitz, H. Baskaran, T.A. Zawodzinski Jr., *Electrochim. Acta*, **54** (2009) 1671.

V.E.5 Open Source FCPEM-Performance and Durability Model: Consideration of Membrane Properties on Cathode Degradation

Shanna Knights (Primary Contact), David Harvey
Ballard Power Systems
9000 Glenlyon Parkway
Burnaby, BC V5J 5J8
Phone: (604) 454-0900
Email: shanna.knights@ballard.com

DOE Manager
Donna Ho
Phone: (202) 586-8000
Email: Donna.Ho@ee.doe.gov

Contract Number: DE-EE0006375

Subcontractors
- K. Karan, University of Calgary, Calgary, AB, Canada
- P. Atanassov, University of New Mexico, Albuquerque, NM

Project Start Date: January 1, 2014
Project End Date: March 31, 2015

Overall Objective

- Develop open source, forward predictive models and conduct systematic cell degradation studies

Fiscal Year (FY) 2015 Objectives

- Complete membrane sub-model development, integration, and validation within Fuel Cell Application Package for Open-source Long-Life Operation (FC-APOLLO)
- Complete open source model hosting for FC-APOLLO
- Complete data analysis for beginning of test (BOT), accelerated stress test (AST), and end of test (EOT) behavior of membranes/membrane electrode assemblies (MEAs)
- Dissemination of data via final report

Technical Barriers

This project addresses the following technical barriers from the Fuel Cell Technologies Office (FCTO) Multi-Year Research, Development, and Demonstration (MYRDD) Plan [1].

(A) Durability

Pt catalyst and Pt catalyst layers degradation

- Effect of cathode structure and composition
- Effect of operational conditions

(B) Performance

- Effect of cathode catalyst structure and composition

(C) Cost (indirect)

Technical Targets

In this project, fundamental studies of the Pt/carbon catalyst degradation mechanisms and degradation rates are conducted and correlated with membrane transport properties and operational conditions. The fundamental studies are used to facilitate the development and refinement of membrane model implementation within the open source software FC-APOLLO. Furthermore, the design curves generated both through model simulations and experimental work, will enable MEA designers to optimize performance, durability, and cost towards the 2020 targets for fuel cell commercialization [1].

- System durability (10% performance loss)
  - Transportation applications: 5,000 h
  - Stationary applications (1–10 kW_e): 60,000 h
- Electrocatalyst (transportation applications)
  - Support stability: <10% mass activity loss after 400 h at 1.2 V in H_2/N_2
  - Electrochemical surface area (ECSA) loss <40%
  - Precious group metal total loading: 0.125 mg/cm^2

FY 2015 Accomplishments

- Completed testing of membrane AST degraded MEAs
- Developed correlations for various behaviors of degraded MEAs and related diagnostics
- Completed hosting and release of the first versions of the open source code, FC-APOLLO
- Revised membrane sub-model and completed first validation against experimental data

✧ ✧ ✧ ✧ ✧

INTRODUCTION

Catalyst/catalyst layer degradation has been identified as a substantial contributor to fuel cell performance degradation and this contribution will most likely increase as MEAs are driven to lower Pt loadings in order to meet the cost targets for full-scale commercialization. Over the past few years significant progress has been made in identifying catalyst degradation mechanisms [1,2] and several key parameters that greatly influence the degradation rates, including electrode potentials, potential cycling, temperature, humidity, and reactant gas composition [2,4–6]. Despite these advancements, many gaps still exist with respect to catalyst layer degradation and an understanding of its driving mechanisms. In particular, acceleration of the mechanisms under different fuel cell operating conditions, due to different structural compositions/neighboring components and as a function of the drive to lower Pt loadings, remains an area not well understood. In order to close these gaps, an understanding is needed of the effect of the membrane properties on the local conditions within the catalyst layer and the subsequent manifestation of those local conditions on performance and durability, in particular the catalyst layer degradation mechanisms and rates.

The focus of this project is to develop open source, forward predictive models and conduct systematic cell degradation studies that enable quantification of the cathode catalyst layer degradation mechanisms and rates and to correlate those rates and the degradation derived changes in catalyst properties/composition to the materials properties of the chosen membranes.

APPROACH

This project addresses the performance and durability of Pt catalysts and catalyst layers which have been identified as key technical barriers in the FCTO MYRDD Plan [1]. The project follows a parallel three-path approach of (1) theoretical simulations, (2) experimental investigations, and (3) material/component characterization (collaborative work) with the overall goal to advance the ability to simulate and design durable fuel cell products and subsequently reduce the iterative design/test cycle process for next generation fuel cell products.

The approach of the project includes (1) refinement of the membrane model that is an integral part of FC-APOLLO in order to describe changes in transport properties as a function of the change in membrane type (material characteristics); (2) experimental assessment of the impact of membrane type, transport and materials properties on the MEA performance loss mechanisms and the Pt dissolution mechanism/rate; and (3) development of correlations that link membrane materials properties and catalyst layer effective properties to MEA/cathode performance and degradation loss mechanisms.

RESULTS

Model Development

During the previous fiscal years a review of existing membrane sub-models and initial implementation was completed in order to down-select, evaluate, and initiate the full development of the membrane sub-model within the FC-APOLLO framework. The relational behavior of several models was evaluated in order to assess the ability to capture and/or predict various trends observed in the experimental data and it was found that the existing membrane sub-models within literature have several short comings in the ability to predict the behaviors observed in various aspects of the experimental data. In particular, many of the membrane sub-models are not implemented in a transient framework and do not adequately describe the rate of exchange between liquid and vapor phases; furthermore, many of the existing models contain parameters that are not tractable to determine, neither analytically nor from an ex situ or in situ experimental basis. Various forms of physics based membrane models do exist within the open literature; however, key coefficients that describe or control the behavior of the materials are generally not measurable or are unknown [7]. This project has adapted the work of Weber and Newman [8] as a starting point for a steady state implementation of the membrane sub-model and work in the last fiscal year has focused on the extension to a general transient, three-dimensional implementation in the context of a unit cell. Figure 1 shows the general schematic of the operating modes that the model captures and the interfacial resistance that exists related to the adsorption/desorption processes that occur at the interface of the ionomeric membrane and porous electrode. The implemented module attempts to capture the observations at steady state and, additionally, the time dependent behavior due to shifts in the chemical potential or state of water in either of the electrode regions over the course of operation. To date, initial implementation of the sub-model framework has been completed and the focus of the ongoing work continues to remain on the development of the interfacial resistance terms in such a way as to continue to capture the steady state

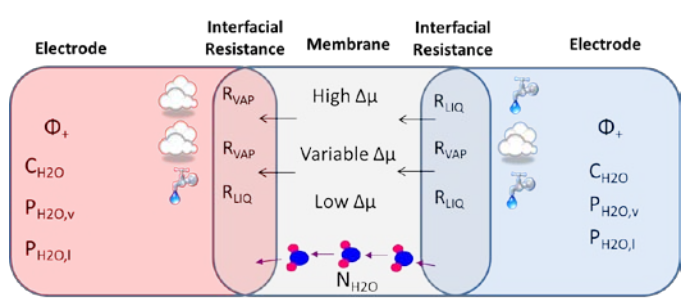

FIGURE 1. Water cross-over transport scenarios for the improved transient sub-model

behavior but additionally provide an explanation/capture the observed transient related effects relevant to AST cycling.

Experimental Parametric Studies

Experimental testing, characterization, and data analysis for the BOT, catalyst AST cycled, and membrane AST/catalyst AST cycled was completed within this fiscal year. The project focused on the following types of membranes: Nafion® 211 (baseline membrane), Nafion® 212 (optional), experimental reinforced perfluorinated sulfonic acid (PFSA) membranes with low and high equivalent weights (EWs), and experimental reinforced partially fluorinated hydrocarbon (R-HFC) membranes of high and low EW. The intention of the testing in the project is to develop characterization and validation data for the simulation and modelling work and to generate data sets that can be used to correlate MEA performance and durability to membrane properties and key transport parameters.

A table of membrane properties/characteristics for the membranes considered in this project is shown in Table 1. Based on the theory/relationships of previous, existing, and to-be-implemented models, the membranes in Table 1 were characterized for behavior and properties related to water transport, uptake, and adsorption/desorption. The characterization of the membranes shown in Table 1 consisted of in-cell and ex situ testing including steady state polarizations, a membrane AST, a cathode catalyst AST, dynamic vapor sorption, and electrochemical impedance spectroscopy in order to elucidate differences and effects due to the use of different membrane materials and the associated effects on the cathode catalyst layer local conditions. The baseline MEA, the test hardware, the cathode AST, and suite of diagnostic tools are described in detail in previous project documentation.

TABLE 1. Properties of Examined Membrane Properties for Model Inputs

Membrane	Acronym Used	EW (g/mol SA)	Density (g/mL)	Dry Thickness (μm)
Baseline: Nafion® NR211	NR211	1,099	2.0	25
Nafion® NR212	NR212	1,099	2.0	50
Reinforced PFSA High EW	R-PFSA-HEW	1,136	2.0	18
Reinforced PFSA Low EW	R-PFSA-LEW	872	2.0	14
Partially Fluorinated Hydrocarbon High EW	R-HFC-HEW	758	1.8	15
Partially Fluorinated Hydrocarbon Low EW	R-HFC-LEW	625	1.8	13

SA – sulfonic acid

In order to establish the effect of the catalyst AST and the combination of the membrane AST (pre-degraded membrane) and subsequent catalyst AST, a BOT performance was established. This test was done for MEAs with the different down-selected membranes at relative humidity (RH) of 60% and 100% and is shown in Figure 2. We see that each of the MEAs has in situ performance greater than 600 mV at current densities less than 1 A/cm^2. At 100% RH the R-PFSA-LEW MEA had similar performance as the baseline NR211 membrane. Lower performance was observed for the R-PFSA-HEW and NR212 MEAs consistent with the increased membrane thickness as compared to the performance of the R-PFSA-LEW and NR211 MEAs, respectively. At 2 A/cm^2 and 100% RH, a difference of 100 mV is observed between the baseline NR211 and the NR212 MEAs with the R-HFC membranes showing similar performance to the NR212 membrane; it is important to note that these membranes were thinner and had lower EW than the baseline. The R-HFC membranes' lower performance may have been a function of the structural pairing of dissimilar ionomers between the catalyst layer and the membrane.

After the BOT testing the MEAs were subjected to a cathode AST for 4,700 cycles. Figure 3 shows the results of the cathode AST on the performance of the MEAs. The range of performance differences observed at the BOT evaluation point was muted following the post-cathode AST performance (except for R-HFC-LEW) creating two pairing groups. This is largely due to the two top performing MEAs (the baseline NR211 and R-PFSA-LEW) having had

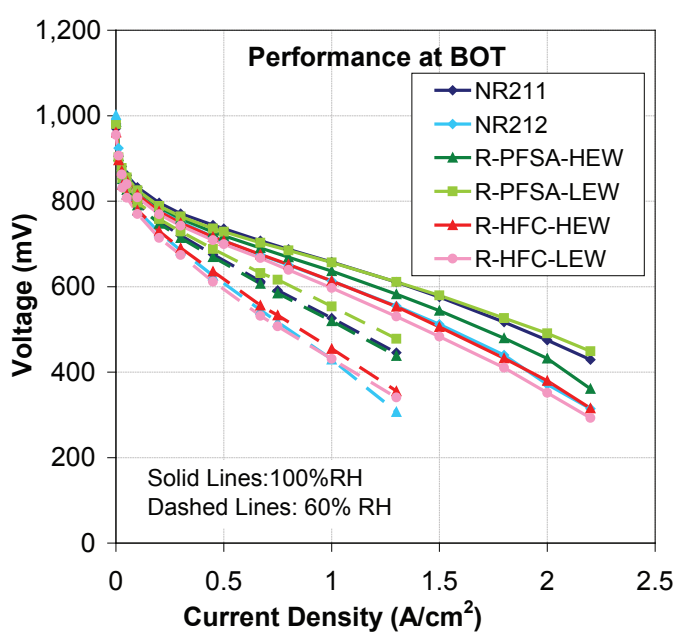

FIGURE 2. MEA performance at 100% and 60% RH at the BOT for the membrane/MEA types

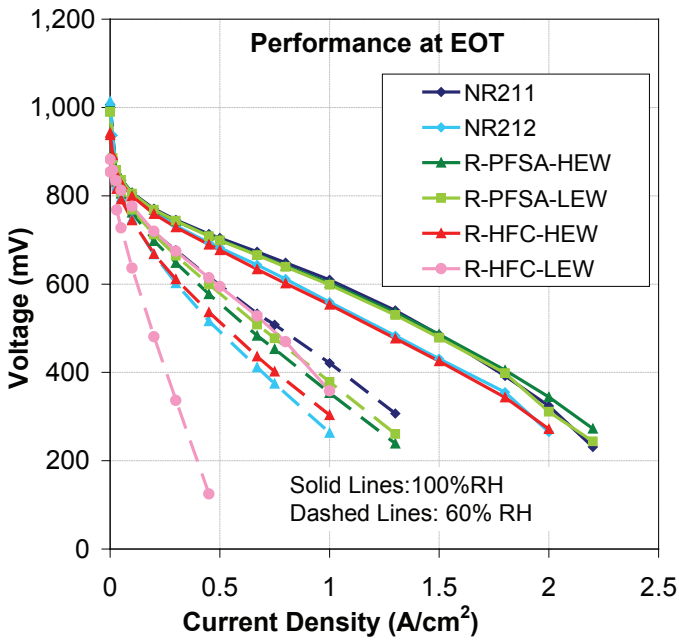

FIGURE 3. MEA performance at 100% and 60% RH after catalyst AST for the membrane/MEA types

higher levels of degradation than their thicker/higher EW counterparts and the R-HFC-LEW having had exceptionally high degradation and overall cell resistance. A voltage loss breakdown technique showed large ohmic loss increases for the R-HFC-LEW suggesting that membrane degradation had occurred during the cathode AST, which was subsequently confirmed by EOT membrane thickness measurements revealing a 50% thickness loss had occurred.

Following evaluation of the BOT and catalyst AST, a combination of membrane AST and catalyst AST was applied to a new set of MEAs (based on three down-selected membranes). These MEAs were subjected to three membrane AST cycles and then to a catalyst AST for up to 4,700 cycles. The ECSA and ECSA loss vs. AST cycles are shown in Figure 4. ECSA loss was observed to occur even during the course of the membrane AST which resulted in a lower starting ECSA entering the catalyst AST protocol. In order to assess the effect of the post-membrane AST state on the catalyst AST, the ECSA loss for post membrane AST samples was normalized to the ECSA at the start of the cathode AST rather than that of the fresh MEA. The results in Figure 4 show that the cyclic open circuit voltage degraded NR211 and R-PFSA membranes had lower ECSA losses after cathode AST cycling than the pristine samples. The NR212 showed similar results up to 700 cycles, but then had much higher ECSA losses for the degraded membrane which in part appears to be due to the development of an internal transfer. Failure analysis of the membranes/MEAs was done to quantify the platinum dissolution mechanism, and it was found that the Pt size did not grow and no platinum in the membrane (PITM) occurred with membrane AST. After both the membrane and cathode AST, the Pt size was higher and the PITM was much lower as compared to the data for the cathode AST alone, suggesting that the platinum migration was hindered by pre-existing membrane degradation and thus resulted in increased Pt agglomeration.

CONCLUSIONS AND FUTURE DIRECTIONS

The interim conclusions are as follows:

- Membrane degradation appears to influence the degree of agglomeration vs. formation of platinum in the membrane as compared to the baseline, catalyst AST only testing.
- Testing was completed on the effect of the combined membrane AST/catalyst AST on low loaded cathode catalyst layers and it was determined that the low loading was more severely affected by the catalyst AST

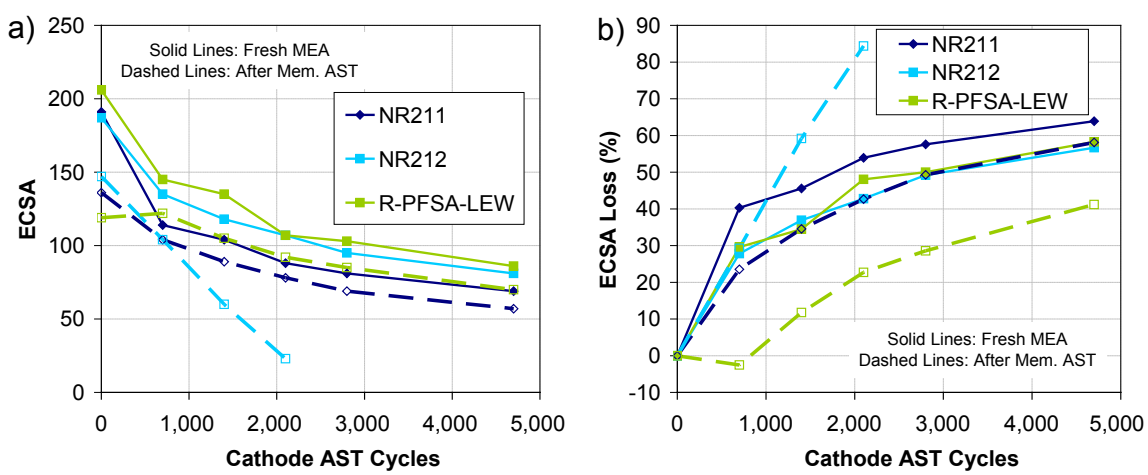

FIGURE 4. ECSA and ECSA loss for the membrane AST degraded MEAs subjected to catalyst AST cycling

as compared to the higher loading samples with the behavior of the samples in the combined membrane/catalyst AST showing similar degradation rates with the fresh samples.

Future directions include the following:

- Complete source code revisions for the improved membrane transport sub-model in FC-APOLLO based on new data for adsorption/desorption processes
- Release the documentation for FC-APOLLO
- Disseminate the validation data set for FC-APOLLO via the public hosting site
- Release revised FC-APOLLO model to www.sourceforge.net/projects/fcapollo
- Complete the project final reporting and publications.

FY 2015 PUBLICATIONS/PRESENTATIONS

1. Conducted FC-APOLLO Tutorial at the June 2015 DOE Annual Merit Review and Peer Evaluation in Arlington, VA.

REFERENCES

1. Hydrogen, Fuel Cells & Infrastructure Technologies Program Multi-Year Research, Development and Demonstration Plan, U.S. Department of Energy, Energy Efficiency and Renewable Energy, 2011 revision http://www.eere.energy.gov/hydrogenandfuelcells/mypp.

2. J. Wu, X.Z. Yuan, J.J. Martin, H. Wang, J. Zhang, J. Shen, S. Wu, W. Merida, "A Review of PEM Fuel Cell Durability: Degradation Mechanisms and Mitigation Strategies." Journal of Power Sources 184, 104–119.

3. R. Borup, J.P. Meyers, B. Pivovar, Y.S. Kim, R. Mukundan, N. Garland, D. Myers, M. Wilson, F. Garzon, D. Wood, P. Zelenay, K. More, K. Stroh, T. Zawodinski, J. Boncella, J.E. McGarth, M. Inaba, K. Miyatake, M. Hori, K. Ota, Z. Ogumi, S. Miyata, A. Nishikata, Z. Siroma, Y. Uchimoto, K. Yasuda, K. Kimijima, N. Iwashita, "Scientific Aspects of Polymer Electrolyte Fuel Cell Durability and Degradation." Chemical Reviews 2007, 107, 3904–3951.

4. Y. Shao, G. Yin, Y. Gao, "Understanding and Approaches for the Durability Issues of Pt-Based Catalysts for PEM Fuel Cell." Journal of Power Sources 2007, 171, 558–566.

5. M.S. Wilson, F. Garzon, K.E. Sickafus, S. Gottesfeld, "Surface Area Loss of Supported Platinum in Polymer Electrolyte Fuel Cells." Journal of the Electrochemical Society 1993, 140, 2872–2876.

6. P.J. Ferreira, G.J. Ia O', Y. Shao-Horn, D. Morgan, R. Makharia, S. Kocha, H. Gasteiger, "Instability of Pt/C Electrocatalysts Membrane Fuel Cells—A Mechanistic Investigation." Journal of the Electrochemical Society 2005, 152, A2256–A2271.

7. G.J.M. Janssen. "A Phenomenological Model of Water Transport in a Proton Exchange Membrane Fuel Cell," ECS 148 (12) A1313–A1323 (2001).

8. A.Z. Weber, J. Newman. "Transport in Polymer-Electrolyte Membranes II. Mathematical Model." ECS 151 (2) A311–A325 (2004).

V.F.1 Optimal Stationary Fuel Cell Integration and Control

Genevieve Saur (Primary Contact),
Chris Ainscough, Matt Post, Jen Kurtz, Sam Sprik
National Renewable Energy Laboratory (NREL)
15013 Denver West Parkway
Golden, CO 80401-3305
Phone: (303) 275-3783
Email: Genevieve.Saur@nrel.gov

DOE Managers
Jason Marcinkoski
Phone: (202) 586-7466
Email: Jason.Marcinkoski@ee.doe.gov

Project Start Date: January 2011
Project End Date: Project continuation and direction determined annually by DOE

Overall Objectives

Build an open source tool (Distributed Generation Build-out Economic Assessment Tool [DG-BEAT]) and simplified web tool (Fuel Cell Tool for Assessing Costs [FCTAC]) that help combined heat and power (CHP) fuel cell developers, end users, and other stakeholders to do the following for their systems, helping to drive economies of scale and cost reduction.

- Determine the appropriate sizing to reduce cost
- Integrate to commercial building control and heating, ventilating, and air conditioning systems to maximize durability
- Compare performance relative to incumbent technologies
- Determine optimum system configuration
- Evaluate potential market penetration

Fiscal Year (FY) 2015 Objectives

- DG-BEAT is undergoing a revision of project scope and vision after being moved under Technology Validation. This revision includes a realignment to focus on grid integration activities. A three-year project plan is in progress.
- FCTAC will have revisions to better represent currently available fuel cell sizes and distinguish between electric only and CHP systems. The modifications will not compromise the ease of use while increasing its validity.

Technical Barriers

This project addresses the following technical barriers from the Technology Validation section of the Fuel Cell Technologies Office Multi-Year Research, Development, and Demonstration Plan:

(B) Lack of Data on Stationary Fuel Cells in Real World Operation

(E) Codes and Standards

Technical Targets

This project is providing a tool to fuel cell manufacturers, end users, and other stakeholders to help them reduce the cost of fuel cell CHP installations by optimizing their sizing, combining them with hybridizing technologies such as thermal energy storage and batteries, dispatching them in cost-optimal ways, and investigating the fuel cell sizes and features to best address the national market. Relevant DOE targets (2020) are:

- Installed cost, natural gas: $1,500/kW
- Operating lifetime: 40,000–80,000 h
- Electrical efficiency at rated power: >50%
- CHP energy efficiency: 90%.

FY 2015 Accomplishments

- DG-BEAT model features:
  - Component library for three types of fuel cells (phosphoric acid fuel cell [PAFC], molten carbonate fuel cell [MCFC], and polymer electrolyte membrane [PEM] fuel cell), two chillers (absorption and electric), thermal storage (heat and cold), batteries, and renewable generation (solar and wind)
  - A total of 1,280 model building profiles covering 16 American Society of Heating, Refrigerating, and Air Conditioning Engineers (ASHRAE) climate regions, 16 building types, and five vintages
  - Utility rate structures for time-of-use (TOU) demand and usage charges, including 20 preloaded rates and state averages; utility rates include options for net metering, fixed sellback, and TOU sellback of electricity
  - Natural gas rates that are forecasted from historical data by state with seasonal variation
  - Geospatially resolved by state emissions data with daily and seasonal variation, which are summed annually

  - Five fuel cell dispatch strategies (baseload, weekend dip, diurnal peaking, load following, and emissions control)
  - Four fuel cell sizing options (fixed size, 100% based on building load, net present value cost minimization, and annual emissions minimization)
- FCTAC accomplishments:
  - Initially released May 2014; has received 437 pages views between September 1, 2014, and April 2015
  - Narrowed the scope of DG-BEAT to be a first step toward making a decision about going forward with a stationary fuel cell installation
  - Reduced inputs to the 12 with the most impact, and carefully chose default values
  - Chose three outputs for FCTAC: net present value cost analysis, greenhouse gas emissions analysis, and criteria pollutant emissions analysis, which are displayed visually and compared to a baseline building performance

✧ ✧ ✧ ✧ ✧

INTRODUCTION

This project aims to create an open source software tool that allows fuel cell developers, their potential customers, and other stakeholders to evaluate the ability of fuel cell installations to save money relative to the grid/natural gas paradigm. The model includes 1,280 model building profiles covering the major ASHRAE climate zones in the United States.

The model can perform design optimizations on single fuel cells and building combinations or campuses of multiple buildings. In addition to fuel cells technologies that can be included in the buildings systems are chillers, energy storage technologies, and onsite renewables such as solar and wind.

APPROACH

The approach taken by the research team is to build a flexible, configurable model that allows users to create modules for the various components that make up a project scenario (fuel cells, energy storage, chillers, buildings, and campuses). NREL has teamed with the University of California, Irvine as a sub-contractor to leverage its extensive expertise in this area. Cost and sizing optimization can now be done for different control strategies utilizing the modules built. In addition, NREL is working cross-center within the laboratory, drawing extensively on the expertise of the Commercial Building group within NREL, to provide model building profiles.

RESULTS

The DG-BEAT project is a full feature tool for analyzing fuel cell integrated building systems (Figure 1). The code is modular and open source by invitation currently. Results include net present value cost analysis that is geospatially resolved with regional data for building profiles, utilities, and natural gas costs. It has a library of building components that include three types of fuel cells (PAFC, MCFC, and PEM), two types of chillers (absorption and electric), hot and cold

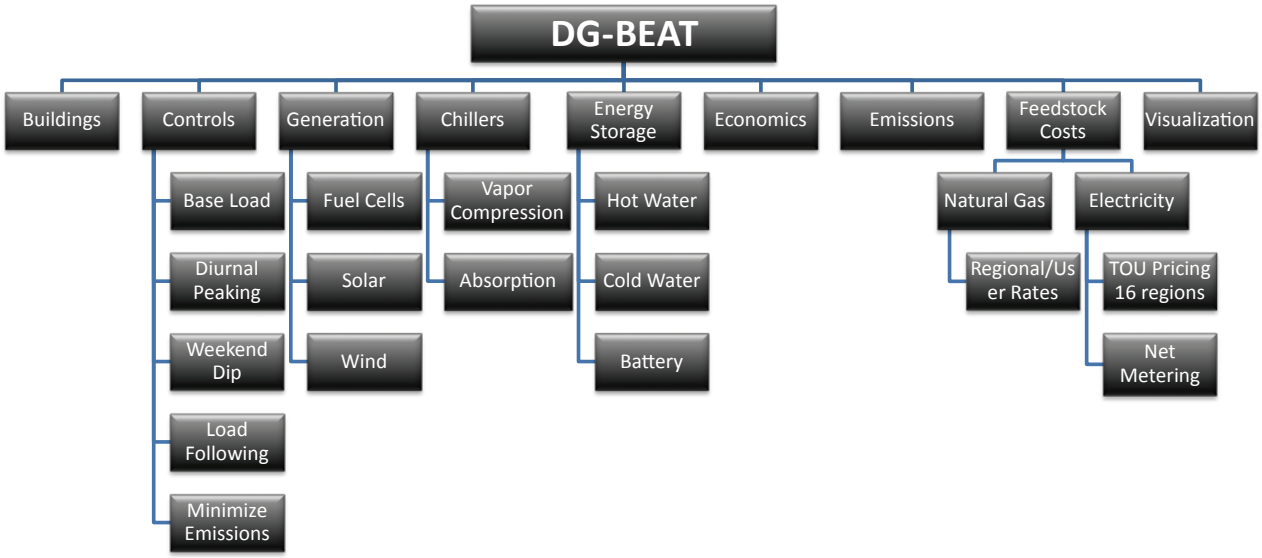

FIGURE 1. Construction of DG-BEAT

thermal storage, batteries, solar, and wind. The building components can be configured with appropriate performance profiles and cost. This year the project has been moved from the DOE Fuel Cell Annual Operating Plan to the Technology Validation section. This move serves to better align the project activities. The project is undergoing a major revision in scope and vision to better align it with grid integration activities. The main activity has been to work on a three-year project plan.

FCTAC had its inaugural year, and after receiving feedback, is undergoing several modifications. The results were revised to better represent currently available fuel cells and to distinguish between electric and CHP systems. The main objective of the web tool is to simplify the complexity of the DG-BEAT model and provide an initial assessment of a fuel cell integrated building (Figure 2). It was originally intended for federal building managers, but the tool is freely accessible at fctac.nrel.gov.

CONCLUSIONS AND FUTURE DIRECTIONS

A strong model foundation is now in place for implementing optimized component sizing optimization. The model can now manage integration of fuel cells into building systems that can include chillers, energy storage technologies, and renewable energy systems. A number of sizing and control strategies are implemented.

Future work includes:

- Real-time optimal dispatch controller.
- Optimum component sizing for use in grid services markets.
- New building interface for communicating with buildings and sending optimized dispatch control schedules, as well as transacting in grid services markets.
- New graphical interface for use by building managers and planners.

FY 2015 PUBLICATIONS/PRESENTATIONS

1. Saur, G., Ainscough, C., Post, M., Kurtz, J., and Sprik, S. "Optimal Stationary Fuel Cell Integration and Control." (June 2015) 2015 DOE Annual Merit Review meeting.

2. Saur, G., and Post, M. "DG-BEAT: Distributed Generation Build-out Economic Analysis Tool, a Stationary Fuel Cell Model." Paper presented at Fuel Cell Seminar, November 2014.

3. Saur, G., Ainscough, C., Kurtz, J., Sprik, S., Post, M., Brouwer, J., McLarty, D., Sullivan, R., Field, K., and Bonnema, E. "Enlarging Potential National Penetration for Stationary Fuel Cell through System Design Optimization." (November 2014) 2014 DOE Annual Progress Report.

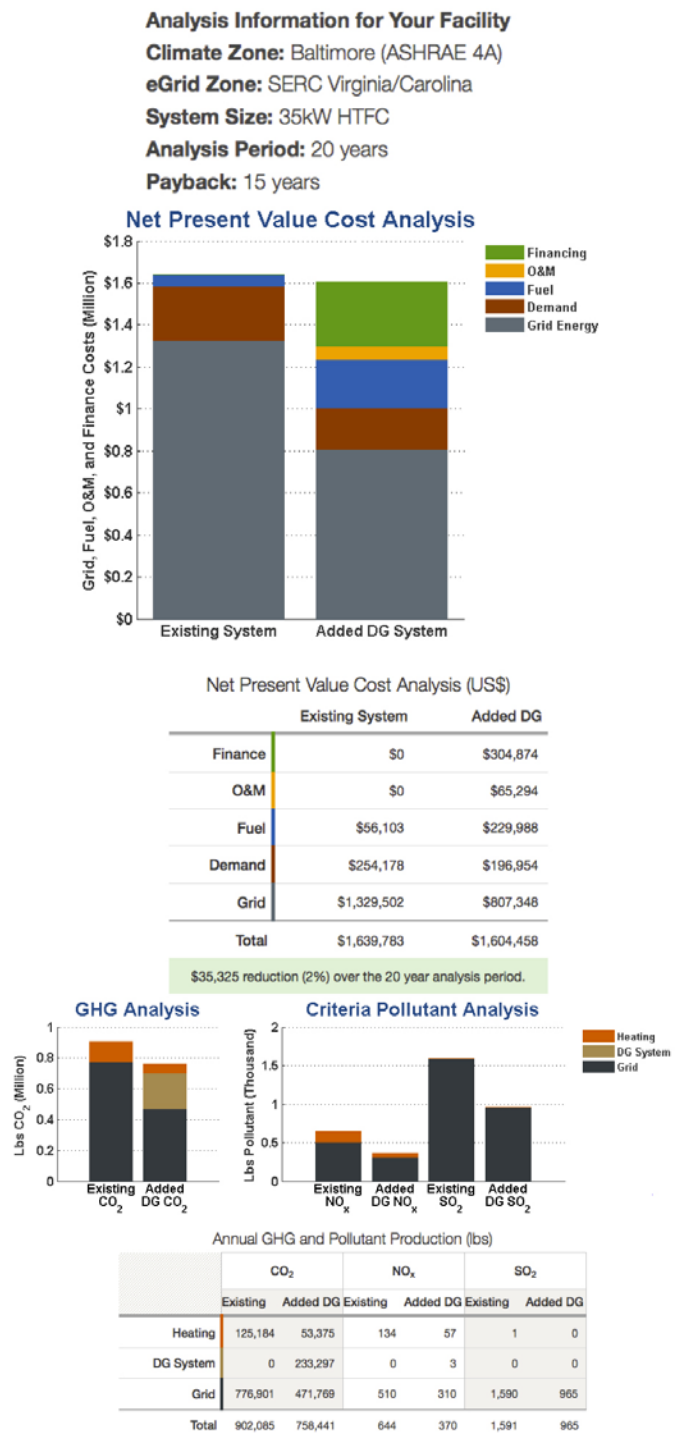

HTFC – High Temperature Fuel Cell; GHG – Greenhouse Gas; DG – Distributed Generation

FIGURE 2. FCTAC example results

V.F.2 Performance and Durability of Advanced Automotive Fuel Cell Stacks and Systems

Rajesh K. Ahluwalia (Primary Contact),
Xiaohua Wang, and J-K Peng
Argonne National Laboratory
9700 South Cass Avenue
Argonne, IL 60439
Phone: (630) 252-5979
Email: walia@anl.gov

DOE Manager
Nancy Garland
Phone: (202) 586-5673
Email: Nancy.Garland@ee.doe.gov

Project Start Date: October 1, 2003
Project End Date: Project continuation and direction determined annually by DOE

Overall Objectives

- Develop a validated model for automotive fuel cell systems and use it to assess the status of the technology
- Conduct studies to improve performance and packaging, to reduce cost, and to identify key research and development issues
- Compare and assess alternative configurations and systems for transportation and stationary applications
- Support DOE and United States Driving Research and Innovation for Vehicle efficiency and Energy (U.S. DRIVE) sustainability automotive fuel cell development efforts

Fiscal Year (FY) 2015 Objectives

- Establish the uncertainties in system performance due to variability in supporting nano-structured thin film (NSTF) cell polarization data
- Extend system analysis to alternate non-NSTF membrane electrode assemblies (MEAs) with conventional platinum on carbon (Pt/C) and advanced platinum alloy on carbon cathode catalysts
- Incorporate durability considerations in system analysis
- Provide modeling support to Eaton's development of roots air supply system

Technical Barriers

This project addresses the following technical barriers from the Fuel Cells section of the Fuel Cell Technologies Office Multi-Year Research, Development, and Demonstration Plan:

(A) Durability

(B) Cost

(C) Performance

Technical Targets

This project is conducting system level analyses to address the following DOE 2020 technical targets for automotive fuel cell power systems operating on direct hydrogen:

- Energy efficiency: 60% at 25% of rated power
- Q/ΔT: 1.45 kW/°C
- Power density: 850 W/L for system, 2,500 W/L for stack
- Specific power: 650 W/kg for system, 2,000 W/kg for stack
- Transient response: 1 s from 10% to 90% of maximum flow
- Start-up time: 30 s from -20°C and 5 s from +20°C ambient temperature
- Precious metal content: 0.125 g/kW_e rated gross power

Accomplishments

- Showed that the simplified model of calculating stack heat load is quite accurate under most conditions except when a significant fraction of the product water forms liquid, releasing the latent heat of condensation
- Established the uncertainties in system performance due to variability in supporting NSTF cell polarization data: 2–5 \$/kW_e fuel cell system (FCS) cost, 0.02–0.05 g Pt/kW_e platinum content, and 10–15% in power density
- Demonstrated that an alternate first generation (GEN I) catalyst system with conventional high surface area carbon support (d-PtNi/C) has promising performance: 54 \$/kW_e FCS cost and 0.21 g Pt/kW_e Pt content
- Identified the dominant NSTF catalyst degradation mechanism and determined the operating conditions for

20% projected voltage loss at rated power density over 5,000 hours

- Determined the parasitic power requirements of the Roots air supply system: 12.7 kW_e at 100% flow (8 kW_e target) and 295 W_e at idle (200 W_e target)

✧ ✧ ✧ ✧ ✧

INTRODUCTION

While different developers are addressing improvements in individual components and subsystems in automotive fuel cell propulsion systems (i.e., cells, stacks, balance of plant components), we are using modeling and analysis to address issues of thermal and water management, design-point and part load operation, and component, system, and vehicle level efficiencies and fuel economies. Such analyses are essential for effective system integration.

APPROACH

Two sets of models are being developed. The GCtool (General Computational toolkit) software is a stand-alone code with capabilities for design, off-design, steady state, transient, and constrained optimization analyses of FCS. A companion code, GCtool-ENG, has an alternative set of models with a built in procedure for translation to the MATLAB®/Simulink® platform commonly used in vehicle simulation codes, such as Autonomie.

RESULTS

In FY 2014, we reported results from a study on an 80 kW_{net} fuel cell system with NSTF ternary catalyst based MEAs, subject to the heat rejection constraint ($Q/\Delta T$ = 1.45 kW/°C) and 40°C ambient temperature [1]. This year, we extended the study to investigate the effect of the stack heat load estimate (Q) on system cost and performance. In our study, Q is the actual stack heat load (AQ) as calculated in the model considering variable $P(O_2)$, $P(H_2)$, $P(H_2O)$, T, and current density along the flow directions. The model includes latent heat released by water condensation (if any) in the stack and the sensible heat transfer to the anode and cathode gases. Besides the cell voltage, AQ should depend on operating conditions such as the operating pressure, temperature, anode/cathode stoichiometry (SR), and rise in coolant temperature (ΔT_c). The heat load in the $Q/\Delta T$ target (simplified Nernst potential [SN]) is written in terms of voltage efficiency ($\eta_V = E/E_N$), defined as the ratio of cell voltage to the Nernst potential (E_N):

$$Q = P_s\left(\frac{1}{\eta_V} - 1\right) = P_s\frac{(E_N - E)}{E},$$

where P_S is the stack gross power required for a fuel cell system that generates 80 kW_e net power; the suggested value of P_S is 90 kW. The target also suggests that, for simplicity, E_N be approximated as 1.25 V, independent of the stack operating conditions [1].

Figures 1a and 1b compare the effect of stack heat load estimates (AQ vs. SN) on the cost and performance of the reference system at different operating pressures. Both sets of results, labeled as $Q/\Delta T$ (AQ) and $Q/\Delta T$ (SN), are for optimized T_c and relative humidity (RH) with specified stack inlet pressure (1.5–3 atm), cathode stoichiometry (1.5), rise in coolant temperature (10°C), and Pt loading in anode and cathode. The results show that, under most conditions, Q(SN) is an acceptable approximation to the actual stack heat load, but it grossly underestimates the heat load for conditions under which liquid water forms in the stack and significant amount of latent heat of condensation is released, as at 3-atm stack inlet pressure.

An extensive data base was developed by running more than 130 polarization and electrochemical characterization tests on multiple cells. The reference conditions at 1.5 atm, 2.5 atm, and 3 atm were visited many times during different test series. Figure 1c shows the variability in polarization curves at 2.5-atm reference pressure in two of the eight cells (23102 and 23272); similar variations were also observed at 1.5 atm and 3 atm reference pressures. The inset in Figure 1c identifies the test series in which the data were taken and the order in which the tests were conducted. Figure 1d indicates that the variability in cell voltage (ΔV) is a function of the current density and is higher at higher current density. We may regard ΔV as a measure of the recoverable losses since the test campaign is not long enough for manifestation of significant irrecoverable losses. In a different study, we confirmed that the voltage losses in Figures 1c and 1d can be recovered by reconditioning the cells by subjecting them to multiple thermal conditioning (TC) cycles. Nevertheless, the variability in cell voltage is representative of the performance variation that may be expected over drive cycles before the onset of permanent degradation mechanisms.

The model discussed in this work is representative (REP) of the average performance in that the kinetic and transport parameters were determined by using the average of all available polarization data. We also developed a model for the best of class (BOC) performance in which we determined the kinetic and transport parameters by using only the best polarization data under different conditions. Figures 1e and 1f compare the FCS cost and performance using the REP and BOC models. Our study shows ~10% improvement in power density (753 mW/cm^2), Pt cost (10.8 $\$/kW_e$) and stack cost (25.7 $\$/kW_e$) if the results for 2.5-atm stack inlet pressure are based on BOC rather than REP polarization data.

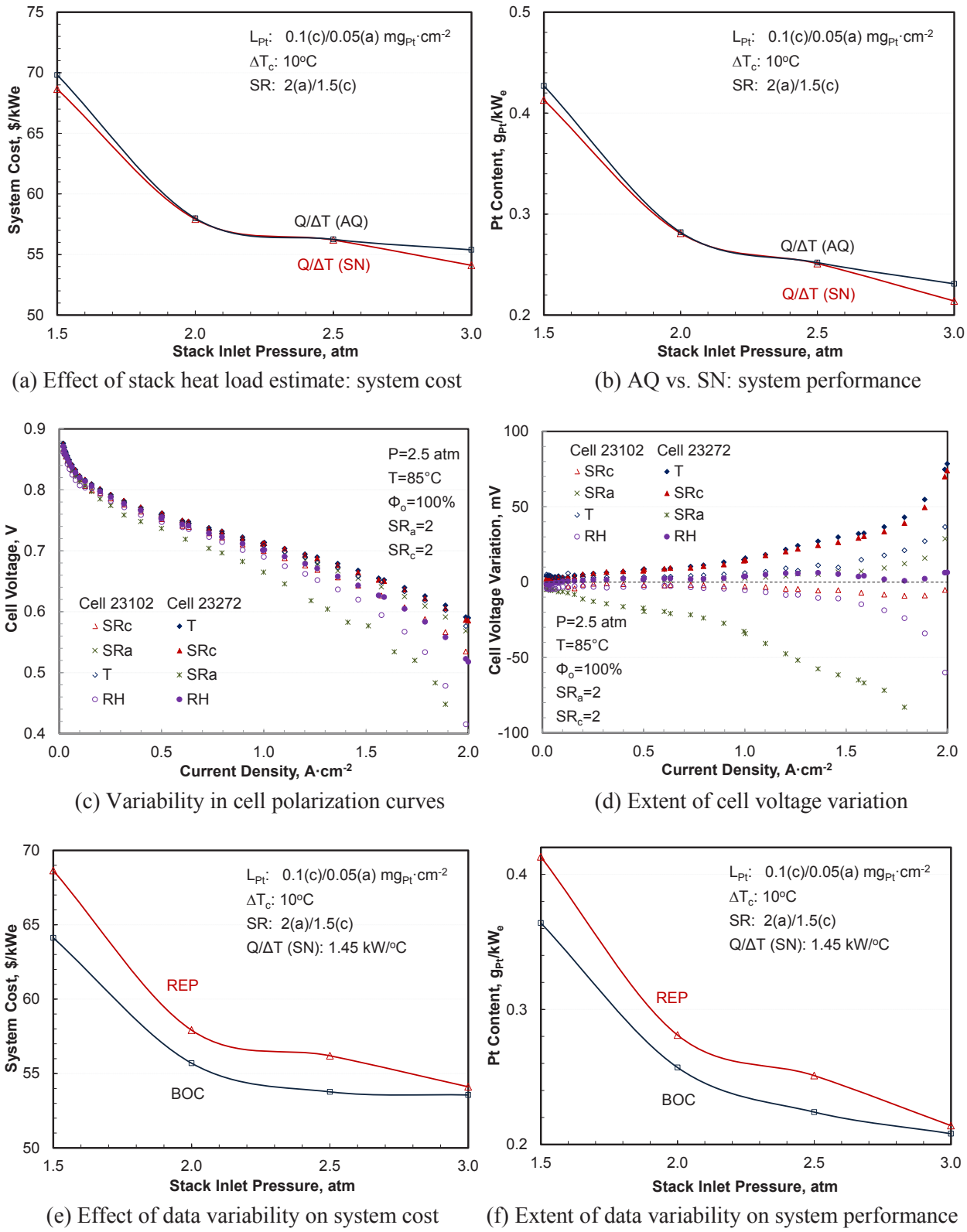

(a) Effect of stack heat load estimate: system cost

(b) AQ vs. SN: system performance

(c) Variability in cell polarization curves

(d) Extent of cell voltage variation

(e) Effect of data variability on system cost

(f) Extent of data variability on system performance

FIGURE 1. FCS cost and performance studies with ternary NSTF catalyst and Q/ΔT constraint, 0.1 (cathode)/0.05 (anode) mg/cm^2 Pt loading, 10°C rise in coolant temperature, 2 (anode)/1.5 (cathode) stoichiometry: (a) effect of stack heat load estimate: system cost; (b) AQ vs. SN: system performance; (c) variability in cell performance; (d): extent of cell voltage variation; (e) effect of data variability on system cost; (f) effect of data variability on system performance

Alternate Catalyst System

We are collaborating with United Technologies Research Center (UTRC) and Johnson Matthey Fuel Cells (JMFC) to evaluate the performance of an MEA with an advanced cathode catalyst, de-alloyed (d) PtNi/C, relative to the targets of 0.44 A/mg-PGM (platinum group metal) mass activity and 720 μA/cm^2-PGM specific activity at 900 mV$_{iR\text{-}free}$, 1,000 mW/cm^2 at rated power, and 300 mA/cm^2 at 800 mV [2].

We analyzed the hydrogen-oxygen polarization data obtained by UTRC on differential cells (12.5 cm^2 active area) with three sets of MEAs supplied by JMFC: d-PtNi/C, high surface area Pt/C, and annealed (a) Pt/C. We developed a step-wise procedure to determine the kinetic parameters of the oxygen reduction reaction (ORR) on d-PtNi/C. Our starting point consisted of using a transmission line model to analyze the hydrogen-air and hydrogen-nitrogen impedance (electrochemical impedance spectroscopy) data for proton conductivity of the membrane (σ_m) and the ionomer in the cathode electrode (σ_i). The second step consisted of developing models for distributed ORR in the cathode electrode and distributed hydrogen oxidation reaction in the anode electrode. The final step involved using the known σ_m and σ_i in these models to determine the ORR kinetic parameters from the measured cell voltage (E) in hydrogen-oxygen (negligible oxygen mass transfer losses) at low current densities (i). An optimization algorithm was required to determine the Tafel slope since the IR-corrected cell voltage ($E + iR_\Omega$) is not linear with $ln(i + i_x)$, where i_x is the hydrogen crossover current onsistent with the experimental data, the modeled mass activities of d-PtNi/C, 0.533–0.583 A/mg Pt, is higher than the target of 0.44 A/mg PGM. Similarly, the measured and modeled specific activities of d-PtNi/C, 935–1,023 μA/cm^2 Pt, are higher than the target of 720 μA/cm^2 PGM.

Knowing the ORR kinetic parameters, we analyzed the hydrogen-air polarization data to determine the limiting current density (i_L), defined as the current density corresponding to 450 mV mass transfer overpotential (η_m). We developed empirical correlations for the dependence of i_L on pressure, temperature, O_2 partial pressure, relative humidity, and flow rate. We also developed empirical correlations for mass transfer overpotentials by representing η_m as a function of the reduced current density (i/i_L), pressure, temperature, relative humidity, and air flow rate.

We incorporated the ORR kinetic and proton/oxygen transport aspects of d-PtNi/C electrodes in our large-area cell model. Figure 2a compares the modeled polarization curves for the three catalysts with 0.3 Pt to C and 0.8 ionomer to carbon ratios under conditions required to satisfy the Q/ΔT constraint at 100% exit RH; the modeled curves include additional 10 mV cell-to-stack voltage loss at 1 A/cm^2. Compared to Pt/C, d-PtNi/C has 66% higher specific activity (914 μA/cm^2 Pt vs. 550 μA/cm^2 Pt) but only 17% higher mass activity (0.530 A/mg Pt vs. 0.453 A/mg Pt) because of lower electrochemical surface area (58 m^2/g Pt vs. 82 m^2/g Pt). Above a critical (crossover) current density, the advantage of higher mass activity of d-PtNi/C is offset by higher mass transfer overpotentials because of smaller surface area and possibly Ni^{2+} contamination. However, in spite of Ni^{2+} leaching out, d-PtNi/C is more durable [3] because its preparation includes an annealing step that grows platinum particles to ~5.1–5.8 nm (~2 nm for Pt/C). Studies have shown that platinum particles smaller than 2 nm are unstable and that the particle diameter needs to be larger than about 4 nm for <30% loss of mass activity after 30,000 potential cycles [4,5].

We analyzed the cost and performance of fuel cell systems with Pt/C, a-Pt/C, and d-PtNi/C cathode catalysts, 1.45 kW/°C Q/ΔT heat rejection constraint, and other assumptions as in Figure 1 for ternary NSTF catalyst. Figure 2b shows that GEN I d-PtNi/C has slight cost ($/kW$_e$) and performance (g Pt/kW$_e$) advantages over Pt/C, especially at low pressures and temperatures. However, as noted above, the high surface area Pt/C is unstable under cyclic potentials, so it may be more appropriate to compare d-PtNi/C with a-Pt/C since the two catalysts have similar Pt particle diameters and should have similar stability. Our model indicates that d-PtNi/C can have 20–30% higher power density than a-Pt/C. Figure 2c shows the relationship between stack inlet pressure and the optimum stack temperature (i.e., coolant exit temperature) for d-PtNi/C. We find that under optimum conditions, d-PtNi/C runs drier at 1.5 atm (88% RH at cathode inlet, 82% at cathode outlet) than at 2.5 atm (82% RH at cathode inlet, 103% at cathode outlet).

Durability of MEAs with NSTF Catalysts

We collaborated with 3M to develop a test protocol for determining the stability of the baseline ternary NSTF catalyst under potentiostatic conditions. The protocol consists of repeatedly degrading the cell for 10 h at constant potential with periodic fluoride collection and partial reconditioning with one TC cycle. Every 20 h of degradation, polarization curves are taken in hydrogen/air. Every 40–80 hours of degradation, the cell is reconditioned more fully with three TC cycles and data are obtained to measure the cathode ORR activity, cathode electrochemical surface area, hydrogen crossover, shorting resistance, and cell polarization in hydrogen/air.

We received data for three tests run using the above protocol with potentiostatic holds at 0.9 V, 0.6 V, and 0.3 V. The tests were run on 50-cm^2 cells with quad serpentine flow fields and ternary catalysts with 0.05 mg/cm^2 Pt loading on anode and 0.15 mg/cm^2 Pt loading on cathode. The cells used 3M, 825 equivalent weight, membrane that was 20 μm thick. The membrane was chemically stabilized with an antioxidant additive but was not mechanically supported. Even without

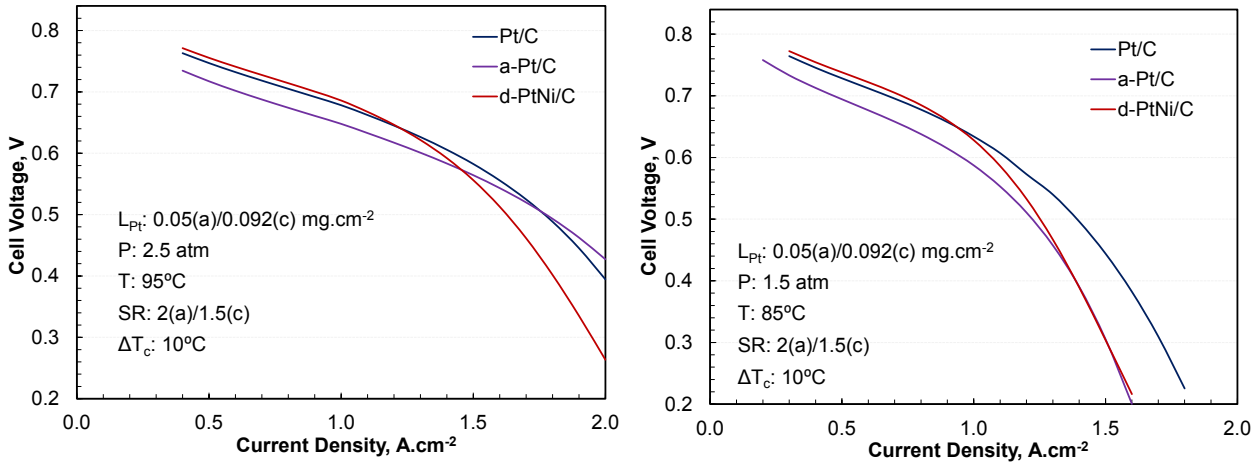

(a) Modeled polarization curves at 2.5 atm (1.5 atm), 95ºC (85ºC), and 100%RH

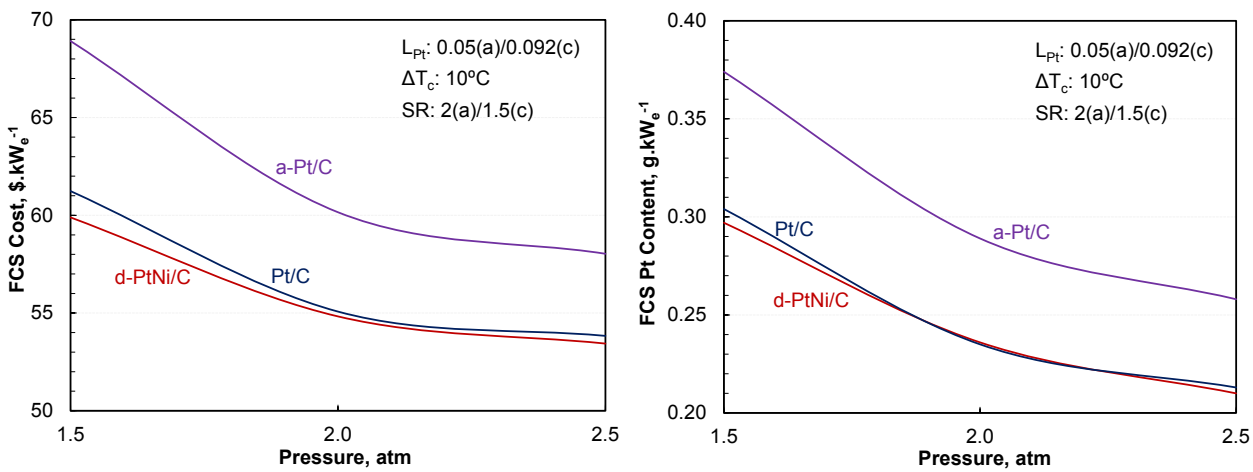

(b) Cost/performance of the three catalyst systems with Q/ΔT constraint (variable P, optimum T_c and RH)

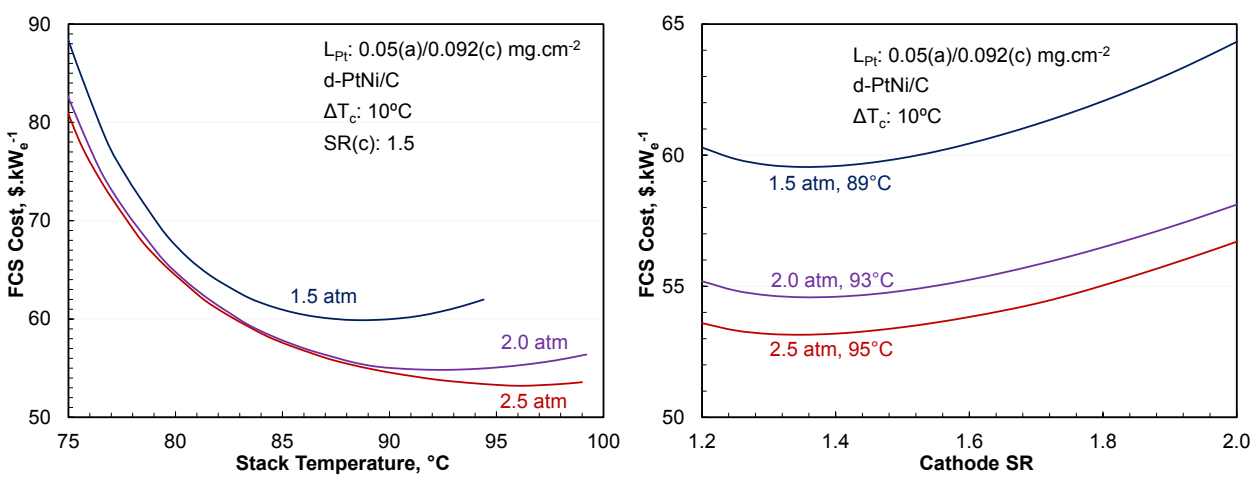

(c) Cost and performance of d-PtNi/C system with Q/ΔT constraint (variable P and T_c, optimized RH)

FIGURE 2. FCS cost and performance studies with dispersed catalysts and Q/ΔT constraint, 0.1 (cathode)/0.05 (anode) mg/cm^2 Pt loading, 10°C rise in coolant temperature, 2 (cathode)/1.5 (anode) stoichiometry: (a) modeled polarization curves at 2.5 atm (1.5 atm), 95°C (85°C), and 100% RH; (b) cost/performance of the three catalyst systems with Q/ΔT constraint (variable P, optimum T and RH); (c) cost and performance of d-PtNi/C system with Q/ΔT constraint (variable P and T_c, optimized RH)

mechanical reinforcement, the chemically stabilized membrane remained healthy in that there was no appreciable change in hydrogen crossover or any systematic change in electronic shorting resistance.

The data show systematic degradation in current density during hold at constant potentials. There is a partial recovery of current density after one TC cycle every 10 h; the recovery is more complete with three TC cycles that were imposed nominally every 60 h. Even with three TC cycles, there are irrecoverable losses suggesting permanent degradation. There are also significant differences between hydrogen/air performance after one TC and three TC cycles. The polarization data show incomplete recovery from reversible losses with one TC cycle. With either recovery method, voltage losses are considerably faster at lower hold potentials and are much higher at higher current densities.

The measured loss in cathode surface area (surface enhancement factor or roughness) is nearly independent of the hold potential (see Figure 3a) and may be associated with the dissolution of whiskerettes and the resulting decrease in surface roughness. The data indicate that the ORR absolute and specific activity losses are higher at 0.3 V than at 0.6 V or 0.9 V.

Figure 3b presents the fluoride release rates (FER) measured by ion chromatography of the collected water samples. The measured FERs are an order-of-magnitude smaller than for dispersed Pt/C catalysts with chemically stabilized and mechanically reinforced membranes. Both cathode and anode FERs are higher at lower cell voltages, consistent with the observed dependence of hydrogen peroxide production on potential in rotating ring disk electrode tests.

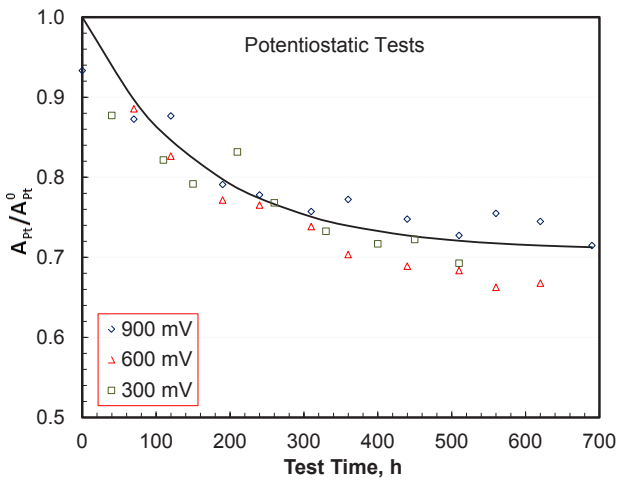

(a) ECSA loss

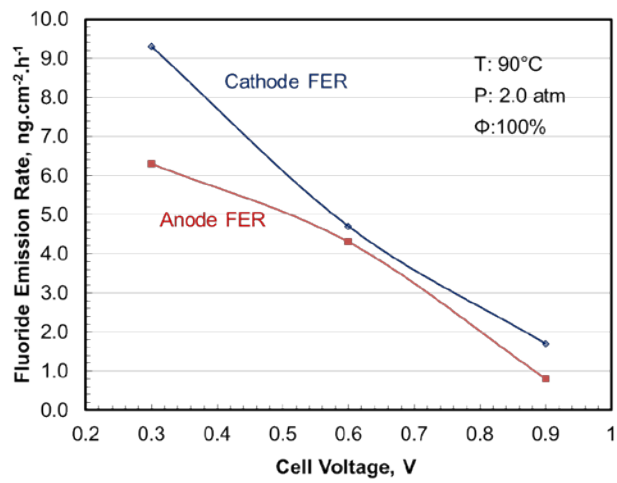

(b) Fluoride emission rate

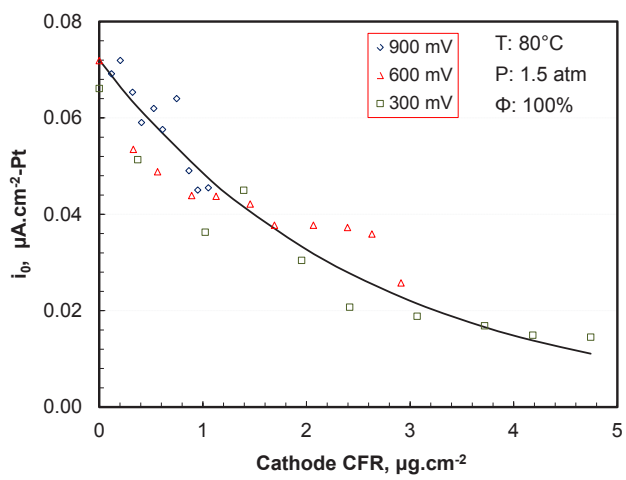

(c) Modeled loss in ORR exchange current density

FIGURE 3. Stability of NSTF catalyst based MEA under potentiostatic conditions: (a) electrochemically active surface area (ECSA) loss; (b) fluoride emission rate; (c) modeled loss in ORR exchange current density

We determined the kinetic parameters from the measured cell voltages at low current densities. We calculated small changes in Tafel slope with ageing at potentiostatic hold. We noted that the increase in ORR overpotential (η_c) is more than the expected increase in η_c due to reduction in surface roughness, suggesting that an additional mechanism exists that accounts for the degradation in specific ORR activity.

We developed a correlation for the increase in ORR overpotential with potentiostatic ageing. Figure 3c presents our correlation of the exchange current density (mA cm^{-2} Pt) assuming that the specific ORR activity is only a function of the cumulative fluoride release (CRF) at cathode. Figure 4a shows a 65 mV irreversible increase in activation overpotential (η_c) during the course of the three tests.

We determined the mass transfer overpotentials (η_m) from the measured cell voltages and the derived ORR kinetic parameters. The data indicate significant increase in η_m with potentiostatic ageing and larger increase in η_m at lower hold potentials. We developed a correlation for the limiting current density (i_L), defined for convenience as the reference current density at which the mass transfer overpotential (η_m) equals 200 mV. Figure 4b shows that i_L decreases as more fluoride is released at cathode, probably because of catalyst contamination (not yet characterized).

We also developed a correlation for the mass transfer overpotential (η_m) assuming that it is only a function of i/i_L and cathode CFR, see Figure 4c. Implicitly, η_m is also a function of the hold potential through its dependence on i_L. Figure 4d indicates that η_m is primarily a function of CFR and current density for 300 mV and 600 mV hold potentials.

In summary, we have confirmed that long potentiostatic hold is a major degradation mechanism for the NSTF catalyst and that the irreversible performance losses are higher at

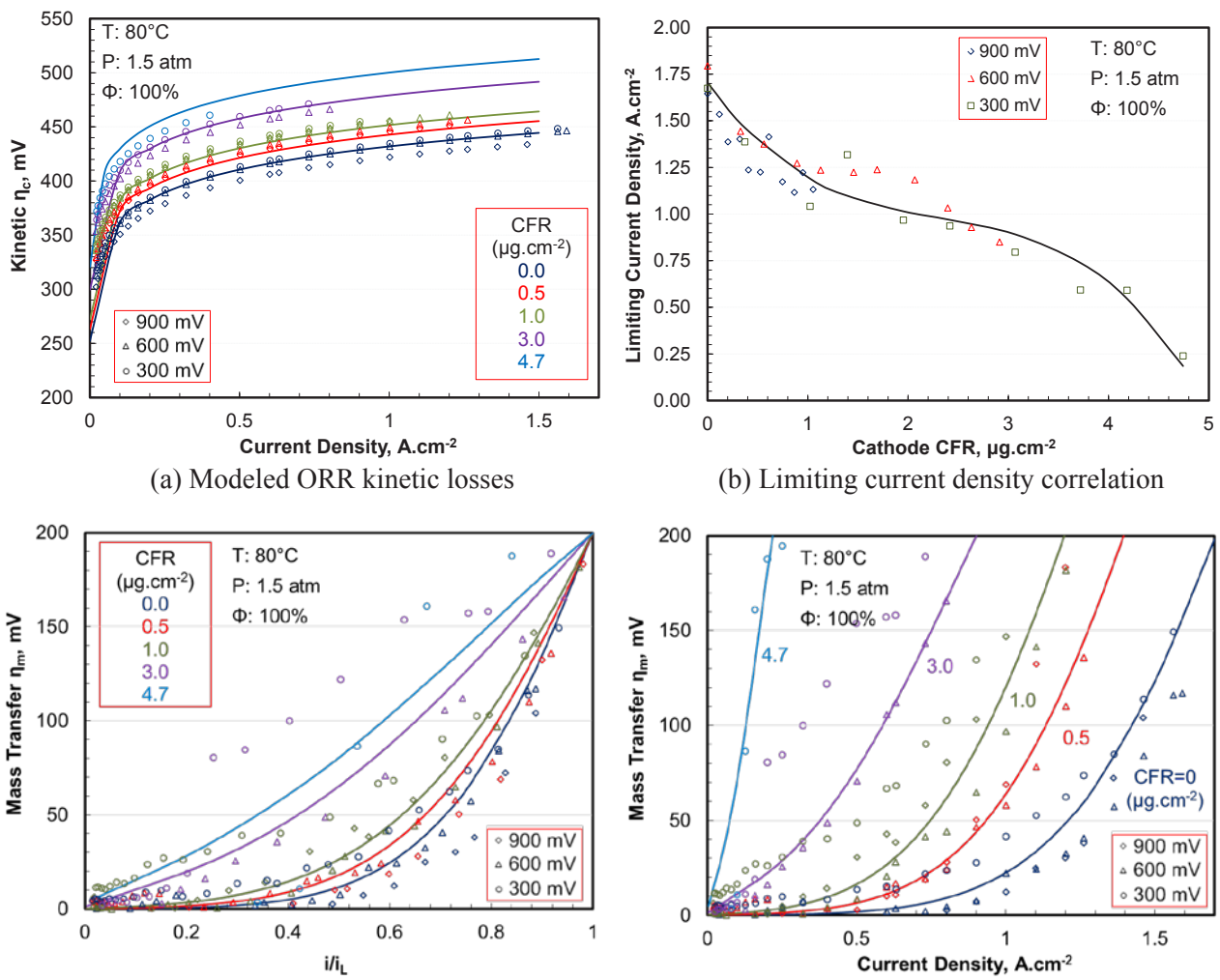

(a) Modeled ORR kinetic losses (b) Limiting current density correlation

(c) Mass transfer correlation (d) Modeled mass transfer losses

FIGURE 4. Degradation model for NSTF catalyst based MEAs: (a) modeled ORR kinetic losses; (b) limiting current density correlation; (c) mass transfer correlation; (d) modeled mass transfer losses

lower cell voltages [6]. Although the measured fluoride release rates are an order-of-magnitude smaller than for Pt/C catalysts with state-of-the-art membranes [7], the resulting losses in cell voltage are much too high. Our next step is to quantify these losses on automotive cycles and develop strategies to mitigate them.

CONCLUSIONS AND FUTURE DIRECTIONS

- Under optimum conditions (2.5-atm stack inlet pressure, 95°C coolant outlet temperature, and 86% cathode exit relative humidity) and using the BOC performance data, the projected platinum content and cost of an 80 kWe fuel cell system that meets the 1.45 kW/°C heat rejection constraint are 0.22 g/kW$_e$ and 53.8 \$/kW$_e$. The stack in this system has ternary PtCoMn/NSTF catalysts with Pt loading of 0.104 mg/cm^2 in the cathode and 0.05 mg/cm^2 in the anode.
- We have shown that GEN I d-PtNi/C has slight cost (\$/kW$_e$) and performance (g Pt/kW$_e$) advantages over Pt/C, especially at low pressures and temperatures. However, since the high surface area Pt/C is unstable under cyclic potentials, it is more appropriate to compare d-PtNi/C with a-Pt/C since the two catalysts have similar Pt particle diameters and should have similar stability. Our model indicates that d-PtNi/C can have 20–30% higher power density than a-Pt/C.
- We have confirmed that long potentiostatic hold is as a major degradation mechanism for the NSTF catalyst and that the irreversible performance losses are higher at lower cell voltages. Our next step is to quantify these losses on automotive cycles and develop strategies to mitigate the performance losses.

FY 2015 PUBLICATIONS/PRESENTATIONS

1. R.K. Ahluwalia, X. Wang, W.B. Johnson, F. Berg, and D. Kadylak, "Performance of a Cross-Flow Humidifier with a High Flux Water Vapor Transport Membrane," J. Power Sources, Vol. 291, pp. 225–238, 2015.

2. D.D. Papadias, R.K. Ahluwalia, J.K. Thomson, H.M. Meyer III, M.P. Brady, H. Wang, R. Mukundan, and R. Borup, "Degradation of SS316L Bipolar Plates in Fuel Cell Environment: Corrosion Rate, Barrier Film Formation Kinetics and Contact Resistance," J. Power Sources, Vol. 273, pp. 1237–1249, 2015.

3. T. Hua, R.K. Ahluwalia, L. Eudy, G. Singer, B. Jermer, N. Asselin-Miller, S. Wessel, T. Patterson, and J. Marcinkoski, "Status of Hydrogen Fuel Cell Electric Buses Worldwide," Journal of Power Sources, Vol. 269, pp. 975–993, 2014.

4. R.K. Ahluwalia, X. Wang, "Performance of an Advanced Automotive MEA with Heat Rejection Constraint," IEA Annex 34 Meeting, Forschungszentrum Jülich, Jülich, Germany, June 24, 2015.

5. D. Myers, N. Kariuki, J. Hammons, R. Ahluwalia, X. Wang, J-K Peng, and D. Fongalland, "Dealloyed Pt-Ni Polymer Electrolyte Fuel Cell Cathodes: Effects of Catalyst-Ionomer Ink Composition on Structure and Performance," 227th ECS Meeting, Chicago, IL, May 24–28, 2015.

6. X. Wang, J-K Peng, R. Ahluwalia, D. Myers, and Z. Yang, "Mass Transfer Overpotentials in Dispersed Pt/C and De-Alloyed PtNi/C Polymer Electrolyte Fuel Cell Cathodes," 227th ECS Meeting, Chicago, IL, May 24–28, 2015.

7. R.K. Ahluwalia, X. Wang, T.Q. Hua, and D. Myers, "Fuel Cell Systems for Transportation: Recent Developments in U.S.A.," IEA Annex 26 Meeting, CEA, Grenoble, France, Dec. 3, 2014.

8. R.K. Ahluwalia, and N. Garland, "Report from the Annexes: Annex 26," IEA AFC ExCo 49th Meeting, CEA, Grenoble, France, Dec. 4–5, 2014.

REFERENCES

1. Fuel cell technical team roadmap, http://energy.gov/sites/prod/files/2014/02/f8/fctt_roadmap_june2013.pdf, June 2013.

2. D. Myers, N. Kariuki, J. Hammons, R. Ahluwalia, X. Wang, J-K Peng, and D. Fongalland, "Dealloyed Pt-Ni polymer electrolyte fuel cell cathodes: Effects of catalyst-ionomer ink composition on structure and performance," 227th ECS Meeting, Chicago, IL, May 24–28, 2015.

3. A. Kongkanand and F. Wagner, "High activity de-alloyed catalyst," 2014 Hydrogen and Fuel Cells Program Review, FC087, June 16–20, 2014.

4. R.K. Ahluwalia, S. Arisetty, X. Wang, X. Wang, R. Subbaraman, S.C. Ball, S. DeCrane, and D. Myers, "Thermodynamics and kinetics of platinum dissolution from carbon-supported electrocatalysts in aqueous media under potentiostatic and potentiodynamic conditions," J. Electrochem. Soc. 160 (2013) F447–F455.

5. R.K. Ahluwalia, S. Arisetty, J-K Peng, R. Subbaraman, X. Wang, N. Kariuki, D.J. Myers, R. Mukundan, R. Borup, and O. Polevaya, "Dynamics of particle growth and electrochemical surface area loss due to platinum dissolution," J. Electrochem. Soc. 161 (2013) F291–F304.

6. A. Kongkanand, J. Zhang, Z. Liu, Y-H Lai, P. Sinha, E.L. Thompson, and R. Makharia, "Degradation of PEMFC observed on NSTF electrodes," J. Electrochem. Soc. 161 (2013) F291–F304.

7. A.J. Steinbach, K. Alade-Lambo, C. Hamilton, M.J. Kurkowski, R. Atanasoski, and M. Debe, "Reversible performance losses of PEM fuel cells," 238th ACS National Meeting and Exposition, Aug. 18, 2009.

V.F.3 Fuel Cell Vehicle and Bus Cost Analysis

Brian D. James (Primary Contact), Jennie M. Moton, Daniel A. DeSantis, Cassidy Houchins
Strategic Analysis (SA), Inc.
4075 Wilson Blvd., Suite 200
Arlington, VA 22203
Phone: (703) 778-7114
Email: bjames@sainc.com

DOE Manager
Jason Marcinkoski
Phone: (202) 586-7466
Email: Jason.Marcinkoski@ee.doe.gov

Contract Number: DE-EE0005236

Project Start Date: September 30, 2011
Project End Date: September 30, 2016

Overall Objectives

- Define low temperature proton exchange membrane (PEM) fuel cell power system operational and physical characteristics that reflect the current status of system performance and fabrication technologies
- Estimate the production cost of the fuel cell systems (FCSs) for automotive and bus applications at multiple rates of annual production
- Identify key cost drivers of these systems and pathways to further cost reduction

Fiscal Year (FY) 2015 Objectives

- Update 2014 automotive and bus fuel cell power system cost projections to reflect latest performance data and system design information
- Define design and analyze cost of PtNi binary catalyst dispersion application methods
- Analyze material processing cost of alternative non-Pt catalyst fabrication
- Re-evaluate and analyze cost of automotive FCS component manufacturing processes at low production volumes

Technical Barriers

This project addresses the following technical barrier from the Fuel Cells section of the Fuel Cell Technologies Office Multi-Year Research, Development, and Demonstration Plan:

(B) Cost

Technical Targets

This project conducts cost modeling to attain realistic, process-based system cost estimates for integrated transportation fuel cell power systems operating on direct hydrogen. These values can help inform future technical targets:

- DOE 2020 fuel cell system cost target: $40/kilowatt-electric (kWe) (net)

FY 2015 Accomplishments

- Projected the fuel cell power system cost for an 80 kWe (net) light-duty vehicle application using a Design for Manufacturing and Assembly (DFMA®) methodology at an annual production rate of 500,000 FCSs per year
- Projected the fuel cell power system cost of a 160 kWe (net) fuel cell power system for a bus at 1,000 systems per year
- Extended multi-variable sensitivity analysis to stack, balance of plant (BOP), and total system at all manufacturing rates for both the automotive and bus systems
- Analyzed a non-platinum catalyst fabrication process as a side study to compare to current platinum catalyst system
- Re-evaluated automotive fuel cell (FC) stack components at low production volume
  - Bipolar plate (BPP) forming and coating
  - Dispersed catalyst coating compared to 3M nano-structured thin film (NSTF)

✧ ✧ ✧ ✧ ✧

INTRODUCTION

Research is ongoing to make fuel cell electric vehicles cost and performance competitive with internal combustion engine vehicles. This work supports that research effort through a DFMA®-style [1] analysis of the cost to manufacture two different transportation FCSs. A detailed system-level cost analysis allows the assessment of individual FC research advancements and therefore provides insight into the most cost beneficial research directions. The cost and performance impact of research advancements on fuel cells for transportation applications is assessed. The systems analyzed are low-temperature (LT) PEM FCSs operating on hydrogen with peak electrical capacities of 80 kWe (net) for light-duty vehicle (automobile) applications and 160 kWe (net) for 40-foot transit bus applications. The onboard

compressed hydrogen storage system is not included in this cost assessment. The impact of annual production rates on the cost of the automotive and bus systems is examined to assess the difference between a nascent and a mature product manufacturing base. The annual production rates analyzed are 1,000, 10,000, 30,000, 80,000, 100,000, and 500,000 FCSs per year for automotive systems and 200, 400, 800, and 1,000 systems per year for the bus systems.

This work focuses primarily on updating the existing automobile FCS DFMA® cost model as well as efforts to design and model the manufacturing cost of bus FCSs. Stack and BOP designs and performance parameters are discussed, and the methods of modeling each are explained. New technologies, materials data, and optimization modeling are incorporated to give an up-to-date value for system cost. Cost trends are evaluated in terms of the capital costs per unit of installed electrical capacity ($/kWe [net]) and system annual production rate.

To assist the DOE and FC companies in charting the transition from prototype and low-volume production to high-volume manufacturing, it is important to understand the crossover point ("break-point") for switching from a low-volume to a high-volume manufacturing process. In 2015, low-volume (1,000–5,000 systems/year) manufacturing techniques were studied for BPP stamping and catalyst deposition to better understand how they differ from high-volume (30,000–500,000 systems/year) manufacturing processes. One goal of this analysis is to better understand the most cost-effective low-volume manufacturing processes and their corresponding break-points.

APPROACH

A DFMA®-style analysis is conducted to estimate the manufacturing cost of PEM FCSs for automobiles and buses at various manufacturing production rates. The optimum stack operating conditions and operating point are selected in collaboration with Argonne National Laboratory (ANL) and the United States Driving Research and Innovation for Vehicle efficiency and Energy sustainability (U.S. DRIVE) Fuel Cell Tech Team. ANL first principles models of fuel cell stack operating conditions [2] and SA DFMA® cost models are used to identify cost and performance optimized conditions, which are vetted by the Fuel Cell Tech Team. Output from the ANL model provides insight into cell voltage, stack pressure, cathode catalyst loading, air stoichiometry, and stack outlet coolant temperature while the DFMA® cost model provides insight into cost and performance tradeoffs. The FCS is sized to provide 80 kWe (net) based on rated power operating parameters. System performance is based on performance estimates of individual components, built up into an overall system energy budget.

DFMA® process-based cost estimation techniques are applied to the major system components (and other specialty components) such as the fuel cell stack, membrane humidifier, air compressor/expander/motor (CEM) unit, and hydrogen recirculation ejectors. For each of these, a manufacturing process train details the specific manufacturing and assembly machinery, and processing conditions are identified and used to assess component cost. For 2015, the full DFMA® analysis was extended to the examination of non-Pt polyaniline-iron-carbon (PANI-Fe-C) catalyst fabrication and alternative manufacturing processes for FC stack components at low production volumes.

RESULTS

As in previous years, the 2015 high-volume manufacturing cost will be reported separately in a DOE data record when available later this year. Final 2014 cost results (reported for the first time) and 2015 component results are described in this report.

2014 Automotive and Bus System Cost

The operating conditions and assumptions used to calculate costs for the 2014 auto and bus systems are summarized in Table 1. The operating conditions and assumptions did not change significantly from 2013. The 2014 automotive system cost at 500,000 systems per year is $54.84/kWe (net) and is similar to the 2013 projected cost of $54.83/kWe (net). While the cost remained stable between 2013 and 2014, the underlying system and modeling assumptions were altered but with nearly exactly offsetting cost impact. Increased power density at a lower operating voltage, higher stack temperature, and higher air stoichiometric ratio contributed to a reduction of $0.37/kWe (net), while updated material costs and component models with improved assumptions contributed to an increase of $0.38/kWe (net). The waterfall chart in Figure 1 shows a potential pathway to meeting the DOE's 2020 automotive fuel cell system cost target of ~$40/kWe (net) from the current status system cost of $54.84/kWe (net). The step improvements are based on U.S. DRIVE cost targets plus additional assumed BOP cost reductions.

Between 2013 and 2014, the bus FCS cost increased from $269.95/kWe (net) to $278.62/kWe (net). The changes between 2013 and 2014 include the same material cost changes that were made to the automotive system, minor changes to the compressor component manufacturing process, and changes to the efficiency of the compressor (from 71% to 58%) and motor (from 80% to 95%) based on recent test data.

In previous years, sensitivity analyses for the automotive and bus FCSs were only conducted at the highest production rates for the total system cost. In 2014, the Monte Carlo analysis was extended to all manufacturing rates with multi-

TABLE 1. PEM FC Auto and Bus System Operating Conditions and Assumptions

	2014 Auto System	2014 Bus System
System Gross Power (kWe)	92.75	187.6
System Net Power (kWe)	80	160
Power Density (mW/cm^2)	834	601
Cell Voltage (mV)	672	676
Stack Temp (Coolant Exit Temp) (˚C)	95	74
Pressure (atm)	2.5	1.8
Platinum Loading (kWe (gross)/g)	92.75	187.6
Air Stoichiometry	2	2.1
Catalyst System	PtCoMn NSTF	PtCoMn NSTF
Cells per System	372	740

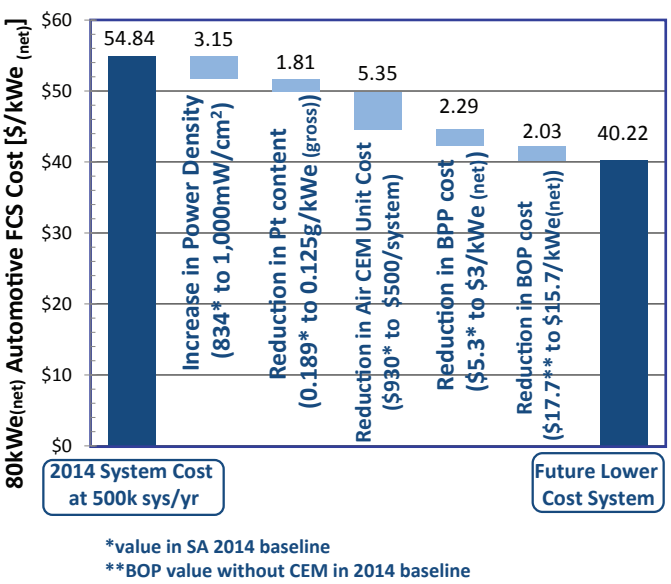

FIGURE 1. Waterfall chart for projection of automotive fuel cell system cost from $54.84/kWe (net) down to $40/kWe (net) [4]

variable sensitivities showing the middle 90% confidence range for stack cost, BOP cost, and total system cost. Figure 2 shows the automotive and bus FCS costs at each manufacturing rate with the Monte Carlo results shown as error bars for the stack and total system. At 500,000 systems per year, the automotive system, with 90% confidence, would be between $50.81/kWe (net) and $63.70/kWe (net). At 1,000 systems per year, the bus system cost range is between $256.92 kWe (net) and $341.49/kWe (net). The larger error bars for the bus system reflect greater uncertainty in the cost projections at low production rates. Indeed, it is surprising that the bus system cost curve falls in line so closely with the automotive system curve given the lower power density and higher platinum loading required in the bus system.

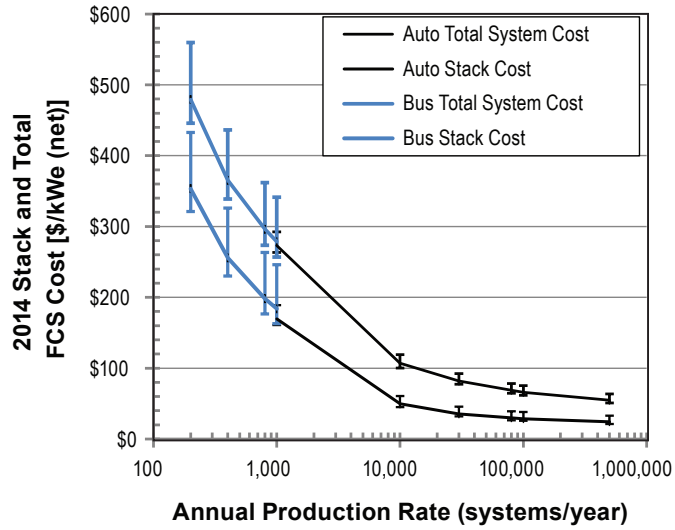

FIGURE 2. Automotive stack and total system cost at all manufacturing rates with error bars based on the Monte Carlo sensitivity results with middle 90% confidence range

Future analysis will seek to improve the confidence in the bus cost results and explore differences between the auto and bus systems at their overlapping manufacturing rate of 1,000 systems per year.

PANI-Fe-C Manufacturing Cost Analysis

For 2015, a DFMA® analysis was completed for a non-Pt PANI-Fe-C catalyst developed by researchers at Los Alamos National Laboratory. The catalyst materials manufacturing process is outlined in Figure 3 and includes seven processing steps: (1) oxidation of carbon, (2) reagent mixing and polymerization, (3) belt drying, (4) grinding, (5) rotary calcining, (6) acid leaching and filtration, and (7) oven pyrolysis. The results show PANI-Fe-C catalyst has a much lower cost per mass of material ($74/kg compared to Pt-based catalysts at ~$41,000/kg); however, the performance of cells using the PANI catalyst is much lower (330 mW/cm^2 at ~0.5 V compared to 834 mW/cm^2 at 0.672 V for PtCoMn catalyst). At such reduced areal power density, and combined with a higher catalyst loading (~4 mg/cm^2 vs. ~0.15 mg/cm^2), 17 times the mass of catalyst powder is required along with substantially larger stack(s) to achieve equal net system power. Total system catalyst cost is still reduced, but the cost of the stack components (membranes, BPP, etc.) is so much larger that the non-Pt PANI-Fe-C stack(s) would cost more than a Pt-based catalyst FC stack.

Low-Volume Cost Analysis

During 2015, multiple component design and manufacturing processes were re-evaluated to assess low-production-rate issues. BPP forming, BPP material and coating, and catalyst ink application (other than NSTF) were each considered.

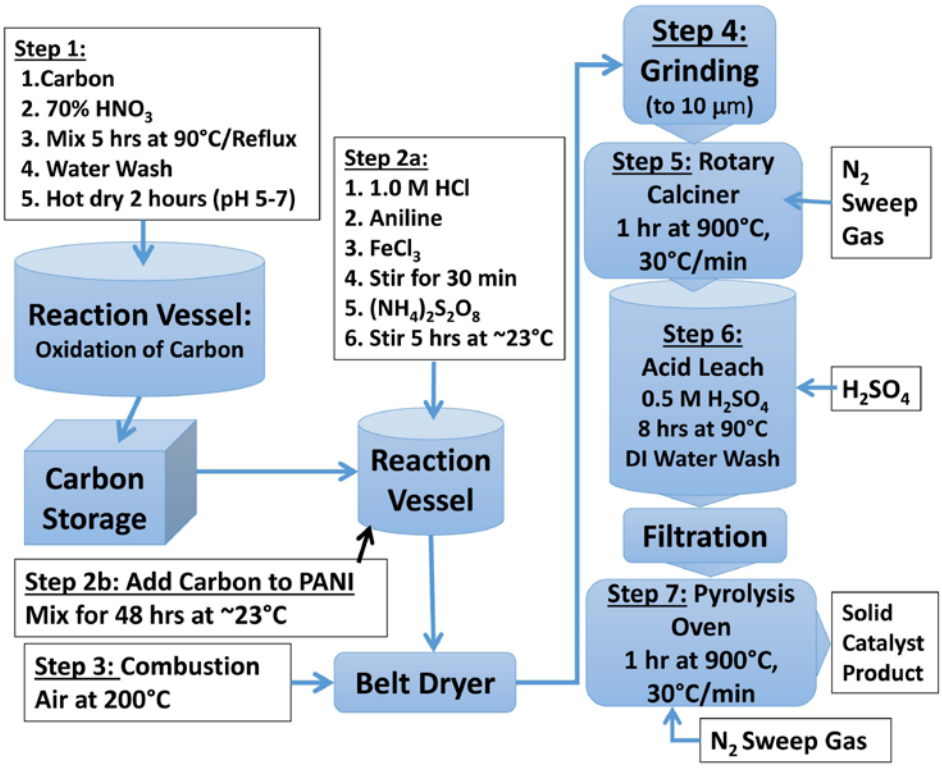

FIGURE 3. Non-Pt-based catalyst PANI-Fe-C material processing flow diagram

The baseline DFMA® model uses progressive die stamping to form the stainless steel (SS) BPP; however, sequential stamping and hydroforming (HF) are viable alternatives to form very thin (76 microns) metal plates. In discussions with stamping and HF equipment manufacturers, HF and stamping (both sequential and progressive) are noted to have significant differences: (1) typical HF cycle times are ~15–20 seconds while stamping is often less than 1 second, and (2) stamping dies (tooling) are typically more expensive (~$40,000) than HF dies (~$10,000–$15,000). Conventional wisdom from HF/stamping vendors suggested that HF would be less expensive than stamping at <50,000 parts per year (about 60 FCS/year) due to lower die costs. This result was confirmed by DFMA® analysis, which showed the manufacturing rate crossover point at which progressive stamping becomes less expensive than sequential stamping or HF is ~100,000 plates per year (~130 FCS per year). This analysis suggests progressive stamping will be less expensive than sequential stamping or HF at all but prototype runs of automotive FCS. Similar results were reported in a Massachusetts Institute of Technology HF/stamping comparison [3]. Non-traditional HF techniques that automate the process can reduce the processing times of HF, potentially reducing the HF cost at low volumes. An analysis of non-traditional HF is expected to be completed in 2016.

Titanium (Ti) BPPs were also investigated in 2015 to determine whether there is a low volume cost benefit to switching from 316 SS with a Treadstone anti-corrosion coating to Ti plates with a gold coating. Since Ti is more expensive per kilogram than SS, such a trade-off appears unlikely unless the cost for coating a SS plate offsets the difference in plate material cost. Commercially pure titanium Grade 2 at 76 microns thickness (quoted at $157/kg Ti) with a gold coating was compared to the baseline 76 micron SS 316 BPP ($11/kg SS 316) with Treadstone coating. At the production volumes specified for the automotive FCS, gold-coated titanium plates are more expensive than SS 316 plates with Treadstone coating. Quotations for thicker titanium sheets (533 microns thick), obtained for comparison, show mill cost (to achieve thin sheets) is a substantial cost contributor. However, use of thicker Ti plates (533 microns) to lower the effective cost of Ti to $27/kg still results in higher cost than the baseline coated SS plates due to the greater mass per area of BPP. Consequently, Ti plates do not appear to be a low-cost alternative to coated SS plates at any production rate of interest based on the current Ti pricing acquired.

Alternative approaches to catalyst application were also considered in 2015. The baseline NSTF catalyst coating approach includes multiple vacuum processes (sublimation of Paralene Red 149 followed by heating and deposition of catalyst metals), which results in high capital cost, particularly for low-volume production. In contrast, slot die coating is an established high-rate, non-vacuum catalyst application technique that is expected to be a lower-cost alternative to NSTF at low volumes. Pricing and operating data from multiple slot die coating companies (two of which

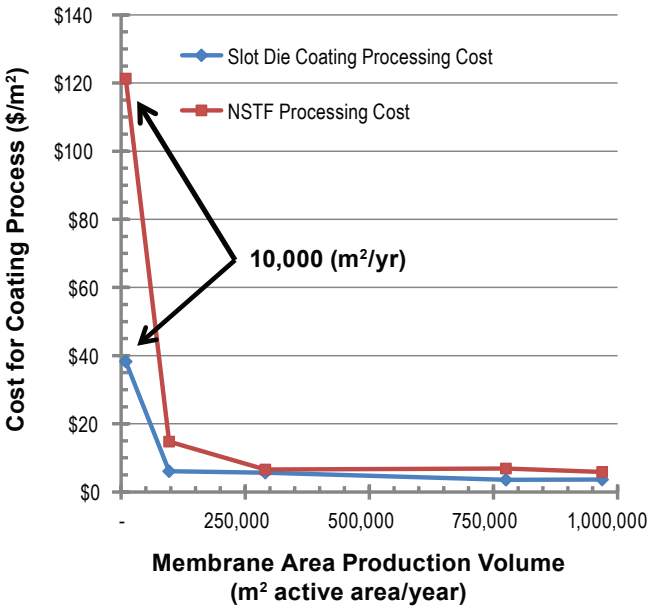

FIGURE 4. Comparison of slot die coating with NSTF coating production cost ($/m^2 active area) over production volume

have supplied fuel cell companies) were collected and used within a DFMA® analysis. As seen in Figure 4 (processing costs only), slot die coating is judged to be the least expensive manufacturing process (per active area of membrane electrode assembly [MEA]) at less than 40,000 m^2 per year (~30,000 FCS per year). Note that this assessment is meant to isolate the cost of catalyst application and is only valid if both catalyst application systems have the same power density. In future analyses, a comparison of dispersed and NSTF catalysts inclusive of all manufacturing and materials costs and power density impacts will be performed to provide a comprehensive assessment of the two catalyst approaches.

CONCLUSIONS AND FUTURE DIRECTIONS

- The 2014 final auto and bus system cost results increased slightly from 2013, due to a series of specific analysis and assumption improvements. The 2015 final system cost analyses for the automotive and bus systems are currently underway.
- The automotive FCS cost for 2014 ($54.84/kWe (net)) did not change significantly from the 2013 analysis ($54.83/kWe (net)). Minor changes were made to material costs, efficiency calculations, and operating conditions.
- The 2014 projected system cost of the 160 kWe (net) LT PEM FC bus system is ~$279/kWe (net), incorporating updated compressor and motor efficiencies.
- The Monte Carlo multi-variable sensitivity analysis was extended to all production volumes and for the stack and BOP for both the auto and bus systems. Future analysis will seek to improve the confidence in the low-production-rate results.
- A 2015 side study of the non-Pt-based catalyst (PANI-Fe-C) revealed a much lower cost per mass ($74/kg), albeit lower performance (330 mW/cm^2) compared to traditional Pt- based catalysts. Higher non-Pt-based catalyst polarization performance is needed to achieve a net stack cost reduction.
- Alternative low-cost processing methods for forming and coating BPP and coating catalyst onto membranes for the automotive system were examined. Hydroforming of the BPP was not found to be less expensive than progressive stamping. Titanium BPPs with gold coatings were not found to be less expensive than SS plates with Treadstone coatings.
- Slot die coating can be a lower-cost method for coating catalyst onto MEAs (on a cost per area basis) for production volumes lower than 300,000 m^2/year. Future analyses will compare dispersed and NSTF catalysts inclusive of all manufacturing and materials costs and power density impacts to provide a comprehensive assessment of the tradeoffs between cost and performance.
- Projections of the overall fuel cell power system cost for both automotive and bus applications will be made for the 2015 analysis and are anticipated to change by substituting auto PtCoMn NSTF ternary catalyst with a binary PtNi-C-based catalyst.

FY 2015 PUBLICATIONS/PRESENTATIONS

1. Moton, J.M., James, B.D., Colella, W.G., "Engineering and Economic Advances in Proton Exchange Membrane (PEM) Fuel Cell Vehicle (FCV) Design," Presented at the 2013 Fuel Cell Seminar and Exposition, Los Angeles, CA, November 13, 2014.

2. "Mass Production Cost Estimation of Direct H_2 PEM Fuel Cell Systems for Transportation Applications: 2014 Update," Strategic Analysis Report prepared by Brian D. James, Jennie M. Moton, and Whitney G. Colella, December 2014.

3. James, B.D., Moton, J.M., Houchins, C., DeSantis, D.A., "2015 DOE Hydrogen and Fuel Cells Program Review: Fuel Cell Vehicle and Bus Cost Analysis," Presented at the 2015 DOE FCTO Annual Merit Review Meeting, Arlington, VA, June 10, 2015.

4. James, B.D., Houchins, C., Moton, J.M., "Transportation Fuel Cells Cost Analysis Update Automotive Cost Analysis," Presented to the Fuel Cell Technical Team, Southfield, MI, July 15, 2015.

REFERENCES

1. Boothroyd, G., P. Dewhurst, and W. Knight. "Product Design for Manufacture and Assembly, Second Edition," 2002.

2. Ahluwalia, R. "Fuel Cell Systems Analysis," Argonne National Laboratory, Presentation to DOE Fuel Cell Tech Team, 16 July 2014, Southfield, MI.

3. Hydroforming Die Cost Assumptions: Matwick, S.E., "An Economic Evaluation of Sheet Hydroforming and Low Volume Stamping and the Effects of Manufacturing Systems Analysis," Masters Thesis for Master of Science in Material Science and Engineering at MIT, pg. 40, February 2003. http://msl.mit.edu/theses/Matwick_S-thesis.pdf

4. U.S. DRIVE Targets: http://energy.gov/sites/prod/files/2014/02/f8/fctt_roadmap_june2013.pdf
U.S. DOE System Targets: http://hydrogen.energy.gov/pdfs/14012_fuel_cell_system_cost_2013.pdf

V.F.4 Characterization of Fuel Cell Materials

Karren L. More (Primary Contact) and
David A. Cullen
Oak Ridge National Laboratory (ORNL)
1 Bethel Valley Road
Oak Ridge, TN 37831-6064
Phone: (865) 574-7788
Email: morekl1@ornl.gov

DOE Manager
Donna Ho
Phone: (202) 586-8000
Email: Donna.Ho@ee.doe.gov

Project Start Date: October 1, 1999
Project End Date: Project continuation and direction determined annually by DOE

Overall Objectives

- Identify, develop, and optimize novel high-resolution imaging and spectroscopy techniques as well as unique specimen preparation methodologies to characterize the material constituents comprising fuel cells (FCs) at the micrometer to sub-angstrom scale (electrocatalysts, catalyst supports, ionomer)
- Understand fundamental relationships between the material constituents within FC membrane electrode assemblies (MEAs), particularly cathode catalyst layers (CCLs), and correlate structural and chemical data with stability, durability, and performance characteristics (with guidance/input from the FC community); apply knowledge gained towards material and CCL optimization
- Integrate microstructural characterization within other DOE projects and establish collaborations with industrial partners
- Apply advanced analytical and imaging techniques for the evaluation of microstructural and microchemical changes resulting from FC testing, including accelerated stress tests (ASTs), to elucidate microstructure-related degradation mechanisms contributing to FC performance loss
- Make capabilities and expertise broadly available to other FC researchers

Fiscal Year (FY) 2015 Objectives

- Establish several new collaborations with FC manufacturers and researchers to identify and quantify FC material degradation mechanisms and characterize new FC materials
- Image (map) and quantify the through-thickness distribution of ionomer dispersions within CCLs; correlate ionomer dispersions with materials constituents within CCLs
- Pursue the development of in situ electrochemical transmission electron microscopy methods to study the degradation of catalyst and support materials
- Interrogate material and MEA structures using three-dimensional (3D) electron tomography and optimize this technique for FC materials analysis

Technical Barriers

This project addresses the following technical barriers from the Fuel Cells section of the Fuel Cell Technologies Office Multi-Year Research, Development, and Demonstration Plan:

(A) Durability

(C) Performance

Technical Targets

This project is focused on conducting fundamental characterization studies to assess the stability and durability of the individual material constituents comprising polymer electrolyte membrane fuel cell (PEMFC) MEAs. These studies include the characterization of newly developed materials (electrocatalysts and catalyst supports), the incorporation of these materials in MEAs, and the correlation of electrode microstructural/material changes that occur during electrochemical aging with measured FC durability and performance. Insights gained through extensive microstructural studies will be applied toward the design and manufacture of catalysts and catalyst supports that meet the DOE 2017 and 2020 targets for integrated PEMFC power systems and FC stacks operating on direct hydrogen for transportation applications (listed in Table 1).

FY 2015 Accomplishments

- Published results from a parametric study with General Motors (GM) to quantify ionomer distributions at multiple length scales within MEAs, e.g., through-thickness distributions within CCLs (100 nm level) and surrounding individual pores within CCLs (<10 nm level) in the *Journal of The Electrochemical Society*, which represent a successful collaboration between ORNL, GM, and Clarkson University

TABLE 1. Technical Targets: Electrocatalysts for Transportation Applications

Characteristic	Unit	2011 Status	2017 Target	2020 Target
PGM Total Content (both electrodes)	g/kW (rated)	0.19	0.125	0.125
PGM Total Loading	mg PGM/cm^3 electrode area	0.15	0.125	0.125
Loss in Initial Catalytic Activity	% mass activity loss	48	<40	<40
Electrocatalyst Support Stability	% mass activity loss	<10	<10	<10
Mass Activity	A/mg Pt at 900 mV	0.24	0.44	0.44
Non-PGM Catalyst Activity per Volume of Supported Catalyst	A/cm^2 at 800 mV	60 (at 0.8 V) 165 (extrapolated from >0.85 V)	300	300

PGM – platinum group metal

- Collaboration continued with Ford Motor Co., to study catalyst dispersions on various catalyst support structures using X-ray photoelectron spectroscopy, high-resolution scanning transmission electron microscopy (STEM), and electron energy loss spectroscopy
- Fully established the capability for mapping ionomer film distributions across CCLs in MEAs using large solid-angle, high collection efficiency STEM-based energy dispersive X-ray spectroscopy (EDS) methods to understand and quantify ionomer aggregation as a function of specific materials components used in CCLs
- Compared results directly with scanning transmission X-ray microscopy data acquired from the same MEAs at McMaster University
- Initiated collaboration with Giner Inc. to study novel oxygen evolution reaction catalysts and support structures ($Ir/W_xTi_{1-x}O_2$) before and after aging
- Performed extensive low-voltage STEM imaging and spectroscopy on C-based materials comprising non-Pt group metal catalysts to identify potential active sites

✧ ✧ ✧ ✧ ✧

INTRODUCTION

PEMFCs are being developed for future use as efficient, zero-emission power sources. However, the performance of PEMFCs degrades with time at elevated temperature and high relative humidity during electrochemical aging in automotive and stationary applications. Performance degradation can be directly attributed to the durability of the individual material constituents comprising the MEA; e.g., the electrocatalyst, the catalyst support, and the ionomer in the CCL. The structural and chemical degradation mechanisms contributing to performance loss have not been fully quantified. The Microstructural Characterization Program at ORNL has focused on forming collaborative relationships with multiple industrial PEMFC developers/manufacturers, universities, and national laboratories to apply ORNL's advanced electron microscopy techniques and expertise to characterize as-fabricated (fresh) FC materials (individual constituents and/or materials incorporated in fresh MEAs), MEAs subjected to ASTs designed to degrade specific MEA components, and field-aged MEAs, with the ultimate goal of establishing critical processing-microstructure-performance correlations and elucidate the individual materials changes contributing to measured MEA degradation, performance loss, and failure. Understanding the structural and compositional changes of the materials comprising MEAs during electrochemical aging will allow for the implementation of materials-based mitigation strategies required for optimizing PEMFC durability and performance.

APPROACH

The task of microstructural characterization requires utilizing advanced electron microscopy imaging and spectroscopy techniques to characterize the individual material components comprising PEMFCs before and after incorporation into MEAs and after electrochemical aging. These studies also include novel materials (primarily electrocatalysts) developed by partner laboratories. Our approach is focused on identifying and optimizing novel high-resolution imaging and compositional/chemical analysis techniques as well as on developing unique specimen preparation methodologies specifically aimed at micrometer- to angstrom-scale characterization of the material constituents within FC CCLs (electrocatalysts, catalyst supports, and ionomer). These advanced analytical and imaging techniques are applied to evaluate the microstructural and microchemical characteristics of each material constituent, and to allow for correlation of these observations with FC performance (aging studies are conducted at the collaborator's laboratories). These studies are designed to elucidate the microstructure-related material degradation mechanisms that contribute to FC performance loss. Most importantly, ORNL is making available the techniques and expertise it has accrued to FC researchers outside of ORNL via several mechanisms: (1) strategic

partnership projects for proprietary research, (2) through the use of ORNL user facilities (e.g., Center for Nanophase Materials Sciences), and (3) by engaging in collaborative non-proprietary research projects via the Microstructural Characterization Project that are consistent with ORNL's research activities.

RESULTS

The ionomer distribution within the CCL plays a critical role in ionic and mass transport, and therefore, controls electrochemical kinetics. In a recent review article by Holdcroft [1], several unresolved challenges regarding the CCL ionomer distribution were identified. One of these challenges was elucidating the ionomer aggregation phenomenon in CCLs and the correlation between catalyst ink processing and solidification on the resultant CCL morphology. Thus, the primary goal of ORNL's research in FY 2015 was to "visualize" the ionomer distributions within PEMFC CCLs using high spatial resolution spectroscopy methods to understand and quantify ionomer film thickness and dispersion as a function of (1) the material constituents comprising the CCL, (2) ionomer loading, (3) the ink preparation method used, and (4) stability during electrochemical aging. An understanding of these relationships will enable optimization of the ionomer distributions within CCLs. In FY 2014, electron microscopy parameters (accelerating voltage, temperature, and electron dose) were optimized as part of a collaboration with GM to minimize damage to the ionomer during imaging analysis [2], and these established "best practices" were applied towards the study of CCL ionomer distributions. These studies also exploited the recent (over the previous two years) development of high-collection-efficiency, large solid-angle silicon drift detectors for EDS. These detectors were integrated within the column of the STEM to map the elemental distribution, specifically of fluorine, across the full thickness of cross-sectioned CCLs (micrometer scale) and at higher resolutions surrounding pores and Pt/C agglomerates (nanometer scale) in very short times (typically <10 minutes).

To demonstrate this ionomer visualization technique, Figure 1 shows a representative high-spatial-resolution STEM-EDS fluorine map, acquired from a CCL with Pt catalyst supported on high surface area carbon (HSAC) and 28% Nafion® ionomer (with corresponding high-angle annular dark field [HAADF] STEM image). The cross-section HAADF-STEM image of the CCL (Figure 1a) shows several levels of contrast that correspond with specific features in the CCL – pores exhibit the darkest contrast (primary and secondary pores are evident), the HSAC support is characterized by medium (grey) contrast, and the Pt nanoparticles exhibit the brightest contrast. The non-homogeneous distribution of fluorine (Figure 1b, shown in green) is clear and is evidence for significant ionomer aggregation within the CCL. There is evidence for the presence of ionomer thin films within the CCL, as well; however, most of the ionomer is concentrated within ionomer aggregates having an average size of ~70 nm (circled in red in Figure 1b). These aggregates are present *between* the Pt/HSAC agglomerates and *within* the Pt/HSAC agglomerates. Additionally, a large fraction of the Pt/HSAC comprising the secondary pore surfaces (pores between Pt/HSAC agglomerates) has no ionomer layers on its surface, which is consistent with the ionomer filling the irregular regions (or pockets) where Pt/HASC agglomerates meet and also filling primary and secondary pores inside the Pt/HSAC agglomerates. The observation of ionomer aggregation is also evident on a CL containing Pt supported on graphitized carbon (low surface area carbon [LSAC]), as shown in Figure 2, except in this case the ionomer aggregation associated with Pt/LSAC is slightly different because the Pt/LSAC agglomerate density is higher (fewer large-sized pores compared to Pt/HSAC agglomerates). In this case,

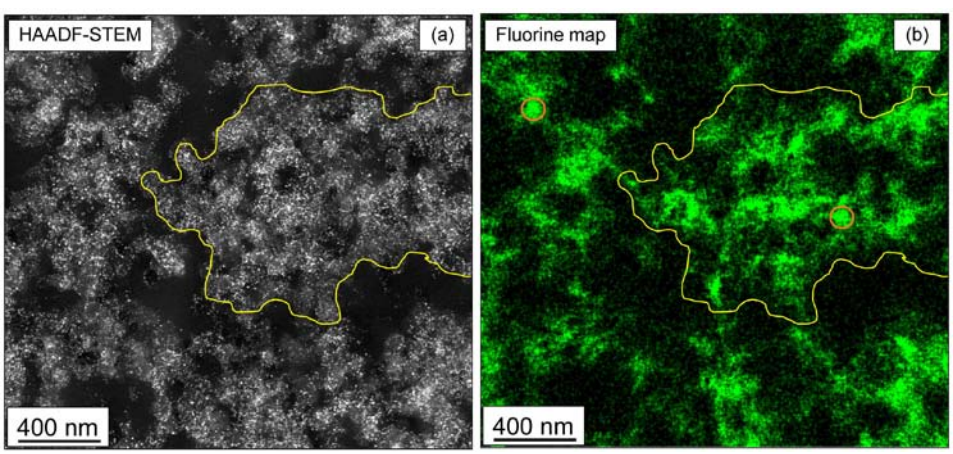

FIGURE 1. (a) HAADF-STEM image and (b) corresponding fluorine map acquired from CCL with Pt/HSAC and 28% Nafion® ionomer

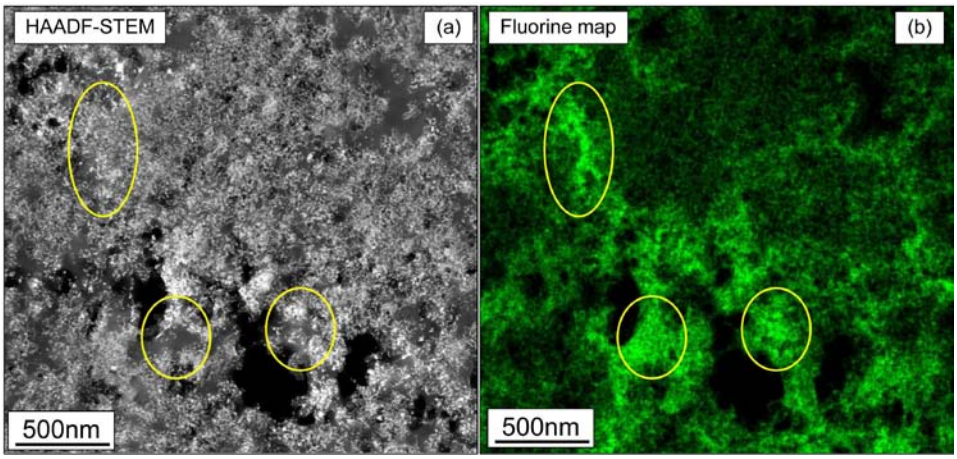

FIGURE 2. (a) HAADF-STEM image and (b) corresponding fluorine map acquired from CCL with Pt/LSAC and 38% Nafion® ionomer

a majority of the large ionomer aggregates were located between Pt/LSAC (circled in yellow in Figure 2), with thinner ionomer films present within the Pt/LSAC agglomerates.

Work is ongoing to establish direct correlations between the observed character of ionomer aggregation and the different types of materials used in CCLs and ink processing methods, with the ultimate goal of preparing CCLs with more uniform ionomer distributions/dispersions.

CONCLUSIONS AND FUTURE DIRECTIONS

ORNL's microstructural studies continue to provide insight regarding the structural and compositional factors of MEA material components that ultimately contribute to the stability and durability of FCs. In FY 2015, studies primarily focused on quantifying ionomer distributions within CCLs and new electrocatalysts. We will continue to support these studies in FY 2016 through collaborations with industrial and academic partners while emphasizing new studies focused on optimizing the interactions and dispersions of the electrocatalyst and ionomer, and on exploiting corrosion-resistant highly graphitized carbon supports by improving catalyst dispersions through surface modification. Specifically, we will:

- Continue to establish new collaborations with FC manufacturers and researchers to identify and quantify FC materials degradation mechanisms and to characterize new FC materials. Input from the Fuel Cell Tech Team, reviewer comments from the Annual Merit Review, and collaborations are key to the success of this microstructural characterization project and identify critical research directions.
- Correlate and quantify interactions between ionomer layers, Pt-based catalysts and their distributions within CCLs, and new/novel catalyst supports; establish relationships between ionomer-Pt-support resulting from various ink preparation methods.
- Characterize ionomer distributions in "real" CCLs through the use of high-resolution 3D electron tomography studies, combining structural and compositional tomography.
- Perform dispersion optimization studies for ionomers and Pt on graphitic supports through surface modification.

FY 2015 PUBLICATIONS/PRESENTATIONS

1. D.A. Cullen, K.L. More, L.L. Atanasoska, and R.T. Atanasoski, "Impact of IrRu Oxygen Evolution Reaction Catalysts on Pt Nanostructured Thin Films under Start-up/Shutdown Cycling," *Journal of Power Sources* 269 671–681 (2014).

2. S.M. Alia, S. Pylypenko, K.C. Neyerlin, D.A. Cullen, S.S. Kocha, and B.S. Pivovar, "Platinum-Coated Cobalt Nanowires as Oxygen Reduction Reaction Electrocatalysts," *ACS Catalysis* 4[8] 2680–2686 (2014).

3. Q. Li, G. Wu, D.A. Cullen, K.L. More, N.H. Mack, H.T. Chung, and P. Zelenay, "Phosphate-Tolerant Oxygen Reduction Catalyst," *ACS Catalysis* 4[9] 3193–3200 (2014).

4. Y.J. Kang, J. Snyder, M. Chi, D.G. Li, K.L. More, N.M. Markovic, and V.R. Stamenkovic, "Multimetallic Core/Interlayer/Shell Nanostructures as Advanced Electrocatalysts," *Nano Letters* 14[11] 6361–6370 (2014).

5. D.A. Cullen, R. Koestner, R.S. Kukreja, Z.Y. Liu, S. Minko, O. Trotsenko, A. Tokarev, L. Guetaz, H.M. Meyer III, C.M. Parish, and K.L. More, "Imaging and Microanalysis of Thin Ionomer Layers by Scanning Transmission Electron Microscopy," *Journal of The Electrochemical Society* 161[10] F1111–F1117 (2014).

6. D.A. Cullen, M. Lopez-Haro, P. Bayle-Guillemaud, L. Guetaz, M.K. Debe, and A.J. Steinbach, "Linking Morphology with Activity through the Lifetime of Pretreated PtNi Nanostructured Thin Film

Catalysts," *Journal of Materials Chemistry A* 3[21] 11660–11667 (2015).

7. J. Zheng, D.A. Cullen, R.V. Forest, J.A. Wittkopft, Z.B. Zhuang, W.C. Sheng, J.G.G. Chen, and Y.S. Yan, "Platinum-Rhuthenium Nanotubes and Platinum-Rhuthenium Coated Copper Nanowires as Efficient Catalysts for Electro-Oxidation of Methanol," *ACS Catalysis* 5[3] 1468–1474 (2015).

8. A. Epshteyn, Y. Garsany, K.L. More, H.M. Meyer III, V. Jain, A.P. Purdy, and K.E. Swider-Lyons, "Effective Strategy for Improving Electrocatalyst Durability by Adhesive Immobilization of Catalyst Nanoparticles on Graphitic Carbon Supports," *ACS Catalysis* 5[6] 3662–3674 (2015).

9. Invited Presentation: K.L. More, D.A. Cullen, and K.S. Reeves, "Correlating Catalyst Stability with Improved Cathode Materials for PEM Fuel Cells," Gordon Research Conference on Fuel Cells, Bryant University, Smithfield, RI, August 3–8, 2014.

10. Contributed Presentation: K.L. More, D.A. Cullen, and K.S. Reeves, "The Effect of Carbon Support Structure on Ionomer Distributions in PEM Fuel Cell Catalyst Layers," 226th ECS Meeting, Cancun, Mexico, October 5–10, 2014.

11. Contributed Presentation: D.A. Cullen, K.L. More, J. Erlebacher, D. van der Vliet, S. Luopa, and A.J. Steinbach, "The Impact of Pretreatments and Conditioning on the Structure and Performance of NSTF ORR Alloy Catalysts," 226th ECS Meeting, Cancun, Mexico, October 5–10, 2014.

12. Invited Presentation: K.L. More and D.A. Cullen, "Understanding Fuel Cell Materials Degradation via Advanced Electron Microscopy Techniques," 227th ECS Meeting, Chicago, IL, May 25–29, 2015.

13. Contributed Presentation: K.L. More, D.A. Cullen, and K.S. Reeves, "Characterization of Ionomer Thin Film Distributions in PEM Fuel Cell Catalyst Layers using Analytical Electron Microscopy," ECS Conference on Electrochemical Energy Conversion & Storage with SOFC-XIV, Glasgow, Scotland, July 26–31, 2015.

REFERENCES

1. S. Holdcroft, "Fuel Cell Catalyst Layers: A Polymer Science Perspective," *Chemistry of Materials* 26[1] 381–393 (2014).

2. D.A. Cullen, R. Koestner, R.S. Kukreja, Z.Y. Liu, S. Minko, O. Trotsenko, A. Tokarev, L. Guetaz, H.M. Meyer III, C.M. Parish, and K.L. More, "Imaging and Microanalysis of Thin Ionomer Layers by Scanning Transmission Electron Microscopy," *Journal of The Electrochemical Society* 161[10] F1111–F1117 (2014).

V.F.5 Neutron Imaging Study of the Water Transport in Operating Fuel Cells

Muhammad Arif (Primary Contact),
David L. Jacobson, Daniel S. Hussey
National Institute of Standards and Technology (NIST)
100 Bureau Drive
Gaithersburg, MD 20899
Phone: (301) 975-6303
Email: arif@nist.gov

DOE Manager
Nancy Garland
Phone: (202) 586-5673
Email: Nancy.Garland@ee.doe.gov

Contract Number: DE-AI-01-01EE50660

Project Start Date: Fiscal Year (FY) 2001
Project End Date: Project continuation and direction determined annually by DOE

Overall Objectives

- Provide state-of-the-art research and testing infrastructure to enable the fuel cell industry to design, test, and optimize prototype to commercial grade fuel cells using in situ neutron imaging techniques
- Provide a secure facility for proprietary research by industry; provide beam time at no cost to non-proprietary research through a competitive proposal process; make open research data available for beneficial use by the general fuel cell community
- Continually improve and develop methods and technology to accommodate rapidly changing industry/academia needs

Fiscal Year (FY) 2015 Objectives

- Collaborate and support groups from the DOE Hydrogen Program performing water transport measurements with neutron imaging at NIST
- Improve fuel cell measurement infrastructure based on needs of the fuel cell community
- Provide support to fuel cell infrastructure to enable testing of automotive-scale test sections
- Explore and develop high resolution neutron imaging methods to enable water transport studies of catalyst and membrane electrode assemblies (MEAs)
- Employ a high resolution imaging method to achieve resolution approaching 1 μm to resolve water concentration in fuel cell electrodes
- Determine and correct systematic effects due to spatial resolution effects

Technical Barriers

This project addresses the following technical barriers from the Fuel Cells section (3.4) of the Fuel Cell Technologies Office Multi-Year Research, Development, and Demonstration Plan:

(A) Durability

(B) Cost

(C) Performance

Technical Targets

This project is conducting fundamental studies of water transport in the fuel cell. Insights gained from these studies will be applied toward the design of components and operational strategies of polymer electrolyte membrane fuel cells that meet the following DOE fuel cell targets:

- Durability with cycling at operating temperature of ≤80°C: 5,000 h
- System energy density: 650 W/L
- System specific power: 850 W/kg
- Energy efficiency: 60% at 25% rated power
- Cost: $30/kWe
- Start-up time to 50% power: 30 s from -20°C, 5 s from 20°C
- Assisted start from low temperatures: -40°C
- Durability with cycling: 5,000 h

FY 2015 Accomplishments

- Performed first user experiments employing the large scale test stand to study water transport and coolant distribution in a five cell stack
- Installed a new, second neutron imaging instrument
- Installed micro-focus X-ray source for simultaneous neutron/X-ray imaging
- Acquired components for new high resolution imaging detector systems

✧ ✧ ✧ ✧ ✧

INTRODUCTION

At NIST, we maintain the premier fuel cell neutron imaging facility in the world and continually seek to

improve its capabilities to meet the changing needs of the fuel cell community. This facility provides researchers with a powerful and effective tool to visualize and quantify water transport inside operating fuel cells. Imaging the water dynamics of a fuel cell is carried out in real time with the required spatial resolution needed for fuel cells that are being developed today. From these images, with freely available NIST-developed image analysis routines, fuel cell industry personnel and researchers can obtain in situ, nondestructive, quantitative measurements of the water content of an operating fuel cell. Neutron imaging is the only in situ method for visualizing the water distribution in a "real-world" fuel cell. Unlike X-rays, whose interaction with materials increases with the number density of electrons, neutrons interact via the nuclear force, which varies somewhat randomly across the periodic table, and is isotopically sensitive. For instance, a neutron's interaction with hydrogen is approximately 100 times greater than that with aluminum and 10 times greater than that with deuterium. It is this sensitivity to hydrogen (and insensitivity to many other materials) that is exploited in neutron imaging studies of water transport in operating fuel cells.

APPROACH

The typical length scales of interest in a fuel cell are: channels approximately 1-mm wide and 1-mm deep, the diffusion media (DM) is 0.1-mm to 0.3-mm thick, the membrane is 0.01-mm to 0.02-mm thick, and the active area of test sections can range from 2 cm^2 to 500 cm^2. Though the study of water transport within these length scales are technically very challenging, the unique capabilities of neutron imaging have already successfully addressed many questions. However, as fuel cell research matures, the water transport questions become increasingly more demanding, requiring for instance resolving the water content in catalyst layers. To meet these demands, based on fuel cell community feedback and need, we continue to develop new facilities and improve existing capabilities for obtaining higher spatial and temporal resolution neutron images. These improvements will enable users to perform even more detailed, nondestructive, and in situ studies of the water and hydrogen transport in fuel cells to meet DOE goals. In addition, employing mathematical models of neutron scattering, we will develop a software suite that enables users to obtain reliable, accurate, quantitative measurements of the water content in an operating fuel cell. Due to the complexity of fuel cells and the large number of remaining open questions regarding water transport, we will develop partnerships with industry, academia, and national laboratories to train them in the use of the facility, seek their feedback, and collaborate with them on research projects, to seek measurement breakthroughs that will facilitate the rapid, efficient, and robust development of fuel cells.

RESULTS

The NIST Neutron Imaging Facility provides year-to-year support for the DOE Hydrogen and Fuel Cell Program projects through beam time and by collaboration with users on a variety of related neutron imaging projects that support the DOE mission. For FY 2015 General Motors (GM), Nissan, Los Alamos National Laboratory (LANL), University of Connecticut, University of California, Merced, Commissariat à l'énergie atomique et aux énergies alternatives (CEA), and University of Tennessee, Knoxville have received project support for experiments at the facility accounting for more than 70 days of beam time. Published results during FY 2015 from these experiments are reflected in the publication list attached to this report.

NIST now provides full support to full sized commercial and automotive grade fuel cell testing at the facility with a large scale fuel cell test stand. This stand was developed through the NIST partnership with GM. The facility technical staff has received extensive onsite training on calibration, operation and validation testing from our testing partners at GM. This test stand is capable of operating fuel cells and small stacks at 800 W, 6–1,000 A at 0.2 V, 0–50 V, hydrogen: 0.065–11.31 SLPM, air: 0.239–26.92 SLPM. The first user experiments employing the test stand were conducted in March, 2015 by researchers from CEA. CEA studied the water content and coolant distribution in a five cell stack.

The University of Tennessee in collaboration with GM have performed an extensive study of how changes to flow channels and diffusion media properties effect thermal transport of water through the cell [1]. One example from this study showed how reducing the number of serpentine flow channels on the anode bipolar plate in order to increase anode flow rates to better facilitate water transport out of the anode could result in more retained water instead of less (see Figure 1). The reason for the anode water content increasing is the fact that decreasing the number of serpentine flows increases the land surface area and thereby increases the thermal transport of heat away from the anode (see Figure 2). This can then result in an increase in the liquid water content on the anode. The study further showed that as the diffusion media saturates the thermal conductivity increases overall and results in a mitigation of the thermally driven transport. Using the diffusion media water saturation profile measured with neutron imaging the study was able to determine that the temperature driven effects are strongest at the inlets (see Figure 3) where the diffusion media is driest and becomes less pronounced near the outlets where the water saturation is the highest due to the flow of product water and humidified water out of the cell.

Normally groups come to NIST with their fuel cells and MEAs and perform testing in person at the facility. This can in some cases be difficult to schedule as travel is

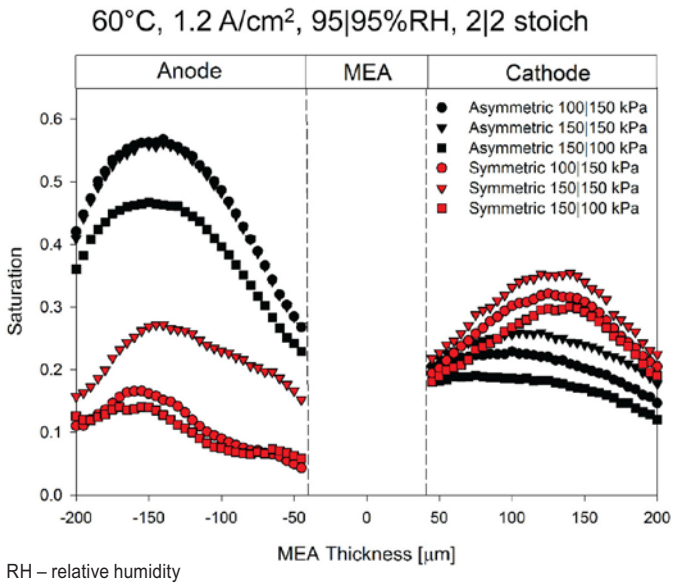

RH – relative humidity

FIGURE 1. Water saturation data measured with neutrons for both symmetric and asymmetric flow field design. More water is retained in the asymmetric design even though the flow velocity is increased.

costly and user schedules must be commensurate with the facility schedule. NIST has been working with LANL to develop a protocol to facilitate users sending MEAs that can be run using standardized fuel cell hardware based on the LANL small scale cell design. This would allow users to reduce travel costs and have more timely results. To test the feasibility of this new capability LANL sent NIST three MEAs with non-precious metal cathode catalysts, each with a different catalyst thicknesses in an effort to determine if flooding of the catalyst support played a significant role in the reduced performance of the MEAs relative to MEAs made purely from platinum catalysts. The neutron imaging results from running the MEAs in the standard small scale hardware were consistent with flooding forming a significant contribution to performance loss. However, due to the lack of in situ impedance testing during the imaging it was not possible to cross validate catalyst flooding with impedance measurements. To address this issue at the facility our testing partners at GM have identified an impedance measurement apparatus that is fully supported by the existing stand software that would allow in situ impedance measurements

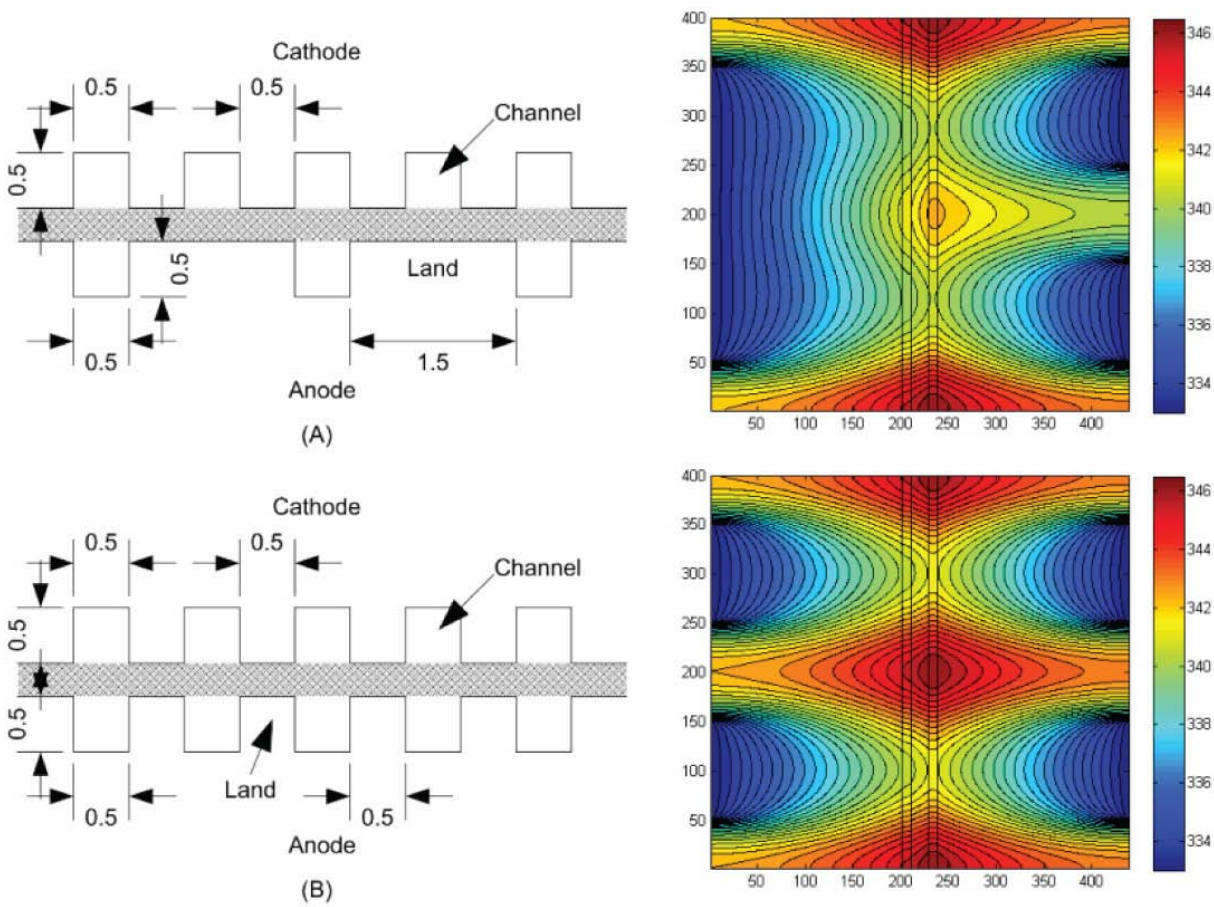

FIGURE 2. Asymmetric flow channels shown in (A) increase contact area on the anode thereby raising the thermal conductivity and decreasing the anode temperature demonstrated by the COMSOL generated temperature model shown on right. In (B) a symmetric flow field design is symmetric in temperature. The net effect if reducing the flow fields in (A) to increase flow rate and reduce water saturation is nullified by the increase in thermal conductivity. In fact the opposite of the desire effect occurs as water saturation increases.

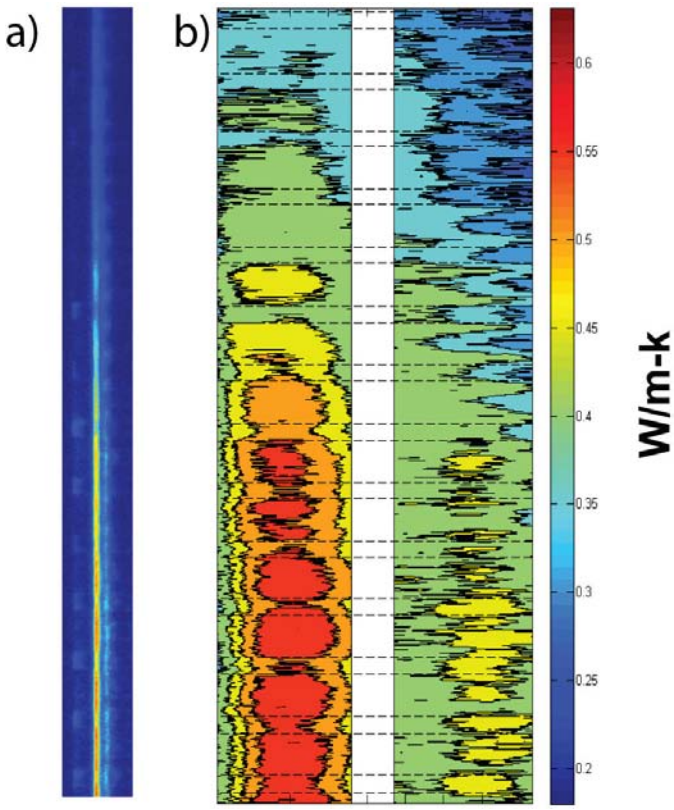

FIGURE 3. Water saturation of the diffusion media increases thermal conductivity and will serve to balance the temperature profile in the cell. The water saturation in a cell measured with neutrons is shown in a) and the calculated thermal conductance based on the measured water saturation profile is shown in b). Here neutrons allow one to directly determine the spatially distributed contributions to temperature driven water transport effects.

at the facility. An impedance measurement apparatus that is fully integrated with the fuel cell test stands at the facility, will be purchased and made available to facility users during FY 2016.

The facility has added a new X-ray modality to the facility capabilities with an X-ray microfocus tube oriented 90 degrees to the neutron beam. This allows one to concurrently image with neutrons and X-rays. This new X-ray imaging capability has spatial resolution approaching 10 µm.

Understanding flooding and degradation issues due to liquid water in the catalyst layers is a critical step towards improving durability and cycling of fuel cells. To study commercial grade platinum based catalysts requires at least a factor of 10 improvement in spatial resolution over current state-of-the-art (about 15 µm). The limiting factor in spatial resolution for current detector systems stems from the range of charged particles (3.5–150 µm) that are used to detect neutrons. To overcome this limit we are exploring several methods. The first method uses nanofabricated neutron absorbing gratings with an opening of ~2 µm or less in width to define the neutron illuminated area of the fuel cell with high spatial resolution in one dimension. By translating the grating across the through-plane direction of the fuel cell, one obtains a high resolution image of the water content from anode to cathode, overcoming the resolution limit of the detector. New gratings with thicker deposits of GadOx particles were obtained, and an image intensifier was purchased, but delivery has been delayed as the vendor addresses problems with the device to meet specifications. It is anticipated that users will have access to this new method by the end of calendar year 2015.

The data from the high resolution fuel cell images show that improvements to the signal to noise ratio are necessary to improve the quality of the data. This can be achieved with longer integration times or more efficient detectors. Longer integration times will limit the number of fuel cell operating conditions that can be measured. Therefore emphasis has been placed on improving the detector efficiency in order to improve the signal quality. Gadox scintillators have similar spatial resolution and four times the stopping power of the microchannel plates currently used for high resolution imaging. However, Gadox produces little light for each stopped neutron and has not been used due to small signal to noise ratios. Modern image intensifiers have been developed that enable high image resolution with stable long-term performance and initial tests showed that an intensifier improved the signal to noise ratio by over a factor of 30. A new detector system based on an intensifier has been designed, and an image intensifier is being procured for fuel cell users. This new system is expected to be available at the facility by January 2015 and is expected to increase the time resolution for high resolution neutron imaging by a factor of four due to the increased neutron detection efficiency. In addition, by magnifying the GadOx scintillation light and taking images at high frame rate, the intensifier may make it possible to obtain higher resolution by calculating the centroid of the emitted light.

By using a neutron lens, it could be possible to increase the neutron intensity by 50 to 100 times than currently available. Previously, practical lenses for neutrons have not been available due to the low neutron refractive power of all materials. However, a new X-ray telescope lens technology using thin nickel foil mirrors developed by the National Aeronautics and Space Administration has shown great promise to provide a practical lens for neutron imaging. By nesting several mirrors, the flux can be increased up to a factor of 100 over BT2. An engineering demonstration lens with 20 µm spatial resolution is expected at the end of calendar year 2016. If successful, a complete optic with 10 nested shells will be produced in 2017 for 20 µm resolution imaging, and in 2018 a magnifying optic to reach ~1 µm resolution. Such "Wolter optics" will be installed at the new cold neutron imaging instrument. This new imaging instrument is being completed in August 2015 and will begin commissioning measurements in September 2015. The new

instrument will also serve as a test bed for new high spatial resolution detector systems and methods and with the lower energy neutron spectrum enable discrimination of ice and water in the fuel cell during freeze operation.

CONCLUSIONS AND FUTURE DIRECTIONS

- NIST Neutron Imaging Facility continues to maintain a robust fuel cell user program with:
  - Eight publications and 10 presentations in FY 2015.
  - Over 50 days of dedicated fuel cell beam time.
- Fuel cell infrastructure supports automotive-scale testing.
  - NIST staff were trained at General Motors to support calibration and use of the test stand.
  - The first user tests were performed by CEA.
- An MEA mail-in program is currently being developed.
  - The program makes use of the standard high resolution fuel cell that is available to users.
  - The first tests with MEAs provided by LANL show it could be a valuable new capability.
  - The program will be fully optimized by new fuel cell test stand supported in situ impedance testing capability.
- With the goal to study catalysts, NIST continues to improve the image spatial resolution. New avenues toward resolving the MEA water content include:
  - Employing a grating method to achieve resolution approaching 1 µm with 12 hour acquisition time (end of 2015).
  - Developing a magnifying neutron lens to reach 1 µm with 20 min acquisition time (2018).
- NIST will improve fuel cell high resolution image time.
  - Time resolution for through-plane water content measurements improved by a factor of four with 20 µm scintillator detector.
  - Future neutron lens will increase time resolution by 50x to achieve image times of 10 s with 10 µm resolution.
- Additional general improvements will be pursued.
  - A second new cold neutron imaging facility will begin operation by Fall of 2015.
  - Improvements to achieve 1 µm imaging will be continued.
    - Develop neutron lens.
    - Improve grating method.

FY 2015 PUBLICATIONS/PRESENTATIONS

1. Rupak Banerjee, Satish G. Kandlikar, "Liquid water quantification in the cathode side gas channels of a proton exchange membrane fuel cell through two-phase flow visualization," Journal of Power Sources, **247**, (2014), Pages 9–19.

2. Jon P. Owejan, Thomas A. Trabold, and Matthew M. Mench, "Oxygen transport resistance correlated to liquid water saturation in the gas diffusion layer of PEM fuel cells," International Journal of Heat and Mass Transfer, **71**, (2014), Pages 585–592.

3. Adam Z. Weber, et al., "A Critical Review of Modeling Transport Phenomena in Polymer-Electrolyte Fuel Cells," Journal of the Electrochemical Society, **161** (12), (2014), Pages F1254–F1299.

4. Jacob M. LaManna, Subhadeep Chakraborty, Jeffrey J. Gagliardo, Matthew M. Mench, "Isolation of transport mechanisms in PEFCs using high resolution neutron imaging," International Journal of Hydrogen Energy, **39**, (2014), Pages 3387–3396.

5. Toshikazu Kotaka, Yuichiro Tabuchi, Ugur Pasaogullari, Chao-Yang Wang, "Impact of Interfacial Water Transport in PEMFCs on Cell Performance," Electrochimica Acta, **146**, (2014), Pages 618–629.

6. Toshikazu Kotaka, Yuichiro Tabuchi, Ugur Pasaogullari, Chao-Yang Wang, "Investigation of Interfacial Water Transport at the Gas Diffusion Media by Neutron Radiography," ECS Transactions, **64**, (2014), Pages 839–851.

7. Thiago Lopes, Jose-Maria Sansiñena, Rangachary Mukundan, Daniel S. Hussey, David L. Jacobson, Fernando H. Garzon, "Diagnosing the Effects of Ammonia Exposure on PEFC Cathodes," Journal of The Electrochemical Society, **161**, (2014) Pages F703–F709.

8. Bradley M. Wood, Kyungmin Ham, Daniel S. Hussey, David L. Jacobson, Adel Faridani, Anders Kaestner, John J. Vajo, Ping Liu, Tabbetha A Dobbins, Leslie G Butler, "Real-time observation of hydrogen absorption by $LaNi_5$ with quasi-dynamic neutron tomography," NIM-A, **324**, (2014), Pages 95–101.

9. D.J. Fenton, J.J. Gagliardo, and T.A. Trabold, "Analysis of Water Morphology in the Active Area and Channel-to-Manifold Transitions of a PEM Fuel Cell," ASME 2014 12th International Conference on Fuel Cell Science, Engineering and Technology, Boston, Massachusetts, USA, June 30–July 2, 2014.

10. J.M LaManna, M.M. Mench, "Comparison of Water Transport Mechanisms Between Commercial and Experimental Virgin and Aged Diffusion Media Using High Resolution Neutron Radiography," The Electrochemical Society Meeting Abstracts, Issue 14 (2014), Pages 646–646.

11. R. Mukundan, R.L Borup, D. Spernjak, G. Wu, A. Steinbach, P. Zelenay, D. Hussey, D. Jacobson, "Neutron Imaging to Optimize PEM Fuel Cell Performance," World Conference on Neutron Radiography, Grindelwald, Switzerland, October 2014.

12. R. Mukundan, D. Spernjak, G. Wu, D.S. Hussey, D.L. Jacobson, A.J. Steinbach, R.L. Borup, P. Zelenay, "Visualizing water in non-precious metal catalyst-based polymer electrolyte fuel cells using neutron imaging," Abstracts of Papers of the American Chemical Society, **248**, August 2014.

13. M. Arif, D.S. Hussey, E. Baltic, and D.L. Jacobson, "Recent Developments at the NIST Neutron Imaging Facility," World Conference on Neutron Radiography, Grindelwald, Switzerland, October 2014.

14. D.S. Hussey, C. Brocker, D.L. Jacobson, E. Baltic, and M. Arif, "A New Cold Neutron Imaging Instrument at NIST," World Conference on Neutron Radiography, Grindelwald, Switzerland, October 2014.

15. D.S. Hussey, D.L. Jacobson, D. Liu, B. Khaykovich, M. Gubarev, M. Arif, "Design of Neutron Microscope Objectives," World Conference on Neutron Radiography, Grindelwald, Switzerland, October 2014.

16. J.M. LaManna, D.S. Hussey, D.L. Jacobson, and M.M. Mench, "Role of Land Drainage on Water Storage in Polymer Electrolyte Fuel Cells Using High Resolution Neutron Imaging," World Conference on Neutron Radiography, Grindelwald, Switzerland, October 2014.

17. Md. A. Uddin, T. Kotaka, U. Pasaogullari, Y. Tabuchi, D.S. Hussey, D.L. Jacobson, "High Resolution Neutron Radiography of the Behavior of Liquid Water at the Interfaces in Polymer Electrolyte Fuel Cells," World Conference on Neutron Radiography, Grindelwald, Switzerland, October 2014.

18. P. Saggu, D.L. Jacobson, D.S. Hussey, D. Pushin, E. Baltic, and M. Arif, "Using Micro-Channel Plates to Achieve Both High Spatial and Temporal Resolution in Neutron Radiography," World Conference on Neutron Radiography, Grindelwald, Switzerland, October 2014.

REFERENCES

1. LaManna, Jacob Michael, "The Role of Channel-Land Architecture, Diffusion Media Transport Properties, and Aging Effects on Water Transport and Storage in Polymer Electrolyte Fuel Cells." PhD diss., University of Tennessee, 2014. (http://trace.tennessee.edu/utk_graddiss/3145).

V.F.6 Stationary and Emerging Market Fuel Cell System Cost Analysis—Primary Power and Combined Heat and Power Applications

Vince Contini (Primary Contact), Fritz Eubanks, Mike Jansen, Paul George, and Mahan Mansouri
Battelle
505 King Avenue
Columbus, OH 43201
Phone: (614) 424-7249
Email: continiv@battelle.org

DOE Manager
Donna Ho
Phone: (202) 586-8000
Email: Donna.Ho@ee.doe.gov

Contract Number: DE-EE0005250/001

Project Start Date: September 30, 2011
Project End Date: September 30, 2016

Overall Objectives

The objective of this project is to assist DOE in developing fuel cell systems for stationary and emerging markets by developing independent cost models for manufacture and ownership.

- Identify the fundamental drivers of system cost and the sensitivity of the cost to system parameters
- Help DOE prioritize investments in research and development of components (e.g., metal bipolar plates versus composite graphite plates in polymer electrolyte membrane [PEM] fuel cells for low volume markets) to reduce the costs of fuel cell systems while considering systems optimization
- Identify manufacturing processes that must be developed to commercialize fuel cells
- Provide insights into the optimization needed for use of off-the-shelf components in fuel cell systems

Fiscal Year (FY) 2015 Objectives

- Finalize cost estimates of 1 kW, 5 kW, 10 kW, and 25 kW PEM and solid oxide fuel cell (SOFC) [1] systems for primary power and combined heat and power (CHP) applications at annual production volumes of 100, 1,000, 10,000 and 50,000 units
- Initiate cost estimates of 100 kW and 250 kW PEM and SOFC systems for primary power and CHP applications at annual production volumes of 100, 1,000, 10,000, and 50,000 units
- Initiate cost estimates of 5 kW PEM fuel cell systems for backup power applications at annual production volumes of 100, 1,000 and 10,000 units

Technical Barriers

This project addresses the following technical barrier from the Fuel Cells section of the Fuel Cell Technologies Office Multi-Year Research, Development, and Demonstration Plan:

(B) Cost

Technical Targets

To widely deploy fuel cells, significant strides must be made in lowering the cost of components and overall systems without compromising reliability and durability. This cost analysis will:

- Identify the fundamental drivers of component and system cost and the sensitivity of the cost to various component and system parameters.
- Provide DOE information on the impact of production volumes on lowering costs of fuel cells and the types of high volume manufacturing processes that must be developed to enable the widespread commercialization.
- Provide insights into the optimization needed for use of off-the-shelf components in fuel cell systems to drive down system costs.
- Analyze the lifecycle costs of owning and operating a fuel cell to estimate primary cost drivers for the end user in applicable markets.

FY 2015 Accomplishments

- Completed manufacturing cost analysis of 1 kW, 5 kW, 10 kW, and 25 kW PEM and SOFC fuel cell systems for primary power and CHP applications
- Completed detailed performance specifications, system requirements, and preliminary system design of 100 kW and 250 kW PEM and SOFC systems for primary power and CHP applications
- Completed detailed performance specifications, system requirements, and preliminary system design of 5 kW PEM fuel cell systems for backup power applications

✧ ✧ ✧ ✧ ✧

INTRODUCTION

Fuel cell power systems may be beneficially used to offset all or a portion of grid-purchased electrical power and supplement on-site heating requirements. For this application, the fuel of choice will usually be pipeline natural gas or on-site propane storage. These fuel sources generally have much higher reliability than utility electric power, being less subject to damage-related outages, and can therefore provide for some continued operation in the event of grid outage—performing both primary power and back-up power functions. Battelle evaluated low temperature polymer electrolyte membrane (LTPEM) and solid oxide fuel cell (SOFC) systems for use as a continuous power supplement (primary power) and to provide auxiliary heating in combined heat and power (CHP) configurations. The power levels considered were 1 kW, 5 kW, 10 kW, and 25 kW. A primary-power/CHP commercial market has not yet developed in this size range; however, our analysis suggests an attractive business opportunity under the right conditions.

APPROACH

Battelle will apply the established methodology used successfully in previous fuel cell cost analysis studies performed for DOE [1–3]. This technical approach consists of four steps, market assessment, system design, cost modeling, and sensitivity analysis (Figure 1). The first step characterizes the potential market and defines the requirements for system design. The second step involves developing a viable system design and the associated manufacturing process vetted by industry. The third step involves building the cost models and gathering inputs to estimate manufacturing costs. Manufacturing costs will be derived using the Boothroyd-Dewhurst Design for Manufacture Assembly (DFMA®) software. Custom manufacturing process models will be defined where necessary and parametrically modeled based on knowledge of the machine, energy and labor requirements for individual steps that comprise the custom process. The fourth step will evaluate the sensitivity of stack and system costs to various design parameters. In addition to the sensitivity analysis, we will conduct a lifecycle cost analysis to estimate total cost of ownership for the target application and markets.

RESULTS

Overall the final cost was analyzed in four distinct categories, the capital cost of manufacturing equipment, the direct cost of material and assembly of the stack, the expense of balance of plant (BOP) hardware, and the final cost of complete system assembly and testing it. BOP was further broken out into two subsets including CHP hardware and fuel cell system BOP hardware.

A sales markup of 50% was integrated at the end and is called out separately in Tables 1–4. At high production volumes, the final ticket prices are estimated to be $4,359/kW and $2,309/kW, respectively, for 5 kW and 25 kW CHP PEM fuel cell systems and $3,615/kW and $1,907/kW for the 5 kW and 25 kW CHP SOFC systems. This work provides a detailed cost breakdown that helps identify key cost drivers and offers insight at various value propositions through the lifecycle cost analyses.

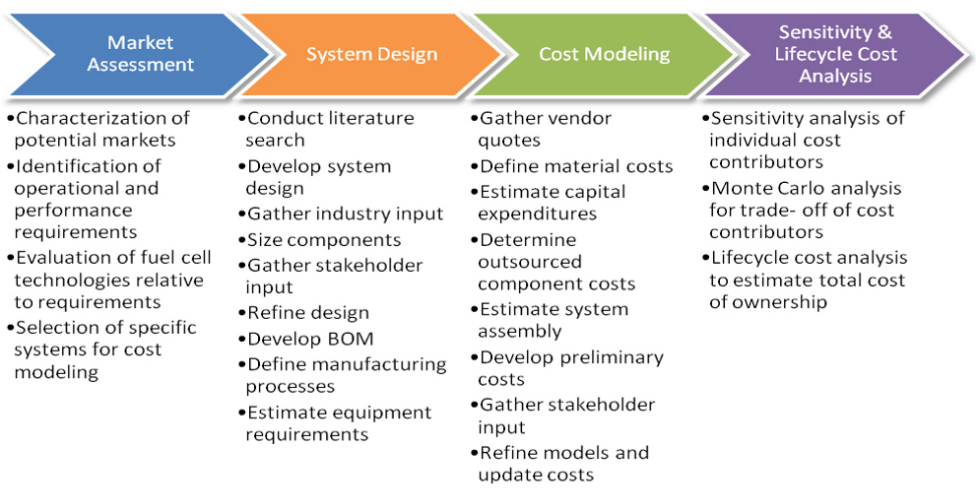

BOM – bill of materials

FIGURE 1. Battelle's cost analysis methodology

TABLE 1. 5 kW CHP PEM Fuel Cell System Cost Summary

Description	100 Units	1,000 Units	10,000 Units	50,000 Units
Total stack manufacturing cost, with scrap	$32,200	$12,967	$7,329	$5,779
Stack manufacturing capital cost	$481	$76	$54	$48
CHP Hardware	$22,325	$18,705	$17,279	$16,298
FC BOP Hardware	$26,658	$20,780	$17,520	$16,097
System assembly, test, and conditioning	$2,777	$452	$283	$257
Total system cost, pre-markup	$84,442	$52,980	$42,465	$38,480
System cost per net kW, pre-markup	$3,378	$2,119	$1,699	$1,539
Sales markup	50.00%	50.00%	50.00%	50.00%
Total system cost, with markup	$126,663	$79,471	$63,697	$57,721
System cost per net kW, with markup	$5,067	$3,179	$2,548	$2,309

TABLE 2. 25 kW CHP PEM Fuel Cell System Cost Summary

Description	100 Units	1,000 Units	10,000 Units	50,000 Units
Total stack manufacturing cost, with scrap	$6,333	$3,923	$2,446	$2,137
Stack manufacturing capital cost	$295	$47	$65	$56
CHP Hardware	$5,112	$4,456	$4,054	$3,838
FC BOP Hardware	$9,311	$7,093	$6,150	$5,856
System assembly, test, and conditioning	$1,946	$316	$178	$162
Total system cost, pre-markup	$22,998	$15,834	$12,893	$12,050
System cost per net kW, pre-markup	$4,600	$3,167	$2,579	$2,410
Sales markup	50.00%	50.00%	50.00%	50.00%
Total system cost, with markup	$34,497	$23,751	$19,339	$18,075
System cost per net kW, with markup	$6,899	$4,750	$3,868	$3,615

TABLE 3. 5 kW CHP SOFC System Cost Summary

Description	100 Units	1,000 Units	10,000 Units	50,000 Units
Total stack manufacturing cost, with scrap	$16,978	$5,847	$2,835	$2,039
Stack manufacturing capital cost	$481	$62	$24	$24
CHP Hardware	$4,915	$4,293	$3,934	$3,719
FC BOP Hardware	$14,231	$11,042	$9,268	$8,497
System assembly, test, and conditioning	$2,737	$433	$274	$252
Total system cost, pre-markup	$39,343	$21,677	$16,335	$14,531
System cost per net kW, pre-markup	$7,869	$4,335	$3,267	$2,906
Sales markup	50.00%	50.00%	50.00%	50.00%
Total system cost, with markup	$59,014	$32,515	$24,503	$21,796
System cost per net kW, with markup	$11,803	$6,503	$4,901	$4,359

FC – fuel cell

TABLE 4. 25 kW CHP SOFC System Cost Summary

Description	100 Units	1,000 Units	10,000 Units	50,000 Units
Total stack manufacturing cost, with scrap	$16,075	$9,600	$6,637	$5,930
Stack manufacturing capital cost	$295	$245	$177	$164
CHP Hardware	$23,134	$19,433	$17,939	$16,939
FC BOP Hardware	$14,426	$10,508	$9,097	$8,546
System assembly, test, and conditioning	$2,211	$442	$238	$198
Total system cost, pre-markup	$56,142	$40,228	$34,087	$31,778
System cost per net kW, pre-markup	$2,246	$1,609	$1,363	$1,271
Sales markup	50.00%	50.00%	50.00%	50.00%
Total system cost, with markup	$84,214	$60,342	$51,131	$47,666
System cost per net kW, with markup	$3,369	$2,414	$2,045	$1,907

CONCLUSIONS AND FUTURE DIRECTIONS

The following lists some of the conclusions drawn from this analysis.

- Electronics and power conversion dominate system cost, particularly as system size increases.
- An attractive value proposition exists under specific utility rate conditions.
- Manufacturing readiness level (MRL) for many BOP components indicates they are not ready for mass production—significant cost driver.
- DFMA® performed on specific components (fuel processing, stack) assumes the technology has an MRL greater than 9.

By the end of FY 2015 Battelle will have completed full cost assessments of 100 kW and 250 kW PEM and SOFC systems for primary power and CHP applications. During FY 2015/2016 Battelle will complete a full cost assessment of 5 kW PEM fuel cell systems for backup power applications.

FY 2015 PUBLICATIONS/PRESENTATIONS

1. V. Contini, F. Eubanks, M. Jansen, P. George, and Mahan Mansouri. June 2015. "Stationary and Emerging Market Fuel Cell System Cost Analysis – Primary Power and Combined Heat and Power Applications." DOE Annual Peer Review. Washington, D.C.

REFERENCES

1. Battelle. 2011. "The High Volume Manufacture Cost Analysis of 5 kW Direct Hydrogen Polymer Electrolyte Membrane (PEM) Fuel Cell for Backup Power Applications." Contract No. DE-FC36GO13110.

2. K. Mahadevan, K. Judd, H. Stone, J. Zewatsky, A. Thomas, H. Mahy, and D. Paul. 2007. "Identification and characterization of near-term direct hydrogen proton exchange membrane fuel cell markets." Contract No. DE-FC36GO13110.

3. H. Stone, K. Mahadevan, K. Judd, H. Stein, V. Contini, J. Myers, J. Sanford, J. Amaya, J. Upton, and D. Paul, 2006. "Economics of Stationary Proton Exchange Membrane Fuel Cells." Contract No. DE-FC36-03GO13110.

V.F.7 A Total Cost of Ownership Model for Design and Manufacturing Optimization of Fuel Cells in Stationary and Emerging Market Applications

Max Wei (Primary Contact), Thomas McKone
Lawrence Berkeley National Laboratory (LBNL)
1 Cyclotron Road, MS 90R-4000
Berkeley, CA 94706
Phone: (510) 486-5220
Email: mwei@lbl.gov

DOE Manager
Donna Ho
Phone: (202) 586-8000
Email: Donna.Ho@ee.doe.gov

Subcontractors
- University of California, Berkeley, CA
- Strategic Analysis, Arlington, VA

Project Start Date: October 1, 2011
Project End Date: September 30, 2016

Overall Objectives

- Develop total cost of ownership (TCO) modeling tool for the design and manufacture of fuel cell systems in emerging markets (e.g., combined heat and power [CHP] and back-up power systems) for low temperature (LT) polymer electrolyte membrane (PEM), high temperature (HT) PEM, and solid oxide fuel cell (SOFC) technologies
- Expand cost modeling framework to include life cycle analysis and possible ancillary financial benefits, including carbon credits, health/environmental externalities, end of life recycling, and reduced costs for building operation
- Perform sensitivity analysis to key cost assumptions, externality valuation, and policy incentive structures

Fiscal Year (FY) 2015 Objectives

- Complete TCO model for HT PEM systems in CHP applications
- Define system design, balance of plant (BOP), bill of materials, and manufacturing process flows for SOFC stationary power and CHP systems
- Develop direct manufacturing cost model for SOFCs in CHP and stationary power applications
- Perform policy and energy system scenario analyses for LT PEM total cost models for CHP and backup power systems

Technical Barriers

This project addresses the following technical barriers from the Fuel Cell Technologies Office Multi-Year Research, Development, and Demonstration Plan:

Fuel Cells (Section 3.4)

(B) Cost: Expansion of the cost envelope to total cost of ownership including full life cycle costs and externalities

Manufacturing R&D (Section 3.5)

(A) Lack of High-Volume Membrane Electrode Assembly Processes

(B) Lack of High-Speed Bipolar Plate Manufacturing Processes

Technical Targets

This project is conducting cost of ownership studies of LT PEM, HT PEM, and SOFC fuel cell systems in nonautomotive applications. Insights gained from these studies can be applied toward the development of lower cost, higher volume manufacturing processes that can meet the following DOE CHP system equipment cost targets (Table 1).

- LT PEM: For reference, the LT PEM cost from earlier work is shown.
- HT PEM: At the annual production volumes shown, HT PEM CHP system costs are estimated to be 15–25% higher than LT PEM systems. Although the 100 kW cost of $2,235/kW at 1,000 units per year meets the 2015 DOE cost target, the automated stack production processes and assumed high yields are more realistic in the 2020 timeframe.
- SOFC: The SOFC CHP system direct equipment manufacturing cost and equipment cost with a 50% markup in price is shown above. At the annual production volumes shown, the SOFC cost per unit kilowatt is estimated to be about 35% lower than for LT PEM systems.
- Although the 10 kW SOFC system cost of $1,655/kW at 50,000 units per year meets the 2015 DOE target, the automated stack production processes and assumed high yields are more realistic in the 2020 timeframe.
- The 10 kW SOFC CHP system meets the 2020 DOE equipment cost at an annual production volume of 50,000 units per year. The 100 kW CHP system exceeds the 2020 DOE target by 14%.

TABLE 1. DOE Cost Targets vs. Modeled Costs in this Work

System	Units/yr	2015 DOE Equipment Cost Target with Markup	2020 DOE Equipment Cost Target with Markup	LT PEM Equipment Cost with 50% Markup	HT PEM Equipment Cost with 50% Markup	SOFC Direct Equipment Cost with 50% Markup
10 kW CHP System	50,000	$1,900/kW	$1,700/kW	$2,585/kW	$2,925/kW	$1,655/kW
100 kW CHP System	1000	$2,300/kW	$1,000/kW	$1,800/kW	$2,235/kW	$1,140/kW

FY 2015 Accomplishments

- Completed TCO model for HT PEM CHP applications
- Completed BOP, bill of materials, and manufacturing process flows definition for SOFC stationary power and CHP systems
- Completed manufacturing cost model for SOFC power and CHP systems

✧ ✧ ✧ ✧ ✧

INTRODUCTION

Over the last decade, DOE has supported several cost analysis studies for fuel cell systems for both automotive [1,2] and nonautomotive systems [3,4]. These studies have primarily focused on the manufacturing costs associated with fuel cell system production. This project expands the scope and modeling capability from existing direct manufacturing cost modeling in order to quantify more fully the benefits of fuel cell systems by taking into account life cycle assessment, air pollutant impacts, and policy incentives. TCO modeling becomes important in a carbon-constrained economy and in a context where health and environmental impacts are increasingly valued. TCO is also critical as an input to industry and government decisions on funding research, development, and deployment as well as an input to organizations and individuals who make long term investment decisions.

The three components of the TCO model are (1) direct manufacturing costs, (2) life cycle or use phase costs such as cost of operations and fuel, and (3) life cycle impact assessment costs such as health and environmental impacts. FY 2015 has been focused on the development of a direct manufacturing cost model for SOFC systems for application in CHP and stationary power and the completion of a TCO cost model for HT PEM CHP applications.

APPROACH

Data for system designs and component costs are derived from (1) existing cost studies where applicable, (2) literature and patent sources, and (3) industry and national laboratory advisors. Stack components that can be made with high-speed roll-to-roll processes, like gas diffusion layer/gas diffusion electrode/catalyst-coated membrane components, and components like BOP components that are largely purchased, are assumed to be part of a vertically integrated manufacturing process. Life cycle or use phase costing utilizes existing LBNL tools [5], a National Renewable Energy Laboratory (NREL) database of commercial building electricity and heating demand profiles by building type and geographical region [6], and earlier CHP modeling work by one of the authors [7].

Life cycle impact assessment is focused on use-phase impacts from energy use, carbon emissions and pollutant emissions [9], and especially on particulate matter (PM) emissions since PM is the dominant contributor to life cycle impacts [10]. Health impact data from PM is disaggregated by geographical region using existing LBNL health impact models [11] and estimates of the amount of displaced grid based electricity and heating fuel that a fuel cell CHP system in that building type and geographical region would provide.

RESULTS

Direct cost model results for PEM CHP systems are shown in Figures 1 and 2. Full details can be found in LT PEM and HT PEM LBNL reports by Wei et al. [12]. Higher stack costs are found for HT PEM systems because of lower power density, larger plate size, higher Pt loading, and different stack design. Somewhat lower BOP/fuel processer costs are found for HT PEM due to a simpler balance of system design that contributes to a lower fraction of system costs. Overall HT PEM system costs are 10–15% higher at low annual production volumes than LT PTEM, and up to 30% higher cost at 100 kW and high volume. For LT PEM systems, nonstack costs dominate the overall system costs. The conclusion that nonstack costs dominate CHP system costs has further been corroborated by industry inputs from both LT PEM and SOFC system vendors.

The TCO model includes New York, Chicago, Minneapolis, Phoenix, Houston, and San Diego settings with various commercial buildings. Fuel cell CHP is found to be most favorable in regions with higher carbon intensity electricity (Chicago and Minneapolis). Figure 2 shows a small hotel in Chicago with a 10 kW HT PEM system that offsets both water heating and space heating costs. An installed cost of $4,400/kW corresponds to an annual production volume of 100 MW (or 10 kW x 10,000 units per year on Figure 1), coupled with a total corporate markup of

(general and administrative, sales and marketing, insurance and fees, and installation) of 100% applied to the direct cost in Figure 1. The total cost of fuel cell provided electricity is seen to drop from 18.8 ¢/kWh to 7.8 ¢/kWh after including heating fuel savings, carbon credits valued at the social cost of carbon ($44/ton of carbon dioxide), and health and environmental savings. This TCO cost of electricity is below the average cost of commercial electricity in Illinois.

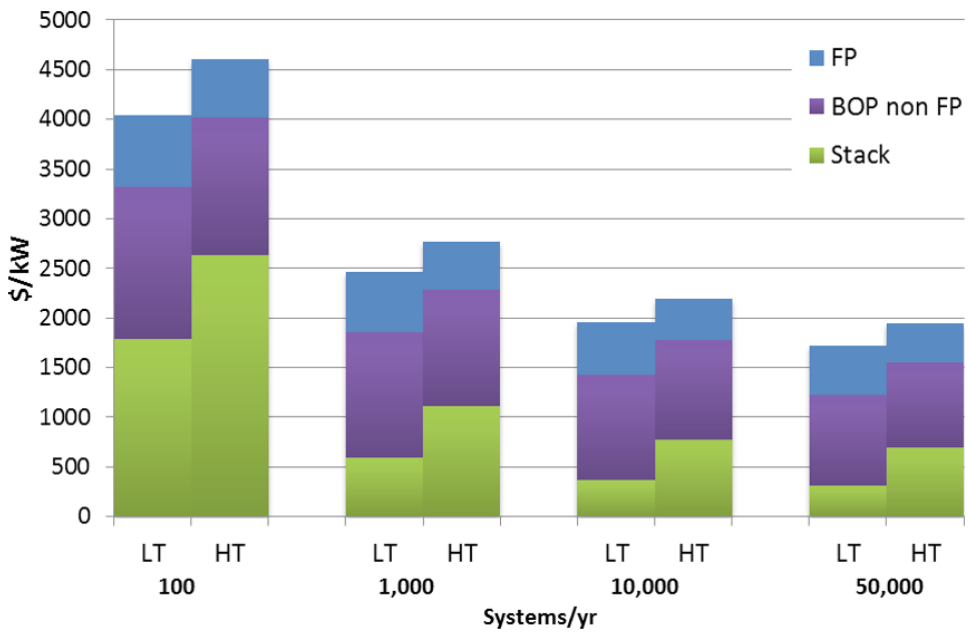

FIGURE 1. Direct cost per kW of 10 kW LT PEM and HT PEM CHP systems vs. annual manufacturing volume (FP = fuel processor; BOP non FP = balance of plant not including FP)

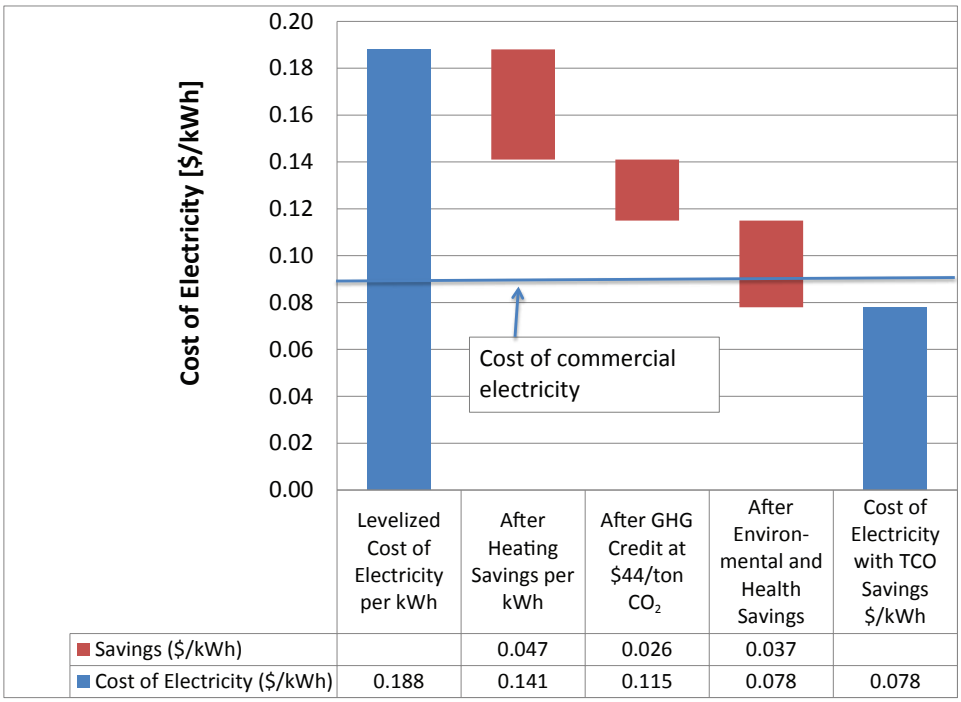

FIGURE 2. Total cost of electricity with 10 kW HT PEM system in a small hotel in Chicago with water heating and space heating offset by the fuel cell system and an installed cost of $4,400/kW (GHG = greenhouse gas)

Figure 3 shows a plot of direct manufacturing costs as a function of annual production volume for a 10 kW SOFC CHP system. The cost drops from $2,677/kW at low volume to $1,103/kW at high volume (50,000 units per year), driven largely by capital cost reduction at high volume as the capital cost is amortized over a greater number of units. At low volume, 39% of the system cost is from the stack, but this contribution drops to 16% of overall cost at high volume as the stack costs drop more rapidly with increasing production volume than do the costs of non-stack BOP and fuel processing equipment.

Figure 4a shows the stack components are dominated by the electrode-electrolyte-electrode assembly as production volumes increase. Interconnects are a larger fraction at low volumes due to high initial tooling costs. Figure 4b shows 10 kW CHP nonstack component costs for the 10 kW CHP system at 10,000 units/year. The fuel processing, heat management, and power conditioning subsystems make up 70% of nonstack component costs. As system sizes increase, power conditioning equipment makes up the largest portion of BOP costs.

CONCLUSIONS AND FUTURE DIRECTIONS

- Direct costs for SOFC CHP 10 kW systems are found to be $3,240/kW at annual production volumes of 100 systems per year and $1,170/kW at 50,000 systems per year (Figure 3).
- For 100 kW CHP systems with reformate, the 2015 DOE cost target at 1,000 units per year can be met with LT

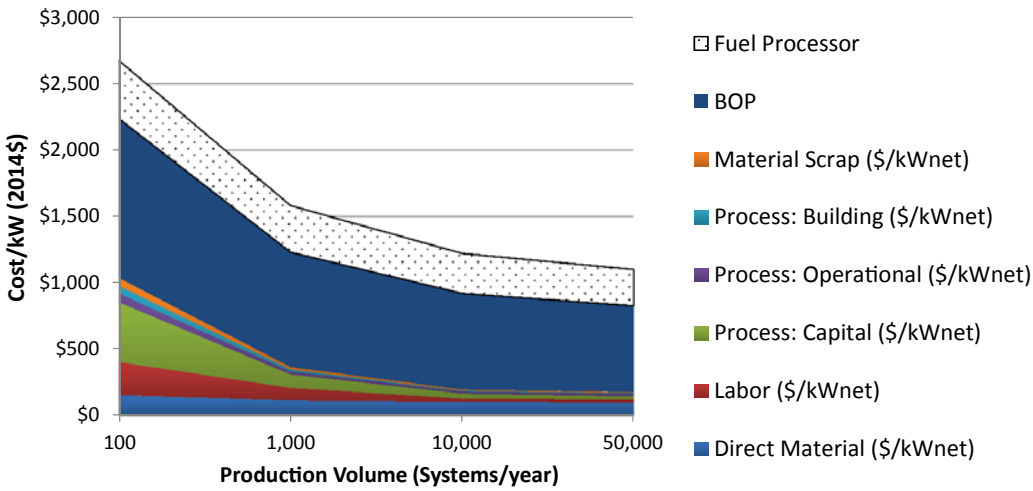

FIGURE 3. Direct system costs vs. production volume for 10 kW SOFC CHP system

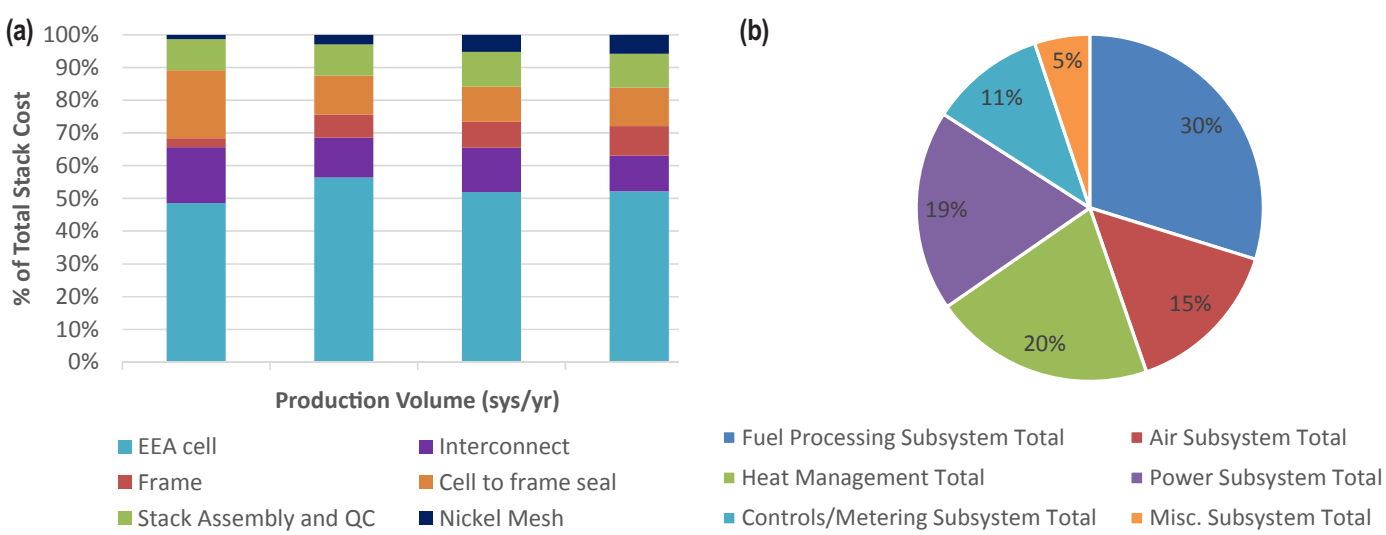

FIGURE 4. (a) Break down of total stack cost and (b) non-stack cost components for a 10 kW SOFC CHP system at annual production volume of 10,000 units per year

PEM, HT PEM, and SOFC systems, but this volume of production is more realistic in the 2020 timeframe and the $1,000/kW cost target for 2020 is not met for any of the three technologies. For 10 kW CHP systems, at 50,000 units per year, both PEM technologies exceed the cost target for both 2015 and 2020 but the SOFC system is close to achieving the $1,700/kW 2020 target.

- Non-stack costs (BOP and fuel processor) are generally found to be the largest component of CHP system costs for LT PEM, HT PEM systems, and SOFC systems. HT PEM CHP systems are projected to be higher cost than LT PEM systems due to lower power density, higher catalyst loading, more complex plate design, and lower process yield assumptions due to less overall technology maturity.
- Total cost of ownership including greenhouse gas, environmental, and health externalities is very dependent on fuel costs, capital costs, waste heat utilization, and the carbon intensity of displaced grid based electricity and conventional heating fuels. Fuel cell systems are most economically competitive from a total cost of ownership perspective in regions with high carbon intensity grid electricity.
- The research team is refining the direct cost modeling and completing the TCO model for SOFC CHP systems in the final quarter of FY 2015.
- Scenario modeling is also being done for fuel cell system lifetime costs vs. the no-fuel cell case of grid electricity and conventional heating as a function of fuel and electricity costs, fuel cell system capital costs, the carbon intensity of grid electricity, and state and federal incentives.

FY 2015 PUBLICATIONS/PRESENTATIONS

1. T. Lipman, M. Wei, Ahmad Mayyas, David Gosselin, Shuk Chan, Hanna Breunig, Tom McKone, "A Total Cost of Ownership Model for Low and High Temperature PEM Fuel Cells in Combined Heat and Power and Backup Power Applications," Fuel Cell Seminar, Los Angeles, CA, November 2014.

2. M. Wei, Timothy Lipman, Ahmad Mayyas, Joshua Chien, Shuk Han Chan, David Gosselin, Hanna Breunig, Michael Stadler, Thomas McKone, Paul Beattie, Patricia Chong, Whitney G. Olella, Brian D. James, "A Total Cost of Ownership Model for Low Temperature PEM Fuel Cells in Combined Heat and Power and Backup Power Applications," Lawrence Berkeley National Lab Report, October 2014.

3. M. Wei, Timothy Lipman, Ahmad Mayyas, Shuk Han Chan, David Gosselin, Hanna Breunig, Michael Stadler, Thomas McKone, "A Total Cost of Ownership Model for High Temperature PEM Fuel Cells in Combined Heat and Power and Backup Power Applications," Lawrence Berkeley National Lab Report LBNL-6772E, October 2014.

REFERENCES

1. James, Brian, Kalinoski, J., and K. Baum, "Mass-Production Cost Estimation for Automotive Fuel Cell Systems," 2010 Annual Merit Review Proceedings, Department of Energy, Hydrogen and Fuel Cells Program. Washington, D.C., June 2010.

2. Sinha, Jayanti, and Y. Yang, "Direct Hydrogen PEMFC Manufacturing Cost Estimation for Automotive Applications," 2010 Annual Merit Review Proceedings, Department of Energy, Hydrogen and Fuel Cells Program. Washington, D.C. June 2010.

3. Mahadevan, Kathya, V. Contini, M. Goshe, J. Price, F. Eubanks, and F. Griesemer, "Economic Analysis of Stationary PEM Fuel Cell Systems," 2010 Annual Merit Review Proceedings, Department of Energy, Hydrogen and Fuel Cells Program. Washington, D.C., June 2010.

4. James, B., Spisak, A., Colella, W., "Manufacturing Cost Analysis of Stationary Fuel Cell Systems," Strategic Analysis Inc., Arlington VA, September 2012.

5. Stadler, Michael, Marnay, C., Gonçalo Cardoso, G. et al., "The Carbon Dioxide Abatement Potential of California's Mid-Sized Commercial Buildings," California Energy Commission, PIER Program. CEC-500-2010-050 (2011).

6. Deru, M., Field, K., Studer, D., Benne, K., Griffith, B., Torcellini, P., Liu, B., Halverson, M., Winiarski, D., Rosenberg, M., Yazdanian, M., Huang, J., Crawley, D. (2011). Reference Building Models of the National Building Stock. NREL Technical Report NREL/TP-5500-46861.

7. Lipman, Timothy E., Jennifer L. Edwards, and Daniel M. Kammen, "Fuel Cell System Economics: Comparing the Costs of Generating Power with Stationary and Motor Vehicle PEM Fuel Cell Systems," Energy Policy 32(1): 101–125 (2004)

8. ACI Technologies, Inc. Manufacturing Fuel Cell Manhattan Project, U.S. Government Contract No. N00014-08-D-0758, November 2011.

9. Van Rooijen, Jaap, "A Life Cycle Assessment of the PureCell™ Stationary Fuel Cell System: Providing a Guide for Environmental Improvement," Center for Sustainable Systems, Report No. CSS06–09 University of Michigan, Ann Arbor, MI, June 30, 2006.

10. National Research Council, "Hidden Costs of Energy: Unpriced Consequences of Energy Production and Use," The National Academies Press: Washington, D.C., 2010.

11. Muller, N.Z., and R.O. Mendelsohn, "The Air Pollution Emission and Policy Analysis Model (APEEP): Technical Appendix [online]," Yale University, New Haven, CT, December 2006. Available at: https://segueuserles.middlebury.edu/nmuller/APEEP_Tech_Appendix.pdf

12. M. Wei, Timothy Lipman, Ahmad Mayyas, Joshua Chien, Shuk Han Chan, David Gosselin, Hanna Breunig, Michael Stadler, Thomas McKone, Paul Beattie, Patricia Chong, Whitney G. Olella, Brian D. James, "A Total Cost of Ownership Model for Low Temperature PEM Fuel Cells in Combined Heat and Power and Backup Power Applications," Lawrence Berkeley National Lab Report, October 2014.

V.F.8 Affordable, High Performance, Intermediate Temperature Solid Oxide Fuel Cells

Bryan Blackburn (Primary Contact),
Thomas Langdo, Dong Ding, Lei Wang,
Luis Correa, and Colin Gore
Redox Power Systems
387 Technology Drive
College Park, MD 20742
Phone: (301) 314-1959
Email: bryan@redoxenergy.com

DOE Manager
David Peterson
Phone: (720) 356-1747
David.Peterson@ee.doe.gov

Contract Number: DE-EE0006735

Subcontractor
University of Maryland, College Park, MD

Project Start Date: October 1, 2014
Project End Date: March 31, 2016

Overall Objectives

Redox Power Systems' overall objectives in this project are to improve the performance and durability of Redox solid oxide fuel cell (SOFC) technology through the:

- Development of an optimized bilayer electrolyte with increased open circuit potential (OCP) and thus greater fuel efficiency for natural gas fueled, intermediate temperature (IT) operation of ~600°C.
- Optimization of compositions and microstructures for the cathode to increase power density, and the anode to improve carbon- and sulfur-tolerance in hydrocarbon fuels for IT operation.
- Use of a custom multiphysics model and advanced materials to optimize the performance of bilayer stack designs for IT operation.
- Creation of bilayer cell performance maps and demonstration of a ~1 kW_e stack for IT operation under combined heat and power (CHP) conditions with natural gas and minimal external reforming.

Fiscal Year (FY) 2015 Objectives

- Validation of multi-physics bilayer cell and stack model to experiment
- Demonstration of a bilayer electrolyte cell with OCP performance of ≥0.9 V in both a button cell and a larger 10 cm by 10 cm cell in operation at ≤600°C
- Demonstration of an advanced SOFC operating at ≤600°C with a cell area specific resistance (ASR) ≤0.2 Ω-cm^2 and power density ≥~1 W/cm^2

Technical Barriers

This project addresses the following technical barriers from the Fuel Cells section of the Fuel Cell Technologies Office Multi-Year Research, Development, and Demonstration Plan:

(A) Durability

(B) Cost

(C) Performance

Technical Targets

This project's goals are focused on stack improvements with increased power density for operation at intermediate temperatures (≤600°C), which supports DOE technical targets. The results of this project can be applied to the design of advanced natural gas fueled power systems in the low and intermediate power range (1–100 kWe). SOFCs with lower operating temperatures can result in simpler, more compact, and lightweight systems with longer lifetimes. Furthermore, higher power densities at lower temperatures result in reduced system and operating costs, while IT operation still maintains sufficient exhaust temperatures for efficient CHP applications. Such systems have the potential to meet or exceed the following 2020 DOE fuel cell technical targets:

- Equipment Cost: ≤\$1,700/kW_{avg}
- Transient Response (10–90% rated power): ≤2 minutes
- Degradation with cycling: ≤0.3%/1,000 h
- Electrical Efficiency: ≥45%
- CHP Efficiency: ≥90%

FY 2015 Accomplishments

- Integrated bilayer electrolyte mechanism into custom Redox multi-physics model for cell and stack, with validation of model using button cell data under different operating conditions (e.g., temperature)
- Demonstrated button cells with OCP ≥0.9 V at ≤600°C using a gadolinium doped ceria (GDC)/erbium-stabilized bismuth oxide (ESB) bilayer

- Demonstrated button cells with power densities exceeding 1.25 W/cm^2 at ≤600°C

✧ ✧ ✧ ✧ ✧

INTRODUCTION

We have previously demonstrated a high power density SOFC technology using advanced materials in a novel bilayer electrolyte design with graded electrode structures at the button cell level. Redox has also been able to scale our base (single layer gadolinia doped ceria, or GDC, electrolyte) cells to a larger 10 cm by 10 cm production size and achieve a degree of performance similar to that of the button cells. Furthermore, we have scaled-up production of the ESB material that together with GDC comprises the bilayer electrolyte. However in addition to integrating the ESB/GDC bilayer into the larger format cells, significant improvements in cell performance/efficiency can still be achieved to make systems based on our technology more commercially viable with lower costs, higher efficiency, and superior durability. Moreover, integrated development of the anode for operation on readily available hydrocarbon fuels with a maximum degree of internal reforming is necessary to take full advantage of SOFC fuel flexibility. Achieving these advancements while maintaining high power density at intermediate temperatures (~600°C) will help us deploy this technology for distributed generation and CHP applications.

APPROACH

Redox's approach involves the synergistic use of two electrolyte materials in a bilayer structure to achieve superior performance (i.e., higher conductivity) at lower temperatures [1]. The first material is cerium oxide based, such as GDC, which has more than five times the ionic conductivity of conventional yttrium-stabilized zirconia (YSZ) at 600°C, but which, due to the electronic leakage that occurs in reducing environments like those in the fuel cell, can result in decreased cell efficiency. The second material is bismuth oxide based, such as ESB, which has 60 times the conductivity of YSZ at 600°C but is unstable in reducing environments. The bilayer electrolyte combines the cerium oxide and bismuth oxide layers (i.e., GDC/ESB) with the latter being situated on the cathode air side of the cell. In this case, the GDC protects the ESB from decomposing while the ESB blocks the electronic leakage in the GDC, thus boosting cell power and efficiency at lower operating temperatures. We have also developed new, bilayer-compatible cathode materials (e.g., composite lanthanum strontium manganite [LSM]-ESB) with exceptionally low ASR and are leveraging past work on infiltration of electrodes to enhance the performance of the cathode and anode. For the anode, catalyst infiltration can significantly increase power density and stability in the presence of hydrocarbon fuels like natural gas, even in the presence of sulfur compounds like H_2S [2]. To assist in the development of cells and stacks for operation at ~600°C, Redox makes use of our advanced multi-physics model that takes into account the unique thermochemical and physical properties of the Redox materials. This model is critical due to variations in conductivity and chemical activity of GDC as a function of temperature and effective oxygen partial pressure P_{O2}, which varies significantly down the channel in SOFC anodes with increasing fuel utilization [3].

RESULTS

During FY 2015, Redox integrated the physics of the GDC/ESB bilayer into our custom single-channel SOFC multiphysics model. The bilayer model employs SOFC layers consisting of Ni-GDC and/or Ni-YSZ anodes, GDC and ESB bilayer electrolytes, and an LSM-ESB cathode. We used the model to simulate both button cells and stack components with outputs consisting of polarization curves, three-dimensional temperature profiles, and composition distributions, based on temperature dependent input kinetic parameters and electrical properties associated with the electrolyte and electrode materials. The bilayer model parameters were fit to the button cell data at 600°C, and validated by correctly predicting performance at 650°C (Figure 1). The only change made to the model input during validation was the operating temperature, which demonstrates that the charge-transfer reaction rate expressions and proposed kinetic parameters are adequate to predict the GDC/ESB bilayer cell performance under different conditions. This validation has also been confirmed with different data generated at higher temperatures and

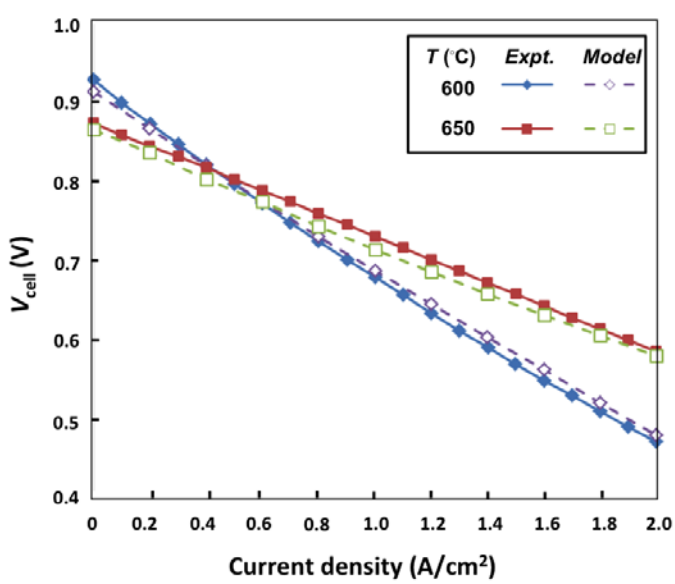

FIGURE 1. Comparison of predicted electrochemical performance of the stack model with experimental I-V curves at 600°C and 650°C

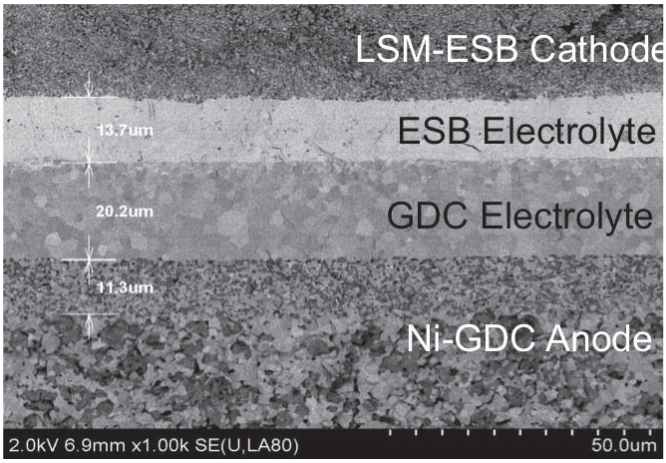

FIGURE 2. Example of SEM micrograph showing bilayer microstructure and geometry for cells

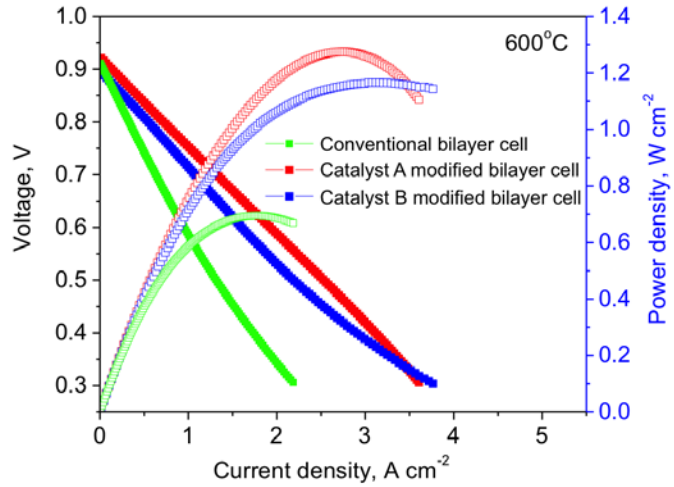

FIGURE 3. Initial results for bilayer button cell showing an OCP ≥0.9 V and a power density of 1.25 W/cm^2 at 600°C in humidified hydrogen

by predicting performance at lower temperatures, as well as with isothermal conditions for variations in the ESB and GDC thickness. The model also captures the kinetics of electrochemical and heterogeneous internal reforming reactions in the anode, and therefore now represents a complete multi-physics tool for cell/stack investigations.

In the first six months of this project, we adjusted the relative and total GDC/ESB bilayer thickness to improve OCP. Figure 2 shows an example scanning electrode microscopy (SEM) micrograph of a GDC/ESB bilayer cell used in the thickness optimization trials. Thicknesses were on the order of 20 µm for the GDC and ~5–20 µm for the ESB. Using these cells we successfully demonstrated a bilayer button cell operating on humidified hydrogen fuel and air (1 atm) with an OCP as high as 0.94 V at 600°C. As shown in Figure 3, we also demonstrated a button cell with an OCP of 0.93 V at 600°C and a maximum power density of 1.27 W/cm^2. The cell also had an ASR of 0.171 Ω-cm^2. These very high power densities at intermediate operating temperatures were accomplished through additional bilayer electrolyte optimization as well as through the introduction of catalyst infiltrants into porous electrodes using methods that are scalable in manufacturing.

CONCLUSIONS AND FUTURE DIRECTIONS

Conclusions from the FY 2015 work include:

- Redox's bilayer electrolyte configuration can effectively boost the open circuit voltage at intermediate operating temperatures (~600°C) and therefore the efficiency of SOFCs when compared to cells consisting of a single cerium oxide electrolyte.
- When the bilayer electrolyte is combined with infiltration of catalysts in the cathode and/or anode, performance can be enhanced further with cells having power densities >1.25 W/cm^2 at 600°C.
- The addition of the bilayer electrolyte to the custom Redox multi-physics model makes it a valuable tool for optimizing designs at both the cell and stack levels.

Future work will include the following:

- The implementation and demonstration of the bilayer electrolyte at the 10 cm by 10 cm cell size with an OCP ≥0.9 V at ≤600°C
- The demonstration of the bilayer 10 cm by 10 cm cells in a ~1 kW$_e$ stack under CHP conditions using natural gas

FY 2015 PUBLICATIONS/PRESENTATIONS

1. Bryan Blackburn, Affordable, High Performance, Intermediate Temperature Solid Oxide Fuel Cells, U.S. Department of Energy's 2015 Annual Merit Review and Peer Evaluation Meetings (AMR) for the Hydrogen and Fuel Cells Program, Arlington, VA, June 11, 2015.

REFERENCES

1. Eric D. Wachsman and Kang Taek Lee, *Science*, **334**, 935–939 (2011).

2. Zhangbo Liu, Beibei Liu, Dong Ding, Mingfei Liu, Fanglin Chen, and Changrong Xia, Fabrication and Modification of Solid Oxide Fuel Cell Anodes Via Wet Impregnation/Infiltration Technique, *Journal of Power Sources*, 237, 243–259 (2013).

3. Lei Wang, Greg S. Jackson, and Bryan M. Blackburn, *ECS Transactions*, 57(1), 2583 (2013).

V.F.9 Smart Matrix Development for Direct Carbonate Fuel Cell

Chao-Yi Yuh (Primary Contact), Abdelkader Hilmi, Arun Surendranath
FuelCell Energy (FCE), Inc.
3 Great Pasture Road
Danbury, CT 06813
Phone: (203) 825-6112
Email: cyuh@fce.com

DOE Manager
Jacob Spendelow
Email: spendelow@lanl.gov

Contract Number: DE-EE0006606

Subcontractors:
- University of Connecticut, Storrs, CT
- Illinois Institute of Technology, Chicago, IL

Project Start Date: September 22, 2014
Project End Date: October 31, 2017

Overall Objectives

Develop an innovative durable DFC® (Direct Fuel Cell) electrolyte matrix ("smart" matrix) to enable >420 kW rated stack power and 10-year (80,000 h) stack service life (current generation: 350 kW rated stack power and 5-year stack service life)

- Increase market penetration for stationary fuel cells
- Enable domestic clean-energy job growth
- Enable technology for hydrogen infrastructure and CO_2 capture

Fiscal Year (FY) 2015 Objectives

- Develop plans to achieve smart matrix technical goals and degradation mechanistic understanding
- Achieve targets of improved beginning of life (BOL) matrix mechanical strength and high-porosity fine-pore microstructure
- Verify smart matrix sealing efficiency and ohmic resistance in >2,000 h cell tests

Technical Barriers

This project addresses the following technical barriers from the Fuel Cells section of the Fuel Cell Technologies Office Multi-Year Research, Development, and Demonstration Plan [1]:

(A) Durability: Incomplete understanding of degradation mechanism and lack of clear long-term degradation mitigation schemes

(B) Cost: cost-effective matrix degradation-mitigation schemes

Technical Targets

This project is developing an innovative electrolyte matrix (smart matrix) to enable combined heat and power (CHP) distributed generation fuel cell systems to meet DOE 2020 research, development, and demonstration (RD&D) technical targets [1] (Table 1).

TABLE 1. FCE Progress towards Meeting DOE RD&D Technical Targets for 100 kW–3 MW CHP Distributed Generation Fuel Cell Systems Operating on Natural Gas

Characteristic	Units	2020 Targets	DFC Baseline
Electrical efficiency at rated power	%	>50	47
CHP energy efficiency	%	90	90
Operating lifetime	Hours	80,000	>44,000

Specific technical targets for the "smart" matrix are established based on multi-year DFC field operation experience:

- >25% BOL mechanical strength increase, >20% porosity increase and improved fine-pore microstructure (>30% reduction on pores larger than 0.2 μm) compared to the baseline
- Stable fine-pore microstructure (<50% pores larger than 0.2 μm at end of life [EOL]) for enhanced capillary electrolyte retention, projected from >5,000 h accelerated cell and technology stack tests
- Understand matrix material degradation mechanism
- Scale-up production of smart matrix for 1 m^2 full-area 30 kW technology stack evaluation

FY 2015 Accomplishments

- Successfully fabricated lab-scale high-porosity smart matrix meeting target of >25% increased BOL mechanical strength
- Verified improved fine-pore microstructure (>30% reduction of pores larger than 0.2 μm) in ~2,000 h cell testing
- Verified smart matrix sealing efficiency in ~2,000 h cell tests

✧ ✧ ✧ ✧ ✧

INTRODUCTION

Worldwide demand for high-efficiency ultra-clean power generation is growing. FCE's efficient DFC products based on high temperature internal reforming carbonate fuel cell technology are striving to meet this growing demand. DFC has already advanced to a single stack capable of producing 350 kW net alternating current power and 5-year service life. Stack power and service life increases will further enhance DFC's commercial competitiveness for larger scale deployment.

The matrix holds a very important key to higher power density operation, longer service life and lower cost. The matrix, a porous microstructure consisting mainly of ultra-fine sub-micro α-$LiAlO_2$ particles sandwiched between two electrodes, immobilizes liquid electrolyte, isolates fuel from oxidant and facilitates ionic transport. However, $LiAlO_2$ slowly coarsens during stack endurance service. Such coarsening lowers capillary force leading to matrix drying and electrolyte redistribution, contributing to performance loss and gas crossover. This program aims to develop a high yield production ready smart matrix with robust and stable fine-pore microstructure to enable DFC meeting targets of DOE 2020 CHP distributed generation fuel cell systems.

APPROACH

The approaches to achieve the technical targets are listed below in Table 2. The technical targets will be validated in long-term >5,000 h cell and full-area 30 kW technology stack tests. Full scale production trials will be conducted to fabricate full area smart matrices for the technology stack tests and to assure the manufacturing process ready for product implementation.

TABLE 2. Approaches to Achieve Smart Matrix Technical Targets

Technical Targets	Approaches
BOL: >25% mechanical strength increase, >20% porosity increase and improved fine-pore microstructure (>30% reduction on pores larger than 0.2 μm) than baseline	Nano-pore former for increased porosity Reinforcement additives to increase mechanical strength
	Optimize slurry formulation and processing for improved particle size distribution, particle packing and production yield
EOL: Stable fine-pore microstructure for enhanced electrolyte retention (<50% pores larger than 0.2 μm)	Stabilized $LiAlO_2$ or additives to slow down coarsening to maintain capillary electrolyte retention
Coarsening mechanistic understanding	Investigate effects of temperature, gas atmosphere, and electrolyte composition on matrix microstructure evolution, $LiAlO_2$ stability, wettability and solubility in single cells/stacks and controlled out-of-cell tests

RESULTS

Examination of long-term operated DFC cells and stacks revealed excellent α-$LiAlO_2$ phase stability but with gradual coarsening. The coarsening process is non uniform, more pronounced at the reducing anode side whereas much slower at the oxidizing cathode side. Figure 1 illustrates $LiAlO_2$ coarsening in accelerated ~250 cm^2 single cells operated for up to ~5,000 hours. Analyses of additional single cells and stacks are continuing to more accurately determine coarsening kinetics and help elucidating mechanism.

$LiAlO_2$ dissolves slightly in the liquid carbonate electrolyte according to:

$CO_3^{2-} \leftrightarrow CO_2 + O^{2-}$ (Reaction 1, dissociation)

$LiAlO_2 + O^{2-} \leftrightarrow Li^+ + AlO_3^{3-}$ (Reaction 2, basic dissolution)

Literature reported the solubility increases with higher temperature, lower CO_2 partial pressure and in strong basic melt [2–4]. Although it is well known that dissolution could cause Ostwald ripening via dissolution-precipitation steps, the causes of the faster reducing anode side coarsening are not yet established. A detailed investigation of the effects of electrolyte chemistry, particle morphology as well as gas atmosphere and temperature on $LiAlO_2$ stability is required to develop fundamental understanding for helping designing mitigation schemes.

A series of controlled out-of-cell tests was initiated to investigate the effect of each parameter on coarsening. The baseline α-$LiAlO_2$ powder immersed in the baseline carbonate electrolyte showed significant coarsening and >90% $\alpha \rightarrow \gamma$ phase transformation at high temperature (700°C) in 150 hours, in the absence of CO_2, explainable by the higher (O^{2-}) (according to Reaction 1) and higher $LiAlO_2$

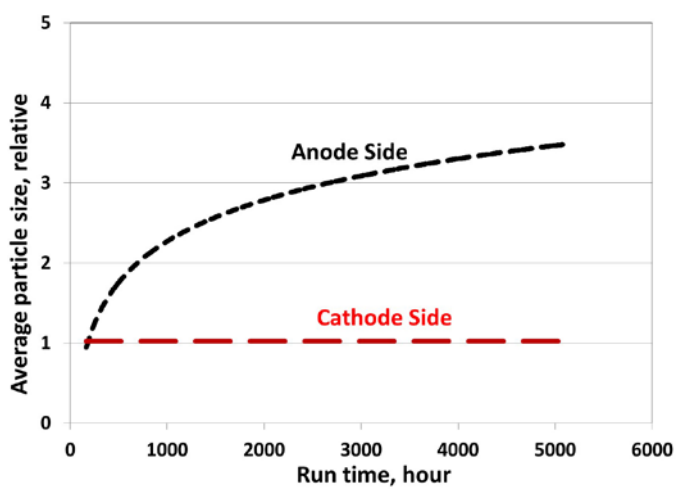

FIGURE 1. Baseline matrix coarsening in accelerated single cells: Reducing anode environment accelerates coarsening.

solubility (according to Reaction 2). These results imply that the dissolved AlO_3^{3-} might rapidly precipitate as γ-$LiAlO_2$ under such an extremely high solubility condition. It is also possible that γ-$LiAlO_2$ may likely nucleate at 700°C [3,4] and faster under the reducing anode atmosphere. The combined high solubility in the absence of CO_2 and more stable γ phase at 700°C may explain the fast simultaneous coarsening and $\alpha \rightarrow \gamma$ transformation. On the other hand, 1–10% CO_2 addition drastically improves phase and particle size stability (no coarsening or phase transformation in 150 h). DFC stack is operated typically between 550°C and 650°C and such $\alpha \rightarrow \gamma$ phase transformation was not observed. It is postulated that such higher-solubility γ or other intermediate phases may still nucleate slowly under the CO_2-containing reducing atmosphere in DFC, promoting Ostwald ripening of the bulk α phase. Further tests to determine the transformation kinetics, wettability and solubility as a function of electrolyte composition, temperature and atmosphere are ongoing to clarify the above hypothesis.

Higher matrix porosity is desired to increase electrolyte storage capacity and reduce cell ohmic resistance. The electrolyte matrix has to remain substantially crack resistant in order to provide effective gas sealing to minimize gas leakage induced electrolyte loss and cell resistance increase. Stronger matrix is desired to withstand thermo-mechanical stress experienced during both initial start-up conditioning and endurance operation. The Ostwald ripening process that contributes to the coarsening and resulting pore-structure degradation needs to be mitigated to maintain a desired stable fine-pore microstructure.

Nano-pore formers meeting key requirements such as particles size, chemical compatibility with the electrolyte, complete removal during conditioning and low sulfur content (<30 ppm) have been utilized. Several promising additives to enhance mechanical strength and to disrupt the Ostwald ripening process have also been selected. In order to achieve an ultra-fine and tighter pore microstructure, matrix formulation and slurry processing were modified to improve dispersion, milling efficiency, particle packing and slurry tape-casting characteristics.

Lab scale (~10 in wide) high-porosity smart matrices with a reinforced fine-pore microstructure have successfully been fabricated. The consistency and reproducibility of the slurry and the matrix physical properties were verified in many lab scale batches (~20 batches). The target of ~20% higher porosity compared to the current baseline has been successfully achieved. Verification of the BOL mechanical strength was conducted in de-bindered matrices from >20 lab scale batches. The debindered matrix before electrolyte filling (during start-up conditioning) is at the mechanically weakest state. Three-point bending tests showed that the smart matrix has >40% higher snap (fracture) strength compared to the current baseline, thus meeting the BOL mechanical strength target (Figure 2). This fracture strength improvement minimizes matrix cracking during conditioning and enables enhanced BOL gas sealing; essentially no gas cross-over (leakage) was detected in ~250 cm^2 bench-scale single cell tests operated for ~2,000 h. The pore structure of the smart matrix in greater than eight single cells operated for up to 1,700 h also meets the BOL target of >30% reduction on pores larger than 0.2 μm (Figures 3 and 4) at the fuel inlet, compared to the baseline. The fuel inlet location was selected for comparison because it is the most reducing location and showing the fastest coarsening, >5,000 h. Endurance cell tests under thermal cycling condition are continuing to evaluate longer term pore-structure stability and matrix sealing capability under transient conditions.

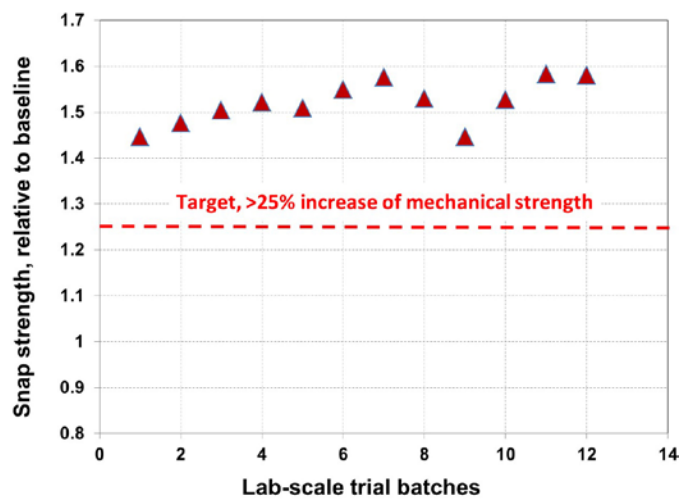

FIGURE 2. BOL mechanical strength of lab-scale smart matrix: Target of >25% increased mechanical strength was achieved.

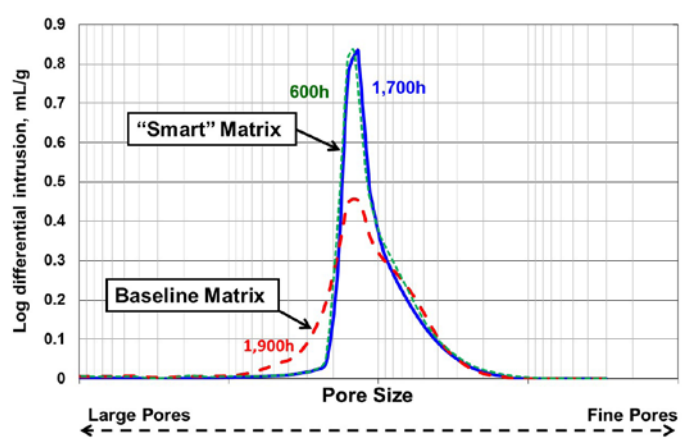

FIGURE 3. Comparison of pore structure of smart matrix vs. baseline in accelerated single cells: >30% reduction of larger pores in smart matrix has been demonstrated.

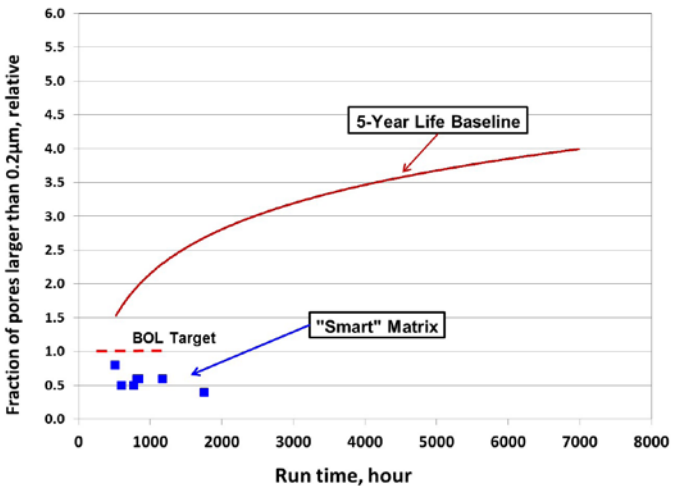

FIGURE 4. Large-pore fraction comparison (pore fraction larger than 0.2 µm): >30% reduction of large pores in smart matrix has been demonstrated in accelerated single cells.

CONCLUSIONS AND FUTURE DIRECTIONS

Lab-scale smart matrix has been successfully verified in single cells operated for ~2,000 h. Accomplishments and conclusions for this reporting period include the following.

- Developed slurry formulation and processing parameters to produce lab-scale (10 in wide) smart matrices with improved fine-particle packing
- Met BOL targets of >20% higher porosity, >25% increase of mechanical strength and >30% reduction on pores larger than 0.2 µm (up to 1,700 h cell testing)
- Degradation mechanistic understanding
  - Identified accelerated coarsening in reducing anode environment
  - Developed hypothesis of accelerated coarsening mechanism

The remainder of the project will focus on optimizing smart matrix formulation, additive improvement, endurance validation and scale-up manufacturing trials.

- Verify smart matrix durability in endurance cell tests (>5,000 h)
- Understand degradation mechanism
- Perform scale-up manufacturing trials and validate smart matrix in 30 kW technology stacks

FY 2015 PUBLICATIONS/PRESENTATIONS

1. Program Kickoff Review, held at FuelCell Energy, Inc., February 26, 2015.

2. Abdelkader Hilmi, Arun Surendranath, and Chao-Yi Yuh, "An Innovative Carbonate Fuel Cell Matrix," Abstract #188, Joint General Session: Battery and Energy Storage-and-Fuel Cells, Electrolytes, and Energy Conversion, paper presented at 227th ECS Meeting, Chicago, IL, May 28, 2015.

3. Chao-Yi Yuh and Abdelkader Hilmi, "Smart Matrix Development for Direct Carbonate Fuel Cell," 2015 DOE Hydrogen and Fuel Cells Program and Vehicle Technologies Office Annual Merit Review and Peer Evaluation Meeting, Arlington, Virginia, June 12–16, 2015.

4. Chao-Yi Yuh, Abdelkader Hilmi, and Ramki Venkataraman, "High-Temperature Direct Fuel Cell Material Experience," paper presented at the 11th International Conference on Ceramic Materials and Components for Energy and Environmental Applications, T1-Ceramics for Energy Conversion, Storage, and Distribution Systems, T1S1: High-Temperature Fuel Cells and Electrolysis, American Ceramic Society, Vancouver, Canada, June 14–19, 2015.

REFERENCES

1. DOE Office of Energy Efficiency and Renewable Energy (EERE) Fuel Cell Technologies Offices Multi-Year Research, Development and Demonstration (MYRDD) Plan, Section 3.4 "Fuel Cells," Updated November 2014, http://energy.gov/sites/prod/files/2014/12/f19/fcto_myrdd_fuel_cells.pdf.

2. Chao-Yi Yuh, Mohammad Farooque, and Hans Maru, "Advances in Carbonate Fuel Cell Matrix and Electrolyte," in *Proc. Symp. Carbonate Fuel Cell Technology V*, The Electrochemical Society, **PV99-20**, 1999: 189–201.

3. Chao-Yi Yuh and Mohammad Farooque, "Materials and Life Considerations," in *Fuel Cells-Molten Carbonate Fuel Cells, Encyclopedia of Electrochemical Power Sources,* 497–507, Elsevier Science, 2009.

4. Chao-Yi Yuh and Mohammad Farooque, "High-Temperature Direct Fuel Cell Material Experience," in *Advances in Solid Oxide Fuel Cells X, Ceramic Engineering and Science Proceedings*, 11th International Symposium on Solid Oxide Fuel Cells (SOFC): Materials, Science and Technology in 38th International Conference and Exposition on Advanced Ceramics and Composites (38th ICACC 2014), American Ceramic Society, **(35)** 9–21, John Wiley & Sons, Hoboken, NJ, 2015.

V.F.10 Fuel Cell Technology Status—Degradation

Jennifer Kurtz (Primary Contact), Huyen Dinh, Chris Ainscough, and Genevieve Saur
National Renewable Energy Laboratory
15013 Denver West Parkway
Golden, CO 80401-3305
Phone: (303) 275-4061
Email: jennifer.kurtz@nrel.gov

DOE Managers
David Peterson
Phone: (720) 356-1747
Email: David.Peterson@ee.doe.gov

Project Start Date: July 1, 2009
Project End Date: Project continuation and direction determined annually by DOE

Overall Objectives

- Conduct an independent assessment to benchmark current fuel cell system cost and price in a non-proprietary method
- Leverage National Fuel Cell Technology Evaluation Center (NFCTEC)
- Collaborate with key fuel cell developers on the voluntary data share and NFCTEC analysis

Fiscal Year (FY) 2015 Objectives

- Receive and analyze new laboratory durability data
- Publish aggregated, current fuel cell voltage durability status

Technical Barriers

This project addresses the following technical barriers from the Fuel Cells section of the Fuel Cell Technologies Office Multi-Year Research, Development, and Demonstration (MYRDD) Plan:

(A) Durability (Lack of data for current fuel cell durability status per targets)

(B) Cost (Lack of data for current fuel cell costs and status per targets)

Technical Targets

This project is conducting an independent assessment of the current fuel cell durability test data from leading fuel cell developers. All results are aggregated to protect proprietary information and are reported on by the system application. Table 1 shows the durability targets.

TABLE 1. Fuel Cell Durability Target and Status Table

Application	2020 Durability Target	Lab Status – Ave. Hours to 10% Voltage Degradation
Light Duty Automotive	5,000 h	3,600
Public Transit	25,000 h	6,200
Forklift	20,000 h Target Under Review	14,600
Backup	10,000 h Target Under Review	2,500
Stationary 1–10 kW	0.3%/1,000 h	11,100
Stationary 100 kW–3 MW	80,000 h	

Per the Fuel Cells section of the Fuel Cell Technologies Office MYRDD Plan, the cost targets are:

- The 2017 transportation fuel cell system cost target is $30/kW.
- The 2020 micro-combined heat and power (CHP) (5 kW) fuel cell system cost target is $1,500/kW.
- The 2020 medium CHP (100 kW–3 MW) fuel cell system cost target is $1,000/kW for natural gas and $1,400/kW for biogas.

FY 2015 Accomplishments

- Collected new fuel cell voltage degradation data sets from fuel cell developers (including data on proton exchange membrane, direct methanol, and solid oxide fuel cell of full active area short stacks and full stacks with systems)
- Analyzed, aggregated, and published current status of fuel cell voltage degradation versus DOE targets
- Published 14 composite data products (CDPs) [1] on
  - Operation time and projected operation time to 10% voltage drop
  - Projected operation time sensitivity to voltage drop levels
  - Comparison of automotive and material handling equipment laboratory and field durability projections
  - Power capability
  - Data sets operated beyond 10% voltage drop
  - Durability projections by configuration and test condition

  - Test configuration and condition breakdowns
  - Time series variation of results
- Updated and published an information pamphlet with participation request and benefits as well as past fuel cell durability CDPs and price/cost CDP
- Updated and published a CDP on low-volume price by backup power, forklift, and prime power applications (split into small and large prime capacity)

✧ ✧ ✧ ✧ ✧

INTRODUCTION

DOE has funded significant research and development activity with universities, national laboratories, and the fuel cell industry to improve the market competitiveness of fuel cells. Most of the validation tests to confirm improved fuel cell stack performance and durability (indicators of market competitiveness) are completed by the research organizations themselves. Although this allows the tests to be conducted by the developers most familiar with their specific technology, it also presents a number of challenges in sharing progress publicly because test conditions and data analysis take many forms and data collected during testing are often considered proprietary.

The National Renewable Energy Laboratory (NREL) is benchmarking the state-of-the-art fuel cell performance, specifically focusing on durability, through independent assessment of current laboratory data sets. NREL's data processing, analysis, and reporting capitalize on capabilities developed in DOE's Fuel Cell Electric Vehicle Learning Demonstration. Fuel cell stack durability status is reported annually and includes a breakdown of status for different applications. A key component of this project is the collaborative effort with key fuel cell developers to understand what is being tested in the laboratory, study analysis results, and expand the included data sets.

APPROACH

The project involves voluntary submission of data from relevant fuel cell developers. NREL is contacting fuel cell developers for fuel cell voltage degradation and cost/price data for multiple fuel cell types to either continue or begin a data sharing collaboration. A continuing effort is to include more data sets, types of fuel cells, quantity of units sold, and developers. The fuel cell voltage degradation data are sent from fuel cell developer testing and studied over time against the DOE's voltage degradation targets.

Raw and processed data are stored in NREL's NFCTEC. The NFCTEC is an off-network room with access provided to a small set of approved users. Processing capabilities are developed or modified for new data sets and then included in the analytical processing of NREL's Fleet Analysis Toolkit (NRELFAT). The incoming raw data may be new or a continuation of data that have already been supplied to NREL. An internal analysis of all available data is completed annually and a set of technical CDPs is published every other year. Publications are uploaded to NREL's technology validation website [1] and presented at industry-relevant conferences. The CDPs present aggregated data across multiple systems, sites, and teams to protect proprietary data and summarize the performance of hundreds of fuel cell systems and thousands of data records. A review cycle is completed before the CDPs are published. This review cycle includes providing detailed data products (DDPs) of individual system- and site-performance results to the specific data provider. DDPs also identify the individual contribution to the CDPs. NRELFAT is an internally developed tool for data processing and analysis structured for flexibility, growth, and simple addition of new applications. Analyses are created for general performance studies as well as application- or technology-specific studies.

RESULTS

Results published in May 2015 were the fifth update for this analysis effort. The annual voltage degradation analysis of state-of-the-art laboratory durability was completed in advance of the milestone to provide an update that could be presented at the DOE's Annual Merit Review. In the current published data set, six applications were covered and 18 fuel cell developers supplied data (more than one data set in many cases). The data sets covered proton exchange membrane, direct methanol, and solid oxide fuel cell stack testing. A total of 145 data sets have been analyzed. Note that a data set represents a short stack, full stack, or system test data. Of the total data sets, 77% have been retired (Figure 1), meaning the system or stack is not accumulating any new operation hours either because of test completion, technology upgrades, or failures. The published data results include 15 CDPs. The power capability illustrates the range of fuel cell power for the data sets by application from less than 2 kW to more than 50 kW. Most of the analyzed data sets are laboratory systems at less than 14 kW power.

The analyzed data sets are from laboratory testing of full active area short stacks (e.g., stacks with fewer cells than the expected full power stack) and test systems with full power stacks. The data sets also vary from one to the other in how the stack/system was tested. Data were generated between 2004 and late 2012 from different testing methods that included constant load, transient load, and accelerated testing. The variability in test conditions and test setups created a group of data that can be difficult to compare. Additional breakdown of the data sets is an important aspect of future work and is dependent on the accumulation of more data sets to not reveal an individual data supplier's contribution to the results or proprietary data.

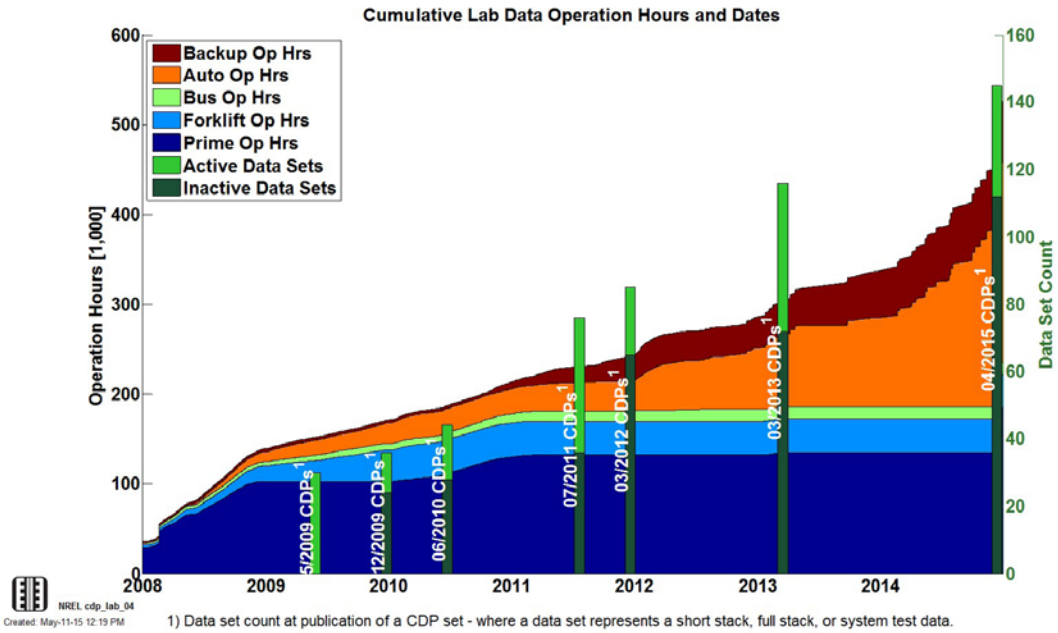

FIGURE 1. Cumulative lab data operation hours and dates

Fuel cell durability is studied at a design-specific current point and measured against a target of 10% voltage drop from beginning of life. The 10% voltage drop metric is used for assessing voltage degradation with a common measurement, but the metric may not be the same as end of life criteria and does not address catastrophic failure modes. Figure 2 is an aggregated set of results separated by application and identifies the percentage of short stacks and how many data sets are still operating (at the time of the results) for each application. Each application has the average, maximum, and 25th and 75th percentile values identified for the operation hours and the projected hours to 10% voltage drop.

The 10% voltage drop level is not necessarily a measurement for end of life or even a significant reduction

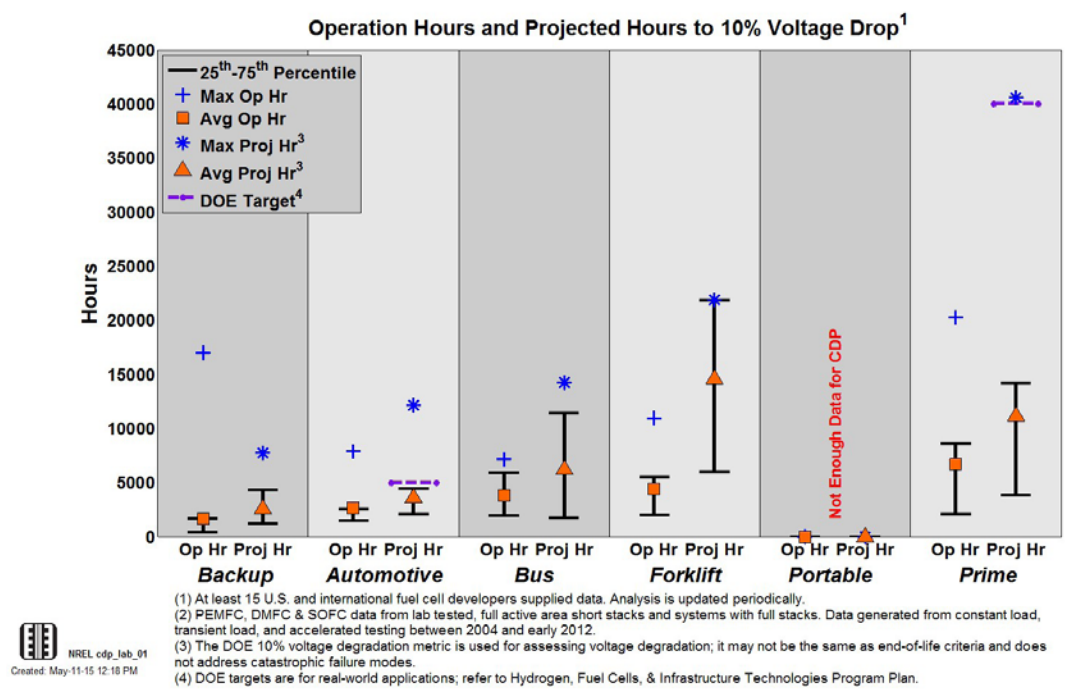

FIGURE 2. Operation hours and projected hours to 10% voltage drop by application category

in performance. Many data sets have not passed (or did not pass) the metric of 10% voltage degradation. The reason data sets operated beyond 10% voltage degradation could be because end of life criteria may be greater than 10% voltage degradation or because the test was designed to operate until a failure occurred. The stack configuration and test conditions can have a significant impact on the projected time to 10% voltage degradation within an application. In general, the average projection decreases with more aggressive test conditions and full systems (Figure 3). Not all applications have data sets in each configuration or test condition group. The test condition groups include:

- Steady—little or no change to load profile
- Duty Cycle—load profile mimics real-world operating conditions
- Accelerated—test profile is more aggressive than real-world operating conditions

The first CDP was published in June 2014 for backup power, forklift, and prime power applications (Figure 4). Statistical details, specifically the median and 25th and 75th percentile range, were identified for each application in dollars per kilowatt. The data are in 2013 dollars without incentives and are from public information, American Recovery and Reinvestment Act deployments, and voluntarily supplied data from fuel cell developers. This includes more than 20 different data points from more than three fuel cell developers.

CONCLUSIONS AND FUTURE DIRECTIONS

This project has leveraged other technology validation projects and existing industry relationships to steadily increase the quantity and depth of reporting on the state-of-the-art fuel cell durability status with a relatively low investment from DOE. U.S. and international developers have voluntarily supplied at least one data set, and it is an ongoing effort to include new data sets, update data sets already included (if applicable), and include new fuel cell developers, applications, and types. The voluntary participation of leading fuel cell developers showcases the fuel cell durability improvements with the current technology and provides an overall technology benchmark (with the published aggregated data) and an individual developer benchmark (with the detailed data products). The data are fully integrated into NRELFAT, and an online interface provides information on the project, contact information for interested collaborators, and all publications. The published results from May 2015 are the sixth update and were completed ahead of the milestone requirement with many new data sets and results. Future work, following the path of degradation and cost/price status updates every other year, includes:

- Continue cultivating existing collaborations and developing new collaborations with fuel cell developers
- Gathering, processing, and reporting on current fuel cell product cost and/or price

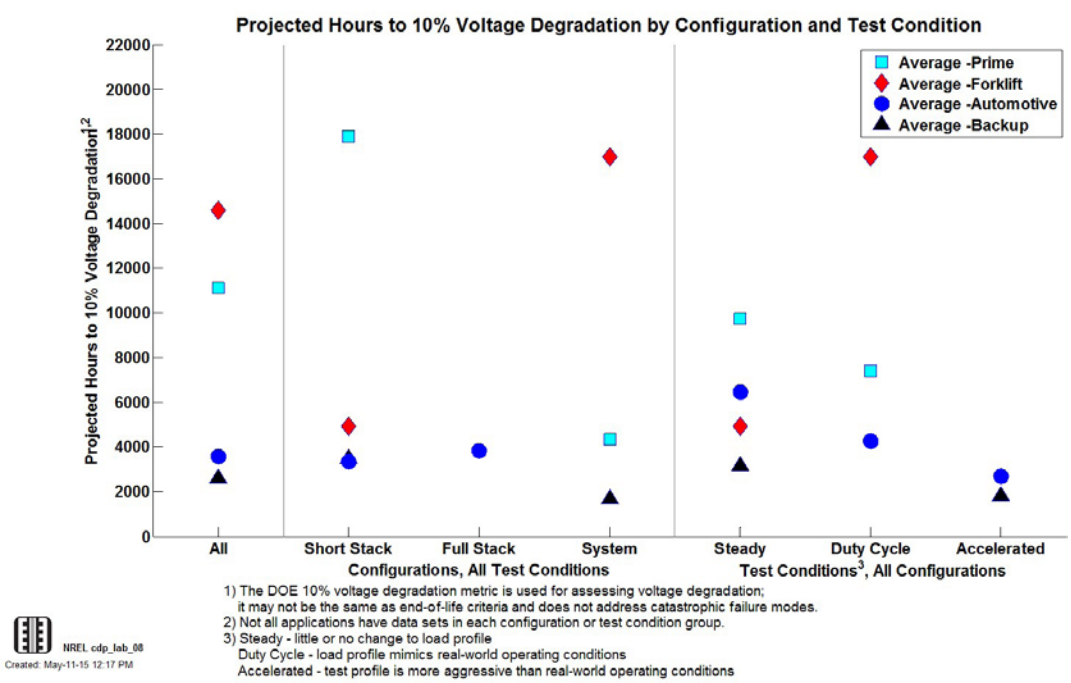

FIGURE 3. Projected hours to 10% voltage drop by configuration and test condition

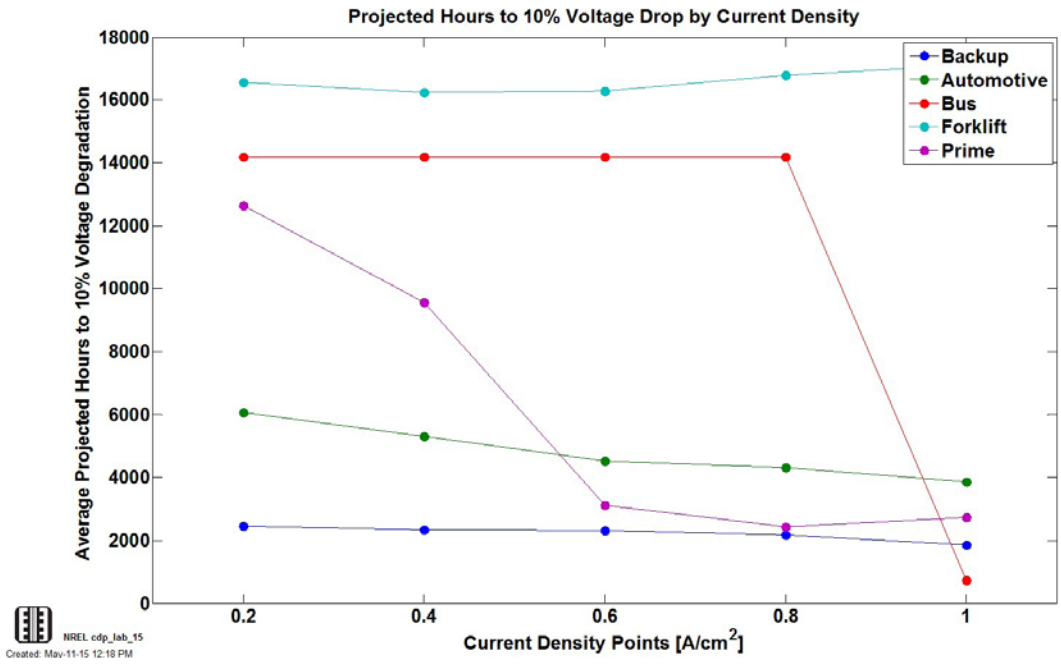

FIGURE 4. Current fuel cell system low volume price by application

FY 2015 PUBLICATIONS/PRESENTATIONS

1. Kurtz, J., and H. Dinh, "Fuel Cell Technology Status – Durability," Presented as a poster at the 2014 Annual Merit Review and Peer Evaluation Meeting, Washington, D.C.,June 2015.

2. Kurtz, J., and H. Dinh, "Current Low Volume Fuel Cell System Price: 2015 Composite Data Product," May 2015.

3. Kurtz, J., H. Dinh, C. Ainscough, and G. Saur, "Current Status of Fuel Cell Voltage Degradation: 2015 Composite Data Product," May 2015.

REFERENCES

1. http://www.nrel.gov/hydrogen/proj_fc_analysis.html

V.F.11 Ionomer Dispersion Impact on Advanced Fuel Cell and Electrolyzer Performance and Durability

Hui Xu (Primary Contact), Jason Willey, and Tom McCallum (Giner), Yu-Seung Kim (LANL)
Giner, Inc.
89 Rumford Ave.
Newton, MA 02466
Phone: (781) 529-0573
Email: hxu@ginerinc.com

DOE Manager
Dimitrios Papageorgopoulos
Phone: (202) 586-5463
Email: Dimitrios.Papageorgopoulos@ee.doe.gov

Contract Number: DE-SC0012409

Subcontractor
Los Alamos National Laboratory (LANL), Los Alamos, NM

Project Start Date: June 9, 2014
Project End Date: March 8, 2015

Overall Objectives

- Validate the scalability and processability (roll to roll production) of membrane and electrode assembly (MEA) fabrication using LANL's ionomer dispersions
- Integrate Giner dimensionally-stabilized membrane (DSM) supports with LANL ionomer dispersion to make mechanically and chemically stable MEAs
- Explore commercial applications of LANL ionomer dispersions in fuel cell or electrolyzer markets

Fiscal Year (FY) 2015 Objectives

The FY 2015 objects are the same as the overall objectives since this is a nine-month Small Business Innovation Research Phase I project.

Technical Barriers

This project addresses the following technical barrier from the Fuel Cells section of the DOE Fuel Cell Technologies Office Multi-Year Research, Development, and Demonstration Plan:

(A) Durability

Technical Targets

The targets of this project are to apply LANL ionomer dispersion technology and Giner DSM technology to make durable fuel cell MEAs that may meet the DOE targets listed in Table 1.

TABLE 1. DOE PEM Fuel Cell MEA Durability Targets

	Units	2020 Target
Platinum group metal (PGM) total content (both electrodes)	g/kW	<0.125
PGM total loading (both electrodes)	mg/cm^2	<0.125
Loss in catalytic (mass) activity	% loss	<40
Loss in performance at 0.8 A/cm^2	mV	30
Loss in performance at 1.5 A/cm^2	mV	30
Mass activity @ 900 $mV_{iR\text{-}free}$	A/mg_{PGM}	0.44

Accomplishments

- Integrated LANL low equivalent weight (EW) ionomer dispersion into Giner DSM platform and created hybrid membranes that exhibit high proton conductivity and good mechanical properties
- Successfully developed DSM-based MEAs that demonstrate both chemical and mechanical stability over extensive voltage and relative humidity (RH) cycling tests
  - One MEA after 30,000 cycles (voltage cycling 0.6 V to 1.0 V) showed 10% to 15% electrochemical surface area (ECSA) loss and minimal performance loss
  - One MEA after 5,000 cycles (RH cycling from dry to fully saturated) showed less than 0.5 mA/cm^2 increase in hydrogen crossover
- Successfully applied ionomer dispersion to PEM and demonstrated high electrolyzer MEA durability in extensive voltage cycling
  - One MEA after 10,000 cycles (voltage cycling 1.4 V to 1.8 V) without any performance loss

✧ ✧ ✧ ✧ ✧

INTRODUCTION

LANL has developed a revolutionary method of building an MEA for PEM fuel cells that can significantly reduce

manufacturing costs and extend MEA lifetimes. This method incorporates unique polymer dispersions in non-aqueous liquids to produce superior electrode performance, stability, and durability during harsh fuel cell operating conditions [1,6]. The LANL-produced MEA has been evaluated and certified using an accelerated stress test (AST) developed by DOE in conjunction with car manufacturers; the voltage loss of LANL's MEA remained below 30 mV even after 70,000 cycles.

The ionomer dispersion work at LANL has a great potential to significantly improve the lifetime of PEM fuel cells [2–4]. However, the ionomer dispersion used was Nafion® 1100 EW; there has been a strong push in the industry towards lower EW membranes that can increase proton conductivity. Low EW ionomers are less dimensionally stable and could benefit more from Giner's well-established dimensionally-stable membrane (DSM™) technology. Also, the work at LANL has been done with dispersions of ionomer in the salt form, rather than in the proton form. This requires additional processing after membrane production to put the membrane in the acid form. Using dispersion from LANL in the acid form and utilizing Giner's DSM technology, this Phase I program validated this technology towards viable commercial applications in advanced fuel cell and electrolyzer systems.

APPROACH

The approach used for this project is shown in Figure 1. First, the ionomer dispersion technology invented by LANL was applied in the platforms of the DSM™ developed at Giner; the impregnation of the novel low EW ionomer dispersion into porous DSM supports has created more durable membranes with excellent proton conductivity for PEM fuel cells. Second, Giner will extend the ionomer dispersion studies to state-of-the-art PEM fuel cell catalysts. Most experiments performed at LANL were based on ETEK 20 wt% Pt supported on VULCAN® 72 (20% Pt/C). Giner will examine the ionomer dispersion technology paired with more advanced catalysts (e.g., Tanaka catalyst). Finally, the project will also investigate the impact of ionomer dispersion on PEM electrolyzer MEAs that generally use unsupported iridium (Ir) catalysts. Giner will perform MEA durability tests following the DOE AST protocols.

RESULTS

The DSM fabrication process [5] is described in Figure 2a. First, the dispersed Nafion® 1100 EW or 3M 825 EW solution was cast onto two pieces of Teflon™ film and then dried at the appropriate temperature (varying by solvent). The porous Kapton® film (DSM substrate) was sandwiched between two cast ionomer films and hot pressed at the appropriate pressure for transfer. The resultant ionomer film was then peeled off from the two Teflon™ substrates. All membranes were dried in a vacuum oven after fabrication at 120°C overnight to ensure complete solvent evaporation. The DSMs fabricated are shown in Figure 2b. These membranes can be placed into two categories (1100 EW and 825 EW) and vary in their thickness from 22 µm to 41 µm. Some of these DSMs were used for subsequent MEA fabrication and testing.

The MEA using Tanaka Pt/C catalyst (46.6 wt%), 3M 825 EW ionomer in dimethylacetamide, and DSM (865-32-1 in Figure 2b) was subjected to voltage cycling followed by AST recommended by DOE's Fuel Cell Technical Team (FCTT). The MEA was cycled from 0.6 V to 1.0 V at 50 mV/s for 30,000 cycles. Cyclic voltammograms (CVs) were obtained at different intervals to examine the ECSA change (see Figure 3a). The ECSA first increased until

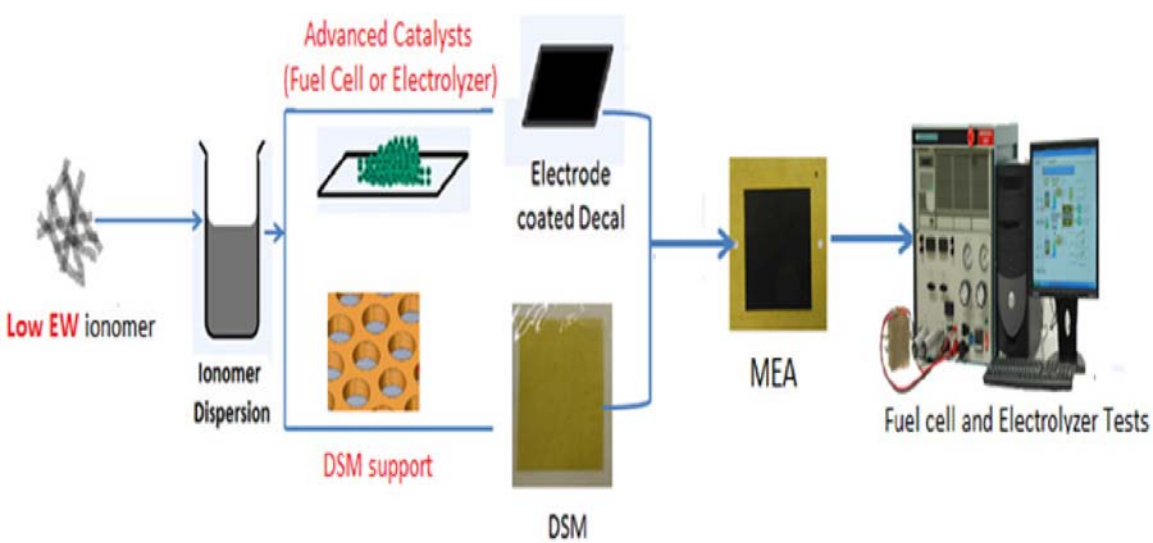

FIGURE 1. Technical approaches for PEM fuel cell and electrolyzer durability tests based on LANL's ionomer dispersion

(a)

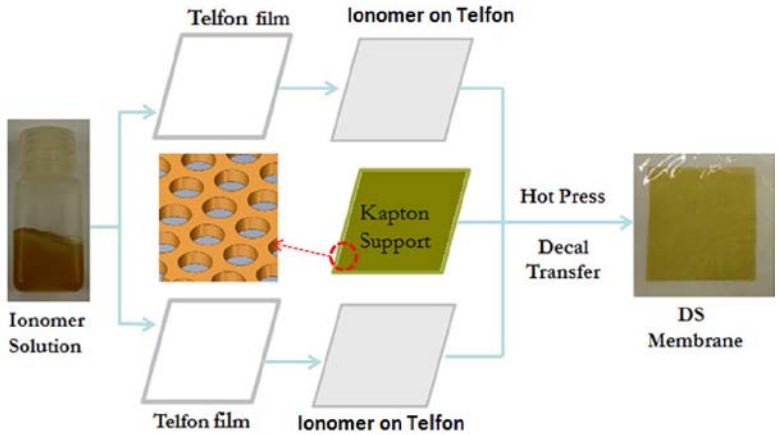

(b)

Membrane ID	865-15-1	865-18-1 865-29-1 865-30-1	865-17-1	865-32-1
Ionomer	5% N1100EW	5% N1100EW	2.5% 3M 825EW	2.5% 3M 825EW
Solvent	1, 2 Pentanediol	NMP	1, 2 Pentanediol	DMAc
Thickness	35 µm	22 µm	24 µm	41 µm
Color	Dark yellowish	Yellow	Yellow	Yellow

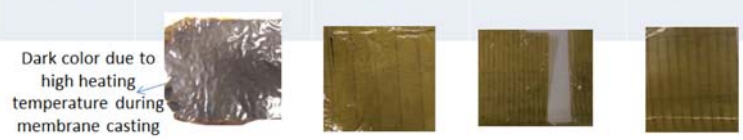

FIGURE 2. Fabrication of DSMs using Giner porous supports and LANL's ionomer dispersion: (a) illustration of DSM fabrication; (b) a list of fabricated DSMs and corresponding compositions

10,000 cycles; it was likely due to the MEA being not fully conditioned at the beginning of voltage cycling. The DSM-based MEA demonstrated outstanding electrochemical stability: the ECSA loss was only 10% from 10,000 cycles to 30,000 cycles. A twin MEA with identical compositions was subject to RH cycling to evaluate its mechanical stability, again following FCTT AST protocol. During the RH-cycling durability testing, the MEA was cycled from dry to oversaturated conditions. Cyclic and linear-sweep voltammograms were performed at certain points during the test to calculate hydrogen crossover. As shown in Figure 3b, the MEA demonstrated excellent mechanical stability after nearly 5,000 cycles, with hydrogen crossover less than 0.5 mA/cm^2, far smaller than FCTT recommended 2 mA/cm^2.

The durability of PEM electrolyzer MEAs using LANL ionomer dispersion was also examined. The anode of these MEAs was made of an oxygen evolution reaction (OER) catalyst and LANL Nafion® 1100 EW ionomer in N-Methyl-2-pyrrolidone. Two categories of OER catalyst were evaluated; one was commercial iridium (Ir) black and the second was a Giner developmental Ir supported on tungsten doped titanium oxide ($Ir/W_xTi_{1-x}O_2$). The latter has higher ECSA and demonstrates much higher mass activity. Both MEAs were subject to a voltage cycling routine Giner developed for electrolyzer stability evaluation: cycling from 1.4 V to 1.8 V with 5 min hold for each voltage. Polarization curves were obtained at regular intervals in the cycling campaign (see Figure 4). Both MEAs demonstrated good durability after 1,500 cycles. In particular, the MEA using $Ir/W_xTi_{1-x}O_2$ catalyst was very stable over the entire course of 10,000 cycles. These data suggests two advantages of the LANL ionomer: good tolerance to high voltage and compatibility between ionomer and Giner's Ir/ $W_xTi_{1-x}O_2$. This is extremely meaningful because the durability and low PGM loading from LANL ionomer and the advanced catalyst will significantly reduce the cost of electrolyzer stacks. Giner has started a 1-MW stack/system development program in collaboration with our major partners and targeting the manufacture and sale of PEM stacks and systems globally. The LANL ionomer dispersion will play a big role for this initiative and will be further studied in our Phase II project.

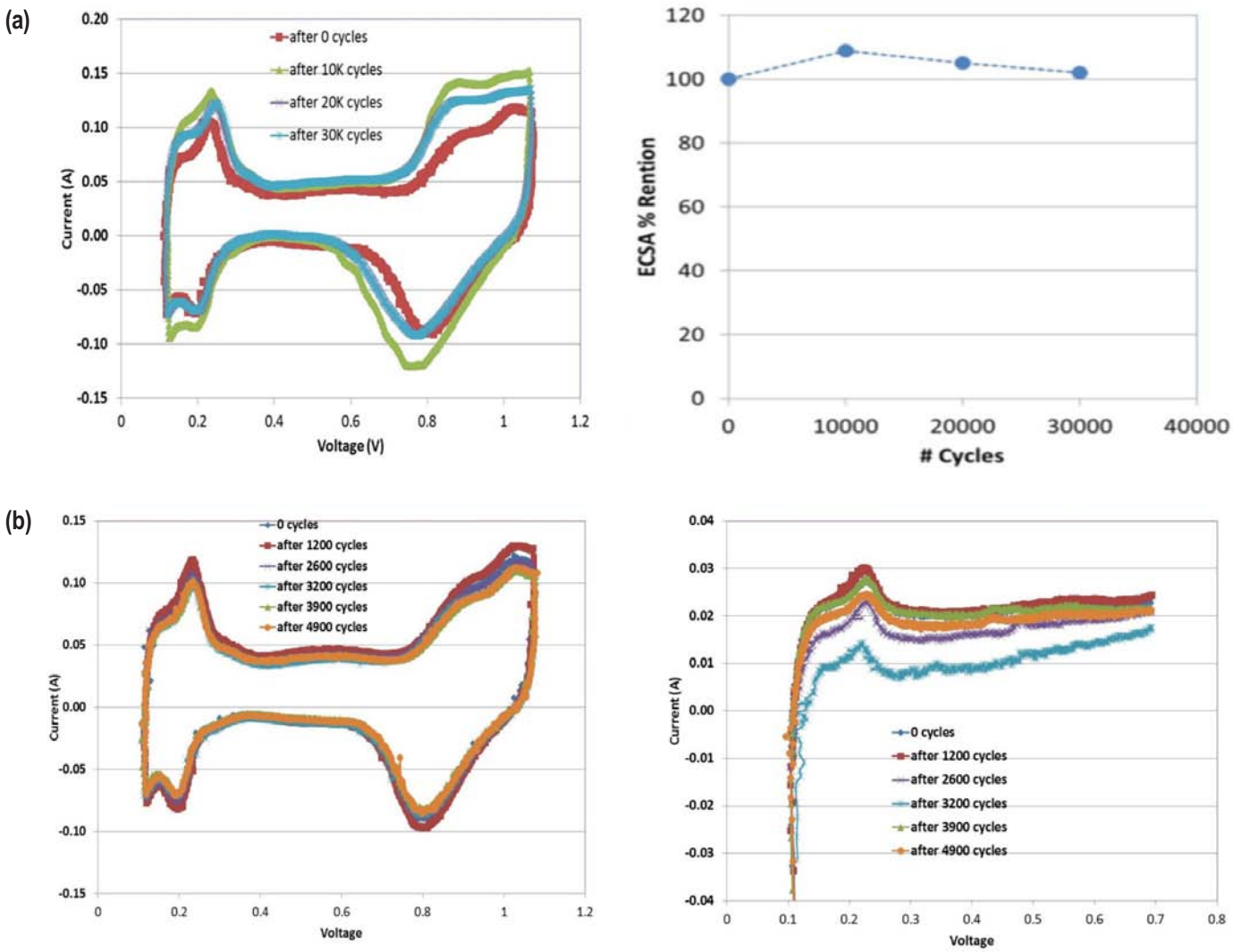

FIGURE 3. Chemical and mechanical durability of MEAs using DSM and LANL ionomer dispersion: (a) CVs and ECSA after voltage cycling: 0.6 V to 1.5 V, 50 mV/s; (b) CVs and hydrogen crossover after RH cycling from dry to saturated condition. Cell area: 50 cm^2; operating temperature: 80°C; cathode Pt loading: 0.4 mg/cm^2 from 46.6 wt% Tanaka Pt/C.

CONCLUSIONS AND FUTURE DIRECTIONS

Conclusions

- LANL non-aqueous ionomer dispersion technology has been validated at Giner in more scalable and processible conditions via DOE AST protocols.
- Hybrid membranes using Giner's DSM supports and LANL ionomer show good conductivity and improved mechanical properties.
- The combination of hybrid membrane and non-aqueous ionomer-based electrodes produces chemically and mechanically stable MEAs.
- The non-aqueous ionomer also demonstrates good compatibility with OER catalysts in electrolyzer, leading to excellent stability upon voltage cycling.

Future Direction

- Scale-up of non-aqueous ionomer dispersion production
- Scale-up of DSM-based MEA fabrication
  - Based on Giner's roll-to-roll DSM technology
- More durability tests in PEM electrolyzers
- Feasibility of licensing and commercializing LANL ionomer dispersion technology

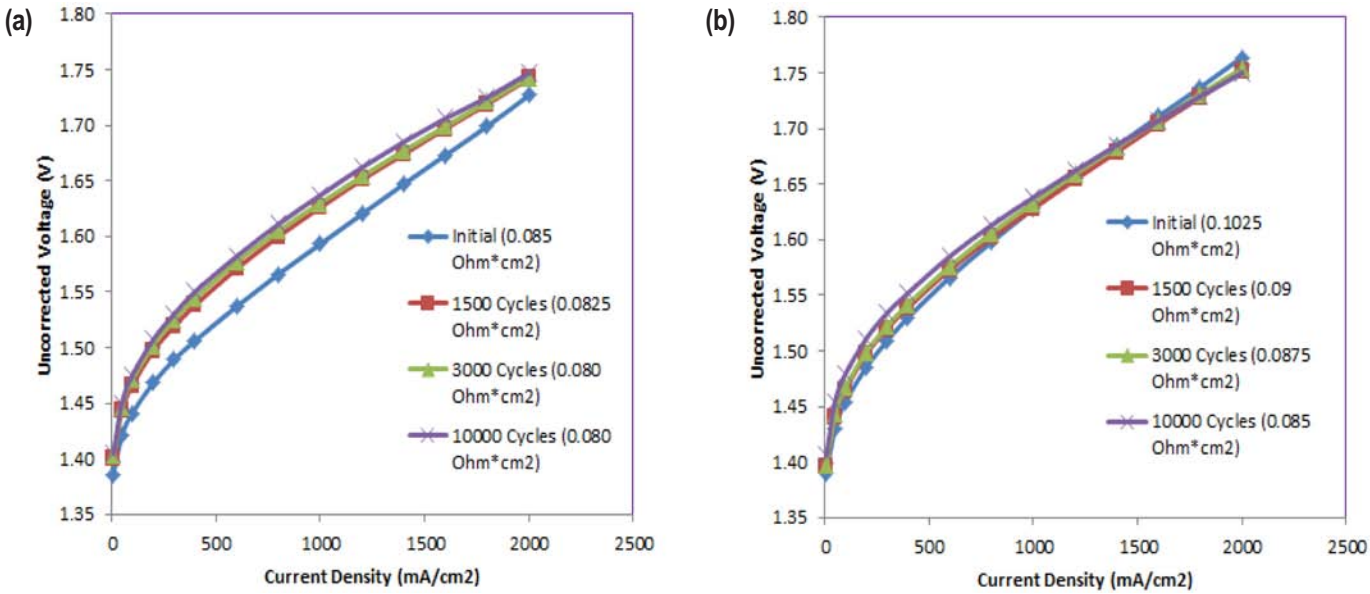

FIGURE 4. Durability of PEM water electrolyzer MEAs using LANL ionomer dispersion. Cell area: 50 cm^2; operating temperature: 80°C; anode catalyst: commercial Ir black or developmental $Ir/W_xTi_{1-x}O_2$, with Ir loading 0.4 mg/cm^2. Voltage cycling from 1.4 V to 1.8V.

FY 2015 PUBLICATIONS/PRESENTATIONS

1. Xu, H., J. Willey, T. McCallum, and Y.S. Kim, "Ionomer Dispersion Impact on Advanced PEM Fuel Cell Performance and Durability," STTR Phase I Final Report, U.S. Department of Energy Grant No. DE-SC0012049, March 2015.

2. Xu, H., "Ionomer Dispersion Impact on Advanced PEM Fuel Cell Performance and Durability," poster presentation in DOE Hydrogen and Fuel Cell Annual Merit Review meeting, Washington, D.C., June 2015.

REFERENCES

1. Brosha, E., F. Garzon, C. Johnston, A. Labourieau, Y.S. Kim, K.-S. Lee, B. Orler, B. Pivovar, D. Torraco, C. Welch, and H. Xu., "Studies Towards Optimizing Fuel Cell Electrode Structure and Composition," Canada to USA Fuel Cell and Hydrogen Cluster Connection Workshop, Vancouver, BC, Canada, February 16–17, 2009.

2. Kim, Y.S.; Lee, K.S.; Rockward T. U.S. Patent 7981319 B2, 2011.

3. Kim, Y.S.; Lee, K.S.; Rockward T. U.S. Patent 8236207 B2, 2012.

4. Kim, Y.S., Labouriau, A., Welch, A, Hjelm, R., and Mack, N., "Solvation and Gelation Process of Nafion," presented in the 216th Meeting of the Electrochemical Society, San Francisco, October 2013.

5. Mittelsteadt, C., Argun, A., Laicer, C., and Willey, J., U.S. Patent 20140342271A.

6. Welch, C., A. Labouriau, R. Hjelm, B. Orler, C. Johnston, and Y.S. Kim, "Nafion in Dilute Solvent Systems: Dispersion or Solution?" *ACS Macro Lett.*, 1, 1403−1407 (2012).

V.F.12 Novel Non-PGM Catalysts from Rationally Designed 3-D Precursors

Di-Jia Liu (Primary Contact), Heather M. Barkholtz
Argonne National Laboratory (ANL)
9700 S. Cass Ave.
Argonne, IL 60439
Phone: (630) 252-3533
Email: djliu@anl.gov

DOE Manager
Nancy Garland
Phone: (202) 586-5673
Email: Nancy.Garland@ee.doe.gov

Project Start Date: July 15, 2014
Project End Date: September 30, 2015

Overall Objectives

- To design, synthesize and evaluate highly efficient nonplatinum group metal (non-PGM) cathode catalysts using rationally designed three dimensional (3-D) precursors with significantly improved fuel cell performance
- To support non-PGM catalyst development through improved understanding on the structure–function relationship

Fiscal Year (FY) 2015 Objectives

- Complete the synthesis and optimization of zeolitic imidazolate framework (ZIF)-based catalysts with new precursor chemistries
  - Achieve membrane electrode assembly (MEA)/ single cell areal current density >200 mA/cm^2 at 0.8 $V_{iR\text{-}free}$ and >25 mA/cm^2 at 0.9 $V_{iR\text{-}free}$ under 1 bar O_2
- Complete the characterizations on precursors and catalysts and improve the understanding of structure–property relationship
- Complete catalyst activity improvement through synthesis and engineering process refinements
  - Achieve volumetric current density >95 A/cm^3 at 0.8 $V_{iR\text{-}free}$ in MEA/fuel cell test under 1 bar O_2

Technical Barriers

This project addresses the following technical barriers from the Fuel Cells section of the Fuel Cell Technologies Office (FCTO) Multi-Year Research, Development, and Demonstration Plan:

(A) Durability (of catalyst and fuel cell)

(B) Cost (replacement of Pt usage at cathode)

(C) Performance (improvement of non-PGM catalyst systems)

Technical Targets

This project aims at developing high efficiency, non-PGM materials as the low cost cathode catalyst replacements for platinum. Technical targets for this project are presented in Table 1.

TABLE 1. Current Status towards Meeting Technical Targets for non-PGM Electrocatalysts for Transportation Applications

Characteristic	Unit	2017/2020 Targets	ANL 2015 Status
Non-Pt catalyst activity per volume of supported catalyst	A /cm^3 at 800 $mV_{iR\text{-}free}$	300/300	108.7[a]

[a] Measured in single fuel cell: 5 cm^2 cell, $P_{O2} = P_{H2}$ = 1 bar at 100% relative humidity (gauge pressure = 7.3 psig); flowrate = 200 ml/min, T = 80°C, cathode loading = 2.5 mg/cm^2, anode loading = 0.3 mg-$_{Pt}$/cm^2, Nafion® membrane = 211.

FY 2015 Accomplishments

- We completed the synthesis and optimization of Fe-doped, ZIF-based non-PGM catalysts. The average areal current density of ten best performing fuel cells reached to 250 mA/cm^2 at 0.8 $V_{iR\text{-free}}$ under 1 bar oxygen, exceeding the goal by 25%. The best performing MEA achieved fuel cell current density of 29.5 mA/cm^2 at 0.9 $V_{iR\text{-free}}$ under 1 bar O_2, exceeding the goal by 18%.
- We completed the ZIF-based precursor and catalyst structure characterizations. A clear correlation between the catalyst surface area and the fuel cell limiting areal current density was observed.
- We completed catalytic activity improvement through alternative ZIF synthesis and engineering process optimization. A volumetric current density of 108 A/cm^3 was also achieved at 0.8 $V_{iR\text{-free}}$, surpassing the project goal.

✧ ✧ ✧ ✧ ✧

INTRODUCTION

Since Pt-based electrode catalyst contribute to nearly half of a fuel cell stack cost, finding inexpensive, earth-abundant materials as replacement of PGMs has been identified as a long-term goal by DOE FCTO for proton exchange membrane fuel cell research. For automotive

applications, DOE's 2017/2020 volumetric activity target for non-PGM catalyst is 300 A/cm^3 and the cost target is less than \$30/kW$_e$. Recently, transition metal doped nitrogen–carbon (TM-N-C) composites received a great deal of attention due to their more promising catalytic activity over other non-PGM materials. Generally, TM-N-C composites are prepared by applying TM-N$_x$ molecular complexes or polymers over amorphous carbon support, followed by thermal activation. Using the catalytically inert carbon support dilutes the active site density therefore limits the catalyst potential to reach the highest possible performance. At Argonne National Laboratory, we developed several new approaches in recent years to circumvent the dilution issue by using "self-supported" transition metal-organic compounds such as metal-organic frameworks (MOFs) or porous organic polymers (POPs) [1-4]. Since MOFs and POPs are intrinsically porous with potential active sites, TM-N$_4$, uniformly distributed and interconnected by organic linker, they have the potentials to produce the highest catalytic site density therefore the most active catalysts [5].

This project focuses on MOF-based non-PGM catalyst development. Although the concept of MOF-based electrocatalyst has been demonstrated, the catalyst preparations have yet to be optimized to reach their full potentials. Under this project, new synthesis and process methods and their operating parameters will be investigated to improve the catalyst performance. The catalysts prepared using the zeolitic imidazolate framework (ZIF, a subclass of MOF) are the focus of the investigation. We will enhance the catalyst activity over our own previous records and the benchmark materials by the others and demonstrate the improvement at the catalyst as well as MEA/fuel cell levels. The goal is to achieve fuel cell areal and volumetric current densities that meet or exceed the project's targets.

APPROACH

This project consists of three main approaches. They are (1) new composition chemistry, exploring new catalyst precursor by applying different organometallic complexes, organic additives and synthetic chemistry; (2) physical property investigation, understanding the structure–performance relationship through precursor and catalyst characterizations; and (3) process optimization, improving catalytic activity by optimizing of ZIF synthesis and posttreatment parameters.

The new composition chemistry focuses on exploring different transition metal complexes and/or nitrogen containing organic compounds as additives to ZIF precursor by infiltration or during direct synthesis. The impact of these additives to the catalyst performance will be evaluated through rotating disk electrode (RDE) and MEA measurements. The physical property study aims at correlating surface–electronic property and morphology between precursor and the catalyst using different characterization tools. The results will serve as guidance for new catalyst design and improvement. The processing optimization targets the controls of precursor and catalyst synthesis conditions to maximize catalyst activity and fuel cell performance.

RESULTS

Our ZIF-based catalyst preparation applies a low cost, "one-pot" solid state synthesis to incorporate transition metal precursor inside of ZIFs with well-defined crystal structure, followed by high temperature pyrolysis. Figure 1 shows an example of preparing Fe-doped non-PGM catalyst via Zn-based ZIF, Zn(mIm)$_2$. Zn(mIm)$_2$ has high porosity and

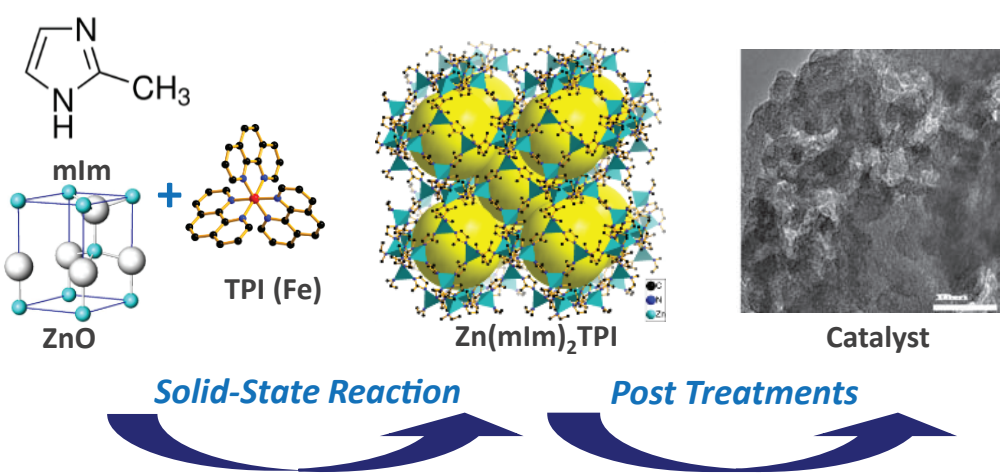

FIGURE 1. Schematics of one-pot synthesis of ANL's ZIF-based non-PGM catalyst by reacting methylimidazole (mIm), zinc oxide (ZnO), tris-1,10-phenanthroline iron(II) perchlorate (TPI) in solid state to form ZIF precursor, Zn(mIm)$_2$TPI, before pyrolyzed to catalyst.

internal surface area, which could serve as host to various TM organometallics or N-containing organic ligands. By incorporating such compounds into ZIF before thermal conversion, one could add additional active sites to further enhance the overall catalytic activity. Under this project, we have investigated several N-containing organic additives such as phenanthroline and polyaniline to $Zn(mIm)_2$. They were incorporated during the "one-pot" synthesis and were uniformly mixed inside or nearby ZIF's cavity. We found that these ligands could indeed enhance the catalyst activity when embedded to $Zn(mIm)_2$ prior to thermal activation, leading to higher oxygen reduction reaction (ORR) onset and halfwave potentials. For example, the addition of phenanthroline increased the catalytic ORR onset potential (E_0) from 0.91 V to 0.96 V and the halfwave potential ($E_{1/2}$) from 0.76 V to 0.82 V, respectively, measured by the RDE experiments.

The performance of non-PGM catalysts derived from ZIF-based precursors could also be influenced by the processing parameters from ZIF crystallization to pyrolysis. We devoted a significant amount of effort in the process optimization under this project. Since the improvement can only be properly gauged by fuel cell performance, we evaluated more than 100 MEAs to evaluate the catalyst activity. Our process optimization has led to substantial improvement in the catalyst and fuel cell performance. For example, Figure 2a shows the current-voltage polarization and power density distribution of a representative MEA prepared during the second quarter of FY 2015. The measurements were conducted under 1 bar oxygen at 80°C. For comparison, we also plotted the polarization and power density curves for the catalyst sample prepared at the project beginning. A major improvement has been achieved. In fact, the average areal current density measured over 10 selected MEAs has reached to 250 mA/cm^2 at 0.8 $V_{iR\text{-}free}$, compared to 178 mA/cm^2 observed at the project inception. This value represents a 40% improvement and exceeds our project target (200 mA/cm^2). We also measured the areal specific activity at 0.9 $V_{iR\text{-}free}$ and obtained the best value of 29.5 mA/cm^2, surpassing the project goal of 25 mA/cm^2. We also measured the volumetric activity of our best performing catalyst in fuel cell and achieved the specific current density of 108 A/cm^3 at 0.8$V_{iR\text{-}free}$ (Figure 2b). This is by far the best value for a non-PGM catalyst to our knowledge. In addition to oxygen, we investigated the catalyst performance in air. Figure 3 shows examples of current-voltage polarization and power density distribution of two MEAs prepared with two of our ZIF-based catalysts identical in composition but different in morphology. The fuel cell measurements were conducted under 1 bar air with 100% relative humidity (RH) at 80°C. The result clearly shows that the morphology has significant impact to fuel cell current and power densities even though good performances were observed in both cases. The best areal current activities were 148 mA/cm^2 at 0.8 $V_{iR\text{-}free}$ and 110 mA/cm^2 at 0.8 $V_{uncorrected}$, respectively.

We also carried out an extensive investigation on the structure–performance relationship of the ZIF-derived catalysts. Specifically, we prepared a series of ZIF-based non-PGM catalysts of different specific surface areas (SSAs) and tested their activities under fuel cell operating condition. Figure 4 shows the areal current densities at both 0.8 $V_{iR\text{-free}}$ and 0.2 $V_{\text{uncorrected}}$ as the functions of catalyst SSA. Positive correlations were found between the current densities and the SSA, particularly at the mass–transport limiting region (0.2 V). Such observation supports the hypothesis that

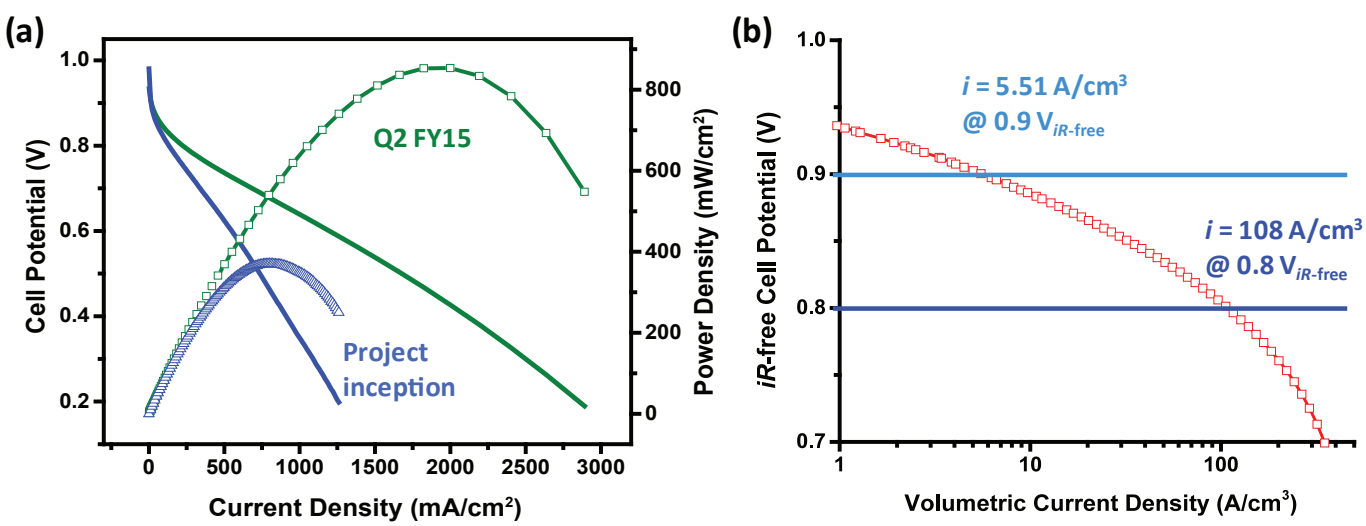

FIGURE 2. (a) Comparison of the current-voltage polarizations and power densities of the fuel cells tested at the project start and at the end of Q2 FY 2015. (b) Volumetric current density of a representative ANL non-PGM catalyst measured in a MEA/fuel cell test. Conditions: $P_{O2} = P_{H2}$ = 1 bar (back pressure = 7.3 psig) fully humidified; Flowrate $_{O2}$ = Flowrate $_{H2}$ = 200 ml/min; T = 80°C; N-211 membrane; 5 cm^2 MEA; cathode catalyst = 3.5~4 mg/cm^2, anode catalyst = 0.4 mg_{Pt}/cm^2.

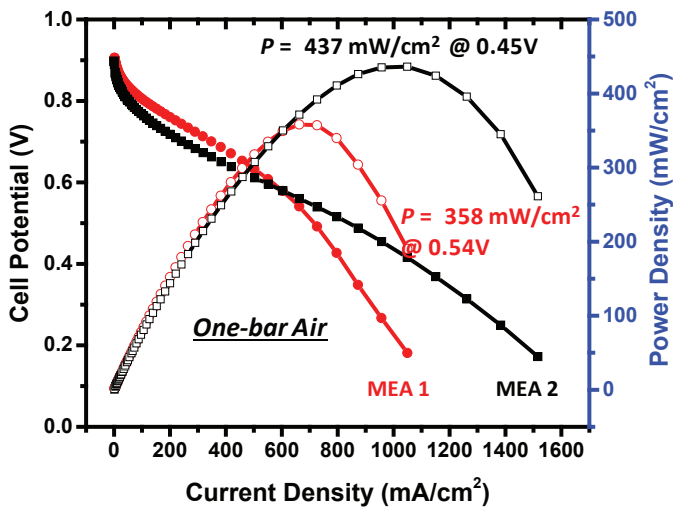

FIGURE 3. The current-voltage polarizations and power densities of two representative MEAs with ZIF-derived cathode catalyst tested in fuel cells. Conditions: $P_{air} = P_{H2}$ = 1 bar (back pressure = 7.3 psig) 100 RH; T = 80°C; N-211 membrane; 5 cm^2 MEA; cathode catalyst = 3.5 mg/cm^2, anode catalyst = 0.4 mg_{Pt}/cm^2.

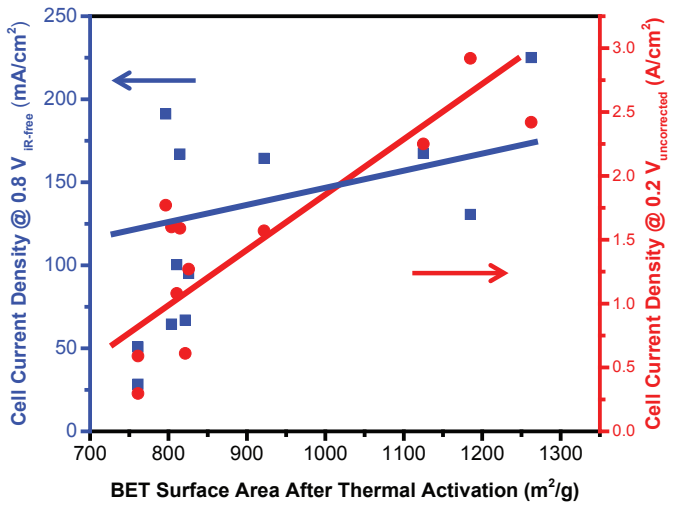

FIGURE 4. Fuel cell areal current densities measured at 0.8 V and 0.2 V as the functions of Brunauer-Emmett-Teller surface area of non-PGM cathode catalysts.

the active sites in the ZIF-derived catalyst are uniformly decorated on the micropore surface with their numbers proportional to the total SSA. This is in contrast to that of Pt-based catalysts.

CONCLUSIONS AND FUTURE DIRECTIONS

- The team has met and exceeded all the project milestones.
- ANL's ZIF-derived non-PGM catalyst achieved areal specific activity of 250 mA/cm^2 at 0.8 $V_{iR\text{-free}}$, 29.5 mA/cm^2 at 0.9 $V_{iR\text{-free}}$ and volumetric activity of 108 A/cm^3 at 0.8 $V_{iR\text{-free}}$ when tested in fuel cell at 80°C under fully humidified 1 bar O_2, all exceeded the project goals.
- Tested under fully humidified 1 bar air at 80°C, ANL's ZIF-derived non-PGM catalyst achieved areal current density of 148 mA/cm^2 at 0.8 $V_{iR\text{-free}}$ or 110 mA/cm^2 at 0.8 $V_{uncorrected}$.
- A structure–property characterization study identified the correlation between the catalyst specific surface area and the fuel cell current density, revealing a key difference in active site distribution between non-PGM and PGM catalysts.
- During the project, ANL team filed three United States patent applications, received two granted United States patents and published three peer-reviewed journal articles.

ANL's ZIF-based non-PGM catalysts open up the following research directions:

- Improving catalytic activity and durability through new organic ligand and organometallics choices including nonferrous metals
- Improving catalyst activity/durability through new MOF/ZIF design, synthesis and conversion
- Better mass/charge transport and water management through new morphology and electrode architecture such as interconnected nano-network

SPECIAL RECOGNITIONS & AWARDS/ PATENTS ISSUED

1. "Non-platinum group metal electrocatalysts using metal organic framework materials and method of preparation," Di-Jia Liu, Shengqian Ma, Gabriel Goenaga, **US Patent 8,835,343**.

2. "Electrocatalysts using porous polymers and method of preparation," Di-Jia Liu, Shengwen Yuan, Gabriel Goenaga, **US Patent 9,012,344**.

3. "Nanofibrous Electrocatalysts," Di-Jia Liu, Jianglan Shui, Chen Chen, **US Patent Application 20140093790**.

4. "Non-Platinum Group Metal Electrocatalysts Using Metal Organic Framework Materials and Method of Preparation," Di-Jia Liu, Shengqian Ma, Gabriel Goenaga, **US Patent Application 20150056536**.

5. "Non-Platinum Group Metal Electrocatalysts Using Metal Organic Framework Materials and Method of Preparation," Di-Jia Liu, Shengqian Ma, Gabriel Goenaga, Dan Zhao, **US Patent Application 20150180045**.

6. "Electrocatalysts Using Porous Polymers and Method of Preparation," Di-Jia Liu, Shengwen Yuan, Gabriel Goenaga, **US Patent Application 20150194681**.

7. Student Poster Award First Place - Solid State Science and Technology to Heather Barkholtz for her research on "Highly Active Non-PGM Catalysts Prepared from Metal-Organic Frameworks," under Di-Jia Liu at Argonne National Laboratory, 227th ECS Spring Meeting, Chicago, IL, May 24–28, 2015

FY 2015 PUBLICATIONS/PRESENTATIONS

1. "High-efficiency non-precious metal catalyst containing metal-organic framework precursor inside of carbon nano-network," Jianglan Shui, Chen Chen, Lauren R. Grabstanowicz, Dan Zhao and Di-Jia Liu, *Proceedings of National Academy of Sciences, USA* (2015), vol. 112, no. 34, 10629–10634.

2. "Highly Active Non-PGM Catalysts Prepared from Metal-Organic Frameworks," Heather M. Barkholtz, Lina Chong, Zachary B. Kaiser, Tao Xu, and Di-Jia Liu, Invited Contribution to Special issue on Polymer Electrolyte Membrane Fuel Cell in *Catalysis 5*, 955-965, (2015) doi:10.3390/catal5020955.

3. "Catalytic Reaction on FeN4/C Site of Nitrogen Functionalized Carbon Nanotubes as Cathode Catalyst for Hydrogen Fuel Cells," Feng Gao, Guang-Lin Zhao, Zhou Wang, Diola Bagayoko, Di-Jia Liu, *Catalysis Communications* 62, 79–82, (2015) doi:10.1016/j.catcom.2015.01.015.

4. "Non-Precious Metal Fuel Cell Catalysts Prepared By Rationally Designed Porous Materials," Heather Barkholtz, Lina Chong, Dan Zhao, Di-Jia Liu, Conference paper at 5th European Fuel Cell Forum, 2015.

5. "MOFs and POPs – Two new classes of porous precursors for highly efficient non-PGM catalyst design and synthesis," Di-Jia Liu, Invited presentation at *Electrocatalysis and Fuel Cell Discussion*, La Grande Motte, France, September 13–16, 2015.

6. "Novel Non-PGM Catalysts from Rationally Designed 3-D Precursors," Di-Jia Liu, Poster presentation at 2015 DOE Hydrogen and Fuel Cells Program and Vehicle Technologies Office Annual Merit Review and Peer Evaluation Meeting, Washington, D.C., June 8–12, 2015.

7. "Highly Active Non-PGM Catalysts Prepared from Metal-Organic Frameworks," Heather M. Barkholtz, Zachary Kaiser, Di-Jia Liu, Poster at 227th Electrochemical Society Meeting, Chicago, IL May 24-28, 2015.

8. "New Material Chemistries and Structural Investigations for Next-Generation Energy Storage and Conversion Applications," Di-Jia Liu, Department of Chemistry Seminar, University of Illinois at Chicago, February 26, 2015.

9. "Oxygen Reduction Reactions in Fuel Cell & Li-Air Battery: Insights of New Catalyst Design & Catalytic Mechanism," Di-Jia Liu, College of Engineering Seminar, Peking University, Beijing, China, Sept. 23, 2014.

10. "Recent Developments in New Materials and Characterization Techniques for Energy Storage and Conversion," Di-Jia Liu, Department of Chemistry Seminar, University of Nebraska - Lincoln, Oct. 20, 2014.

11. "Recent advancements in non-precious metal fuel cell catalysts prepared by rationally designed porous materials," Di-Jia Liu, Plenary talk at *XIV International Congress of the Mexican Hydrogen Society,* Cancun, Mexico, October 2, 2014.

REFERENCES

1. S. Ma, G. Goenaga, A. Call and D.-J. Liu, *Chemistry: A European Journal* **17,** 2063 (2011).

2. D. Zhao, J.-L. Shui, C. Chen, X. Chen, B.M. Reprogle, D. Wang and D.-J. Liu, *Chem. Sci.*, **3** (11), 3200 (2012).

3. D. Zhao, J.-L. Shui, L.R. Grabstanowicz, C. Chen, S.M. Commet, T. Xu, J. Lu, and D.-J. Liu, *Advanced Materials*, **26** 1093 (2014).

4. S. Yuan, J.-L. Shui, L. Grabstanowicz, C. Chen, S. Commet, B. Reprogle, T. Xu, L. Yu and D.-J. Liu, *Angew. Chem. Int. Ed.*, **52**(32), 8349 (2013).

5. E. Proietti, F. Jaouen, M. Lefèvre, N. Larouche, J. Tian, J. Herranz and J.-P. Dodelet, *Nature Comm*. **2**, 416 (2011).

V.F.13 PGM Free Catalysts for PEMFC

Héctor R. Colón-Mercado (Primary Contact),
Jay B. Gaillard
Savannah River National Laboratory
Building 999-2W
Aiken, SC 29808
Phone: (803) 645-7819
Email: Hector.Colon-Mercado@srnl.doe.gov

DOE Manager
Gregory Kleen
Phone: (720) 356-1672
Email: Gregory.Kleen@ee.doe.gov

Project Start Date: July 1, 2014
Project End Date: September 15, 2015

Overall and Fiscal Year (FY) 2015 Objectives

- Synthesize nitrogen activated metal complexes on a novel nanocarbon support in a single step process that is easily scalable and market relevant with highly active, low cost non-platinum group metal (non-PGM) catalysts
- Use chemical vapor deposition (CVD) to produce nitrogen doped carbon nanotube (NCNT) catalysts with surface morphology specifically tailored to maximize oxygen reduction reaction (ORR) catalyst site density
- Use traditional non-PGM preparation techniques to identify and down-select nitrogen and carbon precursors for CVD synthesis
- Increase surface area and enhance catalyst activity by exfoliating the NCNT surface during CVD synthesis using oxidative or catalytic hydrogenation

Technical Barriers

This project addresses the following technical barriers from the Fuel Cells (3.4.5) section of the Fuel Cell Technologies Office Multi-Year Research, Development, and Demonstration (MYRDD) Plan:

(A) Durability (catalyst)

(B) Cost (catalyst)

(C) Performance (catalyst)

Technical Targets

Non-PGM fuel cell catalyst research in this project focuses on the DOE technical targets outlined in Table 3.4.13 (Technical Targets: Electrocatalysts for Transportation Applications) in section 3.4.4 (Technical Challenges) of the Fuel Cell Technologies Office MYRDD Plan. The technical targets of the project are as follows.

- Volumetric catalyst activity in a membrane electrode assembly (MEA) at 0.80 $V_{iR\text{-}free}$, 80°C: ≥300 A cm^{-3} (2020 target)
- Demonstrate performance of non-PGM catalysts prepared using CVD system with the potential to meet 6 A cm^{-3} under rotating ring disk electrode (RRDE) at 0.8 V in acid solutions (near-term)
- Use a single step, highly scalable process to decrease the cost of producing non-PGM catalysts (near-term)
- Demonstrate a favorable $4e^-$ reaction pathway (near term)

FY 2015 Accomplishments

- In situ nitrogen doping of carbon nanotubes was performed using CVD with simultaneously injected liquid and gas nitrogen containing precursors. Using pyridine as the liquid precursor, the ensuing catalyst's ORR onset potential was found to occur at 0.95 V (vs. reversible hydrogen electrode [RHE] in 0.1 M $HClO_4$) as compared to previously reported values of 0.35 V [1]. In addition, high pyridinic nitrogen content (~50%) was measured in the catalyst using X-ray photoelectron spectroscopy (XPS).
- A significant increase in electrochemical surface area (ESA) and ORR activity was observed with increasing CVD growth temperature (750°C to 850°C). A kinetic current density maximum of 1.0 A cm^{-3} at 0.8 V was measured for NCNTs grown at 850°C. The number of electrons transferred for the ORR was measured to be >3.8 showing a high selectivity for the $4e^-$ reaction.
- Oxidative partial unzipping of the 750°C grown NCNTs resulted in a 2.5x increase in ORR kinetic current at 0.8 V and a 10x increase in ESA while maintaining the three dimensional architecture of the pristine carbon nanotubes (CNTs).
- Traditional synthesis techniques were used to optimize CVD precursor formulations. Diazines were identified as a promising nitrogen/carbon precursor for synthesizing electrocatalysts. XPS analysis of Fe-diazine catalysts shows uncommonly high pyridinic nitrogen content (~50%). The catalyst shows high selectivity for the $4e^-$ ORR pathway with the number of electrons measured at >3.6.
- An amination pyrolysis for metal-free graphene-oxide electrocatalysts was demonstrated, resulting in an ESA increase of 50x and an ORR current increase of 2.5x at 0.8 V vs. RHE.

✧ ✧ ✧ ✧ ✧

INTRODUCTION

Reducing the high cost of the proton exchange membrane fuel cell (PEMFC) stack, which accounts for more than 50% of the total system cost, is currently a major focus of fuel cell research. The high stack cost is in large part due to the high cost of platinum catalysts which accounts for approximately half of the stack cost. This platinum-based cost component cannot be reduced through economies of scale, would likely be driven up through increased demand, and introduces geopolitical challenges. Reducing the PEMFC stack cost is typically achieved through decreasing platinum cathode loading, where slow ORR kinetics must be addressed, or by replacing platinum catalysts with non-PGM catalysts.

Eliminating platinum entirely from the cathode is the ideal solution to this problem, as it could result in the most significant reduction in stack cost; however, to date non-PGM catalysts show inferior performance compared to platinum catalysts, particularly in acidic media. The best performing non-PGM catalysts are typically composed of carbon, nitrogen, and transition metals (e.g., iron or cobalt), and usually employ a high temperature thermal treatment. The precise identity of the M-N-C catalysts' ORR site is under debate, but there are indications that the sites are composed of pyridinic or pyrrolic heterocycles coordinated through nitrogen to a transition metal, with pyridinic heterocycles showing the highest activity.

APPROACH

To facilitate an easily scalable and market relevant non-PGM catalyst with high ORR activity, our approach centers on the use of CVD to tailor nitrogen doped carbon nanotubes specifically designed to possess a high density of ORR catalyst sites via in situ doping and in situ surface enhancement treatments. This work differs from traditional methods by synthesizing both catalyst and support with well controlled surface morphology in a highly scalable single step growth process instead of first creating and modifying a support through multiple process-intensive steps, which ultimately leads to poor scalability and high cost. A major benefit of our approach is maintaining economic viability without compromising performance. Current, state-of-the-art, commercial CVD production of multi-walled carbon nanotubes costs approximately $20 per gram, with economy of scale projections estimated as final production costs as low as $0.33 to $1.00 per gram.

Figure 1 shows a simplified schematic that details the catalyst production process. During the production process, metal and nitrogen precursors are injected via spray pyrolysis in to the reaction zone where the carbon based catalysts deposit. It is during the growth that graphene edges are further exposed by oxidation and/or catalytic H_2 opening of the NCNT structure via surface roughening.

RESULTS

During FY 2015, our work focused on preparing and characterizing non-PGM catalysts using traditional synthesis techniques, identifying and down selecting nitrogen and carbon precursors for use in CVD synthesis, assembling and fine tuning a specialized CVD system, and preparing catalysts using CVD. Optimization and development using traditional synthesis techniques provides chemical and structural information on potential precursors that can be utilized in CVD synthesis to make highly active ORR catalysts of the Fe-N-C type. Carbon supports were combined with iron (II) acetate and nitrogen precursors which included amines (primary, secondary), nitrogen heterocycles (pyridine, bipyridine, phenanthroline, diazines, polyazines), urea, selenourea, metal organic framework synthesis templates (polyaniline, polyethylene amine), and macrocycles (functionalized phthalocyanines). Of the screened catalysts, the Fe-diazine catalysts exhibited the highest kinetic current

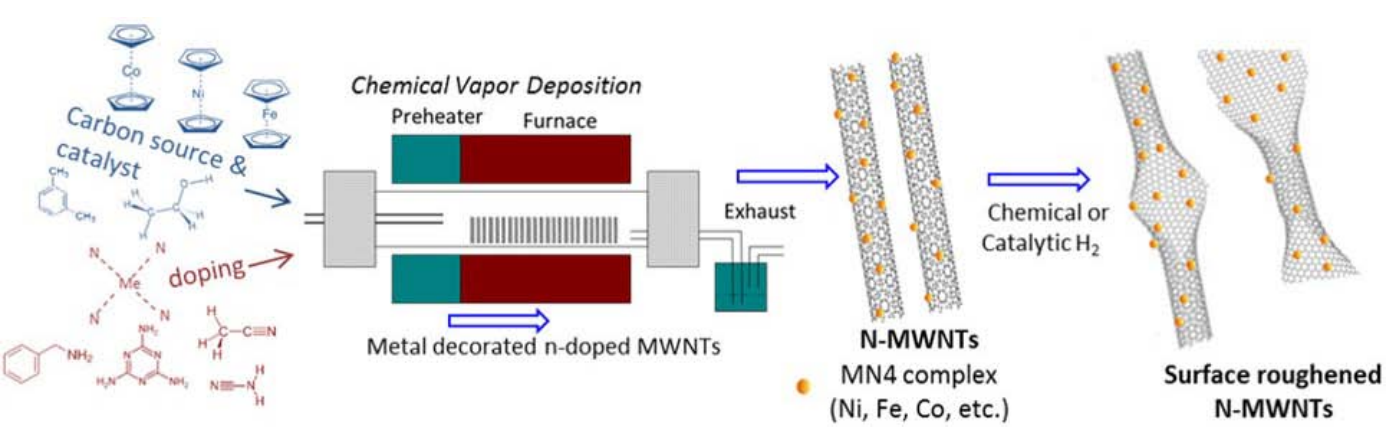

FIGURE 1. Simplified schematic of the one step process for the production of ORR active catalysts

densities (Figure 2), with higher current densities measured following a post synthesis amination pyrolysis. XPS analysis shows the highly active Fe-diazine electrocatalyst has a high atomic percent of pyridinic nitrogen (47.4–51.9%).

In parallel with the traditional synthesis work, the CVD system was assembled and fine-tuned to produce carbon nanotubes using nitrogen and carbon precursors identified through traditional synthesis. Analysis of nanotubes prepared by CVD show excellent performance for the ORR, with initial trends indicating higher performance is achievable once optimization is completed. A major accomplishment during 2015 includes synthesizing catalysts with a one-step CVD growth method that incorporates a high surface concentration of nitrogen (Figure 3), about 5 at%, of which more than 50% is pyridinic. It is noteworthy that there are only a handful of non-PGM catalysts possessing such a high atomic percent of pyridinic nitrogen, and none produced in a single step synthesis.

Scanning electron microscopy (SEM) and transmission electron microscopy (TEM) images (Figure 4a and 4b) show the typical compartmentalized "bamboo"-like morphology of the nitrogen-doped CNTs. The NCNT catalyst grown at 750°C was treated with a mild oxidizer resulting in surface roughening and partial opening of the CNTs, observable by SEM as shown in Figure 4c. Electrochemical analysis of the catalysts prepared via CVD shows high performance in the ORR. As shown in Figure 5 (left), the onset potential for the ORR is around 0.95 V vs. RHE. Catalyst activity increases as a function of pyrolysis temperature. This trend suggests that catalysts with higher activity can be reasonably expected with further optimization of the method. Initial cyclic voltammetry (CV) experiments (cycling 0.05 V to 1.1 V) show unusually high peak current/ESA ratios for the redox couple at 856 mV (Figure 5, left-inset), believed to be of the $Fe^{II/III}N_x$ (x = 2 or 4) type, which is stable even under acidic conditions (0.1 M $HClO_4$). The stability of this moiety is attributed to the formation of stable coordination complexes where pyridinic nitrogen coordinates to Fe^{II} and the pyridine π orbital provides additional stabilization through the sp^2 hybridized carbon support. The surface roughening treatment results in a substantial increase in ESA which can be observed in the CV (Figure 5, right-insert) and increases the number of available active sites resulting in an ORR activity enhancement, shown in Figure 5 (right). Currently, surface roughening treatments for optimizing the higher activity 850°C N-doped CNT samples are underway. The increased onset potential for the ORR at higher growth temperatures as seen in linear sweep voltammetry (LSV) measurements in conjunction with the increased ESA achieved through surface

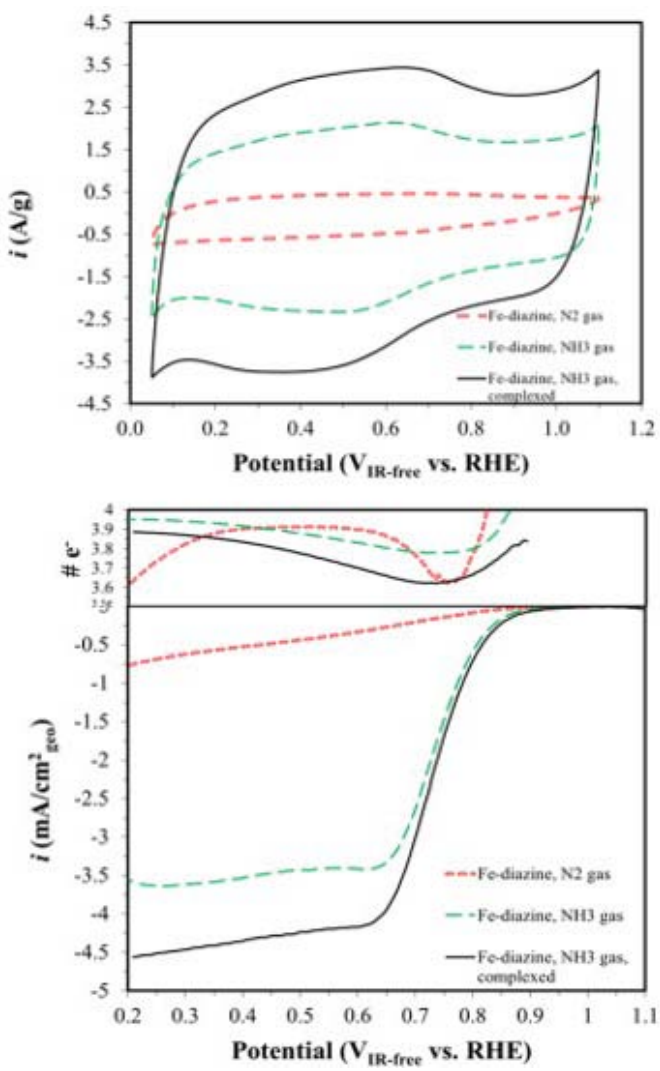

FIGURE 2. Fe-diazine catalyst before and after amination pyrolysis. (top) CV shows ESA and (bottom) RRDE disc current shows ORR activity and number of electron transferred.

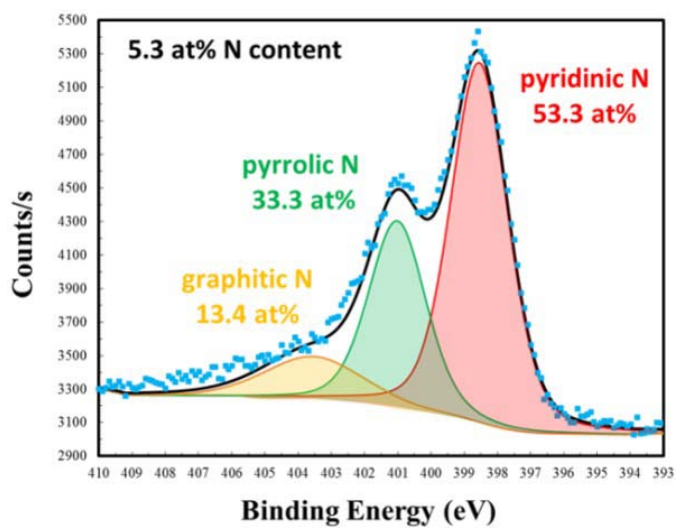

FIGURE 3. XPS N1s spectra of non-PGM catalyst grown in the CVD setup, image shows high pyridinic surface nitrogen

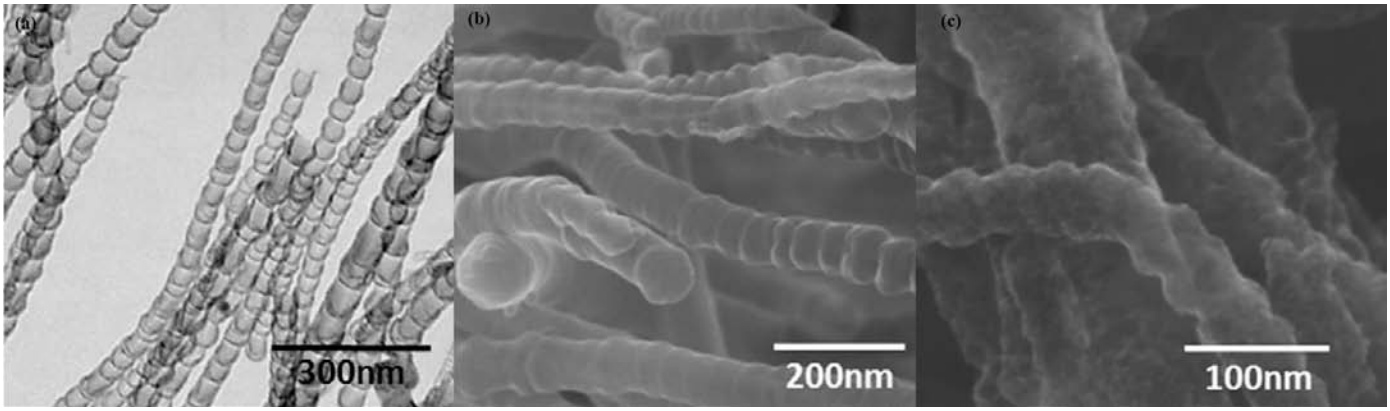

FIGURE 4. (a) TEM and (b) SEM of as grown bamboo-like NCNTs, (c) partially unzipped NCNTs exhibiting surfacing exfoliation with graphene edges

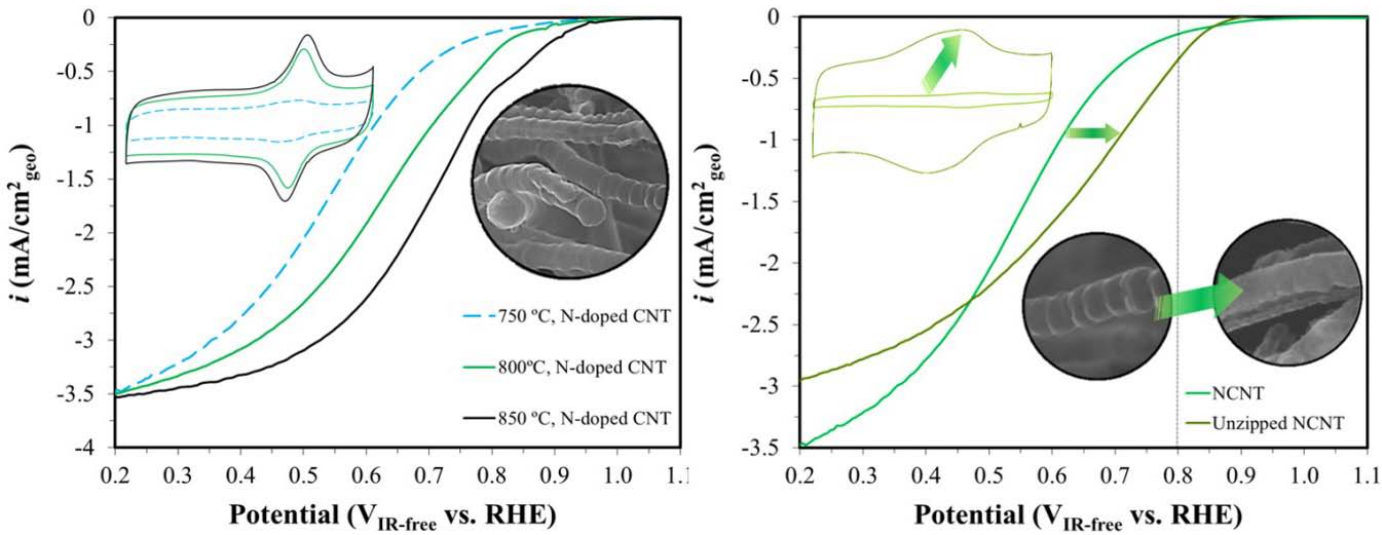

FIGURE 5. (left-inset) CV demonstrates high current/ESA redox couple at ~850 mV. (left) LSV measured ORR activity for the CVD-grown catalysts. (right-inset) CV demonstrates electrochemical active surface area enhancement achieved through chemical roughening methods. (right) ORR activity comparison for the CVD prepared catalyst and after surface roughened catalyst. SEM images show the typical morphology of the tested catalysts.

roughening/unzipping treatments both indicate that further optimization holds potential for producing higher activity catalysts and trends that will approach the DOE performance target.

CONCLUSIONS AND FUTURE DIRECTIONS

- We established a novel non-PGM catalyst production process based on CVD that is highly scalable, economically viable, and produces an active catalyst for the ORR with a high density of catalyst sites and high selectivity for the $4e^-$ reaction (# e^- transferred >3.8).
- Analysis of nanotubes prepared by CVD show excellent performance for the ORR, with initial trends indicating higher performance is achievable once optimization is completed.
- We will continue development of novel CVD growth mechanisms that can accomplish the following.
  - Increase surface area and alter active site morphology through mild surface roughening or opening of nanotubes through in situ gaseous or ex situ mild chemical treatments
  - Characterize the effect of higher temperatures and different nitrogen precursors on active site morphologies, oxidation states, and electrochemically active surface area
  - Incorporate novel non-PGM bimetallic catalysts using in situ and ex situ synthesis techniques

- We will study the high potential redox couple at 850 mV and determine if there is a correlation with the ORR onset potential or the kinetic current using the high peak current/ESA ratio as a handle.

REFERENCES

1. H. Drew, M. Doralice, and C. Zhongwei, *J. Phys. Chem. C*, 114 (2010) 21982–21988.

V.F.14 High Performance and Durable Low PGM Cathode Catalysts

Yong Wang[1] (Primary Contact), Jun Liu[1], Yuyan Shao[1], Yingwen Cheng[1], Rod Borup[2], Tommy Rockward[2], Eric Lanich Brosha[2]
[1]Pacific Northwest National Laboratory
902 Battelle Blvd.
Richland, WA 99352
Phone: (509) 371-6273
Email: yong.wang@pnnl.gov
[2]Los Alamos National Laboratory
Los Alamos, NM 87545

DOE Manager
Donna Ho
Phone: (202) 586-8000
Email: Donna.Ho@ee.doe.gov

Project Start Date: October 1, 2014
Project End Date: September 30, 2015

Overall and Fiscal Year (FY) 2015 Objectives

- Increase mass activity and durability of platinum-based electrocatalysts through three-dimensional (3-D) porous low platinum group metal (PGM) electrocatalysts
- Demonstrate improved performance and durability in fuel cell tests
- Provide pathway to achieve DOE 2020 electrocatalyst target

Technical Barriers

This project addresses the following technical barriers from the Fuel Cells section of the Fuel Cell Technologies Office Multi-Year Research, Development, and Demonstration Plan:

(A) Durability

(B) Cost

Technical Targets

This project addresses fuel cell durability and cost (activity) technical barriers through engineering 3-D porous graphene supported nanocomposite platinum catalysts. The goal of this project is to demonstrate that the enhanced durability and performance of our triple-junction stabilized platinum electrocatalysts obtained from ex situ tests can be successfully achieved in fuel cell device test. The specific targets and status are shown in Table 1.

TABLE 1. Project Targets and Status of Electrocatalysts

	RDE test		MEA test	
	Project Target	Project Status	Project Target	Project Status
ORR Activity	80 mA/mg_{Pt}	137 mA/mg_{Pt}	80 mA/mg_{Pt}	On-going
Durability	20% increase	186% (ESA), 275% (ORR)	<20% loss in activity after 1.2 V hold test.	On-going
Carbon Corrosion	NA	NA	2X reduction in carbon corrosion over baseline	On-going

RDE – rotating disk electrode; MEA – membrane electrode assembly; ORR – oxygen reduction reaction; NA – not applicable; ESA – electrochemical surface area

FY 2015 Accomplishments

- Coated platinum nanoparticles uniformly on porous 3-D indium tin oxide (ITO)-graphene nanocomposite using both vapor deposition method and chemical solution method
- Demonstrated enhanced activity (1.5X) and durability (2X) of Pt-ITO-porous graphene in rotating disk electrode (RDE) test
- Improved the durability further of graphene through thermal annealing (transmission electron microscopy [TEM] imaging indicates no sintering of platinum during thermal annealing)
- In situ fuel cell (MEA) tests show much higher performance of 3-D graphene-based electrocatalysts than that of two-dimensional (2-D) graphene that was obtained in our previous project, but also indicate instability of ITO at elevated temperature.

✧ ✧ ✧ ✧ ✧

INTRODUCTION

There is a strong need to decrease the amount of platinum electrocatalyst used in fuel cells and increase its durability for transportation application. Conventional strategies include platinum nanocrystals and platinum alloy with well-controlled structures, durable carbon support, non-carbon support, etc. We have developed the so-called "metal-metal oxide-carbon" triple junction concept to stabilize platinum and protect carbon from corrosion [1]. It also improved the activity of platinum. Good performance was not achieved in fuel cell testing mainly because of the transport issue due to the use of 2-D graphene. In this project, our main goal is to demonstrate the concept in fuel cell

device test using 3-D porous graphene as support so that the transport issue could be addressed.

APPROACH

Our approach includes engineering 2-D graphene into a 3-D architecture and using directly synthesized 3-D porous graphene from a scalable method to address the transport issue in fuel cell tests while maintaining the advantage of our concept of using the triple-junction structure to stabilize platinum electrocatalysts and protect carbon from corrosion. The chemical solution coating processes of metal oxides and Pt catalysts are scalable.

RESULTS

We have intensively studied the porous 3-D Pt-ITO-graphene electrocatalysts. First, we successfully synthesized uniformly dispersed ITO nanoparticles (5─8 nm) on 3-D porous graphene (Figure 1a). Platinum nanoparticles were uniformly deposited onto ITO-graphene using both the chemical solution method (Figure 1b) and the vapor deposition method (Figure 1c). A close inspection of the porous 3-D Pt-ITO-graphene electrocatalyst reveals its detailed structure. Most of the platinum nanoparticles stay around the ITO nanoparticles, indicating a triple-junction structure is formed (Figure 1d). This result is consistent with what we have achieved on the 2-D graphene substrate.

Further investigation reveals that the 3-D porous Pt-ITO-graphene has very high resistance to thermal annealing (Figures 2a and 2b) while the platinum on carbon support without ITO has severe sintering (Figures 2c and 2d). These results indicate that ITO nanoparticles stabilize platinum nanoparticles against thermal sintering. Thermal annealing is a well-known strategy to improve catalyst performance generally (activity and durability). This provides more room to tune the electrocatalysts.

Ex situ RDE electrochemical test results show high oxygen reduction reaction (ORR) performance of Pt-ITO-graphene, particularly the durability (Figure 3). After thermal annealing, the durability of Pt-ITO-graphene was further increased with only a slight decrease in activity. The electrochemical results are consistent with our TEM analysis. These results indicate the concept of using metal-metal oxide-carbon triple-junction structure to stabilize and improve the performance of platinum electrocatalysts is applicable for porous 3-D substrates. This revelation is significant because the porous 3-D architecture is more applicable in fuel cell devices.

From in situ fuel cell (MEA) tests, the 3-D Pt/graphene shows much better performance than the 2-D Pt/graphene that was obtained in our previous project, which was published in Reference 2. In the high current density operating region—for example, at cell voltage of 0.4 V—the Pt/2-D_graphene from the previous project [2] in an H_2/O_2 cell delivered 310 mA/cm$_2$. The Pt/3-D_graphene from this project delivered 710 mA/cm$_2$ in H_2/air cells (with other testing conditions, such as Pt loading, temperature, relative humidity [RH], and pressure remaining exactly the same or similar). This demonstrates the significantly positive effect of graphene structure engineering from 2-D to 3-D; however, Pt-ITO-graphene is less stable than Pt/graphene (Figure 4a). X-ray diffraction (XRD) patterns of Pt-ITO-graphene before and after an accelerated degradation test (ADT) in an MEA reveal the disappearance of ITO patterns after the ADT

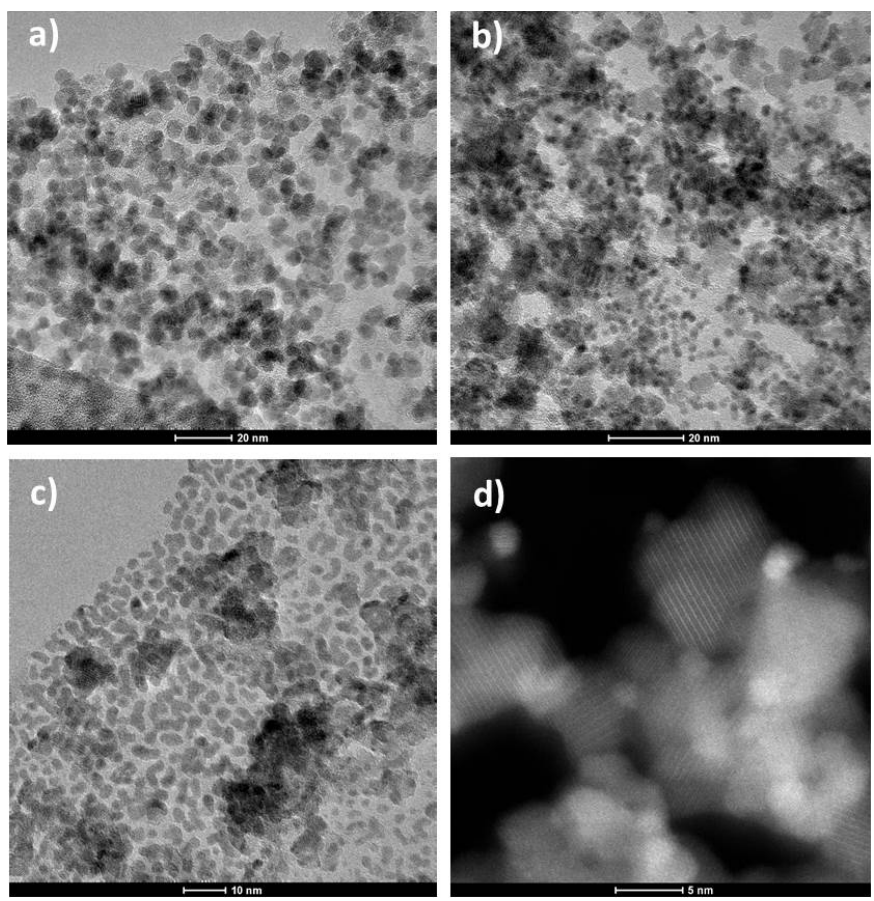

FIGURE 1. TEM images of ITO-graphene (a), Pt-ITO-graphene using chemical solution method (b), Pt-ITO-graphene using vapor deposition method (c), Pt-ITO-graphene using chemical solution method – high resolution dark-field images (d)

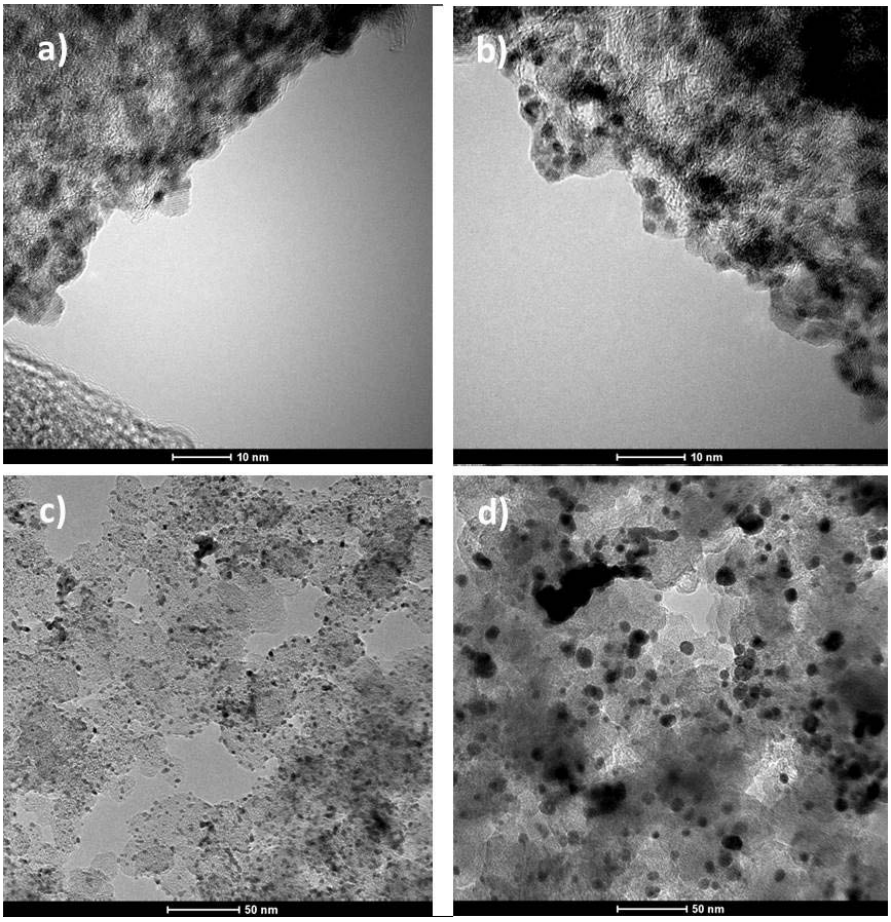

FIGURE 2. TEM images of Pt-ITO-graphene (a, b) and Pt/C (c, d) before (a, c) and after (b, d) thermal annealing

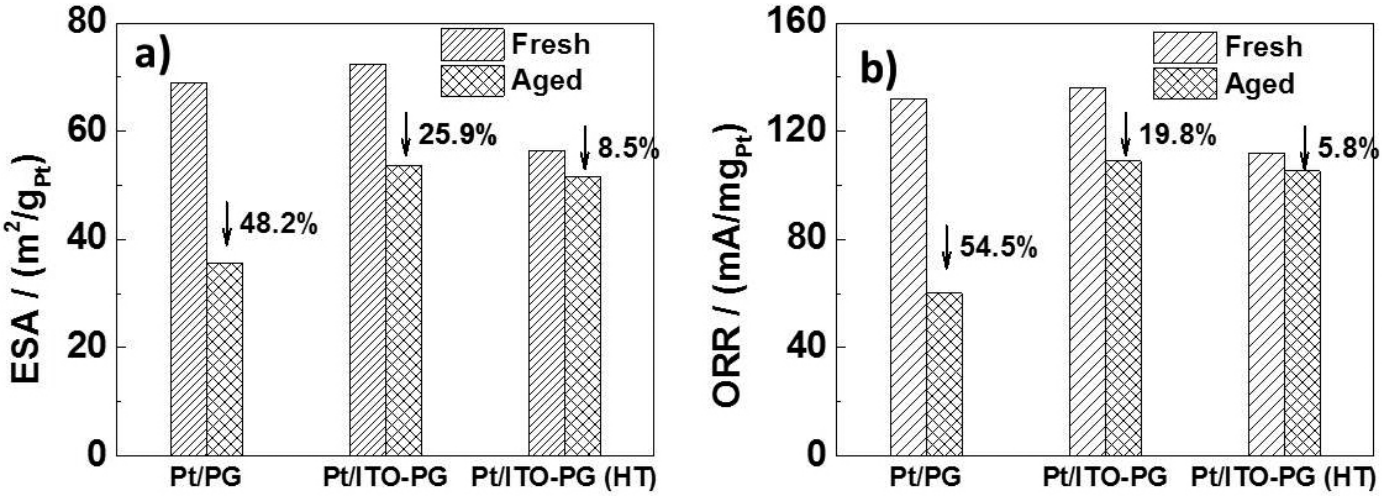

FIGURE 3. Electrochemical surface area (ESA) and ORR activity before and after accelerated degradation test (ADT). ESA1 and ORR1 are values before ADT; ESA2 and ORR2 are values after ADT (PG = porous graphene, HT = heat-treatment/thermal annealing).

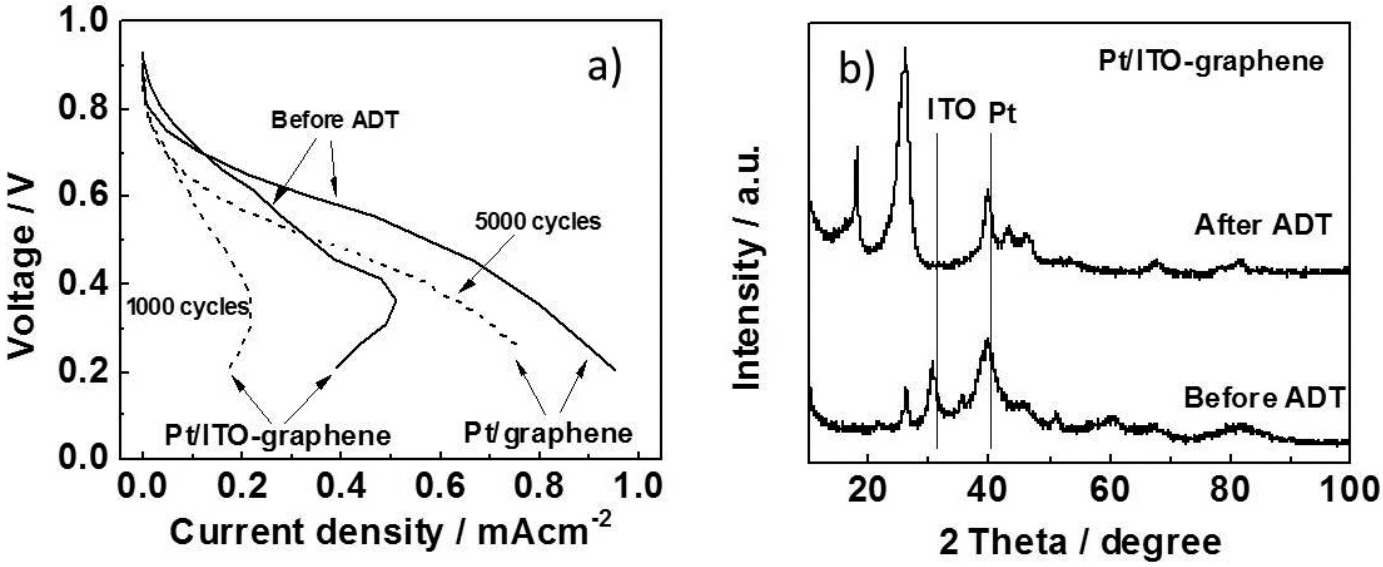

FIGURE 4. a) In situ fuel cell testing results of 3-D Pt/graphene and Pt-ITO-graphene; b) XRD patterns of Pt-ITO-graphene before and after ADT. Testing conditions: 1) Current-voltage curves: A/C: 0.28/0.23 mg Pt/cm$_2$, 80°C, 100% RH, 150 kPa, H_2/air: 200/600 sccm, SGL 25BC; 2) ADT electrochemical stressing protocol: 1.0-1.5 V cyclic voltammetry at 500 mV/s. (a.u. = arbitrary units).

(Figure 4b). This indicates the possible dissolution of ITO during MEA testing (at 80°C) and the urgency of developing alternative metal oxide nano coatings with high stability. In the future, if the well-developed nano-alloys and core-shell electrocatalysts are integrated into the metal oxide coated 3-D graphene, both the performance and durability will be further improved.

CONCLUSIONS AND FUTURE DIRECTIONS

The concept of using metal-metal oxide-carbon triple-junction structure to stabilize and improve the performance of platinum electrocatalysts that we developed previously on a 2-D graphene substrate was successfully demonstrated on a 3-D porous substrate.

- Uniformly dispersed platinum and ITO nanoparticles were successfully deposited on a 3-D porous graphene substrates. TEM characterization revealed that it forms a Pt-ITO-graphene junction structure.
- This junction structure stabilizes platinum nanoparticles and provides high resistance against thermal annealing that can be used to tune electrocatalyst performance.
- Electrochemical test results show enhanced performance of Pt-ITO-graphene, particularly the durability.
- Alternative metal oxides will be investigated to replace ITO so that the instability issue of ITO can be addressed.
- Advanced nano-alloys and core-shell electrocatalysts will be integrated into the metal oxide coated 3-D graphene to further improve both the performance and durability.

FY 2015 PUBLICATIONS/PRESENTATIONS

1. Y. Shao, Y. Cheng, R. Kou, Y. Wang, J. Liu. "Durable Nanostructured Electrocatalysts for Oxygen Reduction Reaction: Materials Design and Testing Protocol." 2015 MRS Spring Meeting & Exhibit April 6–10, 2015, San Francisco, California.

2. Y. Shao, Y. Wang, J. Liu. "Porous nanocomposite from scalable synthesis for electrocatalytic applications." Invention Report filed on December 9, 2014.

3. Y. Shao, Y. Cheng, W. Duan, W. Wang, Y. Lin, Y. Wang, J. Liu. "Nanostructured Electrocatalysts for PEM Fuel Cells and Redox Flow Batteries: a Selected Review." Accepted for publication in ACS Catalysis.

4. Y. Shao, Y. Wang, J. Liu. "Support solution for PEM fuel cell cathode." Invited paper by Nano Energy, to be submitted.

REFERENCES

1. Kou, R.; Shao, Y.Y.; Mei, D.H.; Nie, Z.M.; Wang, D.H.; Wang, C.M.; Viswanathan, V.V.; Park, S.; Aksay, I.A.; Lin, Y.H.; Wang, Y.; Liu, J., Stabilization of Electrocatalytic Metal Nanoparticles at Metal-Metal Oxide-Graphene Triple Junction Points. J. Am. Chem. Soc. 2011, 133 (8), 2541–2547.

2. Park, S.; Shao, Y.Y.; Wan, H.Y.; Rieke, P.C.; Viswanathan, V.V.; Towne, S.A.; Saraf, L.V.; Liu, J.; Lin, Y.H.; Wang, Y., Design of graphene sheets-supported Pt catalyst layer in PEM fuel cells. Electrochem. Commun. 2011, 13 (3), 258–261.

V.F.15 Magnetic Annealing of Pt-Alloy Nanostructured Thin Film Catalysts for Enhanced Activity

David A. Cullen (Primary Contact), Orlando Rios, Craig Bridges, Khorgolkhuu Odbadrakh, and Harry Meyer
Oak Ridge National Laboratory (ORNL)
P.O. Box 2008
Oak Ridge, TN 37831-6064
Phone: (865) 356-3400
Email: cullenda@ornl.gov

DOE Manager
Donna Ho
Phone: (202) 586-8000
Email: Donna.Ho@ee.doe.gov

Subcontractor
- Shyam Kocha and Jason Zack, National Renewable Energy Laboratory (NREL), Golden, CO 80401

Project Start Date: October 1, 2014
Project End Date: October 1, 2015

Overall Objectives

- Explore the potential of high magnetic field annealing to produce highly active surface structures in Pt-alloy oxygen reduction reaction (ORR) catalysts
- Link activity improvements of Pt_3Ni_7 nanostrucutured thin films (NSTF) alloy films measured by rotating disk electrode (RDE) with structural changes measured by X-ray diffraction (XRD), X-ray photoelectron spectroscopy (XPS), and transmission electron microscopy
- Calculate energetics, geometry and electronic structure from first principles to correlate surface structure with surface reactivity

Technical Barriers

This project addresses the following technical barriers from the Fuel Cells section of the Fuel Cell Technologies Office Multi-Year Research, Development, and Demonstration Plan:

(A) Durability

(B) Cost

(C) Performance

Technical Targets

This project is conducting fundamental studies into the effects of magnetic annealing. The technical target is based on RDE-determined mass activity using an as-grown Pt_3Ni_7/NSTF baseline.

- Delivery of best-of-class catalyst via magnetic annealing with 1.5 times the mass activity of baseline

FY 2015 Accomplishments

- Demonstrated magnetic annealing of Pt_3Ni_7/NSTF in a 9 T field at 400°C in Ar and H_2
- Measured specific activity, electrochemical surface area, and mass activity by RDE of both annealed and baseline materials
- Characterized changes in grain size, surface composition, and morphology using XPS, XRD, and scanning transmission electron microscopy (STEM)
- Implemented screened Korringa-Kohn-Rostoker (SKKR) method for advanced density functional theory (DFT) calculations of disordered alloy catalysts

✧ ✧ ✧ ✧ ✧

INTRODUCTION

Replacing a portion of the costly ORR catalyst with transition metals, such as Co or Ni, has not only reduced the overall cost of the electrodes, but has enhanced the initial specific activity through dealloying to form highly active Pt-skin, -shell or -skeleton surface structures. Further, catalyst pretreatments, including dealloying and annealing, can further improve catalyst performance.

In this effort, we explore the effects of high magnetic field annealing as an alternative and innovative approach for tailoring the properties of low precious group metal (PGM) alloy catalysts. This project utilizes unique 9 T magnets in the Advanced Manufacturing Facility at ORNL. Magnetic annealing has been demonstrated in aligning grain growth, modifying surface structures, and even creating new, unexplored structures. This effort explores such possibilities for low PGM alloy cathode catalysts. This work will focus primarily on Pt-transition metal alloys, with an emphasis on 3M's Pt3Ni7/NSTF.

APPROACH

This innovative approach aims to exploit the magnetic properties of these alloys through high magnetic field annealing to modify catalyst surface structures, compositions, and properties under conditions which are both scalable and commercially viable. 3M's Pt_3Ni_7/NSTF has been selected as the primary test structure for these experiments, due to its film-like attributes and high magnetic Ni content. Magnetic annealing (9 T) is performed on thin film samples to establish optimal conditions arising from variables such as field strength, field direction, annealing temperature, annealing time, and environment (H_2 and air).

RDE measurements are used as a screening tool for electrochemical catalyst characterization, and are performed at NREL. These measurements are then compared with structural characterization at ORNL using XRD, XPS, and STEM. As structure-property relationships are unveiled, the data is input into DFT calculations which will identify the source of the activity enhancement and provide guidance for further catalyst design.

RESULTS

The horizontal and vertical magnetics used in this project are shown in Figure 1. A new heating sleeve was designed and fabricated for the horizontal magnetic which allowed for larger sample sizes needed to produce sufficient quantities of material for RDE measurements. The Pt_3Ni_7/NSTF was annealed on the growth substrate in rolled sections of roughly 12 in x 5 in. Following annealing, the NSTF was removed from the substrate and sent as a powder to NREL for RDE analysis. Seven samples were processed and sent to NREL for electrochemical evaluation: two as-grown samples, four specimens annealed at 400°C in Ar or H_2 with and without the magnetic field, and a special sample annealed as a powder at 400°C without the magnet.

As shown in Figure 2a, RDE results show a decline in both specific activity and surface area following annealing both with and without field. Magnetically annealed specimens had a modestly higher mass activity then the field-free annealed specimens. To understand the possible influence of the perylene-red support, which sublimes at these elevated temperatures, Pt_3Ni_7/NSTF was removed from the growth substrate and annealed as a powder. The powder sample showed even lower specific and mass activities. Figures 2b and 2c show the XRD and XPS analysis of the annealed catalysts. XRD showed grain size growth following annealing, with the H_2 annealing leading to a larger grain size. The effect of the magnetic field appears to be a slowing of grain growth, although further experimentation is needed to confirm this result. An increase in C was observed by XPS, indicating perylene-red sublimation with redeposition of C on the NSTF surfaces. More importantly, changes in composition of the surfaces was observed, which would have subsequent effect on the dealloying of the material during RDE, as described later in the report. Consistent with literature reports, annealing led to Pt-rich surfaces. The magnetic field had only a modest effect, showing slightly greater Pt enrichment of the surfaces.

Samples which had been submitted to RDE testing were returned to ORNL for STEM and energy dispersive X-ray spectroscopy (EDS) analysis to understand morphology/composition changes induced by RDE break-in. Such changes are expected based on previous observations with membrane electrode assembly (MEA) samples performed under 3M

FIGURE 1. a) Horizontal and (b) vertical high field magnets in the Advanced Manufacturing Facility at ORNL

projects. Z-contrast STEM images of five of the post-break-in NSTF whiskers are shown in Figure 3. Annealing affected the degree of Ni dissolution during RDE break-in, which in turn affected Pt-skin and pore formation, key morphological factors controlling electrochemical area (ECA) and specific activity.

Perhaps even more telling was the EDS quantification of the Pt at% (relative to Ni) for each sample. When plotted against ECA, there is a clear correlation between the amount of Ni dissolution (leading to increased Pt content), as shown in Figure 4. Previous XRD and XPS results indicated that the presence of the magnetic field tends to slow grain growth and enhance formation of Pt-rich surface structures during annealing, both of which affect the rate of Ni dissolution. Thus, magnetically annealed samples had slightly higher ECA than the non magnetically annealed counterparts. More ambiguous, however, is the connection between composition and specific activity. While greater Pt at% led to generally

(a)

Sample ID	Gas	Process Temp (C°)	Magnet (T)	SA ($\mu A/cm^2_{Pt}$)	MA (mA/mg_{Pt})	ECA (m^2/g_{Pt})
As-Grown	n/a	n/a	n/a	3310	904	28
Ar, 0T	Ar	400	0	2029	251	12
Ar, 9T	Ar	400	9	1927	316	16
H_2, 0T	H_2	400	0	2791	517	18
H2, 9T	H_2	400	9	2653	553	24
Annealed Powder	H_2	400	n/a	1540	186	12
As-Grown Repeat	n/a	n/a	n/a	2774	804	29

(b)

Surface Composition (at.%)

	Pt	Ni	O	C	Cr	N	Ni/Pt
As Received	9.3	27.8	42.5	20.5	0.0	0.0	3.00
Ar_0T	10.5	12.8	10.0	63.7	0.2	2.8	1.22
Ar_9T	9.0	10.4	10.7	66.9	0.3	2.7	1.15
H2_0T	10.2	21.7	25.0	43.0	0.2	0.0	2.13
H2_9T_mid	10.4	21.5	21.8	45.8	0.5	tr	2.07

(c)

Sample	Latt. par. (Å)	Grain size (nm)
Pt (lit.)	3.9231	
As-grown Pt_3Ni_7	3.6977	3.8
Ar 9T	3.6894	4.9
Ar 0T	3.6841	5.6
H_2 9T	3.6779	5.9
H_2 0T	3.6736	6.8

FIGURE 2. (a) RDE measurements of Pt_3Ni_7/NSTF annealed under different conditions. (b) XPS and (c) XRD results from magnetically-annealed sample set

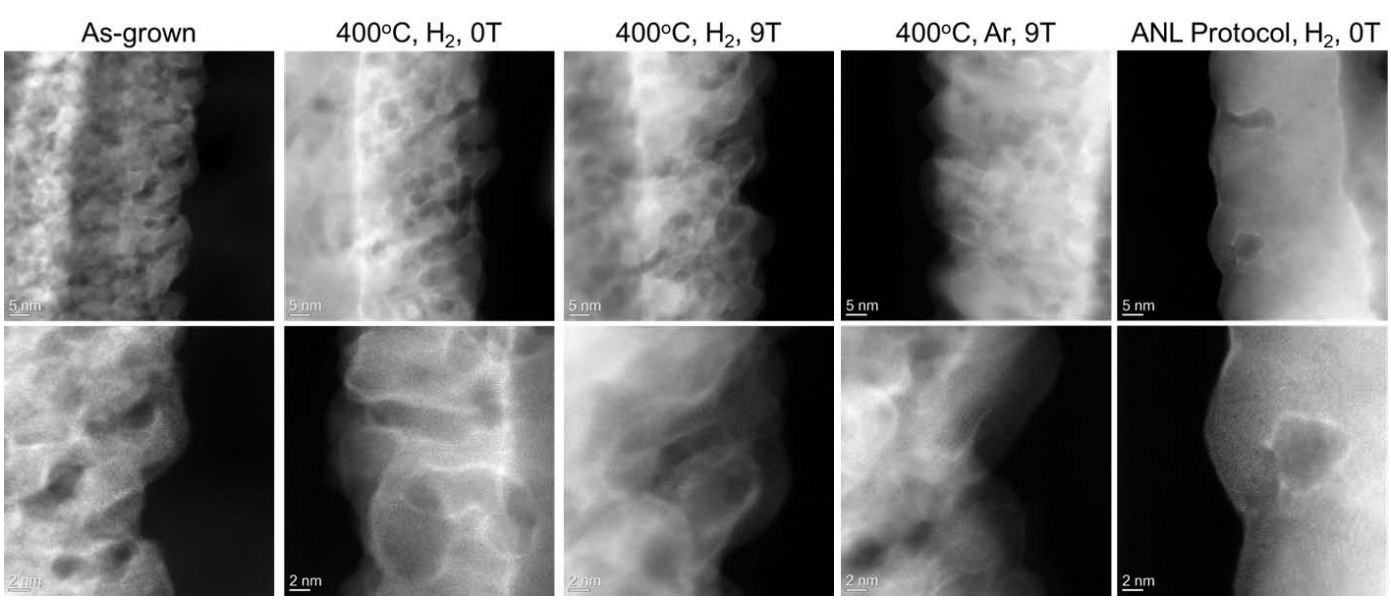

FIGURE 3. Z-contrast STEM images of post-break-in samples for NSTF annealed under different conditions, showing different degrees of pore formation

higher specific activities, the non-magnetically annealed samples (with larger grain sizes) had slightly higher specific activities then their magnetically annealed counterparts. Thus, any increases in ECA from magnetic annealing are being partially countered by drop in specific activity.

We employed a K-space based SKKR method for density functional theory calculations of the Pt-Ni alloys. The SKKR method imposes no periodic boundary conditions for modeling the extended and disordered systems of Pt-Ni alloys. We have calculated electronic structures and ground state magnetism for Pt-Ni and Pt-Co alloys for an entire range of alloying concentrations. Figures 5a and 5b show the electronic structures of $Pt_{0.7}Ni_{0.3}$ and $Pt_{0.3}Ni_{0.7}$ alloys. Exchange splitting, which gives rise to magnetism, is about

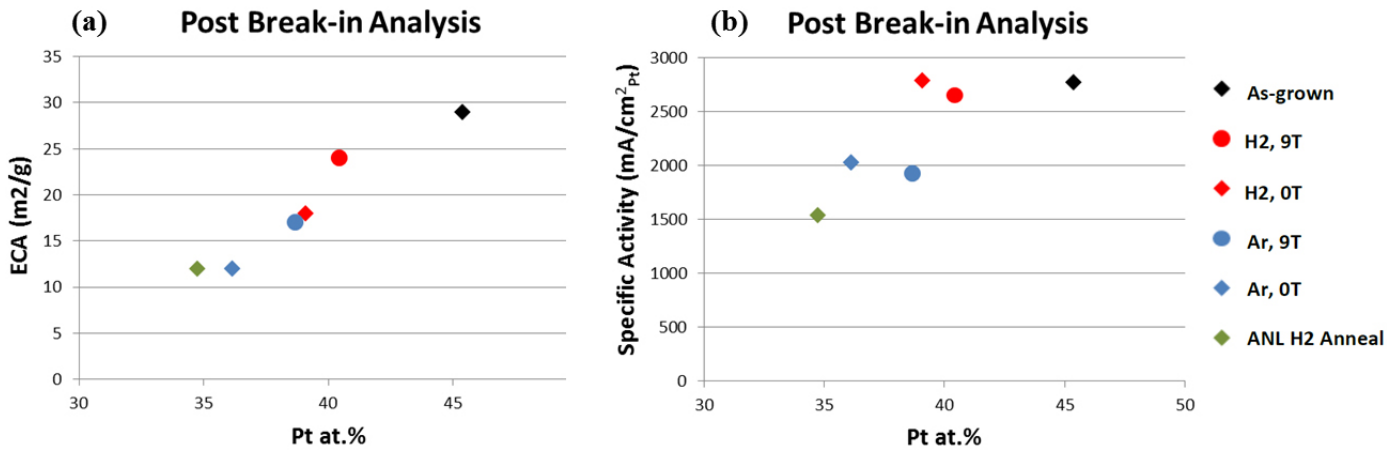

FIGURE 4. Plots of Pt at% after break-in vs (a) ECA and (b) specific activity

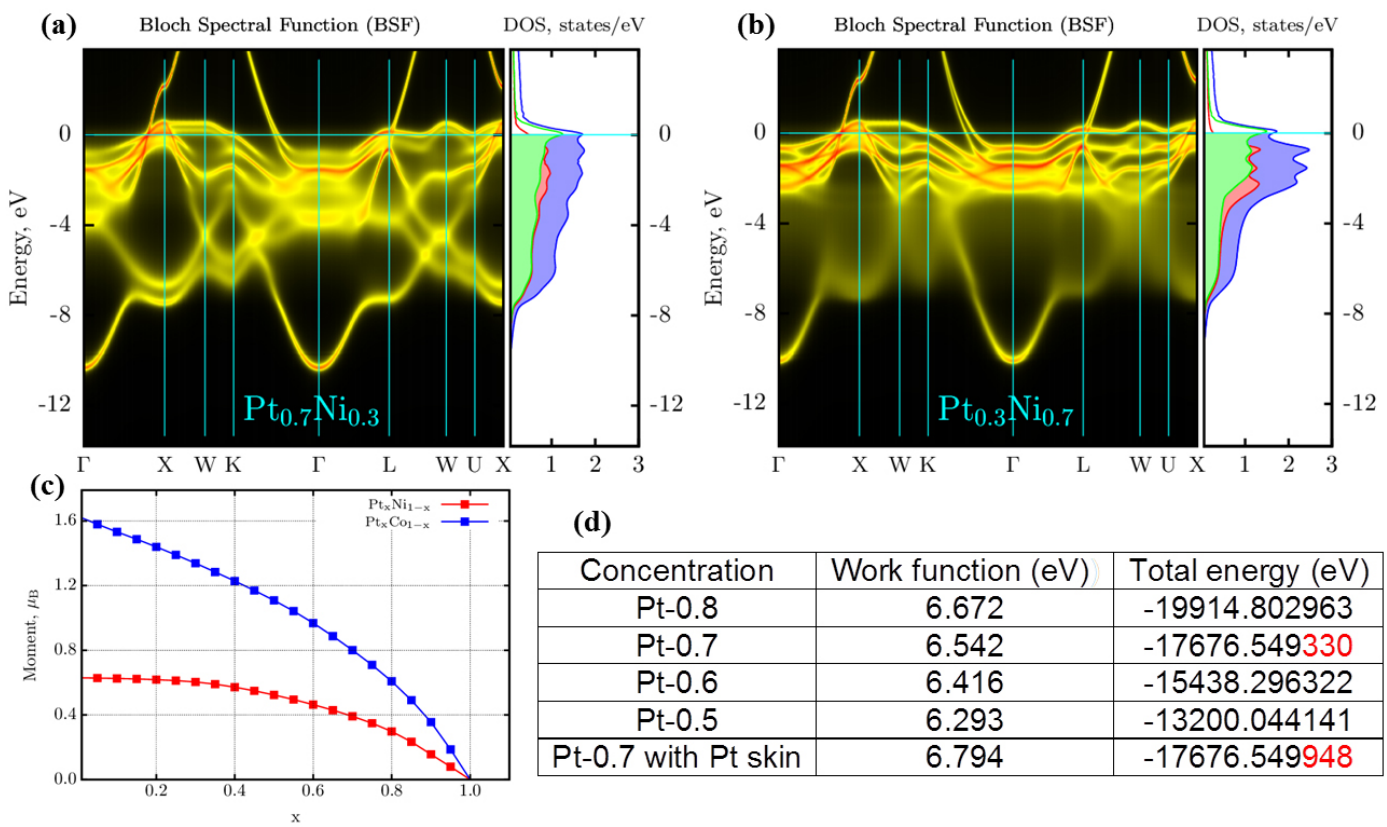

Concentration	Work function (eV)	Total energy (eV)
Pt-0.8	6.672	-19914.802963
Pt-0.7	6.542	-17676.549330
Pt-0.6	6.416	-15438.296322
Pt-0.5	6.293	-13200.044141
Pt-0.7 with Pt skin	6.794	-17676.549948

FIGURE 5. Bloch spectral functions (BLS) and density of states (DOS) for (a) $Pt_{0.7}Ni_{0.3}$ and (b) $Pt_{0.3}Ni_{0.7}$ alloys; (c) Magnetism of Pt-Ni (red) and Pt-Co (blue) alloys at ground state for concentration range from 0.0–1.0; (d) Work function and total energies of Pt-Ni alloy at selected concentrations

the same for both alloys but density of states for $Pt_{0.3}Ni_{0.7}$ alloy are much more pronounced. As a result, $Pt_{0.3}Ni_{0.7}$ alloy has magnetic moment of 0.6 μB per site at T = 0 K while $Pt_{0.7}Ni_{0.3}$ has a moment of 0.39 μB per site. Ground state magnetic moments of Pi-Ni and Pt-Co alloys are shown in Figure 5c for an entire range of alloying concentrations. Pt-Co alloys have more than twice the magnetism of Pt-Ni alloys at all concentrations, suggesting that Pt-Co alloys would respond to magnetic annealing stronger than Pt-Ni alloys.

We have also calculated magnetic ground states for Pt-Ni alloys with surface termination (Figure 5d). The calculations show that $Pt_{0.7}Ni_{0.3}$ alloys with pure Pt skin is energetically favored over pristine $Pt_{0.7}Ni_{0.3}$ surface and lower value of work function. This result suggests that formation of pure Pt skin can be detected through measurement of work functions of samples.

CONCLUSIONS AND FUTURE DIRECTIONS

- Demonstrated magnetic annealing of Pt_3Ni_7/NSTF in a 9 T field at 400°C in Ar and H_2
- Showed magnetic annealing has only modest effect on grain size and surface composition relative to field-free annealing
- Measured specific activity, electrochemical surface area, and mass activity by RDE, which showed, in all cases, annealing leads to a lowering of the mass activity
- Implemented SKKR method for advanced DFT calculations of disordered alloy catalysts, indicating Pt-Co alloys may have greater response to the field

Additional magnetic annealing experiments will be performed at varied temperatures and higher initial Pt concentrations to find the optimal conditions for improving ECA, mass activity, and specific activity. We also plan to begin sputtering Pt-Co alloys onto NSTF to study their behavior under the magnetic field. RDE measurements will add a durability component to test activity of the catalysts over their lifetime.

FY 2015 PUBLICATIONS/PRESENTATIONS

1. D.A. Cullen, "Magnetic Annealing of Pt-alloy Nanostructured Thin Film Catalysts for Enhanced Activity," Oral Presentation, Fuel Cell Tech Team Meeting, Southfield, MI, April 8, 2015.

2. D.A. Cullen, "Magnetic Annealing of Pt-alloy Nanostructured Thin Film Catalysts for Enhanced Activity," Poster Presentation, U.S. Department of Energy Hydrogen and Fuel Cells Program Annual Merit Review and Peer Evaluation Meeting, Washington, D.C., June 15–19, 2015.

V.F.16 High Conductivity Durable Anion Conducting Membranes

Thomas Zawodzinski (Primary Contact), David Wood, Jianlin Li, Jimmy Mays, and Todd Toops
Oak Ridge National Laboratory (ORNL)
Oak Ridge, TN 37831
Phone: (865) 574-1499 (ORNL);
(865) 974-5137 (University of Tennessee, Knoxville)
Email: tzawodzi@utk.edu

DOE Manager
Donna Ho
Phone: (202) 586-8000
Email: Donna.Ho@ee.doe.gov

Project Start Date: September 1, 2014
Project End Date: 2015

Overall and Fiscal Year (FY) 2015 Objectives

The goal of this one-year project is the development of highly conducting durable anion exchange membranes (AEMs) and their demonstration in alkaline fuel cells (AFCs). Outcomes include:

- Synthesizing two classes of anion conducting membranes for use in fuel cells.
- Demonstrating the high conductivity of these membranes.
- Preparing and testing durable membrane electrode assemblies (MEAs) constructed from these new materials.

Technical Barriers

This project addresses the following technical barriers from the Fuel Cells section of the Fuel Cell Technologies Office Multi-Year Research, Development, and Demonstration Plan:

(A) Durability

(B) Cost

(C) Performance

Technical Targets

Second quarter 2017 milestone: Develop AEMs with an area specific resistance (ASR) <0.1 ohm-cm^2 that is maintained for 500 h during testing at 600 mA/cm^2 and at T > 60°C.

FY 2015 Accomplishments

- Produced two classes of highly conductive AEM materials: cross-linked, loaded anion-conducting membranes (CLAMs) and AEMs
- Prepared CLAMs that meet targets for conductivity (>100 mS/cm) at a lower relative humidity (RH) of 50% (**Milestone met)**
- Improved film formation methods for CLAM-type membranes
- Prepared AEMs that meet the conductivity target of >60 mS/cm (**Milestone met)**
- Demonstrated a CLAM-based MEA (>200 µm thick membrane) with an ASR of ~0.09 ohm-cm^2 at 50% RH, exceeding the target of <0.1 ohm-cm^2 (**Milestone met)**
- Prepared and tested first new AEM-based MEA in a fuel cell (FC) with an ASR less than 0.1 ohm-cm^2 and with no precious metal in the cathode
- Demonstrated an AEM lasting >2,500 h at 60°C during ex situ testing

✧ ✧ ✧ ✧ ✧

INTRODUCTION

This project, initiated in August 2014, focuses on improving materials for AFCs. AFCs are a promising technology that can operate without precious metal catalysts on pure hydrogen and CO_2-scrubbed air. To date, the development of high performance AFCs has been somewhat limited by the availability of various materials with suitable performance characteristics as polymer electrolyte binders for electrodes and especially as membranes. Improved conductivity of AEMs and chemical stability of the cationic functional group in hydroxide ion conductors are both areas in which development is lagging.

APPROACH

The project combined several elements for the development of highly conducting, durable membranes and their use in FCs: (i) high-throughput synthesis and physical property evaluation of new materials and processing into AEMs with the key aims of manipulating molecular polarity to aid in OH^- conduction and limit OH^- reactivity and of protecting cationic groups to limit degradation pathways; (ii) accelerated membrane life testing; (iii) 'ink' formulation and catalyst-coated membrane (CCM) preparation; and (iv) FC testing.

RESULTS

We prepared more than a dozen different polymers that were one of two types of membranes. First, we prepared CLAMs from conserved polymer backbones modified with cationic moieties and cross-linking agents. Cross-linking agents were chosen to provide the highest possible conductivity. The cross-linking process was carried out during film formation. This approach required substantial effort devoted to optimizing processing conditions such as temperature, concentration of polymer and cross-linker, and casting medium. A second stream of work was devoted to preparing more conventional AEMs.

In the context of this work, we demonstrated that many CLAM compositions possessed excellent conductivity. One remaining goal lay in showing that this conductivity could be maintained at lower RH. As shown in Figures 1 and 2, conductivity was maintained at >100 mS/cm at reduced RH at both 30ºC and 60ºC. Note that the results were obtained in air; thus, we can assume that the films are saturated with CO_2. Since CO_2 lowers the conductivity of hydroxide conductors, CO_2-free air testing may result in higher values.

One aspect of the CLAMs is the availability of chemical diversity within this class of membranes via modifications of both the cation type and the cross-linker. Given the large number of properties that require optimization beyond conductivity, our current work on the CLAMs is focused on identifying the best compositions for a variety of purposes, including mechanical property optimization and CCM formation. We are also pursuing work to improve film processing to enable us to make thinner films.

AEM-type films, which contain only water in the pores of the membrane, are more conventional than CLAMs. Our synthetic approaches allow us to prepare many different versions of these materials as well. We have varied the backbone polymer chemistry used and have found some compositions that meet the benchmark of 60 mS/cm at 60°C that was set for our milestone.

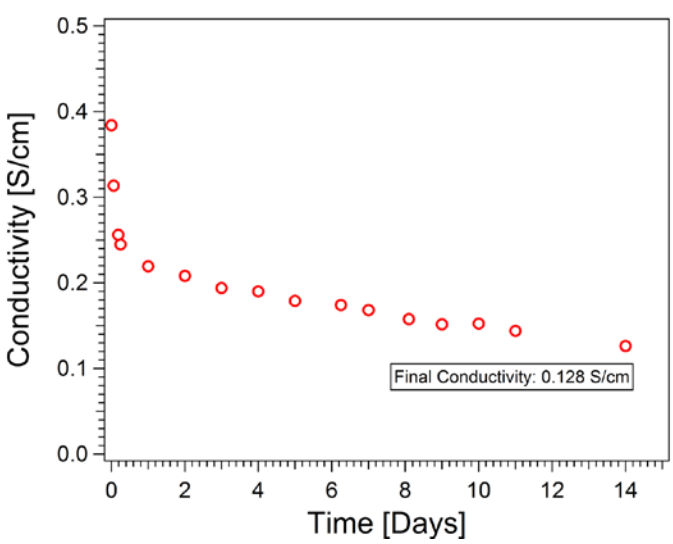

FIGURE 1. CLAM conductivity at 30°C during equilibration at 50% RH

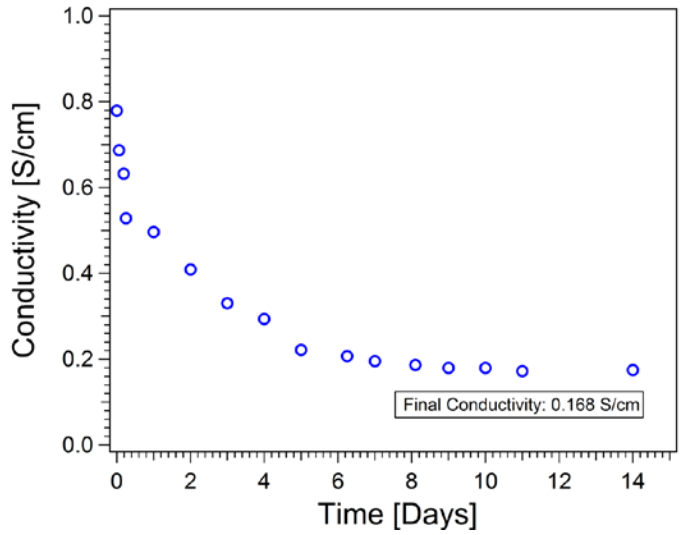

FIGURE 2. Conductivity of CLAM membrane at 50% RH at 60°C

The CLAMs were used to prepare MEAs for testing. An ASR of 0.09 ohm-cm^2 was observed in the fuel cell. Electrode performance, especially anode performance, was rather poor in initial tests. This poor performance necessitated the development of improved materials that are currently being tested.

CONCLUSIONS AND FUTURE DIRECTIONS

- CLAMs can be suitable electrolytes for use in FCs, particularly if RH of 50% or higher is available.
- We are able to readily prepare conventional AEMs with conductivities >60 S/cm.
- Key issues that remain include the development of high performance electrodes for AFCs and the demonstration of significant tolerance to CO_2.
- Water management issues are not adequately defined for AFCs.

SPECIAL RECOGNITIONS & AWARDS/ PATENTS ISSUED

1. Patent application in process.

FY 2015 PUBLICATIONS/PRESENTATIONS

1. Presented poster at the June 2015 U.S. DOE Annual Merit Review and Peer Evaluation.

V.F.17 Advanced Hydroxide Conducting Membranes

Yu Seung Kim (Primary Contact), Kwan-Soo Lee
Los Alamos National Laboratory (LANL)
Materials Physics and Applications Division
Los Alamos, NM 87545
Phone: (505) 667-5782
Email: yskim@lanl.gov

DOE Manager
Nancy Garland
Phone: (202) 586-9811
Email: Nancy.Garland@ee.doe.gov

Subcontractors
- Cy Fujimoto, Michael Hibbs, Sandia National Laboratories, Albuquerque, NM
- Adam Weber, Huai-Suen Shiau, Shouwen Shi, Ahmet Kusoglu, Lawrence Berkeley National Laboratory, Berkeley, CA
- Chul Sung Bae, Angela Mohanty, Woo-Hyung Lee, Rensselaer Polytechnic University, Troy, NY

Project Start Date: August 1, 2014
Project End Date: July 31, 2015

Overall Objectives

- Synthesize highly conductive and stable hydrocarbon anion exchange membranes (AEMs)
- Prepare perfluorinated ionomer dispersions for the fabrication of fuel cell electrodes
- Develop non-precious metal electro-catalysts for hydrogen oxidation reaction (HOR) and oxygen reduction reaction (ORR)
- Demonstrate high performing alkaline membrane fuel cells (AMFCs)
- Demonstrate long-term AMFC performance under steady and accelerated stress conditions

Fiscal Year (FY) 2015 Objectives

- Synthesize highly conductive and alkaline stable AEMs
- Establish design aspects on advanced ionomeric binders
- Predict polarization behaviors through modeling approaches

Technical Barriers

This project addresses the following technical barriers from the Fuel Cells section (3.4) of the Fuel Cell Technologies Office Multi-Year Research, Development, and Demonstration (MYRDD) Plan:

(A) Durability (polymer electrolytes)

(B) Cost (non-precious metal catalysts)

(C) Performance (AMFCs)

Technical Targets

This project is investigating fundamental aspects of AMFCs for practical use in intermediate (10–50 kW) power applications. Insights gained from this project will be applied towards the next stage of advanced AMFC systems. The technical targets for AMFCs in the MYRDD Plan [1] are listed below:

- Develop AEMs with an area specific resistance ≤0.1 ohm cm^2, maintained for 500 hours during testing at 600 mA/cm^2 at T >60°C. (Q2, 2017)
- Demonstrate AMFC peak power performance >600 mW/cm^2 on H_2/O_2 (maximum pressure of 1.5 atm abs) in membrane electrode assembly (MEA) with a total catalyst loading of ≤0.125 mg_{PGM}/cm^2. (Q4, 2017)

FY 2015 Accomplishments

- Developed synthetic routes to produce thin and tough AEMs having no aryl-ether linkage in the polymer backbones; major significant progress on AEM properties include the following:
  - Areal resistance ≤0.1 Ω-cm^2 for FY 2015 AEMs
  - Ex situ alkaline stability <5% degradation after 1–4 M NaOH at ≥80°C for 14–30 days for FY 2015 AEMs
- Demonstrated the excellent alkaline stability of alkyl amide linkage (no apparent degradation after 500 h, 0.5 M NaOH treatment at 80°C) that can be used for the preparation of perfluorinated ionomers
- Developed a membrane + electrode model that takes into account the effect of CO_2 contamination on the AMFC performance; combining with experimental data, benefits of higher temperature operation in the presence of CO_2 were demonstrated

✧ ✧ ✧ ✧ ✧

INTRODUCTION

Preparation of alkaline stable and highly conductive polymers for AMFCs is one of the urgent technical challenges to elevate the AMFC performance/durability to the next level in the DOE MYRDD plan. In the previous research (2008–2014), we identified the two AEM components that readily degrade under high pH conditions, (1) aryl-ether linkage in the polymer backbone [2], and (2) amide group between polymer backbone and cationic functional group [3]. Based on this research, we focused on developing robust and highly conductive AEMs and ionomeric binders in FY 2015. Moreover, we studied the factors that may impact the MEA performance by a modeling study.

APPROACH

Our approach to prepare stable and highly conductive AEMs is to synthesize cation group functionalized aryl-ether-free polymers. Three synthetic routes were developed. The first polymer series is the hexamethyl trimethyl ammonium functionalized Diels-Alder poly(phenylene)s (MRH series). In order to synthesize these polymers, the unfunctionalized Diels-Alder poly(phenylene) (DAPP) was prepared according to the procedure of Fujimoto et al. [4]. The DAPP polymer precursor was reacted with 6-bromohexanoyl chloride in the presence of aluminum chloride. The resultant polymer was reacted with trifluoroacetic acid and triethylsilane to reduce the carbonyl group in alkyl aryl ketones, followed by amination by immersing the polymer in trimethylamine solution [5]. The second polymer series is the hexamethyl trialkyl ammonium functionalized poly(biphenyl alkylene)s (AR series) [6]. These polymers were synthesized by newly developed one-pot, acid-catalyzed Friedel-Crafts polycondensations of biphenyl and trifluoromethyl alkyl ketones. Traditional AEM polymer synthesis via nucleophilic aromatic substitution requires a basic medium for polymerization; thus, it prevents monomers from having a potential leaving group such as alkyl halide. However, the use of acidic conditions in the reaction described in this report allows for the condensation polymerization of a monomer containing bromoalkyl side chains without affecting the quaternary ammonium precursor group. The third polymer series is quaternized ammonium functionalized benzyl trimethyl ammonium functionalized polystyrene-*b*-poly(ethylene-*co*-buthylene)-*b*-polystyrene (SEBS) triblock copolymers. Synthetic methods involving transition metal-catalyzed C-H borylation and Suzuki coupling were utilized to incorporate quaternary ammonium groups to the polystyrene units of SEBS [7].

Our approach to develop anion exchange ionomers includes hydrocarbon based poly(phenylene) and perfluorinated anion exchange ionomers. For poly(phenylene) ionomer, we believe that bulky phenylene groups of DAPPs take advantage of allowing high gas permeability due to the increased free volume. In FY 2015, we compared the electrode performance as a function of ionomer structure to verify this hypothesis. For perfluorinated anion exchange ionomers, we focused on developing stable amide linkage between polymer backbone and cationic functional group. We synthesized multiple perfluorinated amide linkages that include methyl amide, sulfone amide, sulfone methyl amide, alkyl amide and sulfone alkyl amide via condensation reactions. Then, the alkaline stability of the amide linkages was measured under high pH conditions.

Our approach to developing a two-dimensional non-isothermal AMFC model is to predict the response of an AMFC according to variations of the inlet relative humidity (RH), CO_2 concentration in the cathode inlet, and temperature.

RESULTS

Anion Exchange Membranes: The chemical structures of three series of AEMs and the control benzyl trimethyl ammonium functionalized DAPP (ATM-PP) AEM [2] are shown in Figure 1. We successfully prepared tough and ductile AEMs from the synthetic routes described above. We have achieved areal resistance milestone ($\leq$0.1 Ω-cm^2) with FY 2015 AEMs. The mechanical properties of the AEMs were evaluated by tensile tests under controlled humidity and temperatures (50% RH and 50°C). The FY 2015 Diels-Alder poly(phenylene)-based AEMs, MRH series showed similar mechanical properties with the control ATM-PP. The poly(biphenyl alkylene)-based AEMs, AR series, showed higher strain compared to MRH series probably due to the flexible backbone structure. The SEBS series showed much higher strain (>300%) with low stress, reflecting their elastomer-like block copolymer nature. The water uptake of AEMs is ~120% for MRH and AR series. The SEBS series AEM has higher water uptake ca. 220 wt%. The alkaline stability of the AEMs was evaluated under 80–90°C NaOH or KOH conditions. While the FY 2014 ATM-PP series showed ~14% ion exchange capacity (IEC) decrease after 4 M KOH 90°C conditions, the MRH and AR series AEMs did not show degradation at similar conditions. The SEBS series polymers showed only 3% IEC decrease. This improved stability met the FY 2015 AEM stability milestone, *ca.* <10% IEC loss after 500 h, 0.5 M NaOH at 80°C. The alkaline stability of the FY 2015 AEMs was confirmed with fuel cell test. Figure 2 shows the MEA using SEBS AEM before and after 110 h extended-term test. It was noted that high frequency resistance of the MEA slightly decreased in spite of the cell performance loss after the extended-term test. This indicated that the alkaline stability of the AEM was excellent while there was performance degradation. These polymers have potential to meet the DOE FY 2017 stability targets in the MYRDD Plan. The AEM properties are summarized in Table 1.

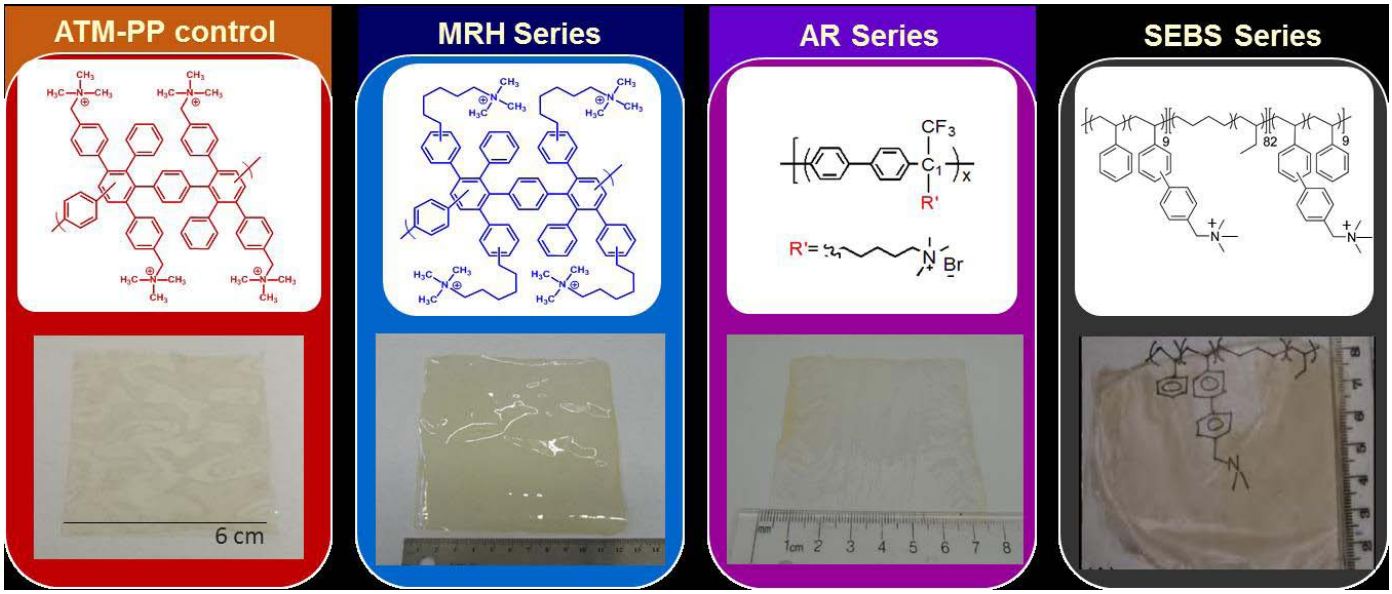

FIGURE 1. The chemical structures of control and FY 2015 membranes. Tough and ductile membranes were prepared from solution cast procedure. Membranes have the thickness 20–60 μm.

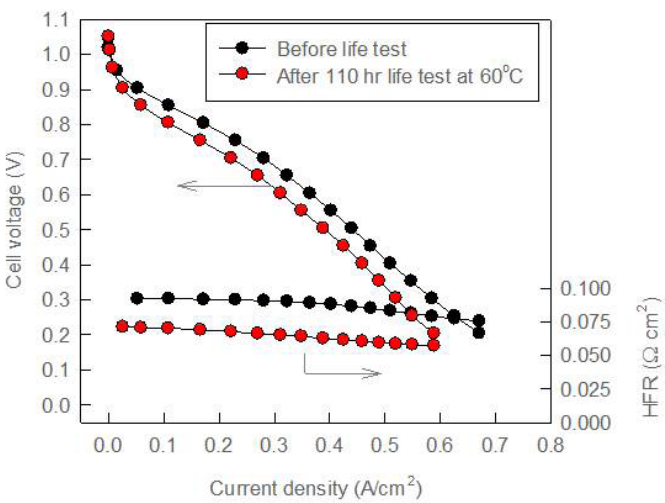

FIGURE 2. H_2/O_2 AMFC performance comparison after 110 h extended-term operation at 60°C. AEM: SEBS series (thickness: 35 μm), ionomeric binder: MRH series, catalyst: 20 wt% Pt/C Pt loading: 0.2 mg/cm^2.

Anion Exchange Ionomer: We prepared a series of poly(phenylene) ionomer dispersion using LANL proprietary dispersion technology [8] and tested in AMFCs. AR series ionomers that have linear structure in the polymer backbone showed inferior cell performance compared to the Diels-Alder poly(phenylene)s, which have bulky phenylene group arrangement in the polymer backbone. Comparing with ATM-PP and AR ionomers, the MEA using MRH ionomer showed a superior cell performance, i.e., peak power density of ~300 mW/cm^2 vs. ~100 mW/cm^2 for ATM-PP (Figure 3). The superior performance with MRH ionomer is perhaps due to the flexible alkyl chain forming a better interface between electrocatalyst and ionomer.

Finding an alkaline stable linkage for perfluorinated ionomers was the main subject for the FY 2015 perfluorinated ionomer development. All methyl substituted amide ($C = ON(CH_3)$) or sulfone amide ($SO_2N(CH_3)$) turned out to be no good or show very limited improvement in terms of alkaline stability. This is probably because the replacement of hydrogen by a methyl group can destroy the resonance structure of amide group that brings instability under

TABLE 1. Summary of the FY 2015 Anion Exchange Membrane Properties

AEM	IEC (meq/g)	AEM thickness (μm)	Hydroxide conductivity (mS/cm)	Areal resistance (Ω-cm^2)	Water uptake (wt%)	Stress (MPa)	Strain (%)	IEC loss (%)
ATM-PP	1.7	60	40	0.17	83	28	20	14[a]
MRH	2.2	30	50	0.07	126	28	23	0[a]
AR	2.0	22	50	0.10	120	36	50	0[b]
SEBS	1.9	35	45	0.08	220	4	>300	3[b]

[a] after 4 M KOH, 90°C for 14 days; [b] after 1 M KOH, 80°C for 28 days.

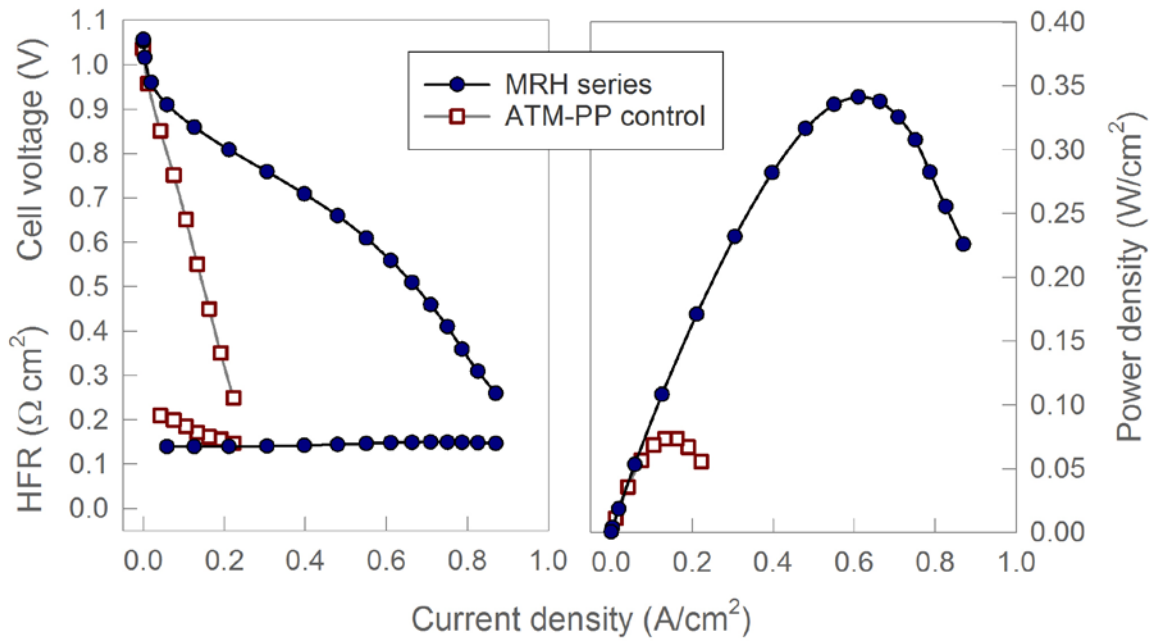

FIGURE 3. Impact of ionomeric binder on H_2/O_2 AMFC performance. Same membrane (MRH-series) with different ionomeric binders (MRH series vs. ATM-PP) were used. Operating temperature: 80°C, catalyst: 20 wt% Pt/C Pt loading: 0.2 mg/cm^2.

alkaline conditions. The best stability of the amide group was obtained with alkyl amide structure ($C = ONH(CH_2)_n$). Figure 4 compared the amide stability after 80°C, 0.5 M NaOH treatment for 500 h. While perfluorinated amide linkage shows notable peak changes, e.g., increased COO^- peak at 1,680 cm^{-1}, decreased NH peak at 1,540 cm^{-1} and decreased benzene C = C peak at 1,515 cm^{-1} due to the hydrolysis of the amide group, the perfluorinated alkyl amide linkage showed no trace of degradation. The exceptional stability of the perfluorinated alkyl amide linkage opens a new strategy to prepare alkaline stable perfluorinated ionomers.

Modeling: The modeling study at different inlet RH from 50% to 100% (without CO_2) showed that the performance is enhanced with increasing anode and cathode humidification. Several voltage losses as a function of current density and inlet RH were observed due to the ORR kinetic loss, ohmic loss through the membrane, and water activity gradient across the AEM. The kinetic loss is lower with higher inlet RH values due to water dependence of ORR kinetics in the alkaline media. Sufficient water supply is needed to avoid dehydration at the cathode. The ohmic and water diffusion losses are reduced with higher inlet RH due to more hydrated membrane. With higher CO_2 concentration in the cathode inlet, the current density decays due to the lowered HOR kinetics and hydroxide ion transport. The carbonate formation by CO_2 at the cathode reduces the number of OH^-, leading to slower HOR in the alkaline media at the anode, as shown by the decrease of current density with increasing $[CO_2]$ at high potentials. OH^- depletion also increases the ion transport resistance through the membrane and catalyst layer ionomer, as indicated by the decreased performance with increasing $[CO_2]$ at low potentials. The modeling study also shows the effect of operating temperature on polarization curves for the air inlet with $[CO_2]$ = 400 ppm. The increase in the operating temperature does have a positive influence on performance. The improvement is attributed to the enhanced electrochemical kinetics of HOR and ORR, and the increased ionic conductivity and water transport coefficient. The decrease of CO_2 solubility in water with higher temperature slightly improves the performance at higher operating temperature.

CONCLUSIONS AND FUTURE DIRECTIONS

- A series of aryl-ether-free AEMs were successfully prepared from various synthetic routes. The FY 2015 AEMs showed not only high hydroxide conductivity and good mechanical properties but also exceptional alkaline stability. The AEMs having hexamethyl trimethyl ammonium groups (MRH and AR) showed the optimal properties. Refining the polymer synthetic process for scale-up production is needed. In addition, long-term membrane stability test in MEA configurations should be done to confirm the ex situ stability results. The SEBS series AEMs showed very promising mechanical properties and good compatibility with catalyst layer. Replacing current benzyl ammonium group to more stable cationic group with more economical synthetic pathway is under investigation.

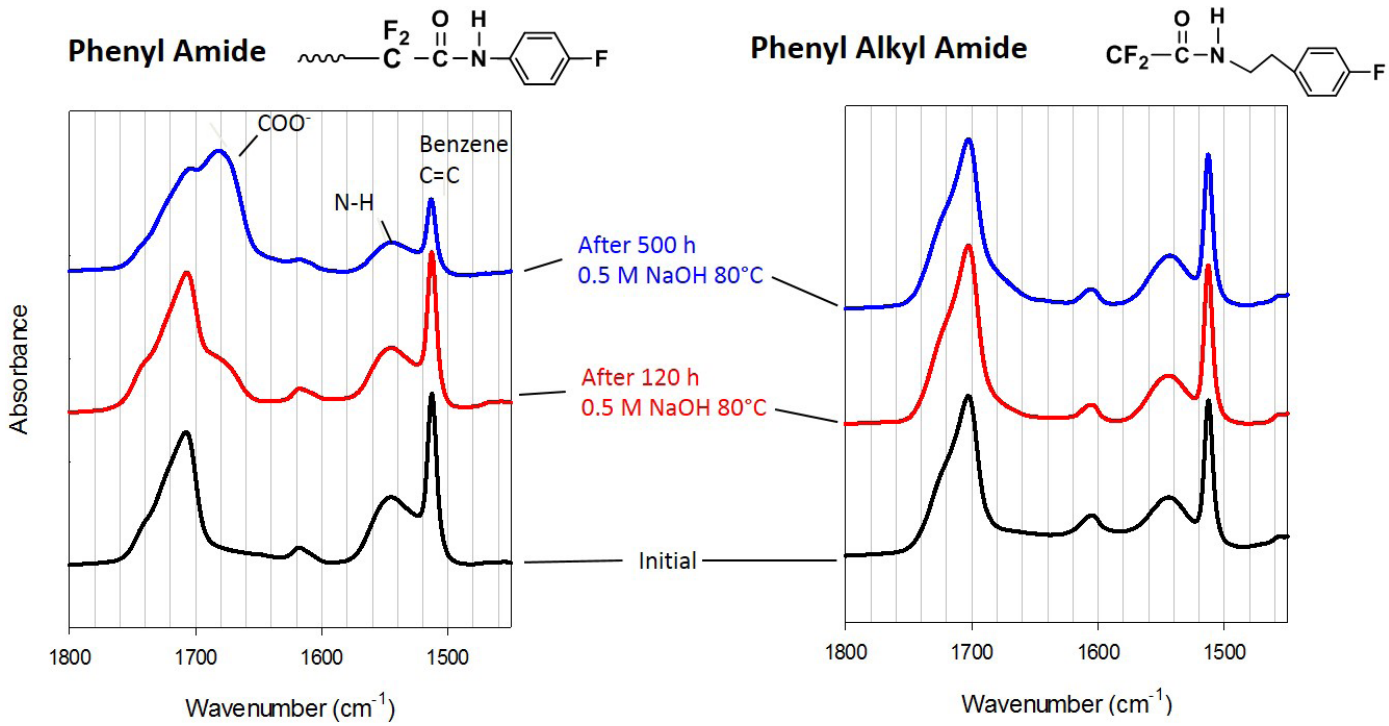

FIGURE 4. Fourier transform infrared spectroscopy change of perfluorinated amide and perfluorinated alkyl amide after ex situ alkaline stability test. Membranes were immersed in 0.5 M NaOH at 80°C for the life test.

- Diels-Alder poly(phenylene) with hexamethyl trimethyl ammonium group showed a promising ionomer performance in the preliminary experiments. Further structural optimization is needed for improving electrode performance. It is of great interest to replace the ammonium group with other cationic groups for better electrode kinetics as our preliminary data showed the cationic group in the ionomer greatly impacts the electrocatalyst activity.
- We have investigated the stability of the amide linkage. Alkaline stability test indicates that alkyl amide is most stable under high pH conditions. Based on this result, perfluorinated ionomers having alkyl amide linkage is being synthesized. Development of dispersion technique of the perfluorinated ionomers in liquid fluid is the future work.
- Fuel cell modeling studies showed the adverse impact of low RH and CO_2 on fuel cell performance. Providing actual fuel cell data with variation of modeling parameters is essential for the verification of modeling works.

SPECIAL RECOGNITIONS & AWARDS/ PATENTS ISSUED

1. Anion Exchange Polymer Electrolytes, D.S. Kim, Y.S. Kim, USP 9,048,480 (2015).

2. Poly(Arylene)-based Anion Exchange Membranes, C.B. Bae, Y.S. Kim, USP 9,051,431 (2015).

3. Robust Hydroxide-Conducting Poly(arylenes) for Anion Exchange Membranes and Ionomers, C. Bae, W.–H. Lee (file on November 18, 2014).

4. Stable Quaternary Ammonium-Containing Styrene Block Copolymers for Anion Exchange Membranes, C. Bae, A.D. Mohanty (file on July 22, 2014).

FY 2015 PUBLICATIONS/PRESENTATIONS

Peer-Reviewed Publications

1. "Alkaline Stability of Benzyl Trimethyl Ammonium Functionalized Polyaromatics: a Computational and Experimental Study," Yoong-Kee Choe, Cy Fujimoto, Kwan-Soo Lee, Luke Dalton, Kathy Ayers, Neil Henson, Yu Seung Kim*, *Chem. Mater.*, 26, (19) 5675–5682 (2014).

2. "Mechanistic Analysis of Ammonium Cation Stability for Anion Exchange Membrane Fuel Cells," *J. Mater. Chem*. A. 2, 17314–17320 (2014).

3. "A Microelectrode Study of Interfacial Reactions at the Platinum-Alkaline Polymer Interface," Sung-Dae Yim, Hoon T. Chung, Jerzy Chlistunoff, Dae-Sik Kim, Cy Fujimoto, Tae-Hyun Yang, Yu Seung Kim*, *J. Electrochem. Soc*. 162 (6) F499–F506 (2015).

4. "Fuel Cell Membrane Characterizations," Yu Seung Kim* and Kwan-Soo Lee, *Polymer Reviews* 55, 330–370 (2015).

5. "Fluorine-Based Hydroxide Ion Conducting Polymers for Chemically Stable Anion Exchange Membrane Fuel Cells," *ACS Macro Lett*. 4, 453–457 (2015).

6. "Robust Hydroxide Ion Conducting Poly(biphenyl alkylene)s for Alkaline Fuel Cell Membranes," Woo-Hyung Lee, Yu Seung Kim, Chulsung Bae, *ACS Macro Lett.* 4, 814–818 (2015).

Conference Presentations

1. "Chemical Degradation Mechanisms of Membranes for Alkaline Membrane Fuel Cells," Y-K. Choe, Neil. J. Henson, Yu Seung Kim, Computational Chemistry Symposium in ICCMSE 2015, March 20–23, 2015, Athens, Greece.

2. "Perfluorinated Anion Exchange Membranes," Y.S. Kim, Advances in Polymers for Fuel Cells, Asilomar Conference Grounds, February 8–11, 2015, Pacific Grove, California.

3. "Synthesis of Highly Ion-Conductive Polymers for Fuel Cells," Bae, C.B., 2015 Asilomar Conference on Fuel Cell, Asilomar Conference Grounds, February 8–11, 2015, Pacific Grove, California.

4. "Anion Exchange Membranes with Improved Chemical Stability," Bae, C.B., New York State Center for Future Energy System 2014–2015 Annual Conference, Hilton Garden Inn, Troy, NY, February 26, 2015.

5. "Perfluorinated Ionomers for Alkaline Membrane Fuel Cells," D.S. Kim, S.D. Yim, K.S. Lee, H. Chung, Y-K. Choe, Y.S. Kim, 226th ECS & SMEQ Joint International Meeting, October 5–10, 2014, Cancun, Mexico.

6. "Degradation Mechanism of Membranes for Alkaline Membrane Fuel Cells," Y-K. Choe, N. Hanson, Y.S. Kim, 226th ECS & SMEQ Joint International Meeting, October 5–10, 2014, Cancun, Mexico.

7. "Development of Ion-Conducting Polymers for Clean Energy Conversion," Bae, C.B. Sukant Tripathy Memorial Symposium, University of Massachusetts Lowell, December 5, 2014.

REFERENCES

1. Fuel Cell Technologies Office Multi-Year Research, Development, and Demonstration Plan 2014. http://energy.gov/sites/prod/files/2014/12/f19/fcto_myrdd_fuel_cells.pdf.

2. C. Fujimoto, D.S. Kim, M. Hibbs, D. Wrobleski, Y.S. Kim, *J. Memb. Sci*. 423, 438 (2012).

3. D.S. Kim, C.H. Fujimoto, M.R. Hibbs, A. Labouriau, Y-K. Choe, Y.S. Kim, *Macromolecules* 46, 7826–7833 (2013).

4. C.H. Fujimoto, M.A. Hickner, C.J. Cornelius, D.A. Loy, *Macromolecules* 38, 5010–5016 (2005).

5. M.R. Hibbs, *Journal of Polymer Science, Part B: Polymer Physics* 51, 1736–1742 (2013).

6. Woo-Hyung Lee, Yu Seung Kim, Chulsung Bae, *ACS Macro Lett.* 4, 814–818 (2015).

7. Angela D. Mohanty, Chang Y. Ryu, Yu Seung Kim, Chulsung Bae, *Macromolecules* 48, 19, 7085–7095 (2015).

8. Y.S. Kim, Patent pending, 2015.

V.F.18 DOE's High Acid Content Diels-Alder Poly(Phenylene)s for High Temperature and Low Humidity Applications

Cy Fujimoto

Sandia National Laboratories (SNL)
Organic Materials Group
Albuquerque, NM 87123
Phone: (505) 844-6432
Email: chfujim@sandia.gov

DOE Manager

Gregory Kleen
Phone: (720) 356-1672
Email: Gregory.Kleen@ee.doe.gov

Subcontractor

Tom Zawodzinski, Oak Ridge National Laboratory (ORNL), Oak Ridge, TN

Project Start Date: August 1, 2014
Project End Date: July 31, 2015

Overall Objectives

- Synthesize polymer exchange membrane block copolymer membranes employing DOE's highly phenylated motif
- Measure proton conductivity of the films at 80°C and 120°C at various relative humidities
- Fabricate membrane electrode assemblies (MEAs) of the block copolymer membranes
- Demonstrate single-cell proton exchange membrane fuel cell (PEMFC) performance of the block copolymer membranes
- Demonstrate long-term PEMFC performance

Fiscal Year (FY) 2015 Objectives

- Synthesize highly conductive, high temperature block copolymers
- Measure performance of new architectures through proton conductivity measurements and fuel cell testing

Technical Barriers

This project addresses the following technical barriers from the Fuel Cells section (3.4) of the Fuel Cell Technologies Office Multi-Year Research, Development, and Demonstration Plan:

(A) Durability

(B) Cost

(C) Performance (over a range of temperatures and humidities)

Technical Targets

The objective of this program is to develop high performance, low cost, durable membranes that will meet the DOE's 120°C membrane technical targets for transportation applications. Insights gained from this project will be applied towards the next generation PEMFC systems. The technical targets are listed below.

- Demonstrate area specific resistance (ASR) of 0.05 ohm cm^2 at 120°C and 50% relative humidity (RH) (or 25 μm film 50 mS/cm)
- Demonstrate 100 h of fuel cell performance under load at 120°C

FY 2015 Accomplishments

- Demonstrated nearly double the conductivity of NRE211 211 at 120°C at approximately 30% RH
- Demonstrated significant fuel cell performance of hydrocarbon block copolymer
  - 85°C at 50% RH 0.6 V–2 A/cm^2, at 25% RH 0.6 V–1 A/cm^2
  - 100°C at 50% RH 0.6 V nearly 1 A/cm^2, at 25% RH 0.6 V–500 A/cm^2
  - 120°C at 35% RH 0.6 V–500 mA/cm^2
- Developed and demonstrated improved wet-dry cycling mechanical properties of a highly conductive hydrocarbon block copolymer
- Developed new intellectual property (IP) that SNL is securing to patent

✧ ✧ ✧ ✧ ✧

INTRODUCTION

Although the current state-of-the-art perfluorinated sulfonic acid (PFSA) membranes, such as Nafion® 211, have shown both good durability and performance, cost still remains an issue. Moreover, transient temperature excursions at or above 120°C can be detrimental to PFSAs due to their low glass transition temperature (90–110°C). The objective of this program is to develop high performance, low cost, durable membranes that will meet the DOE 120°C membrane

technical targets for transportation applications [1]. This program consists of three partners that will be responsible for specific tasks. SNL will perform materials testing, ORNL will perform materials characterization and fuel cell testing, and Automotive Fuel Cell Corporation (AFCC) will act as an industrial consultant.

APPROACH

SNL has developed and patented (U.S. 12/425,413) a first generation, block copolymer structure built by pendant aryl sulfonated Diels-Alder poly(phenylene) as the hydrophilic domain, with a highly fluorinated hydrophobic domain (Figure 1a) [2]. The resultant block copolymer was found to possess conductivities and fuel cell performance similar to PFSAs (Figures 1b and 1c). However, under cyclic humidity conditions, these membranes, mechanically failed after only a short time. It was believed that the high water uptakes of these films (+100%) led to high swelling and deswelling under cyclic humidity. Borrowing innovation strategies from our vanadium redox flow battery work (patent submitted 2014), we have discovered that the phenylene backbone can also be functionalized (Figure 2). In this program, we synthesized block copolymers that contain acid moieties on the pendant and backbone segments of the hydrophilic domain (Figure 3a). We initially focused on employing a hydrophobic domain that did not contain any fluorine to reduce cost and eliminate possible hydrogen fluoride formation. However, in response to a request by the United States Driving Research and Innovation for Vehicle efficiency and Energy sustainability (U.S. DRIVE) team and feedback from the DOE Annual Merit Review, we did ultimately examine a fluorine containing hydrophobic domain (Figure 3b).

Through our unique polymer architecture we hoped to gain both high conductivity at low RH and improved mechanical properties. Our hypothesis is based on recent work by Zawodzinski [3], who has determined that PFSAs

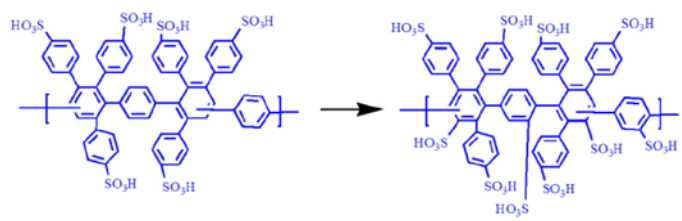

FIGURE 2. High density sulfonation

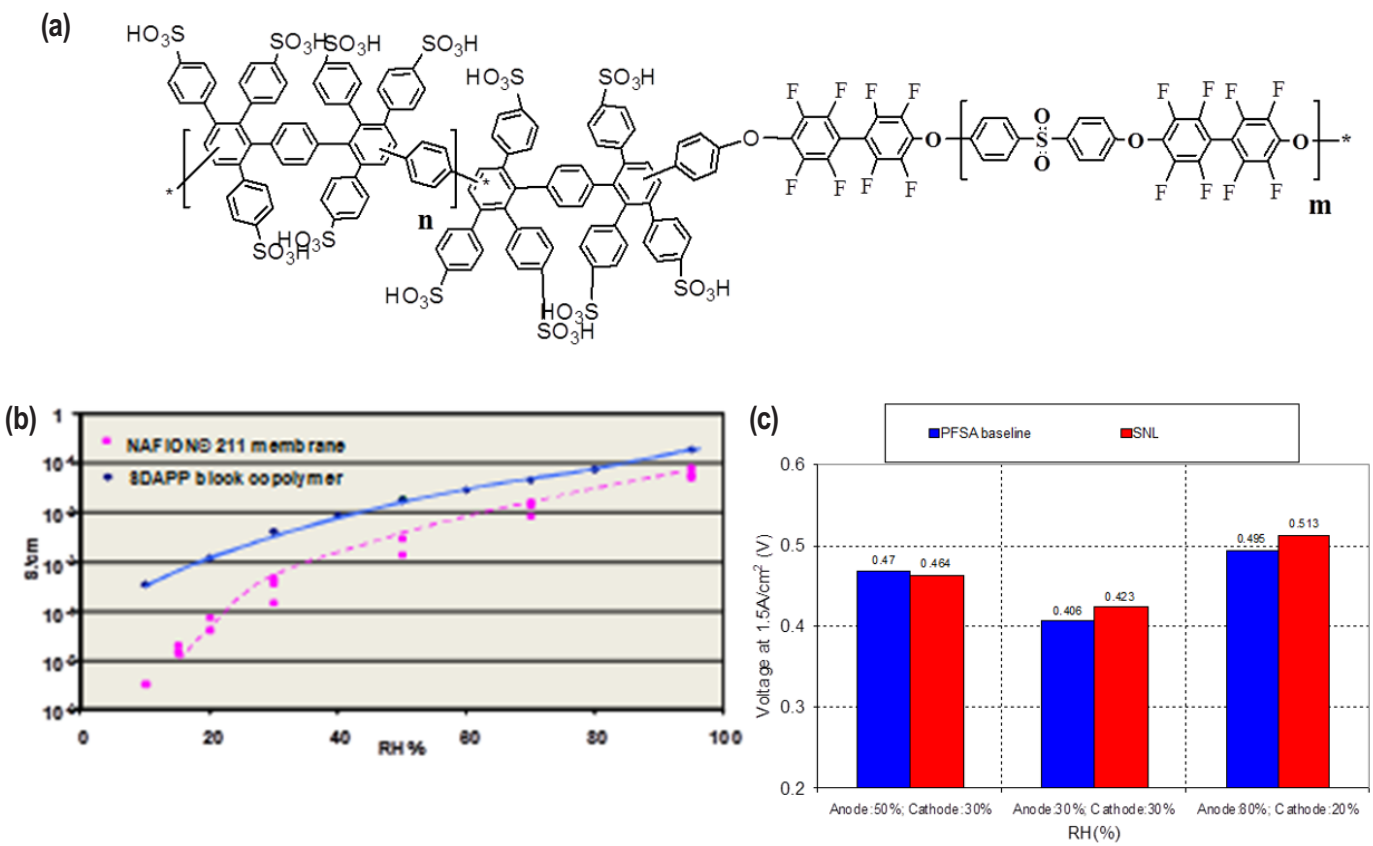

FIGURE 1. First generation block structures: (a) structure of proof of concept block with AFCC; (b) conductivity of first generation vs. Nafion® 211 at 85°C; (c) fuel cell performance of PFSA vs. first generation at 80°C at 1 A/cm²

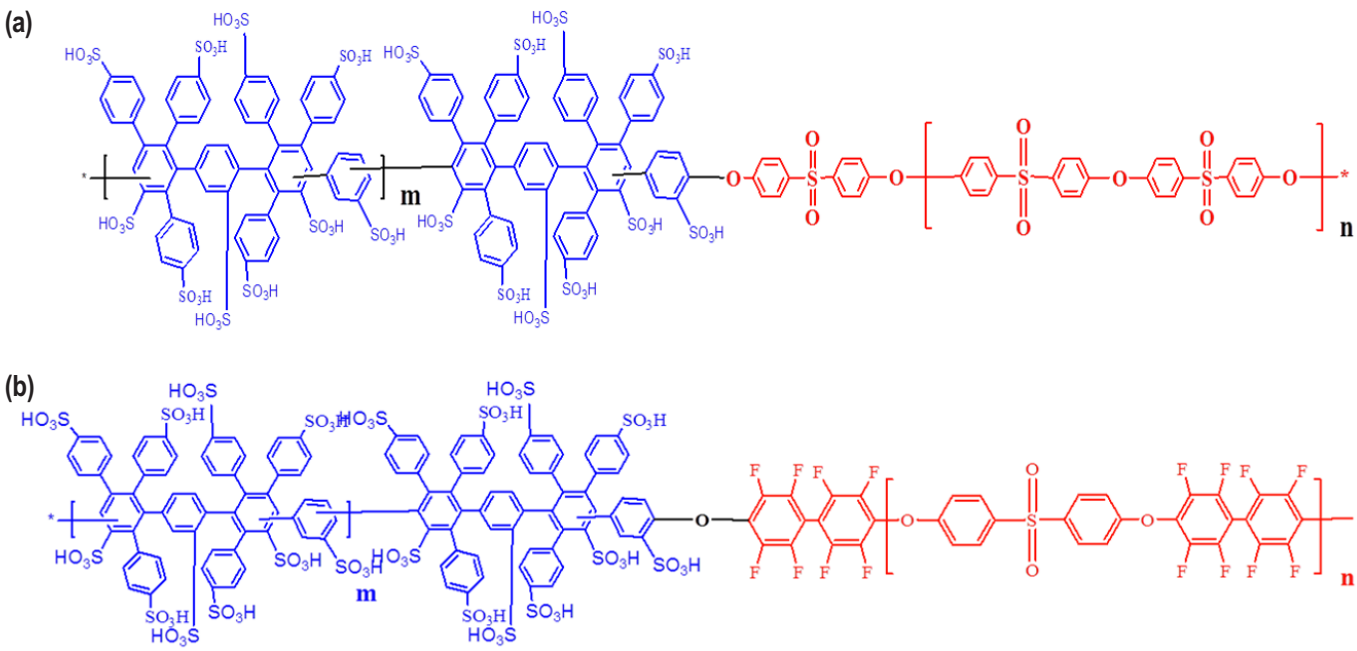

FIGURE 3. (a) Non-fluorinated sulfonic acid FS-DAPP-block copolymer; (b) fluorinated sulfonic acid FS-DAPP-block copolymer

with closely spaced acid moieties enable higher proton mobility at low water content compared to PFSAs of similar equivalent weight that possess longer distances between acid functional groups. We hope to see the same trend in our hydrocarbon block copolymer. Also, by nearly doubling the acid content in the hydrophilic domain we can shorten the hydrophilic segment length relative to the hydrophobic segment; a longer (dominant) hydrophobic segment should strongly influence and improve the mechanical properties of the membranes.

RESULTS

Conductivity of DOE's Block Copolymers

Two of the most critical variables that dictate the physical properties of ionomers in block copolymers are segmental chain length and ion content (ion exchange capacity [IEC] or equivalent weight). From our work with AFCC we have found that an intermediate hydrophilic chain length of m = 10–15 gave promising performance (Figure 1). Therefore, at the start of this project we focused on an intermediate hydrophilic chain length and explored varying the hydrophobic segment length to fine tune the proper ion content for optimal conductivity at high temperatures. Table 1 summarizes the segment lengths tested, resultant ion content, and conductivity of the films.

With exception of the lowest IEC(2.0), all of the block copolymer prepared displayed similar conductivities compared to Nafion® at both low RH and high temperature. Data taken from IEC(3.0) are highlighted in yellow to further emphasize that under all RH and temperature this sample provided the highest conductivities. Moreover, this sample surpassed the first milestone of the program (demonstrate ASR 0.05 ohm cm^2 at 120°C and 50% RH [or 25 µm film 50 mS/cm]); with an average film thickness of 20 µm the ASR for IEC(3.0) is 0.04 ohm cm^2, which is a lower ASR at more aggressive RH conditions (33% instead of 50%)!

TABLE 1. Conductivity of DOE's Block Copolymer vs. Nafion® 211 at Various Temperatures and RH

m Hydrophilic Domain Length	n Hydrophobic Domain Length	IEC meq/g	Conductivity 85°C 95% RH S/cm	Conductivity 85°C 50% RH S/cm	Conductivity 85°C 30% RH S/cm	Conductivity 120°C 33% RH S/cm
15	91	2.0	8.8×10^{-2}	3.7×10^{-3}	8.2×10^{-4}	1.1×10^{-3}
15	72	2.5	2.9×10^{-1}	2.7×10^{-2}	5.0×10^{-3}	2.1×10^{-2}
15	47	3.0	5.8×10^{-1}	5.1×10^{-2}	9.9×10^{-3}	4.7×10^{-2}
Nafion® 211		0.97	1.7×10^{-1}	3.7×10^{-2}	8.5×10^{-3}	2.5×10^{-2}

Fuel Cell Performance of DOE's Block Copolymers

Membrane electrode assembly (MEA) fabrication and testing of IEC(3.0) was performed by Tom Zawodzinski's group at ORNL. Figure 4 displays the polarization curves of both Nafion® 212 (baseline) and IEC(3.0) at 85°C at various RH with H_2/O_2. Oxygen was used initially instead of air to eliminate possible losses from the catalyst layer (e.g., non-optimized catalysts composition/layer) and solely evaluate membrane performance. At 0.6 V IEC(3.0) has a current output of nearly 2 A/cm^2 under all RH conditions! Nafion® 212 however, shows a drop in current density to 1 A/cm^2 at both 50% and 25% RH. Another promising feature of IEC(3.0) is the low ASR under all RH conditions (0.05 ohm cm^2). However, there is also a notable drop in cell voltage at 25% RH at low current density (kinetic region). This loss does not stem from the membrane however, and is instead caused by the dehydration of the catalyst layer. We believe through further optimization of the catalyst layer composition this initial loss can be mitigated.

Since IEC(3.0) outperformed the baseline at 85°C with oxygen, testing under more aggressive real world conditions was initiated. In Figure 5a, IEC(3.0) under H_2/air at 100°C with various RH is plotted. The 75% and 50% RH curves almost overlap and can maintain nearly 1 A/cm^2 at 0.6 V. At 25% RH, the membrane does experience a slight increase in ASR, due to drying of the membrane; however significant loss is again seen in the kinetic region at 25% RH, due to an unoptimized catalyst layer. At 120°C (Figure 5), the data were not as stable as 100°C since the membrane began to self-humidify (by the water product) and dehumidify simultaneously. This makes it difficult for the water content of the membrane to equilibrate. However, in conversations with advisors from General Motors, they expect short temperature excursions up to 120°C that do not necessarily hold at this temperature. At 0.6 V IEC(3.0) can reach a current density of 500 mA/cm^2. Moreover, it is interesting to note that both the infrared (IR) raw and IR free curves are almost identical and may suggest the catalyst layer has water management issues. In this case, further improvements to the catalyst layer composition will further improve performance at these higher temperatures.

We decided not to run IEC(3.0) at 120°C overnight (for durability) since the data were unstable (see water management issue mentioned above) and we were unsure if the carbon gas diffusion layer (GDL) would degrade-combust at 120°C with long term exposure. This brought up safety concerns that will need to be addressed before overnight runs are performed under these conditions. However, we have demonstrated significant fuel cell performance of a hydrocarbon block copolymer ([85°C at 50% RH 0.6 V, 2 A/cm^2, at 25% RH 0.6 V, 1 A/cm^2]; [100°C at 50% RH 0.6 V nearly 1 A/cm^2, at 25% RH 0.6 V, 500 A/cm^2]; [120°C at 35% RH 0.6 V, 500 mA/cm^2]).

Although IEC(3.0) exhibits high conductivity under both high temperature and low relative humidity, its mechanical properties are still an issue. During MEA fabrication, the researchers commented on the large degree of swelling observed when the membrane was exposed to water and the brittleness of the film once it was fully dried. In order to address these concerns we began to develop membranes that would better resist water uptake and mechanical fatigue.

Improved Dimensional Stability of DOE's Block Copolymer

In order to improve the mechanical properties of the block copolymer and reduce water uptake, we modified

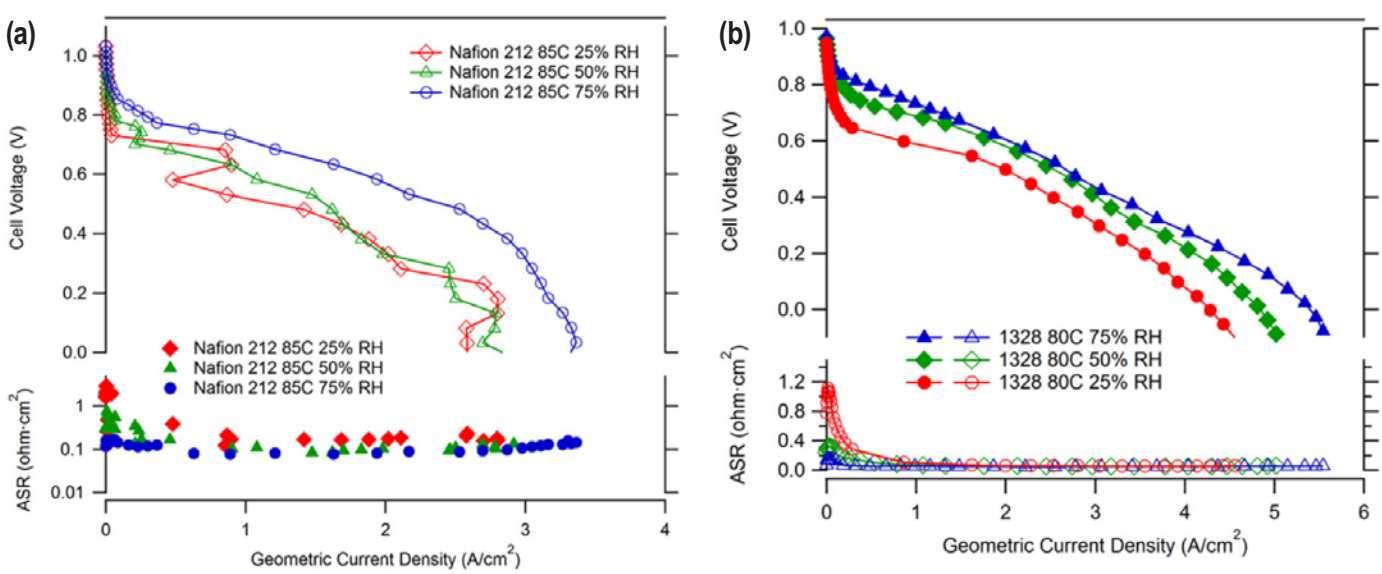

FIGURE 4. Fuel cell polarization H_2/O_2 at 85°C at various RH: (a) Nafion® 212; (b) IEC(3.0)

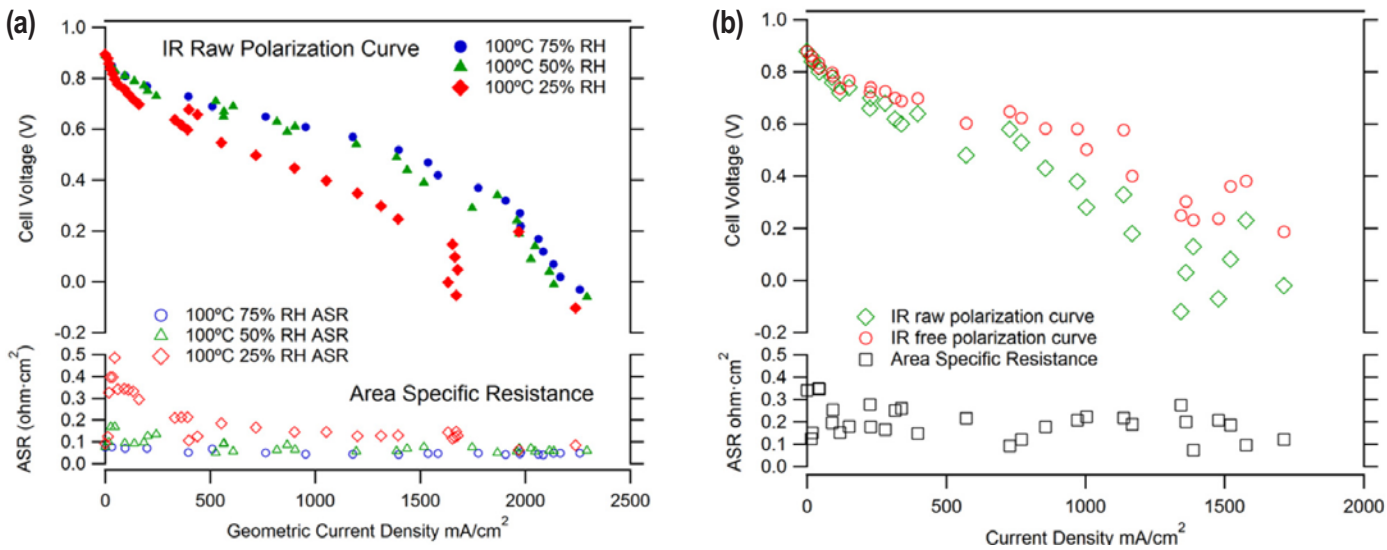

FIGURE 5. Fuel cell polarization H_2/O_2 at 85°C of IEC(3.0): (a) 100°C, various RH; (b) 120°C at 35% RH

the hydrophobic domain to incorporate fluorine. Figure 3b displays the structure of the second block copolymer investigated in this program. The fluorinated block copolymer had a very similar structure to the materials that we previously examined with AFCC (Figure 1a). The main difference between the current and previous materials is that the updated hydrophilic domain has both backbone and pendant sulfonic acid groups. The conductivity data of the fluorinated and non-fluorinated block copolymers and of the Nafion® are summarized Table 2.

Although the conductivity values of the fluorinated block copolymer were slightly lower than both the non-fluorinated block and Nafion® 211, the fluorinated block is promising in that it does not demonstrate a large water uptake (48% compared to 150% between the fluorinated and non-fluorinated). Also, the conductivity drop from 95% RH to 30% RH in the non-fluorinated block is substantial, while the same drop in the fluorinated block is similar to that of Nafion® 211, as shown in Figure 6. This difference is due to the improved water resistance of the fluorinated material and also the more effective water partitioning (water mainly resides in the hydrophilic domain while the hydrophobic domain is better able to resist water). Figure 7 shows the physical expansion of the membranes from dry to wet; the non-fluorinated membrane increased in diameter by 30% while the fluorinated membrane demonstrated a diameter expansion of only 8%.

MEA fabrication and testing of the fluorinated block copolymer was also completed and the results were compared to the non-fluorinated IEC(3.0) membrane in Figure 8. Although the conductivity of the fluorinated membrane

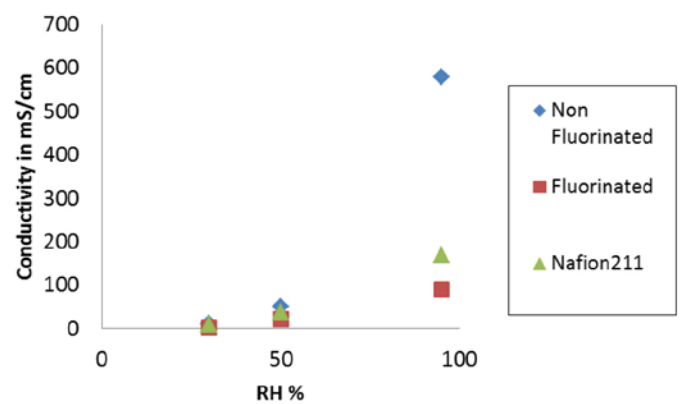

FIGURE 6. Conductivity of the non-fluorinated, fluorinated, and Nafion® 211 at various RH values

TABLE 2. Conductivity of DOE's Fluorinated, Non-Fluorinated Block Copolymer and Nafion® 211 at Various Temperatures and RH

IEC meq/g	Water uptake % RT	Conductivity 85°C 95% RH S/cm	Conductivity 85°C 50% RH S/cm	Conductivity 85°C 30% RH S/cm	Conductivity 120°C 33% RH S/cm
Non-Fluorinated (IEC[3.0])	150%	5.8×10^{-1}	5.1×10^{-2}	9.9×10^{-3}	4.7×10^{-2}
Fluorinated	48%	8.9×10^{-2}	2.1×10^{-2}	2.2×10^{-3}	2.1×10^{-2}
Nafion® 211	34%	1.7×10^{-1}	3.7×10^{-2}	8.5×10^{-3}	2.5×10^{-2}

RT – room temperature

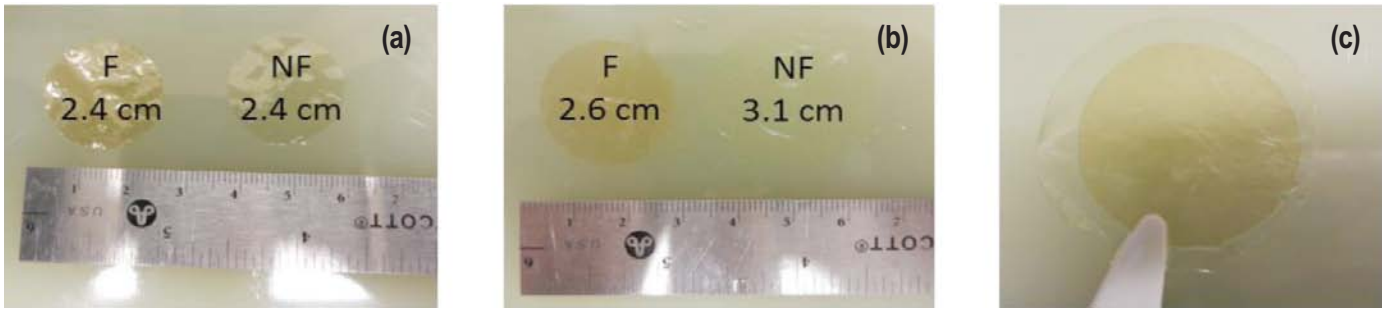

FIGURE 7. Wet-dry dimensional changes of the fluorinated (F) and non-fluorinated (NF) block copolymers: (a) films dry; (b) films wet; (c) overlay of N and NF

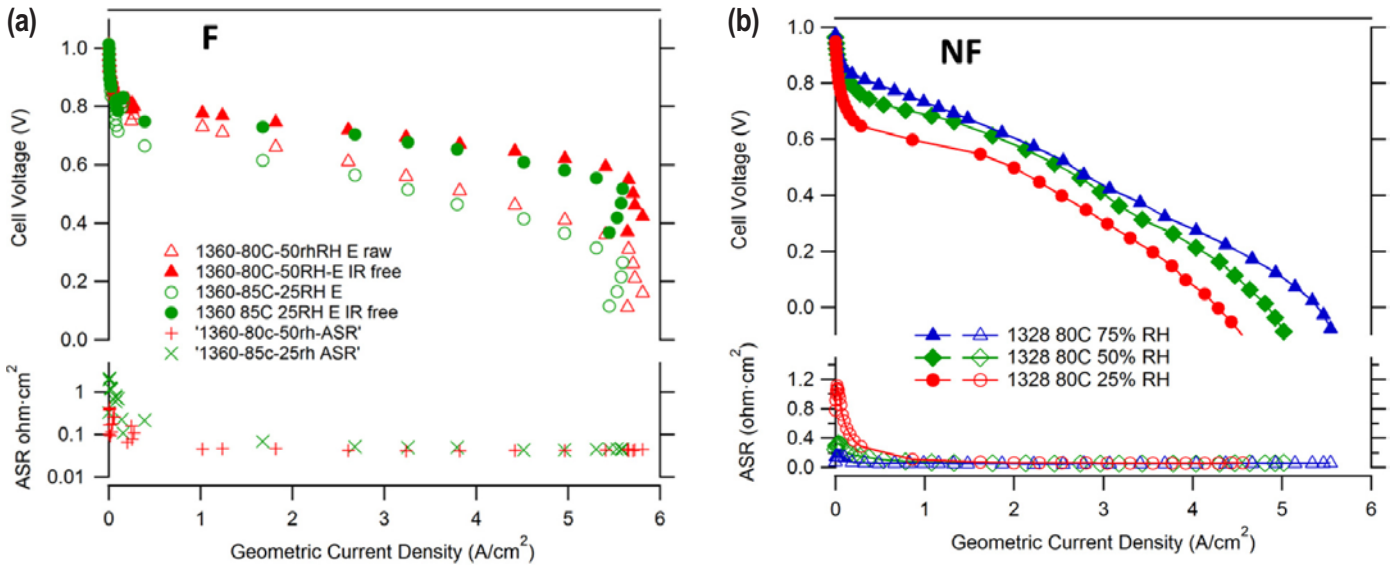

FIGURE 8. Fuel cell polarization H_2/O_2: (a) fluorinated at 80°C at 50% and 25% RH; (b) non fluorinated at 80°C at 50% and 25% RH

was slightly lower than that of the IEC(3.0), the fuel cell performance at both 50% and 25% RH at 80°C was nearly identical, with very similar ASRs.

These results are very encouraging since the fluorinated block copolymer is a rare example of a hydrocarbon displaying high conductivity and low water swelling. We are currently optimizing the hydrophilic-hydrophobic segment length and ion content for transportation use. We believe that this improvement will lead to significant improvement in the durability of the DOE's block copolymer, which was a hurdle in earlier work with AFCC. Finally, Sandia is currently pursuing to patent the fluorinated block copolymer as an improvement over (U.S. 12/425,413).

CONCLUSIONS AND FUTURE DIRECTIONS

- A series of DOE owned, hydrocarbon block copolymers have been synthesized. These materials have shown outstanding conductivities at high temperatures/low RH and achieved the program's initial milestone of 0.05 ohm cm^2 at 120°C at 50% RH.
- The DOE block copolymers were readily fabricated into MEAs. Single cell fuel cell tests of the block copolymers outperformed Nafion® 212, especially in the lower RH regions (50% and 25%). Although the fuel cell tests were very promising, further work in optimizing the catalyst layer composition for the hydrocarbon block copolymers is expected to further improve its performance under these aggressive conditions.
- With concerns about the high degree of water uptake and swelling of the initially tested materials, we modified the polymer architecture to reduce water affinity. The new polymer morphologies showed very promising properties of high conductivities at low RH and low water uptake. SNL is currently securing the IP for this new set of materials.

- We were unable to perform long term durability testing at 120°C with the initial materials that were investigated due to concerns of film brittleness and unstable fuel cell output. However, with the new materials developed within this program and further optimization of the catalyst layer composition, stable fuel cell output and long term testing will become viable.

SPECIAL RECOGNITIONS & AWARDS/ PATENTS ISSUED

We are currently working on submitting a patent on the fluorinated hydrocarbon membrane discussed in this report shortly. We have held off on publishing the new findings of this report until the patent has been submitted.

FY 2015 PUBLICATIONS & PRESENTATIONS

1. High Temperature and Low Humidity Membranes. Fujimoto, C.; Zawodzinski, T; Tang, Z.; Nelson, J. Oral Presentation at the U.S. DRIVE Fuel Cell Meeting. February 2015, Detroit, MI.

2. High Temperature and Low Humidity Membranes. Fujimoto, C.; Zawodzinski, T; Tang, Z.; Nelson, J. Poster Presentation at DOE Hydrogen and Fuel Cell AMR. June 2015, Washington, DC.

REFERENCES

1. Fuel Cell Technologies Office Multi-Year Research, Development and Demonstration Plan 2014. http://energy.gov/sites/prod/files/2014/12/f19/fcto_myrdd_fuel_cells.pdf.

2. Fujimoto, C.; Hibbs, M.; Ambrosini, Andrea. Multi-block sulfonated poly(phenylene) copolymer proton exchange membranes. U.S. (2012), US 8110636 B1 20120207.

3. Maalouf, M.; Sun, C.N.; Pyle, B.; Emery, M.; Haugen, G.; Hamrock, S.; Zawodzinski, T. Factors enabling high mobility of protons and water in perfluorosulfonate membranes under low hydration conditions. International Journal of Hydrogen Energy (2014), 39(6), 2795–2800.

V.F.19 Engineered Low-Pt Catalyst Layers

Mahlon S. Wilson[1] (Primary Contact),
Huai-Suen Shiau,[2] Adam Z. Weber,[2]
Rangachary Mukundan,[1] Yu Seung Kim,[1]
Karren L. More[3]
[1]Los Alamos National Laboratory
PO Box 1663
Los Alamos, NM 87545
Phone: (505) 667-9178
Email: mahlon@lanl.gov
[2]Lawrence Berkeley National Laboratory, Berkeley, CA
[3]Oak Ridge National Laboratory, Oak Ridge, TN

DOE Manager
Nancy Garland
Phone: (202) 586-5673
Email: Nancy.Garland@ee.doe.gov

Project Start Date: October 1, 2014
Project End Date: September 30, 2015

Overall Objectives

- Overcome the "unaccounted" low-Pt loading loss in fuel cell performance by tailoring the topology of the ionomer within an otherwise conventional catalyst layer
- Establish through modeling the theoretical underpinnings and validity of the approach

Fiscal Year (FY) 2015 Objectives

- Develop the techniques necessary to achieve the desired ionomer topologies in catalyst layers formed by conventional ink processing
- Demonstrate recovery of the "unaccounted" performance loss in 0.05 mg Pt/cm^2 50 cm^2 membrane electrode assemblies (MEAs) by comparison with commercial low-Pt MEAs using side-by-side testing

Technical Barriers

This project addresses the following technical barriers from the Fuel Cells section of the Fuel Cell Technologies Office Multi-Year Research, Development, and Demonstration Plan:

(B) Cost

(C) Performance

Technical Targets

The technical target that reflects the catalyst layer development effort is shown in Table 1.

TABLE 1. Technical Targets for Transportation Applications Relevant to this Project

Metric	Units	DOE 2020 Target	Project Status
PGM Total Loading	mg PGM/cm^2	0.125	0.05 (cathode only)

PGM—Precious Group Metals

FY 2015 Accomplishments

- The project team modeled the idealized catalyst layer configuration of ionomer nanofibers with thin ionomer films coating catalyst agglomerates. The modeling predicts that incorporating ionomer nanofibers significantly increases fuel cell performance.
- Two separate high-temperature processes for post-processing of electrospun Nafion® nanofibers for increased durability and insolubility were developed.
- Nafion® coated multi-walled carbon nano-tubes (MWCNTs) as a surrogate for ionomer nanofibers were used to prepare 50 cm^2 MEAs with high and low thin film ionomer compositions. The unoptimized latter showed performance approaching that of commercial low-Pt MEAs.

✧ ✧ ✧ ✧ ✧

INTRODUCTION

When conventional fuel cell MEA cathode Pt loadings are below about 0.1 mg Pt/cm^2, a drop-off in performance occurs, substantially more so than can be ascribed to simple kinetic losses. This negatively impacts efforts to lower Pt loadings to, say, 0.05 mg Pt/cm^2 and still maintain high fuel cell performance. While the reasons are not entirely clear [1], this "unaccounted" loss appears to be primarily manifested as an elevated oxygen transport resistance. One explanation is that the oxygen flux through any ionomer film overlying the catalyst must increase as the amount of catalyst is decreased, resulting in the greater mass transfer barrier. As such, decreasing the ionomer content in conventional-style catalyst layers such that only a very thin film coats the catalyst could alleviate the difficulty by minimizing the transport barrier. However, simply decreasing the amount of Nafion® in the ink formulation is not sufficient as any improvement in reactant transport is negated by the decrease

in ionic conductivity through the catalyst layer. Further, a minimum of ionomer is needed to provide sufficient robustness for conventional catalyst layer ink processing and cell assembly. Consequently, the intention of this project is to engineer the topology of the catalyst layer ionomer to provide low-Pt catalyst layers with low oxygen transport resistance, high bulk conductivity, and structural integrity.

APPROACH

The general approach in this project is to configure the distribution of the ionomer in the catalyst layer to provide the desired combination of properties described above. It is proposed that the optimal configuration consists of two separate "phases" of ionomer in the catalyst layer, a very thin first one coating the catalyst surfaces to provide local conductivity with a minimal oxygen transport barrier, and a second phase of a solid ionomer network to provide bulk ionic conductivity and structural integrity (Figure 1a). Modeling explores the validity of the approach and provides insight into the effects of the relative amounts of the two phases.

To a certain extent, realizing the very thin first ionomer "phase" (light blue in Figure 1a) can be accomplished by adding only enough ionomer to the ink formulation to form a thin film over the catalyst surface area, but the dispersion of this limited amount of ionomer becomes critical for maximizing the electrochemical surface area (ECSA). Consequently, a subsidiary effort in the project is to investigate the synthesis of carbon supports doped with heteroatoms beyond nitrogen to provide greater wettability and corrosion resistance.

The very thin ionomer films will not alone provide sufficient bulk ionic conductivity to the catalyst layer, nor a dried ink layer that will remain intact during processing and assembly. A separate second phase of ionomer in the form of a stable highway network is included to provide

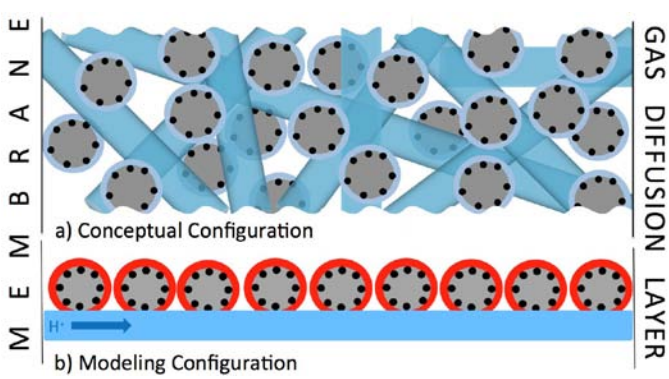

FIGURE 1. (a) The conceptual catalyst layer configuration of thin ionomer film coated agglomerates covering ionomer nanofibers, (b) configuration used for modeling, here the thin-film ionomer is in red

ionic connectivity to catalyst agglomerates and throughout the catalyst layer, shown as medium blue fibers in Figure 1a. Ideally, this solid ionomer addition would have a high-aspect ratio to help with connectivity and binding the catalyst layer together; possibilities include nanofibrillated fibers, fibers formed in the nanopores of sacrificial scaffolds, or electrospun nanofibers. The first two result in discrete fiber "powders" that can be added directly to the catalyst ink, whereas the continuous electrospun fibers formed as a mat need to be milled for ink processing. However, fibers formed by low-temperature recasting such as electrospinning are fragile. Consequently, durability and insolubility, necessary for processing and withstanding the catalyst layer operating environment, will be need to be improved significantly. Otherwise, dissolution, deformation, and compaction result in a low-porosity and densified catalyst layer with poor reactant transport. For conventional catalyst layer ink processing, the toughened electrospun nanofibers are powdered to form small fiber networks for inclusion into the ink (though the formation of uniform dispersions is not without challenges). If successful, a sturdy and durable catalyst layer with high bulk ionic conductivity and low oxygen transport resistance is formed by conventional ink processing. MEAs fabricated in this manner are combined with commercial gas diffusion layers (GDLs) specifically designed for low-Pt loadings for fuel cell testing and side-by-side comparisons with baseline commercial MEAs using similar catalysts, GDL's and hardware.

RESULTS

A multiscale model of the approach has been developed to investigate the effect of ionomer nanofiber-thin film distribution on fuel cell performance. Figure 1b depicts the model configuration of the cathode catalyst layer (CL) with the components situated between the membrane and the GDL. H^+ is transported from the membrane through ionomer nanofibers (blue) to ionomer films (red), ultimately arriving at Pt sites around agglomerate cores. Oxygen diffuses through the red thin films in Figure 1b to reach catalyst sites. The volume fractions of catalysts, ionomers, and pores in the CL are 0.36, 0.34, and 0.30, respectively. The GDL porosity is 30% and the CL and GDL thicknesses are 10 um and 50 um, respectively. The fraction of ionomer in the nanofiber phase is varied from 0% (thin film only) to 90%. The radius of agglomerate cores is 50 nm and the thin film is 5 nm in thickness when no nanofiber phase is present. Assuming the ionomer-wetted surface area of the carbon phase is constant, the thin film thickness, and hence oxygen transport barrier, varies proportionally with the total volume fraction of ionomer film in the CL. The H^+ conductivities employed here are ionomer-film = 10^{-3} S/cm and nanofiber = 10^{-1} S/cm, reflecting the lower value observed in thin ionomer films [2]. Lastly, the O_2 diffusion coefficient through the thin film

= 9.7 x 10^{-6} cm^2/s and the bulk O_2 concentration in the CL macropores is 0.005 mol/m^3.

Figure 2 shows the color-graded distributions of ionic potential of the CL ionomer for scenarios with 10%, 70%, and 90% nanofiber (with the balance comprising the thin film) with the ionic potential fixed at 0.4 V at the membrane interface. With high fiber contents, the drop in fiber ionic potential further away from the membrane is relatively minor, but this benefit is counteracted by increased potential drops in the ionomer films around the (unseen) agglomerates as the films become thinner (variations in film thicknesses not depicted). Since the film ionic potential is a reasonable proxy for the oxygen reduction reaction rate, the far sides of the agglomerates from the fiber are relatively inactive in the 90% case. In the 10% case, the entire periphery of each individual agglomerate contributes fairly equally, but those further away from the membrane less so. The 70% case is a compromise of the two extremes; each agglomerate contributes roughly equally and the potential drop around the agglomerate periphery is not severe.

Figure 3 depicts a series of fuel cell polarization curve simulations with the nanofiber content varied from 0 to 90% of total ionomer. Increasing the second phase nanofiber ionomer content significantly improves performance, with the maximum current densities at 0.6 V occurring with 50–60% nanofiber ionomer contents (Figure 3 inset). At 50% content and below, the oxygen diffusion tangentially through the ionomer thin film is the rate-limiting transport mechanism. At 60% and above, H+ conduction through the thin film is rate-limiting, consequently, the maximum current density occurs where the two limitations are about equal. While the modeling reflects an idealized structure (e.g., all nanofibers in the z-direction, all agglomerates immediately adjacent a nanofiber, etc.), it clearly indicates the potential for substantially increasing CL performance. The nanofibrillation of Nafion® did not produce high-aspect ratio structures, consequently efforts focused on electrospinning to produce precursor mats for subsequent milling to provide a powder for the catalyst layer inks. Nafion® was readily electrospun provided the solution contained ≤0.1% PEO, unfortunate but necessary to provide phase continuity for the electrostatically induced drawing of the fibers. A more severe hindrance was that the essentially low-temperature recast

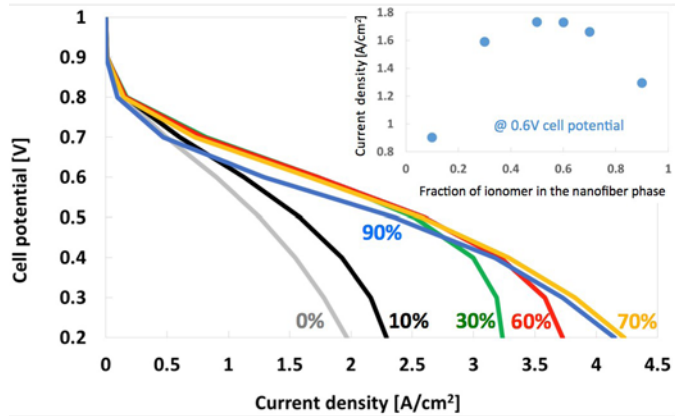

FIGURE 3. Polarization curve simulations for catalyst layers with nanofibers ranging from 0 to 90% of the total ionomer content. Inset depicts the current densities at 0.6 V as a function of nanofiber content.

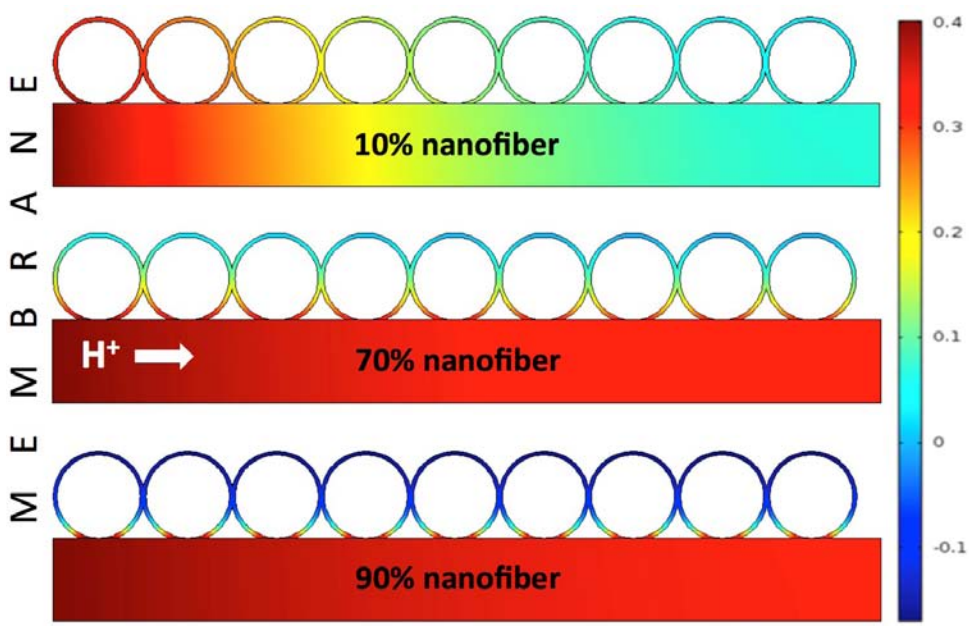

FIGURE 2. Ionomer ionic potential distributions within the thin films surrounding the (unseen) agglomerates and the bulk phase nanofibers for 10%, 70%, and 90% nanofiber ionomer content

electrospun ionomer fibers were both physically fragile and easily redissolved, of concern for withstanding the rigors of ink processing and the operating catalyst layer. The as-spun Nafion® quickly dissolved in solutions typically used for catalyst inks and even fibers annealed at 120°C succumbed.

The initial lack of durable and insoluble fibers stimulated an alternate attempt to demonstrate the proposed ionomer topology. MWCNTs coated with high-temperature recast Nafion® [3] were used as a surrogate for the neat ionomer nanofibers. MEA inks were prepared with standard 20%Pt -XC72 catalysts, surrogate Nafion®/MWCNT fibers, and either low or high solubilized Nafion® levels. The fuel cell performances of 50 cm^2 MEAs with 0.05 mg Pt/cm^2 cathode loadings indicated that the high-solubilized Nafion® ink had a high ECSA but mediocre performance, and the low-solubilized content had a low ECSA but performance that nearly matched that of the commercial baseline MEA in side-by-side testing [4]. Improvements are expected provided stable nanofiber ionomers and improved thin film dispersions (to maximize ECSA/minimize film thickness) can be obtained.

In the side effort to improve ionomer (and catalyst) dispersions on carbon catalyst supports, phosphorus was added to nitrogen as heteroatom dopants as it increases surface energy and stability in supercapacitors [5]. Nanofibers from electrospun polyacrylonitrile + phosphoric acid (PA) solutions were pyrolyzed to obtain doped carbon supports. However, under inert pyrolysis gasses, PA suppressed N and increased O content. Using N_2 or NH_3 gas increased N but O was still high and NH_3 scavenged P at high temperatures. A combination of NH_3 at lower temperatures and N_2 at high maximized P and N content and significantly reduced O.

Returning to the main effort, approaches were pursued to increase nanofiber durability and solvent resistance. One method was to electrospin Nafion® solutions in the tetrabutylammonium form to impart thermoplasticity to the ionomer [6] and thus increase durability and crystallinity after thermal annealing. Indeed, post-spinning annealing substantially improves the properties, but at the risk of the fine thermoplastic fibers fusing into coarse structures. Annealing temperature is consequently critical. A more forgiving and higher temperature approach under development capitalizes upon the increased strength and insolubility imparted by high temperature casting of the ionomer [3]. Since high temperature electrospinning is impractical, the process here entails introducing a low volatility component into the electrospinning solution that is retained within the as-spun fibers (Figure 4a) and then removed in a high temperature "recasting," resulting in some fiber fusion and cross-linking (Figure 4b). If too much agent is used, the high temperature recast again dissolves the fibers into featureless films. With the appropriate amount, fiber morphology is retained and easily handled robust veils

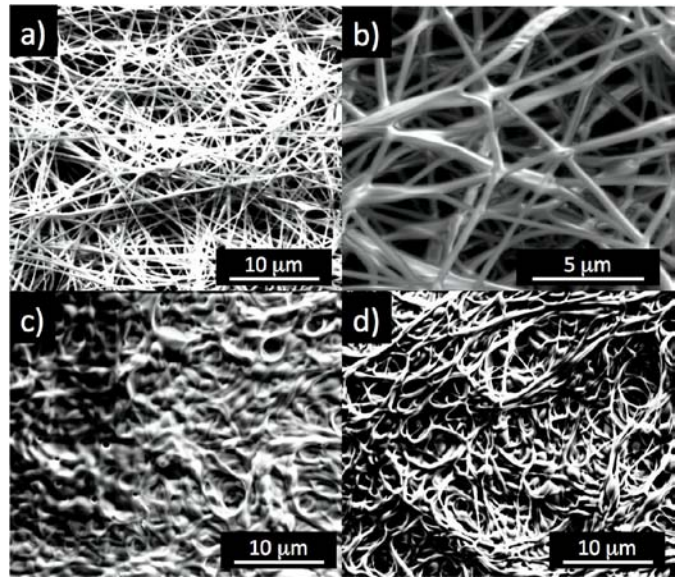

FIGURE 4. (a) As-spun ionomer nanofibers containing a recasting agent (b) Nanofibers after 250°C annealing (c) Milled and cast H^+ nanofibers after heating in neat alcohols (d) Milled and cast H^+ nanofibers after heating in alcohol, water, and ethylene glycol mixture

are formed. After protonation, the mats swell up in alcohols much like cross-linked superabsorbents, but dry again to pliable veils. Milling results in nanofiber suspensions for use in catalyst layer inks, however, solvents plus heating can still degrade the fibers. To test, suspensions were formed and heated in various ink solvent mixtures without catalysts so that cast films can be imaged to evaluate fiber integrity. Figure 4c of one such casting shows substantial dissolution after heating and stirring in neat alcohols, while Figure 4d depicts fibers that have remained intact using a solution also containing water and ethylene glycol (such convoluted and dense-packed morphologies are typical from casting milled suspensions).

CONCLUSIONS AND FUTURE DIRECTIONS

Modeling predicts that the engineered ionomer topology approach has the potential to significantly increase fuel cell performance. The ideal catalyst layer configurations have yet to be achieved, but even the non-ideal surrogates nearly matched commercial baseline MEAs. Success will hinge on the ability to attain the ideal ionomer topology and requisite durability. Before the end of the FY, the best ink formulations (high thin film dispersion and high rate of nanofiber survival) will be used to make a series of 50 cm^2 MEAs of varying nanofiber to thin film ratios to compare to commercial MEAs and the modeling results.

FY 2015 PUBLICATIONS/PRESENTATIONS

1. "Next Generation Catalyst Layers," M.S. Wilson and H.-S. Shiau. Oral presentation to the 8th Meeting of the Transport Modeling Working Group, May 19, 2015, Lawrence Berkeley National Laboratory, Berkeley, CA.

2. "Engineered Low-Pt Catalyst Layers," M.S. Wilson, A.Z. Weber, H.-S. Shiau, Y.S. Kim, D. Langlois, K.S. Lee, R. Mukundan, and K. More. Poster presentation at the DOE Hydrogen and Fuel Cells Program Annual Merit Review, Washington, DC, June 8–12, 2015.

REFERENCES

1. Adam Z. Weber, and Ahmet Kusoglu. "Unexplained Transport Resistances for Low-Loaded Fuel-Cell Catalyst Layers." *Journal of Materials Chemistry A* 2, no. 41 (2014): 17207–17211.

2. Miguel A. Modestino, Devproshad K. Paul, Shudipto Dishari, Stephanie A. Petrina, Frances I. Allen, Michael A. Hickner, Kunal Karan, Rachel A. Segalman, and Adam Z. Weber. "Self-Assembly and Transport Limitations in Confined Nafion Films." *Macromolecules* 46, no. 3 (2013): 867–873.

3. Yu Seung Kim, Cynthia F. Welch, Rex P. Hjelm, Nathan H. Mack, Andrea Labouriau, and E. Bruce Orler. "Origin of Toughness in Dispersion-Cast Nafion Membranes." *Macromolecules* 48, no. 7 (2015): 2161–2172.

4. Mahlon S. Wilson. "Engineered Low-Pt Catalyst Layers." *2015 DOE Hydrogen and Fuel Cells Annual Merit Review* (http://www.hydrogen.energy.gov/pdfs/review15/fc125_wilson_2015_p.pdf).

5. Denisa Hulicova-Jurcakova, Alexander M. Puziy, Olga I. Poddubnaya, Fabian Suarez-Garcia, Juan M. D. Tascon, and Gao Qing Lu. "Highly Stable Performance of Supercapacitors from Phosphorus-Enriched Carbons." *Journal of the American Chemical Society* 131, no. 14 (2009): 5026–5027.

6. Robert B. Moore, Kevin M. Cable, and Timothy L. Croley. "Barriers to Flow in Semicrystalline Ionomers. A Procedure for Preparing Melt-Processed Perfluorosulfonate Ionomer Films and Membranes." *Journal of Membrane Science* 75, no. 1–2 (1992): 7–14.

V.F.20 Semi-Automated MEA Fabrication with Ultra-Low Total PGM Loadings

Stoyan Bliznakov* (Primary Contact), Miomir Vukmirovic, James Wegrzyn*, and Radoslav Adzic
Brookhaven National Laboratory (BNL)
*Sustainable Energy Technology Department
Chemistry Department
Upton, NY 11973
Phone: (631) 344-8865
Email: sbliznakov@bnl.gov

DOE Manager
Nancy Garland
Phone: (202) 586-5673
Email: Nancy.Garland@ee.doe.gov

Project Start Date: November 1, 2014
Project End Date: October 31, 2015

Overall Objectives

- Design, develop, and demonstrate an innovative methodology for fast and facile electrodeposition of Pt monolayer (ML) shell on non-noble refractory metal core electrocatalysts for the oxygen reduction reaction, directly on gas diffusion layers (GDLs)
- Demonstrate the feasibility of developed electrodeposition strategy for scaling up and fabrication of electrodes and membrane electrode assemblies (MEAs) with ultra-low platinum group metal (PGM) loadings and performance that meet or exceed the DOE 2020 technical targets

Fiscal Year (FY) 2015 Objectives

- Develop a semi-automated system for nanoengineering of Pt ML on Pd interlayer on refractory metal alloy (WNi) core catalysts directly on GDLs
- Optimize the composition, structure, and morphology of electrodeposited refractory metal alloy cores and the protocols for deposition of Pt ML shell for fast fabrication of highly active and durable cathodes for cost effective MEAs
- Explore the impact of the structure, morphology, and hydrophobicity of the GDLs from different commercial suppliers on the deposition of the catalysts layer, and optimize the pretreatment protocols to maximize the MEA performance
- Demonstrate the potential of the proposed advanced strategy for preparation of gas diffusion electrodes (GDEs) and fabrication of large MEAs with performance that meet and/or exceed the DOE targets for activity and durability

Technical Barriers

This project addresses the following technical barriers from the Fuel Cells section of the Fuel Cell Technologies Office Multi-Year Research, Development, and Demonstration Plan:

(A) Durability

(B) Cost

(C) Performance

Technical Targets

At BNL we have designed and developed a semiautomated system for electrodeposition of advanced Pt_{ML}/Pd/WNi electrocatalysts with ultra-low PGM loading directly on GDLs. This innovative strategy allows fast and facile preparation of GDEs starting from raw materials (chemicals and GDL) and fabrication of MEAs in less than an hour. The project's technical targets are compared to the DOE 2020 targets in Table 1. The total PGM loading currently attained in 5 cm^2, 25 cm^2, and 50 cm^2 MEAs is 0.120 mg_{PGM}/cm^2 with a projection of achieving less than 0.1 mg_{PGM}/cm^2 by the end of the project. The mass activity target of 0.44 A/mg is achieved on 5 cm^2 MEAs and is approached closely on 50 cm^2 MEAs. Excellent durability performance after 34,000 accelerated stress test (AST) voltage cycles is observed in the MEAs. The loss in the mass activity is 20%, and the voltage loss at 0.8 A/cm^2 is only 19 mV.

TABLE 1. Progress towards Meeting the Technical Targets for Electrocatalysts for Transportation Applications

Characteristic	Units	DOE 2020 Targets	BNL 2015 Status	Project's Targets
PGM total loading (both electrodes)	mg/cm^2	<0.125	0.120	<0.1
Loss in catalytic (mass) activity after 30,000 AST voltage cycles	% loss	<40	20	<30
Loss in performance at 0.8 A/cm^2	mV	30	19	<25
Mass activity @ 900 $mV_{iR\text{-}free}$	A/mg	0.44	0.46; 0.41*	>0.44

*Measured on 50 cm^2 MEA

FY 2015 Accomplishments

The accomplishments for the nine-month period since the beginning of the project are as follows.

- Designed and developed a semiautomated software controlled system for facile fabrication of large GDEs and MEAs with ultra-low total PGM loading, complete Pt utilization, and improved activity and performance stability
- Nanoengineered complex Pt ML shell on Pd interlayer on refractory metal alloy (WNi) core electrocatalysts directly on the GDLs in a single electrochemical cell that allows reproducible fabrication of GDEs with geometrical size of up to 300 cm^2
- Optimized electrochemical protocols and electrolyte compositions for in situ precise control of the catalyst layer structure, thickness, morphology, and composition for improved MEA performance
- The impact of the structure and the surface modification procedure of the GDLs from different suppliers on the catalyst layer structure and utilization was studied, and the best GDL was identified
- Optimized conditions for fabrication of MEAs with geometric areas of up to 50 cm^2, and demonstrated potential for meeting the DOE 2020 targets for activity and durability with ultra-low total PGM loadings

✧ ✧ ✧ ✧ ✧

INTRODUCTION

It has recently been reported [1] that the Pt_{ML} core-shell electrocatalysts ($Pt_{ML}Pd$ /C and $Pt_{ML}Pd_{0.9}Au_{0.1}$/C) are among the most promising candidates that possess a potential to meet the DOE 2020 targets. However, reduction of the PGM loading in the cores, development of scaling up methods for reproducible synthesis, and improving the catalysts' durability are important unresolved challenges that will further reduce the catalysts' cost and improve their performance and durability.

In order to address these challenges, we have developed a semiautomated system for electrodeposition of Pt_{ML} shell on electrodeposited PdWNi nanoparticles core directly on the GDL. In this approach we substitute most of Pd in the core by refractory metal alloy (WNi) and limit the thickness of the Pd interlayer to two to three MLs. This results in reducing the PGM loading and improving the stability of the core. The proposed innovative strategy is not only an alternative to the existing methodology for synthesis of Pt ML core-shell catalysts, but outlines a novel pathway for fast preparation of GDEs, and hence facile fabrication of MEAs with geometric size of industrial significance. As-prepared electrodes are with ultra-low PGM loading and complete Pt utilization. The strategy allows in situ precise control of the structure, composition, thickness, and morphology of the catalyst layer directly on the GDL for fine tuning of the electrode's performance, which is advantageous over the conventional ink spraying methodology.

APPROACH

BNL's unique approach allows facile fabrication of large fuel cell electrodes with ultra-low PGM loadings, starting from raw materials, in less than an hour. The strategy employs two phenomena: (i) induced co-electrodeposition of refractory WNi alloys and (ii) displacement of under-potential deposited (UPD) Cu monolayer by Pt. The as-developed semiautomated system assures software controlled exchange of the solution in the electrochemical cell, where the deposition and displacement processes are taking place under controlled conditions. The catalysts' synthesis is realized in three sequential steps. First, WNi refractory alloy nanoparticles are co-electrodeposited from citrate solution of both metals of interest, and then after exchanging the solution in the cell with Pd^{2+} containing electrolyte, Pd partially displaces the Ni and forms a Pd interlayer over the WNi core. The displacement step is monitored in situ by measuring the open circuit potential, and the amount of the Pd is controlled precisely. In the last step, the solution is exchanged with an electrolyte containing both Pt^{2+} and Cu^{2+} ions, in which the Cu^{2+} concentration is two orders of magnitude higher than that of Pt^{2+}. Pt_{ML} is deposited on top of the Pd interlayer by applying a short pulse in the Cu UPD range to form a Cu ML on Pd. Then after releasing the potential control, the more noble Pt ions displace the Cu atoms. After rinsing the cell with plenty of nanopure water, the electrode is dried and an appropriate amount of liquid Nafion® (5%) ionomer is sprayed over the catalyst layer. The electrode is then dried again. Finally, the electrode is assembled with a Nafion® membrane and an anode, prepared by spraying of commercial Pt catalyst ink onto a GDL, by hot pressing together at 130°C for 1 min. The as-prepared MEA is mounted in a single cell hardware, activated, and its performance is evaluated at real fuel cell operating conditions.

RESULTS

In the first quarter of the project we designed and developed a semiautomated system for electrodeposition of Pt ML core-shell fuel cell electrocatalysts with ultra-low PGM loading (<0.07 mg_{PGM}/cm^2) and complete Pt utilization, directly on GDLs. The system is software controlled and allows fabrication of highly active and durable fuel cell cathodes starting from raw materials (chemical salts and commercial GDLs). A schematic of the system is shown in Figure 1. The system consists of (i) an electrochemical cell that allows fabrication of electrodes with size of up

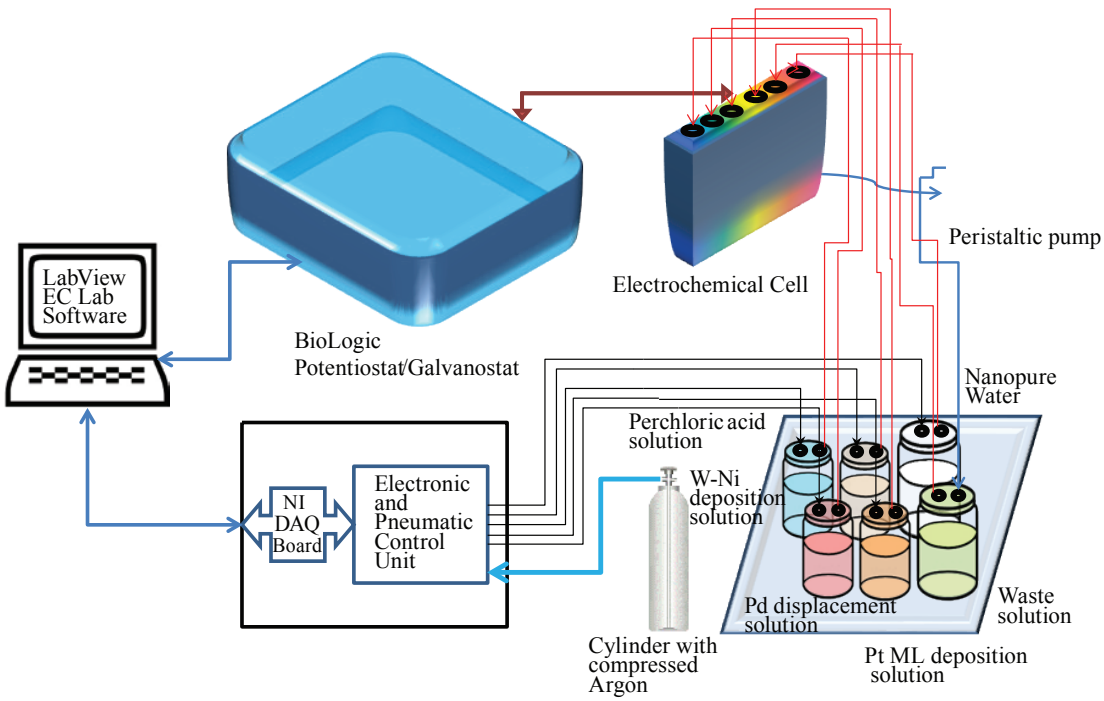

FIGURE 1. Schematic of the semiautomated system for electrodeposition of core-shell (Pt_{ML}/Pd/WNi) fuel cell electrocatalysts, directly on GDL

to 300 cm^2; (ii) a pneumatic control unit with respective electronics that controls the flow of different electrolyte solutions from the deaerated (purged with Ar) stock solutions (WNi plating solution, Pd displacement solution, Pt ML deposition solution, perchloric acid solution, and water) to the cell in a particular order; (iii) an electronic data acquisition board from National Instruments that allows the LabVIEW software to control all the processes step by step; and (iv) a BioLogic potentiostat galvanostat that controls the WNi electrodeposition, Pd displacement, and Cu UPD and Pt ML deposition processes.

Figure 2 presents a picture of the electrochemical cells that have been developed for fabrication of electrodes with geometric area of up to 300 cm^2. We have developed the capabilities to fabricate large electrodes, but, unfortunately, our current fuel cell test station allows us to evaluate the performance of MEAs with a maximum geometric area of 50 cm^2. Larger electrodes and MEAs will be fabricated and tested upon availability of additional funding for purchasing a 2 kW fuel cell test station. The uniform and homogeneous deposition of the catalysts of interest over the entire electrode surface area is defined by the distribution of the electric field in the cell, and as well as from the hydrodynamic flow of the electrolyte in the cell. Both factors strongly depend on the geometry and the volume of the cell, which were optimized. Homogeneous distribution of the electrocatalyst over the electrode area was confirmed for up to 50 cm^2 electrodes. The reproducibility of the catalyst deposition is governed by the repeatability of each step in the multi-step sequence that

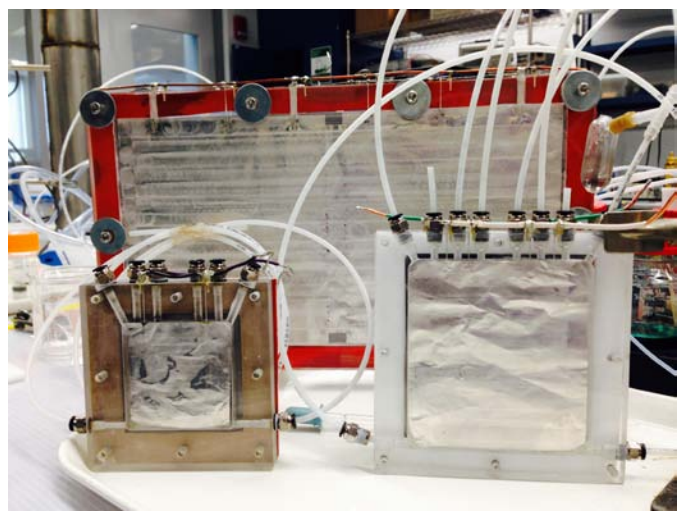

FIGURE 2. Picture of the electrochemical cells designed for fabrication of GDEs with geometric areas of up to 300 cm^2

is programmed in the software controlling the potentiostat. Thus, the software assures exact repeating of each step, and that the reproducibility in the composition, structure, and morphology for the fabricated electrodes exceeds 98%.

The optimization of the electrodeposition protocols, as well as the catalyst layer structure, composition, morphology, and thickness, was first performed on 5 cm^2 electrodes and MEAs, respectively; then, 50 cm^2 MEAs

were fabricated and their performance was evaluated. In addition, GDLs from different commercial suppliers were examined, and Sigracet® 25BC was identified as the best support for the electrodeposited Pt_{ML}/Pd/WNi catalyst layer. The polarization curves measured on 5 cm^2 MEA in H_2/O_2 atmosphere, 80°C and 150 kPa backpressure after different numbers of AST voltage cycles, are presented in Figure 3. The initial mass activity is 0.46 A/mg_{PGM}, and only 20% loss is observed after 34,000 AST voltage cycles. The voltage loss at 0.8 A/cm^2 is only 19 mV after 34,000 cycles. The polarization curves measured on 50 cm^2 MEAs, at the same conditions, but at two different backpressures, are presented in Figure 4. The mass activity at 900 mV (iR-free) is 0.41 A/mg_{PGM}, which is very close to the targeted value of 0.44 A/mg_{PGM}. The results obtained render a developed strategy for direct electrodeposition of Pt ML shell on PdWNi core electrocatalysts on the GDL as a viable methodology for fast and facile fabrication of MEAs that possess the potential to meet and even to exceed the DOE 2020 targets for cost, durability, and performance.

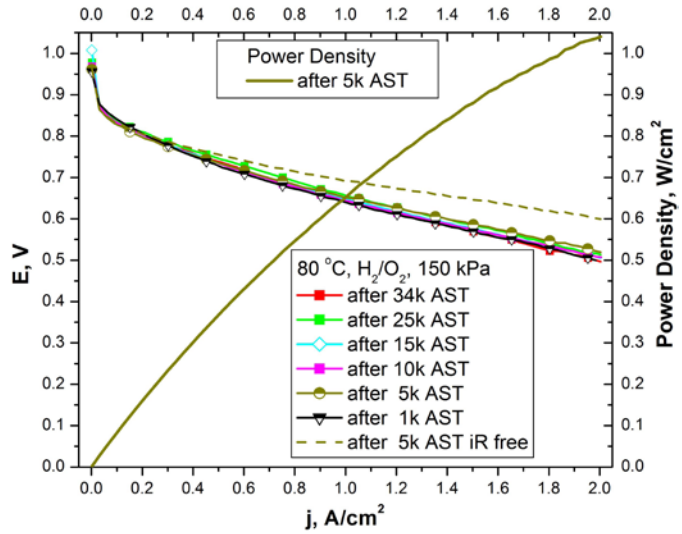

FIGURE 3. Polarization curves measured on 5 cm^2 MEA in H_2/O_2 at backpressure of 150 kPa. The PGM loading on the Pt_{ML}/Pd/WNi/GDL cathode is 0.07 mg_{PGM}/cm^2, and the Pt loading on the anode is 0.05 mg_{Pt}/cm^2 (TKK Pt catalysts). The MEA is assembled with a Nafion® HP membrane

CONCLUSIONS AND FUTURE DIRECTIONS

Conclusions derived from the work in FY 2015 include the following.

- A semiautomated system for fabrication of fuel cell electrodes and MEAs with ultra-low PGM loading has been developed.
- The proposed electrodeposition strategy allows fast and facile preparation of electrodes with a geometric area of up to 300 cm^2.
- Different GDLs were tested, and Sigracet® 25BC GDL was identified as the best support for the Pt_{ML}/Pd/WNi electrocatalysts.
- The performance of the MEAs, with geometric areas of 5 cm^2, 25 cm^2, and 50 cm^2, was examined.
- The mass activity and durability performance of the MEAs of interest meet and in some cases exceed the DOE 2020 targets.

Future directions include the following.

- Explore different electrodeposition protocols to determine the impact of the size and shape of the refractory cores on the activity and durability of 300 cm^2 MEAs
- Reduce MEA fabrication time to less than 30 min by optimizing each step
- Develop a protocol for electrodeposition of anode catalysts with ultra-low Pt loading (less than 30 $\mu g/cm^2$), and thus reduce the total PGM loadings to less than 0.1 mg_{PGM}/cm^2 for both electrodes

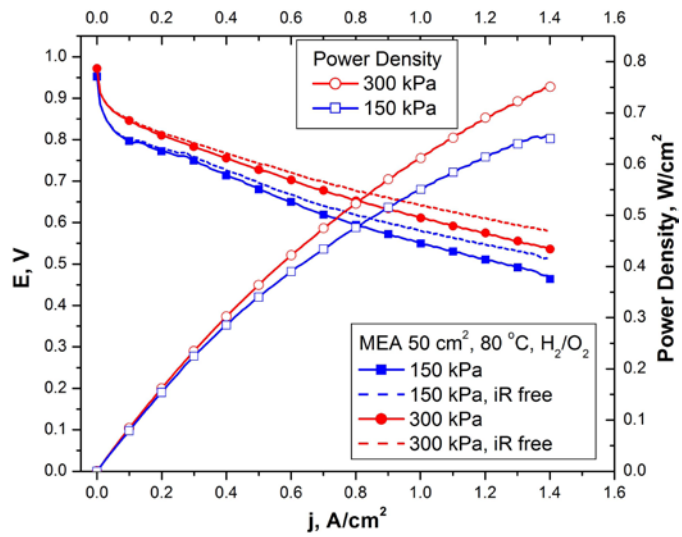

FIGURE 4. Polarization curves measured on 50 cm^2 MEA in H_2/O_2 at backpressures of 150 kPa and 300 kPa. The MEA is assembled with Pt_{ML}/Pd/WNi/GDL cathode (0.09 mg_{PGM}/cm^2), standard Pt/C (TKK Pt catalyst, 0.05 mg_{Pt}/cm^2) anode, and Nafion® XL membrane

- Improve the MEA performance at high power densities and in H_2/air atmosphere
- Conceptualize an automated/low cost roll-to-roll 100% Pt utilization MEA fabrication process in support of fuel cell manufacturing needs, and reduce the time for electrode and MEA fabrication to less than 15 min

FY 2015 PUBLICATIONS/PRESENTATIONS

1. R. Adzic, S. Bliznakov, and M. Vukmirovic, US Patent: Core-Shell Fuel Cell Electrodes, **US2015/0017565 A1**, Jan. 15, 2015.

2. S. Bliznakov, M. Vukmirovic, R. Adzic, Electrochemical Atomic-level Controlled Synthesis of Electrocatalysts for the Oxygen Reduction Reaction, *Atomically-Precise Methods for Synthesis of Solid Catalysts*, S. Hermans and T. Visart de Bocarme, Editors, Chapter 6, p. 144, *The Royal Society of Chemistry*, RCS Catalysis Series No. **22**, (2015).

REFERENCES

1. K. Sasaki, H. Naohara, Y. Choi, Y. Cai, W.-F. Chen, P. Liu, and R.R. Adzic, "Highly Stable Pt Monolayer on PdAu Nanoparticle Electrocatalysts for the Oxygen Reduction Reaction," Nature Communications, **3**, 1115 (2012).

VI.0 Manufacturing R&D Sub-Program Overview

INTRODUCTION

The Manufacturing Research and Development (R&D) sub-program supports activities needed to reduce the cost of manufacturing hydrogen and fuel cell systems and components. Manufacturing R&D will enable the mass production of components in parallel with technology development and will foster a strong domestic supplier base. The sub-program's R&D activities address the challenges of moving today's technologies from the laboratory to high-volume, pre-commercial manufacturing to drive down the cost of hydrogen and fuel cell systems. The sub-program focuses on the manufacturing of components and systems that will be needed in the early stages of commercialization. Research investments are focused on reducing the cost of components currently used or planned for use, as well as reducing overall processing times. Progress toward targets is measured in terms of reductions in the cost of producing fuel cells, increased manufacturing processing rates, and growth of manufacturing capacity.

In Fiscal Year (FY) 2015, manufacturing projects continued in the following areas: use of rolled goods quality control to detect defects in membrane electrode assembly materials; modeling of the effect of defects on fuel cell material properties.

GOAL

Develop innovative technologies and processes that reduce the cost of manufacturing fuel cells and systems for hydrogen production, delivery, and storage.

OBJECTIVES[1]

Key objectives for Manufacturing R&D include the following.

- Develop manufacturing techniques to reduce the cost of automotive fuel cell stacks at high volume (500,000 units per year) from the 2008 value of $38/kW to $20/kW by 2020
- Develop fabrication and assembly processes to produce onboard vehicle hydrogen storage systems achieving 1.8 kWh/kg (5.5 wt% H_2) and 1.3 kWh/L (40 g H_2/L) at a cost of $12/kWh ($400/kg H_2 stored) or less by 2017
- Support efforts to reduce the cost of manufacturing components and systems to produce hydrogen at <$4/gge (gallons gasoline equivalent; 2007 dollars; untaxed, delivered, and dispensed) by 2020

FY 2015 TECHNOLOGY STATUS

Presently, fuel cell systems are fabricated in small quantities. The cost of a 10-kW, low temperature polymer electrolyte membrane (PEM) fuel cell system for backup power is projected to be ~$3,700/$kW_{net}$ at a volume of 100 systems per year[2]. For automotive applications using today's technology, the cost of an 80-kW PEM fuel cell system is projected to be $55/kW for high volume manufacturing (500,000 systems per year)[3]. Projected costs include labor, materials, and related expenditures, but do not account for manufacturing R&D investment.

FY 2015 KEY ACCOMPLISHMENTS

FY 2015 saw a number of advancements in the manufacture of fuel cells and hydrogen storage systems.

- New algorithms for automated defect detection: National Renewable Energy Laboratory (NREL) expanded on its previous demonstration of optical inspection for fuel cell electrodes by developing algorithms that can automatically detect defects of various types from the real-time inspection data (Figure 1). The algorithms were shown to have no false positives on sample materials from General Motors. This work supports improved technology transfer to industry and addresses Manufacturing R&D sub-program milestones for membrane electrode assembly inspection.

[1] Note: Targets and milestones were recently revised; therefore, individual project progress reports may reference prior targets.
[2] http://www.hydrogen.energy.gov/pdfs/review14/fc098_wei_2014_o.pdf
[3] http://www.hydrogen.energy.gov/pdfs/review15/fc018_james_2015_o.pdf

- Component quality control measurement: In FY 2014, NREL demonstrated its reactive impinging flow (RIF) technique in which the reactive gas ($H_2/O_2/N_2$) flows onto conductive fuel cell roll goods; heat from the chemical reaction is then detected. In FY 2015, Lawrence Berkeley National Laboratory (LBNL) modeled the RIF process with gas diffusion electrode material. LBNL predicted the change in temperature of the material (due to the reactive excitation and heat generation) as a function of the width of the defect for three different defect depths, and results can be seen in Figure 2. Clearly at any defect width, the more the catalyst layer thickness is reduced, the higher the temperature change from the bulk material. If the lines are extrapolated down to $\Delta T = 1$ K or 2 K, the width of the minimum detectable defect can be determined.

Funding Opportunity Announcement (FOA): On March 3, 2015, the Office of Energy Efficiency and Renewable Energy (EERE) Fuel Cell Technologies Office (FCTO) released an FOA entitled "Hydrogen and Fuel Cell Technologies Research, Development, and Demonstrations." The FOA included a topic on innovative hydrogen delivery pipeline manufacturing with funding up to $1.5 million. The organizations selected for negotiation will be announced soon.

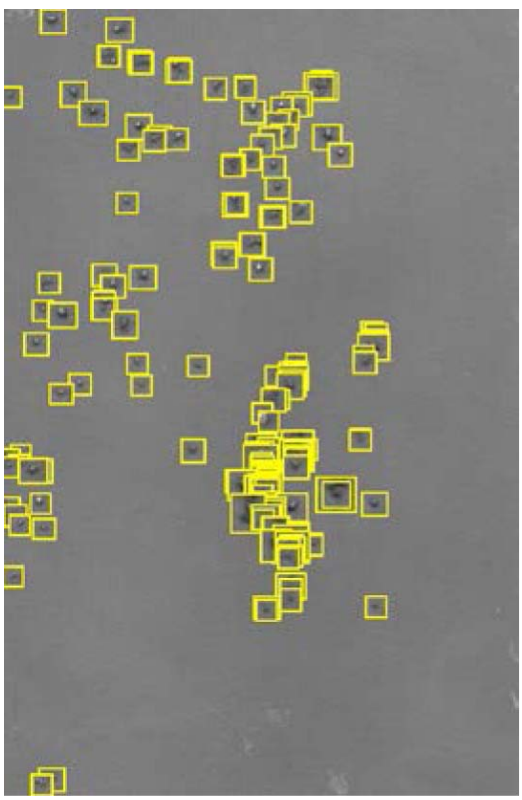

FIGURE 1. Image of intentionally created scuffs and scratches on fuel cell membrane. Defects were detected using optical reflectance. The scanning system operated on sheet materials at 10 fpm. Algorithms were developed and demonstrated for automated detection as illustrated by the yellow boxes. The debris images (dots) were magnified 10x for ease of viewing.

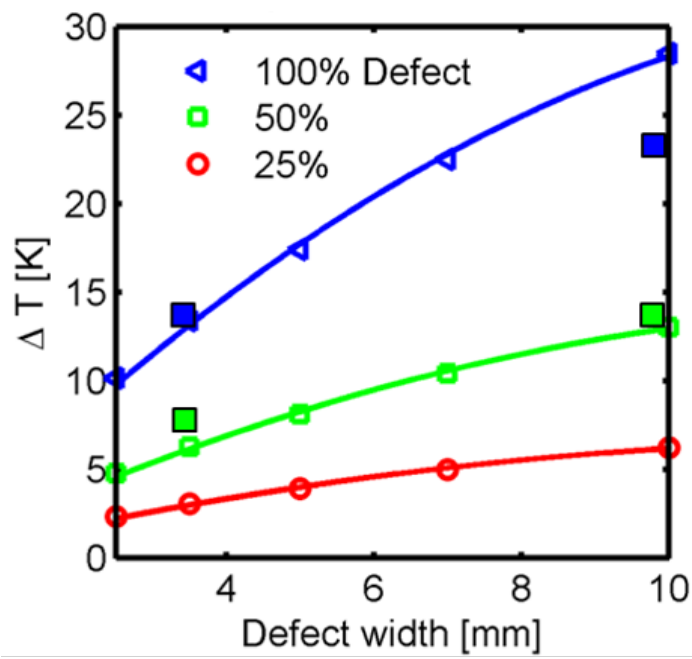

FIGURE 2. Change in temperature of gas diffusion layer material as a function of defect width following reactive excitation for three different defect thicknesses. 100% defect means that all the reactive material is gone and only a bare spot is left. 50% means that the thickness of catalyst layer is reduced by one half, and 25% means the thickness is reduced by one quarter. The solid symbols represent experimental data while the hollow symbols are model predictions. The solid lines were drawn to guide the eye through the modelled data points.

BUDGET

The President's FY 2016 budget request for FCTO includes $4 million for Manufacturing R&D. The FY 2015 appropriation for Manufacturing R&D was $3 million (Figure 3).

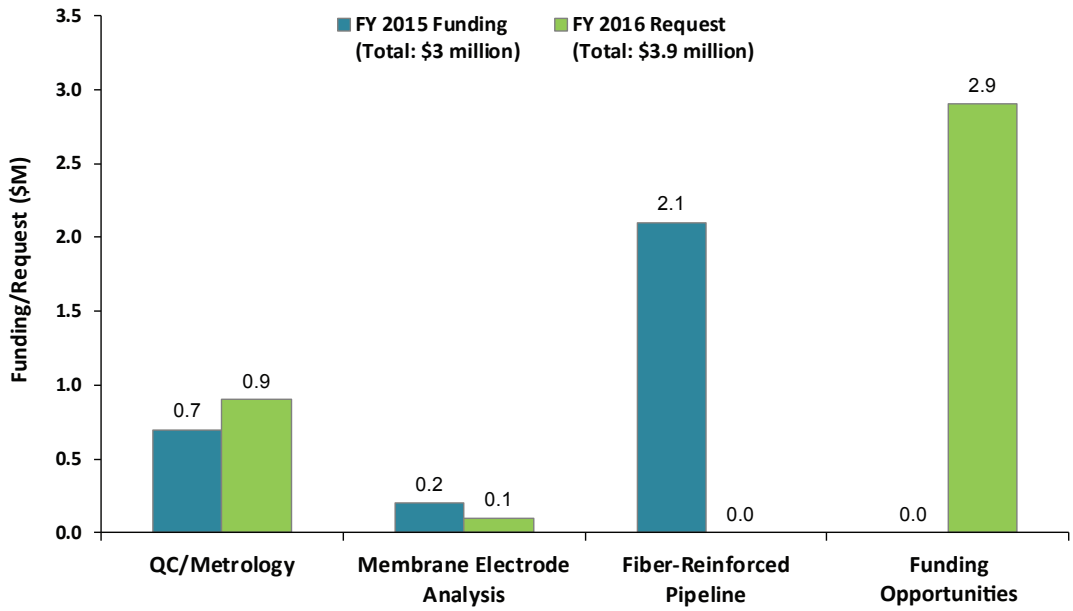

QC – quality control

FIGURE 3. Manufacturing R&D Funding. Subject to appropriations, project go/no-go decisions, and competitive selections. Exact amounts will be determined based on research and development progress in each area and the relative merit and applicability of projects competitively selected through planned funding opportunity announcements.

FY 2016 PLANS

In FY 2016, the Manufacturing R&D sub-program will:

- Continue projects on supply chain development (Ohio Fuel Cell Coalition and Virginia Clean Cities at James Madison University) and global manufacturing competitiveness analysis (GLWN - Westside Industrial Retention & Expansion Network) in collaboration with DOE's Clean Energy Manufacturing Initiative and NREL's Clean Energy Manufacturing Analysis Center.
- Initiate a project to manufacture reliable joints (with very low leak rates) that connect fiber-reinforced pipeline for hydrogen delivery at 100 bar.
- Correlate the size of defects generated during membrane and/or membrane electrode assembly fabrication to loss of fuel cell performance.
- Continue to use predictive modeling and single and segmented cell test methods to assist diagnostic development.
- Develop novel defect detection via infrared detection of the thermal response of material.
- Expand implementation of defect diagnostic techniques on industry production lines to original equipment manufacturers.

FCTO plans to release an FOA that includes topics on hydrogen and fuel cell manufacturing R&D in FY 2016, with awards subject to appropriation and announced later in the fiscal year. FCTO will continue to coordinate with other agencies (including the National Institute of Standards and Technology and the U.S. Department of Defense) and with other technology offices within EERE to identify synergies and leverage efforts.

Nancy Garland
Manufacturing R&D Project Manager
Fuel Cell Technologies Office
Office of Energy Efficiency and Renewable Energy
U.S. Department of Energy
1000 Independence Ave., SW
Washington, D.C. 20585-0121
Phone: (202) 586-5673
Email: Nancy.Garland@ee.doe.gov

VI.1 Fuel Cell Membrane Electrode Assembly Manufacturing R&D

Michael Ulsh (Primary Contact), Guido Bender, Peter Rupnowski
National Renewable Energy Laboratory (NREL)
15013 Denver West Parkway
Golden, CO 80401
Phone: (303) 275-3842
Email: michael.ulsh@nrel.gov

DOE Manager
Nancy Garland
Phone: (202) 586-5673
Email: Nancy.Garland@ee.doe.gov

Partners
- Lawrence Berkeley National Laboratory (LBNL), Berkeley, CA
- Colorado School of Mines, Golden, CO
- New Jersey Institute of Technology, Newark, NJ
- Automotive Fuel Cell Cooperation, Burnaby, BC, Canada
- General Motors, Pontiac, MI
- Ion Power, New Castle, DE
- W.L. Gore and Associates, Elkton, MD

Project Start Date: July 16, 2007
Project End Date: Project continuation and direction determined annually by DOE

Overall Objectives

- Evaluate and develop inline diagnostics for cell and component quality control and validate diagnostics inline
- Investigate the effects of membrane electrode assembly (MEA) component manufacturing defects on MEA performance and durability to understand the required performance of diagnostic systems and contribute to the basis of knowledge available to functionally determine manufacturing tolerances for these materials
- Use established models to predict the effects of local variations in MEA component properties, and integrate modeling of the operational and design characteristics of diagnostic techniques into the design and configuration of inline measurement systems
- These objectives have strong support from the industry. Specifically, the outcomes of the 2011 NREL/DOE Hydrogen and Fuel Cell Manufacturing R&D Workshop, the Office of Naval Research-funded Manufacturing Fuel Cell Manhattan Project, and the 2013 DOE Office of Energy Efficiency & Renewable Energy (EERE) Quality Control Workshop confirmed the importance of continued development of inline quality control techniques for cell manufacturing. Our specific development activities have been and will continue to be fully informed by direct input from industry. As new technologies emerge and as the needs of the industry change, the directions of this project will be adjusted.

Fiscal Year (FY) 2015 Objectives

- Make a go/no-go decision for further work to transition the through-plane infrared/direct-current (IR/DC) technique for industrially relevant MEA constructions from the benchtop roller system to the web-line
- Make a go/no-go decision for further work to transition through-plane reactive excitation (TPRE) of industrially relevant MEA constructions from an enclosed benchtop system to a system design applicable to the web-line
- Complete upgrades on the optical reflectometry prototype system
- Perform in situ performance and failure studies on MEAs with defined defects

Technical Barriers

This project addresses the following technical barriers from the Manufacturing R&D section (3.5) of the Fuel Cell Technologies Office Multi-Year Research, Development, and Demonstration (MYRDD) Plan:

(A) Lack of High-Volume MEA Processes

(E) Lack of Improved Methods of Final Inspection of MEAs

(H) Low Levels of Quality Control

Contribution to Achievement of DOE Manufacturing R&D Milestones

This project contributes to the achievement of the following DOE milestones from the Manufacturing R&D section (3.5) of the MYRDD Plan:

- Milestone 5.1: Establish models to predict the effect of manufacturing variations on MEA performance. (1Q, 2016)
- Milestone 5.2: Demonstrate improved sensitivity, resolution, and/or detection rate for MEA inspection methods. (4Q, 2016).

FY 2015 Accomplishments

NREL accomplished the following in FY 2015:

- Demonstrated the infrared/reactive impinging flow (IR/RIF) technique on our research web-line, including fabrication of a gas diffusion electrode sheet with defined defects, detection of all defects at web speeds up to 30 fpm, and development of noise reduction strategies to improve defect detection
- Performed modeling of the impinging flow dynamics of the IR/RIF technique to help understand the effects of process variables and configurations and to predict potential process improvements
- Developed automated detection algorithms for optical reflectance detection of membrane and electrode defects
- Further refined the through-plane and in-plane IR/DC techniques and verified their applicability to new industry MEA and subassembly constructions
- Developed improved models for cell performance and utilized these models to predict the effects of electrode layer manufacturing variations on cell performance
- Performed in situ studies of performance effects in cells with as-manufactured and/or created defects
- Designed, built and commissioned a new testbed to study the parametric effects of TPRE of MEAs or subassemblies for the detection of membrane pinholes
- Demonstrated the detection of membrane pinholes at least as small as 150 µm diameter in MEAs and membrane-containing subassemblies using TPRE
- Developed an apparatus and methods for creating pinholes at least as small as 50 µm diameter in membranes and membrane-containing subassemblies with high repeatability
- Continued collaboration with our industry partners in accordance with our project charter

✧ ✧ ✧ ✧ ✧

INTRODUCTION

In FY 2005–2007, NREL provided technical support to DOE in developing a new key program activity: manufacturing R&D for hydrogen and fuel cell technologies. This work included a workshop on manufacturing R&D that gathered inputs on technical challenges and barriers from the fuel cell industry, and subsequent development of a roadmap for manufacturing R&D. In late FY 2007, NREL initiated a project to assist the fuel cell industry in addressing these barriers, initially focusing on inline quality control of MEA components.

Defects in MEA components differ in type and extent depending on the fabrication process used. The effects of these defects also differ depending on size, location in the cell relative to the reactant flow field, cell operating conditions, and which component contains the defect. Understanding the effects of these different kinds of defects is necessary in order to specify and/or develop diagnostic systems with the accuracy and data acquisition/processing rates required for the speed and size scales of high volume continuous manufacturing methods. Furthermore, predictive capabilities for manufacturers are critical to assist in the development of tolerances and to enable assessment of the effects of material and process changes.

APPROACH

NREL and its partners are addressing the DOE manufacturing milestones listed above by evaluating, developing, and validating (inline) diagnostics that will support the use of high volume manufacturing processes for the production of MEAs and MEA component materials. Prioritization of this work is based on inputs from our industry partners on their critical manufacturing quality control needs. We are focusing on diagnostic capabilities not addressed by commercially available inline systems; in particular, we are evaluating methods to make areal rather than point measurements such that discrete defects can be identified. We also are developing test methodologies to study the effects of the size and/or extent of each important type of variability or defect. These results will assist our industry partners in validating manufacturing tolerances for these materials, ultimately reducing scrap rates and cost, and improving supply chain efficiency. Finally, predictive models are being used at LBNL to understand the operational and design characteristics of diagnostic techniques by simulating the behavior of MEA components in different excitation modes. These results are being fed back to our design effort in configuring the diagnostics for inline implementation. MEA models are also being utilized to understand the in situ behavior of defected MEAs to guide and further elucidate experiments.

RESULTS

Our major milestone for the past year was the demonstration of our IR/RIF technique on our research web-line. In support of this demonstration, we used an ultrasonic spray coating system to fabricate a 3-ft-long section of electrode on a gas diffusion layer/microporous layer sheet having a series of defects ranging in size from 1 cm^2 to 0.0625 cm^2 and with reductions in thickness from 100% (bare spots) to 25%. All of the defects were detected at web speeds of 10 fpm and 30 fpm. Figure 1 shows an example from the data. Additional post-processing was

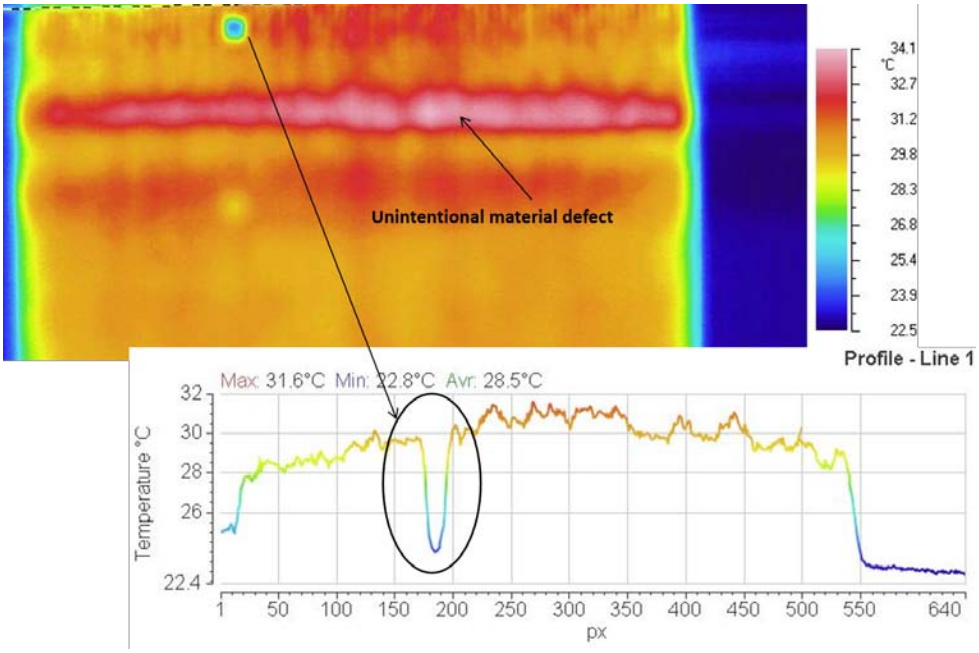

FIGURE 1. IR/RIF data from web-line demonstration, showing detection of a 0.25 cm^2 defect having a 100% reduction in the nominal electrode thickness (a bare spot), at a web speed of 30 fpm. The line graph of cross-web temperature shows the thermal response of this defect. Also shown on the image is indication of an unintentionally created band of thicker electrode coating.

performed to demonstrate the usefulness of a low pass filter to remove high frequency cross web noise in the data and improve sensitivity to small defects. Our partners at LBNL continued to refine their model of the impinging flow configuration, studying detection criteria based on defect size and process parameters, and exploring possible improvements to the technique including different jet array geometries and the addition of a surface behind the gas diffusion electrode (GDE) to increase overall temperature rise for a given excitation. Figure 2 shows the latter modeling result, predicting an increasing temperature differential as the distance between the GDE and the backing surface is decreased.

We completed several optical reflectance studies of GDE and GDE with laminated membrane samples with intentionally created defects in the electrode, including debris particles introduced before and after the electrode coating, pinholes (as small as 150 µm), cuts, scratches, and scuffs in the membrane created before and after lamination of the membrane to the GDE. Figure 3 shows an example of detection of particulates on the GDE surface. All of the defects were successfully detected. In addition, computer algorithms were created to enable automatic detection of these defects during real time post processing of the imaging. The yellow boxes in the image in Figure 3 indicate automated detection of the defects, using the developed algorithm. An associated study was performed to optimize the angle of incident light for these samples.

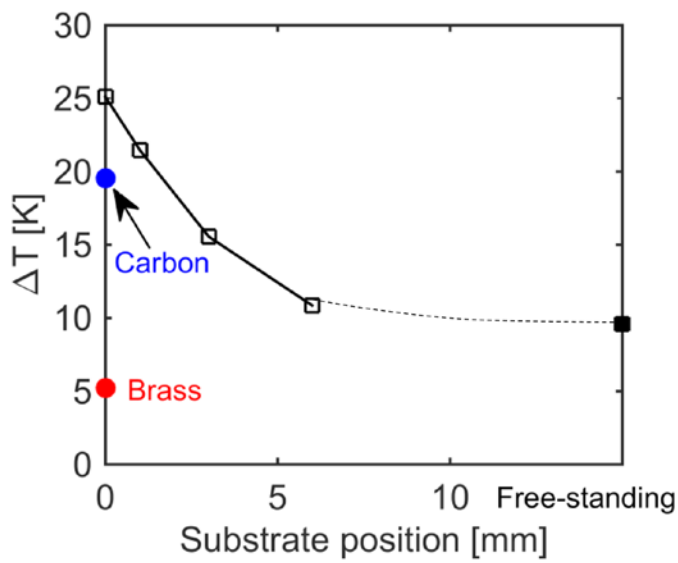

FIGURE 2. IR/RIF modeling result, showing predicted increase in the differential temperature created by a 5 mm electrode bare spot at 10 fpm web speed and 32.5 standard liter per minute jet velocity as a function of backing surface proximity to the back of the GDE.

In preparation for our major milestone at the end of this FY, we designed, built and commissioned a new testbed to study TPRE of MEAs and membrane containing subassemblies for the detection of membrane pinholes. The

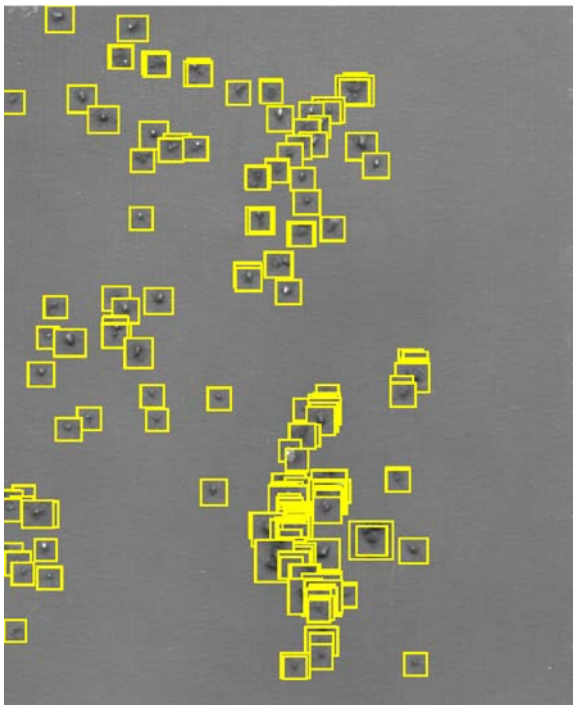

FIGURE 3. Optical reflectance image showing automated detection of particulates on electrode surface of GDE. The individual images of the particles inside the yellow boxes are magnified 10x.

purpose of this testbed is to determine the feasibility of implementing this technique in an inline configuration. As such, the apparatus enables control of reactive gas mixture, flowrate, and exposure time of the sample to the reactive gas. In initial studies, membrane pinholes as small as 150 µm in were detected. In an associated effort, we developed an apparatus and method to create pinholes in membranes and GDEs with laminated membranes with high repeatability. To date, we have been able to create pinholes as small as 50 µm diameter. This technique will be useful for pinhole detection development as well as for in situ studies to understand the effects of pinhole defects.

LBNL used their established cell performance model to perform modeling of electrode defects of different size and location in the cell, and under different operating conditions. These studies continue to guide our experimental in situ work. We continued segmented cell studies of the performance effects of electrode defects, including thin spots and comparison of the effects of defects on the anode vs. on the cathode. Figure 4 gives an example of this work, showing spatially resolved performance data of a MEA with a 1 cm^2 bare spot on the anode. In addition, to support the study of the onset of failure due to defects, we validated an accelerated stress test—based on the development efforts at LANL—that will instigate failure over a period of time.

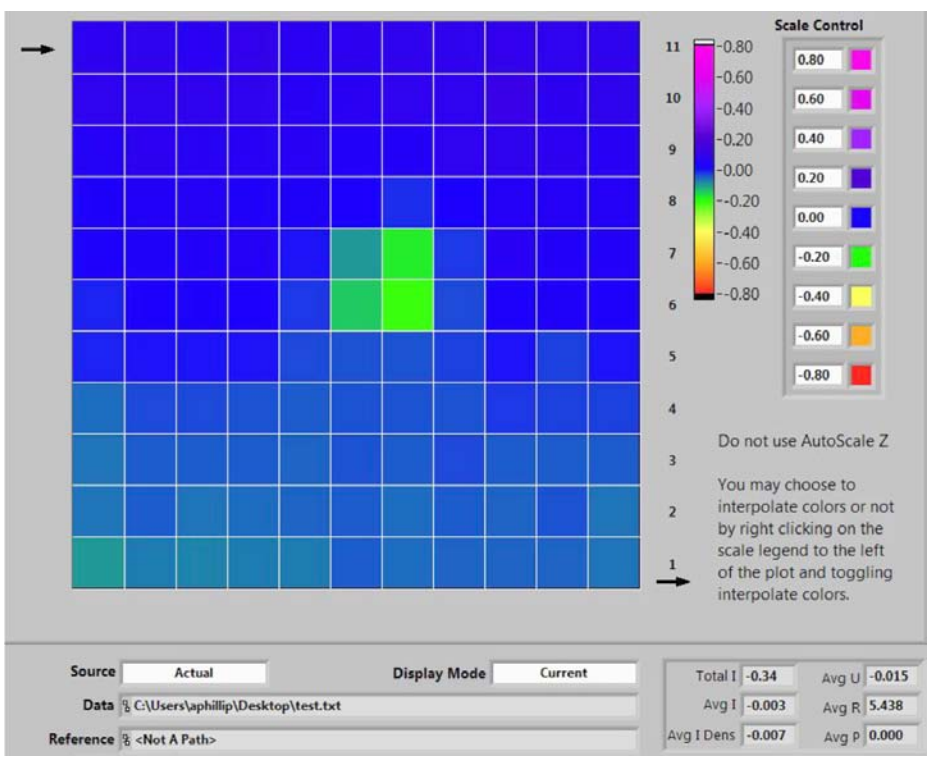

FIGURE 4. Segmented cell data showing the spatially resolved performance effect of a 1 cm^2 bare spot in the anode at a total cell current density of 1.2 A/cm^2. The color scale shows the difference in local current performance between the defected cell and a pristine cell. The cell is operated at anode/cathode conditions of 100/50% relative humidity, 150/150 kPa, 1.5/2.0 stoich, hydrogen/air, and a cell temperature of 80°C.

Based on this work, we will customize a stress test to capture the development of the failure.

FUTURE DIRECTIONS

- Apply our toolbox of techniques to industry-relevant MEA constructions and subassemblies, particularly focusing on near-term commercialization opportunities such as scale up of automotive fuel cells
- Use modeling and experimental studies to refine and improve the performance of the IR/RIF technique for GDE defect detection
- Determine the feasibility of TPRE for web-line implementation
- Continue to use predictive modeling and single and segmented cell test methods to study the effects of as-manufactured defects on MEA performance and lifetime using standard or accelerated stress tests
- Continue to work toward the implementation of more of our techniques on industry production lines

FY 2015 PUBLICATIONS/PRESENTATIONS

1. Rupnowski, P.; Ulsh, M.; Sopori, B. "High Throughput and High Resolution In-line Monitoring of PEMFC Materials by Means of Visible Light Diffuse Reflectance Imaging and Computer Vision," ASME Power and Energy Conversion Conference, San Diego, CA, July, 2015. *PowerEnergy2015-49212*.

2. Ulsh, M. "Fuel Cell MEA Manufacturing R&D," DOE Hydrogen Program Annual Merit Review, Washington, D.C., June, 2015.

3. Ulsh, M. "In-line Quality Control for MEAs," LBNL Energy Technologies Area Seminar, Berkeley, CA, February, 2015.

4. Ulsh, M.; Garland, N. "EERE Quality Control Workshop: Summary and Implications," Fuel Cell Seminar & Exhibition, Los Angeles, CA, November, 2014.

5. Wheeler, D.; Ulsh, M. "Balance of Plant Issues for PEM Fuel Cells," 226th Meeting of the Electrochemical Society, Cancun, Mexico, October, 2014.

6. Wheeler, D.; Ulsh, M. "Manufacturing Readiness and Cost Impacts for PEM Stack and Balance of Plant," *ECS Transactions* (64:3), 2014; pp. 897–908.

7. Ulsh, M. "Fuel Cell Manufacturing R&D," USCAR Fuel Cell Tech Team, Southfield, MI, October, 2014.

8. U.S. Provisional Patent Application 62/130,346, "Batch and Continuous Methods for Evaluating the Physical and Thermal Properties of Thin Films."

VI.2 U.S. Clean Energy Hydrogen and Fuel Cell Technologies: A Competitiveness Analysis

Patrick Fullenkamp
Westside Industrial Retention & Expansion Network NE (dba GLWN)
4855 West 130th Street, Suite 1
Cleveland, OH 44135-5137
Phone: (216) 920-1956
Email: pfullenkamp@glwn.org

DOE Manager
Nancy Garland
Phone: (202) 586-5673
Email: Nancy.Garland@ee.doe.gov

Contract Number: DE-EE0006935

Subcontractors:
- DJW Technologies, Dublin, OH
- E4tech, Lausanne, Switzerland
- Strategic Analysis, Inc. (SAI), Arlington, VA
- eon™ Consultants Ltd., Vancouver, British Columbia, Canada
- Bowen Liu, Markham, Ontario, Canada
- Brent Fourman, New Paris, OH

Project Start Date: June 1, 2015
Project End Date: May 31, 2019

Overall Objectives

- Global competitiveness analysis of hydrogen and fuel cell systems and components manufactured, including 700-bar compressed hydrogen storage system in the United States, Europe, Asia, and other key areas to be identified, to determine the global cost leaders, the best current manufacturing processes, the key factors determining competitiveness, and the potential means of cost reductions. This objective, in close conjunction with the National Renewable Energy Laboratory, will be completed in Period 1 (M1-M18) and the report issued in M18.
- Analysis to assess the status of global hydrogen and fuel cell markets. The analysis of units, megawatts by country, and megawatts by application will focus on polymer electrolyte membrane (PEM) fuel cell systems (automotive and stationary). This objective will be completed annually, and all data for the designated reports will be reported during M12, M24, M36, and M48.

Fiscal Year (FY) 2015 Objectives

- Conduct 30 interviews with fuel cell industry original equipment manufacturers, manufacturers, and industry leaders to make sure the five key components have been identified for this study
- Identify five key component manufacturers in three regions for a total of 15
- Provide a map of industry structure

Technical Barriers

This project addresses the following technical barriers from the Manufacturing R&D section (3.5.5) of the Fuel Cell Technologies Office (FCTO) Multi-Year Research, Development, and Demonstration (MYRDD) Plan through, for example, supply chain development and analysis to understand the competitive landscape for hydrogen and fuel cell component manufacturing:

(A) Lack of High Volume MEA Processes

(B) Lack of High-Speed Bipolar Plate Manufacturing Processes

(C) Lack of High Strength Gas Diffusion Layers.

(K) Lack of Low-Cost Fabrication Techniques for Storage Tanks

✧ ✧ ✧ ✧ ✧

APPROACH

Under FOA-854, GLWN will carry out a detailed manufacturing global competitiveness analysis of hydrogen and fuel cell systems and components manufactured, including 700-bar compressed hydrogen storage systems in the United States, Europe, Asia, and other key areas to be identified, to determine the global cost leaders, the best current manufacturing processes, the key factors determining competitiveness, and the potential means of cost reductions. This objective, in close conjunction with the National Renewable Energy Laboratory, will be completed in Period 1 (M1-M18) and the report issued in M18.

In parallel, GLWN will also carry out an analysis to assess the status of global hydrogen and fuel cell markets. The analysis of units, megawatts by country, and megawatts by application will focus on PEM fuel cell systems (automotive and stationary). This objective will be completed annually, and all data for the designated reports will be reported during M12, M24, M36 and M48.

Three cost analysis methodologies will be applied in this project: CBA (cost breakdown analysis), DFMA® (design for manufacturing and assembly), and VSM (value stream mapping), which will enable a full global competitiveness analysis. A global CBA will be made for the PEM fuel cell and hydrogen storage system and the major components of these systems. Standard design and manufacturing drawings will be generated for an apples-to-apples comparison. Onsite reviews will be held to validate cost and process data. An analysis will be made of all the cost breakdown data, and the manufacturing process will be walked from beginning to end to develop the value stream maps. The categories of the cost breakdown will include materials, labor, burden, SGA (sales, general, administrative), engineering, logistics cost, and profit.

For the assessment of the status of the global hydrogen and fuel cell markets, we will collate shipment data for fuel cells globally using our connections and public data of units, megawatts by country, and megawatts by application. This will be categorized and presented by region, application, etc., to show both amounts and flows.

FY 2015 ACCOMPLISHMENTS

- Project start date was officially June 1, 2015. All forms required by DOE have been completed and submitted.
- All partner subcontracts—SAI, E4tech, Eon, DJW, and Bowen Liu—have been completed as of July 31, 2015.
- Project team meetings have been scheduled for the 2nd and 4th Thursdays of the month. Minutes are published and distributed for each meeting.
- Assignments have been delegated for 1st Quarter Task 1.1 – Supply Chain Evolution and Mapping the Industry, and 1st Quarter Task 1.2 – Questionnaire, Interviews, Top 5 Component Selection.

FY 2015 PUBLICATIONS/PRESENTATIONS

1. DOE Hydrogen and Fuel Cells Technical Advisory Committee Review presentation, P. Fullenkamp, GLWN, and Strategic Analysis, Inc., held April 22, 2015.

2. DOE Annual Merit Review and Peer Evaluation Meeting (AMR) Review presentation, P. Fullenkamp, GLWN, and Strategic Analysis, Inc., held June 11, 2015.

VII.0 Technology Validation Sub-Program Overview

INTRODUCTION

The Technology Validation sub-program demonstrates, tests, and validates hydrogen and fuel cell technologies and uses the results to provide feedback to Fuel Cell Technologies Office (FCTO) research and development (R&D) activities.

Continuing efforts include real-world evaluation and data collection associated with light-duty fuel cell electric vehicles (FCEVs), fuel cell electric buses (FCEBs), hydrogen stations, advanced hydrogen refueling components, and early market applications of fuel cells, such as stationary power and material handling equipment (MHE). The sub-program is also implementing projects that support the advancement of hydrogen infrastructure by developing and validating a prototype device to measure hydrogen dispenser performance, and by developing tools to enhance access to hydrogen station status information. Activities of the sub-program have expanded into examining hydrogen-based energy storage, where electrolyzers may be used as a controllable electrical load that can provide real-time grid services.

GOAL

The goal of the Technology Validation sub-program is to validate the state-of-the-art of fuel cell systems in transportation and stationary applications, as well as hydrogen production, delivery, and storage systems, and assess technology status and progress to determine when technologies should be moved to the market transformation phase.

OBJECTIVES

The objectives of the Technology Validation sub-program are as follows.

- Validate hydrogen FCEVs with greater than 300-mile range and 5,000-hour fuel cell durability by 2019
- Validate a hydrogen fueling station capable of producing and dispensing 200 kg H_2/d (at 5 kg/3 min; 700 bar) to cars and/or buses by 2019
- Validate large-scale systems for grid energy storage that integrate renewable hydrogen generation and storage with fuel cell power generation, operating for more than 10,000 hours, with a round-trip efficiency of 40% by 2020

FISCAL YEAR (FY) 2015 TECHNOLOGY STATUS AND ACCOMPLISHMENTS

FCEV Evaluation

Six major automakers (General Motors, Honda, Hyundai, Mercedes-Benz, Nissan, and Toyota) are demonstrating advanced light-duty FCEVs, where data are being collected from up to 48 vehicles. During the data collection period of October 2012 through December 2014, the 48 FCEVs traveled a total of over 2.4 million miles, demonstrating an average on-road fuel economy of 51 mi/kg and an average fleet voltage durability of 3,930 h. A maximum of 5,605 fuel cell operation hours (which surpasses the 2020 DOE target of 5,000 hours) was also demonstrated[1]. These results, along with previous ones[2], reveal that steady progress has been demonstrated over the past 10 years, with improvements especially in fuel cell durability, range, and fuel economy. (National Renewable Energy Laboratory [NREL])

FCEB Evaluation

During FY 2015, data from 15 FCEBs at two transit agencies, AC Transit (Oakland, California) and SunLine (Thousand Palms, California), were collected and analyzed. The objective of this effort is to determine the status of fuel cell systems for buses and to aid fleets with the implementation of next generation FCEBs. Fuel cell buses continue to show improved fuel economy (ranging from 1.7 to 2.1 times higher) compared to baseline (diesel and compressed natural gas) buses in similar service. The average fuel economy for the FCEBs was 7.26 mi/DGE (diesel gallon equivalent), approaching the Federal Transit Administration's performance target for FCEB fuel economy

[1] However, this vehicle may not meet efficiency and cost targets.
[2] The Learning Demonstration evaluation, 2006-2012, results available at: http://www.nrel.gov/hydrogen/pdfs/54860.pdf

of 8 mi/DGE. The top fuel cell power plant (FCPP) accumulated over 19,000 h of operation, surpassing the DOE/Department of Transportation target of 18,000 h for 2016, while 67% of FCPPs accumulated over 8,000 h. Values for fuel cell system miles between road call—a measure of reliability—surpassed the 2016 target and were found to be approaching the ultimate target. FCEB average availability was found to be 70%. The majority of the road calls were due to bus-related general maintenance, batteries, and hybrid propulsion systems, while fuel cell-related issues made up approximately 10–15% of the road calls. (NREL)

Hydrogen Station Evaluation

The objective of this project is to collect data from state-of-the-art hydrogen fueling facilities, such as those operated by California State University, Los Angeles (CSULA), Proton OnSite, and Gas Technology Institute (GTI), providing valuable feedback on data related to hydrogen infrastructure. Over the period from the first quarter of 2009 to the fourth quarter of 2014, data collected on 10 hydrogen stations revealed that a cumulative 62,784 kg of hydrogen was dispensed (43% improvement over previous year's cumulative), with average dispensing rates of 0.6 kg/min. Average fill time was found to be 5.6 min, with 49% of fills taking less than five minutes and 20% taking less than three minutes. (NREL)

CSULA's electrolyzer-based hydrogen station was commissioned in May 2014. Power meters, flow meters, and buffer tanks were installed, and performance evaluation data are being provided. The station was the *first in the United States* to receive a seal of approval for sale of hydrogen on a per-kilogram basis as of January 2015. Testing was conducted in collaboration with the California Department of Weights and Measures, California Fuel Cell Partnership, and California Air Resources Board. Up to 242 kg H_2/month were sold between October 2014 and March 2015. (CSULA)

Proton OnSite's high pressure (57 bar) electrolyzer at the SunHydro #1 station in Wallingford, Connecticut, was built and tested, and data monitoring is ongoing. The SunHydro #2 station has been designed, and fabrication of components is underway. (Proton OnSite)

GTI's West Sacramento, California, station—using liquid hydrogen and 900 bar ionic compression technology—was commissioned in December 2014, and instrumentation is installed, allowing for data collection. Permits for the San Juan Capistrano, California, site have been granted, and construction is expected to begin mid-2015. For the remaining three sites (Cupertino, California; Mountainview, California; Foster City, California), equipment is being fabricated and construction dates will depend on permitting. (GTI)

Hydrogen Compressor Evaluation

As compressors account for one-third of maintenance hours at hydrogen stations, the main objective of this project is to perform accelerated compressor testing to reproduce component failures, which are correlated to real-world usage with statistical methods. Compressor performance and reliability data (from four compressors) were compared to data collected in the field (through composite data products), and deep dive failure analyses were performed. The compressors demonstrated consistent power consumption with varying pressure and temperature. Seal weakness was found to be the main failure mechanism, with five seal failures occurring (four in compressor heads and one on a check valve seal). Catastrophic seal failure was detected preemptively through a leak detection circuit to continuously monitor leaks (alarms were set at levels above what may indicate the beginning of a failure). NREL found that repairs of common failures are expensive (up to $1,200) and time consuming (up to six weeks parts lead time). In addition, Fourier transform infrared spectroscopy analysis of various contaminants (detected at second stage discharge tube immediately after the head) revealed that the most abundant contaminant is siloxane (mainly from vacuum grease typically applied to elastomer seals), which harms fuel cells by causing membrane embrittlement and crossover issues. A suitable replacement chemical was suggested, with minimal effects on fuel cells. (NREL)

Cryogenic Pressurized Hydrogen Storage and Delivery Evaluation

The use of a 100 kg H_2/h, 875 bar high pressure liquid hydrogen pump is being investigated and validated, as liquid hydrogen pumps have the potential to increase hydrogen storage density (and vehicle driving range) by up to 30%, while enabling five-minute refueling and minimizing delivery costs. A thin-lined vessel with 81% volume ratio (versus 70% for conventional vessels) at 700 bar pressure was manufactured, and its cryogenic strength was demonstrated. The liquid hydrogen pump was instrumented for a power analyzer, boil-off mass flow meter, and outlet temperature sensor. Operational approvals from DOE and Lawrence Livermore National Laboratory (LLNL) were

obtained, and civil construction of a cryogenic hydrogen pressure vessel test facility was completed. The installation of other components, such as containment vessels and heat exchanger, will follow in FY 2016. (LLNL)

Stationary Fuel Cell Evaluation

This project evaluates the deployment and performance of stationary fuel cell systems operating under real-world conditions while reporting on the baseline, progress, and technical challenges. In FY 2015, installation data from California's Self Generation Incentive Program were collected for 397 fuel cell-based units[3] (totaling 161 MW). Deployment of fuel cells (combined heat and power [CHP] and electric only) has exceeded the deployment of internal combustion engines, and most of these fuel cell units use natural gas. However, renewable fuels[4] fare better in terms of installed *capacity* by fuel type, versus *number* of deployments by fuel type. The mean availability of the fuel cell systems was 92%, with about 60% of systems having availability over 90%. The mean electrical efficiency of the fuel cells (>100 kW) exceeded the 2015 DOE target of 43% (on a lower heating value basis). Installed costs ranged from $5,620/kW to $11,275/kW for electric-only fuel cell systems, and from $3,706/kW to $11,303/kW for CHP fuel cell systems, depending on system size and availability of incentives. (NREL)

Early Markets Analysis

Early market analysis of fuel cell technologies includes validating fuel-cell-based MHE performance based on real-world operation data from high-use facilities. By the third quarter of FY 2014, 720 MHE fuel cell units were operating as part of the Technology Validation sub-program, refueling on average in 2.5 min, and operating an average of 3.7 h between fills. Over 350,000 fills took place, with more than 280,000 kg of H_2 dispensed. About one-third of fills were back-to-back (within five minutes), and 60% were within 20 minutes of each other. (NREL)

Hydrogen Station Equipment Performance (HyStEP) Device

The objective of this new effort is developing and validating a prototype device to measure hydrogen dispenser performance, to help accelerate commercial hydrogen station acceptance. The device was co-designed by the HyStEP project team of the H2FIRST project[5]. Powertech Labs fabricated the device. The design and safety aspects of the device were reviewed and approved by the project team, DOE, and the Hydrogen Safety Panel, allowing for a "go" decision on device fabrication. The device will initially be tested at NREL, followed by two pre-deployment tests at California stations. (NREL and Sandia National Laboratories)

Station Operational System Status

Station Operational System Status (SOSS) is a platform designed to use a database to collect, store, and distribute data about the operational status of hydrogen stations. Stations automatically transmit operational data to the database server, and station status is made available to end users. The goal of the current phase (SOSS 3.0 upgrade) of the project is to improve customer satisfaction and station demand by upgrading the software to improve user interface and data quality and improve data transmission interval (which currently ranges from once a day to once every 15 minutes) to 15 minutes. The application has been implemented at five hydrogen stations in California and is planned to be implemented at a station in Boulder, Colorado, plus seven stations in California later in 2015.

Hydrogen Energy Storage/Grid Integration

DOE has established a grid modernization program, which is a cross-cutting effort involving various offices within DOE, with an objective to help set the nation on a cost-effective path to an integrated, secure, and reliable grid that is flexible enough to provide an array of emerging services while remaining affordable to consumers. Hydrogen-based energy storage could provide value to many applications and markets. Electrolyzers may be utilized as a controllable electrical load that can provide real-time grid services. FCTO is exploring these value-added services through related projects. An electrolyzer stack test bed was designed, built, commissioned, and is in operation. The first-of-its-kind real-time digital simulator (RTDS®)-to-RTDS® communications network between labs was established for hardware-in-the-loop simulations, with electrolyzer hardware at NREL and grid simulation at Idaho National Laboratory (INL). High-value locations to implement demand response and ancillary services using hydrogen stations are also to be identified in this project. (NREL and INL)

[3] Fuel cell electric + fuel cell combined heat and power.
[4] Renewable fuels exclude those defined as conventional in Section 2805 of the California Public Utilities Code and are categorized here as gas derived from biomass, digester gas, or landfill gas.
[5] H2FIRST: Hydrogen Fueling Infrastructure Research and Station Technology; see http://www.energy.gov/eere/fuelcells/h2first

BUDGET

The funding portfolio for Technology Validation enables the sub-program to continue to collect and analyze data from fuel cells operating in transportation and stationary applications, as well as hydrogen production and delivery technologies. In FY 2015, $11 million in funding was appropriated for the Technology Validation sub-program, and $7 million was requested for FY 2016 (subject to congressional appropriations).

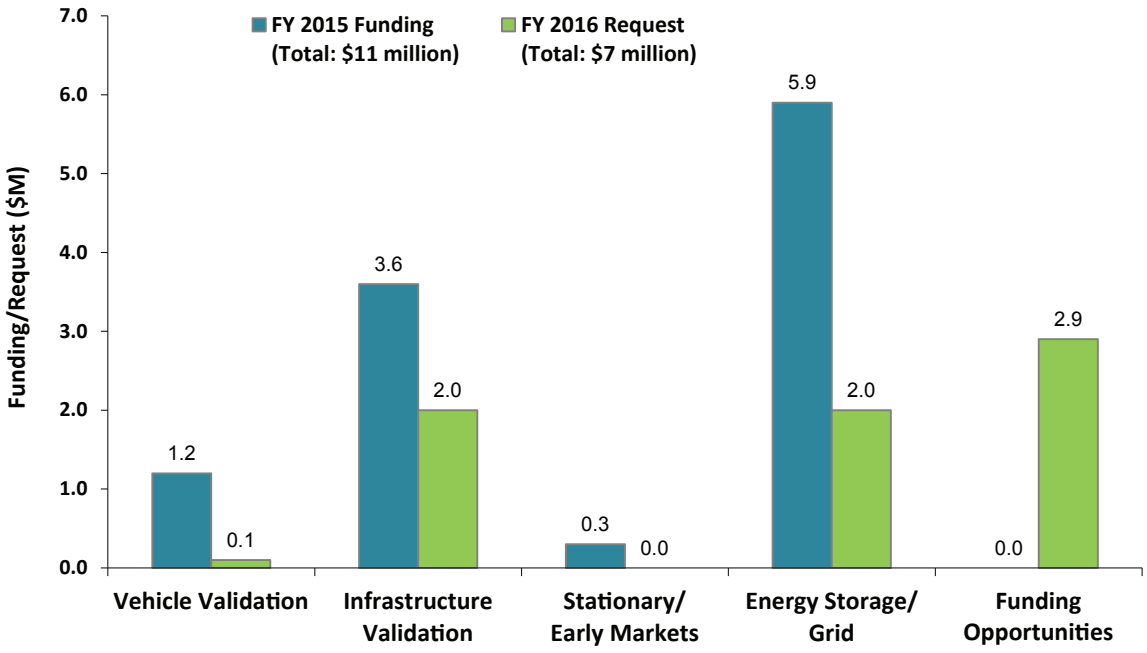

FIGURE 1. Technology Validation R&D Funding. Subject to appropriations, project go/no-go decisions, and competitive selections. Exact amounts will be determined based on research and development progress in each area and the relative merit and applicability of projects competitively selected through planned funding opportunity announcements.

FY 2016 PLANS

In FY 2016, the Technology Validation sub-program will continue its detailed evaluations of FCEVs, FCEBs, hydrogen fueling stations, advanced hydrogen refueling components, stationary power deployments, and early market applications. In coordination with DOE's Office of Energy Efficiency and Renewable Energy and Office of Electricity, a key focus in FY 2016 will be hydrogen-based energy storage and grid integration activities. The design, deployment, and validation of advanced, low cost, mobile hydrogen refuelers will also be pursued, based on selections from a Funding Opportunity Announcement that closed in June 2015. Potential future funding opportunities may emphasize hydrogen refueling station and components validation, subject to appropriations. Prototype fuel cell hybrid electric medium-duty trucks (extending battery electric vehicle range) are expected to be developed and deployed under real-world conditions, and data will be collected to evaluate their performance. Targets are being developed for medium- and heavy-duty fuel cell trucks, and a related request for information is expected to be issued.

Jason Marcinkoski
Technology Validation Project Manager
Fuel Cell Technologies Office
Office of Energy Efficiency and Renewable Energy
U.S. Department of Energy
1000 Independence Ave., SW
Washington, D.C. 20585-0121
Phone: (202) 586-7466
Email: Jason.Marcinkoski@ee.doe.gov

VII.1 Hydrogen Component Validation

Danny Terlip (Primary Contact), Mike Peters, Kevin Harrison
National Renewable Energy Laboratory (NREL)
15013 Denver West Parkway
Golden, CO 80401-3305
Phone: (303) 275-4180
Email: Danny.Terlip@nrel.gov

DOE Manager
Jason Marcinkoski
Phone: (202) 586-7466
Email: Jason.Marcinkoski@ee.doe.gov

Subcontractor
Spectrum Automation, Arvada, CO

Project Start Date: October 20, 2012
Project End Date: Project continuation and direction determined annually by DOE

Overall Objectives

- Operate hydrogen compressors and collect data to understand failure modes, repair and maintenance requirements, and performance in variable conditions
- Perform deep-dive failure analysis and feed results back to component manufacturers
- Collect and analyze contaminants found in hydrogen piping of compressors

Fiscal Year (FY) 2015 Objectives

- Operate compressors for a combined 2,000 h
- Collect contaminant samples from at least three compressors and have them analyzed

Technical Barriers

This project addresses the following technical barriers from the Technology Validation section of the Fuel Cell Technologies Office (FCTO) Multi-Year Research, Development, and Demonstration (MYRDD) Plan:

(D) Lack of Hydrogen Refueling Infrastructure Performance and Availability Data (detailed compressor reliability data and analysis)

Contribution to Achievement of DOE Technology Validation Milestones

This project will contribute to achievement of the following DOE milestones from the Technology Validation section of the FCTO MYRDD Plan:

- Milestone 3.4: Validate station compression technology provided by the delivery team. (4Q, 2018)

FY 2015 Accomplishments

- Generated 800 h of compressor performance and reliability data that can be used to improve station modeling efforts
- Determined seal weakness to be the main cause of failures and communicated this finding to compressor manufacturers
- Identified a mechanism for indicating preemptive seal failure
- Documented repair times and costs to inform station operators and modelers of expected station downtimes and financial burdens due to compressors
- Collected and analyzed composition of contaminant found in process piping

✧ ✧ ✧ ✧ ✧

INTRODUCTION

The Hydrogen Component Validation task tests components used in hydrogen fueling stations at nominal working pressures with the aim of collecting performance and reliability data. Components are integrated into actual fueling stations to replicate field conditions. Testing at NREL's private stations allows engineers to perform deep-dive analyses without inconveniencing fuel cell electric vehicle customers. Findings are communicated to manufacturers to improve designs, to modelers to develop more accurate models, and to DOE to inform research direction.

FY 2015 testing was focused on the leading cause of station downtime, hydrogen compressor failure. Three units—two diaphragms and one air piston—were tested at NREL's two hydrogen stations. One was highly instrumented and operated on a dedicated testing scheme, while the other two were only operated as needed. NREL engineers documented compressor failure and performance data. Failure data was composed of information on failure mechanisms, resulting station downtime, and repair costs. Performance data consisted of information on power and energy consumption

at varying pressure discharge levels and in a range of ambient conditions. This task will increase the scope and breadth of publicly available data regarding compressors.

APPROACH

Each compressor was integrated into a hydrogen production, compression, storage, and dispensing system to best replicate field conditions. Device Under Test 1 (DUT1) was a diaphragm compressor that was highly instrumented to collect internal pressure, temperature, power, and energy data. It was operated under a cooperative research and development agreement with a compressor manufacturer. Testing focused on collecting performance data over long operating periods (up to 20 h/d) at consistent discharge pressures ranging up to 6,000 psi. DUT2 was a diaphragm compressor that operated at pressures similar to those of DUT1. DUT3 was an air-driven compressor that operated at discharge pressures up to 12,500 psi. NREL engineers only operated DUT2 and DUT3 as needed and only collected failure data from these two devices. Compressor failure data was corroborated locally among DUT1, DUT2, and DUT3, and nationally using data from the National Fuel Cell Technology Evaluation Center at NREL.

Additional work was conducted in contaminant analysis. Residue from the inside of process lines on a compressor was sampled and analyzed using Fourier transform infrared spectroscopy. The chemical composition of the residue has been determined from DUT1. NREL engineers are currently reaching out to station operators to obtain field samples of residues for analysis.

RESULTS

Testing in FY 2015 yielded four key results.

- Data logging on DUT1 collected a year's worth of performance and reliability data.
- DUT1, DUT2, and DUT3 tests suggest that seals are the main failure mechanism.
- Seal failures can be detected before catastrophic failure, reducing downtime and repair time.
- Special equipment and lead times were documented for major compressor failures.

DUT1 ran for more than 800 h in FY 2015, compressing more than 1,800 kg of hydrogen. An average efficiency of 3.5 kWh/kg was calculated from the energy consumption[1]. NREL engineers piped a recirculation loop from the discharge of the compressor to the inlet pressure regulator. This allowed for long duration testing without a need for additional hydrogen and made it possible for operators to keep the discharge pressure constant. Figure 1 shows an aggregate of a year's worth of data with DUT1 operating at multiple discharge pressures. Power consumption of the 30 HP motor varied at 200 W/ksi with discharge pressure, averaged 13.1 kW, and had a standard deviation of 0.6 kW over the course of the year.

DUT1 performance was also analyzed over varying ambient temperatures (Figure 2). Power consumption was

[1] Constant suction pressure, power factor of 0.8, includes pump and radiator (1.86 kW).

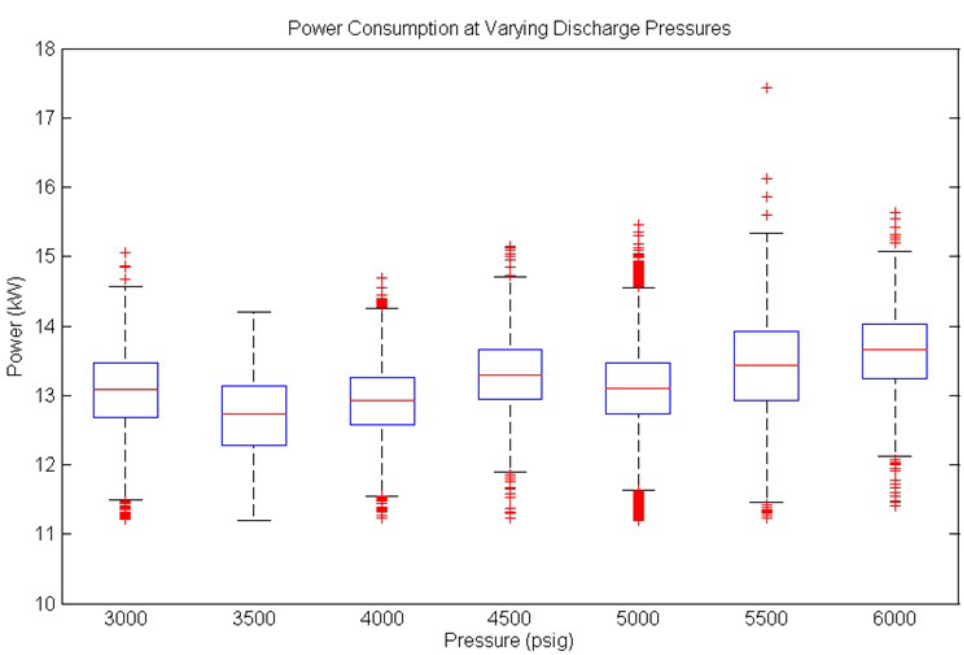

FIGURE 1. DUT1 power consumption in FY 2015 categorized by discharge pressure

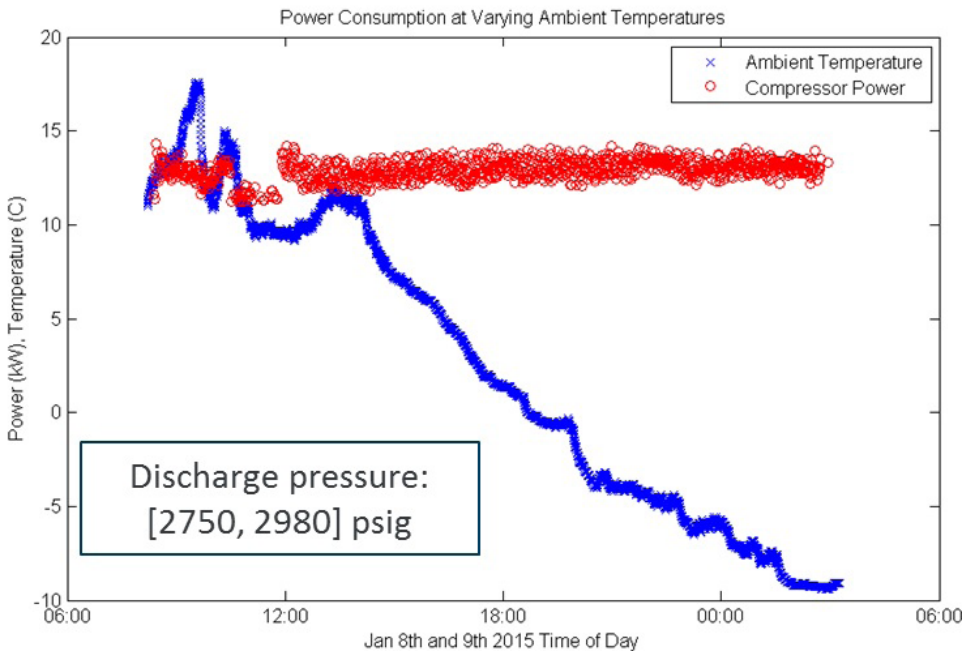

FIGURE 2. DUT1 power consumption (red) and ambient temperature (blue) over a 20-h operating cycle

found to be constant, while the ambient temperature dropped from 18°C to -9°C.

Five major seal failures occurred in FY 2015, with four in compressor heads and one on a check valve. Failures ranged from pieces being severed to discoloration and slight deformation. Seal failures in compressor heads occurred in both diaphragm compressors (DUT1 and DUT2). In three of the four failures, the oil over-pump valves were set to improper values, increasing the pressure and temperature of the compressor heads beyond levels found in normal conditions. Over-pump valves are typically set at the factory, but set points can change during operation.

Leak detection circuits for seals are common on diaphragm compressors, but they do not alert a user of a problem until a major seal failure occurs. NREL engineers found that regular monitoring of leak detection circuits can catch seal failures early reducing repair times by a factor of two. High-resolution data collection on DUT1 allowed for historical analysis of seal failures and significantly contributed to this conclusion. Additionally, following advice from the compressor manufacturer, NREL engineers constructed a pressure manifold for determining set points for in situ over-pump valves. The manifold consists of a check valve for holding pressure, a pressure indicator for showing pressure, and needle valve for releasing pressure.

Repair time effort and documentation is not highly publicized for hydrogen compressors. Repairs often require highly specialized parts and tools that can lead to increased downtime. NREL engineers documented the people, hours, specialized parts, and unique tools required to perform common compressor repairs. Station operators can use this information to reduce downtime by planning repairs and ordering parts with long lead times.

A small sample of black residue found inside process tubing was analyzed for composition. It was found that the sample consisted mostly of a certain type of vacuum grease made from siloxane supplied by the compressor manufacturer. NREL's Fuel Cell System Contaminants Material Screening Data tool indicates that siloxane is harmful to fuel cells, thus different vacuum grease should be used.

CONCLUSIONS AND FUTURE DIRECTIONS

Conclusions derived from work in FY 2015 include the following.

- Compressor performance and reliability data over varying operating pressures and ambient temperature is consistent.
- Seal failures are the most common failure mode for compressors.
- Preemptive detection of seal failures can lead to drastically reduced downtime.
- Keeping certain uncommon spare parts and tools in stock can speed up repair times.
- Vacuum grease containing siloxane should not be used on seals contacting hydrogen.

Future work on this task will include increasing operation hours on all compressors, installing a new linear piston compressor, and incorporating power meters on DUT2 and the new compressor. Additionally, NREL engineers are reaching out to station operators for more samples of contaminants found in compressors for analysis.

FY 2015 PUBLICATIONS/PRESENTATIONS

1. Terlip, D.; Peters, M.; Harrison, K. "Hydrogen Component Validation," 2015 DOE Hydrogen and Fuel Cells Program and Vehicle Technologies Office Annual Merit Review and Peer Evaluation Meeting, June 2015. (presentation)

VII.2 Performance and Durability Testing of Volumetrically Efficient Cryogenic Vessels and High Pressure Liquid Hydrogen Pump

Salvador M. Aceves (Primary Contact), Gene Berry, Francisco Espinosa-Loza, Guillaume Petitpas, Vernon Switzer
Lawrence Livermore National Laboratory (LLNL)
7000 East Avenue, L-792
Livermore, CA 94551
Phone: (925) 422 0864
Email: saceves@llnl.gov

DOE Manager
Jason Marcinkoski
Phone: (202) 586-7466
Email: Jason.Marcinkoski@ee.doe.gov

Subcontractors
- Linde LLC, Hayward, CA
- Spencer Composites Corporation, Sacramento, CA

Project Start Date: January 1, 2014
Project End Date: December 31, 2016

Overall Objectives

- Demonstrate small (63.5 L internal volume), high aspect ratio (34 cm outer diameter and 100 cm length) cryogenic pressure vessels with high volumetric and gravimetric hydrogen storage performance (50 gH_2/L and 9% H_2 weight fraction)
- Demonstrate durability (1,500 thermomechanical cycles) of thin-lined high fiber fraction pressure vessels
- Measure liquid hydrogen (LH_2) pump performance after 6,000 refuelings (24 tonnes of LH_2)

Fiscal Year (FY) 2015 Objectives

- Install sensors for measurement of liquid hydrogen venting, electricity consumption, and hydrogen temperature at pump outlet
- Complete construction of pressure vessel test facility
- Install containment vessel
- Fabricate two thin-lined high fiber fraction vessels
- Cycle and strength test two thin-lined high fiber fraction vessels

Technical Barriers

This project addresses the following technical barriers from the Technology Validation section of the Fuel Cell Technologies Office Multi-Year Research, Development, and Demonstration (MYRDD) Plan:

(C) Hydrogen Storage

(D) Lack of Hydrogen Infrastructure Performance and Availability Data

Contribution to Achievement of DOE Technology Validation Milestones

This project will contribute to achievement of the following DOE milestone from the Technology Validation section of the Fuel Cell Technologies Office MYRDD Plan:

- Milestone 3.4: Validate station compression technology provided by delivery team. (4Q, 2018)

FY 2015 Accomplishments

- Fabricated first thin-lined high fiber fraction vessel
- Pressure tested first thin-lined high fiber fraction vessel
- Instrumented liquid hydrogen pump with venting, electric power, and outlet temperature sensors
- Completed civil construction of pressure vessel test facility
- Received institutional LLNL approval to conduct pressure and cycle testing inside an ASME-rated steel containment vessel
- Wrote a detailed (100+ pages) safety plan and had it reviewed by the DOE Safety Panel

✧ ✧ ✧ ✧ ✧

INTRODUCTION

Cryogenic pressure vessels have demonstrated the highest performance for automotive hydrogen storage, with density (43 gH_2/L), weight fraction (7.3%), cost ($12/kWh), and safety advantages (~8X lower expansion energy than compressed gas and secondary protection from vacuum jacket) [1,2]. This project will explore the potential for reaching high volumetric (50 gH_2/L target) and gravimetric (9% H_2 weight fraction target) storage performance within a small (63.5 L internal volume), high aspect ratio (34 cm outer diameter and 100 cm length) cryogenic pressure vessel with long durability (1,500 thermomechanical cycles) refueled by a liquid hydrogen pump to be tested for degradation after delivery of 24 tonnes of LH_2.

APPROACH

Reaching the very challenging weight and volume targets set for this project demands innovative cryogenic pressure vessel design. Spencer Composites Corporation, in collaboration with LLNL, is developing thin-lined, high fiber fraction cryogenic pressure vessels. At a target liner thickness of 1.5 mm and 80% fiber fraction, these thin-walled vessels may be able to reach the weight and volume targets when installed within a thin vacuum gap and refueled at high density (up to 80 gH_2/L) with the LH_2 pump.

RESULTS

Early in 2015 we were able to produce the first thin-lined (1.8 mm) high volumetric efficiency (81%) Type 3 (metal-lined, fiber-wrapped) 700-bar pressure vessel (Figure 1). Weighing 32 kg, it does have the performance necessary to meet the project targets (50 gH_2/L, 9% H_2 by weight) according to current projections for liquid hydrogen pump and compact vacuum insulation performance.

Soon after manufacture, the thin-lined vessel was pressure tested at cryogenic temperature. The vessel was insulated and then filled with liquid nitrogen inside a containment cell within LLNL's high pressure laboratory (Figure 2). Pressurization then proceeded by pumping compressed ambient temperature nitrogen into the vessel. The vessel underwent three high pressure excursions before eventually failing at 1,560 bar, slightly short of the 1,600 bar target (Figure 3). These high pressure excursions resulted from the relatively small size of LLNL's high pressure cascade vessels, insufficient to pressurize the experimental vessel to the target pressure in a single gas transfer process, and from the difficulty to control the nitrogen input due to temperature variations. Future pressure tests will be conducted with hydrogen at the new pressure vessel test facility and will therefore not be affected by this limitation.

We also instrumented the liquid hydrogen pump with a power analyzer, mass flow meter at the dewar vent line, and temperature sensor at the pump outlet (Figure 4). Investment in these indicators was necessary for a full performance and degradation evaluation.

All civil construction was also completed for the pressure vessel test facility (Figure 5). Construction included a 9.1 m by 9.1 m concrete pad where the containment vessel and heat exchanger (for ambient temperature refueling) will be installed in the future (summer-fall of 2015). In addition to

FIGURE 1. First thin-lined (1.8 mm) high volumetric efficiency (81%) Type 3 (metal-lined, fiber-wrapped) 700-bar experimental pressure vessel prototype

FIGURE 2. Cryogenic pressure test of thin-lined, high volumetric efficiency experimental pressure vessel prototype

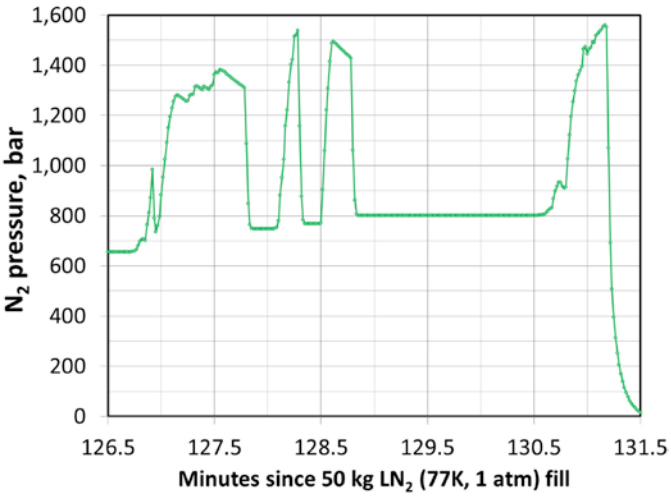

FIGURE 3. Pressure as a function of time during cryogenic strength testing of thin-lined experimental pressure vessel prototype

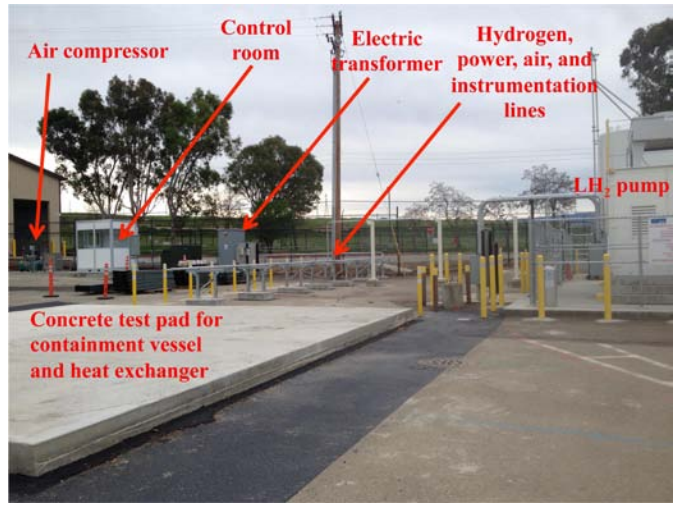

FIGURE 5. Civil construction for LLNL's pressure vessel test facility located next to liquid hydrogen pump. Construction includes an air compressor, a control room, an electric transformer (installed in 2013), and lines for high-pressure cryogenic hydrogen, instrumentation, electricity, and air. The 9.1 m by 9.1 m concrete pad is the future location of the containment vessel and a heat exchanger for ambient temperature refueling.

this, we also installed an air compressor, a control room, and lines for high pressure cryogenic hydrogen, instrumentation, electricity, and air for running explosion-proof pneumatic valves.

Experimental vessels manufactured for this project are not (ASME, Department of Transportation, International Organization for Standardization) certified. We therefore need to test them inside a containment vessel to protect personnel in case of accidental failure. After extensive modeling of blast waves resulting from experimental vessel failure, we specified a 65 bar, ASME rated metallic (SS304) containment vessel with 32 mm wall thickness. Modeling results of blast wave propagation upon experimental vessel failure were presented to LLNL pressure vessel and containment experts, who have approved the operation.

FIGURE 4. New instrumentation installed on the liquid hydrogen pump including (a) power analyzer, (b) vent line mass flow meter, and (c) temperature sensor at the pump outlet

The containment analysis results were documented in a safety note, which is currently undergoing review for final signature.

All aspects of safe operation were also documented in a 100+ page safety plan that includes: failure modes and element analysis, piping and instrumentation diagram, site layout, safety distances for hydrogen, component specifications, and design calculations. The safety plan was reviewed by the DOE Safety Panel, whose members praised it for its completeness and level of detail.

CONCLUSIONS AND FUTURE DIRECTIONS

- This project attempts to identify volumetric and gravimetric performance limits for cryogenic pressurized storage at small size (63.5 liters) and high aspect ratio (34 cm outer diameter and 100 cm length).
- Vessel durability over 1,500 thermomechanical cycles will be demonstrated before pressure testing to minimum burst pressure.
- Durability and strength of the experimental vessel will be tested inside an ASME-rated 65 bar stainless steel containment vessel.
- Pump durability will also be tested by measuring performance after pumping 24 tonnes of LH_2 and comparing it to the initial performance.

SPECIAL RECOGNITIONS AND AWARDS/ PATENTS ISSUED

1. Threaded Insert for Compact Cryogenic-Capable Pressure Vessels, Francisco J. Espinosa-Loza, Timothy O. Ross, Vernon A. Switzer, Salvador M. Aceves, Nicholas J. Killingsworth, Elias Ledesma-Orozco, US Patent 9,057,483 B2, June 16, 2015.

FY 2015 PUBLICATIONS/PRESENTATIONS

1. Salvador M. Aceves, Francisco Espinosa-Loza, Elias Ledesma-Orozco, Guillaume Petitpas, "Compact Hydrogen Storage in Cryogenic Pressure Vessels," in Handbook of Hydrogen Energy, Edited by S.A. Sherif, E.K. Stefanakos, and D.Y. Goswami, CRC Press, Taylor & Francis, ISBN-13: 978-1420054477, 2014.

2. Guillaume Petitpas, Salvador M. Aceves, "The Isentropic Expansion Energy of Compressed and Cryogenic Hydrogen," International Journal of Hydrogen Energy, Volume 39, pp. 20319–20323, 2014.

3. G. Petitpas, P. Benard, L.E. Klebanoff, J. Xiao, S. Aceves, "A Comparative Analysis of the Cryo-Compression and Cryo-Adsorption Hydrogen Storage Methods," International Journal of Hydrogen Energy, Volume 39, pp. 10564–10584, 2014.

4. Guillaume Petitpas, Salvador M. Aceves, Manyalibo J. Matthews, James R. Smith, "Para-H_2 to Ortho-H_2 Conversion in a Full-scale Automotive Cryogenic Pressurized Hydrogen Storage up to 345 bar," International Journal of Hydrogen Energy, Vol. 39, pp. 6533–6547, 2014.

5. Andrew Weisberg, Salvador M. Aceves, "The Potential of Dry Winding for Rapid, Inexpensive Manufacture of Composite Overwrapped Pressure Vessels," International Journal of Hydrogen Energy, Volume 40, pp. 4207–4211, 2015.

6. Salvador M. Aceves, Francisco Espinosa-Loza, John W. Elmer, Robert Huber, "Comparison of Cu, Ti and Ta Interlayer Explosively Fabricated Aluminum to Stainless Steel Transition Joints for Cryogenic Pressurized Hydrogen Storage," International Journal of Hydrogen Energy, Volume 40, pp. 1490–1503, 2015.

REFERENCES

1. Aceves, S.M., Espinosa-Loza, F., Ledesma-Orozco, E., Ross, T.O., Weisberg, A.H., Brunner, T.C., Kircher, O., "High-density automotive hydrogen storage with cryogenic capable pressure vessels," International Journal of Hydrogen Energy, Vol. 35, pp. 1219–1226, 2010.

2. Ahluwalia, R.K., Hua, T.Q., Peng, J.-K., Lasher, S., McKenney, K., Sinha, J., Gardiner, M., "Technical Assessment of Cryo-compressed Hydrogen Storage Tank Systems for Automotive Applications," International Journal of Hydrogen Energy, Vol. 35, pp. 4171–4184, 2010.

VII.3 FCTO INTEGRATE Stack Test Bed and Grid Interoperability

Kevin Harrison (Primary Contact), Owen Smith, Mike Peters, Danny Terlip, Paul Denholm, Marc Mann
National Renewable Energy Laboratory (NREL)
15013 Denver West Parkway
Golden, CO 80401-3305
Phone: (303) 384-7091
Email: Kevin.Harrison@nrel.gov

DOE Manager
Jason Marcinkoski
Phone: (202) 586-7466
Email: Jason.Marcinkoski@ee.doe.gov

Subcontractor
Marc Mann, Spectrum Automation Controls, Inc., Arvada, CO

Project Start Date: June 2014
Project End Date: Project continuation and direction determined annually by DOE

Overall Objectives

INTEGRATE Project Objectives

The Integrated Network Testbed for Energy Grid Research and Technology Experimentation (INTEGRATE) project conducts energy systems integration research by evaluating the benefits and values of energy efficiency, renewable energy, and distributed energy resource technologies at high penetrations into the energy infrastructure at a variety of physical scales (i.e., single location, campus, distribution systems, regional areas).

Fuel Cell Technologies Office (FCTO) Objectives

- Establish an industry-accessible, flexible electrolyzer stack test bed where integrated systems can be modeled, simulated, and evaluated to identify and overcome challenges and accelerate technology deployment
- Gather industry feedback on qualitative and quantitative performance data to identify grid services that can be provided by hydrogen-based technologies (i.e., electrolyzers and fuel cells)

Fiscal Year (FY) 2015 Objectives

- Establish a fully-instrumented, large-active-area electrolyzer stack test bed capable of variable direct current (DC) stack power up to 500 kW (250 V, 2,000 A)
- Use the flexible and fully-instrumented electrolyzer test platform to enable advanced research, development, and demonstration (RD&D) using real time digital simulation (RTDS) and hardware in the loop (HIL) testing between Idaho National Laboratory (INL) and NREL's Energy Systems Integration Facility (ESIF)

Technical Barriers

This project is conducting applied RD&D to reduce the cost and accelerate the deployment of hydrogen production systems via low temperature water electrolysis at the megawatt scale. This project addresses the following technical barrier from the Technology Validation section of the FCTO Multi-Year Research, Development, and Demonstration Plan:

(G) Hydrogen from Renewable Sources

Technical Targets

This project aims to inform DOE and industry of the cost, durability, and efficiency of state-of-the-art, grid-connected electrolyzer and fuel cell systems.

FY 2015 Accomplishments

- NREL designed, built, and began operating an electrolyzer stack test bed capable of hydrogen flow rates in the range of 100 kilograms (kg) per day. Stack power is provided by two programmable DC power supplies with upper limits of 250 V and 2,000 A.
  - Giner Inc. was the first industry stakeholder to partner with NREL to perform factory acceptance testing on three of their newest 150 kW stacks at very high current densities.
- Communications and information, and computation data services were developed for integrated system testing. The work accomplished provides the required hardware and cyber connectivity to establish a fast and secure network connection to enable detailed data exchange between the two RTDS at INL and NREL.
- The first of its kind, bidirectional, high speed simulation between ESIF RTDS and INL RTDS over a secure virtual private network (VPN).

✧ ✧ ✧ ✧ ✧

INTRODUCTION

Electrolyzers, hydrogen storage, and fuel cells may be sited with renewable electricity sources. However, with

appropriate communication, the electrolyzer does not need to be located in the immediate vicinity of the renewable resource to effectively use it. Electrolyzers may be controlled remotely to use inexpensive electricity that is produced when renewable sources are available but demand is not.

The grid must balance generation with demand nearly instantaneously and provide additional capacity to maintain system reliability. Energy and ancillary service markets have been established to procure the necessary resources. Ancillary service markets include load following, fast energy markets, flexibility, regulation, spinning reserve, non-spinning reserve, and other reserves (i.e., replacement or supplemental). Load following, fast energy markets, and flexibility provide similar products by reconciling energy mismatches; these products are often separated into "up" product (increasing generation or reducing demand) and "down" product (reducing generation or increasing demand) [1].

The anticipated value to the electrical utility grid of electrolyzers and fuel cells stems from the fact that they are a controllable load/generator with fast (~1 s) and stable response. In the case of electrolyzers, these systems are typically coupled to hydrogen energy storage. **This allows an integrated system the flexibility to meet hydrogen demand by storing more hydrogen when grid power demand is low and/or renewable energy supply is high, while helping to stabilize the grid by responding to ancillary service requests.**

APPROACH

Projects in Technology Validation are both (1) a "learning demonstration" to help guide and manage the hydrogen and fuel cell component and materials research and development activities and (2) a validation of the technology under real-world operating conditions against durability and performance targets. Specifically, the approach of this project includes the following.

- Develop a flexible industry accessible platform to test large active area electrolyzer stacks (up to 1 MW) and next generation balance of plant (BOP) subsystems to improve system cost and performance
- Provide actionable data to electric utilities and industry stakeholders demonstrating the ability of electrolyzers and fuel cells to participate in ancillary grid support markets
- Develop and demonstrate advanced RTDS, HIL, monitoring, and control of electrolyzer and fuel cell systems to improve overall system efficiency and grid participation effectiveness to enable higher penetrations of renewable electricity generation

RESULTS

Task 1: Design, Build, and Characterize Performance of Electrolyzer Stack Test Bed

NREL completed the design, fabrication, and commissioning of an electrolyzer stack test bed. Multiple beginning-of-life polarization current-voltage (IV) curves were obtained; six of them on three 150 kW polymer electrolyte membrane (PEM) stacks for work covered under a technical services agreement with Giner Inc. and two others on a 120 kW stack procured from Proton Onsite.

The stack test bed provided nearly 1,000 A, controls, and the required BOP to complete the work with Giner Inc. The factory acceptance tests included obtaining polarization curves and individual cell voltages for the three PEM stacks at 70°C, various cathode pressures, and very high current density. In Figure 1, which shows polarization curves for one of the 150 kW stacks at two different pressures, the y-axis values are intentionally removed to protect Giner's data.

NREL also procured a 50-cell, 120 kW, 2.5 kg hydrogen per hour PEM stack from Proton Onsite. A beginning-of-life IV curve was captured at 50°C and 300 psig (Figure 2). Operation of this stack will provide onsite hydrogen production for ESIF fuel cell labs, vehicle refueling, and infrastructure component testing projects (e.g., hoses, pressure relief devices, compressors), as well as a test platform for grid integration, stack decay testing, and BOP optimization under variable power.

Demonstrated grid ancillary services—frequency regulation

In an electric power system, automatic generation control is a system for adjusting the power output of multiple generators at different power plants, in response to changes in the load. An electrolyzer system can quickly reduce or increase its load (stack and BOP) to have the same effect on the grid.

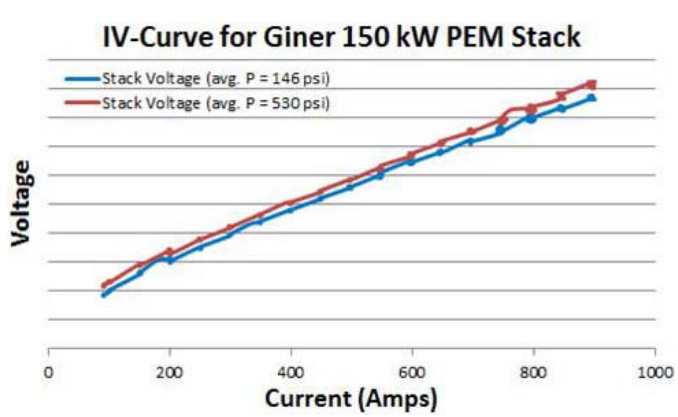

FIGURE 1. Polarization curves (146 psig and 530 psig at 70°C) taken during factory acceptance tests performed on the electrolyzer stack test bed for Giner Inc.

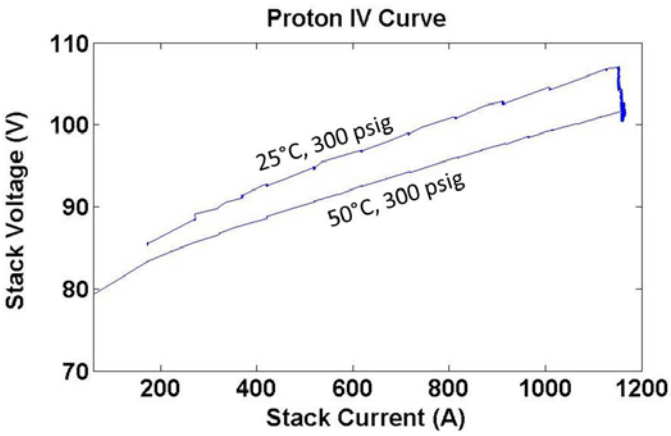

FIGURE 2. Beginning-of-life polarization curves (25°C and 50°C at 300 psig) of a 50-cell, 120 kW PEM electrolyzer stack from Proton Onsite operating on the electrolyzer stack test bed

The large active area stack test bed, operating the 120 kW stack, demonstrated grid ancillary services by following a traditional 4 s simulated frequency regulation signal. The stack DC power supplies were programmed to read a file containing normalized historical frequency regulation signals obtained from Xcel Energy.

Task 2: Develop Communications and Information and Computation Data Services for Integrated System Testing

Communications

The work under this task provided the required hardware and cyber connectivity to establish a VPN to enable detailed data exchange between the two RTDS at INL and NREL from the context of electrolyzers connected to distribution and large scale transmission networks. The data exchange and its properties dictate largely the type of simulations that can be performed under this configuration.

Information and computation data services

In this task, research datasets are collected into secured projects with permissions managed by the principal investigator. Research data can be curated by assigning metadata through the use of tags and classifying the data structure and permissions. Finally, search and filtering capabilities easily locate data across projects and datasets.

This work established two main data connectivity components: (1) the electrolyzer stack test bed data acquisition system was uploaded to the data repository in the ESIF's data center, and (2) data analytics components were developed through a website to visually interpret and share the data with clients. The project takes advantage of the data system components in the ESIF data center—such as a Time Series cluster to manage large amounts of time series data and a file repository that is redundant and backed up—ensuring very secure and reliable data storage and a database for managing metadata.

Task 3: Demonstrate Integrated Systems to Deliver Grid Services

The project team successfully demonstrated a first of its kind, bidirectional, high speed simulation between ESIF RTDS and INL RTDS. The connection between the two RTDS is over the DOE-owned Energy Sciences Network. It was the first time, as we understand, that two RTDS machines communicated over a wide area network. The simulation consisted of the exchange of voltage values between the distribution grid node where the electrolyzer is connected and the electrolyzer input node located on the RTDS at NREL. The data exchange occurs at each time step and simulation proceeds with updated data received at each iteration.

Similarly, the electrolyzer model can be replaced with actual electrolyzer hardware. In this case the data exchange latency would also depend on the internal characteristics of the electrolyzer hardware connected to the RTDS. The time step for simulations in RTDS can be adjusted as per the requirement of a specific simulation to mitigate the effect of data communication latency (~27 ms) and response time. The two parts of the experimental system shown in Figure 3 exchange data across the internet in real time.

CONCLUSIONS AND FUTURE DIRECTIONS

- Conclusion: NREL completed the design, build, and commissioning of an electrolyzer stack test bed and obtained beginning-of-life IV curves on four stacks: three 150 kW PEM stacks under a technical services agreement with Giner and one 120 kW stack procured from Proton Onsite being used for onsite hydrogen production.
  - Future: Operate the 120 kW stack under variable power to demonstrate advanced grid functionality, quantify stack decay rate, and provide a test platform for state-of-the art stacks and BOP optimization
- Conclusion: NREL established connectivity via a VPN to enable detailed data exchange between the two RTDS at INL and NREL. To provide data connectivity, NREL uploaded the electrolyzer stack test bed data acquisition system to the data repository in the ESIF's data center and developed data analytics components through a website to visually interpret and share the data with clients.
  - Future: Improve industry involvement by coordinating meetings with electric utilities to share NREL's electrolyzer stack test bed performance data and understand the value of electrolyzers and fuel

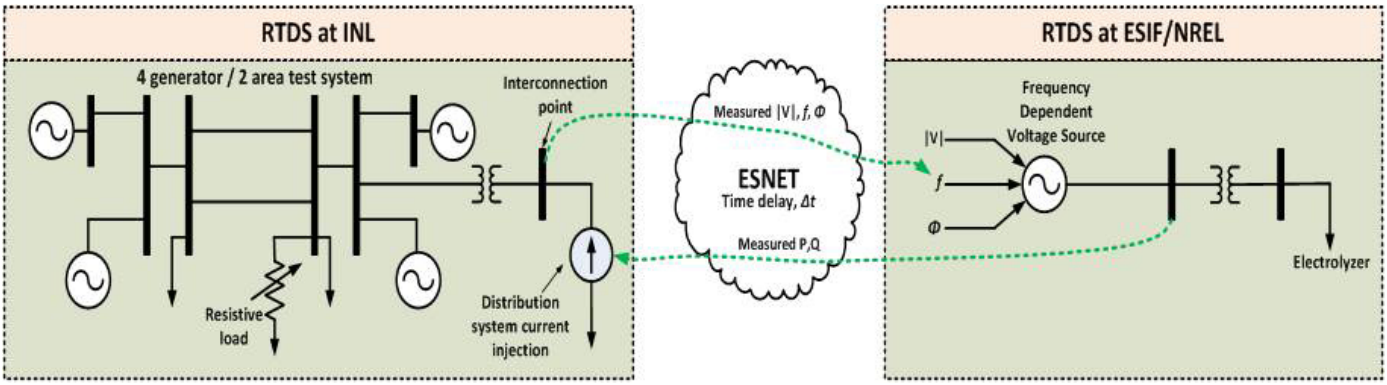

FIGURE 3. The diagram describes the experimental design of the RTDS testing conducted between INL and NREL.

cells if they were to participate in established and potential future markets

  - Future: Attend technical workshops (e.g., energy storage, Smart Grid) that are coordinating national efforts to modernize the grid with advanced monitoring/controls for loads/generators to support the grid enabling the increased penetration of renewable energy

- Conclusion: The project team successfully demonstrated a first of its kind, bidirectional, high speed communication test between the ESIF RTDS and the INL RTDS.
  - Future: Explore new RTDS research applications. Real time simulations by geographically distributed RTDS are a relatively newer concept and require significant efforts to be reliably established. The applications based on geographically distributed RTDS are an unexplored research area for performing dynamic and transient analysis of energy sources. The geographically distributed RTDS can also lead to simulations between remote sites that facilitate testing and characterization. One such application is the ability to utilize real time simulators with standard communication for troubleshooting remote hardware at challenging locations.

FY 2015 PUBLICATIONS/PRESENTATIONS

1. P. Denholm, O. Ma, T. Markel, and J. Eichman, "Summary of Market Opportunities for Electric Vehicles and Dispatchable Load in Electrolyzers" (Technical Report), NREL/TP-6A20-64172 (Golden, CO: National Renewable Energy Laboratory, 2015).

2. K. Harrison, O. Smith, M. Peters, D. Terlip, P. Denholm, and M. Mann, "FCTO INTEGRATE Stack Test Bed and Grid Interoperability," (presented at the DOE Hydrogen and Fuel Cells Program Annual Merit Review and Peer Evaluation Meeting, Arlington, VA, June 10, 2015).

REFERENCES

1. J. Eichman, K. Harrison, and M. Peters, "Novel Electrolyzer Applications: Providing More than Just Hydrogen" (Technical Report), NREL/TP-5400-61758 (Golden, CO: National Renewable Energy Laboratory, 2014).

VII.4 Fuel Cell Electric Vehicle Evaluation

Jennifer Kurtz (Primary Contact), Sam Sprik, Chris Ainscough, and Genevieve Saur
National Renewable Energy Laboratory (NREL)
15013 Denver West Parkway
Golden, CO 80401-3305
Phone: (303) 275-4061
Email: Jennifer.Kurtz@nrel.gov

DOE Manager
Jason Marcinkoski
Phone: (202) 586-7466
Email: Jason.Marcinkoski@ee.doe.gov

Project Start Date: October 1, 2012
Project End Date: Project continuation and direction determined annually by DOE

Overall Objectives

- Validate hydrogen fuel cell electric vehicles (FCEVs) in a real-world setting
- Identify current status and evolution of the technology

Fiscal Year (FY) 2015 Objectives

- Provide a status of FCEV durability compared with the DOE 2020 durability target
- Analyze real-world fuel economy and range
- Report on FCEV specifications as well as driving and fueling trends
- Compare performance data with relevant or past data sets (e.g., FCEV Learning Demonstration, National Household Transportation Survey (NHTS), and typical gasoline fueling trends)
- Make results available through online publication, highlights, and presentations
- Complete two publications cycles (Fall 2014 and Spring 2015).

Technical Barriers

This project addresses the following technical barriers from the Technology Validation section of the Fuel Cell Technologies Office Multi-Year Research, Development, and Demonstration (MYRDD) Plan:

(A) Lack of Fuel Cell Electric Vehicle and Fuel Cell Bus Performance and Durability Data

Contribution to Achievement of DOE Technology Validation

This project contributes to the achievement of the following DOE milestones from the Technology Validation section of the Fuel Cell Technologies Office MYRDD Plan:

- Milestone 2.3: Validate fuel cell electric vehicles achieving 5,000-hour durability (service life of vehicle) and a driving range of 300 miles between fuelings (4Q, 2019).

FY 2015 Accomplishments

- The National Fuel Cell Technology Evaluation Center (NFCTEC) has completed two publication cycles of real-world FCEV operation. The data analyzed has come from 48 vehicles, with model years spanning 2006 to 2012.
- While the 48 vehicles analyzed do not represent all FCEVs on the road today, it is a statistically significant set of data for evaluation with 2,413,340 total miles traveled and 79,468 total fuel cell operation hours. The maximum vehicle odometer is 178,550 miles (approximately 10% of vehicles have passed 100,000 miles) and the maximum fuel cell operation hours is 5,605.
- Compared current FCEV performance with past data from the Learning Demonstration (LD) phases. The comparisons to the LD project have provided insight into the steady progress made over the last eight years, specifically in fuel cell voltage durability, fuel economy, range, and driving trends. The current values are summarized in Table 1.

✧ ✧ ✧ ✧ ✧

INTRODUCTION

Under FOA-625, the DOE has funded projects for the collection and delivery of FCEV data to NREL for analysis, aggregation, and reporting. Multiple real-world sites and customers are included in this FCEV demonstration project. This activity addresses the lack of on-road FCEV data and seeks to validate improved performance and longer durability from comprehensive sets of early FCEVs, including first-production vehicles. NREL's objective in this project is to support DOE in the technical validation of hydrogen FCEVs under real-world conditions. This is accomplished through evaluating and analyzing data from the FCEVs to identify the current status of the technology, comparing it to DOE program targets, and assisting in evaluating progress between

TABLE 1. Current Status against DOE 2020 Targets

Vehicle Performance Metrics	DOE Target (Year 2020)[a]	Current[b]	LD2+[c]	LD2[c]	LD1[c]
Durability					
Max fuel cell durability projection (h)	5,000	3,930	—	2,521	1,807
Average fuel cell durability projection (h)		2,032	1,748	1,062	821
Max fuel cell operation (h)		5,605	1,582	1,261	2,375
Efficiency					
Adjusted dyno (window sticker) range		No update planned	—	196-254 mi	103-190 mi
Median on-road distance between fuelings		119 mi	98 mi	81 mi	56 mi
Fuel economy (window sticker)		51 mi/kg (median)	—	43–58 mi/kg	42–57 mi/kg
Fuel cell efficiency at ¼ power	60%	No update planned	—	53%–59%	51%–58%
Fuel cell efficiency at full power		No update planned	—	42%–53%	30%–54%
Specification					
Specific power (W/kg)	650	240–560		306–406	183–323
Power density (W/L)	850	Planned 2015		300–400	300–400

[a] Fuel Cell Technologies Office Multi-Year Research, Development, and Demonstration Plan [1]
[b] Current results are available at http://www.nrel.gov/hydrogen/proj_fc_vehicle_evaluation.html [3] (updated May 2015)
[c] National Fuel Cell Vehicle Learning Demonstration Final Report (http://www.nrel.gov/hydrogen/pdfs/54860.pdf) [2]

multiple generations of technology, some of which will include commercial FCEVs for the first time.

The project includes six original equipment manufacturers (OEMs): GM, Mercedes-Benz, Hyundai, Nissan, Toyota, and Honda. The latter three OEMs are part of one DOE project with Electricore. Up to 90 vehicles are expected to supply data over potentially two phases, with particular attention on fuel cell stack durability and efficiency, vehicle range and fuel economy, driving behavior, maintenance, on-board storage, refueling, and safety. Previous technology validation work on FCEVs and hydrogen infrastructure was performed through the FCEV LD [2], also known as the Controlled Hydrogen Fleet and Infrastructure Demonstration and Validation Project. Some of the current partners were also part of the LD. Those vehicles and technologies are not necessarily the same as the vehicles currently under evaluation even though some of the platforms are the same. Except where referenced or labeled, all of the data reported here are for the current project.

APPROACH

The project's data collection plan builds on other technology validation activities. Operation, maintenance, and safety data for fuel cell system(s) and accompanying infrastructure are collected on site by project partners. NREL receives the data quarterly and stores, processes, and analyzes the data in NREL's NFCTEC. The NFCTEC is an off-network room with access provided to a small set of approved users. An internal analysis of all available data is completed quarterly and a set of technical composite data products (CDPs) is published every six months. Publications are uploaded to NREL's technology validation website [3] and presented at industry-relevant conferences. The CDPs present aggregated data across multiple systems, sites, and teams in order to protect proprietary data and summarize the performance of hundreds of fuel cell systems and thousands of data records. A review cycle is completed before the CDPs are published. This review cycle includes providing detailed data products (DDPs) of individual system- and site-performance results to the specific data provider. DDPs also identify the individual contribution to the CDPs. The NREL Fleet Analysis Toolkit is an internally developed tool for data processing and analysis structured for flexibility, growth, and simple addition of new applications. Analyses are created for general performance studies as well as application- or technology-specific studies.

RESULTS

The current FCEV evaluation analyses include the following categories: durability, deployment (e.g., number of vehicles included), system specifications, range, fuel economy, efficiency, fill performance, reliability, drive and fill behaviors, power and energy management, fuel cell transients (e.g., frequency of rapid increases or decreases in fuel cell power), and benchmarking against technical targets and typical gasoline vehicle operation.

As of December 2014, NREL has analyzed more than 120,000 trip data files (a cumulative data file size of nearly 11 GB). More than 4,000 analysis files (non-published results)

have been created and submitted to the individual OEMs. All of the public results are available on the NFCTEC website.

The current evaluation includes 48 vehicles with more than 2.4 million miles traveled and nearly 80,000 fuel cell operation hours. As of December 2014, 16 vehicles were retired. The durability target for fuel cell systems is 5,000 hours (equivalent to 150,000 miles), which is on par with light-duty vehicle customer expectations and conventional technologies. Two parameters used in this evaluation project to track and validate system durability are projected operation time to 10% voltage degradation and actual operation hours. Fuel cell durability results were initially published in 2006 (the first generation of the LD project). The voltage durability trend from four unique reporting periods is shown in Figure 1. FCEVs in a fleet and a reporting period are of the same generation and design. The operation time to 10% voltage degradation for each stack in a fleet is averaged to determine the fleet voltage degradation value. The average of the fleets' average operation time to 10% voltage degradation in a reporting period is shown in blue and has increased 147% since the first LD period. The maximum of the fleets' average operation time to 10% voltage degradation, 3,930 hours, has increased 118% since the first reporting value in 2006–2007.

Fuel cell durability has steadily and significantly improved over the last decade. The on-road fuel economy has also increased. The minimum and maximum on-road fuel economy is 41 and 58 miles per kilogram hydrogen, respectively (Figure 2). Overall, the current evaluation indicates an improvement of approximately 30% from the first generation LD (LD1) results (Figure 3).

Another positive trend over the last decade of NFCTEC-analyzed FCEV operation is the actual distance driven between refueling (Figure 4). The results show that the median distance between fueling events was 56 miles for 2005–2007 (light gray), 81 miles for 2007–2009 (dark gray), and 98 miles for 2010–2011 (black). The median distance between refueling in the current evaluation is 119 miles, more than twice as long as the result from the LD1.

In addition to comparisons to past FCEV results, the driving and fueling data have been compared with the NHTS 2009 [4] and typical gasoline fueling trends [5]. Those comparisons include time of day, day of week, daily distance traveled, and average speed. We've found that FCEVs are driven primarily during the work week (Monday through Friday) and have less driving on Saturday and Sunday than the NHTS data indicate. The average speed of all the FCEV trips is just over 28 miles per hour, which is slightly above the NHTS overall average of 25 miles per hour. The percentage of FCEV drive days that are 40 miles or less is 44%, compared with 68% for the NHTS drive days. Relative to the total days of driving for the vehicles in each data set, FCEVs may be driving more in a day than the NHTS vehicles because some of the FCEVs are driven on schedules aimed to accumulate high mileage and operation hours over a variety of conditions, referred to as durability vehicles in this report. Durability vehicles are driven on public roads, in conditions typical for the regions, and will typically accumulate many miles each day.

When comparing the FCEV fills with the typical gasoline fueling profile data, the distribution is most different on Saturday and Sunday. However, the weekend FCEV fills (7–8% of fills) have increased when compared with the

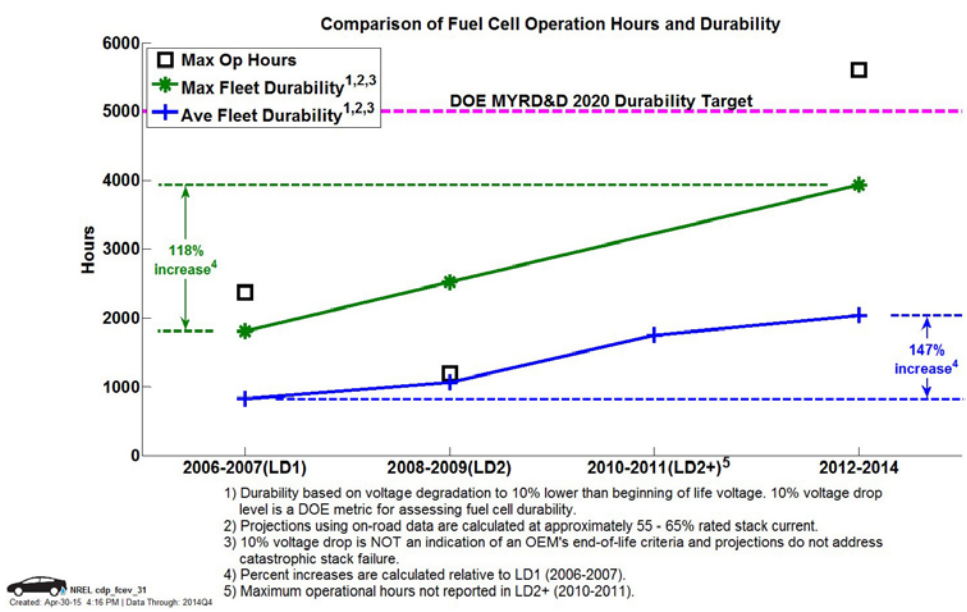

FIGURE 1. FCEV durability trend and comparison

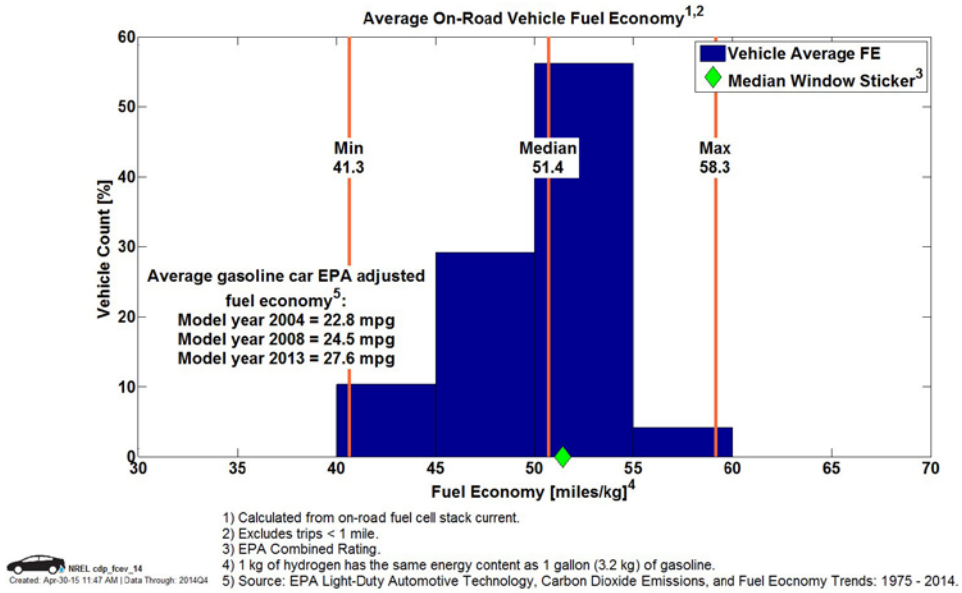

FIGURE 2. FCEV on-road fuel economy

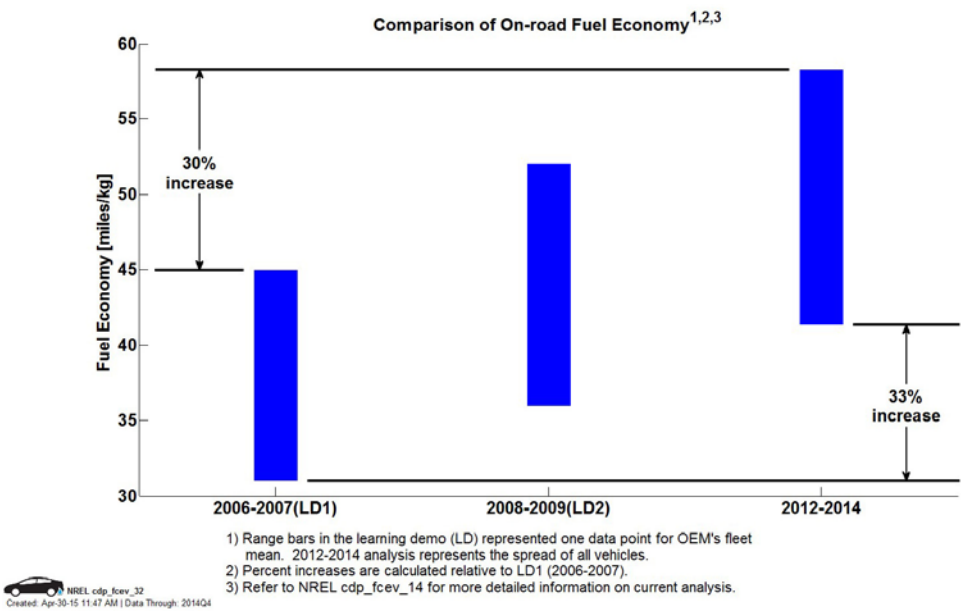

FIGURE 3. FCEV on-road fuel economy trends and comparison

LD fills, where only 2–4% of fills were on Saturdays and Sundays. Almost 80% of all the FCEV fills have occurred between 6 a.m. and 6 p.m., and the FCEV data show a much higher demand early in the day (between 7 a.m. and 10 a.m.) than the typical gasoline Friday fueling profile does.

CONCLUSIONS AND FUTURE DIRECTIONS

NFCTEC has completed two publication cycles of real-world FCEV operation. The data analyzed has come from 48 vehicles, with model years spanning 2006 to 2012. While the 48 vehicles analyzed do not represent all FCEVs on the road today, it is a statistically significant set of data for evaluation with 2,413,340 total miles traveled and 79,468 total fuel cell operation hours. The maximum vehicle odometer is 178,550 miles (approximately 10% of vehicles have passed 100,000 miles) and the maximum fuel cell operation hours is 5,605. Both driving and fueling trends have been compared with conventional gasoline trends. A few differences (like daily distance traveled and weekend fueling) have been observed

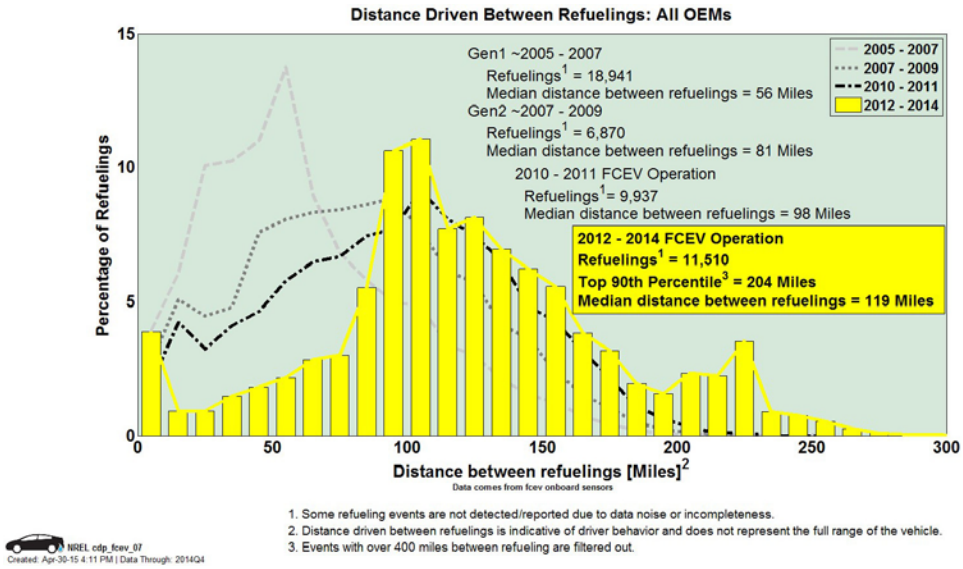

FIGURE 4. FCEV actual driving distance between refueling trend and comparison

in those comparisons. This is an indication that FCEV drivers are utilizing vehicles just as they would any other vehicle except with the advantage of a decreased carbon footprint. There are some FCEVs included in this analysis that are driven based on schedules aimed at accumulating miles and operation hours faster than a typical driver. The future work includes:

- Publish
- Continue analysis on fuel cell durability, fuel economy, and range
- Review key performance trends (durability, fuel economy, and range) over time
- Study the interdependence between FCEV and hydrogen station performance
- Quantify FCEV benefits based on real-world data
- Identify the durability FCEV data trends versus traditional customer FCEVs
- Complete a drive cycle analysis to categorize the different FCEV drive cycles for comparison with standard drive cycles and supply data to R&D community for fuel cell testing

FY 2015 PUBLICATIONS/PRESENTATIONS

1. Kurtz, J., Sprik, S., "Spring 2015 FCEV Evaluation Results," Golden, CO: National Renewable Energy Laboratory, May 2015. Composite data products. (report)

2. Sprik, S., Kurtz, J., "Technology Validation of Fuel Cell Vehicles and Infrastructure," Fuel Cell Seminar 2014, Los Angeles, CA, November 2014. (presentation)

3. Kurtz, J., Sprik, S., "Fall 2014 FCEV Evaluation Results," Golden, CO: National Renewable Energy Laboratory, November 2014. Composite data products. (report)

REFERENCES

1. Fuel Cell Technologies Office Multi-Year Research, Development, and Demonstration Plan. Fuel Cells chapter, Table 3.4.3 Technical targets for automotive application. Washington, D.C.: U.S. Department of Energy, 2012. Accessed October 13, 2014: http://energy.gov/eere/fuelcells/downloads/fuel-cell-technologies-office-multi-year-research-development-and-22.

2. Wipke, K.; Sprik, S.; Kurtz, J.; Ramsden, T.; Ainscough, C.; Saur, G. National Fuel Cell Electric Vehicle Learning Demonstration Final Report. NREL/TP-5600-54860. Golden, CO: National Renewable Energy Laboratory, July 2012. http://www.nrel.gov/hydrogen/pdfs/54860.pdf.

3. NREL's technology validation NFCTEC website (http://www.nrel.gov/hydrogen/proj_tech_validation.html)

4. NHTS 2009 website (http://nhts.ornl.gov)

5. T. Chen. Hydrogen Delivery Infrastructure Options Analysis. http://www1.eere.energy.gov/hydrogenandfuelcells/pdfs/delivery_infrastructure_analysis.pdf

VII.5 Technology Validation: Fuel Cell Bus Evaluations

Leslie Eudy (Primary Contact), Matthew Post
National Renewable Energy Laboratory (NREL)
15013 Denver West Parkway
Golden, CO 80401
Phone: (303) 275-4412
Email: Leslie.Eudy@nrel.gov

DOE Manager
Jason Marcinkoski
Phone: (202) 586-7466
Email: Jason.Marcinkoski@ee.doe.gov

Project Start Date: March 2001
Project End Date: Project continuation and direction determined annually by DOE

Overall Objectives

- Validate fuel cell electric bus (FCEB) performance and cost compared to DOE and U.S. Department of Transportation (DOT) targets and conventional technologies
- Coordinate with the DOT Federal Transit Administration (FTA) on the data collection for the National Fuel Cell Bus Program (NFCBP) and with international work groups to harmonize data collection methods and enable the comparison of a wider set of vehicles

Fiscal Year (FY) 2015 Objectives

- Document performance results from each current FCEB demonstration site
- Complete an annual status report comparing results from the different demonstrations

Technical Barriers

This project addresses the following technical barriers from the Technology Validation section of the Fuel Cell Technologies Office Multi-Year Research, Development, and Demonstration (MYRDD) Plan:

(A) Lack of Fuel Cell Electric Vehicle and Fuel Cell Bus Performance and Durability Data

(D) Lack of Hydrogen Fueling Infrastructure Performance and Availability Data

Contribution to Achievement of DOE Technology Validation Milestones

This project has contributed to achievement of the following DOE milestone from the Technology Validation section of the Fuel Cell Technologies Office MYRDD Plan:

- *Milestone 2.3: Validate fuel cell electric vehicles achieving 5,000-hour durability (service life of vehicle) and a driving range of 300 miles between fuelings. (4Q, 2019)* Through FY 2015, NREL collected data on 18 FCEBs. NREL documented nine fuel cell power plants (FCPP) with operation hours in excess of 10,000 hours. One of these systems has logged more than 19,500 hours in service and a second system has surpassed 12,900 hours. Bus fuel economy is dependent on duty cycle. Based on in-service fuel economies of 6.3 miles per kilogram, the hybrid FCEBs currently in service can achieve a range of approximately 270 miles per fill.

FY 2015 Accomplishments

- Published reports on performance and operational data covering 18 full-size FCEBs in revenue service in the U.S.
- Documented more than 19,500 hours on a single fuel cell power plant

✧ ✧ ✧ ✧ ✧

INTRODUCTION

Transit agencies continue to aid the FCEB industry in developing and optimizing fuel cells for buses. These in-service demonstration programs are vital to validate the performance of fuel cell systems in buses and to determine issues that require resolution. Using fuel cells in a transit application can help accelerate the learning curve for the technology because of the high mileage accumulated in short periods of time. During the last year, the project teams have made progress in improving fuel cell durability, availability, and reliability. More work is still needed to meet the performance needs of transit, lower capital and operating costs, and transition the maintenance to transit staff.

APPROACH

NREL uses a standard evaluation protocol to provide the following.

- Comprehensive, unbiased evaluation results of advanced technology vehicle development and operations

- Evaluations of hydrogen infrastructure development and operation
- Descriptions of facility modifications required for the safe operation of FCEBs
- Detailed FCEB performance and durability results to validate status against technical targets, educate key stakeholders, and further DOE goals

The evaluation protocol includes collecting operation and maintenance data on the bus and infrastructure. The analysis, which consists of economic, technical, and safety factors, focuses on performance and use, including progress over time and experience with vehicle systems and supporting infrastructure. The data are compared to DOE/FTA technical targets and to conventional baseline buses in similar service.

RESULTS

During FY 2015, NREL collected and analyzed data on the following four FCEB demonstrations at three transit agencies in the U.S. and Canada:

- Zero Emission Bay Area (ZEBA) Demonstration—five Bay Area transit agencies led by AC Transit (Oakland, California) are demonstrating twelve 40-foot Van Hool buses with US Hybrid fuel cells in a Siemens hybrid system. The hybrid system was integrated by Van Hool and uses lithium ion batteries from EnerDel.
- American Fuel Cell Bus (AFCB) Project—in December 2012 SunLine began operating an ElDorado National 40-foot bus with a BAE Systems hybrid propulsion system using Ballard Power Systems fuel cells and lithium batteries. This project is part of FTA's NFCBP. SunLine added two more AFCBs in 2014 and a third in 2015. NREL collected data on all four buses.
- Birmingham Fuel Cell Bus Project—Demonstration of one 30-foot EVAmerica bus with an Embedded Power Labs battery-dominant hybrid propulsion system using lithium titanate batteries and a Ballard fuel cell. The bus is being operated by Birmingham-Jefferson County Transit Authority.
- Advanced Composite Fuel Cell Bus: Demonstration of one next-generation battery-dominant Proterra FCEB in Austin, TX, and Washington, DC. The 35-foot bus has a hybrid system from Proterra, lithium titanate batteries, and a Ballard fuel cell power system.

The first two projects involve fuel cell-dominant hybrid buses. NREL's evaluations of these projects were funded by DOE. The remaining two projects involve battery-dominant hybrid buses and were covered by funding from FTA. NREL published results from the first two of these demonstrations. A summary of selected results is included in this report.

The Birmingham bus experienced some issues during the early portion of the demonstration and was not in service for a significant period of time. The Proterra bus went into service in early 2015. NREL will report on these buses once sufficient data are collected.

NREL completed reports on operational and performance data from the FCEBs and from conventional baseline buses at each agency. The results are also compared to technical targets for FCEB performance established by DOE/FTA and published in a Fuel Cell Technologies Program Record in September 2012 [1]. Tables 1 and 2 provide a summary of the reported results from the operation at each agency, including data from the baseline buses.

TABLE 1. 2015 Summary Data Results for ZEBA FCEBs

Vehicle data	FCEB	Diesel (Van Hool)	Diesel (Gillig)
Number of buses	12	3	10
Data period (month, year)	Sept. 2011 – Apr. 2015	Sept. 2011 – Apr. 2015	July 2013 – Apr. 2015
Number of months	36	36	22
Total fleet miles	962,124	490,693	1,030,102
Average miles per month	2,248	4,055	4,682
Total FC hours	112,363	–	–
Fuel economy (mi/kg)	6.36	–	–
Fuel economy (mi/diesel gal equivalent)	7.19	3.92	4.28
Average speed (mph)	8.6	–	–
Availability (%)	74	79	87

FC – fuel cell

TABLE 2. 2015 Summary Data Results for SunLine FCEBs

Vehicle data	AFCB	CNG
Number of buses	4	5
Data period (month, year)	Mar. 2012 – June 2015	Mar. 2012 – June 2015
Number of months	47	47
Total fleet miles	151,935	898,670
Average miles per month	2,491	4,493
Total FC hours	10,297	–
Fuel economy (mi/kg)	6.11	–
Fuel economy (mi/diesel gal equivalent)	6.72	3.20
Average speed (mph)	14.8	16.3
Availability (%)	70	85

CNG – compressed natural gas

Increasing the durability and reliability of the fuel cell system to meet FTA life cycle requirements for a full-size

bus—12 years or 500,000 miles—continues to be a challenge for the fuel cell bus industry. DOE and FTA have set an early FCPP performance target of 4–6 years (or 25,000 hours) durability for the fuel cell propulsion system, which would be approximately half the life of the bus. The FCPP would be rebuilt or replaced at that time—similar to what transit agencies typically do for diesel engines. Over the last year, NREL collected data on 18 FCPPs. Figure 1 shows the total hours accumulated on individual FCPPs for the current projects tracked by NREL. The average of 8,980 hours is shown on the graph as a dashed line. The 2016 and ultimate targets are included on the graph. As of May 2015, the highest-hour FCPP had reached 19,500 hours, surpassing the 2016 target of 18,000 hours. Of the 18 total FCPPs included in the graph, 67% (12) have surpassed 9,000 hours of operation. The FCPPs with the lowest hours accumulated are either newer buses or spare FCPPs that are used periodically. This shows significant improvement in durability toward meeting the 25,000 hour target.

The transit industry measures reliability as mean distance between failures, also known as miles between road call (MBRC). Figure 2 tracks the MBRC over time for the ZEBA and SunLine FCEB demonstrations and includes the MBRC for the bus as a whole and MBRC for the fuel cell system. The targets for each category are included on the chart. Table 3 provides the MBRC by year since 2012. Reliability has shown a marked increase over time, reaching the ultimate targets for both bus MBRC and FC system MBRC. Road calls due to bus-related issues—such as problems with doors, and air conditioning—made up

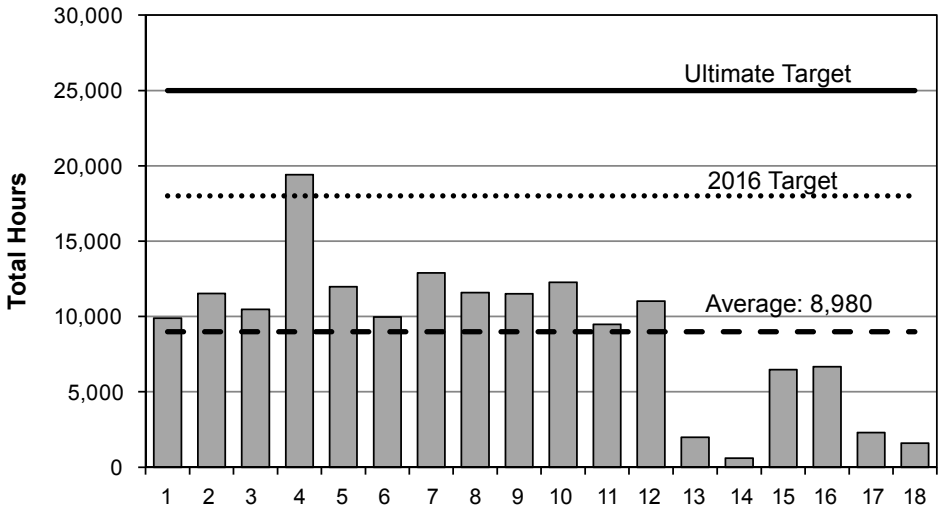

FIGURE 1. Total fuel cell hours accumulated on each FCPP

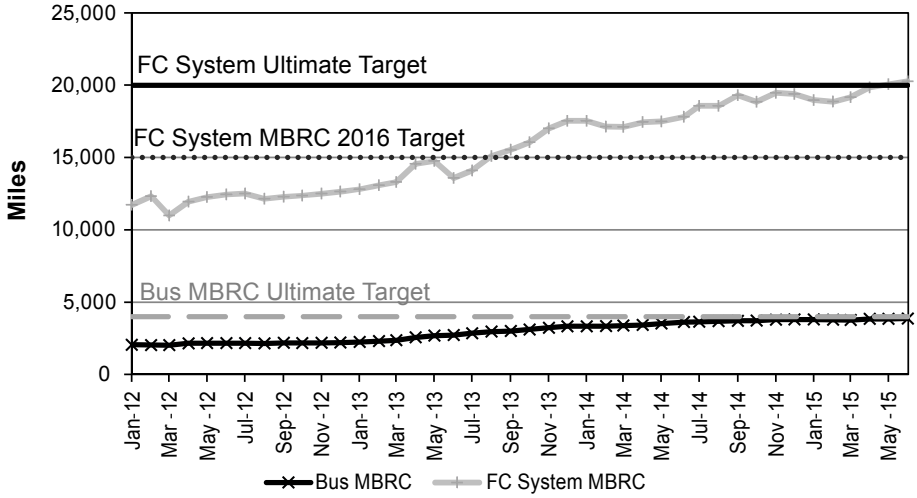

FIGURE 2. Miles between road call

39% of the total failures. Fuel cell-related issues made up approximately 19% of the road calls during the period.

TABLE 3. MBRC by Year through June 2015

	Bus MBRC	FC System MBRC
June 2012	2,160	12,507
June 13	2,730	13,572
June 14	3,625	17,816
June 15	3,873	20,269
% improvement from 2012 to 2015	79	62

CONCLUSIONS AND FUTURE DIRECTION

Fuel cell propulsion systems in buses have continued to show progress in increasing the durability and reliability of FCEBs and the primary components. The current technology already meets fuel economy targets and has now exceeded the fuel cell durability targets. Table 4 summarizes the current status compared to the DOE/DOT performance targets. There are still challenges to overcome before fuel cell buses can match the current performance standard of diesel buses.

- Continuing operation to validate durability and reliability of the fuel cell systems and other components to match transit needs
- Transferring all maintenance work to transit personnel
- Lowering the costs of purchasing, operating, and maintaining buses and infrastructure
- Integrating hydrogen fueling procedures into the existing fueling process
- Transferring the lead role for FC system integration to transit bus builders

Future work by NREL includes the following.

- Continuing data collection, analysis, and reporting on performance data for FCEBs in service at the following sites:
  - ZEBA FCEB Demonstration led by AC Transit
  - SunLine
  - Birmingham-Jefferson County Transit Authority in Birmingham, Alabama
  - Capital Metro, Austin, Texas
  - University of California, Irvine
  - Additional sites as funding allows
- Investigating reliability, durability, and life cycle of FCEBs as a part of ongoing evaluations
- Coordinating with FTA to collect data on the demonstrations funded under the NFCBP
- Coordinating with national and international FCEB demonstration sites

FY 2015 PUBLICATIONS/PRESENTATIONS

1. L. Eudy, M. Post, *Zero Emission Bay Area (ZEBA) Fuel Cell Bus Demonstration: Fourth Results Report*, National Renewable Energy Laboratory, Golden, CO, NREL/TP-5400-63719, July 2015.

2. L. Eudy, *Technology Validation: Fuel Cell Bus Evaluations*, Presentation at the DOE Hydrogen and Fuel Cells Program Annual Merit Review, Washington, DC, June 2015.

3. L. Eudy, *U.S. Fuel Cell Bus Performance*, Presentation at the 9th International Fuel Cell Bus Workshop, February 2015.

4. L. Eudy, *Technology Validation: FCEB Evaluations*, Presentation for the California Fuel Cell Partnership Bus Team meeting, May 2015.

TABLE 4. 2015 Summary of Progress toward Meeting DOE/DOT Targets

	Units	2015 Status	2016 Target	Ultimate Target
Bus lifetime	Years / miles	5/100,000[a]	12/500,000	12/500,000
Power plant lifetime	Hours	600–19,500[a]	18,000	25,000
Bus availability	%	70–74	85	90
Road call frequency (Bus / fuel cell system)	Miles between road call	3,400–4,000 / 17,500–21,300	3,500/15,000	4,000/20,000
Operation time	Hours per day/ days per week	19/7	20/7	20/7
Maintenance cost	$/mile	0.54–1.33	0.75	0.40
Fuel economy	Miles per diesel gallon equivalent	6.7–7.2	8	8
Range	Miles	220–300	300	300

[a] Accumulation of miles and hours to date—not end of life.

5. L. Eudy, C. Gikakis, *Fuel Cell Buses in U.S. Transit Fleets: Current Status 2014*, National Renewable Energy Laboratory, Golden, CO, NREL/TP-5400-62383, December 2014.

REFERENCES

1. Fuel Cell Technologies Program Record #12012, September 2012, www.hydrogen.energy.gov/pdfs/12012_fuel_cell_bus_targets.pdf.

VII.6 Material Handling Equipment Data Collection and Analysis

Chris Ainscough (Primary Contact), Jennifer Kurtz
National Renewable Energy Laboratory (NREL)
15013 Denver West Parkway
Golden, CO 80401-3305
Phone: (720) 431-7296
Email: Chris.Ainscough@nrel.gov

DOE Manager
Jason Marcinkoski
Phone: (202) 586-7466
Email: Jason.Marcinkoski@ee.doe.gov

Project Start Date: October 2012
Project End Date: Project continuation and direction determined annually by DOE

Overall Objectives

- Evaluate fuel cell material handling equipment (MHE) by performing independent technology assessment in real world operation conditions
- Focus on fuel cell system performance and operation
- Leverage data processing and analysis capabilities developed under the fuel cell vehicle learning demonstration project
- Support market growth by providing analyses and results relevant to the market's value proposition
- Report on technology status to fuel cell and hydrogen communities and other key stakeholders like end users

Fiscal Year (FY) 2015 Objectives

- Leverage existing data and results developed under American Recovery and Reinvestment Act (ARRA) to continue the collection of MHE data on new systems on a voluntary basis
- Validate the status of the MHE market, which continues to expand and evolve
- Develop at least 20 updated composite and detailed data products on fuel cell MHE on durability, operation, and infrastructure performance

Technical Barriers

This project addresses the following technical barriers from the Technology Validation section of the Fuel Cell Technologies Office (FCTO) Multi-Year Research, Development, and Demonstration (MYRDD) Plan:

(A) Lack of Fuel Cell Electric Vehicle and Fuel Cell Bus Performance and Durability Data

(D) Lack of Hydrogen Refueling Infrastructure Performance and Availability Data

Contribution to Achievement of DOE Technology Validation Milestones

This project contributes to the achievement of the following DOE milestones from the Technology Validation section of the FCTO MYRDD Plan:

- Milestone 4.2: Updated composite data products for material handling and backup power published. (3Q, 2012)
- Milestone 4.3: Report safety event data and information from ARRA projects. (3Q, 2013)

FY 2015 Accomplishments

- The ninth set of technical composite data products (CDPs) was published on performance and operation for fuel cell MHE with 24 updated results.
- Access to the largest single set of technology validation data in the program's history was negotiated, including hundreds of new-generation vehicles in two different MHE classes, from private commercial sites receiving no direct government funding. This data set represents a 30% increase in total vehicle hours from the ARRA project.
- Some of the key results included:
  - Over 2.6 million hours of MHE operation in commercial distribution facilities, collected from 720 vehicles, including 230 new vehicles, were documented.
  - Dispensing of almost 288,000 kilograms of hydrogen was validated.
  - A B50 time to 10% voltage decay of 10,000 hours was demonstrated.
  - Mean fueling time of 2.5 minutes (which is key to the fuel cell MHE value proposition) was validated.
  - Mean vehicle operating times between fueling of 3.7 hours were validated.

✧ ✧ ✧ ✧ ✧

INTRODUCTION

The U.S. Department of Energy designated more than $40 million in ARRA funds for the deployment of up to

1,000 fuel cell systems. This investment is enabling fuel cell market transformation through development of fuel cell technology, manufacturing, and operation in strategic markets where fuel cells can compete with conventional technologies. The strategic markets include MHE, backup power, stationary power, and portable power, and the majority of the deployed systems are in the MHE and backup power markets. NREL continues to analyze operational data from the MHE sector, because it is the market segment with the most rapid growth and technological evolution. MHE data are provided voluntarily by industry. The data collection has ended for backup power and stationary systems.

The project includes both end users and system developers: Air Products, FedEx, GENCO, Nuvera Fuel Cells, Plug Power, and Sysco Houston. The evaluation focused on fuel cell stack durability, reliability, refueling, safety, and value proposition. The deployment partners provided approximately $53 million in industry cost share [1]. In addition to the ARRA cofunded fuel cell backup power demonstrations, DOE supported additional demonstration projects with other federal agencies through interagency agreements. The Department of Defense and the Federal Aviation Administration are two agencies with fuel cell backup power demonstrations that also submitted operational and deployment data to NREL. All results covered in this report, will include ARRA, and private commercial sites that received no direct government funding. The degradation result, Figure 1, also includes interagency agreement data.

APPROACH

The project's data collection plan builds on other technology validation activities. Project partners collect operation, maintenance, and safety data for fuel cell system(s) and accompanying infrastructure. Then they send data to NREL in a manner consistent with security procedures. NREL receives the data quarterly, then stores, processes, and analyzes data in NREL's National Fuel Cell Technology Evaluation Center (NFCTEC). The NFCTEC is a controlled access, off network analysis facility. An internal analysis of all available data is completed quarterly, and a set of technical CDPs is generally published every six months. Publications are uploaded to NREL's technology validation website [2] and presented at industry relevant meetings. The CDPs present aggregated data across multiple systems, sites, and teams in order to protect proprietary data and summarize the performance of hundreds of fuel cell systems and thousands of data records. A review cycle is completed before the CDPs are published. This review cycle includes providing detailed data products (DDPs) of individual system- and site-performance results to the specific data provider. DDPs also identify the individual contribution to the CDPs.

RESULTS

The initial ARRA funding for MHE kicked off rapid growth of the fuel cell MHE industry. This growth is reflected directly in the large amount of additional data NREL was able to secure from private commercial sites receiving no direct government funding.

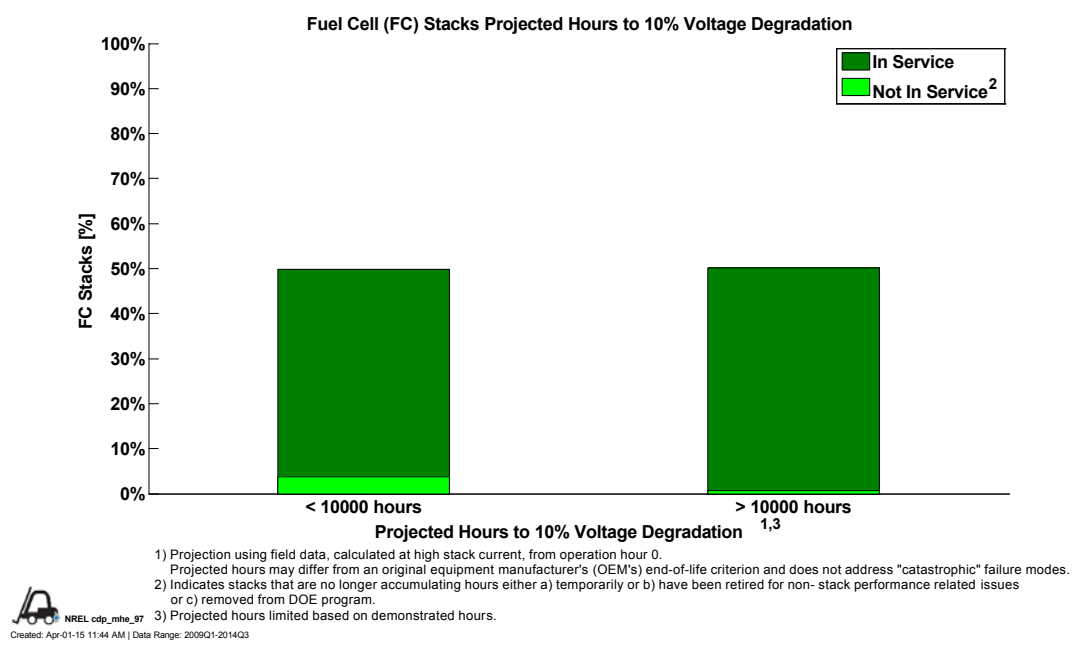

FIGURE 1. Fuel cell stacks projected hours to 10% voltage decay degradation (cdp_mhe_97)

The new data set represents an increase in vehicle operation hours of approximately 30% over the previous ARRA sites, and adds 230 new vehicles to the data set [3]. Yet, these data represent only a piece of the MHE fleet deployed in United States logistics warehouses. Total MHE operating hours tracked in this program now stands at nearly 2.7 million across all fleets and classes. MHE are broken down into classes based on the capabilities of the vehicle. These data represent Classes I (sit-down counterbalance), II (stand-up, high reach, narrow aisle), and III (powered pallet jacks and tow tractors) trucks.

The new fleet data represent newer systems, which are newer generation technologies. This can be seen in Figure 2, represented in a move of the mean operating hours on each vehicle from 4,700 to 4,100. The maximum actual stack hours remains at 16,610, as was reported in previous CDPs under the ARRA program [5].

The projected B50 time to 10% voltage decay for the stacks is 10,000 hours across all vehicle classes. See Figure 1. In other words, half of the vehicles are projected to reach 10% voltage decay of their stacks in 10,000 hours. The 10% decay metric does not represent end of life, but rather a metric for measuring decay in fuel cell stack performance. The fraction of vehicles projected to reach 10% decay before 10,000 hours was increased somewhat by the new data set, partially because some of the machines in operation have design lifetimes less than 10,000 hours.

As reported earlier in this project [4], refueling time is critical to the value proposition for fuel cell MHE. The mean refuel time is just over 2.5 min, with the majority of refuel events completing in less than 5 min. See Figure 3. The mean fuel amount delivered is 0.7 kg, and the mean operating time between fueling is 3.7 h. This does not necessarily represent the vehicle autonomy, as there are other human factors that dictate when fueling is convenient (e.g., breaks, shift changes, or proximity to a fuel dispenser).

One-third of fueling events take place within 5 min of one another, and 73% within 20 min. See Figure 4. This usage pattern has important implications for station design with respect to back-to-back fills, something that light duty vehicle stations also currently struggle with. The fueling largely takes place at 350 bar, which represents a shift from 250 bar used earlier in some applications.

CONCLUSIONS AND FUTURE DIRECTIONS

- NREL has secured an additional new data set, beyond that presented here, that represents a large fraction of the commercial fuel cell MHE installations in the United States. The data includes approximately 2,000 vehicles, or four times the size of the original ARRA project. The source and types of data are different, which may lead to different results and findings.
- NREL wishes to continue to track the progress of this important market segment and report CDPs publicly, while providing important value-added analysis back to industry.

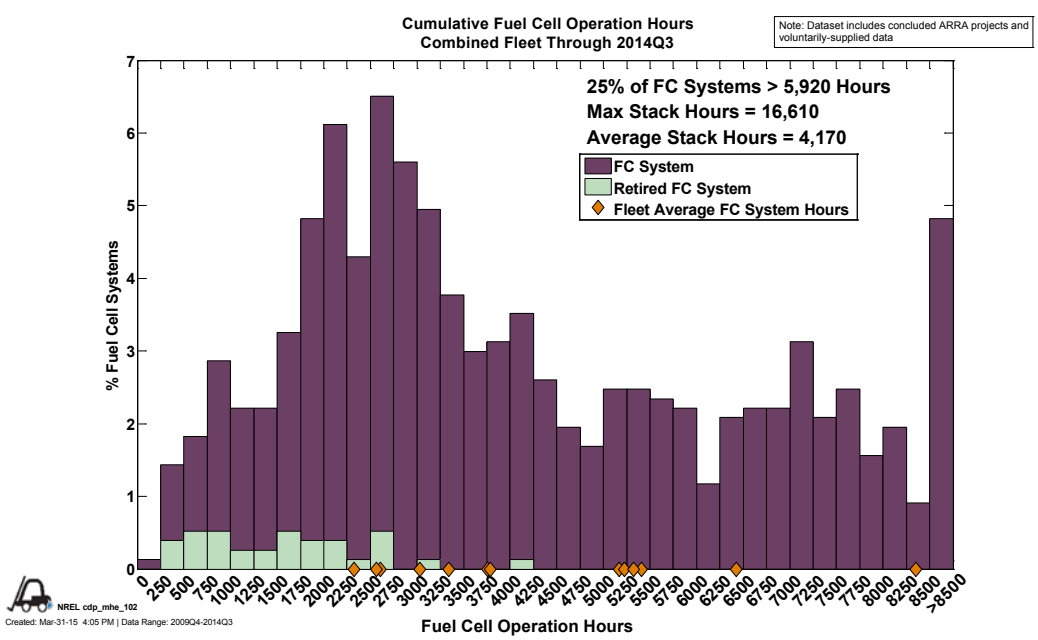

FIGURE 2. Cumulative fuel cell operation hours combined fleet through 2014Q3 (cdp_mhe_102)

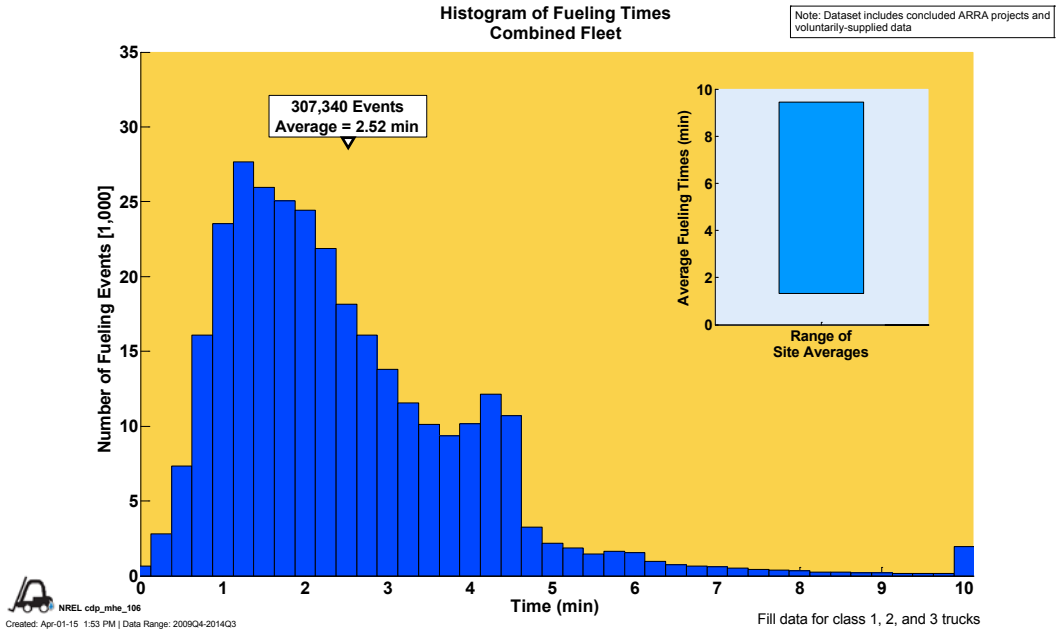

FIGURE 3. Histogram of fueling times, combined fleet (cdp_mhe_106)

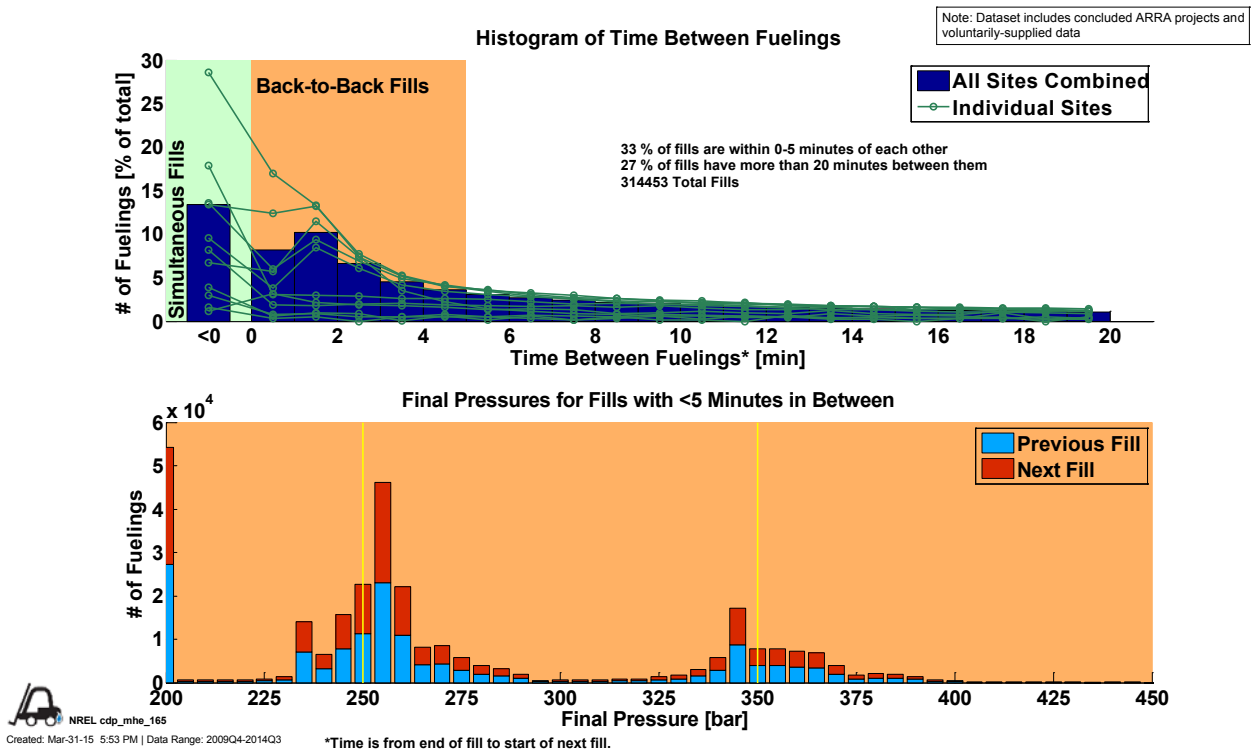

FIGURE 4. Histogram of time between fuelings, relative to the dispensers (cdp_mhe_165)

FY 2015 PUBLICATIONS/PRESENTATIONS

1. Ainscough, C., Kurtz, J., *ARRA Material Handling Equipment Composite Data Products: Data through Quarter 3 of 2014*, Golden, CO: The National Renewable Energy Laboratory, 2015.

2. Ainscough, C., *Material Handling Equipment Data Collection and Analysis,* Washington, DC: U.S. Department of Energy, 2015.

REFERENCES

1. *Highlights from U.S. Department of Energy's Fuel Cell Recovery Act Projects*. Washington, DC: U.S. Department of Energy, February 2014. http://energy.gov/eere/fuelcells/downloads/highlights-us-department-energys-fuel-cell-recovery-act-projects.

2. *Fuel Cell and Hydrogen Technology Validation*. Golden, CO: National Renewable Energy Laboratory. http://www.nrel.gov/hydrogen/proj_tech_validation.html.

3. Kurtz, J., *Forklift and Backup Power Data Collection and Analysis*. Washington, DC: U.S. Department of Energy, 2014, http://www.hydrogen.energy.gov/pdfs/progress14/vii_a_6_kurtz_2014.pdf.

4. Ramsden, T., *An Evaluation of the Total Cost of Ownership of Fuel Cell-Powered Material Handling Equipment*. Golden, CO: National Renewable Energy Laboratory, April 2013.

5. Kurtz, J., et al., *ARRA Material Handling Equipment Composite Data Products: Data through Quarter 4 of 2013*. Golden, CO: National Renewable Energy Laboratory, June 2014. http://www.nrel.gov/docs/fy14osti/62130.pdf.

VII.7 Development of the Hydrogen Station Equipment Performance (HyStEP) Device

Terry Johnson (Primary Contact), Danny Terlip (NREL), Chris Ainscough (NREL)
Sandia National Laboratories (SNL)
7011 East Avenue
Livermore, CA 94551-0969
Phone: (925) 294-2512
Email: tajohns@sandia.gov

DOE Manager
Jason Marcinkoski
Phone: (202) 586-7466
Email: Jason.Marcinkoski@ee.doe.gov

Subcontractor
Powertech Labs Inc., Surrey, B.C., Canada

Project Start Date: September 2014
Project End Date: December 2015

Overall Objectives

- Accelerate commercial hydrogen station acceptance by developing and validating a prototype device to measure hydrogen dispenser performance
- Develop a device capable of testing to the Canadian Standards Association (CSA) HGV 4.3 test method to test dispensers for compliance with the table-based fueling protocol defined by SAE J2601-2014
- Make the device available for use by the state of California to commission existing and new hydrogen stations in the 2016–2017 timeframe

Fiscal Year (FY) 2015 Objectives

- Place a contract with a third party supplier through a competitive bid process for the fabrication of the HyStEP device per a detailed specification developed by the project team
- Co-develop the detailed system design with the supplier including the following
  - Final piping and instrumentation diagram (P&ID)
  - Mechanical layout
  - Electrical diagram
  - Detailed list of mechanical and electrical components
- Finalize the design through a series of reviews, including the following
  - Failure modes effects and criticality analysis (FMECA)
  - Detailed design review
  - Presentation to and review by the Hydrogen Safety Panel
  - Final review and concurrence with Fuel Cell Technologies Office (FCTO) program managers
- Development of safety systems including hardware and software safeguards
- Fabrication, assembly and integration of the HyStEP device (to be performed by the supplier)
- Validation of the HyStEP device performance at National Renewable Energy Laboratory's (NREL's) Energy Systems Integration Facility (ESIF) facility

Technical Barriers

This project addresses the following technical barriers from the Technology Validation section of the FCTO Multi-Year Research, Development, and Demonstration (MYRDD) Plan:

(D) Lack of Hydrogen Refueling Infrastructure Performance and Availability Data

(E) Codes and Standards

Contribution to Achievement of DOE Technology Validation Milestones

This project will contribute to achievement of the following DOE milestones from the Technology Validation section of the FCTO MYRDD Plan:

- Milestone 4.4: Complete evaluation of 700-bar fast fill fueling stations and compare to SAE J2601 specifications and DOE fueling targets. (3Q, 2016)

FY 2015 Accomplishments

- Led a team of stakeholders including NREL, Air Liquide, Boyd Hydrogen, California Air Resources Board (CARB), and Toyota, hereafter called the project team, to co-design the HyStEP device
- Developed a comprehensive specification for the device

- Through a competitive bid process, selected and placed a contract with Powertech Labs to fabricate the HyStEP device
- With Powertech, completed the detailed device design including the H_2 tank selection, P&ID, trailer selection and mechanical layout, electrical equipment selection and layout, and data acquisition, control and safety systems
- Completed a detailed FMECA that identified and analyzed 202 failure modes and effects
- Met the criteria for the first go/no-go milestone by March 31, 2015, to move forward with device fabrication; which included a briefing to and approval from the Hydrogen Safety Panel
- Completed component procurement and fabrication (Powertech)
- Completed mechanical and electrical assembly and integration (Powertech)
- Developed the LabVIEW user interface design, control screen layout, and data reporting templates with Powertech
- Completed the Rev. 1 control and data acquisition software (Powertech and contractor)
- Completed an onsite acceptance test of the device at Powertech
- Coordinated the deployment of the HyStEP device in California with CARB including drafting a contract between Sandia and CARB for the loan of the device

✧ ✧ ✧ ✧ ✧

INTRODUCTION

It is generally agreed that policies and technology solutions need to be developed and implemented to help reduce the time to commission a hydrogen station. The current practice of hydrogen station acceptance, which burdens vehicle original equipment manufacturers (OEMs) with serial testing of stations because each OEM conducts their own testing and evaluation, can take months. This process is not practical or sufficient to support the timely development of a hydrogen fueling station network. This is especially true in the state of California where new stations are coming online currently and as many as 35 new stations are scheduled to be commissioned soon. Ultimately, a hydrogen station test device that can be used to verify station fueling protocol, average daily and peak fueling capacity, and fuel quality would be desirable to commission new stations. In the near-term, a test device designed specifically to test station fueling protocol that is technically effective, safe, robust, and user friendly will accelerate the commissioning of hydrogen stations. This device must be safe and effective to be useful, but also simple enough to design, fabricate, assemble and implement quickly to meet the timetable of current station deployment in California. This project was carried out to develop such a device.

To meet this goal, the project team, along with contractor Powertech Labs, has developed the HyStEP device. The device includes three Type IV 70 MPa tanks capable of storing a total of 9 kg hydrogen that are instrumented with pressure and temperature sensors. The tanks are connected to a 70 MPa receptacle equipped with pressure and temperature sensors as well as Infrared Data Association (IrDA) communications integrated with a data acquisition, analysis, and control system. A valve near the receptacle attached to a vent manifold can be used to both simulate a leak for fault detection tests and for controlled defueling. A nitrogen purge system is also included. Additional temperature sensors will record ambient temperature near the receptacle and various external system temperatures. The HyStEP device is capable of performing key tests defined in CSA HGV 4.3. These include IrDA communication tests, fault detection tests, and communication and non-communication fills.

APPROACH

The project team will select the device supplier through a competitive bid process and collaborate with the supplier on the design and acceptance testing of the HyStEP device. In order to prepare the device for real-world deployment, the device will undergo extensive validation testing at NREL's ESIF facility. This testing will include using the device to carry out many, if not all of the tests defined in CSA HGV 4.3 to ensure safe and reliable operation. The method for data reporting will also be refined during testing and proved out for a real-time report of the results that would be available at a commercial station. Following validation testing at NREL, the device will be shipped to California for pre-deployment testing at two commercial hydrogen stations. The device will then be put into service by the state through a contract between Sandia National Laboratories and CARB.

The device supplier will provide the project team with a comprehensive set of documentation covering device design, operation, maintenance and safety. The required documents will be published by Sandia to a publicly accessible website.

RESULTS

Upon placing the contract, the project team worked closely with Powertech to determine the mobile platform for the device and develop the detailed final P&ID shown in Figure 1. A trailer-based design was chosen and the P&ID was used to develop the list of components for the HyStEP device including valves, tubing and fittings, filter, thermally-activated pressure relief device, hydrogen sensor,

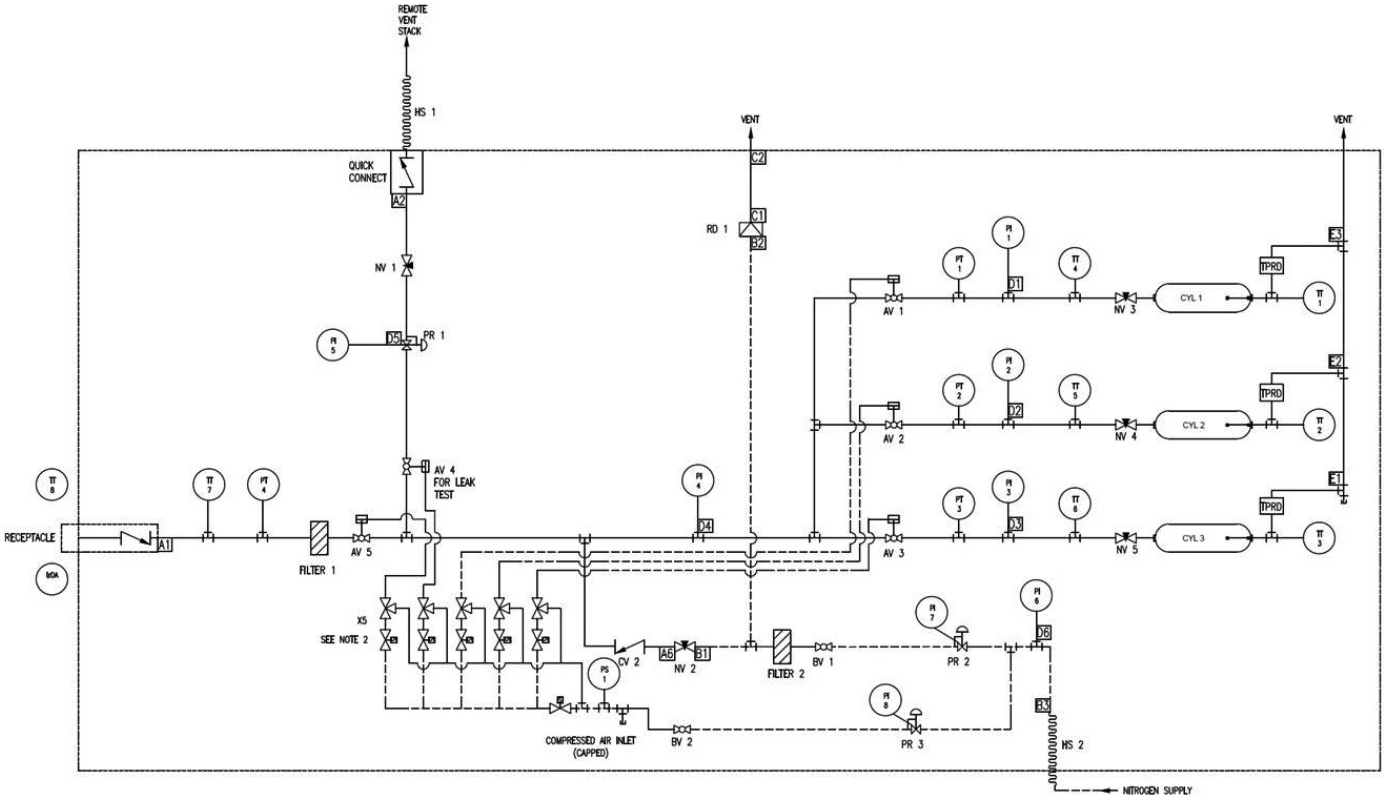

FIGURE 1. HyStEP device piping and instrumentation diagram

tank mounting hardware, IrDA system, receptacle, and instrumentation including pressure transducers, temperature sensors and feedthroughs. The outcome was a comprehensive list of all of the system components, specifications, suppliers and part numbers.

The overall HyStEP device design, including the P&ID, electrical diagrams and component lists, was then reviewed in several ways. Firstly, Powertech and the project team completed a detailed FMECA on the HyStEP design facilitated by Intertek Consulting. The results of the FMECA are summarized as follows:

- 7 functional blocks were analyzed
- 44 functions were defined
- 202 failure modes and effects were identified
- Each effect was assigned severity, occurrence, and detection/prevention ratings
- 47 failure mode effects had severity of 9 or 10 indicating a safety hazard
- 20 failure mode effects had a risk priority number (RPN = severity*occurrence*detection) greater than 100

Following the completion of the FMECA, Powertech and the project team addressed all failure mode effects with RPN values >100 and severity of 9 or 10. Actions were taken to mitigate these risks through design changes, safeguards, and/or operating procedures.

Secondly, a final design review for the HyStEP device was carried out that included a majority of the project team and three engineers from Powertech. Every component on the P&ID was reviewed along with the electrical layout and design as well as the trailer and frame layout and design. Several design changes were made and implemented by Powertech based on this review.

Thirdly, the project team briefed the Hydrogen Safety Panel on the HyStEP device and the results of the FMECA. The team provided the latest design documents at that time. Selected panel members then carried out a more detailed review of these documents. The panel's compiled comments were provided to the project team and Powertech. The project team determined that the panel's comments and recommendations were satisfied by the HyStEP design and prepared a response to the panel, which was accepted.

Based on the FMECA, the project Design Review and the independent review by the Hydrogen Safety Panel, the DOE program management team agreed to move forward with fabrication of the HyStEP device.

With DOE approval, Powertech began the process of procurement and fabrication of the mechanical and electrical hardware for the device. In parallel, Powertech hired a

National Instruments certified LabVIEW programmer to develop the control and data acquisition software and user interface. The project team worked with Powertech to define the requirements for this software including a comprehensive alarm matrix and list of software safeguards based on the FMECA results.

As the major components arrived, Powertech began the mechanical assembly and integration of the system. This included fabricating a custom frame to mount the tanks and hydrogen manifold. A structural finite element analysis was performed on the frame to ensure mechanical stability under shock and vibration. The three hydrogen storage tanks were then mounted to the frame and the tubing manifold was bent and assembled with fittings, valves, and instruments. Instruments and wiring followed. In parallel, a benchtop test apparatus was used to test out the LabVIEW software including the interface to the IRDI Systems infrared communications hardware. Figure 2 shows the nearly complete layout of the interior of the HyStEP trailer with all major systems identified.

At this stage, initial tests in the Powertech lab were carried out including control and data acquisition communications, IrDA operation, leak checks and proof test of the pressure components, and automated procedures. The system was verified to be mechanically sound and leak free and all control and data acquisition functionality was verified using the operator panel shown in Figure 3. These tests were performed at reduced pressure and with nitrogen.

Following the integration and initial checkout and testing by Powertech, Terry Johnson (SNL) and Danny Terlip (NREL) visited Powertech's facility on July 22–23, 2015, to verify the initial checkout. Over the two days, they reviewed the design with the Powertech team and carried out communications and venting tests using the Powertech's commercial hydrogen dispenser (see Figure 4). Fueling tests were not carried out at this time because the system had not been fully pressure tested with hydrogen. A few modifications to the LabVIEW software were identified through this testing that will be completed prior to the device shipping to NREL for validation testing. In addition, a full system leak check at 87.5 MPa hydrogen pressure will be completed before the device ships.

FIGURE 3. HyStEP device operator panel including receptacle, system pressure indicators, touchscreen panel, electro-static discharge, and vent controls

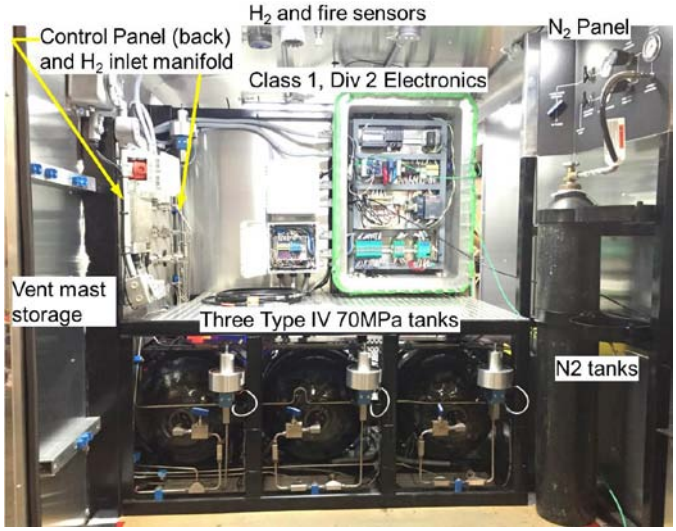

FIGURE 2. Layout of the interior of the HyStEP device trailer showing the major subsystems

FIGURE 4. HyStEP device sited at Powertech's H_2 dispenser with the remote vent stack

CONCLUSIONS AND FUTURE DIRECTIONS

- Final fabrication and assembly—Powertech—through August 7, 2015
- Ship the device to NREL—Powertech—arrival week of August 10, 2015
- Post-shipment leak and functionality checks and communication tests—NREL—week of August 17, 2015
- Onsite training carried out by Powertech; trainees will include NREL staff as well as operators from CARB and California Department of Food and Agriculture Division of Measurement Standards (DMS)—week of August 24, 2015
- Final checkout and verification—NREL/Powertech/SNL—August/September 2015
  - Go/No-Go 15.1: Results of the NREL testing will be reviewed by the project team, DOE HQ, and communicated to H2USA members and additional DOE-approved stakeholders
- Publication of documentation—Powertech/SNL—August 2015
- Pre-deployment test #1—SNL/project team—October 2015
  - Milestone 17.1: Testing has been completed at the first California station
- Pre-deployment test #2—SNL/project team—November 2015
- Performance analysis and report—NREL—November 2015
- Initiate loan to State of California agency (CARB/DMS)—SNL—November 2015

FY 2015 PUBLICATIONS/PRESENTATIONS

1. Johnson, T. "Station Acceptance Project Team," California Fuel Cell Partnership meeting, October 2014. (presentation)

2. Ainscough, C; Pratt, J.; Kurtz, J.; Somerday, B.; Terlip, D.; and Johnson, T. "Hydrogen Fueling Infrastructure Research and Station Technology," DOE Webinar, November 2014. (presentation)

3. Johnson, T. "HyStEP Device Update," Combined Codes and Standards and Hydrogen Delivery Tech Team meeting, January 2015. (presentation)

4. Johnson, T. "HyStEP Device Design and Safety Analysis," 21st Hydrogen Safety Panel meeting, March 2015. (presentation)

5. Johnson, T. "HyStEP Device Update," H2FIRST Coordination Panel Meeting, March 2015. (presentation)

6. Johnson, T. "Development of the Hydrogen Station Equipment Performance (HyStEP) Device," 2015 DOE Hydrogen and Fuel Cells Program and Vehicle Technologies Office Annual Merit Review and Peer Evaluation Meeting, June 2015.

VII.8 Station Operational Status System (SOSS) 3.0 Upgrade

Ben Xiong (Primary Contact), Nico Bouwkamp
California Fuel Cell Partnership (CaFCP)
3300 Industrial Blvd., Suite 1000
West Sacramento, CA 95691
Phone: (916) 371-2870
Email: bxiong@cafcp.org

DOE Manager
Jason Marcinkoski
Phone: (202) 586-7466
Email: Jason.Marcinkoski@ee.doe.gov

Project Start Date: June 1, 2014
Project End Date: May 31, 2015

Overall Objectives

- Increase fuel cell electric vehicle (FCEV) customer satisfaction and thereby station demand by consistently providing relevant station status information so that end users can better assess hydrogen station availability

Fiscal Year (FY) 2015 Objectives

- Improve user interface and data quality
- Increase data transmission interval from stations (once every 15 min at minimum) and data sharing capabilities

Technical Barriers

This project addresses the following technical barrier from the Technology Validation section of the Fuel Cell Technologies Office (FCTO) Multi-Year Research, Development, and Demonstration (MYRDD) Plan:

(D) Lack of Hydrogen Refueling Infrastructure Performance and Availability Data

Contribution to Achievement of DOE Technology Validation Milestones

This project will contribute to achievement of the following DOE milestone from the Technology Validation section of the FCTO MYRDD Plan:

- Milestone 2.3: Validate fuel cell electric vehicles achieving 5,000-hour durability (service life of vehicle) and a driving range of 300 miles between fuelings. (4Q, 2019)

FY 2015 Accomplishments

- Achieved CaFCP member agreement on customer focused criteria
- Implemented code changes on CaFCP's SOSS server
- Improved SOSS interface to better display status information
- Completed integrating SOSS 3.0 at five of eight of the current hydrogen stations
- One new station is publicly open and has SOSS 3.0 implemented at the site

✧ ✧ ✧ ✧ ✧

INTRODUCTION

Argonne National Laboratory/DOE are continuing partners in the California Fuel Cell Partnership. Funds are used to accomplish the goals of the partnership and to provide critical information and data necessary for the DOE to determine the status and prospects for commercialization of fuel cell technology. The partnership supports the Station Operational Status System (SOSS), a mobile web application (Figure 1) [1] that provides status information about each of the available hydrogen stations in California and the National Renewable Energy Laboratory's (NREL's) station in Golden, Colorado.

APPROACH

FCEV customer satisfaction, and thereby station demand, will be increased by consistently providing relevant station status information so that end users can better assess hydrogen station availability. This is accomplished through the SOSS by each station sending a message to CaFCP's server every few minutes, to report on the station operational status (online or offline), available fuel, and available pressures, as well as the station address, contact number, and the Global Positioning System coordinates.

The SOSS 3.0 upgrade creates consistency in timing of data collected and content displayed from hydrogen stations. It also improves the user interface (Figure 1), increases the frequency of operational status updates, and increases data sharing capabilities. Newly built hydrogen stations are solicited to participate in SOSS.

RESULTS

Code changes for SOSS 3.0 have been completed, implemented and tested in the development environment.

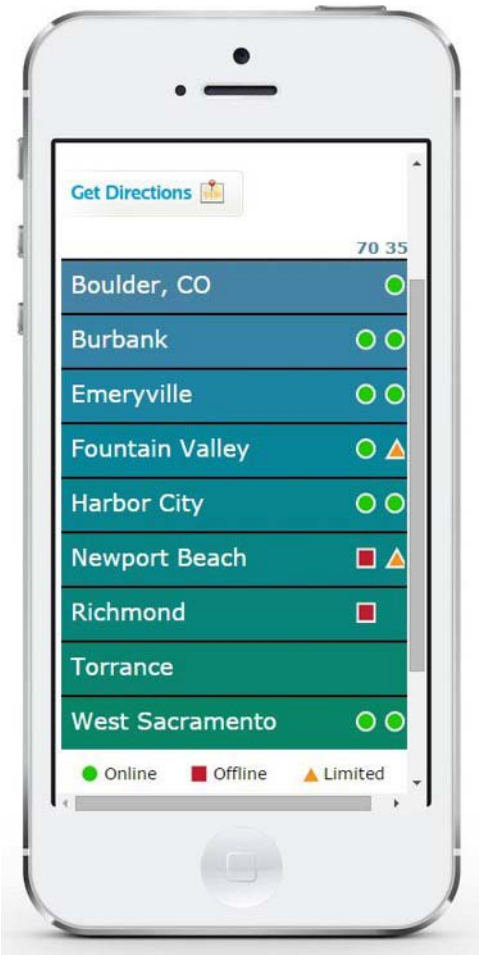

FIGURE 1. SOSS 3.0 interface

Software testing has been performed and the code changes have been implemented on the production environment. The SOSS 3.0 version is being implemented at current stations. Development work is in progress to allow for multiple outgoing feeds to be transmitted from the CaFCP server.

Status of implementation at current stations:

- Burbank (H2 Frontier) development and testing was completed.
- West Los Angeles (Shell/Hydrogenics) was decommissioned.
- Emeryville (Linde) had no upgrade/workaround.
- Fountain Valley (Air Products and Chemicals, Inc. [APCI]) development was completed.
- Boulder, Colorado (NREL) was put on hold.
- Newport Beach (Shell/Powertech) development was completed.
- Torrance (Shell/APCI) development was completed.
- Harbor City (APCI) development was completed.
- H2 Frontier has completed implementation of upgrading their system to be SOSS 3.0 compliant at the Burbank station. Testing has also been completed.
- Linde does not plan to upgrade the Emeryville station to SOSS 3.0. The Linde station does not have separate signals for H35 and H70. When one pressure becomes unavailable, fueling is unavailable for both pressures. This station currently reports in 15-minute intervals.
- APCI has completed initial implementation of upgrading the Fountain Valley station to be SOSS 3.0 compliant. Testing is still in progress to ensure that the station is reporting accurately.
- NREL is considering moving resources from the Boulder, Colorado, station to Golden, Colorado. This would mean no upgrade at the Boulder station, but the Golden station would be developed with SOSS 3.0 capabilities.
- Shell/Powertech has completed implementation of upgrading the Newport Beach station to be SOSS 3.0 compliant. Testing is still in progress to ensure that the station is reporting accurately.
- APCI has completed initial implementation of upgrading the Torrance station to be SOSS 3.0 compliant. Testing is still in progress to ensure that the station is reporting accurately.
- APCI has completed initial implementation of upgrading the Harbor City station to be SOSS 3.0 compliant. Testing is still in progress to ensure that the station is reporting accurately.

Status of implementation at new stations:

- West Sacramento (Linde) development and testing was completed.
- California State University, Los Angeles (Cal State LA) is in progress.
- Diamond Bar (South Coast Air Quality Management District/APCI) has no funding for an upgrade.
- Chino (H2 Frontier/ITM Power) planning is complete.
- Anaheim (Air Liquide) planning is complete.
- Palo Alto (Air Liquide) planning is complete.
- Los Angeles International Airport (LAX) (Air Liquide) planning is complete.
- Linde and Quantum have completed integrating SOSS 3.0 at the West Sacramento station. Testing has been completed and the site is live.
- Cal State LA has completed implementation of SOSS 3.0 at the Cal State LA station. Testing has been postponed. Cal State LA is focused on getting the station to an "open" status.

- APCI and Engineering, Procurement and Construction, LLC, have upgraded the capabilities to program, integrate, and confirm successful communication between station and SOSS that were previously deployed at earlier APCI stations. The station implementers' proposal to procure funding to move forward with implementation has been completed.
- CaFCP continues to be in communication with ITM Power, H2 Frontier, Air Liquide, and First Element to implement SOSS at the Chino, Anaheim, Palo Alto, and LAX stations and other stations not implemented yet.

CONCLUSIONS AND FUTURE DIRECTIONS

Delayed station implementation/rollout has been a barrier for new stations participating on SOSS. Despite the delays, station operators, developers, automakers, and other stakeholders agree that SOSS is critical for customer satisfaction in an early market launch of fuel cell vehicles. Initial proposal of future improvements to SOSS include the following.

- Solicit new hydrogen stations to participate on SOSS
- Implement user interaction and feedback system
- Research mobile native app capabilities and implement if applicable
- Implement backup system
- Implement real-time reporting
- Implement a mobile map interface

REFERENCES

1. (Current) SOSS web interface for FCEV users: http://www.m.cafcp.org/

VII.9 Validation of an Advanced High Pressure PEM Electrolyzer and Composite Hydrogen Storage, with Data Reporting, for SunHydro Stations

Larry Moulthrop (Primary Contact), Luke Dalton
Proton Energy Systems d/b/a Proton OnSite
10 Technology Drive
Wallingford, CT 06492
Phone: (203) 678-2188
Email: lmoulthrop@protononsite.com

DOE Manager
Jason Marcinkoski
Phone: (202) 586-7466
Email: Jason.Marcinkoski@ee.doe.gov

Contract Number: DE-EE0005887

Subcontractors
- SunHydro LLC, Wallingford, CT
- Air Products and Chemicals, Incorporated (APCI), Allentown, PA

Project Start Date: December 1, 2012
Project End Date: June 30, 2015 (go/no go decision for next phase)

Overall Objectives

- Validate energy savings of up to 11 kWh/kg H_2 through system and stack advancements
- Double usable hydrogen storage per unit volume by increasing pressure cycling range
- Provide advanced packaging design to reduce station footprint
- Collect and report station performance for up to 24 months

Fiscal Year (FY) 2015 Objectives

- Quantify full scale advanced cell stack energy savings and performance
- Quantify system portion of energy savings for 55 bar operation of hydrogen dryer and compressor
- Demonstrate higher addressable capacity hydrogen storage tubes
- Validate advanced packaging arrangement
- Conduct reporting of station performance

Technical Barriers

This project addresses the following technical barriers from the Technology Validation section of the Fuel Cell Technologies Office Multi-Year Research, Development, and Demonstration (MYRDD) Plan:

(C) Hydrogen Storage

(D) Lack of Hydrogen Refueling Infrastructure Performance and Availability Data

(E) Codes and Standards

Technical Targets

Advanced Electrolysis-Based Fueling Systems:

There is not a target table in the Technology Validation section of the (MYRDD) Plan specific to hydrogen refueling infrastructure. This project is conducting technology validation of improved cell stack, system, and storage components for an electrolysis-based hydrogen refueling station. These improvements will support the following targets.

- Reduce station energy use by up to 11 kWh/kg
- Reduce the storage volume by 50% per kilogram of hydrogen dispensed
- Package a station based on polymer electrolyte membrane (PEM) electrolysis within a 12 m International Organization for Standardization (ISO) container

FY 2015 Accomplishments

- Operated full scale cell stack utilizing advanced manufacturing process
- Demonstrated SunHydro 1 operation at 55 bar hydrogen generation, drying, and compression
- Quantified performance enhancement of 55 bar operation
- Validated five back to back fills with composite hydrogen storage tubes
- Received SunHydro 2 components
- Validated Sun Hydro 2 compact station code approach with Massachusetts install permit
- Acquired hydrogen station data acquisition system at SunHydro 1

- Reported SunHydro 1 hydrogen energy usage data to the fuel cell electric vehicle (FCEV) infrastructure composite data product (CDP) database

✧ ✧ ✧ ✧ ✧

INTRODUCTION

This project primarily leverages Proton's SunHydro 1 station in Wallingford, Connecticut, with access to over 100 kg/d in generation capacity, and a new containerized SunHydro 2 station for field deployment, for technology validation of improved components for hydrogen fueling stations (Figure 1). Our compact, containerized SunHydro™ station design (Figure 2) embodied by SunHydro 2 can address initial demand for small, manufactured hydrogen fueling infrastructure in a manner that affords rapid, scalable deployment. The SunHydro station product "skid," integrating hydrogen generation, compression, storage, and dispensing in an intermodal transport ISO container, mitigates significant site permitting issues by virtue of its small 40 ft x 8 ft footprint and an innovative application of hydrogen code that drastically reduces required clearances.

Proton and SunHydro are continuing down this pathway to demonstrate advanced generation/compression/storage component technologies, including (1) higher pressure hydrogen generation with electrochemical compression; (2) higher efficiency generation with lower resistance electrolyte and advanced catalyst; (3) higher addressable capacity composite storage, and (4) advanced packaging concepts for reduced footprint.

APPROACH

For higher pressure/higher efficiency PEM cell stacks, Proton has qualified a 30% reduction in PEM membrane thickness for 15 bar and 30 bar hydrogen generator product lines. Furthermore, Proton has been developing advanced

FIGURE 1. SunHydro 1 and SunHydro 2 stations

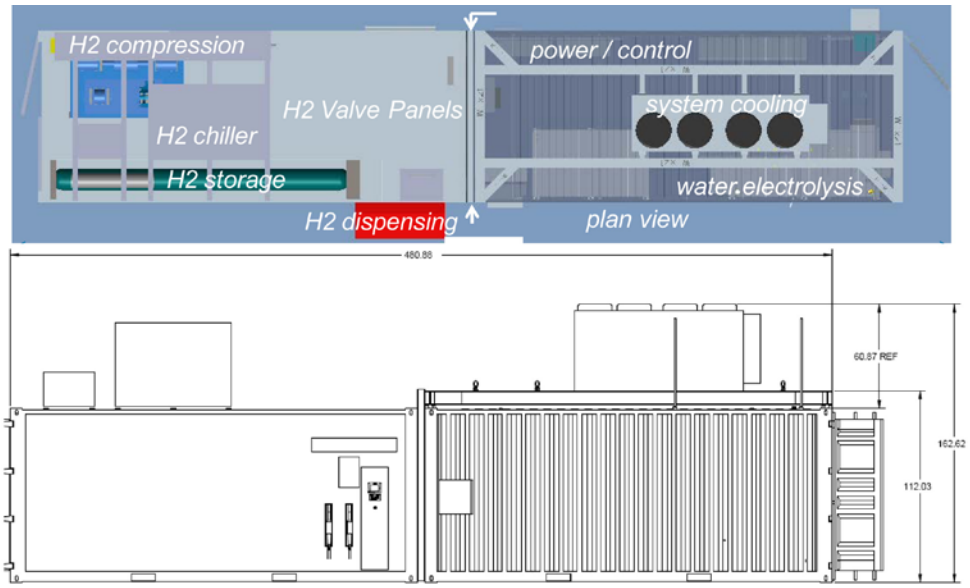

FIGURE 2. Arrangement, H_2 generator container, SunHydro concept, combined containers

catalyst materials and processes that simultaneously reduce the cost of the product and improve the electrochemical performance. A 55 bar militarized cell stack design will be built using the thinner material and advanced catalyst deposition to show the performance improvement at full scale compared to previous technology stacks. We will upgrade a commercial 30 bar C series electrolyzer to operate at 55 bar by strengthening the gas drying components. An increase in hydrogen generation pressure from 30 bar to 55 bar can improve hydrogen fueling system efficiency in two areas – hydrogen gas drying and dried hydrogen compression into station storage. The dryer purge losses can be expected to decrease substantially since the water vapor concentration at 55 bar will be about 55% of the concentration at 30 bar. Higher dry hydrogen pressure into the station mechanical compressor will result in better combined compression energy and higher throughput capability.

For higher addressable capacity storage and reduced station footprint, Proton will install and validate new compact Type II composite storage tubes and apply fresh interpretations of hydrogen safety code to design a complete fueling station within the compact footprint of an ISO container. Proton will apply these new rules to the design of the SunHydro 2 station. The impact of all performance improvements will be reported through instrumentation of the station before and after the design changes. The impact of new compact station arrangements will be reported in site approval time and in station operability data.

RESULTS

Task 1.0 Validate Full Scale 57 bar Higher Efficiency PEM Cell Stack

The project goal was to implement advanced membranes and electrodes in a full scale 57-bar PEM electrolyzer stack to show energy savings approaching 8 kWh/kg H_2 over the 30 bar commercial version. The required improved voltage performance had been previously demonstrated with smaller active area short-stack test articles. Therefore, the challenge was to take the process developed and apply it at a larger scale to the largest stack size currently in production at Proton in the 2013–2014 performance period, the 0.23 ft^2 active area C series cell stack. The expected energy savings based on subscale testing is described by the polarization curves shown in Figure 3. A reduction in voltage from 2.15 VDC/cell to 1.85 VDC/cell at the same current density would yield the estimated 8 kWh/kg H_2 that was targeted.

Achieving the target performance required implementing both thinner membrane as well as advanced catalyst application techniques. As the advanced catalyst application techniques were scaled to support a full production run for the advanced C series cell stack used in Proton's fueling station, some challenges were observed. The larger batch sizes were not as stable during the fabrication process and were more susceptible to variations in ambient environmental conditions. During operation of the stack using the advanced membrane electrode assemblies (MEAs), the performance was approximately equal to the baseline stack. After reviewing the manufacturing process and operating conditions, it was determined that the actual catalyst loading

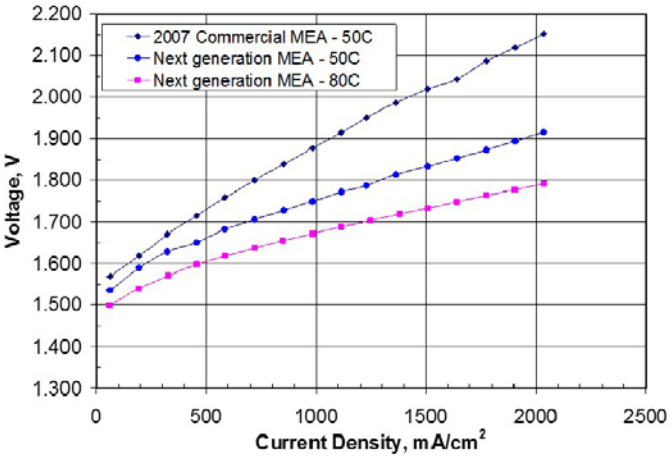

FIGURE 3. Circa 2007 commercial PEM MEA technology is contrasted with next generation MEAs qualified in smaller-scale product lines (performance shown)

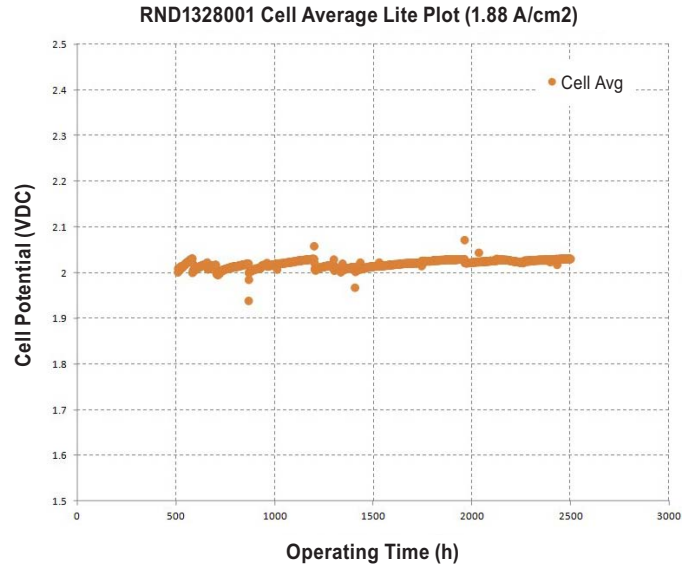

FIGURE 4. With further advances in the fabrication process, demonstrated large-scale active area performance has improved

applied fell below the target level. The performance of the stack was stable over time, indicating that there was not a continuing degradation mechanism. The full scale 55-bar PEM cell stack was successfully installed into the 57-bar capable C series and was operated at 55 bar over 900 hours through the second and third quarter of 2014. The stack has continued to operate stably at both 30 bar and 55 bar operating pressures.

Discussion: As development and demonstration of this advanced MEA with improved efficiency is important to Proton, we made process refinements and continued to demonstrate progress with large active area electrodes. Proton has subsequently introduced to the market a 0.73 ft^2 active area commercial PEM electrolysis cell stack and system, the M series, targeted at power to gas energy storage, fueling, and industrial applications. An example of the further progress we have made is described in Figure 4. With this larger active area electrode, a multi-cell electrolysis stack capable of 10 kg/d H_2 output was produced with the advanced catalyst application technique. This more recent attempt demonstrated an operating voltage of 2.03 VDC/cell, a performance improvement of 120 mV over baseline. Based on this 120 mV/cell improvement, we have demonstrated energy savings of 3.2 kWh/kg H_2. This value represents the current progress toward the 8 kWh/kg target established at the program start.

Task 2.0 Validate Full Scale 57-bar, 65-kg/d Hydrogen Generator

The build of the Proton C Series hydrogen generator that is the test bed for the advanced cell stack was completed in late 2012 and supplies the hydrogen used by the SunHydro 1 station at Proton. The hydrogen gas management portion of Proton's commercial C series 30 bar pressure hydrogen generator is comprised primarily of proprietary design hydrogen–water phase separator and a pressure–swing absorber (PSA). Proton engineering completed a mechanical design analysis of these components in FY 2013 to learn that only minor changes to valve seats, retaining bolts, orifices, and pressure sensors were needed to operate at 55 bar. These modifications were designed to easily revert back to 30 bar operation in the event that Proton product factory support testing was required. Upon a successful system Acceptance Test Plan, work culminated with tuning the PSA regeneration steps to maximize the efficiency gains allowed by higher operating pressures.

Method: The upgraded C series electrolyzer was operated at the elevated pressure for dryer tuning and compressor efficiency testing. The pressure-swing dryer purge stream was tuned to reduce the regenerative hydrogen purge stream volume as guided by calculations and verified by stable dry hydrogen product production at less than 1 ppmv moisture, same as the baseline 30-bar dryer.

Specific energy data from the upgraded 55-bar C series electrolyzer and the fueling station compressor were gathered in kWh/kg H_2 over a period of approximately 30 days in the second and third quarter of 2014. The resulting values were compared to the specific energy data produced under 30 bar operation within a similar time frame. By increasing the PEM water electrolyzer generation pressure from 30 bar to 55 bar, Proton achieved an electrolyzer energy reduction of 1.5 kWh/kg H_2 and a compressor energy reduction of 0.3 kWh/kg H_2 for a total savings of 1.8 kWh/kg H_2, halfway toward the statement of project objectives (SOPO) goal of 3.6 kWh/kg H_2.

Discussion: The specific energy consumed by the C series electrolyzer operating at 55 bar operation decreased

2.6% due to a 45% reduction in the hydrogen dryer purge losses over the 30 bar baseline. The specific energy consumed by the hydrogen compressor decreased more than 13% over the 30 bar baseline. Based on these results, it is evident that operating a C series hydrogen generator at 55 bar produces a noticeable decrease in the specific energy consumed over the 30 bar baseline.

Task 3.0 Validate Higher Addressable Capacity Composite Hydrogen Storage Tubes

Late in FY 2014, the storage tubes were delivered and promptly installed at the SunHydro 1 station. These tubes allow for deeper pressure cycling providing a higher addressable storage capacity. This capability was demonstrated during commissioning with the entire station managing the sequential filling of five vehicles, an increase over the previous filling capability of the SunHydro 1 station of only slightly more than two vehicles back to back.

Storage tube validation continues as the SunHydro 1 station continues to service vehicles. The new tubes serve as the primary bank as they are used first to fill, the other three banks serving to top up. On average the new tubes are pressure cycled three days per week from 870 bar to less than 500 bar based on the demands of an average fleet size of 10 fuel cell vehicles. A second set of storage tubes will enter into validation testing with the deployment of SunHydro 2 station in 2016.

Task 4.0 Validate Compressor Increased Throughput Capacity with 57 bar Input

With the successful completion of Tasks 2 and 3, validation of the anticipated increased throughput capacity of the compressor is completed. By increasing the PEM water electrolyzer generation pressure from 30 bar to 55 bar, Proton achieved an electrolyzer energy reduction of 1.5kWh/kg H_2 and a compressor energy reduction of 0.3 kWh/kg H_2 for a total savings of 1.8 kWh/kg H_2, halfway toward the SOPO goal of 3.6 kWh/kg H_2.

Task 5.0 Hydrogen Station Safety Operation Procedure and EX Zone Review

Results of Chapters 7 and 13 of the National Fire Protection Association (NFPA) 2 "Hydrogen Technologies Code" were used to determine hazardous equipment zones and methods to mitigate code-directed separation distances to develop the novel compact component layout and model in Task 6 with respect to classified and nonclassified areas. Following procedure and zone review, Proton's efforts shifted to actively working the site permitting for SunHydro 2 based on our compact arrangement and addressing several Massachusetts specific issues. An installation plan set was generated to address these issues and a permit application for the 46 kg of hydrogen to be stored in the SunHydro 2 high pressure composite storage tubes was granted by Braintree, Massachusetts authorities in October 2014.

Proton is an industry member of the NFPA 2 Hydrogen Technologies Code technical committee, and has a representative on the Hydrogen Safety Panel (HSP). The technical committee has prepared the 2016 edition of NFPA 2. The HSP, with Proton support, has contributed to a draft public comment concerning hydrogen equipment in enclosures that was reviewed at the second draft meeting for the NFPA 2 committee and subsequently accepted during formal balloting. Creating specific code to address hydrogen processing equipment and storage in prefabricated intermodal enclosures will help code officials with permitting compact containerized hydrogen fueling stations.

Task 6.0 Validate Novel Compact and Non-EX Rated Component Arrangements

An installation permit application for SunHydro 2 was granted by Braintree, Massachusetts, authorities in October 2014. Proton's analysis of compact hydrogen station component arrangements under this work shows an advantage to using the nonclassified area immediately around our PEM hydrogen generator to house almost all electrical power and control equipment. Further, NFPA 2 hydrogen code permits reduction of separation distances to near zero when a 2-h rated firewall is interposed. Our arrangement shows significant space saving advantages in placing this firewall in between the nonclassified electrolyzer generator container space and the classified container space that houses compression, storage, and a built-in dispenser. This approach will be further validated to meet the 8 ft x 40 ft goal in the SunHydro 2 station when installed in the next fiscal year.

Task 7.0 Hydrogen Station Data Acquisition System and Task 8.0 Quarterly Operation Data Reporting

The data acquisition system is installed in SunHydro 1 and has provided operating data for quarterly reports to the FCEV infrastructure CDPs. Identical data acquisition equipment awaits installation in SunHydro 2. Four reports of SunHydro 1 station data were prepared for the FCEV infrastructure CDP during the previous fiscal year, seven in total since the start of our contract.

CONCLUSIONS AND FUTURE DIRECTIONS

Conclusions

- 55 bar generation and compression yields efficiency gains over the 30 bar baseline.
- Compact station arrangements using non-EX rated components can be approved by authorities having jurisdiction (AHJs) for installation using NFPA 2 code.

Future Directions

- Install and validate novel compact and non-EX rated component arrangement of SunHydro 2 with AHJ permit for Washington, DC, site
- Initiate SunHydro 2 data acquisition CDP operational data reporting
- Continue reporting SunHydro 1 CDP operational data reporting

FY 2015 PUBLICATIONS/PRESENTATIONS

1. AMR 2015 moulthrop TV-012.

REFERENCES

1. NFPA 2 Hydrogen Technologies Code, NFPA, 1 Batterymarch, Quincy, MA.

VII.10 Performance Evaluation of Delivered Hydrogen Fueling Stations

Ted Barnes (Primary Contact) and Devin Halliday
Gas Technology Institute (GTI)
1700 S. Mt. Prospect Rd.
Des Plaines, IL 60018
Phone: (847) 544-3405
Email: ted.barnes@gastechnology.org

DOE Manager
Jason Marcinkoski
Phone: (202) 586-7466
Email: Jason.Marcinkoski@ee.doe.gov

Contract Number: DE-EE0005886

Subcontractor
Linde Gas, LLC (Linde), Heyward, CA

Project Start Date: March 1, 2013
Project End Date: April 30, 2018

Overall Objectives

- Integrate non-intrusive data collection systems at five 100 kg/day delivered liquid hydrogen fueling stations located in California for 24-month performance period
- Submit complete sets of the National Renewable Energy Laboratory (NREL) Hydrogen Station Data Templates to National Fuel Cell Technology Evaluation Center (NFCTEC)
- Provide useful data to accurately benchmark and characterize station capacity, utilization, maintenance, and safety

Fiscal Year (FY) 2015 Objectives

- Complete installation of data acquisitions systems on the two hydrogen fueling stations covered under Budget Period 1 (West Sacramento and San Juan Capistrano stations)
- Begin data collection activities at the first two hydrogen fueling stations
- Monitor progress on the other three planned hydrogen fueling stations to ensure data acquisition systems are prepared for installation

Technical Barriers

This project addresses the following technical barriers from the Technology Validation section of the Fuel Cell Technologies Office Multi-Year Research, Development, and Demonstration Plan:

(A) Lack of Fuel Cell Electric Vehicle and Fuel Cell Bus Performance and Durability Data

(D) Lack of Hydrogen Refueling Infrastructure Performance and Availability Data

Contribution to Achievement of DOE Technology Validation Milestones

This project will contribute to the achievement of the following U.S. DOE milestones from the Technology Validation section of the Fuel Cell Technologies Office Multi-Year Research, Development, and Demonstration Plan:

- Milestone 3.2: Validate novel hydrogen compression technologies or systems capable of >200 kg/day that could lead to more cost-effective and scalable (up to 500 kg/day) fueling station solutions for motive applications. (4Q, 2014). The stations currently being constructed will incorporate Linde's patented ionic fluid compressor. This technology utilizes a liquid piston to compress gas rather than a diaphragm or metal piston used in conventional compressor technologies. Linde is optimistic that this technology can be cost effectively scaled to larger capacity stations in the future.
- Milestone 3.4: Validate station compression technology provided by the delivery team. (4Q, 2018). See Milestone 3.2
- Milestone 3.8: Validate reduction of cost of transporting hydrogen from central production to refueling sites to <$0.90/GGE. (4Q, 2019). This project will yield data directly aiding to develop baseline benchmarking and measure improved cost of delivery of liquid hydrogen to fueling stations in California.
- Milestone 4.4: Complete evaluation of 700-bar fast fill fueling stations and compare to Society of Automotive Engineers (SAE) J2601 specifications and U.S. DOE fueling targets. (3Q, 2016). This project will supply data to the NFCTEC that aid the program in the characterization of the stations' storage and delivery capacities, compression performance, fueling transactional data, operational cost, maintenance, and safety. Data supplied will provide points of direct comparison to SAE fueling standards and U.S. DOE fueling targets.

FY 2015 Accomplishments

- Completed installation of the GTI-designed data acquisition system at the newly built West Sacramento hydrogen fueling station (first of five planned stations). This station was commissioned by Linde in December 2014, and is currently open for public use.

- Data collection activities at the West Sacramento station began in January 2015. Two quarters of data have been successfully collected, organized, and reported to NREL.
- Construction of the second fueling station located in San Juan Capistrano began in early June 2015. There was a several month delay in beginning construction due to delays in the permitting process.
- Preparations are complete for the installation of the data acquisition system at San Juan Capistrano. Slight modifications were made to the design to simplify the installation and streamline the data collection process. Installation at this site will occur in 3Q 2015.
- Continuing to coordinate with Linde on the construction timing of the remaining three fueling stations. Construction is expected to begin on the remaining stations around 4Q 2015—1Q 2016.

✧ ✧ ✧ ✧ ✧

INTRODUCTION

The objective of this project is to collect, organize, and report on operational, transactional, safety, and reliability data for five hydrogen fueling stations located in California. Goals of the project are as follows: (1) the data collected will be statistically meaningful and the stations will have sufficient throughput and vehicle fueling frequency to minimize data aberrations; (2) the data collected will be accurate; and (3) the data collected will be comprehensive and timely.

This project will directly assist DOE in assessing the readiness level of current infrastructure and state-of-the-art technologies utilized to support planned fuel cell vehicle deployment within the next five years. The data and observations collected during the performance period of this project will provide NREL with information detailing the operational costs, efficiencies, and reliability of the delivered hydrogen fueling station design. Furthermore, the Linde design utilizes the patented IC90 ionic fluid compressor package; through this project GTI will provide the performance data which will enable DOE and original equipment manufacturers (OEMs) to evaluate real-world efficiencies, further gauging the technology's adequacy in this application. This system is a first of its kind utilized for hydrogen fueling applications in the United States.

APPROACH

Hydrogen station data will be submitted quarterly to the NFCTEC at NREL using the appropriate Hydrogen Station Data Templates. GTI's project partner, Linde, is currently developing delivered hydrogen fueling stations under programs sponsored by the California Energy Commission (CEC). The sites will be accessible to the public for fueling consumer fuel cell vehicles, commercial vehicles, or government-owned vehicles. All five of the sites will be developed at existing or at new sites along with conventional gasoline stations operated by major-branded fuel providers. This provides the project with vehicle fueling data from a broad, cross-section of real-world vehicle applications. The station sites were selected to provide convenient, consumer-friendly vehicle fueling for drivers of fuel cell vehicles. Development of each of these stations has the support of vehicle OEMs and each site has passed stringent location selection requirements of the CEC to ensure the stations will be utilized by a high volume of fuel cell vehicle operators.

The data collection system will utilize a variety of methods in order to provide the entire data requirements set forth by NREL. This system will utilize the existing control architecture of the compressor and dispenser equipment as well as monitor and record signals from a set of installed instrumentation that will supplement information required that is not already captured inherently by the stations' operating system. There are multiple descriptive (as opposed to measured data) deliverables that will be taken manually and submitted to GTI for processing and formatting prior to delivery to NREL. Manually collected data templates include the following:

- NREL Site Log: recording safety drills, training, or public meetings
- Storage & Delivery: compiling liquid hydrogen supplies, delivery quantities, and cost
- Fuel Log: transferring transactional data from monthly reports emanating from fuel management system
- Maintenance: station maintenance and operations reporting
- Hydrogen Cost: collection of utility bills
- Safety: station environmental, health, and safety reporting
- Hydrogen Quality: SAE quality analysis completed annually and submitted

GTI will collaborate with Linde and create a reporting/submittal process to collect this type of data required to populate the NREL templates.

RESULTS

The past year has shown substantial progress including installing the data acquisition system, retrieving data from the first hydrogen station, and making progress toward installing the system at the second station. Figure 1 shows the monthly dispensed hydrogen data collected from the first hydrogen station in West Sacramento. This data shows a

large variability in the station usage for the first half of 2015. This is just a small subset of the large amount of data that is being reported to NREL each quarter. Other data collected includes the energy used in compression and precooling of the hydrogen, maintenance and safety logs, and hydrogen control quality results.

Great progress was made toward construction and commissioning of the second hydrogen station, to be located in San Juan Capistrano. Station construction was started in early June and commissioning activities are planned for late 3Q 2015. With this second installation of the data acquisition system, a review of the performance of the currently installed system was completed to determine if any changes should be made prior to the second installation. During this review, we found the data from two temperature transmitters installed at the West Sacramento station are not being used as inputs to any calculations or data reporting and were therefore removed from the design for subsequent stations (TE-3 and TE-4 in Figure 2). These temperature transmitters are between the compressor, storage, and the dispenser. The TE-4 transmitter was meant to measure storage temperature, but this was found to be more accurate if ambient temperature is used. The TE-3 transmitter was meant to read the 350 bar gas delivery temperature, but modifications made to the pre-cooling system meant this temperature is an intermediate temperature between two coolers, and therefore not useful for data gathering. The delivery temperature will be read from the dispenser instead.

Lastly, progress continues to be made on the installation of the remaining three stations. These installations have progressed slowly due to permitting issues. Components from these remaining stations have begun assembly in preparation for installation, which is targeted to start in 4Q 2015. Geographic diversity and multiple locations should provide an aggregate representation of the stations' performance and operational characteristics. The additional funding allocated to Budget Period 2 will enable the installation of data acquisition systems on these remaining three stations as well as the data collection from all five stations for a two year period. This information will supply the NREL database with accurate representation and characterization of the readiness of delivered hydrogen as a vehicular fuel supply.

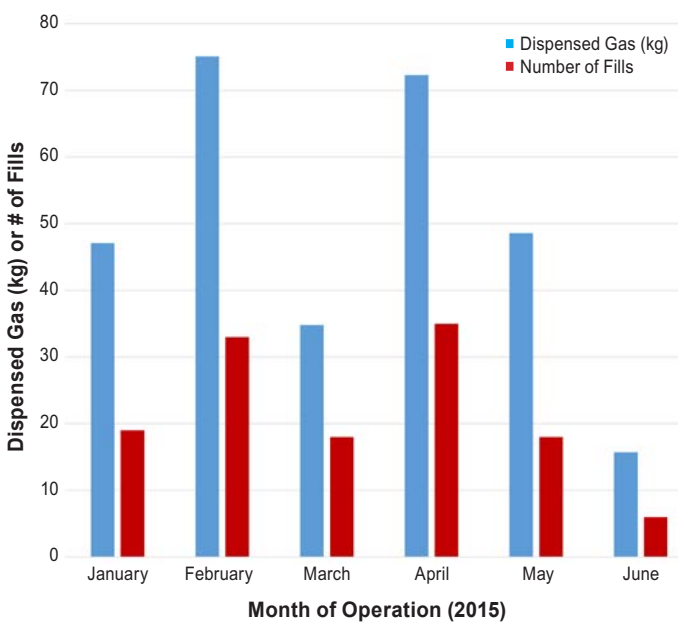

FIGURE 1. Usage data collected from West Sacramento station in first half of 2015

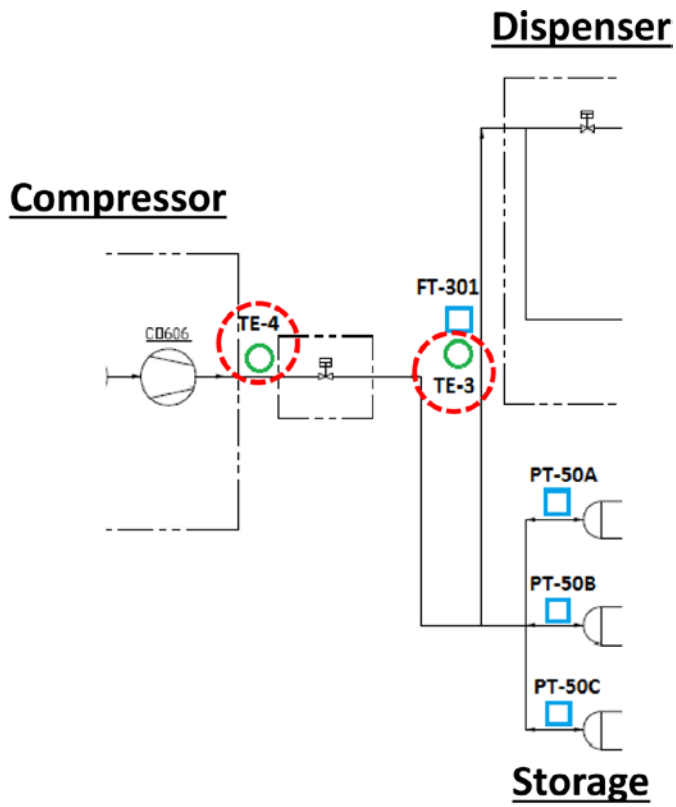

FIGURE 2. Portion of data acquisition system schematic showing thermocouples to be removed (circled in red)

CONCLUSIONS AND FUTURE DIRECTIONS

- Install and commission the second system in Q3 of 2015 at San Juan Capistrano, California, site location
- Produce the complete sets of data for the first two project sites at the end of each quarter after startup and commissioning is completed
- Obtain approval to continue project efforts into Budget Period 2 (Q4 2015)

FY 2015 PUBLICATIONS/PRESENTATIONS

1. tv025_barnes_2015_o.pptx – Oral Presentation 2015 AMR.

VII.11 Hydrogen Station Data Collection and Analysis

Sam Sprik (Primary Contact), Jennifer Kurtz, Chris Ainscough, Genevieve Saur, Matt Post, and Mike Peters
National Renewable Energy Laboratory (NREL)
15013 Denver West Parkway
Golden, CO 80401-3305
Phone: (303) 275-4431
Email: Sam.Sprik@nrel.gov

DOE Manager
Jason Marcinkoski
Phone: (202) 586-7466
Email: Jason.Marcinkoski@ee.doe.gov

Project Start Date: October 1, 2011
Project End Date: Project continuation and direction determined annually by DOE

Overall Objectives

- Analyze current, state-of-the-art hydrogen infrastructure using several metrics including efficiency, performance, cost, and reliability of station components and systems
- Perform an independent assessment of technology in real-world operating conditions, focusing on hydrogen infrastructure for on-road vehicles
- Leverage the data processing and analysis capabilities at the National Fuel Cell Technology Evaluation Center (NFCTEC), originally developed under the Fuel Cell Vehicle Learning Demonstration, as well as from forklift, backup power, and bus projects

Fiscal Year (FY) 2015 Objectives

- Obtain/collect data from state-of-the-art hydrogen fueling facilities that receive funding through DOE Funding Opportunity Announcement (FOA) 626 awards, California Energy Commission (CEC) awards, and others, to enrich the analyses and the set of publicly available composite data products (CDPs) on hydrogen fueling infrastructure
- Work with codes and standards activities and fueling facility owners/operators to benchmark performance of the fueling events relative to current Society of Automotive Engineers (SAE) procedures
- Perform analysis and provide feedback on sensitive data from hydrogen infrastructure for industry and DOE
  - Aggregate these results for publication
- Participate in technical review meetings and site visits with industry partners to discuss results from NREL's analysis
- Maintain an accurate database (location and status) of all online hydrogen stations in the United States, and provide periodic updates to other online resources, specifically the Alternative Fuels Data Center (AFDC) station locator, the Fuel Cell and Hydrogen Energy Association, the California Fuel Cell Partnership (CaFCP), and Pacific Northwest National Laboratory (PNNL)

Technical Barriers

This project addresses the following technical barrier from the Technology Validation section of the Fuel Cell Technologies Office Multi-Year Research, Development, and Demonstration Plan:

(D) Lack of Hydrogen Refueling Infrastructure Performance and Availability Data

Contribution to Achievement of DOE Technology Validation Milestones

This project will contribute to achievement of the following DOE milestone from the Technology Validation section of the Fuel Cell Technologies Office Multi-Year Research, Development, and Demonstration Plan:

- Milestone 4.4: Complete evaluation of 700-bar fast fill fueling stations and compare to SAE J2601 specifications and DOE fueling targets. (3Q, 2016)

FY 2015 Accomplishments

- Internally processed and analyzed quarterly infrastructure data in the NFCTEC for inclusion in CDPs every six months, creating Fall 2014 and Spring 2015 CDPs:
  - Gathered and provided updates on stations under the DOE FOA 626-funded projects
  - Analyzed data from the CEC on their awarded stations
- Provided assistance in filling out and modifying templates for those providing infrastructure data
- Updated NREL's internal database of stations and their locations, submitted updates to AFDC, and synced with PNNL list
- Updated NREL Fleet Analysis Toolkit code to accept and analyze data in multiple formats from stations

- Participated in the CaFCP working group meetings and H_2USA hydrogen fueling station working group
- Presented results at Fuel Cell Seminar 2014 and at the 2015 DOE Annual Merit Review

✧ ✧ ✧ ✧ ✧

INTRODUCTION

In the past decade, approximately 60 hydrogen fueling stations supported a few hundred fuel cell electric vehicles (FCEVs) in the United States. Of these stations, 25 supported the 183 DOE Learning Demonstration vehicles. As we move out of a learning demonstration environment into a commercialization environment, manufacturers are ramping up FCEV production alongside an infrastructure effort to build additional consumer-friendly stations in a retail environment, upgrade existing stations to increase fueling output, and cluster stations to cover areas where vehicles are introduced.

California has been a leader in supporting hydrogen infrastructure with a goal of 100 stations within a carefully planned network. Early efforts in California focus on clusters of stations near population centers in the Los Angeles and the San Francisco Bay areas. Through past funding efforts, eight non-private stations are in place in California with 18 more in near-term development. The most recent awards from the CEC through PON-13-607, which were announced in May of 2014, further support the rollout of FCEVs coming in 2015–2017 and beyond. That effort is funding the building of 28 new stations and a mobile fueler with $46 million of state money through the CEC's Alternative and Renewable Fuel and Vehicle Technology Program. These stations will be included in subsequent evaluations and would bring the California public station count to 54. Besides California, there are efforts in other states, including the northeastern states that will establish hydrogen infrastructure for the upcoming FCEVs.

Keys to success for improving hydrogen fueling availability are selecting the fueling location, ensuring customer-friendly public access, and providing adequate and reliable output to support the vehicles. One concern is the underutilization of the stations while the vehicle market develops, which could be aided by fueling multiple applications such as buses and forklifts at a site. Another idea is to build stations smaller at first with the ability to upgrade the station to higher output once the market develops. Hydrogen output from existing and upcoming facilities varies from 50 kg/day to 350 kg/day, with most new fueling facilities being more than 100 kg/day. Although it is currently most economical to make hydrogen from natural gas, there are efforts and requirements to make hydrogen from renewable sources. Using available biogas from landfills and wastewater treatment plants to generate hydrogen is one way to make use of a renewable feedstock and to lower greenhouse gas emissions. Another renewable pathway is to make hydrogen through electrolysis with the electrical energy coming from a renewable source such as wind or solar. As more vehicles come online, all fueling facilities will need to be accessible to anyone with a hydrogen vehicle. As these fueling facilities are developed, there is a need to continue data collection and analysis to track the progress and determine future technology development needs.

APPROACH

The emphasis of this project is documenting the innovations in hydrogen fueling and how well they meet customer needs. This includes analysis that captures the technology capability (such as back-to-back filling capability, impact of pre-cooling temperature, and radio-frequency identification of vehicles to allow unique fueling profiles) as well as the customer perspective (such as fueling times and rates, safety, and availability). Individual components, such as compressors, are evaluated with the available data to establish current status and research needs. Station locations are evaluated within the context of both available vehicles and future vehicles and their fueling patterns.

Data analysis is performed on sensitive industry hydrogen fueling data in the NFCTEC, supporting DOE in identifying trends from the data that will help guide or supplement R&D activities. Aggregation of the analyzed data allows for creation of composite results for public dissemination and presentation. Some existing CDPs from the previous learning demonstration are updated with new data, as appropriate. All this involves working with industry partners to create and publish CDPs that show the current technology status without revealing proprietary data. Feedback to industry takes form in detailed data products (protected results) and provides direct benefit to them from the NREL analysis performed on their data. NREL will continue exercising the fueling analysis functionality of its Fleet Analysis Toolkit to preserve and archive a snapshot of the analysis results from each quarter. This allows a deeper level of results to be stored in an easy-to-access form within the NFCTEC.

RESULTS

As stations are built or retired, the internal station database is updated and shared with others, including the AFDC. Currently, there are 51 stations in the United States with 46 planned in the near future. Most of the current stations are not available to all original equipment manufacturer customers (only a few are), while most of the future stations will be open to the public and located in California. Using the data reported to NREL by 10 of these stations, 43 CDPs were created by aggregating and analyzing the station data. These results were presented at the Fuel Cell

Seminar and at the DOE Annual Merit Review. Results were also published on NREL's website.

Although the primary goal of the early stations is geographic coverage for FCEV customers to prevent range anxiety, the current analysis includes how these stations are being used. The amount of dispensed hydrogen per day of the week (Figure 1) shows more filling is happening Monday through Friday than on Saturday and Sunday. The highest station shows an average of 31 kg/day on Thursdays. The number of fills per day (Figure 2) at each station ranges from 3 to 11 on average with maximum daily fills at each station ranging from 13 to 31 fills per day. The average amount of hydrogen dispensed per fill (Figure 3) is 2.63 kg ranging mostly between 1.5 kg and 3.5 kg. Some of the lower amounts in the histogram are due to interrupted fills. A look at maintenance by equipment type (Figure 4) shows that hydrogen compressors are the primary items needing maintenance both in terms of number of events and hours. Dispensers, safety items (e.g., false alarms and sensors), and thermal management are the next highest items in terms of number of maintenance events. These results and all the other CDPs are published on NREL's website.

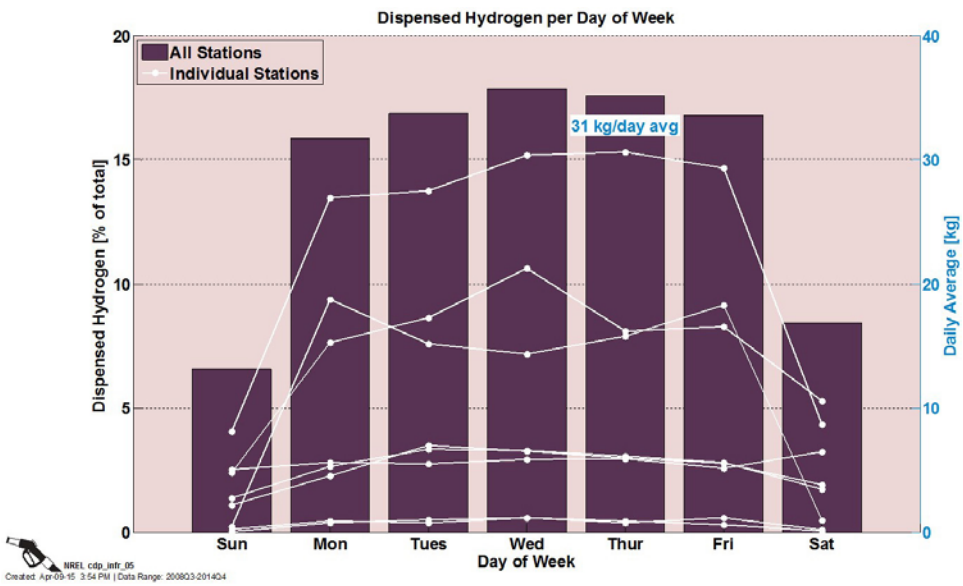

FIGURE 1. Dispensed hydrogen per day of week

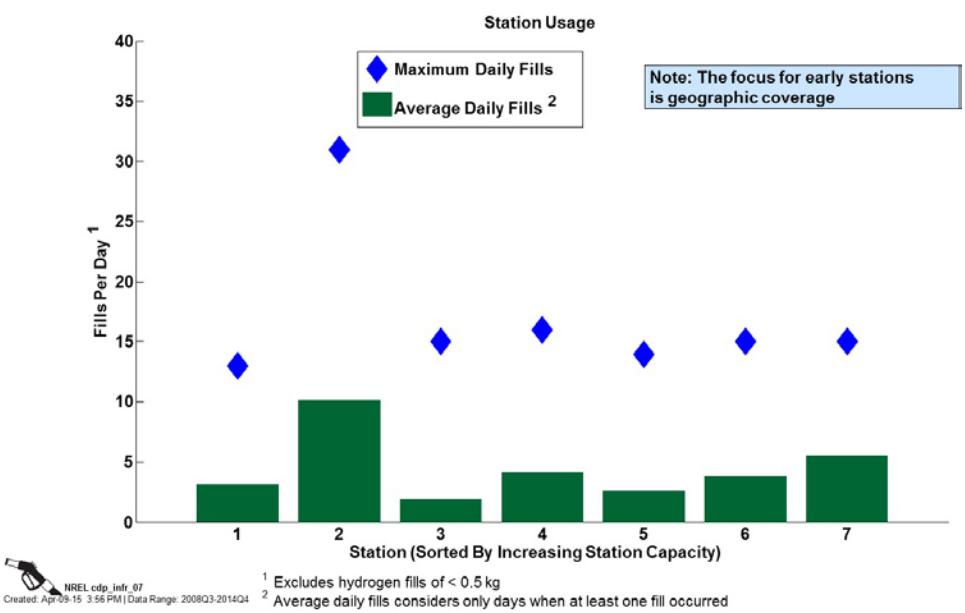

FIGURE 2. Station usage—number of fills per day

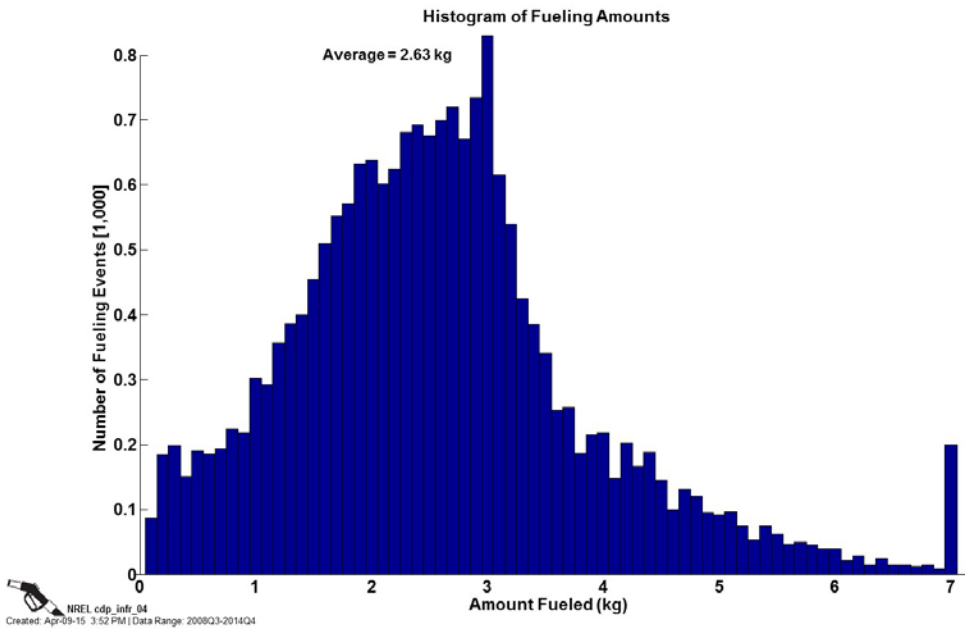

FIGURE 3. Histogram of fueling amounts

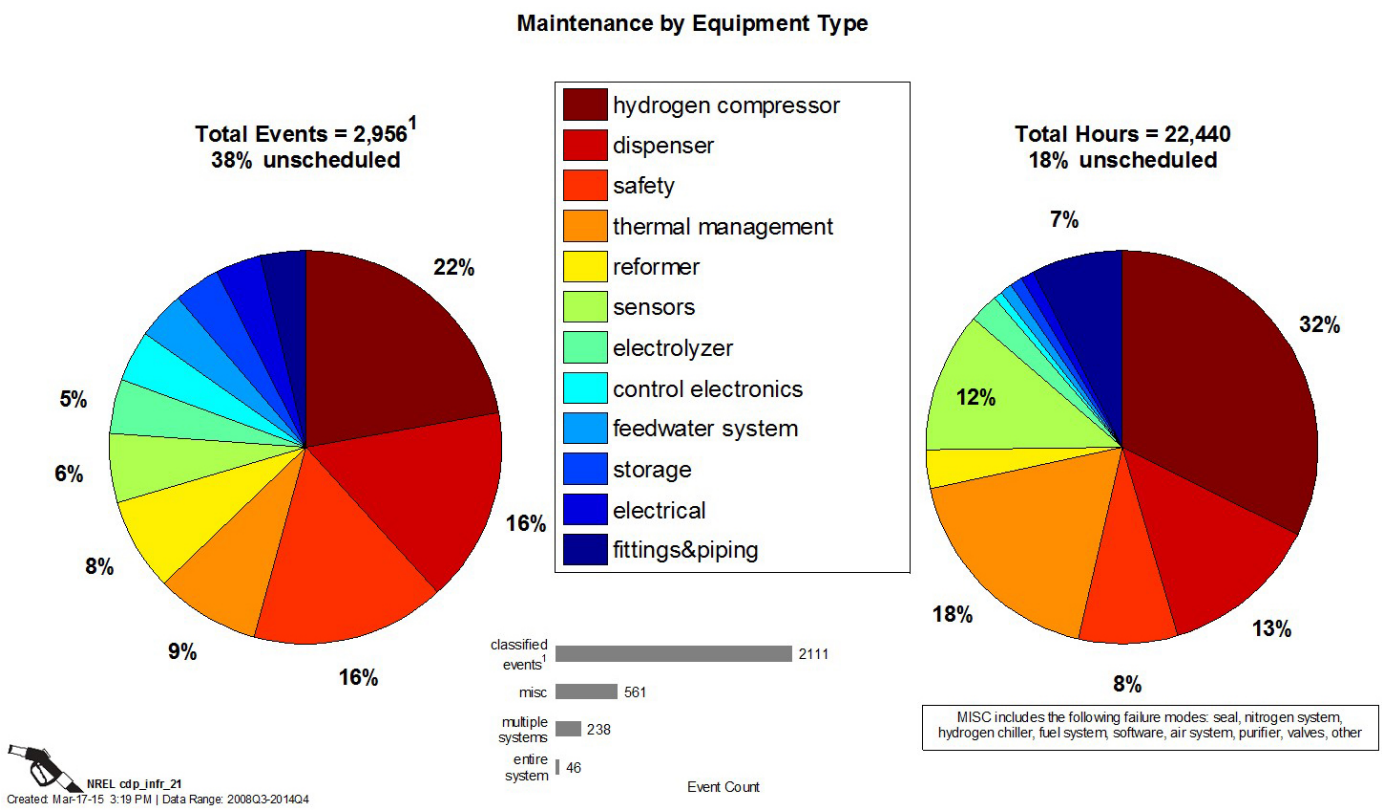

FIGURE 4. Maintenance by equipment type

CONCLUSIONS AND FUTURE DIRECTIONS

As new stations come online or are updated, their performance and availability will affect how successfully they support the current and upcoming fleet of fuel cell vehicles. Continual data collection, analysis, and feedback will provide DOE and the hydrogen and fuel cell community with awareness of the technology readiness and identify areas for improvement that could be research topics. Many new stations are planned to be built and start operating in 2015 and 2016, and will be included in the data set as they report data. Their data will be aggregated and published in CDPs without revealing individual station identity and will help identify general trends for the latest stations. As more data become available from newer stations and as more FCEVs enter the market, there will be an increase in data analysis possibilities to validate the technology for hydrogen infrastructure including focusing on trends over time for usage, reliability, and performance of the stations.

FY 2015 PUBLICATIONS/PRESENTATIONS

1. Sam Sprik, Jennifer Kurtz, Chris Ainscough, Genevieve Saur, and Mike Peters, "TV017: Hydrogen Station Data Collection and Analysis," (presented at the 2015 DOE Annual Merit Review and Peer Evaluation Meeting, Washington, DC, June 2015).

2. Sam Sprik, Jennifer Kurtz, Chris Ainscough, Mike Peters, Matt Post, and Genevieve Saur, "Technology Validation of Fuel Cell Vehicles and Infrastructure," (presented at 2014 Fuel Cell Seminar FCS#222, Los Angeles, California, November 2014.

3. "Hydrogen Fueling Infrastructure Analysis: Composite Data Products," National Renewable Energy Laboratory, http://www.nrel.gov/hydrogen/proj_infrastructure_analysis.html.

VII.12 CSULA Hydrogen Refueling Facility Performance Evaluation and Optimization

David Blekhman
California State University Los Angeles (CSULA)
Los Angeles, CA 90032
Phone: (323) 343-4569
Email: blekhman@calstatela.edu

DOE Manager
Jason Marcinkoski
Phone: (202) 586-7466
Email: Jason.Marcinkoski@ee.doe.gov

Contract Number: DE-EE0005890

Subcontractor
Hydrogenics, Mississauga, ON, Canada

Project Start Date: October 1, 2012
Project End Date: December 31, 2016

Overall Objectives

Technical Objectives:

- Test, collect data, and validate hydrogen refueling architecture deployed at CSULA and its individual components in a real-world operating environment
- Provide the performance evaluations data to the National Fuel Cell Technology Evaluation Center (NFCTEC) at the National Renewable Energy Laboratory (NREL)
- Contribute to the development of new industry standards
- Develop and implement fueling station system performance optimization

Educational Objectives:

- Conduct outreach and training activities promoting the project and hydrogen and fuel cell technologies
- Provide a living-lab environment for engineering and technology students pursuing interests in hydrogen and fuel cell technologies

Fiscal Year (FY) 2015 Objectives

- Perform regular collection of station performance data and submit quarterly reports to NREL
- Conduct outreach and training activities for public and government and engage students in station related activities

Technical Barriers

This project addresses the following technical barriers from the Hydrogen Production and Technology Validation sections of the Fuel Cell Technologies Office Multi-Year Research, Development, and Demonstration Plan:

Hydrogen Production

(L) Operations and Maintenance

(M) Control and Safety

Technology Validation

(D) Lack of Hydrogen Refueling Infrastructure Performance and Availability Data

Contribution to Achievement of DOE Hydrogen Production and Technology Validation Milestones

This project will contribute to achievement of the following DOE milestones from the Hydrogen Production and Technology Validation sections of the Fuel Cell Technologies Office Multi-Year Research, Development, and Demonstration Plan:

Hydrogen Production:

- Milestone 2.6: Verify the total capital investment for a distributed electrolysis system against the 2015 targets using H2A. (Q2, 2016)
- Milestone 2.7: Verify 2015 distributed hydrogen production levelized cost target through pilot scale testing coupled with H2A analysis to project economies of scale cost reduction. (Q3, 2017)

Technology Validation:

- Milestone 3.4: Validate station compression technology provided by delivery team. (4Q, 2018)

FY 2015 Accomplishments

This is the first year of the project. Accomplishments are listed below.

- The station continues to collect and regularly submit performance data to NREL. Station utilization is steadily increasing with over 500 successful fills.
- CSULA became the first station in the United States to receive a seal of approval for commercial sales of hydrogen on a per kilogram basis.

- In addition to fueling light-duty vehicles, the station has also been used to fuel a bus, a mobile refueler, and a mobile fuel cell light source.
- CSULA has performed physical and programming upgrades toward improving safety, meeting fueling standards and per NREL data collection requirements.
- The station has had a steady flow of visitors learning about hydrogen (over 4,000 visitors since May 2014). In addition, three engineering students are interning at the station.

INTRODUCTION

The CSULA hydrogen station deploys the latest technologies with the capacity to produce and dispense 60 kg/d, sufficient to fuel 15–20 vehicles. The station utilizes a Hydrogenics electrolyzer, first and second stage compressors enabling 350 bar and 700 bar fueling, and 60 kg of hydrogen storage. The station is grid-tied and to be supplied by 100% renewable power.

In addition to collecting data per NREL specifications, the comprehensive data collection enhances research opportunities in evaluating and optimizing performance of the hydrogen fueling facility.

APPROACH

To enable effective data collection on the station performance, the team deploys significant number of sensors and meters installed on the station. A custom designed software package is utilized for data collection and reporting to NREL.

As data are collected and analyzed, the station hardware and software is gradually upgraded for optimization and other technical/safety enhancements.

RESULTS

Since its opening in May 2014 CSULA has secured fueling agreements with Hyundai, General Motors, and Volkswagen, providing steady increase in station utilization with more than 500 successful fills, see Figure 1.

Most of the individual equipment is power metered allowing further research into performance efficiency not only of the entire facility but also components. This enables steady data collection and submission to NREL. For example, Figure 2 presents hydrogen cost based on the station energy consumption. In addition, station hardware and programming has been updated to further enhance NREL reporting and improve station safety and compliance with fueling standards.

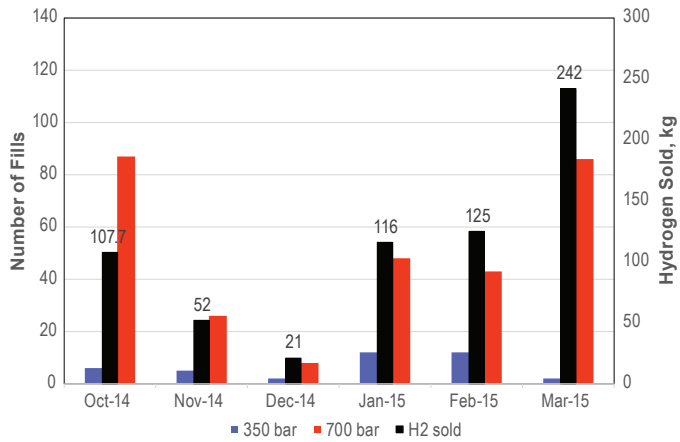

FIGURE 1. CSULA fueling events monthly

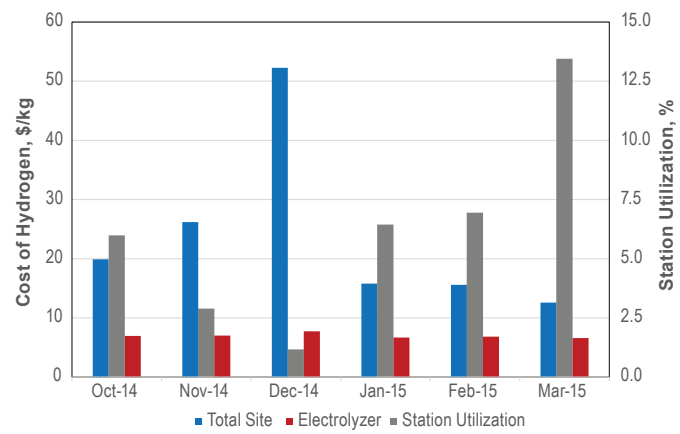

FIGURE 2. Hydrogen costs based on station energy consumption

CSULA became the first station in the United States to receive a seal of approval for commercial sales of hydrogen on a per kilogram basis in January 2015, see Figure 3. Two-phase testing a few months apart was conducted in collaboration with the California Division of Measurement Standards, the California Fuel Cell Partnership, and the California Air Resources Board. This will also enable point of sale using credit cards by individual drivers vs. original equipment manufacturer fueling contracts.

The station has been supporting outreach and collaborative efforts. More than 4,000 visitors have toured the facility with about 85% of them being K–12 and university students. Additionally, CSULA hosted professional meetings and first responder trainings. The facility has accommodated fueling of a bus, see Figure 4, mobile cell tower refueler, and mobile fuel cell lighting unit. The Volkswagen and Audi fuel cell vehicles were fueled during the press days of the Los Angeles Auto Show.

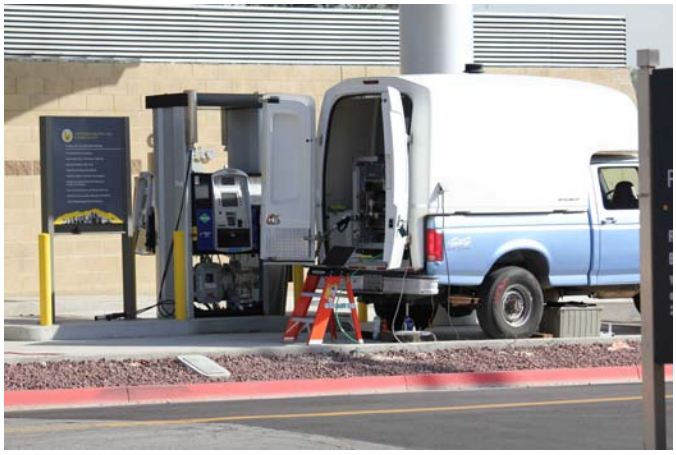

FIGURE 3. CSULA is being tested on the meter accuracy

FIGURE 4. E-bus is fueled at CSULA

CONCLUSIONS AND FUTURE DIRECTIONS

The project has completed Phase I and has transitioned in to Phase II. The station provides reliable fueling experience and generates data that are furnished to NREL. In collaboration with partners, CSULA has received funding from the California Energy Commission to secure two fuel cell shuttles to operate on campus.

SPECIAL RECOGNITIONS & AWARDS

1. Sustainable Transportation Award by 2015 UC and CSU Energy Efficiency and Sustainable Practice Awards Competition. CA Higher Education Sustainability Conference, San Francisco, CA, 2015.

FY 2015 PUBLICATIONS/PRESENTATIONS

1. "An Emerging Culture: Hydrogen Fuel Cell Use in East Los Angeles," C. Ney, D. Blekhman, and M. Dray. CA Higher Education Sustainability Conference, San Francisco, CA, 2015.

2. "Hydrogen Station Performance Evaluation Plan," D. Blekhman, M. Dray and G. Sleiman. Fuel Cell Seminar and Exposition, Los Angeles, CA, 2014.

VII.13 Stationary Fuel Cell Evaluation

Genevieve Saur (Primary Contact), Jennifer Kurtz, Chris Ainscough, Sam Sprik
National Renewable Energy Laboratory (NREL)
15013 Denver West Parkway
Golden, CO 80401-3305
Phone: (303) 275-3783
Email: Genevieve.Saur@nrel.gov

DOE Manager
Jason Marcinkoski
Phone: (202) 586-7466
Email: Jason.Marcinkoski@ee.doe.gov

Project Start Date: October 2011
Project End Date: Project continuation and direction determined annually by DOE

Overall Objectives

- Independently assess, validate, and report operation targets and performance under stationary fuel cell (FC) system real operating conditions

Fiscal Year (FY) 2015 Objectives

- Develop more voluntary data partners, especially for operations data
- Analysis of quarterly data as available
- Publication of 33 technical stationary fuel cell composite data products (CDPs) biannually
- Update of a public website for dissemination of CDPs

Technical Barriers

This project addresses the following technical barriers from the Technology Validation section of the Fuel Cell Technologies Office Multi-Year Research, Development, and Demonstration Plan:

(B) Lack of Data on Stationary Fuel Cells in Real-World Operation - Address gaps in knowledge as stationary fuel cell installations have increased.

(E) Codes and Standards - Provide data and context to codes and standards activities.

Contribution to Achievement of DOE Technology Validation Milestones

This project will contribute to achievement of the following DOE milestones from the Technology Validation section of the Fuel Cell Technologies Office Multi-Year Research, Development, and Demonstration Plan:

- Milestone 1.1: Complete validation of residential fuel cell micro combined heat and power (CHP) systems that demonstrate 40% efficiency and 25,000 hour durability. (4Q, 2015)
- Milestone 1.2: Complete validation of commercial fuel cell CHP systems that demonstrate 45% efficiency and 50,000 hour durability. (4Q, 2017)

FY 2015 Accomplishments

- Published an updated and expanded set of CDPs (http://www.nrel.gov/hydrogen/proj_fc_systems_analysis.html) in April 2015; these included five new CDPs, four of which were for operational criteria, for a total of 33 CDPs
- Validated that commercial stationary fuel cells (>100 kW) exceeded the 2015 DOE technology validation target for electrical efficiency of 43% based on the lower heating value of hydrogen (39% higher heating value of hydrogen)

✧ ✧ ✧ ✧ ✧

INTRODUCTION

This project aims to provide status on stationary fuel cell systems to inform DOE, the public, fuel cell manufacturers, and other stakeholders. This is the only technology validation project working directly on Technical Barrier (B): Lack of Data on Stationary Fuel Cells in Real-World Operation.

APPROACH

The project's data collection plan builds on other technology validation activities. Data (operation, maintenance, and safety) are collected on site by the project partners for the fuel cell system(s) and infrastructure. NREL receives the data quarterly and stores, processes, and analyzes the data in NREL's National Fuel Cell Technology Evaluation Center (NFCTEC).

The NFCTEC is an off-network room with access for a small set of approved users. An internal analysis of all available data is completed quarterly, and a set of technical CDPs is published every six months. The CDPs present aggregated data across multiple systems, sites, and teams in order to protect proprietary data and summarize the performance of hundreds of fuel cell systems.

A review cycle is completed before the publication of CDPs. The review cycle includes providing detailed data products of individual system and site performance results to the individual data provider. Detailed data products also identify the individual contribution to CDPs. The NREL Fleet Analysis Toolkit is an internally developed tool for data processing and analysis structured for flexibility, growth, and simple addition of new applications. Analyses are created for general performance studies as well as application- or technology-specific studies.

RESULTS

In April 2015, a set of 33 CDPs were published, which included updates to 28 CDPs and five new CDPs. The set includes four new operations CDPs to go along with three updated operations CDPs, which cover stoppages, availability, electrical efficiency, load profiles, and cumulative output. The operations CDPs have now been segmented into fuel cells that are less than 100 kW and greater than 100 kW. New load profile CDPs for fuel cell units greater than 100 kW show the frequency of operation time at different load fractions and the ratio of electrical output per rated capacity of the fuel cell unit, separately, for both base load and load following units (Figure 1 and Figure 2). The load profiles show that base load units operate mostly in the 90–100% load fraction as expected, load following units have operation time at a wider range, and some units spend time above 100% rated capacity. We have also validated that the electrical efficiency for fuel cells greater than 100 kW has exceeded the 2015 DOE Technology Validation target of 43% based on the lower heating value of hydrogen (39% higher heating value of hydrogen) (Figure 3).

California's Self-Generation Incentive Program (SGIP) has helped deploy 397 fuel cell systems, for a total of 161 MW, since 2001. The fuel cell deployment increased 25% in 2014. These fuel cell deployments have shown that fuel cells may be applied with a wide variety of fuels, including renewable biogas from landfill, biomass, and digester sources. Natural gas is the dominant fuel type, accounting for 79% of projects and 69% of the capacity. Since 2011, electric-only fuel cell projects have been increasing at a rate (number and capacity) greater than other competing technologies, which include gas turbines, internal combustion turbines, microturbines, and pressure reduction turbines. The fuel cell electric projects now equal the number of internal combustion engines at 279 projects. Deployment numbers have increased even in a climate of declining incentive. Also, in 2014 fuel cell CHP systems neared the cost per kilowatt of gas turbines, and beat the cost when incentives were applied (Figure 4).

The average unit costs in the SGIP are significantly higher than the DOE target of $1,500/kW; however, SGIP costs may include additional costs that are not included in the DOE target. The average range, when differentiating by capacities (0–50 kW, 51–200 kW, 201–400 kW, 401+ kW), is $9,537–$11,275/kW without incentives and $5,620–$8,782/kW with incentives. Generally, larger projects (those with larger capacities) have lower unit costs and also receive more incentives.

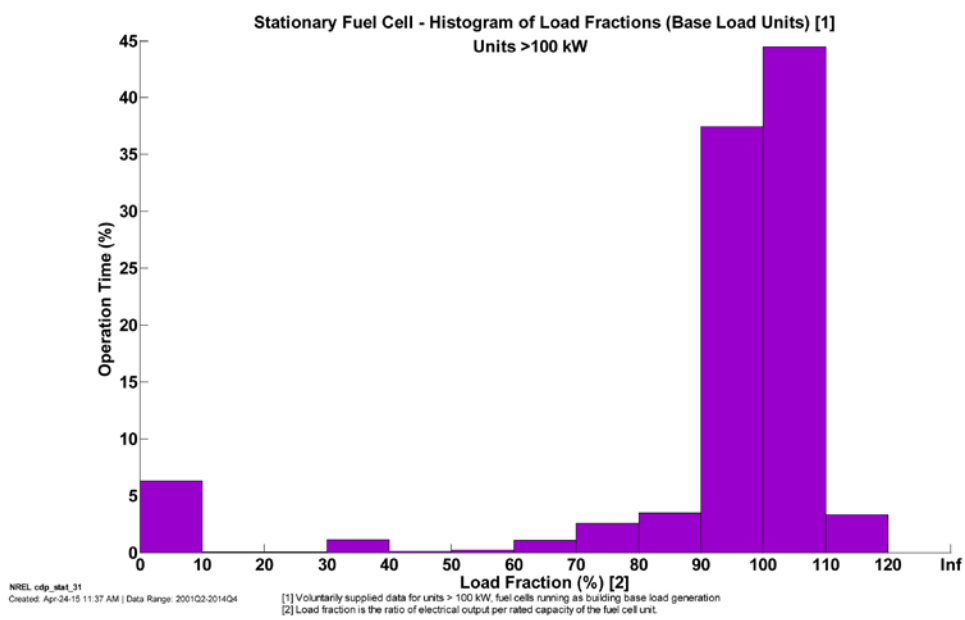

FIGURE 1. Histogram of load fractions for base load units >100 kW

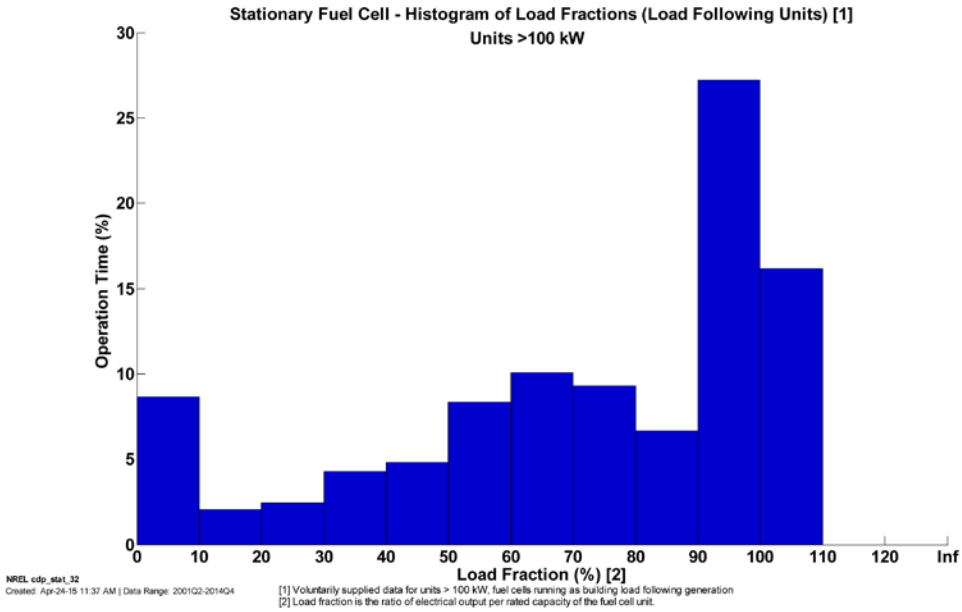

FIGURE 2. Histogram of load fractions for load following units >100 kW

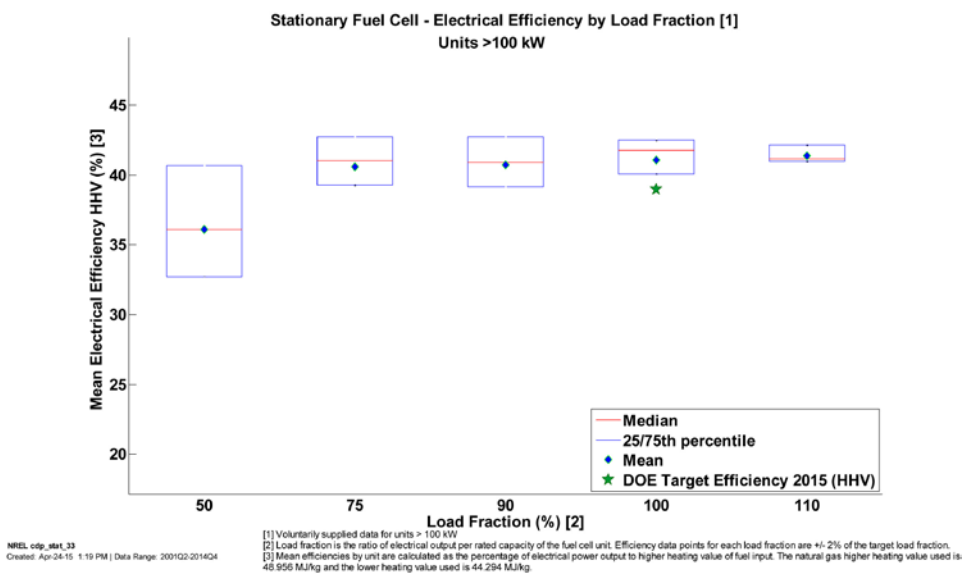

FIGURE 3. Electrical efficiency by load fraction for units >100 kW

All CDPs are available at http://www.nrel.gov/hydrogen/proj_fc_systems_analysis.html.

CONCLUSIONS AND FUTURE DIRECTIONS

The California SGIP has been very successful in installing fuel cell systems. In recent years, fuel cell projects have been installed in greater numbers than other competing technologies, despite generally higher installed costs and decreasing incentive spending. This early market rollout is important for the stationary fuel cell industry in terms of real-world experience and the fuel cell deployments benefit that the SGIP has been extended to run through at least January 1, 2019.

We are exploring more avenues to acquire operations data that will help us expand the analyses and validate other technology validation targets.

Activities for the remainder of FY 2015 will include the following:

- FY 2015 Q4: Update all CDPs with current data from the SGIP and voluntary operations data submissions

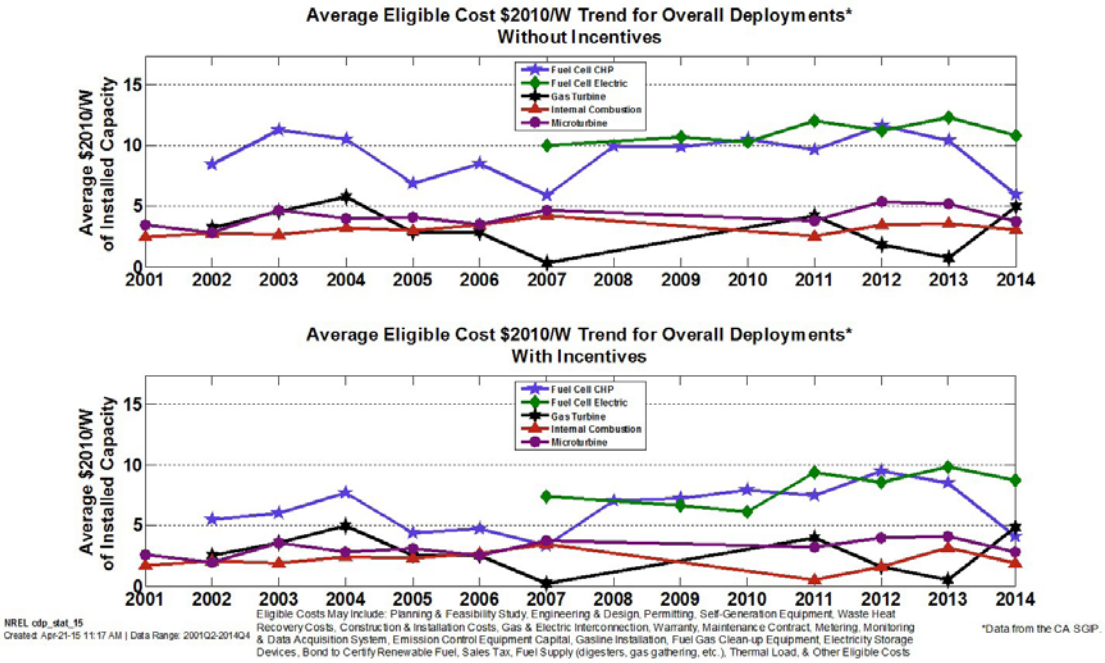

FIGURE 4. Average eligible cost by equipment type, including other distributed generation

- Expand analysis to include new CDPs that address availability and capacity factor of stationary fuel cells
- Look into other data partners (state and federal programs, original equipment manufacturers) for additional data relevant to DOE targets.

FY 2015 PUBLICATIONS/PRESENTATIONS

1. Saur, G., Kurtz, J., Ainscough, C., Sprik, S. "Stationary Fuel Cell Evaluation." DOE Annual Merit Review meeting, June 2015. (presentation)

2. "Stationary Fuel Cell Systems Analysis Project: Partnership Opportunities." Golden, CO: National Renewable Energy Laboratory, published June 2015. (fact sheet)

3. Saur, G., Kurtz, J., Ainscough, C., Sprik, S., Post, M. "Stationary Fuel Cell System Composite Data Products: Data through Quarter 4 of 2014." Golden, CO: National Renewable Energy Laboratory, published April 2015. (report)

4. Saur, G., Kurtz, J., Ainscough, C., Peters, M. "VII.2 Stationary Fuel Cell Evaluation." DOE FY 2014 Annual Merit Review Proceedings. Washington, D.C., published November 2014. (report)

VII.14 Dynamic Modeling and Validation of Electrolyzers in Real Time Grid Simulation

Rob Hovsapian
Idaho National Laboratory (INL)
750 University Blvd.
Idaho Falls, ID 83406
Phone: (208) 526-8217
Email: rob.hovsapian@inl.gov

DOE Manager
Jason Marcinkoski
Phone: (202) 586-7466
Email: Jason.Marcinkoski@ee.doe.gov

Project Start Date: June 29, 2015
Project End Date: September 30, 2017

Overall Objectives

- Validation of the benefits of hydrogen electrolyzers through grid services and hydrogen sale to fuel cell vehicles for full-scale deployment
- Characterization of the potential and highest economic value based on the needs of multiple stakeholders for specific grid regions
- Demonstration of the reliable, fast-reacting performance of hydrogen-producing electrolyzers for at-scale energy storage devices
- Verification of the communications and controls needed for successful participation in electricity markets and demand response programs

Fiscal Year (FY) 2015 Objective

- Develop a geographically distributed testbed for real-time simulation of electrolyzer hardware with models of industry-standard transmission and distribution systems

Technical Barriers

This project addresses the following technical barriers from the Technology Validation section of the Fuel Cell Technologies Office (FCTO) Multi-Year Research, Development, and Demonstration (MYRDD) Plan:

(B) Lack of Data on Stationary Fuel Cells in Real-World Operation

(G) Hydrogen from Renewable Resources

(H) Hydrogen and Electricity Co-Production

Contribution to Achievement of DOE Technology Validation Milestones

This project will contribute to achievement of the following DOE milestones from the Technology Validation section of the FCTO MYRDD Plan:

- Milestone 3.9: Validate large-scale system for grid energy storage that integrates renewable hydrogen generation and storage with fuel cell power generation by operating for more than 10,000 hours with a round-trip efficiency of 40%. (4Q, 2020)

✧ ✧ ✧ ✧ ✧

APPROACH

In order to meet project objectives, a 120-kW electrolyzer is being used, located at the National Renewable Energy Laboratory's (NREL's) Energy Systems Integration Facility. A simulation model of the distribution system is hosted in a computer located at NREL connected to a Real-Time Digital Simulator (RTDS®), and a simulation model of the transmission system is hosted in a computer located at INL, also connected to an RTDS®. RTDS®-to-RTDS® communication is established for simulation of both the transmission and distribution system in real time. A schematic for the distributed co-simulation is shown in Figure 1. In FY 2016, the electrolyzer will be connected to the distribution system. Using this power hardware-in-the-loop (PHIL) strategy, it will be possible to quantify the value of fuel cells and electrolyzers from specific grids and hydrogen refueling stations, and meet other objectives of the project.

FY 2015 ACCOMPLISHMENTS

- Completed the RTDS® model of Institute of Electrical and Electronics Engineers (IEEE) 13 node feeder system with electrolyzer [1,2]
- The model was sent to NREL and was utilized during the RTDS®-to-RTDS® demonstration to Dr. Danielson (Assistant Secretary, U.S. Department of Energy)

FUTURE DIRECTIONS

- Develop and test the 120-kW electrolyzer interface with RTDS® at NREL; develop final details of the locations that will be simulated and tested within the San Francisco Bay area served by Pacific Gas and Electric (PG&E)

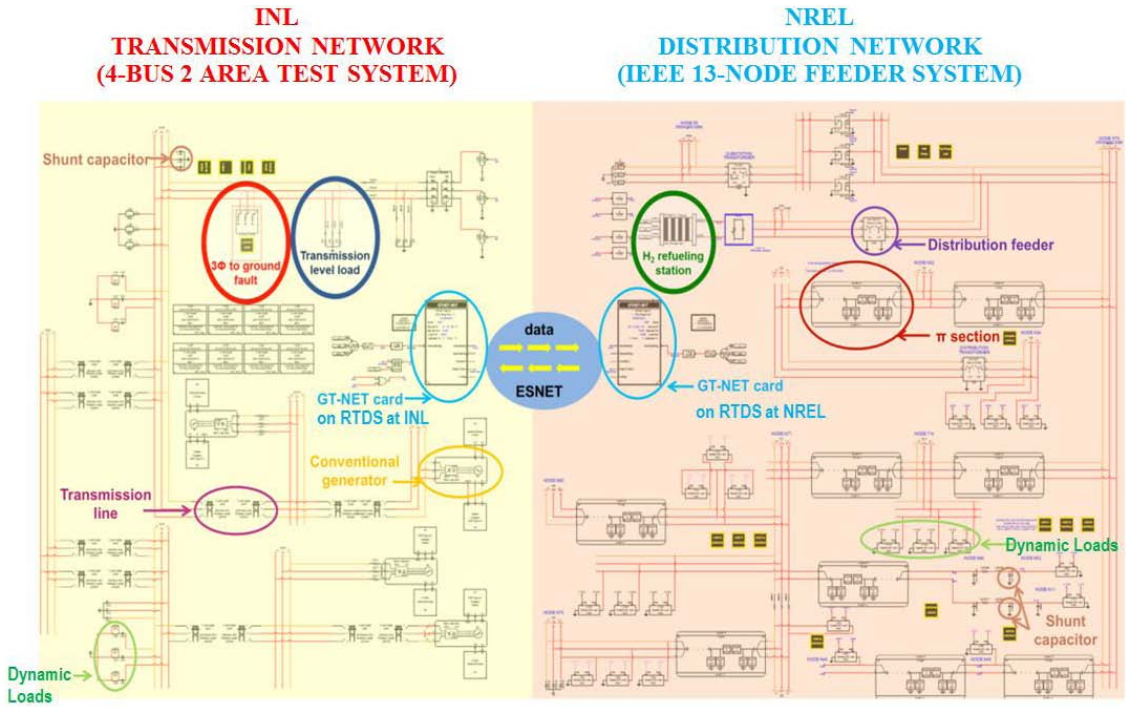

FIGURE 1. Representation of the simulation model spread across INL and NREL

- Perform distributed real-time PHIL simulations with the electrolyzer connected to the IEEE 13 node-based microgrid that is modeled as part of FY 2015 work
- Develop suitable PG&E distribution network model in RTDS® and dynamically test scenarios under existing demand response programs
- Modify the PG&E distribution network model (expand) in RTDS® in order to accommodate future refueling stations as planned in the San Francisco Bay area served by PG&E
- Perform distributed real-time simulation for the expanded distribution networks with future refueling stations under novel demand programs

SPECIAL RECOGNITIONS & AWARDS/ PATENTS ISSUED

1. Geographically distributed co-simulation using RTDS was covered in *SmartGrid News* (May 6, 2015).

REFERENCES

1. Kersting, W.H. "Radial distribution test feeders." *Power Engineering Society Winter Meeting, 2001. IEEE*. Vol. 2. IEEE, 2001.

2. Kuffel, R., et al. "RTDS-a fully digital power system simulator operating in real time." *WESCANEX 95. Communications, Power, and Computing. Conference Proceedings, IEEE*. Vol. 2. IEEE, 1995.

VIII.0 Safety, Codes & Standards Sub-Program Overview

INTRODUCTION

The Safety, Codes and Standards sub-program identifies research and development (R&D) needs and performs high priority R&D to provide an experimentally validated fundamental understanding of the relevant physics, critical data, and safety information needed to define the requirements for technically sound and defensible codes and standards. This information is used to facilitate and enable the widespread deployment and commercialization of hydrogen and fuel cell technologies. In Fiscal Year (FY) 2015, the Sub-Program continued to identify and evaluate safety and risk management measures that can be used to define the requirements and close the gaps in codes and standards in a timely manner.

The sub-program promotes collaboration among government, industry, codes and standards development organizations (CDOs and SDOs), universities, and national laboratories in an effort to harmonize regulations, codes, and standards (RCS) both internationally and domestically. Communication and collaboration among codes and standards stakeholders, the federal government, industry, national labs, and trade associations are emphasized in order to maximize the impact of the sub-program's efforts and activities in international RCS development.

The sub-program has achieved accomplishments in R&D for codes and standards support. In FY 2015, the Hydrogen Risk Assessment Models (HyRAM) were released for alpha testing by various stakeholders, including industry representatives. This software enables quantitative risk assessment (QRA) and performance-based design, and incorporates hydrogen behavior models also developed through the sub-program. A model for release of liquid hydrogen was validated and will be used, along with the QRA tool, to inform separation distances in the 2019 code cycle for National Fire Protection Association (NFPA) 2/55. Development continues for a hydrogen contaminant detector with demonstrated sensitivity to both carbon monoxide (CO) and hydrogen sulfide (H_2S) at Society for Automotive Engineers (SAE) J2719 levels. In addition, the Continuous Codes and Standards Improvement (CCSI) process was initiated, allowing learnings from field deployment to inform code and standard development. One example of CCSI is an NFPA 2/55 task group that was formed to examine the setback distances for both gaseous and liquid hydrogen and to consider possible mitigation strategies that could be implemented to reduce setback distance requirements. Finally, the sub-program is working to support station deployment through utilizing alternative code compliance methods such as those found in NFPA Chapter 5.

The sub-program continues to utilize the expertise of the Hydrogen Safety Panel (HSP) to disseminate relevant information and implement safe practices pertaining to the operation, handling, and use of hydrogen and fuel cell technologies in sub-program-funded projects. HSP, with over 400 years of combined experience in the hydrogen industry, provides recommendations on the safe conduct of Federally-funded project work as well as lessons learned and best practices that can be of broad benefit to the sub-program. The sub-program continues to share current safety information and knowledge with the community through the launch of H2Tools.org, which, in addition to consolidating existing resources (i.e., Hydrogen Lessons Learned Database), serves as a centralized resource for hydrogen safety information, news, and user-specific content.

In addition, extensive external stakeholder input from the fire-protection community, academia, automobile manufacturers, and energy, insurance, and aerospace sectors, is used to create and enhance safety knowledge tools for emergency responders and authorities having jurisdiction (AJHs). The sub-program has renewed its emphasis on ensuring the continual availability of safety knowledge tools, distributed via an array of media outlets, to reach the largest number of safety personnel possible. During FY 2015, the sub-program's training for code officials and first responders reached more than 35,000 individuals through our online and classroom trainings.

GOAL

The sub-program's key goals are to provide the validated scientific and technical basis required for the development of codes and standards, to promulgate safety practices and procedures to allow for the safe deployment of hydrogen and fuel cell technologies, and to ensure that best safety practices are followed in Fuel Cell Technologies Office activities.

OBJECTIVES

The sub-program's key objectives are to:

- Support and facilitate development and promulgation of essential codes and standards to enable widespread deployment and market entry of hydrogen and fuel cell technologies and completion of all essential domestic and international RCS.
- Conduct R&D to provide critical data and information needed to define requirements in developing codes and standards.
- Ensure that best safety practices underlie research, technology development, and market deployment activities supported through DOE-funded projects.
- Develop and enable widespread sharing of safety-related information resources and lessons learned with first responders, AHJs, and other key stakeholders.

FY 2015 STATUS

The sub-program continues to support R&D to provide the technical basis for codes and standards development with projects in a wide range of areas, including fuel specification, separation distances, materials and components compatibility, and hydrogen sensor technologies. Utilizing the results from these R&D activities, the sub-program continues to actively participate in discussions with SDOs such as the NFPA, the International Code Council (ICC), SAE International, the CSA Group, and the International Organization for Standardization (ISO) to promote domestic and international collaboration and harmonization of RCS.

The following websites provide additional, up-to-date information relevant to the status of the sub-program's activities.

- H2Tools (http://h2tools.org/)
  The following resources are available on the H2Tools.org site.
  - Technical Reference for Hydrogen Compatibility of Materials (www.ca.sandia.gov/matlsTechRef/ also available at https://h2tools.org/tech-ref)
  - Hydrogen Lessons Learned Database (https://h2tools.org/lessons)
  - Hydrogen Bibliographic Database (https://h2tools.org/bibliography)
  - Hydrogen Safety Best Practices Manual (https://h2tools.org/bestpractices)
  - National Hydrogen and Fuel Cell Emergency Response Training Resource (https://h2tools.org/fr/nt)
- Hydrogen Safety Training for Researchers (www.h2labsafety.org)
- Introduction to Hydrogen for Code Officials (www.hydrogen.energy.gov/training/code_official_training/)
- Hydrogen Safety for First Responders (www.hydrogen.energy.gov/firstresponders.html)

FY 2015 KEY ACCOMPLISHMENTS

The sub-program continued to make progress in several key areas, including the following.

Hydrogen Behavior, Risk Assessment, and Materials Compatibility (Sandia National Laboratories)

- Released HyRAM v1.0 for alpha testing by industry stakeholders; HyRAM is a first-of-its-kind software tool that enables quantitative risk assessment through reliability data and engineering models and includes a physics mode
- Developed a template of a viable performance-based design (PBD) approach to code compliance that facilitates industry use, AHJ acceptance, and leads to improved PBD requirements in the codes
- Initiated new capability for testing hydrogen embrittlement of stainless steels at sub-ambient temperature

Hydrogen Quality (Los Alamos National Laboratory [LANL])

- Demonstrated sensitivity to CO and H_2S at SAE J2719 levels (0.2 ppm and 4 ppb, respectively) with detection within minutes

Coordination of Codes and Standards Development, Domestic and International (National Renewable Energy Laboratory [NREL])

- Formed a group of code experts through the Fuel Cell Hydrogen Energy Association's Transportation Working Group called the Hydrogen Code Improvement team to address gaps between the International Code Council (I-codes) and NFPA 2
- Developed a plan to revise the liquid hydrogen setback distances in NFPA 2/55 and develop a process for converting mitigation measures into reduced setback distances

Component Testing (NREL)

- Developed a test apparatus for pressure relief valves
- Demonstrated repeatable operation of temperature cycling for accelerated life cycle testing of components

Hydrogen Safety Panel, Databases, Props, and First Responders (Pacific Northwest National Laboratory [PNNL])

- H2Tools.org was launched, consolidating existing safety and knowledge resources into a central location alongside newly added functionality and content.
- PNNL released National Hydrogen and Fuel Cell Emergency Response Training Resource, which is a regularly updated, downloadable resource that allows training for first responders on a local basis with consistent information.
- HSP continues to support best hydrogen safety practices, with 18 project reviews in the past year and supporting state initiatives. HSP's 2013 white paper, "Safety of Hydrogen Systems Installed in Outdoor Enclosures," supported new prescriptive requirements for hydrogen equipment enclosures in the 2016 version of NFPA 2.

Hydrogen Sensors (NREL and LANL)

- Validated hydrogen leak sensor in real-world station environment; investments since 2008 have turned the LANL/Lawrence Livermore National Laboratory-developed solid state electrochemical safety sensor into a commercially ready technology with sensitivity better than commercially available technologies (LANL)
- Developed a test apparatus for verifying tailpipe hydrogen emissions and initiated testing; demonstrated sampling rate of four times per second with accurate readings at low gas levels (NREL)

BUDGET

The sub-program received an appropriation of $7 million in FY 2015 (Figure 1). This allowed for sustained progress in key R&D and codes and standards development work. The President's FY 2016 budget request includes $7 million for Safety, Codes and Standards, which will ensure continuity in key R&D and focus areas as shown below. The R&D category includes such activities as hydrogen behavior, risk assessment and mitigation, materials compatibility, hydrogen fuel quality, metering, sensors, and component testing. The safety management and resources category includes the Hydrogen Safety Panel, databases, training, and training materials. The outreach category includes codes and standards, permitting, continuous codes and standards improvement, and resource dissemination.

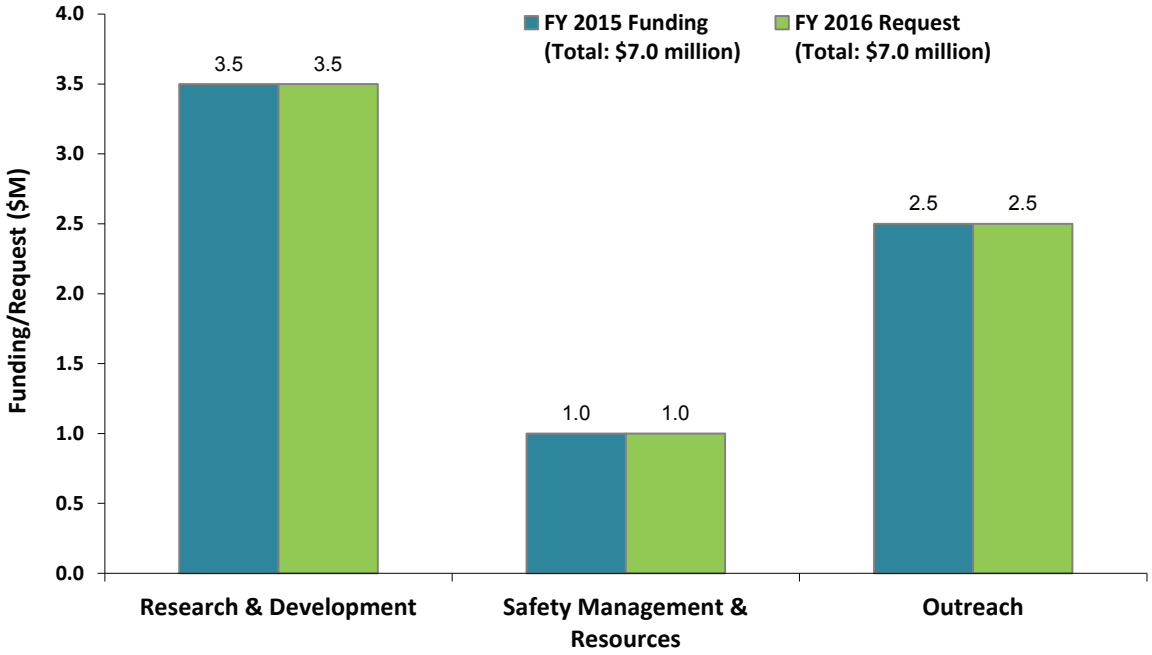

FIGURE 1. Safety, Codes and Standards R&D Funding. Subject to appropriations, project go/no-go decisions, and competitive selections. Exact amounts will be determined based on research and development progress in each area and the relative merit and applicability of projects competitively selected through planned funding opportunity announcements.

FY 2016 PLANS

The Safety, Codes and Standards sub-program will continue to work with CDOs and SDOs to develop technical information and performance data to enhance hydrogen-specific codes and standards. To address these needs, the sub-program will continue to support rigorous technical R&D, including assessment of materials compatibility for component designs and high pressure tank cycle testing, and continue to promote a performance-based QRA approach to assess risks and establish protocols to identify and mitigate risk. Future work will also focus on facilitating the permitting of hydrogen fueling stations and early market applications and testing, measurement, and verification of hydrogen fuel specifications.

The sub-program will continue to promote the domestic and international harmonization of test protocols for qualification and certification as well as the harmonization of RCS for hydrogen fuel quality and other key international standards. This will be enabled by working with the appropriate domestic and international organizations such as the NFPA, ICC, SAE International, the CSA Group, and ISO. The sub-program will also continue to participate in the International Partnership for Hydrogen and Fuel Cells in the Economy's RCS Working Group and the International Energy Agency's Hydrogen Implementing Agreement, both of which are engaged in hydrogen safety work.

Charles James
Safety, Codes & Standards Project Manager
Fuel Cell Technologies Office
Office of Energy Efficiency and Renewable Energy
U.S. Department of Energy
1000 Independence Ave., SW
Washington, D.C. 20585-0121
Phone: (202) 287-6223
Email: Charles.James@ee.doe.gov

VIII.1 Hydrogen Behavior and Quantitative Risk Assessment

Katrina Groth (Primary Contact), Ethan Hecht, Chris LaFleur, Alice Muna, John Reynolds (SAIC)
Sandia National Laboratories (SNL)
P.O. Box 5800 MS 0748
Albuquerque, NM 87185
Phone: (505) 844-6766
Email: kgroth@sandia.gov

DOE Manager
Will James
Phone: (202) 287-6223
Email: Charles.James@ee.doe.gov

Project Start Date: October 2003
Project End Date: Project continuation and direction determined annually by DOE

Overall Objectives

- Build tools to enable industry-led codes and standards revision and safety analyses to be based on a strong science and engineering basis
- Develop and validate hydrogen behavior physics models to address targeted gaps in knowledge
- Develop hydrogen-specific quantitative risk assessment (QRA) tools and methods to support regulations, codes and standards decisions and to enable performance-based design code compliance option

Fiscal Year (FY) 2015 Objectives

- Develop prototype Version 1.0 of the HyRAM toolkit/platform to facilitate use of hydrogen safety research in industry-led safety analyses
- Initiate HyRAM testing activities with external stakeholders by distributing the alpha version of the software to partners from industry, research, and government
- Design and construct laboratory for cold hydrogen release experiments by specifying the modifications needed for the Turbulent Combustion Lab and identifying and purchasing needed equipment
- Experimentally validate an equivalent source model for high pressure hydrogen by conducting release experiments in the Turbulent Combustion Lab

Technical Barriers

This project addresses the following technical barriers from the Hydrogen Safety, Codes and Standards section of the Fuel Cell Technologies Office Multi-Year Research, Development, and Demonstration Plan:

(A) Safety Data and Information: Limited Access and Availability

(F) Enabling National and International Markets Requires Consistent Regulations, Codes and Standards

(G) Insufficient Technical Data to Revise Standards

(L) Usage and Access Restrictions (parking structures, tunnels and other usage areas)

Contribution to Achievement of DOE Safety, Codes & Standards Milestones

This project will contribute to achievement of the following DOE milestones from the Safety, Codes and Standards section of the Fuel Cell Technologies Office Multi-Year Research, Development, and Demonstration Plan:

- Milestone 2.8: Publish risk mitigation strategies. (2Q, 2014)
- Milestone 2.10: Understand flame acceleration leading to transition to detonation. (4Q, 2014)
- Milestone 2.11: Publish a draft protocol for identifying potential failure modes and risk mitigation. (4Q, 2014)
- Milestone 2.13: Develop and validate simplified predictive engineering models of hydrogen dispersion and ignition. (4Q 2015)
- Milestone 2.19: Validate inherently safe design for hydrogen fueling infrastructure. (4Q, 2019)
- Milestone 4.7: Complete risk mitigation analysis for advanced transportation infrastructure systems. (1Q, 2015)
- Milestone 4.8: Revision of NFPA 2 to incorporate advanced fueling storage systems and specific requirements for infrastructure elements such as garages and vehicle maintenance facilities. (3Q, 2016)

FY 2015 Accomplishments

- Developed and copyrighted HyRAM Version 1.0
- Initiated HyRAM user testing by inviting 22 external stakeholders

- Developed detailed design and purchased major equipment needed for lab modifications necessary to conduct experiments on cryogenic hydrogen releases
- Conducted high pressure hydrogen release experiments by conducting experiments with releases up to 60 bar and developed empirical correlations that give boundary conditions to a reduced-order equivalent source model

✧ ✧ ✧ ✧ ✧

INTRODUCTION

DOE has identified safety, codes, and standards as a critical barrier to the deployment of hydrogen, with key barriers related to the availability and implementation of technical information in the development of regulations, codes, and standards. This project provides the technical basis for assessing the safety of hydrogen fuel cell systems and infrastructure using QRA and physics-based models of hydrogen behavior. The risk and behavior tools that are developed in this project are motivated by and shared directly with the committees revising relevant codes and standards, thus forming the scientific basis to ensure that code requirements are consistent, logical, and defensible.

APPROACH

This work leverages Sandia's unique experimental and modeling capabilities and combines these efforts with stakeholder engagement and international leadership. The behavior of hydrogen releases is examined using state-of-the-art diagnostics in the Turbulent Combustion Laboratory. Results of these experiments are used to develop and validate predictive engineering tools for flame initiation, flame sustainment, radiation patterns, and overpressures. The resulting behavior models provide the foundation for QRA modeling efforts, which include scenario analysis, consequence modeling, and quantification of risk. These integrated hydrogen behavior and QRA models are then applied to relevant technologies and systems to provide insight into the risk level and risk mitigation strategies with the aim of enabling the deployment of fuel cell technologies through revision of hydrogen safety, codes, and standards.

RESULTS

HyRAM Toolkit Development

Code committees and industry are both interested in using QRA to enable code development and code compliance for hydrogen systems. Gaps and limited availability of QRA tools for hydrogen form a barrier to this goal. This core research activity addresses the hydrogen QRA tool gap by integrating validated models and data into an engineering tool called HyRAM.

The HyRAM package will enable installation designers, and code and standards development organizations to conduct consequence modeling and QRA with state-of-the-art, validated science and engineering models (see Figure 1). Near-term uses of HyRAM are focused on the needs of codes and standards developers (e.g., National Fire Protection Association [NFPA] 2 and International Organization for Standardization [ISO]-TR-19880). HyRAM can be used to support the establishment of safety distances and other mitigation credits, and furthermore can be used to enable a performance-based compliance option within these codes and standards. Longer-term, HyRAM is anticipated to support development of safety cases and design decisions for user-defined hydrogen installations, and can also be used to demonstrate improvements in facility safety.

HyRAM development was initiated in FY 2014, and during FY 2015 we completed and copyrighted HyRAM Version 1.0 (build number 1.0.0.280). The HyRAM 1.0 toolkit integrates deterministic and probabilistic models for quantifying scenario likelihood, predicting physical effects, and characterizing the impact of hydrogen hazards on people and structures. The current build of HyRAM incorporates generic probabilities for leaks from nine types of hydrogen equipment, generic probabilities for hydrogen ignition, expressions for calculating scenario likelihood and individual risk, probabilistic models for the impact of heat flux on humans and structures, and experimentally validated models of hydrogen jet flames and gaseous hydrogen releases (notional nozzle models and plumes). New modules developed in FY 2015 include the curved flame model (developed and experimentally validated by SNL in 2013) to replace the previous "straight flame" model (developed by SNL in 2007). During FY 2015 work began on integrating the necessary modules to enable calculation of deflagration overpressures resulting from confined hydrogen releases. This overpressure module is being tested internally and is expected to be stable by the end of 2015.

The flexible architecture of the HyRAM framework enables the incorporation of additional physical models, including liquid hydrogen release and dispersion. On the physical model side, future modifications will provide ability to calculate physical effects of liquid hydrogen releases and subsequent ignitions. The models will also be updated to include the effects of a cross wind on plume and flame trajectories, and the submodels (e.g., the jet flame model) will be kept current as scientific consensus changes. For QRA outputs, future modifications will provide cut-sets for Fault Trees and reliability importance measures for risk scenarios.

Initiate HyRAM Testing and Documentation

User feedback is a critical aspect of creating enabling tools and guidance. During FY 2015 we initiated usability

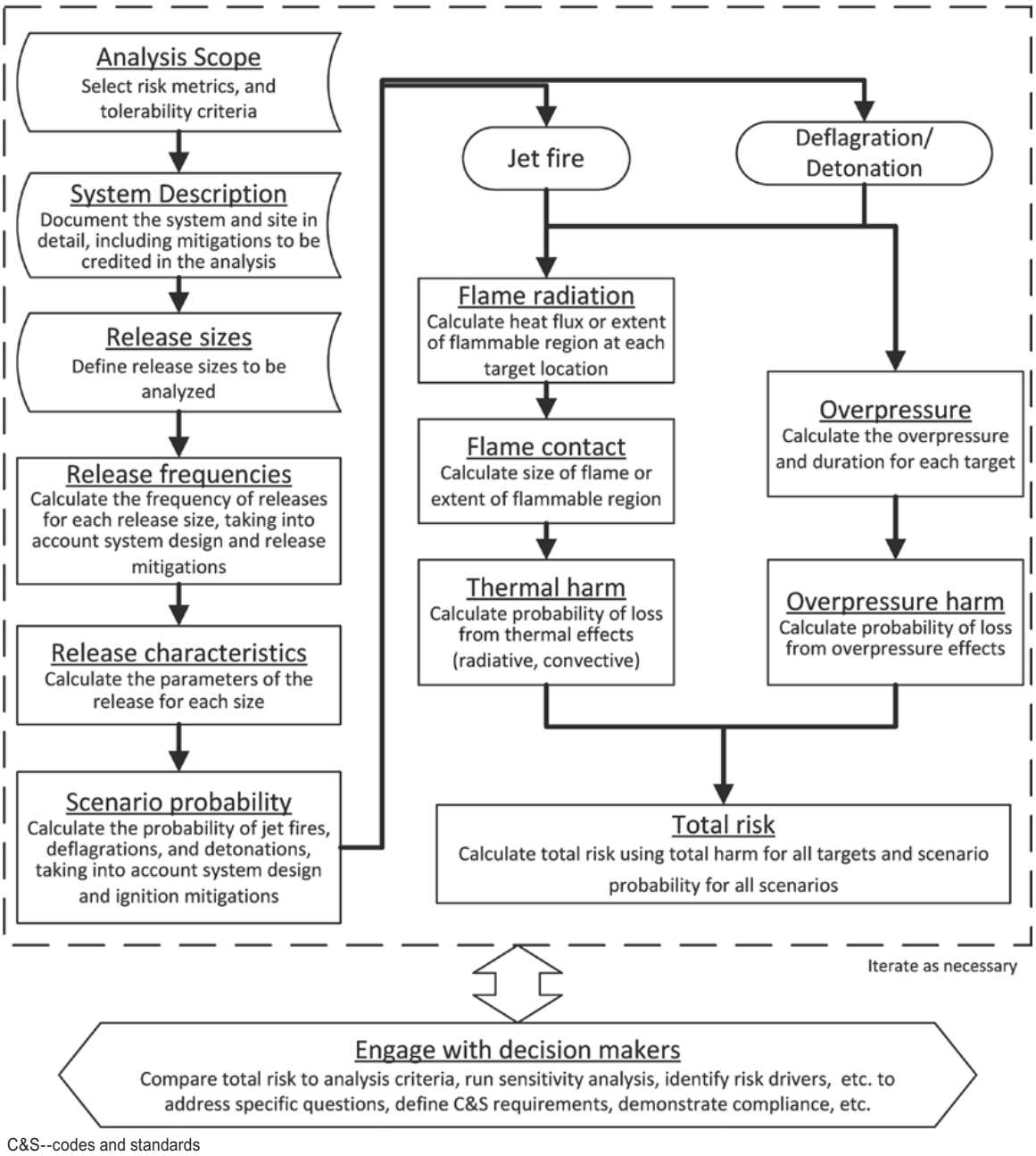

FIGURE 1. Quantitative risk assessment methodology implemented in HyRAM toolkit

testing on HyRAM 1.0.0.280 with a small number of external stakeholders from various aspects of the hydrogen community. Currently, seven stakeholders have signed non-disclosure agreements to gain access to HyRAM 1.0 versions, and Sandia is in various stages of the license process with 15 additional stakeholders. The current alpha testing activities are focused on obtaining unstructured user feedback on the look and feel of the HyRAM prototype. Future external testing activities will include planning for more formal user feedback.

Design and Construct Laboratory for Cold Hydrogen Release Experiments

Stations that have liquid hydrogen delivered and/or store hydrogen cryogenically can serve a larger number of customers per day, and can have favorable economics over stations that have high pressure gas delivered. However, the codes and standards that govern the siting of cryogenic hydrogen have separation distances that are often prohibitively large (e.g., public assembly areas and building openings or air intakes that must be 75 ft away from the

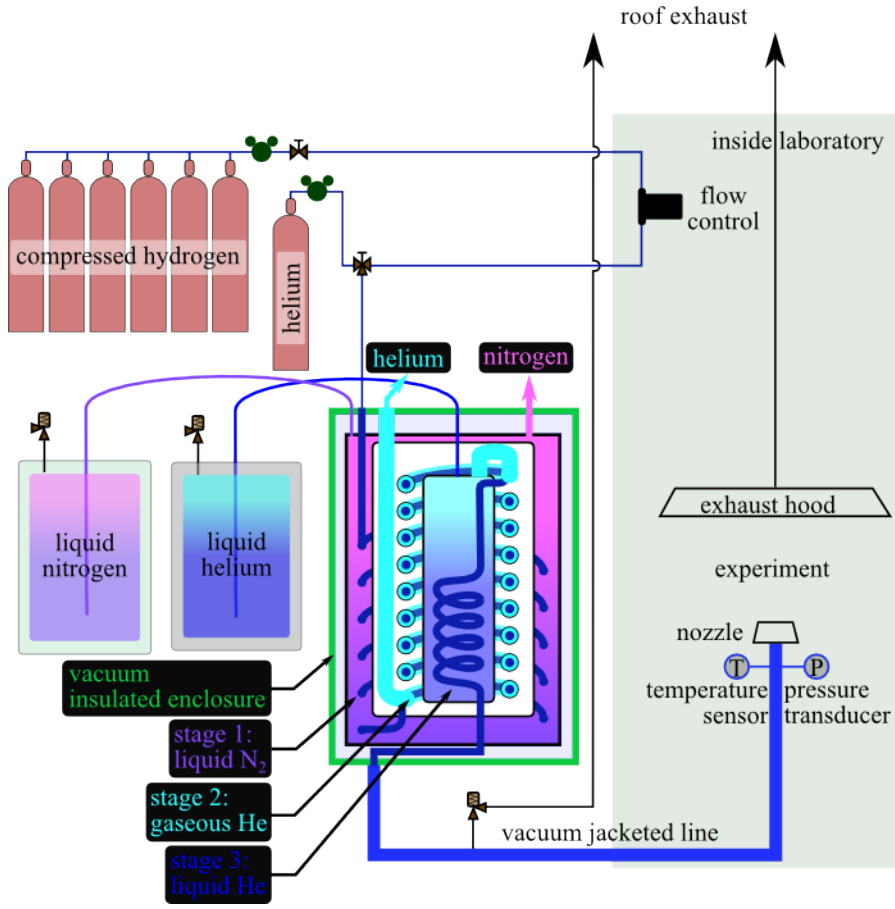

FIGURE 2. Sketch of the planned cryogenic hydrogen release experiment. Compressed hydrogen is cooled in a unique three-stage heat exchanger by liquid nitrogen, cold gaseous helium, and liquid helium.

liquid hydrogen storage). To address this issue, an experiment in the Turbulent Combustion Laboratory has been designed to characterize the dispersion characteristics of cryogenic hydrogen. The experiment will have well controlled releases (i.e., hydrogen temperature, pressure, ambient conditions) characterized by high fidelity diagnostics (e.g., planar laser Rayleigh scattering, Schlieren imaging). This data will be used to develop and validate models for cryogenic hydrogen releases, enabling revision of the safety, codes and standards for cryogenic hydrogen.

In continuation of previous efforts to achieve cryogenic release capabilities, the cryogenic hydrogen release experiment was designed, equipment was ordered, and assembly in the laboratory began in FY 2015. A sketch of the design is shown in Figure 2. A gaseous hydrogen flow will be controlled in the lab using a mass flow controller or pressure drop across a critical flow orifice. This metered gaseous hydrogen will then flow back outside the lab to be cooled in a unique three-stage heat exchanger, first with liquid nitrogen, then with cold gaseous helium, and finally, with liquid helium to near its saturation point. The cold hydrogen will then flow back into the laboratory through a vacuum jacketed line. The temperature and pressure of the hydrogen will be monitored near the release point, and interchangeable orifices, with a range of diameters (around 1 mm) will allow jets/plumes of hydrogen to be studied in the laboratory. Initial experiments will focus on the dispersion characteristics, with other experiments planned to study ignition (using a well-controlled laser-spark) and the impact of barrier walls and other risk mitigation strategies.

Experimentally Validate Equivalent Source Model for High Pressure Hydrogen

When a pressurized gas flowing through a restriction (orifice) is above a critical pressure ratio (1.9 for hydrogen), the flow chokes at the restriction point, and the mass flow rate through the orifice is only dependent on the upstream (high pressure) conditions. Downstream of the flow restriction, this dense gas must expand to the atmospheric conditions. In this expansion region, there are often shocks and complex flow structures that are challenging to model (a high mesh resolution and significant computational resources are required for computational fluid dynamics). For reduced-

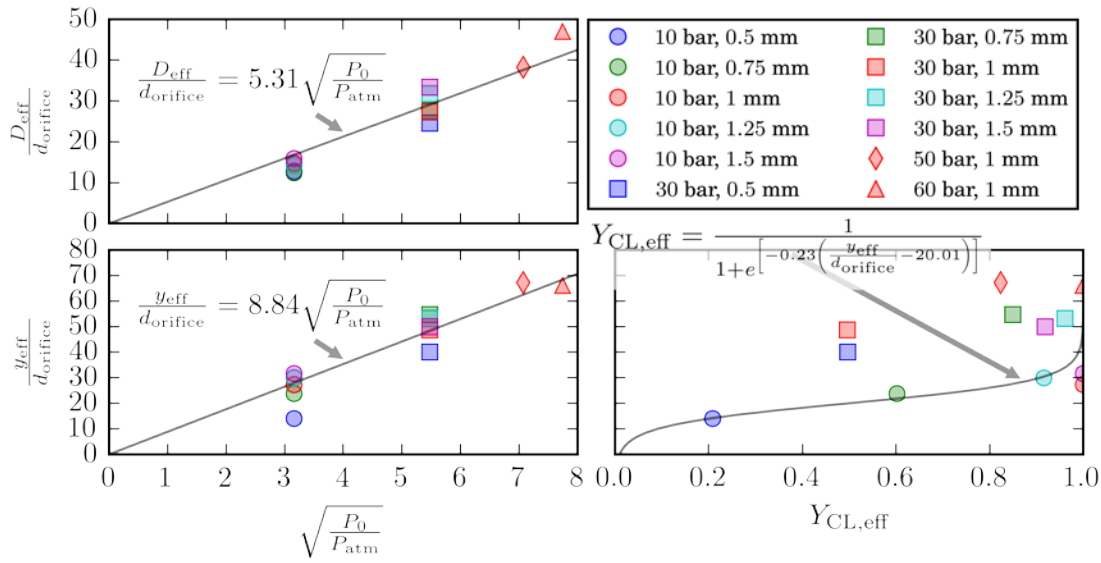

FIGURE 3. Effective leak diameter (upper left), starting point (lower left) and initial mole fraction hydrogen (lower right) for an under-expanded hydrogen jet. Fits to the data are also shown on the figure.

order models, where Gaussian shaped flow characteristics (e.g., mean velocity, mean concentration) are transported along a jet/plume streamline, a constant pressure is often assumed, and the conditions at the orifice cannot be used as inputs to the model. Therefore, in computation fluid dynamics and reduced-order models, an equivalent orifice is commonly used, giving the same downstream characteristics as the high pressure release, but the equivalent source (orifice) is at atmospheric pressure.

Several authors have developed equivalent source models for hydrogen, with varying assumptions and conservation equations. In FY 2015, we took data on hydrogen releases up to 60 bar in collaboration with a visiting researcher from Tsinghua University. This data will enable Sandia to eliminate the ambiguity in these equivalent source models and develop a de facto model. We came up with empirical correlations that scale as the square root of the stagnation pressure to the ambient pressure, to give boundary conditions to a reduced-order model for high pressure releases of hydrogen. The correlations are shown in Figure 3. The data have led to questions regarding several uncertain parameters in the reduced-order model (such as the relative velocity to concentration spreading ratio) and the default values we have been using for these parameters.

CONCLUSIONS AND FUTURE DIRECTIONS

The prototype HyRAM software toolkit provides a platform for modeling the safety of hydrogen systems, which enables industry-led analyses with state-of-the-art hydrogen models. HyRAM development activities are focused on adding capabilities necessary to inform near-term regulations, codes, and standards needs, including those from NFPA 2 and ISO TC197 WG24.

- (future) Extend HyRAM prototype (internal version) to include capability to develop and modify fault trees
- (future) Add visualization capability for the overpressure, plume, and layering behavior models
- (future) Define modules to assess risk-informed separation distances for liquid hydrogen (LH_2)
- (future) Scope initial interface for web-based version of HyRAM for highly accessible (web-based/app) tool for enabling end-users to implement these algorithms

Experiment was designed to develop predictive behavior models for liquefied hydrogen releases which are necessary to improve code requirements limiting the deployment of LH_2 systems.

- (future) Conduct liquid/cryogenic hydrogen release experiments and develop validated LH_2 release model
- (future) Continue experimental work to generate needed validation data and develop new necessary science-based models (e.g., wall interactions)

FY 2015 PUBLICATIONS/PRESENTATIONS

1. K.M. Groth, "Hydrogen behavior and Quantitative Risk Assessment." Presented at the 2015 DOE Hydrogen and Fuel Cells Program Annual Merit Review, June 9, 2015.

2. K.M. Groth. "H2 safety integration toolkit: HyRAM." Presented at the IEA HIA Task 37 Kick-off meeting, Karlsruhe, Germany, April, 2015.

3. E. Hecht, C. LaFleur, I. Ekoto "Cryogenic Hydrogen Release Modeling Validation – Update for Hydrogen Safety Panel." Presentation at Hydrogen Safety Panel Public Meeting, Sacramento, CA, March 2015.

4. K.M. Groth and C. LaFleur "HyRAM demo." Presentation to Kathleen Almand, director of Fire Protection Research Foundation (FPRF), February 2015.

5. K.M. Groth "Hydrogen Quantitative Risk Assessment R&D Needs." Presentation to US DRIVE Hydrogen Codes & Standards Tech Team, February 2015.

6. John T. Reynolds. *HyRAM Testing Strategy and Quality Design Elements*. SAND2014-20676. Sandia National Laboratories, November 2014.

7. Owen T. Parkins. *HyRAM Testing Script*. SAND2014-20522. Sandia National Laboratories, November 2014.

8. E.S. Hecht, I.W. Ekoto. "Vision for validating the liquid hydrogen plume model at temperatures less than 80K." Presentation at HySAFE research priorities workshop, Washington DC, 11 November 2014.

9. K.M. Groth. "HyRAM model integration platform." Presentation at HySAFE research priorities workshop, Washington, DC, 10 November 2014.

10. K.M. Groth. "QRA Tools - Gaps, Methods, Models Tools." Presentation at HySAFE research priorities workshop, Washington, DC, 10 November 2014.

11. E.S. Hecht. "State of the art for gaseous release models." Presentation at HySAFE research priorities workshop, Washington DC, 10 November 2014.

12. C. San Marchi. "Trends in Hydrogen Research in the United States" Presentation at the Korean Society of Mechanical Engineers, GwangJu, Korea, November 2014

13. Ekoto, I.W., Hecht, E., San Marchi, C., Groth, K.M., LaFleur, A.C., Natesan, N., Ciotti, M. & Harris, A. *Liquid Hydrogen Release and Behavior Modeling: State-of-the-Art Knowledge Gaps and Research Needs for Refueling Infrastructure Safety.* SAND2014-18776. Sandia National Laboratories, October, 2014.

VIII.2 Component Standard Research and Development

Robert Burgess (Primary Contact), Matthew Post, Arlen Kostival, William Buttner, Carl Rivkin
National Renewable Energy Laboratory (NREL)
15013 Denver West Parkway
Golden, CO 80401-3305
Phone: (303) 275-3823
Email: robert.burgess@nrel.gov

DOE Manager
Will James
Phone: (202) 287-6223
Email: Charles.James@ee.doe.gov

Subcontractor
- Mark Mann, Spectrum Automation, Denver CO (pressure relief device test apparatus controls support)

Project Start Date: October 1, 2014
Project End Date: Project continuation and direction determined annually by DOE

Overall Objectives

- Accelerate the development of robust codes and standards required for commercialization of hydrogen technologies
- Identify and quantify failure modes exhibited in high pressure hydrogen components by researching operational information and by conducting laboratory controlled testing
- Support the development of hydrogen components through collaborative efforts with industry stakeholders to improve hydrogen dispenser safety and reliability
- Codify standards language that is based on the latest scientific knowledge by providing analytical, technical, and contractual support
- Contribute directly to codes and standards committee efforts to identify technology gaps, then work to define research and development needs required to close those gaps
- Develop laboratory testing capability and conduct research and development aimed at providing the basis for improved code language
- Collaborate with industry, university, and government researchers to develop improved analytical and experimental capabilities

Fiscal Year (FY) 2015 Objectives

- Complete design/build of pressure relief device test apparatus and begin cycle testing
- Plan FY 2016 activities, including hydrogen meter benchmarking project

Technical Barriers

This project addresses the following technical barriers from the Safety, Codes and Standards section of the Fuel Cell Technologies Office Multi-Year Research, Development, and Demonstration (MYRDD) Plan:

(A) Safety Data and Information: Limited Access and Availability

(C) Safety is Not Always Treated as a Continuous Process

(F) Enabling National and International Markets Requires Consistent RCS (Regulations, Codes, and Standards)

(G) Insufficient Technical Data to Revise Standards

(H) Insufficient Synchronization of National Codes and Standards

(J) Limited Participation of Business in the Code Development Process

(K) No Consistent Codification Plan and Process for Synchronization of R&D and Code Development

Contribution to Achievement of DOE Safety, Codes and Standards Milestones

This project will contribute to achievement of the following DOE milestones from the Safety, Codes and Standards sub-program section of the Fuel Cell Technologies Office MYRDD Plan:

- Milestone 2.19: Validate inherently safe design for hydrogen fueling infrastructure. (4Q, 2019)
- Milestone 3.1: Develop, validate, and harmonize test measurement protocols. (4Q, 2014)
- Milestone 4.3: Identify and evaluate failure modes. (Q3, 2013)
- Milestone 4.6: Completion of standards for critical infrastructure components and systems. (Q4, 2014)

FY 2015 Accomplishments

- Designed and built test apparatus for reliability and end of life testing of high pressure hydrogen components under high pressure and cyclic temperature conditions

in the Energy Systems Integration Facility (ESIF) high pressure test laboratory currently conducting testing and generating data for pressure relief devices

- Conducted hydrogen components webinar to disseminate information about high pressure hydrogen applications and current R&D activities at NREL; webinar included open question and answer session for providing feedback on component activities from stakeholders
- Held hydrogen metrology information exchange meeting at NREL to collaborate on issues related to National Institute of Standards and Technology (NIST) Handbook 44 metrology requirements for the sale of vehicle fuel; meeting was focused on collaboration with Japanese stakeholders and included NIST Fluid Metrology Group participation
- Finalized hydrogen meter benchmarking proposal and test plan; test program is designed to measure meter performance as a function of flow, pressure, and temperature
- Developed hydrogen fueling animation as aide for customer understanding of gaseous hydrogen fueling experience
- Continued support of hydrogen standards development through participation on technical committees, including Society of Automotive Engineers (SAE) Fuel Cell Interface, SAE Fuel Cell Safety, and National Fire Protection Association (NFPA) Hydrogen Technologies; NREL hosted a joint technical committee meeting between NFPA 2 and 52 technical committees

✧ ✧ ✧ ✧ ✧

INTRODUCTION

Hydrogen safety, codes and standards topics have been identified in the DOE Multi-Year Program Plan as a subject area where significant barriers need to be addressed. Developing robust codes and standards helps to ensure that hydrogen systems are safe and reliable, thereby enabling the acceptance and growth of hydrogen technologies. NREL is providing research and development support to these codes and standards through validation testing, analytical modeling, and product commercialization efforts. NREL has been tasked with these responsibilities as defined in the DOE MYRDD plan.

APPROACH

Hydrogen safety is being addressed by first identifying safety concerns, then developing appropriate test and analysis tasks that provide a technical basis for improved engineering best practices. Safety concerns are being compiled by direct discussion with key stakeholders, by leveraging existing data available through NREL's Technology Validation Program and by utilizing public outreach activities such as workshops and webinars. Identified safety concerns are prioritized, and then research and development tasks are aligned with the highest risk safety concerns. In general, the risk is defined by the combination of the severity and the likelihood of occurrence. Research and development results are then published for general use by stakeholders. Information is further disseminated through NREL outreach activities. Published results are also being used as a basis for improved hydrogen codes and standards.

NREL is participating on relevant codes and standards committees to help identify gaps and define research and development needs to close those gaps. Working at the committee level allows us to quickly identify areas that need R&D support and to work directly with the technical experts in planning a path forward. This process is instrumental in avoiding delays and setbacks in the development of new codes and standards and in the revision of existing codes and standards. Research and development support is being used to establish codes and standards language with solid technical basis.

RESULTS

NREL has been working toward identifying safety gaps and supporting R&D efforts for developing new and improved hydrogen codes and standards. Results reported here are for efforts specifically directed at component level standards and identified hydrogen safety concerns.

Codes and Standards Technical Committee Support—NREL participated on SAE safety and interface technical committees working on documents under revision including J2601, J2600, and J2579. NREL also supported NFPA 2 Hydrogen Technologies Code by hosting the joint meeting with NFPA 55, July 14–18, 2014. These two standards are on a synchronized revision schedule to simplify hydrogen content improvements.

NREL Hydrogen Component Webinar—NREL held a component webinar on February 4, 2015, to disseminate information on component gaps and R&D programs. Presentation material summarized NREL hydrogen component activities taking place in the Energy Systems Integration Facility (ESIF) laboratory. The webinar provides valuable input for component suppliers and system developers while providing opportunity for feedback to NREL.

Hydrogen Vehicle Fueling Animation – At the request of the SAE J2601 sponsor, NREL prepared a fueling animation that depicts the ramp rates, pressure holds and target conditions required under the SAE J2601 protocol. The animation will help fuel cell electric vehicles (FCEV) users understand the behavior of gaseous motor vehicle fueling.

The animation can be viewed at the following link. http://widgets-stage.nrel.gov/afdc/hydrogen-animation/

Pressure Relief Valve Failure Mode Demonstration—NREL is conducting qualitative reliability testing of hydrogen relief valves to better understand a known failure mode in high pressure hydrogen. This study is focused on determining the necessary and sufficient conditions needed to reproduce the known failure under laboratory controlled conditions. This data will be used as input for developing better performance-based standards. Performance-based standards need to be capable of failing product with known failure modes. This investigation is utilizing the high pressure test cell capability at NREL. Testing has been ongoing since Q2 FY 2015 and is planned to continue into FY 2016. Cycle testing temperature profiles are shown in Figure 1. The thermal transient required to heat and cool the relief valves is a limiting factor for the test design. Convective heat transfer is used in the thermal control box to optimize the number of cycles in a 24-hour period. At this point one valve failure has been detected as shown in Figure 2. During the start of a heating cycle a slow leak was detected, resulting in a system shutdown. Investigation of the leak identified the leak path was through the valve seat. The identified root cause is a valve nozzle–seat interface that was not able to follow the thermal expansion during the start of the heating cycle. Depressurizing and subsequent repressurization resulted in the valve reseating. Pressure relief device seating is a reliability concern and this failure is valuable data for capturing pressure relief device operational issues.

Component Crosscutting Accomplishments—NREL is conducting DOE funded component tasks under other subprograms. This includes a hydrogen meter benchmarking project aimed at quantifying the performance of flow meters and comparing results to NIST Handbook 44 requirements. These efforts have provided an opportunity to leverage safety, codes and standards objectives through crosscutting activities. These activities include regulations, codes, and standards (RCS) guidance for defining test protocols and design requirements for improved code requirements. Crosscutting metrology activities in FY 2015 also included an information exchange meeting with Japanese stakeholders on January 14, 2015. NIST Fluid Metrology Group was also represented at the meetings.

Research and Development Outreach Activities—Numerous outreach activities were conducted in conjunction with the DOE/NREL safety, codes and standards program. Outreach activities are used as a resource in soliciting industry feedback and identifying priorities for research and development tasks. Outreach tasks include contribution to key technical committees and working groups at H2USA, H2FIRST, the California Fuel Cell Partnership, and work with other key stakeholders. Other outreach activities in FY 2015 include participation on the UL Renewable Energy Council meetings being held April 27–29, 2015, and discussions about component testing activities with CSA at their high pressure hydrogen test laboratory in Langley, British Columbia.

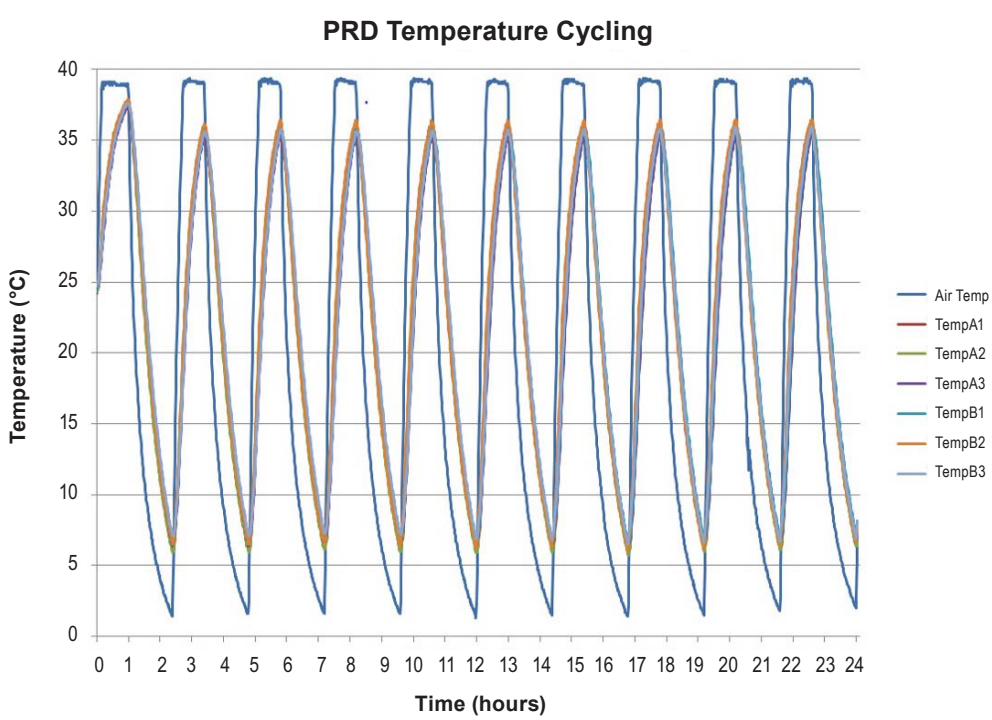

FIGURE 1. Pressure relief device thermal cycles

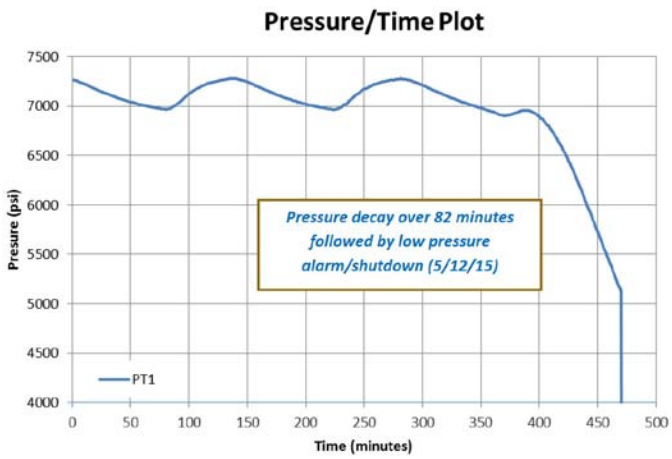

FIGURE 2. Pressure relief device seat failure

CONCLUSIONS AND FUTURE DIRECTIONS

NREL has identified numerous opportunities to further improve the inherent safety of high pressure hydrogen systems that are designed to serve FCEV markets. These opportunities must be pursued through a variety of means, including failure mode testing investigations, root cause analysis and codes and standards development. Future direction will include R&D programs that utilize existing ESIF laboratory facilities for component and system level testing.

FY 2015 PUBLICATIONS/PRESENTATIONS

1. "Component Standard Research and Development," DOE Annual Merit Review, June 9, 2015.

2. NREL Components Open House Presentation, 'Pressure Relief Device Testing R&D," May 28, 2015.

3. NREL Component Webinar Presentation, "Pressure Relief Device Testing R&D", February 4, 2015.

4. "Hydrogen Fueling Station Metrology," Metrology Information Exchange, NREL January 14, 2015.

5. "NREL Component R&D," CSA Langley, B.C. Test Laboratory meetings, January 29, 2015.

6. Hydrogen Fueling Station Animation, http://widgets-stage.nrel.gov/afdc/hydrogen-animation/, Q1 FY 2015.

VIII.3 R&D for Safety, Codes and Standards: Materials and Components Compatibility

Brian Somerday (Primary Contact), Chris LaFleur, Chris San Marchi
Sandia National Laboratories
P.O. Box 969
Livermore, CA 94551-0969
Phone: (925) 294-3141
Email: bpsomer@sandia.gov

DOE Manager
Will James
Phone: (202) 287-6223
Email: Charles.James@ee.doe.gov

Project Start Date: October 1, 2003
Project End Date: Project continuation and direction determined annually by DOE

Overall Objectives

- Optimize the reliability and efficiency of test methods for structural materials and components in hydrogen gas
- Generate critical hydrogen compatibility data for structural materials to enable technology deployment
- Create and maintain information resources such as the "Technical Reference for Hydrogen Compatibility of Materials"
- Demonstrate leadership in the international harmonization of standards for qualifying materials and components for high-pressure hydrogen service

Fiscal Year (FY) 2015 Objectives

- Extend fatigue crack growth testing on Cr-Mo pressure vessels steels in high-pressure hydrogen gas to include data at lower ΔK levels
- In collaboration with vendor, complete engineering drawings and initiate manufacturing of pressure vessel for variable temperature testing in a high-pressure hydrogen system
- Foster growth of international collaboration and leadership on materials science of hydrogen embrittlement, in particular within the International Institute for Carbon-Neutral Energy Research (I2CNER)
- In partnership with Advanced Industrial Science and Technology (AIST), complete fracture threshold measurements on Japanese Cr-Mo pressure vessel steel as a function of hydrogen gas pressure and loading rate

Technical Barriers

This project addresses the following technical barriers from the Safety, Codes and Standards section of the 2012 Fuel Cell Technologies Office Multi-Year Research, Development and Demonstration Plan (MYRDD) (Section 3.8):

(A) Safety Data and Information: Limited Access and Availability

(F) Enabling National and International Markets Requires Consistent RCS (Regulations, Codes, and Standards)

(G) Insufficient Technical Data to Revise Standards

Contribution to Achievement of DOE Safety, Codes & Standards Milestones

This project will contribute to achievement of the following DOE milestones from the Safety, Codes and Standards section of the 2012 Fuel Cell Technologies Office MYRDD Plan:

- Milestone 2.9: Publish technical basis for optimized design methodologies of hydrogen containment vessels to account appropriately for hydrogen attack (4Q, 2013)
- Milestone 2.16: Demonstrate the use of new high-performance materials for hydrogen applications that are cost-competitive with aluminum alloys. (4Q, 2017)
- Milestone 2.3: Implement validated mechanism-based models for hydrogen attack in materials (4Q, 2016)
- Milestone 3.3: Reduce the time required to qualify materials, components, and systems by 50% relative to 2011 with optimized test method development. (1Q, 2017)
- Milestone 3.4: Develop hydrogen material qualification guidelines including composite materials (Q4, 2017)
- Milestone 4.8: Completion of the GTR Phase 2. (1Q, 2017)
- Milestone 5.2: Update materials compatibility technical reference (4Q, 2011-2020)

- Milestone 5.4 Develop and publish database for properties of structural materials in hydrogen gas. (2Q, 2013)

FY 2015 Accomplishments

- Completed measurements of fatigue crack growth rate vs. frequency at two lower ΔK levels for SA-372 Grade J and 34CrMo4 pressure vessel steels in 45 MPa hydrogen gas
- In collaboration with vendor, completed engineering drawings for pressure vessel in variable-temperature testing in hydrogen gas system
- In partnership with AIST, completed fracture threshold measurements on Japanese Cr-Mo steel SCM 435 as a function of hydrogen gas pressure and loading rate

✧ ✧ ✧ ✧ ✧

INTRODUCTION

A principal challenge to the widespread adoption of hydrogen infrastructure is the lack of quantifiable data on its safety envelope and concerns about additional risk from hydrogen. To convince regulatory officials, local fire marshals, fuel suppliers, and the public at large that hydrogen refueling is safe for consumer use, the risk to personnel and bystanders must be quantified and minimized to an acceptable level. Such a task requires strong confidence in the safety performance of high pressure hydrogen systems. Developing meaningful materials characterization and qualification methodologies in addition to enhancing understanding of performance of materials is critical to eliminating barriers to the development of safe, low cost, high performance high-pressure hydrogen systems for the consumer environment.

APPROACH

The Materials and Components Compatibility project leverages decades of experience in high-pressure hydrogen systems, well developed industry partnerships, and an enabling capability in hydrogen materials interactions anchored by the Hydrogen Effects on Materials Laboratory to focus on three critical activities, (1) optimize materials characterization methodologies, (2) generate critical hydrogen compatibility data for materials to enable technology deployment, and (3) provide international leadership by assembling and maintaining a technical reference that is populated with vetted data and includes a technical assessment of the data and its application.

RESULTS

Optimizing Fatigue Crack Growth Measurements in Hydrogen Gas

An activity featured in FY 2013 was fatigue crack growth testing on two commercial Cr-Mo pressure vessel steels as a function of stress-intensity factor range (ΔK), hydrogen gas pressure, and load-cycle frequency. The objective of this testing was to explore an optimized method, in which measurements could be performed over a broad ΔK range while limiting test duration. The proposed approach was to measure the fatigue crack growth rate (da/dN) vs. ΔK relationship at high load-cycle frequency (10 Hz) and then apply a correction based on supplemental da/dN vs. frequency data. During FY 2015, these data were comprehensively analyzed and documented in a manuscript submitted to the ASME 2015 Pressure Vessels & Piping Division Conference. As a result of this analysis, it was determined that the fatigue crack growth data were insufficient for assessing the viability of the proposed modified approach. Specifically, since the baseline da/dN vs. ΔK relationships measured at 10 Hz must be corrected based on da/dN vs. frequency data, the latter data must be measured at appropriate constant-ΔK intervals. The gap in the data set revealed during analysis was the absence of da/dN vs. frequency measurements at lower constant-ΔK levels.

To address this gap, additional da/dN vs. frequency measurements were initiated in FY 2015, focusing on two lower ΔK levels for both pressure vessel steels at 45 MPa hydrogen gas pressure. Figure 1 displays the original data (baseline da/dN vs. ΔK relationships at 10 Hz and da/dN vs. frequency data at two higher constant-ΔK levels) and the latest da/dN vs. frequency measurements at two lower ΔK levels in 45 MPa hydrogen gas. These latest data emphasize that the dependence of fatigue crack growth rate on frequency persists to ΔK levels lower than expected. The implication is that corrections to the baseline da/dN vs. ΔK relationships to reflect upper-bound behavior must include da/dN vs. frequency data in the lower ΔK range. Based on the more comprehensive data sets in Figure 1, a more definitive correction can be applied to the baseline da/dN vs. ΔK relationships to represent upper-bound behavior (dark red dashed lines in Figure 1).

System for Variable-Temperature Testing in Hydrogen Gas

Sandia maintains an enabling capability in hydrogen embrittlement of structural materials, in which the Hydrogen Effects on Materials Laboratory is the central asset. This laboratory features several specialized systems for measuring the mechanical properties of materials in high-pressure hydrogen gas. One essential system for providing

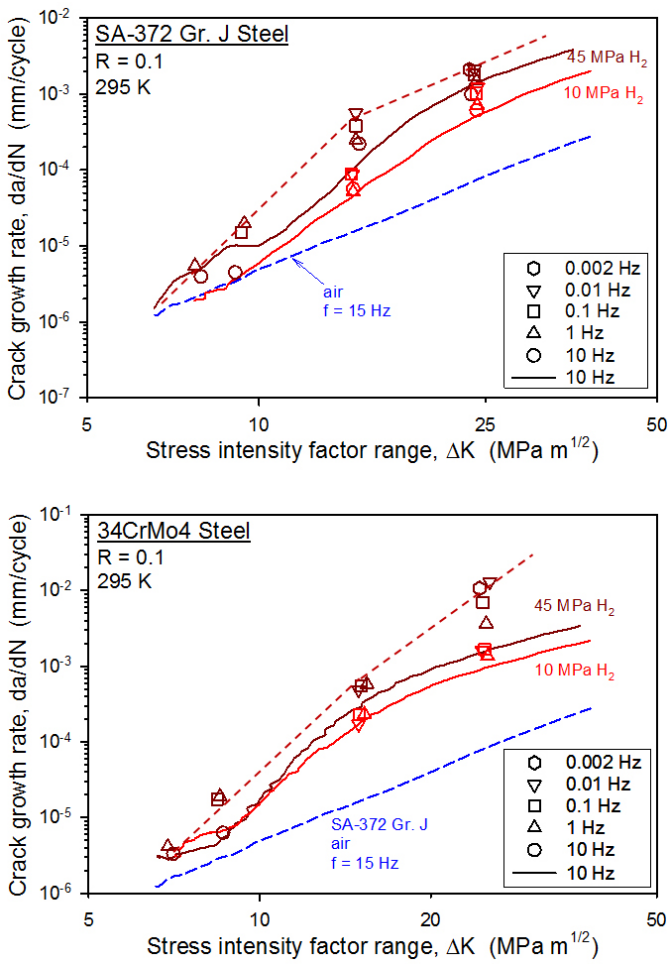

FIGURE 1. Composite data showing fatigue crack growth rate (da/dN) vs. stress-intensity factor range (ΔK) and da/dN vs. frequency for two Cr-Mo pressure vessel steels in 10 MPa and 45 MPa hydrogen gas. The dark red dashed lines indicate corrections applied to the baseline da/dN vs. ΔK relationships to reflect upper-bound behavior based on the da/dN vs. frequency data.

materials data to support hydrogen and fuel cell technology deployment allows dynamic mechanical loading of materials (i.e., fatigue) in high-pressure hydrogen gas at room temperature. However, it is well known that certain materials such as austenitic stainless steels are most susceptible to hydrogen embrittlement at temperatures near 233 K. Thus, it is imperative to develop a system for dynamic mechanical loading of materials in hydrogen gas with a mechanism for varying temperature.

The remaining effort for completing the new materials test system is primarily focused on a pressure vessel with variable-temperature mechanism. In FY 2014, an internal cooling mechanism was identified and validated for the concept pressure vessel. Based on this internal cooling mechanism, the Sandia team has been working collaboratively with a pressure vessel design and manufacturing company to create a set of engineering drawings. These drawings have been completed, and the pressure vessel vendor is determining a cost estimate for the manufacturing.

International Collaboration with I2CNER

On December 20, 2014, Dr. Brian Somerday led a coordination meeting at Sandia National Laboratories in Livermore, CA for the I2CNER Hydrogen Materials Compatibility division. The purpose of this meeting was twofold, (1) promote interaction and coordination among researchers in the Hydrogen Materials Compatibility division and (2) refine research roadmap for the division and ensure research activities align with roadmap. The foundation of the agenda was 12 short overview presentations of research projects in the division. The presenters included professors, postdoctorals, and graduate students having affiliations with I2CNER.

Dr. Brian Somerday served as co-organizer of the Joint HYDROGENIUS and I2CNER International Workshop on Hydrogen-Materials Interactions at the International Hydrogen Energy Development Forum in Fukuoka, Japan, on February 4, 2015. The workshop featured invited presentations on research related to hydrogen effects on mechanical properties of structural metals. The speakers invited to this international workshop represented the United States, Germany, France, Norway, and Japan.

Leveraging Partnership at AIST

AIST (Tsubuka, Japan) and Sandia continued to perform collaborative R&D in FY 2015 to evaluate test methods for measuring fracture thresholds of pressure vessel steels in high-pressure hydrogen gas. The primary testing activity was measuring the fracture thresholds for a Japanese steel (SCM 435) as a function of loading rate and hydrogen gas pressure (Figure 2). These results in conjunction with measurements performed on a U.S. steel (SA-372 Grade J) in FY 2014 constitute the most comprehensive fracture threshold data set for Cr-Mo pressure vessel steels in hydrogen gas. Given the value of these data, Dr. Takashi Iijima from AIST presented the results at the ASTM subcommittee meeting on Environmentally Assisted Cracking (E08.06.02) in November 2014. The data are contributing to the technical basis for formulating an ASTM standard on rising displacement fracture thresholds measurement in hydrogen gas through ASTM subcommittee E08.06.02. Although these fracture threshold measurements are recognized as having relevance for life prediction of pressure vessels in hydrogen gas service, there is currently no ASTM standard guiding such measurements in hydrogen gas. The fracture threshold measurements featured in the AIST-Sandia collaboration have been documented in jointly authored publications submitted to the 2014 and 2015 ASME Pressure Vessels & Piping Division Conference.

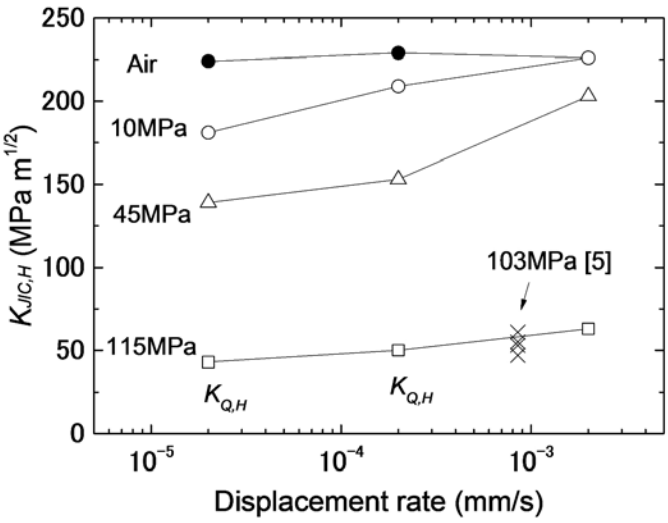

FIGURE 2. Rising-displacement fracture thresholds measured for SCM 435 pressure vessel steel in air and high-pressure hydrogen gas as a function of loading rate. The cross symbols are previous measurements performed at Sandia on a similar Cr-Mo pressure vessel steel (SA-372 Grade J) in 103 MPa hydrogen gas.

CONCLUSIONS AND FUTURE DIRECTIONS

- Establishing an efficient method for measuring the fatigue crack growth relationship for Cr-Mo steels in hydrogen gas over a broad ΔK range can lead to more favorable calculated fatigue lives for hydrogen pressure vessels.
- Progress in completing the variable-temperature testing in hydrogen gas system bolsters the enabling capability in materials compatibility and assures critical testing can be performed on technologically pivotal materials such as stainless steels.
- International partnerships with I2CNER and AIST provide access to basic science related to materials behavior in hydrogen as well as data that enable the development of international standards for materials testing and component qualification.
- (future) In collaboration with the European Commission-supported project MATHRYCE, perform fatigue crack initiation and growth testing on a Cr-Mo pressure vessel steel in 100 MPa hydrogen gas to complement measurements by MATHRYCE partners at lower pressure
- (future) Commission variable-temperature testing in hydrogen gas system: integrate subsystems and demonstrate functionality
- (future) Evaluate suitability of high-hardenability steels for stationary high-pressure hydrogen vessels in partnership with industry stakeholder consortium
- (future) In collaboration with international partners, initiate activity (e.g., round robin testing) to define test methods and augment database for stainless steels in high-pressure hydrogen gas

FY 2015 PUBLICATIONS/PRESENTATIONS

1. C. San Marchi , "Development of Hydrogen Safety Standards in the United States," presentation at Workshop on International Trends in Hydrogen Safety Standards, Seoul, Korea, Nov. 2014.

2. C. San Marchi , "Trends in Hydrogen Research in the United States," presentation at Korean Society of Mechanical Engineers, GwangJu, Korea, Nov. 2014

3. B. Somerday, "Measurements of Subcritical Cracking Thresholds and Fatigue Crack Growth Rates for Steels in H_2 Gas," presentation at Tenaris-Dalmine, Dalmine, Italy, Oct. 2014.

4. B. Somerday, "Enhancing Reliability of Hydrogen Assisted Cracking Properties Measured in Hydrogen Gas," presentation at Hydrogen Embrittlement -Multi-scale Modelling and Measurement: What is the Impact?, National Physical Laboratory, Teddington, UK, Oct. 2014.

5. B. Somerday and C. San Marchi, "R&D for Safety, Codes and Standards: Materials and Components Compatibility," presentation at Joint Delivery-Codes & Standards Tech Team Meeting, Sacramento, CA, Jan. 2015.

6. L. Zhang, B. An, T. Iijima, C. San Marchi, and B. Somerday, "Hydrogen Transport and Hydrogen-Assisted Cracking in SUS304 Stainless Steel During Deformation at Low Temperatures," Proceedings of the ASME2015 Pressure Vessels & Piping Conference, PVP2015-45211, Boston, MA, July 2015.

7. T. Iijima, H. Itoga, B. An, C. San Marchi, and B.P. Somerday, "Fracture Properties of a Cr-Mo Ferritic Steel in High-Pressure Gaseous Hydrogen," Proceedings of the ASME2015 Pressure Vessels & Piping Conference, PVP2015-45328, Boston, MA, July 2015.

8. B. Somerday, P. Bortot, and J. Felbaum, "Optimizing Measurement of Fatigue Crack Growth Relationships for Cr-Mo Pressure Vessel Steels in Hydrogen Gas," Proceedings of the ASME2015 Pressure Vessels & Piping Conference, PVP2015-45424, Boston, MA, July 2015.

VIII.4 Hydrogen Fuel Quality

Tommy Rockward (Primary Contact),
Jacob Valdez, Karen Rau, Eric Brosha,
Mahlon Wilson, and Rangachary Mukundan
Los Alamos National Laboratory (LANL)
P.O. Box 1663
Los Alamos, NM 87545
Phone: (505) 667-9587
Email: trock@lanl.gov

DOE Manager
Will James
Phone: (202) 287-6223
Email: Charles.James@ee.doe.gov

Collaborators/Partners
Japan Automobile Research Institute
European Union
WG-11
ASTM International
Air Liquide
California Fuel Cell Partnership
CONSCI

Project Start Date: October 2006
Project End Date: Project continuation and direction determined annually by DOE

Overall Objectives

To support the Hydrogen Safety, Codes and Standards sub-program through:

- Participation in working groups
- Providing leadership to hydrogen fuel quality efforts
- Performing the research and development (R&D) needed to develop science-based codes and standards
- Develop tools that can remove safety and hydrogen fuel quality barriers to the commercialization of fuel cells

Fiscal Year 2015 Objectives

- To carry out the duties of ASTM sub-committee chair for D03.14 gaseous hydrogen fuel efforts
- To install and validate a hydrogen recirculation system at LANL and evaluate its impact on the carbon monoxide (CO) poisoning of a low platinum loaded membrane electrode assembly (MEA)
- To demonstrate sensitivity of electrochemical analyzer to hydrogen sulfide
- To demonstrate an electrochemical analyzer capable of detecting 4 ppb hydrogen sulfide (H_2S) and 200 ppb CO in hydrogen with a response time <5 min
- Report findings/results to the DOE

Technical Barriers

This project addresses the following technical barriers from the Hydrogen Safety, Codes and Standards section (3.7.5) of the Fuel Cell Technologies Office Multi-Year Research, Development, and Demonstration Plan:

(F) Enabling National and International Markets Requires Consistent RCS (Regulations, Codes, and Standards)

(G) Insufficient Technical Data to Revise Standards

(H) Insufficient Synchronization of National Codes and Standards

(K) No Consistent Codification Plan and Process for Synchronization of R&D and Code Development

FY 2015 Accomplishments

- Testing completed and results coordinated for Interlaboratory Study Program (ILS) 751- *Test Method for Determination of Trace CO_2, Ar, N_2, O_2 and H_20 in Hydrogen Fuel by Jet Pulse Injection and GC/MS Analysis*
- Established ILS for Hydrogen Purity Analysis Using a Continuous Wave Cavity Ring-Down Spectroscopy Analyzer
- Chaired two semiannual ASTM meetings for D03.14 Gaseous Hydrogen Fuel in December 2014 and June 2015
- Improved response time of analyzer to 200 ppb CO to less than 5 minutes
- Tested simultaneous poisoning with CO and H_2S: results indicate short-term exposure favors CO adsorption and poisoning effects are not additive
- Finalized the initial design of the prototype fuel quality analyzer
- Continued international collaborations with the Japan Automobile Research Institute (JARI), CEA, and VTT
- Completed baseline tests with new 25 cm^2 MEAs with results showing excellent agreement with JARI MEAs (membrane: DuPont XL100®, anode: 0.05 mg Pt/cm^2, and cathode: 0.1 mg Pt/cm^2)
- Sent new MEAs to CEA and received first set of data for direct comparison with the LANL-JARI results

✧ ✧ ✧ ✧ ✧

INTRODUCTION

The work performed in this project has been partitioned into three tasks: (1) R&D for fuel quality standards including international interactions, (2) in-line fuel quality analyzer development, and (3) contributions to ASTM standards development.

While steam reforming natural gas will make hydrogen affordable and available, it will produce trace amounts of CO and H_2S. The international team (International Organization for Standardization [ISO] TC197 WG-12) for "development of a hydrogen fuel product specifications for use in proton exchange membrane fuel cell applications for road vehicles;" (ISO 14687-2:2012) [1] and SAE J2719 [2] indicate acceptance levels of several contaminants. Although these contaminants are at sub-ppm levels, their effect on fuel cell performance is uncertain, especially since the total platinum content in the fuel cell MEA has been continuously lowered. Previously conducted fuel cell tests with the fuel specification indicated that ammonia, carbon monoxide, and hydrogen sulfide were the critical constituents most harmful to proton exchange membrane fuel cell performance and/or its durability. In FY 2015 LANL conducted fuel quality testing to evaluate the impact of these critical constituents on current fuel cell MEAs and has continued to engage the international community to incorporate the research results into future updates to these standards.

Although science-based standards for fuel quality have been established [1,2], there is still a need to provide the tools necessary to implement this standard. For example, the ISO and SAE standards have a maximum allowance of 0.2 ppm for CO and 4 ppb for H_2S [1,2]. LANL is helping this effort by providing leadership to ASTM in developing methods to determine the impurity content in the fuel that can be used to certify the hydrogen. Although the hydrogen grade would be certified periodically using these methods, it would be invaluable to have in-line analyzers to protect expensive fuel cell systems and components from these contaminants. LANL demonstrated proof-of-concept for an in-line fuel quality analyzer using various concentrations of CO at or below the levels in the aforementioned standard. In FY 2015 we optimized the MEA to reduce our response time to <5 min and have finalized a design for a prototype in-line fuel quality analyzer. Our goal is to provide a quick and cheap method of detection at various points in the supply chain. The successful commercialization of this product will have a positive impact on the safety of filling stations and the reliability of fuel cell vehicles. This work directly addresses the targets set in Table 3.7.6 of the Safety, Codes and Standards technical plan.

APPROACH

R&D for Fuel Quality Standards

LANL installed a recirculating system on the H_2 side in order to evaluate the impact of impurities while increasing H_2 utilization. This recirculation system was developed under collaboration with VTT (Finland) and represents a significant upgrade in the infrastructure available at LANL for fuel quality testing. In this report we present the first results obtained at LANL using this recirculation system. This system will be used extensively in all our upcoming international collaborations. LANL will continue to engage in collaborations with JARI, CEA (France) and VTT (Finland) to harmonize impurity testing with a view to updating the current fuel quality standards. Finally, LANL scientists were recently invited to participate along with several other countries in the development of an international document entitled, *Single Cell Test Methods –PEFC*.

In-line Fuel Quality Analyzer

The interaction of either H_2S or carbon monoxide in a hydrogen stream over a platinum surface results in inhibition of hydrogen dissociation, and inherently lower current output from an MEA operated at a constant voltage in a H_2 pump mode. The fuel quality analyzer is composed of an active area MEA ≤ 5 cm^2 with platinum-based electrodes. In FY 2015 the electrodes were optimized in order to improve the analyzer's response time. More specifically, by lowering the Pt loading and increasing the Pt particle size we were able to improve the analyzer's response time from a few hours (FY 2014) to <5 min (FY 2015).

RESULTS AND DISCUSSIONS

In-line Analyzer

LANL has continued tests for the development of an in-line hydrogen fuel quality analyzer and has successively made progress towards improving the sensitivity and response time. Our previous results (not shown) using a working electrode loaded with 0.067 mg-Pt/cm^2 and a reference electrode with 0.2 mg-Pt-Ru/cm^2 adhered to a 7-mil thick Nafion® membrane (N117) showed response to CO and H_2S at the SAE J2719 levels only after exposure for >1 h. Using new working electrodes containing 0.04 mg-Pt/cm^2, we tested the response of the analyzer to both CO and also H_2S at the SAE J2719 concentration levels, individually and simultaneously for different time periods. Figure 1 illustrates that this analyzer responds to these low concentration levels of CO and H_2S within minutes. This >100-fold increase in the response time is very encouraging. This analyzer also demonstrated a clear response within minutes after exposure to both CO and H_2S. At short exposure times, the poisoning closely followed the CO only poisoning data while at the

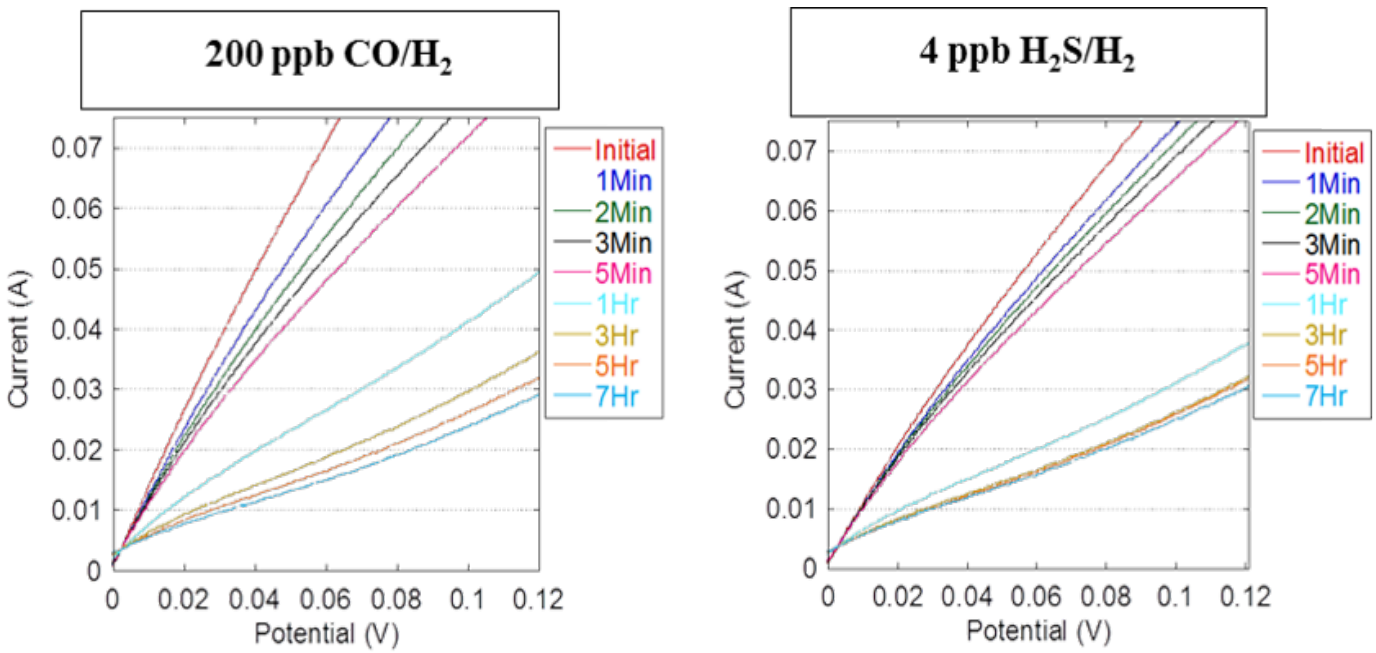

FIGURE 1. Analyzer (0.04 mg-Pt/cm2) response to 200 ppb CO (left) and 4 ppb H_2S (right) at various time intervals

longer exposure times the data is more representative of H_2S poisoning. These tests clearly demonstrate that our analyzer is capable of detecting multiple contaminants at the SAE J2719 levels, simultaneously within the time required for one fill in a station.

We also examined the long-term shelf life of one of our analyzer MEAs. We originally reported in 2014 the response during 7 h of exposure to 200 ppb CO (100 sccm flow rate) from an analyzer with a 0.1 mg-Pt/cm^2 working electrode. After over one year, we retested the same sample under similar conditions. The graphs (Figure 2) show the comparison of the analyzer performance. The baseline data of the analyzer before and after the one year storage is identical (red line) indicating that the membrane shows no sign of degradation and its humidification is identical in both the tests. However the data also indicate some ageing in the electrode resulting in slightly different poisoning effects in these two tests. This could potentially be due to contaminants adsorbed on the electrode during storage. This problem can be alleviated with a clean-up step. This phenomenon will be further examined in the lower loaded (0.04 mg-Pt/cm^2) MEAs in the future to determine analyzer durability.

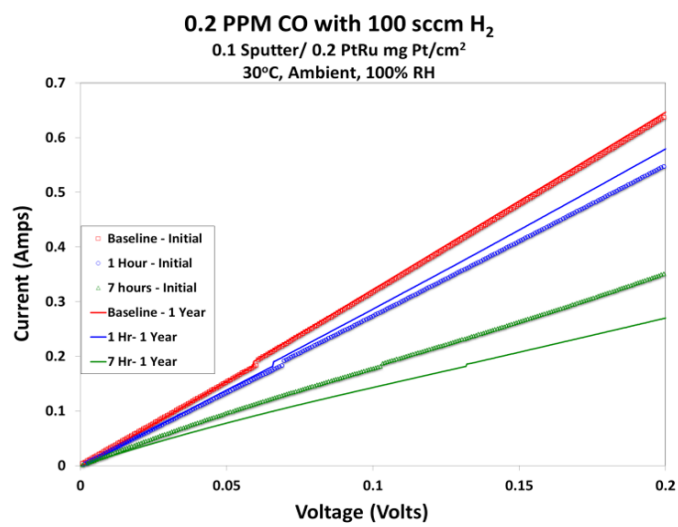

FIGURE 2. Comparison of analyzer response at baseline, and after exposure to 200 ppm for 1 h and 7 h. The data is shown for the initial analyzer response and the response after 1 year of storage of the analyzer MEA.

Hydrogen Fuel Quality: International Collaborations*:*

LANL scientists have continued their efforts within Working Group 11 to advance the *Single Cell Test Methods –PEFC* document in successive stages to be presented as Committee Draft in September 2015 and projected to become a technical specification by November 2016. The document's scope is to provide guidance using performance-based tests to describe fuel cell materials and components. In addition, an internationally accepted document will allow uniform fuel cell testing and provide a basis for comparing test results from around the world. This document also details a standardized way to report test results.

LANL completed baseline fuel cell tests with 25 cm^2 MEAs using both JARI and LANL hardware. These results agree well with those measured by LANL scientists at JARI's testing facility. These tests (graphs shown in Figure 3) confirmed and verified that the MEA performance from

different manufacturers was similar regardless of hardware or test facilities. Figure 3a represents the break-in and polarization data with JARI hardware and LANL MEAs while Figure 3c represents the same data obtained with the newly developed LANL MEA and LANL hardware (blue curve is voltage and red is current density). A comparison of Figures 3a and 3c clearly shows little to no effect of varying hardware with the LANL MEA. Figure 3b shows the current data during the conditioning portion of the break in (first 2 hours of graphs in in Figures 3a and 3c) of the JARI MEA (in blue) and old LANL MEA (yellow). This illustrates that the new LANL MEA (Figures 3a and 3c) performs identical to the JARI MEA irrespective of hardware. The low performance of the old MEA (yellow in Figure 3b) was due to the use of an unoptimized ionomer and has been corrected to obtain these consistent results. This baseline testing is crucial in providing confidence that all future tests at the various tests sites can be directly compared with one another without the need for any extraneous calibration or data manipulation. LANL has now extended these studies to involve CEA and all three organizations will perform impurity testing to harmonize international standards.

In this FY 2015, we installed a hydrogen recirculation system similar to the one developed by VTT (Finland) in their HyCoRA (Hydrogen Contaminant Risk Assessment) project. Here, we report life-test results of a 25 cm^2 polymer electrolyte fuel cell with an anode and cathode of 0.05 and 0.1 mg Pt/cm^2, respectively. The cell was operated at 80°C, 100% relative humidity and 150 kPa in the presence of 200 ppb CO. The hydrogen fuel utilization was initially run at 50% with approximately 90% of the unused H_2 returning into the fuel stream. Under these conditions we observed a 50 mV voltage loss over 100 hours of operation at 1 A/cm^2 (see Figure 4a, left). Under identical test conditions but with no recirculation we observed only a 38 mV voltage loss over the same time period (Figure 4b, right). This demonstrates the effect of recirculation in increasing the impact of impurities on the fuel cell performance. In the single pass system any of the 200 ppb CO that does not adsorb on the Pt is vented while in the recirculation system, this CO is once again sent into the inlet of the fuel stream thus leading to the greater (almost 30%) voltage degradation rate. More systematic studies are planned where we will evaluate the effect of varying the H_2 stoichiometry and recirculation rate on this degradation. Finally we will combine these results with simulated drive cycle operations of fuel cells, to provide better guidance on fuel quality standards.

Contributions to ASTM Standards Development

LANL scientist serves as subcommittee chair for D03.14 Gaseous Fuels. Hydrogen and fuel cells held two semiannual meetings in FY 2015. The ILS 775, ASTM D7649 - *Test Method for Determination of Trace CO_2, Ar, N_2, O_2 and H_20 in Hydrogen Fuel by Jet Pulse Injection and GC/MS Analysis* was completed and the experimental results were discussed by the participating test labs. The results differed between the test sites and it was concluded that unique testing apparatus should not be incorporated into a standardized test methods. Based upon these discussions of the data, a revision of the test method was called for and the new test method will incorporate the findings of the ILS. There is also an additional ILS that is planned to evaluate cavity ring-down spectroscopy which will be initiated as soon as adequate test sites are identified.

CONCLUSIONS AND FUTURE DIRECTIONS

In FY 2015, the analyzer electrode was optimized to improve the response time to 200 ppb CO/4 ppb H_2S from >1 hour to <5 minutes. LANL also installed an H_2 recirculation system and initial results observed a 30% increase in the voltage degradation due to CO poisoning.

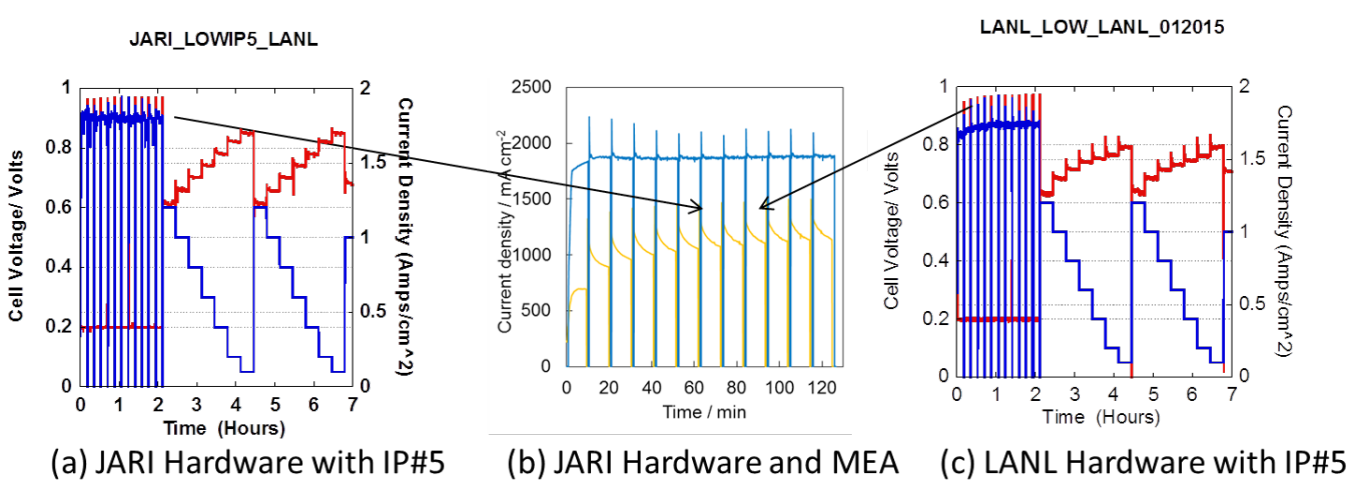

FIGURE 3. Baseline testing shows great agreement (i) MEAs (a) vs. (b); (ii) hardware (a) vs. (c); and (iii) facilities (b) and (c)

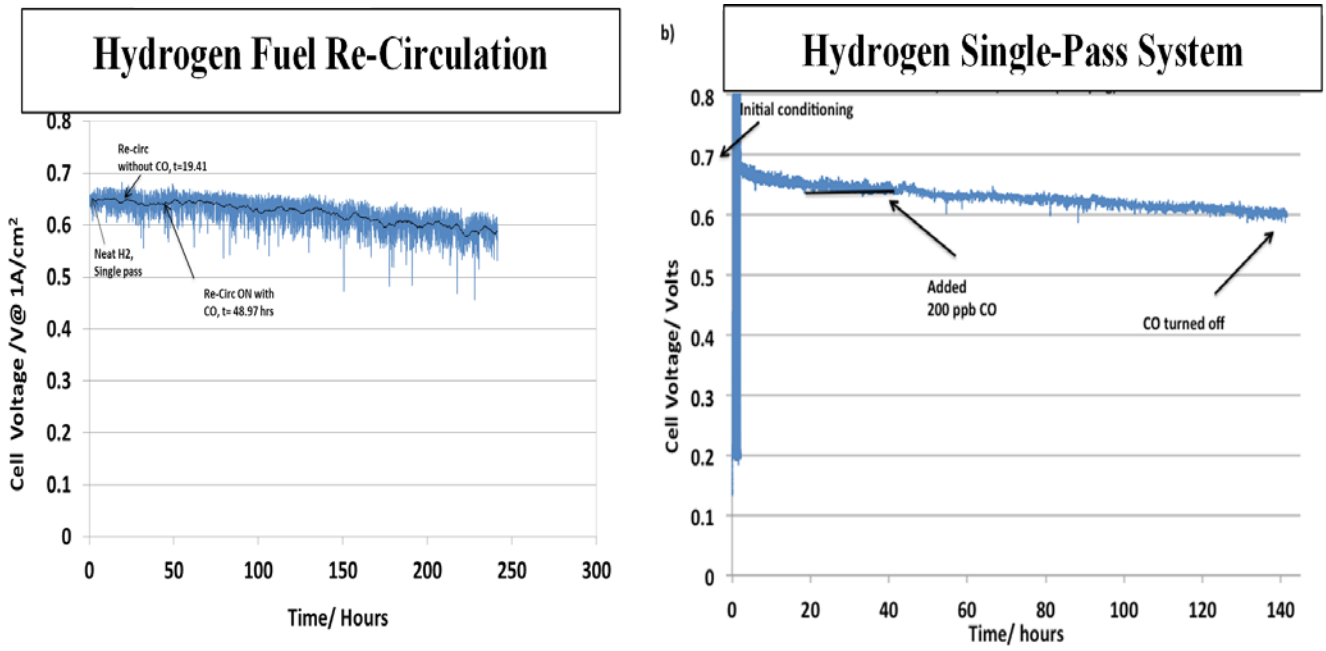

FIGURE 4. Fuel cell voltage at a current of 1 A/cm^2 when operating under H_2 + 200 ppb CO with H_2 recirculation (left) and H_2 single-pass (right)

LANL also completed baseline fuel cell performance testing as part of an international collaboration with JARI and CEA. Finally, in FY 2015 LANL continued to provide leadership to the ASTM subcommittee D03.14 on hydrogen and fuel cells. LANL will work on the following tasks in FY 2015.

- Continue with new standards development – ILS coordination
- Coordinate a workshop on in-line fuel quality, December 2015 ASTM meeting
- Optimize operating conditions of analyzer to further improve sensitivity
- Work with hydrogen fuel suppliers to better understand S-upsets
- Study impact of humidity
- Evaluate long-term durability
- Design and build prototype analyzer by end of FY 2016 to be evaluated at an independent test site
- Continue working with international collaborators
- Initiate an international round robin for impurity testing
- Compare performance degradation with and without **recirculation system** and quantify effect of anode recirculation on CO poisoning of proton exchange membrane fuel cells at different utilizations

REFERENCES

1. Organization, I.S., *Hydrogen fuel — Product specification — Part 2: Proton exchange membrane (PEM) fuel cell applications for road vehicles*, in *ISO TC 197*2012, ISO copyright office: Case postale 56 • CH-1211 Geneva 20.

2. SAE J2719: Hydrogen Fuel Quality for Fuel Cell Vehicles, www.sae.org.

VIII.5 NREL Hydrogen Sensor Testing Laboratory

William Buttner (Primary Contact), Robert Burgess, Carl Rivkin
National Renewable Energy Laboratory (NREL)
15013 Denver West Parkway
Golden, CO 80401-3305
Phone: (303) 275-3903
Email: William.Buttner@nrel.gov

DOE Manager
Will James
Phone: (202) 287-6223
Email: Charles.James@ee.doe.gov

Subcontractor
Element One, Boulder, CO

Project Start Date: October 1, 2010
Project End Date: Project continuation and direction determined annually by DOE

Overall Objectives

- Quantify performance of commercial hydrogen sensors relative to DOE metrics
- Support development and assess performance of advanced sensor technologies
- Support development and updating of hydrogen sensor codes and standards
- Support infrastructure deployment by providing expert guidance on the use of hydrogen sensors and analyzers
- Educate the hydrogen community on the proper use of hydrogen sensors

Fiscal Year (FY) 2015 Objectives

- Support the Department of Transportation/National Highway Traffic Safety Administration (DOT/NHTSA) on the development of the Federal Motor Vehicle Safety Standard (FMVSS) for hydrogen fuel cell vehicles, especially with regards to hydrogen detection requirements identified in the Global Technical Regulation (GTR) for hydrogen-powered vehicles
- Quantify performance metrics of developmental sensor technologies from private organizations and national laboratories, including those supported by DOE as well as privately
- Support infrastructure deployment by providing sensor testing capability and guidance to stakeholders
- Qualify hydrogen safety sensors for specific applications, including those for use in vehicle repair facilities being adapted to accommodate hydrogen vehicles
- Support fuel cell electric vehicle safety through the preparation of a Society of Automotive Engineers (SAE) Technical Information Report (TIR) providing guidance for characterizing on-board hydrogen sensors (J3089, in process)
  - Being developed under the auspices of the SAE Fuel Cell Safety Task Force
- Support of NREL component testing and facility upgrades with sensors for both safety and quantitation of hydrogen releases
- Coordinate international hydrogen safety sensor research and infrastructure deployment through collaboration under the auspices of H2Sense [1], which is a European Union (EU) program funded through the Joint Fuel Cell and Hydrogen Energy (FCH JU)
  - Partners include the Federal Institute for Material Research and Testing (BAM, Berlin, Germany), the Joint Research Centre (JRC) Institute for Energy and Transport (IET, Petten, the Netherlands), and private companies

Technical Barriers

This project addresses the following technical barriers identified in the Hydrogen Safety, Codes and Standards section of the Fuel Cell Technologies Office Multi-Year Research, Development, and Demonstration Plan (MYRDD):

(A) Safety Data and Information: Limited Access and Availability

(C) Safety is Not Always Treated as a Continuous Process

(F) Enabling National and International Markets Requires Consistent Regulations, Codes and Standards

(G) Insufficient Technical Data to Revise Standards

(H) Insufficient Synchronization of National Codes and Standards

(K) No Consistent Codification Plan and Process for Synchronization of R&D and Code Development

Contribution to Achievement of DOE Safety, Codes & Standards Milestones

This project will contribute to achievement of the following DOE milestones from the Hydrogen Safety, Codes and Standards section of the Fuel Cell Technologies Office MYRDD:

- Milestone 2.15: Develop holistic design strategies (4Q, 2017)
- Milestone 2.19: Validate inherently safe design for hydrogen fueling infrastructure. (4Q, 2019)
- Milestone 3.1: Develop, validate, and harmonize test measurement protocols (4Q, 2014)
- Milestone 4.9: Completion of GTR Phase 2 (1Q, 2017)
- Milestone 5.1: Update safety bibliography and incidents databases (4Q, 2011-2020)

FY 2015 Accomplishments

- Implemented or maintained multiple formal agreements with industrial partners, pertaining to the use of sensors in support of infrastructure deployment, on-board vehicle applications, and support of new advanced sensor technology development
- In collaboration with an industrial partner, developed performance requirements for hydrogen sensors used in repair facilities adapted to accommodate fuel cell electric vehicles; developed test protocols to qualify sensors for compliance to the vehicle repair facility requirements, which served as the basis for actual selection of sensors currently being deployed in FCEV repair facilities
- Provide technical support to DOT/NHTSA pertaining to hydrogen detection requirements specified in the GTR
  - Supports the development of the FMVSS
- In collaboration with the JRC, completed an initial study quantifying the impact of potential chemical poisons, identified in the International Organization for Standardization (ISO) 26140 [2] on the major hydrogen sensor platform types
- Working with the SAE Fuel Cell Safety Task Force, completed the first draft of an SAE TIR on hydrogen sensor evaluation protocols for use on board hydrogen vehicles
- Submitted for publication, a book on hydrogen sensors, co-authored with Thomas Hübert/BAM and Lois Boon-Brett/JRC [3]
  - Will be available by the end of 2015

✧ ✧ ✧ ✧ ✧

INTRODUCTION

Safety is a major concern for the emerging hydrogen infrastructure. A reliable safety system is comprised of various elements that can include intrinsic design features (e.g., pressure control systems), engineering controls (e.g., sample size minimization), and the use of hydrogen sensors to monitor for releases. Both the International Fire Code (IFC) 2009 and National Fire Protection Association (NFPA) 2 require hydrogen sensors for numerous applications, and accordingly sensors will be mandatory in all jurisdictions that adopt either the IFC or NFPA 2. To assure the availability of reliable safety sensors, NREL established the sensor testing laboratory. The NREL sensor test facility provides stakeholders (e.g., sensor developers and manufacturers, end users, and code officials) a resource for an independent, unbiased evaluation of hydrogen sensor technologies. Test protocols are guided by the requirements in national and international sensor standards, as well as sensor performance targets established by DOE or by the requirements of the application. In addition to laboratory assessment of sensor performance, a critical mission of the NREL sensor testing laboratory is to educate end users on the proper use of hydrogen sensors. This is achieved, in part, through topical studies designed to illustrate fundamental properties and limitations of various hydrogen sensor technologies, and through outreach activity such as participation on standards development organizations (SDOs) committees and workshops, conference and webinar presentations. The NREL sensor laboratory also facilitates deployment by partnering with end users to assist in the design and deployment of their sensor system.

APPROACH

Evaluation of hydrogen safety sensors is an on-going activity at NREL and supports both sensor developers and end users. The goal of the sensor laboratory is to assure that stakeholders in the hydrogen community have the sensor technology they need. The NREL sensor test apparatus was designed with advanced capabilities, including parallel testing of multiple hydrogen sensors, sub-ambient to elevated temperature, sub-ambient to elevated pressure, active humidity control and accurate control of gas parameters with multiple precision digital mass flow meters operating in parallel. Extended long-term stability testing of sensors is also available. The test apparatus is fully automated for control and monitoring of test parameters and for data acquisition with around-the-clock operation capability. Selected sensors are subjected to an array of tests to quantify the impact of variation of environmental parameters and chemical matrix on performance. Although standard test protocols have been developed [4], these can be adapted for specialized requirements. Results are reported back to the developer or manufacturer to support their future development work[1]. NREL sensor testing also supports end users by qualifying sensor technology for their application and by educating the hydrogen community on the proper use of hydrogen sensors. The importance of hydrogen safety

[1] It is the policy of the NREL sensor laboratory to treat test results as proprietary, and thus results pertaining to specific clients will not be disclosed without permission.

sensors has been internationally recognized, and the NREL sensor laboratory closely collaborates with international test laboratories, sensor developers, and SDOs.

RESULTS

To support hydrogen deployment, the NREL Sensor Test Facility strives to assure the availability of hydrogen sensors to meet stakeholder needs. This is achieved in part by providing an unbiased assessment of performance to sensor developers and manufacturers as well as end users. NREL has also performed numerous topical studies aimed at educating the hydrogen community on the proper use of hydrogen sensors. Results reported here summarize major studies completed in FY 2015 on the characterization and use of hydrogen sensors.

Support of the FMVSS/GTR in collaboration with DOT/NHTSA: Recently, the GTR defining safety requirements for hydrogen vehicles was formally implemented [5]. To harmonize international regulations on the safety features of hydrogen vehicles, the GTR is to serve as the basis for the FMVSS in the United States, which is currently being prepared by NHTSA. Prior to formal implementation, the draft FMVSS will be open to review and comment by stakeholders. The GTR has several requirements on allowable hydrogen levels external to the vehicle fuel system, including maximum hydrogen in vehicle compartments and allowable maximum hydrogen concentration in tail pipe emissions, including the need to detect hydrogen transients of less than 1 s duration. Recently, the NREL sensor laboratory has identified a hydrogen sensor with a manufacturer specified response time of less than 1 s. This sensor is serving as the basis for the development an analyzer by NREL to verify compliance to FCEV tailpipe exhaust requirements specified in the GTR. This work is also of interest to original equipment manufacturers.

Hydrogen Safety Sensor Requirements for Vehicle Repair Facilities: The IFC 2009 edition has specific safety requirements pertaining to repair facilities for hydrogen vehicles, including the use of hydrogen detection systems. Thus, existing repair facilities will likely need modifications so as to accommodate hydrogen vehicles, and an integrated design for repair facilities is being explored for this purpose. One aspect of the upgrade will be the use of hydrogen sensors. The NREL sensor laboratory has been working with KPA, Ltd. and Toyota Motor Sales USA on the deployment of a robust hydrogen sensor system as part of the integrated design. Test protocols, including both laboratory assessment and field deployment, were developed to qualify commercial sensors for this application. Several sensor model types were tested which led to the identification of acceptable sensors. These sensors are now being deployed in repair facilities that are being modified for FCEV maintenance.

International Collaborations: Over the past several years, the NREL sensor laboratory has formally collaborated with the sensor test facility at the JRC under the auspices of a memorandum of agreement. The sensor collaboration expanded to include BAM through an agreement between FCH JU and DOE, which represented the first US-EU project with common objectives. The objectives included

- To evaluate the capability of current sensors to detect hydrogen and to validate performance through independent laboratory tests.
- To ascertain the needs of facility designers, safety engineers, product designers, etc., with respect to their requirements on how hydrogen sensors should perform in different applications and under which conditions.
- To identify ways to facilitate hydrogen sensor innovation by removing barriers which currently hinder sensor use and commercialization.
- To facilitate the safe use and implementation of hydrogen as an alternative fuel by ensuring correct use of effective hydrogen detection devices.

NREL led the United States activity, while the JRC and BAM lead the program in the EU. The EU activity operated under the auspices of H2Sense [1], which was led by BAM and the JRC but included participation by numerous private sensor companies.

Sensor Testing and Evaluation: Sensor testing and evaluation remains a core activity within the NREL sensor laboratory, and is performed for customers with both mature as well as developing sensor technology. The NREL sensor laboratory continues to provide the resources necessary to quantify sensor performance in support of end users. Customers include both infrastructure and vehicle applications.

NREL Hydrogen Component Testing Program: The NREL sensor laboratory is an integral element in the NREL component testing program [6,7]. Hydrogen detection is necessary for safety, an indicator for early detection of a pending component failure, and to quantify hydrogen releases. The NREL sensor laboratory has already provided sensors for the PRD testing and performance assessment and calibration of the hydrogen sensors for the hose test [6].

CONCLUSIONS AND FUTURE DIRECTIONS

In the next year, the NREL sensor laboratory will build off its current accomplishment and capabilities via two main avenues—continued evaluation of commercial and developing sensor technologies and support of deployment by expanded collaborations with end users of sensors.

- End User Support to Support Deployment
  - Guidance on the use of hydrogen sensors in infrastructure deployments, including repair facilities and fueling facilities

  - DOT/NHTSA on the hydrogen vehicle FMVSS and compliance to the GTR, including the development of tools necessary to verify compliance
  - Sensor performance testing protocol standards for vehicles
  - Barriers to sensor certification and the impact
- Manufacture–Developer Support
  - Commercial and developmental sensor technology performance validation
  - Assessment of wide area monitoring/distributed sensor technology (as a topical study with the JRC)
  - Sensors and analytical methods for the detection of contaminants in hydrogen fuel

FY 2015 PUBLICATIONS/PRESENTATIONS

Journal Articles and Proceedings Papers

1. "An assessment on the quantification of hydrogen releases through oxygen displacement using oxygen sensors," Buttner, W.J.; Burgess, R.; Rivkin, C.; Post, M.B.; Boon-Brett, L.; Palmisano, V.; Moretto, P.; International Journal of Hydrogen Energy, volume 39 issue 35, 3 December 2014, 20484-20490.

2. "Evaluation of selectivity of commercial hydrogen sensors," Palmisano, V.; Boon-Brett, L.; Bonato, C.; Harskamp, F.; Buttner, W.J.; Post, M.B.; Burgess, R.; Rivkin, C.; International Journal of Hydrogen Energy 39 issue 35, 3 December 2014, 20491-20496.

3. "Selectivity and resistance to poisons of commercial hydrogen sensors," Palmisano, V.; Weidner, E.; Boon-Brett, L.; Bonato, C.; Harskamp, F.; Moretto, P.; Post, M.B.; Burgess, R.; Rivkin, C.; Buttner, W.J.; International Journal of Hydrogen Energy (2015).

4. Accepted for publication in the proceedings of the Sixth International Conference on Hydrogen Safety (October 19-21), Yokohama, Japan:

5. "Hydrogen Monitoring Requirements in the Global Technical Regulation on Hydrogen and Fuel Cell Vehicles," William Buttner, Carl Rivkin, Robert Burgess, Kevin Hartmann, Ian Bloomfield, Matt Post, Lois Boon-Brett, Eveline Weidner (in press).

6. "Overview of the DOE Hydrogen Safety, Codes and Standards Program--Part 4: Hydrogen Sensors," W.J. Buttner, C. Rivkin, R. Burgess Eric Brosha, Rangachary Mukundan, Will James, Jay Keller (in press).

Reports

1. "An Overview of North American Hydrogen Sensor Standards," K. O'Malley, H. Lopez, R. Wichert, J. Cairns, W.J. Buttner, NREL Technical Report NREL/TP-5400-62062 (2015) in press.

2. (Contributor) International Energy Agency Hydrogen Implementing Agreement Task 31 Hydrogen Safety Final Technical Report W. Hoagland (November 2014).

3. "Hydrogen Technologies Safety Guide," C. Rivkin, R. Burgess, W. Buttner, NREL Technical Report (January 2015), NREL/TP-5400-60948.

Book

1. "Sensors for Safety and Process Control in Hydrogen Technologies," Thomas Hübert, Lois Boon-Brett, William Buttner, CRC Press (2015) in-press.

Presentations

1. "Hydrogen Sensors," W. Buttner, C. Rivkin, R. Burgess, L. Boon-Brett, E. Weidner, T. Hűbert, HySafe Research Priorities Workshop, (November 11-12, 2014), Washington, DC.

2. "Hydrogen Component Testing," C. Rivkin, C. Ainscough, R. Burgess, W. Buttner, M. Peters, H. Dinh, NREL WEBINAR (Feb 4, 2015).

3. "Hydrogen Detectors, Applications and Performance--The NREL Sensor Laboratory," W. Buttner, C. Rivkin, R. Burgess, K. Hartmann, M. Bubar, I. Bloomfield, Hydrogen Safety Panel, Sacramento, CA (March 4, 2015).

4. "H2 Detection and H2 Sensors," P. Moretto, E. Weidner, W. Buttner, IEA-HIA Task 37 Experts Meeting, Karlsruhe, Germany (April 20-22, 2015).

5. "Sensor Testing Lab Overview," W. Buttner, C. Rivkin, R. Burgess, K. Hartmann, M. Bubar, I. Bloomfield, presented to DOE Hydrogen Codes and Standards Tech Team Telecom Meeting (May 14, 2015).

6. "Hydrogen Sensors--Fuel Systems Application," W. Buttner, NREL Component Research Open House (May 28, 2015).

7. "NREL Hydrogen Sensor--Testing Laboratory," W. Buttner, C. Rivkin, R. Burgess, K. Hartmann, M. Bubar, I. Bloomfield, U.S. Department of Energy Hydrogen and Fuel Cell Program Annual Merit Review and Peer Evaluation (June 6-10, 2015) Washington, D.C.

8. To be Presented at the Sixth International Conference on Hydrogen Safety (October 19-21) Yokohama, Japan:

9. "Hydrogen Monitoring Requirements in the Global Technical Regulation on Hydrogen and Fuel Cell Vehicles," William Buttner, Carl Rivkin, Robert Burgess, Kevin Hartmann, Ian Bloomfield, Matt Post, Lois Boon-Brett, Eveline Weidner.

10. "Overview of the DOE Hydrogen Safety, Codes and Standards Program--Part 4: Hydrogen Sensors," W.J. Buttner, C. Rivkin, R. Burgess, Eric Brosha, Rangachary Mukundan, Will James, Jay Keller.

11. "Impact of Environmental Parameters on Hydrogen Safety Sensor Performance," William Buttner, Carl Rivkin, Robert Burgess, Kevin Hartmann, Eveline Weidner, Valerio Palmisano, Christian Bonato.

REFERENCES

1. H2Sense, see http://www.h2sense.bam.de/en/home/index.htm, accessed July 30, 2015.

2. "ISO 26142 Hydrogen Detector for Stationary Apparatus."

3. "Sensors for Safety and Process Control" T. Hűbert, W. Buttner, L. Boon-Brett, CRC Press (2015) in press.

4. "Standard Hydrogen Test Protocols for the NREL Sensor Testing Laboratory" NREL Brochure. (See http://www.nrel.gov/hydrogen/pdfs/53079.pdf, accessed July 30, 2014).

5. Addendum 13: Global technical regulation No. 13 Global Technical Regulation on hydrogen and fuel cell vehicles ECE/TRANS/180/Add.13, July 19, 2013) (see: http://www.unece.org/fileadmin/DAM/trans/main/wp29/wp29wgs/wp29gen/wp29registry/ECE-TRANS-180a13e.pdf, accessed July 30, 2015).

6. "Component Standard Research and Development," R. Burgess, A. Kostival, W. Buttner, C. Rivkin, DOE Annual Merit Review (June 18, 2014), Washington, DC.

7. "700 Bar Hydrogen Dispenser Hose Reliability Improvement," K. Harrison, H. Dinh, M. Peters, DOE Annual Merit Review (June 17, 2014) ,Washington, DC.

VIII.6 Hydrogen Safety Panel, Safety Knowledge Tools and First Responder Training Resources

Nick Barilo
Pacific Northwest National Laboratory (PNNL)
P.O. Box 999
Richland, WA 99354
Phone: (509) 371-7894
Email: nick.barilo@pnnl.gov

DOE Manager
Will James
Phone: (202) 287-6223
Email: Charles.James@ee.doe.gov

Subcontractors
- David J. Farese, Air Products and Chemicals, Inc., Allentown, PA
- William C. Fort, Shell Global Solutions (ret), Fairfax, VA
- Larry Fluer, Fluer, Inc., Paso Robles, CA
- Don Frikken, Becht Engineering, St. Louis, MO
- Jennifer Hamilton, BKi, West Sacramento, CA
- Aaron Harris, Air Liquide, Houston, TX
- Richard A. Kallman, City of Santa Fe Springs, CA
- Larry Moulthrop, Proton OnSite, Wallingford, CT
- Glenn W. Scheffler, GWS Solutions of Tolland, LLC, Tolland, CT
- Steven C. Weiner, Excelsior Design, Inc., Richland, WA
- Robert G. Zalosh, Firexplo, Wellesley, MA

Project Start Date: 2004
Project End Date: Project continuation and direction determined annually by the U.S. DOE

Overall Objectives

- Provide expertise and recommendations to DOE and help identify safety-related technical data gaps, best practices, and lessons learned
- Help DOE integrate safety planning into funded projects to ensure that all projects address and incorporate hydrogen and related safety practices
- Collect information and share lessons learned from hydrogen incidents and near misses to help prevent similar safety events in the future
- Capture vast and growing knowledge base of hydrogen experience and make it publicly available to the hydrogen community and stakeholders
- Support the implementation of hydrogen and fuel cell technologies by providing technically accurate hydrogen safety and emergency response information to first responders

Fiscal Year (FY) 2015 Objectives

- Develop a plan to update first responder training materials with revised and new content, including videos, virtual reality features, and other enhancements
- Develop and deploy a publicly available Hydrogen Tools Portal having at least four resources
- Develop a draft third party hydrogen certification guide to facilitate timely project permitting and approval by code officials

Technical Barriers

This project addresses the following technical barriers from the DOE Fuel Cell Technologies Office (FCTO) Multi-Year Research, Development and Demonstration (MYRDD) Plan [1]:

Safety, Codes and Standards

(A) Safety Data and Information: Limited Access and Availability

(B) Availability and Affordability of Insurance

(C) Safety is Not always Treated as a Continuous Process

(D) Lack of Hydrogen Knowledge by AHJ (Authorities Having Jurisdiction)

(E) Lack of Hydrogen Training Materials and Facilities for Emergency Responders

(G) Insufficient Technical Data to Revise Standards

Education and Outreach

(A) Lack of Readily Available, Objective and Technically Accurate Information

(D) Lack of Educated Trainers and training Opportunities

Contribution to Achievement of DOE Milestones

This project contributes to achievement of the following DOE tasks and milestones from the FCTO MYRDD Plan:

Safety, Codes and Standards

- Task 1: Address Safety of DOE R&D Projects (ongoing)

- Task 5: Dissemination of Data, Safety Knowledge, and Information (ongoing)
- Milestone 5.1: Update safety bibliography and incidents databases (4Q, 2011–2020)

Education and Outreach

- Task 1: Educate Safety and Code Officials (ongoing)
- Milestone 1.1: Update "Introduction to Hydrogen Safety for First Responders" course for first responders (Biannually)

FY 2015 Accomplishments

- The 21st Hydrogen Safety Panel (HSP) meeting in West Sacramento, California, March 3–5, 2015, served to enable the consideration of timely and relevant safety issues and the engagement of key hydrogen infrastructure stakeholders in California.
- Fifteen reviews (including safety plans and project design work) were conducted since July 1, 2014, for projects in fuel cell and hydrogen storage R&D. Particular emphasis was placed on early project involvement, as discussed in the FY 2013 annual progress report [3], in order to identify significant safety-related issues early enough to allow consideration by project teams.
- PNNL and the California Fuel Cell Partnership (CaFCP) collaborated to develop the "National Hydrogen and Fuel Cell Emergency Response Training Resource," which was made publicly available in September 2014.
- Planning sessions involving first responder trainers, facility and equipment providers, and other interested persons identified potential improvements for first responder training resources. Results suggested that improved images and videos, new props, and virtual reality tools could cost-effectively improve the instructional quality and potential reach of such resources.
- The online Hydrogen Tools Portal (http://h2tools.org) was developed and deployed (June 2015) as a publicly available resource. The portal is a transformative step toward disseminating safety information on hydrogen and fuel cell technologies through a variety of tools and web-based content that increase their accessibility, visibility, and value.
- Planning was completed for an outreach and educational session for the International Code Council (ICC) annual business meeting, Long Beach, California, September 27–29, 2015, to include presenting "Safety Considerations for Hydrogen and Fuel Cell Applications."

✧ ✧ ✧ ✧ ✧

INTRODUCTION

Safety is essential for realizing the hydrogen economy—safe operation in all of its aspects from hydrogen production through storage, distribution and use, from research, development and demonstration to deployment and commercialization. As such, safety is given paramount importance in all facets of the research, development, demonstration and deployment work of FCTO. This annual report summarizes activities associated with three project tasks: the Hydrogen Safety Panel, Safety Knowledge Tools, and First Responder Training Resources.

Recognizing the nature of DOE fuel cell technology (FCT) programs and the importance of safety planning, the Hydrogen Safety Panel was formed in December 2003 to bring a broad cross-section of expertise from the industrial, government and academic sectors to help ensure the success of the program as a whole. The panel's experience resides in industrial hydrogen production and supply, hydrogen R&D and applications, process safety and engineering, materials technology, risk analysis, accident investigation, and fire protection. The panel provides expertise and recommendations on safety-related issues and technical data gaps, reviews individual DOE-supported projects and their safety plans and explores ways to develop and disseminate best practices and lessons learned, all broadly benefiting the FCT programs. The panel is currently composed of 14 members having over 400 years of industry and related experience (see Table 1 for FY 2015 panel membership).

TABLE 1. Hydrogen Safety Panel

Nick Barilo, Program Manager	PNNL
Richard Kallman, Chair	City of Santa Fe Springs, CA
David Farese	Air Products and Chemicals
Larry Fluer	Fluer, Inc.
Bill Fort	Shell Global Solutions (ret)
Don Frikken	Becht Engineering
Aaron Harris	Sandia National Laboratories
Chris LaFleur	Sandia National Laboratories
Miguel Maes	NASA White Sands Test Facility
Steve Mathison*	Honda Motor Company
Larry Moulthrop	Proton OnSite
Glenn Scheffler	GWS Solutions of Tolland, LLC
Steven Weiner	Excelsior Design, Inc.
Robert Zalosh	Firexplo

*New panel member; NASA – National Aeronautics and Space Administration

Widespread availability and communication of safety-related information are crucial to ensuring the safe operation of future hydrogen and fuel cell technology systems. The entire hydrogen community benefits if hydrogen safety-related knowledge is openly and broadly shared. To that end,

PNNL continues to improve the safety knowledge software tools and develop new techniques for disseminating this information. This report covers the Hydrogen Tools Portal (http://h2tools.org), the Hydrogen Lessons Learned database (http://h2tools.org/lessons/), the Hydrogen Safety Best Practices online manual (https://h2tools.org/bestpractices), and the Hydrogen Tools iPad and iPhone apps. These resources are key to reaching, educating and informing stakeholders whose contributions will help enable the deployment of new hydrogen and fuel cell technologies.

A suitably trained emergency response force is essential to a viable infrastructure. FCTO has placed a high priority on training emergency response personnel, not only because these personnel need to understand how to respond to a hydrogen incident, but also because firefighters and other emergency responders are influential in their communities and can be a positive force in the introduction of hydrogen and fuel cells into local markets. This report covers hazardous materials emergency response training to provide a tiered hydrogen safety education program for emergency responders. The effort started with development and distribution of the awareness-level online course in FY 2006–2007. An operations-level classroom curriculum was developed in FY 2008–2009, including the design, construction and operation of a fuel cell vehicle prop for hands-on training. PNNL and the California Fuel Cell Partnership (CaFCP) collaborated to develop a national hydrogen safety training resource for emergency responders, which was made publicly available in September 2014.

APPROACH

The HSP strives to raise safety consciousness most directly at the project level through organizational policies and procedures, safety culture, and priority. Project safety plans and design documents are reviewed to encourage thorough and continuous attention to safety aspects of the specific work being conducted. Panel safety reviews focus on engagement, learning, knowledge-sharing and active discussion of safety practices and lessons learned, rather than audits or regulatory exercises. Through this approach, DOE and the HSP are trying to achieve safe operation, handling and use of hydrogen and hydrogen systems for all DOE projects.

The approach for disseminating safety knowledge shifted in FY 2015. While the project retained its current tools—the Hydrogen Lessons Learned database and the Hydrogen Safety Best Practices online manual—the primary focus was a new resource: the Hydrogen Tools Portal. The portal integrates a broader set of hydrogen safety resources into a single location, maximizing their efficacy and impact. Additional discussion of this resource is provided in the Results section of this report.

PNNL collaborates with subject matter experts in hydrogen safety and first responder training to develop, review, and revise training materials as needed. The PNNL project team works with DOE to inform stakeholder groups of training opportunities and to provide "live" training when appropriate. The online awareness-level course provides the student with a basic understanding of hydrogen properties, uses and appropriate emergency response actions. The operations-level classroom/hands-on prop-based course has been presented at the Volpentest Hazardous Material Management and Materials Response (HAMMER) Federal Training Center in Richland, Washington, and at several fire-training centers in California and Hawaii to reach larger audiences in areas where hydrogen and fuel cell technologies are being deployed.

New approaches are needed to meet the needs of first responders and the presentation styles of training organizations and to complement existing training programs. The National Hydrogen and Fuel Cell Emergency Response Training Resource (NTR) will help ensure a consistent source of accurate information and current knowledge. As part of this resource, a training template has been developed to guide the delivery of a variety of training regimens to various audiences.

RESULTS

The 21st meeting of the Hydrogen Safety Panel was held in West Sacramento, California, March 3–5, 2015. The meeting provided opportunities to consider timely and relevant safety issues and provide direct input to FCTO. The topics discussed and outcomes achieved at the meeting are detailed in the minutes [2]. Two panel task groups were formed at the meeting to (1) investigate sources of information for liquid hydrogen releases and provide a summary document and (2) investigate the results from compressed natural gas tank failure incidents, tank testing, SAE J2579 requirements, and other related materials to consider what might be learned for hydrogen.

During the past year, the panel has provided safety reviews and support to projects as noted in Table 2. Since 2004, the panel has participated in 413 project reviews (including safety plans, site visit reviews, follow-up phone interviews, and design review work). Three of these projects used the early project involvement approach discussed in the FY 2013 annual progress report [3], which identified significant project issues early enough to allow consideration by project teams.

A significant panel initiative during FY 2015 was work to develop a certification guide to assist code officials and project proponents with approval of hydrogen systems and facilities when listed equipment is not available. This effort is in response to a gap that the panel identified during the American Recovery and Reinvestment Act of 2009 project

TABLE 2. HSP Project Safety Work since July 1, 2015

Work	Project Title	Contractor
Document Review [4]	Austin Fuel Cell Bus, Hydrogen Purge Failure Analysis Report 1 of 2	Proterra, Inc.
Design Review [5]	Hydrogen Refueling Trailer (Hawaii Maritime Project)	Sandia National Laboratories/Luxfer-GTM
Safety Plan [6]	Smart Matrix Development for Direct Carbonate Fuel Cell	FuelCell Energy
Design Review [7]	HyStEP	Sandia National Laboratories
Safety Plan [8]	Wide Bandgap Chalcopyrite Photoelectrodes for Direct Solar Water Splitting	HNEI
Safety Plan [9]	Linear Motor Reciprocating Compressor (LMRC) for Forecourt Hydrogen Compression	Southwest Research Institute®
Safety Plan [10]	A Novel Hybrid Reformer-Electrolyzer-Purifier (REP) for Distributed Production of Low-Cost, Low Greenhouse Gas Hydrogen	FuelCell Energy
Safety Plan [11]	Affordable, High-Performance, Intermediate Temperature Solid Oxide Fuel Cells	Redox Power Systems, LLC
Safety Plan [12]	Smart Matrix Development for Direct Carbonate Fuel Cell	FuelCell Energy
Safety Plan [13]	Boron-Based Hydrogen Storage – Ternary Borides and Beyond	HRL Laboratories
Safety Plan [14]	Particle Flow Solarthermal RedOx Water Splitting	University of Colorado
Site Visit [15]	LLNL Cryogenic and High Pressure Hydrogen Vessel Testing Facility Safety Plan	LLNL
Safety Plan [16]	Demonstration of a Fuel Cell-powered Transport Refrigeration Unit (TRU) (Safety Plan)	Plug Power
Design Review [17]	Maritime Fuel Cell Generator Project (Second Review)	Sandia National Laboratories
Safety Plan [18]	LLNL Cryogenic and High Pressure Hydrogen Vessel Testing Facility Safety Plan	LLNL

HNEI – Hawaii Natural Energy Institute; LLNL – Lawrence Livermore National Laboratory

reviews [19]. The need for this activity was also identified at a 2014 stakeholder meeting to consider additional tools for supporting hydrogen and fuel cell commercialization [20]. The challenge with certification is that the listing process for rapidly changing products, consistent with developing technologies, tends to be cost-prohibitive for equipment providers (each revision to the equipment requires recertification). The circumstance of new technologies under development and low demand for early market applications results in few components and systems being currently listed. The scarcity of listed equipment places an extraordinary burden on code officials to ensure (and approve) that products include the appropriate inherent or automatic safety measures. The guide will identify listing requirements in the ICC codes and National Fire Protection Association (NFPA) 2 for hydrogen equipment, and suggest criteria for approval when listed equipment is not available. This will provide common criteria for code officials and third parties to use in approving unlisted equipment. It will also ensure that different vendors are considering the same criteria across a variety of projects. A draft of the certification guide is expected to be available in the fall of 2015 [21].

A publicly accessible Hydrogen Safety Panel website (https://h2tools.org/hsp) was made available in March 2015. The website enables visitors to explore the Panel's purpose and activities and download information and resources. A web presence will help reinforce the Panel's position as the go-to resource for serious, informed, and unbiased consideration of relevant safety issues.

The Hydrogen Tools Portal was made publicly available in June 2015. The portal is a transformative step toward disseminating safety information and enabling fuel cell commercialization. It brings together a variety of tools and web-based content on the safety aspects of hydrogen and fuel cell technologies, increasing their accessibility, visibility, and value. The portal is intended to help inform those tasked with designing, approving or using systems and facilities, as well as those responding to incidents. The portal was released with 11 resources, user workspaces, and discussion forums. The workspaces are a first of its kind tool that enables users (code officials, first responders, risk managers, operations and maintenance personnel, project proponents, and researchers) to explore resources side-by-side on a single web page. The resources include a bibliography, lessons learned, best practices, a codes and standards database, a hydrogen compatibility database, and a questions/answers section.

Disseminating safety information continues to be an important aspect of this project. During this reporting period, PNNL primarily focused outreach activities on membership associated with the ICC. ICC members include building, fire, plumbing, mechanical and energy officials representing state, county, municipal and federal governments. Ensuring that this group is informed on hydrogen safety-related issues and resources can help facilitate a safe and timely transition to fuel cell technologies. The project activities during FY 2015 included authoring/coauthoring two online articles for the Building Safety Journal [18] and coordinating a hydrogen safety educational session [22] and outreach event for the ICC's annual business meeting, September 27–29, 2015.

PNNL and the CaFCP are collaborating on the outreach to bring a ride and drive event and booth display for the attendees. Other outreach activities during FY 2015 included a presentation at the National Professional Development Symposium for the National Fire Academy [23], and a presentation at the European Technical School on Hydrogen and Fuel Cells in Crete, Greece [24].

FY 2015 activities directed toward the first responder training task included release and deployment of the NTR, developing a plan for improving first responder training materials, and providing hands-on training. The NTR is intended to serve as a consistent source of accurate and current information to enable trainers to provide their own first responder hydrogen safety training based on their needs and environments. The NTR was made publicly available in September 2014 (http://h2tools/fr/nt), and a webinar was conducted in March 2015 to announce its availability and provide guidance on its use. Early indications are that this will be a valuable resource. The webinar had over 250 attendees and the NTR has been downloaded on six continents and in 35 of 50 states (see Figure 1). The NTR was also translated into Japanese in February 2015 to support hydrogen and fuel cell technology initiatives in Japan. FCTO presented an R&D award to the project manager in charge of this work for "his outstanding efforts in developing comprehensive safety training resources" in this area.

A plan to revise first responder training materials was drafted in FY 2015. The goal of this activity is to consider what types of materials (videos, virtual reality tools, etc.) would enhance the first responder learning experience the most. The effort included collaboration with a variety of first responder trainers, facility and equipment providers and other interested persons. Results suggested that improved images and videos, new props, and virtual reality tools could cost-effectively improve the instructional quality and potential reach of first responder hydrogen safety training resources. Dissemination of training resources was also discussed. As a result of this activity, PNNL has begun discussions with the National Fire Academy to transfer the online awareness training to them in order to:

- Allow a broader distribution of the materials.
- Improve crediting of course completion/continuing education units.
- Provide a good long-term landing spot for the training.

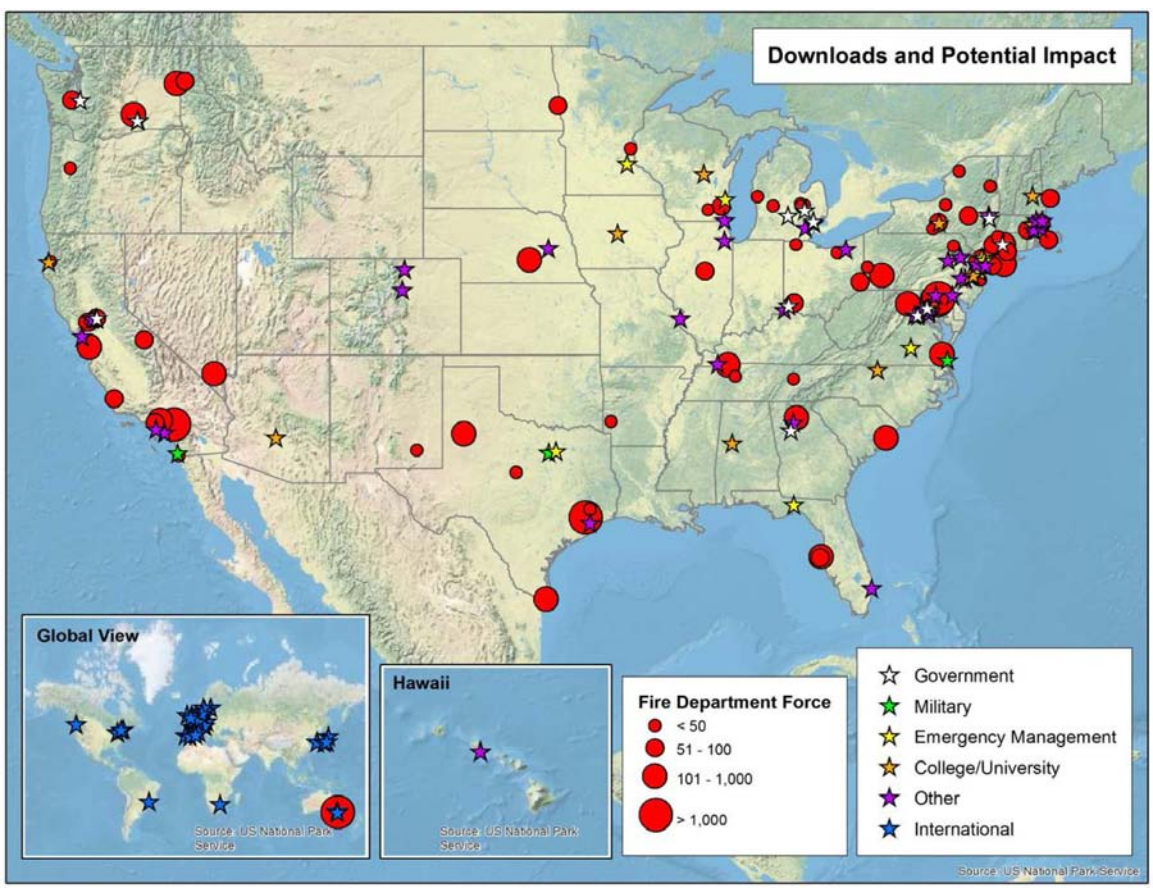

FIGURE 1. NTR Downloads and Potential Impacts

PNNL and CaFCP would continue to provide subject matter expertise on the technical content after the transfer.

First responder outreach and training for FY 2015 included a hydrogen first responder prop demonstration at the Volpentest HAMMER Federal Training Center, Richland, Washington, for the Northwest's International Association of Fire Fighters Fire Ops 101 (approximately 75 participants). Operations-level training, including classroom and prop demonstration, was provided for the Washington State Annual Hazardous Materials Workshop, and was also conducted at HAMMER. For the latter, the NFPA video recorded the prop demonstration for use in their DOE-funded alternative fuels first responder training. NFPA also video recorded the classroom portion of the training for the project to include in the Hydrogen Tools Portal.

CONCLUSIONS AND FUTURE DIRECTIONS

The HSP will continue to focus on how safety knowledge, best practices, and lessons learned can promote the safe conduct of project work and the deployment of hydrogen technologies and systems in applications of interest and priority in FCTO. The Panel can also be used more broadly as an asset for safe commercialization by reaching out to new stakeholders and users involved in early deployment.

HSP initiatives over the next fiscal year will include the following.

- Support project activities with the focus on early engagement, including kickoff meetings, safety plan reviews, site visits, and other interactions with project teams
- Engage non-DOE entities to identify opportunities to use the panel to review hydrogen and fuel cell initiatives and promote safety
- Identify opportunities to support H2USA (H2USA is a public-private partnership to promote the commercial introduction and widespread adoption of fuel cell electric vehicles across the United States with a mission to address hurdles to establishing hydrogen fueling infrastructure)
- Submit a draft hydrogen certification guide to DOE and work with stakeholders, code officials, and other interested parties to review the content in preparation for public release of the document by the end of FY 2016
- Support the H-Prize competition, including a safety planning webinar and participant submittal reviews to ensure that safety is considered and prioritized for this initiative
- Continue to evaluate the panel membership to maintain its leadership role in hydrogen safety through an appropriate mix of safety expertise and perspective to perform safety reviews and address relevant issues
- Seek opportunities to share safety knowledge with new audiences to facilitate the safe deployment of hydrogen and fuel cell technologies
- Meet with code officials, project proponents and stakeholders from recently completed fuel station projects to discuss safety learnings and needs (three to six trips)

Hydrogen safety knowledge tools help remove barriers to the deployment and commercialization of hydrogen and fuel cell technologies. The introduction of the Hydrogen Tools Portal opens new opportunities for sharing safety information and reaching broader audiences. In FY 2016, PNNL will enhance the Hydrogen Tools Portal, including workspace customization, mobile device display improvements, search engine optimization, and improved site performance. PNNL will also explore opportunities to collaborate with other national laboratories, state organizations and industry partners to identify and integrate new resources into this valuable website. Outreach will focus on state fire marshal organizations through focused meetings and key conferences.

The project's first responder training resources address a key H2USA barrier, ensure a safe transition to fuel cell vehicles and hydrogen infrastructure, and pave the way for broader public acceptance. Potential activities for FY 2016 include development of new pictures and videos for use in all first responder training resources and processing the NFPA video for use on the Hydrogen Tools Portal. Onsite operations-level training may also be provided in the Northeast if sufficient resources are available.

International collaboration is important to PNNL's hydrogen safety work. In October 2015, PNNL will participate in the International Conference in Hydrogen Safety in Yokohama, Japan, and present on two topics, "Hydrogen and Fuel Cells – Emphasizing Safety to Enable Commercialization" and "First Responder Training: Supporting Commercialization of Hydrogen and Fuel Cell Technologies." PNNL is also exploring opportunities to collaborate with the International Association on Hydrogen Safety to develop best practices for safety issues related to current and emerging fuel cell technologies.

FY 2015 PUBLICATIONS/PRESENTATIONS

1. Weiner, S.C., "Advancing the Hydrogen Safety Knowledge Base," International Journal of Hydrogen Energy, Vol. 39, Issue 35, December 2014, pp. 20357-20361.

2. Barilo, N.F., "Hydrogen and Fuel Cells Are Coming… Are You Ready?" International Code Council, Online Building Safety Journal, February 2015.

3. Barilo, N.F., "First Responder Training Resources Essential for Transforming Energy Use," H_2FC Newsletter, Issue 2, March 2015 (http://h2fc.eu/files/downloads/e-newsletter/H2FC_e-journal_2-2015_interaktiv.pdf).

4. Barilo, N.F. and Rivkin, C.H., "Hydrogen and Fuel Cells… Focusing on Facility Safety Requirements," Online Building Safety Journal, April 2015.

5. Barilo, N.F. and Weiner, S.C., "Hydrogen and Fuel Cells – Emphasizing Safety to Enable Commercialization," PNNL-SA-108993, International Conference on Hydrogen Safety, Yokohama, Japan, October 19-21, 2015 (manuscript approved May 2015).

6. Barilo, N.F., Hamilton, J.J. and Weiner, S.C., "First Responder Training: Supporting Commercialization of Hydrogen and Fuel Cell Technologies," PNNL-SA-109109, International Conference on Hydrogen Safety, Yokohama, Japan, October 19-21, 2015 (manuscript approved May 2015).

REFERENCES

1. U.S. Department of Energy, "Fuel Cell Technologies Office Multi-Year Research, Development and Demonstration (MYRD&D) Plan," http://energy.gov/eere/fuelcells/downloads/fuel-cell-technologies-office-multi-year-research-development-and-22.

2. Barilo, N.F. to James, C. et al., "Minutes for the 21st Hydrogen Safety Panel Meeting," April 6, 2015.

3. 2013 Annual Progress Report, "VIII.9 Hydrogen Safety Panel and Hydrogen Safety Knowledge Tools," available online at http://www.hydrogen.energy.gov/pdfs/progress13/viii_9_barilo_2013.pdf.

4. Barilo, N.F. to Torr, J., "Hydrogen Safety Panel Review of the Austin Fuel Cell Bus Purge Incident," May 28, 2015.

5. Barilo, N.F. to Pratt, J., "Hydrogen Safety Panel Review of the Luxfer-GTM 1950 Gas Transport Module," June 1, 2015.

6. Barilo, N.F. to Peterson, D., "Re: Hydrogen Safety Panel Review of the FCE Smart Matrix Project, EE0006606," May 15, 2015.

7. Barilo, N.F. to Johnson, T., "Hydrogen Safety Panel Comments on the HyStEP Preliminary Design Review," March 16, 2015.

8. Barilo, N.F. to Peterson, D., "Hydrogen Safety Panel Review of the University of Hawaii Safety Plan for DE-EE0006670," March 30, 2015.

9. Barilo, N.F. to Cierpik, K, "Hydrogen Safety Panel Review of the SwRI Safety Plan for Project DE-EE0006666," March 1, 2015.

10. Barilo, N.F. to Peterson, D., "Hydrogen Safety Panel Review of the FuelCell Energy REP Project Safety Plan (EE0006669)," March 9, 2015.

11. Barilo, N.F. to Peterson, D., "Hydrogen Safety Panel Review of the Safety Plan for Redox Project (EE0006735)," March 9, 2015.

12. Barilo, N.F. to Reginald, T., "Hydrogen Safety Panel Review of the FCE Smart Matrix Project, EE0006606," February 5, 2015.

13. Barilo, N.F. to Cierpik, K., "Hydrogen Safety Panel Review of the HRL Safety Plan (DE-EE0006630)," January 21, 2015.

14. Barilo, N.F. to Randolph, K., "Hydrogen Safety Panel Review of the CU Particle Flow Solarthermal RedOx Water Splitting Project Safety Plan," January 19, 2015.

15. Barilo, N.F. to Petitpas, G., "Hydrogen Safety Panel Site Visit Report – LLNL Cryogenic and High Pressure Hydrogen Vessel Testing Facility," October 31, 2014.

16. Barilo, N.F. to Brooks, K., "Re: Updated TRU Safety Plan/+," August 5, 2014.

17. Barilo, N.F. to Pratt, J.W., "Re: [EXTERNAL] Hydrogen Safety Panel Comments on the Maritime Fuel Cell Generator Project Preliminary Design," July 14, 2014.

18. Barilo, N.F. to Adams, J., "Re: Safety Plan LLNL," July 15, 2014.

19. Barilo, N.F. and Weiner, S.C., "Final Report: Hydrogen Safety Panel Review of DOE Fuel Cell Projects," PNNL-22075, Pacific Northwest National Laboratory, Richland, WA, August 2013.

20. Barilo, N.F., "Electronic Safety Resource Tools – Supporting Hydrogen and Fuel Cell Commercialization, PNNL-23704", Pacific Northwest National Laboratory, Richland, WA, September 2014.

21. Barilo, N.F. and Weiner, S.C., "Hydrogen and Fuel Cells – Emphasizing Safety to Enable Commercialization," PNNL-SA-108993, International Conference on Hydrogen Safety, Yokohama, Japan, October 19-21, 2015. (manuscript approved May 2015)

22. Barilo, N. F., "Safety Considerations for Hydrogen and Fuel Cell Applications," submitted to the ICC Annual Business Meeting and Conference , Long Beach, CA, September 27-29, 2015 (submitted for approval June 12, 2015).

23. Barilo, N.F., "An Introduction to Hydrogen and Fuel Cell Technologies," National Professional Development Symposium, Emmitsburg, MD, June 12, 2015.

24. Barilo, N.F., "Overview of the US Program and Safety Resources," European Technical School on Hydrogen and Fuel Cells, Crete, Greece, June 22, 2015.

VIII.7 Fuel Cell Technologies National Codes and Standards Development and Outreach

Carl Rivkin (Primary Contact), Robert Burgess, and William Buttner
National Renewable Energy Laboratory (NREL)
15301 Denver Parkway West
Golden, CO 80401
Phone: (303) 275-3839
Email: Carl.Rivkin@nrel.gov

DOE Manager
Will James
Phone: (202) 287-6223
Email: Charles.James@ee.doe.gov

Subcontractor
Branded by Media, Orange, CA

Project Start Date: October 1, 2002
Project End Date: Project continuation and direction determined annually by DOE.

Overall Objectives

- Support the deployment of hydrogen technologies for hydrogen fuel cell vehicles and stationary fuel cell applications
- Make critical safety information readily available through webinars, training sessions, safety reports, and technical presentations
- Inform key stakeholders of the safety, codes, and standards requirements for the safe use of hydrogen technologies
- Work with potential infrastructure developers to accelerate the deployment of hydrogen fueling stations and other key infrastructure
- Identify and resolve safety issues associated with hydrogen technologies infrastructure

Fiscal Year (FY) 2015 Objectives

- Publish a paper on progress and accomplishments in the development of codes and standards
- Support the deployment efforts of H2USA through participation in the Market Acceleration and Support Working Group
- Support the development of the next edition of the Nation Fire Protection Association (NFPA) 2 Hydrogen Technologies Code by leading the NFPA Hydrogen Storage Task Group and acting as Principal Committee member of the NFPA Industrial and Medical Gas Technical Committee
- Develop outreach products for permitting hydrogen technologies
- Publish updated National Permit Guide for hydrogen fueling stations
- Present codes and standards information at California hydrogen technologies deployment meetings and workshops
- Implement Continuous Codes and Standards Improvement (CCSI) Process by evaluating field data to determine codes and standards development priorities
- Provide in-person training to code officials and project developers in key jurisdictions in California and other locations where infrastructure projects are planned
- Support the coordination of domestic and international hydrogen standards by participating in International Organization for Standardization (ISO)/TC 197 hydrogen component development projects

Technical Barriers

This project addresses the following technical barriers from the Safety, Codes and Standards section of the Fuel Cell Technologies Office Multi-Year Research, Development, and Demonstration Plan:

(A) Safety Data and Information: Limited Access and Availability

(D) Lack of Hydrogen Knowledge by AHJs. (Authorities Having Jurisdiction)

(F) Enabling National and International Markets Requires Consistent RCS (Regulations, Codes, and Standards)

(G) Insufficient Technical Data to Revise Standards

(H) Insufficient Synchronization of National Codes and Standards

(I) Lack of Consistency in Training of Officials

(K) No Consistent Codification Plan and Process for Synchronization of R&D and Code Development

(L) Usage and Access Restrictions

Contribution to Achievement of DOE Safety, Codes & Standards Milestones

This project will contribute to achievement of the following DOE milestones from the Safety, Codes and Standards section of the Fuel Cell Technologies Office Multi-Year Research, Development, and Demonstration Plan:

- Milestone 4.6: Completion of standards for critical infrastructure components and systems. (4Q, 2014)
- Milestone 4.7: Complete risk mitigation analysis for advanced transportation infrastructure systems. (1Q, 2015)
- Milestone 4.8: Revision of NFPA 2 to incorporate advanced fueling and storage systems and specific requirements for infrastructure elements such as garages and vehicle maintenance facilities. (3Q, 2016)
- Milestone 4.9: Completion of GTR Phase 2. (1Q, 2017)

FY 2015 Accomplishments

- NREL provided broad coordination of codes and standards development.
  - Supported the Codes and Standards Tech Team; gave three presentations on sensors and codes and standards development activities
  - Implemented the CCSI through several projects
    - Supported the Hydrogen Code Improvement (HCI) team through Fuel Cell & Hydrogen Energy Association codes and standards development activities including support of the H2USA codes and standards development efforts
    - Led the NFPA Hydrogen Storage Task Group to develop technical basis for setback distances and safety mitigation measures in NFPA 55 and NFPA 2
- Coauthored an historical perspective on the history of RCS called "Regulations, Codes and Standards (RCS) for Hydrogen Technologies—A Historical Overview," a paper that will be presented at the International Conference on Hydrogen Safety (ICHS) in Yokohama, Japan
- Developed new permitting and codes and standards training modules for hydrogen technologies deployment that include lessons learned from current deployment activities
- Developed a training video titled "Permitting Hydrogen Fueling Station" in collaboration with an AHJ in the Los Angeles metropolitan area where several hydrogen fueling stations will be located
- Presented in-person training sessions for deployment of hydrogen infrastructure in key jurisdictions including Norwalk and Hayward, California; approximately 70 AHJs representing jurisdictions where hydrogen fueling stations will be located attended these training sessions
- Hosted several international researchers in hydrogen safety to leverage similar safety work being conducted in other countries
- Collaborated effectively with other DOE laboratories including Sandia National Laboratories and Pacific Northwest National Laboratory

✧ ✧ ✧ ✧ ✧

INTRODUCTION

The fundamental purpose of this work is to support the safe deployment of hydrogen technologies. To achieve this objective, codes and standards must be in place to protect public safety and any significant safety issues must be resolved.

The work under this project has helped develop a national set of codes and standards to safely deploy hydrogen technologies. Additionally, key safety issues have been identified and are in the process of being resolved. Safety, codes, and standards information has been distributed to interested parties using a variety of techniques including webinars, NREL technical reports, workshops, in-person presentations, videos, online training tools, and web-based products.

APPROACH

The project approach has been to involve as many key stakeholders as possible in codes and standards development and coordination and outreach activities to achieve maximum effectiveness. These stakeholders include industry partners, standards development organizations, research organizations including other national laboratories, authorities having jurisdiction, local government in locations where projects will be deployed, and trade organizations involved in technology development and deployment.

RESULTS

NREL, at the direction of DOE, has helped develop a baseline set of codes and standards for hydrogen technologies. This accomplishment helps meet several DOE milestones, including 4.4 and 4.8.

The next step in this codes and standards development process after the promulgation of the baseline set of codes and standards is monitoring the field performance of these documents, determining where modifications are required, and supporting the implementation of those modifications. This helps DOE meet Milestone 4.5.

This modification process is illustrated in Figure 1. The process consists of evaluating field deployment of hydrogen technologies through use of NREL data and site visits, determining whether there are issues with codes and standards based on this information, and developing modified codes and standards requirements to resolve these issues. This process also integrates NREL laboratory research activities involving hydrogen technologies safety by using this research to address codes and standards issues.

The CCSI process has already begun to produce results in the following areas:

- The NFPA Hydrogen Storage Task Group has revisited the assessment made for bulk gaseous hydrogen setback distances and has developed a plan for revising these distances in the 2018 edition of NFPA 55/2. This plan should produce proposals to NFPA 55/2 in July 2016.
- The HCI team has produced proposals to the Uniform Fire Code (UFC) to coordinate NFPA 2 and the UFC.

NREL developed codes and standards/permitting training tools such as the "Permitting Hydrogen Fueling Stations" video done in collaboration with the Orange County Fire Authority.

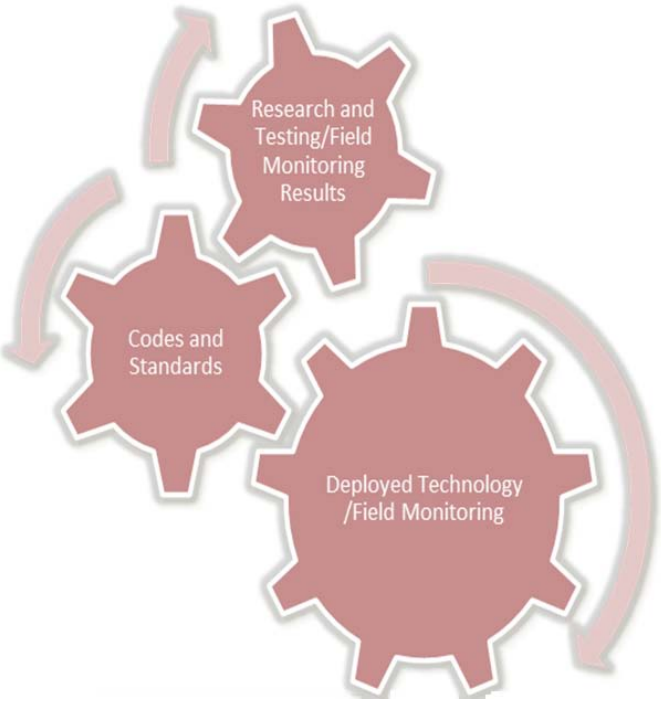

FIGURE 1. Continuous Codes and Standards Improvement (CCSI)

NREL supported the work of H2USA by participating as a member of the Market Acceleration and Support Working Group. This participation included evaluating infrastructure issues such as fuel cell electric vehicle access to tunnels and bridges in New York and Maryland.

NREL supported testing required to develop Federal Motor Vehicle Safety Standards required to implement Global Technical Regulation (GTR) in the United States. This supports DOE Milestone 4.9.

NREL has acted as Task Group Leader for the NFPA Hydrogen Storage Task Group that will develop new requirements for bulk gaseous and liquefied hydrogen and associated safety mitigation measures for the next edition of NFPA 55/2. This supports DOE Milestone 4.9.

CONCLUSIONS AND FUTURE DIRECTIONS

Conclusions

- Codes and Standards
  - Codes and standards development support will continue through direct support of standards development organizations by NREL staff participation on or operation of coordination committees.
  - Ongoing coordination of the fire and building codes and key hydrogen codes and standards is a priority.
  - Field deployment information will help set codes and standards development priorities.
- Outreach
  - Deployment support will be focused on infrastructure at locations with project activity and concrete deployment plans, for example jurisdictions in California.
  - These goals can only be accomplished through collaborations with key stakeholders at all levels.
  - NREL will continue to support deployment of hydrogen and fuel cell technologies through programs such as the technical reports, webinars, safety reviews, and the web-based information compendium.
  - NREL will work with H2 USA to support the efforts of key organizations involved in infrastructure deployment.

Future Directions

- Continue work to coordinate codes and standards on a smaller scale with special focus on taking information from deployment projects back to code development committees
- Resolve infrastructure codes and standards issues such as hydrogen setback distances in NFPA codes
- Continue coordination between National Fire Codes and International Code Council codes, as well as ISO hydrogen component standards and domestic hydrogen component standards
- Support efforts to adopt NFPA 2 Hydrogen Technologies Codes (and other key codes), such as the work done by the California Fire Marshal's Office to adopt NFPA 2 earlier than adoption of the International Fire Code would dictate

Outreach

- Continue to publish NREL technical reports, deliver webinars, and provide web-based information on key safety issues required to support hydrogen technologies deployment
- Assist code officials, project developers, and other interested parties in use of new codes and standards and safety information through outreach activities, with special focus on key jurisdictions such as California
- Utilize NREL hydrogen fueling station for training purposes
- Work with interested parties to provide information to assist in infrastructure deployment
- Provide in-person codes and standards training in key locations such as California and other zero emission vehicles states
- Work with H2USA to support infrastructure development

FY 2015 PUBLICATIONS/PRESENTATIONS

1. C. Rivkin "Deployment of Hydrogen Infrastructure," Hayward Fire Department, Hayward, California, December 9, 2014.

2. C. Rivkin, "Deployment of Hydrogen Infrastructure," Los Cerritos Community College, Norwalk, California, August 9, 2015.

3. C. Rivkin, R. Burgess, and W. "Regulations, Codes and Standards (RCS) for Hydrogen Technologies—A Historical Overview," forthcoming, submitted to ICHS, July 2015.

4. C. Rivkin, R. Burgess, and W. Buttner "Continuous Codes and Standards Improvement (CCSI) Overview," forthcoming, submitted to ICHA, July 2015.

VIII.8 Fuel Cell & Hydrogen Energy Association Codes and Standards Support

Morry Markowitz (Primary Contact), Karen Hall, Connor Dolan
Fuel Cell & Hydrogen Energy Association (FCHEA)
1211 Connecticut Ave. NW, Suite 650
Washington, DC 20033
Phone: (202) 261-1331
Email: mmarkowitz@fchea.org

DOE Manager
Will James
Phone: (202) 287-6223
Email: Charles.James@ee.doe.gov

Contract Number: DE-AC05-00OR22725

Project Start Date: November 16, 2011
Project End Date: Project continuation and direction determined annually by DOE

Overall Objectives

- Support and facilitate development and promulgation of essential codes and standards by 2015 to enable widespread deployment and market entry of hydrogen and fuel cell technologies and completion of all essential domestic and international regulations, codes, and standards (RCS) by 2020
- Ensure that best safety practices underlie research, technology development, and market deployment activities supported through DOE-funded projects
- Conduct research and development (R&D) to provide critical data and information needed to define requirements in developing codes and standards
- Develop and enable widespread sharing of safety-related information resources and lessons learned with first responders, authorities having jurisdiction (AHJs), and other key stakeholders

Fiscal Year (FY) 2015 Objectives

- Participates directly in key domestic and international RCS technical committees and encourage members to participate directly in appropriate technical committees, working groups or discussions
- Optimize information-sharing of precompetitive safety information
  - Hold open discussions during FCHEA Working Group and Task Force meetings between codes and standards development organizations, researchers, government and industry to aid harmonization of requirements and enhance collaboration
  - Identify and schedule Topical Discussions during monthly meetings of the National Hydrogen and Fuel Cell Codes & Standards Coordinating Committee (NHFCCSCC) which FCHEA administers
    - Enables industry priorities to be discussed and synergistic activities to be coordinated
  - Post and/or link data, workshop proceedings, and other informational resources online at www.hydrogenandfuelcellsafety.info
- Conduct forums to identify R&D needs, and engage in dialog with DOE providing a mechanism for input and feedback into DOE R&D plans and activities
- Publish six bimonthly issues of *The Hydrogen and Fuel Cell Safety Report* – a free online newsletter which is read by thousands of interested parties all over the world

Technical Barriers

This project addresses the following technical barriers from the Safety, Codes and Standards section of the Fuel Cell Technologies Office Multi-Year Research, Development, and Demonstration (MYRDD) Plan:

(F) Enabling National and International Markets Requires Consistent RCS

(H) Insufficient Synchronization of National Codes and Standards

(J) Limited Participation of Business in the Code Development Process

Contribution to Achievement of DOE Safety, Codes & Standards Milestones

This project contributes to the achievement of the following DOE milestones from the Safety, Codes and Standards section of the Fuel Cell Technologies Office MYRDD Plan:

- Milestone 4: Development and Harmonization of RCS
- Milestone 5: Dissemination of Data, Safety Knowledge, and Information

FY 2015 Accomplishments

Accomplishments for each working group or task are provided below.

- The Portable Power Working Group
  - Provided United States manufacturers technical input on standards and regulations for micro fuel cells
    - Worked to ensure international standards are inclusive of all fuel types
    - Conducted broad outreach to support International Electrotechnical Commission (IEC) 62282-6-101 Edition 2, and associated "fuel specific" Part 2 documents
  - Provided comment on HM-215L, notice of proposed rulemaking on "Hazardous Materials: Harmonization with International Standards," to ensure harmonization with international standards for fuel cells as carry on and checked baggage
  - Supported objective from the MYRDD, "Enabling National and International Markets Requires Consistent RCS," by ensuring national and international standards for micro fuel cell applications are harmonized, then adopted by international regulations
- The Transportation Working Group
  - Reviewed infrastructure RCS
    - Administers Hydrogen Codes Task Force to review and develop public input for NFPA 2
    - Initiated new task forces for strategic planning to begin to develop comments for next round of model codes
  - Provided and tracked public inputs through the latest National Fire Protection Association (NFPA) 2 development cycle. The public inputs all address harmonizing requirements with other industry accepted standards and codes
  - Supported objective from the Multi-Year Program Plan (MYPP) – Provide consistent RCS and synchronization of national codes and standards
- The Stationary Power Working Group (SPWG)
  - Provided technical input to a fuel cell focus group that was created by the Telecommunications Industry Association (TIA). FCHEA's SPWG provided support and fuel cell experts, and assisted in populating a new draft guideline with relevant information from existing codes, standards, and guides
  - Reviewed and developed input on issues relating to greenhouse gas emissions accounting
  - Supported objective from the MYPP – Develop and enable widespread sharing of safety-related information resources and lessons learned with first responders, AHJs, and other key stakeholders
    - Provides consistency in requirements and reduces duplication of effort
- Coordination
  - NHFCCSCC – facilitated monthly discussion of new key topics of broad interest, such as "Facilitating Deployment"
    - Progress in the development of RCS was reported and captured for the FCHEA Regulatory Matrix, providing an up-to-date overview of current industry priorities and recent progress in RCS
  - Hydrogen and Fuel Cell Safety Report – published every two months, keeping readers informed of the progress and issues encountered in the development of RCS
    - Has introduced industry to the many new working groups in ISO/TC 197 and the call for participation in the United States standards committees
    - Calendar of events aids in scheduling meetings
  - Contributed to DOE goal to develop and enable widespread sharing of safety-related information resources and lessons learned with first responders, AHJs, and other key stakeholders
    - Increases participation of stakeholders in development of harmonized RCS

✧ ✧ ✧ ✧ ✧

INTRODUCTION

FCHEA participates directly in key domestic and international RCS technical committees and encourages members to participate directly in appropriate technical committees, working groups or discussions. Member companies can therefore participate directly or indirectly as appropriate.

FCHEA builds relationships and works directly with stakeholders to identify and address issues in order to ensure

consistency in RCS and facilitate deployment of hydrogen and fuel cell technologies.

APPROACH

FCHEA working groups provide regular opportunities to engage industry in developing RCS. Working groups engage manufacturers, codes and standards developers, users, researchers, and other stakeholders as appropriate, to identify and discuss issues pertinent to transportation, stationary power, and portable power applications for fuel cell technologies and hydrogen infrastructure.

Monthly stakeholder coordination calls provide opportunities for even broader engagement and facilitate coordination of activities to reduce duplication of effort and increase harmonization of technical requirements. Further outreach is accomplished through bimonthly publication of a free, online newsletter, the *Hydrogen and Fuel Cell Safety Report*.

RESULTS

FCHEA's Portable Power Working Group provided United States manufacturers technical input on standards and regulations for micro fuel cells. The working group conducted broad outreach to support IEC 62282-6-101 Edition 2, and associated "fuel specific" Part 2 documents to ensure developing international standards are inclusive of all relevant fuel types. The working group also provided comment on HM-215L, notice of proposed rulemaking on "Hazardous Materials: Harmonization with International Standards," to ensure harmonization with international standards for fuel cells as carry on and checked baggage. This activity supported the objective from the MYRDD, "Enabling National and International Markets Requires Consistent RCS," by ensuring national and international standards for micro fuel cell applications are harmonized, then adopted by international regulations.

FCHEA's Transportation Working Group focused on infrastructure RCS review. The Hydrogen Codes Task Force reviewed and developed public input for NFPA 2. New task forces were initiated for strategic planning to begin to develop comments for the next round of model codes. The task group provided and tracked public inputs through the latest NFPA 2 development cycle. The public inputs all address harmonizing requirements with other industry accepted standards and codes. This activity supported the objective from the MYRDD, provide consistent RCS and synchronization of national codes and standards.

FCHEA's Stationary Power Working Group provided technical input to a fuel cell focus group that was created by the TIA. FCHEA's SPWG provided support and fuel cell experts, and assisted in populating a new draft guideline with relevant information from existing codes, standards, and guides. This activity supported the objective from the MYRDD, develop and enable widespread sharing of safety-related information resources and lessons learned with first responders, AHJs, and other key stakeholders. This provides consistency in requirements and reduces duplication of effort.

FCHEA's coordination activities include facilitation of the NHFCCSCC and publication of the *Hydrogen and Fuel Cell Safety Report*.

In facilitating the NHFCCSCC, FCHEA led monthly discussion of new key topics of broad interest, such as "Facilitating Deployment." Progress in the development of RCS was reported and captured for the FCHEA Regulatory Matrix, providing an up-to-date overview of current industry priorities and recent progress in RCS.

The Hydrogen and Fuel Cell Safety Report is published every two months, keeping readers informed of the progress and issues encountered in the development of RCS. This newsletter has introduced industry to the many new working groups in ISO/TC 197 and the call for participation in United States standards committees. It also includes a calendar of events to aid in scheduling meetings.

FCHEA's coordination activities increase participation of stakeholders in development of harmonized RCS and contribute to the DOE goal to develop and enable widespread sharing of safety-related information resources and lessons learned with first responders, AHJs, and other key stakeholders.

CONCLUSIONS AND FUTURE DIRECTIONS

- The Portable Power Working Group will work to ensure harmonization with international standards for fuel cells as carry on and checked baggage. The Department of Transportation (DOT) continues to not be harmonized with inclusion of division 2.1 and 4.3 fuel cartridges for checked baggage (micro fuel cell applications). FCHEA is pursuing inquiry within the US DOT Pipeline and Hazardous Materials Safety Administration to determine options to have these regulations harmonized.
- The Transportation Working Group: Special Task Force for Strategic Planning will predict potential needs (e.g., low grade storage at a station) in advance of the next round of code revisions. This will be a small task force who can think outside of the box for future needs, as well as come up with proposals for the existing code language and see what other changes/improvements need to be made. The working group will continue dialog with component manufacturers to resolve issues in advance of infrastructure roll-out.
- The Stationary Power Working Group will work with the TIA to complete the guideline for fuel cells in the telecommunications industry. The working group will continue to review United States and international

standards as well as state regulations to ensure consistency with accepted United States requirements and best practices.

- Coordination
  - NHFCCSCC
    - Continue to administer, identify key issues, and document discussions and outcomes
    - Provide industry feedback and other input to the DOE Safety, Codes and Standards subprogram on RCS development needs and priorities; outreach needs and priorities; R&D needs and priorities to support RSC development activities
  - Safety Report
    - Continue to report on the developing RCS to improve coordination of activities and improve information transfer

FY 2015 PUBLICATIONS/PRESENTATIONS

1. Hydrogen and Fuel Cell Safety Report, issues published at www.hydrogenandfuelcellsafety.info for November 2014, January 2015, March 2015, May 2015, and July 2015. Another issue is scheduled for September 2015.

2. 2015 DOE Hydrogen and Fuel Cells Program Annual Merit Review presentation.

VIII.9 Hydrogen Contaminant Detector

Danny Terlip (Primary Contact), Bill Buttner, Chris Ainscough
National Renewable Energy Laboratory
15013 Denver West Parkway
Golden, CO 80401
Phone: (303) 827-9811
Email: danny.terlip@nrel.gov

Scott McWhorter
Savannah River National Laboratory
Aiken, SC 29808

DOE Manager
Will James
Phone: (202) 287-6223
Email: Charles.James@ee.doe.gov

Project Start Date: October 15, 2014
Project End Date: April 17, 2015

Overall Objectives

Ensure high quality fuel is dispensed to fuel cell electric vehicle (FCEV) customers for optimal fuel cell operation by testing for critical contaminants in the fuel before it is dispensed

Fiscal Year (FY) 2015 Objectives

- Define engineering requirements for an in-line hydrogen contaminant detector (HCD)
- Conduct a market survey of the current state of applicable technologies
- Provide a gap analysis that compares requirements to status of current technology

Technical Barriers

This project addresses the following technical barriers from the Safety Codes and Standards section of the Fuel Cell Technologies Office (FCTO) Multi-Year Research, Development, and Demonstration (MYRDD) Plan:

(A) Safety Data and Information: Limited Access and Availability

Contribution to Achievement of DOE Safety, Codes and Standards

This project contributes to achievement of the following DOE milestones from the Safety, Codes and Standards section of the FCTO MYRDD Plan:

- Milestone 3.2: Publish hydrogen quality testing protocols (4Q, 2015)

FY 2015 Accomplishments

- Completed set of engineering requirements for in-line HCD
- Completed market survey of potential HCD technologies
- Published report with engineering requirements, market survey, and gap analysis.

✧ ✧ ✧ ✧ ✧

INTRODUCTION

It is critical that stations deliver high purity hydrogen to FCEV customers to prevent negative impacts on the vehicles. The equipment along the production and dispensing pathway can affect the purity of automotive fuel cell-grade hydrogen. Potential contaminant sources include production equipment, transportation equipment, storage tanks, compressors, chillers, station piping, and dispensing hoses. Each of these sources can introduce different contaminants into the fuel stream. Each station may be subject to different contaminant sources, depending on the configuration and fuel source. Different types and concentrations of contaminants in the dispensed hydrogen have drastically different effects on fuel cell performance. While there may be individual contracts between gas suppliers and station owners, there is no overall agreement on who is responsible for fuel quality along the production-to-dispensing pathway. This combination of factors makes it challenging to guarantee high purity fuel will be dispensed to customers.

An in-line HCD would make it possible to detect contaminants in the fuel stream as or before they are dispensed to an FCEV customer, therefore limiting contamination to at most one FCEV. Currently there is no immediate solution available. Work from this task will be used to inform future efforts on the best path forward for developing and implementing an in-line HCD at commercial hydrogen stations in the near-term.

APPROACH

The list of contaminants and required levels of detection from SAE International (SAE) J2719 make the likelihood of a one size fits all solution infeasible. The first part of this task, which defined a reduced set of engineering requirements for an in-line HCD, considered common station configurations based on input from vehicle original

equipment manufacturers, station operators, industrial gas companies, and government officials. The second part posed a survey to multiple gas analysis technology manufacturers inquiring about current technology and planned development. The final part of this task analyzed the gaps between what is needed for an in-line HCD and the current state of the market. A House of Quality diagram is provided comparing the most promising technologies with customer requests and engineering requirements.

RESULTS

The near-term engineering requirements, developed with input from a wide array of stakeholders, specify a device with capital and operating expenditures that amount to less than 1% of total station costs and are capable of detecting carbon monoxide, water, ammonia, and sulfur at one order of magnitude above SAE J2719 levels (ppbv–ppmv range). (It is impractical to expect a near-term HCD to be able to detect all contaminants listed in SAE J2719.) Device capital cost should be less than $5,000 at high volumes (>1,000 units), and annual operating costs should be less than $1,000. The device should be integrated just upstream of the dispenser to include the greatest possible number of contaminant sources. Because the pressure used in stations is as much as 900 bar, the HCD must employ a pressure reducer and slip stream for sampling. Gas analysis and reporting should occur within the time of a fill, and the results should indicate to a station operator whether the gas meets quality requirements. Routine maintenance and operation of the device should not require a highly specialized technician, and routine maintenance should not be required more frequently than every six months.

The market survey incorporated responses to an HCD survey developed for this project from 10 companies that manufacture analytical equipment with information from previous studies and international workshops related to hydrogen quality. Gas chromatography, mass spectrometry, Fourier transform infrared spectroscopy, non-dispersive infrared spectroscopy, laser absorption, continuous wave cavity ring-down spectroscopy, and concentrator technologies were investigated for detection abilities, cost, availability, and ambient and sampling requirements. Survey responses indicated that current technology is capable of detecting contaminants at lower levels than the requirements specified in SAE J2719. Capital costs ranged from $10,000 to $90,000, while operating costs ranged from $0 to $4,000. The required maintenance schedule varied from annual maintenance for the cavity ring-down technology to daily maintenance for the Fourier transform infrared technology. The cavity ring-down technology specified a sampling and analysis time of one second, which was the fastest response time identified in this survey. The concentrator coupled with mass spectrometry specified the longest response time at 15 minutes.

The gaps between what is currently available and what is required have been identified. As observed, no current technology meets all of the requirements defined here for an HCD. The largest gaps are costs, robustness, skill level needed to operate HCDs, and field validation. This is expected, as the need for such a device is evolving, and existing gas analysis technologies are generally designed for a laboratory setting that requires specially trained operators. Figure 1 gives a visual representation of the gap analysis.

Research into a promising nontraditional gas analysis technology is currently underway at Los Alamos National Laboratory, where an HCD based on a surrogate fuel cell is being developed. This device has the potential to indicate the presence of impurities in a hydrogen stream, but it is not yet ready for commercial deployment.

CONCLUSIONS AND FUTURE DIRECTIONS

- The market survey indicates that there is currently no commercial HCD solution that meets all of the engineering requirements.

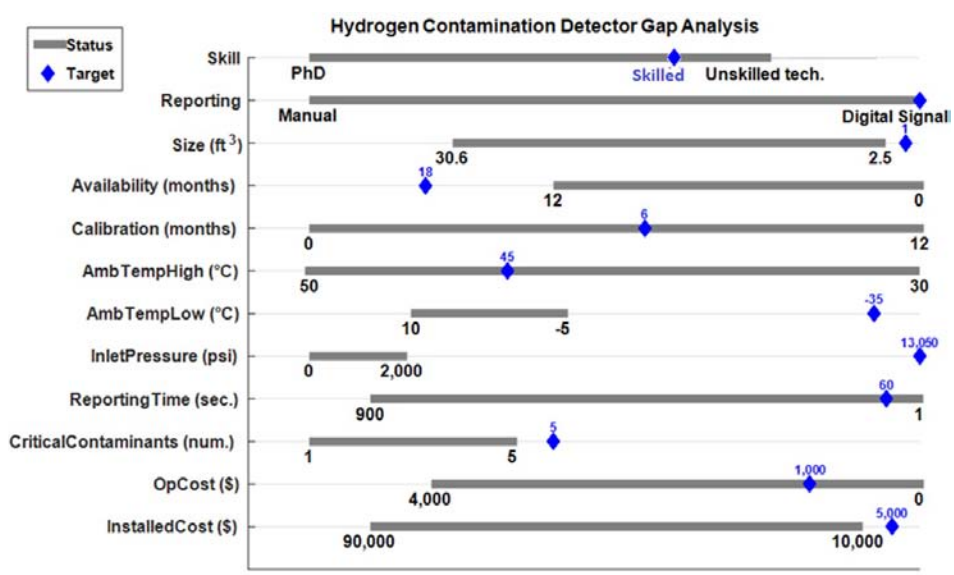

FIGURE 1. Hydrogen contaminant gap analysis with gray bars indicating the current state of the market and blue diamonds indicating engineering requirements

- The capital and operational costs of available analyzers are too high.
- Operation of the current technology is too sophisticated for operators of commercial hydrogen stations and not robust enough to handle the environment.

Hydrogen contaminant detection continues to be an issue of high importance. Plans for continuation of this task will likely involve the installation of new HCD technology in commercial hydrogen stations with the intent of gathering performance and cost data.

FY 2015 PUBLICATIONS/PRESENTATIONS

1. D. Terlip, S. McWhorter, B. Buttner and C. Ainscough, "H2FIRST –Hydrogen Contaminant Detector Task Project Deliverable 1," NREL TP 5400-64063, April 2015.

2. D. Terlip, S. McWhorter, B. Buttner and C. Ainscough, "Hydrogen Contaminant Detector," Presented at the Bi-Annual H2FIRST Coordination Panel Meeting, March 18, 2015.

3. D. Terlip, "Hydrogen Contaminant Detector Project Overview," presented at the California Fuel Cell Partnership Working Group Meeting, 18 September 2014.

VIII.10 Enabling Hydrogen Infrastructure Through Science-Based Codes and Standards

Chris LaFleur (Primary Contact), Alice Muna, Katrina Groth
Sandia National Laboratories
PO Box 5800 MS 0748
Albuquerque, NM 87185
Phone: (505) 844-5425
Email: aclafle@sandia.gov

DOE Manager
Charles (Will) James
Phone: (202) 287-6223
Email: Charles.James@ee.doe.gov

Project Start Date: October 1, 2003
Project End Date: Project continuation and direction determined annually by DOE

Overall Objectives

- Enable the growth of hydrogen infrastructure through science and engineering-based codes and standards
- Enable industry-led codes and standards revision and safety analyses by providing a strong science and engineering basis for code improvements
- Eliminate barriers to deployment of hydrogen fuel cell technologies through scientific leadership in codes and standards development efforts

Fiscal Year (FY) 2015 Objectives

- Apply hydrogen-specific quantitative risk assessment (QRA) tools and methods to support code decisions and to enable risk-equivalent code compliance option
- Optimize cost and time for station permitting by demonstration of alternative approaches to code compliance
- Revise/update codes and standards that address critical limitations to station implementation

Technical Barriers

This project addresses the following technical barriers from the Hydrogen Safety, Codes and Standards section of the Fuel Cell Technologies Office Multi-Year Research, Development, and Demonstration Plan:

(D) Lack of Hydrogen Knowledge by AHJs (Authorities Having Jurisdiction)

(G) Insufficient Technical Data to Revise Standards

(H) Insufficient Synchronization of National Codes and Standards

(K) No Consistent Codification Plan and Process for Synchronization of R&D and Code Development

Contribution to Achievement of DOE Safety, Codes & Standards Milestones

This project will contribute to achievement of the following DOE milestones from the Safety, Codes and Standards section of the Fuel Cell Technologies Office Multi-Year Research, Development, and Demonstration Plan:

- Milestone 2.8: Publish risk mitigation strategies (2Q, 2014)
- Milestone 2.19: Validate inherently safe design for hydrogen fueling infrastructure (4Q, 2019)
- Milestone 4.7: Complete risk mitigation analysis for advanced transportation infrastructure systems (1Q, 2015)
- Milestone 4.8: Revision of NFPA 2 to incorporate advanced fueling storage systems and specific requirements for infrastructure elements such as garages and vehicle maintenance facilities (3Q, 2016)

FY 2015 Accomplishments

- Developed a template of performance-based design of a hydrogen refueling station which demonstrates the use of QRA methods, promotes safety through the use of performance criteria rather than explicit prescriptive requirements, and enables a risk-informed compliance option
- Initiated a hydrogen mitigations forum that identified and prioritized research and development activities for evaluating and crediting safety features that mitigate hydrogen system risks
- Led the development of ISO TR_19880-1 Gaseous Hydrogen-Fueling Stations Part 1: General Requirements by incorporating QRA and safety assessments into the standard

✧ ✧ ✧ ✧ ✧

INTRODUCTION

DOE Fuel Cell Technologies Office has identified safety, codes, and standards as a critical barrier to the deployment of hydrogen, with key barriers related to the availability and implementation of technical information in the development of regulations, codes and standards (RCS). This project provides the technical basis for assessing the safety of hydrogen fuel cell systems and infrastructure using QRA and physics-based models of hydrogen behavior. The risk and behavior tools are used to support both alternate methods of code compliant hydrogen infrastructure as well as direct support of code committees in support of science-based revisions that address critical limitations to refueling station implementation.

This project provides the scientific basis to ensure that code requirements are consistent, logical, and defensible.

APPROACH

State-of-the-art integrated hydrogen behavior and QRA models are applied to relevant technologies and systems to provide insight into the risk level and risk mitigation strategies with the aim of enabling the deployment of fuel cell technologies through revision of hydrogen safety codes and standards. In the short-term focus of providing alternative methods for code compliance, a template demonstrating a credible approach to a performance-based design is developed in order to provide hydrogen information and risk analysis methods to authorities having jurisdiction. This educational effort will enable hydrogen refueling stations that are unable to explicitly meet prescription code requirements to utilize alternate means allowed by the current code. Implementing the template at a real world hydrogen station planned in California will provide precedence for a performance-based design and will allow the cost and schedule for developing this type of station design to be optimized.

Toward the longer term goal of achieving science-based revisions of codes and standards, a mitigations forum of hydrogen experts from industry and research will allow code revisions to account for safety features that are not currently credited in the code requirements. Additionally, a review and revision of the risk-informed code requirements for bulk gaseous hydrogen storage will enable behavior models and technology not available during the 2009 revision to be incorporated in to the risk criteria used to determine these requirements. The bulk liquid hydrogen storage code requirements will also be revised following a similar process once the cold plume release model is validated.

RESULTS

Develop Design Brief to Enable Performance-Based Compliance Option

NFPA 2, Hydrogen Technologies Code, allows for the use of performance-based design (PBD) for hydrogen facilities as a means of complying with the code without strict adherence to the prescriptive code requirements. While Hydrogen Risk Assessment Models (HyRAM) can be used as a means of evaluating the risk of alternate designs, it can also be used to quantitatively evaluate risks associated PBD options. The establishment and demonstration of PBD option will directly increase the availability of locations for hydrogen fueling stations, reduce the effort required by industry to use the PBD approach and lay the groundwork for similar QRA-backed design processes for other alternative fuels. In order to initiate real-world application of science-based risk analysis, a Cooperative Research and Development Agreement was initiated with a major hydrogen fueling station provider.

The HyRAM software was used to calculate the risk metrics for a station that is fully compliant with the prescriptive code requirements in order to establish a baseline for these metrics for a specific station configuration. The performance criteria utilized for each of the required credible scenarios are shown in Figures 1 and 2. Currently, a station design with key modifications to the prescriptive requirements is being evaluated with input from the industry partner for a real-world station that will be processed through the permitting process for a hydrogen station in California. Additionally, lessons learned in applying a performance-based design to a hydrogen refueling station will be used to identify improvements to the current code requirements this type of approach.

Mitigations Forum

With the application of QRA to hydrogen infrastructure, there is a need to characterize and quantify the impact of methods to reduce the risk profile associated with such infrastructure. These methods are commonly referred to as mitigations or safety features. They can be either administrative controls or passive or active engineering controls. Characterizing the risk impacts of these controls is necessary to determine any credit or impact on the separation distances or other code requirements as ongoing code improvements proceed. Currently, a task group under NFPA 2 is actively exploring revisions to the safety distances in the code for bulk liquefied and bulk compressed gaseous hydrogen systems. In order to determine a path forward and identify research gaps, a Hydrogen Mitigations Forum was hosted by SNL.

The forum consisted of a group of hydrogen and risk experts with experience designing and operating hydrogen

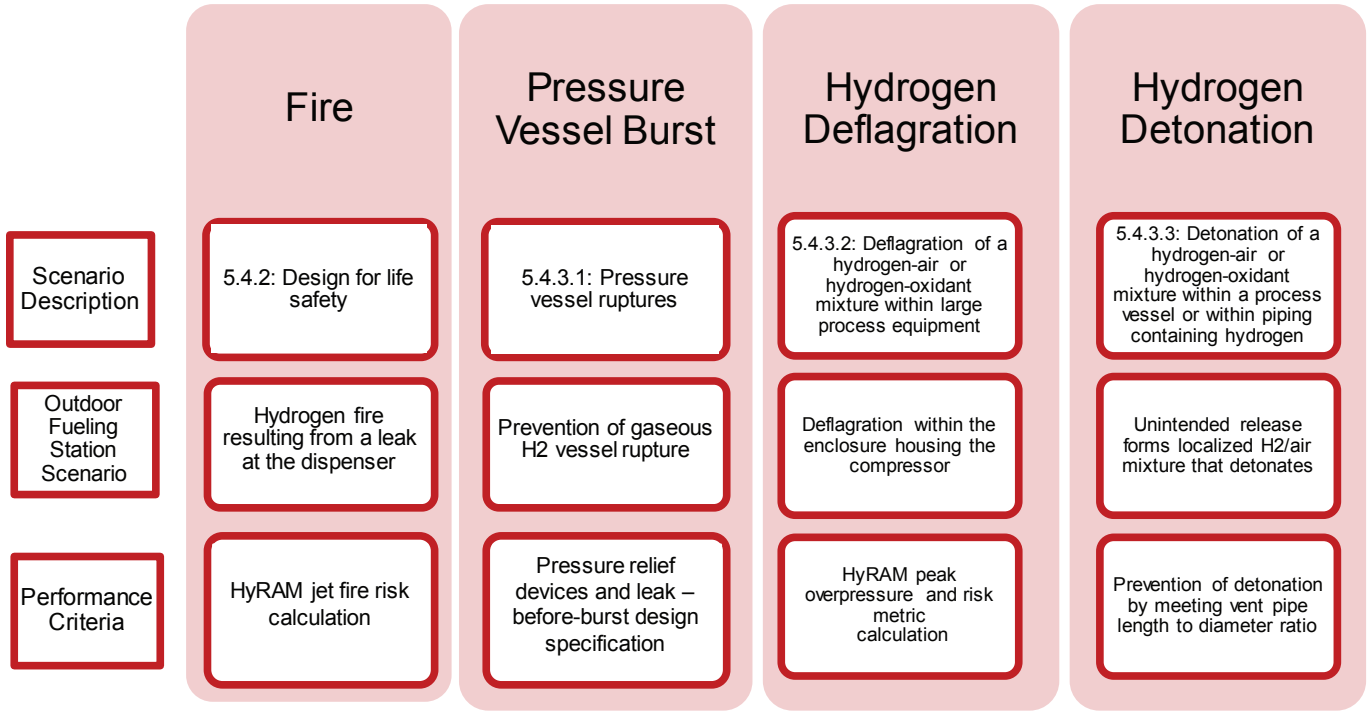

FIGURE 1. Performance criteria utilized for the explosion scenarios in the PBD template

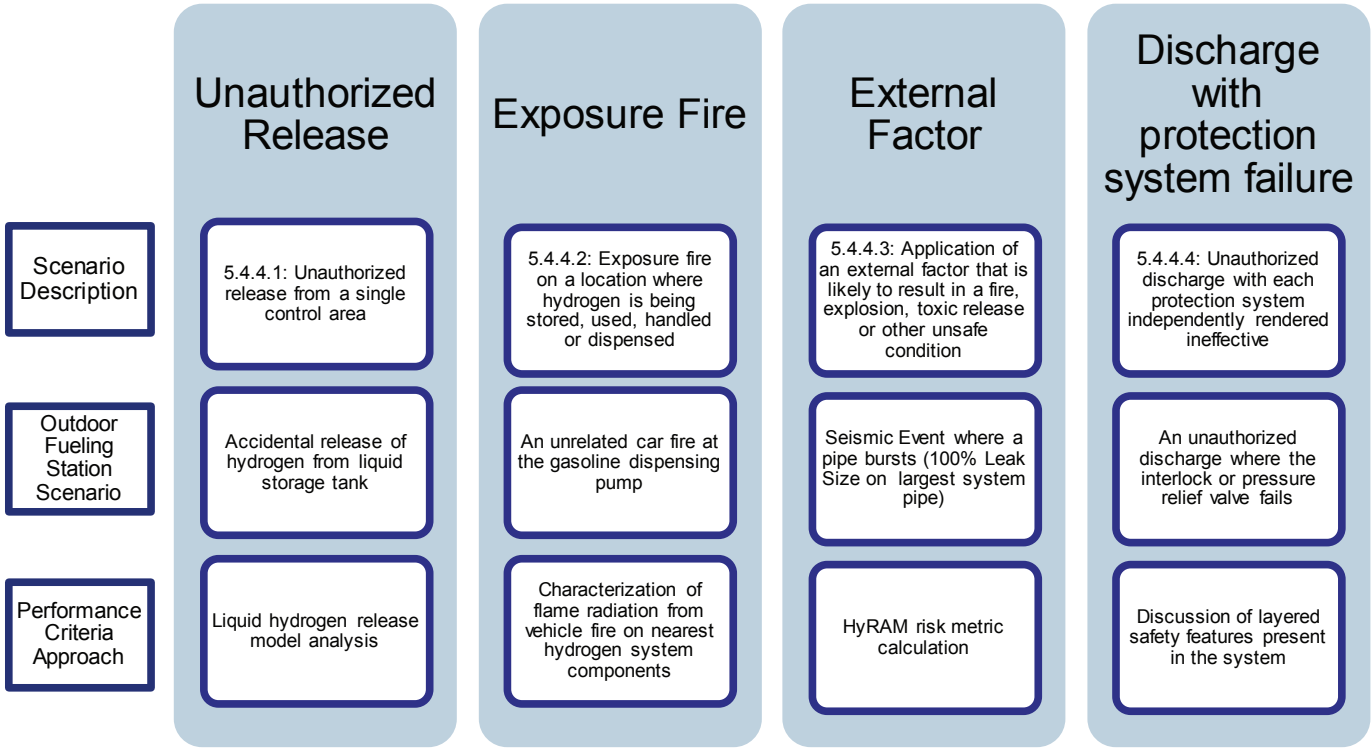

FIGURE 2. Performance criteria utilized for the hazardous material scenarios in the PBD template

systems. Mitigations can be categorized into six groups: release prevention, release detection, release consequence, ignition prevention, ignition detection, and ignition consequence. These groups provide a way to prioritize and credit the safety features based on when they would come into play in a hydrogen release event. It is generally agreed that the closer to the start of an unintentional hydrogen release a feature acts, the smaller the release event and lower potential consequence. In exploring feasible methodologies and strategies for determining these impacts, several gaps in a variety of research areas were identified. In this way, gaps in quantification of risk mitigations can be evaluated and opportunities for advancements in mitigation strategies can be identified. This information will be provided to the code development committees to aid code development activities. Additionally, the gap assessment will provide direction on opportunity to bring science to the code development process, in particular, identification of methods to establish safety credit (e.g., reduction of safety distances) for added mitigations.

Codes and Standards Participation

- CSA HGV 4.9—Hydrogen Fueling Station guidelines has been reviewed by industry and comments received. The CSA standard will be issued following the resolution and dispositioning of all comments and is estimated in FY 2016.
- Hydrogen Safety Panel—SNL participated in several hydrogen safety plan reviews for innovative industrial hydrogen implementations.
- ISO TR-19880-1—SNL has participated in incorporating QRA and safety assessment methodologies into the standard.
- NFPA 2—SNL is providing ongoing technical leadership in the Bulk Hydrogen Storage Task Group of NFPA 2: Hydrogen Technologies Code. The Task group has begun work on revision and update of the prescriptive requirements for both liquefied and gaseous hydrogen separation distances for the next revision cycle of the code.

CONCLUSIONS AND FUTURE DIRECTIONS

- The template for implementing the performance-based approach in NFPA 2 Chapter 5 will be used to demonstrate a credible alternate means of code compliance option and will be utilized as part of the permitting process to demonstrate acceptance of the approach by an authority having jurisdiction.
  - (Future) Extend performance-based design template to other hydrogen application where an alternative solution is needed
- The storage of liquid hydrogen is limited by the existing code requirements and predictive behavior models for liquid hydrogen releases.
  - (Future) Use a validated cold plume release model to characterize the unintended release of liquid-vapor mixed-phase hydrogen releases to revise bulk hydrogen storage code requirements
  - (Future) Identify research gaps in evaluating and prioritizing mitigation features in hydrogen systems
  - (Future) Incorporate recent research and technological advancements into further revisions to the bulk gaseous storage requirements

FY 2015 PUBLICATIONS/PRESENTATIONS

1. LaFleur, C., "Introduction to Hydrogen-Specific Risk Methods and Tools," Presented to Open Public Meeting associated with Hydrogen Safety Panel meeting, March 2, 2015.

2. LaFleur, C., "Performance-Based Approach to Siting Hydrogen Refueling Stations," presentation to DOE H2 CSTT, February 12, 2015.

3. Groth, K.M., "Safety distance working group status update," Presentation to ISO TC197 WG24 sub-team on risk, January 29, 2015.

4. LaFleur, A.C., Muna, A.B., "Draft Fire Protection Engineering Design Brief Template: Hydrogen Refueling Station," Draft Milestone publication, January 2015.

5. LaFleur, C., "Application of Quantitative Risk Assessment (QRA) for Performance-Based Permitting of Hydrogen Fueling Station," Presented at Society of Fire Protection Engineers Annual Meeting, Long Beach, CA, November 14, 2014.

6. San Marchi, C., "Development of Hydrogen Safety Standards in the United States," Presentation at the Workshop on International Trends in Hydrogen Safety Standards, Seoul, Korea, November 14, 2014.

7. Groth, K.M., "Safety distance working group status update," Presentation to ISO TC197 WG24, Munich, Germany, October 13, 2014.

8. Groth, K.M., "Risk-informed method for safety distances," Presentation to ISO TC197 WG24 sub-group on safety distances, Munich, Germany, October 9, 2014.

9. Groth, K.M. "Brief intro to quantitative risk assessment for H_2 C&S." Presentation at ISO TC197, WG24 Meeting, Washington, DC, June 2014.

10. LaFleur, A.C., Muna, A.B., Groth, K.M. "Fire Protection Engineering Design Brief Template: Hydrogen Refueling Station," SAND2015-4500, Sandia National Laboratories, June 2015.

11. LaFleur, A.C., "Enabling Hydrogen Infrastructure Through Science-based Codes and Standards," Presented at the 2015 DOE Hydrogen and Fuel Cells Program and Vehicle Technologies Office Annual Merit Review and Peer Evaluation meeting, June 2015.

VIII.11 Hydrogen Safety, Codes and Standards: Sensors

Eric L. Brosha[1] (Primary Contact),
Christopher J. Romero[1], William Penrose[3],
Todd Williamson[1], Dan Poppe[4], Robert S. Glass[2],
and Rangachary Mukundan[1]

[1]Los Alamos National Laboratory (LANL)
MS D429, P.O. Box 1663
Los Alamos, NM 87545
Phone: (505) 665-4008; Fax: (505) 665-4292
Email: brosha@lanl.gov

[2]Lawrence Livermore National Laboratory (LLNL)
L-103, P.O. Box 808
7000 East Avenue
Livermore, CA 94550
Phone: (925) 423-7140; Fax: (925) 423-4908
Email: glass3@llnl.gov

[3]Custom Sensor Solutions
11786 N. Dragoon Springs Drive
Oro Valley, AZ 85737
Phone: (520) 544-7523
Email: wpenrose@customsensorsolutions.com

[4]Hydrogen Frontier
403 E. Gardena Blvd.
Gardena, CA 90248
dpoppe@hydrogenfrontier.com

DOE Manager
Will James
Phone: (202) 287-6223
Email: Charles.James@ee.doe.gov

Project Start Date: Fiscal Year 2008
Project End Date: Fiscal Year 2015

Overall Objectives

- Develop a low cost, and low power electrochemical hydrogen safety sensor for a wide range of infrastructure and vehicle applications with focus on high durability and reliability
- Continually advance test prototypes guided by materials selection, sensor design, electrochemical research and development investigation, fabrication, and rigorous life testing
- Disseminate packaged sensor prototypes and control systems to DOE laboratories and commercial parties interested in testing and fielding advanced prototypes for cross-validation
- Evaluate manufacturing approaches for commercialization
- Engage an industrial partner and execute technology transfer

Fiscal Year (FY) 2015 Objectives

- Complete construction and testing of prototype field trials units
- Test field trials unit, wireless system, and control software in laboratory setting
- Calibrate unit
- Install first field trials unit at Hydrogen Frontier Inc., Burbank, California location
- Collect data from field trials unit for minimum of one week and continue logging throughout rest of fiscal year
- Prepare follow on field trials units and site at Burbank facility
- Test new H_2 electrochemical sensor elements based on LANL working-electrode improvements

Technical Barriers

This project address the following technical barriers from the Hydrogen Safety, Codes and Standards section (3.8) of the Fuel Cell Technologies Office Multi-Year Research, Development, and Demonstration Plan:

(A) Safety Data and Information: Limited Access and Availability

(C) Safety is Not Always Treated as a Continuous Process

(K) No Consistent Codification Plan and Process for Synchronization of R&D and Code Development

(L) Usage and Access Restrictions

Technical Targets

Technical targets vary depending on the application [1,2], but in general include:

- Sensitivity: 1–4 vol% range in air
- Accuracy: ±1% full scale in the range of 0.04–4 vol%
- Response time: <1 min at 1% and <1 s at 4%; recovery <1 min
- Temperature operating range: -40°C to 60°C
- Durability: Minimal calibration or no calibration required for over sensor lifetime (as defined by particular application)

- Cross-Sensitivity: Minimal interference to humidity, H_2S, CH_4, CO, and volatile organic compounds

FY 2015 Accomplishments

- Field trials were completed using two units, and the units were tested off LANL's site. Wireless communications and GoToMyPC® access to control LabView™ executable software developed by Agile Engineering and Zircoa Corporation were tested. By the end of the fiscal year, two units were installed: a hydrogen safety sensor inside a filling station dispensing island, and another located inside the compressor skid. An equipment-electronics locker was installed to house the LANL data acquisition computer and wireless receiver.
- No evidence of sensor baseline drift was detected during the field trials experiment.
- There were no false alarms or false positives that caused a signal exceeding 4% of H_2 (lower flammability limit). Exposure of sensor enclosure (and sensor) to significant and sometimes severe weather events was confirmed with no deleterious effects to the sensor or stable baseline of the sensor. These data confirm laboratory development data and National Renewable Energy Laboratory (NREL) testing data.
- Hydrogen Frontier station fill logs were obtained from November 7, 2014, through the end of November.
- We found excellent correlation of recorded H_2 release events with customers filling their fuel cell vehicles (FCVs). Multiple fill events were recorded in filling station logs and sensor resolution was good; each FCV fill even when spaced less than 15 min intervals was recorded.
- A statement of work was written and finalized with the South Coast Air Quality Management District (SCAQMD) to initiate a new project to install two sensor field trials units at two additional Los Angeles area hydrogen filling stations in FY 2016 as well as to expand testing at Hydrogen Frontier facilities.
- The FY 2015 Sensor Project milestone was met.

✧ ✧ ✧ ✧ ✧

INTRODUCTION

Recent developments in the search for sustainable and renewable energy coupled with the advancements in FCVs have augmented the demand for hydrogen safety sensors initially to be placed at refueling sites and developed for incorporation on-board vehicles [2]. There are several sensor technologies that have been developed to detect hydrogen, including deployed systems to detect leaks in manned space systems and hydrogen safety sensors for laboratory and industrial usage. Among the several sensing methods commercially available or under development, electrochemical devices that utilize high temperature-based ceramic electrolytes have been shown to be robust, potentially low cost, have high sensitivity and good selectivity, the latter exemplified by tolerance to changes in humidity, and are more resilient to electrode or electrolyte poisoning [3-9]. The desired sensing technique should meet a detection threshold of 1% (10,000 ppm) H_2 and response time of ≤1 min [10], which is a target for infrastructure and vehicular uses. Further, a review of electrochemical hydrogen sensors by Korotcenkov et al. [11] and the report by Glass et al. [10,12] suggest the need for inexpensive, low power, and compact sensors with long-term stability, minimal cross-sensitivity, and fast response. This view has been largely validated and supported by the fuel cell and hydrogen infrastructure industries by the NREL/DOE Hydrogen Sensor Workshop held on June 8, 2011 [13]. Many of the issues preventing widespread adoption of best-available hydrogen sensing technologies available today outside of cost, derive from excessive false positives and false negatives arising from unstable sensor baseline; both of these problems necessitate the need for unacceptable frequent calibration [13]. As part of the Hydrogen Codes and Standards program, LANL and LLNL are working together to develop and test inexpensive, zirconia-based, electrochemical (mixed potential) sensors for H_2 detection in air. Previous work conducted at LLNL showed [9] that indium tin oxide (ITO) electrodes produced a stable mixed potential response in the presence of up to 5% of H_2 in air with very low response to CO_2 and water vapor. The sensor also showed desirable characteristics with respect to response time and resistance to aging, and degradation due to thermal cycling.

APPROACH

In this investigation, the development and testing of an electrochemical H_2 sensor prototype based on ITO/YSZ/Pt configuration is detailed. The device fabricated using commercial ceramic sensor manufacturing methods on an alumina substrate with an integrated Pt resistance heater to achieve precise control of operating temperature while minimizing heterogeneous catalysis and loss of hydrogen sensitivity. Targeting fuel cell vehicle infrastructure, the safety sensor was subjected to interference studies, temperature cycling, operating temperature variations, and long-term testing now exceeding over 6,000 h for some sensor configurations. In FY 2011, FY 2012, and FY 2013 the mixed potential electrochemical technology was independently validated at the hydrogen safety sensor-testing lab at NREL in three separate rounds of testing. In each round, two packaged precommercial prototypes were tested against a standard testing protocol including the effects changes in ambient temperature, pressure, humidity, and oxygen partial pressure and sensor resistance to cross-interferences such as

CO, CO_2, CH_4, and NH_3. In general, NREL testing showed a fast response to H_2 with exceptional low-level sensitivity and high signal-to-noise, very little deviation in sensor response to changes in ambient conditions such as humidity and barometric pressure, and minimal response to some common interference gases. However, potential weakness were found in the first two rounds of testing such as changes in sensor calibration with ambient temperature changes and complete sensor failure under the most harsh operating environment tested (anaerobic conditions, which would only happen under extremely unusual conditions) were identified. These last NREL-identified performance issues were ameliorated in FY 2013 and FY 2014. In FY 2013, a more chemically robust electrode was tested in a wide range of oxygen partial pressures (rich conditions to 100% O_2). The $La_{0.8}Sr_{0.2}CrO_3$ perovskite electrode was incorporated into new ESL devices and tested in FY 2015.

FY 2014 work focused primarily on the design, development, and testing of hardware required for field testing deployment at hydrogen refueling stations in California. In addition to technical work, pursuit of an indemnity agreement, commercial partner outreach, and planning for adherence to codes and standards in designing the prototype units were accomplished. A new circuit board design was prepared by Custom Sensor Solutions Inc. that combined the high impedance buffer circuit and sensor heater control board into one streamlined unit. The first of the new boards was delivered in May 2014 and testing and circuit revisions/optimization continued through June. At the end of June, all of the components were integrated into a commercially sourced, National Electrical Manufacturers Association Class 8 enclosure and systems testing began in July in the laboratory. A dedicated LabVIEW™-based software program was developed by a certified LabVIEW™ developer (Agile Engineering with software-wireless communications testing performed by Zircoa Inc.) This executable code was designed to accommodate up to three independent wireless hydrogen sensors at each deployment location. Given the exposure to outdoor environment at the primary California testing site, a ruggedized industrial computer with solid-state storage was selected and daily performance of the field trials unit will be carried out using remote access communication via the Internet.

The salient features of the H_2 sensor prototype developed by LANL and LLNL are (1) low power consumption, (2) compactness to fit into critical areas for some applications, (3) simple operation, (4) fast response, (5) a direct voltage read-out circumventing the need for complicated signal processing, (6) a low cost sensor platform, and (7) excellent stability and reproducibility all of which are conducive to commercialization using common ceramic manufacturing methods (8) low cost (9) technology readily lends itself to mass manufacturing protocols.

RESULTS REPORTED IN FY 2015

The sensor unit and data collection system were shipped to the Burbank filling station location and LANL staff members arrived several days after Hydrogen Frontier received the equipment. Installation began on November 4, 2014, and the sensor was brought online on November 5, 2014. The data acquisition system was installed inside of a properly rated steel enclosure above the existing control electronics bay for the filling station. The wireless system was brought online and the sensor was tested using a calibration gas provided by Hydrogen Frontier. The data acquisition computer was connected to a 1 GB/s Internet connection and control of the computer using GoToMyPC® software was tested using a laptop with cell modem communications. Figure 1 shows pictures of the installation.

FIGURE 1. (Left) Sensor unit installed inside dispensing island with cover closed. (Center) Cover open showing wireless transmitter and sensor and metal shielded power supply. (Right) Completed installation with dispenser unit enclosure sealed and ready for service.

The field trials experiment went online on November 5th and a new data file was typically started on each morning of each subsequent day of testing. After two to three days of testing, the LabVIEW™ program was remotely closed and the data files were downloaded to a laptop computer in New Mexico using the File Transfer Protocol provision in the GoToMyPC® program. Several characteristics in the sensor data were immediately apparent; the sensor baseline was stable and did not drift however there was some sensor activity that could not be attributed to noise. Also, several sharp responses were recorded almost immediately. Three significant releases of H_2 were detected in the first 20 hours and two of these exceeded 1,000 ppm. The same behavior was seen in the next 25 hours of data collection; five release events were recorded with one pair occurring within 20 minutes of each other and one exceeding 2,500 ppm. The sensor baseline on the second day, in between these spikes in H_2 concentration, was exceptionally stable with no drift. We requested that the station filling log data be made available and Hydrogen Frontier sent LANL data for November 7th. Several positive correlations to station filling activities were immediately noted and we requested more station filling log data. Figure 2 shows the sensor data collected for the file that was started in the morning of November 7, 2014, and continuous sensor logging was carried out for 34 hours. As indicated, each of the H_2 releases detected by the field trials sensor corresponded to a station customer filling his/her FCV. Every release detected is accounted for by matching the time that the sensor recorded an H_2 release and when the customer began or ended the FCV fill. Another significant observation to note is that there are no H_2 peaks that are not unaccounted for despite that fact that the filling station is located in a heavily congested downtown city environment. The facility is adjacent to the City of Burbank's facility for waste and municipal government operations that include heavy vehicle access to their facilities in close proximity to the station and sensor location. Since the computer software does not record a date/time stamp in the data file, the correlation of sensor time and station filling log time must be manually synchronized and there is a cumulative error of perhaps 2–3 minutes between the sensor log and station dispenser log however the error is much smaller than the average 12–15 minutes that the typical FCV fill would take. It is speculated that the H_2 releases being recorded are the result of H_2 diffusing from the vent line located well above the dispensing island enclosure after depressurization of the filling hose and nozzle. The station operators did not anticipate or expect these frequent incursions of H_2 inside the dispensing island enclosure and they have been made aware of these occurrences. To our knowledge, the commercial H_2 sensor located less than 12 inches from the LANL-LLNL field trials sensor, did not record these events.

A closer analysis of the event, the peak shape illustrates the detail that the field trials sensor unit was able to capture when FCV customers filled their hydrogen tanks. Figure 3 is an expanded view of the hydrogen dispensed on November 7, 2014, at 17:36. Figure 3 shows a deviation from the sensor baseline occurring within the time error of the station's filling log. There was a slow increase in sensor output for approximately 11 minutes at which time there was a large, rapid increase in H_2 to 1,300 ppm and then rapid decay in H_2 as the H_2 dissipated. Since the station filling log indicated that recharging the FCV storage tanks took 12 minutes, we believe that the field trials sensor accurately captures the pressurization of the delivery hose (and was sensitive enough to measure the hydrogen either diffusing through

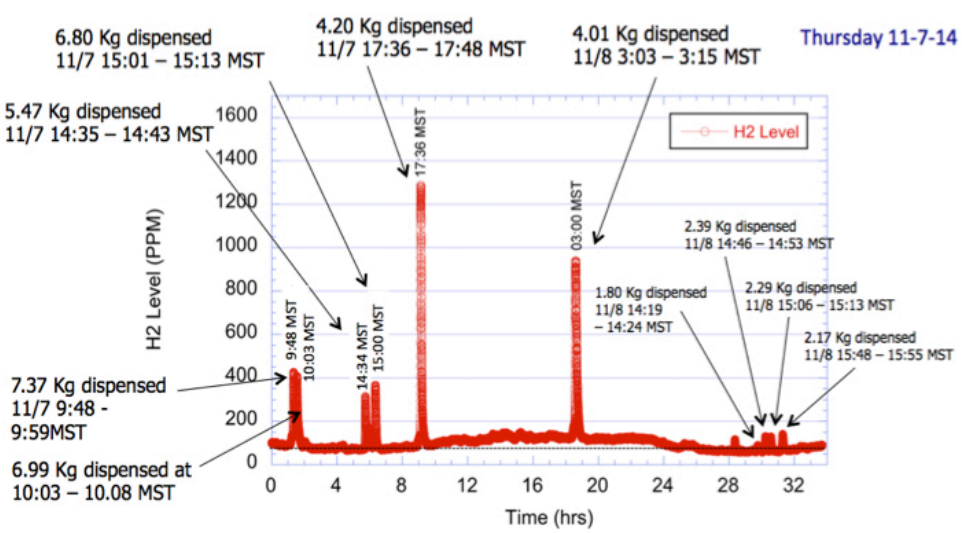

FIGURE 2. Data recorded from Thursday, November 7, 2014 field trials sensor unit. Each release of H_2 recorded (>100 ppm) is matched to the Hydrogen Frontier station filling log data for customers filling their FCVs. The station time and amount of H_2 dispensed is indicated.

the walls of the hose or is an indication of small leaks in the internal connections of the dispensing station) and the depressurization/venting of the system before the dispensing hose was decoupled from the vehicle.

These types of sensor behavior were seen throughout the next week of logging sensor data. Around November 12, 2014, the data became increasingly noisy and wireless communications dropouts began to be detected. This was apparent to us whenever the recorded sensor voltage would spike to +10 V, the default voltage produced by the Omega wireless received when the signal is lost from the Omega transmitter. By November 19, 2014, the signal was lost entirely for almost two weeks. On November 29th, communications were reestablished and sensor logging was restarted. Over the course of the next 280 hours of field trials data logging, there was a change in the behavior of the H_2 releases recorded by the sensor. These data are shown in Figure 4. An elevated and oscillating sensor baseline was seen; the concentration fluctuated between 200 ppm and 400 ppm of H_2 with a periodicity of about 24 hours. This behavior was seen for over 280 hours of continuous monitoring with several large releases of H_2 recorded (as high as 8,000 ppm). As before, the sensor baseline showed no drift over the course of this interval; the periodicity was very regular – suggesting this was a man-made cause – and the concentration of H_2 releases was much larger than any of the FCV-related activity.

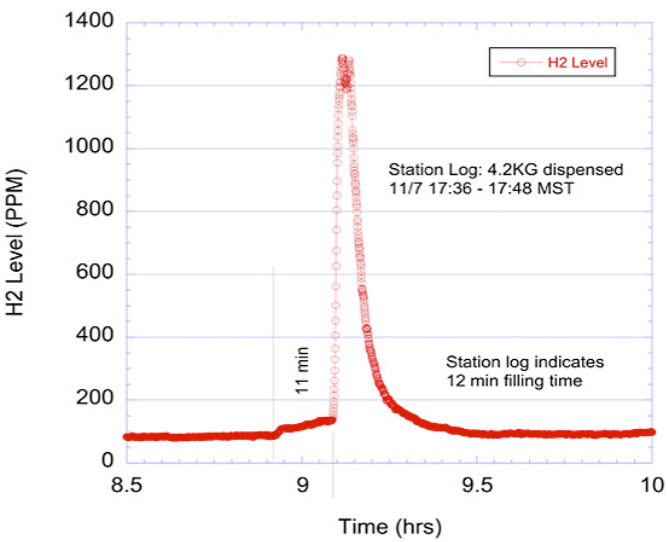

FIGURE 3. Expanded axes of the hydrogen release recorded on November 7, 201414 at 17:36 MST. There are two different sensor behaviors captured in these data showing FCV fueling and depressurization-hose release from the vehicle.

We contacted Hydrogen Frontier to discuss possible causes for this sensor behavior. We were informed that that station had gone back to onsite-generation of hydrogen using the station's methane reformer. When this occurs, the reformer operates continuously on a 600-hour duty cycle with periodic compression of the synthesized H_2 using the station's compressor systems. Moreover, during this enhanced level of station activity, the Burbank and Greater Los Angeles Area received significant severe weather over the course of a week that included high winds, downpours (leading to standing water inside the filling station dispenser enclosure) and even a recorded tornado. Time correlations of these events are indicated in Figure 4. Once again, the behavior of the field trials sensor can be explained by station activities. The fact that the periodic sensor baseline was not affected

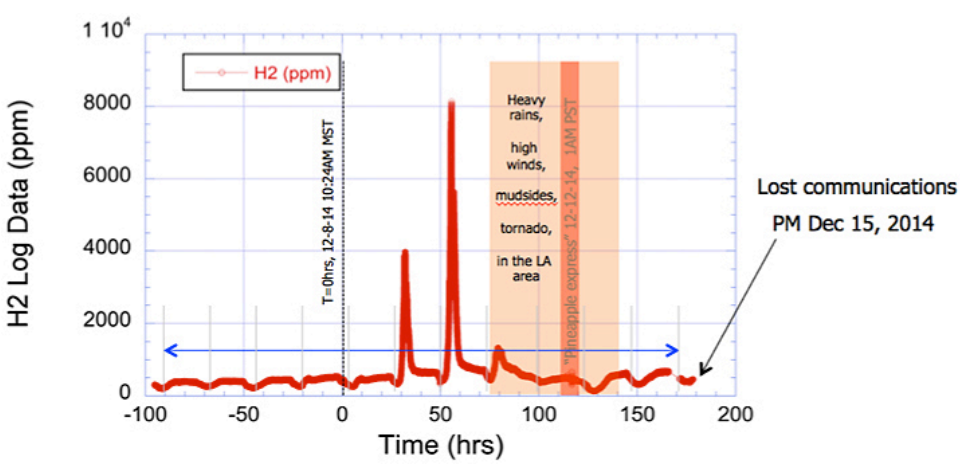

FIGURE 4. After communications were reestablished on November 29, 2014, a continuous run of 280 hours was successfully achieved that overlapped with known, significant weather events in the Burbank area. Elevated baseline and periodic oscillations are attributed to the Hydrogen Frontier station producing H_2 onsite with their methane steam reformer system.

by severe weather (arrival of a "Pineapple Express" weather phenomena indicated) is an excellent confirmation of our reported laboratory findings during the sensor development phase of this project and confirmation of NREL sensor testing results. Communications with the field trials unit went offline permanently on December 15, 2014. The FY 2015 milestone for the field trials experiment was achieved.

At the end of FY 2014, discussions were initiated with our sensor manufacturing partner, ESL Electroscience to design the next generation of H_2 safety sensor to further reduce sensor cost, increase performance, and to simplify the construction of future field trials test units. The present sensors are designed using an indium tin oxide-working electrode identified by LLNL early in this safety, codes and standards project. Since this material is not compatible with ESL's manufacturing process, the working electrode and solid electrolyte must be deposited at LANL subsequent to delivery of the substrates from ESL. As discussed before, this increases cost and complexity of making the H_2 safety sensors. A new La-Sr-Cr-O working electrode identified by LANL was substituted for the LLNL ITO electrode. Furthermore, it was identified in FY 2014 that some commercial alumina tape varieties in use by ESL could permit sufficient ionic or electronic leakage currents between the Pt resistive heater and the electrodes/electrolyte of the sensor as to cause anomalous behavior from the high-impedance buffer circuit. Work began at ESL on 20 complete devices in December using a new sensor design leveraged off of LANL NO_x/NH_3 sensor technology projects. These complete devices, as prepared, are fabricated using ESL's commercial high temperature co-fired ceramic method. The devices will supply subsequent field trials operations through FY 2015 and beyond.

CONCLUSIONS

- The FY 2015 milestone was completed this year.
- Field trials testing at Burbank, California, Hydrogen Frontier Inc. were successful with H_2 exposure results almost perfectly correlated to station activities; both FCV filling and on-site production of hydrogen could be tracked by examination of the field trials sensor response.
- No false positives or false negatives were detected during period of performance.
- There was no evidence of or obvious drift in sensor baseline voltage over the course of testing and known severe weather events did not affect the sensor.
- The on-site commercial sensor did not report recorded hydrogen releases/exposures.
- The Hydrogen Frontier dispensing island enclosure was selected because of anticipated quiescent conditions but hydrogen was present during normal station operations.
- The station's filling log data support conclusions that H_2 releases appear to be related to filling FCVs and production-compression activities.
- Changes in ambient relative humidity, temperature, and pressure did not appear to have an effect on sensor performance.
- The mixed potential, electrochemical sensor technology performed as designed.

FUTURE DIRECTIONS

- Return to Burbank site to install second field trials unit and to upgrade sensor element of the first field trials unit to a new sensor prepared entirely by ESL using the new, LANL-derived working electrode
- Install computer controlled weather station to correlate atmospheric conditions with sensor data
- Reorient/reposition system antenna of commercial wireless units to reduce signal dropouts
- Begin work with SCAQMD to expand field-testing at other California H_2 filling station locations
- Continue with commercialization/technology transfer efforts with webinars and commercial outreach
  - Responded to NineSigma call for H_2 sensing technology for fuel cell infrastructure

REFERENCES

1. W.J. Buttner, M.B. Post, R. Burgess, C. Rivkin, *Int. J. Hydrogen Energy*, **36**, 2462 (2011).

2. L. Boon-Brett, J. Bousek, G. Black, P. Moretto, P. Castello, T. Hübert, and U. Banach, Identifying performance gaps in hydrogen safety sensor technology for automotive and stationary applications, International Journal of Hydrogen Energy, 35 (2010), 373-384.

3. H.Iwahara, H. Uchida, K. Ogaki and H. Nagato, Nernstian Hydrogen Sensor Using $BaCeO_3$-Based, Proton-Conducting Ceramics Operative at 200-900^0 C, Journal of The Electrochemical Society, 138 (1991), 295-299.

4. Y. Tan and T.C. Tan, Characteristics and Modeling of a Solid State Hydrogen Sensor, The Journal of Electrochemical Society, 141 (1994), 461-466.

5. Z. Samec, F. Opekar, and G.J.E.F. Crijns, Solid-state Hydrogen Sensor Based on a Solid-Polymer Electrolyte, Electroanalysis, 7 (1995), 1054-1058.

6. Y-C. Liu, B-J. Hwang, and I.J. Tzeng, Solid-State Amperometric Hydrogen Sensor Using Pt/C/Nafion Composite Electrodes Prepared by a Hot-Pressed Method, Journal of The Electrochemical Society, 149 (2002), H173-H178.

7. L.B. Kriksunov, and D.D. Macdonald, Amperometric hydrogen sensor for high-temperature water, Sensors and Actuators B, 32 (1996), 57-60.

8. G. Lu, N. Miura, and N. Yamazoe, High-temperature hydrogen sensor based on stabilized zirconia and a metal oxide electrode, Sensors and Actuators B, 35-36 (1996), 130-135.

9. L. P. Martin and R. S. Glass, Hydrogen Sensor Based on Yttria-Stabilized Zirconia Electrolyte and Tin-Doped Indium Oxide Electrode, Journal of The Electrochemical Society, 152 (2005), H43-H47.

10. R.S. Glass, J. Milliken, K. Howden, R. Sullivan (Eds.), Sensor Needs and Requirements for Proton-Exchange Membrane Fuel Cell Systems and Direct-Injection Engines, 2000, pp. 7 – 15. DOE, UCRL-ID-137767.

11. G. Korotcenkov, S.D. Han and J.R. Stetter, Review of Electrochemical Hydrogen Sensors, Chemical Review, 109 (2009), 1402-1433.

12. L.P. Martin and R.S. Glass, Electrochemical Sensors for PEMFC Vehicles, presented at The 2004 DOE Hydrogen, Fuel Cells, and Infrastructure Technologies Program Review, Philadelphia, PA (May 27, 2004).

13. NREL/DOE Hydrogen Sensor Workshop, June 8, 2011, Chicago IL. http://www.hydrogen.energy.gov/pdfs/progress11/viii_3_burgess_2011.pdf

14. F.H. Garzon, R. Mukundan, and E.L. Brosha, Solid state mixed potential gas sensors: theory, experiments and challenges, Solid State Ionics, 136-137 (2000), 633-638.

15. P.K. Sekhar, E.L. Brosha, R. Mukundan, M.A. Nelson and F.H. Garzon, Application of Commercial Automotive Sensor Manufacturing Methods for NO_x/NH_3 Mixed Potential Sensors for Emission Control, ECS Transactions. 19 (2009), 45-49.

VIII.12 Hands-On Hydrogen Safety Training

Salvador M. Aceves (Primary Contact),
Gregg Holtmeier, Vernon Switzer
Lawrence Livermore National Laboratory (LLNL)
7000 East Avenue, L-792
Livermore, CA 94550
Phone: (925) 422 0864
Email: saceves@llnl.gov

DOE Manager
Will James
Phone: (202) 287-6223
Email: Charles.James@ee.doe.gov

Project Start Date: October 1, 2010
Project End Date: Project continuation and direction determined annually by DOE

Overall Objectives

- Maintain and update web-based safety training materials for researchers running hydrogen laboratory experiments
- Teach hands-on safety training to personnel in charge of hydrogen systems

Fiscal Year (FY) 2015 Objectives

- Complete class materials for hands-on safety training

Technical Barriers

This project addresses the following technical barriers from the Hydrogen Safety, Codes and Standards section of the Fuel Cell Technologies Office (FCTO) Multi-Year Research, Development and Demonstration (MYRDD) Plan:

(D) Lack of Hydrogen Knowledge by AHJs (Authorities Having Jurisdiction)

(E) Lack of Hydrogen Training Materials and Facilities for Emergency Responders

Contribution to Achievement of DOE Safety, Codes & Standards Milestones

This project will contribute to achievement of the following DOE milestones from the Hydrogen Safety, Codes and Standards section of the FCTO MYRDD Plan:

- Milestone 5.3: Enhance hydrogen safety training props and deliver classroom curriculum for emergency response training

Accomplishments

- Completed three modules of classroom training for hands-on hydrogen safety class
- Registered over 400 completions in web-based hydrogen safety class (www.h2labsafety.org)

✧ ✧ ✧ ✧ ✧

INTRODUCTION

LLNL has been conducting hydrogen research for more than 50 years, starting with national security applications and continuing with energy research. For many of these years, LLNL was designated as the pressure safety training facility for the whole DOE complex and other government institutions. Many technicians and researchers visited LLNL to receive training on many aspects of pressure safety, including hydrogen technology, cryogenics, leak detection, and vacuum technology.

This unique training expertise is still available and is now being applied for hydrogen energy research through the development of training materials that may contribute to safe operation within the many institutions working on hydrogen technology.

APPROACH

We are developing a two-pronged approach to hydrogen safety training.

- Researchers conducting laboratory experiments can benefit from basic training on hydrogen and pressure safety. This web-based training can be completed in approximately four hours.
- Technical personnel in charge of setting up experimental equipment require comprehensive hands-on training on all aspects of hydrogen systems. This extensive training is planned for three full days.

RESULTS

Publicly released in 2010, the web-based hydrogen safety class (www.h2labsafety.org) reached 400 total completions and it is standard training material in many universities, government institutions, and private companies. The class is, however, not well publicized, and targeted advertisement may contribute to more widespread utilization.

In addition to the web-based fundamentals class, we are developing a hands-on hydrogen safety class for pressure operators. This comprehensive training will be conducted

during a three-day session at Lawrence Livermore National Laboratory or at remote institutions if appropriate facilities (classroom, compressed gas supply, and pressure test laboratory) exist.

The hands-on training class starts with a full day of classroom instruction covering essential topics of pressure system assembly and operation (Table 1). Classroom instruction focuses on identifying hazards, safety precautions, personal protective equipment, and pressurized hydrogen system components and their function. This class greatly expands the descriptions from the online hydrogen safety class, going into detailed operational information about every component in pressure systems, describing their inner functionality, applicability, and recommended use.

Days two and three will be spent in the laboratory for practical application of the classroom information from day one. On day two, students will be handed a safety document and instructed to assemble the pressure system described therein. Students will have to select, inspect and install pressure components, bend tube, install pipe and compression fittings, and assemble the entire system.

On day three this system will be leak checked with a mass spectrometer helium leak detector with a leak rate of no more than 10^{-5} atm-cc/s helium. The pressure system will then be connected to the data acquisition system and pressure tested remotely at 150% of the maximum allowable working pressure. The last leak test will be conducted using liquid leak detection fluid at the system's maximum operating pressure. Finally, the students will operate the system to reach a desired pressure.

The hands-on class is nearly complete. Three of the five modules for classroom instruction (Table 1) have been completed (Figures 1 and 2). The remaining two modules will be completed before the end of the fiscal year.

Common Hydrogen Gas Cylinder Sizes

Cylinder Name	Contents (ft^3)	Pressure (psig)	CGA Connection	Cylinder Diameter x Height (in)
300, T, 1L, 49	261	2,400	350	9.25 x 55
200, K, 1A, 44	215	2,000	350	9 x 51
80, Q, 2, 16	65	2,000	350	7 x 31
Lecture Bottle	2	1,800	170 or 180	2 x 15

Note: Cylinder name, contents and pressure will vary between gas suppliers
CGA – Compressed Gas Association

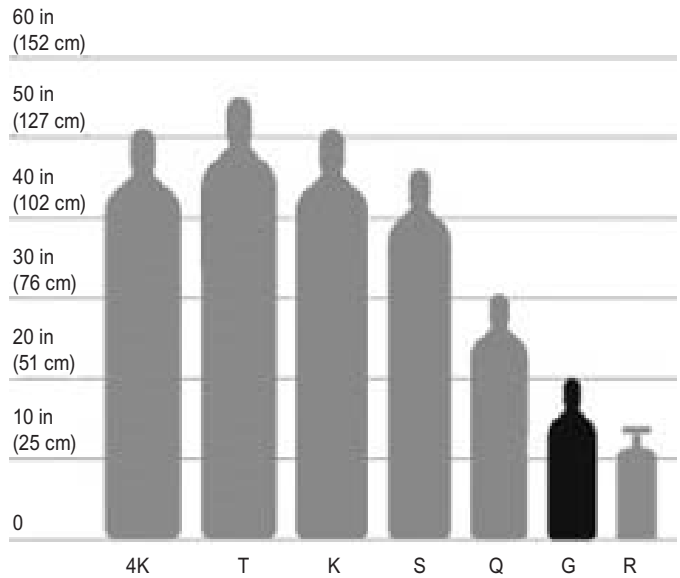

FIGURE 1. Gas cylinder information from the "Gas Cylinders and CGA Fittings" module of the classroom training section for the hands-on hydrogen safety class

CONCLUSIONS AND FUTURE DIRECTIONS

Lawrence Livermore National Laboratory is contributing to safe hydrogen operations by developing instructional materials for researchers and technical operators.

- *Laboratory researchers* can obtain basic hydrogen safety information from a four-hour web-based class (free online access at http://www.h2labsafety.org/) addressing hydrogen fundamentals: properties, pressure and cryogenic safety, emergency response, and codes and standards.
- *Technical operators* in charge of building and testing experimental hydrogen equipment require more in-depth information than provided by the web-based class. We are therefore preparing a three-day hands-on safety class that presents detailed information for installation, testing, and operation of hydrogen pressurized systems. The hands-on class includes a full day of classroom instruction followed by two days of laboratory work where students assemble, test and operate a pressure system based on a schematic and component description.

We anticipate completing the hands-on safety class in FY 2015 and performing a peer review of the class before releasing it to the public.

TABLE 1. Hands-on safety class structure. Modules 2, 3 and 5 are now complete and remaining modules will be completed before the end of the fiscal year.

	Modules	
Day 1	**Classroom Teaching**	
	1	Concepts Hazards Personal Protective Equipmen
	2	Gas Cylinders CGA fittings Supply manifolds Flash arrestors
	3	Pressure Reducing Regulators
	4	Gauges/Pressure Transducers Relief Devices Valves Flash Arrestors
	5	Fittings (VCR, bite, NPT, VCO, DIN) Tubing and Piping
	6	Quiz
Day 2	**Pressure system assembly**	
		Given a system schematic and description, select components, inspect and install, cut and bend tube, apply various fittings, and assemble full system
Day 3	**System leak test and operation**	
		Leak test using a mass spectrometer leak detector; setup data acquisition; conduct remote pressure test; leak test at maximum operating pressure using leak detection fluid; operate system to reach a desired pressure

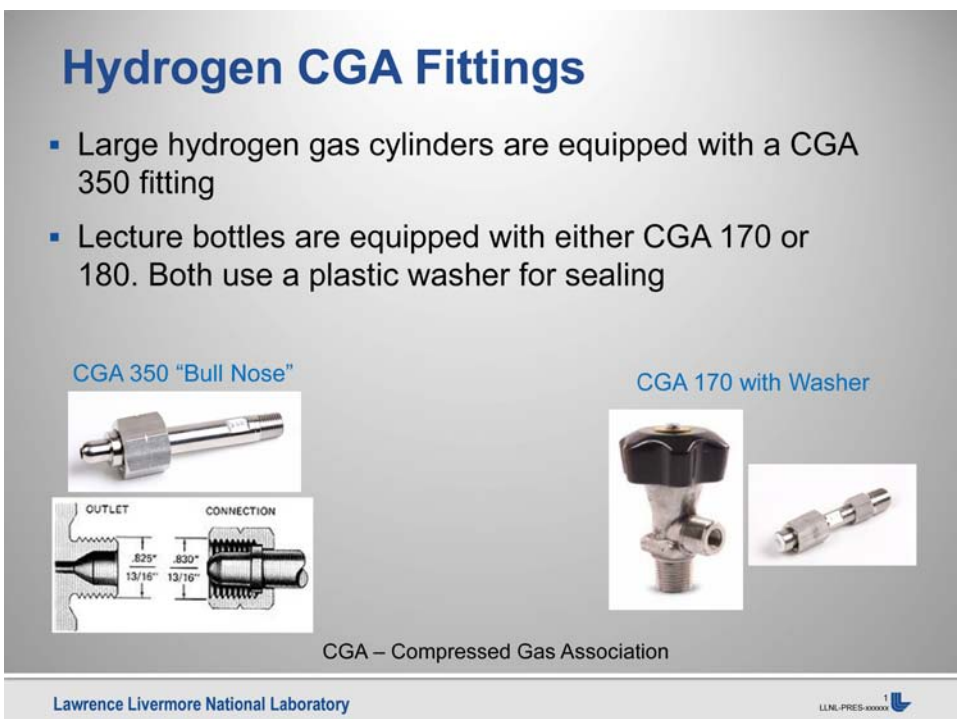

FIGURE 2. CGA fitting information from the "Gas Cylinders and CGA Fittings" module of the classroom training section for the hands-on hydrogen safety class

IX.0 Systems Analysis Sub-Program Overview

INTRODUCTION

Systems Analysis supports decision making of the U.S. Department of Energy's (DOE's) Fuel Cell Technologies Office (FCTO) by providing a greater understanding of technology gaps, options and risks, and the contribution of individual technology components to the overall system, i.e., from fuel production to utilization, as well as the interaction of the components and their effects on the system. Analysis is also conducted to assess cross-cutting issues, such as integration of hydrogen and fuel cells with the electrical sector for energy storage and hydrogen infrastructure development.

The Systems Analysis sub-program made several significant contributions to FCTO during Fiscal Year (FY) 2015. The Hydrogen Financial Analysis Scenario Tool (H2FAST) was developed to provide in-depth financial analysis of hydrogen refueling stations. The impact of improving the fuel cell efficiency on the costs of the fuel cell and storage systems and the fuel cell electric vehicle (FCEV) performance was studied. The JOBS model, developed by Argonne National Laboratory (ANL) and RCF Economic and Financial Consulting, Inc., was used to assess employment and economic impacts of infrastructure development for the early market penetration of fuel cell vehicles in California. The Greenhouse gases, Regulated Emissions, and Energy use in Transportation (GREET) model continues to be enhanced for the analysis of greenhouse gas emissions, petroleum use, and water consumption for conventional and renewable hydrogen pathways on a life-cycle basis.

GOAL

The goal of the Systems Analysis sub-program is to provide system-level analysis to support hydrogen and fuel cell technology development and technology readiness by evaluating technologies and pathways, including resource and infrastructure issues; guiding the selection of research, development, and demonstration (RD&D) projects; and estimating the potential value of RD&D efforts.

OBJECTIVES

- By 2015–2016, complete analysis of milestones and technology targets, including risk analysis, independent reviews, financial evaluations, and environmental analysis to identify technology gaps and risk mitigation strategies.
- By 2017, complete assessment of potential employment impacts and establish linkages with the United States veteran community for growing hydrogen and fuel cell industries.
- By 2017, complete sustainability analysis and develop a framework for incorporating metrics (such as greenhouse gas [GHG] emissions, ecological footprint, economic/societal impact, etc.) into hydrogen production and infrastructure assessments.
- By 2017, complete analysis of program performance, cost status, and potential for use of fuel cells for a portfolio of commercial applications.
- By 2019, complete analysis of the potential for hydrogen, stationary fuel cells, fuel cell vehicles, and other fuel cell applications such as material handling equipment. The analysis will address necessary resources, hydrogen production, transportation infrastructure, performance of stationary fuel cells and vehicles, and the system effects resulting from the growth of fuel cell market shares in the various sectors of the economy.
- Provide milestone-based analysis, including risk analysis, independent reviews, financial evaluations, and environmental analysis, to support the Office's needs prior to technology readiness.
- Periodically update the life-cycle energy, petroleum use, GHG emissions, and criteria emissions analysis for technologies and pathways for FCTO to include technological advances or changes.

FY 2015 STATUS

The Systems Analysis sub-program focuses on examining the economics, benefits, opportunities, and impacts of fuel cells and renewable fuels with a consistent and comprehensive analytical framework. Analysis conducted

in FY 2015 included examination of socio-economic impacts such as increased employment from early market infrastructure development in California, development of the financial analysis tool (H2FAST), assessment of the cost improvement of the fuel cell and storage system costs as a result of improved fuel cell efficiency, development of an interim hydrogen cost target for early markets, identification of the impacts of station utilization and fueling pressure on dispensed hydrogen cost, and analysis of life-cycle water use for multiple hydrogen and conventional fuel/vehicle pathways. The Systems Analysis sub-program leverages key models shown in Figure 1 that were developed with sub-program funding in prior years for critical program analyses, as evidenced by the completed and ongoing analysis activities in the accomplishment section.

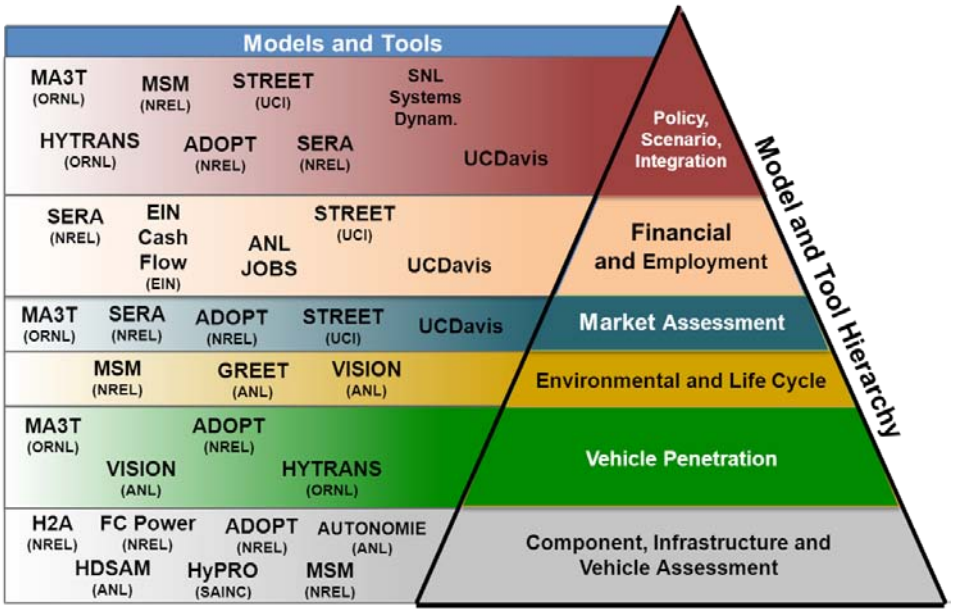

Source: Argonne National Laboratory
ORNL – Oak Ridge National Laboratory; NREL – National Renewable Energy Laboratory;
UCI – University of California, Irvine; EIN – Energy Independence Now; SAINC – Strategic Analysis, Inc.;
SNL – Sandia National Laboratories; UCDavis – University of California, Davis

FIGURE 1. Key models for critical program analyses performed in the Systems Analysis sub-program

FY 2015 ACCOMPLISHMENTS

Models and Systems Integration

Employment Analysis

ANL, with assistance from RCF Economic and Financial Consulting, Inc., continues to enhance and apply the JOBS H2 model. The model was created to estimate employment and revenue impacts of infrastructure development to support the early market penetration of FCEVs. The JOBS H2 model uses the same model structure and input-output methodology as developed for the JOBS FC (fuel cell) model to estimate changes in industry expenditures as a result of hydrogen fueling infrastructure deployment and calculates the effects of those changes throughout the economy. Recently, the model has been used to estimate the jobs creation and economic impacts of the early market FCEV and supporting infrastructure rollout in California. (ANL)

Figure 2 shows that the development of 25 hydrogen fueling stations over five years, as projected by the California vehicle rollout plans, will create or retain approximately 1,300 jobs. Note that jobs will start to decline once the station construction is completed, but operation-related jobs will be retained.

Water Life-Cycle Analysis

ANL continued to enhance the GREET model's life-cycle analysis capabilities in FY 2015 to examine water consumption for hydrogen production and delivery pathways from natural gas, water electrolysis, and other fuels such

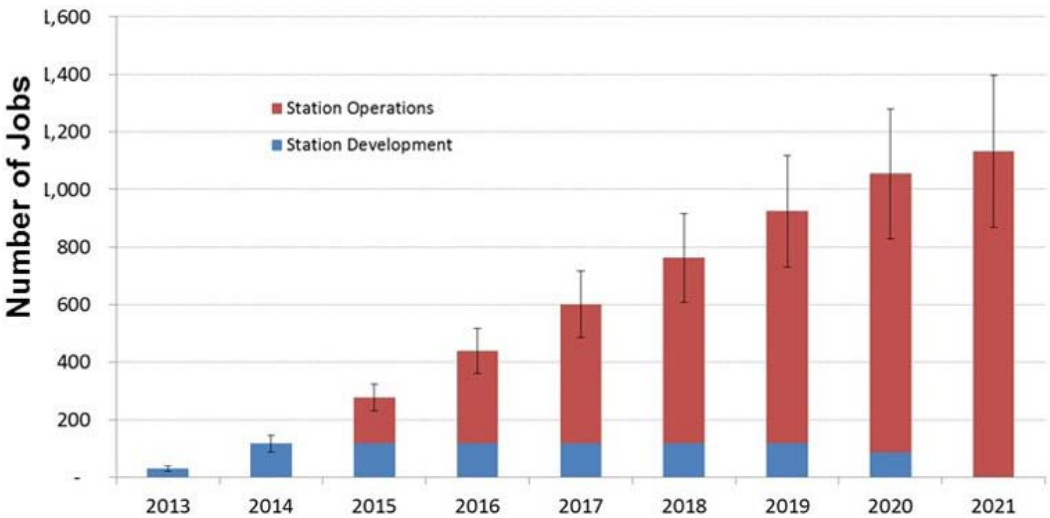

Source: Argonne National Laboratory

FIGURE 2. Job creation from station development in California

as gasoline and ethanol. ANL developed water consumption factors for hydrogen production from biogas and from coal and biomass gasification and updated the water consumption factors for hydrogen production via steam methane reforming (SMR) and electrolysis. A methodology for allocating water consumption to hydropower generation was developed. ANL expanded the GREET model to include the water consumption factors for the new and updated hydrogen production pathways. The water consumption quantities per 100 miles for various fuel/vehicle combinations were compared (Figure 3) to identify the stages with major contribution to life-cycle water consumption. The outstanding issues include the use of different water consumption evaluation methods with respect to system boundary and allocation. Also, the variability of water consumption by region and the water consumption during purification need to be assessed. (ANL)

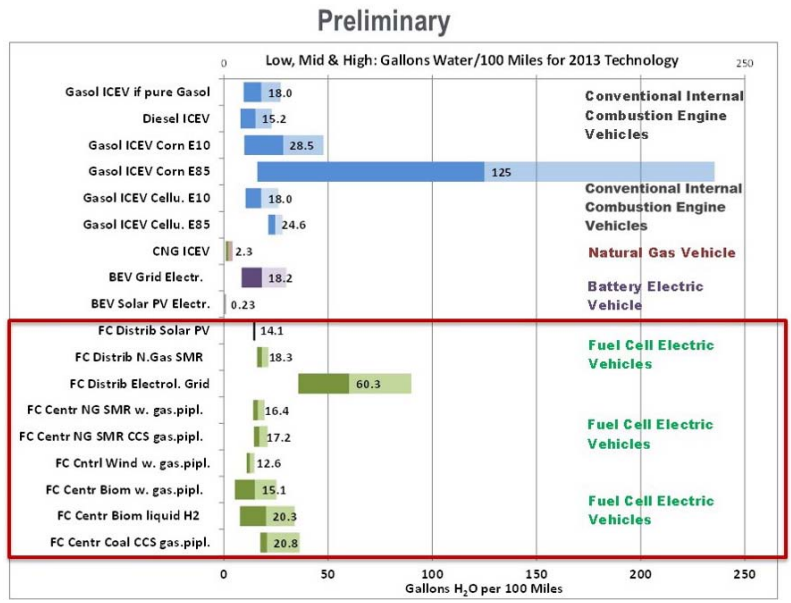

Source: Argonne National Laboratory
ICEV – internal combustion engine vehicle; CNG – compressed natural gas;
BEV – battery electric vehicle; FC – fuel cell; PV – photovoltaic; NG – natural gas;
CCS – carbon capture and sequestration

FIGURE 3. Life-cycle water consumption of fuels and vehicle technologies comparable to conventional fuels

The Hydrogen Financial Analysis Scenario Tool (H2FAST)

NREL developed the H2FAST tool to provide quick and convenient in-depth financial analysis of hydrogen fueling stations. H2FAST is available in two formats: an interactive online tool and a downloadable Excel spreadsheet. The spreadsheet version of H2FAST offers basic and advanced user interface modes for modeling individual stations or groups of up to ten stations. It provides users with detailed annual finance projections in the form of income statements, cash flow statements, and balance sheets; graphical presentation of financial performance parameters for 65 common metrics; life-cycle cost breakdown for each analysis scenario; and common ratio analysis results such as debt/equity position, return on equity, and debt service coverage ratio. The online H2FAST can be used to explore the impact of basic financial performance metrics by varying up to 20 user inputs, as illustrated in the model input screen

shown in Figure 4. The tool was thoroughly peer reviewed and issued to the public through the following Web address: http://www.nrel.gov/hydrogen/h2fast/. (NREL)

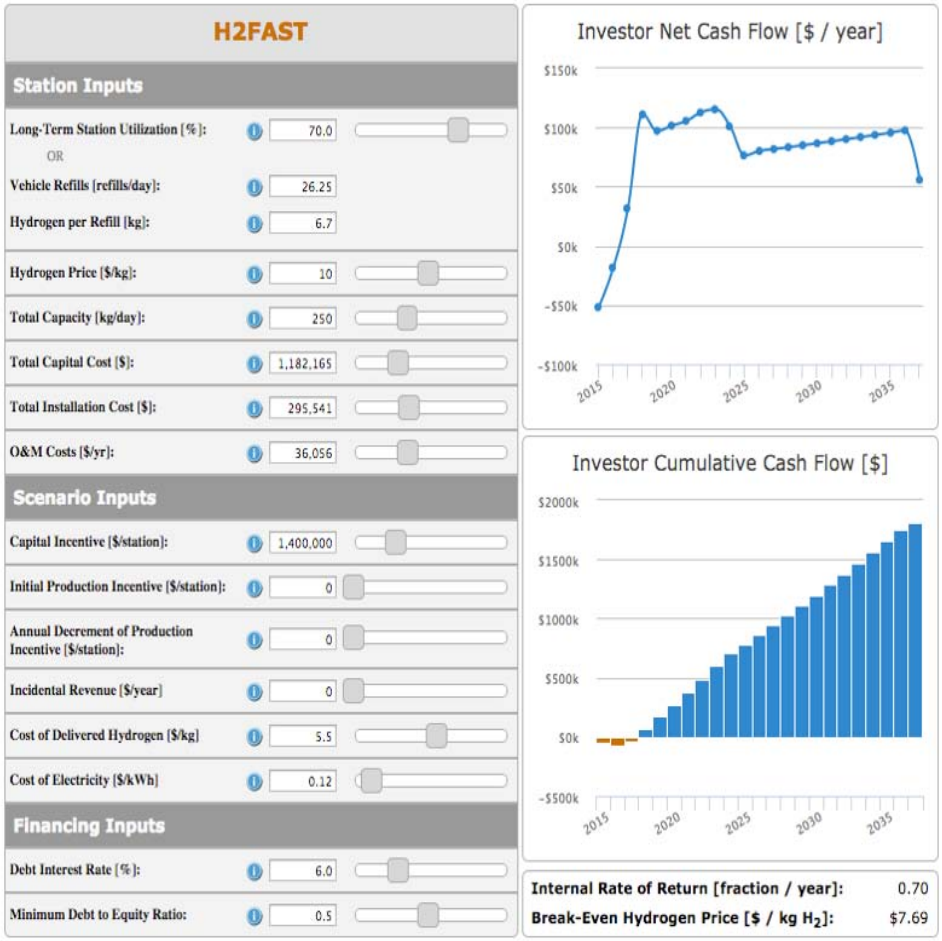

FIGURE 4. H2FAST financial scenario analysis tool input module

Infrastructure Analysis

Fueling Pressure Analysis

ANL evaluated the cost of multiple delivered hydrogen pressures (350 bar, 500 bar, and 700 bar) for refueling FCEVs. The project assessed the performance of the refueling system and the impact of fueling pressure and precooling requirements on the tank fill time and refueling cost. Also, the refueling costs for stations with high and low utilization factors with a capacity of 200 kg/d were evaluated, as exhibited in Figure 5. The refueling cost savings with the lower fueling pressures is much greater as a result of the reduced compressor needs and smaller storage equipment costs. (ANL)

Environmental Analysis

Well-to-Wheels (WTW) GHG Emissions for Methanol-to-Hydrogen Pathways

The methanol hydrogen fuel cell vehicle and direct methanol fuel cell (DMFC) vehicle pathways were estimated to have 30% to 35% less GHG emissions as compared to today's gasoline ICEV. In comparison, the natural gas hydrogen fuel cell vehicle pathways have 45% to 50% less GHG emissions as compared to today's gasoline ICEV. The analysis

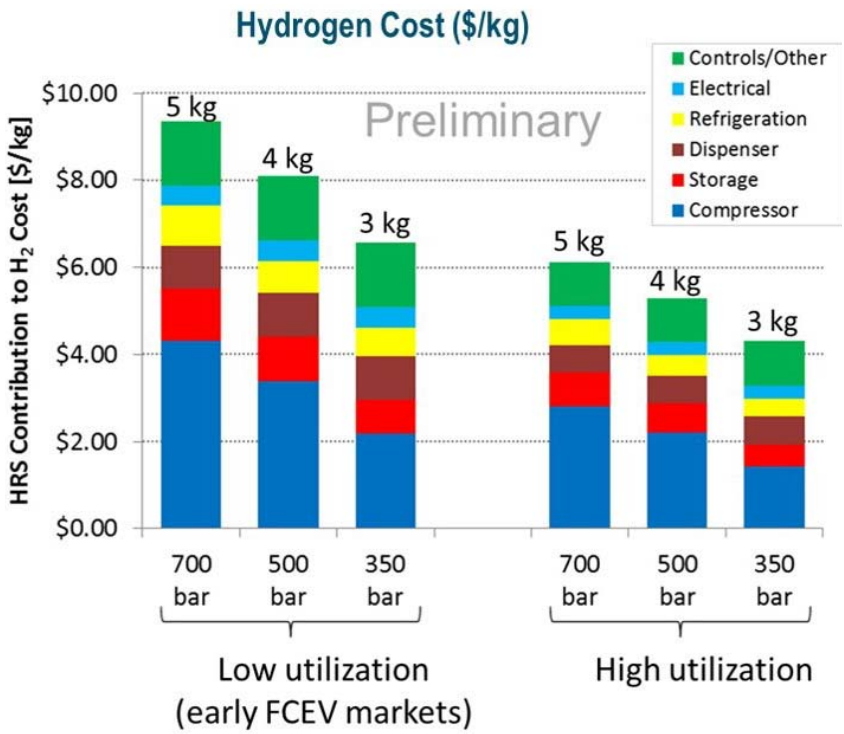

Source: Argonne National Laboratory
HRS – hydrogen refueling station

FIGURE 5. Impact of fueling pressure on hydrogen refueling cost

was carried out by expanding and modifying the 2014 version of the GREET model. Figure 6 compares the GHG emissions associated with the production and use of hydrogen in FCEVs and of methanol (MeOH) in DMFC vehicles to the GHG emissions associated with the production and use of petroleum gasoline and CNG in ICEVs and hybrid electric vehicles (HEVs). Figure 6 also shows a renewable pathway for hydrogen production via electrolysis using electricity generated from wind power. The small GHG emissions associated with that pathway are due to compression energy at refueling stations using a United States average generation mix. Note that gasoline is a mix of 10%

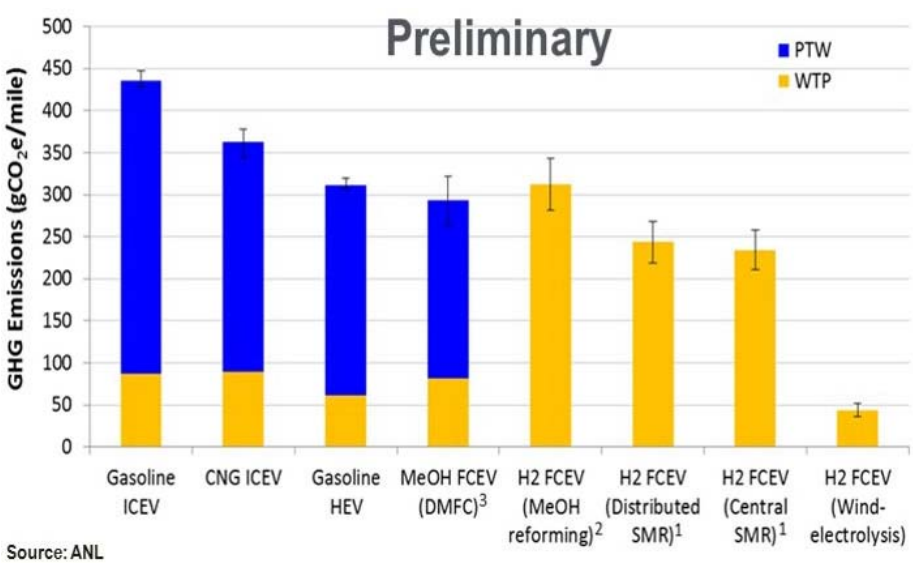

FIGURE 6. WTW GHG emissions of hydrogen FCEV pathways compared to gasoline and CNG ICEV pathways

corn-based ethanol and 90% gasoline blendstock by volume (also known as E10). The figure shows two main stages for the WTW GHG emissions: well-to-pump (WTP) and pump-to-wheels (PTW). (ANL)

Programmatic Analysis

Impact of Fuel Cell System Peak Efficiency on Fuel Consumption and Cost

ANL studied the impact of different fuel cell targets on the vehicle energy consumption and cost using the Autonomie model and compared the energy consumption and cost to those of conventional gasoline internal combustion powertrains. In addition, the impact of fuel cell system improvements on the potential onboard storage requirements and cost was analyzed. The findings of the study indicate the fuel economy of the FCEV could be improved by 10–14% by increasing the fuel cell peak efficiency from 60% to 68%. When the FCEV improvements are compared to conventional vehicles, the FCEV's fuel economy is found to be five times higher than that of the conventional vehicle in the 2030 timeframe. The fuel economy improvements for the FCEV are illustrated in Figure 7. (ANL)

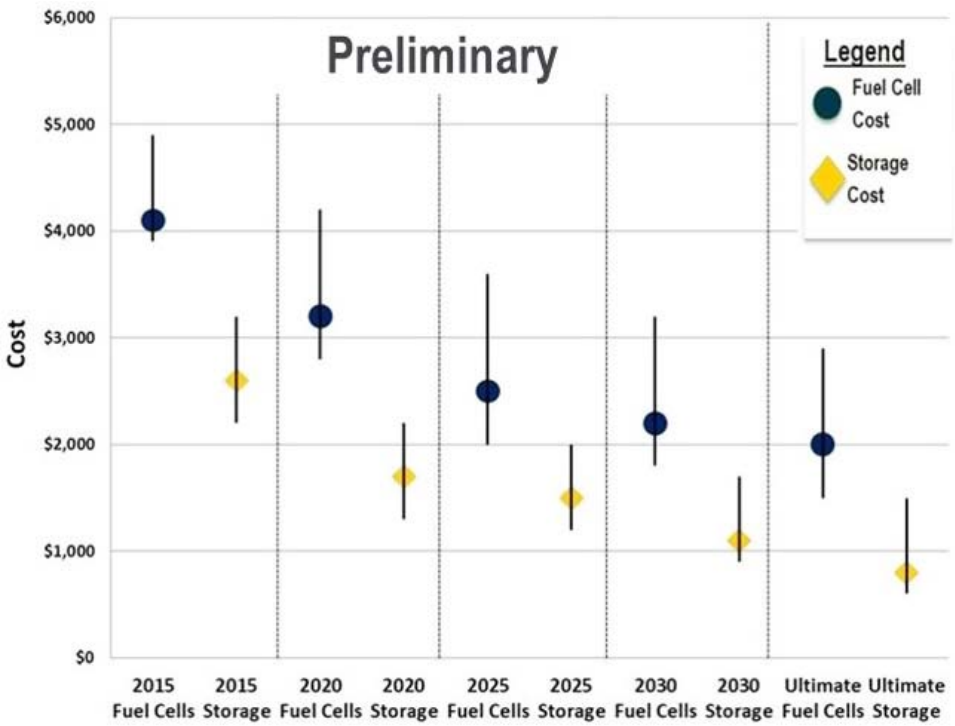

Source: Argonne National Laboratory

FIGURE 7. Improvement in fuel economy and onboard fuel storage costs for FCEVs over time

Interim Cost Target

An early market cost target was developed to guide and prioritize R&D for FCTO. The early market hydrogen cost target, a pathway independent target to guide R&D for production and delivery technologies for hydrogen fuel, is set at $7/gge, untaxed and dispensed at the pump. This target is based on a "top-down" analysis of the cost at which hydrogen fuel for FCEVs is projected to be competitive on a cost per mile basis with gasoline fuel for gasoline ICEVs in the early market timeframe of 2015 to 2020, as exhibited in Figure 8. The target considers a range of vehicle technologies, performance, fuel economy values (for both FCEVs and the competing ICEVs), and the federal and regional incentives currently in place, as well as the gasoline market prices in the regions analyzed. DOE record #14013 was developed, peer reviewed, and issued. http://hydrogen.energy.gov/pdfs/14013_hydrogen_early_market_cost_target.pdf

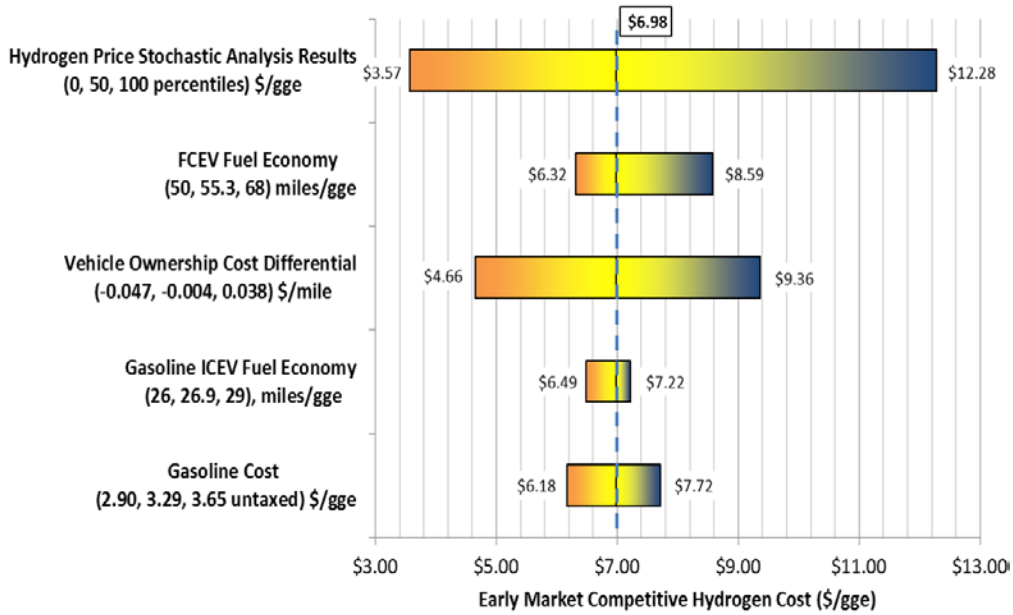

FIGURE 8. Sensitivity of the early market hydrogen cost (untaxed) to gasoline cost, vehicle ownership cost differential, and vehicle fuel economy

Commercial Products and Patents Resulting from DOE-Sponsored R&D

Pacific Northwest National Laboratory (PNNL) continues to analyze the commercial benefits of FCTO by tracking the commercial products and technologies, and patents developed from FCTO R&D funding. The benefits of DOE-funded projects continue to grow, as illustrated in Figures 9 and 10. Over 510 patents were awarded and 40 products were commercialized by 2015 as a result of research funded by FCTO in the areas of storage, production, delivery, and fuel cells, which will be highlighted in the FY 2015 Pathways to Commercial Success report. (PNNL)

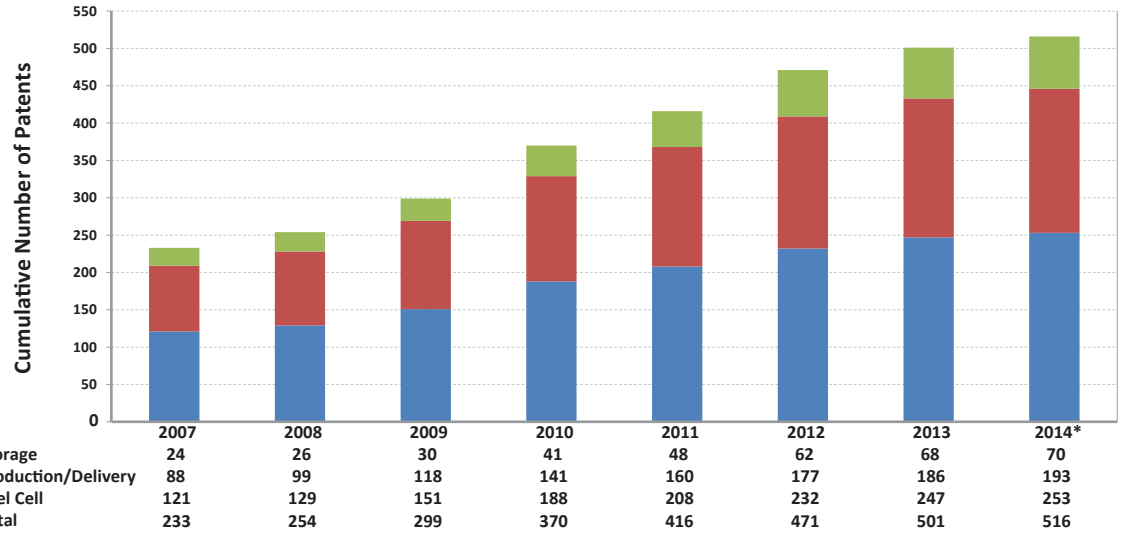

Source: Pacific Northwest National Laboratory

FIGURE 9. Cumulative number of patents awarded for FCTO-funded projects

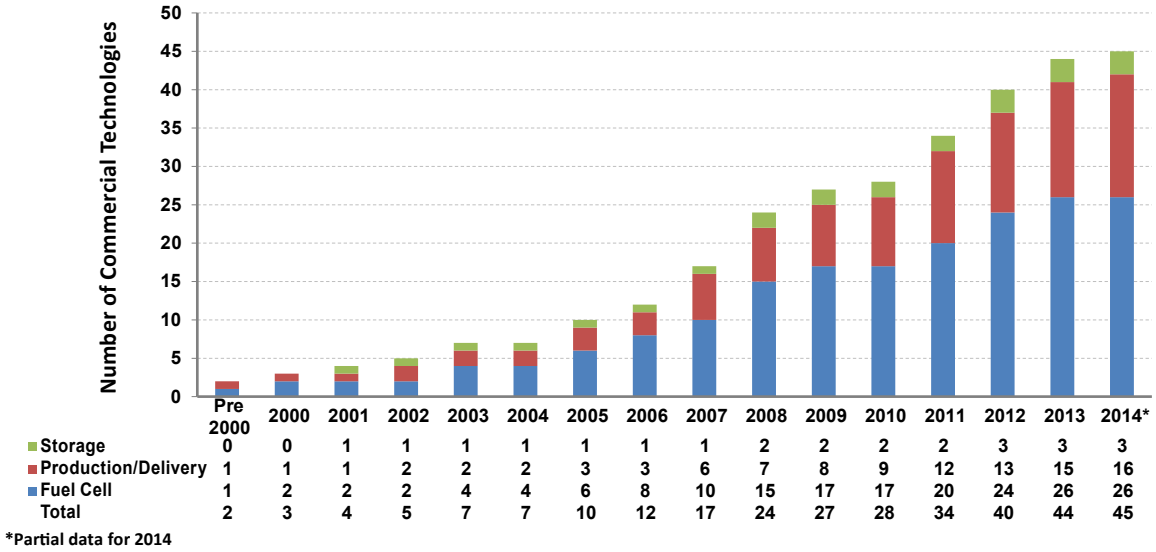

Source: Pacific Northwest National Laboratory

FIGURE 10. Cumulative number of commercial products entering the market from FCTO-funded projects

BUDGET

The budget for the Systems Analysis sub-program is consistent with the goals and objectives of FCTO and is responsive to assessing hydrogen and fuel cell applications for energy storage, stationary power generation, specialty applications, and light-duty transportation. The FY 2015 appropriation for the Systems Analysis sub-program was $3 million (Figure 11). Funding for the sub-program continues to focus on conducting analysis using the models developed by the program. In particular, projects are concentrated on analysis of hydrogen for energy storage and transmission, analysis of early market adoption of fuel cells, continued life-cycle analysis of water use for advanced

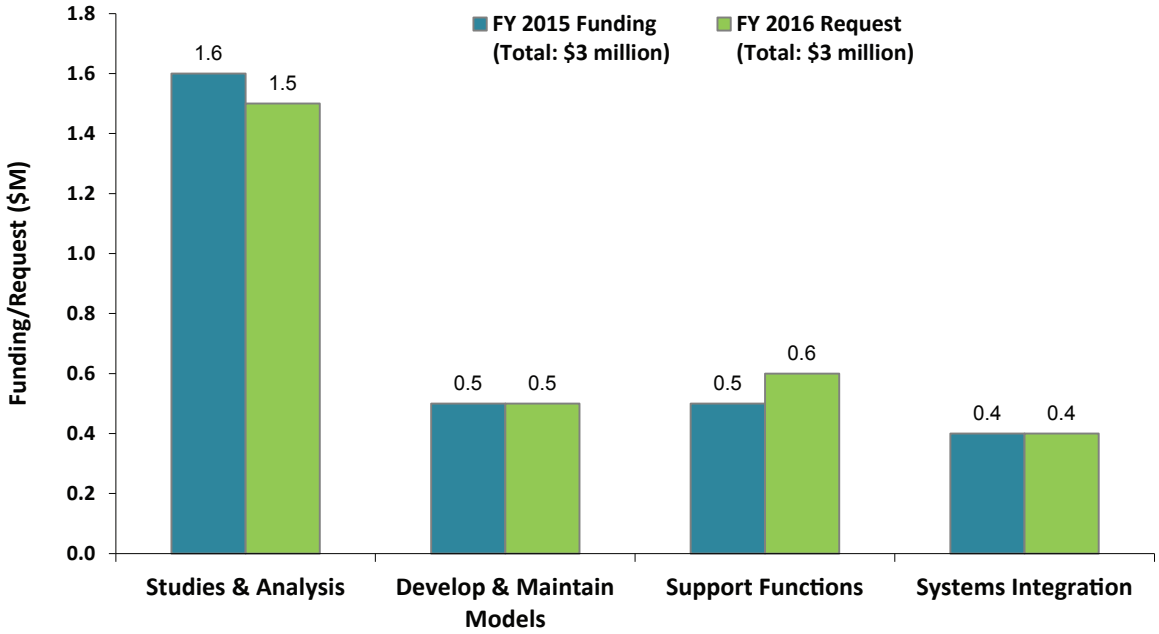

FIGURE 11. Systems Analysis R&D Funding. Subject to appropriations, project go/no-go decisions, and competitive selections. Exact amounts will be determined based on research and development progress in each area and the relative merit and applicability of projects competitively selected through planned funding opportunity announcements.

hydrogen production technology pathways, analysis of the levelized cost of hydrogen from emerging hydrogen production pathways, assessment of the impacts of consumer behavior, analysis of the cost of onboard hydrogen storage options and associated greenhouse gas emissions and petroleum use, and hydrogen fueling station business assessment.

FY 2016 PLANS

The FY 2016 request of $3 million, subject to congressional appropriation, provides greater emphasis on analysis of employment impacts of hydrogen and fuel cell technologies, sustainability, early market adoption of fuel cells, life-cycle analysis of GHG emissions and petroleum use for future hydrogen production technology pathways such as photoelectrochemical and solar thermal chemical hydrogen production, levelized cost of hydrogen from emerging hydrogen production pathways, and impacts of consumer behavior.

Fred Joseck
Systems Analyst
Fuel Cell Technologies Office
Office of Energy Efficiency and Renewable Energy
U.S. Department of Energy
1000 Independence Ave., SW
Washington, D.C. 20585-0121
Phone: (202) 586-7932
Email: Fred.Joseck@ee.doe.gov

IX.1 Impact of Fuel Cell System Peak Efficiency on Fuel Consumption and Cost

Aymeric Rousseau (Primary Contact),
Neeraj Shidore, and Namdoo Kim
Argonne National Laboratory (ANL)
9700 South Cass Avenue, Building 362
Lemont, IL 60439
Phone: (630) 252-7261
Email: arousseau@anl.gov

DOE Manager
Fred Joseck
Phone: (202) 586-7932
Email: Fred.Joseck@ee.doe.gov

Project Start Date: October 1, 2014
Project End Date: September 30, 2015

Overall Objectives

- Quantify fuel displacement and cost of advanced hydrogen storage and fuel cell systems, in conjunction with advancements in the rest of the powertrain, as part of DOE Baseline and Scenario Analysis (BaSce)
- Quantify the fuel displacement and cost of advanced hydrogen storage and fuel cell systems, without considering advancements in the rest of the powertrain

Fiscal Year (FY) 2015 Objectives

- Build vehicle simulations using the individual component assumptions
- Run the simulations as part of the BaSce process over advancements in hydrogen tank, fuel cell, and the rest of the vehicle powertrain (the detailed analysis and report generation will be performed in FY 2016)
- Run simulations with advances in hydrogen tank and fuel cell technology while not considering advances in the rest of the powertrain
  - Provide detailed analysis on impact of fuel cell and hydrogen tank assumptions on the energy consumption, cost, component sizing, and vehicle weight

Technical Barriers

This project addresses the following technical barriers from the Systems Analysis section of the Fuel Cell Technologies Office Multi-Year Research, Development, and Demonstration Plan:

(A) Future Market Behavior

(C) Inconsistent Data, Assumptions and Guidelines

(D) Insufficient Suite of Models and Tools

(E) Unplanned Studies and Analysis

Contribution to Achievement of DOE Systems Analysis Milestones

This project will contribute to achievement of the following DOE milestones from the Systems Analysis section of the Fuel Cell Technologies Office Multi-Year Research, Development, and Demonstration Plan:

- Milestone 1.1: Complete an analysis of the hydrogen infrastructure and technical target progress for hydrogen fuel and vehicles. (2Q, 2011)
- Milestone 1.11: Complete analysis of the impact of hydrogen quality on the hydrogen production cost and the fuel cell performance for the long range technologies and technology readiness. (2Q, 2015)
- Milestone 1.12: Complete an analysis of the hydrogen infrastructure and technical target progress for technology readiness. (4Q, 2015)
- Milestone 1.16: Complete analysis of program performance, cost status, and potential use of fuel cells for a portfolio of commercial applications. (4Q, 2018)
- Milestone 1.17: Complete analysis of program technology performance and cost status, and potential to enable use of fuel cells for a portfolio of commercial applications. (4Q, 2018)
- Milestone 2.2: Annual model update and validation. (4Q, 2011 through 4Q, 2020)

FY 2015 Accomplishments

- Full vehicle simulations were performed to assess the vehicle energy consumption and cost of current and future fuel cell vehicles compared to conventional powertrains for different fuel cell systems.
- Compared to current conventional vehicles, fuel cell vehicles achieve similar weight and a fuel economy up to 4.5 times higher by 2025 or 1.7 times higher (if compared to same-year conventional vehicle).

- Current DOE targets for both fuel cell peak power (80 kW) and onboard hydrogen weight (5.6 kg) will exceed the requirements for most of the vehicle classes by 2025.
- Midsize fuel cell vehicles with advances in hydrogen tank and fuel cell technology were sized and simulation was performed to evaluate the benefits of fuel cells and storage without improvements from the DOE Vehicle Technologies Office (VTO).
- Advances in the fuel cell system alone lead to a fuel consumption benefit of 6.8 to 10.5%, a vehicle manufacturing cost reduction of 6.2 to 6.5%, and a reduction of hydrogen fuel mass of 6.2 to 9.1% by 2020.
- Advances in hydrogen storage alone lead to a fuel consumption benefit up to 0.2% and a vehicle manufacturing cost reduction of 2.6 to 2.9% by 2020.

✧ ✧ ✧ ✧ ✧

INTRODUCTION

Autonomie has been used by the U.S. Department of Energy to evaluate the vehicle energy consumption and benefits of a wide range of powertrain configurations, component technologies, and control strategies. In this study, the objective is to quantify the vehicle energy consumption and cost of fuel cell hybrid vehicles compared to conventional powertrains using two target scenarios: current and aggressive. The current scenario is based on a 60% peak efficiency fuel cell system while the aggressive scenario relies on higher fuel cell system efficiencies (up to 70%).

APPROACH

To properly assess the benefits of future technologies, different vehicle classes were considered: compact car, midsize car, small sport utility vehicle (SUV), medium SUV, and pickup truck. Different timeframes representing different sets of assumptions were simulated. For this report, we will show 'lab years' 2010, 2020, and 2045. It should be noted that lab year 2010 would reflect a vehicle available in the market in 2015 (current technology). Similarly, lab or simulation year 2020 would reflect a vehicle in the market in 2025, and a 2045 simulation vehicle would be in the market in 2050. For the actual study, lab years 2010, 2020, 2025, 2030, and 2045 were simulated, which would reflect model years 2015 (current technology), 2025, 2030, 2035, and 2050, respectively.

Additionally, to address uncertainties, a triangular distribution approach (low, medium, and high) was employed. For each component, assumptions (e.g., regarding efficiency, power density) were made, and three separate values were defined to represent the (1) 90th percentile, (2) 50th percentile, and (3) 10th percentile. A 90% probability means that the technology has a 90% chance of being available at the time considered. For each vehicle considered, the cost assumptions also follow the triangular uncertainty. For each vehicle case (particular class, technology uncertainty, simulation/show-case year), simulations were performed with evolution of all vehicle technology simultaneously. The above simulations were performed as a part of DOE VTO's BaSce process.

In addition, simulations were performed which involved evolution of the fuel cell and hydrogen tank with time (up to 2045) while maintaining technology of the rest of the powertrain at 2010 levels. This isolated the vehicle-level impacts of advancements in fuel cell and hydrogen tank technologies, contrasting the BaSce results where all technologies were evolving at the same time.

RESULTS

Baseline and Scenario Analysis

Based on assumptions of technology improvement for fuel cells and hydrogen storage, it can be seen that fuel cell system power required to meet the vehicle technical specification decreases significantly with time. Also, the required hydrogen fuel mass could drop by 50% by year 2045 (Figure 1). By 2045, the cost of fuel cell hybrid vehicles is comparable to conventional vehicles (Figure 2a). This cost decrease is mainly due to the decrease in the cost of the hydrogen tank. Due to the compounding effects of fuel cell improvements, hydrogen technology improvements, and improvement in the rest of the powertrain, fuel cell vehicles retain a fairly constant fuel economy advantage compared to conventional vehicles up to 160% over time (Figure 2b). Both figures show results for midsize class.

Fuel Cell and Hydrogen Storage System Only Analysis

In order to evaluate the potential of fuel cell and hydrogen tank technologies in isolation, the simulations of fuel cell vehicles for midsize class were performed in four iterations: with all technologies being 2015 (Ref.) (from BaSce results), improved hydrogen storage (H2) only (iteration 1), only improved fuel cell system (FC) (iteration 2), then both improved fuel cell and hydrogen storage (H2 + FC) (iteration 3), and finally all technologies (All: FC + H2 + electric machine + battery + lightweighting…) (iteration 4, from BaSce). Fuel cell vehicle weight decreases by 1 to 4% by 2045 without lightweighting or improvement in other component technology. The vehicle hydrogen storage has been sized to provide a range of 320 miles on the combined driving cycle (Urban Dynamometer Driving Schedule and Highway Fuel Economy Driving Schedule). Required onboard hydrogen fuel mass could drop by 15% due to the

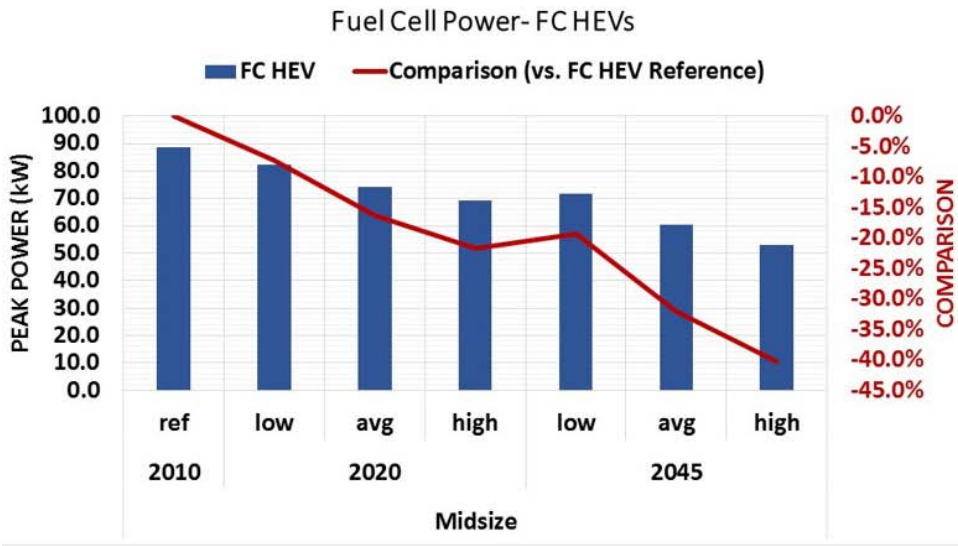

(a) Fuel cell peak power, kW

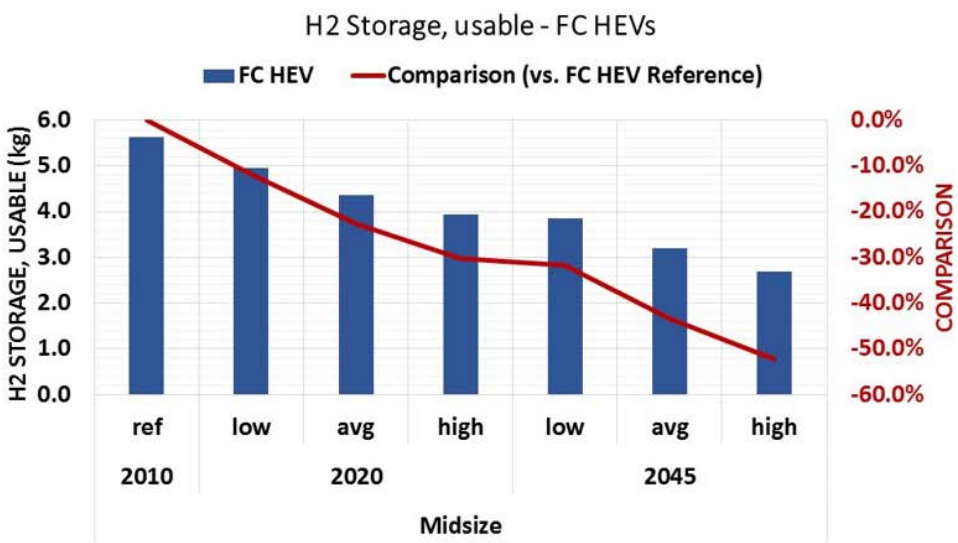

(b) Hydrogen storage usable, kg

FC – fuel cell
HEV – hybrid electric vehicle
ref – reference

FIGURE 1. Evolution of fuel cell peak power and usable hydrogen storage for BaSce scenario

fuel cell system technology improvements only (Figure 3) by lab year 2020, i.e., showroom year 2025. Figure 4a shows the fuel cell system cost with the advances in hydrogen tank only, fuel cell technology only, and all technology improvements. The results show that fuel cell system cost could decrease by 50% due to the fuel cell system technology improvements only. As shown in Figure 4b, the fuel cell system improvements lead to significant fuel savings on the U.S. Environmental Protection Agency combined driving procedure. While better batteries, electric machine, and lightweighting help, fuel cell system improvements lead to significant fuel savings of about 40% by 2045.

CONCLUSIONS AND FUTURE DIRECTIONS

Two sets of vehicle simulations were performed to assess the vehicle energy consumption and cost of fuel cell vehicles compared to conventional powertrains. Different timeframes, fuel cell system peak efficiencies, and hydrogen storage assumptions were considered. For one set of simulations, all

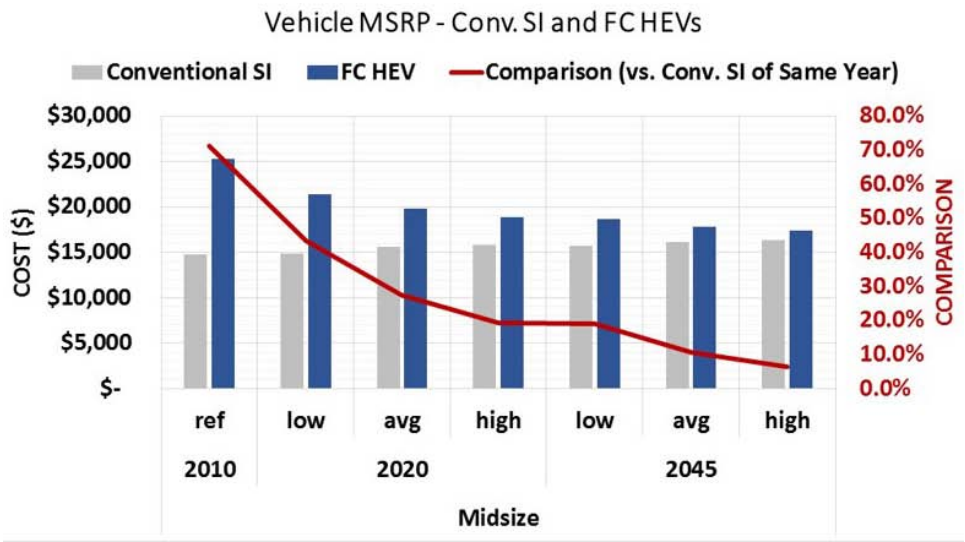

(a) Vehicle cost – Conv. SI and FC HEVs, $

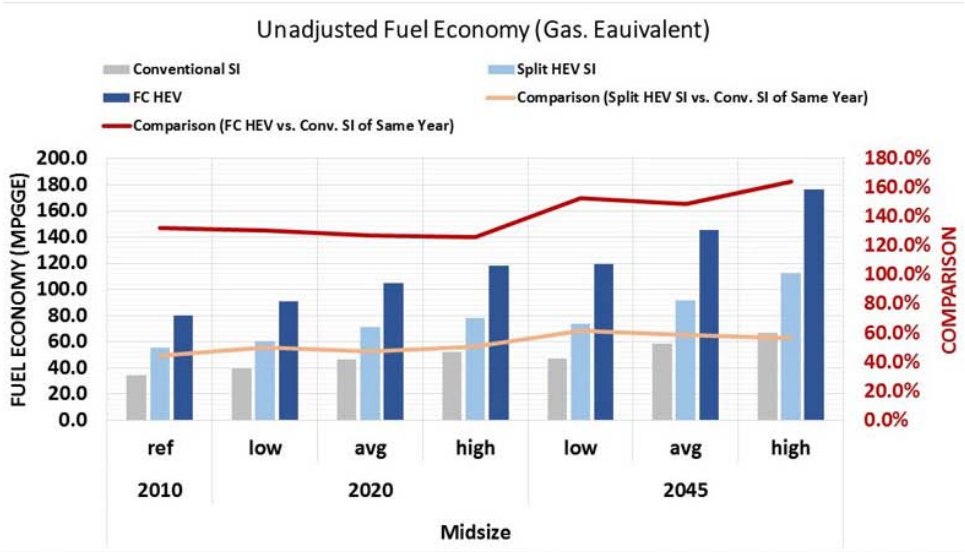

(b) Fuel economy – Conv. SI, SI HEVs and FC HEVs, MPGGE

MSRP – manufacturer's suggested retail price
SI – spark ignition
Conv. – conventional
MPGGE – miles per gallon gasoline equivalent

FIGURE 2. Evolution of fuel cell vehicle cost and fuel economy for BaSce scenario

vehicle assumptions (including drag coefficient, frontal area, glider mass, etc.) were varied with time (BaSce simulations), and for the second set of simulations, only fuel cell and hydrogen storage assumptions were varied with time.

- The BaSce simulation results showed that required hydrogen fuel mass could drop by 50% by showroom year 2050.
- With evolution in the fuel cell system, hydrogen tank, and the rest of the powertrain, by 2045 the cost of the fuel cell hybrid vehicles will be comparable to conventional vehicles, mainly due to the decrease in the cost of the hydrogen tank.
- When considering the impact of fuel cell and hydrogen storage system technology only (without considering

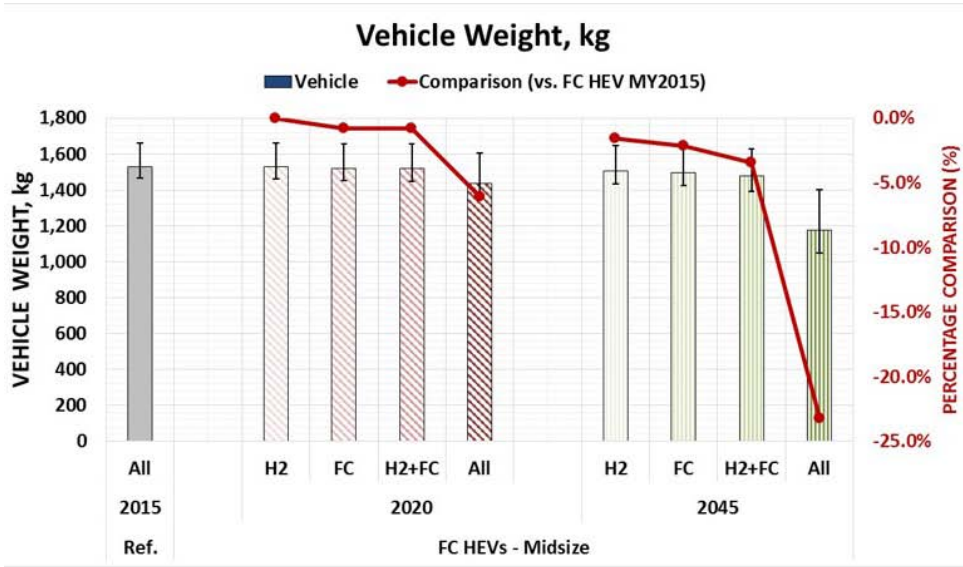

(a) Vehicle curb weight, kg

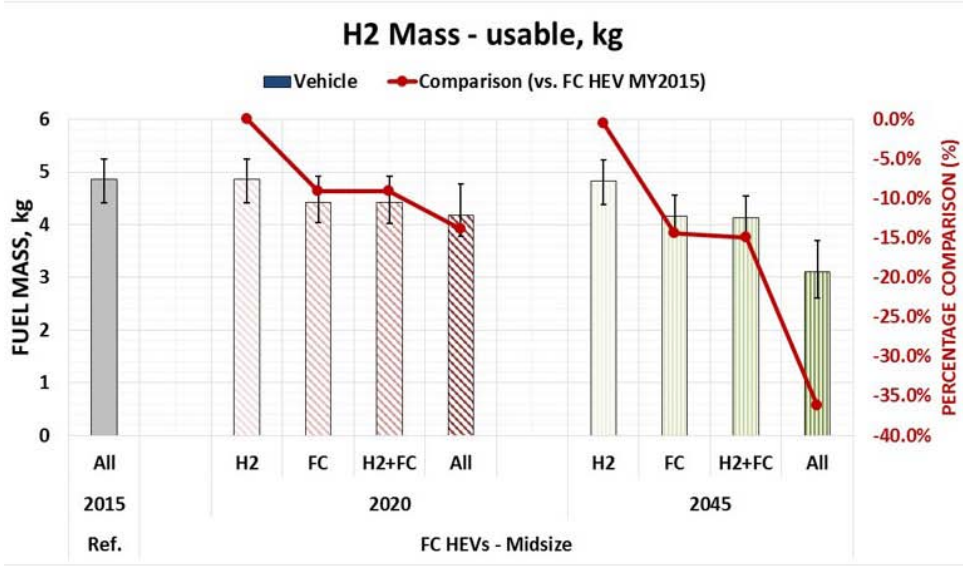

(b) Hydrogen storage usable, kg

FIGURE 3. Progression in vehicle curb weight and usable hydrogen storage due to improvements in fuel cell and hydrogen storage technology

improvements in the rest of the powertrain), required hydrogen mass could drop by 1 to 4% by 2045.

- Under the same scenario (development fuel cell system only), fuel cell system cost could decrease by 50%.

For FY 2016, a thorough analysis of assumptions, component (fuel cell) and vehicle operation, and fuel economy benefits of fuel cell vehicles (compared to conventional and other advanced powertrains) will be published in the form of a comprehensive report for the BaSce simulations. In addition, requests for further analysis will be supported as part of the project.

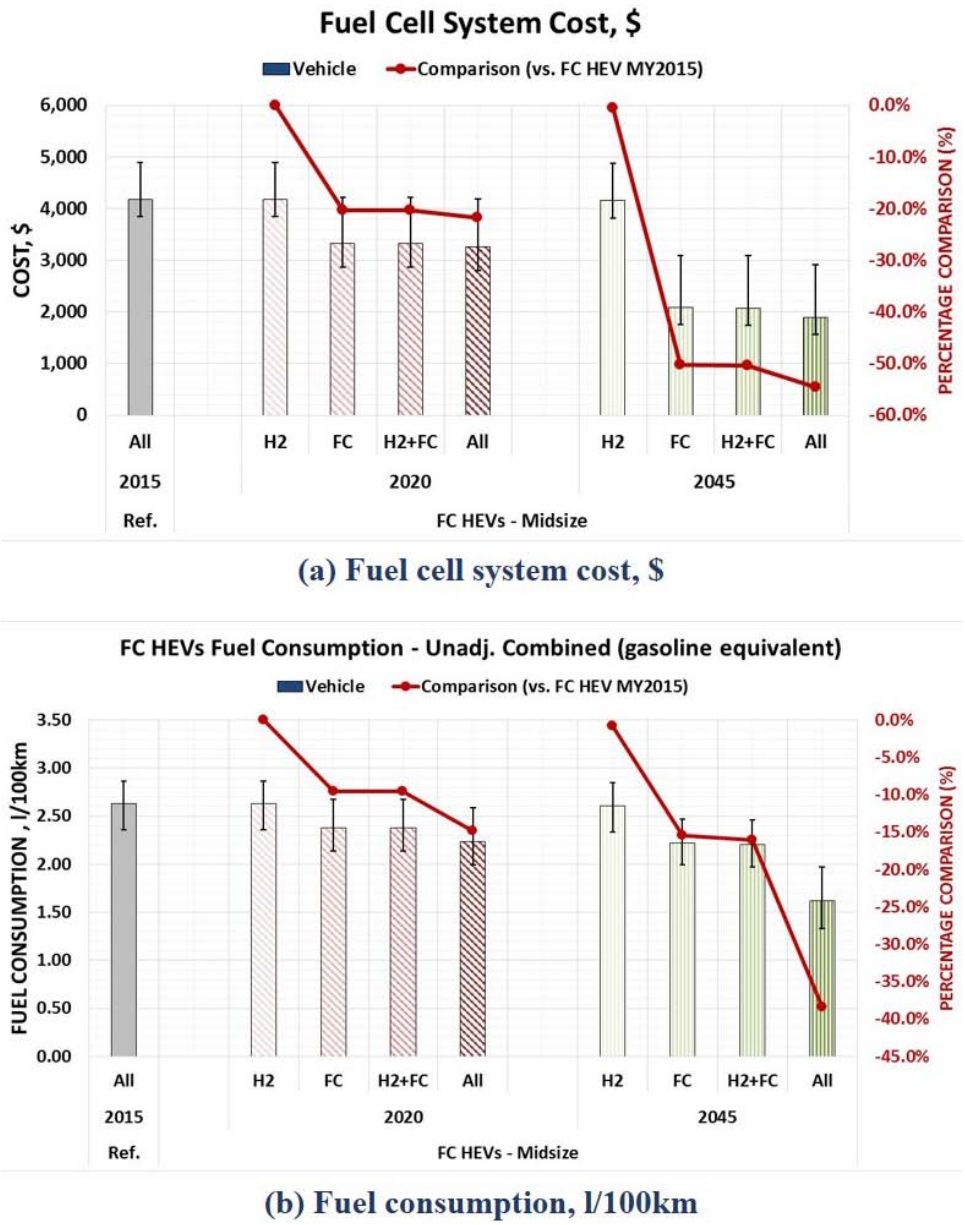

FIGURE 4. Progression in fuel cell system cost and vehicle fuel consumption considering improvements in fuel cell and hydrogen storage technology

FY 2015 PUBLICATIONS/PRESENTATIONS

1. Aymeric Rousseau, "Impact of Fuel Cell System Efficiency on Vehicle Energy Consumption and Cost." Presentation at the Annual Merit Review.

REFERENCES

1. ANL Report: Potential of Technologies for Displacing Gasoline Consumption by Light-Duty Vehicles through 2045 – September 2014.

IX.2 GPRA Analysis: Impact of Program Targets on Vehicle Penetration and Benefits

Zhenhong Lin (Primary Contact), Changzheng Liu
Oak Ridge National Laboratory (ORNL)
2360 Cherahala Boulevard
Knoxville, TN 37932
Phone: (865) 946-1308
Email: linz@ornl.gov

DOE Manager
Fred Joseck
Phone: (202) 586-7932
Email: Fred.Joseck@ee.doe.gov

Project Start Date: October 1, 2013
Project End Date: Project continuation and direction determined annually by DOE

Overall Objectives

- Quantify impacts of DOE Fuel Cell Technologies Office (FCTO) program targets on market penetration and societal benefits of fuel cell electric vehicles (FCEVs)
- Estimate FCEV market share and the resulting reduction in petroleum use and greenhouse gas (GHG) emissions
- Support United States Driving Research and Innovation for Vehicle efficiency and Energy sustainability (U.S. DRIVE) goals and FCTO activities

Fiscal Year (FY) 2015 Objectives

- Update fuel cell vehicle data and hydrogen cost data
- Construct appropriate hydrogen station roll-out scenarios
- Coordinate assumptions and data with program offices, national labs, and/or industry
- Report updated benefit analysis results

Technical Barriers

This project addresses the following technical barriers from the Systems Analysis section of the FCTO Multi-Year Research, Development, and Demonstration Plan:

(A) Future Market Behavior

(C) Inconsistent Data, Assumptions and Guidelines

(D) Insufficient Suite of Models and Tools

(E) Unplanned Studies and Analysis

Contribution to Achievement of DOE Systems Analysis Milestones

This project will contribute to achievement of the following DOE milestones from the Systems Analysis section of the FCTO Multi-Year Research, Development, and Demonstration Plan:

- Milestone 1.13: Complete environmental analysis of the technology environmental impacts for hydrogen and fuel cell scenarios and technology readiness. (4Q, 2015)
- Milestone 1.15: Complete analysis of program milestones and technology readiness goals - including risk analysis, independent reviews, financial evaluations, and environmental analysis - to identify technology and risk mitigation strategies. (4Q, 2015)

FY 2015 Accomplishments

- Constructed 44 alternative scenarios to reflect uncertainty in fuel cell costs ($40/kW or $30/kW by 2020), hydrogen storage cost ($10/kWh or $8/kWh by 2020), oil prices, hydrogen station roll-out speed, and hydrogen prices
- Generated results of the above 44 scenarios on FCEV sales, petroleum consumption, and GHG emissions
- Found FCEV sales impact of program targets depends on oil price, infrastructure roll-out speed, and hydrogen price, but overall is significant
- Found FCEVs, battery electric vehicles (BEVs), and long-range plug-in hybrid electric vehicles (PHEVs) benefit the most from the program targets
- Found the $30/kW fuel cell target and the $8/kWh hydrogen storage target reduce petroleum use by 0.23 MMbpd by 2030, 1.1 MMbpd by 2050
- Found the $30/kW fuel cell target and the $8/kWh hydrogen storage target reduce GHG emissions by 12–31 $MMtCO_2e$ by 2030 and 29–163 $MMtCO_2e$ by 2050, depending on supply share of renewable hydrogen

✧ ✧ ✧ ✧ ✧

INTRODUCTION

The Government Performance and Results Act (GPRA) is a United States law enacted in 1993, as one of a series of laws designed to improve management of government-funded projects. The GPRA requires agencies to engage in project management tasks such as setting goals, measuring results, and reporting progress. In order to comply with the GPRA, agencies are required to prepare annual performance plans that establish the performance goals for the applicable fiscal year and must prepare annual performance reports that review the agency's success or failure in meeting its targeted performance goals.

The DOE's Market Acceptance of Advanced Automotive Technologies (MA3T) model has been extensively used by the Vehicle Technologies Office (VTO) and FCTO to assess and analyze the potential market success of advanced automotive technologies. MA3T was used by the VTO in its GPRA analysis for FY 2012–FY 2014, and was used in FY 2013 in two studies for FCTO on the hydrogen fuel cell vehicle market, resulting in two articles published in International Journal of Hydrogen Energy.

This study aims at quantifying impacts of FCTO program targets (fuel cell costs and hydrogen storage costs) on FCEV sales, the light-duty vehicle (LDV) petroleum consumption, and GHG emissions, in both the near and long terms.

The objectives of this project are to:

- Construct appropriate scenarios to capture key transition uncertainties and reasonably reflect consensus understandings or assumptions.
- Generate simulation results to quantify the FCEV sales impact and LDV-related societal impacts of FCTO program targets.

APPROACH

The ORNL MA3T model was used to quantify FCEV sales, LDV petroleum use, and GHG emissions as a result of alternative assumptions. MA3T endogenously estimates market share of FCEVs among competing LDV technologies by including up to 300 vehicle choices and over 9,000 consumer segments. It explicitly considers range limitation, hydrogen refueling availability, technology learning, and vehicle make/model availability.

A total of 44 alternative scenarios were constructed to reflect the fuel cell (FC) cost targets of $40/kW or $30/kW by 2020, hydrogen storage (HS) cost targets of $10/kWh or $8/kWh by 2020, oil prices of Reference and High from Annual Energy Outlook (AEO) 2014 (a publication of the DOE Energy Information Administration), hydrogen station roll-out speed of Reference and Optimistic from the National Renewable Energy Laboratory's Scenario Evaluation, Regionalization and Analysis (SERA) model, and hydrogen prices of $8/kg, $4/kg, and $2/kg by assumption.

The Base case vehicle data in MA3T from the Low-Low scenario of the Argonne National Laboratory Autonomie output is modified to reflect the isolated effect of FCTO program targets on fuel cell and hydrogen storage costs. As in Figure 1, the FC and HS costs and capacity values in the Base case are used to calculate the FC and HS Base unit costs, which are compared to the FC and HS target unit costs. The comparison yields a vehicle cost difference that, when added to the Base vehicle cost, results in the target-adjusted vehicle cost in an alternative scenario.

This project also contributes to the broader DOE program benefit analysis, Baseline and Scenario Analysis (BaSce), by providing MA3T simulation results on two scenarios— "NoProgram" that assumes the "Low-Low" scenario of the most recent Autonomie vehicle simulation

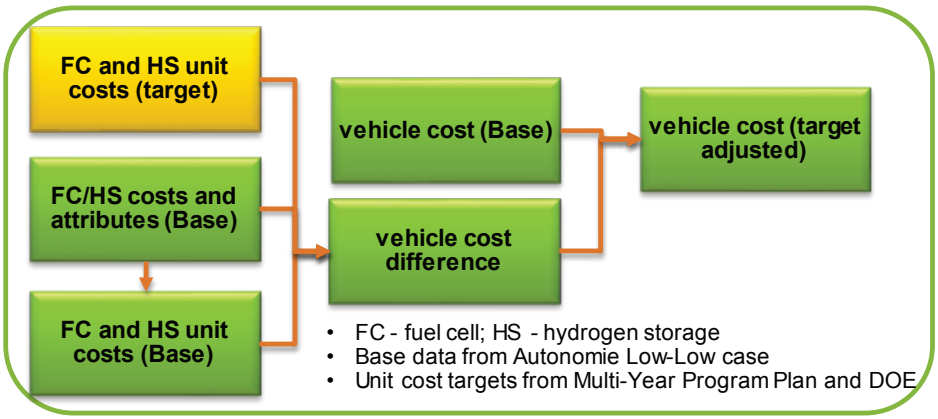

FIGURE 1. Target adjustment of vehicle costs

data on fuel economy and costs, representing no active pursuit of DOE VTO or FCTO program activities, and "ProgramSuccess" that assumes all DOE program targets are met on time plus an optimistic roll-out of both hydrogen refueling and electric vehicle charging infrastructure. Both scenarios assume AEO 2014 Reference energy prices.

RESULTS

Between the NoProgram and ProgramSuccess scenarios, the program targets seem to have greater positive impacts on market shares of powertrain choices that have a larger component targeted by DOE R&D activities. As shown in Figure 2, FCEVs, BEVs, and long-range PHEVs benefit the most from the program targets. As a result of program targets, FC hybrid electric vehicles (HEVs) have greater market shares both in the near and long terms. So do PHEV40s, while PHEV10s have smaller market shares both in the near and long terms and BEV100s have a larger near-term market share and a smaller long-term market share.

The FCTO program targets are found to result in significant reduction in LDV petroleum consumption. As shown in Figure 3, while the effect is much smaller by 2030, the long-term effect in 2050 is significant, especially when both FC and HS targets are combined. The FC $30/kW and HS $8/kWh targets are found to reduce petroleum use by 0.23 MMbpd by 2030 and 1.1 MMbpd by 2050.

The GHG benefits of FCTO program targets are more uncertain. For simplification, we assume 0.51 kg CO_2/kWh electricity based on AEO estimated 2015 United States average grid carbon intensity and 9.22 kg CO_2/kg H_2 based on central reforming of natural gas at current technology without carbon capture and sequestration, but expect greater GHG benefits from deeper decarbonization of electricity and hydrogen supply. As shown in Figure 4, the FC $30/kW and HS $8/kWh targets reduce GHG emissions by 12–31 $MMtCO_2e$ by 2030 and 29–163 $MMtCO_2e$ by 2050, depending on supply share of renewable hydrogen.

CONCLUSIONS AND FUTURE DIRECTIONS

- FCEV sales impacts of program targets were found to be significant and dependent on oil price, station roll-out speed, and hydrogen price.
- The petroleum reduction benefit of program targets is significant, especially in the long run. The FCTO targets reduce petroleum use by 0.12 MMbpd or 2% by 2030, 0.68 MMbpd or 16% by 2050.
- The GHG reduction benefit of program targets is significant only in the long run and with decarbonization of hydrogen supply. The FC $40/kW and HS $10/kWh targets reduce GHG emissions by 0.8%–2% by 2030 and 3%–18% 2050, depending on supply share of renewable hydrogen.
- Recommended future work includes vehicle data updates to reflect recent views of future technology trends, cluster strategy to capture potential targeted markets, business model analysis to assist private sector investments, and consumer segmentation to understand niche and mass markets for FCEVs.

FY 2015 PUBLICATIONS/PRESENTATIONS

1. Zhenhong Lin, Changzheng Liu, GPRA Analysis: Impact of Program Targets on Vehicle Penetration and Benefits. Presented at the 2015 DOE Annual Merit Review meeting.

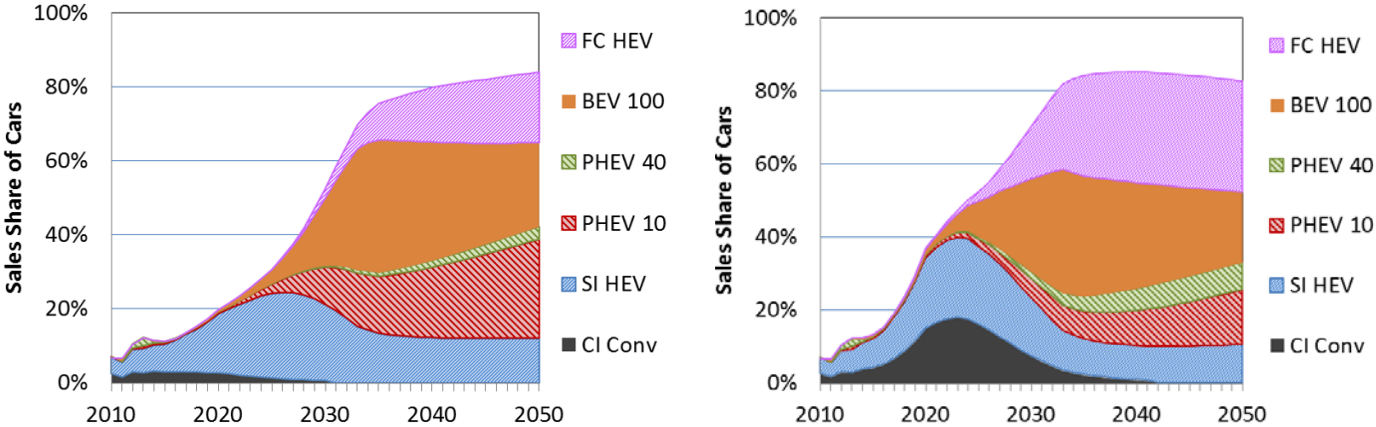

SI – spark ignition; CI – compression ignition; Conv – conventional

FIGURE 2. Technology market share impact of program targets (midsize cars and crossovers only)

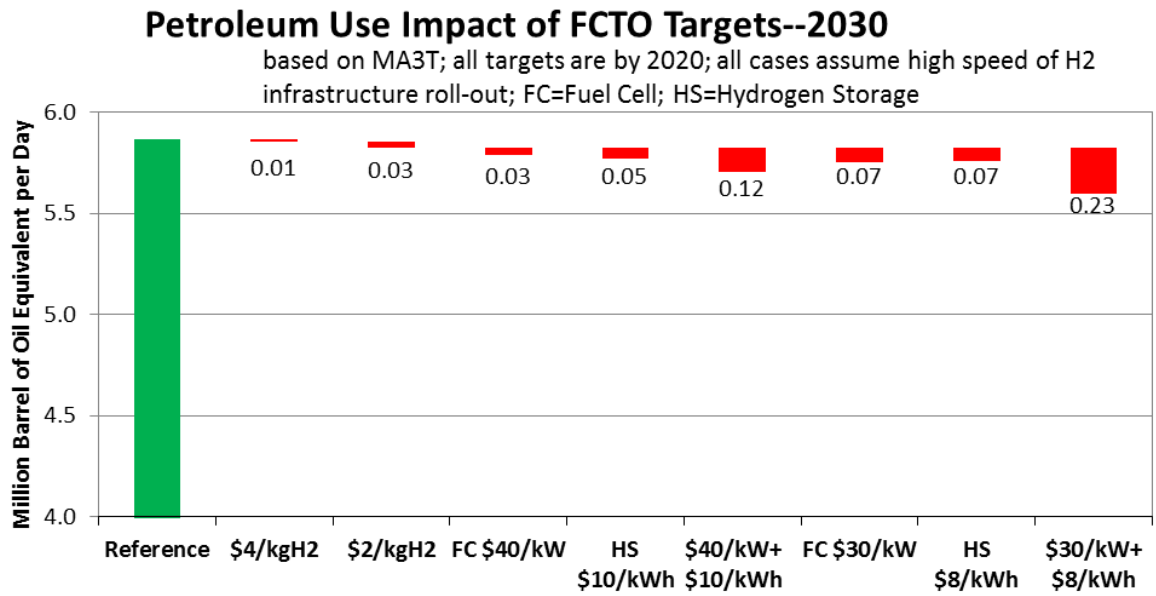

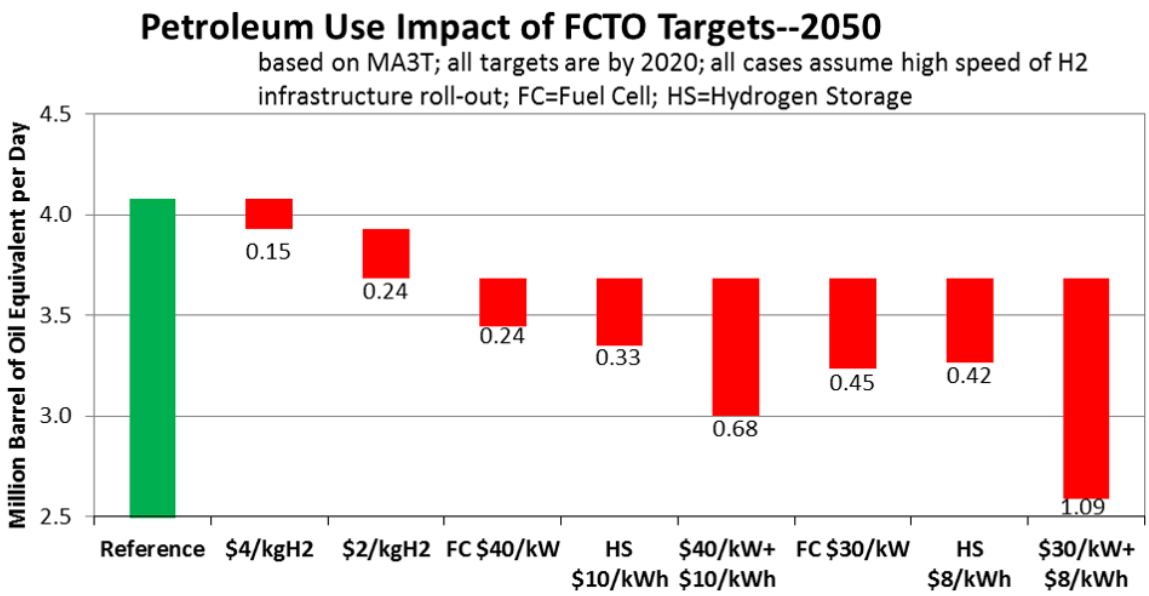

FIGURE 3. FCTO target impacts on LDV petroleum use

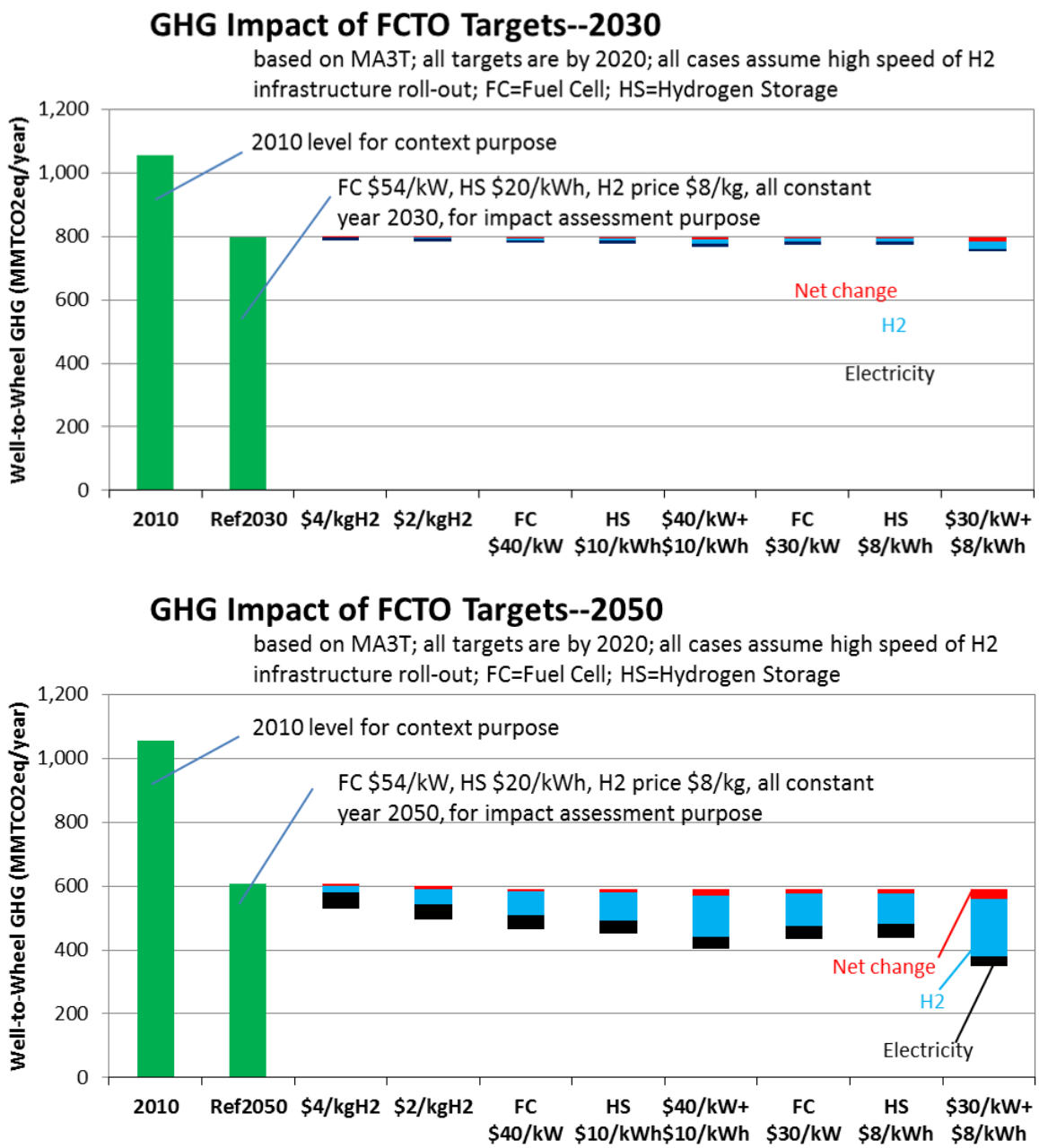

FIGURE 4. FCTO target impacts on LDV GHG emissions

IX.3 Pathway Analysis: Projected Cost, Lifecycle Energy Use and Emissions of Emerging Hydrogen Technologies

Todd Ramsden (Primary Contact), Victor Diakov, Neil Popovich
National Renewable Energy Laboratory
15013 Denver West Pkwy.
Golden, CO 80401
Phone: (303) 275-3704
Email: todd.ramsden@nrel.gov

DOE Manger
Fred Joseck
Phone: (202) 586-7932
Email: Fred.Joseck@ee.doe.gov

Project Start Date: March 1, 2014
Project End Date: September 30, 2015

Overall Objectives

- Conduct cost and lifecycle energy and emissions analyses of complete future and emerging technology hydrogen pathways to evaluate hydrogen cost, energy requirements, and greenhouse gas (GHG) emissions
- Provide detailed reporting of assumptions and data used to analyze hydrogen production, delivery, and dispensing technologies, enabling consistent and transparent understanding of results
- Report on upstream energy and feedstock usage and GHG emissions on a full lifecycle basis, including vehicle cycle and well-to-wheels fuel cycle
- Understand lifecycle costs, energy, and emissions of hydrogen technologies to inform research and development (R&D) decision-making process
- Evaluate potential of future hydrogen technologies to meet the $4/kg hydrogen cost target
- Validate the DOE Fuel Cell Technologies Office's (FCTO's) Macro-System Model (MSM) and its underlying component models (in particular, the Hydrogen Analysis [H2A] Production model, the Hydrogen Delivery Scenario Analysis Model [HDSAM], and the Greenhouse Gases, Regulated Emissions, and Energy Use in Transportation [GREET] model) through industry review

Fiscal Year (FY) 2015 Objectives

- Conduct an evaluation of complete hydrogen production, delivery, and dispensing pathways based on the cost and performance of future and emerging technologies expected to be available in the 2020 to 2030 timeframe, assessing the impact technology improvements and developments will have on lifecycle cost, energy use, and emissions
  - FY 2015 evaluation focused on emerging, low-carbon hydrogen production paths
- Conduct detailed sensitivity analyses, including cost, energy use, and emissions analyses, based on a fuel cell electric vehicle (FCEV) on-road fuel economy of 58 miles per gasoline gallon equivalent (GGE) and 68 miles per GGE (mpgge)
- Conduct a detailed review of the evaluation framework, component models, input parameters, and results with DOE and industry stakeholders through the United States Driving Research and Innovation for Vehicle efficiency and Energy sustainability (U.S. DRIVE) partnership with a goal of assessing technology progress and remaining technology gaps where further R&D is needed

Technical Barriers

This project addresses the following technical barriers from the Systems Analysis section of the FCTO Multi-Year Research, Development, and Demonstration Plan:

(B) Stove-piped/Siloed Analytical Capability

(C) Inconsistent Data, Assumptions and Guidelines

(D) Insufficient Suite of Models and Tools

Contribution to Achievement of DOE Systems Analysis Milestones

This project will contribute to achievement of the following DOE milestones from the Systems Analysis section of the FCTO Multi-Year Research, Development, and Demonstration Plan:

- Milestone 1.12: Complete an analysis of the hydrogen infrastructure and technical target progress for technology readiness. (4Q, 2015)
- Milestone 1.13: Complete environmental analysis of the technology environmental impacts for hydrogen and fuel cell scenarios and technology readiness. (4Q, 2015)
- Milestone 1.15: Complete analysis of program milestones and technology readiness goals - including risk analysis, independent reviews, financial evaluations, and environmental analysis - to identify technology and risk mitigation strategies. (4Q, 2015)
- Milestone 1.18: Complete life cycle analysis of vehicle costs for fuel cell electric vehicles compared to other vehicle platforms. (4Q, 2019)

- Milestone 2.2: Annual model update and validation. (4Q, 2011 through 4Q, 2020)
- Milestone 3.4: Review Hydrogen Threshold Cost status. (4Q, 2014; 4Q, 2017; 4Q, 2020)

FY 2015 Accomplishments

- Estimated the lifecycle costs, energy use, and emissions from four complete emerging technology hydrogen fuel pathways, including a total cost of fuel cell vehicle ownership that considers the cost of hydrogen fuel and FCEV purchase and operating costs
  - Of the emerging production technology pathways evaluated, hydrogen production from natural gas reformation with carbon capture and sequestration (CCS) resulted in the lowest total pathway cost, with a cost of $0.10 per mile driven for hydrogen fuel and a total vehicle ownership and operational cost of $0.72 per mile (in a mature market)
- Assessed the total pathway costs and well-to-wheels (WTW, or fuel-cycle) energy use and GHG emissions of the emerging-technology pathway scenarios
  - Estimated the cost of hydrogen in a mature market, with costs ranging from $5.60/kg H_2 for the natural gas reformation with carbon sequestration pathway to over $12/kg H_2 for the photo-biological production pathway
  - Estimated the total fuel-cycle (WTW) and lifecycle GHG emissions of all pathways, including upstream fuel- and feedstock-related emissions and vehicle-production-related emissions
  - Emerging carbon sequestration technologies are predicted to lower WTW emissions of the central natural gas reformation pathway from about 210 g carbon dioxide (CO_2)-equivalent per mile to 90 g CO_2-equivalent per mile at 68 mpgge fuel economy (110 g CO_2/mi at 58 mpgge)
- Completed extensive industry review of overall results, modeling results, and input parameters, providing external validation of the MSM and the related component models
- Conducted an initial assessment of emerging, onboard hydrogen storage technologies

✧ ✧ ✧ ✧ ✧

INTRODUCTION

DOE's Fuel Cell Technologies Office had identified a need to understand the cost, energy use, and emissions tradeoffs of various hydrogen fuel infrastructure technologies under consideration for fuel cell vehicles. This particular study is part of a broader assessment of complete hydrogen production, delivery, and dispensing scenarios. This evaluation considers the cost and performance of future and emerging hydrogen technologies expected to be available in the 2020 to 2030 timeframe, focusing particularly on the impact emerging, low-carbon hydrogen production technologies will have on lifecycle cost, energy use, and emissions. The study considers the potential of future and emerging hydrogen technologies if they were brought to commercial scale in a mature fuel cell vehicle market; it is not an assessment of transition scenarios where equipment may not be fully utilized. This emerging technology pathway analysis is a companion analysis to the current and future technology hydrogen pathway assessments conducted previously in FY 2012–2014.

This study will help FCTO evaluate the potential of emerging, low-carbon hydrogen production technologies to meet the $4/kg cost target for dispensed hydrogen. By providing a common framework for modeling using consistent data and assumptions, this study provides a detailed and transparent understanding of hydrogen technologies and will assist FCTO with goal setting and R&D decisions. Finally, this analysis will aid in understanding and assessing technology needs and progress, potential environmental impacts, and the energy-related economic benefits of various hydrogen pathways.

APPROACH

This study evaluated four complete hydrogen production, delivery, and dispensing pathways with the potential to be available in the 2020-2030 timeframe, assessing the cost and performance of emerging, low-carbon production technologies coupled with future hydrogen delivery and dispensing technologies (see Table 1). The study assessed the impact technology developments and improvements will have on hydrogen cost, energy requirements, and GHG emissions. Considering plausible hydrogen production and delivery scenarios for mature hydrogen transportation fuel markets combined with market penetration of hydrogen fuel cell vehicles, the study uses a common set of assumptions to provide a consistent assessment of all pathways. Major assumptions include:

- A 2025 start-up year for hydrogen fuel infrastructure
- Future (2020-2030) hydrogen technologies, projected to a commercial scale
- Costs reported in 2007$ (to be consistent with FCTO's cost target of $4/kg in 2007$)
- A 40-year analysis period for central production facilities
- Feedstock and utility costs from the DOE Energy Information Administration's Annual Energy Outlook (AEO) 2009, based on national averages

- On-road FCEV fuel economy of 58 mpgge (with sensitivity analyses at 68 mpgge)
- Urban demand area with a population of 1.25 million (nominally Indianapolis)
- A 15% FCEV penetration
- Mid-sized FCEV, chassis comparable to conventional vehicle
- 15,000 miles/year vehicle miles traveled per FCEV
- Hydrogen dispensed for 700 bar, high-pressure storage

TABLE 1. Emerging-Technology Hydrogen Pathways Evaluated

Path	Production Feedstock / Technology	Delivery Mode	Dispensing Mode
1	Natural Gas Reforming with CCS	Gaseous H_2 in Pipelines	700 bar, gaseous
2	Photo-biological	Gaseous H_2 in Pipelines	700 bar, gaseous
3	Photo-Electrochemical	Gaseous H_2 in Pipelines	700 bar, gaseous
4	Solar Thermo-Chemical	Gaseous H_2 in Pipelines	700 bar, gaseous

The analysis was conducted using the MSM, which acts as a central transfer station, linking together the H2A Production model, HDSAM, GREET, and the Cost-Per-Mile (CPM) tool. Making use of the discounted cash flow, rate of return features of H2A Production and HDSAM, the MSM provides cost results in terms of a levelized cost of hydrogen (incorporating a 10% real rate of return on investments) in a $/kg basis. The MSM also outputs well-to-pump, pump-to-wheels, and well-to-wheels efficiencies, GHG emissions, and energy use for each pathway. Emissions and energy use results include upstream energy use required for feedstock production, processing, and delivery.

RESULTS

The MSM evaluation of the four emerging technology hydrogen pathways presents the cost of hydrogen and the performance of the pathways in terms of total energy use, fossil energy use, and GHG emissions. For all pathways evaluated, the key assumptions, modeling parameters, analysis inputs, and results were reviewed by industry partners through the U.S. DRIVE Fuel Pathway Integration Technical Team (FPITT). Figure 1 shows the levelized cost of hydrogen from the emerging-technology pathways. DOE's Fuel Cell Technologies Office has set a hydrogen cost target of $4.00 per GGE (approximately equivalent to 1 kg of hydrogen), dispensed at the pump. Of the low-carbon production pathways evaluated, the natural gas reformation with CCS pathway offers the lowest cost, with a dispensed hydrogen cost of $5.60/kg. (Previous pathway analysis studies found that only the distributed natural gas reformation pathway is expected to meet the $4/kg target,

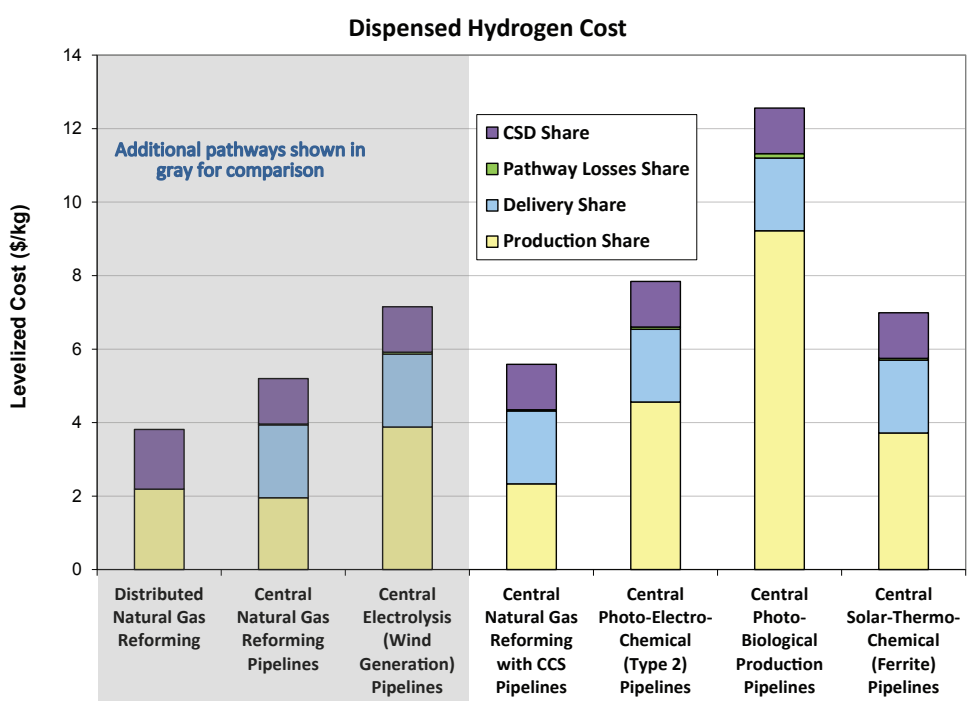

CSD – compression, storage, and dispensing

FIGURE 1. Cost of dispensed hydrogen from all pathways

with a projected dispensed hydrogen cost of $3.80/kg.) The renewable solar production pathways (photo-biological, solar-thermochemical, and photo-electrochemical hydrogen production) have higher dispensed hydrogen costs, ranging from $7/kg to over $12/kg, indicating the need for further R&D into these emerging technologies.

The pathway assessment evaluated the hydrogen cost contribution of capital costs, operations and maintenance (O&M) costs, and feedstock costs of the various pathways. As shown in Figure 2, the renewable solar production pathways have significant capital contribution costs, with costs of $3–5/kg attributable to production capital costs alone. This again points to the need for additional R&D to reduce these capital and O&M costs. It should be noted, however, that as low-technology-readiness-level pathways, renewable solar technologies are evolving rapidly and the latest research into these pathways is not necessarily reflected in the published H2A Production case studies used in this analysis.

The study also evaluated the total cost of FCEV ownership, including the costs of the hydrogen fuel and the costs of vehicle purchase and operation. Of the emerging technology pathways evaluated, the lowest cost of FCEV ownership resulted from hydrogen fuel produced from natural gas reformation coupled with carbon capture and sequestration. Assuming a 5-year ownership period and fuel economy of 58 mpgge, the natural gas reformation with CCS pathway resulted in total ownership costs of $0.72 per mile. With fuel costs of $0.10/mi, the cost of hydrogen fuel represents almost 15% of ownership costs. The purchase of the FCEV (represented as finance and depreciation costs) accounts for about 50% of ownership costs.

All of the emerging technology pathways were evaluated for lifecycle GHG emissions and energy use. Results of these investigations were discussed in depth with DOE and industry partners through the FPITT. The analysis shows that the addition of CCS to the central natural gas reformation pathway reduces fuel-cycle GHG emissions from about 210 g CO_2-equivalent/mi to 90 g CO_2-equivalent/mi at 68 mpgge fuel economy (110 g CO_2-equivalent/mi at 58 mpgge). This represents a significant improvement over the greater than 450 g CO_2-equivalent/mi emissions of a comparable conventional gasoline vehicle. The lifecycle emission results of the renewable solar hydrogen production pathways are expected to be lower than the natural gas with CCS pathway. (Preliminary results of these pathways have been developed and reviewed with DOE and industry, but are not being reported publicly as they are considered preliminary awaiting official published GREET cases for these pathways.)

CONCLUSIONS AND FUTURE DIRECTIONS

The lifecycle analysis shows that the emerging-technology hydrogen production, delivery, and dispensing

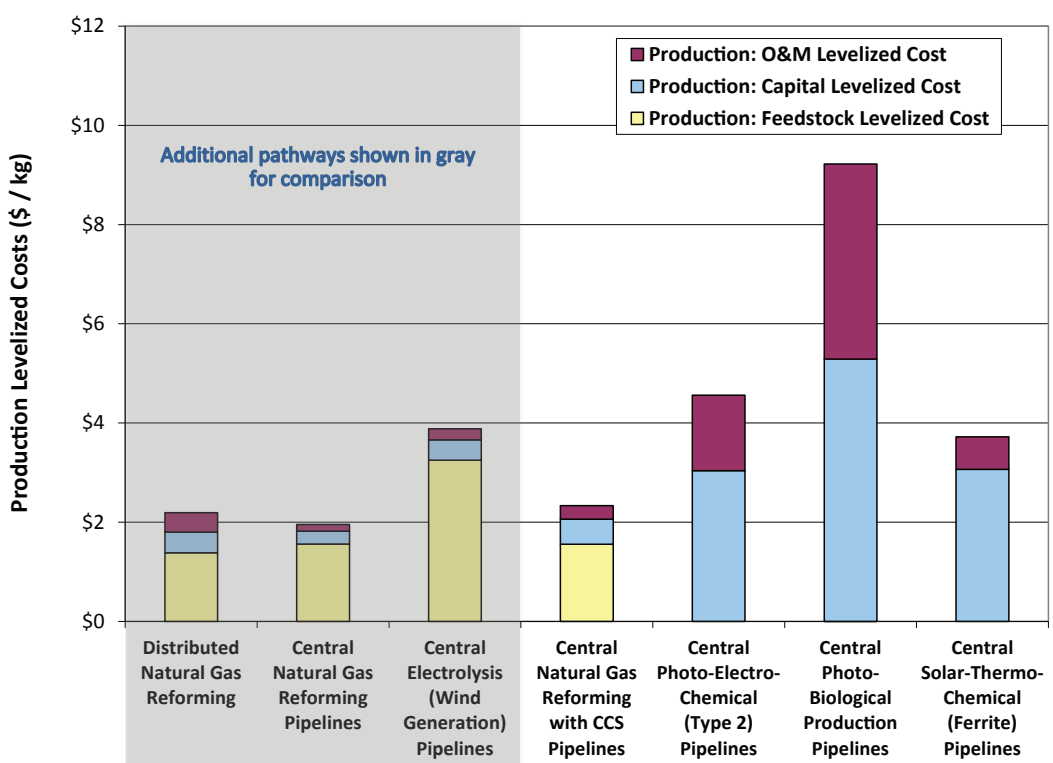

FIGURE 2. Hydrogen production cost contributions of capital, O&M, and feedstock for all pathways

pathways are expected to significantly reduce lifecycle GHG emissions, but all pathways are expected to result in costs above DOE's $4/kg target, indicating that further R&D into these emerging technologies is needed.

In the latter part of FY 2015 and in FY 2016, the hydrogen pathways analysis will be extended to consider emerging hydrogen delivery and onboard vehicle storage technologies. This will include an assessment of high-pressure gaseous truck delivery and emerging onboard hydrogen storage technologies such as cold hydrogen gas storage and sorbent storage.

FY 2015 PUBLICATIONS/PRESENTATIONS

1. Ramsden, T., Diakov, V., and Popovich, N., 2015 [expected]. *Hydrogen Pathways: Updated Cost, Well-to-Wheels Energy Use, and Emissions for the Future Technology Status of Nine Hydrogen Production, Delivery, and Distribution Scenarios*, National Renewable Energy Laboratory, Technical Report, Golden, CO (Draft report under DOE review).

2. Todd Ramsden, 2014. "Pathway Analysis: Emerging Hydrogen Production Pathways." U.S. DRIVE Fuel Pathway Integration Technical Team Meeting, Shell, Houston, TX (December).

3. Todd Ramsden, 2015. "Pathway Analysis: Emerging Hydrogen Production Pathways [Update]." U.S. DRIVE Fuel Pathway Integration Technical Team Meeting, Air Products, Allentown, PA (March).

4. Todd Ramsden, 2015. "Pathway Analysis: Initial Storage and Emerging Hydrogen Production Pathways." U.S. DRIVE Fuel Pathway Integration Technical Team Meeting, National Renewable Energy Laboratory, Golden, CO (July).

IX.4 Performance and Cost Analysis for a 300 kW Tri-Generation Molten Carbonate Fuel Cell System

Shabbir Ahmed (Primary Contact),
Rajesh Ahluwalia, Dennis Papadias, Thanh Hua,
H-S Roh
Argonne National Laboratory
9700 South Cass Avenue
Argonne, IL 60439
Phone: (630) 252-4453
Email: ahmeds@anl.gov

DOE Manager
Fred Joseck
Phone: (202) 586-7932
Email: Fred.Joseck@ee.doe.gov

Project Start Date: October, 2015
Project End Date: October 2016

Overall Objectives

- Examine strategies for improving the performance and reducing the cost relative to the one-off Orange County Sanitation District (OCSD) tri-generation system
- Explore scenarios in which the molten carbonate fuel cell (MCFC) tri-generation system has particular cost benefits including the scenario for charging electric vehicles

Fiscal Year (FY) 2015 Objectives

- Develop meaningful definitions for cell, stack, electrical, hydrogen production efficiencies in tri-generation modes
- Formulate cost models for MCFC stack, mechanical and electrical balance of plant (BOP), pressure swing adsorption (PSA), compression, storage, dispensing (CSD), and vehicle charging system
- Determine the performance and cost benefits of a MCFC plant that can co-produce electric power, hydrogen, and heat
- Explore strategies to improve the performance of the system in combined heat and power (CHP) and combined heat, hydrogen, and power (CHHP) modes

Technical Barriers

This project addresses the following technical barriers from the Systems Analysis section of the Fuel Cell Technologies Office Multi-Year Research, Development, and Demonstration (MYRDD) Plan.

(A) Future Market Behavior

(C) Inconsistent Data, Assumptions and Guidelines

(E) Unplanned Studies and Analysis

Contribution to Achievement of DOE Systems Analysis Milestones

This project will contribute to achievement of the following DOE milestones from System Analysis section of the Fuel Cell Technologies Office MYRDD Plan.

- Milestone 1.17: Complete analysis of program technology performance and cost status, and potential to enable use of fuel cells for a portfolio of commercial applications (4Q, 2018)
- Complete analysis of the potential for hydrogen, stationary fuel cells, fuel cell vehicles, and other fuel cell applications such as material handling equipment including resources, infrastructure and system effects resulting from the growth in hydrogen market shares in various economic sectors. (4Q, 2020)

FY 2015 Accomplishments

- Formulated a consistent system performance model of thermally-integrated natural gas (NG) fuel processor and MCFC stack in the electricity and hydrogen generation mode (CHHP)
- Set up cost models and performed cost analysis of the MCFC tri-generation system, showing installed capital costs of $510,000 for the MCFC system, $615,000 for CSD and PSA, $55,000 for auxiliary heater and water distribution, and $37,000 for electric vehicle (EV) charging
- Conducted sensitivity analysis to determine the required price for H_2; for fixed electricity price of $0.103/kWh (U.S. average), hydrogen can be priced at $6.50/kg for 125 kg/day co-production
- Integrated EV charging in the revenue stream shows that the cost of hydrogen can be reduced by ~$0.80/kg for each $0.10/kWh premium applied to EV charging

✧ ✧ ✧ ✧ ✧

INTRODUCTION

The demand for lower-volume hydrogen production systems at dispersed locations is projected to increase to meet the needs of fuel cell cars and other applications. Tri-gen systems that can produce electricity, heat, and hydrogen, are being proposed and developed. One example of such a system is the molten carbonate fuel cell based tri-gen plant installed at the OCSD water treatment facility in Fountain Valley, California. This system operates on NG or digester gas to nominally produce up to 250 kW of electricity, 200 kW of useful heat (as low pressure steam), and 100 kg-H_2/d. This study sets up a generic model of a tri-gen plant that can sell hydrogen, sell the power to the grid or recharge EVs. The analysis calculates efficiencies that account for the values of the products (power, hydrogen, and heat), and estimates the earning potential of the plant and future cost reductions.

APPROACH

The analysis is conducted using systems modeling and cost estimation. The performance evaluation is based on metrics that include energy efficiencies and cost of the system over the lifecycle.

- Identifies the technology, component, or design criteria that limit the system performance (efficiency, emissions), in both the CHP and tri-gen modes of operation
- Identifies and quantifies the major cost contributors, potential cost reduction opportunities, and projects future costs based on advances in component technology, capacity scale-up, and volume production

RESULTS

A generic tri-gen system was analyzed for the performance and cost analysis, Figure 1. The case selected for the analyses is based on a 300 kW molten carbonate fuel cell to serve as a direct comparison with the one of a kind system at OCSD. In our case, the system is operating solely with NG as fuel. The natural gas passes through a high temperature polisher for sulfur removal and is pre-reformed before entering the anode side of the MCFC. The reformate leaving the stack passes through a low temperature shift and further compressed to 10 bar. A four-bed PSA unit separates and purifies the hydrogen before the hydrogen is further compressed and stored for delivery. Revenue sources include hydrogen for fuel cell electric vehicles, electricity to grid or directly to EV charging stations, and waste heat recovery.

Considering the stack and system performance, the model was tuned to match current performance metrics given the available open information in the literature on the existing plant. Table 1 summarizes the system performance for the tri-gen system modeled for (a) pure electric mode and (b) combined electric and H_2 mode for a maximum hydrogen

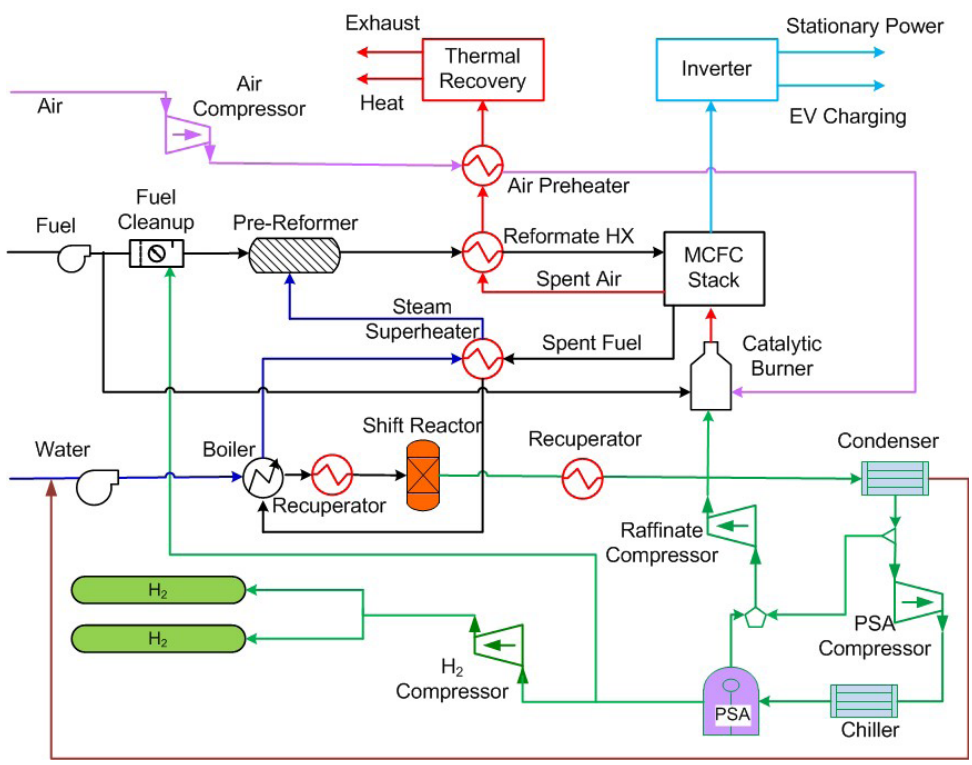

HX - heat exchanger

FIGURE 1. MCFC tri-gen system performance model

TABLE 1. Summary of system performance for CHP and CHHP modes

	Pure Electric	Combined Electric and H_2 Mode	Comments for Performance in Combined Electric and H_2 Mode
Net H_2 Production (kg/d)	**0**	**125**	79 kW_t supplemental fuel to burner
Net Electrical Power (kW_e)	258.1	183.1	5% increase in fuel input to stack
Fuel Utilization (%)	73.0	60.0	Terminal limits of fuel utilization (U_F)
Oxygen Utilization (%)	60	60	Fixed O_2 utilization, variable U_F
Cell Voltage (mV)	768.9	816.4	Higher Nernst potential at lower U_F
Stack DC Gross (kW_e)	300.0	274.9	
Stack Actual Efficiency (%)	51.1	51.1	Stack efficiency does not increase because of higher burner load
Gross Electrical Efficiency (%)	46.4	42.6	Lower gross electrical efficiency in spite of higher cell voltage
H_2 Production Efficiency (%)	87.3	89.4	
PSA Efficiency (%)		43.0	Efficiencies inclusive of electric power consumed in PSA and H_2 compressors
H_2 Storage Efficiency (%)		83.9	
Net Electrical Efficiency (%)	46.4	27.6	
Fuel Processor Efficiency (%)	0.0	26.2	
Thermal Efficiency (%)	32.7	23.2	Waste heat used to raise hot water. Lower if steam is raised.

production rate of 125 kg/d. Through several iterations as well as input from industry, we calibrated the model such as the fuel input to the stack and burner as more hydrogen is co-produced. As the hydrogen production level increases beyond 50 kg/d, the fuel utilization is kept constant at 60%. More fuel is introduced to the stack and burner with the constraint of maintaining the stack temperature at 650°C. At 125 kg/d, a net electrical power of 183 kW can be produced which is 40% more for the case of constant fuel input. Electrical efficiencies decrease as more hydrogen is co-produced. The net efficiency is the power supplied to the grid relative to all fuel input to the station and all parasitic power including reformate compressor to the PSA and hydrogen compression to storage.

The net electrical efficiency decreases from ~47% when no hydrogen is produced to ~28% at rated hydrogen production. The net hydrogen efficiency is the ratio of the hydrogen produced to the total fuel energy content. At rated hydrogen generation of 125 kg/d and available at the refueling pressure, the net hydrogen efficiency increases to 26%. Not accounting for the waste heat, at rated hydrogen production the hydrogen and electrical efficiencies sum up to 54%.

Figure 2 shows the estimated capital costs for the 300 kW tri-gen system analyzed. A process flow based approach to estimate the MCFC stack cost was employed in the present study. First, all major process steps required in the manufacture of all components of the stack are identified.

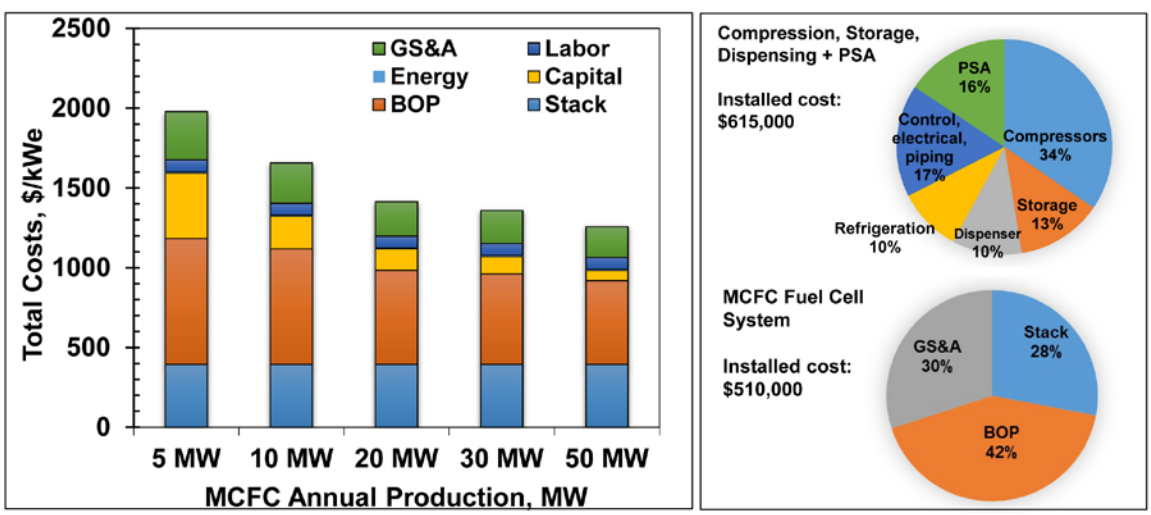

FIGURE 2. Estimated capital costs for MCFC stack and BOP

The key technical details of each manufacturing step (material mass, process temperature, machine cycle time, labor requirement) are used to develop a cost estimate for that step. Process flows, materials and equipment requirements have been identified in the literature, especially patents. Cost of materials and equipment has been found in literature and from direct inquiries with vendors. BOP estimates were determined through a combination of direct manufacturing analysis, component specification calculations, supplier quotations, literature searches, and scaling factors. Hydrogen supply and dispensing is designed for 125 kg/d cascade dispensing and cooling for on-board storage at 700 bar. For compression and storage of hydrogen, we consider a minimal station design without back-up compressors. The model assumes two compressors; each compressor operates at 50% of the designed flow. For lower volume and cost reduction, the pressure of the low pressure storage tank is increased to 482 bar. Low and high pressure cascade tanks are used with pressures of 482 bar and 875 bar, respectively. All storage is designed based on Type IV composite tanks and refrigeration unit is used to allow fast filling rates. Considering the materials and designated flow rates, the cost for a similar system for compression storage and dispensing of hydrogen as the OCSD can be reduced to $500,000. Since the OCSD compressors were oversized, we used the H2A model to calculate the cost of two 31 kW units. The cost of compressors were reduced to approximately $200,000. Considering a one of a kind demonstration unit, costs are bound to be high, partly because of learning experience and components that are only available for specific flows. In our present base case analysis, components are assumed to exist at reasonable high production volume at rated capacities. The installed costs between stack and hydrogen purification and storage are similar, costing $510,000 for the stack (annual production rate of 20 MW) and $615,000 for purification and storage. Compressors account for the main capital cost contribution.

The cost of hydrogen has been evaluated based on H2A FCPower tool. For a facility with hydrogen co-production and a fixed charge of electricity at 10.3 ¢/kWh, hydrogen needs to be priced at $6.50/kg, as shown in Figure 3, for maximum production capacity of 125 kg/d. For 75 kg/d, the cost increases to over $9/kg. The minimum price of hydrogen depends, however, strongly on the price of electricity and feedstock costs. Revenues from a higher electricity price can offset the price of co-produced hydrogen; for instance, at electricity prices of 18 ¢/kWh the hydrogen cost is reduced to $4/kg. The higher revenue from electricity alone will also make the price of hydrogen less sensitive to capacity changes. For the base case, a hydrogen price of $6.50/kg, the tornado chart in Figure 3 shows the sensitivity for the hydrogen price, with $1 cost reduction possible with capital expenditure reduction, stack replacement frequency to 10 years or feedstock price reduction. Further capital cost reductions of stack compression and storage may reduce the price by the same amount.

We are considering that the facility or business owner will provide electric vehicle charging for employees of customers. In addition to electric power being delivered to the grid or to a facility, some of the power can be used for electric vehicle charging. For EV charging, the assumptions for our base case and cost estimates consider four 6-kW units costing $3,000 each and two 50-kW fast charging stations at $10,000 each. Assuming 10 hours of operation per day, charging capacity of 12 kWh/vehicle and for 125 kg-H_2/d co-production, the facility can charge up to 150 vehicles/day. At full charging capacity utilization, the price of hydrogen is reduced by ~$0.80/kg for each $0.10/kWh premium[11] for EV charging.

[1] A 10 ¢/kWh premium means the station charges 10 cents more per kilowatthour than the residential rate available at that location.

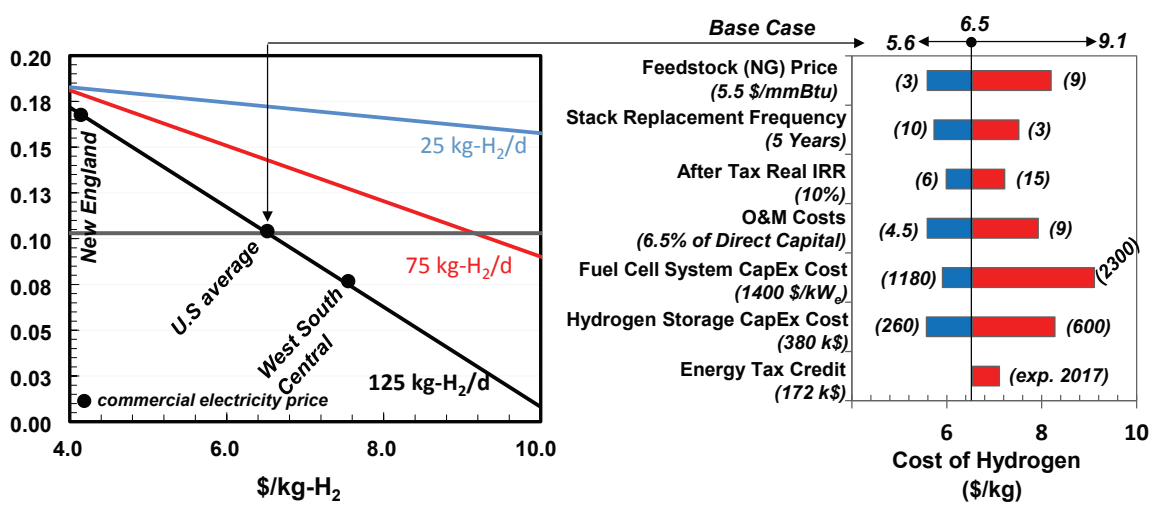

FIGURE 3. Sensitivity of hydrogen price versus the price of electricity, the amount of hydrogen co-produced, and capital costs

CONCLUSIONS AND FUTURE DIRECTIONS

This study analyzed a 300 kW tri-gen plant that can sell hydrogen, sell the power to the grid or recharge electric vehicles. The analysis conducted has defined efficiencies that account for the values of the products (power, hydrogen, and heat), capital cost and the earning potential of the plant.

- The high temperature fuel cell subsystem generates hydrogen by reforming the supplied fuel within the stack. The combined efficiency for the production of electric power and hydrogen can exceed 54%.
- For a facility with hydrogen co-production and a fixed charge of electricity at 10.3 ¢/kWh, hydrogen needs to be priced at $6.50/kg. Revenues from a higher electricity price can offset the price of co-produced hydrogen.
- The cost of hydrogen can be reduced by selling the EV charging power at a rate higher than the prevalent commercial rate.

In the remaining part of FY 2015, the analysis will explore strategies to improve the performance and economics of the tri-gen system considering the following.

- Electrochemical separation and compression and trade-off between PSA compressor, H_2 recovery and compression
- Analyze larger, 1,000 kW and 1,500 kW MCFC systems to improve the economics and increase revenues by adapting the production of power and hydrogen relative to peak hour demand

FY 2015 PUBLICATIONS/PRESENTATIONS

1. Ahmed, S., Papadias, D., Ahluwalia, R., Hua, T., Roh, H-S., "Performance and Cost Analysis for a 300 kW Tri-generation Molten Carbonate Fuel Cell System," 2015 U.S. DOE Hydrogen and Fuel Cells Program and Vehicle Technologies Office Annual Merit Review and Peer Evaluation Meeting, June 9, 2015.

IX.5 Employment Impacts of Infrastructure Development for Hydrogen and Fuel Cell Technologies

Marianne Mintz
Argonne National Laboratory (ANL)
9700 S. Cass Ave.
Argonne, IL 60439
Phone: (630) 252-5627
Email: mmintz@anl.gov

DOE Manager
Fred Joseck
Phone: (202) 586-7932
Email: Fred.Joseck@ee.doe.gov

Subcontractors
- RCF Economic & Financial Consulting, Inc., Chicago, IL
- Northwestern University, Evanston, IL

Project Start Date: October 2012
Project End Date: Project continuation and direction determined annually by DOE

Overall Objectives

- Facilitate early market deployment of fuel cells (FCs) by developing a downloadable, user-friendly tool to estimate economic impacts associated with the deployment of FCs and related infrastructure
- Develop a consistent framework to identify opportunities to enhance the economic impact of FC production and deployment by better understanding where and how impacts occur and how infrastructure deployment produces economic benefits
- Meet stakeholder needs for estimating impacts of FC and infrastructure deployment on state, regional, and national employment, earnings, and economic output

Fiscal Year (FY) 2015 Objectives

- Launch JOBS H2
- Analyze economic impacts associated with the hydrogen station deployment roadmap [1] developed by the California Fuel Cell Partnership (CaFCP)
- Add a stochastic simulation capability to JOBS H2 to enable it to explicitly account for uncertainty in key input variables

Challenges/Technical Barriers

This project addresses the following technical barriers from the Systems Analysis section of the Fuel Cell Technologies Office (FCTO) Multi-Year Research, Development and Demonstration (MYRDD) Plan.

(A) Future Market Behavior

(B) Stove-piped/Siloed Analytical Capability

(C) Inconsistent Data, Assumptions, and Guidelines

(D) Insufficient Suite of Models and Tools

Contribution to Achievement of DOE Systems Analysis Milestones

This project contributes to achieving the following milestones from the Systems Analysis section of the FCTO MYRDD Plan:

- Milestones 2.3–2.6: Develop and maintain models and tools
- Milestones 1.7, 1.10, and 1.14: Perform studies and analyses of job impacts

FY 2015 Accomplishments

- Launched JOBS H2 1.0 in an Office of Energy Efficiency & Renewable Energy (EERE)-sponsored webinar on June 24, 2014
- Continued a program of close collaboration with stakeholders, hydrogen and fuel cell producers, and other researchers via a series of teleconferences and review of interim results
- Analyzed economic impacts associated with the CaFCP's hydrogen station deployment roadmap and published a report documenting the methodology and results of that analysis
- Developed a stochastic procedure for estimating the effect of uncertainty in key parameters of JOBS H2
- Expanded access to JOBS H2 (as well as JOBS FC) by providing links from the Alternative Fuels Data Center (AFDC) website and via smartphone readable Quick Response (QR) cards distributed by the Clean Cities Program

✧ ✧ ✧ ✧ ✧

INTRODUCTION

The project is developing and applying a computer model to estimate economic impacts of deploying FCs and associated infrastructure in early markets. Insights from this work will assist FCTO and its stakeholders in estimating employment and other economic impacts from DOE technology development and in identifying FC markets and regions that are most likely to generate jobs and economic activity.

In earlier work, ANL and RCF Economic & Financial Consulting designed and implemented a tool to calculate state, regional and national economic impacts of FC production, installation, and utilization in early markets. Known as JOBS FC (JOBS and economic impacts of fuel cells) that tool is a user friendly, spreadsheet based model. In FY 2013, work began on a companion tool, JOBS H2, using the same methodology. FY 2015 activities focused on enhancing JOBS H2.

APPROACH

JOBS H2 is an Excel-based model that estimates economic impacts of activities associated with hydrogen station deployment based on user specified scenarios. Activities include station design, engineering, and permitting; site preparation; equipment production, shipping and installation; station operation and maintenance (O&M); and hydrogen production and delivery. The model calculates economic impacts along supply chains and from induced or ripple effects using input-output relationships from the U.S. Department of Commerce Bureau of Economic Analysis' Regional Input-output Modeling System. JOBS H2 can be run with default values (based on stakeholder input and engineering estimates from the published literature) or user inputs.

RESULTS

JOBS H2 calculates the effect of hydrogen infrastructure deployment on any of 60 geographies—50 states, nine census regions, or the nation as a whole—by adjusting dollar flows among economic sectors within the relevant geography. As hydrogen infrastructure is deployed, those expenditures send dollars up the supply chain for station equipment (e.g., compressor packages, dispensers) and H_2 fuel, as well as to the relevant supply chains for system integrators, installers, fuel suppliers and businesses providing O&M services. In the aggregate, the resulting web of transactions represents a nascent H_2 retailing sector. Purchases include not only the H_2 itself, but all transactions required to install, fuel and operate the station.

Analysis

In FY 2015 JOBS H2 was employed to estimate economic impacts associated with the CaFCP's hydrogen station roadmap within the state of California. As shown in Figure 1, stations grow from 23 in 2015 to 123 in 2023 under the roadmap. Thus, the JOBS H2 analysis included the development of 100 new hydrogen stations of different sizes over the next eight years, the operation of those new stations as they came on line and their utilization evolved, and the operation of 23 existing hydrogen stations over the next eight years. As shown in Figure 2, employment rises in response to the rate of station deployment, increasing as more stations come online, and eventually leveling off when all stations are online. Induced jobs account for 30–40% of the total. Once all 123 stations in the roadmap are online, station operation jobs level off at ~1,000/year.

Model Development

In FY 2015 JOBS H2 also was enhanced with a stochastic simulation capability to permit it to explicitly

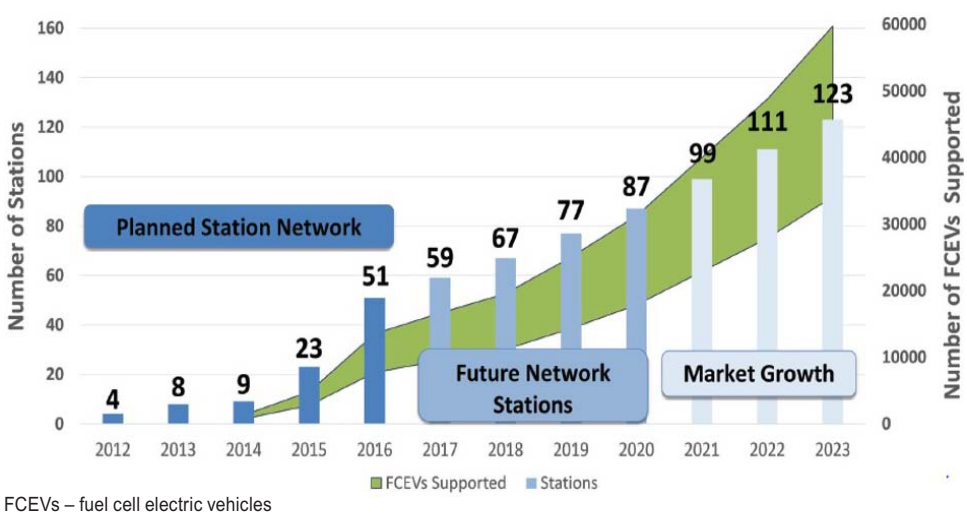

FCEVs – fuel cell electric vehicles

FIGURE 1. California Fuel Cell Partnership station roadmap (CaFCP 2014)

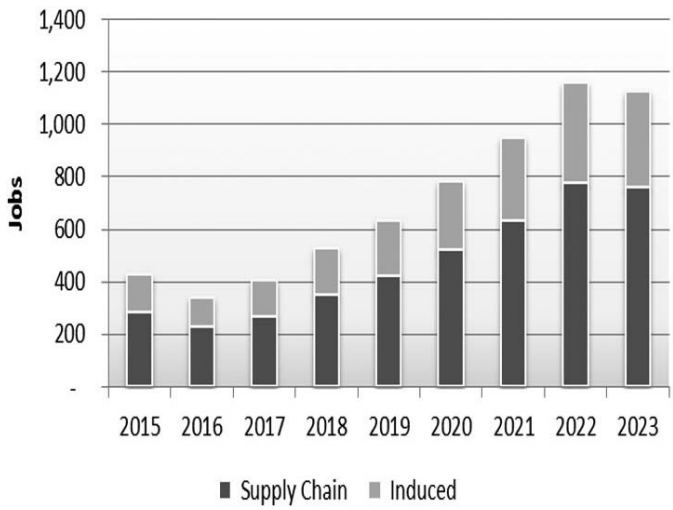

FIGURE 2. JOBS H2 estimate of California employment associated with the CaFCP H_2 station roadmap

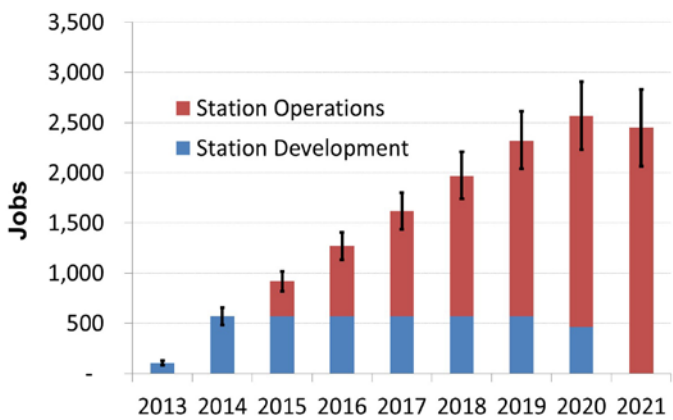

FIGURE 3. JOBS H2 estimate of United States employment associated with a station rollout similar to the CaFCP roadmap

account for uncertainty in key input parameters. Probability density functions were specified for a number of development, equipment, and operational expense categories and the model was configured to sample inputs from those distributions for thousands of simulations. The resulting outputs can be displayed as a range of results bounded by 10% and 90% probabilities. In Figure 3 those ranges are shown as bars surrounding most probable (or mean) estimates of United States employment for a scenario similar to the CaFCP roadmap.

User Resources

Stakeholders have been heavily involved in the development of JOBS H2. An advisory group consisting of representatives from the hydrogen and FC industry, station developers and state/local agencies assisted in data validation, requirements specification/review of the user interface, and beta testing of JOBS H2. Outreach included one-on-one conversations, webinars, links from EERE's AFDC and QR cards, and a website (http://jobsmodels.es.anl.gov). The latter features user access to the model itself along with video user guides, links to EERE-sponsored webinars, and copies of publications and presentations.

CONCLUSIONS AND FUTURE DIRECTIONS

FY 2015 work focused on enhancement of the JOBS H2 model. Work included the initial model launch, development of a stochastic capability to estimate uncertainty, and analysis of the CaFCP hydrogen station roadmap. FY 2016 work will build on these efforts, including expanding the model to include liquid hydrogen delivery and larger capacity stations, examining station rollout plans in the northeast, and validating California results with a more detailed analysis of the CaFCP program.

Potential future model enhancements include expanding hydrogen delivery and dispensing options to include distributed production and mobile fuelers, and analyzing the impacts of alternative hydrogen station rollout scenarios.

SPECIAL RECOGNITIONS & AWARDS

1. 2015 DOE Hydrogen and Fuel Cells Program Team R&D Award, June 2015.

FY 2015 PUBLICATIONS/PRESENTATIONS

1. Mintz, M., J. Gillette, C. Mertes, and E. Stewart, "Economic Impacts Associated with Commercializing Fuel Cell Electric Vehicles in California: An Analysis of the California Roadmap Using the JOBS H2 Model," Argonne National Laboratory Report, ANL/ESD-15/1, Dec. 31, 2014.

2. Mintz, M., C. Mertes, and E. Stewart, "Employment and Economic Impacts of Hydrogen Station Deployment," EERE webinar, June 24, 2014 (http://energy.gov/eere/fuelcells/2014-webinar-archives#date062414).

REFERENCES

1. CaFCP, 2014. *A California Roadmap, 2014 Update*, "Hydrogen Progress, Priorities and Opportunities," July.

IX.6 Life Cycle Analysis of Water Use for Hydrogen Production Pathways

Amgad Elgowainy (Primary Contact),
David Lampert, Hao Cai, Jeongwoo Han,
Jennifer Dunn, and Michael Wang
Argonne National Laboratory
9700 South Cass Avenue
Argonne, IL 60439
Phone: (630) 252-3074
Email: aelgowainy@anl.gov

DOE Manager
Fred Joseck
Phone: (202) 586-7932
Email: Fred.Joseck@ee.doe.gov

Project Start Date: April 2013
Project End Date: Project continuation and direction determined annually by DOE

Overall Objectives

- Incorporate water consumption as a new sustainability metric for evaluating hydrogen as a transportation fuel for use in fuel cell electric vehicles (FCEVs) and other fuel/vehicle systems on a life cycle basis

Fiscal Year (FY) 2015 Objectives

- Review and update water consumption for baseline petroleum fuels and current hydrogen production technologies, including natural gas steam methane reforming (SMR) and electrolysis
- Incorporate water consumption for low-carbon hydrogen production pathways of biomass gasification and biogas purification and reforming
- Address outstanding water consumption issues for hydrogen production such as impact of water treatment for SMR and electrolysis, and indirect water consumption associated with hydropower electricity generation (for electrolysis pathway)
- Examine impact of various cooling technologies (wet cooling vs. dry cooling)

Technical Barriers

This project directly addresses Technical Barriers C, D, and E in the Systems Analysis section of the Fuel Cell Technologies Office Multi-Year Research, Development, and Demonstration (MYRDD) Plan.

(C) Inconsistent Data, Assumptions, and Guidelines

(D) Insufficient Suite of Models and Tools

(E) Unplanned Studies and Analysis

Technical Targets

This project expands the Greenhouse Gases, Regulated Emissions, and Energy Use in Transportation (GREET) Model to include water consumption factors for the various life cycle stages of hydrogen and other fuels, and to compare the life cycle water consumption of the various fuel/vehicle systems on a consistent basis.

Contribution to Achievement of DOE System Analysis Milestones

This project contributes to achievement of the following DOE milestone from the Systems Analysis section of the Fuel Cell Technologies Office MYRDD Plan:

- Task 1.13: Complete environmental analysis of the technology, environmental impacts for hydrogen and fuel cell scenarios and technology readiness. (4Q, 2015)
- Task 2.2: Annual model update and validation. (4Q, 2011 through 4Q, 2020)

FY 2015 Accomplishments

- Developed water consumption factors for hydrogen production from biogas reforming, and from coal and biomass gasification
- Updated water consumption factors for hydrogen production via SMR and electrolysis
- Updated water consumption for petroleum pathways
- Developed methodology for allocating water consumption to hydropower generation
- Examined tradeoff between water saving and energy use of dry cooling vs. wet cooling
- Expanded the GREET model to include updated and new water consumption factors
- Compared water consumption per mile for various fuel/vehicle combinations
- Documented approach, data, methodology, and analysis in a report

✧ ✧ ✧ ✧ ✧

INTRODUCTION

One emerging sustainability metric of interest to the lifecycle analysis of alternative fuel/vehicle systems is water consumption. The production of most energy feedstocks and

fuels require significant water use. Fossil feedstock sources such as natural gas, crude oil, and oil sands require the use of water and steam for extraction, processing, refining, and upgrading. Similarly, biofeedstocks such as corn need water for growth. Converting these feedstocks to fuels consumes additional water. Producing electricity at thermal power plants requires a substantial amount of water to cool the equipment and complete the power cycle. Large amounts of water evaporation are reported from water reservoirs used for hydropower generation.

Water withdrawal is the water uptake from a source by any given process, while water consumption is the withdrawal amount minus the amount returned to the same withdrawal source. Argonne developed water consumption factors for petroleum fuels (e.g., gasoline and diesel), conventional natural gas and shale gas, corn ethanol, various electric power generation technologies, and hydrogen production via SMR, water electrolysis, biogas reforming, and biomass gasification. Water consumption factors for hydrogen production were developed from open literature data as well as data provided by industrial sources. Water consumption factors for hydrogen production included water rejection during the preproduction treatment processes, steam use in the SMR process, water use as a feedstock for the electrolysis process, and water consumption with the various cooling technologies.

RESULTS

Table 1 shows the updated water consumption factors for hydrogen production via SMR and electrolysis in central production and distributed locations based on information acquired from industry. The stoichiometric steam-to-carbon ratio (S/C) on a molar basis is 2, which translates to 1.2 gallon of water per kilogram of hydrogen. However, an S/C ratio of 2.5–3 is used in large industrial production to maximize methane conversion. For small scale distributed SMR production, the S/C is higher to increase the hydrogen yield at the expense of small efficiency reduction. Cooling can be performed with either wet cooling or dry cooling.

TABLE 1. Water Consumption Factors for Central and Distributed SMR Hydrogen Production [gal/kg $_{H2}$]

Production technology	SMR	
Production scale	Central	Distributed
S/C ratio	2.5–3	4–5
Production process	1.6 (1.5–1.8)	2.5 (2.4–3.0)

Argonne also investigated the water consumption associated with biogas upgrading since the CH_4 content in raw biogas is typically 60–70% while the rest of the raw biogas is largely CO_2 along with other impurities, such as H_2S and NH_3. For biogas upgrading, six processes are used: chemical scrubber, water scrubber, organic physical scrubber, pressure swing adsorption, membrane separation, and cryogenic separation. Among them, chemical scrubber, water scrubber and organic physical scrubber use an absorption technique with a different absorbent. Water scrubbers utilize the higher water solubility of CO_2 relative to CH_4 for separation and thus consume more water than the other upgrading technologies. Water scrubbers are the most commonly used technology in the world but are less common in the United States, thus most information collected on water scrubbers is based on European plants. Depending on the water recovery employed by different plants, the range of make-up water consumption for scrubbers covers a wide range (4 to 192 gal/mmBtu), with a production weighted average of 59 gal/mmBtu. We assume that the water consumption of water scrubbers in the United States is consistent with that in Europe. Water consumption by the other biogas upgrading technologies is assumed to be small since no water-intensive process is used. Thus, their water consumption is assumed to be similar to that of fossil natural gas processing at 1.7 gal/mmBtu. Taking account for the biogas upgrading capacity by each technology in the United States, a production weighted average water consumption for total biogas upgrading in the U.S. is estimated at 9.3 gal/mmBtu, with a range from 2 to 27 gal/mmBtu.

Argonne investigated the water consumption associated with gasification of biomass to hydrogen. Gasification processes require water both to drive the process and for cooling. The cooling required in a gasification facility can be wet, dry, or some combination of the two. Additionally, the process efficiency can be improved using heat recovery that impacts the overall process water consumption rate. A water consumption rate of 38.1 gal/mmBtu was developed using the material balance from a detailed process of a woodchip gasification facility.

Argonne developed an allocation method to update the water consumption factor for hydropower generation. The approach included merging the eGRID and National Inventory of Dams databases. The gross reservoir evaporation was estimated based on pan evaporation data, while the background evapotranspiration was deducted from the gross evaporation. The reservoirs were divided into two categories: multipurpose and dedicated to hydropower generation. An allocation methodology was developed to allocate the water consumption burden in multipurpose reservoirs. Figure 1 shows a schematic of the allocation approach that resulted in a weighted average net water consumption factor for hydropower generation of 9.85 gal/kWh.

Figure 2 shows the life cycle water consumption for hydrogen production via natural gas and renewable natural gas (biogas) SMR, water electrolysis, and gasification of coal and woody biomass. The hydrogen production stage dominates the life cycle water consumption for all pathways

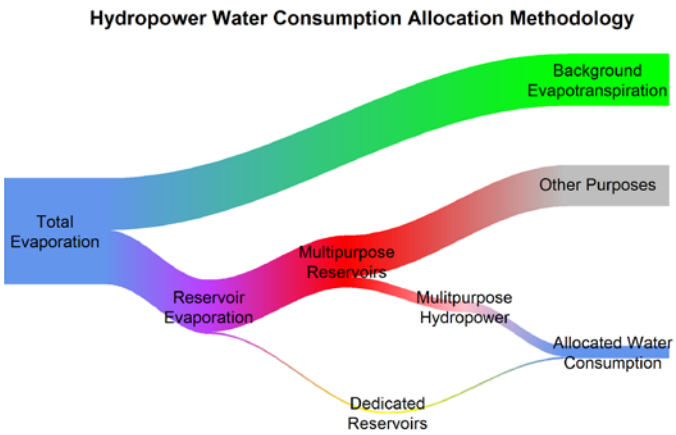

FIGURE 1. Hydropower water consumption allocation methodology

with the exception of electrolysis using United States electricity grid mix due to its high water consumption factor and the significant use of electricity. The water embedded in the electricity used for hydrogen compression at the station is also significant contributor to the life cycle water consumption for all pathways.

Figure 3 shows a chart of the life cycle water consumption per 100 mile for various fuel/vehicle systems of the midsize vehicle class with the fuel economy of various fuel/vehicle systems shown in the upper chart of the figure.

Figure 3 shows the significant impact of the large water consumption factors of corn ethanol on the E85. The figure also shows the significant impact of water embedded in the United States electricity grid mix on the electrolysis and battery electric vehicle (BEV) pathways, even after revising the hydropower water consumption factor from 18 to 9.85 gal/kWh based on the allocation methodology discussed above.

CONCLUSIONS AND FUTURE DIRECTIONS

Argonne developed water consumption factors for hydrogen production from biogas and from coal and biomass gasification and updated the water consumption factors for hydrogen production via SMR and electrolysis. A methodology for allocating water consumption to hydropower generation was developed. Argonne expanded the GREET model to include the water consumption factors for the new and updated hydrogen production pathways. The water consumption per 100 miles for various fuel/vehicle combinations was compared to identify the stages with major contribution to life cycle water consumption. The outstanding issues include the use of different water consumption evaluation methods with respect to system boundary and allocation. Also the variability of water consumption by region and the water consumption during purification need to be assessed.

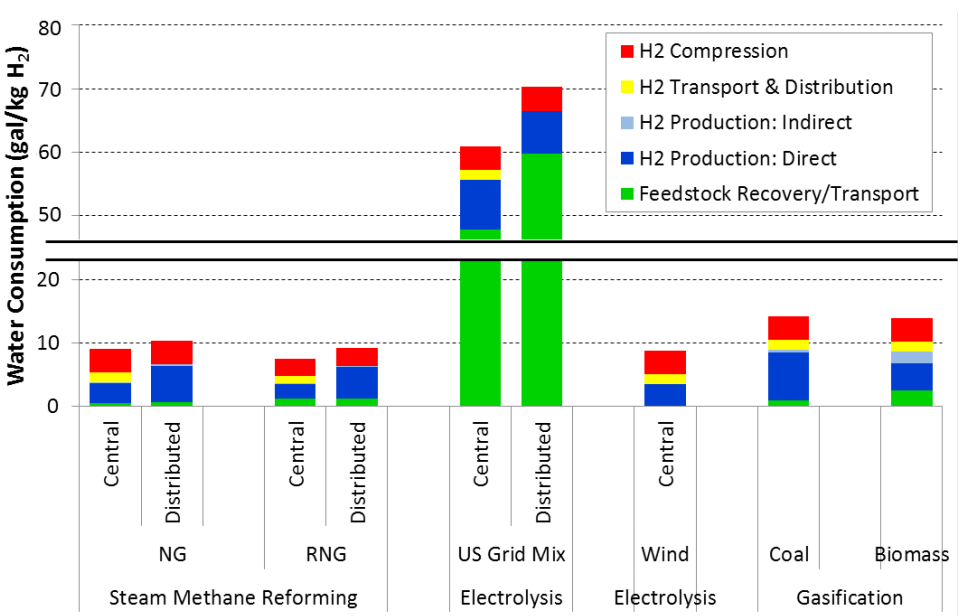

FIGURE 2. Life cycle water consumption for various hydrogen production pathways

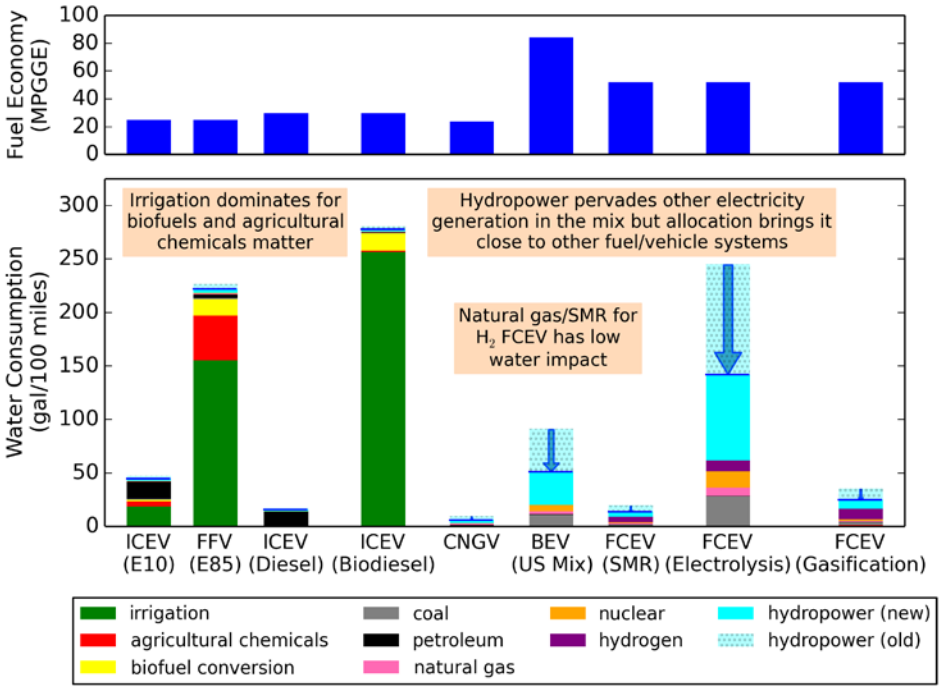

BEV – battery electric vehicle; CNGV – compressed natural gas vehicle; FFV – flexible fuel vehicle; ICEV – internal combustion engine vehicle; mpgge – miles per gallon of gasoline equivalent; NG – natural gas; RNG – renewable natural gas

FIGURE 3. Life cycle water consumption for alternative fuel/vehicle systems

IX.7 Hydrogen Analysis with the Sandia ParaChoice Model

Todd West (Primary Contact), Dawn Manley, Rebecca Levinson
Sandia National Laboratories
7011 East Avenue
Livermore, CA 94550
Phone: (925) 294-3145
Email: thwest@sandia.gov

DOE Manager
Fred Joseck
Phone: (202) 586-7932
Email: Fred.Joseck@ee.doe.gov

Project Start Date: October 1, 2014
Project End Date: Project continuation and direction determined annually by DOE

Overall Objectives

- ParaChoice captures changes to the light-duty vehicle (LDV) stock through 2050 and its dynamic, economic relationship to fuels and energy sources
- Model occupies a system-level analysis layer with input from other DOE models to explore the uncertainty and trade space (with 10,000s of model runs) that is not accessible in individual scenario-focused studies
- Model dynamics and competition among LDV powertrains and fuels using regional-level feedback loops from vehicle use to energy source
- Identify set of conditions that must be true to reach performance goals and sensitivities and tradeoffs between technology investments, market incentives, and modeling uncertainty

Fiscal Year 2015 Objectives

- Add hydrogen production and fuel cell electric vehicles (FCEVs) to existing Sandia ParaChoice model to further the Fuel Cell Technologies Office (FCTO) mission
- Determine how FCEVs compete in the fleet with conventional and other alternative energy vehicles
- Determine effects of FCEV and hydrogen adoption on petroleum usage and greenhouse gas (GHG) emissions
- Evaluate hydrogen production and consequences for hydrogen pricing, FCEV adoption, and GHG emissions

Technical Barriers

This project addresses the following technical barriers from the Systems Analysis section of the FCTO Multi-Year Research, Development, and Demonstration (MYRDD) Plan:

(A) Future Market Behavior

(B) Stove-piped/Siloed Analytical Capability

(C) Inconsistent Data, Assumptions and Guidelines

(D) Insufficient Suite of Models and Tools

Contribution to Achievement of DOE Systems Analysis Milestones

This project will contribute to achievement of the following DOE milestones from the Systems Analysis section of the FCTO MYRDD Plan:

- Milestone 1.15: Complete analysis of program milestones and technology readiness goals—including risk analysis, independent reviews, financial evaluations, and environmental analysis—to identify technology and risk mitigation strategies. (4Q, 2015)
- Milestone 1.16: Complete analysis of program performance, cost status, and potential use of fuel cells for a portfolio of commercial applications. (4Q, 2018)
- Milestone 1.18: Complete life cycle analysis of vehicle costs for fuel cell electric vehicles compared to other vehicle platforms. (4Q, 2019)

Specifically, this project models the life cycle costs of fuel cell electric vehicles compared to conventional and alternative LDVs. Sensitivity analyses were performed to identify where FCEVs can successfully compete with current and potential future LDV options.

FY 2015 Accomplishments

- Added FCEVs and a range of hydrogen production pathways to the existing Sandia ParaChoice model
- Updated ParaChoice model to use most recent Annual Energy Outlook and Autonomie projections as well as the most recent vehicle registration data and state incentives for FCEVs and hydrogen production
- Completed initial analysis of FCEV adoption, hydrogen production pathways, and sensitivity analysis
- Presented initial analyses at DOE Annual Merit Review

✧ ✧ ✧ ✧ ✧

INTRODUCTION

In the coming decades, light-duty vehicle options and their supporting infrastructure must undergo significant transformations to achieve aggressive national targets for reducing petroleum consumption and lowering greenhouse gas emissions. Hydrogen FCEVs, battery and hybrid electric vehicles, and biofuels are among the promising advanced technology options. In addition, natural gas vehicles, fueled with domestically produced natural gas, have significant potential to displace petroleum use in the light-duty vehicle mix.

The parametric analysis of factors that influence adoption of hydrogen vehicles and infrastructure for light duty transportation is assessing the evolving market penetration potential of FCEVs. Specifically, this analysis is examining options for the evolving light duty vehicle mix from the present to 2050 to include FCEVs, conventional internal combustion engines (ICEs), battery electric vehicles (BEVs) of various ranges, plug-in hybrid electric vehicles which have an electric range of either 10 or 40 miles (PHEV-10 or PHEV-40), natural gas vehicles (both dedicated and bi-fuel vehicles), as well as E85 flex fuel vehicles.

APPROACH

ParaChoice captures changes to the LDV stock through 2050 and its dynamic, economic relationship to fuels and energy sources. The model occupies a system-level analysis layer with input from other DOE models to explore the uncertainty and trade space (with 10,000s of model runs) that is not accessible in individual scenario-focused studies. By conducting parametric analyses, this sensitivity study identifies the set of conditions that must be true to reach performance goals and tradeoffs between technology investments, market incentives, and modeling uncertainty.

In particular, this project is examining the market penetration of FCEVs as a function of (1) various hydrogen production and distribution pathways, as well as public infrastructure availability; (2) fuel (gasoline, natural gas, hydrogen) and electricity cost; (3) vehicle cost; (4) home filling (natural gas) or charging (BEV, PHEV) cost; and (5) fuel economy.

RESULTS

The parametric approach taken in this analysis allows exploration of broad range of scenarios and tradeoffs. Analysis of which factors have the greatest impact on FCEV adoption and GHG emissions is ongoing, but preliminary results are highlighted below.

Using baseline input parameters, we find that FCEVs are a significant fraction of fleet sales by 2050 (Figure 1). These results however are sensitive to specific assumptions on future costs of FCEVs from the Argonne National Laboratory *Autonomie* model. Initial results using an updated version of *Autonomie* show much less adoption of FCEVs by 2050.

ParaChoice models vehicle adoption and use at the state and urban/suburban/rural level. For example, model outputs show the effects of different state incentives on 2050 FCEV sales (Figure 2). State incentives and fuel prices appear to drive regional variation in FCEV adoption.

Hydrogen pump fuel prices drop with increasing demand, ultimately becoming competitive with gasohol prices on a per mile basis (Figure 3).

For baseline inputs, hydrogen is provided by industrial sources until mid-2030s (Figure 4). Hydrogen production then transitions to distributed production via steam methane

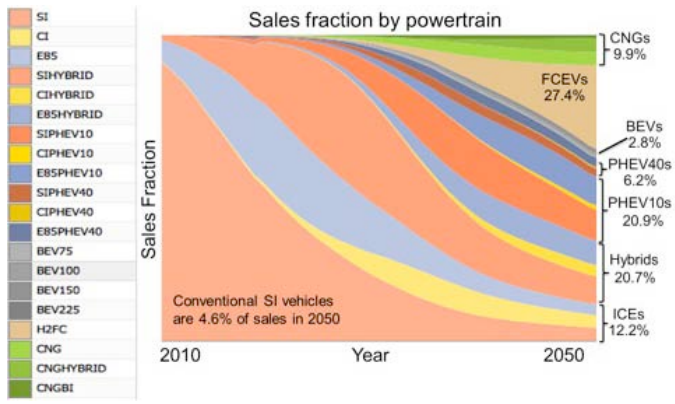

FIGURE 1. Sales fraction by powertrain for baseline scenario, using costs and efficiencies from Autonomie 2011

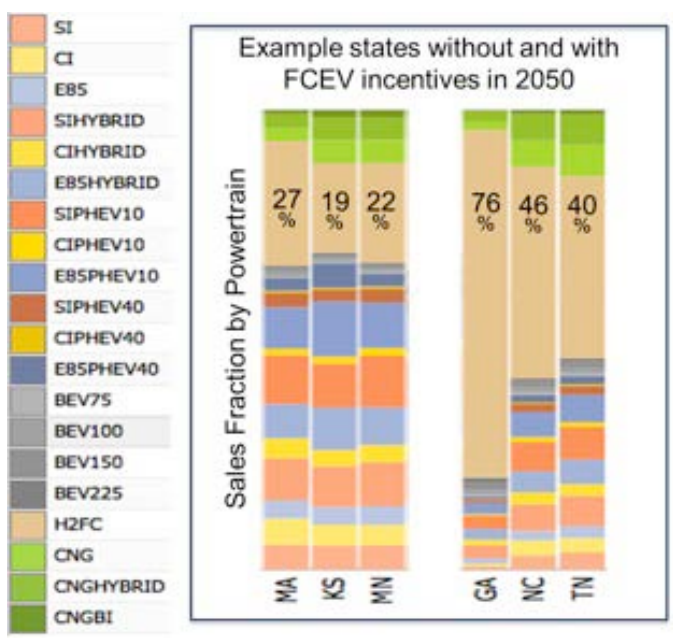

FIGURE 2. FCEV adoption differs between states with and without incentives

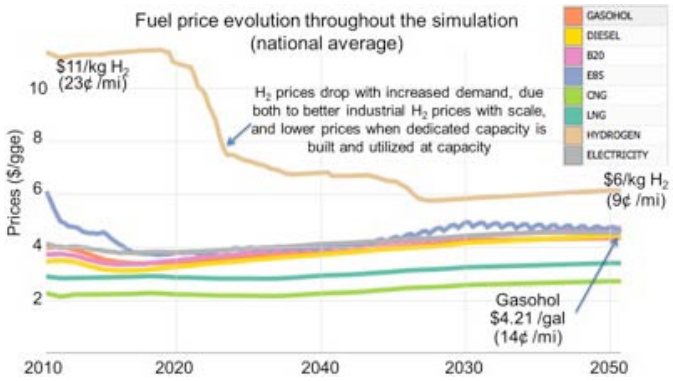

FIGURE 3. National average fuel prices through 2050 for baseline scenario

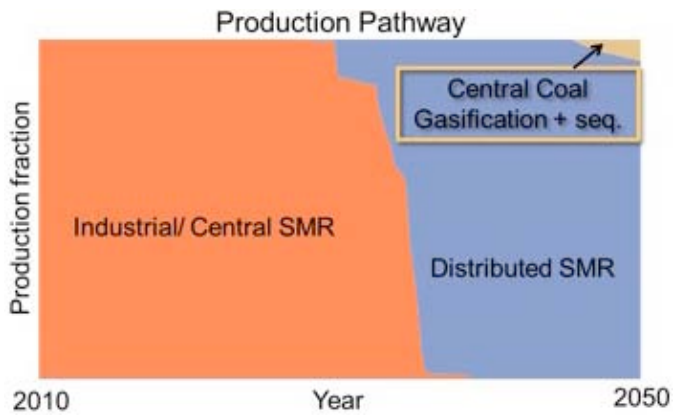

FIGURE 4. Hydrogen production pathways through 2050 in the baseline scenario

reforming (SMR). By 2045, centralized production using coal plus sequestration becomes the cheapest option for some states. Consequently, greenhouse gas emissions are not strongly affected by the substantial FCEV adoption in the absence of low carbon mandates or other incentives.

CONCLUSIONS AND FUTURE DIRECTIONS

FCEVs and hydrogen fuel production are now part of the Pathways ParaChoice model. This model's parametric approach allows exploration of a broad range of scenarios and tradeoffs. Initial findings include the following.

- Hydrogen can play a large role in the 2050 fleet.
- If market forces are the only drivers of hydrogen production pathways, FCEVs will have a carbon neutral effect on the fleet out through 2050.
- FCEVs have the potential to reduce GHG emissions if carbon taxes, technology improvements, or incentives steer hydrogen production towards low-carbon pathways.

Future work will expand on this analysis of FCEVs in the vehicle fleet and on the pathways used to produce hydrogen as a vehicle fuel. In particular, the analysis will examine the market penetration of FCEVs in a range of specific market segments to determine under what conditions FCEVs can best compete with other alternative fuel vehicles.

FY 2015 PUBLICATIONS/PRESENTATIONS

1. Levinson, Rebecca. "Hydrogen Analysis with the Sandia ParaChoice Model." 2015 Annual Merit Review. Crystal City Marriott, Arlington, VA. 9 June 2015.

IX.8 Status and Prospects of the N.A. Non-Automotive Fuel Cell Industry: 2014 Update

David L. Greene
The University of Tennessee
Howard H. Baker, Jr. Center for Public Policy
1640 Cumberland Avenue
Knoxville, TN 37996-3340
Phone: (865) 974-3839
Email: dlgreene@utk.edu

DOE Manager
Fred Joseck
Phone: (202) 586-7932
Email: Fred.Joseck@ee.doe.gov

Contract Number: ANL 4F-30621 GREENE

Project Start Date: October 1, 2013
Project End Date: September 30, 2016

Overall Objectives

- Quantify the North American (N.A.) non-automotive fuel cell industry's progress in terms of reduction in costs of products and improvements in performance
- Quantify the impact of the American Recovery and Reinvestment Act (ARRA) and Investment Tax Credit (ITC) on the N.A. non-automotive fuel cell industry
- Estimate the timing and conditions under which the industry is likely to become self-sustaining without further policy support
- Assist DOE and Argonne National Laboratory (ANL) with planning and analysis of the transition to hydrogen fuel cell vehicles in the United States

Fiscal Year (FY) 2015 Objectives

- Estimate the total costs of nationwide, vehicle refueling or recharging infrastructure for (1) gasoline and diesel, (2) hydrogen, (3) electricity, (4) natural gas, (5) propane and (6) E85
- Prepare a draft report reviewing the literature on how consumers' evaluate novel vehicle technologies, quantifying key factors as the literature permits
- Provide analytical support to DOE's participation in H_2USA, as requested by DOE

Technical Barriers

This project addresses the following technical barriers from the Systems Analysis section of the Fuel Cell Technologies Office Multi-Year Research, Development, and Demonstration Plan:

(A) Future Market Behavior

(C) Inconsistent Data Assumptions and Guidelines

(D) Insufficient Suite of Models and Tools

(E) Unplanned Studies and Analysis

Contribution to Achievement of DOE Systems Analysis Milestones

This project contributes to achievement of the following DOE milestones from the Systems Analysis section of the Fuel Cell Technologies Office Multi-Year Research, Development, and Demonstration Plan:

- Milestone 3.3: Complete review of status and outlook of non-automotive fuel cell industry. (biennially from 4Q, 2011 through 4Q, 2019)
- Milestone 1.15: Complete analysis of program milestones and technology readiness goals—including risk analysis, independent reviews, financial evaluations, and environmental analysis—to identify technology and risk mitigation strategies. (4Q, 2015)
- Milestone 1.16: Complete analysis of program performance, cost status, and potential use of fuel cells for a portfolio of commercial applications. (4Q, 2018)
- Milestone 1.19: Complete analysis of the potential for hydrogen, stationary fuel cells, fuel cell vehicles, and other fuel cell applications such as material handling equipment including resources, infrastructure and system effects resulting from the growth in hydrogen market shares in various economic sectors. (4Q, 2020)

FY 2015 Accomplishments

- Through interviews with original equipment manufacturers (OEMs) and analysis of financial reports and published literature, developed updated estimates of scale economies, rates of learning-by-doing, annual technological progress, and costs of fuel cell material handling equipment (MHE) and backup power (BuP) systems manufactured in North America

- Updated the N.A. Non-Automotive Fuel Cell Market Model to reflect 2014 industry restructuring, technological advances and market conditions, including deployments under ARRA
- Completed an evaluation of the additional impacts of the ARRA and ITC on the domestic fuel cell industry and estimated the impacts of ending or phasing out the ITC after 2016

✧ ✧ ✧ ✧ ✧

INTRODUCTION

North American firms have been producing fuel cell BuP and MHE systems for demonstration and commercial sales for about a decade. Fuel cell technologies typically compete with battery and diesel generator systems in the BuP market, and battery-powered forklifts in indoor, warehousing MHE applications where emission-free operation is a priority. Over the past five years, the industry has made enormous progress improving the performance of its products and reducing their costs. The industry has benefited from government policies that provide tax credits and other subsidies, as well as direct purchases.

This project estimates the impact of government subsidies provided by ARRA and ITC on the sales of fuel cell BuP and MHE (i.e., forklifts) by North American firms. The objective is to estimate the additional impact of those policies and their effects on the outlook for the industry in the future.

APPROACH

The N.A. Non-Automotive Fuel Cell Market Model [2] was updated and revised based on information obtained via confidential interviews with hydrogen fuel cell OEMs, as well as from published sources and the internet. Past sales and cost projections of the model were compared with data collected during 2014 to evaluate its performance and identify parameters in need of recalibration. The updated model was then used to estimate the impacts of ARRA and ITC on the North American fuel cell industry and to develop conditional projections of its prospects.

DOE reports that the ARRA partially funded sales of 524 MHE units and 824 BuP units (see Table 1) [5,6]. The ARRA expenditures for fuel cell MHE support was $9.7 million, while the industry cost share was $11.8 million. The corresponding numbers for ARRA funded BuP sales were $18.5 million from DOE and $30.8 million from industry. In addition, DOE has subsidized 83 BuP units and 189 MHE units out of its departmental appropriations. Thus, total DOE-subsidized fuel cell sales amount to 907 BuP units and 713 MHE units. Since 2009, firms have purchased 5,568 BuP units and 8,340 MHE units without DOE support.

TABLE 1. Fuel Cell Unit Sales (Delivered and Planned) by North American OEMs since 2009

Equipment Type	DOE ARRA	DOE Budget	DOE Total	Industry	Total
Backup Power	824	83	907	5,568	6,475
Material Handling	524	189	713	8,340	9,053

Source: Devlin and Kiuru [5,6].

However, these sales also benefitted from ITC and possibly state subsidies.

The customer choice model of the Market Model was recalibrated to exactly predict the sales of fuel cell MHE and BuP units not supported by ARRA for the period 2005 to 2014. Purchases directly supported by ARRA were added making the sum of the two exactly equal to total sales for the period. ARRA sales thereby influenced scale economies and learning in the model. Sales were predicted through 2025. Purchases directly supported by ARRA were then subtracted from the actual purchases and the model was rerun, providing an estimate of what sales would have been in the absence of the ARRA program during the 2009 to 2013 period, as well as the impact on projected sales through 2025. The additional impact of ARRA was estimated by the difference between non-ARRA supported sales given ARRA and the predicted sales without ARRA. Sensitivity analysis was used to explore the effect of assuming that none of the ARRA sales would have occurred in the absence of the program.

RESULTS

Sales predictions made by the 2011 study were compared with estimated actual sales for MHE and BuP. Given the many factors, including ARRA and industry consolidation, influencing sales from 2010 to 2014, the MHE projections are satisfactory but generally underestimate estimated actual sales. BuP sales projections, on the other hand, generally overestimated estimated actual sales, although the data for 2013 and 2014 are incomplete due to the absence of data for one firm in 2013 and two firms in 2014. In both cases the model's predictions are of the correct order of magnitude but the accuracy in any given year is not much better than +/- 50%

Cost analyses published since 2011 and discussions with OEMs in 2014 suggest scale economies for fuel cell stack production in the range of -0.07 to -0.1 [3]. For fuel cell stacks for material handling equipment, cost estimates by Contini et al. imply scale elasticities of -0.04 to -0.07 [1]. Scale elasticities inferred from their cost estimates for the balance of plant are -0.11 for 100 to 1,000 units per year and -0.07 for 1,000 to 10,000. Recent data is consistent with progress ratios for learning by doing of approximately 0.95. Rates of cost reduction due to technological progress are averaging about 2% per year.

The recalibrated market model predicts a price of $33,000–$34,000 for the MHE stack and balance of plant in 2010 but with a wide range of uncertainty (Figure 1). Prices and uncertainty decline sharply in 2011 and continued progress is predicted through 2014. The prediction for 2013 ($17,000) is close to HD Systems' estimate of $15,000–$16,000 for that year, based on manufacturer interviews, company annual reports, and other public sources [3]. The model's cost estimates for BuP also show that 2014 costs are approximately half of the 2010 level (Figure 2). In contrast to Contini et al., HD Systems assumes that the markup over direct manufacturing cost for a fuel cell OEM unit was only 10–15% because market conditions in 2013 did not allow full cost recovery [1,3].

The 504 ARRA MHE deployments were estimated to induce an additional 1,500 MHE sales through 2025 (Figure 3). The 852 ARRA BuP deployments were estimated to produce 3,000 additional BuP unit sales through 2025. Sensitivity analysis predicted that even if as many as 50% of the ARRA deployments would have occurred in the absence of ARRA support, the ARRA-supported deployments would induce 1,000 additional sales of fuel cell MHE and 1,500 additional sales of BuP fuel cell units.

Ending ITC abruptly after 2016 was estimated to have a disruptive effect on the N.A. non-automotive fuel cell market, reducing sales in 2017 to approximately half the 2016 level. Sales could be sustained at approximately the 2016 level through 2020 by a linear phase-out of ITC.

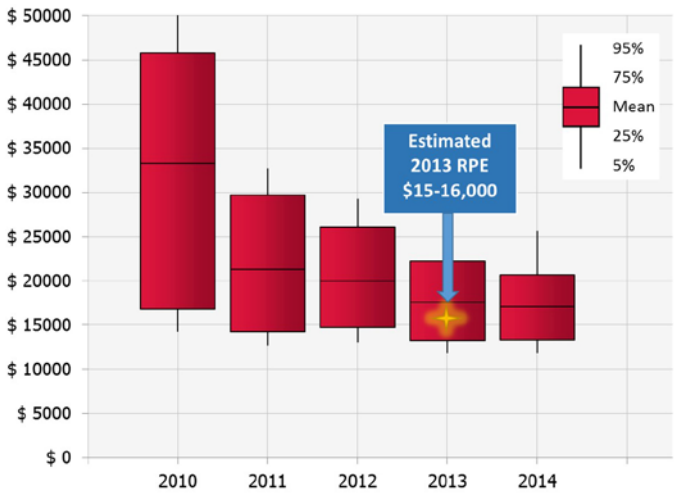

FIGURE 1. Predicted retail price equivalent (RPE) of fuel cell stack and balance of plant for a representative 5 kW forklift

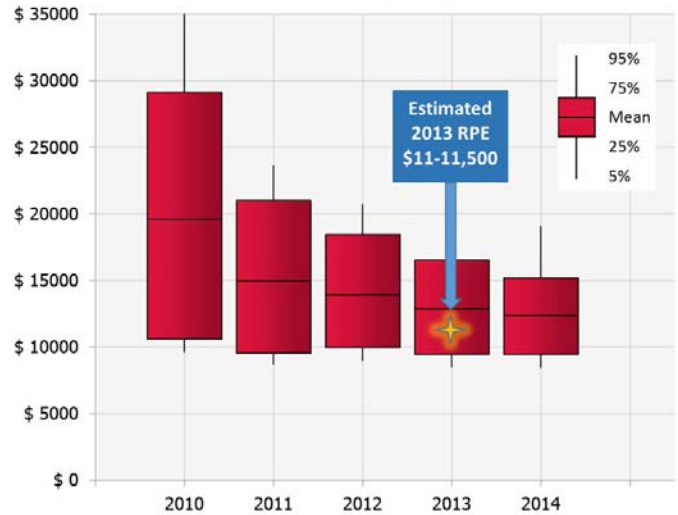

FIGURE 2. Predicted retail price of fuel cell stack and balance of plant for a representative 5 kW backup power unit

FIGURE 3. Estimated additional impact of ARRA on sales of fuel cell (FC) MHE and BuP in North America through 2020

CONCLUSIONS AND FUTURE DIRECTIONS

- The N.A. non-automotive fuel cell industry made substantial progress between 2010 and 2014, cutting costs by approximately half while improving durability and performance.
- Deployment of fuel cell MHE and BuP systems directly supported by ARRA will induce approximately three times as many additional sales of fuel cell systems by N.A. manufacturers through 2025.
- Throughscale economies and learning by doing, the ARRA deployments reduced the cost of fuel cells systems manufactured in N.A. by several hundred dollars per unit.
- Terminating ITC abruptly after 2016 will likely have a disruptive effect on N.A. fuel cell manufacturers. The negative impact could likely be eliminated by gradually phasing out the tax credit by 2020.
- Previous model predictions for the N.A. non-automotive fuel cell industry appear to have underestimated rates of technological progress while overestimating scale economies and learning by doing. Substantial future progress is likely to make the industry self-sustaining without public policy support before 2025.

Future model development should improve the representation of domestic and international markets and increase the level detail in representing fuel cell products. Another review of industry status and prospects, to obtain updated information and continue validation of the industry model should be carried out in 2016–17.

FY 2015 PUBLICATIONS/PRESENTATIONS

1. Greene, D.L., 2015. "Potential Applications of Scale Economies and Learning Curves in Modeling the Transition to Hydrogen Fuel Cell Technologies," Joint FPITT-HDTT-PHTT Meeting, National Renewable Energy Laboratory, Golden, CO, July 14, 2015.

2. Greene, D.L., "Status and Prospects of the N.A. Non-Automotive Fuel Cell Industry: 2014 Update," Project SA056, 2015 U.S. DOE Hydrogen and Fuel Cells Program and Vehicle Technologies Office Annual Merit Review and Peer Evaluation Meeting, Arlington, VA, June 9, 2015.

REFERENCES

1. Contini, V., K. Mahadevan, F. Eubanks, J. Smith, G. Stout, and M. Jansen, 2013. "Manufacturing Cost Analysis of Fuel Cells for Material Handling Applications," Battelle, 5/14/2013, http://www.hydrogen.energy.gov/pdfs/review13/fc097_mahadevan_2013_o.pdf .

2. Greene, D.L., K.G. Duleep, and G. Upreti, 2011. "Status and Outlook for the U.S. Non-Automotive Fuel Cell Industry: Impacts of Government Policies and Assessment of Future Opportunities," ORNL/TM-2011/101, Oak Ridge National Laboratory, Oak Ridge, Tennessee.

3. H-D Systems, 2015. "Non Automotive Fuel Cell Applications: Analysis of Technology, Cost and Markets," Draft Final Report to Oak Ridge National Laboratory, Washington, D.C., January 15.

4. Upreti, G., D.L. Greene, K.G. Duleep, and R. Sawhney, 2012. "Fuel cells for non-automotive uses: status and prospects," International Journal of Hydrogen Energy, Volume 37, Issue 8, pp. 6339–6348, 2012.

5. P. Devlin and K. Kiuru, 2015a. "Industry Deployed Fuel Cell Backup Power (BuP)," DOE Hydrogen and Fuel Cells Program Record 15004, U.S. Department of Energy, Washington, DC.

6. P. Devlin and K. Kiuru, 2015b. "Industry Deployed Fuel Cell Powered Lift Trucks," DOE Hydrogen and Fuel Cells Program Record 15003, U.S. Department of Energy, Washington, DC.

IX.9 Tri-Generation Fuel Cell Technologies for Location-Specific Applications

Kersey S. Manliclic, Brendan P. Shaffer (Primary Contact), G. Scott Samuelsen
Advanced Power and Energy Program
University of California, Irvine
Engineering Laboratory Facility, Bldg. 323
Irvine, CA 92697-3350
Phone: (949) 824-7302 ext. 11127
Email: bps@apep.uci.edu

DOE Manager
Fred Joseck
Phone: (202) 586-7932
Email: Fred.Joseck@ee.doe.gov

Contract Number: XFC-4-23067-01

Project Start Date: January 1, 2014
Project End Date: March 31, 2015 (Final Report in Progress)

Overall Objectives

- Assess potential number and location of tri-generation (Tri-Gen) fuel cell systems, producing electricity, high quality waste heat, and hydrogen, in an early fuel cell electric vehicle (FCEV) market scenario (circa 2015) in New York, New Jersey, Connecticut, and Massachusetts
  - Consider use of natural gas and anaerobic digester gas as feedstock
  - Consider viability of the Tri-Gen units serving as a local hub for hydrogen production

Fiscal Year (FY) 2015 Objectives

- Conduct sensitivity studies:
  - Assess the effect that vehicle sales data selection/market distribution has on the resulting necessary tri-generation and/or hydrogen refueling infrastructure. Spanning scenarios:
    - Temporal deployment of fuel cell electric vehicles (e.g., 10,000−50,000+ FCEVs)
    - Spatial deployment of hydrogen refueling stations (e.g., 108, 313, and 774 to cover the top 25%, top 50%, and top 75% of the alternative vehicle sales market based on zip codes)
    - Varied drive time service coverage (e.g., 6, 10, and 15 minutes)
- Complete the identification of candidate Tri-Gen sites using anaerobic digester gas from wastewater treatment plants as a feedstock and operating as either: (1) a hydrogen refueling station dispensing the hydrogen produced, or (2) central hub of hydrogen production
- Complete the identification of candidate Tri-Gen sites using conventional natural gas as a feedstock and operating as either: (1) a hydrogen refueling station dispensing the hydrogen produced, or (2) a central hub of hydrogen production
- Estimate the hydrogen, electricity, and heat production from the aforementioned identified Tri-Gen sites
- Conduct an economic analysis to compare cost of hydrogen across the different scenarios
- Assess the greenhouse gas (GHG) and oxides of nitrogen (NO_X) emissions from the Tri-Gen systems

Technical Barriers

This project addresses the following technical barriers from the Systems Analysis section of the Fuel Cell Technologies Office Multi-Year Research, Development and Demonstration Plan (MYRDDP):

(A) Future Market Behavior

(B) Stove-piped/Siloed Analytical Capability

(E) Unplanned Studies and Analysis

This project will contribute to achievement of the following DOE milestones from the Systems Analysis section of the MYRDDP:

- Milestone 1.9: Complete analysis and studies of resource/feedstock, production/delivery, and existing infrastructure for technology readiness. (4Q, 2014)
- Milestone 1.12: Complete an analysis of the hydrogen infrastructure and technical target progress for technology readiness. (4Q, 2015)
- Milestone 1.13: Complete environmental analysis of the technology environmental impacts for hydrogen and fuel cell scenarios and technology readiness. (4Q, 2015)

FY 2015 Accomplishments

- Completed economic analysis for Tri-Gen system sited at the largest wastewater treatment plants (WWTPs) and supplying hydrogen to an on-site hydrogen dispenser
- Completed economic analysis for Tri-Gen system sited at the largest WWTPs, acting as a central hub of hydrogen

production, and supplying hydrogen to various roll outs of hydrogen refueling stations

- Completed economic analysis for Tri-Gen system operating on conventional natural gas and supplying hydrogen to an on-site hydrogen dispenser
- Completed economic analysis for Tri-Gen system operating on conventional natural gas, acting as a central hub of hydrogen production, and supplying hydrogen to various roll outs of hydrogen refueling stations

✧ ✧ ✧ ✧ ✧

INTRODUCTION

Zero-emission FCEVs are one of the pieces in a portfolio of solutions for the transportation sector to reduce its GHG emissions and lower its negative impacts on air quality. With gaseous hydrogen fuel combined with the oxygen in the air, electricity is generated in the fuel cell to power the vehicle, and the vehicle emits nothing but water in the process. Even though it has zero-emissions at the tailpipe, for the vehicle to truly be zero-emissions, every effort must be made to reduce and minimize the GHGs emitted during the production of the hydrogen fuel.

Tri-Gen fuel cell systems are a distributed generation technology with the capability of producing the three useful products of electricity, high quality waste heat, and hydrogen that could be used to refuel FCEVs. The northeastern United States is currently being touted as the next stationary and mobile fuel cell market after California. As such, this research effort recognizes and capitalizes on the opportunity to strategically site Tri-Gen fuel cell systems while the hydrogen refueling infrastructure in the Northeast is burgeoning.

APPROACH

As a first step, the Spatial and Temporally Resolved Energy and Environment Tool (STREET), in conjunction with geographic information systems, was employed to plan out the location and number of hydrogen refueling stations needed in the aforementioned region based on alternative vehicle sales registration data (STREET was the tool used to plan out the roadmap of hydrogen refueling stations for California). Subsequently, various scenarios of Tri-Gen fuel cell deployments to provide hydrogen to the theoretical hydrogen refueling stations will be assessed with the goal being to minimize delivery distances. Since the number of potential fuel cell vehicles can be estimated and which fuel cell systems are supplying hydrogen to given stations is known, the appropriate size and corresponding economics of the Tri-Gen fuel cell systems can be determined. Any viable site with access to the natural gas pipeline (e.g. the Northeast Interstate/Intrastate natural gas pipeline) will be treated as a candidate for the installation of a Tri-Gen system, and water treatment facilities will serve as the candidate locations for Tri-Gen fuel cell system operating on renewable anaerobic digester gas.

RESULTS

Using alternative vehicles sales registration data as an input, this study estimates that approximately 108, 313, and 774 hydrogen refueling stations would be needed to serve and enable the top 25%, top 50%, and top 75% of the alternative vehicles market, respectively, in the states of New York, New Jersey, Connecticut, and Massachusetts taken as a whole (Figure 1).

In assessing how and where Tri-Gen fuel cell systems producing high quality waste heat, electricity, and hydrogen could support this network, a total of four scenarios were investigated:

- Tri-Gen system supplying an on-site hydrogen dispenser; anaerobic digester gas feedstock
- Tri-Gen system acting as a central hub of hydrogen production supplying nearby hydrogen stations with hydrogen; anaerobic digester gas feedstock
- Tri-Gen system supplying an on-site hydrogen dispenser; natural gas feedstock
- Tri-Gen system acting as a central hub of hydrogen production supplying nearby hydrogen stations with hydrogen; natural gas feedstock.

The location of water treatment facilities (WTF) in the aforementioned states was ascertained from the EPA Enforcement and Compliance History Online (ECHO) database. The 25 largest water treatment facilities in those four states were chosen as candidates for the installation of a Tri-Gen fuel cell system supplying an on-site hydrogen dispenser. The smallest of these 25 can support a Tri-Gen system approximately 1.8 MW in size based on potential biogas supply. Therefore, treatment plants smaller than this size will become less viable for the installation of a Tri-Gen system.

The potential hydrogen demand from FCEVs at WTFs varies widely from site to site. For example, some WTFs may be large in size, but too far away from potential vehicles. To ascertain the potential number of FCEVs within proximity of the top 25 WTFs, the dataset of ~95,000 alternative vehicles were treated as proxy FCEVs and the number of those proxy FCEVs within 6, 10, and 15 minutes of the WTFs were counted. The results are presented in Table 1. One important realization is whether a stakeholder defines his/her market based on the number of FCEVs within 6, 10, or 15 minutes greatly affects what size Tri-Gen system they may want to install and, subsequently, what price of hydrogen they can deliver.

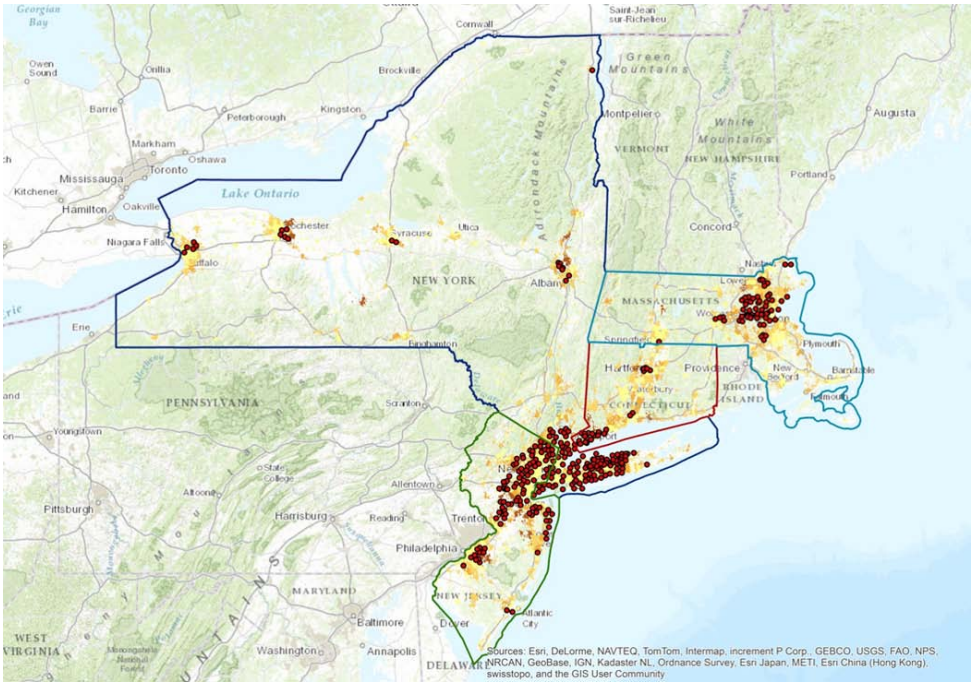

FIGURE 1. Three hundred thirteen stations would be needed to ensure 6 min service coverage to a hydrogen refueling station for the top 50% of zip codes based on alternative vehicle sales registration data. Source: Manliclic et al. [1].

TABLE 1. The top 25 water treatment facilities in terms of millions of gallons per day (MGD) influent size. The number of alternative vehicles (out of the 95,048 total in the alternative vehicle sales registration dataset) within 6 minutes, 10 minutes, and 15 minutes is shown. Source: EPA ECHO

Name	City	State	Rated MGD	6 minutes	10 minutes	15 minutes
MWRA DEER ISLAND TREATMENT PLANT	BOSTON	MA	480	0	31	82
BOSTON WATER AND SEWER COMM, CSO	BOSTON	MA	330	585	2013	4616
PASSAIC VALLEY SEWERAGE COMM	NEWARK	NJ	330	7	111	1512
NYCDEP - NEWTOWN CREEK WPCP	NEW YORK	NY	310	198	1296	2985
NYCDEP - WARD'S ISLAND WPCP	NEW YORK	NY	275	65	602	2497
NYCDEP - HUNT'S POINT WPCP	BRONX	NY	200	5	164	1643
BIRD ISLAND STP	BUFFALO	NY	180	54	133	376
NYCDEP - NORTH RIVER WPCP	NEW YORK	NY	170	10	339	1562
NYCDEP - BOWERY BAY WPCP	ASTORIA	NY	150	140	580	2417
MIDDLESEX CNTY UA	SAYREVILLE	NJ	147	51	144	361
FRANK E VAN LARE STP	ROCHESTER	NY	135	51	105	397
YONKERS JOINT WWTP	YONKERS	NY	120	217	582	2126
NYCDEP - OWLS HEAD WPCP	BROOKLYN	NY	120	161	721	1757
NYCDEP - CONEY ISLAND WPCP	BROOKLYN	NY	110	257	545	1259
NYCDEP - JAMAICA WPCP	JAMAICA	NY	100	100	622	2414
NYCDEP - 26TH WARD WPCP	BROOKLYN	NY	85	108	545	1988
BERGEN CNTY WTP	LITTLE FERRY	NJ	84.28	0	3	92
METROPOLITAN SYRACUSE WWTP	SYRACUSE	NY	84.2	53	272	584
NYCDEP - TALLMAN ISLAND WPCP	COLLEGE POINT	NY	80	134	527	1982
DELAWARE #1 WATER POL CON FAC	CAMDEN	NJ	80	9	126	506
JT MGT OF ESSEX & UNION CNTY	ELIZABETH	NJ	75	10	184	877
CEDAR CREEK WPCP	WANTAGH	NY	72	120	798	1853
BAY PARK STP	EAST ROCKAWAY	NY	70	557	1218	2350
SPRINGFIELD W W T P	AGAWAM	MA	67	41	212	379
HARTFORD WPCF	HARTFORD	CT	60	42	253	927

With respect to Tri-Gen fuel cell systems sited at WTFs and acting as central hubs of hydrogen production, due to the limited biogas potential from WTFs, sometimes a network of 10 or more Tri-Gen central hubs is needed to supply and support the given number of hydrogen refueling stations. Thus, effectively, there are size limitations to the Tri-Gen systems that can be installed, and therefore, a limit on economies of scale, which drop the price of hydrogen that can be offered and be taken advantage of. An example is shown in Figure 2 where 10 Tri-Gen systems sited at WTFs struggle and cannot support a scenario of about 774 refueling stations with ~95,000 FCEVs in the four states.

Conversely, there is a lot more flexibility afforded to a stakeholder when operating a Tri-Gen fuel cell system on conventional natural gas. Candidate sites for the installation of such a system included points along the inter/intrastate natural gas pipeline as well as at the theoretically planned hydrogen refueling stations – i.e., the 108, 313, and 774 stations. Assuming that an unlimited amount of natural gas can be tapped into and ascertained, the resulting effect is that the Tri-Gen systems can be sized as large as needed to meet the FCEV hydrogen demand. As such, scenarios where 1, 5, and 10 hubs set to serve the entire hydrogen station refueling network were analyzed and deemed possible. Due to economies of scale, in all cases, having one large Tri-Gen central hub was the cheapest option (cost of producing the hydrogen plus the cost of delivery). For the most part, this result is due to the capital cost of a Tri-Gen system dropping off faster than the increase in delivery costs as a function of distance. The case of five hubs delivering to the 108 station solution is shown in Figure 3 (a full range of the results will be reported in the project's final report). Moreover, though from a cost perspective, a large single Tri-Gen hub is the most favorable, early results are showing that the long delivery distances from one, or even five, Tri-Gen central hubs to the corresponding stations that are rolled out (i.e., 108, 313, or 774) may be resulting in more NO_X and/or GHG emissions than the emissions offset by the FCEVs driving on the road.

# of WWTP Central Hubs	10*	20	29	40
H2 Fuel Production Cost (Tri-Gen System)	128,157.44	187,455.00	216,368.85	465,510.78
Total Delivery Cost (Gaseous)	50,986.66	72,365.74	72,072.92	69,293.64
Total Delivery Cost (Liquid)	76,070.30	102,290.05	108,567.89	108,245.93
Total Delivery Cost (Pipeline)	107,778.82	154,233.17	151,683.11	147,290.01
kg H2 produced per day	34,802.44	48,311.38	49,739.16	49,739.16
*Hub(s) unable to serve entire H2 station network				

Note: In this instance, 20 hubs are very close to being (but not fully) sufficient to service the network

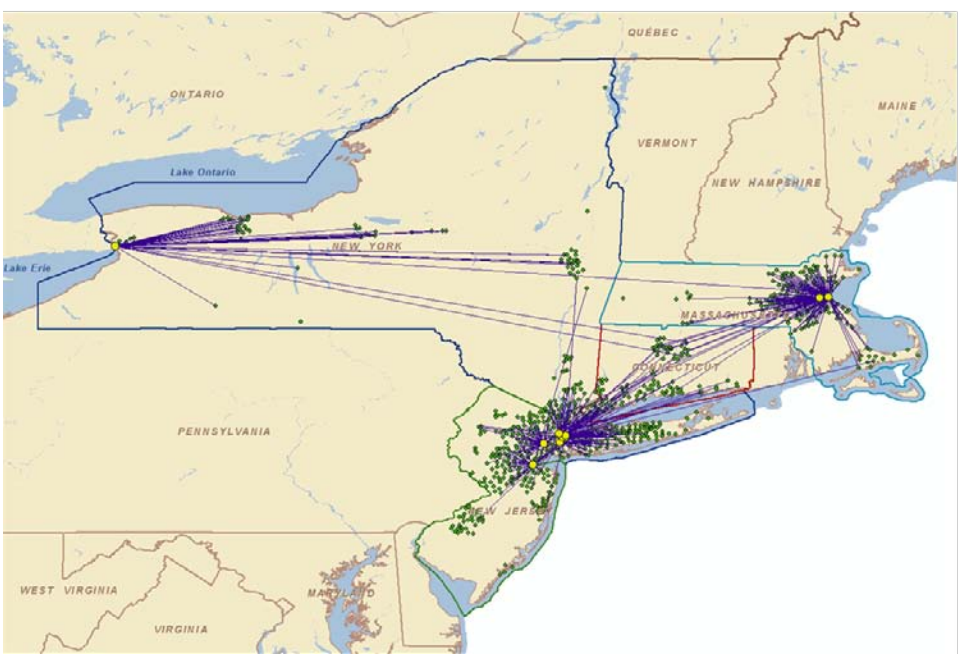

FIGURE 2. Ten hubs can only deliver to 419 of the 774 stations

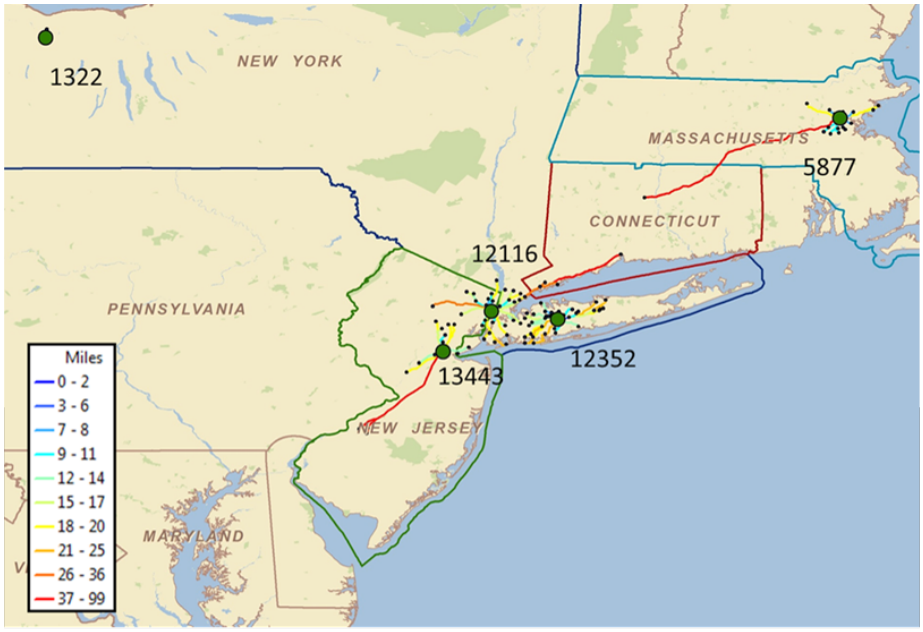

5 Hubs	# of Vehicles	kg H2	Fuel Cell Capacity (kW)	Electricity Produced (kW)	Heat Produced (kW)	Total Capital Cost ($)	Price of H2 ($/kg)	Fuel Input (kW)
1322	53.29	37.30	83.60	66.10	19.98	993,906	15.41	200.30
5877	806.87	564.81	1,265.74	1,000.73	302.57	4,805,973	6.60	3,032.63
12116	1,249.87	874.91	1,960.67	1,550.16	468.69	7,046,920	5.76	4,697.64
12352	979.68	685.77	1,536.82	1,215.05	367.37	5,680,126	6.21	3,682.12
13443	399.06	279.34	626.01	494.94	149.64	2,743,013	8.22	1,499.87

H2 Fuel Production Cost (Tri-Gen System)	**15,895.32**
Total Delivery Cost (Gaseous)	3,235.46
Total Delivery Cost (Liquid)	5,295.59
Total Delivery Cost (Pipeline)	6,969.96
kg H2 produced per day	2,442.14

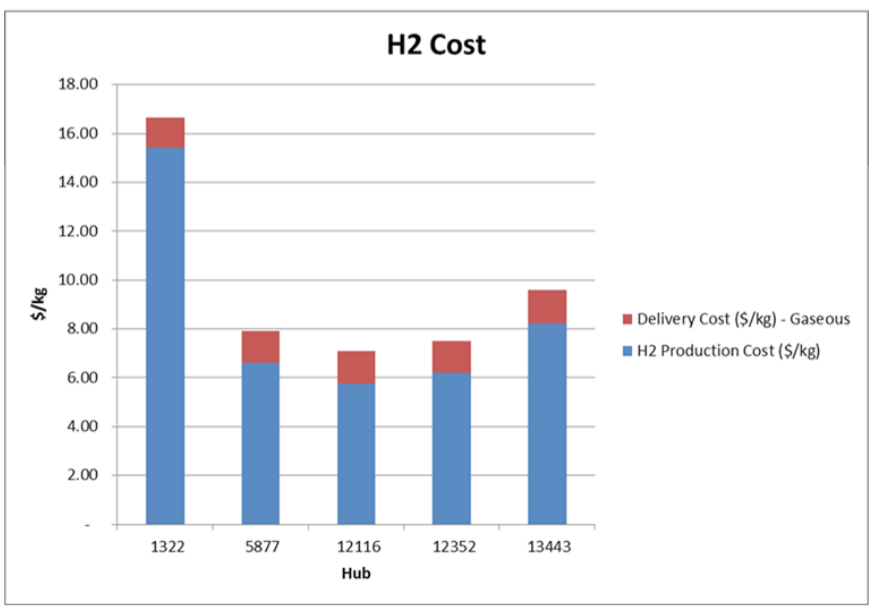

FIGURE 3. Five hubs delivering to the 108 station solution, which serves 25% of the market – i.e., 25% of the 10,000 fuel cell electric vehicles deployed

CONCLUSIONS AND FUTURE DIRECTIONS

- Whether stakeholders interested in installing a Tri-Gen fuel cell system with an on-site hydrogen dispenser deems their customer base to be FCEV drivers within six or, more generously, 15 minutes of their site greatly impacts the size of the system they will want to install as well as the capital cost investment that will need to be made.
- Operating on conventional natural gas offers the greatest opportunity to install large-sized Tri-Gen systems, thereby resulting in the lowest cost of hydrogen. However, the long delivery routes from these "Tri-Gen central hubs" could produce GHG and NO_X emissions (if diesel trucks are used) that are greater than the GHG and NO_X emissions that the FCEVs are offsetting.
- No additional work is planned, but future directions could include:
  - Looking at landfill gas as a Tri-Gen system feedstock
  - Exploring the sale of the electricity to the grid
  - Using the hydrogen as a means of energy storage – e.g., Power-2-Gas
  - Looking at how dairy waste could augment the biogas supply.

FY 2015 PUBLICATIONS/PRESENTATIONS

1. K.S. Manliclic, B.P. Shaffer (presenter), G.S. Samuelsen. Tri-Generation Fuel Cell Technologies for Location-Specific Applications. U.S. Department of Energy. 2015 Annual Merit Review. Washington D.C., June 8–15, 2015.

2. K.S. Manliclic, B.P. Shaffer, G.S. Samuelsen. Tri-Generation Fuel Cell Technologies for Infrastructure Applications in the Northeastern United States. Fuel Cell Seminar and Energy Exposition. Los Angeles, CA. November 13, 2014.

REFERENCES

1. K.S. Manliclic, T.M. Brown, G.S. Samuelsen. The Optimized Siting of Hydrogen Refueling Stations for the New York Tri-State Area. Fuel Cell Seminar and Energy Exposition. Columbus, Ohio. October 22, 2013.

IX.10 Analysis of Incremental Fueling Pressure Cost

Amgad Elgowainy (Primary Contact) and Krishna Reddi
Argonne National Laboratory
9700 South Cass Avenue
Argonne, IL 60439
Phone: (630) 252-3074
Email: aelgowainy@anl.gov

DOE Manager
Fred Joseck
Phone: (202) 586-7932
E-mail: Fred.Joseck@ee.doe.gov

Project Start Date: October 2013
Project End Date: September 2015

Overall Objective

- Provide a platform for comparing the impact of alternative refueling protocols, fueling pressures, and precooling temperatures on hydrogen refueling cost

Fiscal Year (FY) 2015 Objectives

- Evaluate the impact of fueling pressure on fill time and refueling cost
- Incorporate implications of Society of Automotive Engineers (SAE) J2601 Lookup Tables (L/T) and MC Default fill refueling protocol methods in the modeling of hydrogen refueling stations (HRS)
- Estimate the temperature rise due to heat gain between the dispenser breakaway and vehicle's onboard tank and account for this temperature rise in other project goals
- Identify cost drivers of various fueling technologies and configurations

Technical Barriers

This project directly addresses Technical Barriers A, D, and E in the Systems Analysis section of the Fuel Cell Technologies Office Multi-Year Research, Development, and Demonstration (MYRDD) Plan.

(A) Future Market Behavior

(D) Insufficient Suite of Models and Tools

(E) Unplanned Studies and Analysis

Technical Targets

The project employs the Hydrogen Station Cost Optimization and Performance Evaluation (H2SCOPE) simulation tool to simulate the performance of the SAE J2601 L/T and MC Default fill methods and to investigate the impact of fueling pressure and precooling requirement on the fill duration and refueling cost. The project also examines the tradeoff between the fueling pressure (fill amount) and refueling cost for a target fill time of three minutes.

Contribution to Achievement of DOE Systems Analysis Milestones

This project contributes to the following DOE milestone from the Systems Analysis section of the Fuel Cell Technologies Office MYRDD Plan:

- Milestone 1.12: Complete an analysis of the hydrogen infrastructure and technical target progress for technology readiness. (4Q, 2015)
- Milestone 2.2: Annual model update and validation. (4Q, 2011 through 4Q, 2020)

FY 2015 Accomplishments

- Updated and used H2SCOPE to evaluate the performance of SAE J2601 L/T and MC Default fill fueling protocol methods at different initial conditions and precooling temperature profiles
- Used H2SCOPE to study the impact of various fueling pressures and precooling temperatures on refueling time and cost
- Evaluated the impact of various combinations of fueling pressures and precooling temperatures on refueling cost of early market stations

✧ ✧ ✧ ✧ ✧

INTRODUCTION AND APPROACH

Previous studies have indicated that compression, refrigeration, and storage account for more than 75% of the refueling equipment cost. Additionally, refrigeration and compression are the two major components with significant operational costs. While the refueling station compression and storage requirements depend on the fueling pressure and demand profile, the cooling requirement depends on the precooling temperature and performance requirements in the fueling protocol. The precooling temperature and fueling protocol largely decide the fill rate for a given fueling pressure and initial vehicle tank condition. In this project,

we studied the performance of the SAE J2601 L/T and MC Default fill fueling methods for various combinations of vehicle tank boundary conditions and precooling profiles. The impact of various combinations of fueling pressures and precooling temperatures on the refueling cost of hydrogen was also evaluated.

The H2SCOPE simulation model tracks the transient temperature, pressure, and mass at all the points between the hydrogen source and the vehicle's tank. The model provided the opportunity to simulate the SAE J2601 L/T and MC Default fill fueling methods, in addition to conducting a parametric study, examining the highest fill rate possible with any combination of fueling pressure and precooling temperature within limits set by SAE J2601 protocol on pressure, temperature, and state of charge. The temperature rise inside the vehicle's tank is influenced by various parameters, including the tank's physical size and configuration, the tank thermal properties, and the initial and boundary conditions of the tank. The physical size, thermal properties, and initial and boundary conditions of the fill process simulated by the H2SCOPE model are provided in Tables 1, 2, and 3, respectively. The primary difference between the SAE J2601 L/T and MC Default fills is that the MC Default fill uses the actual pre-cooling temperature at the dispenser to control fueling process, while the SAE J2601 L/T fill uses the worst case boundary temperature (e.g., -33°C for T40 station) to decide fill rate. The refueling performance difference between the SAE J2601 L/T and MC Default fill methods was quantified for various boundary conditions, and the associated fueling costs for various combinations of fueling pressures and precooling temperatures were estimated.

TABLE 1. Vehicle Tank Characteristics

Tank Physical Properties	Fill Pressure [bar]		
	700	500	350
Capacity [kg]	5	4	3
Outer Diameter [in]	19.5		
Thickness [in]	1.83		
Tank Length [in]	49.2		
Liner Thickness [in]	0.2		
Volume [L]	129		

TABLE 2. Thermal Properties of Type IV Vehicle Tank

	Composite	Liner (Polyethylene)
Temperature Range [°C]	-100 to 140	-100 to 140
Density [kg/m^3]	1,550	975
Specific Heat [J/kg-K]	500–1,500	1,000–3,000
Thermal Conductivity [W/m-K]	0.3–0.8	0.3–0.8
Thermal Diffusivity [cm^2/s]	0.001–0.009	0.001–0.009

TABLE 3. Initial and Boundary Conditions of the Vehicle Tank System

Initial Pressure [bar]	20
Initial Temperature (Ambient Temperature) [K]	313
Hot Soak Condition [K]	No soak
Maximum Pressure [bar]	875
Maximum Temperature [K]	358
Convective Heat Transfer Coefficient [W/m^{2}K]	325 (Inside), 5 (Outside)
Inlet (Dispensing) Temperature [K]	263, 253, 243, 233
Fill Strategy	Constant Pressure Ramp Rate

RESULTS

MC Default fill compares favorably to the SAE J2601 L/T in terms of the fill duration for any set of boundary conditions. Figure 1 shows the fill duration and state of charge (SOC) at various precooling temperatures for SAE J2601 L/T and MC Default Fill methods for non-communication fueling. The MC Default fill takes advantage of the actual precooling temperatures at the dispenser by allowing a higher pressure ramp rate for lower precooling temperatures, while the SAE J2601 L/T has the same pressure ramp rate defined by the warmest temperature allowed for a station type (e.g., -33°C for T40 station).

Figure 2 shows the minimum fill times possible for different fueling pressures at various precooling temperatures. It also shows that the 700 bar refueling in type IV tanks would require at least -40°C precooling to fill 5 kg within 3 minutes. Additionally, precooling to -20°C and -10°C is required to fill the vehicle's tank in approximately 3 minutes for fueling pressures of 500 bar and 350 bar, respectively. Figure 3 shows the estimated refueling costs for filling the vehicle's tank at different fueling pressures in approximately 3 minutes for a 200 kg/d station. It can be seen from the figure that with partial fill of vehicle's tank (i.e., with lower fueling pressures), the refueling cost is significantly reduced. These lower fueling costs are due to the reduced cooling, compression, and storage costs at refueling stations designed to dispense hydrogen at these lower fueling pressures. The figure shows the refueling costs with increasing and constant annual utilization scenarios. With the ramp-up utilization scenario, a refueling cost reduction of about $3/kg can be achieved by partial fueling (up to 350 bar) compared to 700 bar fueling. These savings reduce to $2/kg when the station has constant high utilization throughout the analysis period.

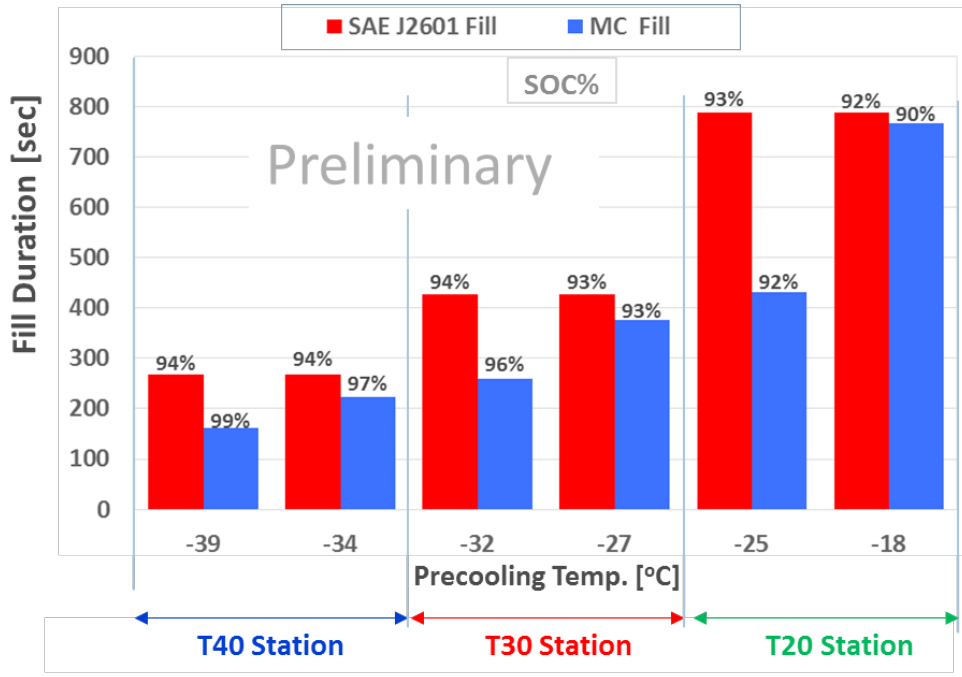

FIGURE 1. Fill duration of SAE J2601 L/T and MC Default fill methods at different pre-cooling temperatures

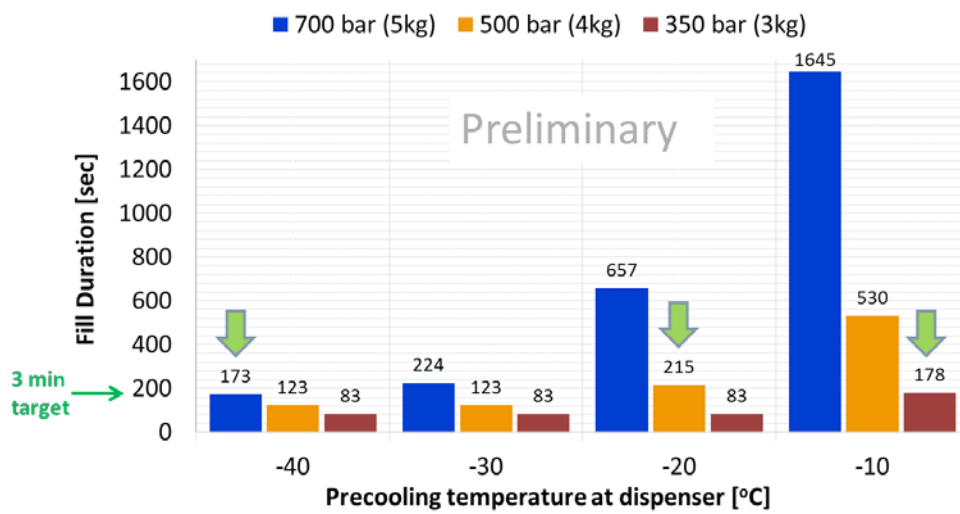

FIGURE 2. Estimated fill duration for various fueling pressures and precooling temperatures

CONCLUSIONS

In general, the MC Default fill method has the potential to provide faster fill rates compared to the SAE J2601 L/T method. The dynamic control of the MC Default fill method provides faster fills with lower temperatures within the precooling temperature window. The fueling pressure greatly impacts the fill duration, especially with higher precooling temperatures. Filling the vehicle with lower pressures (partial fills) reduces the associated refueling costs. The reduction in refueling cost with lower fueling pressures is greater with lower station utilizations.

PATENT APPLICATION

1. Elgowainy, A., Reddi, K., "Enhanced Methods for Operating Refueling Station Tube-trailers to Reduce Refueling Cost," United States Patent and Trademark Office Application Number: US 14/039,120, Published on April 2, 2015.

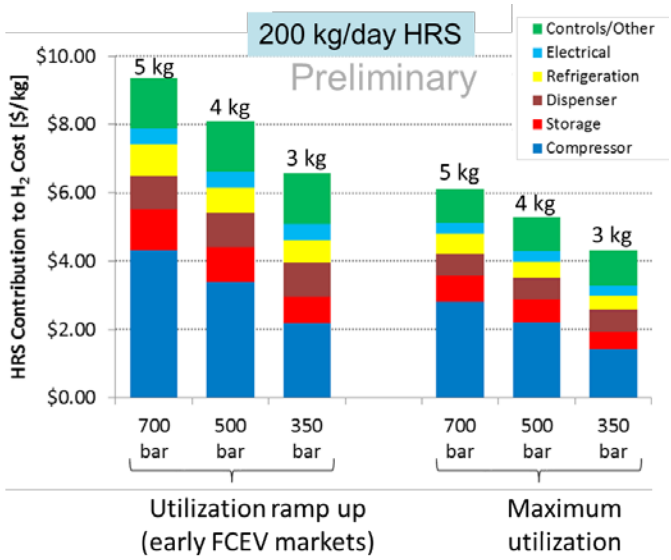

FIGURE 3. Estimated refueling cost for various fueling pressures for two station utilization scenarios of a 200 kg/d station

PUBLICATIONS

1. Elgowainy, A., Reddi, K., Sutherland, E., and Joseck, F., 2014. Tube-trailer consolidation strategy for reducing hydrogen refueling station costs. International Journal of Hydrogen Energy, 39(35), pp. 20197–20206.

2. Reddi, K., Elgowainy, A., and Sutherland, E., 2014. Hydrogen refueling station compression and storage optimization with tube-trailer deliveries. International Journal of Hydrogen Energy, 39(33), pp. 19169–19181.

IX.11 Analysis of Optimal On-Board Storage Pressure for Hydrogen Fuel Cell Vehicles

Zhenhong Lin (Primary Contact), Changzheng Liu
Oak Ridge National Laboratory
2360 Cherahala Boulevard
Knoxville, TN 37932
Phone: (865) 946-1308
Email: linz@ornl.gov

DOE Manager
Fred Joseck
Phone: (202) 586-7932
Email: Fred.Joseck@ee.doe.gov

Project Start Date: October 1, 2012
Project End Date: Project continuation and direction determined annually by DOE

Overall Objectives

- Optimize delivered hydrogen pressure
- Analyze sensitivity of optimal pressure
- Compare different pressure options for California

Fiscal Year (FY) 2015 Objectives

- Represent the ZEV (zero emission vehicle) mandate in optimization
- Consider mixed storage pressure
- Consider travel pattern daily variation and driver heterogeneity
- Quantify range limitation cost
- Conduct California case studies

Technical Barriers

This project addresses the following technical barriers from the Hydrogen Storage section of the Fuel Cell Technologies Office Multi-Year Research, Development, and Demonstration Plan (MYRDDP):

(B) System Cost

(G) Codes and Standards

(X) System Life-Cycle Assessments

This project also addresses the following technical barrier from the Market Transformation section of the Fuel Cell Technologies Office MYRDDP:

(B) High hydrogen fuel infrastructure capital costs for Polymer Electrolyte Membrane (PEM) fuel cell applications

Contribution to Achievement of DOE Hydrogen Storage and Market Transformation Milestones

This project will contribute to achievement of the following DOE milestones from the Hydrogen Storage and Market Transformation sections of the Fuel Cell Technologies Office MYRDDP:

- Hydrogen Storage 3.3: Transportation: Complete economic evaluation of cold hydrogen storage against targets. (4Q, 2015)
- Hydrogen Storage 3.6: Update early market storage targets. (4Q, 2017)
- Hydrogen Storage 3.7: Transportation: Complete analysis of onboard storage options compared to ultimate targets. (4Q, 2020)
- Market Transformation 1.13: Deploy, test, and develop business cases for renewable hydrogen energy systems for power, building, and transportation sectors. (1Q, 2015)

FY 2015 Accomplishments

- The Hydrogen Optimal Pressure (HOP) model was upgraded to include range limitation cost and ZEV credits in its objective function. Six types of daily driving patterns were derived to represent California drivers and on which to base the quantitative analysis of range limitation costs.
- The pressure of 700 bar is found to be especially valuable for consumers with frequent long-distance and away-from-station-cluster trips. These consumers may still face range limitation even with a 300-mile driving range.
- The value of the ZEV credits for 700-bar tanks (enabling >300-mile range) is significant enough to overshadow other determining factors.

✧ ✧ ✧ ✧ ✧

INTRODUCTION

The pressure of hydrogen delivered to hydrogen vehicles can be an important parameter that has great impact on the

delivered cost of hydrogen and the range limitation obstacle of hydrogen vehicles. Higher hydrogen pressure allows more hydrogen to be stored on board, enabling a longer driving range between hydrogen refills, but the cost of hydrogen supply infrastructure, and therefore the delivered cost of hydrogen, will be higher. While lower hydrogen pressure shortens the driving range and results in higher refueling frequency, the delivered hydrogen cost can be lower. Also importantly, the lower capital cost of low-pressure stations may encourage investment activities in developing more stations, resulting in better refueling convenience for consumers.

The objectives of this project are to:

- Develop an optimization model to identify the delivered pressure of hydrogen that reflects tradeoff among hydrogen cost, infrastructure capital cost requirement, driving range, refueling frequency, and refueling convenience. The motivation of optimization is to maximize consumer acceptance of hydrogen vehicles.
- Analyze and recommend the delivered hydrogen pressure as a function of technology cost, regional geography, hydrogen demand, and driving patterns.

APPROACH

The optimization model is formulated to reflect tradeoff between consumer refueling convenience, onboard storage cost, infrastructure costs, range limitation cost, and ZEV compliance value. Higher pressure increases hydrogen storage volume, driving range, and time between hydrogen refills, but increases the cost of delivery and storage infrastructure (thereby increasing the cost of hydrogen) and the capital cost of the onboard storage system. Long driving range decreases the chance of needing a substitute vehicle for long-distance trips. A driving range exceeding 300 miles is eligible for maximum ZEV credits, based on the current ZEV policy. Both region-wide optimal infrastructure roll-out strategies and cluster strategies are considered.

Specifically, the optimal pressure is solved for by equating the marginal value of increased range due to increased pressure to the sum of the marginal H_2 delivered cost and the marginal onboard storage capital cost, also due to increased pressure. This approach is equivalent to minimization of combined costs of refueling inconvenience, onboard storage system, and stations. The marginal value of increased range due to higher pressure includes three components—the reduced need for using a backup vehicle for long and away-from-station trips, the increased units of ZEV credits, and the reduction of net present value of total refueling time over five years. Refueling time includes access time to station (depends on availability), refueling time at station, and annoyance amplification. The marginal cost of increased pressure includes the resulting increased cost of pumps, tanks, and energy use. Based on discussions with the Fuel Pathways Integration Technical Team (FPITT) of the United States Driving Research and Innovation for Vehicle efficiency and Energy sustainability (U.S.DRIVE) partnership, the published work by University of California, Davis, the DOE's Hydrogen Analysis (H2A) model, and the National Household Travel Survey 2009, the following parameter assumptions are used for the baseline: mid-sized fuel cell electric vehicles (FCEVs) with fuel economy of 60 miles per gallon gasoline equivalent; a representative driver who drives 13,000 miles per year and values refueling travel time at $50/hour; a dispenser linger time of 2.4 minutes; hydrogen filling rate of 1.6 kg/min; $3.27/kg delivered hydrogen cost at 700 bar at 200 kg/d and $2.21/kg at 350 bar at 200 kg/d, both with full utilization (based on H2A models); and Southern California as the regional context and the city of Santa Monica in California as the cluster strategy context.

RESULTS

The optimal pressure found from the study has evolved during the three project years due to modification of optimization scope and context. In summary, FY 2013 results found 700 bar to be more desirable in many region-strategy scenarios. FY 2014 results show that 350 bar or 500 bar can be more competitive in reducing system cost in certain cluster-strategy scenarios. FY 2015 results show strong preferences for 700 bar over 350 bar or 500 bar, because 700 bar is the only one among three pressure levels to enable an over 300-mile range required for maximum ZEV credits. The ZEV credit, based on available credit trading information, is so valuable that the ZEV credit value becomes a dominating factor in the optimization, regardless of driver types.

The pressure of 700 bar can be valuable for consumers with frequent long-distance and away-from-station-cluster trips. To capture driving pattern and driver heterogeneity, six types of drivers and their driving patterns are derived to represent California drivers, as shown in Figure 1, based on the 2009 National Household Travel Survey. In our calculation, 350 bar and 700 bar result in 210 miles and 360 miles of driving range, respectively. For most drivers, they are both adequate in meeting daily travel needs. For FSC (frequent and short commute) drivers who concentrate a substantial portion of the annual 31,100 miles on long-distance trips and require a rental car (an equivalent concept for a substitute vehicle) at $50/day, it could result in a significant penalty, i.e., range limitation cost (which is usually a concern for short-range battery electric vehicles), as much as $205/year for 700 bar and $1,428/year for 350 bar.

The newly added value component on ZEV credits seems to be the dominating factor for the optimal pressure level. A 700 bar pressure enables a driving range of 360 miles, making the vehicle eligible for nine ZEV credits, while driving ranges for vehicles with 350 bar and 500 bar

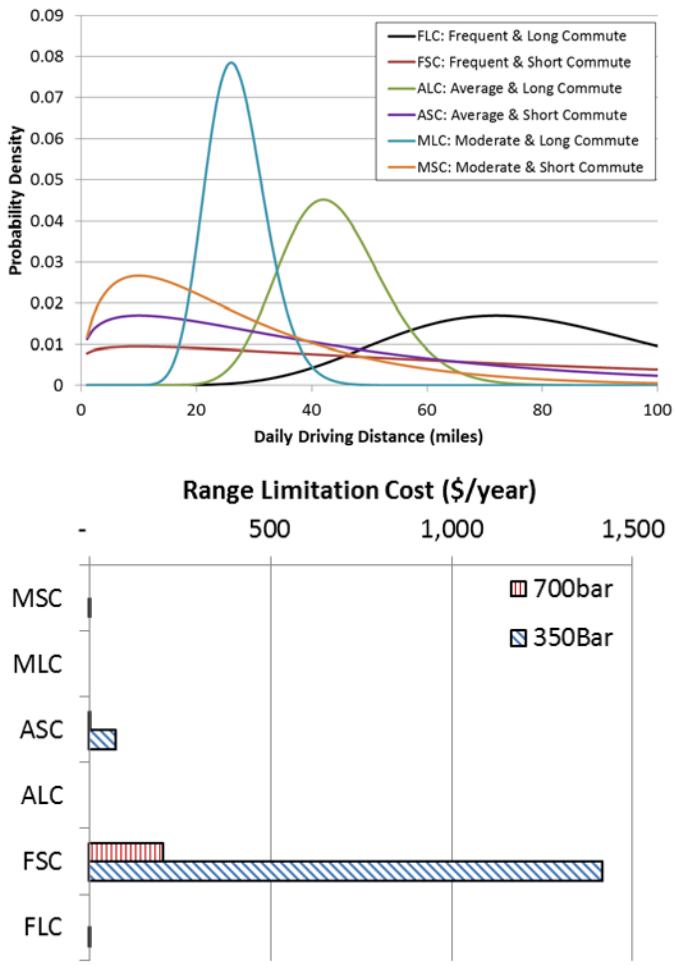

FIGURE 1. Range limitation cost of heterogeneous drivers

tanks are 200–300 miles qualifying the vehicles for only five ZEV credits. If $4,000 is assumed for the value of each ZEV credit, the four-credit gap means $16,000 in revenue lost per vehicle for original equipment manufacturers. This is a significant advantage of 700 bar. As shown in Figure 2, without considering ZEV credits, 350 bar would result in the lowest system cost among the three pressure levels with the cluster strategy for station roll-out, for the FLC (frequent & long commute) drivers. Using nine ZEV credits as the reference and assuming $4,000 as the value of each ZEV credit, we found significant ZEV loss (due to not gaining the full nine ZEV credits) for 350 bar and 500 bar. As a result, 700 bar is a clear winner of the three.

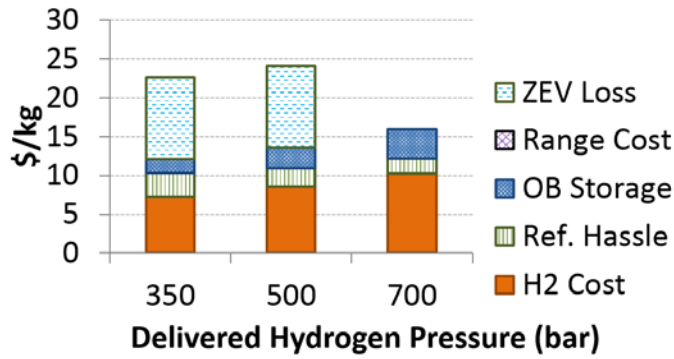

assume cluster strategy in Santa Monica, 1x12 kg/day station (5% fuel availability), 130 FCEVs, $100/hr time value
OB – Onboard

FIGURE 2. Cost components of optimization objective function (FLC drivers)

CONCLUSIONS AND FUTURE DIRECTIONS

The HOP model was upgraded to include range limitation cost and ZEV credits in its objective function. Six types of daily driving patterns were derived to represent California drivers and on which to base the quantitative analysis of range limitation costs.

The pressure of 700 bar is found to be especially valuable for consumers with frequent long-distance and away-from-station-cluster trips. These consumers may still face range limitation even with a 300 mile driving range.

The ZEV value of 700 bar (enabling >300-mile range) is significant enough to overshadow other determining factors.

In-depth optimal pressure analysis for early adopters and integration with consumer choice models is recommended. More research is needed on identifying the optimal pressure for early adopters, for maximizing FCEV market acceptance, and for standardization concerns. Uncertainty of key parameters also requires more analysis.

FY 2015 PUBLICATIONS/PRESENTATIONS

1. Zhenhong Lin, Changzheng Liu, Analysis of Optimal On-Board Storage Pressure for Hydrogen Fuel Cell Vehicles. Presented at the 2015 DOE Annual Merit Review meeting.

IX.12 Infrastructure Investment and Finance Scenario Analysis

Marc Melaina (Primary Contact), Brian Bush, Dan Getman, Jonathan Duckworth, Michael Penev
National Renewable Energy Laboratory
15013 Denver West Parkway
Golden, CO 80401
Phone: (303) 275-3836
Email: Marc.Melaina@nrel.gov

DOE Manager
Fred Joseck
Phone: (202) 586-7932
Email: Fred.Joseck@ee.doe.gov

Subcontractor:
DBA Consulting

Project Start Date: September 1, 2013
Project End Date: Project continuation and direction determined annually by DOE

Overall Objectives

- Provide an independent financial assessment capability that incorporates multiple real-world influences on hydrogen station investments
- Develop a financial analysis tool designed to meet the needs of a range of end users
- Adhere to standard financial analysis methods
- Provide user-friendly and readily accessible tools

Fiscal Year (FY) 2015 Objectives

- Provide analysis capability in the form of an interactive online tool and downloadable spreadsheet
- Develop interface formats that highlight priority results of interest to end users
- Develop a beta version of a visualization tool for full supply chain network financing

Technical Barriers

This project addresses the following technical barriers from the Systems Analysis section of the Fuel Cell Technologies Office Multi-Year Research, Development, and Demonstration Plan:

(A) Future Market Behavior

(E) Unplanned Studies and Analysis

Technical Targets

This project will help facilitate investments in hydrogen refueling stations and improve policy design decisions to support early hydrogen station and fuel cell electric vehicle (FCEV) market development. Ultimately, as early markets evolve, more informed investment decisions will increase station availability and may result in reduced hydrogen costs to consumers. In this way the project facilitates commercialization of FCEVs and contributes to stakeholder coordination efforts to expand hydrogen station networks.

FY 2015 Accomplishments

- A financial analysis framework for hydrogen stations, called the Hydrogen Financial Analysis Scenario Tool (H2FAST), has been developed as an extension of the Hydrogen Analysis (H2A) suite of cost estimation tools. The framework employs standard financial accounting methods, reporting income statements, cash flows, balance statements, as well as a wide range of financial metrics that are readily comprehensible and meaningful to users with a finance background.
- H2FAST has been implemented in website and spreadsheet (Microsoft Excel) tools as well as in a beta version Business Case Scenario (BCS) visualization tool. Each H2FAST tool has been designed for distinct end-user types and needs and has been carefully validated.
  - The web version of H2FAST is simple to use and provides quick, first-cut analyses of multiple station financing options. The intuitive, user-friendly interface provides instant visual and numerical results.
  - The spreadsheet version of H2FAST allows users more control over a larger set of inputs, and it allows for analysis of multiple stations and financial options. It is intended for more advanced users with more detailed information about one or more station projects. The user interface is highly annotated and easy to navigate, and it allows for both basic and advanced modes of interaction.
  - The BCS version of H2FAST, which is in beta development, is intended for more advanced users interested in full supply chain financing and regional or national scenarios of infrastructure dynamics. The interface is based on a general multivariate visualization framework, allowing users access to large volumes of data from detailed scenarios. Additional knowledge of end user requirements is needed to refine this tool.

- The H2FAST scenario is fully integrated with the scenario development and cost optimization capabilities of the Scenario Evaluation, Regionalization, and Analysis (SERA) model. Therefore, all national station and infrastructure rollout scenarios developed using SERA are easily analyzed across the full range of H2FAST financial metrics, and they can be assessed for a wide range of financial strategies and policy support mechanisms.

✧ ✧ ✧ ✧ ✧

INTRODUCTION

Limited availability of hydrogen stations is a significant barrier to the successful commercialization of FCEVs. Investment risk is one of the factors that may inhibit the expansion of hydrogen stations in advance of widespread FCEV adoption. While the U.S. Department of Energy's Fuel Cell Technologies Office has supported extensive cost estimation tools based on engineering principles and vetted by industry experts, these tools have been limited in their ability to explore finance options. This is a barrier to conveying the relevance of hydrogen station investment opportunities to key stakeholders and project partners through existing assessments of station costs and deployment.

Multiple studies have examined hydrogen infrastructure in terms of financial metrics. A 2008 National Academies study conveyed costs in terms of cash flows, highlighting the shortfall period—or "valley of death"—between initial market growth and net positive cash flow [3]. A 2013 Energy Independence Now report incorporated greater detail at the individual station level and examined policy support mechanisms [1]. A 2013 National Academies study examined cash flows in terms of private and social costs and compared a hydrogen scenario with success scenarios for other alternative fuels, with a study goal of examining light-duty vehicle greenhouse gas emission reductions of 80% by 2050 [2]. The development of H2FAST builds on these previous studies, providing a rigorous framework and set of tools that can be used alongside or in conjunction with standard financial tools used in the private sector.

APPROACH

The H2FAST framework is based on the discounted cash flow framework originally implemented in the H2A suite of cost estimation models. This cash flow basis allows future capital costs, such as component replacements or station upgrades, to be treated consistently with upfront capital and annual operating costs. H2FAST extends the financial calculations to develop a much broader range of outputs than is contained in the H2A models. The financial calculations are consistent with Generally Accepted Accounting Principles, and the format and terms used to convey financial results are consistent with standard reports used by private companies. One important difference between H2A and H2FAST is that hydrogen price is a user-defined input in H2FAST, as opposed to a profited-cost result in H2A. (H2FAST does, however, estimate the break-even hydrogen price at which investors would achieve their desired rate of return.) In addition, H2FAST is not a cost estimation tool; users must bring reliable input cost data to the model to obtain meaningful results.

The user interfaces of the web and spreadsheet versions of H2FAST have been designed for financial end users. Reviews of the model interface were completed with members of the H2USA Investment and Finance Working Group, and modifications were made to highlight metrics of greatest interest to target end users. The interfaces enable users to perform many iterations and variations on station financing assumptions and scenarios quickly.

RESULTS

The input panel of the web version of H2FAST is shown in Figure 1. These inputs are a subset of the total range of possible inputs in the analysis framework. A review process identified them as high-priority inputs for the target audience, and their limited number enables use of a simple, easily navigated interface within a web browser. As shown, these inputs are categorized as station inputs, scenario inputs, and financial inputs. Values can be entered directly into input cells or adjusted with sliders. The website opens with default values, taken from Argonne National Laboratory's H2A Refueling Station Analysis Model, which can be restored by clicking on the "reset inputs" button at the bottom of the panel.

The results panel of the web version of H2FAST is shown in Figure 2. The key numerical results shown at the top of the panel are internal rate of return, breakeven hydrogen price, first year of positive earnings before interest, tax, and depreciation, investor payback period, and net present value. In addition, the results panel provides graphs illustrating trends over time; users can select from among 20 different graphs to visualize a wide variety of results. The values and graphs in the results panel update automatically in response to changes in the input panel. Full financial tables can be downloaded for any station scenario simply by clicking a "download results" button, and a brief user's guide is accessible through the "about" link. H2FAST can easily be embedded into other websites as a widget. The version on the National Renewable Energy Laboratory website is located at http://www.nrel.gov/hydrogen/h2fast/.

For financial analyses beyond the capabilities of the web version, users can turn to the spreadsheet version of

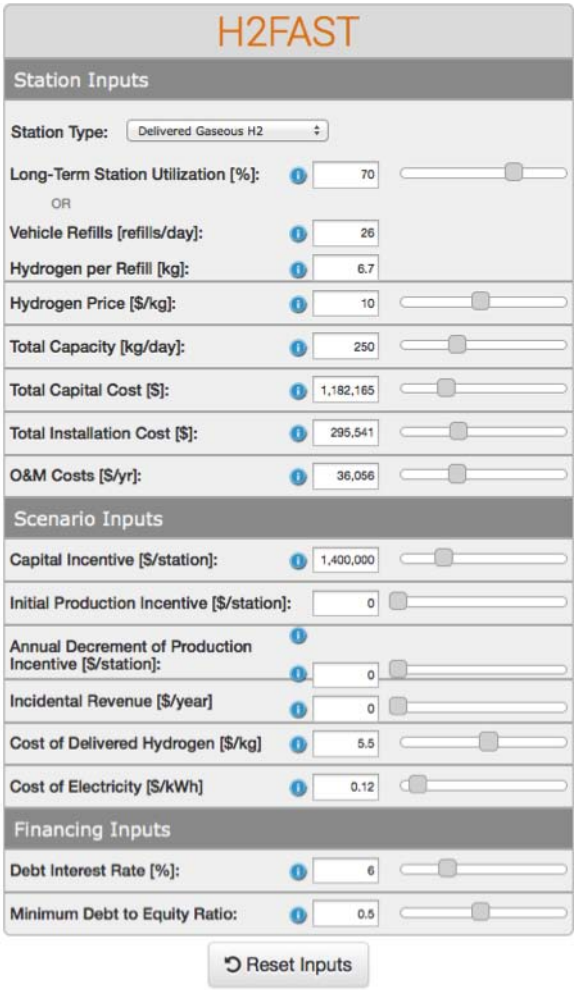

O&M - operating and maintenance

FIGURE 1. Input panel for the website version of H2FAST

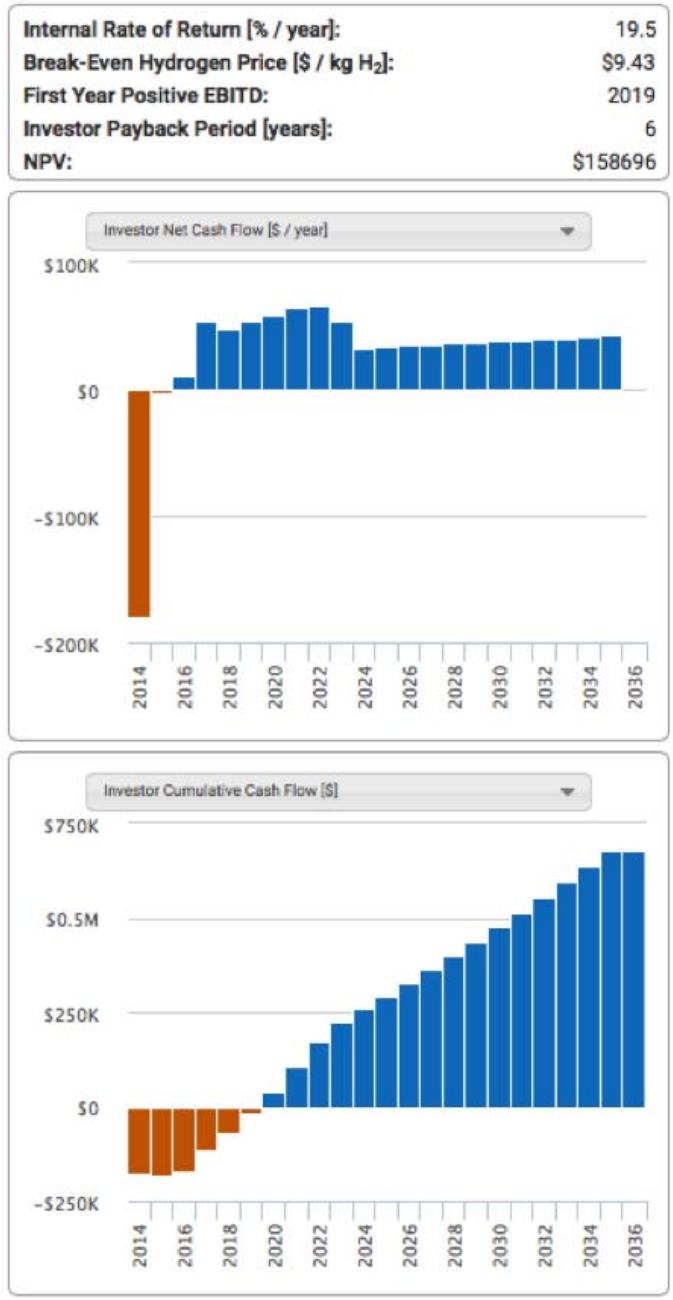

NPV - net present value; EBITD - earnings before interest, taxes, and depreciation

FIGURE 2. Results panel for the website version of H2FAST

H2FAST, which can be downloaded directly from the website version. The spreadsheet version contains many hover-over annotations to orient users, and a draft user's manual is available through the website "about" link. Key capabilities unique to the spreadsheet version include the ability to assess multiple stations individually or as a group, a broader range of inputs that enable more customized financial assessments, and the flexibility of working within a spreadsheet environment. The number of input values can be expanded from basic to advanced mode, depending on the needs of the user. The standard financial calculations have been resolved in closed form, allowing use of other spreadsheet functions, such as Excel's "Goal Seek," for determining relationships between input values and results. For example, a particular subsidy level can be determined precisely for a target (goal) internal rate of return.

Although the H2FAST framework has been deployed across all aspects of the SERA model, results from national or regional scenarios of hydrogen infrastructure rollout can be very data intensive and multifaceted. One means of exploring these results is the BCS visualization version of H2FAST. This map- and web-based tool has only been developed as a beta version, but it may be refined in future work as additional end-user requirements are clarified. The general platform and features of this multivariate visualization tool are reviewed in a brief demonstration video: http://youtu.be/J7y51c-dldo.

CONCLUSIONS AND FUTURE DIRECTIONS

The H2FAST financial framework has been implemented consistently across multiple analysis tools. Because these independently developed tools provide financial assessment capabilities consistent with standard practices within the finance sector, they will be useful to stakeholders involved in real-world hydrogen station projects, including individual companies, government agencies, and project partnerships with multiple stakeholders. User comments on the first version of H2FAST will inform the development of updated versions, and future work may involve applying the framework to other components along the hydrogen supply chain.

SPECIAL RECOGNITIONS & AWARDS/ PATENTS ISSUED

1. Annual Merit Review Award 2015, Systems Analysis: Marc Melaina, Brian Bush, and Michael Penev. http://www.hydrogen.energy.gov/annual_review15_awards.html

FY 2015 PUBLICATIONS/PRESENTATIONS

1. Melaina, M., B. Bush, and M. Penev. 2015. "Overview of Station Analysis Tools Developed in Support of H2USA: Overview of the Hydrogen Financial Analysis Scenario Tool (H2FAST)." Presentation as part of EERE Webinar Series, May 12, 2015. http://energy.gov/eere/fuelcells/downloads/overview-station-analysis-tools-developed-support-h2usa

2. Melaina, M. 2015. "Infrastructure Investment and Finance Scenario Analysis." Presentation at 2015 Annual Merit Review Meeting, June 8-12, Washington, DC. http://www.hydrogen.energy.gov/annual_review15_analysis.html

3. Bush, B., M. Penev, M. Melaina, and J. Zuboy. 2015. *Hydrogen Financial Analysis Scenario Tool (H2FAST): Web Tool User's Manual*. NREL/TP-5400-64020. Golden, CO: National Renewable Energy Laboratory. http://www.nrel.gov/docs/fy15osti/64020.pdf

4. Penev, M., M. Melaina, B. Bush, and J. Zuboy. 2015. *Hydrogen Financial Analysis Scenario Tool (H2FAST): Spreadsheet Tool User's Manual*. Draft Technical Report. Golden, CO: National Renewable Energy Laboratory. http://www.nrel.gov/hydrogen/h2fast/assets/pdfs/h2fast_spreadsheet_user_manual.pdf

REFERENCES

1. Eckerle, T., and R. Garderet. 2013. *Hydrogen Network Investment Plan*. Energy Independence Now. http://www.einow.org/images/stories/factsheets/h2nip_full_paper_final.pdf

2. NRC (National Research Council). 2013. *Transitions to Alternative Vehicles and Fuels*. Washington, D.C.: National Academies Press.

3. NRC (National Research Council). 2008. Transitions to Alternative Transportation Technologies: A Focus on Hydrogen. Washington, D.C.: National Academies Press.

IX.13 The Business Case for Hydrogen-Powered Passenger Cars: Competition and Solving the Infrastructure Puzzle

R. Rosner[1] (Primary Contact), R. Topel[2]
[1]Energy Policy Institute of Chicago [EPIC] and Harris School of Public Policy Studies
[2]EPIC and Booth School of Business
The University of Chicago
Chicago, IL 60637
Phone: (773) 702-0560
Email: rrosner@uchicago.edu

DOE Manager
Fred Joseck
Phone: (202) 586-7932
Email: Fred.Joseck@ee.doe.gov

Project Start Date: February 2015
Project End Date: Project continuation and direction determined annually be DOE

Overall Objectives

- Cost and business case analyses of various key sub-sectors of the hydrogen fuel-based transport sector

Fiscal Year (FY) 2015 Objectives

- A competitive analysis of a variety of alternative fuel passenger cars, focusing on the total cost of ownership, with a particular emphasis on the current and expected competitive posture of hydrogen-powered passenger cars
- A business case analysis for commercial hydrogen filling stations that serve the prospective hydrogen passenger car market

Technical Barriers

- Uncertain learning curves for hydrogen-based vehicle manufacturing, especially for fuel cells
- Uncertainties regarding marketplace acceptance

Contribution to Achievement of DOE Milestones

- Establishment of the current and prospective competitive posture of hydrogen-powered passenger vehicles vis-à-vis passenger vehicles using other fuel technologies
- Establishment of investment opportunities for commercial hydrogen fueling stations aimed at the passenger car market

FY 2015 Accomplishments

- Completed competitive total cost of ownership analysis for hydrogen-powered vehicles, as compared to cars using other fuel technologies
- Completed cost data collection for a business case analysis for investing in hydrogen fueling stations

✧ ✧ ✧ ✧ ✧

INTRODUCTION AND APPROACH

Our analyses entail two distinct procedures. First, we are engaged in a broad effort to collect extant cost data for both vehicles and hydrogen fueling stations, focusing in particular on both bounding costs from above and below (e.g., most and least expensive), as well as obtaining statistical information, when available, for the uncertainties in these cost estimates. Second, we have developed a costing model for establishing the lifetime total cost of vehicle ownership (TCO), used in our competitive vehicle cost analysis. In addition, we are using the National Renewable Energy Laboratory's (NREL's) Hydrogen Financial Analysis Scenario Tool (H2FAST) to compute the investment picture for building and operating hydrogen filling stations, based on the cost parameters we have been establishing. In all cases, we are vetting our analyses with experts versed in the hydrogen-based transport sector at Argonne National Laboratory, as well as with one of the key automobile vendors active in the hydrogen transport sector.

RESULTS

As part of the lifetime competitive cost analysis for hydrogen-powered vehicles, we have expanded beyond our presentation at the DOE Annual Merit Review and Peer Evaluation meeting (AMR) [1] by developing a Monte Carlo-based statistical analysis that now allows us to conduct error analyses of our results. That is, based on our assessment of the uncertainties associated with the various cost components for car ownership, we are now able to provide uncertainties for the TCO. The results of this analysis are presented in Figure 1.

As part of a related sensitivity analysis, we have identified the purchase price of the vehicles as the key contributor to TCO uncertainties in the out years. In the case of hydrogen-powered vehicles, this uncertainty appears to be dominated by uncertainties related to the cost of the hydrogen fuel cell. We are currently investigating what is currently

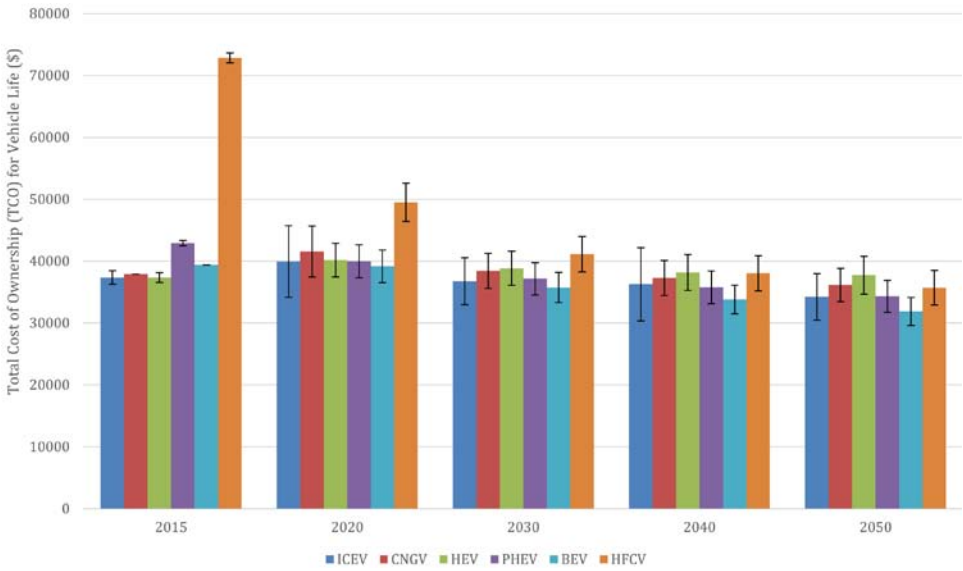

FIGURE 1. Total cost of ownership for vehicle life. This figure shows the results of our new uncertainty analysis for the TCO for vehicles acquired in 2015 through 2050 (internal combustion engine vehicle [ICEV] = Toyota Camry, gasoline-powered; compressed natural gas vehicle [CNGV] = Honda Civic natural gas-powered; hybrid electric vehicle [HEV] = Toyota Camry hybrid; plug-in hybrid electric vehicle [PHEV] = Chevy Volt hybrid plug-in; battery electric vehicle [BEV] = Ford Focus battery-powered; hydrogen fuel cell vehicle [HFCV] = Toyota Mirai hydrogen-powered). Error bars indicate the results of a Monte Carlo statistical analysis, based on uncertainties in our model's input cost data.

understood about potential cost reductions in fuel cells, based both on recourse to alternate membrane technologies as well as the cost reductions associated with 'learning' as production of fuel cells ramps up.

We are using a combination of NREL's H2FAST investment tool and our own analysis of the various cost factors entering into the building and operation of a commercial hydrogen filling station, to build a first analysis of the investment picture for such a facility. Because commercial exploitation of this market is relatively recent, there are insufficient data to develop a statistical uncertainty analysis; instead, we are developing bounds on the various cost factors, based on the most expensive and least expensive cost numbers to be found in the extant literature.

CONCLUSIONS AND FUTURE DIRECTIONS

By the end of FY 2015, we will finish our TCO competitive cost analysis. Two memos will be prepared: one detailing the input data used in our cost analysis, the second providing the detailed results of our TCO analysis.

In the case of the hydrogen filling station business plan, we are completing our investment analysis using H2FAST. This analysis will result in a memo, to be completed by the end of FY 2015, detailing the business case, including our bounding analysis for the various cost factors entering into the construction and operation of hydrogen filling stations.

REFERENCES

1. R. Rosner and R. Topel, *The Business Case for Hydrogen--powered Passenger Cars: Competition and Solving the Infrastructure Puzzle,* Presented at the 2015 DOE Hydrogen and Fuel Cells Program Annual Merit Review, June 2015.

IX.14 Retail Marketing Analysis: Hydrogen Refueling Stations

Kent Schlesselman (Primary Contact),
Debbie Miggins, Selen Onel
Kalibrate
4343 S. 118th E. Ave., Suite C
Tulsa, OK 74146
Phone: (918) 877-6974
Email: Kent.Schlesselman@Kalibrate.com

DOE Manager
Fred Joseck
Phone: (202) 586-7932
Email: Fred.Joseck@ee.doe.gov

NREL Subcontract Number: AFC-4-23056-01

Project Start Date: December 17, 2013
Project End Date: December 17, 2014

Overall Objectives

- Develop an analytic approach to prioritize and identify the best locations for hydrogen refueling stations
- Apply this framework to California to prioritize station network expansion beyond existing and planned locations

Fiscal Year (FY) 2015 Objectives

This project is complete.

Technical Barriers

This project addresses the following technical barriers from the Systems Analysis section (4.5) of the Fuel Cell Technologies Office Multi-Year Research, Development, and Demonstration Plan:

(A) Future Market Behavior

(D) Insufficient Suite of Models and Tools

(E) Unplanned Studies and Analysis

FY 2015 Accomplishments

- Objectively evaluated locations
  - Determined supply and demand variables
  - Determined dependent and independent variables
  - Identified competitive area or trading area size for aggregating data
  - Established weights on variables
  - Ranked 30,620 traffic points
- As a complement to Spatially & Temporally Resolved Energy & Environmental Tool (STREET) and cluster studies, proposed locales for refueling stations based on rankings
  - Identified attractive areas outside a competitive distance from current/existing and planned hydrogen refueling stations (Coverage Network)
  - Identified attractive areas in the major urban areas of Los Angeles and San Francisco, offering minimal competition with current/existing and planned hydrogen refueling stations (Urban Incremental Network)

✧ ✧ ✧ ✧ ✧

INTRODUCTION

The availability and proper placement of retail hydrogen refueling stations is critical to the successful market adoption of fuel cell electric vehicles (FCEVs) by consumers and to ensure successful transition to hydrogen as a viable transportation fuel. It is important to establish a network of hydrogen refueling stations that will instill confidence in consumers that they can travel throughout the marketplace with minimal concern about where they can refuel their FCEVs. As of October 6, 2014, there were only 10 hydrogen refueling stations available to the public in the state of California and 42 planned stations that were not yet operational. The only other states having at least one public hydrogen refueling station were South Carolina and Connecticut. In September 2013, the California state legislature approved a bill to fund at least 100 hydrogen refueling stations in California with a commitment of up to $20 million a year to 2023 through the California Energy Commission's Alternative and Renewable Fuel and Vehicle Technology Program (ARFVTP).

For this project, Kalibrate is challenged with determining the key factors for introducing the hydrogen refueling station infrastructure so that FCEVs can gradually replace gasoline internal combustion engine vehicles. As an application of this analytic capability, these key factors are used to determine the number of hydrogen refueling stations required to establish a refueling infrastructure in California, prioritizing the best locations for new station networks. Results from this analytic capability can contribute to stakeholder efforts to determine the best locations for additional hydrogen refueling stations in preparation for the widespread release of FCEVs to the public.

APPROACH

- Through detailed statistical analysis, determine a set of supply and demand variables suitable for evaluating locations for hydrogen refueling stations
- Then, using a ranking tool, rank locations throughout the State of California based on these variables
- Apply the ranking to determine areas most attractive for hydrogen refueling stations

RESULTS

- Identified dependent and independent variables necessary to develop model for ranking locations for hydrogen refueling stations
- Ranked 30,620 geographic points across the State of California according to their attractiveness for hydrogen fuel cell electric vehicle refueling (Figure 1)
- Building on the STREET model results and cluster strategies, used the rankings of 30,620 points to identify attractive areas that are unlikely to compete with current/existing and planned hydrogen refueling stations (Coverage Network) (Figure 2) and to identify attractive areas in the major urban areas of Los Angeles and San

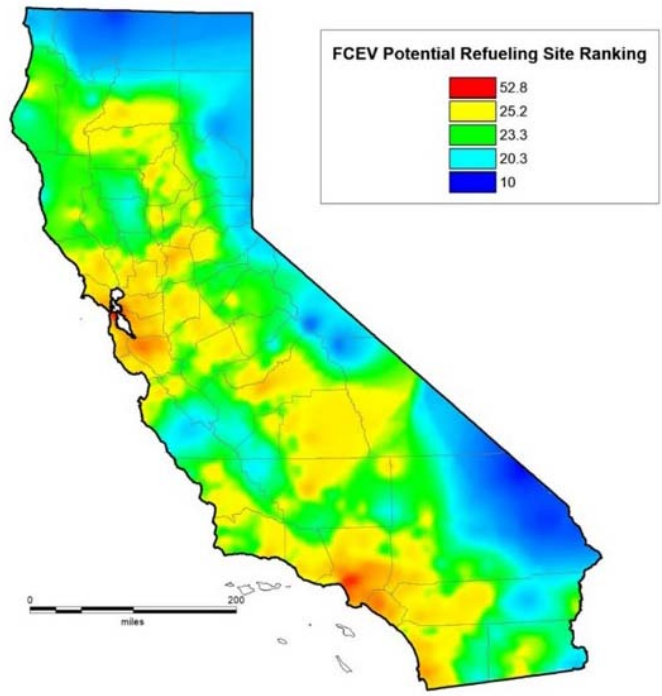

FIGURE 1. Thermal map of ranked locations across the State of California

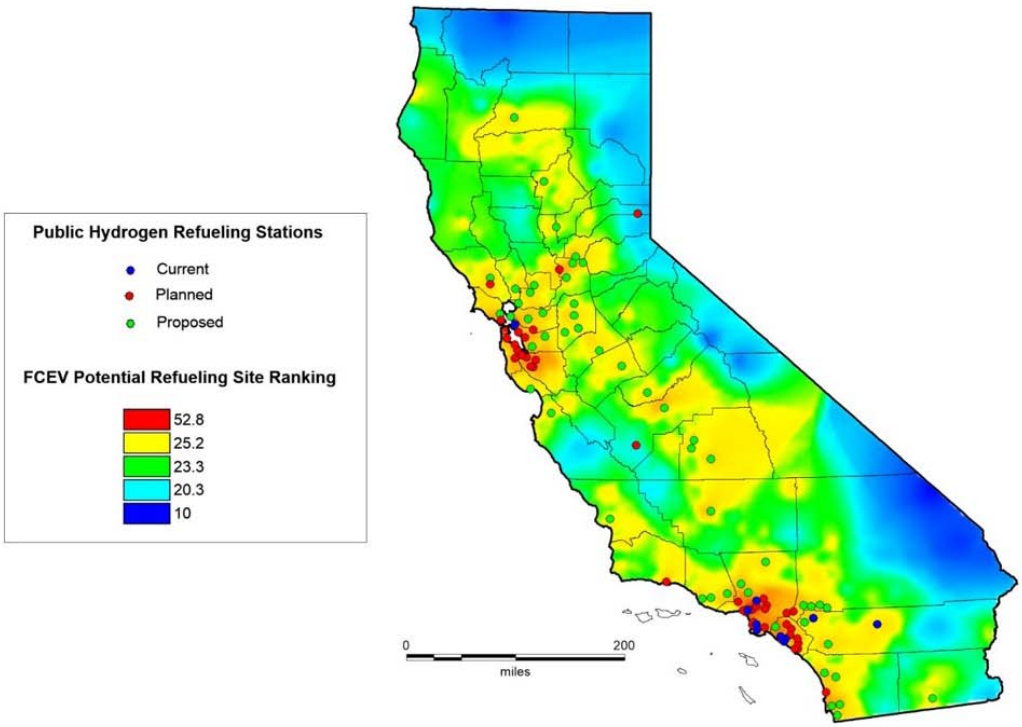

FIGURE 2. Thermal map of ranked locations with proposed coverage network as a complement to current and planned stations

Francisco, offering minimal competition with current/existing and planned hydrogen refueling stations (Urban Incremental Network) (Figure 3 and 4)

CONCLUSIONS AND FUTURE DIRECTIONS

This specific project, "Retail Marketing Analysis: Hydrogen Refueling Stations" for the State of California, is complete.

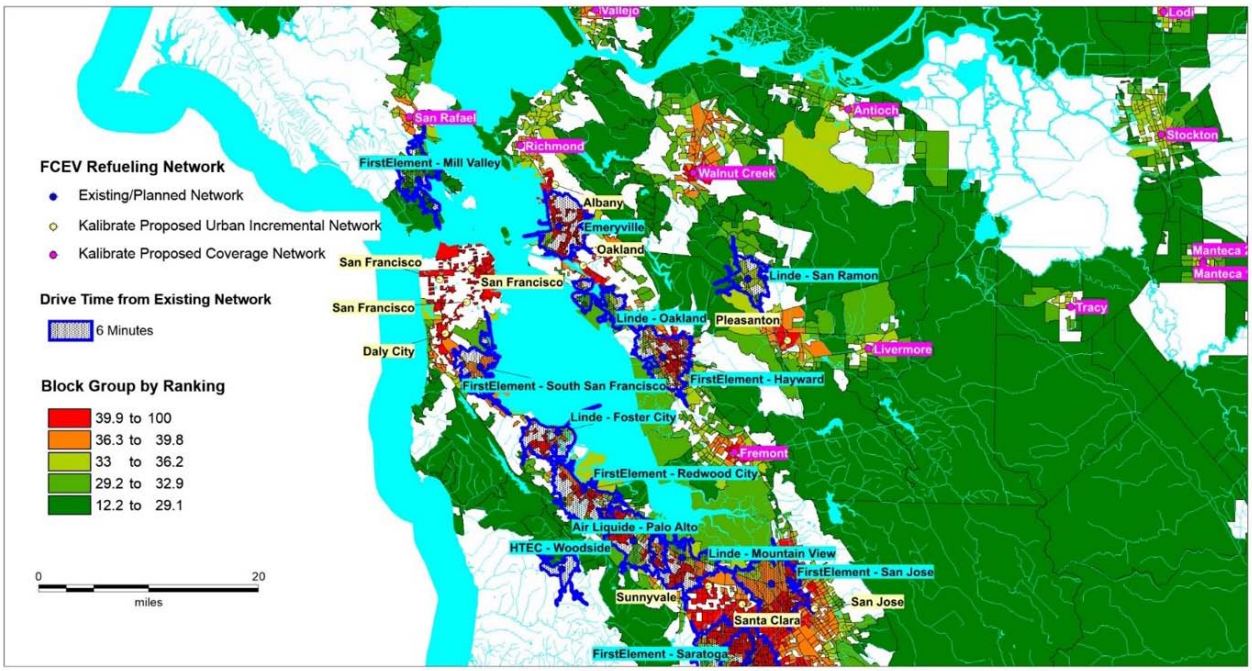

FIGURE 3. Urban Incremental Network and Coverage Network relative to six minute drive time around existing and planned hydrogen refueling stations in San Francisco Bay Area

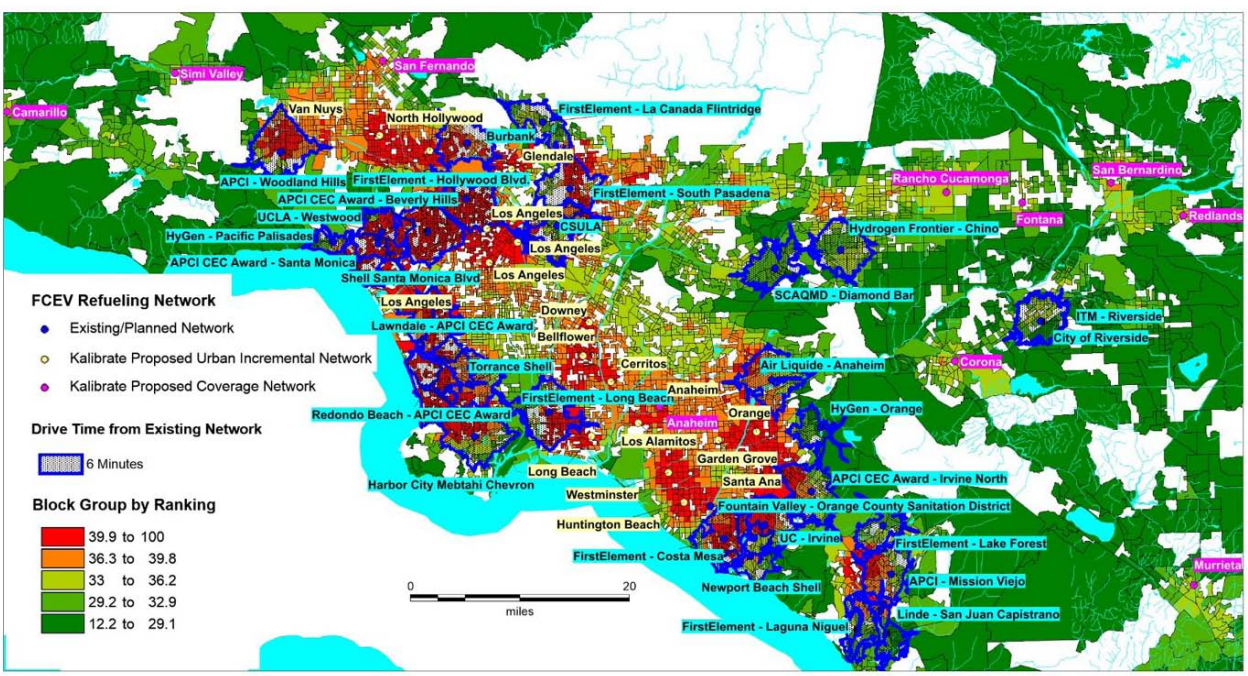

FIGURE 4. Urban Incremental Network and Coverage Network relative to six minute drive time around existing and planned hydrogen refueling stations in Greater Los Angeles Area

Given the opportunity for additional work, Kalibrate can assist with additional projects.

- Similar work in other geographies, other U.S. states or regions
- Develop a tool to provide instant analysis of ranked map points
- Given a sufficiently developed infrastructure of hydrogen refueling stations, creation of a full featured network planning tool for the industry
- Contribute to National Renewable Energy Laboratory infrastructure simulation capabilities by improving on station sizing, footprint restrictions, market saturation, and inter-station demand shifting algorithms

FY 2015 PUBLICATIONS/PRESENTATIONS

1. Thompson, I., "Retail Marketing Analysis: Hydrogen Refueling Stations," 2015 DOE Hydrogen and Fuel Cells Program Annual Merit and Peer Evaluation Meeting, June 2015 (presentation).

2. Kalibrate Technologies plc, "Retail Marketing Analysis Hydrogen Refueling Stations," NREL Subcontract No.: AFC-4-23056-01, December 2014 (report).

X.0 Market Transformation Sub-Program Overview

INTRODUCTION

The purpose of the Market Transformation sub-program is to spur market growth for domestically produced hydrogen and fuel cell systems. The Market Transformation sub-program is conducting activities to help promote and implement commercial and pre-commercial hydrogen and fuel cell systems in real-world operating environments and to provide feedback to research programs, United States industry manufacturers, and potential technology users. By supporting increased technology operations testing and use in key early applications, this sub-program helps to identify and overcome non-technical barriers to commercial deployment and to reduce the life-cycle costs of fuel cell power by helping to achieve manufacturing economies of scale. These early market deployments will also address other market acceptance factors, resulting in further expansion of technology opportunities.

The Market Transformation sub-program aims to replicate past successes in material handling equipment (MHE) (e.g., lift trucks) and emergency backup power applications that were part of the American Recovery and Reinvestment Act of 2009 (Recovery Act). For example, Market Transformation has projects in applications like fuel-cell-powered airport ground support baggage tractors and fuel cell electric medium-duty hybrid trucks for parcel delivery applications. These projects are highly leveraged, with an average of more than half of the projects' funds being provided by DOE's partners. Partners providing resources and financial investment to these projects show their high level of interest in continuing to explore these applications and markets, and this level of industry interest is very promising for the potential growth of the domestic fuel cell industry. Market Transformation also partners with other federal agencies and various stakeholders to deploy new applications such as auxiliary power for ships in port and onboard ocean-going vessels in collaboration with the U.S. Department of Transportation Maritime Administration.

GOAL

Market Transformation activities provide financial and technical assistance for the use of hydrogen and fuel cell systems in early market applications, with the key goals of achieving sales volumes that will enable cost reductions through economies of scale, supporting the development of a domestic industry, and providing feedback to testing programs, manufacturers, and potential technology users.

OBJECTIVES

The objectives of the Market Transformation sub-program are as follows.

- Evaluate the status against target performance metrics for commercially available emergency backup, MHE, and other systems and provide feedback to component suppliers regarding cost reduction opportunities
- Test emerging approaches to grid management using renewable hydrogen
- Advance the knowledge and expertise of waste-to-energy fuel, shipboard, and truck auxiliary power units (APUs), fuel cell electric truck parcel delivery, and aviation ground support applications through targeted testing and evaluation efforts in coordination with the Technology Validation sub-program and in partnership with the U.S. Navy, the U.S. Marine Corps, and civilian agencies such as the U.S. Department of Transportation's Maritime and Federal Aviation Administrations
- Identify lessons learned from promulgated policies and regulations and promote the development of the most effective and applicable incentives for hydrogen and fuel cell technologies
- Conduct market transformation deployment projects to enable life-cycle cost and performance of fuel-cell-powered lift trucks and emergency backup power systems to be on par with conventional technologies

FISCAL YEAR (FY) 2015 TECHNOLOGY STATUS AND ACCOMPLISHMENTS

Fuel cells have been enjoying growing success in key early markets, particularly in MHE and backup power applications. The sub-program's early market deployment efforts, including Market Transformation funding and Recovery Act funding, have successfully catalyzed a significant level of market activity in these areas, which has been accompanied by substantial reductions in the price of fuel cells. For example, material handling and backup power

orders are up 18% this year (see DOE Records 15003 and 15004) from the cumulative total orders in 2009 through 2014. Ongoing activities and additional areas of interest include the following.

- **Hydrogen Energy Storage Project:** This project is supporting the demonstration of a hydrogen energy storage system as a grid management tool. While hydrogen produced from the system could be used in a variety of value-added applications, the initial phase of the project will use the hydrogen in fuel cell buses operated by the County of Hawaii Mass Transportation Agency and the National Park Service. This year, site planning and preparation were finalized in preparation for installing and operating the system. (Naval Research Laboratory and the State of Hawaii)
- **Ground Support Equipment (GSE) Demonstration Project:** This project is demonstrating the value proposition of using fuel-cell-powered tow tractors as a cost-competitive and more energy efficient solution compared to incumbent internal combustion engine (ICE)-powered vehicles. This effort will address concerns regarding the weatherproofing of fuel-cell-powered GSE and enable end users at a Federal Express terminal to accomplish their daily tasks while reducing consumption of gasoline and diesel fuels. This project commissioned a fleet of 15 GSE units, which are now operating at the Federal Express hub at the airport in Memphis, Tennessee. (Plug Power)
- **Maritime Fuel Cell Generator Project:** This project is demonstrating the use of fuel cell power for refrigeration APUs onboard sea vessels and at pier side to reduce petroleum use and greenhouse gas emissions. Design development has been accomplished and a prototype unit has been assembled and installed and is now in active operations at the Honolulu, Hawaii, port. (Sandia National Laboratories)
- **Fuel Cells in Hybrid Electric Trucks Project:** This project is demonstrating the value of using fuel-cell-powered parcel delivery trucks as a more energy efficient solution compared to incumbent ICE-powered vehicles. This year, the project completed the modeling of duty cycle and a power system preliminary design for the prototype truck. (Center for Transportation and the Environment)

BUDGET

The FY 2015 appropriation was $3 million, and $3 million was requested again for FY 2016 (Figure 1).

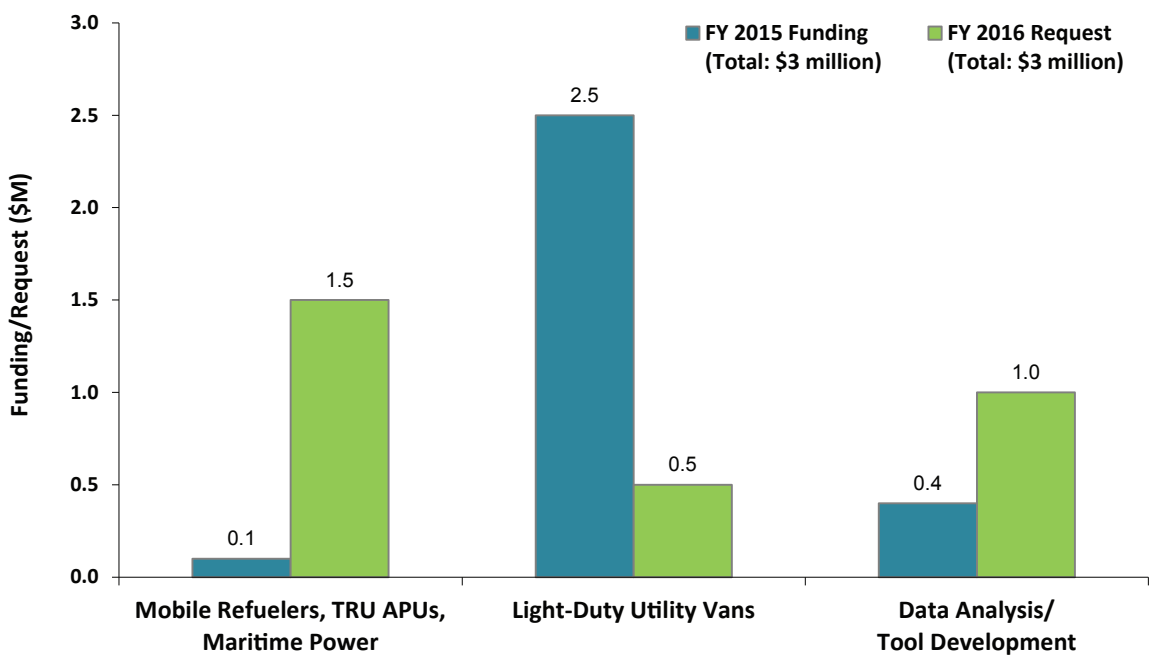

FIGURE 1. Market Transformation R&D Funding. Subject to appropriations, project go/no-go decisions, and competitive selections. Exact amounts will be determined based on research and development progress in each area and the relative merit and applicability of projects competitively selected through planned funding opportunity announcements.

FY 2016 PLANS

In FY 2016, the sub-program will continue to collect and analyze data for on-going and completed projects. A new activity will be initiated to design and deploy fuel-cell-battery-powered hybrid light-duty vehicles for commercial uses such as dispatch utility applications. Strategies for road vehicle market entry and refueling station development, including risk management with respect to safety, environmental, and siting requirements, will be a priority. Business analysis and case studies for newly developed applications will be developed. Collection and evaluation of data from these projects will provide the basis for verifying the business cases for various early market fuel cell systems, as well as providing an assessment of the performance of these integrated systems. Data will be made publicly available so that more potential customers will become aware of the benefits of integrated hydrogen and fuel cell systems. In addition, a near-term priority will be to continue collaborating with other federal agencies—in accordance with existing interagency cooperative agreements such as the DOE-Department of Defense memorandum of understanding—to increase the use of fuel cells in market-ready applications and to increase awareness of the benefits of these deployments. A potential new activity that could be initiated subject to Congressional appropriations is the deployment of mobile refueling trucks subscription refueling use to support the commercialization of fuel-cell-battery-powered light-duty automobiles in various part of the country.

Pete Devlin
Market Transformation Project Manager
Fuel Cell Technologies Office
Office of Energy Efficiency and Renewable Energy
U.S. Department of Energy
1000 Independence Ave., SW
Washington, D.C. 20585-0121
Phone: (202) 586-4905
Email: Peter.Devlin@ee.doe.gov

X.1 Ground Support Equipment Demonstration

Jim Petrecky
Plug Power
968 Albany-Shaker Road
Latham, NY 12110
Phone: (518) 817-9124
Email: James_Petrecky@plugpower.com

DOE Manager
Peter Devlin
Phone: (202) 586-4905
Email: Peter.Devlin@ee.doe.gov

Contract Number: DE-EE0006093

Project Start Date: January 2013
Project End Date: April 2017

Overall Objectives

- To create a hydrogen fuel cell-based solution as a cost-competitive and more energy-efficient baggage tow tractors (airport vehicle) compared to the incumbent internal combustion engine-powered vehicles
- To enable airport end users to accomplish their daily tasks with a hydrogen fuel cell solution while reducing consumption of gasoline and diesel fuels, reducing demand for petroleum in the United States
- To demonstrate lower carbon emissions with fuel cells
- To demonstrate a value proposition that shows decreased energy expenditures when compared to diesel-powered airport vehicles

The project objectives are listed in Table 1.

Fiscal Year (FY) 2015 Objectives

- Develop the 80-V fuel cell product for baggage tow tractor (BTT)
- Test with Charlatte CT5E baggage tow tractor
- Perform factory acceptance test to demonstrate equivalent operation as battery/internal combustion engine tow tractors
- Conduct site planning to install hydrogen at host site
- Start of the demonstration

Technical Barriers

- Upsizing GenDrive architecture from current 48-V product to 80-V product
- Weatherproofing for outdoor application

Technical Targets

Technical targets for this project are listed in Table 2.

FY 2015 Accomplishments

- Conducted operator and fire safety training on fuel cell systems and hydrogen infrastructure
- Hosted Memphis Fire Services Bureau for review
- Received permitting for hydrogen site
- Commissioned the fleet of 15 fuel cell cargo tractors and liquid hydrogen infrastructure site
- Conducted a site event including the DOE, FedEx Express, Plug Power, and Steve Cohen (US Congressman for Tennessee, 9th District)

✧ ✧ ✧ ✧ ✧

TABLE 1. Specific Project Objectives and Expectations

DOE Project Objectives	Plug Power-FedEx Project Expectations
Reduce petroleum consumption	Each BTT uses ~2 gal/hr. Total BTT run time of 15 BTT's over 2 years will be upwards of **175,200 gallons of diesel fuel reduced.**
Reduce emissions at airports	AT 9.8 kg CO2 per gal of diesel, there will be upwards of **1717 metric tonnes of CO2 eliminated at airports.**
Operate 10 hrs/day & 5,000+ hours	BTT operation occurs during two shifts: day (10AM-2 PM) and night (10PM-2AM). The total clock day is 10AM-2PM (16 hours). **Actual BTT activity is 8 hours per day. Total run time of 15 BTT's over 2 years will be upwards of 87,600 fleet hours.**
Towing capability of 3,000 to 6,000 lbs.	The BTT will be able to tow 4 FedEx containers each weighing 40,000 lbs. The corresponding **drawbar capacity of the fuel cell-powered BTT is 5,000 lbs.**
Accelerated development of FC-powered GSE	**Fleet of 15 80V fuel cell systems in real world application in 2013 gaining significant field experience while allowing a premier BTT end user to evaluate for larger deployments.**

FC - fuel cell; GSE - ground support equipment

TABLE 2. Project Technical Targets

Comparison of BTT Specifications (Fuel Cells vs. Diesel and Battery)					
Specifications	**Units**	**Current GenDrive (48V MHE)**	**Proposed GenDrive (80V BTT)**	**Diesel[1] (Tug MA Model)**	**Battery (80V)**
Startup Time[2]	min @ 0 °C	0	0	15	0
Maximum Output Power (kW) [3]	kW	10	~20	36.5 - 64 [4]	10 @ 5 hrs
Minimum Output Power (kW) [5]	kW	0	0	3.6 - 6.4	
Energy Storage Capacity @ Rated Efficiency [6]	kW-hr	26.7	37.1	147.1	29
Run Time [7]	hrs	~ 8	8-10 (full shift)	7.75	~ 4-6
Operating Temperature Range [8]	deg C	-22°–104°F	-22°–140°F	See note 8.	-4°–140°F
Durability (power degradation with time) [9]	%	10%	10%	Minimal	80%
Fuel Cell Stack and Battery Voltage Degradation [10]	%	0%	0%	-	14%
Cycle Life	cycles	NA	NA	NA	1000 - 1200
Electrical Efficiency	%	45%	45%	20%	58% from grid
Refueling / Recharging Time	minutes	2	2	5	480
Availability	%	> 95% (~98.5%)	> 95% (~98.5%)	> 80%	> 95%
Scheduled Maintenance [11]	hrs	2,000	1,000	1000	200
Estimated Mean Time Between Failure (MTBF) [12]	hrs	425	250-500	250	1000
Emissions (CO) Level @ BTT	kg CO / unit	0	0	9.8 / gallon	0

[1] Diesel Tug MA model used a representative diesel BTT. This is a very popular model in used in the BTT market.
[2] Diesel generally need to be started for 15 to 20 minutes before usage at freezing or below. (Customer engagement interviews)
[3] Maximum output for batteries is rated at 5 hours. Battery capacity assumed to be 625 A-hr.
[4] Net brake hp at governed RPM. The range represents the different engines that can be selected.
[5] No minimum turndown for GenDrive or battery. Minimum turndown for diesel engines is typically 10% of rated power.
[6] Energy Storage * Efficiency = Storage Capacity. Diesel BTT holds 15.5 gallons. Diesel has 37.95 kW-hr per gallon. Hydrogen has 33 kW-hr per kg.
[7] Run time for diesel is calculated by dividing 15.5 gallon tank by 2 gallons per hour consumption. Significant energy is consumed by idlng.
[7] The batteries and fuel cell don't need as much energy onboard because energy is only consumed when needed (little idling) and due to regenerative braking.
[8] See note 2. Diesel engine needs to warm up before usage in freezing temps. Available energy run time drops by 40-60% in freezing conditions.
[8] At very cold temps, diesel engines use resistive heaters in the intake manifold to warm the inlet air for starting or until the engine is warm.
[8] Diesel fuel is also prone to waxing or gelling in cold weather. Number 2 diesel begins to cloud at 32 deg F due to the paraffin in the fuel solidifying.
[9] By definition, battery voltage (power) degrades to 20% of the state of charge at fully charged condition.
[10] Fuel cells are able to maintain output voltage throughout the shift. Batteries will drop 14% from 100% state of charge (SOC) to 20% SOC.
[11] Scheduled maintenance for fuel cells is air filter replacement. This will increase in frequency for BTT from MHE due to additional contaminants at airport.
[11] Diesel engine maintenance include oil changes, oil filters, and air filters. Battery maintenance include equalization charges once per month at a minimum.
[12] Demonstration-level fuel cells will have roughly 10 maintenance calls per year. This is expected to decrease to 5-6 with field experience

INTRODUCTION

This project will deploy 15 fuel cell-powered units for two years at FedEx Express' busiest airport. The project is planned for two phases. The first is a one-year development phase where Plug Power develops, builds and tests the 80-V (~20 kW) fuel cell system for the BTT application. The second is a two-year demonstration where a fleet of BTTs are integrated into Charlatte CT5E electric tow tractors and deployed at the FedEx locations under real world conditions. The fuel cell fleet will be fueled by a GenFuel hydrogen compression, storage, and dispensing solution.

APPROACH

Plug Power will design an 80-V fuel cell system as a drop in place replacement of an electric Charlatte tug (see Figure 1).

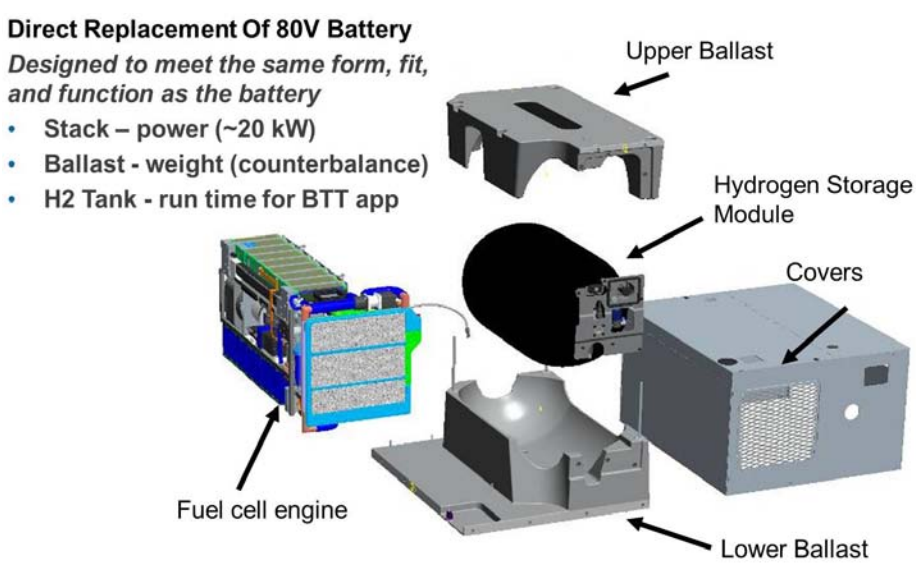

FIGURE 1. Direct replacement of 80-V battery

Hydrogen will be supplied to the tugs via GenFuel hydrogen infrastructure that will provide onsite hydrogen at 350 bar to be dispensed directly to the fuel cell in the tug (see Figure 2).

- Definition of Requirements – complete
- Alpha Prototype – complete
- BTT Beta Builds – complete
- BTT Testing and Certification – complete
- Site Preparation – complete
- Commissioning – complete
- First Year of Demonstration – second quarter (Q2) of 2015 to Q2 2016
- Assessment after Year 1 – Q2 2016
- Demonstration – Q2 2016 to Q2 2017
- Assessment after Year 2 – fourth quarter 2017

FIGURE 2. Hydrogen solution

RESULTS

The kickoff of the project occurred on March 27, 2013. Results will be communicated in quarterly reports later this year.

CONCLUSIONS AND FUTURE DIRECTIONS

The first year of the demonstration is underway. Data and field performance are being collected. Conclusions will be drawn as the demonstration continues on. Future directions will depend on performance and will be reported on in the 2016 update.

X.2 Maritime Fuel Cell Generator Project

Joe Pratt (Primary Contact)
Sandia National Laboratories
PO Box 969, MS-9051
Livermore, CA 94551
Phone: (925) 294-2133
Email: jwpratt@sandia.gov

DOE Manager
Peter Devlin
Phone: (202) 586-4905
Email: Peter.Devlin@ee.doe.gov

Subcontractor
Hydrogenics, Mississauga, Ontario, Canada

Project Start Date: September 15, 2013
Project End Date: March 31, 2015

Overall Objectives

- Lower the technology risk of future port fuel cell deployments by providing performance data of hydrogen polymer electrolyte membrane (PEM) fuel cell technology in this environment
- Lower the investment risk by providing a validated business case assessment for this and future potential projects
- Enable easier permitting and acceptance of hydrogen fuel cell technology in maritime applications by assisting U.S. Coast Guard (USCG) and the American Bureau of Shipping (ABS) develop hydrogen and fuel cell codes and standards
- Act as a stepping stone for more widespread shipboard fuel cell auxiliary power unit deployments
- Reduce port emissions with this and future deployments

Fiscal Year (FY) 2015 Objectives

- Enable new maritime-specific regulations for hydrogen and fuel cells
- Enable new user experiences
- Lower technology and business risk
- Maintain hydrogen infrastructure capability on Oahu in support of this and future strategic projects

Technical Barriers

This project addresses the following technical barriers from the Market Transformation section of the Fuel Cell Technologies Office Multi-Year Research, Development, and Demonstration Plan:

(A) Inadequate standards and complex and expensive permitting procedures

(E) A lack of flexible, simple, and proven financing mechanisms

(F) Inadequate user experience for many hydrogen and fuel cell applications

Technical Targets

No specific technical targets have been set.

FY 2015 Accomplishments

- Finished prototype design
- Completed hydrogen supply plan
- Finished site preparations
- Satisfactorily completed Factory Acceptance Testing of the prototype
- Performed site-specific quantitative risk assessment
- Began broad outreach campaign
- Obtained final USCG design and operating approval
- Performed on-site hydrogen safety and awareness training for over 200 Young Brothers Ltd. (YB) personnel, first responders, the USCG, and other stakeholders
- Provided product development leverage for technology supplier
- Supported Hickam hydrogen fueling station
- Provided leverage for a new, high capacity hydrogen delivery trailer

✧ ✧ ✧ ✧ ✧

INTRODUCTION

Fuel costs and emissions in maritime ports are an opportunity for transportation energy efficiency and emissions reduction efforts. For example, a 2004 study showed the Port of Los Angeles had average daily emissions exceeding that of 500,000 vehicles [1]. Diesel fuel costs continue to rise as low-sulfur limits are imposed, making

power generation more expensive for fleets. Hydrogen fuel cells have the potential to meet the electrical demands of vessels in the port as well as supply power for other port uses such as yard trucks, forklifts, and other material handling specialty equipment. Validation of the commercial value proposition of both the application and the hydrogen supply infrastructure is the next step towards widespread use of hydrogen fuel cells in the maritime environment, and is determined by meeting necessary equipment and operating costs and customer expectations such as reliability, form and function.

Sandia National Laboratories' recent report, "Vessel Cold-Ironing Using a Barge Mounted PEM Fuel Cell: Project Scoping and Feasibility," identified several opportunities for demonstrating technical and commercial viability of a fuel cell in the maritime environment [2]. One identified opportunity is in Honolulu Harbor at the YB wharf. YB provides barge transport of goods between Oahu and the Hawaiian neighbor islands and is an ideal demonstration location because of their high fuel costs and corporate interest in low emission, low environmental impact solutions (Figure 1). YB uses refrigerated containers ("reefers"), which keep perishable goods cold while on the dock and on the barge by using dedicated diesel generators mounted inside mobile 20-foot containers. Sandia's report concluded that it is technically feasible to build a containerized hydrogen fuel cell generator to replace the diesel generator in YB operations (Figure 2).

APPROACH

This project develops and demonstrates a nominally 100 kW, integrated fuel cell prototype for marine applications. This project brings together industry partners in this prototype development as a first step towards eventual commercialization of the technology. To be successful, the project incorporates interested industry and regulatory stakeholders: an end user, technology supplier and product integrator, and land- and maritime-based safety and code authorities. Project costs have been shared by the primary stakeholders in the form of funds, in-kind contribution, and material/equipment either loaned or donated to the project. Funding provided by the Department of Transportation's Maritime Administration (MARAD) is used to provide assistance with the integrated system and packaging designs, data collection and assistance during the demonstration period, and technical assistance and project management throughout the project. In addition, some MARAD funds are used to purchase specialized equipment needed to construct the prototype. DOE funds are used to provide overall project management, technical design assistance, and deployment facilitation, and are used via subcontract to the prototype manufacturer for the design, build, and testing of the final product.

The project has four phases:

1. Establishment and specification (September 2013–December 2013)
2. Detailed design and engineering (January 2014–March 2015)
3. Prototype fabrication/site construction (October 2014–June 2015)
4. Deployment (on-site demonstration) and analysis (August 2015–March 2016)

FIGURE 1. The Maritime Fuel Cell Generator will be used on the dock and over the ocean on barges such as this one, providing power for refrigerated containers during transit.

FIGURE 2. The Maritime Fuel Cell Generator contains 75 kg of compressed hydrogen storage and produces over 100 kW net electricity, packaged in a 20-foot shipping container.

RESULTS

Key prototype build-related accomplishments (by subcontractor Hydrogenics) in FY 2015:

- Completed hydrogen storage tank factor certification testing and delivery
- Completed inverter factory testing
- Completed draft failure mode effects analysis (FMEA), and resolved potential operational handling issues.
- Designed and built hydrogen storage rack and ruggedized fuel cell rack
- Completed fuel cell module assembly
- Finalized procurement for container
- Finalized FMEA
- Submitted complete design package the USCG and ABS for review
- Built and commissioned all four 30 kW fuel cell modules.
- Released detailed container design drawings to subcontractor and completed 75% of container modifications
- Completed electrical system testing: fuel cell rack + inverter + ultracapacitor
- Completed hydrogen storage rack
- Completed container build
- Completed equipment mounting within container
- Completed all interconnecting piping and wiring
- Finished complete build
- Completed shakedown testing
- Completed Factory Acceptance Testing
- Shipped to Honolulu for deployment

The project team finalized the Data Collection and Analysis Plan, which describes how the project's work will be captured and made useful to fulfil the objectives of the sponsors and stakeholders. There are three categories of data to be collected during the deployment: technical, business, and regulatory. The technical data includes both prototype performance and usage as well as hydrogen supply and refueling information. Working with the National Renewable Energy Laboratory, the project team was able to ensure that data collected will be directly comparable with other DOE efforts.

The YB-preferred method of fueling the prototype at the Hickam station was finalized. In this arrangement the prototype is placed on a container handling trailer ("chassis") and a truck will drive it to the Hickam station where it will be filled by the Hickam station operator. This method is also anticipated to be able to fill the prototype to 100% in less than one hour. Currently, YB prefers this method because of its apparent logistical simplicity and will begin the demonstration refueling the trailer by this method. In FY 2015 Sandia, the Hawaii Center for Advanced Transportation Technologies (HCATT), and YB formulated the logistics (primarily timing) for this arrangement. YB also finalized an arrangement with a local trucker to perform this service.

Sandia engaged its in-house safety and risk experts, and DOE's Fuel Cell Technologies Office Safety, Codes and Standards subprogram to perform an analysis of the prototype's operation in the specific context of YB operations. The goal of this analysis was to quantitatively determine the impact of any usage restrictions on safety risk and was necessary because of the lack of applicable codes and standards on this type of equipment in these environments (on the dock and on the barge). The assessment consisted of three parts: (1) identification of scenarios where the prototype's operation may present a hazard in the context of YB operations, (2) fluid dynamics simulations of hydrogen releases into the environment to assess the distribution and extent of flammable hydrogen concentrations, and (3) quantitative risk assessment to quantify the risk to personnel. The accomplishment of these three tasks enabled the project team to confidently recommend minimal operational restrictions on the prototype. (More detail is contained within the project's "Safety Features Integrated into Design and Use of System" fact sheet and the project's Safety Plan).

The project team engaged Pacific Northwest National Laboratory (PNNL) to administer Hydrogen Safety Training to local first responders and YB personnel. In the second quarter, the training materials were solidified through a combination effort by PNNL, their subcontractor Jennifer Hamilton of the California Fuel Cell Partnership, YB,

Hydrogenics, and Sandia. The result was a customized training package that included not only the general first responder information from PNNL's National Training Program but also specific information on the prototype's safety features and operation as well as information for YB personnel on special handling and usage instructions. The training was given April 9–11, at the YB facility in Honolulu, Oahu, and April 15–17, at the Kahului Fire Station, Maui and reached over 200 personnel. A summary of the training was published by PNNL [3].

The training was videotaped and during the third quarter (Q3) the videographer worked on final editing of two versions of the training: a full-length version that captures all aspects of the training, and a shorter version which focuses on hydrogen familiarity and the prototype's use and operation. The shorter version will be used in the fourth quarter by YB to train their operational personnel who were not able to attend the April training in person. Both versions of the video can also be used in subsequent deployments of this prototype at other locations.

In Q3 the Sandia outreach team produced two project fact sheets, one that overviews the project and one that explains the safety features of the prototype. The outreach team also stood up a project website (maritime.sandia.gov), organized a blog post announcing the shipping from Hydrogenics, and has been responsible for organizing a project "ribbon cutting" ceremony for the project on August 28, at YB's Honolulu facility. To ensure all project partners continue to be part of these efforts, the outreach team established an ongoing bi weekly call with appropriate partner personnel.

CONCLUSIONS AND FUTURE DIRECTIONS

The Maritime Fuel Cell Project is a wholly-collaborative effort with early and continuous stakeholder feedback that is breaking down non technical barriers to hydrogen and fuel cell use. Future work in FY 2016 includes:

- Finish deployment and data collection
- Produce technical and business case analyses
- Continue outreach based on project results

FY 2015 PUBLICATIONS/PRESENTATIONS

1. M. Elmore and J. Hamilton, "Final Report: Maritime Fuel Cell Project Hydrogen Safety and Emergency Response Training, Honolulu, Oahu and Kahului, Maui – Hawaii," Pacific Northwest National Laboratory, PNNL-24327, April 2015.

2. "Maritime Hydrogen Fuel Cell – Hydrogen Fuel Cell Demonstration Project at Port of Honolulu," Sandia National Laboratories Fact Sheet, SAND2015-2566 M, April 2015.

3. "Maritime Hydrogen Fuel Cell – Safety Features Integrated into Design and Use of System," Sandia National Laboratories Fact Sheet, SAND2015-2559 M, April 2015.

4. "Hydrogen Fuel Cells Help Ports Meet Environmental Goals," Partnerships Annual Report FY 2014, Sandia National Laboratories, April 2015.

REFERENCES

1. D. Bailey, T. Plenys, G.M. Solomon, T.R. Campbell, G.R. Feuer, J. Masters, and B. Tonkonogy, "Harboring Pollution - Strategies to Clean Up U.S. Ports," National Resources Defense Council, NY, August, 2004.

2. J.W. Pratt and A.P. Harris, "Vessel Cold Ironing Using a Barge Mounted PEM Fuel Cell: Project Scoping and Feasibility," Sandia National Laboratories, Report SAND2013-0501, available at http://energy.gov/eere/fuelcells/downloads/vessel-cold-ironing-using-barge-mounted-pem-fuel-cell-project-scoping-and.

3. M. Elmore and J. Hamilton, "Final Report: Maritime Fuel Cell Project Hydrogen Safety and Emergency Response Training, Honolulu, Oahu and Kahului, Maui – Hawaii," Pacific Northwest National Laboratory, PNNL-24327, April 2015.

X.3 Fuel Cell Hybrid Electric Delivery Van Project

Jason Hanlin
Center for Transportation and the Environment (CTE)
730 Peachtree Street, Suite 760
Atlanta, GA 30308-1209
Phone: (404) 808-6489
Email: Jason@cte.tv

DOE Manager
Pete Devlin
Phone: (202) 586-4905
Email: Peter.Devlin@ee.doe.gov

Contract Number: DE-EE0006523

Subcontractors
- United Parcel Service (UPS), Sandy Springs, GA
- University of Texas Center for Electromechanics (UT-CEM), Austin, TX
- Unique Electric Solutions, Stony Brook, NY
- Hydrogenics, Mississauga, Ontario, Canada
- Valence, Austin, TX

Project Start Date: July 15, 2014
Project End Date: October 15, 2018

Overall Objectives

- Increase the zero emission driving range and commercial viability of medium-duty trucks
- Phase 1 – develop a fuel cell hybrid electric delivery van and validate its design and construction through in-service operation
- Phase 2 – build the Phase 1 delivery van at precommercial volume (up to 16 vehicles) and perform at least 5,000 operation hours of in-service demonstration
- Develop an Economic/Market Opportunity Assessment for medium-duty fuel cell hybrid electric trucks

Fiscal Year (FY) 2015 Objectives

- Perform application specific modeling and simulation to guide component selection and predict vehicle performance on delivery routes
- Perform trade study of vehicle powertrain and energy storage components to optimize commercial viability
- Complete vehicle design, order long lead time components, and begin fabrication
- Coordinate fueling infrastructure needs at demonstration site

Technical Barriers

This project addresses the following technical barriers from the following sections of the Fuel Cell Technologies Office Multi-Year Research, Development, and Demonstration Plan:

Technology Validation

(A) Lack of Fuel Cell Electric Vehicle and Fuel Cell Bus Performance and Durability Data

Market Transformation

(D) Market uncertainty around the need for hydrogen infrastructure versus timeframe and volume of commercial fuel cell applications

(F) Inadequate user experience for many hydrogen and fuel cell applications

Technical Targets

This project directly addresses Section 3.9.4 Sub-Program Targets. This project lays out a very specific and rational pathway for the introduction of fuel cell technologies into the medium-duty vehicle market. The project has a technology validation phase and a follow-on deployment of precommercial volumes of the vehicles. The project is built upon the initial structure that DOE prescribed in the funding opportunity announcement and is augmented by the active participation and guidance of a major commercial fleet operator, UPS. UPS operates 46,000 medium-duty vehicles worldwide. Further, the vehicles will be deployed in California to take advantage of that state's focused growth of fueling infrastructure and desire to deploy zero emission vehicles. CTE has coordinated with station providers early in the project in order to identify and overcome fueling station barriers for this emerging application of fuel cell technologies, such as the limitation of SAE J2601 fueling protocol described below. This project further leverages the resources and support of the State of California. The project team has also focused on upfront design to ensure that (1) selection the fuel cell size will take advantage of volume growth from other applications and markets, and (2) that the design will meet the needs of our commercial fleet operator by matching the performance of incumbent technologies, while meeting the range requirements for over 97% of delivery van duty cycles.

FY 2015 Accomplishments

- Collected real-world duty cycle data, modeled various fuel cell hybrid electric vehicle configurations, and simulated vehicle performance on anticipated delivery routes

- Defined the vehicle specifications
- Developed vehicle solid models and completed preliminary physical layout of battery, fuel cell, and hydrogen storage system
- Identified an absence of accepted standards for fueling medium-duty vehicles with greater than 7 kg of hydrogen storage (at 350 bar) at public fueling stations utilizing SAE J2601 protocol
  - Issue has been brought to the attention of several industry partners, and solutions are being discussed with Linde Industrial Gases and SAE J2601 committee members, among others
- Developed maps and proximity data that relate existing or expected hydrogen fueling stations with UPS service centers
  - Long-term commercialization will see fueling stations deployed by and at fleet properties, properly selecting fueling station locations and organizing the associated infrastructure is vital to the precommercial viability of these zero emission vans

✧ ✧ ✧ ✧ ✧

INTRODUCTION

Parcel delivery van fleets are currently dominated by diesel- and compressed natural gas (CNG)-powered Class 3–6 trucks. In recent years, some parcel delivery services have integrated battery-electric trucks into their fleet; however, these battery-electric vehicles have been unable to match the performance of existing delivery vans and their limited range significantly impacts deployment strategy. The intent of this project is to develop a hydrogen fuel cell hybrid electric van that provides fleet operators with a zero emission vehicle capable of meeting route range requirements while matching the performance characteristics of its existing fleet vehicles. According to Fleet DNA data compiled by the National Renewable Energy Laboratory (NREL), a vehicle with a 125-mile range will meet 97% of Class 3–6 daily delivery driving distances [1]. Meeting this 125-mile range threshold will increase the attractiveness of zero emission trucks to fleet operators and increase their commercial viability.

APPROACH

This project develops and demonstrates a hydrogen fuel cell hybrid electric van with a 125-mile operational range, which will be validated through in-service deployment in a California UPS fleet. This project has two phases:

- Develop a fuel cell hybrid electric delivery van and validate its design and construction through in-service operation.
- Build the Phase 1 delivery van at precommercial volume (up to 16 vehicles) and perform at least 5,000 operation hours of in-service demonstration.

During Phase 1, real-world delivery van route data are collected to define the expected duty cycle requirements. All potential fuel cell hybrid electric van powertrain configurations are then modeled and simulated on the duty cycles to assess vehicle performance and aid final design. Trade studies (including cost and projected costs at high volumes) are accomplished and vehicle components are then down-selected and the physical layout is completed. The first delivery van can then be built and validated through in-service operation. If the delivery van meets Phase 1 performance requirements, the project team will build and deploy up to 16 additional vans in Phase 2. All of the vans will be demonstrated in California. Vehicle performance data during the demonstration periods will be collected and provided to NREL's National Fuel Cell Technology Evaluation Center for analysis.

The project team benefits from having members with extensive hydrogen fuel cell experience, including UT-CEM and Hydrogenics, and one of the largest medium-duty truck fleet operations in the world, UPS. UPS has deployment experience with delivery vans powered by various fuels, including gasoline, diesel, CNG, and battery-electric. This experience gives them a unique perspective on the commercial viability of alternative fueled vehicles and their project contributions are invaluable. Project funding is provided by the DOE, the California Energy Commission, and the South Coast Air Quality Management District. UPS is providing cost share during the demonstration periods by supplying operation, maintenance, and fueling costs.

RESULTS

The teams' modeling activity showed that a 32 kW fuel cell module, 45 kWh battery energy storage, and 10–15 kg of hydrogen are required to meet the 125-mile driving range objective on actual UPS delivery routes. These propulsion system configuration will allow the van to outperform existing battery-electric vans in UPS' fleet, as shown in the example simulation results in Figure 1. The simulated fuel cell van operates for over 500 minutes and drives 125 miles. The comparable battery electric van cannot reach 400 minutes of operation and only travels 70 miles.

After the modeling activity, the team established the vehicle specifications listed in Table 1.

Initial solid models of the van's physical layout and component packaging are shown in Figures 2 and 3.

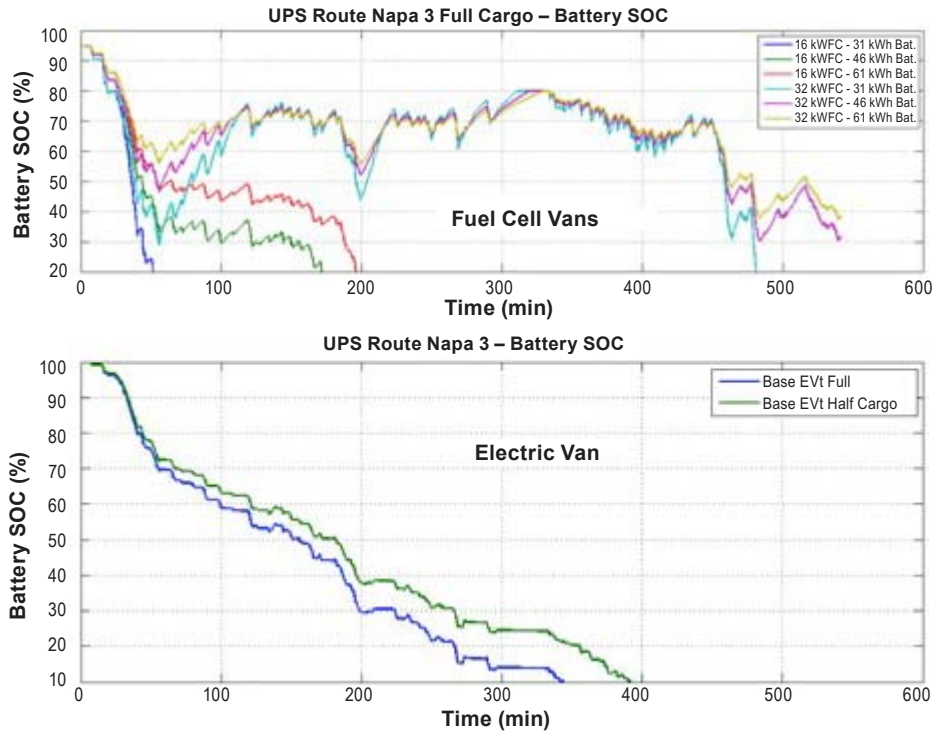

FIGURE 1. Simulated performance of fuel cell and battery electric vans on UPS delivery route

TABLE 1. Vehicle Specifications for Hydrogen Fuel Cell Hybrid Electric Van from Modeling Activity

Physical Specifications	
Vehicle Chassis	Navistar International 1652SC 4X2
Maximum Speed	65 mph
Maximum Range	125 mi
Acceleration (0–60 mph)	26 s at 19,500 lb
Gross Vehicle Weight	Class 6 (23,000 lb)
Wheel Base	176 in
Capacity	970 ft^3
Battery System	
Chemistry	$LiFeMgPO_4$
	45 kWh
	110 Volts Alternating Current
	1,500 cycles / 5 years
Fuel Cell	
Rated Power	32 kW continuous
Peak Efficiency	55%
Hydrogen Storage	
Capacity	9.78 kg
Pressure	350 bar

FIGURE 2. Physical layout and component packaging with van body

CONCLUSIONS AND FUTURE DIRECTIONS

The Fuel Cell Hybrid Electric Delivery Van project is utilizing team member experience with hydrogen fuel cell technologies, alternate fuel vehicle fleet familiarity, and

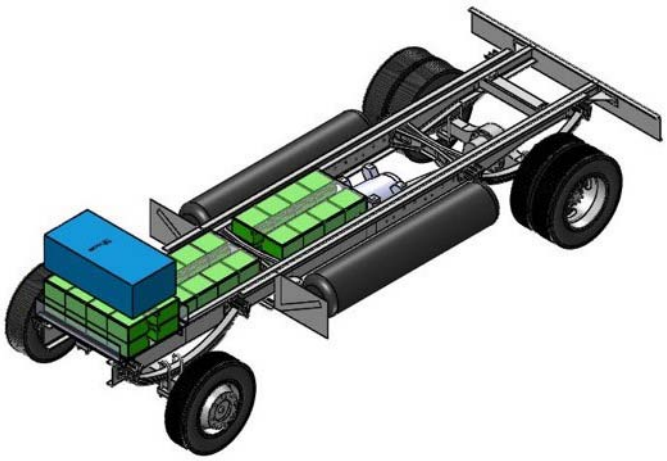

FIGURE 3. Energy storage system locations in van chassis frame

stakeholder feedback to develop commercially viable zero emission medium-duty trucks. The team has developed:

- Vehicle specifications to promote commercial acceptance.
- Component selection to ensure performance on real-world delivery duty cycles.
- Solid models of major components within vehicle body.
- Strategy to ease UPS fleet acceptance and fueling procedures.

Future work includes:

- Completing safety hazard analysis with support from the Hydrogen Safety Panel.
- Coordinating fueling availability and continue coordinating the development of medium-duty hydrogen fueling protocol.
- Completing the final design for the vehicle.
- Building and commissioning initial van design.
- Validating prototype van through in-service operation.
- Building final van design at precommercial volume (up to 16 vehicles).
- Training and educating end-user fleet operations personnel.
- Deploying and supporting vans in UPS California fleets.
- Collecting and evaluating in-service data during demonstration period.
- Developing an economic/market opportunity assessment for the vehicles.

FY 2015 PUBLICATIONS/PRESENTATIONS

1. J. Hanlin, "Fuel Cell Hybrid Electric Delivery Van Project," presented at the DOE Annual Merit Review, Washington, DC, June 8–12, 2015.

REFERENCES

1. Walkowicz, K.; Kelly, K.; Duran, A.; Burton, E. (2014). *Fleet DNA Project Data*. National Renewable Energy Laboratory. http://www.nrel.gov/fleetdna

X.4 Hydrogen Energy Systems as a Grid Management Tool

Richard (Rick) E. Rocheleau (Principal Investigator),
Mitch Ewan (Primary Contact)
Hawaii Natural Energy Institute (HNEI)
School of Ocean and Earth Science and Technology
University of Hawaii at Manoa
1680 East-West Road, POST 109
Honolulu, HI 96822
Phone: (808)956-2337; (808) 956-8346
Email: ewan@hawaii.edu; rochelea@hawaii.edu

DOE Manager
Pete Devlin
Phone: (202) 586-4905
Email: Peter.Devlin@ee.doe.gov

Technical Advisor
Karen Swider-Lyons
Naval Research Laboratory
Phone: (202) 404-3314
Email: karen.lyons@nrl.navy.mil

Contract Number: DE-EE0002811

Project Start Date: September 30, 2010
Project End Date: September 29, 2015

Overall Objectives

- Demonstrate the use of electrolyzers to mitigate the impacts of intermittent renewable energy by regulating grid frequency
- Characterize performance/durability of commercially available electrolyzers under dynamic load conditions
- Supply hydrogen to fuel cell shuttle buses operated by County of Hawaii Mass Transit Agency (MTA), and Hawaii Volcanoes National Park (HAVO)
- Conduct performance/cost analysis to identify benefits of integrated system including grid ancillary services and off-grid revenue streams
- Evaluate effect on reducing overall hydrogen costs offset by value-added revenue streams

Fiscal Year (FY) 2015 Objectives

- Relocate the project from the Puna Geothermal Venture (PGV) power plant to the Natural Energy Laboratory Hawaii Authority (NELHA) site at Kailua-Kona on the Island of Hawaii
- Execute a Facility Use Agreement (lease) with NELHA for the test site
- Install site improvements and utilities at NELHA to support the operation of the hydrogen system
- Conduct a hydrogen site safety review utilizing an independent third party consultant
- Install, commission, and operate the hydrogen system at NELHA
- Install a 350 bar hydrogen fuel dispenser at NELHA to fuel the MTA fuel cell shuttle bus
- Develop electrolyzer system cycling test protocols based on operational data collected from a 1 MW battery energy storage system installed on the HELCO grid for frequency regulation
- Characterize performance/durability of the electrolyzer system under dynamic load conditions at Powertech Labs facilities in Vancouver, Canada, prior to shipping equipment to Hawaii
- Conduct performance/cost analysis to identify benefits of integrated systems including grid services and off-grid revenue streams

Technical Barriers

This project addresses the following technical barriers from the Market Transformation section of the Fuel Cell Technologies Office Multi-Year Research, Development, and Demonstration Plan:

Section 3.9.5 – Market Transformation Barriers

(A) Inadequate standards and complex and expensive permitting procedures

(B) High hydrogen infrastructure capital costs for Polymer Electrolyte Membrane (PEM) fuel cell applications

(C) Inadequate private sector resources available for infrastructure development

(F) Inadequate user experience for many hydrogen and fuel cell applications

(G) Lack of knowledge regarding the use of hydrogen inhibits siting

(H) Utility and other stakeholders lack awareness of potential renewable hydrogen storage application

Technical Targets

No specific technical targets have been set.

FY 2015 Accomplishments

- Relocated the project from the PGV geothermal power plant to the NELHA site at Kailua-Kona on the Island of Hawaii
- Executed a Facility Use Agreement (lease) with NELHA for the test site
- Designed site improvements and utilities at NELHA to support the operation of the hydrogen system; prepared construction bid package for installation of the site improvements
- Conducted a NELHA hydrogen site safety review utilizing Boyd Hydrogen
- Developed electrolyzer system cycling test protocols based on operational data collected from a 1 MW battery energy storage system installed on the Hawaii Electric Light Company grid for frequency regulation
- Designed, fabricated and installed a programmable logic controller (PLC) and power monitoring system for control of the electrolyzer system
- Commissioned the electrolyzer system and characterized performance/durability under dynamic load conditions at Powertech Labs facilities in Vancouver, Canada
- Conducted five months of testing at Powertech Labs supervised by on-site HNEI staff

✧ ✧ ✧ ✧ ✧

INTRODUCTION

While solar and wind resources offer a major opportunity for supplying energy for electrical grid electricity production and delivery systems, their variability and intermittency can raise challenges for the cost effective and high reliability integration of these renewable sources on electrical grids. In Hawaii, the curtailment and grid management-related challenges experienced by these renewable sources are a challenge at today's level of generation capacity, and these costs will hinder the substantive additional penetration of electricity generation supplied by these renewable resources. Hydrogen production through electrolysis may provide an opportunity to mitigate curtailment and grid management costs by serving as a controllable load allowing real-time control in response to changes in electricity production. The renewable hydrogen product can also create new and incremental revenue streams to the power producers through the sale of hydrogen products to customers outside of the electricity delivery system. Accordingly, hydrogen energy production at a utility scale offers the potential for increasing the levels of variable renewable energy that can be harnessed by the power producers or systems operators.

APPROACH

This project evaluates the value proposition of using utility-scale electrolyzers to both regulate the grid and using the product hydrogen for transportation applications. An electrolyzer system will be installed at NELHA on the Big Island. The electrolyzer will be ramped up and down to provide frequency regulation. Data will be collected to analyze the optimum electrolyzer ramp rates and determine its durability and performance under dynamic operating conditions. The hydrogen produced by the system will be used to fuel three hydrogen-fueled buses. It is planned to deliver hydrogen to HAVO as per the original plan to support two HAVO buses. The third bus will be operated from Kona instead of Hilo. A schematic of the project concept is shown in Figure 1.

RESULTS

Due to a lava flow that threatened to cut off access to the original project site, the decision was made to move the project from Puna to NELHA located on the West Coast of the Big Island as shown in Figure 1. A lease was executed with NELHA and a new infrastructure design was developed and reviewed by a third party hydrogen safety consultant (Boyd Hydrogen). A construction bid package was prepared and will go out to pubic tender. In parallel to the site work, HNEI developed electrolyzer system cycling test protocols based on operational data collected from a 1 MW battery energy storage system installed on the

FIGURE 1. Hydrogen Production and Delivery System

HELCO grid for frequency regulation. A PLC and power monitoring system for control of the electrolyzer system was designed and installed on the electrolyzer system to facilitate implementation of the electrolyzer testing protocols, and support data collection. The electrolyzer system was commissioned at Powertech Labs facilities in Vancouver, Canada, in January/February 2015 and on-site HNEI staff conducted a testing program. The electrolyzer system has been characterized and performance and durability testing is being conducted in accordance with the test plan. Several technical issues were identified in the course of operations at Powertech and are being rectified as they are discovered. The electrolyzer has presented many technical challenges. This six-month test phase at the manufacturer's facility is proving to be very beneficial and will result in a true "plug and play" when the system is installed at NELHA with most of the bugs resolved.

CONCLUSIONS AND FUTURE DIRECTIONS

The Hydrogen Energy Systems as a Grid Management Tool project has coordinated the efforts of a diverse group of stakeholders to provide a technology solution to facilitate integration of intermittent renewable energy sources on an electrical grid while producing hydrogen for transportation. The project has identified and provided valuable solutions to the many nontechnical barriers associated with introducing hydrogen technology into a community for the first time. Lessons learned from this project will make the way easier for projects that follow. Future work includes the following:

- Installing and operating hydrogen production systems and dispensing infrastructure at the NELHA site. It is projected the site will be operational in February 2016.
- Operating the 26-passenger fuel cell electric vehicle (FCEV) bus based at the NELHA site.
- Transporting hydrogen in hydrogen transport trailers from the production site to dispensing HAVO to support the two park service FCEV buses.
- Collecting and analyzing hydrogen system and FCEV bus performance data.
- Preparing performance reports and sharing it with project sponsors and industry.
- Conducting outreach activities with the public to inform them about hydrogen technologies.

FY 2015 PUBLICATIONS/PRESENTATIONS

1. Ewan M., Rocheleau, R., Oral presentation at US DOE Annual Merit Review, "Hydrogen Energy Systems as a Grid Management Tool," Washington, DC, June 10, 2015.

X.5 Demonstration and Deployment of a Fuel Cell-Electric Refuse Truck for Waste Transportation

Abas Goodarzi
US Hybrid Corporation
445 Maple Avenue
Torrance, CA 90503
Phone: (310) 212-1200
Email: abas@ushybrid.com

DOE Manager
Pete Devlin
Phone: (202) 586-4905
Email: Peter.Devlin@ee.doe.gov

Contract Number: DE-SC00011854

Subcontractor
Mitch Ewan, Honolulu, HI

Project Start Date: June 9, 2014
Project End Date: March 8, 2015

Overall Objectives

- Design and technical analysis of zero emission, fuel cell-powered refuse powertrain system architectures for refuse truck operation in Honolulu, Hawaii
- Evaluate its environmental benefits in terms of reducing emissions and fossil fuel consumption
- Explore the commercial viability of a zero emission, fuel cell-powered, heavy-duty, electric hybrid truck for waste hauling applications

Fiscal Year (FY) 2015 Objectives

- Analyze best route of refuse truck operation based on existing fueling infrastructure
- Evaluate commercial viability and next steps for Phase II demonstration build and deployment
- Establish a commercialization plan for Phase II deployment containing market analysis and commercialization strategy

Technical Barriers

This project addresses the following technical barriers from the Market Transformation section of the Fuel Cell Technologies Office Multi-Year Research, Development, and Demonstration Plan:

(D) Market uncertainty around the need for hydrogen infrastructure versus timeframe and volume of commercial fuel cell applications

(E) A lack of flexible, simple, and proven financing mechanisms

(F) Inadequate user experience for many hydrogen and fuel cell applications

Technical Targets

No specific technical targets have been set.

FY 2015 Accomplishments

- Proposed deployment route from Honolulu Collection Yard to neighborhood collection area based on existing hydrogen infrastructure
- Calculated total energy use for route is 53.17 kWh, with 3.9 kWh/mi energy consumption
- Determined that total hydrogen consumption is 2.7 kg, with 0.2 kg/mi fuel consumption
- Designed packaging in conjunction with refuse truck body original equipment manufacturer (OEM)
- Projected a cost analysis indicating that the cost premium for commercial volume production could have a payback time of five years based on a hydrogen cost of $6/kg

✧ ✧ ✧ ✧ ✧

INTRODUCTION

Urban refuse collection is a major industry in North America, with a fleet estimated at approximately 179,000 waste-hauling trucks. Due to the continuous start and stop behavior of waste collection, refuse trucks, which are typically diesel fueled, operate at low speeds. This results in significant greenhouse gases (GHG) and exposure to diesel exhaust, which is comprised primarily of particulate matter (PM) and oxides of nitrogen (NOx). The refuse truck duty cycle engine operation translates to a very poor fuel economy averaging 3 miles per gallon (mpg) and hearing-damaging noise exceeding decibel levels of 100. Nationally, refuse trucks use 1 billion gallons of diesel fuel annually, representing 3% of the United States' total diesel fuel consumption. As such, US Hybrid Corporation teamed with Hawaii Center for Advanced Transportation Technologies (HCATT) and Hawaii Natural Energy Institute to perform a

Phase I analysis to explore the potential of a fuel cell electric system for refuse truck propulsion.

Based on the initial technical and economic analysis and performance data, the fuel cell-powered zero emission refuse truck is a viable product for refuse truck operators that want to experience lower lifetime operating cost, significant noise reductions, better acceleration and handling, and zero tailpipe GHG or criteria pollutant emissions. In the short run, the fuel cell refuse truck may initially be focused on niche markets, where eliminating emissions or the operating noise is critical, due to its higher capital cost. Eventually, economies of scale will reduce the cost, so the zero emission truck will provide a lower lifetime operating cost while eliminating emissions and allowing full utilization of renewable energy for transportation.

APPROACH

This project explored the technical and commercial viability of a zero emission, fuel cell-powered, heavy-duty, electric hybrid truck for waste hauling application. The scope of the project included the design and technical analysis of zero emission, fuel cell-powered refuse powertrain system architectures for refuse truck operation in Honolulu, Hawaii. This incorporated both analytical and computational evaluation, that latter of which was done with a simulation that measured performance and energy consumption. Our analysis of performance characteristics of various refuse drive cycles identified the required fuel cell, energy storage capacity, electric powertrain, and the electrohydraulic drive system component size required to meet or exceed the performance criteria set for conventional refuse trucks. Using the component sizing results, we were able to do a preliminary packaging study with OEM body builder, Heil. We also explored ways to establish a business case and an optimized route for the refuse hauler based on current station development.

RESULTS

Our analysis of performance characteristics of various refuse drive cycles identified the required fuel cell, energy storage capacity, electric powertrain, and the electrohydraulic drive system component size required to meet or exceed the performance criteria set for conventional refuse trucks. The baseline vehicle assumed for the analysis was a 54,000 lb gross vehicle weight restriction model built on a Navistar WorkStar® with a Heil body with a 370 hp MaxxForce® engine. The study indicated that the minimum traction motor power is 240 kW, fuel cell power is 68 kW and the hydraulic drive power is 80 hp. The vehicle also included 24 kWh of battery storage to provide transient power and fully recover braking energy on a typical Honolulu route and other refuse routes. The refuse truck's duty cycle is characterized by high power demand and relatively low energy demand. The energy needs on a typical route are under 45 kWh with a peak power of up to 240 kW. The fuel efficiency of the fuel cell refuse truck was simulated using the actual Honolulu residential district route profile provided by the City and County of Honolulu.

The refuse truck starts its day at the Honolulu Collection Yard and commences its refuse route in Waikiki. As shown in Figure 1, Joint Base Pearl Harbor-Hickam (JPBHH) is in

FIGURE 1. JBPHH hydrogen station location relative to Honolulu Collection Yard and neighborhood for refuse collection (image courtesy of Google Maps)

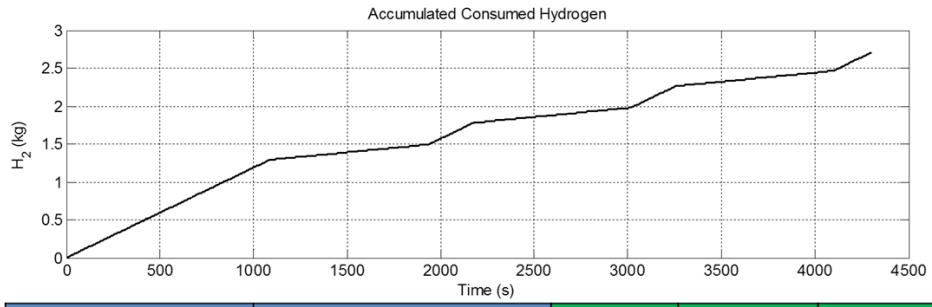

Total energy used (kWh)	Energy used per mile (kWh/mile)	H_2 (kg)	H_2 (Kg/mile)	H_2 (Kg/hour)
53.17	3.9	2.7	0.2	2.26
Distance=13.7 miles, Time=4300 seconds (1.2 hours)				

FIGURE 2. Performance data and energy efficiency and consumption for 24,500 kg refuse truck

close proximity to the yard. This study concluded that the preferred operation would consist of driving the refuse truck from the Honolulu Collection Yard and fuel it at the HCATT hydrogen production and fueling station at JBPHH. The truck would then complete its daily operations and then return to the Honolulu Collection Yard in the evening.

The results of the simulations indicated that the fuel cell hybrid electric refuse truck consumes about 3 kg of hydrogen per hour. Given 20 kg of hydrogen storage, this provides about seven hours of continuous operation, which is much longer than a full day's operation of current diesel trucks. This represents more than 42 gallons of diesel fuel saving per day. The current average fuel use is about 31 gallons per day. The performance data and energy efficiency and consumption for the fuel cell hybrid electric truck are shown in Figure 2.

The economic analysis of the viability of the fuel cell electric hybrid refuse truck accounted for the cost of the additional components, development costs, and increased labor to integrate the system into the vehicle. The cost analysis indicated that the cost premium for commercial volume production has a payback time of five years based on a hydrogen cost of $6/kg. Such prices will arise with matured hydrogen generation technologies. In the long run, fuel cell hybrid electric systems may offer lower costs and shorter payback times and better return on investments, while improving truck productivity by continuous compacting, better truck and hydraulic performance, lower noise, simpler packaging, and reduced hydraulic equipment load with an electrically driven pump.

CONCLUSIONS AND FUTURE DIRECTIONS

Based on the initial technical and economic analysis and performance data, the fuel cell-powered, zero emission refuse truck is a viable product; however, it may initially be focused on niche markets, where eliminating emissions or the operating noise is critical, due to its higher capital cost. Eventually, economies of scale will reduce the cost, so the zero emission truck will provide a lower lifetime operating cost while eliminating emissions and allowing full utilization of renewable energy for transportation.

Future work includes:

- Phase II prototype build and deployment
- Determine logistical and environmental impact of actual vehicle fuel cell powertrain development, modeling, and fabrication
- On site commissioning and training with refuse truck operator
- Begin deployment testing and collect operational and cost data
- Phase III technical and business discussions with OEMs and distributors for deployment beyond initial demonstration

FY 2015 PUBLICATIONS/PRESENTATIONS

1. G.A. Goodarzi, "Demonstration and Deployment of a Fuel Cell-Electric Refuse Truck for Waste Transportation," presented at the DOE Annual Merit Review, Washington, DC, June 8–12, 2015.

REFERENCES

1. Inform (2003). Greening Garbage Trucks: New Technologies for Cleaner Air [Online]. Available: http://www.informinc.org/reportpdfs/st/GreeningGarbageTrucks.pdf.

2. U.S. Energy Information Administration. (2015). Hawaii Profile Overview [Online]. Available: http://www.eia.gov/state/?sid=HI.

XI. SMALL BUSINESS INNOVATION RESEARCH (SBIR) FUEL CELL TECHNOLOGIES OFFICE NEW PROJECTS AWARDED IN FY 2015

XI.0 Small Business Innovation Research (SBIR) Fuel Cell Technologies Office New Projects Awarded in FY 2015

The Small Business Innovation Research (SBIR) program provides small businesses with opportunities to participate in DOE research activities by exploring new and innovative approaches to achieve research and development (R&D) objectives. The funds set aside for SBIR projects are used to support an annual competition for Phase I awards of up to $225,000 each for about nine months to explore the feasibility of innovative concepts. Phase II R&D efforts further demonstrate the technologies to move them into the marketplace, and these awards are up to $1,500,000 over a two-year period. Small Business Technology Transfer (STTR) projects include substantial (at least 30%) cooperative research collaboration between the small business and a non-profit research institution.

Table 1 lists the SBIR Phase I projects, and Table 2 lists the SBIR Phase II projects awarded in FY 2015 related to the Hydrogen and Fuel Cells Program. Brief descriptions of each project follow.

TABLE 1. FY 2015 SBIR Phase I Projects Related to the Hydrogen and Fuel Cells Program

Title	Company	City, State
XI.1 Fuel Cell-Battery Electric Hybrid for Utility or Municipal MD or HD Bucket Trucks (H2BT)	US Hybrid Corporation	Torrance, CA
XI.2 Cross-polarized Near-UV Detector for In-line Quality Control of PEM Materials	Mainstream Engineering Corporation	Rockledge, FL
XI.3 Non-Platinum Group Metal OER/ORR Catalysts for Alkaline Membrane Fuel Cells and Electrolyzers	Proton Energy Systems	Wallingford, CT
XI.4 Non-Precious Metal Bi-Functional Catalysts	PH Matter, LLC	Columbus, OH
XI.5 Diode Laser Sensor for Contaminants in Hydrogen Fuel	Southwest Sciences, Inc.	Santa Fe, NM
XI.6 Hydrogen Contamination Detection	Sustainable Innovations, LLC	East Hartford, CT

TABLE 2. FY 2015 SBIR Phase II Projects Related to the Hydrogen and Fuel Cells Program

Title	Company	City, State
XI.7 Ionomer Dispersion Impact on Advanced Fuel Cell and Electrolyzer Performance and Durability	Giner, Inc.	Newton, MA
XI.8 New High Performance Water Vapor Membranes to Improve Fuel Cell Balance of Plant Efficiency and Lower Costs	Tetramer Technologies, LLC	Pendleton, SC
XI.9 Flexible Barrier Coatings for Harsh Environments	GVD Corp.	Cambridge, MA
XI.10 High Performance Long Lifetime Catalyst for Proton Exchange Membrane Electrolysis	Giner, Inc.	Newton, MA
XI.11 New Approaches to Improved PEM Electrolyzer Ion Exchange Membranes	Tetramer Technologies, LLC	Pendleton, SC

PHASE I PROJECTS

XI.1 Fuel Cell-Battery Electric Hybrid for Utility or Municipal MD or HD Bucket Trucks (H2BT)

US Hybrid Corporation
445 Maple Ave.
Torrance, CA 90503-3807

The project will develop and demonstrate polymer electrolyte membrane (PEM) fuel cell-battery electric hybrid trucks for medium- or heavy-duty (MD or HD) bucket trucks with drivetrain-integrated electric power take-off systems. The fuel cell bucket truck has no emission and saves 1,400 gallons of diesel fuel per year. It is cleaner, quieter, and friendlier to operate, with a fuel cell power plant enabling mobility via renewable energy.

XI.2 Cross-polarized Near-UV Detector for In-line Quality Control of PEM Material

Mainstream Engineering
200 Yellow Place
Rockledge, FL 32955-5327

Mainstream Engineering Corporation of Rockledge, Florida, will develop a real-time, in-line optical detector for the measurement of fuel cell membrane thickness. Previously, the Fuel Cell Technologies Office funded the National Renewable Energy Laboratory (NREL) to develop non-destructive in-line quality control techniques for membrane electrode assembly components production. Mainstream Engineering's project involves technical transfer of NREL intellectual property on optical techniques. Mainstream will design and fabricate a quality control device that is readily implementable in a roll-to-roll production line for the production of one or more membrane electrode assembly component materials. Their quality control device will help to drive down the costs of fuel cells by reducing waste and improving the process efficiency of roll-to-roll manufacturing of PEMs.

XI.3 Non-Platinum Group Metal OER/ORR Catalysts for Alkaline Membrane Fuel Cells and Electrolyzers

Proton OnSite
10 Technology Drive
Wallingford, CT 06492

The project will develop a non-precious metal catalyst based on doped cobalt oxides for use as an oxygen catalyst in reversible alkaline membrane fuel cells. This project also aims to develop a more efficient bidirectional alkaline exchange membrane cell stack which can ultimately be deployed for low cost and lightweight energy storage requirements. The innovation will provide a cost-effective and simpler system approach to generating hydrogen via electrolysis, and converting it back to electricity in fuel cell mode.

XI.4 Non-Precious Metal Bi-Functional Catalysts

PH Matter, LLC
1275 Kinnear Rd.
Columbus, OH 43212

The project will develop a non-precious metal catalyst based on phosphorus-doped carbon–nitrogen materials for use as an oxygen catalyst in reversible alkaline membrane fuel cells. The technology will be used for stationary energy storage applications.

XI.5 Diode Laser Sensor for Contaminants in Hydrogen Fuel

Southwest Sciences, Inc.
1570 Pacheco Street
Santa Fe, NM 87505

The project will develop a diode laser sensor for detection of typical impurities found in hydrogen fuel at the refueling station. A contaminant detector for hydrogen fuel is needed to prevent fouling of fuel cell vehicle propulsion systems.

XI.6 Hydrogen Contamination Detection

Sustainable Innovations, LLC
111 Roberts Street, Suite J
East Hartford, CT 06854

Sustainable Innovations has teamed with the University of Connecticut to develop an innovative multi-channel hydrogen fuel quality monitor to detect multiple impurities at low levels in hydrogen. Successful development of a low-cost hydrogen contaminant sensor will prove critically important in expanding markets for hydrogen used in industrial and fueling applications.

PHASE II PROJECTS

XI.7 Ionomer Dispersion Impact on Advanced Fuel Cell and Electrolyzer Performance and Durability

Giner Inc.
89 Rumford Avenue
Newton, MA 02466-1311

The project will develop advanced membrane and electrode components that may significantly enhance the durability and performance of proton exchange membrane fuel cells and electrolyzers. Enhanced durability and performance will lead to cost reductions for fuel cells and for hydrogen and accelerate public acceptance of hydrogen vehicles.

XI.8 New High Performance Water Vapor Membranes to Improve Fuel Cell Balance of Plant Efficiency and Lower Costs

Tetramer Technologies, LLC
657 South Mechanic Street
Pendleton, SC 29670

Tetramer Technologies has developed an advanced water vapor transport membrane (WVT) for fuel cell vehicles. This new technology showed no anhydride formation and produced a higher WVT performance with a lower cost. This project will focus on optimizing the polymer synthesis, characterization, film formation through roll coating, testing, and manufacturing scale-up unit operations. The new membranes will improve the humidifier durability and increase balance of plant efficiency.

XI.9 Flexible Barrier Coatings for Harsh Environments

GVD Corporation
45 Spinelli Place
Cambridge, MA 02138

The project will develop a barrier coating for o-rings and other high pressure hydrogen seals to prevent hydrogen from permeating the seal, even at 200°C and 700 bar. GVD Corporation is partnered with Green Tweed and Massachusetts Institute of Technology. The new barrier coating will reduce permeability of the seals by 10x compared to the uncoated baseline performance.

XI.10 High Performance Long Lifetime Catalyst for Proton Exchange Membrane Electrolysis

Giner Inc.
89 Rumford Ave.
Newton, MA 02466

The project addresses high capital and operating costs of PEM electrolysis. It will help commercialize advanced water electrolysis catalysts that are more active and require an order of magnitude less precious metal than industry standards. This effort will make water electrolysis more efficient and competitive compared to other hydrogen production technologies.

XI.11 New Approaches to Improved PEM Electrolyzer Ion Exchange Membranes

Tetramer Technologies, LLC
657 S. Mechanic Street
Pendleton, SC 29670

Tetramer Technologies, LLC, has developed a new membrane molecular architecture, which has demonstrated equivalent or better performance compared to the current Nafion® materials at 50% lower cost. These attributes directly address the high electrolyzer cost and performance issues. Key attributes of Tetramer's technology vs. the current Nafion® electrolyzer membranes are improved physical performance properties, 50% lower hydrogen permeability, and equal or higher conductivity. This technology will provide thinner membranes, which can lower costs and increase performance directly through decreased ionic resistance, and indirectly through the reduction of the overall cell potential. Tetramer's membranes can also provide 50% less hydrogen crossover loss, thus improving the electrolyzer yield and lowering costs.

XII. Acronyms, Abbreviations, and Definitions

α-AlH_3	Alpha polymorph of aluminum hydride
~	Approximately
@	At
°C	Degrees Celsius
°F	Degrees Fahrenheit
Δ	Change, delta
ΔG	Gibbs free energy of reaction
ΔH	Enthalpy of reaction, Enthalpy of hydrogenation
$\Delta H°_{des}$	Desorption enthalpy
ΔK	Stress intensity factor
ΔP	Pressure drop, pressure change
≈	Equals approximately
ε	Average pristine fiber failure strain
>	Greater than
≥	Greater than or equal to
<	Less than
≤	Less than or equal to
µm	Micrometer(s), micron(s)
η	Viscosity
#	Number
Ω	Ohm(s)
Ω/cm^2	Ohm(s) per square centimeter
Ω-cm^2	Ohm-square centimeter
ρ	Average fiber density
%	Percent
®	Registered trademark
σ_f	Average pristine fiber strength
$	United States dollars
1-D, 1D	One-dimensional
1Q	First quarter of the fiscal year
2-D, 2D	Two-dimensional
2Q	Second quarter of the fiscal year
3-D, 3D	Three-dimensional
3Q	Third quarter of the fiscal year
4Q	Fourth quarter of the fiscal year
A	Ampere, amps
A	Alkali
Å	Angstrom
AB	Ammonia-borane, NH_3BH_3
Abs	Absolute
ABS	American Bureau of Shipping
AC	Alternating current
A-CCS	Activated carbon composite support
AD	Adsorbent
ADF	Annular dark-field imaging
ADT	Accelerated degradation test
Ae	Alkaline earth
AEM	Anion exchange membrane; Analytical electron microscopy
AEMFC	Anion exchange membrane fuel cell
AEO	Annual Energy Outlook
AFC	Automotive fuel cell
AFCB	American Fuel Cell Bus Project
AFCC	Automotive Fuel Cell Cooperation
AFDC	Alternative Fuels Data Center
AFM	Atomic force microscopy
AFMBR	Anaerobic fluidized bed membrane reactor
Ag	Silver
AHJ	Authorities having jurisdiction
AIST	Japanese National Institute of Advanced Industrial Science and Technology
Al	Aluminum
Al_2O_3	Aluminum oxide
ALD	Atomic layer deposition
AlH_3	Aluminum hydride; Alane
ALS	Advanced Light Source at Lawrence Berkeley National Laboratory
AM1.5G	Air Mass 1.5 Global (solar spectrum)
A/m^3	Amps per cubic meter
AMFC	Anion exchange membrane fuel cell; Alkaline membrane fuel cell
AMR	Annual Merit Review
AMR	Active magnetic regenerator
AMS	Air Management System
ANL	Argonne National Laboratory
ANOVA	Analysis of variance
ANSI	American National Standards Institute
APCI, APCi	Air Products and Chemicals, Inc.
API	American Petroleum Institute
APRR	Average pressure ramp rates
APU	Auxiliary power units
AQ	Actual stack heat load
Ar	Argon
AR	As received

AR	Hexamethyl trimethyl ammonium functionalized poly(biphenyl alkylene)
ARPA-E	Advanced Research Projects Agency–Energy
ARRA	American Recovery and Reinvestment Act
As	Arsenic
ASHRAE	American Society of Heating, Refrigerating, and Air-Conditioning Engineers
ASME	American Society of Mechanical Engineers
ASPEN	Modeling software, computer code for process analysis
ASR	Area-specific resistance; areal surface resistance
AST	Accelerated stress test
ASTM	ASTM International, originally known as the American Society for Testing and Materials
at%	Atomic percent
atm	Atmosphere
ATM-PP	Benzyl trimethyl ammonium functionalized Diels-Alder poly(phenylene)
a.u.	Arbitrary units
Au	Gold
AuS	Gold sulfide
B	Boron
Ba	Barium
BAM	Federal Institute for Material Research and Testing
bara	Bar absolute
BaSce	Baseline and Scenario Analysis
BCS	Business Case Scenario
Be	Beryllium
BES	Basic Energy Sciences office within the DOE Office of Science
BET	Brunauer-Emmett-Teller surface area analysis method
BETO	Bioenergy Technologies Office
BEV	Battery electric vehicle
B-H, BH, BH_4	Borohydride
Bi	Bismuth
BM	Base metal
BN	Boron-nitrogen
BNL	Brookhaven National Laboratory
Boc	Tert-butoxycarbonyl
BOC	Best of class
BOL	Beginning of life
BOP, BoP	Balance of plant
BOT	Beginning of test
BPP	Bipolar plate
BPV	Boiler and Pressure Vessel
Br	Bromine
BSA	Bovine serum albumin
BSF	Bloch spectral function
BTT	Baggage tow tractor
BTU, Btu	British thermal unit(s)
BuP	Backup power
BVPC	Boiler and pressure vessel code (ASME)
C	Carbon
Ca	Calcium
CAD	Computer-aided design
CaFCP	California Fuel Cell Partnership
cal	Calorie(s)
CalTech	California Institue of Technology
CARB	California Air Resources Board
CB	Conduction band
CBA	Cost breakdown analysis
CBET	Division of Chemical, Bioengineering, Environmental, and Transport Systems
CBN	Carbon-boron-nitrogen
CBS	Casa Bonita strain; Complete basis set
cc	Cubic centimeter(s)
CCL	Cathode catalyst layer
CCM	Catalyst-coated membrane
Cc/min, ccm	Cubic centimeters per minute
CCS	Carbon capture and sequestration
CCSD(T)	coupled cluster theory with single and double excitations plus a perturbative correction for triple excitations
CCSI	Continuous Codes and Standards Improvement
Cd	Cadmium
CDO	Codes Development Organization
CDP	Constant dew point
CDP	Composite data product
CdS	Cadmium sulfide
Ce	Cerium
CEA	Commissariat à l'Energie Atomique
CEC	California Energy Commission
CEM	Compressor/expander motor (module)
CeO_2	Ceric oxide
CF	Carbon fiber; Carbon foam
CFD	Computational fluid dynamics
cfm	Cubic feet per minute
CGA	Compressed Gas Association
CH	Chemical hydride

cH_2	Compressed hydrogen gas
CH_4	Methane
CH-AB	Chemical hydride-ammonia borane
CHE	Computational hydrogen electrode
CHEX	Cold heat exchanger
CHG	Compressed hydrogen gas
CHHP	Combined heat, hydrogen, and power
CHP	Combined heat and power
CI	Combustion ignition
Cl	Chlorine
CL	Catalyst layer
cm	Centimeter
CM	Cyanamide
cm^2	Square centimeter
CM-PANI	Cyanamide-polyaniline
CMU	Carnegie Mellon University
CNG	Compressed natural gas
CNGV	Compressed natural gas vehicle
CNT	Carbon nanotube
Co	Cobalt
CO	Carbon monoxide
CO_2	Carbon dioxide
CO_{2e}	Carbon dioxide equivalent
COCV	Cyclic open circuit voltage
COD	Chemical oxygen demand
COMSOL	Multiphysics modeling and engineering simulation software
COP	Cooefficient of performance
COPV	Composite overwrapped pressure vessel
COV	Coefficient of variation
cP	Centipoise
C/P	Conductivity to permeability (ratio)
CPM	Cost per thousand impressions; Cycles per minute; Cost per mile
CPR2	Cascading pressure receiver reactor
CPU	Computer processing unit
Cr	Chromium
CRF	cumulative fluoride release
Cs	Cesium
CS	Carbon steel
C&S	Codes and standards
CSA	Canadian Standards Association
CSD	Compression, storage, and delivery
CSM	Colorado School of Mines; Combined structure & material
CSU	California State University
CSULA	California State University Los Angeles
CT	Computed tomography
CTD	Composite Technology Development, Inc.
CTE	Coefficient of thermal expansion
CTE	Center for Transportation and the Environment
Cu	Copper
CU	University of Colorado
cu in	Cubic inch
$CuInGaS_2$	Copper indium gallium sulfide
cu yd	Cubic yard(s)
CV	Cyclic voltammatry; Cyclic voltammogram
CVD	Chemical vapor deposition
CWG	Catalysis Working Group
d	Day(s)
D_2	Deuterium
DAPP	Diels-Alder poly(phenylene)
DC	Direct current
DDP	Detailed Data Product
ΔG	Gibbs free energy of reaction
ΔH	Enthalpy of reaction
ΔK	Stress intensity factor
DFC®	Direct fuel cell
DFMA®	Design for Manufacturing and Assembly
DFT	Density functional theory
DG	Distributed generation
DG-BEAT	Distributed Generation Build-out Economic Assessment Tool
DGE	Diesel gallon equivalent
DM	Diffusion media
DMA	Dynamic mechanical analysis
DMFC	Direct methanol fuel cell
DMR	De-acetylation and mechanically refined
DMS	Division of Measurement Standards
DNA	Deoxyribonucleic acid
DOE	Department of Energy
DOS	Density of states
DOT	Department of Transportation
DR	Demand response
DSC	Differential scanning calorimetry
DSM™	Dimensionally stable membrane
DUT	Device under test
e^-	Electron
E85	85%–15% blend of ethanol with gasoline

$E_{1/2}$	Half–wave potential
ECA	Electrochemical area
ECHO	Enforcement and compliance history online
ECSA	Electrochemically active surface area; Electrochemical surface area; Effective catalyst surface area
EDA	Ethylene diamine; Energy decomposition analysis
EDS	Energy dispersive X-ray spectroscopy; Energy dispersive spectrum
EDX	Energy dispersive X-ray
EELS	Electron energy loss spectroscopy
EERE	U.S. DOE Office of Energy Efficiency and Renewable Energy
EFP	Effective fragment potential
e.g.	*Exempli gratia*: for example
EHC	Electrochemical hydrogen compressor
EIA	Energy Information Administration of the U.S. Department of Energy
EIS	Electrochemical impedance spectroscopy
ENG	Enhanced natural graphite; expanded natural graphite
EOL	End of life
EPA	Environmental Protection Agency
EPIC	Energy Policy Institute of Chicago
ePTFE	Expanded polytetrafluoroethylene
ESA	Electrochemical surface area
ESB	Erbium-stabilized bismuth oxide
ESD	Electro-static discharge
ESIF	Energy Systems Integration Facility
et al.	*Et Alii:* and others
etc.	*Et cetera*: and so on
E-TEK	Division of De Nora North America, Inc.
ETFECS	Extended thin-film electrocatalyst structures
EU	European Union
eV	Electron volt
EV	Electric vehicle
EW	Equivalent weight
EXAFS	Extended X-ray absorption fine structure analysis
F	Fluorine
FC	Fuel cell
FC1	Fluoropolymer nanofiber
FC-APOLLO	Fuel Cell Application Package for Open-source Long-Life Operation software
FCB	Fuel cell bus
FCE	FuelCell Energy
FCEB	Fuel cell electric bus
FCEV	Fuel cell electric vehicle
FCHEA	Fuel Cell Hydrogen Energy Association
FCH JU	Joint Fuel Cell and Hydrogen Energy
FC-PAD	Fuel Cell Performance and Durability
FCPP	Fuel cell power plant
FCS	Fuel cell system
FCT	Fuel Cell Technologies
FCTAC	Fuel Cell Tool for Assessing Costs
FCTO	Fuel Cell Technologies Office
FCTT	Fuel Cell Technical Team
FCV	Fuel cell vehicle
Fd	Ferredoxin
Fe	Iron
FE	U.S. DOE Office of Fossil Energy
Fe_2O_3	Ferric oxide
FEA	Finite element analysis
FEM	Finite element model
FER	Fluoride emission rate
FFV	Flexible fuel vehicle
FID	Flame ionization detector
FLC	Frequent and long commute
FMC	Ford Motor Company
FMEA	Failure modes and effects analysis
FMECA	Failure Modes Effects and Criticality Analysis
FMVSS	Federal Motor Vehicle Safety Standards
FOA	Funding opportunity announcement
FOM	Figure of merit
FPITT	Fuel Pathway Integration Technical Team (U.S. DRIVE)
fpm	Feet per minute
FRP	Fiber-reinforced composite piping; Fiber-reinforced polymer; Full rate production
FSC	Frequent and short commute
FSW	Friction stir welding
ft	Feet
ft^2	Square feet
ft^3	Cubic feet
FTA	Federal Transit Administration
FT-IR, FTIR	Fourier transform infrared
FTO	Fluorine-doped tin oxide
FWS	Fixed-window scan
FY	Fiscal year
FZ	Fusion zone

g	Gram; acceleration of gravity
G	Graphite
Ga	Gallium
GaAs	Gallium arsenic
gal	Gallon
GaP	Gallium phosphide
GB	Gigabyte
GC	Glassy, or vitreous carbon
g/cc	Grams per cubic centimeter
GCMS	Gas chromatograph-mass spectroscopy
Gd	Gadolinium
GDC	Gadolinium-doped ceria
GDE	Gas diffusion electrode
GDL	Gas diffusion layer
Ge	Germanium
GEN I	First generation
GEN II	Second generation
GEN III	Third generation
GGE, gge	Gasoline gallon equivalent
GHG	Greenhouse gas
GHSV	Gas hourly space velocity
GJ	Gigajoule(s)
GKB	Grapitized Ketjenblack®
g/kW	Gram(s) per kilowatt
GLWN	Westside Industrial Retention & Expansion Network
gm	Gram(s)
GM	General Motors
gm/day	Gram(s) per day
g/min	Gram(s) per minute
GOI	Gene of interest
GPa	Gigapascal(s)
GPRA	Government Performance and Results Act
GREET	Greenhouse gases, Regulated Emissions and Energy use in Transportation model
g/s	Grams per second
GSE	Ground support equipment
GTI	Gas Technology Institute
GTR	Global Technical Regulations
GUI	Graphical user interface
GVW	Gross vehicle weight
GWe, GW_e	Gigawatt(s) electric
h	Hour(s)
H	Hydrogen
H^-	Hydride
H+	Proton
H_2	Diatomic hydrogen
H2A	Hydrogen Analysis project sponsored by DOE
H2FAST	Hydrogen Financial Analysis Scenario Tool
H_2O	Water
H_2O_2	Hydrogen peroxide
H_2S	Hydrogen sulfide
H2SCOPE	Hydrogen Station Cost Optimization and Performance Evaluation
H_2SO_4	Sulfuric acid
H2ST2	Hydrogen Storage Tech Team
H2USA	Hydrogen Technology Learning Centers (for CA, FL, and NY)
HAADF	High-angle annular dark-field
HAADF-STEM	High angle annular dark field scanning transmission electron microscopy
HAMMER	Hazardous Materials Management and Emergency Response
HAVO	Hawaii Volcanoes National Park
HAZ	Heat-affected zone
HCATT	Hawaii Center for Advanced Transportation Technologies
HCC	Hybrid cathode catalyst
HCD	Hydrogen contaminant detector
HCI	Hydrogen Code Improvement
HCl	Hydrochloric acid
$HClO_4$	Perchloric acid
HDPE	High-density polyethylene
HDSAM	Hydrogen Delivery Scenario Analysis Model
HDTT	Hydrogen Delivery Technical Team
He	Helium
HE	Hydrogen embrittlement
HER	Hydrogen evolution reaction
HEV	Hybrid electric vehicle
HEX	Heat exchanger
Hf	Hafnium
HF	Hydrogen fluoride
HF	Hydroforming
HFCV	Hydrogen fuel cell vehicle
HFE	Hydrofluoro ether
HFR	High-frequency resistance
HFSWG	Hydrogen Fueling Station Working Group of H2USA
HGV	Hydrogen gaseous vehicle
HHV	Higher heating value
HIB	High-impedance buffer

HIL	Hardware in loop
HITRF	Hydrogen Infrastructure Testing and Research Facility
HNEI	Hawaii Natural Energy Institute
HOP	Hydrogen Optimal Pressure model
HOR	Hydrogen oxidation reaction
HPA	Heteropoly acid
HPTB	High powered test bay at NREL
hr	Hour(s)
HRS	Hydrogen refueling station
HRSAM	Hydrogen refueling station analysis model
HRT	Hydraulic retention time
HR-TEM	High resolution transmission electron microscopy
HS	Hydrogen storage
HSA	High surface area
HSAC	High surface area carbon
HSC	Database name derived from the letters for enthalpy, entropy and heat capacity
HSCoE	Hydrogen Sorption Center of Excellence
HSDC	Hydrogen Secure Data Center
HSECoE	Hydrogen Storage Engineering Center of Excellence
HSP	Hydrogen Safety Panel
HT	High throughput; High temperature; heat-treatment/thermal annealing
HTF	Heat transfer fluid
HTFC	High-temperature fuel cell
HX	Heat exchanger
HyCoRA	Hydrogen Contaminant Risk Assessment
HyRam	Hydrogen Risk Assessment Models
HyS	Hybrid sulfur
HyStEP	Hydrogen Station Equipment Performance
Hz	Hertz
I	Current
I_2	Diatomic iodine
I2CNER	International Institute for Carbon-Neutral Energy Research
I/C	Ionomer to catalyst
ICC	International Code Council
ICE	Internal combustion engine
ICEV	Internal combustion engine vehicle
ICHS	International Conference on Hydrogen Safety
i.e.	*id est*: that is
IEC	International Electrotechnical Commission
IEC	Ion exchange capacity, milliequivalents of acid groups per gram of material
IEEE	Institute of Electrical and Electronics Engineers, Inc.
IET	Institute for Energy and Transport
IFC	International Fire Code
IIT	Illinois Institute of Technology
IL	Illinois
ILS	Inter-laboratory studies; Integrated laboratory scale, Instrument landing systems
IMM	Inverted metamorphic multijunction
In	Indium
In., in	Inch
in^2	Square inch
INL	Idaho National Laboratory
INTEGRATE	Integrated Network Testbed for Energy Grid Research and Technology Experimentation
IP	Intellectual property
IR	Infrared
iR	Internal resistance
Ir	Iridium
IR/DC	Infrared diagnostic system with direct current excitation
IrDA	Infrared Data Association
IrO_x	Iridium oxide
IR/RIF	Infrared/reactive impinging flow
ISO	International Organization for Standardization
ISO TC197	International Standards Organization Technical Committee
IT	Information technology
ITC	Investment tax credit
ITO	Indium tin oxide
IV, iV	Current-voltage
J	Current
J	Joule(s)
JARI	Japan Automobile Research Institute
JPBHH	Joint Base Pearl Harbor-Hickman (Hawaii)
JPL	Jet Propulsion Laboratory
JRC	Joint Research Centre
J-V, JV	Current density-voltage
K	Kelvin, absolute temperature
K	Potassium
kÅ	1,000 angstroms
kA/m^2	Kilo-ampere(s) per square meter
kcal	Kilocalorie(s)

kcal/mol	Kilocalorie(s) per mole
kg	Kilogram(s)
kg/d	Kilogram(s) per day
kg/hr	Kilogram(s) per hour
kg/m^3	Kilogram(s) per cubic meter
kHz	Kilohertz
kJ	Kilojoule(s)
kJ/mol	Kilojoule(s) per mole
km	Kilometer(s)
kN	Peak load
KOH	Potassium hydroxide
kPa	Kilopascal(s)
kph	Kilometer(s) per hour
ksi	1,000 pound-force per square inch
kW	Kilowatt(s)
kWe, kW_e	Kilowatt(s) electric
kWh	Kilowatt-hour(s)
kWh/kg	Kilowatt-hour(s) per kilogram
kWh/L	Kilowatt-hour(s) per liter
kW/kg	Kilowatt(s) per kilogram
L, l	Liter(s)
La	Lanthanum
λ	Lambda, hydration number
LAMOX	Lanthanum molybdenum oxide (*e.g.*, $La_2Mo_2O_9$)
LANL	Los Alamos National Laboratory
LAX	Los Angeles International Airport
lb	Pound(s)
lb mol	Pound-mole(s)
LBNL	Lawrence Berkeley National Laboratory
LCA	Life cycle assessment; Life-cycle analysis
L/D	Length to diameter ratio
LD	Learning demonstration
LDV	Light-duty vehicle
L/h, l/h	Liter(s) per hour
LH2, LH_2	Liquid hydrogen
LHV	Lower heating value
LI	Leaching index
Li	Lithium
Li_3N	Lithium nitride
	$LiBH_4$ Lithium borohydride
LiH	Lithium hydride
LLC	Limited Liability Company
LLNL	Lawrence Livermore National Laboratory
L/min, l/min	Liter(s) per minute
LMRC	Linear motor reciprocating compressor
LN_2	Liquid nitrogen
LNG	Liquefied natural gas
LP	Lattice parameter
LSAC	Low surface area carbon
LSM	Lanthanum strontium manganate
LSV	Lanthanum strontium vanadate; Linear sweep voltammetry
LT	Low-temperature
L/T	Lookup tables
LTC	Low temperature coolant
LTPEM	Low temperature polymer electrolyte membrane
m	Meter(s)
M	Mole, molar
M	Million
m^2	Square meter(s)
m^2/g	Square meter(s) per gram
m^2/s	Square meter(s) per second
m^3	Cubic meter(s)
MA	Mass activity
MA3T	Market Acceptance of Advanced Automotive Technologies
μA	Micro ampere(s)
mA	MilliAmps (s)
MA	Mass activity
$\mu A/cm^2$	Micro ampere(s) per square centimeter
mA/cm^2	Milliamp(s) per square centimeter
MARAD	Department of Transportation Maritime Administration
MAS	Magic angle spinning
MASC	Multi-acid side-chain
MAS NMR	Magic angle spinning nuclear magnetic resonance
MATI	Modular Adsorption Tank Insert
MAWP	Maximum allowable working pressure
MB	Megabyte
MBRC	Miles between roadcall
MCFC	Molten carbonate fuel cell
m-CFDE	Multi-electrode channel flow double electrode
MCHL	Magnetocaloric hydrogen liquefier
MD	Molecular dynamics
MEA	Membrane electrode assembly
MEC	Microbial electrolysis cellMeOHMethanol
meq	Milliequivalents

meq/g	Milliequivalents/gram
MES	Microstructered electrode scaffold
MeV	Mega electron volt
MFC	Microbial fuel cell, Mass flow controller
Mg	Megagram(s)
µg	Microgram(s)
mg	Milligram(s)
mg/cm^2	Milligram(s) per square centimeter
mg Pt/cm^2	Milligram (s) of platinum per square centimeter
MH	Metal hydride
MHE	Material handling equipment
MHz	Megahertz
mi	Mile(s)
mi/kg	Mile(s) per kilogram
mil	Millimeter(s)
min	Minute(s)
MJ	Megajoule(s)
mL, ml	Milliliter(s)
ML	Monolayer
µm	Micrometer(s); micron(s)
µM	Micromolar
mM	Millimolar
mm	Millimeter(s)
MMBtu	Million British thermal units
mmol	Millimole(s)
µmol	Micromole(s)
Mn	Manganese
mΩ	Milli-ohm(s)
MΩ	Mega-ohm(s)
$m\Omega/cm^2$	Milli-ohm(s) per square centimeter
$\mu\Omega\text{-}cm^2$	Micro-ohm(s) - square centimeter
Mo	Molybdenum
MOF	Metal-organic framework
mol	Mole(s)
mol%	Mole percent
mol/min	Mole(s) per minute
MPa	Megapascal(s)
MPG, mpg	Mile(s) per gallon
MPGGE	Miles per gasoline gallon equivalent
mph	Mile(s) per hour
MPL	Microporous layer
MREC	Microbial reverse-electrodialysis electrolysis cell
MRH	Hexamethyl trimethyl ammonium functionalized Diels-Alder poly(phenylene)
MRL	Manufacturing readiness level
ms	Millisecond(s)
mS/cm	Milli-Siemen(s) per centimeter
MSM	Macro-System Model
MSRP	Manufacturer's suggested retail price
MSTF	Mesostructured thin films
MSU	Montana State University
MTA	Mass Transportation Agency
mtorr	Millitorr
MTU	Michigan Technological University
µV	Microvolt(s)
mV	Millivolt(s)
mW	Milliwatt(s)
MW	Megawatt(s)
MW	Molecular weight
mW/cm^2	Milliwatt(s) per square centimeter
MWCNT	Multiple-wall carbon nanotube
MWe	Megawatt(s) electric
MWh	Megawatt-hour(s)
MWNT	Multi-wall carbon nanotube
MYPP	Multi-Year Program Plan (the Fuel Cell Technologies Program's Multi-Year Research, Development and Demonstration Plan)
MYRDD, MYRD&DP	Multi-Year Research, Development and Demonstration Plan
N	Nitrogen atom
N	Newton (unit of force)
N112	Nafion® 1100 equivalent weight, 2 millimeter thick membrane
N_2	Diatomic nitrogen
N_2O	Nitrous oxide
Na	Sodium
NA	North American
Nafion®	Registered Trademark of E.I. DuPont de Nemours
NaOH	Sodium hydroxide
NASA	National Aeronautics and Space Administration
Nb	Niobium
N/cm^2	Newton(s) per square centimeter
NCNT	Nitrogen doped carbon nanotube
NDE	Non-destructive examination
NE	U.S. DOE Office of Nuclear Energy, Science and Technology

NEU	Northeastern University
NFCBP	National Fuel Cell Bus Program
NFCTEC	National Fuel Cell Technology Evaluation Center, at NREL
NFPA	National Fire Protection Association
ng	Nanogram
NG	Natural gas
NGNP	Next Generation Nuclear Plant
NG-SR	Natural gas steam reforming
NGV	Natural gas vehicle
NH_3	Ammonia
NHTS	National Household Transportation Survey
NHTSA	National Highway Traffic Safety Administration of the U.S. Department of Transportation
Ni	Nickel
NIST	National Institute of Standards and Technology
NIST FACT	National Institute of Standards and Technology, Facility for Adsorbent Characterization and Testing
nm	Nanometer(s)
NM	Noble metal; nanomaterial
nmol	Nanomole(s)
NMR	Nuclear magnetic resonance
Non-PGM	Non-precious metal group
NOx, NO_x	Oxides of nitrogen
NP	Nanoparticle
NPD	Neutron powder diffraction
NPT	Normal pressure and temperature
NR211	Nafion® 211 membrane
NR212	Nafion® 212 membrane
NREL	National Renewable Energy Laboratory
NRELFAT	NREL Fleet Analysis Toolkit
NRVS	Nuclear resonance vibrational spectroscopy
NSF	National Science Foundation
NSTF	Nano-structured thin-film
NT	Nanotube
NTCNA	Nissan Technical Center, North America
NTR	National Hydrogen and Fuel Cell Emergency Response Training Resource
NV	Neutron vibrational
NVS	Neutron vibrational spectroscopy
NW	Nanowire
Ω	Ohm(s)
Ωcm^2	Ohm(s) - square centimeter
O	Oxygen
O_2	Diatomic oxygen
OCP	Open circuit potential
OCSD	Orange County Sanitation District
OCV	Open-circuit voltage
o.d.,OD	Outer diameter
OEM	Original equipment manufacturer
OER	Oxygen evolution reaction
O&M	Operation and maintenance
ORNL	Oak Ridge National Laboratory
ORR	Oxygen reduction reaction
OSU	Ohio State University
OSU	Oregon State University (Microproducts Breakthrough Institute)
P	Phosphorus
Pa	Pascal(s)
PA	Polyamide
PAFC	Phosphoric acid fuel cell
PAN	Peroxyacetyl nitrate; Polyacrylonitrile
P&D	Production and delivery
P&ID	Piping and instrumentation diagram
PANI	Polyaniline
PAN-MA	Polyacrylonitrile with methyl acrylate
Pb	Lead
PBCTF	Pressurized button cell test facility
PBD	Performance-based design
PBI	Polybenzimidazole
PC	Precharged (hydrogen)
PCR	Polymerase chain reaction
PCT	Pressure-composition-temperature
Pd	Palladium
Pd/C	Palladium on carbon
PEC	Photoelectrochemical
PEFC	Proton exchange fuel cell; Polymer electrolyte fuel cell
PEGS	Prototype electrostatic ground state
PEM	Proton exchange membrane; Polymer electrolyte membrane
PEMFC	Polymer electrolyte membrane fuel cell; Proton exchange membrane fuel cell
PEO	Poly(ethylene oxide)
PF	Perfluoro; Phenolic
PFCB	Perfluorocyclobutyl
PFCT	Porvair Fuel Cell Technology, Inc.
PFD	Process flow diagram
PFIA	Perfluoroimide acid

PFICE	Perfluoro ionene chain extended
PFSA	Perfluorinated sulfonic acid, perfluorosulfonic acid, poly(fluorosulfonic acid)
PF-SFP	Perfluoro sulfonyl fluoride precursor
PG	Porous graphene
PG&E	Pacific Gas and Electric Company
PGM	Precious group metal; Platinum-group metal
PGV	Puna Geothermal Ventures
PHEV	Plug-in hybrid electric vehicle
PHIL	Power hardware in the loop
PI	Principal investigator
P&ID	Process and instrumentation diagram
PID	Proportional, integral, derivative
PITM	Platinum in the membrane
PLC	Programmable logic controller
PLD	Pulsed laser deposition
PM	Particulate matter
PMMA	Poly(methyl methacrylate)
PNNL	Pacific Northwest National Laboratory
POM	Polyoxometallate
POP	Porous organic polymers
PPA	Polyphthalamide
ppb	Part(s) per billion
ppbv	Part(s) per billion by volume
PPC	Pajarito Powder
ppm, PPM	Part(s) per million
ppmv	Part(s) per million by volume
ppmw	Part(s) per million by weight
PRD	Pressure relief device
PSA	Pressure swing adsorption, adsorber
PSD	Particle size distribution, pore size distribution
psi, PSI	Pound(s) per square inch
psia	Pound(s) per square inch absolute
psig, PSIG	Pound(s) per square inch gauge
Pt	Platinum
Pt/C	Platinum/carbon
PTFE	Teflon® – poly-tetrafluoroethylene
PtO	Platinum oxide
PtO_2	Platinum dioxide
PtRu	Platinum ruthenium
PUC	Public Utility Commission
PV	Photovoltaic; Present value
PVD	Physical vapor deposition
PXRD	Powder X-ray diffraction
Q	Heat load estimate
Q1, Q2, Q3, Q4	Quarters of the fiscal year
Q/ΔT	Heat rejection constraint
QC	Quality control
QE	Quantum efficiency
QENS	Quasielastic neutron scattering
QMED	Quantum based materials exploration and design
QR	Quick response
QRA	Quantitative risk assessment
R	Universal or ideal gas constant, $8.314472\ J \cdot K^{-1} \cdot mol^{-1}$
RBS	Ribosome binding site
RCS	Regulations codes and standards
R&D	Research and development
RD&D, R,D&D	Research, development, and demonstration
RDE	Rotating disk electrode
Re	Rhenium
Ref	Reference
REP	Reformer-Electrolyzer-Purifier; Representative performance
RF, rf	Radio frequency
RGA	Residual gas analyzer (analysis)
rGO	Reduced graphene oxide
Rh	Rhodium
RH	Relative humidity
R-HC-HEW	Partially fluorinated hydrocarbon high equivalent weight
R-HC-LEW	Partially fluorinated hydrocarbon low equivalent weight
RHE	Reference hydrogen electrode; Reversible hydrogen electrode
RIE	Reactive ion etching
RIF	Reactive impinging flow
RNG	Renewable natural gas
ROI	Return on investment
R-PFSA-HEW	Reinforced perfluorinated sulfonic acid high equivalent weight membrane
R-PFSA-LEW	Reinforced perfluorinated sulfonic acid low equivalent weight membrane
rpm	Revolution(s) per minute
RPN	Risk priority number
RRDE	Rotating ring disc electrode
RT	Room temperature
RTDS®	Real time digital simulation
RTO	Ruthenium-titanium oxide

Ru	Ruthenium
s	Second(s)
S	Siemen(s)
S	Sulfur
SA	Solvay Amodel PPA; Strategic Analysis, Inc.
SAE	SAE International, originally known as the Society of Automotive Engineers
SBIR	Small Business Innovation Research
Sc	Scandium
S/C	Steam to carbon ratio
SCAQMD	South Coast Air Quality Management District
sccm, SCCM	Standard cubic centimeter(s) per minute
SCCV	Steel/concrete composite vessel
SCF, scf	Standard cubic feet
scfd	Standard cubic feet per day
SCFH, scfh	Standard cubic feet per hour
SCFM	Standard cubic feet per minute
S/cm	Siemen(s) per centimeter
SDAPP	Sulfonated Diels-Alder polyphenylene
SDAPPe	Sulfonated Diels-Alder polyphenylene ether
SDD	Si-drift detector
SDE	SO_2-depolarized electrolyzer
SDO	Standards development organization
SD/SU	Shut-down/start-up
Se	Selenium
SEBS	Benzyl trimethyl ammonium functionalized polystyrene-*b*-poly(ethylene-*co*-buthylene)-*b*-polystyrene triblock copolymers
sec	Second(s)
SEM	Scanning electron microscopy; Scanning electron microscope
SEM	Secondary electron microscopy
SERA	Scenario Evaluation, Regionalization and Analysis
SFE	Stacking fault energy
SFR	Stagnation flow reactor
SGA	Sales, general, administration
SGIP	Self-Generation Incentive Program
SHE	Standard hydrogen electrode
Si	Silicon
S-I	Sulfur-iodine
SI	Spark ignition
SiO_2	Silicon dioxide
SKKR	Screened Korringa-Kohn-Rostoker method
sL	Standard liter (0°C, 1 atm)
slpm, slm, sL/min	Standard liter(s) per minute
SMR	Steam methane reformer; Steam methane reforming
Sn	Tin
SNL	Sandia National Laboratories
SnO	Tin oxide
SnO_2	Tin oxide
SO_2	Sulfur dioxide
SOC	State-of-charge
SOEC	Solid oxide electrolyzer cell
SOFC	Solid oxide fuel cell
SOPO	Statement of project objectives
SOSS	Station Operational Status System
SPWG	Stationary Power Working Group
sq. in.	Square inch(es)
Sr	Strontium
SR	Stoichometric ratio
SRNL	Savannah River National Laboratory
SrO	Strontium oxide
SS	Stainless steel
SSA	Specific surface area
STCH	Solar thermochemical hydrogen
STEM	Scanning transmission electron microscopy
STH	Solar-to-hydrogen
STREET	Spatially and Temporally Resolved Energy and Environment Tool
STWS	Solar thermal water splitting
STXM	Scanning transmission X-ray microscopy
SwRI®	Southwest Research Institute®
T	Temperature
T, t	Ton, tonne
T	Tesla (unit of magnetic induction)
t	Time
Ta	Tantalum
TAMU	Texas A&M University
TBD	To be determined
TC	Thermal conductivity
TC	Thermocouple; Thermal conditioning
TCO	Transparent conductive oxide; Total cost of ownership
Te	Tellurium
TEDA	Triethylenediamine
TEM	Transmission electron microscopy
TFVE	Trifluorovinyl ether

TGA	Thermal gravimetric analysis; Thermogravimetric analysis; Thermogravimetric analyzer
Ti	Titanium
TIA	Telecommunications Industry Association
TIR	Technical information report
TKK	Tanaka Kikinzoku Kogyo K. K.
TM	Transition metal
TMB	Trimethylborate
TOC	Total organic carbon
TOS	Time on stream
TOU	Time of use
TPD	Tonne(s) per day
TPD	Thermally programmed desorption; Temperature-programmed desorption
TPR	Through plate resistance; Temperature programmed reaction
TPRD	Thermally-activated pressure relief device
TPRE	Through-plane reactive excitation
TPS	Transient plane source
TRL	Technology readiness level
TRU	Trailer refrigeration unit
TTS	Time-temperature superpositioning
TVS	Twin Vortices Series
UAV	Unmanned aerial vehicle
UCB	University of California, Berkeley
UCSD	University of California, San Diego
U_F	Fuel Utilization
UFC	Uniform Fire Code
UH	University of Hawaii
µm	Micrometer(s)
UM	University of Michigan
UNLV	University of Nevada, Las Vegas
UNM	University of New Mexico
UPD	Underpotential deposition
UPS	United Parcel Service
UQTR	Université du Québec à Trois-Rivières
URFC	Unitized regenerative fuel cell
U.S.	United States
USAXS	Ultra-small angle X-ray scattering
USC	University of South Carolina
USCAR	United States Council for Automotive Research, U.S. Cooperative Automotive Research
USCG	U.S. Coast Guard
U.S. DRIVE	United States Driving Research and Innovation for Vehicle efficiency and Energy sustainability
UTRC	United Technologies Research Center
UTS	Ultimate tensile strength
UV	Ultraviolet
UV-vis	Ultraviolet-visual
V	Vanadium
V	Volt
VAC	Volts alternating current
VB	Valence band
VC	Volumetric capacity
VDC	Volts direct current
V-I, V/I	Voltage – current
Vol., vol.	Volume
vol%	Volume percent
VPN	Virtual private network
VSM	Value stream mapping
VTO	Vehicles Technologies Office
W	Tungsten
W	Watt(s)
W/cm^2	Watt(s) per square centimeter
We, W_e	Watt(s) electric
WG	Working group
Wh	Watt-hour(s)
W-h/kg	Watt-hour(s) per kilogram
W-h/L, Wh/liter, Wh/L	Watt-hour(s) per liter
W/kg	Watt(s) per kilogram
W/L, W/l	Watt(s) per liter
W/m-K, W/m.K, W/mK	Watt(s) per meter-Kelvin (unit of thermal conductivity)
Wppm	Weight part(s) per million
WS	Water splitting
wt	Weight
Wt	Watt(s) thermal
wt%, wt.%	Weight percent (percent by weight)
WTE	Well-to-engine
WTF	Water treatment facility
WTT	Well-to-tank
WTW	Well-to-wheels
WWTP	Waste water treatment plant
XAFS	X-ray absorption fine structure

XANES	X-ray absorption near-edge spectroscopy
XAS	X-ray absorption spectroscopy
XES	X-ray emission spectroscopy
XPS	X-ray photoelectron spectroscopy, X-ray photon spectroscopy, X-ray photoemission spectroscopy, X-ray photoluminescence spectroscopy
XRD	X-ray diffraction
XRF	X-ray fluorescence
XRPD	X-ray powder diffractions
XRT	X-ray tomography
Y	Yttrium
YB	Young Brothers Ltd.
yr, YR	Year
YSZ	Yttria-stablized zirconia
ZEBA	Zero Emission Bay Area
ZEV	Zero emission vehicle
ZIF	Zeolitic imidazolate framework
Zn	Zinc
ZnO	Zinc oxide
ZPE	Zero point energy
Zr	Zirconium
ZrO_2	Zirconium dioxide

XIII. Primary Contacts Index

A

Aceves, Salvador. IV–113, VII–13, VIII–60
Adzic, Radoslav V–20
Ahluwalia, Rajesh. IV–11, V–133
Ahmed, Shabbir IX–29
Ainscough, Chris VII–31
Anton, Donald. IV–22
Arif, Muhammad V–152
Ayers, Katherine II–28

B

Baldwin, Don III–25
Barilo, Nick. VIII–31
Barnes, Ted VII–50
Blackburn, Bryan V–167
Blekhman, David VII–58
Bliznakov, Stoyan V–223
Borup, Rod V–101
Broerman, Eugene III–33
Brooks, Kriston. IV–44
Brosha, Eric VIII–53
Burgess, Robert VIII–13
Buttner, William VIII–26

C

Cai, Mei. IV–59
Colón-Mercado, Héctor V–189
Contini, Vince. V–158
Cullen, David V–198

D

Danilovic, Nemanja V–56
Deutsch, Todd II–50
Dinh, Huyen V–113
Dismukes, G. Charles II–72
Drost, Kevin IV–32

E

Edgecombe, Brian IV–122
Elgowainy, Amgad III–9, III–57, IX–37, IX–54
Eudy, Leslie VII–26
Ewan, Mitch X–18

F

Feng, Zhili. III–13, III–40
Fujimoto, Cy V–211
Fullenkamp, Patrick VI–12

G

Gaillard, Nicolas II–56
Goodarzi, Abas X–21
Gotthold, David IV–118
Greene, David IX–44
Groth, Katrina. VIII–7

H

Haight, Andrea IV–138
Hanlin, Jason X–14
Harrison, Kevin III–60, VII–17
Herring, Andrew. V–69
Holladay, Jamie. III–65
Hovsapian, Rob. VII–65

J

Jahnke, Fred II–90
James, Brian II–11, IV–17, V–141
Jena, Puru IV–146
Johnson, Terry VII–36

K

Kim, Yu Seung V–205
Knights, Shanna V–125
Kurtz, Jennifer V–174, VII–21

L

LaFleur, Chris. VIII–49
Lalli, Jennifer III–28
Li, Hong IV–134
Lin, Zhenhong IX–19, IX–58
Lipp, Ludwig. III–50
Liu, Di-Jia V–184
Liu, Shih-Yuan IV–92
Liu, Wei. II–84
Long, Jeffrey. IV–63

M
Maness, Pin-Ching II–76, II–81
Markowitz, Morry VIII–42
Martin, Richard IV–88
Matter, Paul. V–60
McDaniel, Anthony II–35
Melaina, Marc. IX–61
Mintz, Marianne. IX–34
Mittelsteadt, Cortney II–31
More, Karren V–147
Moulthrop, Larry VII–44
Mukerjee, Sanjeev V–29
Musgrave, Charles II–60
Myers, Deborah V–51, V–80

N
Newhouse, Norman IV–53

P
Parilla, Philip IV–70
Paulauskas, Felix IV–126
Pecharsky, Vitalij IV–81, IV–143
Peters, Mike II–18
Petrecky, Jim. X–7
Pivovar, Bryan V–9, V–92
Popov, Branko. V–37
Power, Philip. IV–145
Prakash, Amit. III–45
Pratt, Joe III–53, X–10

R
Ramani, Vijay. V–25
Ramsden, Todd. IX–24
Rawls, George. III–22
Rivkin, Carl VIII–38
Rockward, Tommy VIII–21
Rosner, R. IX–65
Rousseau, Aymeric. IX–13

S
San Marchi, Chris. IV–108
Saur, Genevieve V–130, VII–61
Schlesselman, Kent. IX–67
Semelsberger, Troy IV–56
Shaffer, Brendan. IX–48
Somerday, Brian III–18, VIII–17
Sprik, Sam VII–53
Stamenkovic, Vojislav V–13
Steinbach, Andrew V–73
St-Pierre, Jean. V–119
Stretch, Dale V–96
Summers, William II–46

T
Terlip, Danny VII–9, VIII–46
Thornton, Matthew. IV–49

U
Udovic, Terrence. IV–76
Ulsh, Michael VI–7

V
Vajo, John IV–97
van Hassel, Bart IV–36
Veenstra, Michael. IV–27

W
Wang, Conghua “CH” V–86
Wang, Yong. V–194
Weber, Adam V–108
Wei, Max. V–162
Weimer, Alan II–41
West, Todd II–41
Wilson, Mahlon V–218
Wood, Brandon. IV–101

X
Xiong, Ben VII–41
Xu, Hui II–23, V–179

Y
Yandrasits, Michael V–64
Yan, Yanfa. II–67
Yuh, Chao-Yi V–170

Z
Zawodzinski, Thomas V–203
Zelenay, Piotr V–43
Zidan, Ragaiy IV–84, IV–144

XIV. Hydrogen and Fuel Cells Program Contacts

Sunita Satyapal
Director
Fuel Cell Technologies Office
Office of Energy Efficiency and Renewable Energy
U.S. Department of Energy
Phone: (202) 586-2336
Email: Sunita.Satyapal@ee.doe.gov

Rick Farmer
Operations Supervisor
Fuel Cell Technologies Office
Office of Energy Efficiency and Renewable Energy
U.S. Department of Energy
Phone: (202) 586-1623
Email: Richard.Farmer@ee.doe.gov

John Vetrano
Materials Sciences and Engineering Division
Basic Energy Sciences Program
Office of Science
U.S. Department of Energy
Phone: (301) 903-5976
Email: John.Vetrano@science.doe.gov

Bhima Sastri
Advanced Combustion & Fuel Cells Program Manager
Office of Fossil Energy
U.S. Department of Energy
Phone: (202) 586-2561
Email: Bhima.Sastri@hq.doe.gov

Carl Sink
Office of Gas Cooled Reactor Technologies
Office of Nuclear Energy
U.S. Department of Energy
Phone: (301) 903-5131
Email: Carl.Sink@nuclear.energy.gov

HYDROGEN PRODUCTION AND DELIVERY

Eric Miller
Hydrogen Production and Delivery Program Manager
Fuel Cell Technologies Office
Office of Energy Efficiency and Renewable Energy
U.S. Department of Energy
Phone: (202) 287-5829
Email: Eric.Miller@ee.doe.gov

HYDROGEN STORAGE

Ned Stetson
Hydrogen Storage Program Manager
Fuel Cell Technologies Office
Office of Energy Efficiency and Renewable Energy
U.S. Department of Energy
Phone: (202) 586-9995
Email: Ned.Stetson@ee.doe.gov

FUEL CELLS

Dimitrios Papageorgopoulos
Fuel Cells Program Manager
Fuel Cell Technologies Office
Office of Energy Efficiency and Renewable Energy
U.S. Department of Energy
Phone: (202) 586-5463
Email: Dimitrios.Papageorgopoulos@ee.doe.gov

MANUFACTURING R&D

Nancy Garland
Manufacturing R&D Project Manager
Fuel Cell Technologies Office
Office of Energy Efficiency and Renewable Energy
U.S. Department of Energy
Phone: (202) 586-5673
Email: Nancy.Garland@ee.doe.gov

TECHNOLOGY VALIDATION

Jason Marcinkoski
Technology Validation Project Manager
Fuel Cell Technologies Office
Office of Energy Efficiency and Renewable Energy
U.S. Department of Energy
Phone: (202) 586-7466
Email: Jason.Marcinkoski@ee.doe.gov

SAFETY, CODES & STANDARDS

Charles James, Jr.
Safety, Codes & Standards Project Manager
Fuel Cell Technologies Office
Office of Energy Efficiency and Renewable Energy
U.S. Department of Energy
Phone: (202) 287-6223
Email: Charles.James@ee.doe.gov

EDUCATION

Gregory J. Kleen
Education Project Manager
Fuel Cell Technologies Office
Golden Field Office
U.S. Department of Energy
Phone: (720) 356-1672
Email: Gregory.Kleen@ee.doe.gov

MARKET TRANSFORMATION

Pete Devlin
Market Transformation Project Manager
Fuel Cell Technologies Office
Office of Energy Efficiency and Renewable Energy
U.S. Department of Energy
Phone: (202) 586-4905
Email: Peter.Devlin@ee.doe.gov

SYSTEMS ANALYSIS

Fred Joseck
Systems Analysis Project Manager
Fuel Cell Technologies Office
Office of Energy Efficiency and Renewable Energy
U.S. Department of Energy
Phone: (202) 586-7932
Email: Fred.Joseck@ee.doe.gov

AMERICAN RECOVERY AND REINVESTMENT ACT (ARRA) ACTIVITIES

Jim Alkire
Project Manager and Recovery Act Activities Lead
Fuel Cell Technologies Office
Office of Energy Efficiency and Renewable Energy
U.S. Department of Energy
Phone: (720) 356-1426
Email: James.Alkire@ee.doe.gov

XV. Project Listings by State

Alabama

IV.C.7 The University of Alabama: Novel Carbon(C)-Boron(B)-Nitrogen(N)-Containing H_2 Storage Materials IV–92

IV.D.3 Toray Composites America: Enhanced Materials and Design Parameters for Reducing the Cost of Hydrogen Storage Tanks IV–118

Arizona

II.C.1 Arizona State University: High Efficiency Solar Thermochemical Reactor for Hydrogen Production II–35

VIII.11 Custom Sensor Solutions: Hydrogen Safety, Codes and Standards: Sensors VIII–53

Arkansas

III.9 Ashok Saxena: Low Cost Hydrogen Storage at 875 Bar Using Steel Liner and Steel Wire Wrap III–45

California

II.C.1 Sandia National Laboratories: High Efficiency Solar Thermochemical Reactor for Hydrogen Production II–35

II.C.1 Stanford University: High Efficiency Solar Thermochemical Reactor for Hydrogen Production II–35

II.C.5 Stanford University: Wide Bandgap Chalcopyrite Photoelectrodes for Direct Solar Water Splitting II–56

II.C.5 Lawrence Livermore National Laboratory: Wide Bandgap Chalcopyrite Photoelectrodes for Direct Solar Water Splitting II–56

II.F.2 University of California, Irvine: Reformer-Electrolyzer-Purifier (REP) for Production of Hydrogen II–90

III.3 Sandia National Laboratories: Hydrogen Embrittlement of Structural Steels III–18

III.8 Bevilacqua Knight, Inc.: Steel Concrete Composite Vessel for 875 bar Stationary Hydrogen Storage III–40

III.8 LightSail: Steel Concrete Composite Vessel for 875 bar Stationary Hydrogen Storage III–40

III.11 Sandia National Laboratories: Reference Station Design III–53

IV.B.1 Jet Propulsion Laboratory: Hydrogen Storage Engineering Center of Excellence IV–22

IV.B.1 California Institute of Technology: Hydrogen Storage Engineering Center of Excellence IV–22

IV.C.1 Lawrence Berkeley National Laboratory: Hydrogen Storage in Metal-Organic Frameworks IV–63

IV.C.2 H2 Technology Consulting LLC: Hydrogen Sorbent Measurement Qualification and Characterization IV–70

IV.C.2 University of California, Berkeley: Hydrogen Sorbent Measurement Qualification and Characterization . . IV–70

IV.C.2 University of California, San Diego: Hydrogen Sorbent Measurement Qualification and Characterization IV–70

IV.C.6 Ardica Technologies: Low-Cost α-Alane for Hydrogen Storage IV–88

IV.C.6 SRI International: Low-Cost α-Alane for Hydrogen Storage IV–88

IV.C.8 HRL Laboratories, LLC: Boron-Based Hydrogen Storage: Ternary Borides and Beyond IV–97

IV.C.8 Sandia National Laboratories: Boron-Based Hydrogen Storage: Ternary Borides and Beyond IV–97

IV.C.9 Lawrence Livermore National Laboratory: Improving the Kinetics and Thermodynamics of $Mg(BH_4)_2$ for Hydrogen Storage IV–101

IV.C.9 Sandia National Laboratories: Improving the Kinetics and Thermodynamics of $Mg(BH_4)_2$ for Hydrogen Storage IV–101

IV.D.1 Sandia National Laboratories: Innovative Development, Selection and Testing to Reduce Cost and Weight of Materials for BOP Components IV–108

IV.D.2 Lawrence Livermore National Laboratory: Thermomechanical Cycling of Thin Liner High Fiber Fraction Cryogenic Pressure Vessels Rapidly Refueled by LH_2 Pump to 700 Bar IV–113

IV.D.2 Spencer Composites Corporation: Thermomechanical Cycling of Thin Liner High Fiber Fraction Cryogenic Pressure Vessels Rapidly Refueled by LH_2 Pump to 700 Bar IV–113

California (Continued)

IV.D.2 Linde LLC: Thermomechanical Cycling of Thin Liner High Fiber Fraction Cryogenic Pressure Vessels Rapidly Refueled by LH_2 Pump to 700 Bar . . . IV–113

IV.D.4 Materia: Next Generation Hydrogen Storage Vessels Enabled by Carbon Fiber Infusion with a Low Viscosity, High Toughness System . . . IV–122

IV.D.4 Spencer Composites Corporation: Next Generation Hydrogen Storage Vessels Enabled by Carbon Fiber Infusion with a Low Viscosity, High Toughness System. . . . IV–122

IV.E.2 Savannah River National Laboratory: Elucidation of Hydrogen Interaction Mechanisms with Metal-Doped Carbon Nanostructures . . . IV–144

IV.E.3 University of California, Davis: Activation of Hydrogen Under Ambient Conditions by Main Group Molecules . . . IV–145

V.C.1 Lawrence Berkeley National Laboratory: High Performance, Durable, Low Cost Membrane Electrode Assemblies for Transportation Applications . . . V–73

V.D.1 Electricore, Inc.: Roots Air Management System with Integrated Expander . . . V–96

V.E.1 Lawrence Berkeley National Laboratory: Durability Improvements Through Degradation Mechanism Studies . . . V–101

V.E.2 Lawrence Berkeley National Laboratory: Fuel-Cell Fundamentals at Low and Subzero Temperatures . . . V–108

V.F.7 Lawrence Berkeley National Laboratory: A Total Cost of Ownership Model for Design and Manufacturing Optimization of Fuel Cells in Stationary and Emerging Market Applications . . . V–162

V.F.7 University of California, Berkeley: A Total Cost of Ownership Model for Design and Manufacturing Optimization of Fuel Cells in Stationary and Emerging Market Applications. . . . V–162

V.F.17 Lawrence Berkeley National Laboratory: Advanced Hydroxide Conducting Membranes . . . V–205

V.F.19 Lawrence Berkeley National Laboratory: Engineered Low-Pt Catalyst Layers . . . V–218

VI.1 Lawrence Berkeley National Laboratory: Fuel Cell Membrane Electrode Assembly Manufacturing R&D . . . VI–7

VII.2 Lawrence Livermore National Laboratory: Performance and Durability Testing of Volumetrically Efficient Cryogenic Vessels and High Pressure Liquid Hydrogen Pump . . . VII–13

VII.2 Linde LLC: Performance and Durability Testing of Volumetrically Efficient Cryogenic Vessels and High Pressure Liquid Hydrogen Pump . . . VII–13

VII.2 Spencer Composites Corporation: Performance and Durability Testing of Volumetrically Efficient Cryogenic Vessels and High Pressure Liquid Hydrogen Pump . . . VII–13

VII.7 Sandia National Laboratories: Development of the Hydrogen Station Equipment Performance (HyStEP) Device . . . VII–36

VII.8 California Fuel Cell Partnership: Station Operational Status System (SOSS) 3.0 Upgrade . . . VII–41

VII.10 Linde Gas, LLC: Performance Evaluation of Delivered Hydrogen Fueling Stations . . . VII–50

VII.12 California State University, Los Angeles: CSULA Hydrogen Refueling Facility Performance Evaluation and Optimization . . . VII–58

VIII.3 Sandia National Laboratories: R&D for Safety, Codes and Standards: Materials and Components Compatibility . . . VIII–17

VIII.6 Fluer, Inc.: Hydrogen Safety Panel, Safety Knowledge Tools and First Responder Training Resources . . . VIII–31

VIII.6 BKi: Hydrogen Safety Panel, Safety Knowledge Tools and First Responder Training Resources . . . VIII–31

VIII.6 City of Santa Fe Springs: Hydrogen Safety Panel, Safety Knowledge Tools and First Responder Training Resources. . . . VIII–31

VIII.7 Branded by Media: Fuel Cell Technologies National Codes and Standards Deployment and Outreach . . . VIII–38

VIII.11 Lawrence Livermore National Laboratory: Hydrogen Safety, Codes and Standards: Sensors . . . VIII–53

VIII.11 Hydrogen Frontier: Hydrogen Safety, Codes and Standards: Sensors . . . VIII–53

VIII.12 Lawrence Livermore National Laboratory: Hands-on Hydrogen Safety Training . . . VIII–60

IX.7 Sandia National Laboratories: Hydrogen Analysis with the Sandia ParaChoice Model . . . IX–44

California (Continued)

IX.9 University of California, Irvine: Tri-Generation Fuel Cell Technologies for Location-Specific Applications (FY 2015) . . . IX–54

X.2 Sandia National Laboratories: Maritime Fuel Cell Generator Project . . . X–10

X.5 US Hybrid Corporation: Demonstration and Deployment of a Fuel Cell-Electric Refuse Truck for Waste Transportation . . . X–21

Colorado

II.B.1 National Renewable Energy Laboratory: Renewable Electrolysis Integrated System Development and Testing . . . II–18

II.B.1 Spectrum Automation Controls: Renewable Electrolysis Integrated System Development and Testing . . . II–18

II.B.2 National Renewable Energy Laboratory: High-Performance, Long-Lifetime Catalysts for Proton Exchange Membrane Electrolysis . . . II–23

II.C.1 Colorado School of Mines: High Efficiency Solar Thermochemical Reactor for Hydrogen Production . . . II–35

II.C.2 University of Colorado Boulder: Flowing Particle Bed Solarthermal Redox Process to Split Water . . . II–41

II.C.2 National Renewable Energy Laboratory: Flowing Particle Bed Solarthermal Redox Process to Split Water. . . . II–41

II.C.4 National Renewable Energy Laboratory: High-Efficiency Tandem Absorbers for Economical Solar Hydrogen Production . . . II–50

II.C.5 National Renewable Energy Laboratory: Wide Bandgap Chalcopyrite Photoelectrodes for Direct Solar Water Splitting . . . II–56

II.C.6 University of Colorado Boulder: Accelerated Discovery of Advanced RedOx Materials for Solar Thermal Water Splitting to Produce Renewable Hydrogen . . . II–60

II.E.1 National Renewable Energy Laboratory: Fermentation and Electrohydrogenic Approaches to Hydrogen Production . . . II–76

II.E.2 National Renewable Energy Laboratory: Improving Cyanobacterial O_2-Tolerance using CBS Hydrogenase for H_2 Production . . . II–81

III.6 National Renewable Energy Laboratory: Cryogenically Flexible, Low Permeability H_2 Delivery Hose . . . III–28

III.11 National Renewable Energy Laboratory: Reference Station Design . . . III–53

III.13 Spectrum Automation Controls: 700-Bar Hydrogen Dispenser Hose Reliability Improvement. . . . III–60

III.13 National Renewable Energy Laboratory: 700-Bar Hydrogen Dispenser Hose Reliability Improvement . . . III–60

IV.B.1 National Renewable Energy Laboratory: Hydrogen Storage Engineering Center of Excellence . . . IV–22

IV.B.6 National Renewable Energy Laboratory: System Design, Analysis, and Modeling for Hydrogen Storage Systems. . . . IV–49

IV.C.2 National Renewable Energy Laboratory: Hydrogen Sorbent Measurement Qualification and Characterization . . . IV–70

IV.D.7 Composite Technology Development: Optimizing the Cost and Performance of Composite Cylinders for H_2 Storage using a Graded Construction . . . IV–138

V.A.1 National Renewable Energy Laboratory: Extended, Continuous Pt Nanostructures in Thick, Dispersed Electrodes . . . V–9

V.A.1 Colorado School of Mines: Extended, Continuous Pt Nanostructures in Thick, Dispersed Electrodes . . . V–9

V.B.2 Colorado School of Mines: Advanced Hybrid Membranes for Next Generation PEMFC Automotive Applications . . . V–69

V.B.2 National Renewable Energy Laboratory: Advanced Hybrid Membranes for Next Generation PEMFC Automotive Applications . . . V–69

V.C.4 National Renewable Energy Laboratory: Advanced Ionomers & MEAs for Alkaline Membrane Fuel Cells . . . V–92

V.C.4 Colorado School of Mines: Advanced Ionomers & MEAs for Alkaline Membrane Fuel Cells . . . V–92

Colorado (Continued)

V.E.3 National Renewable Energy Laboratory: Effect of System Contaminants on PEMFC Performance and Durability . . . V–113

V.E.3 Colorado School of Mines: Effect of System Contaminants on PEMFC Performance and Durability . . . V–113

V.F.1 National Renewable Energy Laboratory: Optimal Stationary Fuel Cell Integration and Control. . . . V–130

V.F.10 National Renewable Energy Laboratory: Fuel Cell Technology Status--Degradation . . . V–174

V.F.15 National Renewable Energy Laboratory: Magnetic Annealing of Pt-Alloy Nanostructured Thin Film Catalysts for Enhanced Activity . . . V–198

VI.1 National Renewable Energy Laboratory: Fuel Cell Membrane Electrode Assembly Manufacturing R&D. . . VI–7

VI.1 Colorado School of Mines: Fuel Cell Membrane Electrode Assembly Manufacturing R&D. . . VI–7

VII.1 National Renewable Energy Laboratory: Hydrogen Component Validation . . . VII–9

VII.1 Spectrum Automation Controls: Hydrogen Component Validation. . . VII–9

VII.3 National Renewable Energy Laboratory: FCTO INTEGRATE Stack Test Bed & Grid Interoperability. . . .VII–17

VII.3 Spectrum Automation Controls: FCTO INTEGRATE Stack Test Bed & Grid Interoperability VII–17

VII.4 National Renewable Energy Laboratory: Fuel Cell Electric Vehicle Evaluation. . . .VII–21

VII.5 National Renewable Energy Laboratory: Technology Validation: Fuel Cell Bus Evaluations VII–26

VII.6 National Renewable Energy Laboratory: Material Handling Equipment Data Collection and Analysis VII–31

VII.11 National Renewable Energy Laboratory: Hydrogen Station Data Collection and Analysis VII–53

VII.13 National Renewable Energy Laboratory: Stationary Fuel Cell Evaluation VII–61

VIII.2 National Renewable Energy Laboratory: Component Standard Research & Development . . . VIII–13

VIII.2 Spectrum Automation Controls: Component Standard Research & Development . . . VIII–13

VIII.5 National Renewable Energy Laboratory: NREL Hydrogen Sensor Testing Laboratory. . . .VIII–26

VIII.5 Element One: NREL Hydrogen Sensor Testing Laboratory VIII–26

VIII.7 National Renewable Energy Laboratory: Fuel Cell Technologies National Codes and Standards Deployment and Outreach VIII–38

VIII.9 National Renewable Energy Laboratory: Hydrogen Contaminant Detector VIII–46

IX.3 National Renewable Energy Laboratory: Pathway Analysis: Projected Cost, Lifecycle Energy Use and Emissions of Emerging Hydrogen Technologies . . . IX–24

IX.12 National Renewable Energy Laboratory: Infrastructure Investment and Finance Scenario Analysis IX-61

Connecticut

II.B.3 Proton OnSite: Low-Noble-Metal-Content Catalysts/Electrodes for Hydrogen Production by Water Electrolysis . . . II–28

II.F.2 FuelCell Energy, Inc.: Reformer-Electrolyzer-Purifier (REP) for Production of Hydrogen . . . II–90

III.10 FuelCell Energy, Inc.: Electrochemical Hydrogen Compressor. . . . III–50

III.10 Sustainable Innovations, LLC: Electrochemical Hydrogen Compressor. . . . III–50

IV.B.1 United Technologies Research Center: Hydrogen Storage Engineering Center of Excellence . . . IV–22

IV.B.4 United Technologies Research Center: Advancement of Systems Designs and Key Engineering Technologies for Materials Based Hydrogen Storage . . . IV–36

V.A.9 Proton OnSite: Non-Platinum Group Metal OER/ORR Catalysts for Alkaline Membrane Fuel Cells and Electrolyzers. . . . V–56

V.C.2 United Technologies Research Center: Rationally Designed Catalyst Layers for PEMFC Performance Optimization. . . . V–80

V.E.2 United Technologies Research Center: Fuel-Cell Fundamentals at Low and Subzero Temperatures. . . . V–108

V.E.4 University of Connecticut: The Effect of Airborne Contaminants on Fuel Cell Performance and Durability . . . V–119

V.E.4 WPCSOL: The Effect of Airborne Contaminants on Fuel Cell Performance and Durability. . . . V–119

Connecticut (Continued)

V.F.9 FuelCell Energy, Inc.: Smart Matrix Development for Direct Carbonate Fuel Cell V–170

V.F.9 University of Connecticut: Smart Matrix Development for Direct Carbonate Fuel Cell V–170

VII.9 Proton OnSite: Validation of an Advanced High Pressure PEM Electrolyzer and Composite Hydrogen Storage, with Data Reporting, for SunHydro Stations VII–44

VII.9 SunHydro LLC: Validation of an Advanced High Pressure PEM Electrolyzer and Composite Hydrogen Storage, with Data Reporting, for SunHydro Stations VII–44

VIII.6 Proton OnSite: Hydrogen Safety Panel, Safety Knowledge Tools and First Responder Training Resources VIII–31

VIII.6 GWS Solutions of Tolland, LLC: Hydrogen Safety Panel, Safety Knowledge Tools and First Responder Training Resources. VIII–31

Delaware

V.A.1 University of Delaware: Extended, Continuous Pt Nanostructures in Thick, Dispersed Electrodes V–9

V.E.1 Ion Power: Durability Improvements Through Degradation Mechanism Studies V–101

VI.1 Ion Power: Fuel Cell Membrane Electrode Assembly Manufacturing R&D. VI–7

Georgia

X.3 Center for Transportation and the Environment: Fuel Cell Hybrid Electric Delivery Van Project. X–14

X.3 United Parcel Service: Fuel Cell Hybrid Electric Delivery Van Project X–14

Hawaii

II.C.4 University of Hawaii: High-Efficiency Tandem Absorbers for Economical Solar Hydrogen Production II–50

II.C.5 University of Hawaii: Wide Bandgap Chalcopyrite Photoelectrodes for Direct Solar Water Splitting. II–56

V.C.3 University of Hawaii: Novel Structured Metal Bipolar Plates for Low Cost Manufacturing V–86

V.E.4 Hawaii Natural Energy Institute: The Effect of Airborne Contaminants on Fuel Cell Performance and Durability V–119

X.4 Hawaii Natural Energy Institute: Hydrogen Energy Systems as a Grid Management Tool X–18

Idaho

VII.14 Idaho National Laboratory: Dynamic Modeling and Validation of Electrolyzers in Real Time Grid Simulation VII–65

Illinois

II.C.1 Northwestern University: High Efficiency Solar Thermochemical Reactor for Hydrogen Production II–35

III.1 Argonne National Laboratory: Hydrogen Delivery Infrastructure Analysis. III–9

III.11 Argonne National Laboratory: Reference Station Design III–53

III.12 Argonne National Laboratory: Hydrogen Fueling Station Pre-Cooling Analysis. III–57

IV.A.1 Argonne National Laboratory: System Analysis of Physical and Materials-Based Hydrogen Storage IV–11

V.A.2 Argonne National Laboratory: Nanosegregated Cathode Alloy Catalysts with Ultra-Low Platinum Loading. V–13

V.A.4 Illinois Institute of Technology: Synthesis and Characterization of Mixed-Conducting Corrosion Resistant Oxide Supports. V–25

V.A.8 Argonne National Laboratory: High-Throughput Synthesis, ORR Activity Modeling, and Testing of non-PGM PEMFC Cathode Catalysts V–51

V.C.1 Argonne National Laboratory: High Performance, Durable, Low Cost Membrane Electrode Assemblies for Transportation Applications. V–73

V.C.2 Argonne National Laboratory: Rationally Designed Catalyst Layers for PEMFC Performance Optimization. V–80

Illinois (Continued)

V.E.1 Argonne National Laboratory: Durability Improvements Through Degradation Mechanism Studies. V–101
V.F.2 Argonne National Laboratory: Fuel Cells Systems Analysis. V–133
V.F.9 Illinois Institute of Technology: Smart Matrix Development for Direct Carbonate Fuel Cell V–170
V.F.12 Argonne National Laboratory: Novel Non-PGM Catalysts from Rationally Designed 3-D Precursors. V–184
VII.10 Gas Technology Institute: Performance Evaluation of Delivered Hydrogen Fueling Stations VII–50
IX.1 Argonne National Laboratory: Impact of Fuel Cell System Peak Efficiency on Fuel Consumption and Cost IX–13
IX.4 Argonne National Laboratory: Performance and Cost Analysis for a 300 kW Tri-generation Molten Carbonate Fuel Cell System. IX–29
IX.5 Argonne National Laboratory: Employment Impacts of Infrastructure Development for Hydrogen and Fuel Cell Technologies IX–34
IX.5 RCF Economic & Financial Consulting: Employment Impacts of Infrastructure Development for Hydrogen and Fuel Cell Technologies IX–34
IX.5 Northwestern University: Employment Impacts of Infrastructure Development for Hydrogen and Fuel Cell Technologies IX–34
IX.6 Argonne National Laboratory: Life-Cycle Analysis of Water Consumption for Hydrogen Production IX–41
IX.10 Argonne National Laboratory: Analysis of Incremental Fueling Pressure Cost IX–54
IX.13 University of Chicago: The Business Case for Hydrogen-powered Passenger Cars: Competition and Solving the Infrastructure Puzzle IX–65

Indiana

III.8 AccerlorMittal: Steel Concrete Composite Vessel for 875 bar Stationary Hydrogen Storage. III–40
V.C.2 Indiana University Purdue University: Rationally Designed Catalyst Layers for PEMFC Performance Optimization. V–80

Iowa

IV.C.4 Ames Laboratory: High-Capacity Hydrogen Storage Systems via Mechanochemistry IV–81
IV.E.1 Ames Laboratory: Complex Hydrides - A New Frontier for Future Energy Applications IV–143

Maryland

IV.C.1 National Institute of Standards and Technology: Hydrogen Storage in Metal-Organic Frameworks. IV–63
IV.C.2 National Institute of Standards and Technology: Hydrogen Sorbent Measurement Qualification and Characterization. IV–70
IV.C.3 National Institute of Standards and Technology: Neutron Characterization in Support of the DOE Hydrogen Storage Sub-Program IV–76
V.C.1 Johns Hopkins University: High Performance, Durable, Low Cost Membrane Electrode Assemblies for Transportation Applications. V–73
V.F.5 National Institute of Standards and Technology: Neutron Imaging Study of the Water Transport in Operating Fuel Cells V–152
V.F.8 Redox Fuel Cells, Inc.: Affordable, High Performance, Intermediate Temperature Solid Oxide Fuel Cells V–167
V.F.8 University of Maryland: Affordable, High Performance, Intermediate Temperature Solid Oxide Fuel Cells V–167
VI.1 W.L. Gore & Associates: Fuel Cell Membrane Electrode Assembly Manufacturing R&D VI–7

Massachusetts

II.B.2 Giner Electrochemical Systems: High-Performance, Long-Lifetime Catalysts for Proton Exchange Membrane Electrolysis. II–23
II.B.4 Giner Electrochemical Systems: High Temperature, High Pressure Electrolysis II–31
IV.C.7 Boston College: Novel Carbon(C)-Boron(B)-Nitrogen(N)-Containing H_2 Storage Materials IV–92

Massachusetts (Continued)

IV.C.7 Protonex Technology Corporation: Novel Carbon(C)-Boron(B)-Nitrogen(N)-Containing H_2 Storage Materials . . . IV–92

V.A.5 Northeastern University: Development of Novel Non-PGM Electrocatalysts for Proton Exchange Membrane Fuel Cell Applications . . . V–29

V.F.11 Giner, Inc.: Ionomer Dispersion Impact on Advanced Fuel Cell and Electrolyzer Performance and Durability . . . V–179

VIII.6 Firexplo: Hydrogen Safety Panel, Safety Knowledge Tools and First Responder Training Resources . . . VIII–31

Michigan

IV.B.1 General Motors Company: Hydrogen Storage Engineering Center of Excellence . . . IV–22

IV.B.1 Ford Motor Company: Hydrogen Storage Engineering Center of Excellence . . . IV–22

IV.B.1 University of Michigan: Hydrogen Storage Engineering Center of Excellence . . . IV–22

IV.B.2 Ford Motor Company: Ford/BASF-SE/UM Activities in Support of the Hydrogen Storage Engineering Center of Excellence . . . IV–27

IV.B.2 University of Michigan: Ford/BASF-SE/UM Activities in Support of the Hydrogen Storage Engineering Center of Excellence . . . IV–27

IV.B.9 General Motors Company: Testing, Modeling, and Evaluation of Innovative Hydrogen Storage System Designs . . . IV–59

IV.C.1 General Motors Company: Hydrogen Storage in Metal-Organic Frameworks . . . IV–63

IV.C.9 University of Michigan: Improving the Kinetics and Thermodynamics of $Mg(BH_4)_2$ for Hydrogen Storage . . . IV–101

IV.D.3 Ford Motor Company: Enhanced Materials and Design Parameters for Reducing the Cost of Hydrogen Storage Tanks . . . IV–118

V.A.4 Nissan Technical Center, North America: Synthesis and Characterization of Mixed-Conducting Corrosion Resistant Oxide Supports . . . V–25

V.A.5 Michigan State University: Development of Novel Non-PGM Electrocatalysts for Proton Exchange Membrane Fuel Cell Applications . . . V–29

V.A.5 Nissan Technical Center, North America: Development of Novel Non-PGM Electrocatalysts for Proton Exchange Membrane Fuel Cell Applications . . . V–29

V.A.7 General Motors Company: Non-Precious Metal Fuel Cell Cathodes: Catalyst Development & Electrode Structure Design . . . V–43

V.B.1 General Motors Company: New Fuel Cell Membranes with Improved Durability and Performance . . . V–64

V.B.2 Nissan Technical Center, North America: Advanced Hybrid Membranes for Next Generation PEMFC Automotive Applications . . . V–69

V.C.1 Michigan Technological University: High Performance, Durable, Low Cost Membrane Electrode Assemblies for Transportation Applications . . . V–73

V.C.1 General Motors Company: High Performance, Durable, Low Cost Membrane Electrode Assemblies for Transportation Applications . . . V–73

V.D.1 Kettering University: Roots Air Management System with Integrated Expander . . . V–96

V.E.3 General Motors Company: Effect of System Contaminants on PEMFC Performance and Durability . . . V–113

VI.1 General Motors Company: Fuel Cell Membrane Electrode Assembly Manufacturing R&D . . . VI–7

Minnesota

II.B.2 3M Company: High-Performance, Long-Lifetime Catalysts for Proton Exchange Membrane Electrolysis . . . II–23

V.B.1 3M Company: New Fuel Cell Membranes with Improved Durability and Performance . . . V–64

V.B.2 3M Company: Advanced Hybrid Membranes for Next Generation PEMFC Automotive Applications . . . V–69

V.C.1 3M Company: High Performance, Durable, Low Cost Membrane Electrode Assemblies for Transportation Applications . . . V–73

Minnesota (Continued)

V.C.4 3M Company: Advanced Ionomers & MEAs for Alkaline Membrane Fuel Cells V–92
V.E.2 3M Company: Fuel-Cell Fundamentals at Low and Subzero Temperatures V–108

Missouri

IV.C.4 University of Missouri: High-Capacity Hydrogen Storage Systems via Mechanochemistry IV–81
IV.C.8 University of Missouri: Boron-Based Hydrogen Storage: Ternary Borides and Beyond IV–97
VIII.6 Becht Engineering: Hydrogen Safety Panel, Safety Knowledge Tools and First Responder Training Resources VIII–31

Montana

IV.D.4 Montana State University: Next Generation Hydrogen Storage Vessels Enabled by Carbon Fiber Infusion with a Low Viscosity, High Toughness System IV–122

Nebraska

III.5 Hexagon Lincoln: Development of High Pressure Hydrogen Storage Tank for Storage and Gaseous Truck Delivery III–25
IV.B.1 Hexagon Lincoln: Hydrogen Storage Engineering Center of Excellence IV–22
IV.B.7 Hexagon Lincoln: Development of Improved Composite Pressure Vessels for Hydrogen Storage. IV–53
IV.D.3 Hexagon Lincoln: Enhanced Materials and Design Parameters for Reducing the Cost of Hydrogen Storage Tanks IV–118
IV.D.6 Hexagon Lincoln: Achieving Hydrogen Storage Goals through High-Strength Fiber Glass IV–134

Nevada

II.C.4 University of Nevada, Las Vegas: High-Efficiency Tandem Absorbers for Economical Solar Hydrogen Production II–50
II.C.5 University of Nevada, Las Vegas: Wide Bandgap Chalcopyrite Photoelectrodes for Direct Solar Water Splitting II–56

New Hampshire

III.6 New England Wire Technologies: Cryogenically Flexible, Low Permeability H_2 Delivery Hose III–28
III.8 SustainX: Steel Concrete Composite Vessel for 875 bar Stationary Hydrogen Storage III–40

New Jersey

II.D.2 Rutgers, the State University of New Jersey: Tunable Photoanode-Photocathode-Catalyst Interface Systems for Efficient Solar Water Splitting II–72
V.A.9 Rutgers, the State University of New Jersey: Non-Platinum Group Metal OER/ORR Catalysts for Alkaline Membrane Fuel Cells and Electrolyzers V–56
V.C.3 TreadStone Technologies, Inc.: Novel Structured Metal Bipolar Plates for Low Cost Manufacturing. V–86
VI.1 New Jersey Institute of Technology: Fuel Cell Membrane Electrode Assembly Manufacturing R&D VI–7

New Mexico

IV.B.1 Los Alamos National Laboratory: Hydrogen Storage Engineering Center of Excellence. IV–22
IV.B.8 Los Alamos National Laboratory: Chemical Hydrogen Rate Modeling, Validation, and System Demonstration IV–56
IV.C.2 Los Alamos National Laboratory: Hydrogen Sorbent Measurement Qualification and Characterization . . . IV–70
IV.D.7 Adherent Technologies, Inc.: Optimizing the Cost and Performance of Composite Cylinders for H_2 Storage using a Graded Construction IV–138
V.A.5 University of New Mexico: Development of Novel Non-PGM Electrocatalysts for Proton Exchange Membrane Fuel Cell Applications V–29

New Mexico (Continued)

V.A.5 Pajarito Powder, LLC: Development of Novel Non-PGM Electrocatalysts for Proton Exchange Membrane Fuel Cell Applications . . . V–29

V.A.7 Los Alamos National Laboratory: Non-Precious Metal Fuel Cell Cathodes: Catalyst Development & Electrode Structure Design . . . V–43

V.A.7 IRD Fuel Cells: Non-Precious Metal Fuel Cell Cathodes: Catalyst Development & Electrode Structure Design. . . . V–43

V.A.8 Los Alamos National Laboratory: High-Throughput Synthesis, ORR Activity Modeling, and Testing of non-PGM PEMFC Cathode Catalysts . . . V–51

V.C.1 Los Alamos National Laboratory: High Performance, Durable, Low Cost Membrane Electrode Assemblies for Transportation Applications . . . V–73

V.E.1 Los Alamos National Laboratory: Durability Improvements Through Degradation Mechanism Studies . . . V–101

V.E.2 Los Alamos National Laboratory: Fuel-Cell Fundamentals at Low and Subzero Temperatures . . . V–108

V.E.5 University of New Mexico: Open Source Performance and Durability Model: Consideration of Membrane Properties on Cathode Degradation . . . V–125

V.F.11 Los Alamos National Laboratory: Ionomer Dispersion Impact on Advanced Fuel Cell and Electrolyzer Performance and Durability. . . . V–179

V.F.14 Los Alamos National Laboratory: High Performance and Durable Low PGM Cathode Catalysts . . . V–194

V.F.17 Los Alamos National Laboratory: Advanced Hydroxide Conducting Membranes. . . . V–205

V.F.17 Sandia National Laboratories: Advanced Hydroxide Conducting Membranes . . . V–205

V.F.18 Sandia National Laboratories: DOE's High Acid Content Diels Alder Poly(Phenylene)s for High Temperature and Low Humidity Applications . . . V–211

V.F.19 Los Alamos National Laboratory: Engineered Low-Pt Catalyst Layers . . . V–218

VIII.1 Sandia National Laboratories: Hydrogen behavior and Quantitative Risk Assessment . . . VIII–1

VIII.4 Los Alamos National Laboratory: Hydrogen Fuel Quality . . . VIII–21

VIII.10 Sandia National Laboratories: Enabling Hydrogen Infrastructure Through Science-based Codes and Standards . . . VIII–49

VIII.11 Los Alamos National Laboratory: Hydrogen Safety, Codes and Standards: Sensors . . . VIII–53

New York

II.B.3 Brookhaven National Laboratory: Low-Noble-Metal-Content Catalysts/Electrodes for Hydrogen Production by Water Electrolysis. . . . II–28

V.A.3 Brookhaven National Laboratory: Contiguous Platinum Monolayer Oxygen Reduction Electrocatalysts on High-Stability-Low-Cost Supports. . . . V–20

V.A.7 University of Rochester: Non-Precious Metal Fuel Cell Cathodes: Catalyst Development & Electrode Structure Design . . . V–43

V.F.17 Rensselaer Polytechnic University: Advanced Hydroxide Conducting Membranes. . . . V–205

V.F.20 Brookhaven National Laboratory: Semi-Automated MEA Fabrication with Ultra-Low Total PGM Loadings. . . . V–223

X.1 Plug Power: Ground Support Equipment Demonstration. . . . X–7

X.3 Unique Electric Solutions: Fuel Cell Hybrid Electric Delivery Van Project . . . X–14

North Carolina

II.F.1 Cormetech, Inc.: Monolithic Piston-Type Reactor for Hydrogen Production through Rapid Swing of Reforming/Combustion Reactions. . . . II–84

Ohio

II.D.1 University of Toledo: New Metal Oxides for Efficient Hydrogen Production via Solar Water Splitting . . . II–67

III.6 Swagelok: Cryogenically Flexible, Low Permeability H_2 Delivery Hose . . . III–28

Ohio (Continued)

III.7 Norm Shade: Hydrogen Compression Application of the Linear Motor Reciprocating Compressor (LMRC) . . . III–33

III.9 N & R Engineering: Low Cost Hydrogen Storage at 875 Bar Using Steel Liner and Steel Wire Wrap . . . III–45

V.A.10 pH Matter, LLC: Non-Precious Metal Bi-Functional Catalysts . . . V–60

V.F.6 Battelle: Stationary and Emerging Market Fuel Cell System Cost Analysis—Primary Power and Combined Heat and Power Applications . . . V–158

VI.2 GLWN – Westside Industrial Retention & Expansion Network: U.S. Clean Energy Hydrogen and Fuel Cell Technologies: A Competitiveness Analysis . . . VI–12

VI.2 DJW Technologies: U.S. Clean Energy Hydrogen and Fuel Cell Technologies: A Competitiveness Analysis . . . VI–12

Oklahoma

IX.14 Kalibrate: Retail Marketing Analysis: Hydrogen Refueling Stations . . . IX–67

Oregon

III.2 Harris Thermal Transfer Products: Vessel Design and Fabrication Technology for Stationary High-Pressure Hydrogen Storage. . . . III–13

IV.B.1 Oregon State University: Hydrogen Storage Engineering Center of Excellence . . . IV–22

IV.B.3 Oregon State University: Microscale Enhancement of Heat and Mass Transfer for Hydrogen Energy Storage . . . IV–32

IV.D.1 Hy-Performance Materials Testing LLC: Innovative Development, Selection and Testing to Reduce Cost and Weight of Materials for BOP Components . . . IV–108

Pennsylvania

II.C.1 Bucknell University: High Efficiency Solar Thermochemical Reactor for Hydrogen Production . . . II–35

II.E.1 Pennsylvania State University: Fermentation and Electrohydrogenic Approaches to Hydrogen Production . . . II–76

III.2 Temple University: Vessel Design and Fabrication Technology for Stationary High-Pressure Hydrogen Storage . . . III–13

III.8 Temple University: Steel Concrete Composite Vessel for 875 bar Stationary Hydrogen Storage . . . III–40

III.9 C P Industries: Low Cost Hydrogen Storage at 875 Bar Using Steel Liner and Steel Wire Wrap . . . III–45

IV.D.6 PPG Industries, Inc.: Achieving Hydrogen Storage Goals through High-Strength Fiber Glass . . . IV–134

V.A.7 Carnegie Mellon University: Non-Precious Metal Fuel Cell Cathodes: Catalyst Development & Electrode Structure Design . . . V–43

VII.9 Air Products and Chemicals, Inc.: Validation of an Advanced High Pressure PEM Electrolyzer and Composite Hydrogen Storage, with Data Reporting, for SunHydro Stations . . . VII–44

VIII.6 Air Products and Chemicals, Inc.: Hydrogen Safety Panel, Safety Knowledge Tools and First Responder Training Resources . . . VIII–31

South Carolina

II.C.3 Savannah River National Laboratory: Electrolyzer Component Development for the HyS Thermochemical Cycle . . . II–46

II.C.3 Savannah River Consultants: Electrolyzer Component Development for the HyS Thermochemical Cycle. . . II–46

III.4 Savannah River National Laboratory: Fiber Reinforced Composite Pipelines . . . III–22

IV.B.1 Savannah River National Laboratory: Hydrogen Storage Engineering Center of Excellence . . . IV–22

IV.C.5 Savannah River National Laboratory: Electrochemical Reversible Formation of α-Alane . . . IV–84

V.A.6 University of South Carolina: Development of Ultra-Low Doped-Pt Cathode Catalysts for PEM Fuel Cells . . . V–37

South Carolina (Continued)

V.E.3 University of South Carolina: Effect of System Contaminants on PEMFC Performance and Durability . . . V–113

V.F.13 Savannah River National Laboratory: PGM Free Catalysts for PEMFC V–189

Tennessee

III.2 Oak Ridge National Laboratory: Vessel Design and Fabrication Technology for Stationary High-Pressure Hydrogen Storage III–13

III.8 Oak Ridge National Laboratory: Steel Concrete Composite Vessel for 875 bar Stationary Hydrogen Storage III–40

III.9 Oak Ridge National Laboratory: Low Cost Hydrogen Storage at 875 Bar Using Steel Liner and Steel Wire Wrap III–45

IV.D.3 AOC, LLC: Enhanced Materials and Design Parameters for Reducing the Cost of Hydrogen Storage Tanks IV–118

IV.D.5 Oak Ridge National Laboratory: Melt Processable PAN Precursor for High Strength, Low-Cost Carbon Fibers (Phase II) IV–126

V.A.2 Oak Ridge National Laboratory: Nanosegregated Cathode Alloy Catalysts with Ultra-Low Platinum Loading. V–13

V.A.7 Oak Ridge National Laboratory: Non-Precious Metal Fuel Cell Cathodes: Catalyst Development & Electrode Structure Design V–43

V.B.1 Vanderbilt University: New Fuel Cell Membranes with Improved Durability and Performance V–64

V.E.1 Oak Ridge National Laboratory: Durability Improvements Through Degradation Mechanism Studies V–101

V.F.4 Oak Ridge National Laboratory: Characterization of Fuel Cell Materials V–147

V.F.15 Oak Ridge National Laboratory: Magnetic Annealing of Pt-Alloy Nanostructured Thin Film Catalysts for Enhanced Activity V–198

V.F.16 Oak Ridge National Laboratory: High Conductivity Durable Anion Conducting Membranes V–203

V.F.18 Oak Ridge National Laboratory: DOE's High Acid Content Diels Alder Poly(Phenylene)s for High Temperature and Low Humidity Applications V–211

V.F.19 Oak Ridge National Laboratory: Engineered Low-Pt Catalyst Layers V–218

IX.2 Oak Ridge National Laboratory: GPRA Analysis: Impact of Program Targets on Vehicle Penetration and Benefits IX–19

IX.8 University of Tennessee: Status and Prospects of the N.A. Non-Automotive Fuel Cell Industry: 2014 Update IX–48

IX.11 Oak Ridge National Laboratory: Analysis of Optimal On-Board Storage Pressure for Hydrogen Fuel Cell Vehicles. IX–58

Texas

III.2 Hanson Pressure Pipe: Vessel Design and Fabrication Technology for Stationary High-Pressure Hydrogen Storage. III–13

III.7 Southwest Research Institute®: Hydrogen Compression Application of the Linear Motor Reciprocating Compressor (LMRC) III–33

III.8 Air Liquide: Steel Concrete Composite Vessel for 875 bar Stationary Hydrogen Storage III–40

III.8 Hanson Pressure Pipe: Steel Concrete Composite Vessel for 875 bar Stationary Hydrogen Storage III–40

III.9 Pressure Science, Inc.: Low Cost Hydrogen Storage at 875 Bar Using Steel Liner and Steel Wire Wrap . . . III–45

IV.C.2 Texas A&M University: Hydrogen Sorbent Measurement Qualification and Characterization IV–70

V.C.2 University of Texas at Austin: Rationally Designed Catalyst Layers for PEMFC Performance Optimization. V–80

VIII.6 Air Liquide: Hydrogen Safety Panel, Safety Knowledge Tools and First Responder Training Resources . . VIII–31

X.3 University of Texas: Fuel Cell Hybrid Electric Delivery Van Project X–14

X.3 Valence: Fuel Cell Hybrid Electric Delivery Van Project X–14

Utah

III.2 MegaStir Technologies, LLC: Vessel Design and Fabrication Technology for Stationary High-Pressure Hydrogen Storage . . . III–13

III.8 MegaStir Technologies, LLC: Steel Concrete Composite Vessel for 875 bar Stationary Hydrogen Storage . . . III–40

Virginia

II.A.1 Strategic Analysis, Inc.: Hydrogen Pathways Analysis for Solid Oxide Fuel Cell (SOFC) and Dark Fermentation. . . . II–11

II.B.4 Virginia Polytechnic Institute: High Temperature, High Pressure Electrolysis . . . II–31

III.6 Nanosonic: Cryogenically Flexible, Low Permeability H_2 Delivery Hose . . . III–28

III.8 WireTough Cylinders: Steel Concrete Composite Vessel for 875 bar Stationary Hydrogen Storage . . . III–40

III.9 WireTough Cylinders: Low Cost Hydrogen Storage at 875 Bar Using Steel Liner and Steel Wire Wrap. . . . III–45

IV.A.2 Strategic Analysis, Inc.: Hydrogen Storage Cost Analysis. . . . IV–17

IV.D.5 Virginia Polytechnic Institute: Melt Processable PAN Precursor for High Strength, Low-Cost Carbon Fibers (Phase II) . . . IV–126

IV.E.4 Virginia Commonwealth University: Elucidation of Hydride Interaction Mechanisms with Carbon Nanostructures and the Formation of Novel Nanocomposites . . . IV–146

V.F.3 Strategic Analysis, Inc.: Fuel Cell Vehicle and Bus Cost Analysis . . . V–141

V.F.7 Strategic Analysis, Inc.: A Total Cost of Ownership Model for Design and Manufacturing Optimization of Fuel Cells in Stationary and Emerging Market Applications . . . V–162

VI.2 Strategic Analysis, Inc.: U.S. Clean Energy Hydrogen and Fuel Cell Technologies: A Competitiveness Analysis . . . VI–12

Washington

II.F.1 Pacific Northwest National Laboratory: Monolithic Piston-Type Reactor for Hydrogen Production through Rapid Swing of Reforming/Combustion Reactions . . . II–84

II.F.1 Washington State University: Monolithic Piston-Type Reactor for Hydrogen Production through Rapid Swing of Reforming/Combustion Reactions . . . II–84

II.F.1 Dason Technology, Inc.: Monolithic Piston-Type Reactor for Hydrogen Production through Rapid Swing of Reforming/Combustion Reactions. . . . II–84

III.2 Global Engineering and Technology, LLC: Vessel Design and Fabrication Technology for Stationary High-Pressure Hydrogen Storage. . . . III–13

III.8 Global Engineering and Technology, LLC: Steel Concrete Composite Vessel for 875 bar Stationary Hydrogen Storage . . . III–40

III.14 Pacific Northwest National Laboratory: Magnetocaloric Hydrogen Liquefaction . . . III–65

III.14 Emerald Energy NW LLC: Magnetocaloric Hydrogen Liquefaction . . . III–65

IV.B.1 Pacific Northwest National Laboratory: Hydrogen Storage Engineering Center of Excellence . . . IV–22

IV.B.5 Pacific Northwest National Laboratory: Systems Engineering of Chemical Hydrogen Storage and Cryo-Sorbent Storage, Pressure Vessel, and Balance of Plant for Onboard Hydrogen Storage . . . IV–44

IV.C.7 Pacific Northwest National Laboratory: Novel Carbon(C)-Boron(B)-Nitrogen(N)-Containing H_2 Storage Materials . . . IV–92

IV.D.3 Pacific Northwest National Laboratory: Enhanced Materials and Design Parameters for Reducing the Cost of Hydrogen Storage Tanks . . . IV–118

IV.D.6 Pacific Northwest National Laboratory: Achieving Hydrogen Storage Goals through High-Strength Fiber Glass . . . IV–134

V.F.14 Pacific Northwest National Laboratory: High Performance and Durable Low PGM Cathode Catalysts . . . V–194

VIII.6 Pacific Northwest National Laboratory: Hydrogen Safety Panel, Safety Knowledge Tools and First Responder Training Resources . . . VIII–31

Washington (Continued)

VIII.6 Excelsior Design, Inc.: Hydrogen Safety Panel, Safety Knowledge Tools and First Responder Training Resources VIII–31

Washington, D.C.

VIII.8 Fuel Cell & Hydrogen Energy Association: Fuel Cell & Hydrogen Energy Association Codes and Standards Support VIII–42

Wisconsin

V.D.1 Eaton Corporation: Roots Air Management System with Integrated Expander V–96

Foreign Countries

Canada

IV.B.1 Université du Québec à Trois-Rivières: Hydrogen Storage Engineering Center of Excellence IV–22

V.A.7 University of Waterloo: Non-Precious Metal Fuel Cell Cathodes: Catalyst Development & Electrode Structure Design V–43

V.D.1 Ballard Power Systems: Roots Air Management System with Integrated Expander. V–96

V.E.4 Ballard Power Systems: The Effect of Airborne Contaminants on Fuel Cell Performance and Durability . . V–119

V.E.5 Ballard Power Systems: Open Source Performance and Durability Model: Consideration of Membrane Properties on Cathode Degradation. V–125

V.E.5 University of Calgary: Open Source Performance and Durability Model: Consideration of Membrane Properties on Cathode Degradation. V–125

VI.1 Automotive Fuel Cell Corporation: Fuel Cell Membrane Electrode Assembly Manufacturing R&D VI–7

VI.2 eon™ Consultants Ltd.: U.S. Clean Energy Hydrogen and Fuel Cell Technologies: A Competitiveness Analysis VI–12

VII.7 Powertech Labs, Inc.: Development of the Hydrogen Station Equipment Performance (HyStEP) Device. . .VII–36

VII.12 Hydrogenics: CSULA Hydrogen Refueling Facility Performance Evaluation and Optimization. VII–58

X.2 Hydrogenics: Maritime Fuel Cell Generator Project X–10

X.3 Hydrogenics: Fuel Cell Hybrid Electric Delivery Van Project. X–14

Germany

IV.B.2 BASF SE: Ford/BASF-SE/UM Activities in Support of the Hydrogen Storage Engineering Center of Excellence. IV–27

Israel

V.C.4 CellEra, Inc.: Advanced Ionomers & MEAs for Alkaline Membrane Fuel Cells V–9

Japan

III.2 Kobe Steel, LTD: Vessel Design and Fabrication Technology for Stationary High-Pressure Hydrogen Storage III–13

South Korea

III.8 POSCO: Steel Concrete Composite Vessel for 875 bar Stationary Hydrogen Storage III–40

Switzerland

VI.2 E4tech: U.S. Clean Energy Hydrogen and Fuel Cell Technologies: A Competitiveness Analysis VI–12

United Kingdom

V.C.2 Johnson Matthey Fuel Cells: Rationally Designed Catalyst Layers for PEMFC Performance Optimization. V–80

XVI. Project Listings by Organization

3M Company

II.B.2 High-Performance, Long-Lifetime Catalysts for Proton Exchange Membrane Electrolysis II–23
V.B.1 New Fuel Cell Membranes with Improved Durability and Performance V–64
V.B.2 Advanced Hybrid Membranes for Next Generation PEMFC Automotive Applications V–69
V.C.1 High Performance, Durable, Low Cost Membrane Electrode Assemblies for Transportation Applications . . . V–73
V.C.4 Advanced Ionomers & MEAs for Alkaline Membrane Fuel Cells V–92
V.E.2 Fuel-Cell Fundamentals at Low and Subzero Temperatures. V–108

AccerlorMittal

III.8 Steel Concrete Composite Vessel for 875 bar Stationary Hydrogen Storage III–40

Adherent Technologies, Inc.

IV.D.7 Optimizing the Cost and Performance of Composite Cylinders for H_2 Storage using a Graded Construction IV–138

Air Liquide

III.8 Steel Concrete Composite Vessel for 875 bar Stationary Hydrogen Storage III–40
VIII.6 Hydrogen Safety Panel, Safety Knowledge Tools and First Responder Training Resources VIII–31

Air Products and Chemicals, Inc.

VII.9 Validation of an Advanced High Pressure PEM Electrolyzer and Composite Hydrogen Storage, with Data Reporting, for SunHydro Stations. VII–44
VIII.6 Hydrogen Safety Panel, Safety Knowledge Tools and First Responder Training Resources VIII–31

Ames Laboratory

IV.C.4 High-Capacity Hydrogen Storage Systems via Mechanochemistry IV–81
IV.E.1 Complex Hydrides - A New Frontier for Future Energy Applications IV–143

AOC, LLC

IV.D.3 Enhanced Materials and Design Parameters for Reducing the Cost of Hydrogen Storage Tanks IV–118

Ardica Technologies

IV.C.6 Low-Cost α-Alane for Hydrogen Storage IV–88

Argonne National Laboratory

III.1 Hydrogen Delivery Infrastructure Analysis III–9
III.11 Reference Station Design III–53
III.12 Hydrogen Fueling Station Pre-Cooling Analysis III–57
IV.A.1 System Analysis of Physical and Materials-Based Hydrogen Storage IV–11
V.A.2 Nanosegregated Cathode Alloy Catalysts with Ultra-Low Platinum Loading V–13
V.A.8 High-Throughput Synthesis, ORR Activity Modeling, and Testing of non-PGM PEMFC Cathode Catalysts V–51
V.C.1 High Performance, Durable, Low Cost Membrane Electrode Assemblies for Transportation Applications V–73
V.C.2 Rationally Designed Catalyst Layers for PEMFC Performance Optimization. V–80
V.E.1 Durability Improvements Through Degradation Mechanism Studies V–101

Argonne National Laboratory (Continued)

V.F.2 Fuel Cells Systems Analysis V–133
V.F.12 Novel Non-PGM Catalysts from Rationally Designed 3-D Precursors V–184
IX.1 Impact of Fuel Cell System Peak Efficiency on Fuel Consumption and Cost. IX–13
IX.4 Performance and Cost Analysis for a 300 kW Tri-generation Molten Carbonate Fuel Cell System IX–29
IX.5 Employment Impacts of Infrastructure Development for Hydrogen and Fuel Cell Technologies IX–34
IX.6 Life-Cycle Analysis of Water Consumption for Hydrogen Production. IX–41
IX.10 Analysis of Incremental Fueling Pressure Cost IX–54

Arizona State University

II.C.1 High Efficiency Solar Thermochemical Reactor for Hydrogen Production II–35

Ashok Saxena

III.9 Low Cost Hydrogen Storage at 875 Bar Using Steel Liner and Steel Wire Wrap. III–45

Automotive Fuel Cell Corporation

VI.1 Fuel Cell Membrane Electrode Assembly Manufacturing R&D VI–7

Ballard Power Systems

V.D.1 Roots Air Management System with Integrated Expander V–96
V.E.4 The Effect of Airborne Contaminants on Fuel Cell Performance and Durability V–119
V.E.5 Open Source Performance and Durability Model: Consideration of Membrane Properties on Cathode Degradation V–125

BASF SE

IV.B.2 Ford/BASF-SE/UM Activities in Support of the Hydrogen Storage Engineering Center of Excellence. IV–27

Battelle

V.F.6 Stationary and Emerging Market Fuel Cell System Cost Analysis—Primary Power and Combined Heat and Power Applications V–158

Becht Engineering

VIII.6 Hydrogen Safety Panel, Safety Knowledge Tools and First Responder Training Resources VIII–31

Bevilacqua Knight, Inc.

III.8 Steel Concrete Composite Vessel for 875 bar Stationary Hydrogen Storage III–40

BKi

VIII.6 Hydrogen Safety Panel, Safety Knowledge Tools and First Responder Training Resources VIII–31

Boston College

IV.C.7 Novel Carbon(C)-Boron(B)-Nitrogen(N)-Containing H_2 Storage Materials IV–92

Branded by Media

VIII.7 Fuel Cell Technologies National Codes and Standards Deployment and Outreach VIII–38

Brookhaven National Laboratory

II.B.3 Low-Noble-Metal-Content Catalysts/Electrodes for Hydrogen Production by Water Electrolysis II–28
V.A.3 Contiguous Platinum Monolayer Oxygen Reduction Electrocatalysts on High-Stability-Low-Cost Supports V–20

Brookhaven National Laboratory (Continued)
V.F.20 Semi-Automated MEA Fabrication with Ultra-Low Total PGM Loadings V–223

Bucknell University
II.C.1 High Efficiency Solar Thermochemical Reactor for Hydrogen Production II–35

C P Industries
III.9 Low Cost Hydrogen Storage at 875 Bar Using Steel Liner and Steel Wire Wrap. III–45

California Fuel Cell Partnership
VII.8 Station Operational Status System (SOSS) 3.0 Upgrade. VII–41

California Institute of Technology
IV.B.1 Hydrogen Storage Engineering Center of Excellence IV–22

California State University, Los Angeles
VII.12 CSULA Hydrogen Refueling Facility Performance Evaluation and Optimization VII–58

Carnegie Mellon University
V.A.7 Non-Precious Metal Fuel Cell Cathodes: Catalyst Development & Electrode Structure Design V–43

CellEra, Inc.
V.C.4 Advanced Ionomers & MEAs for Alkaline Membrane Fuel Cells V–92

Center for Transportation and the Environment
X.3 Fuel Cell Hybrid Electric Delivery Van Project X–14

City of Santa Fe Springs
VIII.6 Hydrogen Safety Panel, Safety Knowledge Tools and First Responder Training Resources VIII–31

Colorado School of Mines
II.C.1 High Efficiency Solar Thermochemical Reactor for Hydrogen Production II–35
V.A.1 Extended, Continuous Pt Nanostructures in Thick, Dispersed Electrodes. V–9
V.B.2 Advanced Hybrid Membranes for Next Generation PEMFC Automotive Applications V–69
V.C.4 Advanced Ionomers & MEAs for Alkaline Membrane Fuel Cells V–92
V.E.3 Effect of System Contaminants on PEMFC Performance and Durability V–113
VI.1 Fuel Cell Membrane Electrode Assembly Manufacturing R&D VI–7

Composite Technology Development
IV.D.7 Optimizing the Cost and Performance of Composite Cylinders for H_2 Storage using a Graded Construction. IV–138

Cormetech, Inc.
II.F.1 Monolithic Piston-Type Reactor for Hydrogen Production through Rapid Swing of Reforming/Combustion Reactions II–84

Custom Sensor Solutions
VIII.11 Hydrogen Safety, Codes and Standards: Sensors VIII–53

Dason Technology, Inc.
II.F.1 Monolithic Piston-Type Reactor for Hydrogen Production through Rapid Swing of Reforming/Combustion Reactions. II–84

DJW Technologies
VI.2 U.S. Clean Energy Hydrogen and Fuel Cell Technologies: A Competitiveness Analysis VI–12

E4tech
VI.2 U.S. Clean Energy Hydrogen and Fuel Cell Technologies: A Competitiveness Analysis VI–12

Eaton Corporation
V.D.1 Roots Air Management System with Integrated Expander V–96

Electricore, Inc.
V.D.1 Roots Air Management System with Integrated Expander V–96

Element One
VIII.5 NREL Hydrogen Sensor Testing Laboratory VIII-26

Emerald Energy NW LLC
III.14 Magnetocaloric Hydrogen Liquefaction III–65

eon™ Consultants Ltd.
VI.2 U.S. Clean Energy Hydrogen and Fuel Cell Technologies: A Competitiveness Analysis VI–12

Excelsior Design, Inc.
VIII.6 Hydrogen Safety Panel, Safety Knowledge Tools and First Responder Training Resources VIII–31

Firexplo
VIII.6 Hydrogen Safety Panel, Safety Knowledge Tools and First Responder Training Resources VIII–31

Fluer, Inc.
VIII.6 Hydrogen Safety Panel, Safety Knowledge Tools and First Responder Training Resources VIII–31

Ford Motor Company
IV.B.1 Hydrogen Storage Engineering Center of Excellence IV–22
IV.B.2 Ford/BASF-SE/UM Activities in Support of the Hydrogen Storage Engineering Center of Excellence IV–27
IV.D.3 Enhanced Materials and Design Parameters for Reducing the Cost of Hydrogen Storage Tanks IV–118

Fuel Cell & Hydrogen Energy Association
VIII.8 Fuel Cell & Hydrogen Energy Association Codes and Standards Support. VIII–42

FuelCell Energy, Inc.
II.F.2 Reformer-Electrolyzer-Purifier (REP) for Production of Hydrogen II–90
III.10 Electrochemical Hydrogen Compressor III–50
V.F.9 Smart Matrix Development for Direct Carbonate Fuel Cell V–170

Gas Technology Institute
VII.10 Performance Evaluation of Delivered Hydrogen Fueling Stations VII–50

General Motors Company
IV.B.1 Hydrogen Storage Engineering Center of Excellence IV–22
IV.B.9 Testing, Modeling, and Evaluation of Innovative Hydrogen Storage System Designs. IV–59
IV.C.1 Hydrogen Storage in Metal-Organic Frameworks. IV–63

General Motors Company (Continued)

V.A.7 Non-Precious Metal Fuel Cell Cathodes: Catalyst Development & Electrode Structure Design V–43
V.B.1 New Fuel Cell Membranes with Improved Durability and Performance V–64
V.C.1 High Performance, Durable, Low Cost Membrane Electrode Assemblies for Transportation Applications V–73
V.E.3 Effect of System Contaminants on PEMFC Performance and Durability V–113
VI.1 Fuel Cell Membrane Electrode Assembly Manufacturing R&D VI–7

Giner Electrochemical Systems, LLC

II.B.4 High Temperature, High Pressure Electrolysis II–31

Giner, Inc.

II.B.2 High-Performance, Long-Lifetime Catalysts for Proton Exchange Membrane Electrolysis II–23
V.F.11 Ionomer Dispersion Impact on Advanced Fuel Cell and Electrolyzer Performance and Durability V–179

Global Engineering and Technology, LLC

III.2 Vessel Design and Fabrication Technology for Stationary High-Pressure Hydrogen Storage III–13
III.8 Steel Concrete Composite Vessel for 875 bar Stationary Hydrogen Storage III–40

GLWN – Westside Industrial Retention & Expansion Network

VI.2 U.S. Clean Energy Hydrogen and Fuel Cell Technologies: A Competitiveness Analysis VI–12

GWS Solutions of Tolland, LLC

VIII.6 Hydrogen Safety Panel, Safety Knowledge Tools and First Responder Training Resources VIII–31

H2 Technology Consulting LLC

IV.C.2 Hydrogen Sorbent Measurement Qualification and Characterization IV–70

Hanson Pressure Pipe

III.2 Vessel Design and Fabrication Technology for Stationary High-Pressure Hydrogen Storage III–13
III.8 Steel Concrete Composite Vessel for 875 bar Stationary Hydrogen Storage III–40

Harris Thermal Transfer Products

III.2 Vessel Design and Fabrication Technology for Stationary High-Pressure Hydrogen Storage III–13

Hawaii Natural Energy Institute

V.E.4 The Effect of Airborne Contaminants on Fuel Cell Performance and Durability V–119
X.4 Hydrogen Energy Systems as a Grid Management Tool X–18

Hexagon Lincoln

III.5 Development of High Pressure Hydrogen Storage Tank for Storage and Gaseous Truck Delivery III–25
IV.B.1 Hydrogen Storage Engineering Center of Excellence IV–22
IV.B.7 Development of Improved Composite Pressure Vessels for Hydrogen Storage IV–53
IV.D.3 Enhanced Materials and Design Parameters for Reducing the Cost of Hydrogen Storage Tanks IV–118
IV.D.6 Achieving Hydrogen Storage Goals through High-Strength Fiber Glass IV–134

HRL Laboratories, LLC

IV.C.8 Boron-Based Hydrogen Storage: Ternary Borides and Beyond IV–97
VIII.11 Hydrogen Safety, Codes and Standards: Sensors VIII–53

Hydrogenics
VII.12 CSULA Hydrogen Refueling Facility Performance Evaluation and Optimization VII–58
X.2 Maritime Fuel Cell Generator Project X–10
X.3 Fuel Cell Hybrid Electric Delivery Van Project X–14

Hy-Performance Materials Testing LLC
IV.D.1 Innovative Development, Selection and Testing to Reduce Cost and Weight of Materials for BOP Components IV–108

Idaho National Laboratory
VII.14 Dynamic Modeling and Validation of Electrolyzers in Real Time Grid Simulation VII–65

Illinois Institute of Technology
V.A.4 Synthesis and Characterization of Mixed-Conducting Corrosion Resistant Oxide Supports V–25
V.F.9 Smart Matrix Development for Direct Carbonate Fuel Cell V–170

Indiana University Purdue University
V.C.2 Rationally Designed Catalyst Layers for PEMFC Performance Optimization. V–80

Ion Power
V.E.1 Durability Improvements Through Degradation Mechanism Studies V–101
VI.1 Fuel Cell Membrane Electrode Assembly Manufacturing R&D VI–7

IRD Fuel Cells
V.A.7 Non-Precious Metal Fuel Cell Cathodes: Catalyst Development & Electrode Structure Design V–43

Jet Propulsion Laboratory
IV.B.1 Hydrogen Storage Engineering Center of Excellence IV–22

Johns Hopkins University
V.C.1 High Performance, Durable, Low Cost Membrane Electrode Assemblies for Transportation Applications. . . V–73

Johnson Matthey Fuel Cells
V.C.2 Rationally Designed Catalyst Layers for PEMFC Performance Optimization. V–80

Kalibrate
IX.14 Retail Marketing Analysis: Hydrogen Refueling Stations IX–67

Kettering University
V.D.1 Roots Air Management System with Integrated Expander. V–96

Kobe Steel, LTD
III.2 Vessel Design and Fabrication Technology for Stationary High-Pressure Hydrogen Storage III–13

Lawrence Berkeley National Laboratory
IV.C.1 Hydrogen Storage in Metal-Organic Frameworks. IV–63
V.C.1 High Performance, Durable, Low Cost Membrane Electrode Assemblies for Transportation Applications. . . V–73
V.E.1 Durability Improvements Through Degradation Mechanism Studies V–101
V.E.2 Fuel-Cell Fundamentals at Low and Subzero Temperatures. V–108

Lawrence Berkeley National Laboratory (Continued)

V.F.7 A Total Cost of Ownership Model for Design and Manufacturing Optimization of Fuel Cells in Stationary and Emerging Market Applications . . . V–162
V.F.17 Advanced Hydroxide Conducting Membranes . . . V–205
V.F.19 Engineered Low-Pt Catalyst Layers . . . V–218
VI.1 Fuel Cell Membrane Electrode Assembly Manufacturing R&D . . . VI–7

Lawrence Livermore National Laboratory

II.C.5 Wide Bandgap Chalcopyrite Photoelectrodes for Direct Solar Water Splitting . . . II–56
IV.C.9 Improving the Kinetics and Thermodynamics of $Mg(BH_4)_2$ for Hydrogen Storage . . . IV–101
IV.D.2 Thermomechanical Cycling of Thin Liner High Fiber Fraction Cryogenic Pressure Vessels Rapidly Refueled by LH_2 Pump to 700 Bar . . . IV–113
VII.2 Performance and Durability Testing of Volumetrically Efficient Cryogenic Vessels and High Pressure Liquid Hydrogen Pump . . . VII–13
VIII.11 Hydrogen Safety, Codes and Standards: Sensors . . . VIII–53
VIII.12 Hands-on Hydrogen Safety Training . . . VIII–60

LightSail

III.8 Steel Concrete Composite Vessel for 875 bar Stationary Hydrogen Storage . . . III–40

Linde Gas, LLC

VII.10 Performance Evaluation of Delivered Hydrogen Fueling Stations . . . VII-50

Linde LLC

IV.D.2 Thermomechanical Cycling of Thin Liner High Fiber Fraction Cryogenic Pressure Vessels Rapidly Refueled by LH_2 Pump to 700 Bar . . . IV–113
VII.2 Performance and Durability Testing of Volumetrically Efficient Cryogenic Vessels and High Pressure Liquid Hydrogen Pump . . . VII–13

Los Alamos National Laboratory

IV.B.1 Hydrogen Storage Engineering Center of Excellence . . . IV–22
IV.B.8 Chemical Hydrogen Rate Modeling, Validation, and System Demonstration . . . IV–56
IV.C.2 Hydrogen Sorbent Measurement Qualification and Characterization . . . IV–70
V.A.7 Non-Precious Metal Fuel Cell Cathodes: Catalyst Development & Electrode Structure Design . . . V–43
V.A.8 High-Throughput Synthesis, ORR Activity Modeling, and Testing of non-PGM PEMFC Cathode Catalysts . . . V–51
V.C.1 High Performance, Durable, Low Cost Membrane Electrode Assemblies for Transportation Applications . . . V–73
V.E.1 Durability Improvements Through Degradation Mechanism Studies . . . V–101
V.E.2 Fuel-Cell Fundamentals at Low and Subzero Temperatures . . . V–108
V.F.11 Ionomer Dispersion Impact on Advanced Fuel Cell and Electrolyzer Performance and Durability . . . V–179
V.F.14 High Performance and Durable Low PGM Cathode Catalysts . . . V–194
V.F.17 Advanced Hydroxide Conducting Membranes . . . V–205
V.F.19 Engineered Low-Pt Catalyst Layers . . . V–218
VIII.4 Hydrogen Fuel Quality . . . VIII–21
VIII.11 Hydrogen Safety, Codes and Standards: Sensors . . . VIII–53

Materia

IV.D.4 Next Generation Hydrogen Storage Vessels Enabled by Carbon Fiber Infusion with a Low Viscosity, High Toughness System . . . IV-122

MegaStir Technologies, LLC

III.2 Vessel Design and Fabrication Technology for Stationary High-Pressure Hydrogen Storage III–13
III.8 Steel Concrete Composite Vessel for 875 bar Stationary Hydrogen Storage III–40

Michigan State University

V.A.5 Development of Novel Non-PGM Electrocatalysts for Proton Exchange Membrane Fuel Cell Applications V–29

Michigan Technological University

V.C.1 High Performance, Durable, Low Cost Membrane Electrode Assemblies for Transportation Applications . . . V–73

Montana State University

IV.D.4 Next Generation Hydrogen Storage Vessels Enabled by Carbon Fiber Infusion with a Low Viscosity, High Toughness System IV–122

N & R Engineering

III.9 Low Cost Hydrogen Storage at 875 Bar Using Steel Liner and Steel Wire Wrap. III–45

Nanosonic

III.6 Cryogenically Flexible, Low Permeability H_2 Delivery Hose. III–28

National Institute of Standards and Technology

IV.C.1 Hydrogen Storage in Metal-Organic Frameworks. IV–63
IV.C.2 Hydrogen Sorbent Measurement Qualification and Characterization IV–70
IV.C.3 Neutron Characterization in Support of the DOE Hydrogen Storage Sub-Program IV–76
V.F.5 Neutron Imaging Study of the Water Transport in Operating Fuel Cells V–152

National Renewable Energy Laboratory

II.B.1 Renewable Electrolysis Integrated System Development and Testing II–18
II.B.2 High-Performance, Long-Lifetime Catalysts for Proton Exchange Membrane Electrolysis II–23
II.C.2 Flowing Particle Bed Solarthermal Redox Process to Split Water II–41
II.C.4 High-Efficiency Tandem Absorbers for Economical Solar Hydrogen Production II–50
II.C.5 Wide Bandgap Chalcopyrite Photoelectrodes for Direct Solar Water Splitting II–56
II.E.1 Fermentation and Electrohydrogenic Approaches to Hydrogen Production. II–76
II.E.2 Improving Cyanobacterial O_2-Tolerance using CBS Hydrogenase for H_2 Production II–81
III.6 Cryogenically Flexible, Low Permeability H_2 Delivery Hose. III–28
III.11 Reference Station Design III–53
III.13 700-Bar Hydrogen Dispenser Hose Reliability Improvement. III–60
IV.B.1 Hydrogen Storage Engineering Center of Excellence IV–22
IV.B.6 System Design, Analysis, and Modeling for Hydrogen Storage Systems. IV–49
IV.C.2 Hydrogen Sorbent Measurement Qualification and Characterization IV–7
V.A.1 Extended, Continuous Pt Nanostructures in Thick, Dispersed Electrodes. V–9
V.B.2 Advanced Hybrid Membranes for Next Generation PEMFC Automotive Applications V–69
V.C.4 Advanced Ionomers & MEAs for Alkaline Membrane Fuel Cells V–92
V.E.3 Effect of System Contaminants on PEMFC Performance and Durability V–113
V.F.1 Optimal Stationary Fuel Cell Integration and Control V–130
V.F.10 Fuel Cell Technology Status—Degradation V–174
V.F.15 Magnetic Annealing of Pt-Alloy Nanostructured Thin Film Catalysts for Enhanced Activity V–198

National Renewable Energy Laboratory (Continued)

VI.1 Fuel Cell Membrane Electrode Assembly Manufacturing R&D VI–7
VII.1 Hydrogen Component Validation. VII–9
VII.3 FCTO INTEGRATE Stack Test Bed & Grid Interoperability VII–17
VII.4 Fuel Cell Electric Vehicle Evaluation VII–21
VII.5 Technology Validation: Fuel Cell Bus Evaluations VII–26
VII.6 Material Handling Equipment Data Collection and Analysis VII–31
VII.11 Hydrogen Station Data Collection and Analysis VII–53
VII.13 Stationary Fuel Cell Evaluation VII–61
VIII.2 Component Standard Research & Development VIII–13
VIII.5 NREL Hydrogen Sensor Testing Laboratory VIII–26
VIII.7 Fuel Cell Technologies National Codes and Standards Deployment and Outreach VIII–38
VIII.9 Hydrogen Contaminant Detector VIII–46
IX.3 Pathway Analysis: Projected Cost, Lifecycle Energy Use and Emissions of Emerging Hydrogen Technologies IX–24
IX.12 Infrastructure Investment and Finance Scenario Analysis IX–61

New England Wire Technologies

III.6 Cryogenically Flexible, Low Permeability H_2 Delivery Hose. III–28

New Jersey Institute of Technology

VI.1 Fuel Cell Membrane Electrode Assembly Manufacturing R&D VI–7

Nissan Technical Center, North America

V.A.4 Synthesis and Characterization of Mixed-Conducting Corrosion Resistant Oxide Supports V–25
V.A.5 Development of Novel Non-PGM Electrocatalysts for Proton Exchange Membrane Fuel Cell Applications V–29
V.B.2 Advanced Hybrid Membranes for Next Generation PEMFC Automotive Applications V–69

Norm Shade

III.7 Hydrogen Compression Application of the Linear Motor Reciprocating Compressor (LMRC) III–33

Northeastern University

V.A.5 Development of Novel Non-PGM Electrocatalysts for Proton Exchange Membrane Fuel Cell Applications V–29

Northwestern University

II.C.1 High Efficiency Solar Thermochemical Reactor for Hydrogen Production II–35
IX.5 Employment Impacts of Infrastructure Development for Hydrogen and Fuel Cell Technologies IX–34

Oak Ridge National Laboratory

III.2 Vessel Design and Fabrication Technology for Stationary High-Pressure Hydrogen Storage III–13
III.8 Steel Concrete Composite Vessel for 875 bar Stationary Hydrogen Storage III–40
III.9 Low Cost Hydrogen Storage at 875 Bar Using Steel Liner and Steel Wire Wrap. III–45
IV.D.5 Melt Processable PAN Precursor for High Strength, Low-Cost Carbon Fibers (Phase II) IV–126
V.A.2 Nanosegregated Cathode Alloy Catalysts with Ultra-Low Platinum Loading V–13
V.A.7 Non-Precious Metal Fuel Cell Cathodes: Catalyst Development & Electrode Structure Design V–43
V.E.1 Durability Improvements Through Degradation Mechanism Studies V–101

Oak Ridge National Laboratory (Continued)

V.F.4 Characterization of Fuel Cell Materials . . . V–147
V.F.15 Magnetic Annealing of Pt-Alloy Nanostructured Thin Film Catalysts for Enhanced Activity . . . V–198
V.F.16 High Conductivity Durable Anion Conducting Membranes . . . V–203
V.F.18 DOE's High Acid Content Diels Alder Poly(Phenylene)s for High Temperature and Low Humidity Applications . . . V–211
V.F.19 Engineered Low-Pt Catalyst Layers . . . V–218
IX.2 GPRA Analysis: Impact of Program Targets on Vehicle Penetration and Benefits . . . IX–19
IX.11 Analysis of Optimal On-Board Storage Pressure for Hydrogen Fuel Cell Vehicles . . . IX–58

Oregon State University

IV.B.1 Hydrogen Storage Engineering Center of Excellence . . . IV–22
IV.B.3 Microscale Enhancement of Heat and Mass Transfer for Hydrogen Energy Storage . . . IV–32

Pacific Northwest National Laboratory

II.F.1 Monolithic Piston-Type Reactor for Hydrogen Production through Rapid Swing of Reforming/Combustion Reactions . . . II–84
III.14 Magnetocaloric Hydrogen Liquefaction . . . III-65
IV.B.1 Hydrogen Storage Engineering Center of Excellence . . . IV–22
IV.B.5 Systems Engineering of Chemical Hydrogen Storage and Cryo-Sorbent Storage, Pressure Vessel, and Balance of Plant for Onboard Hydrogen Storage . . . IV–44
IV.C.7 Novel Carbon(C)-Boron(B)-Nitrogen(N)-Containing H_2 Storage Materials . . . IV–92
IV.D.3 Enhanced Materials and Design Parameters for Reducing the Cost of Hydrogen Storage Tanks . . . IV–118
IV.D.6 Achieving Hydrogen Storage Goals through High-Strength Fiber Glass . . . IV–134
V.F.14 High Performance and Durable Low PGM Cathode Catalysts . . . V–194
VIII.6 Hydrogen Safety Panel, Safety Knowledge Tools and First Responder Training Resources . . . VIII–31

Pajarito Powder, LLC

V.A.5 Development of Novel Non-PGM Electrocatalysts for Proton Exchange Membrane Fuel Cell Applications . . . V–29

Pennsylvania State University

II.E.1 Fermentation and Electrohydrogenic Approaches to Hydrogen Production . . . II–76

pH Matter, LLC

V.A.10 Non-Precious Metal Bi-Functional Catalysts . . . V–60

Plug Power

X.1 Ground Support Equipment Demonstration . . . X–7

POSCO

III.8 Steel Concrete Composite Vessel for 875 bar Stationary Hydrogen Storage . . . III–40

Powertech Labs, Inc.

VII.7 Development of the Hydrogen Station Equipment Performance (HyStEP) Device . . . VII–36

PPG Industries, Inc.

IV.D.6 Achieving Hydrogen Storage Goals through High-Strength Fiber Glass . . . IV–134

Pressure Science, Inc.

III.9 Low Cost Hydrogen Storage at 875 Bar Using Steel Liner and Steel Wire Wrap. III–45

Proton Energy Systems d/b/a Proton OnSite

II.B.3 Low-Noble-Metal-Content Catalysts/Electrodes for Hydrogen Production by Water Electrolysis II–28

V.A.9 Non-Platinum Group Metal OER/ORR Catalysts for Alkaline Membrane Fuel Cells and Electrolyzers V–56

VII.9 Validation of an Advanced High Pressure PEM Electrolyzer and Composite Hydrogen Storage, with Data Reporting, for SunHydro Stations. VII–44

VIII.6 Hydrogen Safety Panel, Safety Knowledge Tools and First Responder Training Resources VIII–31

Protonex Technology Corporation

IV.C.7 Novel Carbon(C)-Boron(B)-Nitrogen(N)-Containing H_2 Storage Materials IV–92

RCF Economic & Financial Consulting

IX.5 Employment Impacts of Infrastructure Development for Hydrogen and Fuel Cell Technologies IX–34

Redox Fuel Cells, Inc.

V.F.8 Affordable, High Performance, Intermediate Temperature Solid Oxide Fuel Cells. V–167

Rensselaer Polytechnic University

V.F.17 Advanced Hydroxide Conducting Membranes V–205

Rutgers, the State University of New Jersey

II.D.2 Tunable Photoanode-Photocathode-Catalyst Interface Systems for Efficient Solar Water Splitting II–72

V.A.9 Non-Platinum Group Metal OER/ORR Catalysts for Alkaline Membrane Fuel Cells and Electrolyzers V–56

Sandia National Laboratories

II.C.1 High Efficiency Solar Thermochemical Reactor for Hydrogen Production II–35

III.3 Hydrogen Embrittlement of Structural Steels III–18

III.11 Reference Station Design. III–53

IV.C.8 Boron-Based Hydrogen Storage: Ternary Borides and Beyond IV–97

IV.C.9 Improving the Kinetics and Thermodynamics of $Mg(BH_4)_2$ for Hydrogen Storage. IV–101

IV.D.1 Innovative Development, Selection and Testing to Reduce Cost and Weight of Materials for BOP Components IV–108

V.F.17 Advanced Hydroxide Conducting Membranes V–205

V.F.18 DOE's High Acid Content Diels Alder Poly(Phenylene)s for High Temperature and Low Humidity Applications V–211

VII.7 Development of the Hydrogen Station Equipment Performance (HyStEP) Device VII–36

VIII.1 Hydrogen behavior and Quantitative Risk Assessment. VIII–1

VIII.3 R&D for Safety, Codes and Standards: Materials and Components Compatibility VIII–17

VIII.10 Enabling Hydrogen Infrastructure Through Science-based Codes and Standards VIII–49

IX.7 Hydrogen Analysis with the Sandia ParaChoice Model IX–44

X.2 Maritime Fuel Cell Generator Project X–10

Savannah River Consultants

II.C.3 Electrolyzer Component Development for the HyS Thermochemical Cycle II–46

Savannah River National Laboratory

II.C.3 Electrolyzer Component Development for the HyS Thermochemical Cycle II–46

III.4 Fiber Reinforced Composite Pipelines. III–22

Savannah River National Laboratory (Continued)

IV.B.1 Hydrogen Storage Engineering Center of Excellence IV–22
IV.C.5 Electrochemical Reversible Formation of α-Alane IV–84
IV.E.2 Elucidation of Hydrogen Interaction Mechanisms with Metal-Doped Carbon Nanostructures. IV–144
V.F.13 PGM Free Catalysts for PEMFC V–189

Southwest Research Institute®

III.7 Hydrogen Compression Application of the Linear Motor Reciprocating Compressor (LMRC) III–33

Spectrum Automation Controls

II.B.1 Renewable Electrolysis Integrated System Development and Testing II–18
III.13 700-Bar Hydrogen Dispenser Hose Reliability Improvement. III–60
VII.1 Hydrogen Component Validation. VII–9
VII.3 FCTO INTEGRATE Stack Test Bed & Grid Interoperability VII–17
VIII.2 Component Standard Research & Development VIII–13

Spencer Composites Corporation

IV.D.2 Thermomechanical Cycling of Thin Liner High Fiber Fraction Cryogenic Pressure Vessels Rapidly Refueled by LH_2 Pump to 700 Bar. IV–113
IV.D.4 Next Generation Hydrogen Storage Vessels Enabled by Carbon Fiber Infusion with a Low Viscosity, High Toughness System. IV–122
VII.2 Performance and Durability Testing of Volumetrically Efficient Cryogenic Vessels and High Pressure Liquid Hydrogen Pump VII–13

SRI International

IV.C.6 Low-Cost α-Alane for Hydrogen Storage IV–88

Stanford University

II.C.1 High Efficiency Solar Thermochemical Reactor for Hydrogen Production II–35
II.C.5 Wide Bandgap Chalcopyrite Photoelectrodes for Direct Solar Water Splitting II–56

Strategic Analysis, Inc.

II.A.1 Hydrogen Pathways Analysis for Solid Oxide Fuel Cell (SOFC) and Dark Fermentation II–11
IV.A.2 Hydrogen Storage Cost Analysis IV–17
V.F.3 Fuel Cell Vehicle and Bus Cost Analysis. V–141
V.F.7 A Total Cost of Ownership Model for Design and Manufacturing Optimization of Fuel Cells in Stationary and Emerging Market Applications V–162
VI.2 U.S. Clean Energy Hydrogen and Fuel Cell Technologies: A Competitiveness Analysis VI–12

SunHydro LLC

VII.9 Validation of an Advanced High Pressure PEM Electrolyzer and Composite Hydrogen Storage, with Data Reporting, for SunHydro Stations. VII–44

Sustainable Innovations, LLC

III.10 Electrochemical Hydrogen Compressor III–50

SustainX

III.8 Steel Concrete Composite Vessel for 875 bar Stationary Hydrogen Storage III–40

Swagelok
III.6 Cryogenically Flexible, Low Permeability H_2 Delivery Hose. III–28

Temple University
III.2 Vessel Design and Fabrication Technology for Stationary High-Pressure Hydrogen Storage III–13
III.8 Steel Concrete Composite Vessel for 875 bar Stationary Hydrogen Storage III–40

Texas A&M University
IV.C.2 Hydrogen Sorbent Measurement Qualification and Characterization IV–70

The University of Alabama
IV.C.7 Novel Carbon(C)-Boron(B)-Nitrogen(N)-Containing H_2 Storage Materials IV–92

Toray Composites America
IV.D.3 Enhanced Materials and Design Parameters for Reducing the Cost of Hydrogen Storage Tanks IV–118

TreadStone Technologies, Inc.
V.C.3 Novel Structured Metal Bipolar Plates for Low Cost Manufacturing. V–86

Unique Electric Solutions
X.3 Fuel Cell Hybrid Electric Delivery Van Project X–14

United Parcel Service
X.3 Fuel Cell Hybrid Electric Delivery Van Project X–14

United Technologies Research Center
IV.B.1 Hydrogen Storage Engineering Center of Excellence IV–22
IV.B.4 Advancement of Systems Designs and Key Engineering Technologies for Materials Based Hydrogen Storage IV–36
V.C.2 Rationally Designed Catalyst Layers for PEMFC Performance Optimization. V–80
V.E.2 Fuel-Cell Fundamentals at Low and Subzero Temperatures. V–108

University of Connecticut
V.E.4 The Effect of Airborne Contaminants on Fuel Cell Performance and Durability V–119

University of Texas at Austin
V.C.2 Rationally Designed Catalyst Layers for PEMFC Performance Optimization. V–80

Université du Québec à Trois-Rivières
IV.B.1 Hydrogen Storage Engineering Center of Excellence IV–22

University of Calgary
V.E.5 Open Source Performance and Durability Model: Consideration of Membrane Properties on Cathode Degradation V–125

University of California, Berkeley
IV.C.2 Hydrogen Sorbent Measurement Qualification and Characterization IV–70
V.F.7 A Total Cost of Ownership Model for Design and Manufacturing Optimization of Fuel Cells in Stationary and Emerging Market Applications V–162

University of California, Davis

IV.E.3 Activation of Hydrogen Under Ambient Conditions by Main Group Molecules IV–145

University of California, Irvine

II.F.2 Reformer-Electrolyzer-Purifier (REP) for Production of Hydrogen II–90

IX.9 Tri-Generation Fuel Cell Technologies for Location-Specific Applications (FY 2015) IX–54

University of California, San Diego

IV.C.2 Hydrogen Sorbent Measurement Qualification and Characterization IV–70

University of Chicago

IX.13 The Business Case for Hydrogen-powered Passenger Cars: Competition and Solving the Infrastructure Puzzle IX–65

University of Colorado Boulder

II.C.2 Flowing Particle Bed Solarthermal Redox Process to Split Water II–41

II.C.6 Accelerated Discovery of Advanced RedOx Materials for Solar Thermal Water Splitting to Produce Renewable Hydrogen II–60

University of Connecticut

V.F.9 Smart Matrix Development for Direct Carbonate Fuel Cell V–170

University of Delaware

V.A.1 Extended, Continuous Pt Nanostructures in Thick, Dispersed Electrodes. V–9

University of Hawaii

II.C.4 High-Efficiency Tandem Absorbers for Economical Solar Hydrogen Production II–50

II.C.5 Wide Bandgap Chalcopyrite Photoelectrodes for Direct Solar Water Splitting II–56

V.C.3 Novel Structured Metal Bipolar Plates for Low Cost Manufacturing. V–86

University of Maryland

V.F.8 Affordable, High Performance, Intermediate Temperature Solid Oxide Fuel Cells. V–167

University of Michigan

IV.B.1 Hydrogen Storage Engineering Center of Excellence IV–22

IV.B.2 Ford/BASF-SE/UM Activities in Support of the Hydrogen Storage Engineering Center of Excellence. IV–27

IV.C.9 Improving the Kinetics and Thermodynamics of $Mg(BH_4)_2$ for Hydrogen Storage. IV–101

University of Missouri

IV.C.4 High-Capacity Hydrogen Storage Systems via Mechanochemistry IV–81

IV.C.8 Boron-Based Hydrogen Storage: Ternary Borides and Beyond IV–97

University of Nevada, Las Vegas

II.C.4 High-Efficiency Tandem Absorbers for Economical Solar Hydrogen Production II–50

II.C.5 Wide Bandgap Chalcopyrite Photoelectrodes for Direct Solar Water Splitting II–56

University of New Mexico

V.A.5 Development of Novel Non-PGM Electrocatalysts for Proton Exchange Membrane Fuel Cell Applications V–29

V.E.5 Open Source Performance and Durability Model: Consideration of Membrane Properties on Cathode Degradation V–125

University of Rochester
V.A.7 Non-Precious Metal Fuel Cell Cathodes: Catalyst Development & Electrode Structure Design V–43

University of South Carolina
V.A.6 Development of Ultra-Low Doped-Pt Cathode Catalysts for PEM Fuel Cells V–37
V.E.3 Effect of System Contaminants on PEMFC Performance and Durability V–113

University of Tennessee
IX.8 Status and Prospects of the N.A. Non-Automotive Fuel Cell Industry: 2014 Update. IX–48

University of Texas
X.3 Fuel Cell Hybrid Electric Delivery Van Project X–14

University of Toledo
II.D.1 New Metal Oxides for Efficient Hydrogen Production via Solar Water Splitting. II–67

University of Waterloo
V.A.7 Non-Precious Metal Fuel Cell Cathodes: Catalyst Development & Electrode Structure Design V–43

US Hybrid Corporation
X.5 Demonstration and Deployment of a Fuel Cell-Electric Refuse Truck for Waste Transportation X–21

Valence
X.3 Fuel Cell Hybrid Electric Delivery Van Project X–14

Vanderbilt University
V.B.1 New Fuel Cell Membranes with Improved Durability and Performance V–64

Virginia Commonwealth University
IV.E.4 Elucidation of Hydride Interaction Mechanisms with Carbon Nanostructures and the Formation of Novel Nanocomposites. IV–146

Virginia Polytechnic Institute
II.B.4 High Temperature, High Pressure Electrolysis II–31
IV.D.5 Melt Processable PAN Precursor for High Strength, Low-Cost Carbon Fibers (Phase II) IV–126

W.L. Gore & Associates
VI.1 Fuel Cell Membrane Electrode Assembly Manufacturing R&D VI–7

Washington State University
II.F.1 Monolithic Piston-Type Reactor for Hydrogen Production through Rapid Swing of Reforming/Combustion Reactions II–84

WireTough Cylinders
III.8 Steel Concrete Composite Vessel for 875 bar Stationary Hydrogen Storage III–40
III.9 Low Cost Hydrogen Storage at 875 Bar Using Steel Liner and Steel Wire Wrap. III–45

WPCSOL
V.E.4 The Effect of Airborne Contaminants on Fuel Cell Performance and Durability V–119

U.S. DEPARTMENT OF
ENERGY

www.hydrogen.energy.gov